November 2009

Technical Note of the National Research Institute for Earth Science and Disaster Prevention No.336

Technical Reports on National Seismic Hazard Maps for Japan

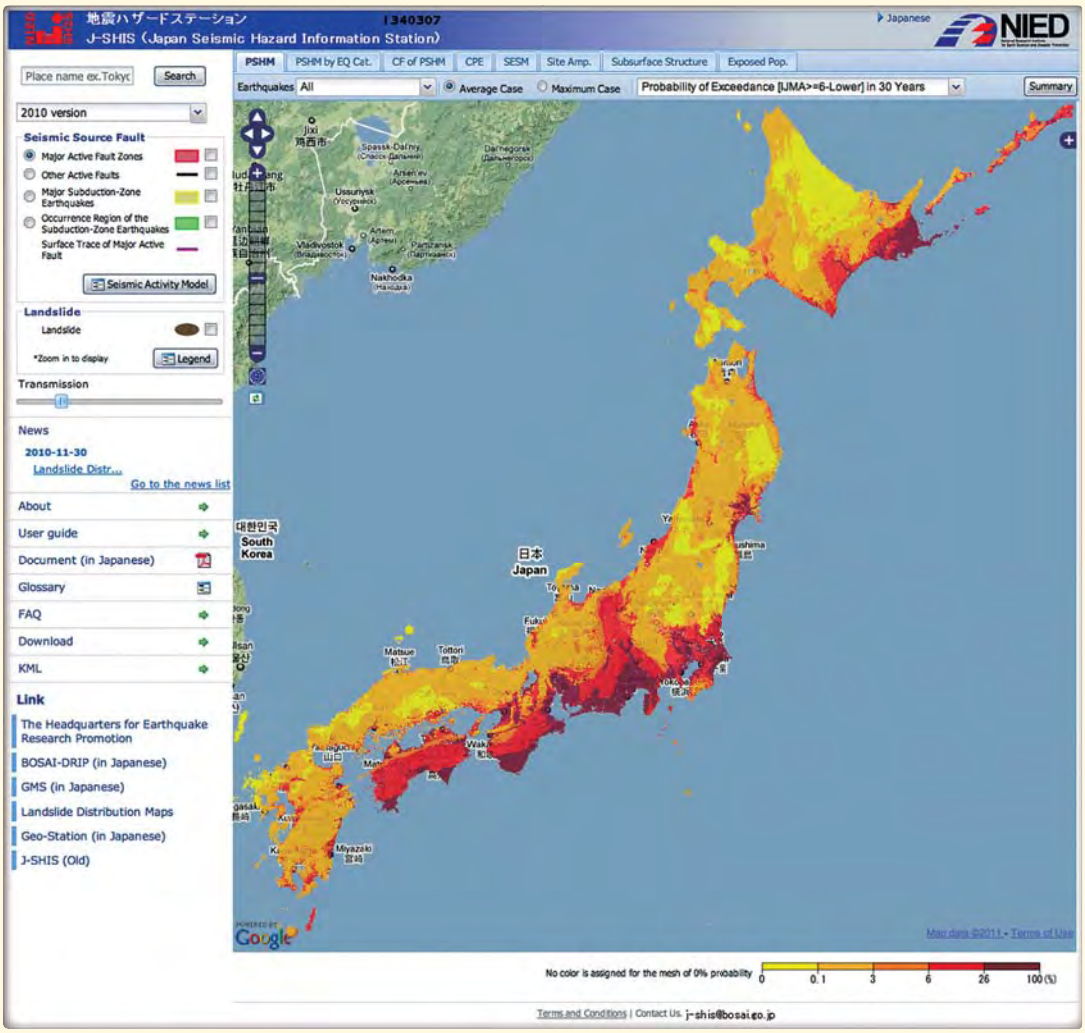

NIED 独立行政法人 防災科学技術研究所

National Research Institute for Earth Science and Disaster Prevention, Japan

Technical Reports on National Seismic Hazard Maps for Japan

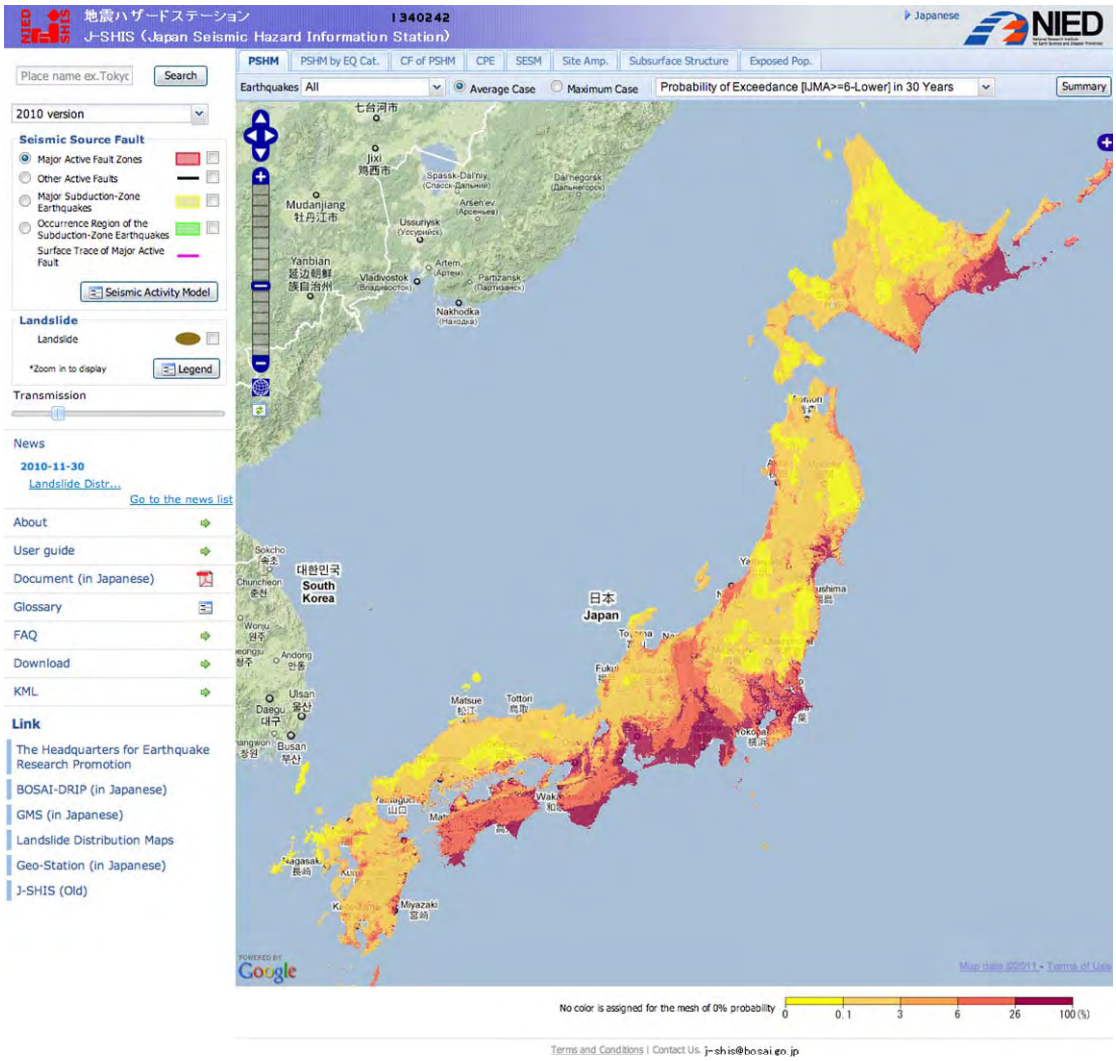

Explanation of the Cover Page

Example of a National Seismic Hazard Map for Japan (Map of probability of ground motions equal to or larger than JMA intensity 6 Lower) displayed at the Japan Seismic Hazard Information Station (J-SHIS) (http://www.j-shis.bosai.go.jp).

Technical Reports on National Seismic Hazard Maps for Japan

Hiroyuki FUJIWARA, Shinichi KAWAI, Shin AOI, Nobuyuki MORIKAWA, Shigeki SENNA, Nobuaki KUDO, Masahiro OOI, Ken Xiansheng HAO, Kazue WAKAMATSU, Yutaka ISHIKAWA, Toshihiko OKUMURA, Toru ISHII, Shinichi MATSUSHIMA, Yuzuru HAYAKAWA, Nobuhiko TOYAMA, and Akira NARITA

Technical Reports on National Seismic Hazard Maps for Japan

Table of Contents

1. Introduction

1.1 Background

1.2 Outline of the National Seismic Hazard Maps for Japan (2009)

1.2.1 Probabilistic seismic hazard maps

1.2.2 Seismic hazard maps for specified seismic source faults

1.2.3 Japan Seismic Hazard Information Station (J-SHIS)

2. Seismic Source Fault Models for Characteristic Earthquakes in Long-Term Evaluation

2.1 Characteristic Earthquakes Occurring in Major Active Fault Zones

2.1.1 Seismic source fault models in previous strong motion evaluation

2.1.2 Seismic source fault models by the standardized procedural modeling method applicable nationwide

2.1.3 Seismic source fault models for super-long faults

2.2 Characteristic Earthquakes Occurring in the Subduction-Zone and Eastern Margin of the Japan Sea

3. Probabilistic Seismic Hazard Maps (PSHM)

3.1 Evaluation Procedure and Its Result Representation

3.1.1 Outline of the seismic hazard evaluation method

3.1.2 Hazard curve calculation method

3.1.3 Representation of the results

3.2 Area Covered by the PSHM and Map Specifications

3.2.1 Area covered by the maps

3.2.2 Map specifications

3.3 Seismic Activity Evaluation Models

3.3.1 Characteristic earthquakes occurring in major active fault zones

3.3.2 Subduction-zone earthquakes

3.3.3 Earthquakes occurring in active faults other than major active fault zones

3.3.4 Earthquakes without specified source faults

3.4 Earthquake Category

3.5 Ground Motion Evaluation Models

3.5.1 Attenuation relation for the peak ground velocityon the engineering bedrock

3.5.2 Correction method for regions of anomalous seismic intensity

3.5.3 Evaluation of the peak ground velocity on the ground surface
3.5.4 Evaluation of the instrumental seismic intensity on the ground surface
3.5.5 Variance of the attenuation relation
3.6 Change Logs for the Used Parameters of Probabilistic Seismic Hazard Maps
3.7 Evaluation Results
3.7.1 List of evaluation maps
3.7.2 Evaluation results
3.7.3 Exceedance Probability of JMA Seismic Intensity 6 Lower Within 30 Years at Representative Sites
4. Seismic Hazard Maps (SHM) for Specified Seismic Source Faults
4.1 Procedure and Results of Evaluation and Presentation Method
4.1.1 Target earthquakes
4.1.2 Outline of the evaluation method
4.1.3 Method for presenting the results
4.2 Areas Covered by the SHM and Its Specifications
4.2.1 Areas covered by the SHM
4.2.2 Map specifications
4.3 Determination of the Inner Source Parameters and Others of Characteristic Earthquakes Occurring in Major Active Fault Zones
4.3.1 Determination of inner source parameters
4.3.2 Determination of other source parameters
4.4 Subsurface Structure Models
4.4.1 Crustal structure of the seismic bedrock and deeper
4.4.2 Deep subsurface structure models
4.4.3 Shallow subsurface structure models
4.5 Method of Strong Motion Simulation
4.5.1 Simulation of waveforms on the "engineering bedrock in the detailed method"
4.5.2 Simulation of the peak velocity on the engineering bedrock using an attenuation relation
4.5.3 Evaluation of the peak ground velocity on ground surface
4.5.4 Evaluation of the JMA instrumental seismic intensity on ground surface
4.5.5 Conditional exceedance probability
4.6 Evaluation Results
4.6.1 Characteristic earthquakes occurring in major active fault zones
4.6.2 Subduction-zone earthquakes and earthquakes in the eastern margin of the Japan Sea

5. Japan Seismic Hazard Information Station (J-SHIS)
5.1 Outline
5.2 Objectives
5.3 Technical Background
5.4 J-SHIS System
5.4.1 Functions
5.4.2 Public data
5.4.3 Seismic hazard map numerical database
5.4.4 Hardware configuration
5.4.5 Software configuration
5.5 Toward Sending Information on Earthquake Risk

6. Toward the Future

7. Closing Remarks

Acknowledgments

Appendix Strong Ground Motion Prediction Method ("Recipe") for Earthquakes with Specified Source Faults

1. Introduction

1.1 Background

The Hyogo-ken Nanbu (Kobe) Earthquake, which struck on January 17, 1995, claimed the lives of more than 6,400 victims and brought to light many problems to be solved in Japan's earthquake disaster prevention measures. In particular, regarding earthquake research, it was pointed out that the research results were not being sufficiently conveyed to people and disaster prevention agencies. Based on the lessons learned from this Earthquake, the Diet enacted a House member bill, the Act on Special Measures concerning Earthquake Disaster Management, in July 1995 in order promote comprehensive earthquake disaster prevention measures nationwide. Pursuant to this Act, the government established the Headquarters for Earthquake Research Promotion (HERP) under the Prime Minister's Office (currently in place under the Ministry of Education, Culture, Sports, Science and Technology (MEXT)) as the government's special agency, with the aim of clarifying the sharing of responsibilities concerning earthquake research which should be directly linked with administrative measures, and promoting such research in a centralized manner. HERP has a Policy Committee and an Earthquake Research Committee (ERC), and is designed to undertake the following roles: (1) planning of comprehensive and basic policies; (2) coordination of budgets and other administrative works with related governmental organizations; (3) establishment of comprehensive survey and observation plans; (4) collection, arrangement, analysis, and comprehensive evaluation of survey results by related governmental organizations, universities, etc.; and (5) public announcements based on the comprehensive evaluations.

In April 1999, HERP formulated "The Promotion of Earthquake Research: Basic comprehensive policy for the promotion of earthquake observation, measurement, surveys and research" (hereinafter referred to as the "Basic Comprehensive Policy") as the basic policy for the promotion of earthquake research during the next ten years and a guideline for HERP's activities. The Basic Comprehensive Policy sets as its basic aim to promote earthquake research that contributes to the strengthening of earthquake disaster prevention measures, especially to reducing damage caused by earthquakes. It indicates that earthquake research on the following four issues needs to be promoted immediately, and that surveys, observations, and research required for addressing these issues should be promoted. The four issues are as follows: (1) preparation of maps showing predicted seismic activity (seismic hazard maps) which consolidate surveys of active faults, long-term evaluation of the probability of earthquake occurrence, and strong motion prediction; (2) promotion of real-time transmission of earthquake information; (3) improvement of observation and other research in the areas of intensified earthquake disaster prevention measures determined by the Act on Special Measures Concerning Countermeasures for Large-Scale Earthquakes and their vicinity; and (4) promotion of observation and research for earthquake prediction.

Among these priority issues, preparation of seismic hazard maps was mentioned at the top of the list. Accordingly, HERP's ERC started preparation of the *Zenkoku Wo Gaikan Shita Jisindo Yosoku Chizu* (National Seismic Hazard Maps for Japan (2005)), and completed and published the 2005 version in March 2005. Since then, the National Seismic Hazard Maps for Japan have been updated every year by incorporating new evaluation results. In July 2009, the Committee summarized the studies over the past ten years and published dramatically improved maps under a new Japanese name, *Zenkoku Jishindo Yosoku Chizu* (National Seismic Hazard Maps for Japan (2009)). By adding various new data and adopting more advanced preparation methods, notable improvements were made, including the change of the mesh resolution of the maps from 1 km to a finer 250 m.

In order to contribute to preparation of seismic hazard maps, the National Research Institute for Earth Science and Disaster Prevention (NIED) launched a special project called the "National Seismic Hazard Mapping Project of Japan" in April 2001, and has made technical studies that contribute to preparation of seismic hazard maps, and has prepared maps. In NIED's Second Five-year Period as well, it has implemented research that contributes to advancement of seismic hazard maps through research called "Strong Motion Prediction and Seismic Hazard Evaluation" (FY2006-FY2007) and the "Research Project on the Disaster Risk Information Platform" (FY2008-). This report sums up NIED's studies on seismic hazard mapping techniques over the past decade.

1.2 Outline of the National Seismic Hazard Maps for Japan (2009)

The National Seismic Hazard Maps for Japan published by the ERC consist of two types of maps different in nature: the Probabilistic Seismic Hazard Maps that combine long-term probabilistic evaluations of earthquake occurrence and evaluation of strong motions predicted at the time of earthquake occurrence, and the Seismic Hazard Maps for Specified Seismic Source Faults which are based on detailed strong motion evaluation for scenarios assumed for specific earthquakes. Whereas HERP was established based on the lessons learned from the Hyogo-ken Nanbu (Kobe) Earthquake, the National Seismic Hazard Maps for Japan can be regarded as a comprehensive compilation of HERP's past ten years of achievements in its activities related to long-term evaluation and strong motion evaluation. Therefore, including the data required for mapping, they contain an enormous amount of information. The following part briefly outlines the National Seismic Hazard Maps for Japan.

1.2.1 Probabilistic seismic hazard maps

Evaluation of earthquake occurrence and ground motions incidental thereto (seismic hazard evaluation) involves many uncertainties at present. With the current level of seismology and

earthquake engineering, it is difficult to derive a single deterministic prediction about the date, time, place, magnitude, or ground motions of an earthquake that could occur in the future. A technical framework that is considered to be promising for quantitatively evaluating such uncertainties is the probabilistic approach. For preparing Probabilistic Seismic Hazard Maps, seismic hazard evaluation based on the following method is adopted. Seismic hazard evaluation analyzes the relationship between the following three parameters: the "ground motion intensity" that occur in the future at a given site; the "target period"; and "target probability." The brief outline of the procedure of seismic hazard evaluation in preparation of Probabilistic Seismic Hazard Maps is shown below.

(1) Model the earthquake activities around a target site according to the ERC's earthquake classification.
(2) For each earthquake modeled, evaluate the probability of the earthquake magnitude, the probability of the distance from the target site, and the probability of earthquake occurrence.
(3) Set a probability model for presuming the ground motion intensity for an earthquake of a given magnitude and distance. For each modeled earthquake, evaluate the probability of the intensity of the ground motions caused by that earthquake within the target period exceeding a certain value. Use empirical attenuation relations for strong motion evaluation. Specifically, first derive the peak velocity on the engineering bedrock based on an attenuation relation using the shortest distance from the target site to the fault plane, then multiply the derived value by the site amplification factor to obtain the peak velocity, and finally use the relation between the peak velocity and the instrumental seismic intensity to evaluate the seismic intensity on the ground surface.
(4) Repeat the operation above for the same number of times as the number of the modeled earthquakes, and sum up the results to obtain the probability of the intensity of the ground motions occurring within the target period exceeding a certain value by at least one degree, when all earthquakes are taken into consideration.

In this manner, seismic hazard evaluation is conducted for each site, and by fixing any two parameters of the ground motion intensity, period, and probability, the value of the remaining parameter are obtained. The Probabilistic Seismic Hazard Maps show the distribution of such values.

1.2.2 Seismic hazard maps for specified seismic source faults

For earthquakes that occur at major active fault zones, in addition to probabilistic seismic hazard evaluation, certain scenarios are assumed and detailed strong motion evaluation is used to prepare Seismic Hazard Maps for Specified Seismic Source Faults. Seismic Hazard Maps for Specified Seismic Source Faults are prepared by using a seismic waveform synthesis method called the hybrid method for detailed strong motion evaluation. The hybrid method is a complicated waveform synthesis method consisting of multiple elemental technologies. Therefore, studies have been made to standardize the method as much as possible and to develop such a method that could produce the same results for anyone. As a result, the ERC developed the "strong ground motion prediction method ("Recipe") for earthquakes with specified source faults." Meanwhile, detailed ground motion evaluation requires modeling of the subsurface structure. Therefore, deep subsurface structure models are being developed for the whole of Japan.

For earthquakes that occur at major active fault zones, earthquakes that occur at any other active faults, and subduction-type earthquakes of which seismic sources are specified are individually made subject to strong motion evaluation (expected ground motions and conditional exceedance probability) through a simple method using empirical attenuation relations, in addition to detailed strong motion evaluation.

1.2.3 Japan Seismic Hazard Information Station (J-SHIS)

The National Seismic Hazard Maps for Japan are regarded as a comprehensive compilation of HERP's past ten years of achievements of seismic hazard evaluation, and, including the data required for mapping such as seismic activity models, seismic source fault models, and subsurface structure models, they contain an enormous amount of information. As a part of its studies on utilization of seismic hazard maps, NIED has set up the Study Committee on Engineering Application of the National Seismic Hazard Program (Chair: Hiroyuki Kameda) to explore into the issue. The Committee's report recommends that the seismic hazard maps should be considered as seismic hazard information sharing bases by regarding the maps as a group of information incorporating the underlying data used in the evaluation process, such as the seismic activity models, seismic source models, and subsurface structure models, rather than mere maps as final products. In order to put this recommendation into practice, NIED developed an online disclosure system for seismic hazard maps, and started its operation in May 2005 under the name “Japan Seismic Hazard Information Station (J-SHIS),” which was the name proposed in the report above.

Four years have passed since the launch of operation of the J-SHIS. During that time, remarkable progress has been made in the technology to distribute map data via the Internet. By incorporating such latest technology, NIED developed a new J-SHIS system. The new system manages various data in an integrated manner, including the new National Seismic Hazard Maps for Japan which consist of the Probabilistic Seismic Hazard Maps for the whole of Japan with a 250 m mesh resolution and the Seismic Hazard Maps for Specified Seismic Source Faults based on detailed strong motion prediction of earthquakes that occur at major active fault zones, as well as the deep subsurface structure models for the whole of Japan and 250 m mesh geomorphological land classification models used for the required calculations. The system is also capable of providing these data in a user-friendly

manner by showing them over background maps. This new J-SHIS system is a web mapping system based on open source software which allows general users to easily view various data on their Internet browsers. Notable new functions available include the following: image overlapping functions such as the layer transparency function between the seismic hazard maps and Google Maps, a scroll function that allows users to move the maps and to freely scale the maps zoom in or out, the seismic hazard map viewing function supporting a 250 m mesh resolution, a detailed location search function using addresses and postal codes, a function to display/select a seismic source fault on the browser, and a function to display attribute values for each mesh. The new system has been in operation since July 2009. (http://www.j-shis.bosai.go.jp)

2. Seismic Source Fault Models for Characteristic Earthquakes in Long-Term Evaluation

This Chapter describes the methods for modeling seismic source faults and indicates the parameters used for earthquakes to be evaluated in both the Probabilistic Seismic Hazard Maps and the Seismic Hazard Maps for Specified Seismic Source Faults. The target earthquakes are those subject to the Seismic Hazard Maps for Specified Seismic Source Faults, in other words, characteristic earthquakes occurring in major active fault zones, subduction-zone characteristic earthquakes, and characteristic earthquakes that occur in the eastern margin of the Japan Sea subject to long-term evaluation.

2.1 Characteristic Earthquakes Occurring in Major Active Fault Zones

Previously, in seismic hazard maps, the magnitude of earthquakes occurring in major active fault zones had not been treated in a unified manner between long-term evaluation and strong motion evaluation. Therefore, a method for building fault models through a series of processes based on results of long-term evaluation was added to the "strong ground motion prediction method ('Recipe') for earthquakes with specified source faults" (ERC, 2008b; hereinafter referred to as the "Recipe") in April 2008, in which the methods for building source fault models were reviewed so that the earthquake magnitude will be the same in both evaluations, and asperity locations were simplified so that multiple faults can be treated together as a group. In the 2009 version of the National Seismic Hazard Maps for Japan, the Probabilistic Seismic Hazard Maps and strong motion waveforms were to be calculated by building fault models for the 105 major active fault zones for which long-term evaluation had been carried out by the end of 2008 based on such revised Recipe, in principle. The following basic policy was set for building fault models.

(1) For a fault zone that strong motion evaluation was made on it, the fault model and parameters used before shall be used as far as possible.
(2) If multiple fault models overlap and no clear information about such overlapping is available at present, fault models can cross each other.
(3) For a fault zone that is more than roughly 80 km long, consideration shall be made about a separate model as a super-long fault.
(4) If the probability of earthquake occurrence in the case where multiple faults are activated simultaneously has not been obtained in long-term evaluation, such case of simultaneous activity shall not be modeled. Consideration shall be made about separately modeling such case if earthquake occurrence has been observed in the past, but the faults shall be evaluated individually for the Probabilistic Seismic Hazard Maps.

Table 2.1-1 shows a list of the models of major active fault zones. Table 2.1-2 and Figure 2.1-1 indicate the determined fault plane locations and parameters. The specific modeling methods are described in the following sections. For the Uemachi fault zone, a straight fault model (one plane) as well as a bent fault model (two planes) are built in consideration of the modeling by the Central Disaster Prevention Council (2006). However, only the straight fault model is used for the Probabilistic Seismic Hazard Maps.

2.1.1 Seismic source fault models in previous strong motion evaluation

By the end of 2008, strong motion evaluation was carried out for 12 major active fault zones, and the results have been published by HERP. These seismic source fault models have been built through detailed analysis when carrying out the strong motion evaluation, and the modeling method is summarized in the current Recipe under the section "(A) The cases of estimating a seismic source fault based on historical earthquake records and based on detailed research results". These models have also been used as-is in the Probabilistic Seismic Hazard Maps. Therefore, with regard to fault zones for which strong motion evaluation has been carried out, the parameters determined for the strong motion evaluation were used as far as possible, in compliance with the above basic policy (1). As a result, only very minor changes were made, such as setting the depth of the upper edge of the fault models deeper than the seismic bedrock of deep subsurface structure models (see Section 4.4.2) and adjusting the modeled fault length and width to multiples of the fault model mesh size indicated in the following section. However, for the Yamagata-bonchi fault zone (ERC, 2007) and the Tonami-heiya fault zone (eastern part) (ERC, 2008c) of which fault locations and shapes have been changed as a result of revision of the long-term evaluation after the publication of the strong motion evaluation, new seismic source fault models were built by the standardized procedural modeling method applicable nationwide that is indicated in the following section. In addition, verification of the strong motion evaluation method (Recipe) targeting the 2005 West off Fukuoka Earthquake has already been carried out for the Kego fault zone (northwestern part) (ERC, 2008a), but the fault was separately modeled for the Probabilistic Seismic Hazard Maps in consideration of consistency in earthquake magnitude and other factors. Further, for the Itoigawa-Shizuoka-kozosen fault zone (northern part/central part), the super-long fault modeling method indicated in Section 2.1.3 was also examined.

2.1.2 Seismic source fault models by the standardized procedural modeling method applicable nationwide

Previously, the Recipe had been compiled for the purpose of carrying out detailed strong motion evaluation for individual fault zones. However, in order to enable calculation of strong motion waveforms even when targeting multiple fault zones together as a group or when the target fault zone lacks detailed information, a method that has simplified the determination of some fault

parameters while being based on the conventional Recipe was added to the Recipe updated in April 2008, as "(B) The case of estimating a seismic source fault by a simplified method based on ground surface active fault information" (ERC, 2008b). This method is applied to build seismic source fault models for major active fault zones which are not super-long faults and have not undergone strong motion evaluation. Figure 2.1.2-1 (Appended Figure 3 of the Recipe) shows the overall flow chart of the modeling.

The dip angle of a seismic source fault uses the value obtained in long-term evaluation, in principle, but if the dip angle is not clearly indicated in long-term evaluation, the value is determined by following the flow chart shown in the Recipe (Figure 2.1.2-2; Appended Figure 4 of the Recipe). The depth of the upper edge of the fault model (H_s [km]) is determined by taking into account the depth of the seismic bedrock around the fault zone based on the deep subsurface structure models formulated in this study (see Section 4.4.2), and the depth of the lower edge of the seismogenic layer (H_d [km]) by taking into account the source depth distribution of microearthquakes (Figure 2.1.2-3). Figure 2.1.2-3 shows the deepest source depth of microearthquakes in each 0.2-degree resolution that have been selected from the Japan Meteorological Agency (JMA) unified earthquake catalog for the period from October 1, 2000 to March 31, 2008, based on the following criteria: depth free (obtained by inversion); 25 km deep or shallower; not a low-frequency earthquake; and five or more events within a 0.2-degree resolution. Outer fault parameters are determined by the following procedure, using the JMA magnitude M derived from the active fault length L obtained in long-term evaluation (active fault length formed through repeated seismic activity) as a fixed parameter.

i. Active fault length L [km]

The active fault length L is deemed to be the length of a surface earthquake fault (a surface fault generated by a single seismic event), and uses the fault length obtained in long-term evaluation.

ii. JMA magnitude M (M_j)

The JMA magnitude M is obtained using the following relation by Matsuda (1975):

$$M = (\log L + 2.9)/0.6 \qquad (2.1.2\text{-}1)$$

iii. Seismic moment M_0 [Nm]

The seismic moment M_0 is obtained using the following relation by Takemura (1990) (Formula (4) of the Recipe):

$$\log M_0 = 1.17 \cdot M + 10.72 \qquad (2.1.2\text{-}2)$$

iv. Moment magnitude M_w

The moment magnitude M_w is obtained using the following relation by Kanamori (1977):

$$M_w = (\log M_0 - 9.1)/1.5 \qquad (2.1.2\text{-}3)$$

v. Fault area S [km^2] (provisionally determined)

The fault area is obtained using the relation between seismic moment and fault area by Irikura and Miyake (2001) (Formula (3)' or (2)' of the Recipe).

$$S = \begin{cases} 4.24\times10^{-11}\cdot(M_0\times10^7)^{1/2} & (M_0 \geq 7.5\times10^{18}) \\ 2.23\times10^{-15}\cdot(M_0\times10^7)^{2/3} & (M_0 < 7.5\times10^{18}) \end{cases} \qquad (2.1.2\text{-}4)$$

vi. Fault width W [km] (provisionally determined)

The fault width is obtained by the following formula (Formula (5) of the Recipe):

$$W = S/L \qquad (2.1.2\text{-}5)$$

Then, fault model parameters for ground motion simulation are determined. These parameters are distinguished from the parameters above by using the suffix "model".

vii. Modeled fault width W_{model} [km] and modeled fault length L_{model} [km]

The modeled fault width W_{model} and the modeled fault length L_{model} are obtained by taking into account the relation between the depth of the lower edge of the fault obtained by the fault width W derived in vi. above, the depth of the upper edge of the fault (H_s), and the dip angle δ, and the depth of the lower edge of the seismogenic layer. If the lower edge of the fault goes deeper beyond the lower edge of the seismogenic layer, the maximum allowable depth of the lower edge of the fault model will be the lower edge of the seismogenic layer plus 2 km.

$$W_{model} = N_W \cdot L_{mesh} \leq \min\{W, (T_S + 2)/\sin\delta\} \qquad (2.1.2\text{-}6)$$

$$L_{model} = N_L \cdot L_{mesh} \geq S/W_{model} \geq L$$

(Maximum L_{model} is L + 5 km.)

(2.1.2-7)

In the formulae above, T_S represents the thickness of the seismogenic layer (=H_d-H_s), N_W and N_L represent the largest and smallest integers that satisfy the above relation, and L_{mesh} represents the mesh size of the fault model. L_{mesh} corresponds to the mesh size used in the calculation for the later-mentioned stochastic Green's function method, but in this study, 2 km is used in consideration of employing a 1-second filter frequency for the waveform simulation by the hybrid method. The M_0 obtained by Formulae (2.1.2-1) and (2.1.2-2) and S obtained by Formula (2.1.2-4) hold when W is about 18 km. Therefore, when using this modeling method, W_{model} will be 18 km even when the value of W can be made larger in light of the relation between the seismogenic layer and the dip angle.

viii. Modeled fault area S_{model} [km^2]

The modeled fault area S_{model} is obtained by the following formula (Formula (7) of the Recipe):

$$S_{\mathrm{model}} = L_{\mathrm{model}} \times W_{\mathrm{model}} \qquad (2.1.2\text{-}8)$$

ix. Average slip of the fault model D_{model} [m]

The average slip of the fault model D_{model} is obtained by the following relation (Formula (9) of the Recipe):

$$D_{\mathrm{model}} = M_0 / (\mu \cdot S_{\mathrm{model}}) \qquad (2.1.2\text{-}9)$$

where μ is the rigidity of the seismogenic layer, which is calculated by the following relation using density ρ (kg/m^3) and shear wave velocity β (km/s) (Formula (10) of the Recipe):

$$\mu = \rho \cdot \beta^2 \qquad (2.1.2\text{-}10)$$

According to the Recipe, this rule is to be applied to building a seismic source fault model for an *M*7 or larger earthquake (a fault length of 20 km or more), but here it is applied also to fault zones with a length of 15 km or more and less than 20 km.

2.1.3 Seismic source fault models for super-long faults

The relation between the fault length L and the earthquake magnitude M by Matsuda (1975) (Formula (2.1.2-1)) is based on data for faults with a length of 80 km or less. Thus, it is not applicable to faults that are longer than 80 km. Meanwhile, for an earthquake occurring at a super-long active fault with a length of over 100 km, the fault displacement at the time of an earthquake is known to become saturated, so the relation between the fault length and the earthquake magnitude is likely to differ from that of an earthquake occurring at a shorter active fault. Accordingly, it is difficult to directly apply Formula (2.1.2-1) to such earthquakes occurring at super-long faults through extrapolation. Therefore, as mentioned in basic policy (3), a major active fault that is more than about 80 km long is regarded as a super-long fault, and a seismic source fault model is built separately without using the procedural method described in the preceding section, but instead, using a method based on the relation between the seismic moment and the fault size, which has been used in the current strong motion evaluation. In that process, adjustment is made in order to prevent contradiction with the observational facts of the fault length L and displacement D_{surf} indicated by long-term evaluation. In this study, two types of adjustment methods explained below were adopted. Figure 2.1.3-1 shows the overall flow chart of modeling seismic source faults for super-long faults.

<u>Adjustment method I</u>: a method based on (A) in the Recipe

This adjustment method is the method for building a source fault model which has conventionally been used in strong motion evaluation. The modeled fault length L_{model} and the modeled fault width W_{model}, which are multiples of the fault model mesh size (2 km in this case), are determined from the active fault length L and the fault width W obtained from the thickness of the seismogenic layer and the dip angle of the fault. Using the derived modeled fault area S_{model} (see Formula (2.1.2-8)), M_0 is obtained by the relation between the fault size and seismic moment M_0. The relation should desirably one derived or examined specifically for a super-long fault, but at present, the following formula by Irikura and Miyake (2001) (Formula (3) of the Recipe) is used:

$$M_0 = \left(\frac{S}{4.24} \times 10^{11}\right)^2 \times 10^{-7} \qquad (2.1.3\text{-}1)$$

The relation between the average slip of the fault $D_{\mathrm{sub_ave}}(=M_0/(\mu \cdot S)$, equivalent to Formula (2.1.2-9) and Formula (9) of the Recipe) obtained thereby and the ground surface displacement D_{surf} by a single seismic event is confirmed. Since a recent analysis of super-long faults shows that D_{surf} is about twice to three times the value of $D_{\mathrm{sub_ave}}$ (Figure 2.1.3-2), if the value of D_{surf} differs substantially from this, M_0 is adjusted to make the value match. Consideration is given so that the seismic moment does not become smaller than the value derived in the adjustment method II shown below. In this process, the modeled fault area S_{model} is fixed, so the relation between the fault size and the seismic moment in Formula (2.1.3-1) does not apply as a result.

<u>Adjustment method II</u>: the segmenting and aggregating method

In adjustment method II, a super-long fault zone is deemed to be multiple activity areas where seismic activity occurs simultaneously to cause an earthquake. By introducing the concept of "unit segments" to a target fault zone, the entire fault zone is divided into "segments for assuming earthquake magnitude", each of which consists of multiple "unit segments" with a total length not exceeding about 80 km (Figure 2.1.3-3). For each "segment for assuming earthquake magnitude", parameters are determined by the method shown in the preceding section (the method of (B) in the Recipe). The overall seismic moment is obtained by adding up the seismic moment of each "segment for assuming earthquake magnitude". This can be considered as a method combining the ideas of scaling law and cascade model. When multiple combinations of "unit segments" can be assumed, the combination which produces the largest overall seismic momentum is used. This method is not applied to a fault zone which needs no M_0 adjustment in adjustment method I.

Based on the above policy, seismic source fault models were built for the following six super-long faults: the Chuo-kozosen fault zone (Sanuki-sanmyaku-nan'en-Ishizuchi-sanmyaku-hokuen-tobu (S-I part)), the Chuo-kozosen fault zone (Ishizuchi-sanmyaku-hokuen-seibu-Iyonada (I-I part)), the Itoigawa-Shizuoka-kozosen fault zone (central part/northern part), the Nagaoka-heiya-seien fault zone, the Kanto-heiya-hokuseien fault zone, and the Tokachi-heiya fault zone. Figure 2.1.3-2 also shows the relation between D_{surf} and $D_{\mathrm{sub_ave}}$ for each fault zone before the adjustment of the seismic momentum. Meanwhile, only

models using adjustment method I are applied in creating the Probabilistic Seismic Hazard Maps.

(1) Chuo-kozosen fault (S-I part)

D_{surf} is about 1.2 times the value of D_{sub_ave}. Thus, in order to make D_{surf} about twice the value of D_{sub_ave} under adjustment method I, the seismic moment is multiplied by 0.6 (=1.2/2) times.

The Chuo-kozosen fault zon (S-I part; 131 km long in total) can be divided into the following four unit segments: the Naruto/Itano/Kanda fault segment (29 km long), the Chichio/Iguchi fault segment (22 km long), the Mino/Hashikura/Ikeda fault segment (53 km long), and the Sangawa/Ishizuchi fault segment (27 km long) (Figure 2.1.3-4). The "segments for assuming earthquake magnitude" under adjustment method II are the 51 km long segment consisting of the Naruto/Itano/Kanda and Chichio/Iguchi fault segments and the 80 km long segment consisting of the Mino/Hashikura/Ikeda and Sangawa/Ishizuchi fault segments.

(2) Chuo-kozosen fault (I-I part)

D_{sub_ave} is almost the same as D_{surf}. In order to make D_{surf} about twice the value of D_{sub_ave} under adjustment method I, the seismic moment needs to be multiplied by about 0.5. In this case, however, the seismic moment becomes smaller than that under adjustment method II. Thus, the seismic moment is multiplied by 1.0 times, with no M_0 adjustment.

The Chuo-kozosen fault zone (I-I part; 129 km long in total) can be divided into the following three unit segments: the Kawakami/Shigenobu fault segment (40 km long), the Iyo fault segment (37 km long), and the Iyonada fault segment (52 km long) (Figure 2.1.3-4). The "segments for assuming earthquake magnitude" under adjustment method II are the 77 km long segment consisting of the Kawakami/Shigenobu and Iyo fault segments and the 52 km long segment consisting of the Iyonada fault segment alone.

(3) Itoigawa-Shizuoka-kozosen fault zone (central part/northern part), Kanto-heiya-hokuseien fault zone

Since these two fault zones generally satisfy the relation between D_{surf} and D_{sub_ave}, they are directly used as seismic source fault models with no M_0 adjustment.

(4) Nagaoka-heiya-seien fault zone

D_{sub_ave} is larger than D_{surf}. However, as the displacement indicated in long-term evaluation was "2 m or more" (ERC, 2004d), no M_0 adjustment is made due to sufficient likelihood that D_{surf} is larger than 2m.

(5) Tokachi-heiya fault zone

Since long-term evaluation results indicated that "no direct data have been obtained about displacement by a single seismic event" (ERC, 2005b), no M_0 adjustment is made due to lack of direct information about D_{surf}.

As a result, adjustment methods I and II are only applied to the two fault zones in the Chuo-kozosen fault zone.

Table 2.1-1 List of models of major active fault zones (part 1)

	Active faults subject to fundamental surveys and observations		Models of major active fault zones (165 faults)
No.	Fault name	Code	Fault model name
1	Shibetsu fault zone	0101	Shibetsu fault zone
2	Tokachi-heiya fault zone	0201	Tokachi-heiya fault zone (main part)
		0202	Kochien fault
3	Furano fault zone	0301	Furano fault zone (western part)
		0302	Furano fault zone (eastern part)
4	Mashike-sanchi-toen/Numata-Sunagawa area fault zone	0401	Mashike-sanchi-toen fault zone
		0402	Numata-Sunagawa area fault zone
5	Tobetsu fault	0501	Tobetsu fault
6	Ishikari-teichi-toen fault zone	0601	Ishikari-teichi-toen fault zone (main part)
		0602	Ishikari-teichi-toen fault zone (southern part)
7	Kuromatsunai-teichi fault zone	0701	Kuromatsunai-teichi fault zone
8	Hakodate-heiya-seien fault zone	0801	Hakodate-heiya-seien fault zone
9	Aomori-wan-seigan fault zone	0901	Aomori-wan-seigan fault zone
10	Tsugaru-sanchi-seien fault zone	1001	Tsugaru-sanchi-seien fault zone (northern part)
		1002	Tsugaru-sanchi-seien fault zone (southern part)
11	Oritsume fault	1101	Oritsume fault
12	Noshiro fault zone	1201	Noshiro fault zone
13	Kitakami-teichi-seien fault zone	1301	Kitakami-teichi-seien fault zone
14	Shizukuishi-bonchi-seien/Mahiru-sanchi-toen fault zone	1401	Shizukuishi-bonchi-seien fault zone
		1402	Mahiru-sanchi-toen fault zone (northern part)
		1403	Mahiru-sanchi-toen fault zone (southern part)
15	Yokote-bonchi-toen fault zone	1501	Yokote-bonchi-toen fault zone (northern part)
		1502	Yokote-bonchi-toen fault zone (southern part)
16	Kitayuri fault	1601	Kitayuri fault
17	Shinjo-bonchi fault zone	1701	Shinjo-bonchi fault zone
18	Yamagata-bonchi fault zone	1801	Yamagata-bonchi fault zone (northern part)
		1802	Yamagata-bonchi fault zone (southern part)
19	Shonai-heiya-toen fault zone	1901	Shonai-heiya-toen fault zone
20	Nagamachi-Rifu-sen fault zone	2001	Nagamachi-Rifu-sen fault zone
21	Fukushima-bonchi-seien fault zone	2101	Fukushima-bonchi-seien fault zone
22	Nagai-bonchi-seien fault zone	2201	Nagai-bonchi-seien fault zone
23	Futaba fault	2301	Futaba fault
24	Aizu-bonchi-seien/-toen fault zone	2401	Aizu-bonchi-seien fault zone
		2402	Aizu-bonchi-toen fault zone
25	Kushigata-sanmyaku fault zone	2501	Kushigata-sanmyaku fault zone
26	Tsukioka fault zone	2601	Tsukioka fault zone
27	Nagaoka-heiya-seien fault zone	2701	Nagaoka-heiya-seien fault zone
28	Tokyo-wan-hokuen fault	-	-
29	Kamogawa-teichi fault zone	2901	Kamogawa-teichi fault zone
30	Sekiya fault	3001	Sekiya fault
31	Kanto-heiya-hokuseien fault zone	3101	Kanto-heiya-hokuseien fault zone (main part)
		3102	Hirai-Kushibiki fault zone
32	Motoarakawa fault zone	-	-
33	Arakawa fault	-	-
34	Tachikawa fault zone	3401	Tachikawa fault zone
35	Isehara fault	3501	Isehara fault

Table 2.1-1 List of models of major active fault zones (part 2)

	Active faults subject to fundamental surveys and observations		Models of major active fault zones (165 faults)
No.	Fault name	Code	Fault model name
36	Kannawa/Kozu-Matsuda fault zone	3601	Kannawa/Kozu-Matsuda fault zone
37	Miura-hanto fault group	3701	Miura-hanto fault group (Kinugasa/Kitatake fault zone of the main part)
		3702	Miura-hanto fault group (Takeyama fault zone of the main part)
		3703	Miura-hanto fault group (southern part)
38	Kitaizu fault zone	3801	Kitaizu fault zone
39	Tokamachi fault zone	3901	Tokamachi fault zone (western part)
		3902	Tokamachi fault zone (eastern part)
40	Shinanogawa fault zone (Nagano-bonchi-seien fault zone)	4001	Nagano-bonchi-seien fault zone
41 44	Itoigawa-Shizuoka-kozosen fault zone (central part) Itoigawa-Shizuoka-kozosen fault zone (northern part)	4101	Itoigawa-Shizuoka-kozosen fault zone (central part/northern part)
42	Itoigawa-Shizuoka-kozosen fault zone (southern part)	4201	Itoigawa-Shizuoka-kozosen fault zone (southern part)
43	Fujikawa-kako fault zone	4301	Fujikawa-kako fault zone
45	Kiso-sanmyaku-seien fault zone	4501	Kiso-sanmyaku-seien fault zone (northern segment of the main part)
		4502	Kiso-sanmyaku-seien fault zone (southern segment of the main part)
		4503	Seinaiji-toge fault zone
46	Sakaitoge/Kamiya fault zone	4601	Sakaitoge/Kamiya fault zone (main part)
		4602	Mutoyama-Narai fault zone
47	Atotsugawa fault zone	4701	Atotsugawa fault zone
48	Takayama/Oppara fault zone	4801	Kokufu fault zone
		4802	Takayama fault zone
		4803	Inohana fault zone
49	Ushikubi fault	4901	Ushikubi fault zone
50	Shokawa fault zone	5001	Shokawa fault zone
51	Inadani fault zone	5101	Inadani fault zone (main part)
		5102	Inadani fault zone (southeastern part)
52	Atera fault zone	5201	Atera fault zone (northern segment of the main part)
		5202	Atera fault zone (southern segment of the main part)
		5203	Sami fault zone
		5204	Shirakawa fault zone
53 54	Byobuyama/Enasan fault zone and Sanageyama fault zone	5301	Byobuyama fault zone
		5302	Ako fault zone
		5303	Enasan-Sanageyama-kita fault zone
		5304	Sanage-Takahama fault zone
		5305	Kagiya fault zone
55	Ochigata fault zone	5501	Ochigata fault zone
56	Tonami-heiya fault zone/Kurehayama fault zone	5601	Tonami-heiya fault zone (western part)
		5602	Tonami-heiya fault zone (eastern part)
		5603	Kurehayama fault zone

Table 2.1-1 List of models of major active fault zones (part 3)

	Active faults subject to fundamental surveys and observations		Models of major active fault zones (165 faults)
No.	Fault name	Code	Fault model name
57	Morimoto/Togashi fault zone	5701	Morimoto/Togashi fault zone
58	Fukui-heiya-toen fault zone	5801	Fukui-heiya-toen fault zone (main part)
		5802	Fukui-heiya-toen fault zone (western part)
59	Nagaragawa-joryu fault zone	5901	Nagaragawa-joryu fault zone
60	Nobi fault zone	6001	Nukumi fault (northwestern part)
		6002	Nukumi fault (southeastern part)
		6003	Nobi fault zone (Neodani fault zone of the main part)
		6004	Nobi fault zone (Umehara fault zone of the main part)
		6005	Nobi fault zone (Mitabora fault zone of the main part)
		6006	Ibigawa fault zone
		6007	Mugigawa fault
61 62	Yanagase/Sekigahara fault zone	6101	Yanagase/Sekigahara fault zone (northern segment of the main part)
		6102	Yanagase/Sekigahara fault zone (central segment of the main part)
		6103	Yanagase/Sekigahara fault zone (southern segment of the main part)
		6104	Urazoko-Yanagaseyama fault zone
63	Nosaka/Shufukuji fault zone	6301	Nosaka fault zone
		6302	Shufukuji fault
64	Kohoku-sanchi fault zone	6401	Kohoku-sanchi fault zone (northwestern part)
		6402	Kohoku-sanchi fault zone (southeastern part)
65	Biwako-seigan fault zone	6501	Biwako-seigan fault zone
66	Gifu-Ichinomiya fault zone	-	-
67	Yoro-Kuwana-Yokkaichi fault zone	6701	Yoro-Kuwana-Yokkaichi fault zone
68	Suzuka-toen fault zone	6801	Suzuka-toen fault zone
69	Suzuka-seien fault zone	6901	Suzuka-seien fault zone
70	Tongu fault	7001	Tongu fault
71	Nunobiki-sanchi-toen fault zone	7101	Nunobiki-sanchi-toen fault zone (western part)
		7102	Nunobiki-sanchi-toen fault zone (eastern part)
72	Kizugawa fault zone	7201	Kizugawa fault zone
73	Mikata/Hanaore fault zone	7301	Mikata fault zone
		7302	Hanaore fault zone (northern part)
		7303	Hanaore fault zone (central-southern part)
74	Yamada fault zone	7401	Yamada fault zone (main part)
		7402	Gomura fault zone
75	Kyoto-bonchi-Nara-bonchi fault zone (southern part) (Nara-bonchi-toen fault zone)	7501	Nara-bonchi-toen fault zone
76	Arima-Takatsuki fault zone	7601	Arima-Takatsuki fault zone
77	Ikoma fault zone	7701	Ikoma fault zone
78	Mitoke/Kyoto-Nishiyama fault zone	7801	Kanbayashigawa fault
		7802	Mitoke fault
		7803	Kyoto-Nishiyama fault zone

Table 2.1-1 List of models of major active fault zones (part 4)

	Active faults subject to fundamental surveys and observations		Models of major active fault zones (165 faults)
No.	Fault name	Code	Fault model name
79	Rokko/Awajishima fault zone	7901	Rokko/Awajishima fault zone (Rokko-sanchi-nan'en-Awajishima-togan segment of the main part)
		7902	Rokko/Awajishima fault zone (Awajishima-seigan segment of the main part)
		7903	Senzan fault zone
80	Uemachi fault zone	8001	Uemachi fault zone
81 83 85 86 89	Chuo-kozosen fault zone (Izumi-sanmyaku-nan'en-Kongo-sanchi-toen) Chuo-kozosen fault zone (Kitan-kaikyo-Naruto-kaikyo) Chuo-kozosen fault zone (Sanuki-sanmyaku-nan'en-Ishizuchi-sanmyaku-hokuen-tobu) Chuo-kozosen fault zone (Ishizuchi-sanmyaku-hokuen) Chuo-kozosen fault zone (Ishizuchi-sanmyaku-hokuen-seibu-Iyonada)	8101	Chuo-kozosen fault zone (Kongo-sanchi-toen-Izumi-sanmyaku-nan'en)
		8102	Chuo-kozosen fault zone (Kitan-kaikyo-Naruto-kaikyo)
		8103	Chuo-kozosen fault zone (S-I part)
		8104	Chuo-kozosen fault zone (Ishizuchi-sanmyaku-hokuen)
		8105	Chuo-kozosen fault zone (I-I part)
82	Yamasaki fault zone	8201	Nagisen fault zone
		8202	Yamasaki fault zone (northwestern segment of the main part)
		8203	Yamasaki fault zone (southeastern segment of the main part)
		8204	Kusatani fault
84	Nagao fault zone	8401	Nagao fault zone
87	Itsukaichi fault zone	8701	Itsukaichi fault
		8702	Koi-Hiroshima-seien fault zone
88	Iwakuni fault zone	8801	Iwakuni fault zone
90	Kikukawa fault zone	9001	Kikukawa fault zone
91	Nishiyama fault zone	9101	Nishiyama fault zone
92	Beppu-Haneyama fault zone	9201	Beppu-wan-Hijiu fault zone (eastern part)
		9202	Beppu-wan-Hijiu fault zone (western part)
		9203	Oita-heiya-Yufuin fault zone (eastern part)
		9204	Oita-heiya-Yufuin fault zone (western part)
		9205	Noinedake-Haneyama fault zone
		9206	Kuenohirayama-Kameishiyama fault zone
93	Futagawa/Hinagu fault zone	9301	Futagawa/Hinagu fault zone (northeastern part)
		9302	Futagawa/Hinagu fault zone (central part/southwestern part)*
94	Minou fault zone	9401	Minou fault zone
95	Unzen fault group	9501	Unzen fault group (northern part)
		9502	Unzen fault group (southeastern part)
		9503	Unzen fault group (northern segment of the southwestern part)
		9504	Unzen fault group (southern segment of the southwestern part)
96	Izumi fault zone	9601	Izumi fault zone

Table 2.1-1 List of models of major active fault zones (part 5)

	Active faults subject to fundamental surveys and observations		Models of major active fault zones (165 faults)
No.	Fault name	Code	Fault model name
97	Ise-wan fault zone	9701	Ise-wan fault zone (northern segment of the main part)
		9702	Ise-wan fault zone (southern segment of the main part)
		9703	Shirako-Noma fault
98	Osaka-wan fault zone	9801	Osaka-wan fault zone
99	Sarobetsu fault zone	9901	Sarobetsu fault zone
101	Hanawa-higashi fault zone	10101	Hanawa-higashi fault zone
104	Sone-kyuryo fault zone	10401	Sone-kyuryo fault zone
105	Uozu fault zone	10501	Uozu fault zone
106	Ube-Oki fault group (Suonada fault group)	10601	Suonada fault zone (main part)
		10602	Aio-Oki fault zone
		10603	Ube-nanpo-Oki fault zone
108	Kego fault zone	10801	Kego fault zone (northwestern part)
		10802	Kego fault zone (southeastern part)
109	Hitoyoshi-bonchi-nan'en fault	10901	Hitoyoshi-bonchi-nan'en fault

(Notes) – Among the active faults subject to fundamental surveys and observations, those for which long-term evaluation results were published together as a group are given a single code as a group.

- The Tokyo-wan-hokuen fault zone (28), the Arakawa fault (33), and the Gifu-Ichinomiya fault zone (66) were excluded from the modeling, since they were determined not to be active faults as a result of the long-term evaluation.
- With regard to the Motoarakawa fault zone (32), the northern part is included in the evaluation of the Kanto-heiya-hokuseien fault zone (31). The southern part was excluded from the modeling, since it was determined not to be an active fault as a result of the long-term evaluation.
- Since two cases were presented in the long-term evaluation of the Futagawa/Hinagu fault zone (central part/southwestern part) (9302), those cases are taken into account in the modeling.

Table 2.1-2 Magnitudes and fault plane parameters of major active fault zones (part 1)

Code	Fault name	Fault type		M_j	Fault length	Fault plane width	Fault plane dip	Seismogenic layer depth
0101	Shibetsu fault zone	Northwest-dipping reverse fault	Long-term evaluation	Around 7.7 or more	About 52 km or more	Unknown	NW	Lower edge: around 15 km
			Model	M_w 7.1	56 km	18 km	45° NW	3-15 km
0201	Tokachi-heiya fault zone (main part)	East-dipping reverse fault	Long-term evaluation	Around 8.0	About 84 km	Unknown	E	Lower edge: around 20 km
			Model	M_w 7.5	84 km	24 km	45° E	4-19 km
0202	Kochien fault	East-dipping reverse fault	Long-term evaluation	Around 7.2	About 26 km	Unknown	E	Lower edge: around 20 km
			Model	M_w 6.7	28 km	18 km	45° E	3-20 km
0301	Furano fault zone (western part)	West-dipping reverse fault	Long-term evaluation	Around 7.2	About 27 km	Unknown	W	Lower edge: around 15 km
			Model	M_w 6.7	28 km	18 km	45° W	2-15 km
0302	Furano fault zone (eastern part)	East-dipping reverse fault	Long-term evaluation	Around 7.2	About 25 km	Unknown	E	Lower edge: around 15 km
			Model	M_w 6.7	28 km	18 km	50° E	2-15 km
0401	Mashike-sanchi-toen fault zone	West-dipping reverse fault	Long-term evaluation	Around 7.8	About 60 km	Unknown	W	Lower edge: around 20 km
			Model	M_w 7.2	64 km	18 km	45° W	3-20 km
0402	Numata-Sunagawa area fault zone	East-dipping reverse fault	Long-term evaluation	Around 7.5	About 38 km	Unknown	E	Lower edge: around 20 km
			Model	M_w 6.9	40 km	18 km	45° E	3-20 km
0501	Tobetsu fault	West-dipping reverse fault	Long-term evaluation	Around 7.0	About 20 km	Unknown	Around 30-50° W	Lower edge: around 20 km
			Model	M_w 6.5	22 km	18 km	40° W	3-20 km
0601	Ishikari-teichi-toen fault zone (main part)	East-dipping reverse fault	Long-term evaluation	(Modeled based on the fault model used in the strong motion evaluation) (ERC, 2004e)				
			Model	M_w 7.3	39.3 km 23.3 km	24 km	45° E	7-30 km
0602	Ishikari-teichi-toen fault zone (southern part)	East-dipping reverse fault	Long-term evaluation	Around 7.1 or more	23 km or more	Unknown	E (low angle)	Deeper than around 30 km
			Model	M_w 6.6	24 km	18 km	30° E	7-30 km
0701	Kuromatsunai-teichi fault zone	West-dipping reverse fault	Long-term evaluation	Around 7.3 or more	About 32 km or more	Unknown	W	Lower edge: around 15 km
			Model	M_w 6.8	34 km	18 km	45° W	2-15 km
0801	Hakodate-heiya-seien fault zone	West-dipping reverse fault	Long-term evaluation	Around 7.0-7.5	24 km	Unknown	W	15 km or shallower
			Model	M_w 6.6	26 km	18 km	45° W	2-15 km
0901	Aomori-wan-seigan fault zone	West-dipping reverse fault	Long-term evaluation	Around 7.3	About 31 km	Unknown	W (high angle)	Lower edge: around 15 km
			Model	M_w 6.8	32 km	18 km	60° W	3-18 km
1001	Tsugaru-sanchi-seien fault zone (northern part)	East-dipping reverse fault	Long-term evaluation	Around 6.8-7.3	About 16 km	Unknown	E	Lower edge: around 15 km
			Model	M_w 6.4	18 km	18 km	45° E	3-18 km
1002	Tsugaru-sanchi-seien fault zone (southern part)	East-dipping reverse fault	Long-term evaluation	Around 7.1-7.3	About 23 km	Unknown	E	Lower edge: around 15 km
			Model	M_w 6.6	24 km	18 km	45° E	3-18 km

Table 2.1-2 Magnitudes and fault plane parameters of major active fault zones (part 2)

Code	Fault name	Fault type		M_j	Fault length	Fault plane width	Fault plane dip	Seismogenic layer depth
1101	Oritsume fault	West-dipping reverse fault	Long-term evaluation	Up to around 7.6	Up to around 47 km	Unknown	W	Lower edge: around 15 km
			Model	M_w 7.0	48 km	18 km	45° W	2-15 km
1201	Noshiro fault zone	East-dipping reverse fault	Long-term evaluation	Around 7.1 or more	About 22 km or more	Unknown	E	Lower edge: around 15 km
			Model	M_w 6.6	24 km	18 km	45° E	3-18 km
1301	Kitakami-teichi-seien fault zone	West-dipping reverse fault	Long-term evaluation	Around 7.8	62 km	20-30 km	20-30°, 30-40° W	Lower edge: around 15 km
			Model	M_w 7.2	64 km	18 km	35° W	3-14 km
1401	Shizukuishi-bonchi -seien fault zone	West-dipping reverse fault	Long-term evaluation	Around 6.9	About 17 km	Unknown	W	Lower edge: around 15 km
			Model	M_w 6.4	18 km	18 km	45° W	2-14 km
1402	Mahiru-sanchi-toen fault zone (northern part)	West-dipping reverse fault	Long-term evaluation	Around 6.7-7.0	About 14-21 km (21 km)	Unknown	About 40° W (near the ground surface)	Lower edge: around 15 km
			Model	M_w 6.6	22 km	18 km	40° W	3-17 km
1403	Mahiru-sanchi-toen fault zone (southern part)	West-dipping reverse fault	Long-term evaluation	Around 6.9-7.1	About 17-23 km (17 km)	Unknown	W	Lower edge: around 15 km
			Model	M_w 6.4	18 km	18 km	45° W	3-19 km
1501	Yokote-bonchi-toen fault zone (northern part)	East-dipping reverse fault	Long-term evaluation	Around 7.2	About 26 km	Unknown	20-30° E (near the ground surface)	Lower edge: around 15 km
			Model	M_w 6.7	28 km	18 km	25° E	3-17 km
1502	Yokote-bonchi-toen fault zone (southern part)	East-dipping reverse fault	Long-term evaluation	Around 7.3	About 30 km	Unknown	E	Lower edge: around 15 km
			Model	M_w 6.8	32 km	18 km	45° E	3-15 km
1601	Kitayuri fault	East-dipping reverse fault	Long-term evaluation	Around 7.3	About 30 km	Unknown	E	Lower edge: around 20 km
			Model	M_w 6.8	32 km	18 km	45° E	3-24 km
1701	Shinjo-bonchi fault zone	East-dipping reverse fault	Long-term evaluation	Around 6.6-7.1	11-23 km	Unknown	E	Lower edge: around 15 km
			Model	M_w 6.6	24 km	18 km	45° E	3-20 km
1801	Yamagata-bonchi fault zone (northern part)	West-dipping reverse fault	Long-term evaluation	Around 7.3	About 29 km	Unknown	W	Lower edge: around 15 km
			Model	M_w 6.8	30 km	18 km	45° W	4-16 km
1802	Yamagata-bonchi fault zone (southern part)	West-dipping reverse fault	Long-term evaluation	Around 7.3	About 31 km	Unknown	W	Lower edge: around 15 km
			Model	M_w 6.8	32 km	18 km	45° W	4-16 km
1901	Shonai-heiya-toen fault zone	East-dipping reverse fault	Long-term evaluation	Around 7.5	About 38 km	Unknown	E	Lower edge: around 20 km
			Model	M_w 6.9	40 km	18 km	45° E	3-20 km
2001	Nagamachi-Rifu-sen fault zone	Northwest-dipping reverse fault	Long-term evaluation	Around 7.0-7.5	21-40 km	About 15-25 km	35-45° W	Lower edge: around 13 km
			Model	M_w 6.9	42 km	18 km	40° W	3-16 km

Table 2.1-2 Magnitudes and fault plane parameters of major active fault zones (part 3)

Code	Fault name	Fault type		M_j	Fault length	Fault plane width	Fault plane dip	Seismogenic layer depth
2101	Fukushima-bonchi -seien fault zone	West-dipping reverse fault	Long-term evaluation	Around 7.8	About 57 km	Unknown	Around 30-60° NW (200 m deep or shallower)	Lower edge: around 15 km
			Model	M_w 7.1	60 km	18 km	45° NW	2-15 km
2201	Nagai-bonchi-seien fault zone	West-dipping reverse fault	Long-term evaluation	Around 7.7	About 51 km	Unknown	W	Lower edge: around 15 km
			Model	M_w 7.1	54 km	18 km	45° W	2-15 km
2301	Futaba fault	Left-lateral strike-slip fault dipping west	Long-term evaluation	Around 6.8-7.5	About 16-40 km	Around 15 km	E (vertical – high angle)	Lower edge: around 15 km
			Model	M_w 6.9	42 km	18 km	90°	2-19 km
2401	Aizu-bonchi-seien fault zone	West-dipping reverse fault	Long-term evaluation	Around 7.4	About 34 km	Unknown	W	Lower edge: around 15 km
			Model	M_w 6.8	36 km	18 km	45° W	2-20 km
2402	Aizu-bonchi-toen fault zone	East-dipping reverse fault	Long-term evaluation	Around 7.7	About 49 km	Unknown	E	Lower edge: around 15 km
			Model	M_w 7.0	50 km	18 km	45° E	2-18 km
2501	Kushigata-sanmyaku fault zone	West-dipping reverse fault	Long-term evaluation	Around 6.8	About 16 km	Unknown	Around 45° W (less than 20 m deep)	Lower edge: about 15-20 km
			Model	M_w 6.4	18 km	18 km	45° W	3-23 km
2601	Tsukioka fault zone	West-dipping reverse fault	Long-term evaluation	Around 7.3	About 30 km	Around 15-20 km	50-60° W (20-300 m deep)	Lower edge: around 15 km
			Model	M_w 6.8	32 km	18 km	55° W	3-24 km
2701	Nagaoka-heiya-seien fault zone	West-dipping reverse fault	Long-term evaluation	Around 8.0	About 83 km	Unknown	Around 50-60° W	Lower edge: around 25 km
			Model	M_w 7.5	84 km	24 km	55° W	6-23 km
2901	Kamogawa-teichi fault zone	South-dipping fault	Long-term evaluation	Roughly 7.2	Roughly 25 km	Unknown	Unknown	Lower edge: around 15 km
			Model	M_w 6.7	26 km	18 km	90°	2-18 km
3001	Sekiya fault	West-dipping reverse fault	Long-term evaluation	Around 7.5	About 38 km	Unknown	About 15-40° W	Lower edge: around 15 km
			Model	M_w 6.9	40 km	18 km	30° W	2-13 km
3101	Kanto-heiya-hokuseien fault zone (main part)	Southwest-dipping reverse fault	Long-term evaluation	Around 8.0	About 82 km	Around 20-25 km	50-70° SW (500 m deep or shallower)	Lower edge: about 20 km
			Model	M_w 7.4	82 km	20 km	60° SW	5-20 km
3102	Hirai-Kushibiki fault zone	Left-lateral strike-slip fault (with a northeast-dipping component)	Long-term evaluation	Around 7.1	About 23 km	Around 20 km	High angle (near the ground surface)	Lower edge: about 20 km
			Model	M_w 6.6	24 km	18 km	90°	2-20 km
3401	Tachikawa fault zone	Northeast-dipping fault with a left-lateral strike-slip component in the northwestern part	Long-term evaluation	Around 7.4	About 33 km	Unknown	Very high angle	Unknown
			Model	M_w 6.8	34 km	18 km	90°	2-18 km

Table 2.1-2 Magnitudes and fault plane parameters of major active fault zones (part 4)

Code	Fault name	Fault type		M_j	Fault length	Fault plane width	Fault plane dip	Seismogenic layer depth
3501	Isehara fault	East-dipping reverse fault	Long-term evaluation	Around 7.0	About 21 km	Around 15-20 km	About 60° E	Lower edge: about 15 km
			Model	M_w 6.6	22 km	18 km	60° E	1-15 km
3601	Kannawa/Kozu -Matsuda fault zone	North-northeast-dipping reverse fault	Long-term evaluation	Around 7.5	25 km or more	Around 10 km Around 10-15 km	70-80° N 40-60° NE	Lower edge: about 10 km
			Model	7.5	15 km 10 km 27 km	10 km 13 km 13 km	75° N 50° E 50° E	3-10 km
3701	Miura-hanto fault group (Kinugasa/Kitatake fault zone of the main part)	Right-lateral strike-slip fault	Long-term evaluation	(Modeled based on the fault model used in the strong motion evaluation) (ERC, 2003c)				
			Model	M_w 6.7	28 km	18 km	45° NE	3-15 km
3702	Miura-hanto fault group (Takeyama fault zone of the main part)	Right-lateral strike-slip fault	Long-term evaluation	(Modeled based on the fault model used in the strong motion evaluation) (ERC, 2003c)				
			Model	M_w 6.5	20 km	18 km	45° NE	3-15 km
3703	Miura-hanto fault group (southern part)	Right-lateral strike-slip fault with a south-dipping component	Long-term evaluation	Around 6.1 or more	About 6 km or more	Unknown	High angle	(No description)
			Model	7.0	20 km	12 km	90°	3-15 km
3801	Kitaizu fault zone	Left-lateral strike-slip fault	Long-term evaluation	Around 7.3	About 32 km	Around 10 km	Nearly vertical – high angle	Lower edge: about 10 km
			Model	M_w 6.8	36 km	10 km	90°	3-11 km
3901	Tokamachi fault zone (western part)	West-dipping reverse fault	Long-term evaluation	Around 7.4	About 33 km	Unknown	W	Lower edge: around 15 km
			Model	M_w 6.8	34 km	18 km	45° W	5-25 km
3902	Tokamachi fault zone (eastern part)	East-dipping reverse fault	Long-term evaluation	Around 7.0	About 19 km	Unknown	E	Lower edge: around 15 km
			Model	M_w 6.5	20 km	20 km	45° E	5-20 km
4001	Nagano-bonchi-seien fault zone	West-dipping reverse fault	Long-term evaluation	Around 7.4-7.8	About 58 km	Unknown	W	Lower edge: around 15 km
			Model	M_w 7.1	60 km	18 km	45° W	4-18 km
4101	Itoigawa-Shizuoka -kozosen fault zone (central part/northern part)	Dominant east-dipping reverse fault component (northern part), dominant left-lateral strike-slip component (central part)	Long-term evaluation	(Modeled based on the fault model used in the strong motion evaluation) (ERC, 2002)				
			Model	M_w 7.4	25.5 km 35.5 km 15.5 km 33.5 km	20 km 20 km 14 km 14 km	40° E 40° E 80° E 80° E	2-15 km
4201	Itoigawa-Shizuoka -kozosen fault zone (southern part)		Long-term evaluation	(No detailed description)				
			Model	7.3	30 km	20 km	45° W	2-15 km
4301	Fujikawa-kako fault zone		Long-term evaluation	Around 8.0	(No detailed description)			
			Model	8.0	20 km (land area)	8 km	45° W	3-10 km

Table 2.1-2 Magnitudes and fault plane parameters of major active fault zones (part 5)

Code	Fault name	Fault type		M_j	Fault length	Fault plane width	Fault plane dip	Seismogenic layer depth
4501	Kiso-sanmyaku-seien fault zone (northern segment of the main part)	[Northern half] East-dipping reverse fault / [Southern half] Right-lateral strike-slip fault	Long-term evaluation	Around 7.5	About 40 km	Unknown / Around 20 km	About 40° or lower angle, E / high angle	Lower edge: about 20 km
			Model	M_w 6.9	30 km 14 km	18 km 16 km	40° E 90°	2-16 km
4502	Kiso-sanmyaku-seien fault zone (southern segment of the main part)	Right-lateral strike-slip fault	Long-term evaluation	Around 6.3	About 8 km	Around 20 km	High angle	Lower edge: about 20 km
			Model	6.3	9 km	9 km	90°	2-16 km
4503	Seinaiji-toge fault zone	Right-lateral strike-slip fault	Long-term evaluation	Around 7.4	About 34 km	Around 20 km	High angle	Lower edge: about 20 km
			Model	M_w 6.8	38 km	16 km	90°	2-16 km
4601	Sakaitoge/Kamiya fault zone (main part)	Left-lateral strike-slip fault (with a dip slip component)	Long-term evaluation	Around 7.6	About 47 km	Around 15 km	High angle (dipping east at a high angle in the northern part)	Lower edge: about 15 km
			Model	M_w 7.0	52 km	16 km	90°	2-16 km
4602	Mutoyama-Narai fault zone	Right-lateral strike-slip fault	Long-term evaluation	Around 7.2	About 28 km	15 km	High angle	Lower edge: about 15 km
			Model	M_w 6.7	32 km	16 km	90°	2-16 km
4701	Atotsugawa fault zone	Right-lateral strike-slip fault (with a northwest-dipping component)	Long-term evaluation	Around 7.9	About 69 km	About 15 km	Nearly vertical	Lower edge: about 15 km
			Model	M_w 7.2	74 km	16 km	90°	2-16 km
4801	Kokufu fault zone	Right-lateral strike-slip fault	Long-term evaluation	(Modeled based on the fault model used in the strong motion evaluation) (ERC, 2004c)				
			Model	M_w 6.6	28 km	14 km	90°	2-17 km
4802	Takayama fault zone	Right-lateral strike-slip fault	Long-term evaluation	(Modeled based on the fault model used in the strong motion evaluation) (ERC, 2004c)				
			Model	M_w 6.9	48 km	14 km	90°	2-17 km
4803	Inohana fault zone	Right-lateral strike-slip fault	Long-term evaluation	(Modeled based on the fault model used in the strong motion evaluation) (ERC, 2004c)				
			Model	M_w 6.5	24 km	14 km	90°	2-17 km
4901	Ushikubi fault zone	Right-lateral strike-slip fault (with a southeast-dipping component in the northeastern part, with a northwest-dipping component in the southwestern part)	Long-term evaluation	Around 7.7	About 54 km	Around 15 km	Nearly vertical – high angle	Lower edge: about 15 km
			Model	M_w 7.1	58 km	16 km	90°	2-16 km

Table 2.1-2 Magnitudes and fault plane parameters of major active fault zones (part 6)

Code	Fault name	Fault type		M_j	Fault length	Fault plane width	Fault plane dip	Seismogenic layer depth
5001	Shokawa fault zone	Left-lateral strike-slip fault (with an east-dipping component in Kazura fault, with a west-dipping component in Shirakawa fault and Miogo fault)	Long-term evaluation	Around 7.9	About 67 km	Around 15 km	High angle	Lower edge: about 15 km
			Model	M_w 7.2	72 km	14 km	90°	2-15 km
5101	Inadani fault zone (main part)	West-dipping reverse fault	Long-term evaluation	Around 8.0	79 km	Around 25-60 km	20-40° W	Lower edge: about 15-20 km
			Model	M_w 7.3	41.5 km 37.5 km	18 km 18 km	70° W 70° W	2-20 km
5102	Inadani fault zone (southeastern part)	West-dipping reverse fault	Long-term evaluation	Around 7.3	About 32 km	Unknown	W (high angle)	Lower edge: about 15-20 km
			Model	M_w 6.8	34 km	18 km	60° W	2-20 km
5201	Atera fault zone (northern segment of the main part)	Left-lateral strike-slip fault (with an east-dipping component)	Long-term evaluation	Around 6.9	About 17 km	Around 15 km	High angle	Lower edge: about 15 km
			Model	M_w 6.4	20 km	16 km	90°	2-17 km
5202	Atera fault zone (southern segment of the main part)	Left-lateral strike-slip fault (with a northeast-dipping component)	Long-term evaluation	Around 7.8	About 60 km	Around 15 km	High angle	Lower edge: about 15 km
			Model	M_w 7.2	64 km	16 km	90°	2-17 km
5203	Sami fault zone	Right-lateral strike-slip fault	Long-term evaluation	Around 7.2	About 25 km	Around 15 km	High angle	Lower edge: about 15 km
			Model	M_w 6.7	28 km	16 km	90°	2-17 km
5204	Shirakawa fault zone	Right-lateral strike-slip fault (with a southeast-dipping component)	Long-term evaluation	Around 7.3	About 31 km	Around 15 km	High angle	Lower edge: about 15 km
			Model	M_w 6.8	34 km	16 km	90°	2-17 km
5301	Byobuyama fault zone	Southeast-dipping reverse fault	Long-term evaluation	Around 6.8	About 15 km	Unknown	SE (high angle)	Lower edge: about 20 km
			Model	M_w 6.4	20 km	18 km	60° SE	2-22 km
5302	Ako fault zone	Southwest-dipping fault	Long-term evaluation	Around 7.1	About 23 km	Unknown	High angle	Lower edge: about 15 km
			Model	M_w 6.6	24 km	18 km	60° SW	2-20 km

Table 2.1-2 Magnitudes and fault plane parameters of major active fault zones (part 7)

Code	Fault name	Fault type		M_j	Fault length	Fault plane width	Fault plane dip	Seismogenic layer depth
5303	Enasan-Sanageyama -kita fault zone	[Eastern half] Southeast-dipping reverse fault with a right-lateral strike-slip component / [Western half] Right-lateral strike-slip fault (with a dip-slip component)	Long-term evaluation	Around 7.7	About 51 km	Unknown / Around 20 km	30-50° SE / High angle	Lower edge: about 20 km
			Model	M_w 7.2	38 km 22 km	18 km 18 km	40° SE 90°	2-20 km
5304	Sanage-Takahama fault zone	West-dipping reverse fault (northern part/southern part)	Long-term evaluation	Around 7.7	About 51 km	Unknown	About 50-80° W	Lower edge: about 20 km
			Model	M_w 7.1	34 km 18 km	18 km 18 km	65° W 65° W	2-22 km
5305	Kagiya fault zone	[Northern half] West-dipping reverse fault / [Southern half] East-dipping reverse fault	Long-term evaluation	Around 7.4	About 35 km	Unknown	W (high angle) / E	Lower edge: about 20 km
			Model	M_w 6.9	12 km 26 km	18 km 18 km	60° W 45° E	2-16 km
5501	Ochigata fault zone	Southeast-dipping reverse fault	Long-term evaluation	Around 7.6	About 44 km	Unknown	About 30° SE (200 m deep or shallower)	Lower edge: about 20 km
			Model	M_w 7.0	46 km	18 km	30° SE	2-18 km
5601	Tonami-heiya fault zone (western part)	West-dipping reverse fault	Long-term evaluation	(Modeled based on the fault model used in the strong motion evaluation) (ERC, 2004a)				
			Model	M_w 6.8	26 km	22 km	45° W	4-20 km
5602	Tonami-heiya fault zone (eastern part)	East-dipping reverse fault	Long-term evaluation	Around 7.0	21 km	Unknown	SE	Lower edge: Around 15-20 km
			Model	M_w 6.6	22 km	18 km	45° E	4-20 km
5603	Kurehayama fault zone	West-dipping reverse fault	Long-term evaluation	(Modeled based on the fault model used in the strong motion evaluation) (ERC, 2004a)				
			Model	M_w 6.9	30 km	22 km	45° W	4-20 km
5701	Morimoto/Togashi fault zone	East-dipping reverse fault	Long-term evaluation	(Modeled based on the fault model used in the strong motion evaluation) (ERC, 2003a)				
			Model	M_w6.6	26 km	20 km	45° E	4-18 km
5801	Fukui-heiya-toen fault zone (main part)	Left-lateral strike-slip with east-dipping reverse fault	Long-term evaluation	Around 7.6	About 45 km	Around 15 km	50° E - nearly vertical	Lower edge: about 15 km
			Model	M_w 7.0	48 km	16 km	90°	2-17 km

Table 2.1-2 Magnitudes and fault plane parameters of major active fault zones (part 8)

Code	Fault name	Fault type		M_j	Fault length	Fault plane width	Fault plane dip	Seismogenic layer depth
5802	Fukui-heiya-toen fault zone (western part)	Left-lateral strike-slip fault (with an east-dipping component in the central-northern part, with a west-dipping component in the southern part)	Long-term evaluation	Around 7.1	About 33 km	Around 15 km	High angle, E - nearly vertical	Lower edge: about 15 km
			Model	M_w 6.8	36 km	16 km	90°	2-17 km
5901	Nagaragawa-joryu fault zone	Left-lateral strike-slip fault which is an west-dipping fault	Long-term evaluation	Around 7.3	About 29 km	Unknown	High angle	Lower edge: around 15 km
			Model	M_w 6.8	32 km	16 km	90°	2-17 km
6001	Nukumi fault (northwestern part)	Left-lateral strike-slip fault (with a northeast-dipping component)	Long-term evaluation	Around 6.8	About 16 km	Around 15 km	High angle	Lower edge: about 15 km
			Model	M_w 6.4	20 km	12 km	90°	2-13 km
6002	Nukumi fault (southeastern part)	Left-lateral strike-slip fault (with a southwest-dipping component)	Long-term evaluation	Around 7.0	About 21 km	Around 15 km	High angle	Lower edge: about 15 km
			Model	M_w 6.6	22 km	18 km	90°	2-18 km
6003	Nobi fault zone (Neodani fault zone of the main part)	Left-lateral strike-slip fault	Long-term evaluation	Around 7.3	About 30 km	About 15 km	High angle	Lower edge: about 15 km
			Model	M_w 6.8	34 km	14 km	90°	2-15 km
6004	Nobi fault zone (Umehara fault zone of the main part)	Left-lateral strike-slip fault (with a northeast-dipping component in a part of the northwestern part, with a southwest-dipping component in the southeastern part)	Long-term evaluation	Around 7.4	About 36 km	About 20 km	High angle	Lower edge: about 20 km
			Model	M_w 6.9	40 km	18 km	90°	2-19 km
6005	Nobi fault zone (Mitabora fault zone of the main part)	Left-lateral strike-slip fault (with a southwest-dipping component)	Long-term evaluation	Around 7.0	About 19 km	About 20 km	High angle	Lower edge: about 20 km
			Model	M_w 6.5	22 km	18 km	90°	2-19 km
6006	Ibigawa fault zone	Left-lateral strike-slip fault (with a southwest-dipping component in the southeastern part)	Long-term evaluation	Around 7.1	About 24 km	About 15 km	High angle	Lower edge: about 15 km
			Model	M_w 6.6	28 km	14 km	90°	2-15 km
6007	Mugigawa fault	Left-lateral strike-slip fault (with a northeast-dipping component in the southeastern part)	Long-term evaluation	Around 7.3	About 29 km	Around 20 km	High angle	Lower edge: about 20 km
			Model	M_w 6.8	32 km	18 km	90°	2-19 km

Table 2.1-2 Magnitudes and fault plane parameters of major active fault zones (part 9)

Code	Fault name	Fault type		M_j	Fault length	Fault plane width	Fault plane dip	Seismogenic layer depth
6101	Yanagase/Sekigahara fault zone (northern segment of the main part)	East- and northeast-dipping reverse fault	Long-term evaluation	Around 7.6	About 48 km	About 25 km	E 40° NE	Lower edge: around 15 km
			Model	M_w 7.0	23.9 km 23.9 km	18 km 18 km	40° 40°	2-15 km
6102	Yanagase/Sekigahara fault zone (central segment of the main part)	Left-lateral strike-slip fault	Long-term evaluation	Around 6.6	About 12 km	About 15 km	Nearly vertical	Lower edge: around 15 km
			Model	6.6	13 km	12 km	90°	2-17 km
6103	Yanagase/Sekigahara fault zone (southern segment of the main part)	Left-lateral strike-slip fault, Northeast- or east-dipping reverse fault	Long-term evaluation	Around 7.6	About 45 km	About 15 km	Nearly vertical	Lower edge: around 15 km
			Model	M_w 7.0	48 km	16 km	90°	2-17 km
6104	Urazoko -Yanagaseyama fault zone	Left-lateral strike-slip fault	Long-term evaluation	Around 7.2	About 25 km	About 15 km	Nearly vertical	Lower edge: around 15 km
			Model	M_w 6.7	26 km	18 km	90°	2-22 km
6301	Nosaka fault zone	Left-lateral strike-slip fault which is a northeast-dipping reverse fault	Long-term evaluation	Around 7.3	About 31 km	About 15 km	NE (high angle)	Lower edge: around 15 km
			Model	M_w 6.8	34 km	16 km	90°	2-17 km
6302	Shufukuji fault	Left-lateral strike-slip fault (with northeast-dipping and dip-slip components)	Long-term evaluation	Around 6.5	About 10 km	About 15 km	Nearly vertical	Lower edge: about 15 km
			Model	6.5	10 km	10 km	90°	2-17 km
6401	Kohoku-sanchi fault zone (northwestern part)	Right-lateral strike-slip fault which is a southeast-dipping reverse fault	Long-term evaluation	Around 7.2	About 25 km	About 15 km	SE (high angle)	Lower edge: around 15 km
			Model	M_w 6.7	26 km	18 km	90°	2-22 km
6402	Kohoku-sanchi fault zone (southeastern part)	Right-lateral strike-slip fault partially dipping northwest	Long-term evaluation	Around 6.8	About 16 km	About 15 km	Nearly vertical	Lower edge: around 15 km
			Model	M_w 6.4	20 km	16 km	90°	2-16 km
6501	Biwako-seigan fault zone	West-dipping reverse fault	Long-term evaluation	(Modeled based on the fault model used in the strong motion evaluation) (ERC, 2004b)				
			Model	M_w 7.1	60 km	16 km	70° W	3-18 km
6701	Yoro-Kuwana -Yokkaichi fault zone	West-dipping reverse fault	Long-term evaluation	Around 8	About 60 km	About 30-40 km	About 30° W	Lower edge: about 15-20 km
			Model	M_w 7.2	38.2 km 20.2 km	18 km 18 km	30° W 30° W	2-17 km
6801	Suzuka-toen fault zone	West-dipping reverse fault	Long-term evaluation	Around 7.5	About 34-47 km	Around 20-25 km	Boundary: high angle Frontal part: 30-60°	Lower edge: around 20 km
			Model	M_w 7.0	48 km	18 km	60° W	2-17 km

Table 2.1-2 Magnitudes and fault plane parameters of major active fault zones (part 10)

Code	Fault name	Fault type		M_j	Fault length	Fault plane width	Fault plane dip	Seismogenic layer depth
6901	Suzuka-seien fault zone	East-dipping reverse fault	Long-term evaluation	Around 7.6	About 44 km	About 30-40 km	30-40° E	Lower edge: about 20 km
			Model	M_w 7.0	46 km	18 km	35° E	1-20 km
7001	Tongu fault	East-dipping reverse fault	Long-term evaluation	Around 7.3	About 31 km	Unknown	50-80° E	Lower edge: about 15 km
			Model	M_w 6.8	32 km	18 km	65° E	1-17 km
7101	Nunobiki-sanchi-toen fault zone (western part)	West-dipping reverse fault	Long-term evaluation	Around 7.4	About 33 km	Around 20 km	50-60° W	Lower edge: about 15 km
			Model	M_w 6.8	34 km	18 km	55° W	2-17 km
7102	Nunobiki-sanchi-toen fault zone (eastern part)	West-dipping reverse fault	Long-term evaluation	Around 7.6	About 48 km	Unknown	Around 45° W	Lower edge: about 20 km
			Model	M_w 7.0	50 km	18 km	45° W	2-20 km
7201	Kizugawa fault zone	North-dipping reverse fault with a right-lateral strike-slip component	Long-term evaluation	Around 7.3	About 31 km	Unknown	40-60° N	Lower edge: about 15 km
			Model	M_w 6.8	32 km	18 km	50° N	1-14 km
7301	Mikata fault zone	East-dipping reverse fault	Long-term evaluation	Around 7.2	About 26 km	Unknown	E (high angle)	Lower edge: around 15 km
			Model	M_w 6.7	28 km	18 km	60° E	1-16 km
7302	Hanaore fault zone (northern part)	Right-lateral strike-slip fault	Long-term evaluation	Around 7.2	About 26 km	About 15-20 km	Nearly vertical	Lower edge: around 15-20 km
			Model	M_w 6.7	30 km	18 km	90°	1-20 km
7303	Hanaore fault zone (central-southern part)	Central part: right-lateral strike-slip fault Southern part: east-dipping reverse fault partially dipping west	Long-term evaluation	Around 7.3	About 20 km (central part), about 15 km (southern part)	15- 20 km (central part) 20-45 km (southern part)	Central part: nearly vertical Southern part: 50, 25-55°	Lower edge: around 15-20 km
			Model	M_w 6.9	22 km 16 km	18 km 18 km	90° 50° E	1-20 km
7401	Yamada fault zone (main part)	Right-lateral strike-slip fault with a northwest-dipping component	Long-term evaluation	Around 7.4	About 33 km	Unknown	NW	Lower edge: about 10 km
			Model	M_w 6.8	38 km	16 km	90°	1-15 km
7402	Gomura fault zone	Left-lateral strike-slip fault with a southwest-dipping component	Long-term evaluation	Around 7.4 or more	About 34 km or more	Around 15 km	SW (high angle)	Lower edge: about 15 km
			Model	M_w 6.8	38 km	16 km	90°	1-16 km
7501	Nara-bonchi-toen fault zone	East-dipping reverse fault	Long-term evaluation	Around 7.4	About 35 km	Unknown	50-60° E	Lower edge: around 15 km
			Model	M_w 6.9	36 km	18 km	55° E	1-15 km
7601	Arima-Takatsuki fault zone	Right-lateral strike-slip fault with a vertical displacement	Long-term evaluation	7.5±0.5	About 55 km	Unknown	N (high angle)	Unknown
			Model	M_w 7.1	60 km	16 km	90°	1-16 km
7701	Ikoma fault zone	East-dipping reverse fault	Long-term evaluation	Around 7.0-7.5	About 38 km	Unknown	30-40° E	Lower edge: around 15 km
			Model	M_w 6.9	40 km	18 km	35° E	2-15 km

Table 2.1-2 Magnitudes and fault plane parameters of major active fault zones (part 11)

Code	Fault name	Fault type		M_j	Fault length	Fault plane width	Fault plane dip	Seismogenic layer depth
7801	Kanbayashigawa fault	Right-lateral strike-slip fault (with a northwest-dipping component)	Long-term evaluation	Around 7.2	About 26 km	Unknown	High angle	Lower edge: about 15 km
			Model	M_w 6.7	30 km	16 km	90°	1-15 km
7802	Mitoke fault	Left-lateral strike-slip fault (with a northeast-dipping component)	Long-term evaluation	Around 7.2	About 26 km	Unknown	High angle	Lower edge: about 15 km
			Model	M_w 6.7	30 km	16 km	90°	1-15 km
7803	Kyoto-Nishiyama fault zone	[Northwestern half] Left-lateral strike-slip fault with a northeast-dipping reverse fault component / [Southeastern half] West-dipping reverse fault	Long-term evaluation	Around 7.5	About 42 km	Unknown	Partially dipping northeast (high angle) / W	Lower edge: about 15 km
			Model	M_w 7.0	30 km 18 km	18 km 18 km	90° 45° W	1-19 km
7901	Rokko/Awajishima fault zone (Rokko-sanchi-nan'en-Awajishima-togan segment of the main part)	Mainly right-lateral strike-slip fault with a northwest-dipping reverse fault component	Long-term evaluation	Around 7.9	About 71 km	Around 15-20 km, around 15 km	50-70° NW, NW (high angle)	Lower edge: 15 km
			Model	M_w 7.3	74 km	18 km	60° NW	1-16 km
7902	Rokko/Awajishima fault zone (Awajishima-seigan segment of the main part)	Right-lateral strike-slip fault with a southeast-dipping reverse fault component	Long-term evaluation	Around 7.1	About 23 km	Around 15 km	About 80° SE	Lower edge: 15 km
			Model	M_w 6.6	28 km	16 km	80° SE	1-16 km
7903	Senzan fault zone	Northwest-dipping reverse fault	Long-term evaluation	Around 6.6	About 12 km	Unknown	NW	Lower edge: 15 km
			Model	6.6	11 km	11 km	45° NW	1-16 km
8001	Uemachi fault zone	East-dipping reverse fault	Long-term evaluation	Around 7.5	About 42 km	15-20 km	65-70° E	Lower edge: around 15 km
			Model	M_w 7.0	46 km	16 km	70° E	2-15 km
8101	Chuo-kozosen fault zone (Kongo-sanchi-toen-Izumi-sanmyaku-nan'en)	Right-lateral strike-slip fault with a dip-slip component Kongo-toen: west-dipping reverse fault	Long-term evaluation	(Modeled based on the fault model used in the strong motion evaluation) (ERC, 2005c)				
			Model	M_w 7.1	60 km 12 km	16 km 16 km	43° N 43° W	4-15 km
8102	Chuo-kozosen fault zone (Kitan-kaikyo-Naruto-kaikyo)	Right-lateral strike-slip fault with a dip-slip component	Long-term evaluation	Around 7.7	About 43-51 km	20-60 km	15-45° N	Lower edge: around 15 km
			Model	M_w 7.1	54 km	18 km	30° N	4-15 km

Table 2.1-2 Magnitudes and fault plane parameters of major active fault zones (part 12)

Code	Fault name	Fault type		M_j	Fault length	Fault plane width	Fault plane dip	Seismogenic layer depth
8103	Chuo-kozosen fault zone (S-I part)	Right-lateral strike-slip fault with a dip-slip component	Long-term evaluation	Around 8.0 or more	About 130 km	20-30 km	30-40° N	Lower edge: 1around 5 km
			Model	M_w 7.6 (M_w 7.4)	132 km (136 km)	24 km (18 km)	35° N	4-16 km
8104	Chuo-kozosen fault zone (Ishizuchi-sanmyaku -hokuen)	Right-lateral strike-slip fault with a dip-slip component	Long-term evaluation	Around 7.3-8.0	About 30 km	Unknown	High angle	Lower edge: around 15 km
			Model	M_w 6.8	34 km	14 km	90°	4-17 km
8105	Chuo-kozosen fault zone (I-I part)	Right-lateral strike-slip fault with a dip-slip component	Long-term evaluation	Around 8.0 or more	About 130 km	Unknown	N (high angle)	Lower edge: around 15 km
			Model	M_w 7.4 (M_w 7.4)	130 km (138 km)	14 km (14 km)	90°	4-16 km
8201	Nagisen fault zone	North-dipping fault	Long-term evaluation	(Modeled based on the fault model used in the strong motion evaluation) (ERC, 2005a)				
			Model	M_w 7.0	32 km	26 km	45° N	2-21 km
8202	Yamasaki fault zone (northwestern segment of the main part)	Left-lateral strike-slip fault	Long-term evaluation	(Modeled based on the fault model used in the strong motion evaluation) (ERC, 2005a)				
			Model	M_w 7.1	52 km	18 km	90°	Model
8203	Yamasaki fault zone (southeastern segment of the main part)	Left-lateral strike-slip fault	Long-term evaluation	(Modeled based on the fault model used in the strong motion evaluation) (ERC, 2005a)				
			Model	M_w 6.7	30 km	18 km	90°	2-21 km
8204	Kusatani fault	Right-lateral strike-slip fault	Long-term evaluation	Around 6.7	(Modeled based on the fault model used in the strong motion evaluation) (ERC, 2005a)			
			Model	6.7	12 km	12 km	90°	2-21 km
8401	Nagao fault zone	South-dipping reverse fault with a right-lateral strike-slip component	Long-term evaluation	Around 7.1	About 24 km	25-30 km	30-40° S	Lower edge: around 15 km
			Model	M_w 6.6	26 km	18 km	35° S	3-12 km
8701	Itsukaichi fault	Right-lateral strike-slip fault (with a west-dipping reverse fault component)	Long-term evaluation	Around 7.0	About 20 km	About 25 km	W (high angle)	Lower edge: around 25 km
			Model	M_w 6.5	22 km	18 km	90°	2-23 km
8702	Koi-Hiroshima-seien fault zone	Right-lateral strike-slip fault	Long-term evaluation	Around 6.5	About 10 km	Unknown	Nearly vertical	Lower edge: around 25 km
			Model	6.5	10 km	10 km	90°	2-25 km
8801	Iwakuni fault zone	Right-lateral strike-slip fault (with a northwest-dipping component)	Long-term evaluation	Around 7.6	About 44 km	About 20 km	NW (high angle)	Lower edge: around 20 km
			Model	M_w 7.0	46 km	18 km	90°	2-18 km
9001	Kikukawa fault zone	Left-lateral strike-slip fault with a northeast-dipping reverse fault component	Long-term evaluation	Around 7.6 or more	About 44 km or more	Unknown	NE (high angle)	Lower edge: around 10-15 km
			Model	M_w 7.0	48 km	16 km	90°	2-16 km

Table 2.1-2 Magnitudes and fault plane parameters of major active fault zones (part 13)

Code	Fault name	Fault type		M_j	Fault length	Fault plane width	Fault plane dip	Seismogenic layer depth
9101	Nishiyama fault zone	Fault mainly with a left-lateral strike-slip component	Long-term evaluation	Around 7.3	About 31 km	About 15 km	Nearly vertical	Lower edge: about 15 km
			Model	M_w 6.8	36 km	16 km	90°	2-16 km
9201	Beppu-wan-Hijiu fault zone (eastern part)	Normal fault relatively dipping mainly to the south	Long-term evaluation	Around 7.6	About 43 km	Around 15 km	Mainly dipping south at a high angle	Lower edge: about 15 km
			Model	M_w 7.0	48 km	14 km	60° S	3-14 km
9202	Beppu-wan-Hijiu fault zone (western part)	Normal fault relatively dipping mainly to the south	Long-term evaluation	Around 7.3	About 32 km	Unknown	Mainly dipping south at a high angle	Lower edge: about 15 km
			Model	M_w 6.8	36 km	14 km	60° S	3-14 km
9203	Oita-heiya-Yufuin fault zone (eastern part)	Normal fault relatively dipping north	Long-term evaluation	Around 7.2	About 27 km	Around 15 km	Mainly dipping north at a high angle	Lower edge: about 15 km
			Model	M_w 6.7	32 km	14 km	60° N	3-14 km
9204	Oita-heiya-Yufuin fault zone (western part)	Normal fault relatively dipping north	Long-term evaluation	Around 6.7	About 14 km	Unknown	Mainly dipping north at a high angle	Lower edge: about 15 km
			Model	M_w 6.3	18 km	14 km	60° N	3-14 km
9205	Noinedake-Haneyama fault zone	Normal fault relatively dipping mainly to the south	Long-term evaluation	Around 7.3	About 30 km	Unknown	Mainly dipping south at a high angle	Lower edge: around 10 km
			Model	M_w 6.8	34 km	14 km	60° S	3-14 km
9206	Kuenohirayama -Kameishiyama fault zone	Normal fault relatively dipping mainly to the north	Long-term evaluation	Around 7.4	About 34 km	Unknown	Mainly dipping north at a high angle	Lower edge: around 10 km
			Model	M_w 6.8	38 km	14 km	60° N	3-14 km
9301	Futagawa/Hinagu fault zone (northeastern part)	Right-lateral strike-slip fault with southeast-dipping and dip-slip components	Long-term evaluation	Around 7.2	About 27 km	Unknown	High angle near the ground surface	Lower edge: around 15 km
			Model	M_w 6.7	32 km	14 km	90°	3-16 km
9302	Futagawa/Hinagu fault zone (central part)	Right-lateral strike-slip fault with southeast-dipping and dip-slip components	Long-term evaluation	(Modeled based on the fault model used in the strong motion evaluation) (ERC, 2003b)				
			Model	M_w 7.0	52 km	16 km	60° W	3-16 km
9302	Futagawa/Hinagu fault zone (southwestern part)	Right-lateral strike-slip fault with southeast-dipping and dip-slip components	Long-term evaluation	Around 7.2	(Modeled based on the fault model used in the strong motion evaluation) (ERC, 2003b)			
			Model	M_w 6.7	32 km	16 km	60° W	3-16 km
9302	Futagawa/Hinagu fault zone (central part/southwestern part simultaneous)	Right-lateral strike-slip fault with southeast-dipping and dip-slip components	Long-term evaluation	(Modeled based on the fault model used in the strong motion evaluation) (ERC, 2003b)				
			Model	M_w7.3	52 km 32 km	16 km 16 km	60° W 60° W	3-16 km
9401	Minou fault zone	North-dipping normal fault	Long-term evaluation	Around 7.2	About 26 km	Around 15 km	N (high angle)	Lower edge: around 15 km
			Model	M_w 6.7	30 km	14 km	60° N	3-14 km

Table 2.1-2 Magnitudes and fault plane parameters of major active fault zones (part 14)

Code	Fault name	Fault type		M_j	Fault length	Fault plane width	Fault plane dip	Seismogenic layer depth
9501	Unzen fault group (northern part)	Mainly south-dipping normal fault	Long-term evaluation	Around 7.3 or more	Around 30 km or more	Unknown	S (high angle)	Lower edge: around 15 km
			Model	M_w 6.8	32 km	18 km	60° S	3-18 km
9502	Unzen fault group (southeastern part)	North-dipping normal fault	Long-term evaluation	Around 7.1	Around 23 km	Unknown	N (high angle)	Lower edge: around 15 km
			Model	M_w 6.6	26 km	18 km	60° N	3-18 km
9503	Unzen fault group (northern segment of the southwestern part)	Mainly north-dipping normal fault	Long-term evaluation	Around 7.3	Around 30 km	Unknown	N (high angle)	Lower edge: around 15 km
			Model	M_w 6.8	34 km	18 km	60° N	3-18 km
9504	Unzen fault group (southern segment of the southwestern part)	Mainly south-dipping normal fault	Long-term evaluation	Around 7.1	Around 23 km	Unknown	S (high angle)	Lower edge: around 15 km
			Model	M_w 6.6	26 km	18 km	60° S	3-18 km
9601	Izumi fault zone	Northwest-dipping normal fault with a right-lateral strike-slip displacement	Long-term evaluation	Around 7.0	About 20 km	Unknown	About around 40-50° NW	Lower edge: about 15 km
			Model	M_w 6.5	22 km	18 km	45° NW	3-15 km
9701	Ise-wan fault zone (northern segment of the main part)	East-dipping reverse fault	Long-term evaluation	Around 7.2	About 25 km	Around 15-25 km	60-70° E	Lower edge: around 15-20 km
			Model	M_w 6.7	26 km	18 km	65° E	3-23 km
9702	Ise-wan fault zone (southern segment of the main part)	North-dipping fault (normal or reverse unknown)	Long-term evaluation	Around 6.9	About 17 km	Unknown	Unknown	Lower edge: around 15-20 km
			Model	M_w 6.4	18 km	18 km	45° N	2-19 km
9703	Shirako-Noma fault	Fault with a north-dipping reverse fault component	Long-term evaluation	Around 7.0	About 21 km	Around 15-20 km	N (high angle)	Lower edge: around 15-20 km
			Model	M_w 6.6	22 km	18 km	60° N	2-21 km
9801	Osaka-wan fault zone	Northwest-dipping reverse fault	Long-term evaluation	Around 7.5	About 39 km	About 15-20 km	60-80° W	Lower edge: around 15 km
			Model	M_w 6.9	44 km	12 km	70° W	4-15 km
9901	Sarobetsu fault zone	East-dipping reverse fault	Long-term evaluation	Around 7.6	About 44 km	Unknown	Mainly dipping east at a low angle	Lower edge: around 25 km
			Model	M_w7.0	44 km	18 km	30° E	7-25 km
10101	Hanawa-higashi fault zone	East-dipping reverse fault	Long-term evaluation	Around 7.0	About 19 km	Unknown	About 40-50° E	Lower edge: around 15 km
			Model	M_w6.5	20 km	20 km	45° E	3-15 km
10401	Sone-kyuryo fault zone	Southeast-dipping reverse fault	Long-term evaluation	Around 7.3	About 32 km	Unknown	About 30° SE	Lower edge: around 20 km
			Model	M_w6.8	34 km	18 km	30° SE	2-16 km
10501	Uozu fault zone	Southeast-dipping reverse fault (with a right-lateral strike-slip component)	Long-term evaluation	Around 7.2	About 32 km	Unknown	SE	Lower edge: around 15 km
			Model	M_w6.8	24 km 7.9 km	18 km 18 km	43° SE 43° SE	3-18 km

Table 2.1-2 Magnitudes and fault plane parameters of major active fault zones (Part 15)

Code	Fault name	Fault type		M_j	Fault length	Fault plane width	Fault plane dip	Seismogenic layer depth
10601	Suonada fault zone (main part)	Right-lateral strike-slip fault	Long-term evaluation	Around 7.6	About 44 km	Unknown	High angle	Lower edge: around 15-20 km
			Model	M_w7.0	46 km	18 km	90°	2-18 km
10602	Aio-Oki fault zone	Right-lateral strike-slip fault	Long-term evaluation	Around 7.1	About 23 km	Unknown	High angle	Lower edge: around 15-20 km
			Model	M_w6.6	24 km	18 km	90°	2-18 km
10603	Ube-nanpo-Oki fault zone	Strike-slip fault	Long-term evaluation	Around 7.1	About 22 km	Unknown	High angle	Lower edge: around 15-20 km
			Model	M_w6.6	12 km 12 km	18 km 18 km	90° 90°	2-18 km
10801	Kego fault zone (northwestern part)	Left-lateral strike-slip fault	Long-term evaluation	Around 7.0	About 25 km	Around 15 km	High angle (nearly vertical)	Lower edge: around 15 km
			Model	M_w6.7	30 km	16 km	90°	2-19 km
10802	Kego fault zone (southeastern part)	Left-lateral strike-slip fault (with a southwest-dipping component)	Long-term evaluation	Around 7.2	About 27 km	Around 15 km	SW (high angle)	Lower edge: around 15 km
			Model	M_w6.7	32 km	16 km	90°	2-17 km
10901	Hitoyoshi-bonchi -nan'en fault	Northwest-dipping normal fault	Long-term evaluation	Around 7.1	About 22 km	Unknown	NW (high angle)	Lower edge: around 15 km
			Model	M_w6.6	24 km	18 km	60° NW	2-17 km

(Notes)

- The fault length of the model does not always coincide with that in long-term evaluation. The red characters indicate values changed from the 2008 version.
- The dip angle used for the Tobetsu fault (0501) is 40°, which is the median angle.
- The modeled fault length for the Ishikari-teichi-toen fault zone (main part) (0601) is re-determined so that the upper and lower edges of two faults continue underground, and therefore differs from the value in long-term evaluation.
- For the Hakodate-heiya-seien fault zone (0801), M_w is calculated by assuming the magnitude to be 7.3 based on the active fault length.
- For the Tsugaru-sanchi-seien fault zone (northern part) (1001) and (southern part) (1002), M_w is calculated by assuming the magnitudes to be 6.8 and 7.1, respectively, based on the active fault length.
- The dip angle used for the Kitakami-teichi-seien fault zone (1301) is 35°.
- For the Mahiru-sanchi-toen fault zone (northern part) (1402), M_w is calculated by assuming the magnitude to be 7.0 based on an estimated fault length of the northern part of 21 km.
- For the Mahiru-sanchi-toen fault zone (southern part) (1403), M_w is calculated by assuming the magnitude to be 6.9 based on an estimated fault length of the southern part of 17 km.
- The model of the Shinjo-bonchi fault zone (1701) covers the entire fault. Thus, M_w is calculated by assuming the magnitude to be 7.1.
- The model of the Nagamachi-Rifu-sen fault zone (2001) covers the entire fault. Thus, M_w is calculated by assuming the magnitude to be 7.5. The dip angle used is 40°, which is the median angle.
- The dip angle used for the Fukushima-bonchi-seien fault zone (2101) is 45°, which is the median angle.
- The model of the Futaba fault (2301) covers the entire fault. Thus, M_w is calculated by assuming the magnitude to be 7.5.
- The dip angle used for the Tsukioka fault zone (2601) is 55°, which is the median angle.
- The dip angle used for the Nagaoka-heiya-seien fault zone (2701) is 55°, which is the median angle.
- The dip angle used for the Kamogawa-teichi fault zone (2901) is 90°, which is the median angle.
- The dip angle used for the Sekiya fault (3001) is 30°, which is the rounded median angle.
- The Kannawa/Kozu-Matsuda fault zone (3601) is extended by about 27 km into the sea.
- Both ends of the Miura-hanto fault group (southern part) (3703) are extended on both ends into the sea to make the total length 20 km, and the magnitude is assumed to be 7.0.

- For the Nagano-bonchi-seien fault zone (4001), M_w is calculated by assuming the magnitude to be 7.8 based on the active fault length.
- For the Itoigawa-Shizuoka-kozosen fault zone (southern part) (4201), the length of about 31 km south of Kobuchizawa up to the Ichinose fault group is assumed to be a southwest-dipping reverse fault. The magnitude is assumed to be 7.3 based on the length. The seismogenic layer is assumed to be the same as that of the northerly adjacent Itoigawa-Shizuoka-kozosen fault zone (northern part/central part).
- For the Fujikawa-kako fault zone (4301), long-term evaluation indicated that "the active segments (source area) were inferred as not being limited to this fault zone (land area), but extending within Suruga Bay, and mostly overlapping with the source area assumed for a future Tokai earthquake". However, only the land area is modeled, deeming the model to be independent from the Tokai earthquake. The lower edge and the dip angle of the fault plane are so determined as to connect to the source area of the Tokai earthquake.
- The modeled fault length for the Inadani fault zone (main part) (5101) is re-determined so that the upper and lower edges of two faults continue underground, and therefore differs from the value in long-term evaluation. The dip angle used is 70° so as to converge with the Kiso-sanmyaku-seien fault zone.
- The dip angle used for the east half of the Enasan-Sanageyama-kita fault zone (5303) is 40°, which is the median angle.
- The dip angle used for the Sanage-Takahama fault zone (5304) is 65°, which is the median angle.
- The dip angle used for the Fukui-heiya-toen fault zone (main part) (5801) is 90°.
- The modeled fault length for the Yanagase/Sekigahara fault zone (northern segment of the main part) (6101) is re-determined so that the upper and lower edges of two faults continue underground, and therefore differs from the value in long-term evaluation.
- The modeled fault length for the Yoro-Kuwana-Yokkaichi fault zone (6701) is re-determined so that the upper and lower edges of two faults continue underground, and therefore differs from the value in long-term evaluation.
- The active fault length used for the Suzuka-toen fault zone (6801) is 47 km.
- The dip angle used for the Suzuka-seien fault zone (6901) is 35°, which is the median angle.
- The dip angle used for the Tongu fault (7001) is 65°, which is the median angle.
- The dip angle used for the Nunobiki-sanchi-toen fault zone (western part) (7101) is 55°, which is the median angle.
- The dip angle used for the Kizugawa fault zone (7201) is 50°, which is the median angle.
- The dip angle used for the southern segment of the Hanaore fault zone (central-southern part) (7303) is 50°.
- The dip angle used for the Nara-bonchi-toen fault zone (7501) is 55°, which is the median angle.
- The model of the Ikoma fault zone (7701) covers the entire fault. Thus, M_w is calculated by assuming the magnitude to be 7.5.
- The Rokko/Awajishima fault zone (Rokko-sanchi-nan'en-Awajishima-togan segment of the main part) (7901) is modeled as a single fault plane, and uses the dip angle of 60°.
- The dip angle used for the Uemachi fault zone (8001) is 70°, which is the rounded median angle.
- The Chuo-kozosen fault zone (Kongo-sanchi-toen-Izumi-sanmyaku-nan'en) (8101) is modeled based on deliberation materials for the strong motion evaluation.
- The dip angles used for the Chuo-kozosen fault zone (Kitan-kaikyo-Naruto-kaikyo) (8102) and (Sanuki-sanmyaku-nan'en-Ishizuchi-sanmyaku-hokuen-tobu) (8103) are 30° and 35°, respectively, which are the median angles. For the Chuo-kozosen fault zone (Ishizuchi-sanmyaku-hokuen) (8104), M_w is calculated by assuming the magnitude to be 7.3 based on the active fault length.
- The parameters used for the modeling of the Chuo-kozosen fault zone (S-I part) (8103) and (Ishizuchi-sanmyaku-hokuen-seibu-Iyonada) (8105) based on adjustment method II (segmenting and aggregating method) are shown in parentheses.
- The dip angle used for the Nagao fault zone (8401) is 35°, which is the median angle.
- The dip angle used for the Izumi fault zone (9601) is 45°, which is the median angle.
- The dip angle used for the Ise-wan fault zone (northern segment of the main part) (9701) is 65°, which is the median angle.
- Since it is unknown whether the Ise-wan fault zone (southern segment of the main part) (9702) is a normal fault or a reverse fault, the fault zone is modeled as a north-dipping fault, assuming it to be a reverse fault.
- The dip angle used for the Osaka-wan fault zone (9801) is 70°, which is the median angle.
- The modeled fault length and the dip angle for the Uozu fault zone (10501) are re-determined so that the upper and lower edges of two faults continue underground, and therefore differ from the values in long-term evaluation.

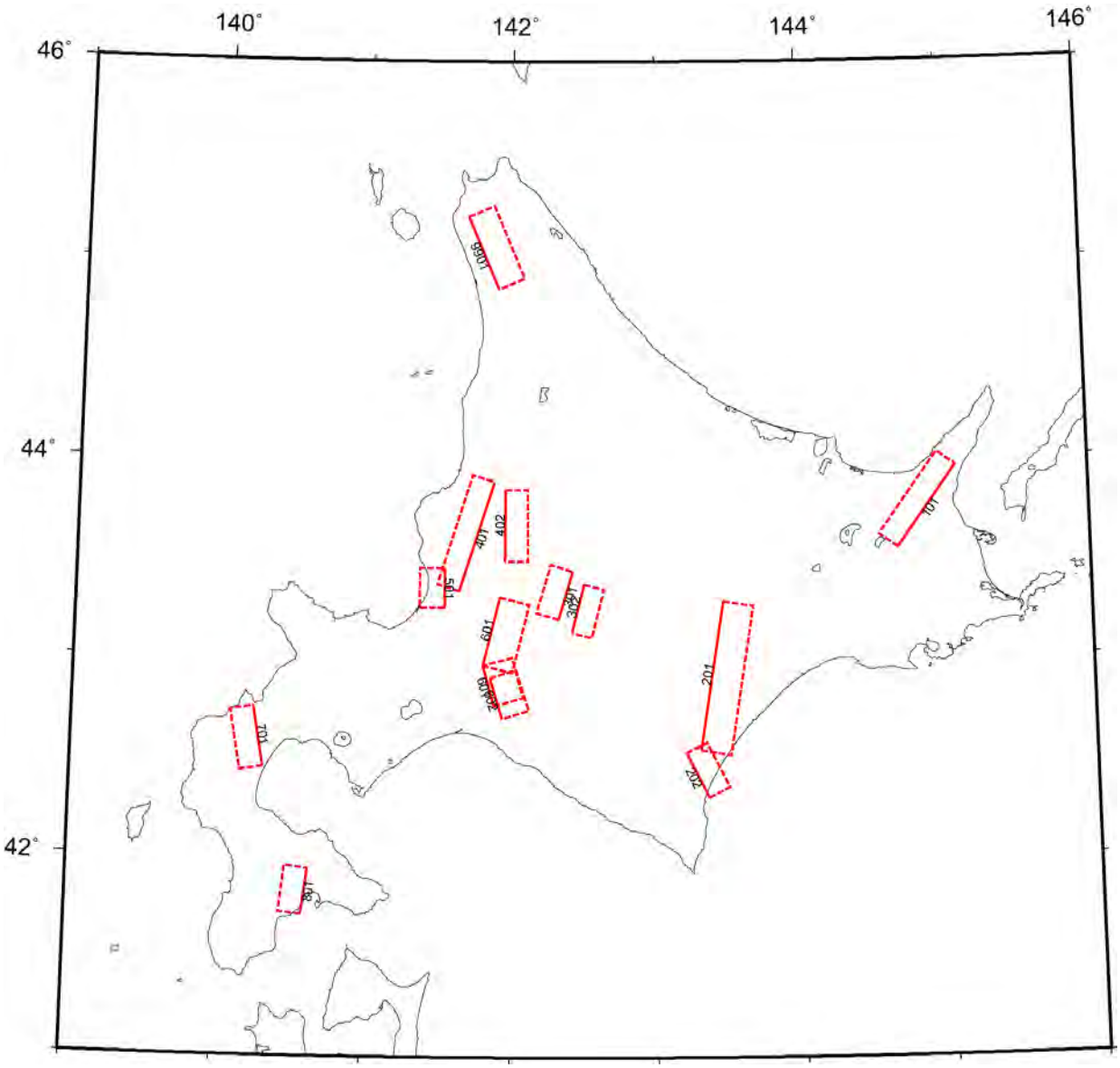

Figure 2.1-1 Models of major active fault zones (part 1)

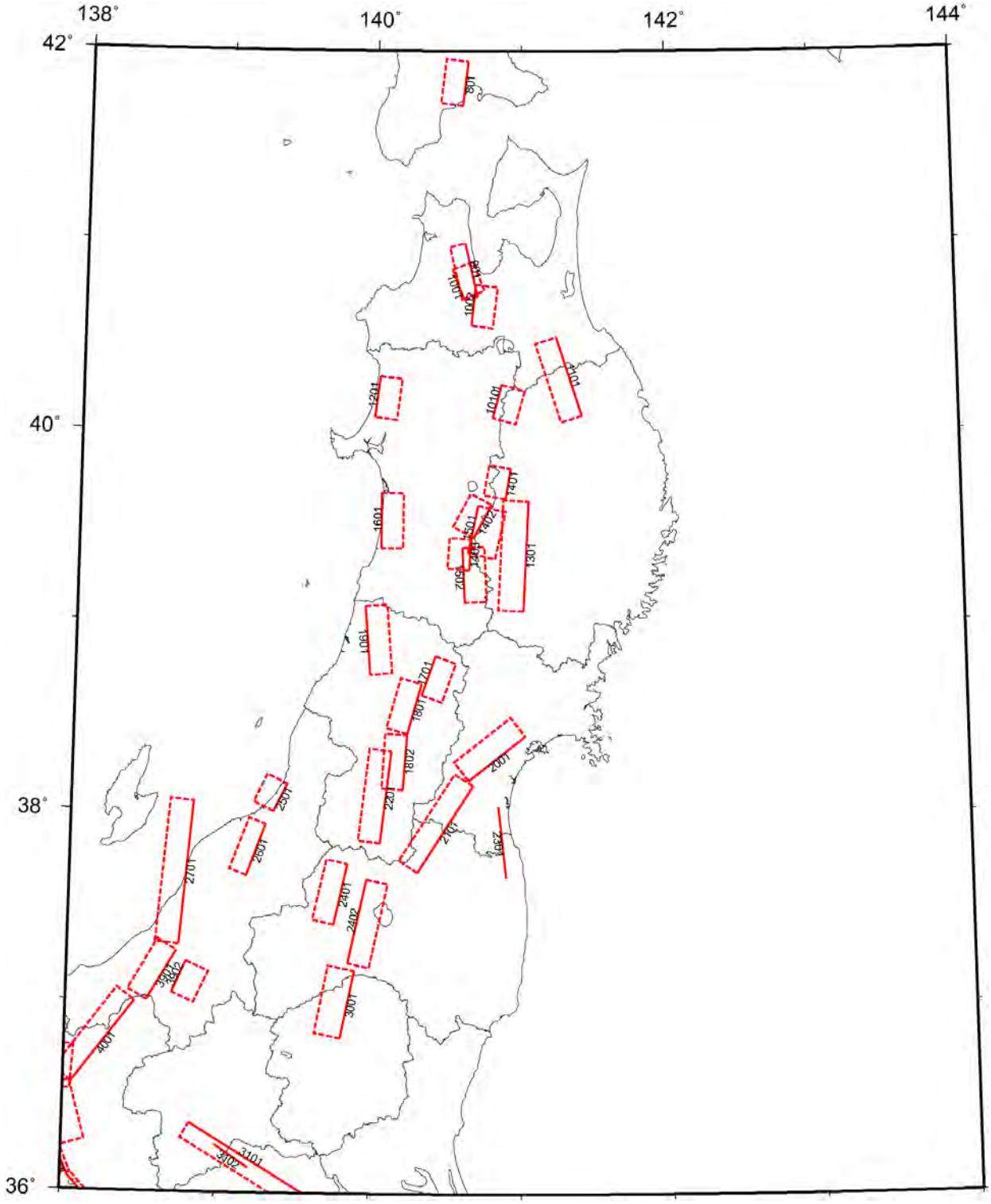

Figure 2.1-1 Models of major active fault zones (part 2)

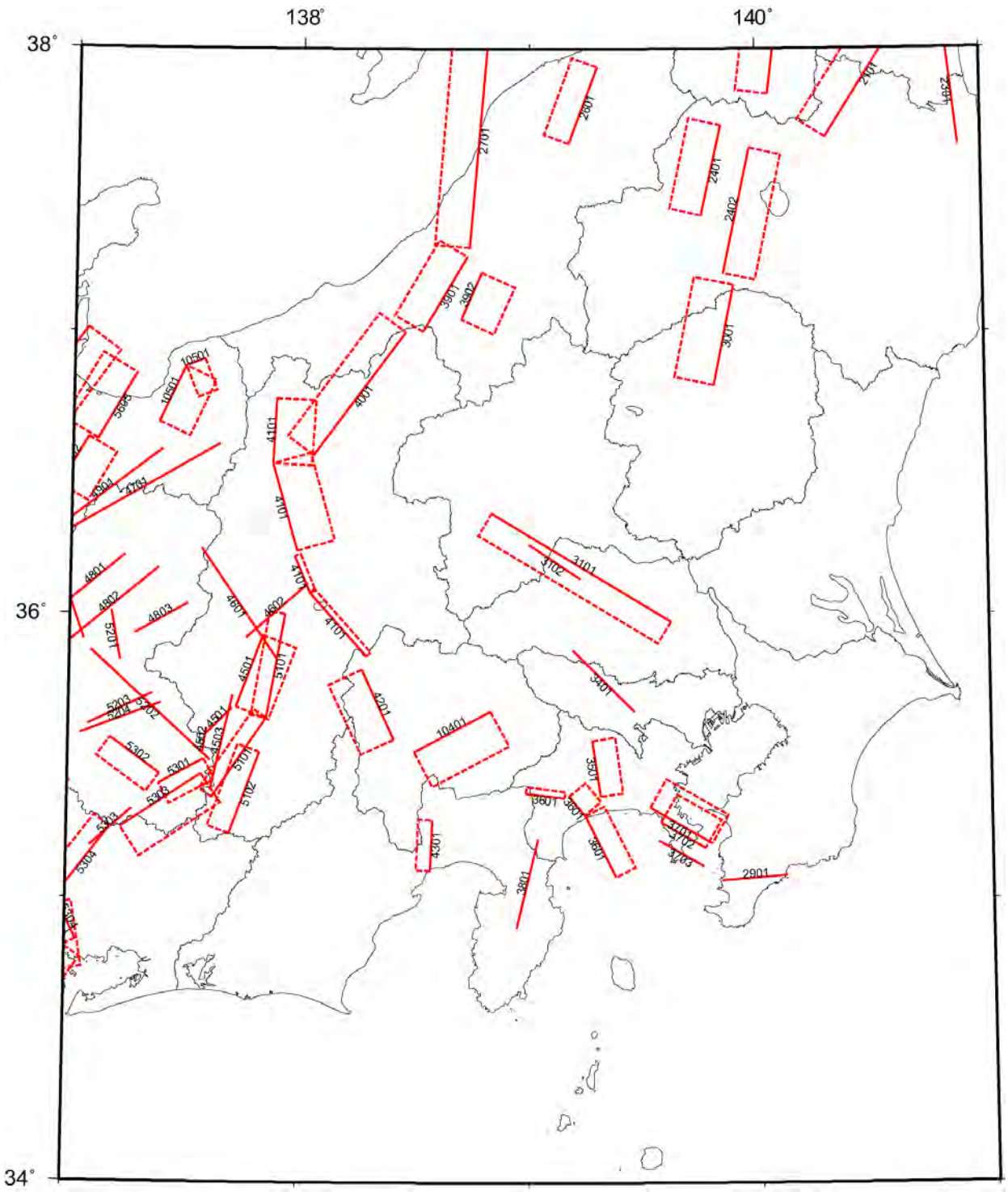

Figure 2.1-1 Models of major active fault zones (part 3)

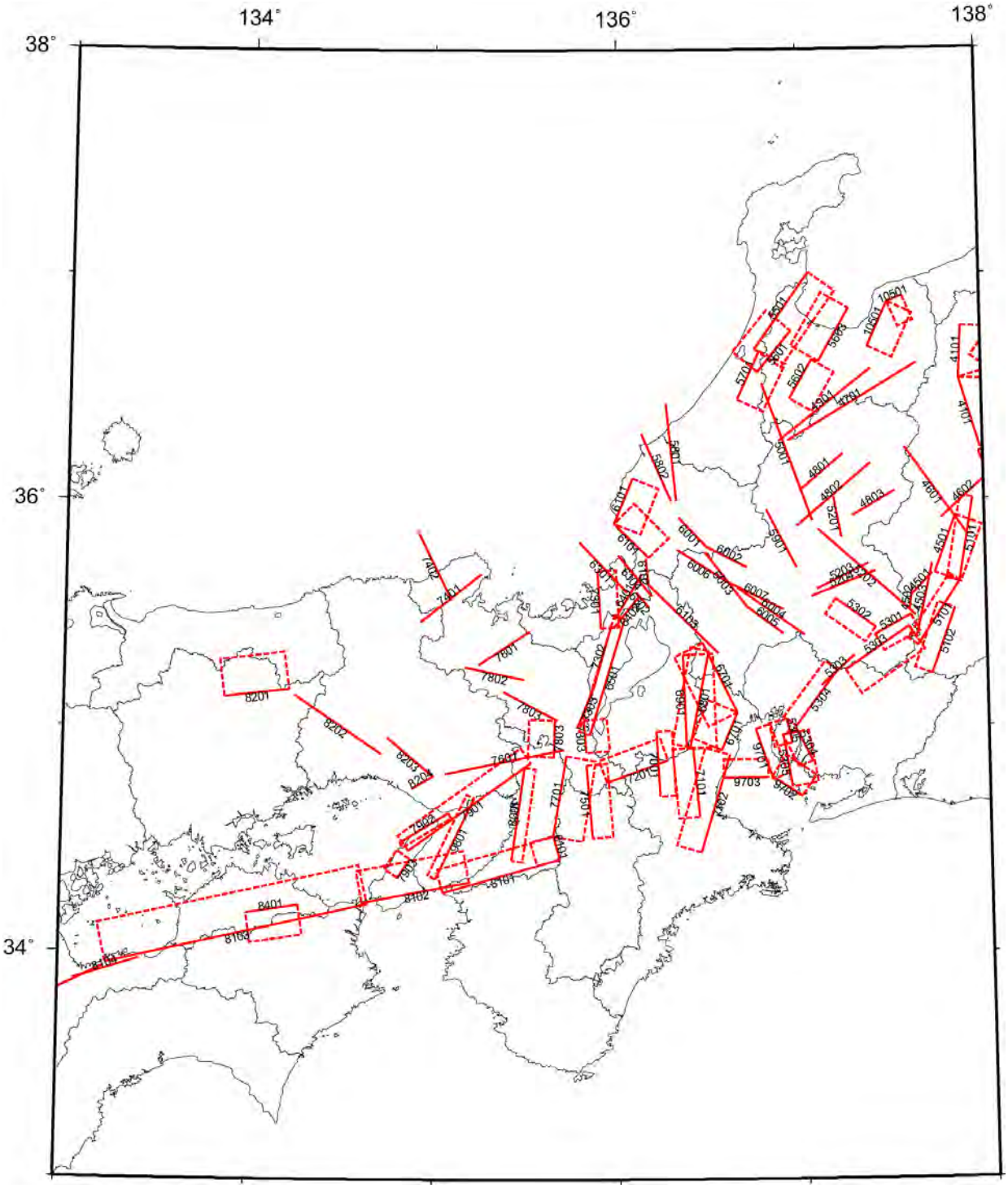

Figure 2.1-1 Models of major active fault zones (part 4)

* Only the rectilinear fault is shown for the Uemachi fault zone (8001) and the model based on adjustment method I for the Chuo-kozosen fault zone (8103).

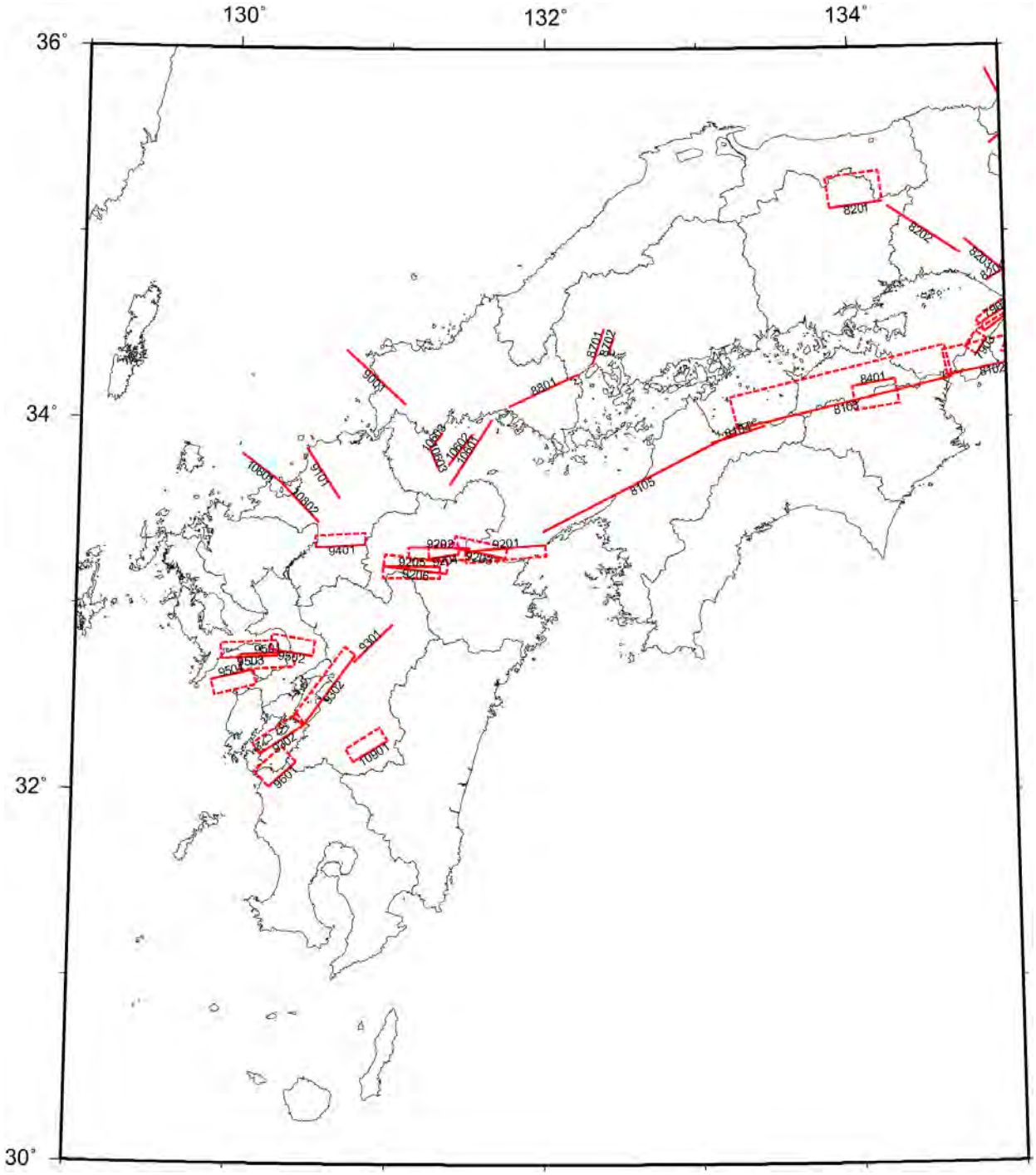

Figure 2.1-1 Models of major active fault zones (part 5)

* Only the models based on adjustment method I are shown for the Chuo-kozosen fault zone (8103, 8105).

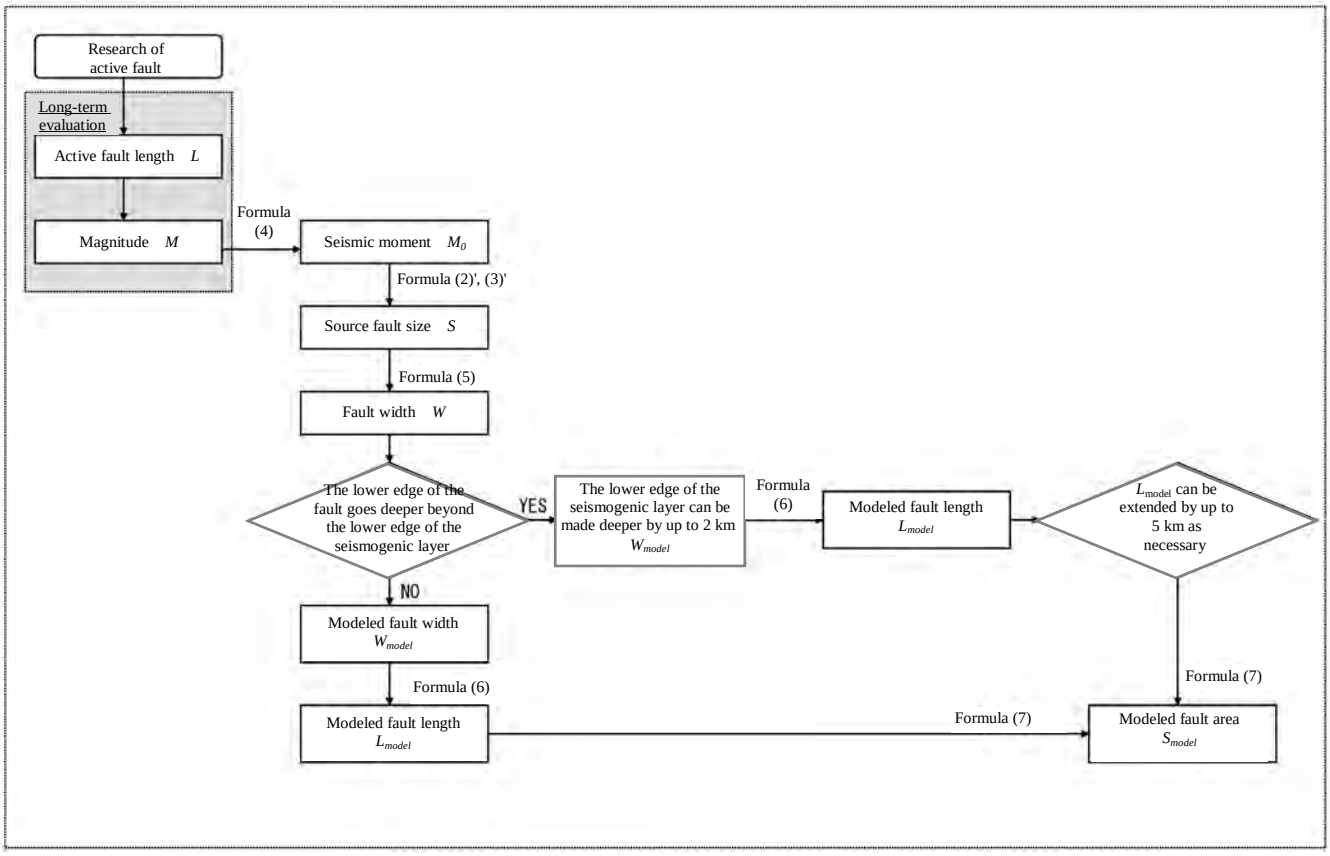

Figure 2.1.2-1 Flow chart of determination of outer source parameters under the procedural method (Source: Appended Figure 3 of the Recipe)

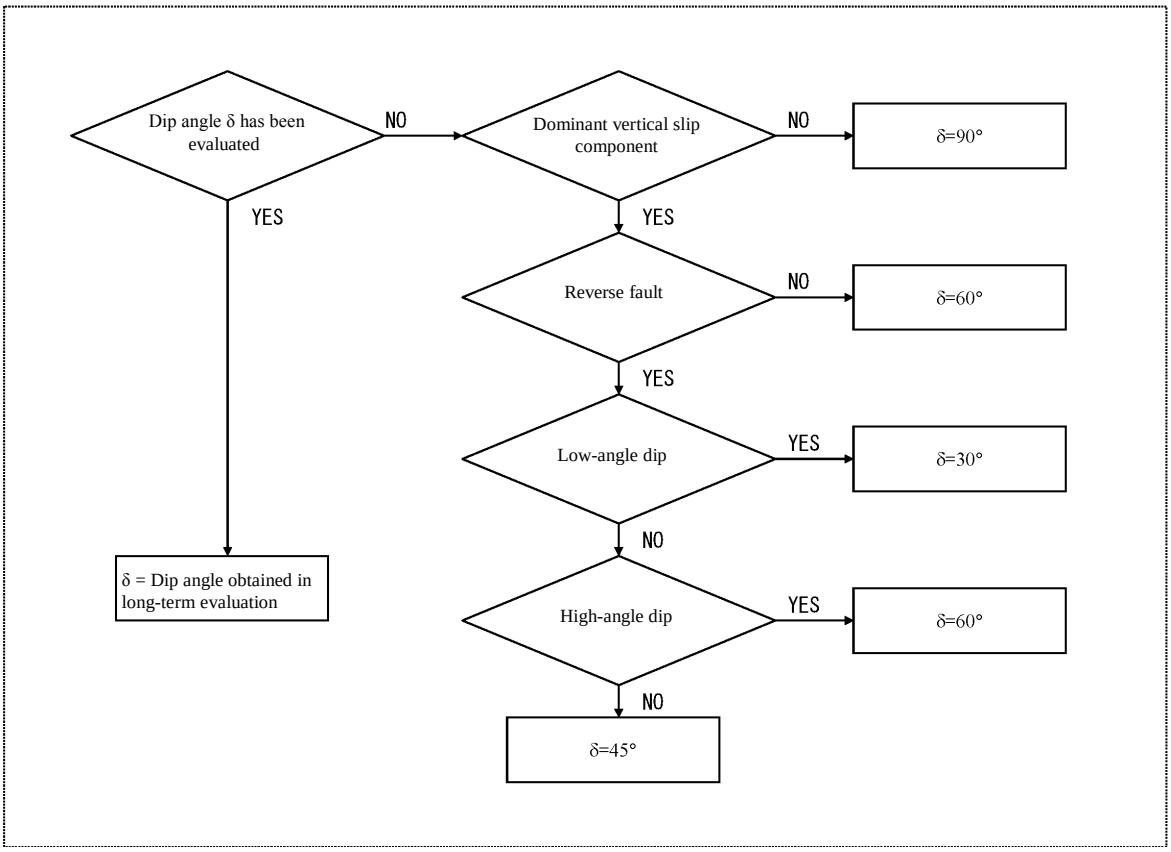

Figure 2.1.2-2 Flow chart of determination of fault plane dip angle (Source: Appended Figure 4 of the Recipe)

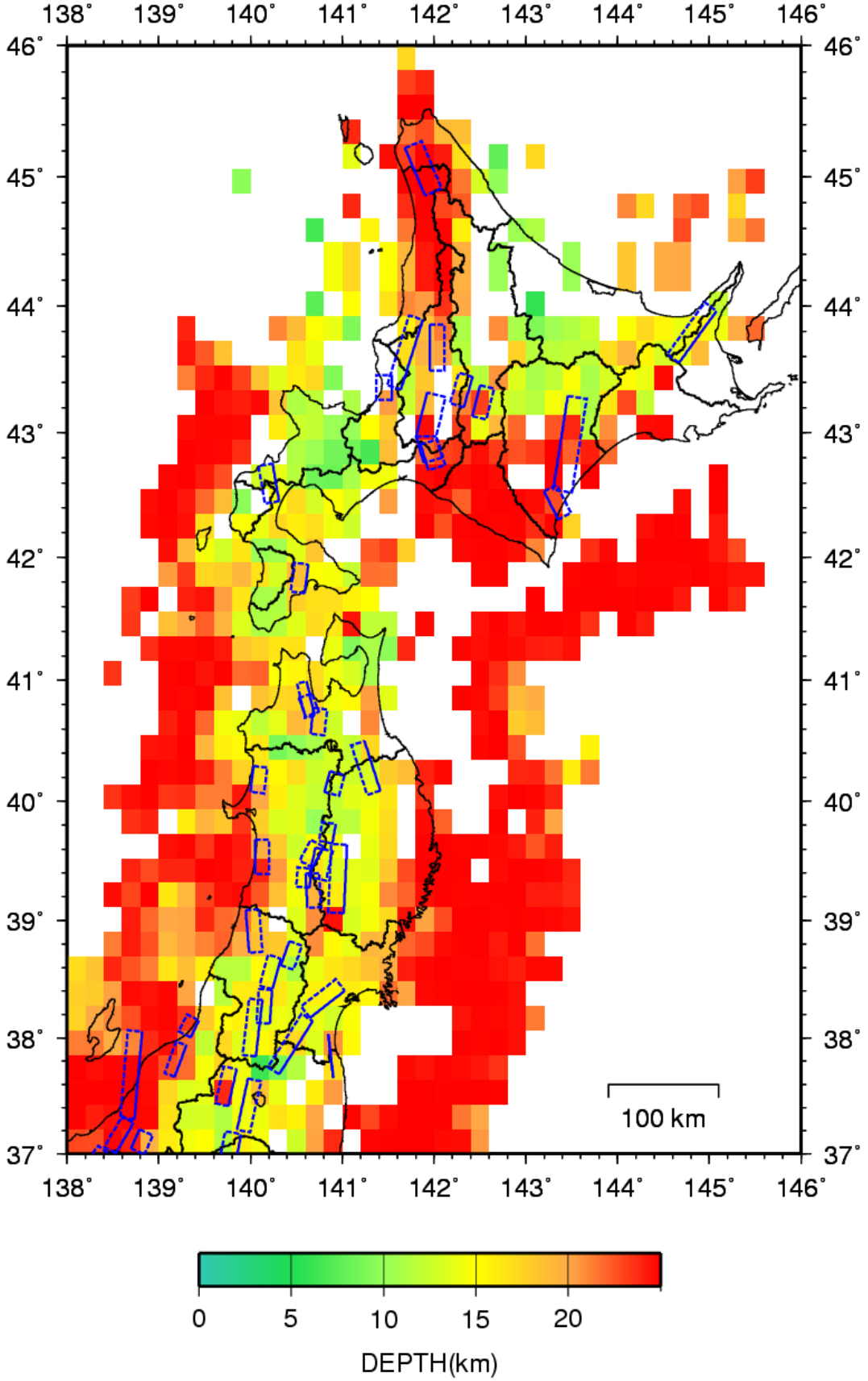

Figure 2.1.2-3 Distribution of the deepest source depth of microearthquakes in each 0.2-degree resolution obtained from the JMA unified earthquake catalog (part 1)

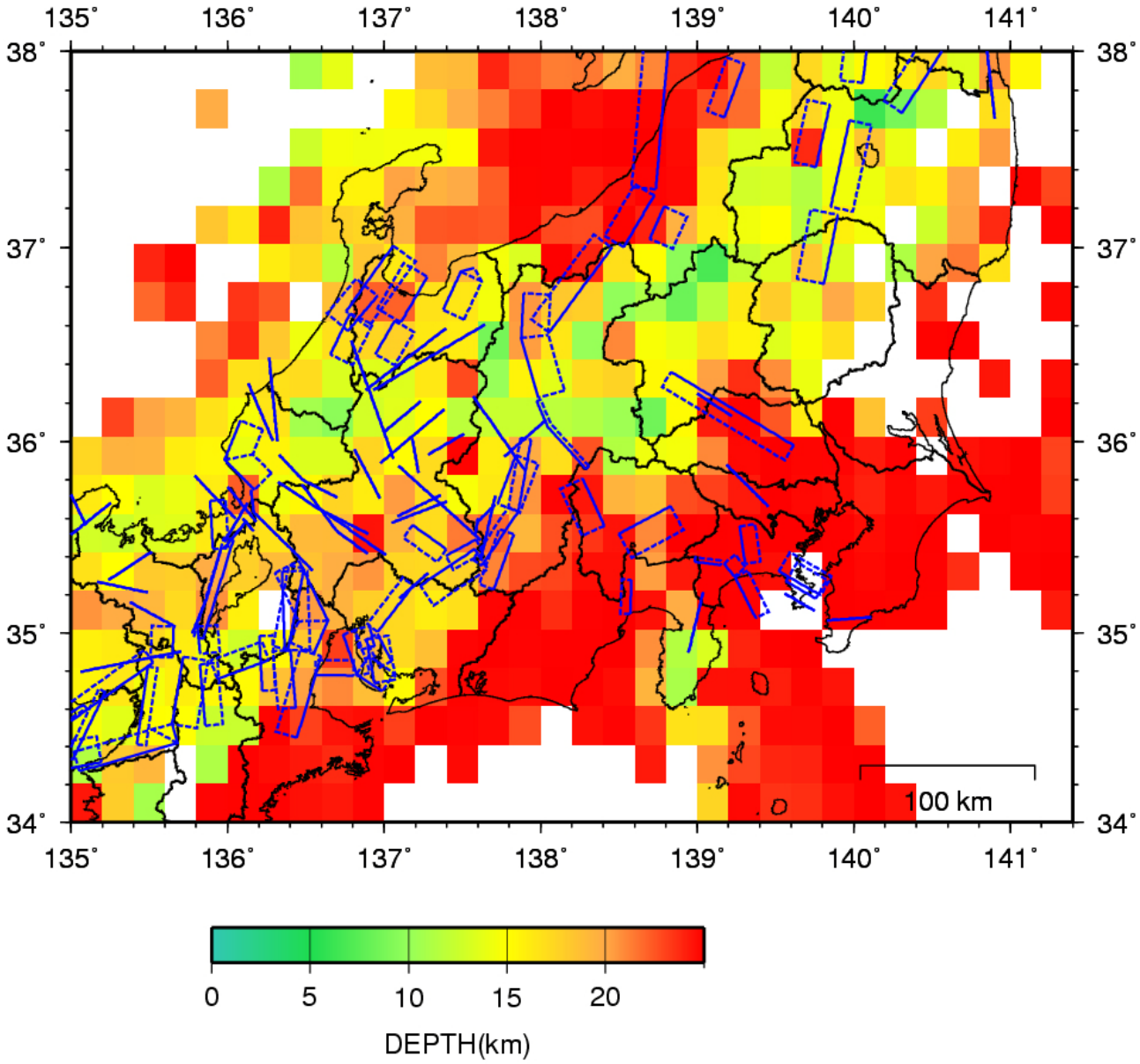

Figure 2.1.2-3 Distribution of the deepest source depth of microearthquakes in each 0.2-eegree resolution obtained from the JMA unified earthquake catalog (part 2)

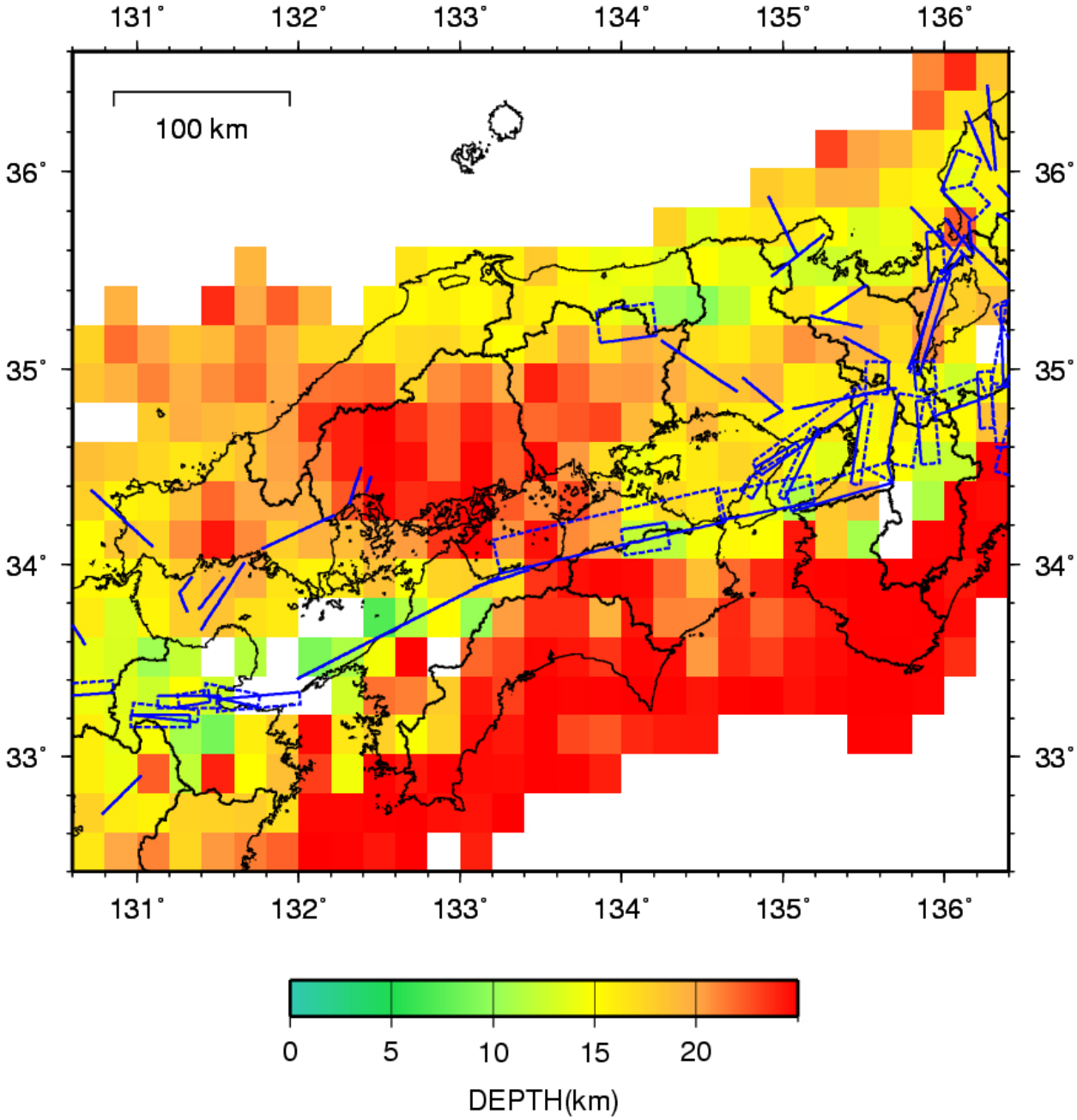

Figure 2.1.2-3 Distribution of the deepest source depth of microearthquakes in each 0.2-degree resolution obtained from the JMA unified earthquake catalog (part 3)

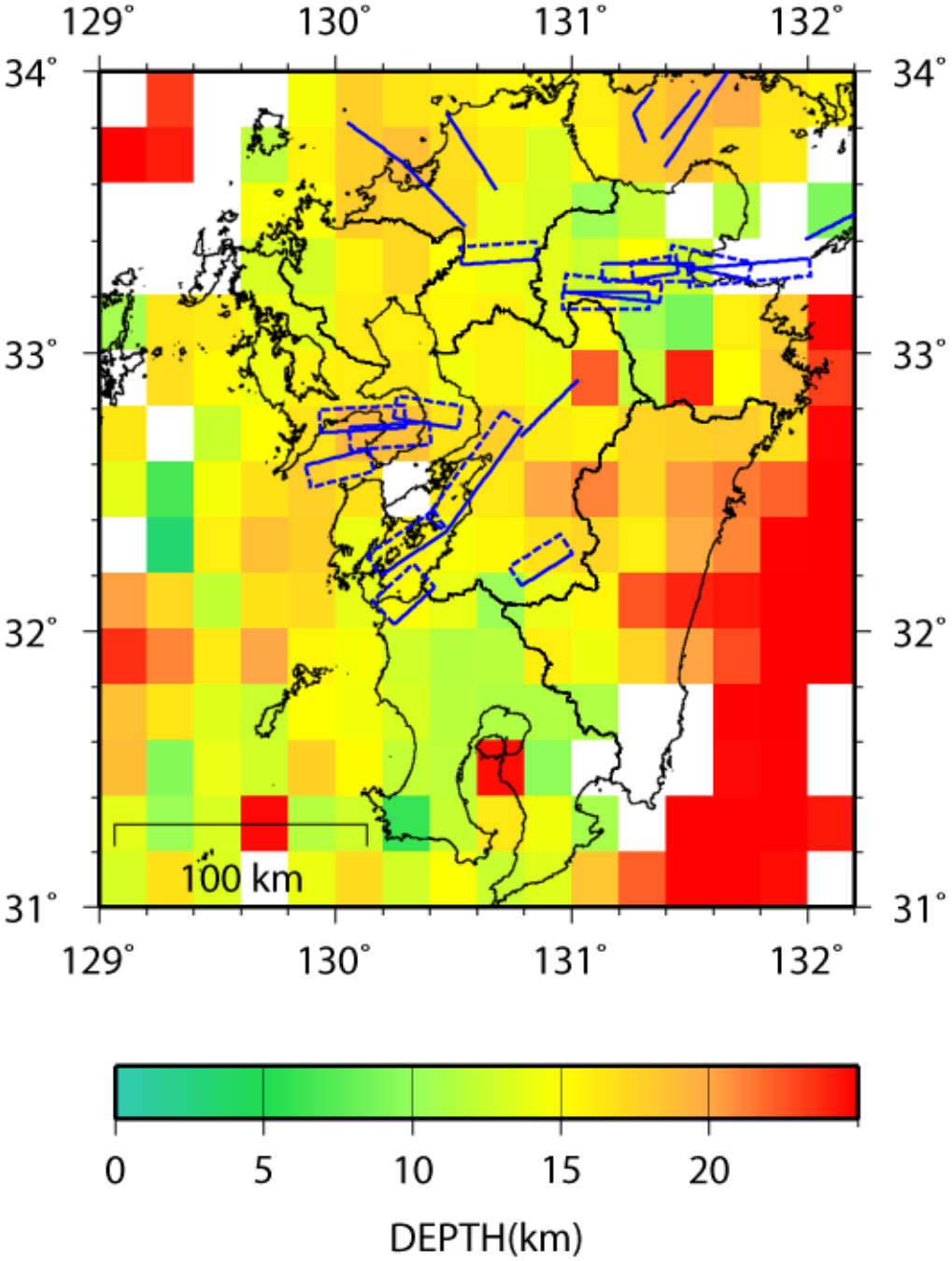

Figure 2.1.2-3 Distribution of the deepest source depth of microearthquakes in each 0.2-degree resolution obtained from the JMA unified earthquake catalog (part 4)

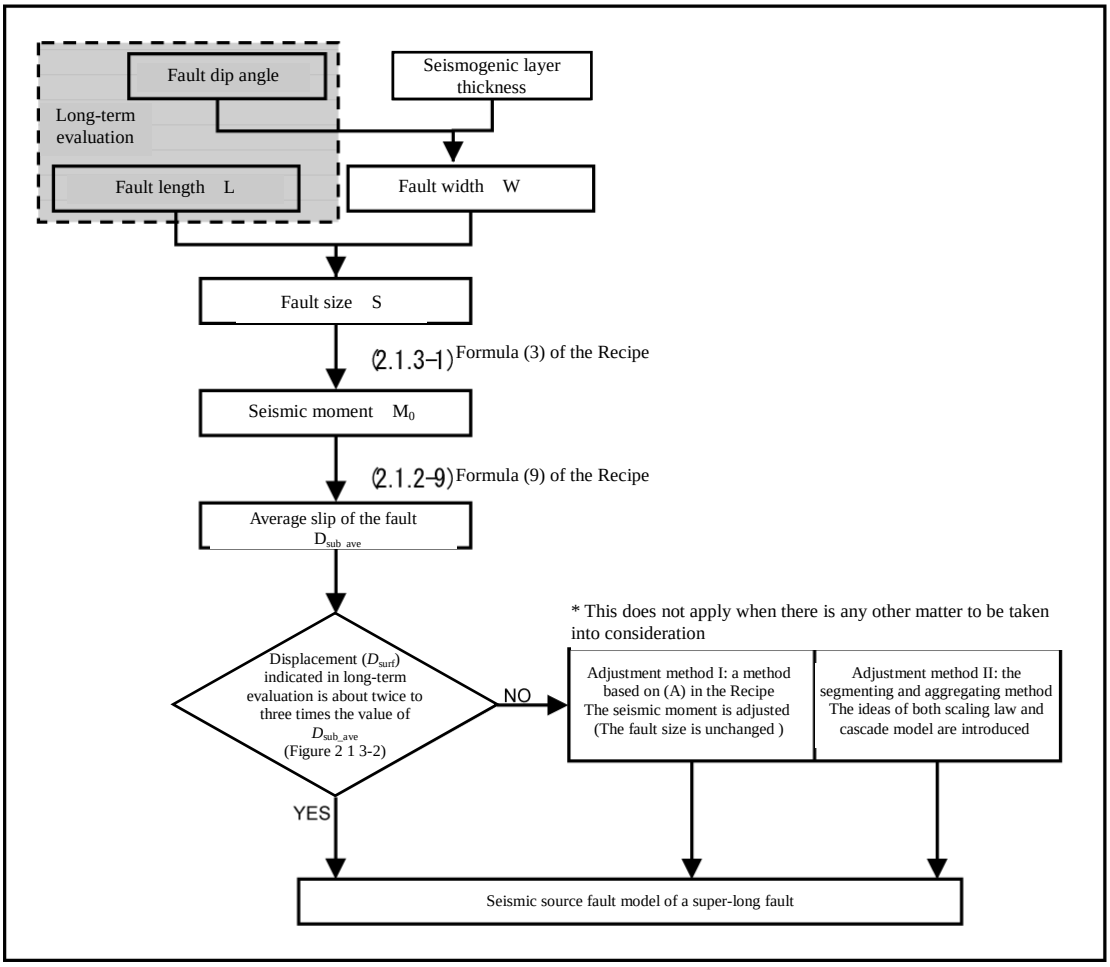

Figure 2.1.3-1 Flow chart of modeling seismic source faults for super-long faults

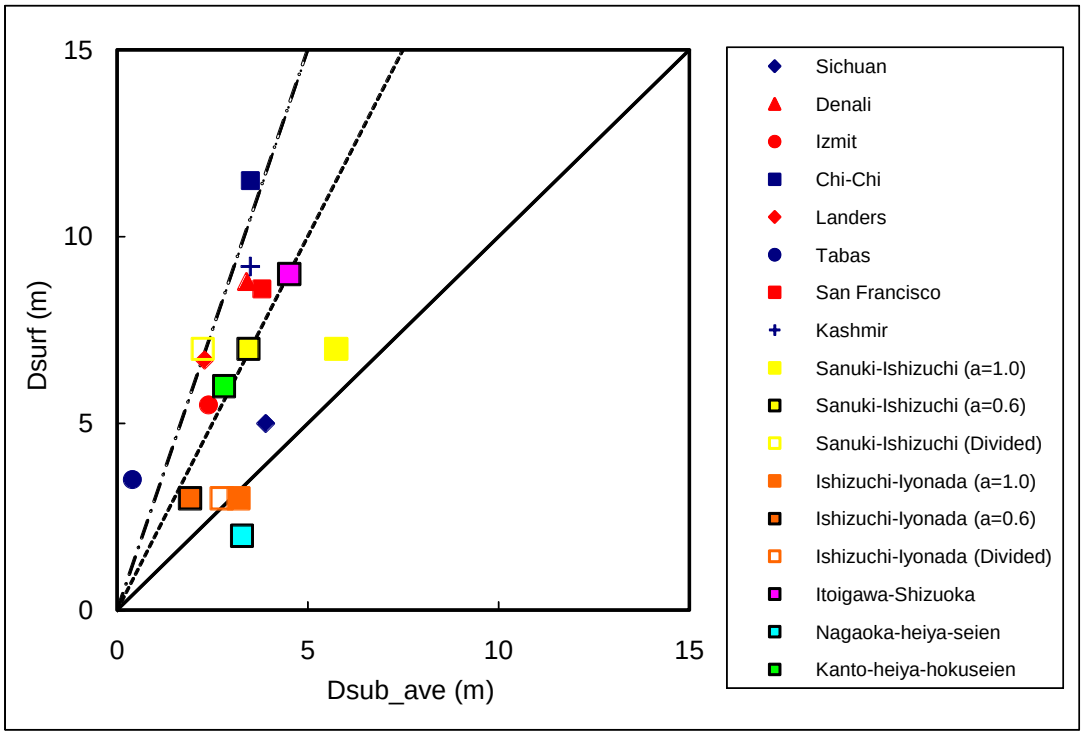

Figure 2.1.3-2 Relation between ground surface displacement (D_{surf}) and average slip of a fault plane (D_{sub_ave}) (Source: Compiled from data of the ERC)

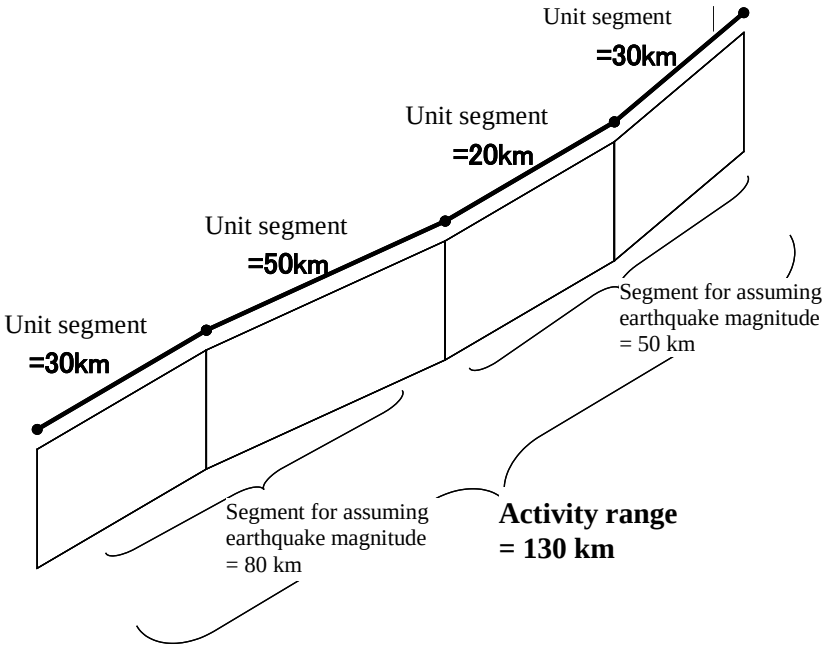

Figure 2.1.3-3 Concept of unit segment, segment for assuming earthquake magnitude, and activity range

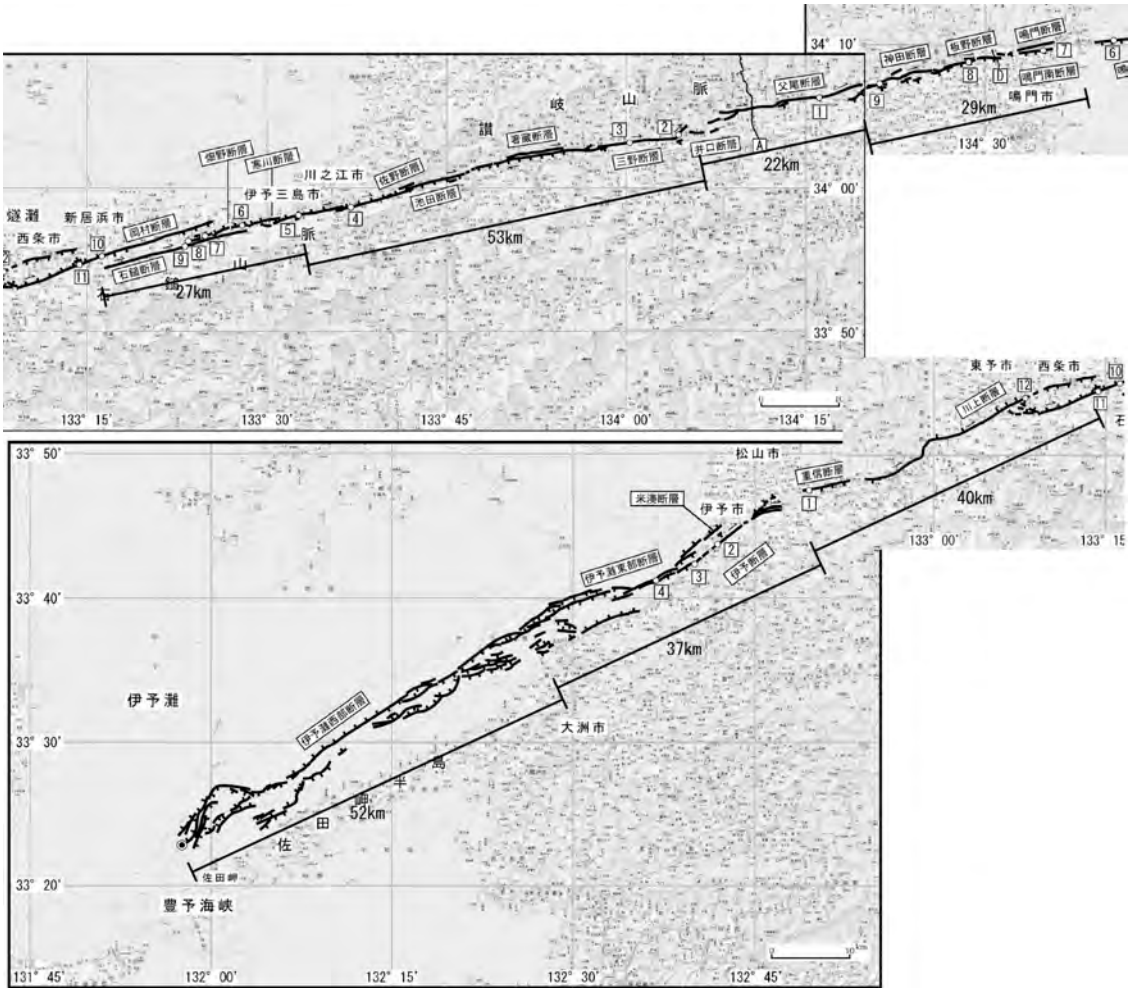

Figure 2.1.3-4 Segments for assuming earthquake magnitude in the Chuo-kozosen fault zone.
Above: S-I part
Below: I-I part

2.2 Characteristic Earthquakes Occurring in the Subduction-Zone and in the Eastern Margin of the Japan Sea

In this section, a subduction-zone earthquake which occurs at specified seismic source fault is treated as a characteristic earthquake. These characteristic earthquakes include "Category I" earthquakes as indicated in Section 3.4, and the earthquakes that occur at specified seismic source faults in the eastern margin of the Japan Sea as indicated the areas (11) to (15) in Figure 2.2-1 and Table 2.2-1. The latter ones are (11) Hokkaido-seiho-Oki Earthquake, (12) Hokkaido-nansei-Oki Earthquake, (13) Aomori-ken-seiho-Oki Earthquake, (14) Yamagata-ken-Oki Earthquake, and (15) Niigata-ken-hokubu-Oki Earthquake. The seismic source fault models for these characteristic earthquakes have been basically those inherited from the past Probabilistic Seismic Hazard Maps. However, Ibaraki-ken-Oki Earthquake, an espcecial case which was belong "Category II", is treated with characteristic earthquake as indicated (10) in Figure 2.2-1 and Table 2.2-1, after the May 8, 2008 (M7.0) Ibaraki-ken-Oki earthquake occurred.The long-term evaluation (e.g., ERC, 2009) for the past earthquakes and the areas where they occurred were reviewed to determine the area where earthquakes resemble characteristic earthquakes. With reference to the earthquakes for which slip distribution on the fault plane has been obtained by seismic waveform analysis, namely, the May 8, 2008 earthquake (Nagoya University, 2008) and the July 23, 1982 earthquake (Murotani et al., 2003; Mochizuki et al., 2008), such area is so determined to surround the entire rupture area including the asperities of those earthquakes. The earthquake magnitude is determined to be M=M_w=7.0 by again referring to the two earthquakes. The above treatment adopts some of the contents of deliberations for the revision of long-term evaluation (ERC, 2009) ahead of the actual revision (Working Group for Advancement of Seismic Hazard Maps (WGASHM), Subcommittee for Long-term Evaluations/Subcommittee for Evaluation of Strong Ground Motion (SLTE/SESGM), ERC, 2008). Figure 2.2-1 and Table 2.2-1 show the locations and moment magnitudes of seismic source fault models for all of the target characteristic earthquakes.

References for Chapter 2

1) Central Disaster Prevention Council (2006): "Chubu-ken/Kinki-ken no nairiku jishin no shindo bunpu to ni tsuite – Zuhyoshu –" (Seismic intensity distribution, etc. of inland earthquakes in the Chubu and Kinki zones: Collection of figures), Special investigation council concerning Tonankai and Nankai earthquakes, etc. (No. 26), Material 2 (in Japanese).
2) Irikura, K. and Miyake, H. (2001): “Prediction of Strong Ground Motions for Scenario Earthquakes", *Journal of Geography*, **110**, 849-875 (in Japanese with English abstract).
3) Earthquake Research Committee (2002): "Itoigawa-Shizuoka-kozosen dansotai (hokubu, chubu) no jishin wo sotei shita kyoshindo hyoka ni tsuite" (Strong motion evaluation assuming earthquakes at the Itoigawa-Shizuoka-kozosen fault zone (northern part, central part)), published on October 31, 2002 (in Japanese).
4) Earthquake Research Committee (2003a): "Morioto/Togashi dansotai no jishin wo sotei shita kyoshindo hyoka ni tsuite" (Strong motion evaluation assuming earthquakes at the Morimoto/Togashi fault zone), published on March 12, 2003 (in Japanese).
5) Earthquake Research Committee (2003b): "Futagawa/Hinagu dansotai no jishin wo sotei shita kyoshindo hyoka ni tsuite" (Strong motion evaluation assuming earthquakes at the Futagawa/Hinagu fault zone), published on July 31, 2003 (in Japanese).
6) Earthquake Research Committee (2003c): "Miura-hanto dansogun no jishin wo sotei shita kyoshindo hyoka ni tsuite" (Strong motion evaluation assuming earthquakes at the Miura-hanto fault group), published on October 28, 2003 (in Japanese).
7) Earthquake Research Committee (2004a): "Tonami-haiya dansotai/Kurehayama dansotai no jishin wo sotei shita kyoshindo hyoka ni tsuite" (Strong motion evaluation assuming earthquakes at the Tonami-heiya fault zone/Kurehayama fault zone), published on March 22, 2004 (in Japanese).
8) Earthquake Research Committee (2004b): "Biwako-seigan dansotai no jishin wo sotei shita kyoshindo hyoka ni tsuite" (Strong motion evaluation assuming earthquakes at the Biwako-seigan fault zone), published on June 21, 2004 (in Japanese).
9) Earthquake Research Committee (2004c): "Takayama/Oppara dansotai no jishin wo sotei shita kyoshindo hyoka ni tsuite" (Strong motion evaluation assuming earthquakes at the Takayama/Oppara fault zone), published on September 27, 2004 (in Japanese).
10) Earthquake Research Committee (2004d): "Nagaoka-heiya-seien dansotai no choki hyoka ni tsuite" (Long-term evaluation of the Nagaoka-heiya-seien fault zone), published on October 13, 2004 (in Japanese).
11) Earthquake Research Committee (2004e): "Ishikari-teichi-toen dansotai no jishin wo sotei shita kyoshindo hyoka ni tsuite" (Strong motion evaluation assuming earthquakes at the Ishikari-teichi-toen fault zone), published on November 29, 2004 (in Japanese).
12) Earthquake Research Committee (2005a): "Yamasaki dansotai no jishin wo sotei shita kyoshindo hyoka ni tsuite" (Strong motion evaluation assuming earthquakes at the Yamasaki fault zone), published on January 31, 2005 (in Japanese).
13) Earthquake Research Committee (2005b): "Tokachi-heiya dansotai no choki hyoka ni tsuite" (Long-term evaluation of the Tokachi-heiya fault zone), published on April 13, 2005 (in Japanese).
14) Earthquake Research Committee (2005c): "Chuo-kozosen

dansotai (Kongo-sanchi-toen-Izumi-sanmyaku-nan'en) no jishin wo sotei shita kyoshindo hyoka ni tsuite" (Strong motion evaluation assuming earthquakes at the Chuo-kozosen fault zone (Kongo-sanchi-toen-Izumi-sanmyaku-nan'en)), published on July 19, 2005 (in Japanese).

15) Earthquake Research Committee (2007): "Yamagata-bonchi dansotai no choki hyoka no ichibu kaitei ni tsuite" (Partial revision of long-term evaluation of the Yamagata-bonchi fault zone), published on August 23, 2007 (in Japanese).

16) Earthquake Research Committee (2008a): "2005 nen Fukuoka-ken-seiho-Oki no jishin no kansoku kiroku ni motozuku kyoshindo yosoku hyoka no kensho ni tsuite" (Verification of strong motion prediction/evaluation based on observation records of the 2005 West off Fukuoka Earthquake), published on April 11, 2008 (in Japanese).

17) Earthquake Research Committee (2008b): "Shingen danso wo tokutei shita jishin no kyoshindo yosoku shuho ('Reshipi')" (Strong ground motion prediction method ("Recipe") for earthquakes with specified source faults) (updated on April 11, 2008), published on April 11, 2008 (in Japanese).

18) Earthquake Research Committee (2008c): "Tonami-heiya dansotai/Kurehayama dansotai no choki hyoka no ichibu kaitei ni tsuite" (Partial revision of long-term evaluation of the Tonami-heiya fault zone/Kurehayama fault zone), published on May 16, 2008 (in Japanese).

19) Earthquake Research Committee (2009): "Sanriku-Oki kara Boso-Oki ni kakete no jishin katsudo no choki hyoka no ichibu kaitei ni tsuite" (Partial revision of long-term evaluation of seismic activity from Sanriku-Oki to Boso-Oki), published on March 9, 2009 (in Japanese).

20) Working Group for Advancement of Seismic Hazard Maps, Subcommittee for Long-term Evaluations/Subcommittee for Evaluation of Strong Ground Motion, Earthquake Research Committee (2008): "Zenkoku jishindo yosoku chizu ni okeru Ibaraki-ken-Oki no jishin no atsukai ni tsuite" (Treatment of the Ibaraki-ken-Oki Earthquake in the National Seismic Hazard Maps for Japan) (conference material, Map 25 (7)), December 17, 2008 (in Japanese).

21) Kanamori, H. (1977): "The energy release in great earthquakes", *J. Geophys. Res.*, **82**, 2981-2987.

22) Matuda, T. (1975): "Magnitude and Recurrence Interval of Earthquakes from a Fault", *Journal of the Seismological Society of Japan* (Second Series), **28**, 269-283 (in Japanese with English abstract).

23) Mochizuki, K., Yamada, T., Shinohara, M., Yamanaka, Y. and Kanazawa, T. (2008): "Weak interplate coupling by seamounts and repeating M~7 earthquakes", *Science*, **321**, 1194-1197.

24) Murotani, T., Kikuchi, M., and Yamanaka, Y (2003): "Source process of the 1982 Ibaraki ken oki earthquake inferred from JMA strong motion records", *Seismological Society of Japan 2003 Fall Meeting*, P029 (in Japanese).

25) Nagoya University (2008): “Source process of Off-Ibaraki earthquake on May 8, 2008 (Mj6,4, 7.0)", *Report of the Coordinating Committee for Earthquake Prediction, Japan*, **80**, 101-110 (in Japanese).

26) Takemura, M. (1990): “Magnitude-seismic moment relations for the shallow earthquakes in and around Japan", *Journal of the Seismological Society of Japan* (Second Series), **43**, 257-265 (in Japanese with English abstract).

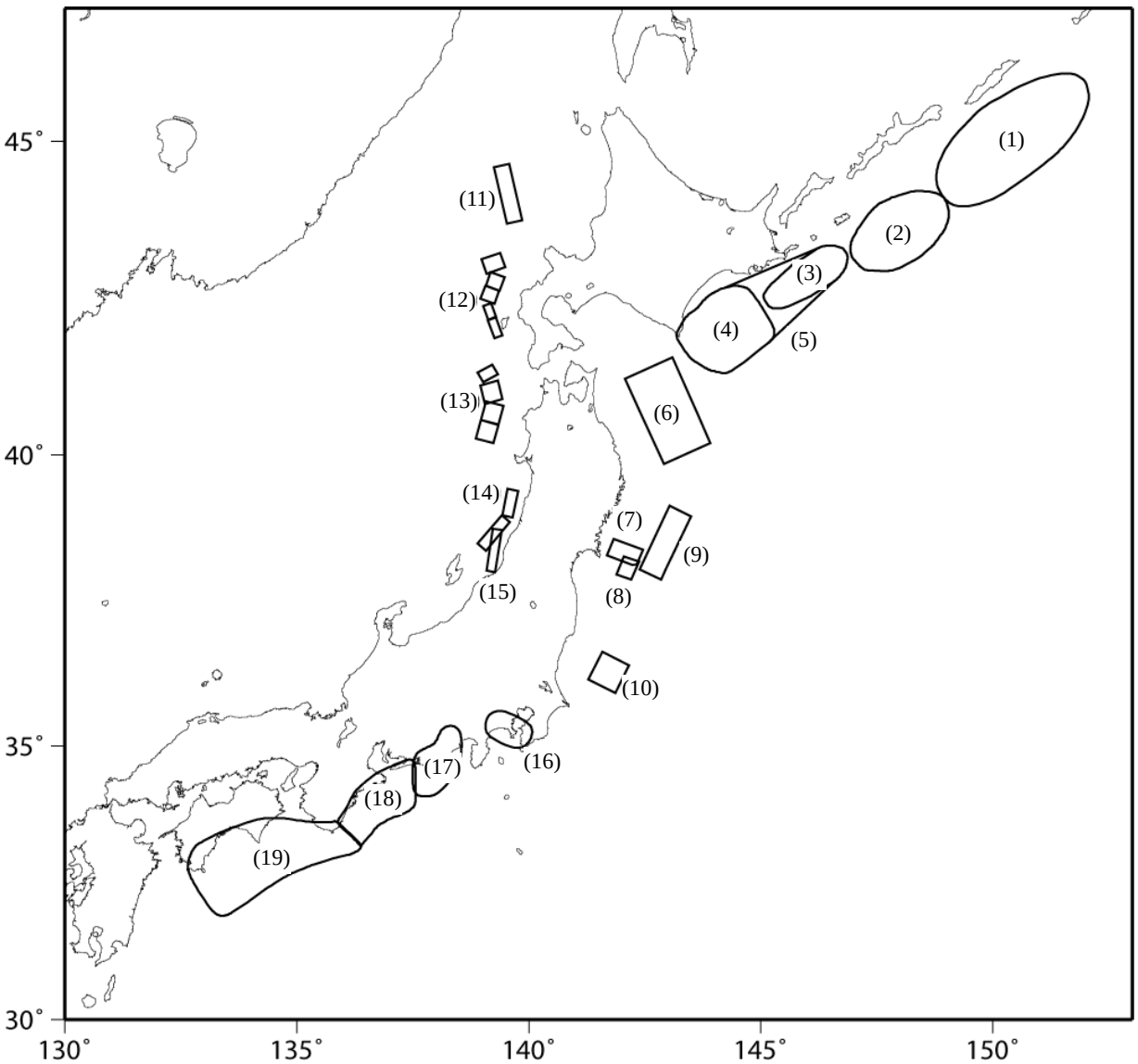

Figure 2.2-1 Locations of the seismic source faults of subduction-zone characteristic earthquakes and characteristic earthquakes that occur in the eastern margin of the Japan Sea

See Table 2.2-1 for the earthquakes corresponding to the respective numbers.

Table 2.2-1 Corresponding area numbers and the moment magnitudes (M_w) of subduction-zone characteristic earthquakes and characteristic earthquakes that occur in the eastern margin of the Japan Sea

Areas	Earthquakes	M_w	Areas	Earthquakes	M_w
(1)	Etorofuto-Oki Earthquake	8.1	(11)	Hokkaido-seiho-Oki Earthquake	7.5
(2)	Shikotanto-Oki Earthquake	7.8	(12)	Hokkaido-nansei-Oki Earthquake	7.8
(3)	Nemuro-Oki Earthquake	7.9	(13)	Aomori-ken-seiho-Oki Earthquake	7.7
(4)	Tokachi-Oki Earthquake	8.1	(14)	Yamagata-ken-Oki Earthquake	7.7
(5)	Tokachi-Oki Earthquake + Nemuro-Oki Earthquake	8.3	(15)	Niigata-ken-hokubu-Oki Earthquake	7.5
(6)	Large interplate earthquakes in Northern Sanriku-Oki	8.3	(16)	Kanto Earthquake of "1923 Taisho" type	7.9
(7)	Miyagi-ken-Oki Earthquake (A1)	7.6	(17)	Assumed Tokai Earthquake	8.0
(8)	Miyagi-ken-Oki Earthquake (A2)	7.4	(18)	Tonankai Earthquake	8.1
(9)	Earthquakes close to the offshore trenches in Southern Sanriku-Oki (B)	7.8	(19)	Nankai Earthquake	8.4
(7) (9)	Miyagi-ken-Oki Earthquake (A1+B)	7.9	(17) (18)	Tonankai Earthquake + Assumed Tokai Earthquake	8.4
(8) (9)	Miyagi-ken-Oki Earthquake (A2+B)	7.9	(18) (19)	Nankai Earthquake + Tonankai Earthquake	8.5
(7) (8) (9)	Miyagi-ken-Oki Earthquake (A1+A2+B)	8.0	(17) (18) (19)	Nankai Earthquake + Tonankai Earthquake + Assumed Tokai Earthquake	8.5
(10)	Interplate earthquakes in Ibaraki-ken-Oki (characteristic)	7.0			

3. Probabilistic Seismic Hazard Maps (PSHM)

3.1 Evaluation Procedure and Its Result Representation

3.1.1 Outline of the seismic hazard evaluation method

Seismic hazard evaluation calculates the relation between the ground motion intensity at a specific site and the probability of exceeding that intensity within a specific period (such relation is called a hazard curve). Generally, evaluation follows the flow chart shown in Figure 3.1.1-1. The brief outline of the procedure is given below.

1) The seismic activity around the target site is modeled. For computing the PSHM for the whole of Japan, the all of earthquakes to be considered were modeled by classiging them into the following groups:
   a) Characteristic earthquakes occurring in major active fault zones
   b) Subduction-zone earthquakes
   c) Other earthquakes (earthquakes not considered in the long-term evaluation)
      [1] Earthquakes with specified source faults
         (1) Earthquakes occurring in active faults other than major active fault zones
         (2) Earthquakes occurring in major active fault zones excluding the characteristic events
      [2] Earthquakes without specified source faults
         (1) Earthquakes on the plate boundaries, but other than large events
         (2) Earthquakes within subducting (or subducted) plates, but other than large events
         (3) Earthquakes occurring at onshore locations where active faults have not been specified
         (4) Earthquakes without specified source faults but in Urakawa-Oki
         (5) Earthquakes without specified source faults but in the eastern margin of the Japan Sea
         (6) Earthquakes without specified source faults but in the southern area of Izushoto islands
         (7) Earthquakes without specified source faults but in the vicinity of Nanseishoto islands

   Note: the c)[1](2) above is an exception of evaluation for the PSHM.
2) For each modeled earthquake, the probabilities of earthquake magnitude, distance, and earthquake occurrence (or frequency) are evaluated.
3) A probability model is built for evaluating the ground motion intensity of an earthquake under a given magnitude and distance. Usually, the model is built based on an attenuation relation of ground motion and with variance.
4) For each modeled earthquake, the probability that the ground motions caused by that earthquake within the target period exceed a certain value is evaluated.
5) This process is repeated for the same number times as the number of the modeled earthquakes, and the results are summarized to calculate the probability that the ground motion intensity exceeds a certain level at least once within the target period, when all earthquakes are taken into consideration.

Seismic hazard evaluation is conducted for each site through the procedure above, and by fixing any two parameters of the period, ground motion intensity, and probability, the value of the remaining parameter is obtained. The PSHM show the regional distribution of such values.

3.1.2 Hazard curve calculation method

The probability that the ground motion intensity exceeds level y at least once within t years as a result of earthquakes (or earthquake clusters) that occur around a target site is generally called a hazard curve, and is expressed as $P(Y>y;t)$. A hazard curve is evaluated by subtracting from 1 the probability that the ground motion intensity does not exceed level y by any of the earthquakes (earthquake clusters) that occur around the target site, as shown in the following formula:

$$P(Y > y;t) = 1 - \prod_k \{1 - P_k(Y > y;t)\} \qquad (3.1.2\text{-}1)$$

where $P_k(Y>y;t)$ is the probability that the ground motion intensity exceeds level y at least once within t years as a result of the k-th earthquake (earthquake cluster), which is calculated as shown in (1) and (2) below. Discrete representations are used below for the earthquake magnitude and distance.

(1) Earthquakes with specified source faults (earthquakes occurring subduction-zones, and either in major active fault zones, or other fault zones)

The occurrence probability of some of such earthquakes is calculated based on a model representing nonstationary seismic activity such as a renewal process or a time-predictable model, and that of the other earthquakes is evaluated by assuming a stationary Poisson process. In this case, probability $P_k(Y>y;t)$ that the ground motion intensity exceeds level y at least once within t years as a result of the k-th earthquake can be calculated as follows.

a) When the earthquake occurrence probability is calculated based on a nonstationary seismic activity model

When considering multiple earthquake occurrences within period t, if the ground motion intensity Y during each earthquake is assumed to be independent from each other, probability $P_k(Y>y;t)$ that the ground motion intensity Y exceeds level y at least once within t years is expressed by

$$P_k(Y > y;t) = 1 - \sum_{l=0}^{\infty} \{P(E_k^{[l]};t)[1 - P(Y > y \mid E_k)]^l\} \qquad (3.1.2\text{-}2).$$

Here, $P(E_k^{[l]};\ t)$ is the probability of earthquakes occurring l times within period t. $P(Y>y|E_k)$ is the conditional probability that the ground motion intensity Y exceeds level y where

earthquake k occurs once, defined as

$$P(Y > y \mid E_k) = \sum_i \sum_j P(Y > y \mid m_i, r_j) P_k(m_i) P_k(r_j \mid m_i) \tag{3.1.2-3}$$

where $P_k(m_i)$ is a probability function of the magnitude of the k-th earthquake, $P_k(r_j|m_i)$ is a probability function of the distance where the magnitude is m_i, and $P(Y>y|m_i, r_j)$ is the conditional probability that the ground motion intensity Y exceeds level y where the earthquake magnitude is m_i and the distance is r_j. When evaluating the ground motion intensity by using an attenuation relation, $P(Y>y| m_i, r_j)$ is written as

$$P(Y > y \mid m_i, r_j) = 1 - F_U\left(\frac{y}{\overline{Y}(m_i, r_j)}\right) \tag{3.1.2-4}$$

using the mean value $\overline{Y}(m_i, r_j)$ obtained by an attenuation relation and the variance (often expressed as U, which is a logarithmic normal distribution where the mean value is 1). $F_U(u)$ is a cumulative distribution function of U.

When the probability that earthquakes occur more than once within period t can be ignored, Formula (3.1.2-2) can be simplified to

$$\begin{aligned} P_k(Y > y; t) &= P(E_k; t) P(Y > y \mid E_k) \\ &= P(E_k; t) \sum_i \sum_j P(Y > y \mid m_i, r_j) P_k(m_i) P_k(r_j \mid m_i) \end{aligned} \tag{3.1.2-5}$$

where $P(E_k; t)$ is the occurrence probability of the k-th earthquake within period t, which is evaluated by using the Brownian passage time distribution based on a renewal process or time-predictable model (ERC, 2001a).

b) When the earthquake occurrence probability is calculated based on a stationary Poisson process

When modeling earthquake occurrence by a Poisson process, the probability $P_k(Y>y; t)$ that the ground motion intensity exceeds level y within t years can be expressed as

$$P_k(Y > y; t) = 1 - \exp\{-\nu_k(Y > y) \cdot t\} \tag{3.1.2-6}$$

where $\nu_k(Y>y)$ is the annual frequency that the ground motion intensity Y exceeds level y by earthquakes at the k-th source area and can be written as

$$\begin{aligned} \nu_k(Y > y) &= \nu(E_k) P(Y > y \mid E_k) \\ &= \nu(E_k) \sum_i \sum_j P(Y > y \mid m_i, r_j) P_k(m_i) P_k(r_j \mid m_i) \end{aligned} \tag{3.1.2-7}$$

where $\nu(E_k)$ is the annual frequency of earthquakes at the k-th source area and the other parameters are the same as those in a) above.

(2) Earthquakes without specified source faults

Unlike in the case of (1) above, in the case of earthquakes without specified source faults, the target earthquakes need to be treated as a group of earthquakes of different magnitudes and distances. These earthquakes are evaluated by using both a zoning method and a non-zoning method. Seismic activity is assumed to be uniform in each seismic activity area in the case of the zoning method, and in each mesh in the case of the non-zoning method. Because of this, earthquake magnitudes and locations are independent from each other as long as individual seismic activity areas or meshs are targeted. The probability distribution of earthquake magnitude can be obtained by a Gutenberg-Richter relation with an upper limit, and the probability distribution of distance can be obtained by the geometric relationship between the location of the site and that of the seismic activity area or mesh. The time series of earthquake occurrence is modeled by a stationary Poisson model.

Based on the above, the probability $P_n(Y>y; t)$ that the ground motion intensity Y exceeds level y within t years as a result of group n earthquakes can be calculated by the following formula:

$$P_n(Y > y; t) = 1 - \exp(-\nu_n(Y > y) \cdot t) \tag{3.1.2-8}$$

Here, $\nu_n(Y>y)$ is the annual frequency that the ground motion intensity exceeds level y by group n earthquakes, which can be written as

$$\begin{aligned} \nu_n(Y > y) &= \sum_k \nu(E_k) P(Y > y \mid E_k) \\ &= \sum_k \nu(E_k) \sum_i \sum_j P(Y > y \mid m_i, r_j) P_k(m_i) P_k(r_j \mid m_i) \end{aligned} \tag{3.1.2-9}$$

where $\nu(E_k)$ is the annual frequency of earthquakes with magnitude exceeding the minimum magnitude (=5.0) that occur at the k-th seismic activity area or mesh constituting the group n earthquakes, $P(Y>y|E_k)$ is the conditional probability that the ground motion intensity at the site exceeds level y where a single earthquake occurs at the k-th seismic activity area or mesh constituting the group n earthquakes, $P_k(m_i)$ is a probability function of the magnitude at the k-th seismic activity area or mesh, $P_k(r_j|m_i)$ is a probability function of the distance where the magnitude is m_i, and $P(Y>y|m_i, r_j)$ is the conditional probability that the ground motion intensity exceeds level y where the earthquake magnitude is m_i and the distance is r_j.

For earthquakes without specified source faults, the probability distribution of earthquake magnitude is modeled by a model based on a Gutenberg-Richter relation (so-called b-value model), as described above. Strictly speaking, it is a b-value model with an upper limit (a truncated b-value model), since the maximum magnitude is set for each area. The b-value model with an upper limit (and lower limit) to the magnitude uses

$$N(m_l \le M \le m_u) = N(M \ge m_l) - N(M \ge m_u) \tag{3.1.2-10}$$

$$N(m_l \le M \le m) = N(M \ge m_l) - N(M \ge m) \qquad (3.1.2\text{-}11)$$

and the Gutenberg Richter relation

$$N(M \ge m) = 10^{a-bm} \qquad (3.1.2\text{-}12)$$

to derive the distribution function of magnitude M, which is written as

$$\begin{aligned} F_M(m) &= P(M \le m) \\ &= \frac{N(M \ge m_l) - N(M \ge m)}{N(M \ge m_l) - N(M \ge m_u)} \\ &= \frac{1-10^{-b(m-m_l)}}{1-10^{-b(m_u-m_l)}} \\ &= \frac{1-\exp(-b\ln 10(m-m_l))}{1-\exp(-b\ln 10(m_u-m_l))} \end{aligned} \qquad (3.1.2\text{-}13).$$

Here, m_l and m_u are the minimum and maximum magnitudes, respectively. Generally, magnitude interval Δm is set at 0.1. In that case, if the minimum magnitude (indicated by 0.1 intervals) is 5.0, 5.0 − Δm/2=4.95 is used as m_l, and similarly, the maximum magnitude indicated by 0.1 intervals＋Δm/2 is used as m_u. Using Formula (3.1.2-13) above, the probability of magnitude M becoming m_i is given by

$$P(m_i) = P(m_1 \le m_i \le m_2) = F_M(m_2) - F_M(m_1) \qquad (3.1.2\text{-}14)$$

where we put $m_i - \Delta m/2 = m_1 \le m_i < m_2 = m_i + \Delta m/2$. It should be noted that, in a b-value model without an upper limit, the cumulative frequency of occurrence by magnitude level forms a straight line on a semi-logarithmic axis, but when an upper limit is set, the cumulative frequency of occurrence by magnitude level does not form a straight line.

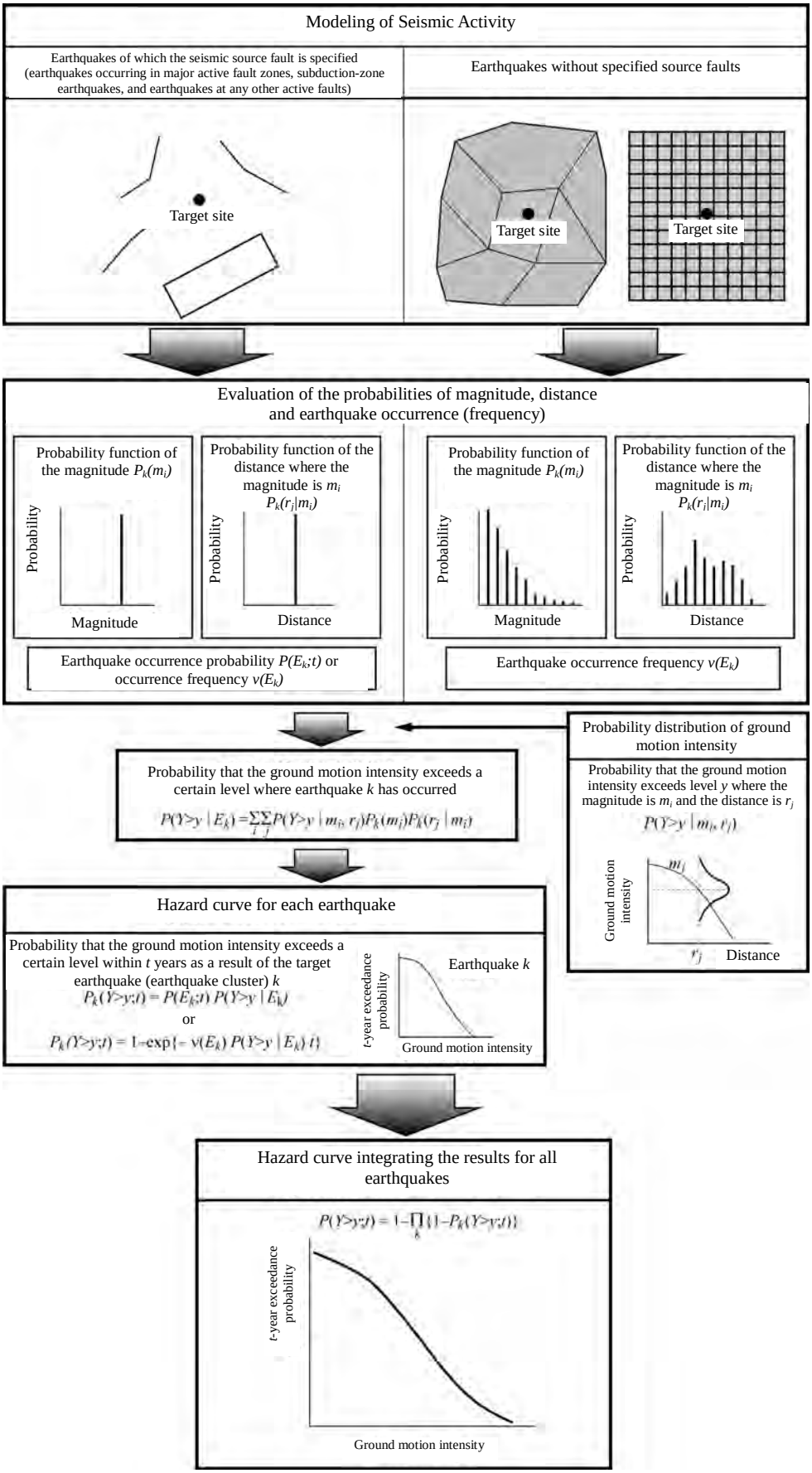

Figure 3.1.1-1 Flow chart of seismic hazard evaluation

3.1.3 Representation of the results

(1) Hazard curve

A hazard curve indicates the relation between ground motion intensity and the probability of exceeding that intensity within a specific period, and it is calculated as described in Section 3.1.2. In practice, the exceedance probability is calculated for each discretely determined ground motion intensity, and the results are plotted on a figure exemplified by Figure 3.1.3-1 by connecting the data by straight lines.

The probability of exceeding a given ground motion intensity and the ground motion intensity corresponding to a given exceedance probability are respectively calculated through linear interpolation in Figure 3.1.3-1. In this way, it is easy to calculate the probability for a given ground motion intensity and the ground motion intensity for a given probability over a fixed target period by using a single hazard curve. On the other hand, it is difficult to calculate the period for given ground motion intensity and probability when using a nonstationary earthquake occurrence model. However, if all earthquake occurrences are assumed to follow a stationary Poisson process, the derived hazard curve can be converted into an exceedance probability for a different period, so the calculation will be possible by using such relation.

(2) Representation of PSHM

The following two types of PSHM are created, based on the hazard curve for t years calculated independently for each site:

a) Map showing distribution of the ground motion intensity for a given probability obtained for each site
b) Map showing distribution of the exceedance probability for a given ground motion intensity obtained for each site.

As shown in Figure 3.1.3-1, the only difference between these two PSHM is from which direction the hazard curve is read.

(3) Results and degree of influence by earthquake category

This time, earthquakes are classified into three categories, and PSHM are also created for each category (Ishikawa et al., 2008). The earthquakes included in each category are indicated in 3.4. In addition, the "degree of influence" is used as an index that shows which category of earthquakes have an outstanding influence at a specific probability level (seismic intensity level), and the degree of influence is also presented. The degree of influence is defined below.

There have been studies proposing the idea of "probabilistic scenario earthquakes" as a methodology for selecting earthquakes that are highly likely to cause ground motion intensity that corresponds to the target probability level as scenario earthquakes (Kameda et al., 1997; Ishikawa and Okumura, 2001). Those studies define the degree of influence (the term "contribution factor" is used in the original articles) of each earthquake as an index representing the relative occurrence probability of earthquakes that could cause such ground motions. The degree of influence changes according to the target probability level and the ground motion indices. Earthquakes with a larger degree of influence are to be emphasized in selecting scenario earthquakes.

Using the symbols indicated in 3.1.2, the degree of influence is defined as

$$c_k(p;t) = \frac{P_k(Y > y;t)}{\sum_k P_k(Y > y;t)} \qquad (3.1.3\text{-}1)$$

where $c_k(p;\ t)$ is the degree of influence of the k-th earthquake (earthquake cluster) of which the exceedance probability within t years corresponds to probability level p, and $P_k(Y>y;\ t)$ is the probability that the ground motion intensity exceeds level y at least once within t years by the k-th earthquake. When the probability that earthquakes occur more than once within t years can be ignored, the probability can be broken down into the earthquake occurrence probability and the ground motion exceedance probability as

$$c_k(p;t) = \frac{P(E_k, t)\cdot P_k(Y > y \mid E_k)}{\sum_k P(E_k, t)\cdot P_k(Y > y \mid E_k)} \qquad (3.1.3\text{-}2)$$

where $P(E_k,\ t)$ is the occurrence probability of the k-th earthquake within t years, and $P_k(Y>y \mid E_k)$ is the conditional probability that the ground motion intensity exceeds level y where the k-th earthquake occurs.

As clear from the formula above, for each probability level, the degree of influence of all earthquakes sums up to 1 (100%). The degree of influence of the same earthquake changes according to the probability level. Conversely, even if the site and the probability level are the same, the degree of influence varies if the target ground motion indices differ.

The degree of influence is defined for each earthquake, but it is also applicable to an earthquake cluster consisting of multiple earthquakes. This time, three degrees of influence are evaluated for each earthquake category according to the probability levels (seismic intensity levels) for each site, and the category that has the strongest influence (the "highest degree of influence") is extracted for each site. The "Map of Earthquake Category with the Highest Degree of Influence" which shows such extracted results on a map is also created.

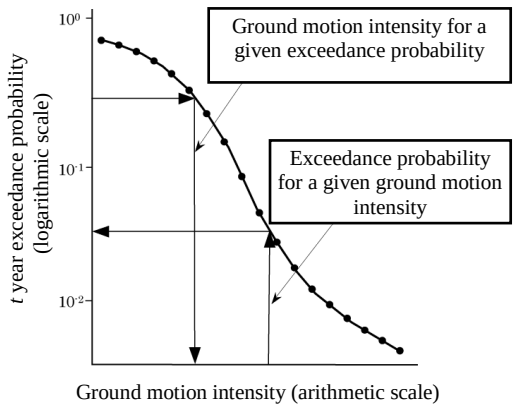

Figure 3.1.3-1 Conceptual graph of a hazard curve

3.2 Area Covered by the PSHM and Map Specifications

3.2.1 Area covered by the PSHM

The PSHM covers 47 prefectures, from Hokkaido to Okinawa, for the whole of Japan. However, while Etorofu, Kunashiri, Shikotan and Habomai Islands are covered by the maps, Okinotorishima Island and Minamitorishima Island are not evaluated due to the lack of information for modeling seismic activity. The number of 250 m meshs (each being 1/16 of the 3rd grid of the Grid Square System) included in the area covered totals to about 5,955,000.

3.2.2 PSHM Map specifications

The peak ground velocity derived using an attenuation relation by Si and Midorikawa (1999) and the JMA instrumental seismic intensity based on it are used as ground motion indices for the maps. The target periods are 30 years and 50 years from January 2009. The following two types of PSHM are created.

1) Distribution map of ground motion intensity where the period and the exceedance probability are fixed

The ground intensities where the exceedance probabilities within 30 years from January 2009 are 6% and 3%, and those within 50 years are 39%, 10%, 5%, and 2% at the center of the 250 m mesh included in the area covered are calculated and presented in a color scale for each mesh. The presented ground motion intensity is the JMA seismic intensity at the ground surface.

2) PSHM distribution map of exceedance probability where the period and the ground motion intensity are fixed

The probabilities that ground motions with JMA seismic intensity of 5 Lower or more, 5 Upper or more, 6 Lower or more, and 6 Upper or more occur at ground surface within 30 years from January 2009 at the center of the 250 m mesh included in the area covered are calculated and presented in a color scale for each mesh.

As for the PSHM distribution map of in terms of JMA seismic intensity and of exceedance probability within 30 years, the maps by earthquake category are indicated in addition to the previous-version maps that took into consideration all earthquakes. Earthquakes had previously been classified into earthquakes occurring in major active fault zones, subduction-zone earthquakes, and other earthquakes, but this time, maps for three newly defined earthquake categories are indicated. The categorization of earthquakes is discussed later in 3.4. In addition, the PSHM differential distribution maps, between the results of the 2008 version and 2009 version, are created in terms of the exceedance probability within 30 years and in terms of the peak ground velocity at the engineering bedrock where the exceedance probabilities are 6% and 3% within 30 years. Since the occurrence probability of earthquakes in major active fault zones is evaluated for both the average case and the maximum case, the maps for the maximum case are also presented. The results are shown in Section 3.7.

The latitudes and longitudes of the maps are based on the Tokyo Datum before the revision of the Survey Act.

3.3 Seismic Activity Evaluation Models

From among the evaluation conditions for creating PSHM, this section describes the seismic activity evaluation models.

The seismic activity evaluation models used are basically the same as those used for the PSHM published in March 2005, September 2006, April 2007, and April 2008 (ERC, 2005b, 2006b, 2007b, 2008b). However, the long-term evaluation results that were revised and published after that are incorporated, and changes in the earthquake occurrence probability in line with the passage of one year are taken into consideration. Also, the earthquake catalog for determining the occurrence frequency of earthquakes without specified source faults has been updated. Moreover, as a result of introducing a new method for seismic source fault modeling for major active fault zones, seismic source fault models have been updated for a large number of active faults.

Based on long-term evaluation results of earthquakes that occur at active faults and subduction-zone earthquakes, earthquakes that occur around the Japanese archipelago are classified as follows:

"Characteristic earthquakes occurring in major active fault zones"
"Subduction-zone earthquakes"
"Other earthquakes (earthquakes not considered in the long-term evaluation)"

- Earthquakes with specified source faults
  1) Earthquakes occurring in active faults other than major active fault zones
  2) Earthquakes occurring in major active fault zones excluding the characteristic events
- Earthquakes without specified source faults
  3) Earthquakes on the plate boundaries, but other than large events
  4) Earthquakes within subducting (or subducted) plates, but other than large events
  5) Earthquakes occurring at onshore locations where active faults have not been specified
  6) Earthquakes without specified source faults but in Urakawa-Oki
  7) Earthquakes without specified source faults but in the eastern margin of the Japan Sea
  8) Earthquakes without specified source faults but in the southern area of Izushoto islands
  9) Earthquakes without specified source faults in the vicinity of Nanseishoto islands

The following section outlines the respective seismic activity

models. Among the above, earthquakes of group 2) are included in group 5) when modeled.

3.3.1 Characteristic earthquakes occurring in major active fault zones

(1) Basic policy for modeling

[1] Basic policy

For the seismic activity of characteristic earthquakes occurring in major active fault zones, the earthquake occurrence probability, the magnitude, and the fault plane parameters are modeled based on long-term evaluation results. For determining the magnitude and the seismic source fault parameters, the newly examined seismic source fault modeling method (see Section 2.1 for details) is applied. For active faults for which strong motion evaluation (Seismic Hazard Maps for Specified Seismic Source Faults) has been conducted, the seismic source fault information considered in that evaluation is taken into account.

With regard to the Futagawa/Hinagu fault zone (central part/southwestern part) for which multiple results have been given in long-term evaluation, a hazard curve is calculated by a weighted mean of the multiple results. The active fault zones targeted this time are those for which long-term evaluation results have been revised and published by the end of December 2008.

[2] Determination of the earthquake occurrence probability

The occurrence probability of earthquakes in major active fault zones is calculated according to the method indicated in ERC(2001a), using Brownian Ｐassage Ｔime (BPT) distribution as the probability distribution of activity intervals, and using 0.24 as variance α. However, for some active fault zones for which the time of the latest event and other factors are unknown, the occurrence probability is calculated based on a Poisson process.

The mean recurrence interval and the time of the latest event for calculating the probability are based on long-term evaluation results (ERC, 2005a, 2006a, 2007a, 2008a, 2009a). The starting point of the time is January 2009. In long-term evaluation, the earthquake occurrence probability is not clearly indicated for some active faults since the mean recurrence interval or the time of the latest event is unknown. In such case, the mean recurrence interval is assumed based on individual information such as the fault length or the average slip rate, and the earthquake occurrence probability is determined based on a Poisson process. When the average slip rate is unknown, 0.25 mm/y is assumed as a general average slip rate for active faults of Class B activity level (Okumura and Ishikawa, 1998), while the class border values 1 mm/y and 0.1 mm/y are respectively assumed as general average slip rates for Class A-B and Class B-C active faults (Matsuda, 1975). When the activity level is unknown, it is assumed to be Class B.

Sometimes, the earthquake occurrence probability is indicated in a range of values in long-term evaluation. Here, the models are built using the earthquake occurrence probability based on the median values of the respective ranges of the recurrence interval and the time of the latest event (hereinafter referred to as the "average case").

When the long-term evaluation results for major active fault zones were published, the faults were classified into a "group with a high probability of occurrence," a "group with a fairly high probability of occurrence," and "others" by relative comparison of the values of earthquake occurrence probability within 30 years. It should be noted that the maximum value of earthquake occurrence probability is used in that categorization, which differs from the probability value used in the "average case" above. Therefore, in order to compare the differences in results, a study is also made for the case of using the maximum value of earthquake occurrence probability (hereinafter referred to as the "maximum case").

Where the mean recurrence interval is evaluated only in one side of the range of values (XX years or more), the mean recurrence interval shall be "XX years" for both the "average case" and the "maximum case."

Where the time of the latest event is given only in one side of the range of values (year XX or later), the other end of the range is determined by considering the recent period over which definitely no event has occurred and the median value of the time of the latest event is determined ("average case").

Where there is a range of values in the mean recurrence interval since multiple fault segments have been presented, the fault segments which make the fault length the longest (which make the earthquake magnitude the greatest) are modeled, and the mean recurrence interval is determined to match that, in principle.

[3] Determination of the magnitude

As for the magnitude of an earthquake that occurs at an active fault, JMA magnitude M_j is calculated by the Matsuda formula (Matsuda, 1975) using the seismic source fault length based on the long-term evaluation results (ERC, 2005a, 2006a, 2007a, 2008a, 2009a). Then, after converting JMA magnitude M_j to seismic moment based on Takemura (1990), moment magnitude M_w is obtained, and that value is used, in principle. Where the magnitude has been indicated in a range of values, the median value of the range is used. Where there is a range of values in the magnitude since multiple fault segments have been presented, the magnitude is determined to match the determined fault segments.

[4] Determination of the fault plane parameters

The fault plane of each active fault is modeled either as single or multiple rectangular planes. The parameters defining a model are the location of the edges, the length, the width, the strike, the dip angle, and the depth of the upper edge of the fault. While the details of the modeling method are as described in Section 2.1, the brief outline of the procedure is as shown below.

i) Magnitude M_j is calculated based on Matsuda (1975) using fault length L that has been indicated in long-term evaluation.

ii) Seismic moment M_0 is calculated based on Takemura

(1990) using magnitude M_j.

iii) Fault area S is calculated based on Irikura and Miyake (2001) using seismic moment M_0.

iv) Fault width W is calculated by the formula $W=S/L$.

v) The depth of upper edge of the fault is determined by taking into account the depth of the seismic bedrock in the deep subsurface structure model used for strong motion evaluation, and the depth of the lower edge of the fault is determined by taking into consideration the depth of the deep end of the seismogenic layer based on the source depth distribution of microearthquakes.

vi) The dip angle uses the value obtained in long-term evaluation, if any, but if no value is available, it shall be 90 degrees for a dominant strike-slip component, 60 degrees for a reverse fault, 30 degrees for a low angle, and 60 degrees for a high angle, and if none of them applies, it shall be 45 degrees.

vii) The width and length are adjusted based on the positional relationship between the lower edge of the fault model and the lower edge of the seismogenic layer to derive the final shape.

However, faults are modeled separately in the case of a super-long fault of which the length exceeds roughly 80 km, the case where the active fault length is less than 15 km, and the case where the active fault length and the earthquake magnitude are unclear.

[5] Active segments

Basically, seismic activities are assumed to occur simultaneously at all segments of an active fault when an earthquake occurs. However, if multiple combinations of faults that cause earthquakes have been indicated for a single fault zone in the long-term evaluation results, the fault combination which is most likely to cause an earthquake is determined as the active segments.

(2) Active fault parameters of major active fault zones used for creating the PSHM

The major active fault zones used for creating PSHM are shown in Table 2.1-1 and Figure 2.1-1. The number of faults is 165. Table 2.1-2 shows the magnitudes and fault plane parameters of these faults. Table 3.3.1-1 shows the earthquake occurrence probability (within 30 years and 50 years from January 2009). Notes about individual active faults concerning the modeling of the earthquake occurrence probability and fault plane parameters are indicated at the end of each relevant table.

The left-hand column of Table 2.1-1 shows the fault names used when they were listed as active faults subject to fundamental surveys and observations. It should be noted that, at the time of publication of long-term evaluation results, different fault names are used in some cases, such as where the results for multiple active faults are published in a combined manner.

(3) Modeling of the Futagawa/Hinagu fault zone (central part/southwestern part)

In the long-term evaluation of the Futagawa/Hinagu fault zone (ERC, 2002a), two cases have been presented concerning the mean recurrence interval and the time of the latest event for evaluation of the central part/southwestern part of the fault zone, based on interpretation of the recurrence history. Thus, the hazard curve for the Futagawa/Hinagu fault zone (central part/southwestern part) is calculated as a weighted mean of the three cases shown in Table 3.3.1-2 which give consideration to those two cases. Table 3.3.1-3 shows the earthquake occurrence probability and the magnitude of each case. The sum of products with earthquakes other than the Futagawa/Hinagu fault zone (central part/southwestern part) is done not for the individual cases below, but by using a hazard curve obtained as a weighted mean.

Table 3.3.1-1 Occurrence probability of earthquakes in major active fault zones (part 1)

Code	Fault name		Long-term evaluation result (* indicates shape evaluation)	Occurrence probability average case	Occurrence probability maximum case
0101	Shibetsu fault zone *L*=52 km	Mean recurrence interval (Interval)	Unknown	17,000 years	17,000 years
		Latest event	Unknown	(Poisson process)	
		Occurrence probability within 30 years (30 years)	-	0.18%	0.18%
		Occurrence probability within 50 years (50 years)	-	0.29%	0.29%
0201	Tokachi-heiya fault zone (main part)	Interval	Around 17,000-22,000 years	19,500 years	17,000 years
		Latest event	Unknown	(Poisson process)	
		30 years	0.1%-0.2%	0.15%	0.18%
		50 years	0.2%-0.3%	0.26%	0.29%
0202	Kochien fault	Interval	About around 7,000-21,000 years	14,000 years	7,000 years
		Latest event	Cannot be specified	(Poisson process)	
		30 years	0.1%-0.4%	0.21%	0.43%
		50 years	0.2%-0.7%	0.36%	0.71%
0301	Furano fault zone (western part)	Interval	Around 4,000 years	4,000 years	4,000 years
		Latest event	2nd century-AD 1739	1,090 years ago	1,909 years ago
		30 years	Nearly 0%-0.03%	Nearly 0%	0.029%
		50 years	Nearly 0%-0.05%	Nearly 0%	0.052%
0302	Furano fault zone (eastern part)	Interval	Around 9,000-22,000 years	15,500 years	9,000 years
		Latest event	About 4,300-2,400 years ago	3,350 years ago	4,300 years ago
		30 years	Nearly 0%-0.01%	Nearly 0%	0.012%
		50 years	Nearly 0%-0.02%	Nearly 0%	0.021%
0401	Mashike-sanchi -toen fault zone	Interval	Around 5,000 years or more	5,000 years	5,000 years
		Latest event	Unknown	(Poisson process)	
		30 years	0.6% or less	0.60%	0.60%
		50 years	1% or less	1.0%	1.0%
0402	Numata-Sunagawa area fault zone *L*=38 km	Interval	Unknown	12,000 years	12,000 years
		Latest event	Unknown	(Poisson process)	
		30 years	—	0.25%	0.25%
		50 years	—	0.42%	0.42%
0501	Tobetsu fault	Interval	Around 7,500-15,000 years	11,250 years	7,500 years
		Latest event	About 11,000-2,200 years ago	6,600 years ago	11,000 years ago
		30 years	Nearly 0%-2%	0.082%	2.5%
		50 years	Nearly 0%-4%	0.14%	4.1%
0601	Ishikari-teichi-toen fault zone (main part)	Interval	About 3,300-6,300 years	4,800 years	3,300 years
		Latest event	About 5,200-3,300 years ago or later	4,250 years ago	5,200 years ago
		30 years	0.05%-6% or less	1.7%	5.8%
		50 years	0.09%-10% or less	2.8%	9.5%
0602	Ishikari-teichi-toen fault zone (southern part) *L*=23 km *s*=0.2 mm/y	Interval	Unknown	9,100 years	9,100 years
		Latest event	Unknown	(Poisson process)	
		30 years	—	0.33%	0.33%
		50 years	—	0.55%	0.55%
0701	Kuromatsunai -teichi fault zone	Interval	Around 3,600-5,000 years or more	4,300 years	3,600 years
		Latest event	5,900-4,900 years ago	5,400 years ago	5,900 years ago
		30 years	2%-5% or less	3.7%	5.5%
		50 years	3%-9% or less	6.0%	9.0%

Table 3.3.1-1 Occurrence probability of earthquakes in major active fault zones (part 2)

Code	Fault name		Long-term evaluation result (* indicates shape evaluation)	Occurrence probability average case	Occurrence probability maximum case
0801	Hakodate-heiya -seien fault zone	Mean recurrence interval (Interval)	13,000-17,000 years	15,000 years	13,000 years
		Latest event	14,000 years ago or later (-AD1611)	7,199 years ago	14,000 years ago
		Occurrence probability within 30 years (30 years)	Nearly 0%-1%	0.0077%	0.98%
		Occurrence probability within 50 years (50 years)	Nearly 0%-2%	0.013%	1.6%
0901	Aomori-wan-seigan fault zone	Interval	Around 3,000-6,000 years	4,500 years	3,000 years
		Latest event	Unknown	(Poisson process)	
		30 years	0.5%-1%	0.66%	1.0%
		50 years	0.8%-2%	1.1%	1.7%
1001	Tsugaru-sanchi -seien fault zone (northern part)	Interval	Unknown	—	—
		Latest event	Earthquake in AD 1766	—	—
		30 years	—	Nearly 0%	Nearly 0%
		50 years	—	Nearly 0%	Nearly 0%
1002	Tsugaru-sanchi -seien fault zone (southern part)	Interval	Unknown	—	—
		Latest event	Earthquake in AD 1766	—	—
		30 years	—	Nearly 0%	Nearly 0%
		50 years	—	Nearly 0%	Nearly 0%
1101	Oritsume fault *L*=47 km	Interval	Unknown	15,000 years	15,000 years
		Latest event	Unknown	(Poisson process)	
		30 years	—	0.20%	0.20%
		50 years	—	0.33%	0.33%
1201	Noshiro fault zone	Interval	Around 1,900-2,900 years	2,400 years	1,900 years
		Latest event	AD 1694 Noshiro Earthquake	315 years ago	315 years ago
		30 years	Nearly 0%	Nearly 0%	Nearly 0%
		50 years	Nearly 0%	Nearly 0%	Nearly 0%
1301	Kitakami-teichi -seien fault zone	Interval	16,000-26,000 years	21,000 years	16,000 years
		Latest event	Around 4,500 years ago	4,500 years ago	4,500 years ago
		30 years	Nearly 0%	Nearly 0%	Nearly 0%
		50 years	Nearly 0%	Nearly 0%	Nearly 0%
1401	Shizukuishi-bonchi -seien fault zone *L*=17 km	Interval	Unknown	5,400 years	5,400 years
		Latest event	2,800 years ago-14th century	(Poisson process)	
		30 years	—	0.55%	0.55%
		50 years	—	0.92%	0.92%
1402	Mahiru-sanchi-toen fault zone (northern part)	Interval	Around 6,300-31,000 years	18,650 years	6,300 years
		Latest event	AD 1896 Rikuu Earthquake	113 years ago	113 years ago
		30 years	Nearly 0%	Nearly 0%	Nearly 0%
		50 years	Nearly 0%	Nearly 0%	Nearly 0%
1403	Mahiru-sanchi-toen fault zone (southern part) *L*=17 km	Interval	Unknown	5,400 years	5,400 years
		Latest event	Unknown	(Poisson process)	
		30 years	—	0.55%	0.55%
		50 years	—	0.92%	0.92%
1501	Yokote-bonchi-toen fault zone (northern part)	Interval	Around 3,400 years	3,400 years	3,400 years
		Latest event	AD 1896 Rikuu Earthquake	113 years ago	113 years ago
		30 years	Nearly 0%	Nearly 0%	Nearly 0%
		50 years	Nearly 0%	Nearly 0%	Nearly 0%

Table 3.3.1-1 Occurrence probability of earthquakes in major active fault zones (Part 3)

Code	Fault name		Long-term evaluation result (* indicates shape evaluation)	Occurrence probability average case	Occurrence probability maximum case
1502	Yokote-bonchi-toen fault zone (southern part) *L*=30 km	Mean recurrence interval (Interval)	Unknown	9,500 years	9,500 years
		Latest event	About 6,000-5,000 years ago	(Poisson process)	
		Occurrence probability within 30 years (30 years)	—	0.32%	0.32%
		Occurrence probability within 50 years (50 years)	—	0.52%	0.52%
1601	Kitayuri fault	Interval	Around 3,400-4,000 years	3,700 years	3,400 years
		Latest event	About 2,800 years ago or later	1,400 years ago	2,800 years ago
		30 years	2% or less	Nearly 0%	1.9%
		50 years	3% or less	0.0019%	3.2%
1701	Shinjo-bonchi fault zone	Interval	Around 2,000-4,000 years	4,000 years	4,000 years
		Latest event	Unknown	(Poisson process)	
		30 years	0.7%-1%	0.75%	0.75%
		50 years	1%-2%	1.2%	1.2%
1801	Yamagata-bonchi fault zone (northern part)	Interval	Around 2,500-4,000 years	3,250 years	2,500 years
		Latest event	About 3,900-1,600 years ago (-1,609 years ago)	2,755 years ago	3,900 years ago
		30 years	0.002%-8%	2.2%	7.6%
		50 years	0.004%-10%	3.6%	12%
1802	Yamagata-bonchi fault zone (southern part)	Interval	Around 2,500 years	2,500 years	2,500 years
		Latest event	Unspecified	(Poisson process)	
		30 years	1%	1.2%	1.2%
		50 years	2%	2.0%	2.0%
1901	Shonai-heiya-toen fault zone	Interval	Around 2,400-4,600 years	3,500 years	2,400 years
		Latest event	3,000 years ago-the end of the 18th century	1,605 years ago	3,000 years ago
		30 years	Nearly 0%-6%	0.020%	6.5%
		50 years	Nearly 0%-10%	0.037%	11%
2001	Nagamachi-Rifu -sen fault zone	Interval	Around 3,000 years or more	5,000 years	5,000 years
		Latest event	Cannot be specified sufficiently	(Poisson process)	
		30 years	1% or less	0.60%	0.60%
		50 years	2% or less	1.0%	1.0%
2101	Fukushima-bonchi -seien fault zone	Interval	Around 8,000 years	8,000 years	8,000 years
		Latest event	About 2,200 years ago-3rd century	1,955 years ago	2,200 years ago
		30 years	Nearly 0%	Nearly 0%	Nearly 0%
		50 years	Nearly 0%	Nearly 0%	Nearly 0%
2201	Nagai-bonchi-seien fault zone	Interval	Around 5,000-6,300 years	5,650 years	5,000 years
		Latest event	About 2,400 years ago or later	1,200 years ago	2,400 years ago
		30 years	0.02% or less	Nearly 0%	0.024%
		50 years	0.04% or less	Nearly 0%	0.043%
2301	Futaba fault	Interval	Around 8,000-12,000 years	10,000 years	8,000 years
		Latest event	About 2,400 years ago-2nd century	2,105 years ago	2,400 years ago
		30 years	Nearly 0%	Nearly 0%	Nearly 0%
		50 years	Nearly 0%	Nearly 0%	Nearly 0%
2401	Aizu-bonchi-seien fault zone	Interval	About 7,400-9,700 years	8,550 years	7,400 years
		Latest event	AD 1611 Aizu Earthquake	398 years ago	398 years ago
		30 years	Nearly 0%	Nearly 0%	Nearly 0%
		50 years	Nearly 0%	Nearly 0%	Nearly 0%

Table 3.3.1-1 Occurrence probability of earthquakes in major active fault zones (part 4)

Code	Fault name		Long-term evaluation result (* indicates shape evaluation)	Occurrence probability average case	Occurrence probability maximum case
2402	Aizu-bonchi-toen fault zone	Mean recurrence interval (Interval)	About 6,300-9,300 years	7,800 years	6,300 years
		Latest event	About 3,000-2,600 years ago	2,800 years ago	3,000 years ago
		Occurrence probability within 30 years (30 years)	Nearly 0%-0.02%	Nearly 0%	0.017%
		Occurrence probability within 50 years (50 years)	Nearly 0%-0.03%	Nearly 0%	0.030%
2501	Kushigata -sanmyaku fault zone	Interval	2,800-4,200 years	3,500 years	2,800 years
		Latest event	About 3,200-2,600 years ago	2,900 years ago	3,200 years ago
		30 years	0.3%-5%	1.9%	4.9%
		50 years	0.6%-8%	3.1%	8.1%
2601	Tsukioka fault zone	Interval	7,500 years or more	7,500 years	7,500 years
		Latest event	About 6,500-900 years ago (-909 years ago)	3,705 years ago	6,500 years ago
		30 years	Nearly 0%-1%	0.022%	1.0%
		50 years	Nearly 0%-2%	0.039%	1.7%
2701	Nagaoka-heiya -seien fault zone	Interval	About 1,200-3,700 years	2,450 years	1,200 years
		Latest event	13th century or later	405 years ago	809 years ago
		30 years	2% or less	Nearly 0%	2.2%
		50 years	4% or less	Nearly 0%	4.0%
2901	Kamogawa-teichi fault zone *L*=25 km	Interval	Unknown	7,900 years	7,900 years
		Latest event	Unknown	(Poisson process)	
		30 years	—	0.38%	0.38%
		50 years	—	0.63%	0.63%
3001	Sekiya fault	Interval	About 2,600-4,100 years	3,350 years	2,600 years
		Latest event	14th-17th century	509 years ago	709 years ago
		30 years	Nearly 0%	Nearly 0%	Nearly 0%
		50 years	Nearly 0%	Nearly 0%	Nearly 0%
3101	Kanto-heiya -hokuseien fault zone (main part)	Interval	Around 13,000-30,000 years	21,500 years	13,000 years
		Latest event	About 6,200-2,500 years ago	4,350 years ago	6,200 years ago
		30 years	Nearly 0%-0.008%	Nearly 0%	0.0083%
		50 years	Nearly 0%-0.01%	Nearly 0%	0.014%
3102	Hirai-Kushibiki fault zone *L*=23 km	Interval	Unknown	7,000 years	7,000 years
		Latest event	Unknown	(Poisson process)	
		30 years	—	0.43%	0.43%
		50 years	—	0.71%	0.71%
3401	Tachikawa fault zone	Interval	Around 10,000-15,000 years	12,500 years	10,000 years
		Latest event	About 20,000-13,000 years ago	16,500 years ago	20,000 years ago
		30 years	0.5%-2%	1.3%	2.2%
		50 years	0.8%-4%	2.2%	3.7%
3501	Isehara fault	Interval	Around 4,000-6,000 years	5,000 years	4,000 years
		Latest event	5th century-the early 18th century	959 years ago	1,609 years ago
		30 years	Nearly 0%-0.003%	Nearly 0%	0.0026%
		50 years	Nearly 0%-0.005%	Nearly 0%	0.0047%
3601	Kannawa/Kozu -Matsuda fault zone	Interval	About 800-1,300 years	1,050 years	800 years
		Latest event	12th century-the first half of the 14th century (AD 1350)	784 years ago	909 years ago
		30 years	0.2%-16%	4.3%	16%
		50 years	0.4%-30%	7.4%	26%

Table 3.3.1-1 Occurrence probability of earthquakes in major active fault zones (part 5)

Code	Fault name		Long-term evaluation result (* indicates shape evaluation)	Occurrence probability average case	Occurrence probability maximum case
3701	Miura-hanto fault group (Kinugasa/Kitatake fault zone of the main part)	Mean recurrence interval (Interval)	Around 1,900-4,900 years	3,400 years	1,900 years
		Latest event	6th-7th century	1,409 years ago	1,509 years ago
		Occurrence probability within 30 years (30 years)	Nearly 0%-3%	0.0050%	3.0%
		Occurrence probability within 50 years (50 years)	Nearly 0%-5%	0.0093%	5.0%
3702	Miura-hanto fault group (Takeyama fault zone of the main part)	Interval	Around 1,600-1,900 years	1,750 years	1,600 years
		Latest event	About 2,300-1,900 years ago (-1,909 years ago)	2,105 years ago	2,300 years ago
		30 years	6%-11%	8.4%	11%
		50 years	10%-20%	14%	18%
3703	Miura-hanto fault group (southern part) *L*=20 km *S*=1.0 mm/y	Interval	Unknown	1,600 years	1,600 years
		Latest event	About 26,000-22,000 years ago	(Poisson process)	
		30 years	—	1.9%	1.9%
		50 years	—	3.1%	3.1%
3801	Kitaizu fault zone	Interval	About 1,400-1,500 years	1,450 years	1,400 years
		Latest event	AD 1930 Kitaizu Earthquake	79 years ago	79 years ago
		30 years	Nearly 0%	Nearly 0%	Nearly 0%
		50 years	Nearly 0%	Nearly 0%	Nearly 0%
3901	Tokamachi fault zone (western part)	Interval	Around 2,000-3,000 years	2,500 years	2,000 years
		Latest event	Unknown	(Poisson process)	
		30 years	1%	1.2%	1.5%
		50 years	2%	2.0%	2.5%
3902	Tokamachi fault zone (eastern part)	Interval	Around 4,000-8,000 years	6,000 years	4,000 years
		Latest event	Unknown	(Poisson process)	
		30 years	0.4%-0.7%	0.50%	0.75%
		50 years	0.6%-1%	0.83%	1.2%
4001	Nagano-bonchi -seien fault zone	Interval	800-2,500 years	1,650 years	800 years
		Latest event	AD 1847 Zenkoji Earthquake	162 years ago	162 years ago
		30 years	Nearly 0%	Nearly 0%	Nearly 0%
		50 years	Nearly 0%	Nearly 0%	Nearly 0%
4101	Itoigawa-Shizuoka -kozosen fault zone (central part/northern part)	Interval	About 1,000 years	1,000 years	1,000 years
		Latest event	About 1,200 years ago (about 1,209 years ago)	1,209 years ago	1,209 years ago
		30 years	14%	14%	14%
		50 years	20%	23%	23%
4201	Itoigawa-Shizuoka -kozosen fault zone (southern part) *L*=31 km *s*=2 mm/y	Interval	Unknown	1,200 years	1,200 years
		Latest event	Unknown	(Poisson process)	
		30 years	—	2.5%	2.5%
		50 years	—	4.1%	4.1%
4301	Fujikawa-kako fault zone	Interval	1,500-1,900 years	1,700 years	1,500 years
		Latest event	About 2,100-1,000 years ago (-1,009 years ago)	1,555 years ago	2,100 years ago
		30 years	0.2%-11%	5.2%	11%
		50 years	0.4%-20%	8.7%	18%

Table 3.3.1-1 Occurrence probability of earthquakes in major active fault zones (part 6)

Code	Fault name		Long-term evaluation result (* indicates shape evaluation)	Occurrence probability average case	Occurrence probability maximum case
4501	Kiso-sanmyaku -seien fault zone (northern segment of the main part)	Mean recurrence interval (Interval)	About 6,400-9,100 years	7,750 years	6,400 years
		Latest event	Around the 13th century	759 years ago	809 years ago
		Occurrence probability within 30 years (30 years)	Nearly 0%	Nearly 0%	Nearly 0%
		Occurrence probability within 50 years (50 years)	Nearly 0%	Nearly 0%	Nearly 0%
4502	Kiso-sanmyaku -seien fault zone (southern segment of the main part)	Interval	About 4,500-24,000 years	14,250 years	4,500 years
		Latest event	About 6,500-3,800 years ago	5,150 years ago	6,500 years ago
		30 years	Nearly 0%-4%	Nearly 0%	4.0%
		50 years	Nearly 0%-7%	Nearly 0%	6.6%
4503	Seinaiji-toge fault zone *L*=34 km	Interval	Unknown	11,000 years	11,000 years
		Latest event	Unknown	(Poisson process)	
		30 years	—	0.27%	0.27%
		50 years	—	0.45%	0.45%
4601	Sakaitoge/Kamiya fault zone (main part)	Interval	About 1,800-5,200 years	3,500 years	1,800 years
		Latest event	About 4,900-2,500 years ago	3,700 years ago	4,900 years ago
		30 years	0.02%-13%	3.5%	13%
		50 years	0.04%-20%	5.8%	20%
4602	Mutoyama-Narai fault zone *L*=28 km Class AB	Interval	Unknown	2,200 years	2,200 years
		Latest event	Unknown	(Poisson process)	
		30 years	—	1.4%	1.4%
		50 years	—	2.2%	2.2%
4701	Atotsugawa fault zone	Interval	About 2,300-2,700 years	2,500 years	2,300 years
		Latest event	AD 1858 Hietsu Earthquake	151 years ago	151 years ago
		30 years	Nearly 0%	Nearly 0%	Nearly 0%
		50 years	Nearly 0%	Nearly 0%	Nearly 0%
4801	Takayama/Oppara fault zone Kokufu fault zone	Interval	About 3,600-4,300 years	3,950 years	3,600 years
		Latest event	About 4,700-300 years ago (-309 years ago)	2,505 years ago	4,700 years ago
		30 years	Nearly 0%-5%	0.43%	4.6%
		50 years	Nearly 0%-7%	0.74%	7.5%
4802	Takayama/Oppara fault zone Takayama fault zone	Interval	Around 4,000 years	4,000 years	4,000 years
		Latest event	Unknown	(Poisson process)	
		30 years	0.7%	0.75%	0.75%
		50 years	1%	1.2%	1.2%
4803	Takayama/Oppara fault zone Inohana fault zone *L*=24 km	Interval	Unknown	7,600 years	7,600 years
		Latest event	Unknown	(Poisson process)	
		30 years	—	0.39%	0.39%
		50 years	—	0.66%	0.66%
4901	Ushikubi fault zone	Interval	About 5,000-7,100 years	6,050 years	5,000 years
		Latest event	11th-12th century	909 years ago	1,009 years ago
		30 years	Nearly 0%	Nearly 0%	Nearly 0%
		50 years	Nearly 0%	Nearly 0%	Nearly 0%
5001	Shokawa fault zone	Interval	About 3,600-6,900 years	5,250 years	3,600 years
		Latest event	11th-16th century	709 years ago	1,009 years ago
		30 years	Nearly 0%	Nearly 0%	Nearly 0%
		50 years	Nearly 0%	Nearly 0%	Nearly 0%

Table 3.3.1-1 Occurrence probability of earthquakes in major active fault zones (part 7)

Code	Fault name		Long-term evaluation result (* indicates shape evaluation)	Occurrence probability average case	Occurrence probability maximum case
5101	Inadani fault zone (main part)	Mean recurrence interval (Interval)	Around 5,200-6,400 years	5,800 years	5,200 years
		Latest event	14th-18th century	459 years ago	709 years ago
		Occurrence probability within 30 years (30 years)	Nearly 0%	Nearly 0%	Nearly 0%
		Occurrence probability within 50 years (50 years)	Nearly 0%	Nearly 0%	Nearly 0%
5102	Inadani fault zone (southeastern part) *L*=32 km Class BC	Interval	Unknown	25,000 years	25,000 years
		Latest event	Unknown	(Poisson process)	
		30 years	—	0.12%	0.12%
		50 years	—	0.20%	0.20%
5201	Atera fault zone (northern segment of the main part)	Interval	About 1,800-2,500 years	2,150 years	1,800 years
		Latest event	About 3,400-3,000 years ago	3,200 years ago	3,400 years ago
		30 years	6%-11%	8.4%	11%
		50 years	10%-20%	14%	18%
5202	Atera fault zone (southern segment of the main part)	Interval	About 1,700 years	1,700 years	1,700 years
		Latest event	AD 1586 Tensho Earthquake	423 years ago	423 years ago
		30 years	Nearly 0%	Nearly 0%	Nearly 0%
		50 years	Nearly 0%	Nearly 0%	Nearly 0%
5203	Atera fault zone Sami fault zone *L*=25 km	Interval	Unknown	7,900 years	7,900 years
		Latest event	Unknown	(Poisson process)	
		30 years	—	0.38%	0.38%
		50 years	—	0.63%	0.63%
5204	Atera fault zone Shirakawa fault zone *L*=31 km	Interval	Unknown	9,800 years	9,800 years
		Latest event	Unknown	(Poisson process)	
		30 years	—	0.31%	0.31%
		50 years	—	0.51%	0.51%
5301	Byobuyama/Enasan fault zone and Sanageyama fault zone Byobuyama fault zone	Interval	Around 4,000-12,000 years	8,000 years	4,000 years
		Latest event	Unknown	(Poisson process)	
		30 years	0.2%-0.7%	0.37%	0.75%
		50 years	0.4%-1%	0.62%	1.2%
5302	Ako fault zone *L*=23 km	Interval	Unknown	7,300 years	7,300 years
		Latest event	Unknown	(Poisson process)	
		30 years	—	0.41%	0.41%
		50 years	—	0.68%	0.68%
5303	Enasan -Sanageyama-kita fault zone	Interval	About around 7,200-14,000 years	10,600 years	7,200 years
		Latest event	About 7,600-5,400 years ago	6,500 years ago	7,600 years ago
		30 years	Nearly 0%-2%	0.12%	1.7%
		50 years	Nearly 0%-3%	0.21%	2.8%
5304	Sanage-Takahama fault zone	Interval	Around 40,000 years	40,000 years	40,000 years
		Latest event	About around 14,000 years ago	14,000 years ago	14,000 years ago
		30 years	Nearly 0%	Nearly 0%	Nearly 0%
		50 years	Nearly 0%	Nearly 0%	Nearly 0%
5305	Kagiya fault zone	Interval	Around 30,000 years	30,000 years	30,000 years
		Latest event	Unknown	(Poisson process)	
		30 years	0.1%	0.10%	0.10%
		50 years	0.2%	0.17%	0.17%

Table 3.3.1-1 Occurrence probability of earthquakes in major active fault zones (Part 8)

Code	Fault name		Long-term evaluation result (* indicates shape evaluation)	Occurrence probability average case	Occurrence probability maximum case
5501	Ochigata fault zone	Mean recurrence interval (Interval)	Around 1,200-1,900 years	1,550 years	1,200 years
		Latest event	(About 3,200 years ago-9th century)	(Poisson process)	
		Occurrence probability within 30 years (30 years)	2%	1.9%	2.5%
		Occurrence probability within 50 years (50 years)	3%-4%	3.2%	4.1%
5601	Tonami-heiya fault zone (western part)	Interval	About 6,000-12,000 years or less	9,000 years	6,000 years
		Latest event	About 6,900 years ago-1st century	4,405 years ago	6,900 years ago
		30 years	Nearly 0%-2% or more	0.017%	2.3%
		50 years	Nearly 0%-4% or more	0.028%	3.9%
5602	Tonami-heiya fault zone (eastern part)	Interval	Around 3,000-7,000 years	5,000 years	3,000 years
		Latest event	About 4,300-3,600 years ago	3,950 years ago	4,300 years ago
		30 years	0.04%-6%	1.1%	5.9%
		50 years	0.06%-10%	1.8%	9.7%
5603	Kurehayama fault zone	Interval	Around 3,000-5,000 years	4,000 years	3,000 years
		Latest event	About 3,500 years ago-7th century	2,405 years ago	3,500 years ago
		30 years	Nearly 0%-5%	0.29%	4.8%
		50 years	Nearly 0%-8%	0.50%	7.8%
5701	Morimoto/Togashi fault zone	Interval	About 2,000 years	2,000 years	2,000 years
		Latest event	About 2,000-200 years ago (about 2,009-209 years ago)	1,109 years ago	2,009 years ago
		30 years	Nearly 0%-5%	0.31%	5.5%
		50 years	Nearly 0%-9%	0.56%	9.1%
5801	Fukui-heiya-toen fault zone (main part)	Interval	Around 7,000-18,000 years or less	12,500 years	7,000 years
		Latest event	Unknown	(Poisson process)	
		30 years	0.2%-0.4% or more	0.24%	0.43%
		50 years	0.3%-0.7% or more	0.40%	0.71%
5802	Fukui-heiya-toen fault zone (western part)	Interval	Unknown	—	—
		Latest event	AD 1948 Fukui Earthquake	—	—
		30 years	—	Nearly 0%	Nearly 0%
		50 years	—	Nearly 0%	Nearly 0%
5901	Nagaragawa-joryu fault zone *L*=29 km	Interval	Unknown	9,200 years	9,200 years
		Latest event	Unknown	(Poisson process)	
		30 years	—	0.33%	0.33%
		50 years	—	0.54%	0.54%
6001	Nukumi fault (northwestern part)	Interval	About 2,200-2,400 years	2,300 years	2,200 years
		Latest event	AD 1891 Nobi Earthquake	118 years ago	118 years ago
		30 years	Nearly 0%	Nearly 0%	Nearly 0%
		50 years	Nearly 0%	Nearly 0%	Nearly 0%
6002	Nukumi fault (southeastern part) *L*=21 km Class AB	Interval	Unknown	1,700 years	1,700 years
		Latest event	Unknown	(Poisson process)	
		30 years	—	1.7%	1.7%
		50 years	—	2.9%	2.9%
6003	Nobi fault zone (Neodani fault zone of the main part)	Interval	About 2,100-3,600 years	2,850 years	2,100 years
		Latest event	AD 1891 Nobi Earthquake	118 years ago	118 years ago
		30 years	Nearly 0%	Nearly 0%	Nearly 0%
		50 years	Nearly 0%	Nearly 0%	Nearly 0%

Table 3.3.1-1 Occurrence probability of earthquakes in major active fault zones (part 9)

Code	Fault name		Long-term evaluation result (* indicates shape evaluation)	Occurrence probability average case	Occurrence probability maximum case
6004	Nobi fault zone (Umehara fault zone of the main part)	Mean recurrence interval (Interval)	About 14,000-15,000 years	14,500 years	14,000 years
		Latest event	AD 1891 Nobi Earthquake	118 years ago	118 years ago
		Occurrence probability within 30 years (30 years)	Nearly 0%	Nearly 0%	Nearly 0%
		Occurrence probability within 50 years (50 years)	Nearly 0%	Nearly 0%	Nearly 0%
6005	Nobi fault zone (Mitabora fault zone of the main part) *L*=19 km, Class BC	Interval	Unknown	15,000 years	15,000 years
		Latest event	Unknown	(Poisson process)	
		30 years	—	0.20%	0.20%
		50 years	—	0.33%	0.33%
6006	Ibigawa fault zone *L*=24 km	Interval	Unknown	7,600 years	7,600 years
		Latest event	1st-10th century	(Poisson process)	
		30 years	—	0.39%	0.39%
		50 years	—	0.66%	0.66%
6007	Mugigawa fault *L*=29 km	Interval	Unknown	9,200 years	9,200 years
		Latest event	Unknown	(Poisson process)	
		30 years	—	0.33%	0.33%
		50 years	—	0.54%	0.54%
6101	Yanagase/Sekigahara fault zone (northern segment of the main part)	Interval	About 2,300-2,700 years	2,500 years	2,300 years
		Latest event	Around the 17th century	359 years ago	409 years ago
		30 years	Nearly 0%	Nearly 0%	Nearly 0%
		50 years	Nearly 0%	Nearly 0%	Nearly 0%
6102	Yanagase/Sekigahara fault zone (central segment of the main part) *L*=12 km	Interval	Unknown	3,800 years	3,800 years
		Latest event	About 7,200-7,000 years ago	(Poisson process)	
		30 years	—	0.79%	0.79%
		50 years	—	1.3%	1.3%
6103	Yanagase/Sekigahara fault zone (southern segment of the main part) *L*=45 km	Interval	Unknown	14,000 years	14,000 years
		Latest event	About 4,900 years ago-15th century	(Poisson process)	
		30 years	—	0.21%	0.21%
		50 years	—	0.36%	0.36%
6104	Urazoko-Yanagaseyama fault zone *L*=25 km, Class BC	Interval	Unknown	20,000 years	20,000 years
		Latest event	Unknown	(Poisson process)	
		30 years	—	0.15%	0.15%
		50 years	—	0.25%	0.25%
6301	Nosaka fault zone	Interval	About 5,600-7,600 years or less	6,600 years	5,600 years
		Latest event	15th-17th century	459 years ago	609 years ago
		30 years	Nearly 0% or more	Nearly 0%	Nearly 0%
		50 years	Nearly 0% or more	Nearly 0%	Nearly 0%
6302	Shufukuji fault *L*=10 km	Interval	Excluded from detailed evaluation	3,200 years	3,200 years
		Latest event		(Poisson process)	
		30 years	—	0.93%	0.93%
		50 years	—	1.6%	1.6%
6401	Kohoku-sanchi fault zone (northwestern part)	Interval	About 3,000-4,000 years	3,500 years	3,000 years
		Latest event	11th-14th century	809 years ago	1,009 years ago
		30 years	Nearly 0%	Nearly 0%	Nearly 0%
		50 years	Nearly 0%	Nearly 0%	Nearly 0%

Table 3.3.1-1 Occurrence probability of earthquakes in major active fault zones (part 10)

Code	Fault name		Long-term evaluation result (* indicates shape evaluation)	Occurrence probability average case	Occurrence probability maximum case
6402	Kohoku-sanchi fault zone (southeastern part)	Mean recurrence interval (Interval)	Roughly around 7,000 years	7,000 years	7,000 years
		Latest event	15th-17th century	459 years ago	609 years ago
		Occurrence probability within 30 years (30 years)	Nearly 0%	Nearly 0%	Nearly 0%
		Occurrence probability within 50 years (50 years)	Nearly 0%	Nearly 0%	Nearly 0%
6501	Biwako-seigan fault zone	Interval	About 1,900-4,500 years	3,200 years	1,900 years
		Latest event	About 2,800-2,400 years ago	2,600 years ago	2,800 years ago
		30 years	0.09%-9%	1.9%	9.4%
		50 years	0.2%-20%	3.2%	15%
6701	Yoro-Kuwana -Yokkaichi fault zone	Interval	1,400-1,900 years	1,650 years	1,400 years
		Latest event	13th-16th century	609 years ago	809 years ago
		30 years	Nearly 0%-0.7%	0.0019%	0.66%
		50 years	Nearly 0%-1%	0.0043%	1.2%
6801	Suzuka-toen fault zone	Interval	6,500-12,000 years	9,250 years	6,500 years
		Latest event	About 3,500-2,800 years ago	3,150 years ago	3,500 years ago
		30 years	Nearly 0%-0.07%	Nearly 0%	0.066%
		50 years	Nearly 0%-0.1%	Nearly 0%	0.11%
6901	Suzuka-seien fault zone	Interval	About 18,000-36,000 years	27,000 years	18,000 years
		Latest event	Unknown	(Poisson process)	
		30 years	0.08%-0.2%	0.11%	0.17%
		50 years	0.1%-0.3%	0.19%	0.28%
7001	Tongu fault	Interval	About 10,000 years or more	10,000 years	10,000 years
		Latest event	About 10,000 years ago-7th century	5,655 years ago	10,000 years ago
		30 years	1% or less	0.067%	1.1%
		50 years	2% or less	0.11%	1.8%
7101	Nunobiki-sanchi -toen fault zone (western part)	Interval	Around 17,000 years	17,000 years	17,000 years
		Latest event	About 28,000-400 years ago (-409 years ago)	14,205 years ago	28,000 years ago
		30 years	Nearly 0%-1%	0.39%	1.2%
		50 years	Nearly 0%-2%	0.66%	2.0%
7102	Nunobiki-sanchi -toen fault zone (eastern part)	Interval	Around 25,000 years	25,000 years	25,000 years
		Latest event	Around 11,000 years ago	11,000 years ago	11,000 years ago
		30 years	0.001%	0.0014%	0.0014%
		50 years	0.002%	0.0024%	0.0024%
7201	Kizugawa fault zone	Interval	About 4,000-25,000 years	14,500 years	4,000 years
		Latest event	AD 1854 Iga-Ueno Earthquake	155 years ago	155 years ago
		30 years	Nearly 0%	Nearly 0%	Nearly 0%
		50 years	Nearly 0%	Nearly 0%	Nearly 0%
7301	Mikata fault zone	Interval	About 3,800-6,300 years	5,050 years	3,800 years
		Latest event	Earthquake in AD 1662	347 years ago	347 years ago
		30 years	Nearly 0%	Nearly 0%	Nearly 0%
		50 years	Nearly 0%	Nearly 0%	Nearly 0%
7302	Hanaore fault zone (northern part)	Interval	Unknown	—	—
		Latest event	Earthquake in AD 1662 (15th-17th century)	—	—
		30 years	—	Nearly 0%	Nearly 0%
		50 years	—	Nearly 0%	Nearly 0%

Table 3.3.1-1 Occurrence probability of earthquakes in major active fault zones (part 10)

Code	Fault name		Long-term evaluation result (* indicates shape evaluation)	Occurrence probability average case	Occurrence probability maximum case
7303	Hanaore fault zone (central-southern part)	Mean recurrence interval (Interval)	4,200-6,500 years	5,350 years	4,200 years
		Latest event	2,800 yeasr ago-6th century	2,105 years ago	2,800 years ago
		Occurrence probability within 30 years (30 years)	Nearly 0%-0.6%	0.0013%	0.56%
		Occurrence probability within 50 years (50 years)	Nearly 0%-1%	0.0023%	0.95%
7401	Yamada fault zone (main part) *L*=33 km	Interval	Unknown	10,000 years	10,000 years
		Latest event	3,300 years ago or earlier	(Poisson process)	
		30 years	—	0.30%	0.30%
		50 years	—	0.50%	0.50%
7402	Gomura fault zone	Interval	Around 10,000-15,000 years	12,500 years	10,000 years
		Latest event	AD 1927 Kitatango Earthquake	82 years ago	82 years ago
		30 years	Nearly 0%	Nearly 0%	Nearly 0%
		50 years	Nearly 0%	Nearly 0%	Nearly 0%
7501	Nara-bonchi-toen fault zone	Interval	About 5,000 years	5,000 years	5,000 years
		Latest event	About 11,000-1,200 years ago (-1,209 years ago)	6,105 years ago	11,000 years ago
		30 years	Nearly 0%-5%	3.1%	4.5%
		50 years	Nearly 0%-7%	5.0%	7.4%
7601	Arima-Takatsuki fault zone	Interval	1,000-2,000 years	1,500 years	1,000 years
		Latest event	AD 1596 Keicho-Fushimi Earthquake	413 years ago	413 years ago
		30 years	Nearly 0%-0.02%	Nearly 0%	0.024%
		50 years	Nearly 0%-0.06%	Nearly 0%	0.060%
7701	Ikoma fault zone	Interval	3,000-6,000 years	4,500 years	3,000 years
		Latest event	Around 1,600-1,000 years ago (1,609-1,009 years ago)	1,309 years ago	1,609 years ago
		30 years	Nearly 0%-0.1%	Nearly 0%	0.14%
		50 years	Nearly 0%-0.3%	Nearly 0%	0.26%
7801	Kanbayashigawa fault *L*=26 km	Interval	Unknown	8,300 years	8,300 years
		Latest event	Unknown	(Poisson process)	
		30 years	—	0.36%	0.36%
		50 years	—	0.60%	0.60%
7802	Mitoke fault	Interval	Around 5,000-7,000 years	6,000 years	5,000 years
		Latest event	3rd century or earlier (Cannot be specified sufficiently)	(Poisson process)	
		30 years	0.4%-0.6%	0.50%	0.60%
		50 years	0.7%-1%	0.83%	1.0%
7803	Kyoto-Nishiyama fault zone	Interval	About 3,500-5,600 years	4,550 years	3,500 years
		Latest event	About 2,400 years ago-2nd century	2,105 years ago	2,400 years ago
		30 years	Nearly 0%-0.8%	0.017%	0.80%
		50 years	Nearly 0%-1%	0.030%	1.4%
7901	Rokko/Awajishima fault zone (Rokko-sanchi -nan'en-Awajishima -togan segment of the main part)	Interval	Around 900-2,800 years	1,850 years	900 years
		Latest event	16th century	459 years ago	509 years ago
		30 years	Nearly 0%-0.9%	Nearly 0%	0.94%
		50 years	Nearly 0%-2%	Nearly 0%	1.8%

Table 3.3.1-1 Occurrence probability of earthquakes in major active fault zones (part 11)

Code	Fault name		Long-term evaluation result (* indicates shape evaluation)	Occurrence probability average case	Occurrence probability maximum case
7902	Rokko/Awajishima fault zone (Awajishima-seigan segment of the main part)	Mean recurrence interval (Interval)	Around 1,800-2,500 years	2,150 years	1,800 years
		Latest event	AD 1995 Hyogo-ken Nanbu (Kobe) Earthquake	14 years ago	14 years ago
		Occurrence probability within 30 years (30 years)	Nearly 0%	Nearly 0%	Nearly 0%
		Occurrence probability within 50 years (50 years)	Nearly 0%	Nearly 0%	Nearly 0%
7903	Senzan fault zone	Interval	Around 5,000-10,000 years	7,500 years	5,000 years
		Latest event	11th century-the early 17th century	709 years ago	1,009 years ago
		30 years	Nearly 0%	Nearly 0%	Nearly 0%
		50 years	Nearly 0%	Nearly 0%	Nearly 0%
8001	Uemachi fault zone	Interval	Around 8,000 years	8,000 years	8,000 years
		Latest event	About 28,000-9,000 years ago	18,500 years ago	28,000 years ago
		30 years	2%-3%	2.9%	3.1%
		50 years	3%-5%	4.8%	5.1%
8101	Chuo-kozosen fault zone (Kongo-sanchi-toen -Izumi-sanmyaku -nan'en)	Interval	About 2,000-12,000 years	7,000 years	2,000 years
		Latest event	1st-4th century	1,809 years ago	2,009 years ago
		30 years	Nearly 0%-5%	Nearly 0%	5.5%
		50 years	Nearly 0%-9%	Nearly 0%	9.1%
8102	Chuo-kozosen fault zone (Kitan-kaikyo -Naruto-kaikyo)	Interval	About 4,000-6,000 years	5,000 years	4,000 years
		Latest event	About 3,100-2,600 years ago	2,850 years ago	3,100 years ago
		30 years	0.005%-1%	0.15%	1.3%
		50 years	0.009%-2%	0.25%	2.1%
8103	Chuo-kozosen fault zone (S-I part)	Interval	About 1,000-1,600 years	1,300 years	1,000 years
		Latest event	16th century	459 years ago	509 years ago
		30 years	Nearly 0%-0.3%	0.0012%	0.31%
		50 years	Nearly 0%-0.6%	0.0033%	0.64%
8104	Chuo-kozosen fault zone (Ishizuchi -sanmyaku-hokuen)	Interval	About 1,000-2,500 years	1,750 years	1,000 years
		Latest event	16th century	459 years ago	509 years ago
		30 years	Nearly 0%-0.3%	Nearly 0%	0.31%
		50 years	Nearly 0%-0.6%	Nearly 0%	0.64%
8105	Chuo-kozosen fault zone (I-I part)	Interval	About 1,000-2,900 years	1,950 years	1,000 years
		Latest event	16th century	459 years ago	509 years ago
		30 years	Nearly 0%-0.3%	Nearly 0%	0.31%
		50 years	Nearly 0%-0.6%	Nearly 0%	0.64%
8201	Nagisen fault zone	Interval	About 30,000-40,000 years	35,000 years	30,000 years
		Latest event	Unknown	(Poisson process)	
		30 years	0.07%-0.1%	0.086%	0.10%
		50 years	0.1%-0.2%	0.14%	0.17%
8202	Yamasaki fault zone (northwestern segment of the main part)	Interval	About 1,800-2,300 years	2,050 years	1,800 years
		Latest event	AD 868 Harimanokuni Earthquake	1,141 years ago	1,141 years ago
		30 years	0.09%-1%	0.31%	0.99%
		50 years	0.2%-2%	0.56%	1.7%
8203	Yamasaki fault zone (southeastern segment of the main part)	Interval	Around 3,000 years	3,000 years	3,000 years
		Latest event	About 3,600 years ago-6th century	2,505 years ago	3,600 years ago
		30 years	0.03%-5%	2.2%	4.9%
		50 years	0.06%-8%	3.8%	8.1%

Table 3.3.1-1 Occurrence probability of earthquakes in major active fault zones (part 12)

Code	Fault name		Long-term evaluation result (* indicates shape evaluation)	Occurrence probability average case	Occurrence probability maximum case
8204	Kusatani fault	Mean recurrence interval (Interval)	Around 5,000 years	5,000 years	5,000 years
		Latest event	5th-12th century	1,209 years ago	1,609 years ago
		Occurrence probability within 30 years (30 years)	Nearly 0%	Nearly 0%	Nearly 0%
		Occurrence probability within 50 years (50 years)	Nearly 0%	Nearly 0%	Nearly 0%
8401	Nagao fault zone	Interval	Roughly around 30,000 years	30,000 years	30,000 years
		Latest event	9th-16th century	809 years ago	1,209 years ago
		30 years	Nearly 0%	Nearly 0%	Nearly 0%
		50 years	Nearly 0%	Nearly 0%	Nearly 0%
8701	Itsukaichi fault *L*=20 km	Interval	Unknown	6,400 years	6,400 years
		Latest event	7th-12th century	(Poisson process)	
		30 years	—	0.47%	0.47%
		50 years	—	0.78%	0.78%
8702	Koi-Hiroshima-seien fault zone *L*=10 km, Class BC	Interval	Unknown	7,900 years	7,900 years
		Latest event	About 23,000 years ago or earlier	(Poisson process)	
		30 years	—	0.38%	0.38%
		50 years	—	0.63%	0.63%
8801	Iwakuni fault zone	Interval	About 9,000-18,000 years	13,500 years	9,000 years
		Latest event	About 11,000-10,000 years ago	10,500 years ago	11,000 years ago
		30 years	0.03%-2%	0.38%	1.7%
		50 years	0.05%-3%	0.63%	2.8%
9001	Kikukawa fault zone *L*=44 km	Interval	Unknown	14,000 years	14,000 years
		Latest event	About 8,500-2,100 years ago	(Poisson process)	
		30 years	—	0.21%	0.21%
		50 years	—	0.36%	0.36%
9101	Nishiyama fault zone *L*=31 km	Interval	Unknown	9,800 years	9,800 years
		Latest event	About 12,000-roughly 2,000 years ago (-2,009 years ago)	(Poisson process)	
		30 years	—	0.31%	0.31%
		50 years	—	0.51%	0.51%
9201	Beppu-wan-Hijiu fault zone (eastern part)	Interval	About 1,300-1,700 years	1,500 years	1,300 years
		Latest event	AD 1596 Keicho-Bungo Earthquake	413 years ago	413 years ago
		30 years	Nearly 0%	Nearly 0%	Nearly 0%
		50 years	Nearly 0%	Nearly 0%	Nearly 0%
9202	Beppu-wan-Hijiu fault zone (western part)	Interval	Around 13,000-25,000 years	19,000 years	13,000 years
		Latest event	About 7,300 years ago-6th century	4,355 years ago	7,300 years ago
		30 years	Nearly 0%-0.05%	Nearly 0%	0.048%
		50 years	Nearly 0%-0.08%	Nearly 0%	0.081%
9203	Oita-heiya-Yufuin fault zone (eastern part)	Interval	About 2,300-3,000 years	2,650 years	2,300 years
		Latest event	About 2,200 years ago-6th century	1,805 years ago	2,200 years ago
		30 years	0.03%-4%	1.0%	4.3%
		50 years	0.06%-7%	1.8%	7.1%
9204	Oita-heiya-Yufuin fault zone (western part)	Interval	About 700-1,700 years	1,200 years	700 years
		Latest event	Unknown (Two events between about 2,000 years ago-the early 18th century)	(Poisson process)	
		30 years	2%-4%	2.5%	4.2%
		50 years	3%-7%	4.1%	6.9%

Table 3.3.1-1 Occurrence probability of earthquakes in major active fault zones (part 13)

Code	Fault name		Long-term evaluation result (* indicates shape evaluation)	Occurrence probability average case	Occurrence probability maximum case
9205	Noinedake -Haneyama fault zone	Mean recurrence interval (Interval)	Around 4,000 years	4,000 years	4,000 years
		Latest event	About 3,900 years ago-6th century	2,655 years ago	3,900 years ago
		Occurrence probability within 30 years (30 years)	Nearly 0%-3%	0.57%	2.6%
		Occurrence probability within 50 years (50 years)	Nearly 0%-4%	0.98%	4.3%
9206	Kuenohirayama -Kameishiyama fault zone	Interval	About 4,300-7,300 years	5,800 years	4,300 years
		Latest event	13th century or later	405 years ago	809 years ago
		30 years	Nearly 0%	Nearly 0%	Nearly 0%
		50 years	Nearly 0%	Nearly 0%	Nearly 0%
9301	Futagawa/Hinagu fault zone (northeastern part)	Interval	About 11,000-27,000 years	19,000 years	11,000 years
		Latest event	About 1,500-1,200 years ago (about 1,509-1,209 years ago)	1,359 years ago	1,509 years ago
		30 years	Nearly 0%	Nearly 0%	Nearly 0%
		50 years	Nearly 0%	Nearly 0%	Nearly 0%
9302	Futagawa/Hinagu fault zone (central part) (Case 1)	Interval	About 3,500-11,000 years	7,250 years	3,500 years
		Latest event	About 7,500-2,200 years ago	4,850 years ago	7,500 years ago
		30 years	Nearly 0%-6%	0.33%	6.3%
		50 years	Nearly 0%-10%	0.55%	10%
9302	Futagawa/Hinagu fault zone (central part) (Case 2)	Interval	About 7,000-14,000 years	10,500 years	7,000 years
		Latest event	About 8,000-7,500 years ago	7,750 years ago	8,000 years ago
		30 years	0.03%-2%	0.38%	2.0%
		50 years	0.05%-3%	0.64%	3.3%
9302	Futagawa/Hinagu fault zone (southwestern part) (Case 1: simultaneous activity with the central part)	Interval	Unknown		
		Latest event	About 7,500-2,000 years ago	(Same occurrence probability as in the central part)	
		30 years	—	0.33%	6.3%
		50 years	—	0.55%	10%
9302	Futagawa/Hinagu fault zone (southwestern part) (Case 1: independent activity from the central part)	Interval	Unknown	8,600 years	8,600 years
		Latest event	About 7,500-2,200 years ago	(Poisson process)	
		30 years	—	0.35%	0.35%
		50 years	—	0.58%	0.58%
9302	Futagawa/Hinagu fault zone (southwestern part) (Case 2) *L*=27 km	Interval	Unknown	8,600 years	8,600 years
		Latest event	About 7,500-1,300 years ago (-1,309 years ago)	(Poisson process)	
		30 years	—	0.35%	0.35%
		50 years	—	0.58%	0.58%
9401	Minou fault zone	Interval	Around 14,000 years	14,000 years	14,000 years
		Latest event	AD 679 Tsukushi Earthquake	1,330 years ago	1,330 years ago
		30 years	Nearly 0%	Nearly 0%	Nearly 0%
		50 years	Nearly 0%	Nearly 0%	Nearly 0%
9501	Unzen fault group (northern part) *L*=30 km Class AB	Interval	Unknown	2,400 years	2,400 years
		Latest event	About 5,000 years ago or later	(Poisson process)	
		30 years	—	1.2%	1.2%
		50 years	—	2.1%	2.1%

Table 3.3.1-1 Occurrence probability of earthquakes in major active fault zones (part 14)

Code	Fault name		Long-term evaluation result (* indicates shape evaluation)	Occurrence probability average case	Occurrence probability maximum case
9502	Unzen fault group (southeastern part) *L*=23 km Class AB	Mean recurrence interval (Interval)	Unknown	1,800 years	1,800 years
		Latest event	About 7,300 years ago or later	(Poisson process)	
		Occurrence probability within 30 years (30 years)	—	1.7%	1.7%
		Occurrence probability within 50 years (50 years)	—	2.7%	2.7%
9503	Unzen fault group (northern segment of the southwestern part)	Interval	About 2,500-4,700 years	3,600 years	2,500 years
		Latest event	About 2,400 years ago-11th century	1,655 years ago	2,400 years ago
		30 years	Nearly 0%-4%	0.020%	4.0%
		50 years	Nearly 0%-7%	0.037%	6.6%
9504	Unzen fault group (southern segment of the southwestern part)	Interval	About 2,100-6,500 years	4,300 years	2,100 years
		Latest event	(About 4,500 years ago-16th century)	(Poisson process)	
		30 years	0.5%-1%	0.70%	1.4%
		50 years	0.8%-2%	1.2%	2.4%
9601	Izumi fault zone	Interval	Roughly 8,000 years	8,000 years	8,000 years
		Latest event	About 7,300-2,400 years ago	4,850 years ago	7,300 years ago
		30 years	Nearly 0%-1%	0.15%	1.1%
		50 years	Nearly 0%-2%	0.25%	1.8%
9701	Ise-wan fault zone (northern segment of the main part)	Interval	Around 10,000-15,000 years	12,500 years	10,000 years
		Latest event	Roughly 1,000-500 years ago (1,009-509 years ago)	759 years ago	1,009 years ago
		30 years	Nearly 0%	Nearly 0%	Nearly 0%
		50 years	Nearly 0%	Nearly 0%	Nearly 0%
9702	Ise-wan fault zone (southern segment of the main part)	Interval	Around 5,000-10,000 years	7,500 years	5,000 years
		Latest event	Roughly 2,000-1,500 years ago (2,009-1,509 years ago)	1,759 years ago	2,009 years ago
		30 years	Nearly 0%-0.002%	Nearly 0%	0.0019%
		50 years	Nearly 0%-0.004%	Nearly 0%	0.0035%
9703	Shiroko-Noma fault	Interval	Around 8,000 years	8,000 years	8,000 years
		Latest event	Roughly 6,500-5,000 years ago	5,750 years ago	6,500 years ago
		30 years	0.2%-0.8%	0.44%	0.76%
		50 years	0.3%-1%	0.74%	1.3%
9801	Osaka-wan fault zone	Interval	About 3,000-7,000 years	5,000 years	3,000 years
		Latest event	About the 9th century or later	605 years ago	1,209 years ago
		30 years	0.004% or less	Nearly 0%	0.0037%
		50 years	0.007% or less	Nearly 0%	0.0071%
9901	Sarobetsu fault zone	Interval	About 4,000-8,000 years	6,000 years	4,000 years
		Latest event	About 5,100-4,500 years ago	2,550 years ago	5,100 years ago
		30 years	4% or less	0.0038%	4.0%
		50 years	7% or less	0.0068%	6.6%
10101	Hanawa-higashi fault zone	Interval	Around 3,000-5,000 years	4,000 years	3,000 years
		Latest event	Cannot be specified sufficiently	(Poisson process)	
		30 years	0.6%-1%	0.75%	1.0%
		50 years	1%-2%	1.2%	1.7%
10401	Sone-kyuryo fault zone	Interval	Roughly 2,000-3,000 years	2,500 years	2,000 years
		Latest event	About 10,000 years ago or later (cannot be specified sufficiently)	(Poisson process)	
		30 years	1%	1.2%	1.5%
		50 years	2%	2.0%	2.5%

Table 3.3.1-1 Occurrence probability of earthquakes in major active fault zones (part 15)

Code	Fault name		Long-term evaluation result (* indicates shape evaluation)	Occurrence probability average case	Occurrence probability maximum case
10501	Uozu fault zone	Mean recurrence interval (Interval)	Around 8,000 years or less	8,000 years	8,000 years
		Latest event	Unknown	(Poisson process)	
		Occurrence probability within 30 years (30 years)	0.4% or more	0.37%	0.37%
		Occurrence probability within 50 years (50 years)	0.6% or more	0.62%	0.62%
10601	Suonada fault zone (main part)	Interval	Roughly 5,800-7,500 years	6,650 years	5,800 years
		Latest event	About 11,000-10,000 years ago	10,500 years ago	11,000 years ago
		30 years	2%-4%	2.9%	3.7%
		50 years	4%-6%	4.8%	6.1%
10602	Aio-Oki fault zone *L*=23 km *s*=0.1 mm/y	Interval	Unknown	18,300 years	18,300 years
		Latest event	Unknown	(Poisson process)	
		30 years	—	0.16%	0.16%
		50 years	—	0.27%	0.27%
10603	Ube-nanpo-Oki fault zone *L*=22 km *s*=0.1 mm/y	Interval	Unknown	17,500 years	17,500 years
		Latest event	Unknown	(Poisson process)	
		30 years	—	0.17%	0.17%
		50 years	—	0.29%	0.29%
10801	Kego fault zone (northwestern part)	Interval	Unknown	—	—
		Latest event	AD 2005 West off Fukuoka Earthquake	4 years ago	4 years ago
		30 years	—	Nearly 0%	Nearly 0%
		50 years	—	Nearly 0%	Nearly 0%
10802	Kego fault zone (southeastern part)	Interval	About 3,100-5,500 years	4,300 years	3,100 years
		Latest event	About 4,300-3,400 years ago	3,850 years ago	4,300 years ago
		30 years	0.3-6%	1.9%	5.6%
		50 years	0.4-9%	3.2%	9.2%
10901	Hitoyoshi-bonchi -nan'en fault	Interval	About 8,000 years or more	8,000 years	8,000 years
		Latest event	About 7,300-3,200 years ago	5,250 years ago	7,300 years ago
		30 years	1% or less	0.26%	1.1%
		50 years	2% or less	0.44%	1.8%

(Notes)

- The earthquake occurrence probability is the value for the period starting in AD 2009. The values in red are those that have changed from the values for the period starting in AD 2008, and the values in blue are those that have changed, but are indicated as being the same as the values for the period starting in AD 2008 as a result of the rounding.
- Where the time of the latest event is in AD, it is indicated as a specific year no later than AD 2009. For the "average case" as well, the time of the latest event is rounded to a specific year.
- Where the time of the latest event has been evaluated as "XX years ago" in long-term evaluation, and that year is in AD, such value is deemed to have been evaluated as of AD 2000, and a value for the period starting in AD 2009 is calculated.
- Where the time of the latest event has been indicated in century, which covers multiple years, the year which makes the range of the time of the latest event the broadest is used (e.g., "AD 400-AD 600" in the case of "5th century-6th century"), and the value for the period starting in AD 2009 is calculated. However, where there was an explanation such as "at the beginning of" or "in the first half of," 100 years and 50 years were respectively subtracted from such year.
- Where the probability is 10^{-3}% or less, it is indicated as "Nearly 0%."
- When calculating the earthquake occurrence probability using the BPT distribution, 0.24 is used as variance α.
- For an active fault of which the earthquake occurrence probability was unknown in the long-term evaluation, the mean recurrence interval is obtained based on the fault length and the average slip rate, and the occurrence probability is given by a Poisson process. The values of fault length *L* and average slip rate *s* used for the calculation are indicated in the fault name column. Where the average slip

rate was unknown, an average slip rate based on activity level (Class AB = 1 m/1000 years, Class B = 0.25 m/1000 years, Class BC = 0.1 m/1000 years) is assumed. The activity level is assumed to be Class B, in principle, but when Class AB or Class BC is assumed, a statement to that effect is indicated in the fault name column. The average slip rate was determined based on activity level for the following active faults:

(Class AB) Kiritoyama-Narai fault zone (4602), Nukumi fault zone (southeastern part) (6002), Unzen fault group (northern part) (9501), Unzen fault group (southeastern part) (9502)

(Class B) Shibetsu fault zone (0101), Numata-Sunagawa area fault zone (0402), Oritsume fault (1101), Shizukuishi-bonchi-seien fault zone (1401), Mahiru-sanchi-toen fault zone (southern part) (1403), Yokote-bonchi-toen fault zone (southern part) (1502), Aizu-bonchi-toen fault zone (2402), Kamogawa-teichi fault zone (2901), Hirai-Kushibiki fault zone (3102), Seinaiji-toge fault zone, (4503), Inohana fault zone (4803), Sami fault zone (5203), Shirakawa fault zone (5204), Akako fault zone (5302), Nagaragawa-joryu fault zone (5901), Ibigawa fault zone (6006), Mugigawa fault zone (6007), Yanagase/Sekigahara fault zone (central segment of the main part) (6102), Yanagase/Sekigahara fault zone (southern segment of the main part) (6103), Shufukuji fault (6302), Yamada fault zone (main part) (7401), Kanbayashigawa fault (7801), Itsukaichi fault (8701), Kikukawa fault zone (9001), Nishiyama fault zone (9101), Futagawa/Hinagu fault zone (southwestern part) (9302)

(Class BC) Nobi fault zone (Mitabora fault zone of the main part) (6005), Urazoko-Yanagaseyama fault zone (6104), Koi-Hiroshima-seien fault zone (8702), Inadani fault zone (southeastern part) (5102)

- For the Mashike-sanchi-toen fault zone (0401), the mean recurrence interval used is 5,000 years for both the "average case" and the "maximum case."
- For the Ishikari-teichi-toen fault zone (main part) (0601), the time of the latest event used is 4,250 years ago for the "average case" and 5,200 years ago for the "maximum case."
- For Hakodate-heiya-seien fault zone (0801), since the long-term evaluation explained about the time of the latest event that "no event is considered to have occurred at this fault zone within the last 390 years," the time of the latest event used for the "average case" is 7,199 years ago, which is the median value of 14,000-398 years ago.
- For the Tsugaru-sanchi-seien fault zone (northern part) (1001) and the Tsugaru-sanchi-seien fault zone (southern part) (1002), the long-term predictability has not been evaluated since the mean recurrence interval is unknown. Given that, at both fault zones, the last event occurred in 1766 and the long-term evaluation has indicated that "the possibility of earthquake occurrence in the near future is considered to be low," the earthquake occurrence probability used is nearly 0% for both the probability within 30 years and 50 years.
- While the length of the Mahiru-sanchi-toen fault zone (southern part) (1403) has been indicated in a range of values, the length is assumed to be 17 km in determining the mean recurrence interval.
- The time of the latest event used for the "average case" of the Kitayuri fault (1601) is 1,400 years ago.
- The mean recurrence interval used for the Shinjo-bonchi fault zone (1701) is 4,000 years for both the "average case" and the "maximum case," based on the displacement per event (about 2 m) and the average slip rate (about 0.5 m/1000 years) assumed from the fault length which is determined to be 23 km, adopting the longer end of the range of the length.
- The mean recurrence interval used for the Yamagata-bonchi fault zone (northern part) (1801) is 3,250 years for the "average case" and 2,500 years for the "maximum case," and the time of the latest event used is 2,755 years ago (the median value of 3,900-1,609 years ago) for the "average case" and 3,900 years ago for the "maximum case."
- The mean recurrence interval used for the Yamagata-bonchi fault zone (southern part) (1802) is 2,500 years for both the "average case" and the "maximum case,"
- The mean recurrence interval used for the Nagamachi-Rifu-sen fault zone (2001) is 5,000 years for both the "average case" and the "maximum case," based on the displacement per event (about 3 m) and the average slip rate (about 0.6 m/1000 years) assumed from the fault length which is determined to be 40 km, adopting the longer end of the range of the length.
- The time of the latest event used for the Nagai-bonchi-seien fault zone (2201) is 1,200 years ago for the "average case."
- The time of the latest event used for the Aizu-bonchi-seien fault zone (2401) is 398 years ago for both the "average case" and the "maximum case."
- The mean recurrence interval used for the Tsukioka fault zone (2601) is 7500 years for both the "average case" and the "maximum case."
- The time of the latest event used for the Nagaoka-heiya-seien fault zone (2701) is 405 years ago for the "average case."
- The time of the latest event used for the Isehara fault (3501) is 959 years ago for the "average case" and 1,609 years ago for the "maximum case."
- The mean recurrence interval used for the Itoigawa-Shizuoka-kozosen fault zone (southern part) (4201) is 1,200 years for both the "average case" and the "maximum case," assuming the fault length to be 31 km and the average slip rate to be 2 m/1000 years. Based on this, the earthquake occurrence probability is given by a Poisson model.
- The time of the latest event used for the Kiso-sanmyaku-seien fault zone (northern segment of the main part) (4501) is 759 years ago for the "average case" and 809 years ago for the "maximum case."
- The mean recurrence interval used for the Tonami-heiya fault zone (western part) (5601) is 9,000 years for the "average case" and 6,000 years for the "maximum case."

- The mean recurrence interval used for the Fukui-heiya-toen fault zone (main part) (5801) is 12,500 years for the "average case" and 7,000 years for the "maximum case."
- For the Fukui-heiya-toen fault zone (western part) (5802), the long-term predictability has not been evaluated since the mean recurrence interval is unknown. Given that, at both fault zones, the last event occurred in 1948 and the long-term evaluation has indicated that "the earthquake occurrence probability within the next 30 years is nearly 0%, and the earthquake occurrence probability within the next 300 years is also judged to be extremely low," the earthquake occurrence probability used is nearly 0% for both the probability within 30 years and 50 years.
- The time of the latest event used for the Yanagase/Sekigahara fault zone (northern segment of the main part) (6101) is 359 years for the "average case" and 409 years ago for the "maximum case."
- The mean recurrence interval used for the Nosaka fault zone (6301) is 6,600 years for the "average case" and 5,600 years for the "maximum case."
- The mean recurrence interval used for the Tongu fault (7001) is 10,000 years for both the "average case" and the "maximum case."
- For the Hanaore fault zone (northern part) (7302), the long-term predictability has not been evaluated since the mean recurrence interval is unknown, but it is noted in the long-term evaluation results that "the time span from the latest event until the time of the evaluation is slightly over 300 years, which is shorter than the recurrence interval of general active faults in Japan, (omitted) thus the probability of earthquake occurrence in the immediate future is considered to be low." Therefore, the earthquake occurrence probability used is nearly 0% for both the probability within 30 years and 50 years.
- The time of the latest event used for the Rokko/Awajishima fault zone (Rokko-sanchi-nan'en-Awajishima-togan segment of the main part) (7901) is 459 years ago for the "average case" and 509 years ago for the "maximum case."
- The time of the latest event used for the Senzan fault zone (7903) is 709 years ago for the "average case" and 1,009 years ago for the "maximum case."
- The time of the latest event used for the Chuo-kozosen fault zone (S-I part) (8103), Chuo-kozosen fault zone (Ishizuchi-sanmyaku-hokuen) (8104), Chuo-kozosen fault zone (I-I part) (8105) is 459 years ago for the "average case" and 509 years ago for the "maximum case."
- The time of the latest event used for the Kuenohirayama-Kameishiyama fault zone (9206) is 405 years ago for the "average case."
- The Futagawa/Hinagu fault zone (central part/southwestern part) (9302) is evaluated as an average of Case 1 and Case 2. The long-term evaluation results indicate that the mean recurrence interval is unknown for the southwestern part. For the case where seismic activities occur simultaneously at the southwestern part and the central part, the earthquake occurrence probability for the central part is used. However, for the case where seismic activities occur separately at the southwestern part and the central part, the mean recurrence interval is assumed to be 8,600 years based on the length of the southwestern part (27 km) and the general average slip rate of a Class B active fault (0.25 m/1000 years), and the future earthquake occurrence probability is given by a Poisson model.
- The time of the latest event used for the Osaka-wan fault zone (9801) is 605 years ago for the "average case."
- For the Sarobetsu fault zone (9901), the long-term evaluation indicated that the time of the latest event (5,100 years ago or later, 4,500 years ago or earlier) "cannot be specified as the latest event," but the time of the latest event used for the average case is 2,550 years ago (half of 5,100 years) and that used for the maximum case is 5,100 years ago.
- For the Uozu fault zone (10501), the long-term evaluation indicated that the mean recurrence interval is "about 8,000 years of less," so the mean recurrence interval used is "8,000 years" for both the average case and the maximum case.
- The mean recurrence interval used for the Aio-Oki fault zone (10602) is 18,300 years for both the "average case" and the "maximum case," based on the displacement per event (about 1.83 m) and the average slip rate (about 0.1 m/1000 years) assumed from the fault length which is determined to be 23 km.
- The mean recurrence interval used for the Ube-nanpo-Oki fault zone (10603) is 17,500 years for both the "average case" and the "maximum case," based on the displacement per event (about 1.75 m) and the average slip rate (about 0.1 m/1000 years) assumed from the fault length which is determined to be 22 km.
- For the Kego fault zone (northwestern part) (10801), the long-term evaluation indicated that, while the mean recurrence interval is unknown, "given that the latest event was the 2005 West off Fukuoka Earthquake, only an extremely short time has elapsed compared to the general recurrence interval of major active faults in Japan, thus the probability that an earthquake which matches the one evaluated this time will occur at the northwestern part of the fault zone in the immediate future is considered to be low." Therefore, the occurrence probability used is "nearly 0%."

Table 3.3.1-2 Proposed cases for the Futagawa/Hinagu fault zone (central part/southwestern part)

Case	Basis for determination of the occurrence probability	Seismic activities at the central part/southwestern part	M_j	Weight
Case 1-1	Case 1 in the long-term evaluation	Simultaneous activities	M_w 7.3	0.25
Case 1-2	Case 1 in the long-term evaluation	Separate activities	M_w 7.0, M_w 6.7	0.25
Case 2	Case 2 in the long-term	Separate activities	M_w 7.0, M_w 6.7	0.5

Table 3.3.1-3 Earthquake occurrence probability and magnitude for each case of the Futagawa/Hinagu fault zone (central part/southwestern part)

Case	Segment	Occurrence probability within 30 years		Occurrence probability within 50 years		M
Case 1-1	Central part/southwestern part	Average 0.33%	Maximum 6.3%	Average 0.55%	Maximum 10%	M_w 7.3
Case 1-2	Central part	Average 0.33%	Maximum 6.3%	Average 0.55%	Maximum 10%	M_w 7.0
	Southwestern part	Average 0.35%	Maximum 0.35%	Average 0.58%	Maximum 0.58%	M_w 6.7
Case 2	Central part	Average 0.38%	Maximum 2.0%	Average 0.64%	Maximum 3.3%	M_w 7.0
	Southwestern part	Average 0.35%	Maximum 0.35%	Average 0.58%	Maximum 0.58%	M_w 6.7

Note: "Average" denotes the average case and "Maximum" denotes the maximum case. See Table 2.1-2 for the fault plane parameters.

3.3.2 Subduction-zone earthquakes

Since long-term evaluation results for subduction-zone earthquakes have been indicated for individual groups consisting of multiple areas, the outline of the modeling is described in the following order.

(1) Nankai Trough earthquakes (ERC, 2001b)
(2) Miyagi-ken-Oki Earthquake (ERC, 2000) and earthquakes from Sanriku-Oki to Boso-Oki (ERC, 2002b; Working Group for Advancement of Seismic Hazard Maps (WGASHM), Subcommittee for Long-term Evaluations/Subcommittee for Evaluation of Strong Ground Motion (SLTE/SESGM), ERC, 2008)
(3) Earthquakes along the Kuril Trench (ERC, 2003a; ERC, 2004d)
(4) Earthquakes in the eastern margin of the Japan Sea (ERC, 2003c)
(5) Earthquakes in Hyuganada and in the vicinity of the Nansei-shoto Trench (ERC, 2004a)
(6) Earthquakes along the Sagami Trough (ERC, 2004c)

Table 3.3.2-1 shows the magnitude and the earthquake occurrence probability of each modeled earthquake (within 30 years and 50 years from January 2009).

In order to accurately figure out the long-term evaluation result of the SLTE, ERC, following the evaluation terms are technically defined and digitized in detail.

In the calculation of the earthquake occurrence probability, if the mean recurrence interval or variance α of the recurrence interval has been indicated in a range of values, the median value of the parameter is used. If the mean recurrence interval is given only in one side of the range (XX years or more), the earthquake occurrence probability is calculated using XX years.

If the magnitude has been indicated to be approximately XX or about XX, the magnitude of the earthquake is assumed to be XX. If the magnitude has been indicated in a range of values, the occurrence probability is given in 0.1 intervals to fit the Gutenberg Richter relation with b=0.9.

In evaluation of the ground motion intensity, $M_w = M_j$ is assumed for all earthquakes unless otherwise noted.

Table 3.3.2-2 shows the annual changes in the occurrence probabilities for major subduction-zone earthquakes from 2005 through 2009.

Table 3.3.2-1 List of occurrence probabilities for subduction-zone earthquakes (part 1)

	Area or earthquake name	Parameter	Long-term evaluation result	Model
Nankai Trough earthquakes	Nankai Earthquake*1	Magnitude	Approx. M8.4	M_w 8.4
		Mean recurrence interval	90.1 years*2	90.1 years
		Latest event	December 1946	62.0 years ago
		Variance α	0.20-0.24	0.20
		Occurrence probability within 30 years	50%-60%	56%
		Occurrence probability within 50 years	80%-90%	88%
	Tonankai Earthquake*1	Magnitude	Approx. M8.1	M_w 8.1
		Mean recurrence interval	86.4 years*2	86.4 years
		Latest event	December 1944	64.1 years ago
		Variance α	0.18-0.24	0.20
		Occurrence probability within 30 years	60%-70%	68%
		Occurrence probability within 50 years	Around 90% or more	93%
	Assumed Tokai Earthquake*1	Magnitude	-	M_w 8.0
		Mean recurrence interval	-	118.8 years
		Latest event	-	154.0 years ago
		Variance α	-	0.20
		Occurrence probability within 30 years	-	87%
		Occurrence probability within 50 years	-	97%
Earthquakes from Sanriku-Oki to Boso-Oki	Miyagi-ken-Oki Earthquake*1*3	Magnitude	Approx. M7.5	M_w 7.6, 7.4*5
		Mean recurrence interval	37.1 years	37.1 years
		Latest event	June 1978	30.6 years ago
		Variance α	0.177*4	0.177
		Occurrence probability within 30 years	99%	Nearly 100%
		Occurrence probability within 50 years	-	Nearly 100%
	Earthquakes close to the offshore trenches in Southern Sanriku-Oki*1	Magnitude	Approx. M7.7	M_w7.8*5
		Mean recurrence interval	Around 105 years	104.5 years
		Latest event	August 1897	111.4 years ago
		Variance α	0.19-0.24	0.22
		Occurrence probability within 30 years	80%-90%	80%
		Occurrence probability within 50 years	90%-98%	95%

Table 3.3.2-1 List of occurrence probabilities for subduction-zone earthquakes (part 2)

	Area or earthquake name	Parameter	Long-term evaluation result	Model
Earthquakes from Sanriku-Oki to Boso-Oki	Large Interplate earthquakes in Northern Sanriku-Oki	Magnitude	Approx. *M*8.0	M_w8.3[*5]
		Mean recurrence interval	About 97.0 years	97.0 years
		Latest event	May 1968	40.6 years ago
		Variance α	0.11-0.24	0.18
		Occurrence probability within 30 years	0.2%-10%	4.5%
		Occurrence probability within 50 years	30%-40%	39%
	Large interplate earthquakes close to the offshore trenches in the Sanriku-Oki to Boso-Oki regions (Tsunami earthquakes)	Magnitude	Approx. M_t8.2	M_w6.8[*6]
		Mean recurrence interval	Around 3 times in 400 years	133.3 years
		Latest event	(Poisson process)	-
		Variance α	-	-
		Occurrence probability within 30 years	Around 20%	20%
		Occurrence probability within 50 years	Around 30%	31%
	Large intraplate earthquakes close to the offshore trenches in the Sanriku-Oki to Boso-Oki regions (normal fault type)	Magnitude	Approx. *M*8.2	M_w8.2
		Mean recurrence interval	1 time in 400-750 years	575 years
		Latest event	(Poisson process)	-
		Variance α	-	-
		Occurrence probability within 30 years	4%-7%	5.1%
		Occurrence probability within 50 years	6%-10%	8.3%
	Interplate earthquakes other than characteristic earthquakes in Northern Sanriku-Oki	Magnitude	*M*7.1-*M*7.6	M_w7.1-7.6[*7]
		Mean recurrence interval	Around 1 time in 11.3 years	11.3 years
		Latest event	(Poisson process)	-
		Variance α	-	-
		Occurrence probability within 30 years	Around 90%	93%
		Occurrence probability within 50 years	-	99%
	Interplate earthquakes in Fukushima-ken-Oki[*8]	Magnitude	Approx. *M*7.4	M_w7.4
		Mean recurrence interval	Once in 400 years or less	400 years
		Latest event	(Poisson process)	-
		Variance α	-	-
		Occurrence probability within 30 years	Around 7% or less	7.2%
		Occurrence probability within 50 years	Around 10% or less	12%
	Interplate earthquakes in Ibaraki-ken-Oki[*10]	Magnitude	-	M_w7.0
		Mean recurrence interval	-	21.7 years
		Latest event	-	0.7 years ago
		Variance α	-	0.21
		Occurrence probability within 30 years	-	96%
		Occurrence probability within 50 years	-	Nearly 100%
Earthquakes along the Kuril Trench	Tokachi-Oki Earthquake[*1]	Magnitude	Approx. *M*8.1	M_w8.1
		Mean recurrence interval	72.2 years	72.2 years
		Latest event	September 2003	5.3 years ago
		Variance α	0.24-0.32	0.28
		Occurrence probability within 30 years	0.2%-2%	0.62%
		Occurrence probability within 50 years	Around 20%	20%
	Nemuro-Oki Earthquake[*1*3]	Magnitude	Around *M*7.9	M_w7.9
		Mean recurrence interval	72.2 years	72.2 years
		Latest event	Junr 1973	35.5 years ago
		Variance α	0.24-0.32	0.28
		Occurrence probability within 30 years	Around 40%	41%
		Occurrence probability within 50 years	Around 80%	77%
	Shikotanto-Oki Earthquake[*3]	Magnitude	Approx. *M*7.8 (approx. M_w8.2)	M_w7.8
		Mean recurrence interval	72.2 years	72.2 years
		Latest event	August 1969	39.4 years ago
		Variance α	0.24-0.32	0.28
		Occurrence probability within 30 years	Around 50%	49%
		Occurrence probability within 50 years	Around 80%	82%

Table 3.3.2-1 List of occurrence probabilities for subduction-zone earthquakes (part 3)

	Area or earthquake name	Parameter	Long-term evaluation result	Model
Earthquakes along the Kuril Trench	Etorofuto-Oki Earthquake[*3]	Magnitude	Approx. *M*8.1 (Approx. M_w8.5)	M_w8.1
		Mean recurrence interval	72.2 years	72.2 years
		Latest event	October 1963	45.2 years ago
		Variance α	0.24-0.32	0.28
		Occurrence probability within 30 years	Around 60%	59%
		Occurrence probability within 50 years	80%-90%	86%
	Relatively small interplate earthquakes in the Tokachi-Oki and Nemuro-Oki regions	Magnitude	Approx. *M*7.1	M_w7.1
		Mean recurrence interval	1 time in 17.5 years	17.5 years
		Latest event	(Poisson process)	-
		Variance α	-	-
		Occurrence probability within 30 years	Around 80%	82%
		Occurrence probability within 50 years	Around 90%	94%
	Relatively small interplate earthquakes in the Shikotanto-Oki and Etorofuto-Oki regions	Magnitude	Around *M*7.1 (approx. M_w7.7)	M_w7.1
		Mean recurrence interval	1 time in 10.5 years	10.5 years
		Latest event	(Poisson process)	-
		Variance α	-	-
		Occurrence probability within 30 years	Around 90%	94%
		Occurrence probability within 50 years	Around 90% or more	99%
	Relatively shallow earthquakes within a subducted plate	Magnitude	Approx. *M*8.2	M_w8.2
		Mean recurrence interval	1 time in 82.8 years	82.8 years
		Latest event	(Poisson process)	-
		Variance α	-	-
		Occurrence probability within 30 years	Around 30%	30%
		Occurrence probability within 50 years	Around 50%	45%
	Relatively deep earthquakes within a subducted plate	Magnitude	Around *M*7.5	M_w7.5
		Mean recurrence interval	1 time in 27.3 years	27.3 years
		Latest event	(Poisson process)	-
		Variance α	-	-
		Occurrence probability within 30 years	Around 70%	67%
		Occurrence probability within 50 years	Around 80%	84%
Earthquakes in the eastern margin of the Japan Sea	Hokkaido-hokusei-Oki Earthquake	Magnitude	Around *M*7.8	M_w7.8
		Mean recurrence interval	Around 3,900 years	3,900 years
		Latest event	Around 2,100 years ago	2,100 years ago
		Variance α	0.17-0.24	0.21
		Occurrence probability within 30 years	0.006%-0.1%	0.046%
		Occurrence probability within 50 years	0.01%-0.2%	0.082%
	Hokkaido-seiho-Oki Earthquake	Magnitude	Approx. *M*7.5	M_w7.5
		Mean recurrence interval	Around 1,400-3,900 years	2,650 years
		Latest event	August 1940	68.4 years ago
		Variance α	0.17-0.24	0.21
		Occurrence probability within 30 years	Nearly 0%	0%
		Occurrence probability within 50 years	Nearly 0%	0%
	Hokkaido-nansei-Oki Earthquake	Magnitude	Approx. *M*7.8	M_w7.8
		Mean recurrence interval	Around 500-1,400 years	950 years
		Latest event	July 1993	15.5 years ago
		Variance α	0.17-0.24	0.21
		Occurrence probability within 30 years	Nearly 0%	0%
		Occurrence probability within 50 years	Nearly 0%	0%
	Aomori-ken-seiho-Oki Earthquake	Magnitude	Approx. *M*7.7	M_w7.7
		Mean recurrence interval	Around 500-1,400 years	950 years
		Latest event	June 1983	25.6 years ago
		Variance α	0.17-0.24	0.21
		Occurrence probability within 30 years	Nearly 0%	0%
		Occurrence probability within 50 years	Nearly 0%	0%

Table 3.3.2-1 List of occurrence probabilities for subduction-zone earthquakes (part 4)

	Area or earthquake name	Parameter	Long-term evaluation result	Model
Earthquakes in the eastern margin of the Japan Sea	Akita-ken-Oki Earthquake	Magnitude	Around *M*7.5	M_w7.5
		Mean recurrence interval	Around 1,000 years or more	1,000 years
		Latest event	(Poisson process)	-
		Variance α	-	-
		Occurrence probability within 30 years	Around 3% or less	3.0%
		Occurrence probability within 50 years	Around 5% or less	4.9%
	Yamagata-ken-Oki Earthquake	Magnitude	Approx. *M*7.7	M_w7.7
		Mean recurrence interval	Around 1,000 years or more	1,000 years
		Latest event	December 1833	175.1 years ago
		Variance α	0.17-0.24	0.21
		Occurrence probability within 30 years	Nearly 0%	0%
		Occurrence probability within 50 years	Nearly 0%	0%
	Niigata-ken-hokubu-Oki Earthquake	Magnitude	Approx. *M*7.5	M_w7.5
		Mean recurrence interval	Around 1,000 years or more	1,000 years
		Latest event	June 1964	44.5 years ago
		Variance α	0.17-0.24	0.21
		Occurrence probability within 30 years	Nearly 0%	0%
		Occurrence probability within 50 years	Nearly 0%	0%
	Sadogashima-hoppo-Oki Earthquake	Magnitude	Around *M*7.8	M_w7.8
		Mean recurrence interval	Around 500-1,000 years	750 years
		Latest event	(Poisson process)	-
		Variance α	-	-
		Occurrence probability within 30 years	3%-6%	3.9%
		Occurrence probability within 50 years	5%-10%	6.4%
Earthquakes in Hyuganada and in the vicinity of the Nansei-shotoTrench	Intraplate earthquakes in Akinada-Iyonada-Bungosuido	Magnitude	*M*6.7-7.4	M_w6.7-7.4[*7]
		Mean recurrence interval	About 1 time in 67 years	67 years
		Latest event	(Poisson process)	-
		Variance α	-	-
		Occurrence probability within 30 years	Around 40%	36%
		Occurrence probability within 50 years	Around 50%	53%
	Interplate earthquakes in Hyuganada	Magnitude	Approx. *M*7.6	M_w7.6
		Mean recurrence interval	About 1 time in 200 years	200 years
		Latest event	(Poisson process)	-
		Variance α	-	-
		Occurrence probability within 30 years	Around 10%	14%
		Occurrence probability within 50 years	Around 20%	22%
	Relatively small interplate earthquakes in Hyuganada	Magnitude	Approx. *M*7.1	M_w7.1
		Mean recurrence interval	About 1 time in 20-27 years	23 years
		Latest event	(Poisson process)	-
		Variance α	-	-
		Occurrence probability within 30 years	70%-80%	73%
		Occurrence probability within 50 years	80%-90%	89%
	Earthquakes in the vicinity of Yonaguni-jima	Magnitude	Around *M*7.8	M_w7.8
		Mean recurrence interval	About 1 time in 100 years	100 years
		Latest event	(Poisson process)	-
		Variance α	-	-
		Occurrence probability within 30 years	Around 30%	26%
		Occurrence probability within 50 years	Around 40%	39%
Sagami Trough	Kanto Earthquake of "1923 Taisho" type[*9]	Magnitude	Around *M*7.9	M_w7.9
		Mean recurrence interval	200-400 years	219.7 years[*9]
		Latest event	September 1923	85.3 years ago
		Variance α	0.17-0.24	0.21
		Occurrence probability within 30 years	Nearly 0%-1%	0.12%
		Occurrence probability within 50 years	Nearly 0%-6%	1.3%

Table 3.3.2-1 List of occurrence probabilities for subduction-zone earthquakes (part 5)

	Area or earthquake name	Parameter	Long-term evaluation result	Model
Sagami Trough	Other *M*7 class earthquakes in Southern Kanto	Magnitude	Around *M*6.7-7.2	M_w6.7-7.2*7
		Mean recurrence interval	1 time in 23.8 years	23.8 years
		Latest event	(Poisson process)	-
		Variance α	-	-
		Occurrence probability within 30 years	Around 70%	72%
		Occurrence probability within 50 years	Around 90%	88%

Notes: The earthquake occurrence probability is the value for the period starting in January 2009. The values in red are those that have changed from the values for the period starting in 2008. "Variance α" in the table denotes the variance at the time of calculating the earthquake occurrence probability by the BPT distribution.

*1 The Nankai Earthquake, the Tonankai Earthquake, the Assumed Tokai Earthquake, the Miyagi-ken-Oki Earthquake, the earthquakes close to the offshore trenches in Southern Sanriku-Oki, the Tokachi-Oki Earthquake, and the Nemuro-Oki Earthquake are modeled while taking into consideration their correlated occurrence.

*2 For the Nankai Earthquake and the Tonankai Earthquake, the mean recurrence interval used is the typical recurrence interval with the next event.

*3 The Miyagi-ken-Oki Earthquake, the Nemuro-Oki Earthquake, the Shikotanto-Oki Earthquake, and the Etorofuto-Oki Earthquake are modeled while taking into consideration the case of occurring twice.

*4 For the Miyagi-ken-Oki Earthquake, the variance α of the recurrence interval is based on the report "Regarding methods for evaluating long-term probability of earthquake occurrence" (ERC, 2001a).

*5 For the Miyagi-ken-Oki Earthquake, the earthquakes close to the offshore trenches in Southern Sanriku-Oki, and the large interplate earthquakes in Northern Sanriku-Oki, M_w is based on the strong motion evaluation.

*6 For the large interplate earthquakes close to the offshore trenches in the Sanriku-Oki to Boso-Oki regions (Tsunami earthquakes), the magnitude used for ground motion evaluation is M_w=6.8.

*7 For the interplate earthquakes other than characteristic earthquakes in Northern Sanriku-Oki, the intraplate earthquakes in Akinada-Iyonada-Bungosuido, and the other *M*7 class earthquakes in Southern Kanto, the recurrence frequency by magnitude is evaluated to fit the Gutenberg Richter relation with b=0.9.

*8 The earthquakes in Fukushima-ken-Oki are modeled while taking into consideration the case of occurring three times successively.

*9 The Kanto Earthquake of "1703 Genroku" type is not modeled as an earthquake along the Sagami Trough. The mean recurrence interval used for the Kanto Earthquake of "1923 Taisho" type is 219.7 years based on the interval between the Genroku Earthquake (December 1703) and the Kanto Earthquake (September 1923).

*10 The earthquakes in Ibaraki-ken-Oki are newly modeled based on the earthquake on May 8, 2008 (WGASHM, SLTE/SESGM, ERC, 2008).

Table 3.3.2-2 Changes in the occurrence probability of major subduction-zone earthquakes

(a) Occurrence probability within 30 years

	2005	2006	2007	2008	2009
Nankai Earthquake	48%	50%	53%	55%	56%
Tonankai Earthquake	61%	62%	64%	66%	68%
Assumed Tokai Earthquake	86%	87%	87%	87%	87%
Miyagi-ken-Oki Earthquake	99%	99%	Nearly 100%	Nearly 100%	Nearly 100%
Earthquakes close to the offshore trenches in southern Sanriku-Oki	79%	79%	80%	80%	80%
Large interplate earthquakes in northern Sanriku-Oki	2.2%	2.6%	3.2%	3.8%	4.5%
Tokachi-Oki Earthquake	0.15%	0.22%	0.32%	0.45%	0.62%
Nemuro-Oki Earthquake	33%	35%	37%	39%	41%
Shikotanto-Oki Earthquake	41%	43%	45%	47%	49%
Etorofuto-Oki Earthquake	52%	54%	56%	57%	59%
Kanto Earthquake of "1923 Taisho" type	0.065%	0.076%	0.089%	0.10%	0.12%

(b) Occurrence probability within 50 years

	2005	2006	2007	2008	2009
Nankai Earthquake	84%	85%	86%	87%	88%
Tonankai Earthquake	90%	91%	92%	92%	93%
Assumed Tokai Earthquake	97%	97%	97%	97%	97%
Miyagi-ken-Oki Earthquake	Nearly 100%	Nearly 100%	Nearly 100%	Nearly 100%	Nearly 100%
Earthquakes close to the offshore trenches in southern Sanriku-Oki	94%	95%	95%	95%	95%
Large interplate earthquakes in northern Sanriku-Oki	29%	32%	34%	36%	39%
Tokachi-Oki Earthquake	14%	15%	17%	19%	20%
Nemuro-Oki Earthquake	72%	73%	75%	76%	77%
Shikotanto-Oki Earthquake	77%	78%	79%	80%	82%
Etorofuto-Oki Earthquake	83%	84%	85%	86%	86%
Kanto Earthquake of "1923 Taisho" type	0.85%	0.94%	1.0%	1.1%	1.3%

Note: Both tables show the occurrence probabilities for the periods starting in January of the respective years.

(1) Nankai Trough earthquakes

The Nankai Earthquake, the Tonankai Earthquake, and the Assumed Tokai Earthquake are modeled as the Nankai Trough earthquakes. The earthquakes are modeled while referring to "Long-term Evaluation of Nankai Trough Earthquakes" (ERC, 2001b) and "Report of the Special Survey Committee for the Tokai Earthquake" (Central Disaster Prevention Council, 2001).

Here, the earthquakes of which the source areas are the respective areas shown in Figure 3.3.2-1 are called by the names shown below. The correspondence between past earthquakes and the source areas are indicated in Table 3.3.2-3.

- Nankai Earthquake: off Ashizuri-misaki – off Shiono-misaki (area *X*)
- Tonankai Earthquake: off Shiono-misaki – off Hamana-ko (area *Y*)
- Assumed Tokai Earthquake: off Hamana-ko – Suruga-wan (area *Z*)

For the modeling of seismic activities of the Nankai-Tonankai-Assumed Tokai Earthquakes, the following is assumed on the basis of the past seismic activities shown in Table 3.3.2-3 and the fact that the Assumed Tokai Earthquake is considered to be caused by the portion that remains unruptured in the source area of the 1854 Ansei Tokai Earthquake.

<u>The Nankai Earthquake, the Tonankai Earthquake, and the Assumed Tokai Earthquake are assumed to occur sequentially according to separate, independent renewal processes. However, where multiple earthquakes occur within the target period, those earthquakes occur in a correlated manner (occur simultaneously) with the predetermined probability.</u>

The parameters for calculating the occurrence probabilities of the respective earthquakes are determined as shown in Table 3.3.2-4, based on the long-term evaluation. The latest event of the Assumed Tokai Earthquake is assumed to be the 1854 Ansei Tokai Earthquake.

Under the conditions above, the occurrence probabilities of the respective earthquakes within 30 years and 50 years from January 2009 are derived as indicated in Table 3.3.2-5. (Note: The probability of occurring twice within 50 years is not considered for any of the earthquakes.)

As for the source areas, it is assumed that the respective earthquakes occur independently or that multiple earthquakes occur in a correlated manner. The source area of each earthquake shall be the predetermined model within each relevant area, and the case where only one part of the model constitutes the source area is not assumed.

Figure 3.3.2-2 shows the modeled source areas of the respective earthquakes. The source areas of the Nankai Earthquake and the Tonankai Earthquake are based on the long-term evaluation, and the source area of the Assumed Tokai Earthquake is based on the Report of the Special Survey Committee for the Tokai Earthquake, Central Disaster Prevention Council.

The probability of correlated occurrence of multiple earthquakes is determined on the assumption that possible events all occur with equal probabilities. The specific determination method is as follows:

- Case where the Nankai Earthquake and the Tonankai Earthquake occur, but the Assumed Tokai Earthquake does not occur
  - Probability that the Nankai and Tonankai Earthquakes occur independently: 1/2 (50%)
  - Probability that the Nankai-Tonankai Earthquakes occur in a correlated manner: 1/2 (50%)
- Case where the Tonankai Earthquake and the Assumed Tokai Earthquake occur, but the Nankai Earthquake does not occur
  - Probability that the Tonankai and Assumed Tokai Earthquakes occur independently: 1/2 (50%)
  - Probability that the Tonankai-Assumed Tokai Earthquakes occur in a correlated manner: 1/2 (50%)
- Case where all three earthquakes occur
  - Probability that the respective earthquakes occur independently: 1/4 (25%)
  - Probability that the Nankai and Tonankai Earthquakes occur in a correlated manner: 1/4 (25%)
  - Probability that the Tonankai-Assumed Tokai Earthquakes occur in a correlated manner: 1/4 (25%)
  - Probability that the Nankai-Tonankai-Assumed Tokai Earthquakes occur in a correlated manner: 1/4 (25%)

The magnitudes of the respective earthquakes and the cases of correlated occurrence are assumed as shown in Table 3.3.2-6.

Under the conditions above, the 13 cases shown in Table 3.3.2-7 can be derived as the occurrence patterns of the Nankai-Tonankai-Assumed Tokai Earthquakes. The table also shows the probabilities that the respective cases occur within 30 years or 50 years from 2009.

Since the cases shown in Table 3.3.2-7 are mutually-exclusive and cover all cases, the seismic hazard is calculated by obtaining the sum of products of the occurrence probability for each case and the exceedance probability of the ground motion intensity for the case regarding the 13 cases shown below.

In the sea area along the Suruga Trough to the Nankai Trough, an Assumed Tokai Earthquake is expected to occur at any time, being an area that remains unruptured in the 1944 Tonankai Earthquake and the 1946 Nankai Earthquake. Whereas large earthquakes have occurred repeatedly at intervals of 100 to 150 years in this sea area, the area of the Assumed Tokai Earthquake has never ruptured in an isolated manner in the occurrence pattern of historical earthquakes that has been taken into consideration in the modeling. In that sense, it is difficult to evaluate the long-term

probability of earthquake occurrence based on past events.

A desirable approach would be to evaluate the probability of future occurrence of earthquakes by modeling the time series of events while taking into consideration factors including the interaction with neighboring areas. However, the mechanism of correlation between areas where earthquakes occur and that of the time series of the occurrence are still largely unclear. Therefore, it is currently difficult to quantitatively evaluate the earthquake occurrence probability by taking the physics of such elements into consideration.

At present, long-term observation and research have been continued for the Assumed Tokai Earthquake based on the Act on Special Measures Concerning Countermeasures for Large-Scale Earthquakes enforced in 1978. For the Tonankai/Nankai Earthquakes as well, long-term survey and observation of earthquake recurrence intervals and a mechanism of correlated occurrences are planned based on the "Plan for Strengthening Survey and Observation of the Tonankai/Nankai Earthquakes (First Report)" (Subcommittee for Survey and Observation Plans of the Policy Committee, 2003). If more appropriate modeling of seismic activity becomes possible based on the results of such survey, observation, and research or development of theories concerning areas that remain unruptured, correlated occurrences, and sequential occurrences, the earthquake occurrence probability for the area needs to be reconsidered based on such achievements.

If the Assumed Tokai Earthquake does not occur for some time, there is a possibility that the area of that earthquake will rupture simultaneously with the next Tonankai Earthquake. Regarding this point, the earthquake occurrence probability and the occurrence pattern need to be reconsidered at an appropriate point of time in the future.

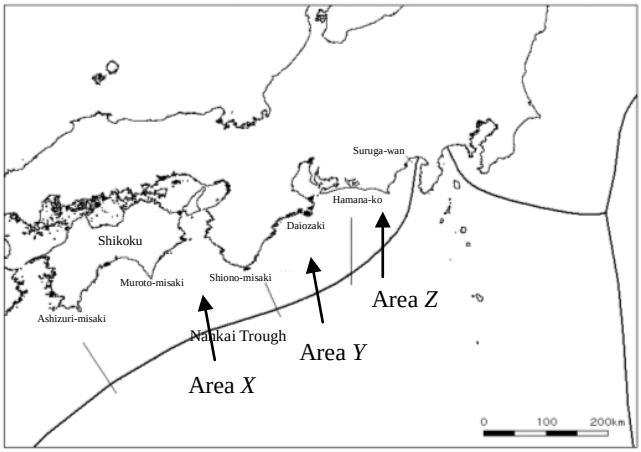

Figure 3.3.2-1 Locational relationship between source areas of the Nankai Trough Earthquakes

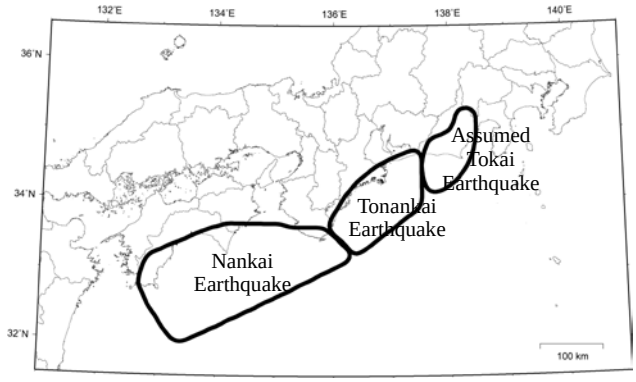

Figure 3.3.2-2 Modeled source area of each earthquake

Table 3.3.2-3 Source areas of past Nankai Trough Earthquakes

Date of occurrence	Earthquake name	Area *X*	Area *Y*	Area *Z*
Sep. 20, 1498	1498 Meio Tokai Earthquake		○	△
Feb. 3, 1605	1605 Keicho Earthquake	○	○	△
Oct. 28, 1707	1707 Hoei Earthquake	○	○	△-○
Dec. 23, 1854	1854 Ansei Tokai Earthquake		○	○
Dec. 24, 1854	1854 Ansei Nankai Earthquake	○		
Dec. 7, 1944	1944 Showa Tonankai Earthquake		○	
Dec. 21, 1946	1946 Showa Nankai Earthquake	○		

Note: ○ denotes that almost the entire area constituted the source area, and △ denotes that only a part of the area constituted the source area.

Table 3.3.2-4 Parameters concerning recurrence interval of each earthquake

	Recurrence interval	Latest event	Variance α
Nankai Earthquake	90.1 years	Dec. 1946	0.20
Tonankai Earthquake	86.4 years	Dec. 1944	0.20
Assumed Tokai Earthquake	118.8 years	Dec. 1854	0.20

Notes: The parameters for the Nankai Earthquake and the Tonankai Earthquake are based on the long-term evaluation. Variance α for the two earthquakes are both 0.20. The recurrence interval of the Assumed Tokai Earthquake is the mean value of Meio-Keicho (106.4 years), Keicho-Hoei (102.7 years), and Hoei-Ansei (147.2 years), and variance α is the same value as that for the Nankai Earthquake and the Tonankai Earthquake.

Table 3.3.2-5 Occurrence probability of each earthquake

	Time elapsed	Probability within 30 years	Probability within 50 years
Nankai Earthquake	62.0 years	56%	88%
Tonankai Earthquake	64.1 years	68%	93%
Assumed Tokai Earthquake	154.0 years	87%	97%

Note: Time elapsed denotes the time elapsed as of January 2009.

Table 3.3.2-6 Magnitude of each earthquake

Earthquake	M_w
Nankai Earthquake	8.4
Tonankai Earthquake	8.1
Assumed Tokai Earthquake	8.0
Nankai Earthquake + Tonankai Earthquake	8.5
Tonankai Earthquake + Assumed Tokai Earthquake	8.4
Nankai Earthquake + Tonankai Earthquake + Assumed Tokai Earthquake	8.5

Notes: In applying the attenuation relation by Si and Midorikawa (1999), when the earthquake magnitude is M_w8.3 or more, the peak ground velocity is assumed not to increase in proportion to M_w (saturation of magnitude).

Table 3.3.2-7 Occurrence pattern and occurrence probability of Nankai-Tonankai-Assumed Tokai Earthquakes

No.	Nankai Earthquake	Tonankai Earthquake	Assumed Tokai Earthquake	Probability within 30 years	Probability within 50 years
(1)	×	×	×	1.8%	0.025%
(2)	↔	×	×	2.4%	0.18%
(3)	×	↔	×	3.8%	0.31%
(4)	×	×	↔	12%	0.86%
(5)	↔	↔	×	2.5%	1.1%
(6)	↔	↔	×	2.5%	1.1%
(7)	↔	×	↔	16%	6.2%
(8)	×	↔	↔	13%	5.5%
(9)	×	↔	↔	13%	5.5%
(10)	↔	↔	↔	8.3%	20%
(11)	↔	↔	↔	8.3%	20%
(12)	↔	↔	↔	8.3%	20%
(13)	↔	↔	↔	8.3%	20%
	Total			100%	100%

Notes: For example, the probability within 30 years for (9) is obtained as follows. According to Table 3.3.2-5, the probability that the Nankai Earthquake does not occur is 1-0.56=0.44, the occurring probabilities of the Tonankai Earthquake and Assumed Tokai Earthquake are 0.67 and 0.87. Thus, the probability that the Tonankai Earthquake and the Assumed Tokai Earthquake occur without the occurrence of the Nankai Earthquake is 0.44*0.68*0.87=0.26. The probability of correlated occurrence of the Tonankai Earthquake and the Assumed Tokai Earthquake under these conditions is 0.5. Hence, the probability of occurrence of Pattern (9) within the next 30 years is 0.26*0.5=0.13 (13%).

(2) Miyagi-ken-Oki Earthquake and earthquakes in the Sanriku-Oki to Boso-Oki regions

The areas covered in the evaluation of the Miyagi-ken-Oki Earthquake (ERC, 2000) and the earthquakes in the Sanriku-Oki to Boso-Oki regions (ERC, 2002b) are shown in Figure 3.3.2-3.

The brief outline of the modeling of subduction-zone earthquakes that occur in these areas is shown below.

The following basic policy was set for modeling faults.

- For the Miyagi-ken-Oki Earthquake and the earthquakes close to the offshore trenches in Southern Sanriku-Oki (Areas A and E in Figure 3.3.2-3), the possibility of correlated occurrence of both earthquakes shall be taken into consideration in the modeling.
- The magnitude used for the large interplate earthquakes close to the offshore trenches in Northern Sanriku-Oki to Boso-Oki regions (Tsunami earthquakes: Area C in Figure 3.3.2-3) shall be M_w 6.8, taking into account the magnitude of the 1896 Meiji Sanriku Earthquake derived by Usami (1996, Materials for comprehensive list of destructive earthquakes in Japan).
- Since earthquakes of a magnitude class 7 or more are not assumed for earthquakes in Central Sanriku-Oki (Area D in Figure 3.3.2-3), they are not modeled as subduction-zone earthquakes (but are modeled as earthquakes without specified source faults).
- For earthquakes in Fukushima-ken-Oki (Area F in Figure 3.3.2-3), multiple earthquakes are assumed to occur successively within a short period. So, the time series of occurrence is expressed by a Poisson process with a mean recurrence interval of 400 years, and the influence of the sequential occurrence is taken into consideration by assuming that earthquakes occur three times on the same fault plane when evaluating the exceedance probability of the ground motion intensity.
- As for the location of the source area, specific fault planes are determined for the Miyagi-ken-Oki Earthquake (Area A in Figure 3.3.2-3), the earthquakes close to the offshore trenches in Southern Sanriku-Oki (Area E in Figure 3.3.2-3), and the large interplate earthquakes in Northern Sanriku-Oki (Area B in Figure 3.3.2-3). However, for other earthquakes, multiple fault planes are allocated along the plate boundaries within the proposed areas, and earthquakes are assumed to occur on those fault planes with an equal probability, except that for the large intraplate earthquakes close to the offshore trenches in the Northern Sanriku-Oki to Boso-Oki regions (normal fault type), the fault plane is modeled as a normal fault with a dip angle of 45º and of which the upper edge is 0 km deep. The western end of Areas B, F, and G in Figure 3.3.2-3 are determined based on Umino et al. (1990).

The parameters of the seismic activity model of each earthquake are shown below.

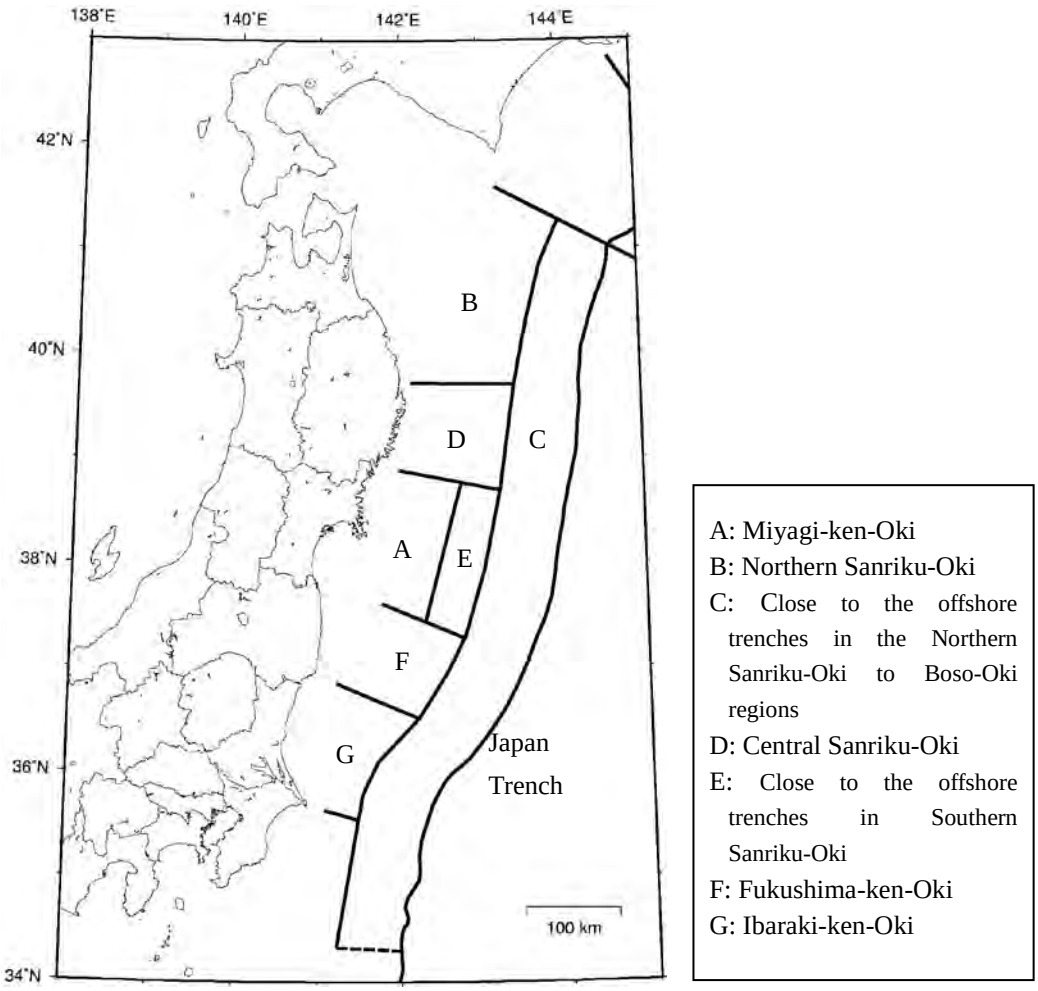

Figure 3.3.2-3 Areas covered in evaluation of the Miyagi-ken-Oki Earthquake and earthquakes in the Sanriku-Oki to Boso-Oki regions.

1) Miyagi-ken-Oki Earthquake and earthquakes close to the offshore trenches in Southern Sanriku-Oki

According to the “Long-term Evaluation of the Miyagi-ken-Oki Earthquake” (ERC, 2000) and “Evaluation for seismic activity from Sanriku-Oki to Boso-Oki” (ERC, 2002b), the past events of the Miyagi-ken-Oki Earthquake and the earthquakes close to the offshore trenches in Southern Sanriku-Oki are as shown in Figure 3.3.2-4.

As for the Miyagi-ken-Oki Earthquake, one out of six past events was correlated with an earthquake close to the offshore trenches in Southern Sanriku-Oki. Regarding the earthquakes close to the offshore trenches in Southern Sanriku-Oki, one of the two past events was correlated with the Miyagi-ken-Oki Earthquake.

Based on such data, the long-term evaluation report mentioned above indicates the values in Table 3.3.2-8 as parameters concerning recurrence interval.

When the earthquake occurrence probabilities within 30 years and 50 years from January 2009 are obtained based on these parameters by applying a renewal process using the BPT distribution for the recurrence interval, the results are as shown in Table 3.3.2-9. With regard to the Miyagi-ken-Oki Earthquake, due to the short mean recurrence interval, the probability of occurrence of two events cannot be ignored in the probabilistic seismic hazard evaluation for the next 30 years and 50 years. Therefore, evaluation is carried out while taking such fact into consideration (Ishikawa et al., 2002).

Meanwhile, the long-term evaluations of the two earthquakes indicate that it cannot be determined at present whether the next Miyagi-ken-Oki Earthquake and earthquake close to the offshore trenches in Southern Sanriku-Oki occur independently or in a correlated manner.

The "Evaluation of the Seismic Source Fault Shape of the Next Miyagi-ken-Oki Earthquake" (SLTE, ERC, 2002b) and "Strong Motion Evaluation Assuming the Miyagi-ken-Oki Earthquake" (ERC, 2003b) assume a "case of independent occurrence" where the source area of the Miyagi-ken-Oki Earthquake is Area A1 or A2 shown in Figure 3.3.2-5, and a "case of correlated occurrence" where the source areas are Area A1 or A2, and Area B.

Based on the data above, the Miyagi-ken-Oki Earthquake and the earthquakes close to the offshore trenches in Southern Sanriku-Oki are modeled, taking into consideration correlated occurrence.

Here, based on the fact that one of the two past events of the earthquakes close to the offshore trenches in Southern Sanriku-Oki was correlated with the Miyagi-ken-Oki Earthquake, the following is assumed as the condition for correlated occurrence of the two earthquakes.

<u>Where the Miyagi-ken-Oki Earthquake and earthquakes close to the offshore trenches in Southern Sanriku-Oki both occur within the target period (within 30 years or 50 years), they occur in a correlated manner with a 50% probability (once out of two times).</u>

The source areas and the magnitude of each earthquake are modeled as below according to "Evaluation of the Seismic Source Fault Shape of the Next Miyagi-ken-Oki Earthquake" (Subcommittee for Long-term Evaluations, ERC, 2002b) and the "Strong Motion Evaluation Assuming the Miyagi-ken-Oki Earthquake" (ERC, 2003b).

In the "case of independent occurrence" of the Miyagi-ken-Oki Earthquake, the source area is assumed to be either Area A1 or A2 shown in Figure 3.3.2-5, and the probability of occurrence is assumed to be equal between the two source areas (the probability of 50% for each source area). The magnitude is assumed to be M_w=7.6 in the case of independent occurrence in Area A1, and M_w=7.4 in the case of independent occurrence in Area A2.

In the case of independent occurrence of an earthquake close to the offshore trenches in Southern Sanriku-Oki, the source area is assumed to be Area B shown in Figure 3.3.2-5. The magnitude is assumed to be M_w=7.8 based on the determined fault plane area, using a relation between the fault plane area and the magnitude.

The source areas in the case of correlated occurrence of the Miyagi-ken-Oki Earthquake and an earthquake close to the offshore trenches in Southern Sanriku-Oki are assumed to be Areas A1+B, Areas A2+B, or Areas A1+A2+B shown in Figure 3.3.2-5. The probability of occurrence is assumed to be equal between the three combinations of source areas (the probability of 1/3 for each combination). By referring to the fault plane area of each combination of source areas, the magnitude is assumed to be M_w=7.9 in the case of Areas A1+B, M_w=7.9 in the case of Areas A2+B, and M_w =8.0 in the case of Areas A1+A2+B.

Under the conditions above, the occurrence patterns of the Miyagi-ken-Oki Earthquake and earthquakes close to the offshore trenches in Southern Sanriku-Oki total to the 21 cases shown in Table 3.3.2-10, considering the frequency of the Miyagi-ken-Oki Earthquake, the presence or absence of correlation, and the differences in the source areas of each earthquake. The probability of occurrence of each case within the next 30 years or 50 years can be derived as shown in Table 3.3.2-10 by using the occurrence probability of each earthquake (Table 3.3.2-9), the probability of correlation based on the assumptions above, and the probability of occurrence in the respective source areas.

Since the cases shown in Table 3.3.2-10 are mutually-exclusive and cover all cases, the seismic hazard is calculated by obtaining the sum of products of the occurrence probability for each case and the exceedance probability of the ground motion intensity for the case regarding all of the cases above.

The degree of influence (contribution factor) of each earthquake on the seismic hazard evaluation results is indicated as a value that combines the two earthquakes.

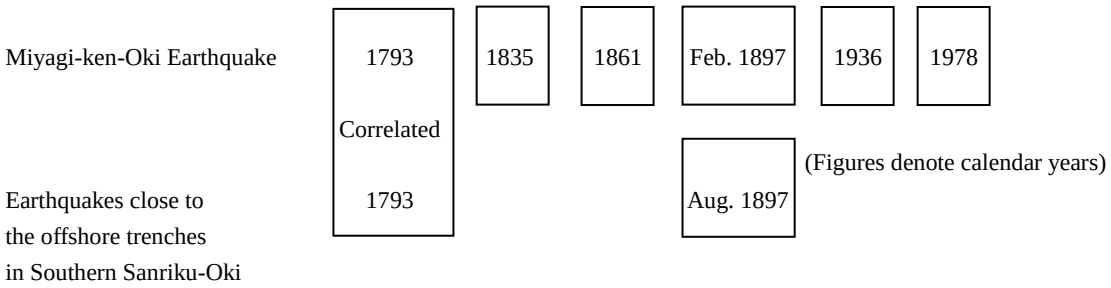

Figure 3.3.2-4 History of occurrence of the Miyagi-ken-Oki Earthquake and earthquakes close to the offshore trenches in southern Sanriku-Oki

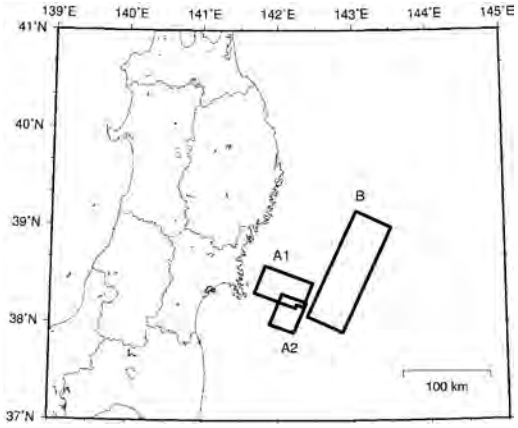

Figure 3.3.2-5 Modeled source area of each earthquake

Table 3.3.2-8 Parameters concerning recurrence interval of the Miyagi-ken-Oki Earthquake and earthquakes close to the offshore trenches in southern Sanriku-Oki

	Mean recurrence interval	Time elapsed from the latest event	Recurrence interval variance α
Miyagi-ken-Oki Earthquake	37.1 years	30.6 years	0.177
Earthquakes close to the offshore trenches in southern Sanriku-Oki	104.5 years	111.4 years	0.19-0.24

Notes: Time elapsed from the latest event denotes the time elapsed as of January 2009. Variance α for the Miyagi-ken-Oki Earthquake is based on the report "Regarding methods for evaluating long-term probability of earthquake occurrence" (ERC, 2001a).

Table 3.3.2-9 Occurrence probabilities of the Miyagi-ken-Oki Earthquake and earthquakes close to the offshore trenches in southern Sanriku-Oki

	Occur. prob. within 30 years			Occur. prob. within 50 years		
	None	Once	Twice	None	Once	Twice
Miyagi-ken-Oki Earthquake	0.23%	98%	2.1%	Nearly 0%	27%	73%
Earthquakes close to the offshore trenches in southern Sanriku-Oki	20%	80%	Nearly 0%	5.1%	95%	Nearly 0%

Notes: Variance α used for the earthquakes close to the offshore trenches in Southern Sanriku-Oki is 0.22 (the median value of the range). Probability less than 10^{-3}% is indicated as "Nearly 0%". The occurrence probability is that for the period starting January 2009.

Table 3.3.2-10 Occurrence probabilities of the Miyagi-ken-Oki Earthquake and earthquakes close to the offshore trenches in southern Sanriku-Oki

	Case	Probability within 30 years	Probability within 50 years
(1)	"Miyagi" 0 times * "Sanriku" 0 times	0.045%	Nearly 0%
(2)	"Miyagi" 0 times * "Sanriku" once independent	0.19%	Nearly 0%
(3)	"Miyagi" once independent A1 * "Sanriku" 0 times	9.6%	0.70%
(4)	"Miyagi" once independent A2 * "Sanriku" 0 times	9.6%	0.70%
(5)	"Miyagi" once independent A1 * "Sanriku" once independent	20%	6.5%
(6)	"Miyagi" once independent A2 * "Sanriku" once independent	20%	6.5%
(7)	"Miyagi" once + "Sanriku" once correlated A1+B	13%	4.3%
(8)	"Miyagi" once + "Sanriku" once correlated A2+B	13%	4.3%
(9)	"Miyagi" once + "Sanriku" once correlated A1+A2+B	13%	4.3%
(10)	"Miyagi" twice independent A1 * A1 * "Sanriku" 0 times	0.10%	0.93%
(11)	"Miyagi" twice independent A1 * A2 * "Sanriku" 0 times	0.20%	1.9%
(12)	"Miyagi" twice independent A2 * A2 * "Sanriku" 0 times	0.10%	0.93%
(13)	"Miyagi" twice independent A1 * A1 * "Sanriku" once independent	0.21%	8.6%
(14)	"Miyagi" twice independent A1 * A2 * "Sanriku" once independent	0.42%	17%
(15)	"Miyagi" twice independent A2 * A2 * "Sanriku" once independent	0.21%	8.6%
(16)	"Miyagi" twice - once correlated with "Sanriku" A1+B * once independent A1	0.14%	5.7%
(17)	"Miyagi" twice – once correlated with "Sanriku" A2+B * once independent A1	0.14%	5.7%
(18)	"Miyagi" twice - once correlated with "Sanriku" A1+A2+B * once independent A1	0.14%	5.7%
(19)	"Miyagi" twice - once correlated with "Sanriku" A1+B * once independent A2	0.14%	5.7%
(20)	"Miyagi" twice – once correlated with "Sanriku" A2+B * once independent A2	0.14%	5.7%
(21)	"Miyagi" twice – once correlated with "Sanriku" A1+A2+B * once independent A2	0.14%	5.7%
	Total	100%	100%

Notes: "Miyagi" denotes the Miyagi-ken-Oki Earthquake, and "Sanriku" denotes earthquakes close to the offshore trenches in southern Sanriku-Oki. The occurrence probability is that for the period starting January 2009. Recurrence interval variance α used for earthquakes close to the offshore trenches in southern Sanriku-Oki is 0.22 (the median value of the range). Probability less than 10^{-3}% is indicated as "Nearly 0%".

For example, the probability within 30 years for (7) above is calculated to be about 13%, by combining (a) the probability that the Miyagi-ken-Oki Earthquake will occur once within 30 years (98%) and (b) the probability that an earthquake close to the offshore trenches in southern Sanriku-Oki will occur once within 30 years (80%) shown in Table 3.3.2-9, as well as (c) the probability that the two earthquakes occur in a correlated manner (50%), and (d) the probability that the source areas will be Areas A1 + B in the case of correlated occurrence (33%).

2) Large interplate earthquakes in northern Sanriku-Oki

The parameters of the seismic activity model are shown in Table 3.3.2-11. The locations of the fault planes are shown in Figure 3.3.2-6. The fault planes are those used in the strong motion evaluation (ERC, 2004b).

Table 3.3.2-11 Parameters of large interplate earthquakes in northern Sanriku-Oki

	Long-term evaluation	Model
Occur. prob. within 30 years	0.2%-10%	4.5%
Occur. prob. within 50 years	30%-40%	39%
Magnitude	Approx. *M*8.0	M_w 8.3
Source area	Location of the assumed source area is shown in the figure.	Fault planes used in the strong motion evaluation

Notes: The earthquake occurrence probability is that for the period starting January 2009. In calculating the probabilities for the model, the recurrence interval is assumed to follow the BPT distribution where the mean recurrence interval=97.0 years, the time of the latest event=40.6 years ago, and variance α=0.18 (the median value of 0.11-0.24). M_w is assumed to be equal to M_j.

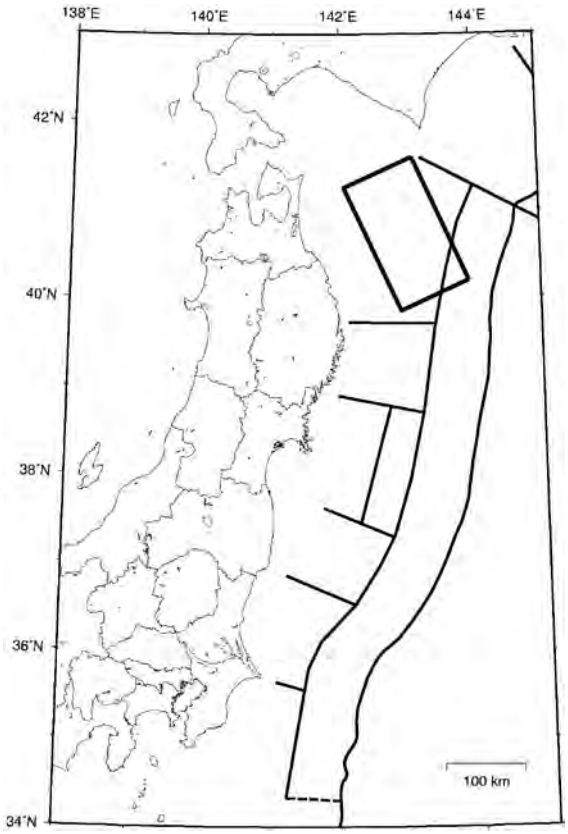

Figure 3.3.2-6 Fault plane of large interplate earthquakes in northern Sanriku-Oki

3) Large interplate earthquakes close to the offshore trenches in the Northern Sanriku-Oki to Boso-Oki regions (Tsunami earthquakes)

The parameters of the seismic activity model are shown in Table 3.3.2-12. The magnitude used is M_w 6.8, taking into account the magnitude of the 1896 Meiji Sanriku Earthquake derived by Usami (1996).

Regarding the location of the source area, the long-term evaluation has indicated that "an earthquake could occur anywhere within the area", but here, rectangular fault planes each of which is 200 km long and 50 km wide are arranged along the plate boundaries within the area, seven rows in the North-South direction and two rows in the East-West direction, and an earthquake is assumed to occur with equal probability on any of those planes. Figure 3.3.2-7 shows the location of those planes.

Table 3.3.2-12 Parameters of large interplate earthquakes close to the offshore trenches in northern Sanriku-Oki to Boso-Oki regions (Tsunami earthquakes)

	Long-term evaluation	Model
Occur. prob. within 30 years	Around 20%	20%
Occur. prob. within 50 years	Around 30%	31%
Magnitude	Approx. *Mt*8.2	M_w 6.8
Source area	Within Area C shown in Figure 3.3.2-3, but the source area cannot be specified; about 200 km long and about 50 km wide	Rectangular fault planes each of which is 200 km long and 50 km wide are arranged along the plate boundaries within the area, seven rows in the North-South direction and two rows in the East-West direction, and an earthquake is assumed to occur with equal probability on any of those planes (no. of faults: 14)

Notes: In calculating the probabilities for the model, a Poisson process is assumed where the mean recurrence interval=133.3 years. M_w is assumed to be equal to M_j, which is 6.8.

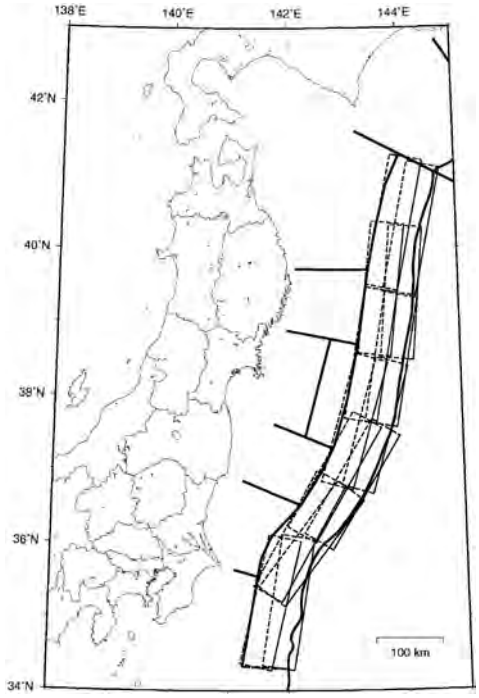

Figure 3.3.2-7 Fault planes of large interplate earthquakes close to the offshore trenches in the northern Sanriku-Oki to Boso-Oki regions (Tsunami earthquakes)

4) Large intraplate earthquakes close to the offshore trenches in the Northern Sanriku-Oki to Boso-Oki regions (normal fault type)

The parameters of the seismic activity model are shown in Table 3.3.2-13. Regarding the location of the source area, the long-term evaluation has indicated that "an earthquake could occur anywhere within the area", but here, rectangular fault planes each of which is 200 km long and 100 km wide, with a dip angle of 45° and the depth of the upper edge being 0km, are arranged within the area, seven rows in the North-South direction, and an earthquake is assumed to occur with equal probability on any of those planes. Figure 3.3.2-8 shows the location of those planes.

Table 3.3.2-13 Parameters of large intraplate earthquakes close to the offshore trenches in northern Sanriku-Oki to Boso-Oki regions (normal fault type)

	Long-term evaluation	Model
Occur. prob. within 30 years	4%-7%	5.1%
Occur. prob. within 50 years	6%-10%	8.3%
Magnitude	Approx. *M*8.2	M_w 8.2
Source area	Within Area C shown in Figure 3.3.2-3, but the source area cannot be specified; about 200 km long and about 100 km wide	Rectangular fault planes each of which is 200 km long and 100 km wide, with a dip angle of 45° and the depth of the upper edge being 0km, are arranged within the area, seven rows in the North-South direction, and an earthquake is assumed to occur with equal probability on any of those planes (no. of faults: 7)

Notes: In calculating the probabilities for the model, a Poisson process is assumed where the mean recurrence interval=575 years (the median value of 400 – 750 years). *Mw* is assumed to be equal to *Mj*.

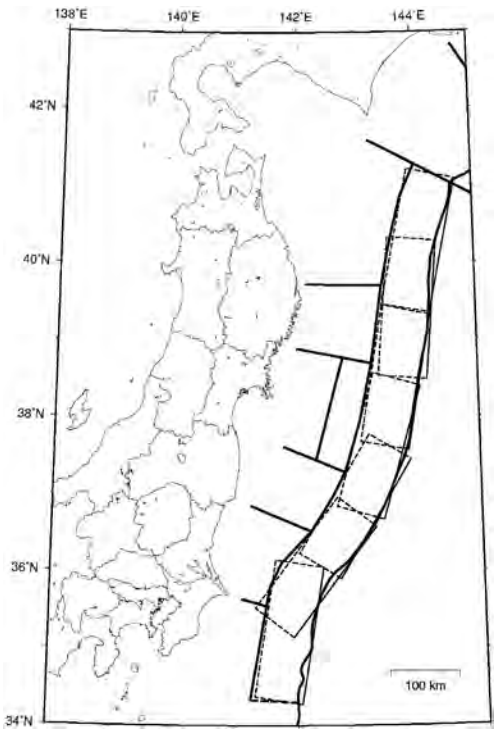

Figure 3.3.2-8 Fault planes of large intraplate earthquakes close to the offshore trenches in the northern Sanriku-Oki to Boso-Oki regions (normal fault type)

5) Interplate earthquakes other than characteristic earthquakes in northern Sanriku-Oki

The parameters of the seismic activity model are shown in Table 3.3.2-14. Regarding the magnitude, the long-term evaluation has indicated that M=7.1-7.6, but here, earthquakes of M=7.1-7.6 (0.1 intervals) are assumed to occur with the following percentages (relative probabilities) to fit the Gutenberg-Richter relation with b=0.9.

M=7.1:26.3%, M=7.2:21.4%, M=7.3:17.4%,
M=7.4:14.1%, M=7.5:11.5%, M=7.6:9.3%

Regarding the location of the source area, the long-term evaluation has indicated that "an earthquake could occur anywhere within the area", but here, for earthquakes of M_w=7.1-7.3, rectangular fault planes each of which is 40 km long and 40 km wide are arranged along the plate boundaries within the area, nine rows in the North-South direction and six rows in the East-West direction, and an earthquake is assumed to occur with equal probability on any of those planes. For earthquakes of M_w=7.4-7.6, rectangular fault planes each of which is 60 km long and 60 km wide are arranged along the plate boundaries within the area, seven rows in the North-South direction and four rows in the East-West direction, and an earthquake is assumed to occur with equal probability on any of those planes. Figure 3.3.2-9 shows the location of those planes.

Table 3.3.2-14 Parameters of interplate earthquakes other than characteristic earthquakes in northern Sanriku-Oki

	Long-term evaluation	Model
Occur. prob. within 30 years	About 90%	93%
Occur. prob. within 50 years	-	99%
Magnitude	M7.1 – M7.6	M_w 7.1-7.6
Source area	Within Area B shown in Figure 3.3.2-3	For earthquakes of M_w=7.1-7.3, rectangular fault planes each of which is 40 km long and 40 km wide are arranged along the plate boundaries within the area, nine rows in the North-South direction and six rows in the East-West direction (no. of faults: 54); for earthquakes of M_w=7.4-7.6, rectangular fault planes each of which is 60 km long and 60 km wide are arranged along the plate boundaries within the area, seven rows in the North-South direction and four rows in the East-West direction (no. fault planes: 28); an earthquake is assumed to occur with equal probability on any of those planes.

Notes: In calculating the probabilities for the model, a Poisson process is assumed where the mean recurrence interval=11.3 years. The occurrence probability within 50 years is not indicated in the long-term evaluation. M_w is assumed to be equal to M_j.

(a) Earthquakes of *M*7.1-7.3

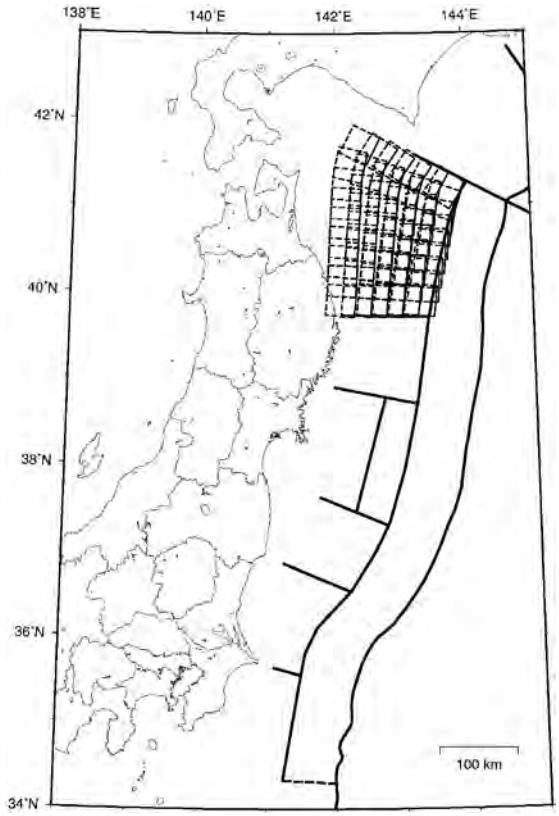

(b) Earthquakes of *M*7.4-7.6

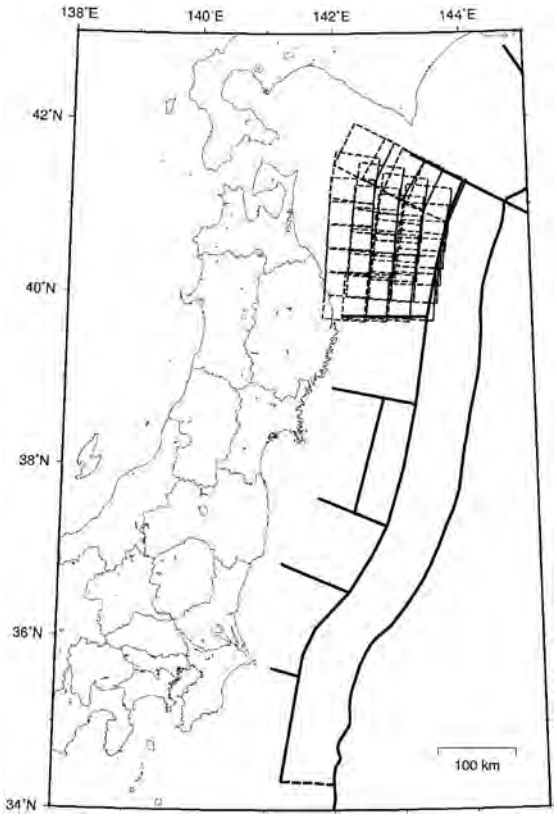

Figure 3.3.2-9 Fault planes of interplate earthquakes other than characteristic earthquakes in northern Sanriku-Oki

6) Interplate earthquakes in Fukushima-ken-Oki

The parameters of the seismic activity model are shown in Table 3.3.2-15. The long-term evaluation has indicated that the mean recurrence interval is 400 years or more, but here, it is assumed to be 400 years. Since there has been a case where multiple large earthquakes occurred successively during a period of about two days, it is assumed that multiple earthquakes would occur successively during a short period at the time of the next earthquake. However, they are treated as a single event in terms of time series. The influence of the successive occurrence is taken into consideration by assuming that three earthquakes occur on the same fault plane when evaluating the exceedance probability of the ground motion intensity.

Regarding the location of the source area, the long-term evaluation has indicated that "an earthquake could occur anywhere within the area", but here, rectangular fault planes each of which is 50 km long and 50 km wide are arranged along the plate boundaries within the area, three rows in the North-South direction and five rows in the East-West direction, and an earthquake is assumed to occur with equal probability on any of those planes. Figure 3.3.2-10 shows the location of those planes.

Table 3.3.2-15 Parameters of interplate earthquakes in Fukushima-ken-Oki

	Long-term evaluation	Model
Occur. prob. within 30 years	About 7% or less	7.2%
Occur. prob. within 50 years	About 10% or less	12%
Magnitude	Approx. *M*7.4; successive occurrence of multiple earthquakes	M_w 7.4 (Successive occurrence is taken into consideration in the ground motion evaluation)
Source area	Within Area F shown in Figure 3.3.2-3	Rectangular fault planes each of which is 50 km long and 50 km wide are arranged along the plate boundaries within the area, three rows in the North-South direction and five rows in the East-West direction, and an earthquake is assumed to occur with equal probability on any of those planes (no. of faults: 15)

Notes: In calculating the probabilities for the model, a Poisson process is assumed where the mean recurrence interval=400 years. M_w is assumed to be equal to M_j.

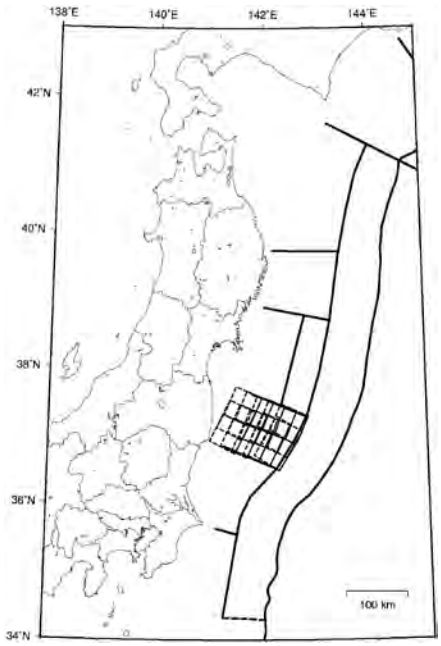

Figure 3.3.2-10 Fault planes of interplate earthquakes in Fukushima-ken-Oki

7) Interplate earthquakes in Ibaraki-ken-Oki

In the past, the occurrence probability of subduction-zone earthquakes in Ibaraki-ken-Oki had been calculated by assuming a Poisson process, and in the modeling process, an earthquake had been assumed to occur anywhere within the target area. However, taking into account the earthquake of May 8, 2008, a fault plane where earthquakes resemble characteristic earthquakes was newly determined (WGASHM, SLTE/SESGM, ERC, 2008).

During the 68 years from 1940 when the influence of the 1923 Kanto Earthquake on seismic activities in the surrounding area began to diminish until July 1, 2008, earthquakes with nearly the same seismic source as the earthquake of May 8, 2008 and with a magnitude of *M*6.7 or more occurred five times, in 1943, 1961, 1965, 1982, and 2008 (Table 3.3.2-16). Among these, the earthquakes in 1961 and 1965 are treated as a single characteristic earthquake, considering the locations of their seismic sources and their magnitude. As a result, four earthquakes of a similar size as characteristic earthquakes have occurred during the period of about 68 years, and the mean recurrence interval is 21.7 years. The assumed magnitude is 7.0, since the magnitude of the 1982 earthquake and the 2008 earthquake were 7.0, and that of the 1961 earthquake and the 1965 earthquake would total to about *M*7.0 if they are regarded as a single earthquake.

As for the location of the fault plane, a single flat plane along the plate boundary is determined in such a manner as to incorporate areas where substantial slip was observed (asperities) in the slip distribution of the 1982 earthquake (Murotani et al., 2003 ; Mochizuki et al., 2008) and in the slip distribution of the 2008 earthquake (Nagoya University, 2008) derived through seismic source inversion analysis. The size of the determined fault plane has been confirmed to generally correspond to the fault size that is assumed from the earthquake magnitude (7.0) (Murotani et al., 2008).

The parameters of the seismic activity model are shown in Table 3.3.2-17. The locations of the fault planes are shown in Figure 3.3.2-11. Here, some of the contents of deliberations for the revision of long-term evaluation are adopted ahead of the actual revision, in modeling. The later-revised long-term evaluation slightly differs from the model in this study, since the mean recurrence interval in the long-term evaluation is obtained by also considering the 1923 earthquake as a characteristic earthquake, although the 1923 earthquake had not been considered in the past due to being regarded as an earthquake on which the influence of the 1923 Kanto Earthquake remains (ERC, 2009b).

Table 3.3.2-16 Earthquakes treated as characteristic earthquakes in Ibaraki-ken-Oki (based on data from the ERC).

Date of occurrence	*M*
Apr. 11, 1943	6.7
Jan. 16, 1961	6.8
Sep. 18, 1965	6.7
Jul. 23, 1982	7.0
May 8, 2008	7.0

Note: The 1961 earthquake is included in the 1965 earthquake to be treated as a characteristic earthquake.

Table 3.3.2-17 Parameters of interplate earthquakes in Ibaraki-ken-Oki

	Long-term evaluation	Model
Occur. prob. within 30 years	-	96% (once: 95%, twice: 1.1%)
Occur. prob. within 50 years	-	Nearly 100% (once: 13%, twice: 85%, three times: 2.2%)
Magnitude	-	M_w 7.0
Source area	-	Fault planes are determined while taking into account the earthquake of May 8, 2008

Notes: The earthquake occurrence probability is that for the period starting January 2009. In calculating the probabilities for the model, the recurrence interval is assumed to follow the BPT distribution where the mean recurrence interval=21.7 years, the time of the latest event=0.7 years ago, and variance α=0.21 (the median value of 0.18-0.24).

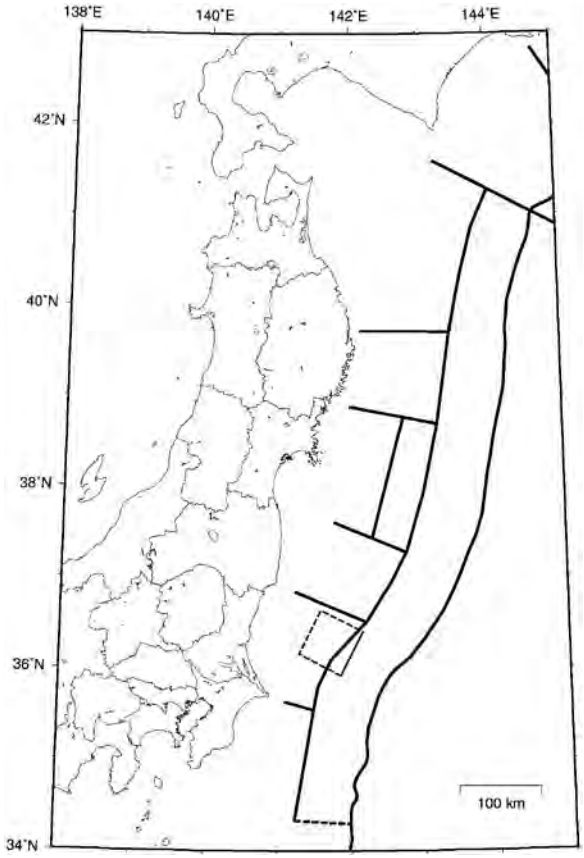

Figure 3.3.2-11 Fault plane of interplate earthquakes in Ibaraki-ken-Oki

(3) Earthquakes along the Kuril Trench

With regard to seismic activities of subduction-zone earthquakes along the Kuril Trench, the "Long-term Evaluation of Seismic Activity Along the Kuril Trench" (ERC, 2003a) was published in March 2003. Later, as the Tokachi-Oki Earthquake (*M*8.0) occurred on September 26, 2003 and the Kushiro-Oki Earthquake (*M*7.1) occurred on November 29, 2004, the "Long-term Evaluation of Seismic Activity Along the Kuril Trench [Second Edition]" (ERC, 2004d) was published in December 2004, by also incorporating the subsequent survey and research results.

Figure 3.3.2-12 shows the areas covered in evaluation of subduction-zone earthquakes along the Kuril Trench. Here, earthquakes are grouped as follows based on the results of the long-term evaluation mentioned above.

1) Interplate earthquakes (*M*8 class and *M*7 class)
- *M*8 class interplate earthquakes: the Tokachi-Oki Earthquake, the Nemuro-Oki Earthquake, the Shikotanto-Oki Earthquake, the Etorofuto-Oki Earthquake (including correlated occurrence of the Tokachi-Oki Earthquake and the Nemuro-Oki Earthquake)
- Relatively small interplate earthquakes: the Tokachi-Oki and Nemuro-Oki regions and the Shikotanto-Oki and Etorofuto-Oki regions

2) Intraplate earthquakes
- Relatively shallow earthquakes within a subducted plate (about 50 km deep, about *M*8)
- Relatively deep earthquakes within a subducted plate (about 100 km deep, about *M*7.5)

The following policy was set for modeling.

- For "*M*8 class interplate earthquakes", characteristic earthquakes are assumed to occur on specific fault planes in the four areas shown in Figure 3.3.2-12. However, for the Tokachi-Oki Earthquake and the Nemuro-Oki Earthquake, the case of independent occurrence and the case of correlated occurrence between the two earthquakes are both considered. The probability of correlated occurrence is assumed that "where the two earthquakes both occur within the target period (within 30 years or 50 years), they occur in a correlated manner with a 16.7% probability (once out of six times)". This probability (once out of six times) has been determined based on the mean recurrence interval of *M*8 class interplate earthquakes (72.2 years) and the approximate mean recurrence interval of correlated occurrence of the two earthquakes (about 400-500 years).
- Regarding the location of the source area, specific fault planes are determined for "*M*8 class interplate earthquakes", but for "relatively small interplate earthquakes", "relatively shallow earthquakes within a subducted plate", and "relatively deep earthquakes within a subducted plate", multiple fault planes are arranged within the proposed areas, and an earthquake is assumed to occur with equal probability on any of those planes. The area where "relatively small interplate earthquakes" occur shall be an area where the upper surface of the plate is between 20-60 km deep. For "relatively shallow earthquakes within a subducted plate", the fault plane of the 1994 Eastern Hokkaido-Oki Earthquake is taken into account, and for "relatively deep earthquakes within a subducted plate", the fault plane of the 1993 Kushiro-Oki Earthquake is taken into account.

The parameters of the seismic activity model of each earthquake are shown below.

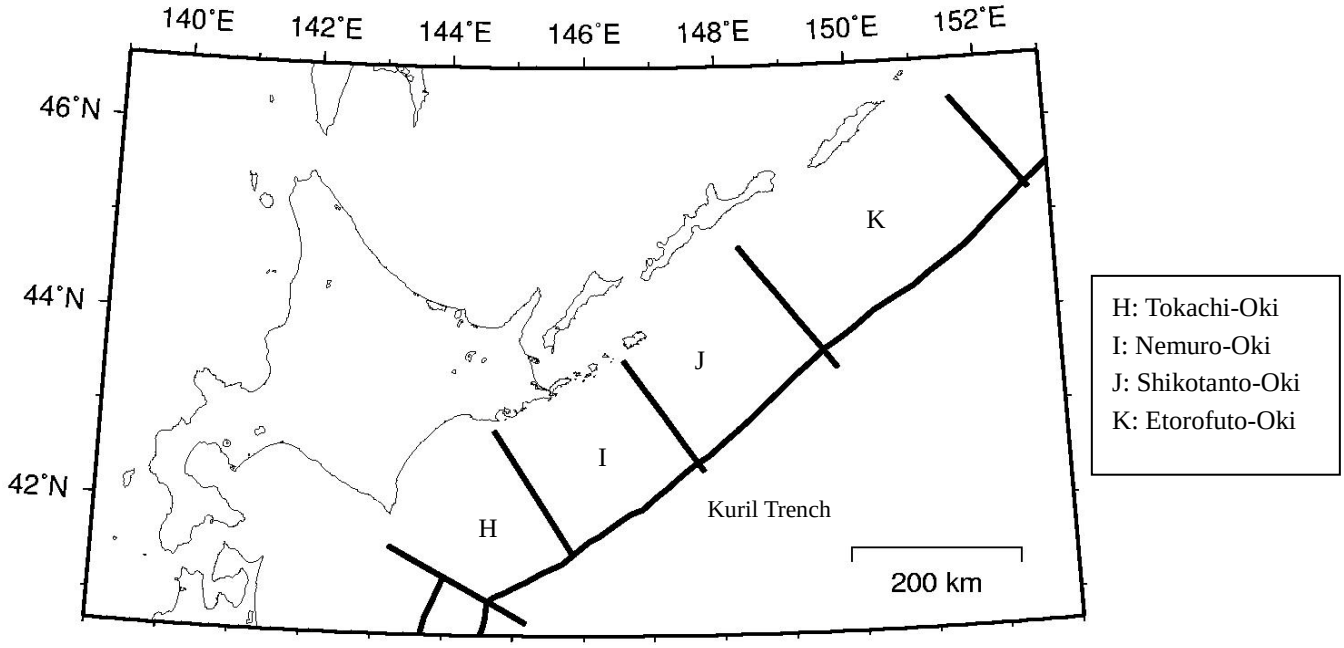

Figure 3.3.2-12 Areas covered in evaluation of subduction-zone earthquakes along the Kuril Trench

1) Tokachi-Oki Earthquake/Nemuro-Oki Earthquake

For the Tokachi-Oki Earthquake and the Nemuro-Oki Earthquake, the case of independent occurrence and the case of correlated occurrence between the two earthquakes are both considered. The probability of correlated occurrence of the two earthquakes is assumed as follows.

<u>When the two earthquakes both occur within the target period (30 years or 50 years), they occur in a correlated manner with a 16.7% probability (once out of six times)</u>

This probability of correlated occurrence (once out of six times) has been determined based on the mean recurrence interval of *M*8 class interplate earthquakes (72.2 years) and the approximate mean recurrence interval of the two earthquakes (about 400-500 years).

Table 3.3.2-18 shows the occurrence probabilities of the two earthquakes. For the Nemuro-Oki Earthquake, the probability of occurring twice within 50 years is not "nearly 0%". Under the conditions above, the occurrence patterns of the three earthquakes (Tokachi-Oki Earthquake independent, Nemuro-Oki Earthquake independent, and Tokachi-Oki Earthquake + Nemuro-Oki Earthquake) total to the eight cases shown in Table 3.3.2-19.The probability of occurrence of each case is also shown in Table 3.3.2-19.

As for the location of the fault plane, a specific fault plane is determined for each of the three earthquakes above. The magnitude for the case of correlated occurrence directly uses the earthquake magnitude (*M*8.3) used in the long-term evaluation of the Tokachi-Oki/Nemuro-Oki Earthquake.

The magnitudes of these earthquakes are shown in Table 3.3.2-20 and the locations of the fault planes are shown in Figure 3.3.2-14.

Table 3.3.2-18 Occurrence probabilities of the Tokachi-Oki Earthquake/Nemuro-Oki Earthquake

Earthquake	Evaluation period of occurrence probability	Long-term evaluation	Model	
			Occurring once	Occurring twice
Tokachi-Oki Earthquake	Within 30 years	0.2%-2%	0.62%	Nearly 0%
	Within 50 years	About 20%	20%	Nearly 0%
Nemuro-Oki Earthquake	Within 30 years	About 40%	41%	Nearly 0%
	Within 50 years	About 80%	77%	0.37%

Notes: The earthquake occurrence probability is that for the period starting January 2009. In calculating the probabilities for the model, the recurrence interval is assumed to follow the BPT distribution where the mean recurrence interval=72.2 years, the time of the latest event=5.3 years ago (Tokachi-Oki) and 35.5 years ago (Nemuro-Oki), and variance α=0.28 (the median value of 0.24-0.32) based on the long-term evaluation results. Probability less than 10^{-3}% is indicated as "Nearly 0%".

Table 3.3.2-19 Occurrence probabilities of the Tokachi-Oki Earthquake/Nemuro-Oki Earthquake (including the case of correlated occurrence)

	Case	Probability within 30 years	Probability within 50 years
(1)	"Tokachi-Oki" 0 times * "Nemuro-Oki" 0 times	58%	18%
(2)	"Tokachi-Oki" 0 times * "Nemuro-Oki" once independent	41%	61%
(3)	"Tokachi-Oki" once independent * "Nemuro-Oki" 0 times	0.37%	4.7%
(4)	"Tokachi-Oki" once independent * "Nemuro-Oki" once independent	0.21%	13%
(5)	"Tokachi-Oki" once + "Nemuro-Oki" once correlated	0.043%	2.6%
(6)	"Tokachi-Oki" 0 times * "Nemuro-Oki" twice independent	Nearly 0%	0.30%
(7)	"Tokachi-Oki" once independent * "Nemuro-Oki" twice independent	Nearly 0%	0.063%
(8)	"Tokachi-Oki" once + "Nemuro-Oki" twice – once correlated	Nearly 0%	0.012%
	Total	100%	100%

Notes: "Tokachi-Oki" denotes the Tokachi-Oki Earthquake, and "Nemuro-Oki" denotes the Nemuro-Oki Earthquake. The occurrence probability is that for the period starting January 2009. Probability less than 10^{-3}% is indicated as "Nearly 0%".

For example, the probability within 50 years for (4) above is calculated to be about 13%, by combining (a) the probability that the Tokachi-Oki Earthquake will occur once within 50 years (20%) and (b) the probability that the Nemuro-Oki Earthquake will occur once within 50 years (77%) shown in Table 3.3.2-18, as well as (c) the probability that the two earthquakes will not correlate (100-16.7=83.3%).

Table 3.3.2-20 Magnitude of the Tokachi-Oki/Nemuro-Oki Earthquake (including the case of correlated occurrence)

	Long-term evaluation	Model
Tokachi-Oki Earthquake: independent	Approx. *M*8.1	M_w 8.1
Nemuro-Oki Earthquake: independent	About *M*7.9	M_w 7.9
Tokachi-Oki Earthquake+ Nemuro-Oki Earthquake	About *M*8.3	M_w 8.3

Notes: For the cases of independent occurrence, M_w is assumed to be equal to M_j. The magnitude for the case of correlated occurrence directly uses the earthquake magnitude used in the long-term evaluation of the Tokachi-Oki/Nemuro-Oki Earthquake.

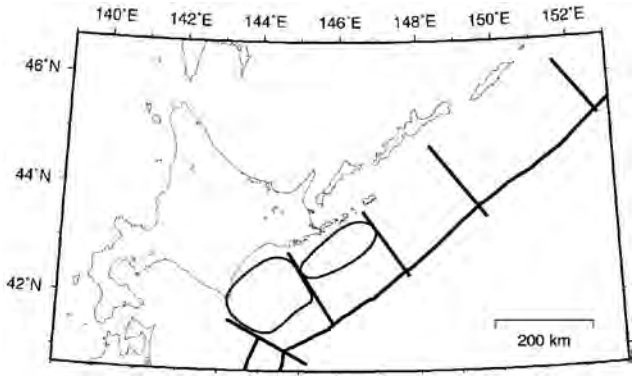

Figure 3.3.2-13 Fault planes of the Tokachi-Oki/Nemuro-Oki Earthquake (for the case of independent occurrence)

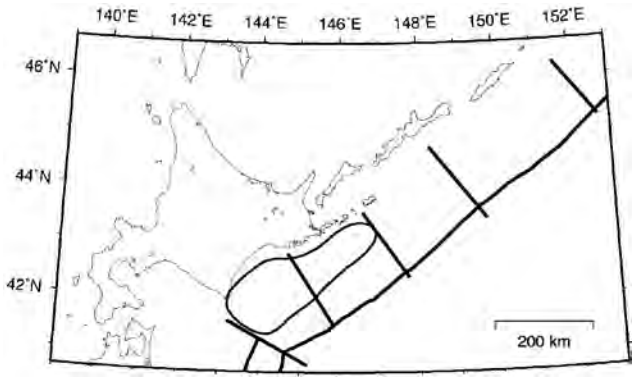

Figure 3.3.2-14 Fault plane of the Tokachi-Oki/Nemuro-Oki Earthquake (for the case of correlated occurrence)

2) Shikotanto-Oki Earthquake/Etorofuto-Oki Earthquake

For the Shikotanto-Oki Earthquake and the Etorofuto-Oki Earthquake, models are built according to the long-term evaluation results. The parameters of the seismic activity model are shown in Table 3.3.2-21 and Table 3.3.2-22. The locations of the fault planes are shown in Figure 3.3.2-15.

Table 3.3.2-21 Parameters of the Shikotanto-Oki Earthquake

	Long-term evaluation	Model
Occur. prob. within 30 years	Around 50%	49%
Occur. prob. within 50 years	Around 80%	82% (once: 81%, twice: 0.60%)
Magnitude	Approx. *M*7.8	M_w 7.8
Source area	Location of the assumed source area is shown in the figure.	Specific fault planes that comply with the source area assumed in the long-term evaluation are determined.

Notes: The earthquake occurrence probability is that for the period starting January 2009. In calculating the probabilities for the model, the recurrence interval is assumed to follow the BPT distribution where the mean recurrence interval=72.2 years, the time of the latest event=39.4 years ago, and variance α=0.28 (the median value of 0.24-0.32) based on the long-term evaluation results. For the probability within 50 years, the case of occurring twice is also considered. M_w is assumed to be equal to M_j.

Table 3.3.2-22 Parameters of the Etorofuto-Oki Earthquake

	Long-term evaluation	Model
Occur. prob. within 30 years	Around 60%	59%
Occur. prob. within 50 years	80%-90%	86% (once: 85%, twice: 1.0%)
Magnitude	Approx. *M*8.1	M_w 8.1
Source area	Location of the assumed source area is shown in the Figure 3.3.2-15.	Specific fault planes that comply with the source area assumed in the long-term evaluation are determined.

Notes: The earthquake occurrence probability is that for the period starting January 2009. In calculating the probabilities for the model, the recurrence interval is assumed to follow the BPT distribution where the mean recurrence interval=72.2 years, the time of the latest event=45.2 years ago, and variance α=0.28 (the median value of 0.24-0.32) based on the long-term evaluation results. For the probability within 50 years, the case of occurring twice is also considered. M_w is assumed to be equal to M_j.

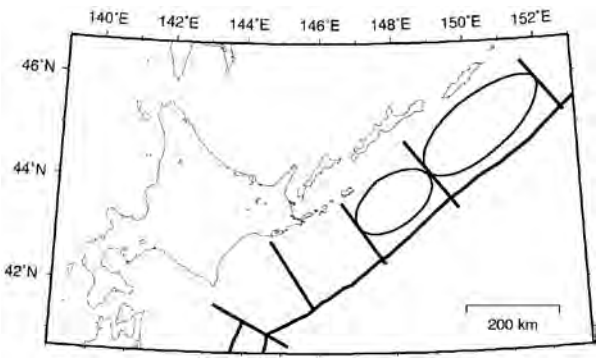

Figure 3.3.2-15 Fault planes of the Shikotanto-Oki Earthquake/Etorofuto-Oki Earthquake

3) Relatively small interplate earthquakes

With regard to the relatively small interplate earthquakes, those in the Tokachi-Oki and Nemuro-Oki regions and those in the Shikotanto-Oki and Etorofuto-Oki regions are modeled separately according to the long-term evaluation results. Table 3.3.2-23 shows the parameters of the seismic activity model of relatively small interplate earthquakes in the Tokachi-Oki and Nemuro-Oki regions, and Table 3.3.2-24 shows the parameters of the seismic activity model of relatively small interplate earthquakes in the Shikotanto-Oki and Etorofuto-Oki regions.

Regarding the location of the source area, the long-term evaluation has indicated that "an earthquake could occur anywhere" within the area", but here, rectangular fault planes each of which is 35 km long and 35 km wide (equivalent to M_j 7.1) are arranged along the plate boundaries within each area, where the upper plane of the plate is between 20-60 km. For the Tokachi-Oki and Nemuro-Oki regions, 149 of such planes are arranged (18-22 rows × 7-9 rows), and for the Shikotanto-Oki and Etorofuto-Oki regions, 156 of such planes are arranged (29 rows × 5-7 rows), and an earthquake is assumed to occur with equal probability on any of those planes. The locations of the fault planes of earthquakes in the respective regions are shown in Figure 3.3.2-16 and Figure 3.3.2-17.

Table 3.3.2-23 Parameters of relatively small interplate earthquakes in the Tokachi-Oki and Nemuro-Oki regions

	Long-term evaluation	Model
Occur. prob. within 30 years	Around 80%	82%
Occur. prob. within 50 years	Around 90%	94%
Magnitude	Approx. *M*7.1	M_w 7.1
Source area	Within Area H or I shown in Figure 3.3.2-12, but the source area cannot be specified	Rectangular fault planes each of which is 35 km long and 35 km wide are arranged along the plate boundaries within the area, 18-22 rows horizontally to the trench and 7-9 rows vertically to the trench, and an earthquake is assumed to occur with equal probability on any of those planes (no. of faults: 149)

Notes: In calculating the probabilities for the model, a Poisson process is assumed where the mean recurrence interval=17.5 years (five times within 105 years). M_w is assumed to be equal to M_j.

Table 3.3.2-24 Parameters of relatively small interplate earthquakes in the Shikotanto-Oki and Etorofuto-Oki regions

	Long-term evaluation	Model
Occur. prob. within 30 years	Around 90%	94%
Occur. prob. within 50 years	Around 90% or more	99%
Magnitude	Approx. *M*7.1	M_w 7.1
Source area	Within Area J or K shown in Figure 3.3.2-12, but the source area cannot be specified	Rectangular fault planes each of which is 35 km long and 35 km wide are arranged along the plate boundaries within the area, 29 rows horizontally to the trench and 5-7 rows vertically to the trench, and an earthquake is assumed to occur with equal probability on any of those planes (no. of faults: 156)

Notes: In calculating the probabilities for the model, a Poisson process is assumed where the mean recurrence interval=10.5 years (four times within 42 years). M_w is assumed to be equal to M_j.

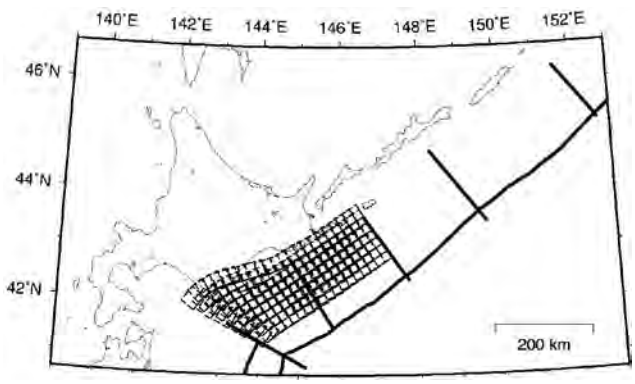

Figure 3.3.2-16 Fault planes of relatively small interplate earthquakes in the Tokachi-Oki and Nemuro-Oki regions

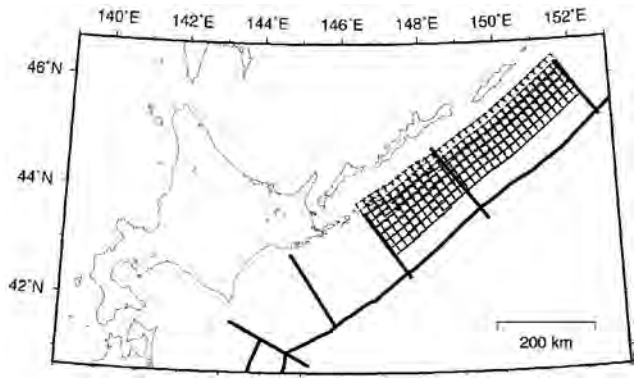

Figure 3.3.2-17 Fault planes of relatively xmall interplate earthquakes in the Shikotanto-Oki and Etorofuto-Oki regions

4) Intraplate earthquakes

With regard to the intraplate earthquakes (*M*8 class), relatively shallow earthquakes within a subducted plate (about 50 km deep) and relatively deep earthquakes within a subducted plate (about 100 km deep) are modeled separately according to the long-term evaluation results. Table 3.3.2-25 and Table 3.3.2-26 show the parameters of the respective types of earthquakes.

In determining the fault planes for relatively shallow earthquakes, the model of the 1994 Eastern Hokkaido-Oki Earthquake by Kikuchi and Kanamori (1995) is taken into account, and fault planes each of which is 120 km long and 60 km wide, with a dip angle of 75°, and positioned so that its upper edge is aligned with the 20 km depth contour of the plate boundary are arranged at random (half overlapped) along the depth contour within the four areas from Tokachi-Oki to Etorofuto-Oki.

Table 3.3.2-25 Parameters of relatively shallow earthquakes within a subducted plate

	Long-term evaluation	Model
Occur. prob. within 30 years	Around 30%	30%
Occur. prob. within 50 years	Around 50%	45%
Magnitude	Approx. *M*8.2	M_w 8.2
Source area	Depth of the source area is roughly around 50 km, but the source area cannot be specified	Fault planes each of which is 120 km long and 60 km wide, with a dip angle of 75°, and positioned so that its upper edge is aligned with the 20 km depth contour of the plate boundary are arranged at random along the depth contour within the four areas from Tokachi-Oki to Etorofuto-Oki (no. of faults: 13)

Notes: In calculating the probabilities for the model, a Poisson process is assumed where the mean recurrence interval=82.8 years (twice within 165.7 years). M_w is assumed to be equal to M_j.

Table 3.3.2-26 Parameters of relatively deep earthquakes within a subducted plate

	Long-term evaluation	Model
Occur. prob. within 30 years	Around 70%	67%
Occur. prob. within 50 years	Around 80%	84%
Magnitude	Approx. *M*7.5	M_w 7.5
Source area	Depth of the source area is roughly around 100 km, but the source area cannot be specified	Fault planes, each of which is 60 km long and 40 km wide, horizontal, and positioned so that the 100 km depth line directly below the 60 km depth contour of the upper surface of the plate comes in the middle of the fault plane, are arranged at random along the depth contour within the four areas from Tokachi-Oki to Etorofuto-Oki (no. of faults: 29)

Notes: In calculating the probabilities for the model, a Poisson model is assumed where the mean recurrence interval=27.3 years (three times within 82 years). M_w is assumed to be equal to M_j.

For relatively deep earthquakes, the model of the 1993 Kushiro-Oki Earthquake by Ide and Takeo (1995) is taken into account, and fault planes, each of which is 60 km long and 40 km wide, horizontal, and positioned so that the 100 km depth line directly below the 60 km depth contour of the upper surface of the plate comes in the middle of the fault plane, are arranged at random (half overlapped) along the depth contour within the four areas from Tokachi-Oki to Etorofuto-Oki. Figure 3.3.2-18 illustrates the positions of the fault planes. Figure 3.3.2-19 and Figure 3.3.2-20 show the resulting fault plane models.

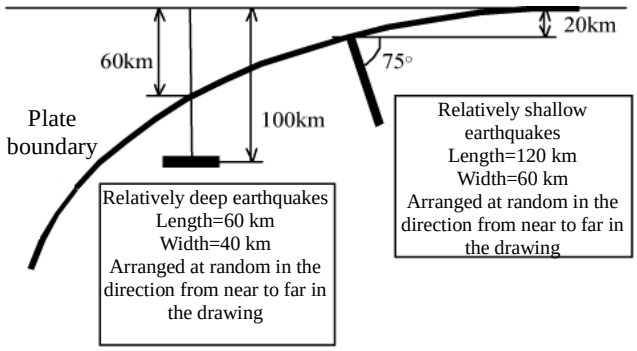

Figure 3.3.2-18 Schematic drawing of positions of fault planes of intraplate earthquakes (*M*8 class)

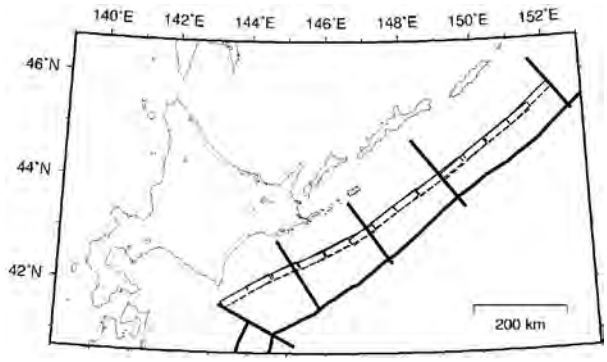

Figure 3.3.2-19 Fault planes of relatively shallow earthquakes within a wubducted plate

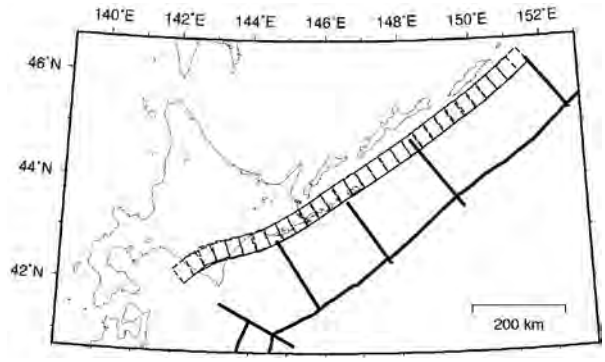

Figure 3.3.2-20 Fault planes of relatively deep earthquakes within a subducted plate

(4) Earthquakes in the eastern margin of the Japan Sea

With regard to subduction-zone earthquakes in the eastern margin of the Japan Sea, seismic activities are modeled based on the "Long-Term Evaluation of Seismic Activity in the Eastern Margin of the Japan Sea" (ERC, 2003c). Figure 3.3.2-21 shows the areas covered in evaluation of subduction-zone earthquakes in the eastern margin of the Japan Sea along with fault planes of past earthquakes.

The following policy was set for modeling.

- The areas covered in evaluation are, from the north, Hokkaido-hokusei-Oki (Area L shown in Figure 3.3.2-21), Hokkaido-seiho-Oki (Area M in Figure 3.3.2-21: 1940 Shakotan-hanto-Oki Earthquake), Hokkaido-nansei-Oki (Area N in Figure 3.3.2-21: 1993 Hokkaido-nansei-Oki Earthquake), Aomori-ken-seiho-Oki (Area O in Figure 3.3.2-21: 1983 Nihonkai-chubu Earthquake), Akita-ken-Oki (Area P in Figure 3.3.2-21), Yamagata-ken-Oki (Area Q in Figure 3.3.2-21: 1833 Shonai-Oki Earthquake), Niigata-ken-hokubu-Oki (Area R in Figure 3.3.2-21: 1964 Niigata Earthquake), and Sadogashima-hoppo-Oki (Area S in Figure 3.3.2-21). Among these, areas that have earthquake names in parentheses, namely, Hokkaido-seiho-Oki, Hokkaido-nansei-Oki, Aomori-ken-seiho-Oki, Yamagata-ken-Oki, and Niigata-ken-hokubu-Oki, are known to have experienced an earthquake of *M*7.5 or more in the past. Hokkaido-hokusei-Oki, Akita-ken-Oki, and Sadogashima-hoppo-Oki are not known to have experienced an earthquake of *M*7.5 or more in the past.
- In the calculation of the earthquake occurrence probability, if the mean recurrence interval or variance α of the recurrence interval has been indicated in a range of values, the median value of the parameter is used. As for Akita-ken-Oki, Yamagata-ken-Oki, and Niigata-ken-hokubu-Oki for which the mean recurrence interval is indicated to be around 1,000 years or more, the mean recurrence interval is assumed to be 1,000 years in calculating the earthquake occurrence probability.
- Regarding the location of the source area, for areas that are known to have experienced a large earthquake in the past, fault planes are determined based on the fault models of those earthquakes. For areas that are not known to have experienced a large earthquake in the past, rectangular fault planes each of which has the following dimension and angle are positioned so that the upper edge of the fault planes is 3 km deep: 140 km long and 24 km wide with a dip angle of 45° for Hokkaido-hokusei-Oki, 90 km long and 24 km wide with a dip angle of 45° for Akita-ken-Oki, and 140 km long and 34 km wide with a dip angle of 30° for Sadogashima-hoppo-Oki. As for the dip direction, all of these fault planes are assumed to either dip east or dip west with equal probability. Regarding Hokkaido-hokusei-Oki and Sadogashima-hoppo-Oki, it has been indicated that an earthquake could occur anywhere within the area. Here, three faults are arranged within each area, and an earthquake is assumed to occur with equal probability on any of those faults.

The parameters of the seismic activity model of each earthquake are shown below.

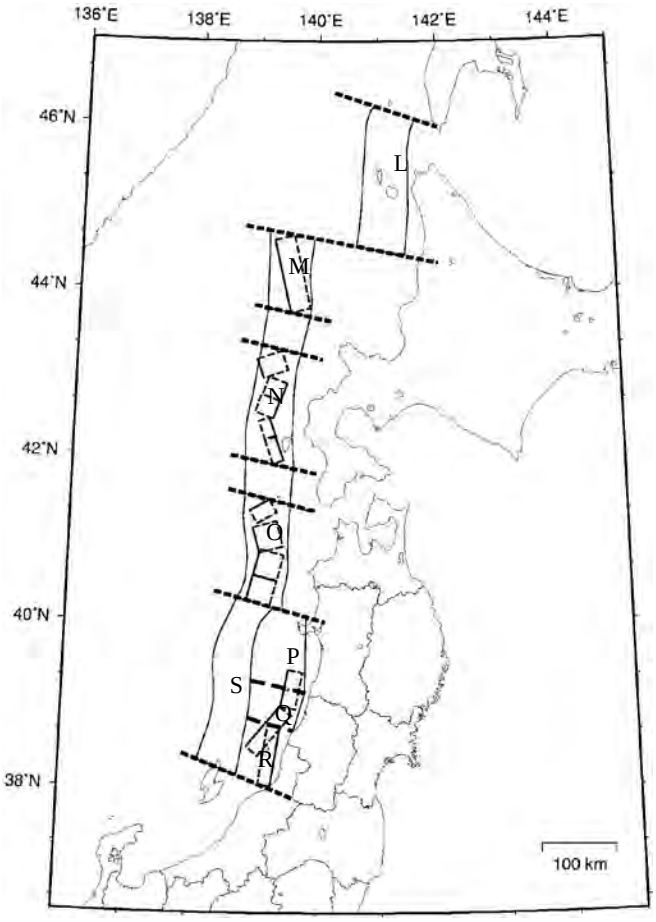

L: Hokkaido-hokusei-Oki
M: Hokkaido-seiho-Oki
N: Hokkaido-nansei-Oki
O: Aomori-ken-seiho-Oki
P: Akita-ken-Oki
Q: Yamagata-ken-Oki
R: Niigata-ken-hokubu-Oki
S: Sadogashima-hoppo-Oki

Fault planes of past earthquakes
- Area M: 1940 Shakotan-hanto-Oki Earthquake
- Area N: 1993 Hokkaido-nansei-Oki Earthquake
- Area O: 1983 Nihonkai-chubu Earthquake
- Area Q: 1833 Shonai-Oki Earthquake
- Area R: 1964 Niigata Earthquake

Figure 3.3.2-21 Areas covered in evaluation of subduction-zone earthquake in the eastern margin of the Japan Sea and fault planes of past earthquakes

1) Hokkaido-hokusei-Oki Earthquake

The parameters of the seismic activity model are shown in Table 3.3.2-27, and the locations of the fault planes are shown in Figure 3.3.2-22. Regarding the location of the source area, the long-term evaluation has indicated that "an earthquake could occur anywhere within the area", but here, rectangular fault planes each of which is 140 km long and 24 km, with a dip angle of 45° and the depth of the upper edge being 3 km, are arranged within the area, three rows in the North-South direction (either east-dipping or west-dipping), and an earthquake is assumed to occur with equal probability (1/6) on any of those planes.

Table 3.3.2-27 Parameters of the Hokkaido-hokusei-Oki Earthquake

	Long-term evaluation	Model
Occur. prob. within 30 years	0.006%-0.1%	0.046%
Occur. prob. within 50 years	0.01%-0.2%	0.082%
Magnitude	Around *M*7.8	M_w 7.8
Source area	Location of the assumed source area is shown in the figure Figure 3.3.2-22.	Rectangular fault planes each of which is 140 km long and 24 km wide (dip angle: 45°, east-dipping or west-dipping) are arranged within the area, three rows in the North-South direction, and an earthquake is assumed to occur with equal probability on any of those planes.

Notes: The earthquake occurrence probability is that for the period starting January 2009. In calculating the probabilities for the model, the recurrence interval is assumed to follow the BPT distribution where the mean recurrence interval=3,900 years, the time of the latest event=2,100 years ago, and variance α=0.21 (the median value of 0.17-0.24). M_w is assumed to be equal to M_j.

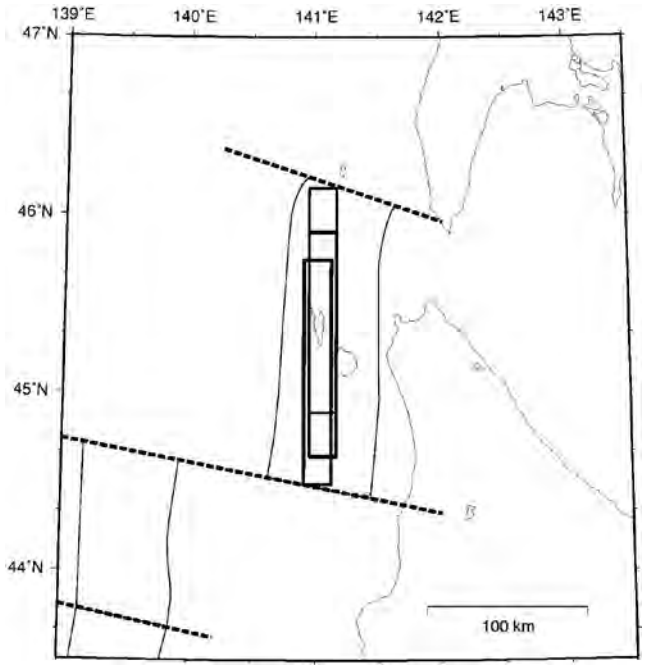

Figure 3.3.2-22 Fault planes of the Hokkaido-hokusei-Oki Earthquake

2) Hokkaido-seiho-Oki Earthquake

The parameters of the seismic activity model are shown in Table 3.3.2-28. The parameters of the fault planes are those used in the fault model of the 1940 Shakotan-hanto-Oki Earthquake (Satake (1986)) (Figure 3.3.2-21).

3) Hokkaido-nansei-Oki Earthquake

The parameters of the seismic activity model are shown in Table 3.3.2-29. The parameters of the fault planes are those used in the fault model of the 1993 Hokkaido-nansei-Oki Earthquake (Tanioka et al. (1995)) (Figure 3.3.2-21).

4) Aomori-ken-seiho-Oki Earthquake

The parameters of the seismic activity model are shown in Table 3.3.2-30. The parameters of the fault planes are those used in the fault model of the 1983 Nihonkai-chubu Earthquake (main shock=Sato (1985), aftershock=Abe (1987)) (Figure 3.3.2-21).

Table 3.3.2-28 Parameters of the Hokkaido-seiho-Oki Earthquake

	Long-term evaluation	Model
Occur. prob. within 30 years	Nearly 0%	Nearly 0%
Occur. prob. within 50 years	Nearly 0%	Nearly 0%
Magnitude	Approx. *M*7.5	M_w 7.5
Source area	Fault plane of the 1940 Shakotan-hanto-Oki Earthquake	Fault plane of the 1940 Shakotan-hanto-Oki Earthquake

Table 3.3.2-29 Parameters of the Hokkaido-nansei-Oki Earthquake

	Long-term evaluation	Model
Occur. prob. within 30 years	Nearly 0%	Nearly 0%
Occur. prob. within 50 years	Nearly 0%	Nearly 0%
Magnitude	Approx. *M*7.8	M_w 7.8
Source area	Fault planes of the 1993 Hokkaido-nansei-Oki Earthquake	Fault planes of the 1993 Hokkaido-nansei-Oki Earthquake

Table 3.3.2-30 Parameters of the Aomori-ken-seiho-Oki Earthquake

	Long-term evaluation	Model
Occur. prob. within 30 years	Nearly 0%	Nearly 0%
Occur. prob. within 50 years	Nearly 0%	Nearly 0%
Magnitude	Approx. *M*7.7	M_w 7.7
Source area	Fault planes of the 1983 Nihonkai-chubu Earthquake	Fault planes of the 1983 Nihonkai-chubu Earthquake

Notes: In all tables from Table 3.3.2-28 to Table 3.3.2-30, the earthquake occurrence probability is that for the period starting January 2009. In calculating the probabilities for the model, the recurrence interval is assumed to follow the BPT distribution where the mean recurrence interval=2,650 years (the Hokkaido-seiho-Oki Earthquake; the median value of 1,400-3,900 years) and 950 years (the Hokkaido-nansei-Oki Earthquake and the Aomori-ken-seiho-Oki Earthquake; the median value of 500-1,400 years), the time of the latest event=68.4 years ago (the Hokkaido-seiho-Oki Earthquake), 15.5 years ago (the Hokkaido-nansei-Oki Earthquake), 25.6 years ago (the Aomori-ken-seiho-Oki Earthquake), and variance α=0.21 (the median value of 0.17-0.24). Probability less than 10^{-3}% is indicated as "Nearly 0%". M_w is assumed to be equal to M_j.

5) Akita-ken-Oki Earthquake

The parameters of the seismic activity model are shown in Table 3.3.2-31 and the locations of the fault planes are shown in Figure 3.3.2-23. Regarding the location of the source area, rectangular fault planes each of which is 90 km long and 24 km wide, with a dip angle of 45° and the depth of the upper edge being 3 km, are arranged within the area (either east-dipping or west-dipping), and an earthquake is assumed to occur with equal probability (1/2) on any of those planes.

Table 3.3.2-31 Parameters of the Akita-ken-Oki Earthquake

	Long-term evaluation	Model
Occur. prob. within 30 years	Around 3% or less	3.0%
Occur. prob. within 50 years	Around 5% or less	4.9%
Magnitude	Around *M*7.5	M_w 7.5
Source area	Location of the assumed source area is shown in the Figure 3.3.2-23.	Rectangular fault planes each of which is 90 km long and 24 km wide (dip angle: 45°, east-dipping or west-dipping) are arranged within the area, and an earthquake is assumed to occur with equal probability on any of those planes.

Notes: In calculating the probabilities for the model, a Poisson process is assumed where the mean recurrence interval=1,000 years (long-term evaluation: around 1,000 years or more). M_w is assumed to be equal to M_j.

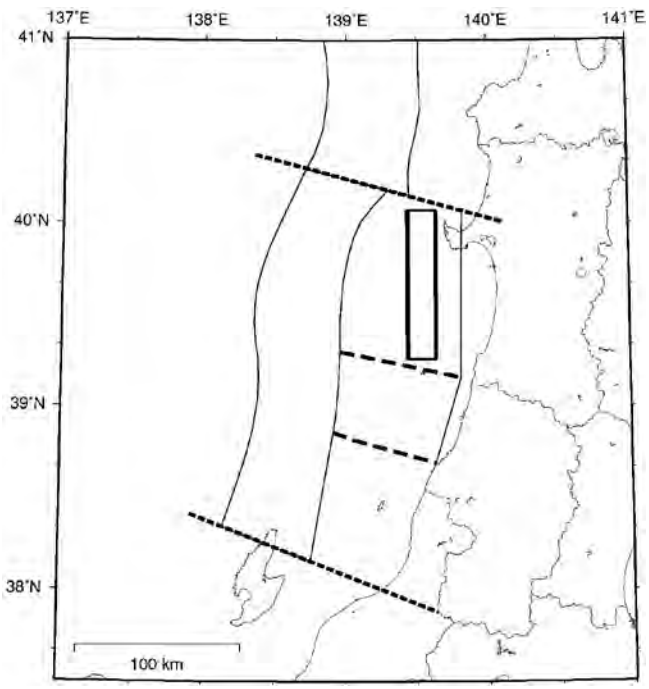

Figure 3.3.2-23 Fault planes of the Akita-ken-Oki Earthquake

6) Yamagata-ken-Oki Earthquake

The parameters of the seismic activity model are shown in Table 3.3.2-32. The parameters of the fault planes are those used in the fault model of the 1833 Shonai-Oki Earthquake (Aida (1989)) (Figure 3.3.2-21).

Table 3.3.2-32 Parameters of the Yamagata-ken-Oki Earthquake

	Long-term evaluation	Model
Occur. prob. within 30 years	Nearly 0%	Nearly 0%
Occur. prob. within 50 years	Nearly 0%	Nearly 0%
Magnitude	Approx. *M*7.7	M_w 7.7
Source area	Fault planes of the 1833 Shonai-Oki Earthquake	Fault planes of the 1833 Shonai-Oki Earthquake

Notes: The earthquake occurrence probability is that for the period starting January 2009. In calculating the probabilities for the model, the recurrence interval is assumed to follow the BPT distribution where the mean recurrence interval=1,000 years (long-term evaluation: around 1,000 years or more), the time of the latest event=175.1 years ago, and variance α=0.21 (the median value of 0.17-0.24). Probability less than 10^{-3}% is indicated as "Nearly 0%". M_w is assumed to be equal to M_j.

7) Niigata-ken-hokubu-Oki Earthquake

The parameters of the seismic activity model are shown in Table 3.3.2-33. The parameters of the fault planes are those used in the 1964 Niigata Earthquake (Abe (1975)) (Figure 3.3.2-21).

Table 3.3.2-33 Parameters of the Niigata-ken-hokubu-Oki Earthquake

	Long-term evaluation	Model
Occur. prob. within 30 years	Nearly 0%	Nearly 0%
Occur. prob. within 50 years	Nearly 0%	Nearly 0%
Magnitude	Approx. *M*7.5	M_w7.5
Source area	Fault planes of the 1964 Niigata Earthquake	Fault planes of the 1964 Niigata Earthquake

Notes: The earthquake occurrence probability is that for the period starting January 2009. In calculating the probabilities for the model, the recurrence interval is assumed to follow the BPT distribution where the mean recurrence interval=1,000 years (long-term evaluation: around 1,000 years or more), the time of the latest event=44.5 years ago, and variance α=0.21 (the median value of 0.17-0.24). Probability less than 10^{-3}% is indicated as "Nearly 0%". M_w is assumed to be equal to *M*j.

8) Sadogashima-hoppo-Oki Earthquake

The parameters of the seismic activity model are shown in Table 3.3.2-34 and the locations of the fault planes are shown in

Figure 3.3.2-24. Regarding the location of the source area, the long-term evaluation has indicated that "an earthquake could occur anywhere within the area", but here, rectangular fault planes each of which is 140 km long and 34 km with, with a dip angle of 30° (east dipping or west dipping) and the depth of the upper edge being 3 km, are arranged within the area, three rows in the North-South direction, and an earthquake is assumed to occur with equal probability (1/6) on any of those planes.

Table 3.3.2-34 Parameters of the Sadogashima-hoppo-Oki Earthquake

	Long-term evaluation	Model
Occur. prob. within 30 years	3-6%	3.9%
Occur. prob. within 50 years	5-10%	6.4%
Magnitude	Around *M*7.8	M_w 7.8
Source area	Location of the assumed source area is shown in the Figure 3.3.2-24.	Rectangular fault planes each of which is 140 km long and 34 km wide (dip angle: 30°; east-dipping or west-dipping) are arranged within the area, three rows in the North-South direction, and an earthquake is assumed to occur with equal probability on any of those planes.

Notes: In calculating the probabilities for the model, a Poisson process is assumed where the mean recurrence interval=750 years (long-term evaluation: around 500-1,000 years). M_w is assumed to be equal to M_j.

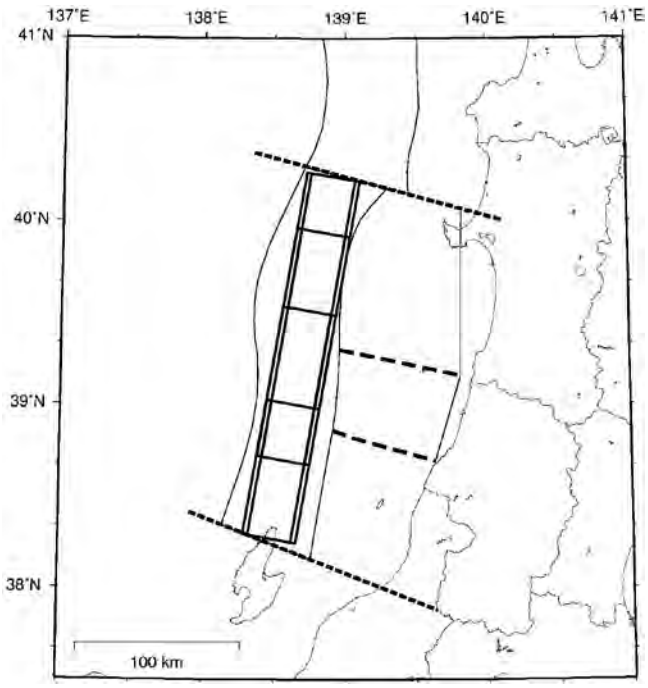

Figure 3.3.2-24 Fault planes of the Sadogashima-hoppo-Oki Earthquake

(5) Earthquakes in Hyuganada and in the vicinity of the Nansei-shotoTrench

Based on "Long-term Evaluation of Seismic Activity Along Hyuganada and the Vicinity of Nanseishoto Trench" (ERC, 2004a), intraplate earthquakes in Akinada-Iyonada-Bungosuido, interplate earthquakes in Hyuganada, relatively small interplate earthquakes in Hyuganada, and earthquakes in the vicinity of Yonaguni-jima are modeled.

Regarding the location of the source area in modeling these earthquakes, for all of the earthquakes, multiple fault planes are arranged within the proposed area, and earthquakes are assumed to occur on those fault planes with an equal probability. If the fault size has not been clearly indicated, a square fault of which the length of one side is determined by using fault size S corresponding to magnitude *M* (log*S*=*M*-4; Utsu and Seki, 1955) as a rough guide.

1) Intraplate earthquakes in Akinada-Iyonada-Bungosuido

The parameters of intraplate earthquakes in Akinada-Iyonada-Bungosuido are shown in Table 3.3.2-35. The locations of the determined fault planes are shown in Figure 3.3.2-25.

The magnitude of each earthquake is based on a Gutenberg-Richter relation with b=0.9, and is assumed to occur with the following relative probabilities (percentages).

M_w 6.7:23.1% M_w 6.8:18.8% M_w 6.9:15.3%
M_w 7.0:12.4% M_w 7.1:10.1% M_w 7.2:8.2%
M_w 7.3:6.7% M_w 7.4:5.4%

Table 3.3.2-35 Parameters of intraplate earthquakes in Akinada-Iyonada-Bungosuido

	Long-term evaluation	Model
Occur. prob. within 30 years	Around 40%	36%
Occur. prob. within 50 years	Around 50%	53%
Magnitude	M6.7-7.4	M_w 6.7-7.4
Source area	Location of the assumed source area is shown in the Figure 3.3.2-25.	Taking into consideration the 2001 Geiyo Earthquake, rectangular fault planes striking north-south and dipping west at a dip angle of 55° are arranged within the area, so that the middle of the upper edge of the plane is aligned with the depth of the upper surface of the plate, and an earthquake is assumed to occur with equal probability on any of those planes. The fault planes are assumed to be 30 km long and 30 km wide (no. of faults: 38) for earthquakes of M_w 6.7-7.0, and 40 km long and 40 km wide (no. of faults: 22) for earthquakes of M_w 7.1-7.4.

Notes: In calculating the probabilities for the model, a Poisson process is assumed where the mean recurrence interval=67 years (six times within 400 years). M_w is assumed to be equal to M_j.

(a) Earthquakes of M6.7-7.0

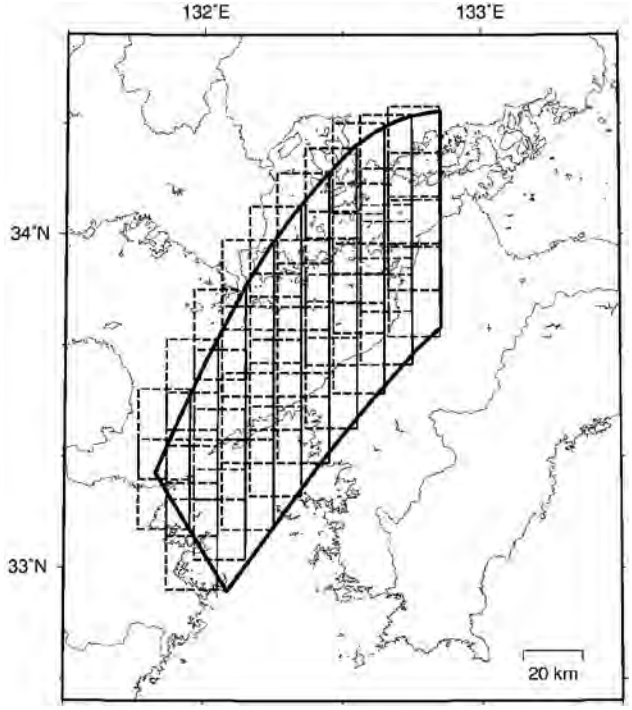

(b) Earthquakes of M7.1-7.4

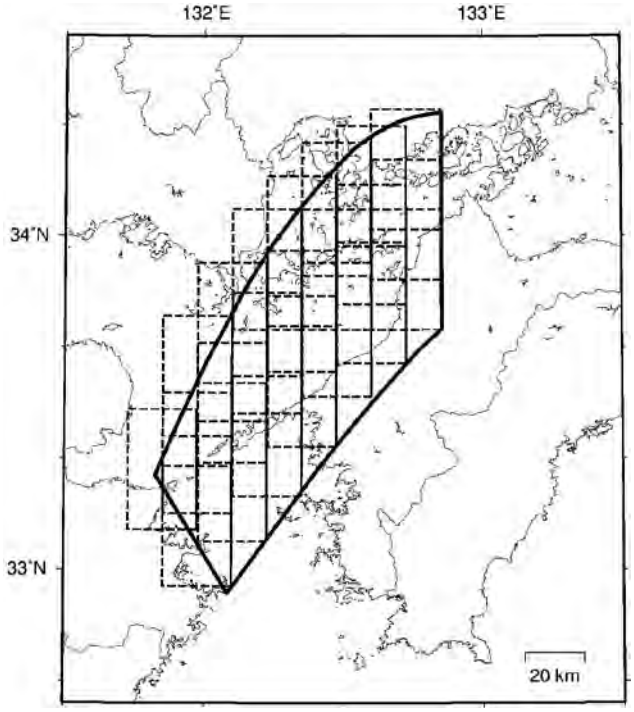

Figure 3.3.2-25 Fault planes of intraplate earthquakes in Akinada-Iyonada-Bungosuido

2) Interplate earthquakes in Hyuganada

The parameters of the model of interplate earthquakes in Hyuganada are shown in Table 3.3.2-36. The locations of the determined fault planes are shown in Figure 3.3.2-26.

Table 3.3.2-36 Parameters of interplate earthquakes in Hyuganada

	Long-term evaluation	Model
Occur. prob. within 30 years	Around 10%	14%
Occur. prob. within 50 years	Around 20%	22%
Magnitude	Approx. *M*7.6	M_w 7.6
Source area	Location of the assumed source area is shown in the Figure 3.3.2-26.	Rectangular fault planes each of which is 65 km long and 65 km wide (equivalent to *M*7.6) (no. of faults: 10) are arranged within the area, along the plate boundaries, and an earthquake is assumed to occur with equal probability on any of those planes.

Notes: In calculating the probabilities for the model, a Poisson process is assumed where the mean recurrence interval=200 years (twice within 400 years). M_w is assumed to be equal to M_j.

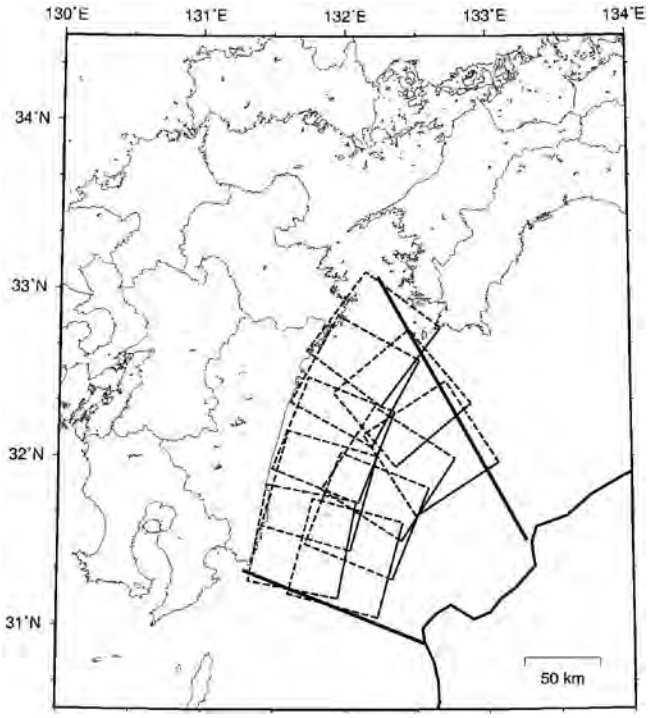

Figure 3.3.2-26 Fault planes of interplate earthquakes in Hyuganada

3) Relatively small interplate earthquakes in Hyuganada

The parameters of the model of relatively small interplate earthquakes in Hyuganada are shown in Table 3.3.2-37. The locations of the determined fault planes are shown in Figure 3.3.2-27.

Table 3.3.2-37 Parameters of relatively small interplate earthquakes in Hyuganada

	Long-term evaluation	Model
Occur. prob. within 30 years	70%-80%	73%
Occur. prob. within 50 years	80%-90%	89%
Magnitude	Approx. *M*7.1	M_w 7.1
Source area	Location of the assumed source area is shown in the Figure 3.3.2-27.	Rectangular fault planes each of which is 35 km long and 35 km wide (equivalent to *M*7.1) (no. of faults: 44) are arranged within the area, along the plate boundaries, and an earthquake is assumed to occur with equal probability on any of those planes.

Notes: In calculating the probabilities for the model, a Poisson process is assumed where the mean recurrence interval=23 years (three to four times within 80 years). M_w is assumed to be equal to M_j.

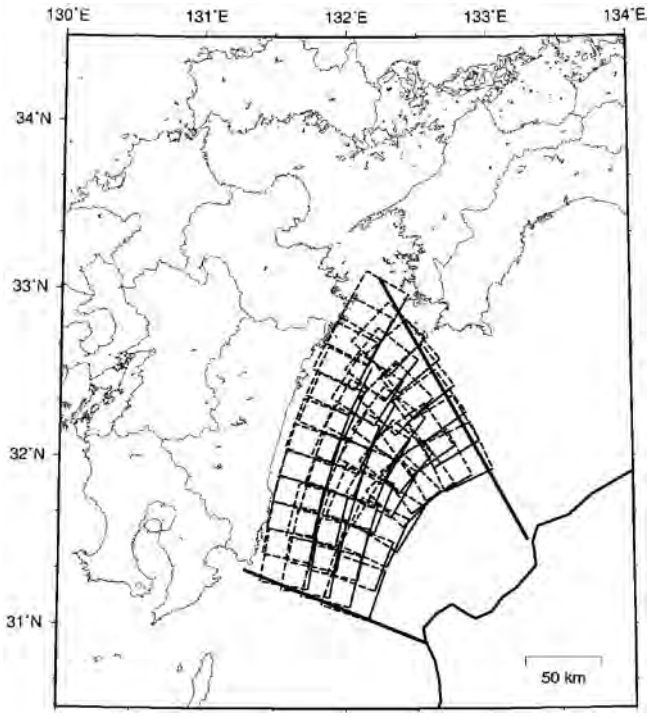

Figure 3.3.2-27 Fault planes of relatively small interplate earthquakes in Hyuganada

4) Earthquakes in the vicinity of Yonaguni-jima

The parameters of the model of earthquakes in the vicinity of Yonaguni-jima are shown in Table 3.3.2-38. The locations of the determined fault planes are shown in Figure 3.3.2-28.

Table 3.3.2-38 Parameters of earthquakes in the vicinity of Yonaguni-jima

	Long-term evaluation	Model
Occur. prob. within 30 years	Around 30%	26%
Occur. prob. within 50 years	Around 40%	39%
Magnitude	Around *M*7.8	M_w 7.8
Source area	Location of the assumed source area is shown in the Figure 3.3.2-28.	Rectangular fault planes, each of which is 80 km long and 80 km wide (equivalent to *M*7.8) and is striking east-west and dipping north at a dip angle of 45° (no. of faults: 8), are arranged within the area so that the depth of the middle of the fault is 40 km, and an earthquake is assumed to occur with equal probability on any of those planes.

Notes: In calculating the probabilities for the model, a Poisson process is assumed where the mean recurrence interval=100 years (once within 100 years). M_w is assumed to be equal to M_j.

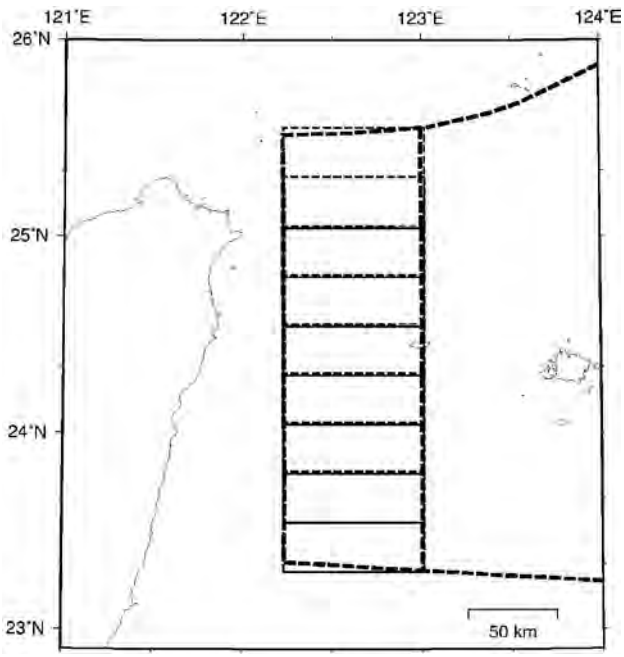

Figure 3.3.2-28 Fault planes of earthquakes in the vicinity of Yonaguni-jima

(6) Earthquakes along the Sagami Trough

Based on "Long-term Evaluation of Seismic Activity Along the Sagami Trough" (ERC, 2004c), the Kanto Earthquake of "1923 Taisho" type and other *M*7 class earthquakes in Southern Kanto are modeled. The Kanto Earthquake of "1703 Genroku" type is not modeled, because the possibility of occurrence in the near future (within 30 years or 50 years) is extremely low.

The following policy was set for modeling.

- The mean recurrence interval used for the Kanto Earthquake of "1923 Taisho" type is 219.7 years based on the interval between the 1703 Genroku Earthquake (Dec. 1703) and the 1923 Kanto Earthquake (Sep. 1923).
- With regard to the location of the source area, a specific fault plane is determined for the Kanto Earthquake of "1923 Taisho" type. For other *M*7 class earthquakes in Southern Kanto, the earthquakes are classified into three types: earthquakes on the upper surface of the Philippine Sea plate, earthquakes within the Philippine Sea plate, and earthquakes on the upper surface of the Pacific plate. For each type of earthquake, multiple fault planes are arranged within the proposed area, and an earthquake is assumed to occur with equal probability on any of those planes. If the fault size has not been clearly indicated, a square fault of which the length of one side is determined by using fault size S corresponding to magnitude *M* (log*S*=*M*-4; Utsu and Seki, 1955) as a rough guide.

1) Kanto Earthquake of "1923 Taisho" type

The parameters of the model of the Kanto Earthquake of "1923 Taisho" type are shown in Table 3.3.2-39. The locations of the determined fault planes are shown in Figure 3.3.2-29. The mean recurrence interval of the Kanto Earthquake of "1923 Taisho" type has been indicated to be 200-400 years in the long-term evaluation, but here, it is 219.7 years based on the interval between the 1703 Genroku Earthquake (Dec. 1703) and the 1923 Kanto Earthquake (Sep. 1923).

Table 3.3.2-39 Parameters of the Kanto Earthquake of "1923 Taisho" type

	Long-term evaluation	Model
Occur. prob. within 30 years	Nearly 0%-1%	0.12%
Occur. prob. within 50 years	Nearly 0%-6%	1.3%
Magnitude	Around *M*7.9	M_w 7.9
Source area	Location of the assumed source area is shown in the Figure 3.3.2-29.	A specific fault plane that matches the source area assumed in the long-term evaluation is determined.

Notes: The earthquake occurrence probability is that for the period starting January 2009. In calculating the probabilities for the model, the recurrence interval is assumed to follow the BPT distribution where the mean recurrence interval=219.7 years, the time of the latest event=85.3 years ago, and variance α=0.21 (the median value of 0.17-0.24). M_w is assumed to be equal to M_j.

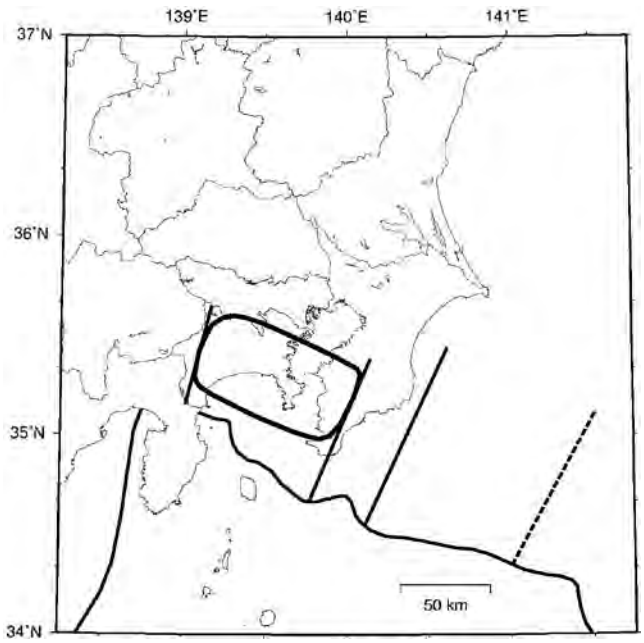

Figure 3.3.2-29 Fault planes of the Kanto Earthquake of "1923 Taisho" type

2) Other *M*7 class earthquakes in southern Kanto

For other *M*7 class earthquakes in Southern Kanto, the following three types of earthquakes are modeled: a) earthquakes on the upper surface of the Philippine Sea plate, b) earthquakes within the Philippine Sea plate, and c) earthquakes on the upper surface of the Pacific plate. Earthquakes within the Pacific plate are not modeled since the depth of the area covered in evaluation is 80 km or more. However, they are taken into consideration as earthquakes without specified source faults.

The areas where the fault planes are arranged are shown in Figure 3.3.2-30. Fault planes are arranged within the area where the depth is 30 km or more for a) earthquakes on the upper surface of the Philippine Sea plate, and within the entire area covered in evaluation for b) earthquakes within the Philippine Sea plate, and within the area where the depth is 80 km or less for c) earthquakes on the upper surface of the Pacific plate. For earthquakes on the upper surface of the Philippine Sea plate and earthquakes on the upper surface of the Pacific plate, the fault planes are arranged along the plate boundaries. For earthquakes within the Philippine Sea plate, the fault planes are arranged parallel to the upper surface of the plate at a depth 10 km below the upper surface of the plate. However, when the depth of the area covered in evaluation is 30 km or less, the fault plane is arranged 30 km deep. Earthquakes are assumed to occur on those fault planes with an equal probability.

The fault planes are assumed to be 25 km long and 25 km wide for earthquakes of M_w 6.7-6.9, and 35 km long and 35 km wide for earthquakes of M_w 7.0-7.2.

The magnitude of each earthquake is assumed to occur with the following percentages (relative probabilities) to fit a Gutenberg-Richter relation with b=0.9.

M_w 6.7:26.3%　M_w 6.8:21.4%　M_w 6.9:17.4%
M_w 7.0:14.1%　M_w 7.1:11.5%　M_w 7.2:9.3%

Table 3.3.2-40 Parameters of other *M*7 class earthquakes in southern Kanto

	Long-term evaluation	Model
Occur. prob. within 30 years	Around 70%	72%
Occur. prob. within 50 years	Around 90%	88%
Magnitude	Around *M*6.7-7.2	M_w 6.7-7.2
Source area	Locations of the areas covered in evaluation are shown in the Figure.3.3.2-30	Fault planes are arranged for the following three types of earthquakes: a) earthquakes on the upper surface of the Philippine Sea plate (depth: 30 km or more), b) earthquakes within the Philippine Sea plate, and c) earthquakes on the upper surface of the Pacific plate (depth: 80 km or less). An earthquake is assumed to occur with equal probability on any of those planes. Fault planes are assumed to be 25 km long and 25 km wide for earthquakes of M_w 6.7-6.9, and 35 km long and 35 km wide for earthquakes of M_w 7.0-7.2.

Notes: In calculating the probabilities for the model, a Poisson process is assumed where the mean recurrence interval=23.8 years (five times within 119 years). M_w is assumed to be equal to M_j. The number of faults allocated is shown in Figure 3.3.2-31.

The parameters of other *M*7 class earthquakes in Southern Kanto are shown in Table 3.3.2-40. The locations of the determined fault planes are shown in Figure 3.3.2-31.

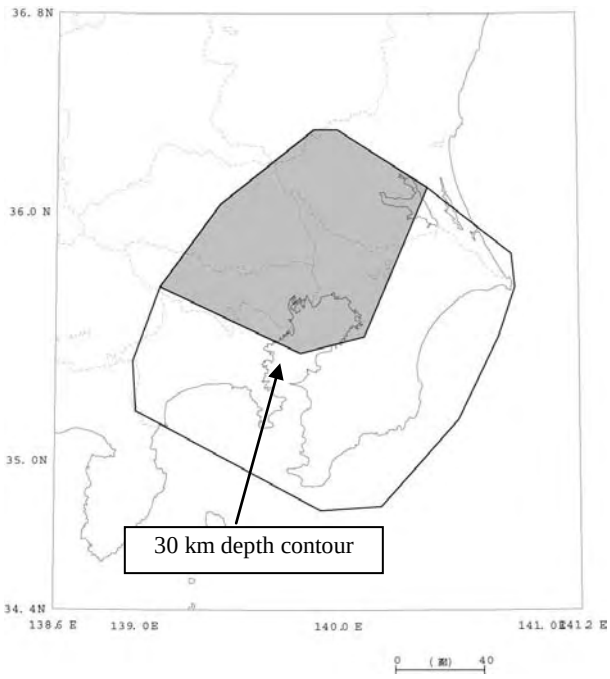

(a) Earthquakes on the upper surface of the Philippine Sea plate

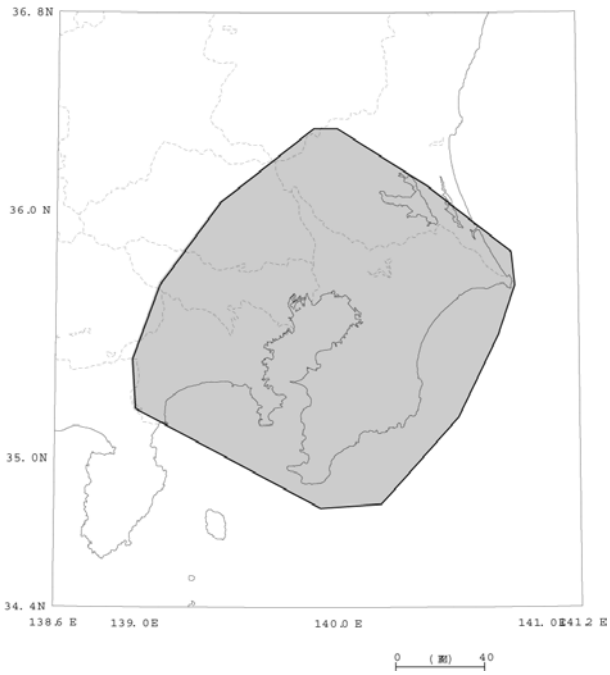

(b) Earthquakes within the Philippine Sea plate

Note: Fault planes are arranged within the shaded area.

Figure 3.3.2-30 Areas in which fault planes of other *M*7 class earthquakes in southern Kanto are arranged (Part 1)

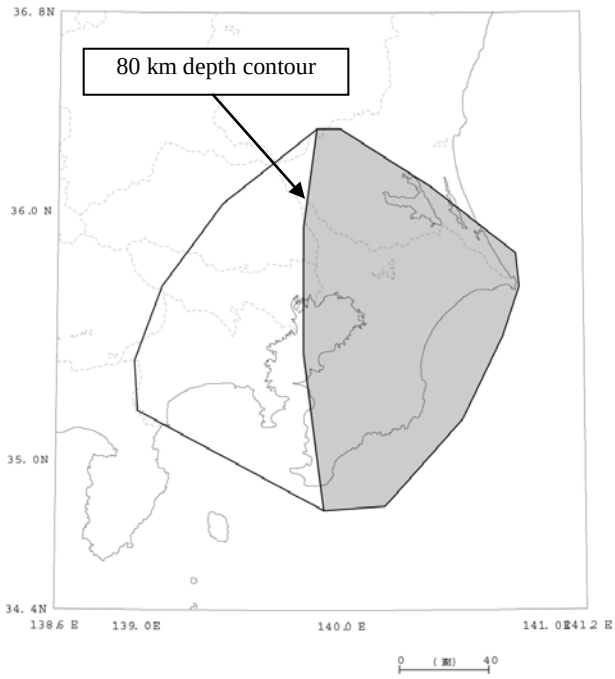

(c) Earthquakes on the upper surface of the Pacific plate

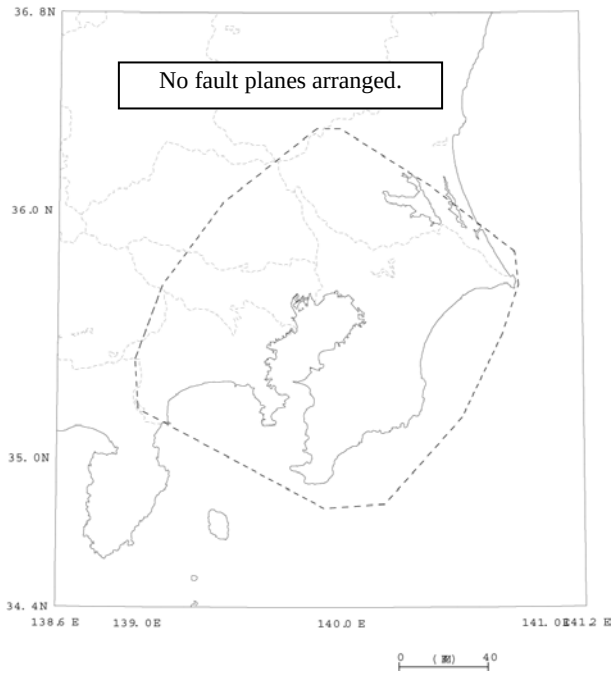

(d) Earthquakes within the Pacific plate

Note: Fault planes are arranged within the shaded area.

Figure 3.3.2-30 Areas in which fault planes of other *M*7 class earthquakes in southern Kanto are arranged (Part 2)

(a) Earthquakes on the upper surface of the Philippine Sea plate

○ Earthquakes of *M*6.7-6.9

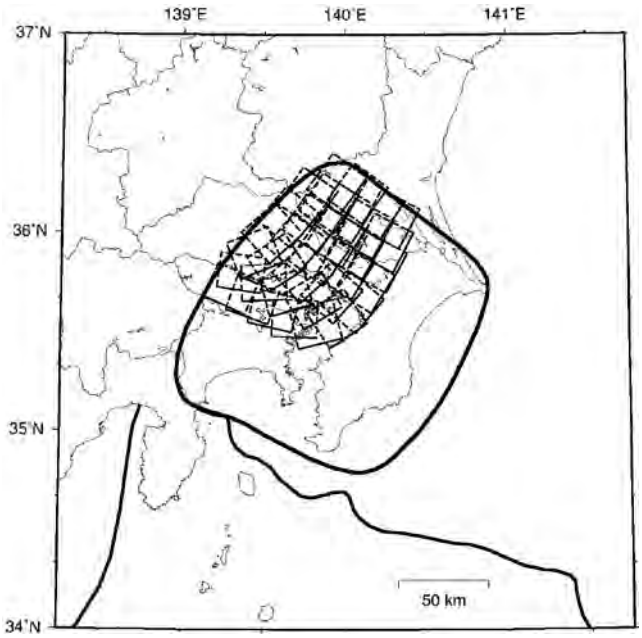

No. of faults: 34

○ Earthquakes of *M*7.0-7.2

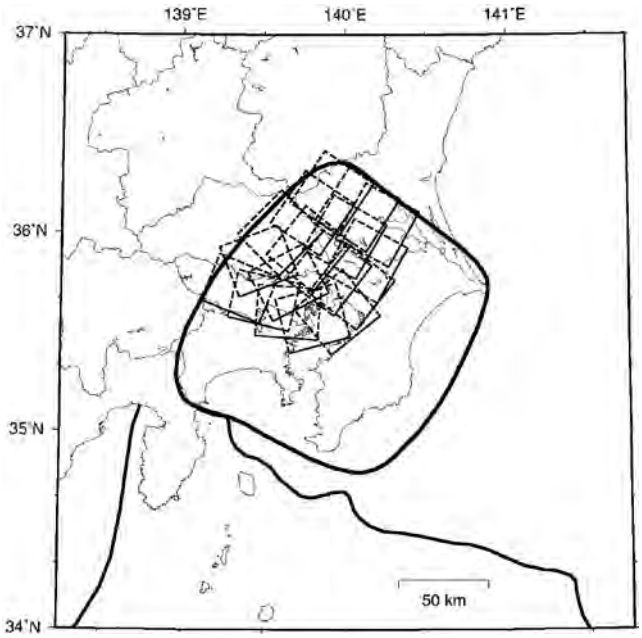

No. of faults: 17

Figure 3.3.2-31 Fault planes of other *M*7 class earthquakes in southern Kanto (Part 1)

(b) Earthquakes within the Philippine Sea plate

○ Earthquakes of *M*6.7-6.9

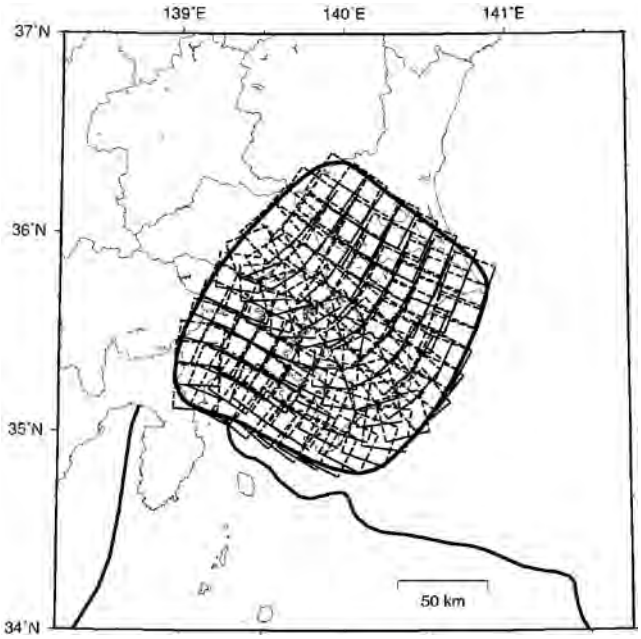

No. of faults: 106

○ Earthquakes of *M*7.0-7.2

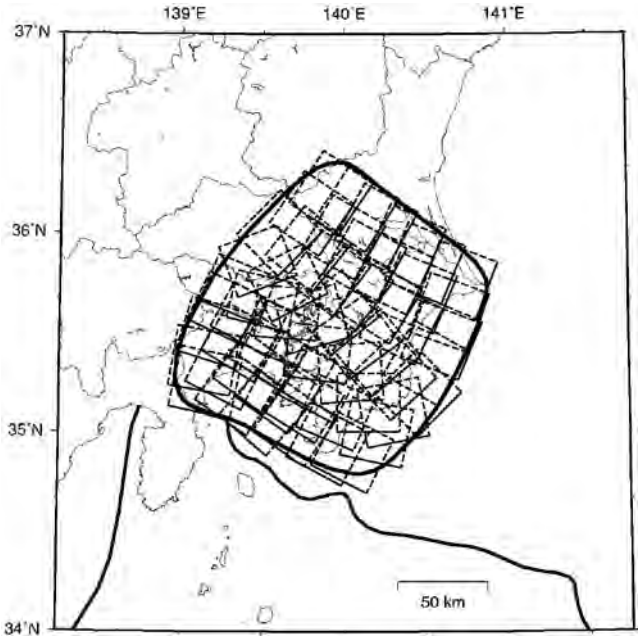

No. of faults: 56

Figure 3.3.2-31 Fault planes of other *M*7 class earthquakes in southern Kanto (Part 2)

(c) Earthquakes on the upper surface of the Pacific plate

○ Earthquakes of *M*6.7-6.9

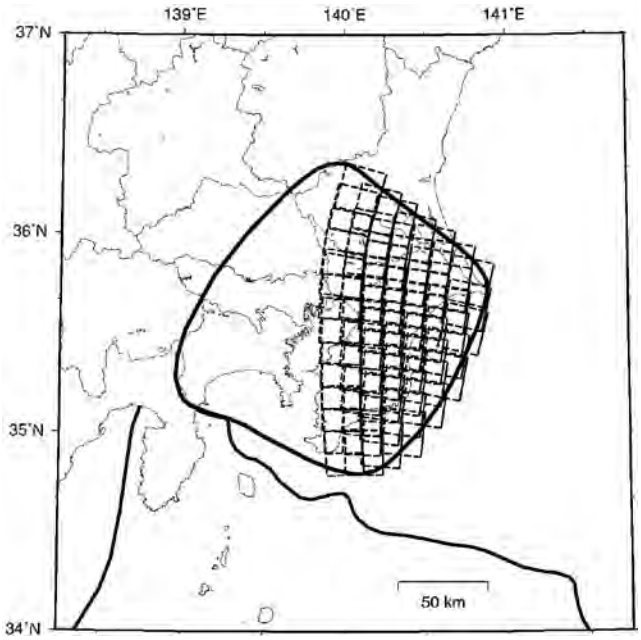

No. of faults: 63

○ Earthquakes of *M*7.0-7.2

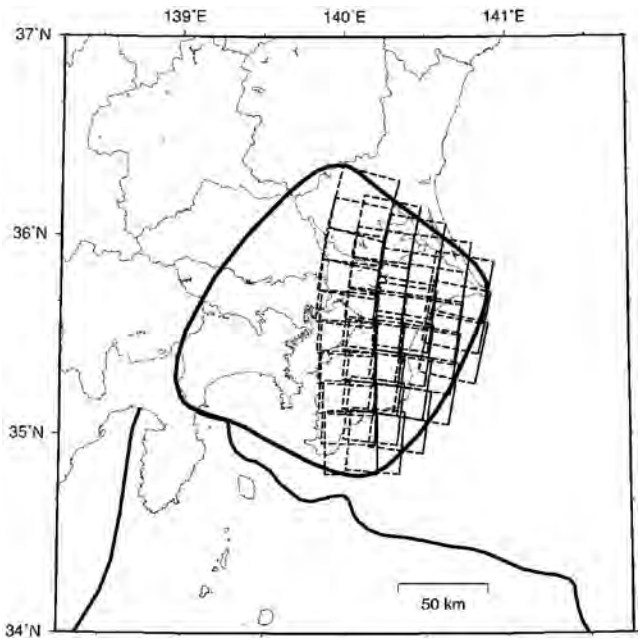

No. of faults: 31

Figure 3.3.2-31 Fault planes of other *M*7 class earthquakes in southern Kanto (Part 3)

3.3.3 Earthquakes occurring on active faults other than major active fault zones[1]

1) Basic policy

Among the faults which satisfy the criteria for seismogenic faults by Matsuda et al. (2000), those other than major active fault zones are extracted as target earthquakes. Also, faults that were considered in the long-term evaluation of major active fault zones but were not evaluated due to failing to satisfy the criteria for the fundamental surveys and observations are modeled under this earthquake category if they satisfy the criteria for seismogenic faults.

2) Seismogenic fault extraction process

- Using "New Edition: Active Faults of Japan" (The Research Group for Active Faults of Japan ed., 1991) and "Digital Active Fault Map of Japan" (Nakata and Imaizumi ed., 2002) as databases, seismogenic faults with a total length of 10 km or more are extracted from those databases based on the criteria by Matsuda et al. (2000). The edge points of the faults and the fault lengths were reviewed based on the two databases.
  - An isolated fault of which the length is 10 km or more where no other active fault line exists within a distance of 5 km
  - A group of faults with approximately the same strike which are located within a distance of 5 km from each other
  - A fault with a different strike from the main fault line where the mid-point of the fault line is located 5 km or more away from the main fault line
- Faults that are classified under certainty level III in "New Edition: Active Faults of Japan" are treated as follows.
  - If a fault of certainty level III with a length of 5 km or less continues from the edge of a seismogenic fault, such fault is included in the length of the seismogenic fault.
  - If a fault of certainty level III with a length of 5 km or less is included in the middle of a seismogenic fault and joins fault lines of certainty level II or more, such fault is included in the length of the seismogenic fault.
  - A fault line of certainty level III which is longer than 5 km is excluded.
- The presumed active faults in "Digital Active Fault Map of Japan" are made subject to extraction of seismogenic faults. Although they are not made subject to extraction of seismogenic faults in the digital map, presumed active faults are also extracted as target faults in the long-term evaluation of major active fault zones. Thus, presumed

[1] The modeling of earthquakes occurring on active faults other than major active fault zones was carried out by the Secretariat of HERP. NIED used such data provided by HERP for creating the PSHM.

active faults are made subject to extraction of seismogenic faults here in order to achieve consistency.

- For a seismogenic fault that is covered in both databases, the one with the longer fault length is adopted. For a seismogenic fault that is covered in only one of the databases, the parameters in that database are used directly.

3) Determination of the earthquake occurrence probability

According to the method indicated in "Regarding methods for evaluating long-term probability of earthquake occurrence" (ERC, 2001a), the occurrence probability is calculated from a general recurrence interval based on a Poisson process.

The mean recurrence interval R (year) for calculating the probability can be obtained by the following formula, using the average slip rate S (mm/year) and the displacement D (m) per event:

$$R = D / S * 1000 \qquad (3.3.3\text{-}1)$$

Using the relations between M (magnitude) and D, and between M and fault length L (km) (Matsuda, 1975),

$$\log L = 0.6\,M - 2.9 \qquad (3.3.3\text{-}2)$$

$$\log D = 0.6\,M - 4.0 \qquad (3.3.3\text{-}3)$$

the mean recurrence interval is presumed as follows from the length and the average slip rate:

$$\log R = \log L/S + 1.9 \qquad (3.3.3\text{-}4)$$

For active faults of which the average slip rate is unknown, an average slip rate is assumed according to the activity level indicated in "New Edition: Active Faults of Japan". For an active fault which is short and that has a high level of activity, the mean recurrence interval calculated by the method adopted this time becomes several hundred years to less than 1,000 years. While the evaluation method for the recurrence interval of such active fault is a matter that needs to be studied further in the future, here, the average slip rates shown below are given to active faults for which the average slip rate has been indicated and of which the activity levels are grouped as Class A or Class A-B, in order to avoid the recurrence interval from becoming unrealistic. It should be noted that these values differ from those used for major active fault zones.

Class A: 1 mm/y	(Lowest value for Class A)
Class A-B: 0.5 mm/y	(Half the value for Class A)
Class B: 0.25 mm/y	(Okumura and Ishikawa, 1998)
Class B-C: 0.1 mm/y	(Border value between Class B and C)
Class C: 0.047 mm/y	(Okumura and Ishikawa, 1998)

If the activity level is unknown, it is assumed to be less than Class C, and the average slip rate is assumed to be 0.024 mm/y as half the value of the average slip rate for Class C shown above. If the activity level is indicated as being less than Class B or less than Class C, the average slip rate is assumed to be 0.1 mm/y or 0.024 mm/y as the average slip rate for Class B-C or less than Class C.

4) Determination of the magnitude

The magnitude of an earthquake that occurs on an active fault is obtained from the fault length according to Formula (3.3.3-2).

5) Determination of the parameters of the fault planes

The fault plane of each active fault is modeled either as single or multiple rectangular planes. The parameters defining a model are the location of the edges, the length, the width, the strike, the dip angle, and the depth of the upper edge of the fault. Among these, the dip angle is determined to be 90° (vertical plane) for all faults. The depth of the upper edge is determined to be 3 km, taking into account the research from the viewpoint of ground motion evaluation (Ito, 1997). The width is assumed to be the same as the length for active faults that are up to 15 km long. For active faults that are more than 15 km long, the width is determined to be 15 km, assuming the depth of the seismogenic layer to be 3-18 km.

6) Active segments

Seismic activities are assumed to occur simultaneously at all segments of an active fault.

7) Parameters of the modeled active faults

The parameters of active faults other than major active fault zones that are used for creating the PSHM are shown in Table 3.3.3-1, and maps that show the locations of the active faults together with the locations of major active fault zones are shown in Figure 3.3.3-1. The number of faults is 175. Of the Ube-Oki fault group (Suonada fault group), three faults with a fault length of less than 20 km (Ube-tobu fault-Shimogo fault (30180), Ube-nanto-Oki fault zone (30181), and Himeshima-hokuto-Oki fault zone (30182)) newly became targeted. Hanawa-bonchi fault zone (30017) became non-targeted under the group of "other active faults" since it is to be evaluated as a major active fault zone.

Table 3.3.3-1 Parameters for modeling active faults other than major active fault zones (part 1)

Code	Modeled fault name (note 1)	Fault length (note 2)	*M*	Recurrence interval	Basis for calculation of recurrence interval (note 3)	Occur. prob. within 30 years	Occur. prob. within 50 years
30001	Rausu-dake fault zone	12 km	6.6	1,000 years	Class A	3.0%	4.9%
30002	Shari-dake-higashi fault zone	13 km	6.7	1,500 years	0.7 mm/y	2.0%	3.3%
30003	Abashiri-ko fault zone	15 km	6.8	4,800 years	Class B	0.62%	1.0%
30004	Tokoro-gawa-togan fault	10 km	6.5	3,200 years	Class B	0.93%	1.6%
30005	Toikanbetsu fault zone	20 km	7.0	12,200 years	0.13 mm/y	0.25%	0.41%
30006	Horonobe fault zone	22 km	7.1	3,500 years	0.5 mm/y	0.85%	1.4%
~~30007~~	~~Sarobetsu-flexure zone~~	~~39 km~~	~~7.5~~	~~15,500 years~~	~~0.2 mm/y~~	~~0.19%~~	~~0.32%~~
30008	Ponnitashibetsu fault	11 km	6.6	3,500 years	Class B	0.85%	1.4%
30009	Mitsuishi-Urakawa fault zone	12 km	6.6	3,800 years	Class B	0.79%	1.3%
30010	Karumai fault (Ishikari zanbu)	14 km	6.7	23,700 years	Class C	0.13%	0.21%
30011	Nopporo-kyuryo fault zone	20 km	7.0	7,900 years	0.2 mm/y	0.38%	0.63%
30012	Shiribetsu-gawa fault zone	25 km	7.2	7,900 years	0.25 mm/y	0.38%	0.63%
30013	Yakumo fault zone	10 km	6.5	800 years	1 mm/y	3.7%	6.1%
30014	Noheji fault zone	20 km[Note 4)]	7.0	6,400 years	Class B	0.47%	0.78%
30015	Tsugaru-sanchi-seien fault zone (hokubu hoppo-encho) (Tsugaru-sanchi-seien fault zone [hokubu/chubuzan])	15 km	6.8	49,600 years	? (Less than Class C)	0.060%	0.10%
30016	Iwaki-san-nanroku fault zone	11 km	6.6	3,500 years	Class B	0.85%	1.4%
~~30017~~	~~Hanawa-bonchi fault zone~~	~~17 km~~	~~6.9~~	~~4,500 years~~	~~0.3 mm/y~~	~~0.66%~~	~~1.1%~~
30018	Takizawaukai-nishi fault (Kitakami zanbu)	17 km	6.9	28,700 years	Class C	0.10%	0.17%
30019	Tazawa-ko fault zone	10 km	6.5	2,000 years	0.4 mm/y	1.5%	2.5%
30020	Kitaguchi fault zone	16 km	6.8	5,100 years	Class B	0.59%	0.98%
30021	Yokote-bonchi-seinan fault zone	21 km	7.0	35,500 years	Class C	0.084%	0.14%
30022	Toridame fault zone	24 km[Note 4)]	7.1	7,600 years	Class B	0.39%	0.66%
30023	Kamagadai fault zone	11 km	6.6	3,500 years	Class B	0.85%	1.4%
30024	Kisakata fault zone	10 km	6.5	800 years	1 mm/y	3.7%	6.1%
30025	Asahiyama flexure zone	23 km	7.1	36,500 years	0.05 mm/y	0.082%	0.14%
30026	Medeshima estimated fault	11 km	6.6	36,400 years	? (Less than Class C)	0.082%	0.14%
30027	Sakunami-Yashikidaira fault zone	10 km	6.5	26,500 years	0.03 mm/y	0.11%	0.19%
30028	Togatta fault zone	11 km	6.6	2,900 years	0.3 mm/y	1.0%	1.7%
30029	Obanazawa fault zone	14 km	6.7	2,200 years	0.5 mm/y	1.4%	2.2%
30030	Sakekawa fault (Shinjo-bonch-seien fault zone zanbu)	23 km	7.1	3,700 years	0.5 mm/y	0.81%	1.3%
30031	Kotaru-gawa fault zone	10 km	6.5	3,200 years	Class B	0.93%	1.6%
30032	Futaba fault nanbu (Haramachi-shi Ohara inan) (Futaba fault nanbu C-class zanbu)	48 km	7.6	120,000 years	(Note 5)	0.025%	0.042%
30033	Osaka-Ashizawa fault zone	16 km	6.8	12,700 years	Class B-C	0.24%	0.39%
30034	Futatsuya fault	10 km	6.5	3,200 years	Class B	0.93%	1.6%
30035	Sangunmori fault zone	18 km	6.9	5,700 years	Class B	0.52%	0.87%
30036	Yunotake fault	12 km	6.6	3,800 years	Class B	0.79%	1.3%
30037	Idosawa fault	19 km	7.0	62,900 years	? (Less than Class C)	0.048%	0.079%
30038	Takahagi-fukin estimated fault	17 km	6.9	56,300 years	? (Less than Class C)	0.053%	0.089%
30039	Tanagura fracture zone seien fault	20 km	7.0	66,200 years	? (Less than Class C)	0.045%	0.076%
30040	Adatara-yama-toroku fault zone	15 km	6.8	2,400 years	0.5 mm/y	1.2%	2.1%
30041	Kawageta-yama fault zone	15 km	6.8	11,900 years	0.1 mm/y	0.25%	0.42%

Table 3.3.3-1 Parameters for modeling active faults other than major active fault zones (part 2)

Code	Modeled fault name (note 1)	Fault length (note 2)	*M*	Recurrence interval	Basis for calculation of recurrence interval (note 3)	Occur. prob. within 30 years	Occur. prob. within 50 years
30042	Shirakawa-seiho fault zone	18 km	6.9	59,600 years	? (Less than Class C)	0.050%	0.084%
30043	Hinoemata-nishi fault	15 km	6.8	25,400 years	Class C	0.12%	0.20%
30044	Kokuzoyama-toho fault	11 km	6.6	3,500 years	Class B	0.85%	1.4%
30045	Hanezu fault zone	14 km	6.7	3,200 years	0.35 mm/y	0.93%	1.6%
30046	Numakoshi-toge fault	16 km	6.8	5,100 years	Class B	0.59%	0.98%
30047	Yoshinoya fault	12 km	6.6	4,800 years	0.2 mm/y	0.62%	1.0%
30048	Yukyu-zan fault zone	22 km	7.1	5,800 years	0.3 mm/y	0.52%	0.86%
30049	Jorakuji fault	11 km	6.6	3,500 years	Class B	0.85%	1.4%
30050	Osado-seigan fault zone	14 km	6.7	11,100 years	0.1 mm/y	0.27%	0.45%
30051	Kuninaka-heiya-minami fault	10 km	6.5	1,600 years	0.5 mm/y	1.9%	3.1%
30052	Muikamachi fault zone	24 km	7.1	3,800 years	0.5 mm/y	0.79%	1.3%
30053	Hirataki-Busuno-toge fault	10 km	6.5	3,200 years	Class B	0.93%	1.6%
30054	Takada-heiya-toen fault zone	14 km	6.7	800 years	1.4 mm/y	3.7%	6.1%
30055	Takada-heiya-seien fault zone	15 km	6.8	11,900 years	0.1 mm/y	0.25%	0.42%
30056	Togakushi-yama fault	11 km	6.6	3,500 years	Class B	0.85%	1.4%
30057	Jonen-dake-higashi fault zone	28 km	7.2	22,200 years	Class B-C	0.14%	0.22%
~~30058~~	~~Kurobishi-yama fault zone~~	~~28 km~~	~~7.2~~	~~2,200 years~~	~~1 mm/y~~	~~1.4%~~	~~2.2%~~
30059	Saotome-dake fault	16 km	6.8	12,700 years	Class B-C	0.24%	0.39%
30060	Noto fault zone	18 km	6.9	5,700 years	Class B	0.52%	0.87%
30061	Kirigamine fault zone	20 km	7.0	1,600 years	Class A	1.9%	3.1%
30062	Kamogawa-teichi fault zone kita fault	15 km	6.8	10,000 years	(Note 5)	0.30%	0.50%
30063	Ogose fault	13 km	6.7	22,000 years	Class C	0.14%	0.23%
30064	Tsurukawa fault	28 km[Note 4)]	7.2	47,300 years	Class C	0.063%	0.11%
30065	Ogiyama fault	21 km	7.0	16,700 years	Class B-C	0.18%	0.30%
30066	Kurokura-Shiozawa fault zone	16 km	6.8	5,100 years	Class B	0.59%	0.98%
30067	Hadano fault zone	13 km	6.7	700 years	1.5 mm/y	4.2%	6.9%
~~30068~~	~~Kofu-bonchi nan'en fault zone~~	~~38 km~~	~~7.5~~	~~3,000 years~~	~~1 mm/y~~	~~1.0%~~	~~1.7%~~
30069	Tanna fault zone nantan group	14 km	6.7	5,600 years	0.2 mm/y	0.53%	0.89%
30070	Daruma-yama fault zone	11 km	6.6	2,900 years	0.3 mm/y	1.0%	1.7%
30071	Iro-zaki fault	14 km	6.7	2,200 years	0.5 mm/y	0%[Note 6)]	0%[Note 6)]
30072	Nihondaira fault zone	12 km	6.6	4,800 years	0.2 mm/y	0.62%	1.0%
30073	Hatanagi-san fault	13 km	6.7	22,000 years	Class C	0.14%	0.23%
30074	Chuo-kozosen-Akaishi-sanchi-seien fault zone	52 km[Note 4)]	7.7	16,500 years	Class B	0.18%	0.30%
30075	Shimoina-ryuto fault zone	27 km	7.2	8,600 years	Class B	0.35%	0.58%
30076	Hiraoka fault	20 km	7.0	15,900 years	Class B-C	0.19%	0.31%
~~30077~~	~~Niino fault~~	~~13 km~~	~~6.7~~	~~10,300 years~~	~~Class B-C~~	~~0.29%~~	~~0.48%~~
30078	Suzugasawa fault	10 km	6.5	3,200 years	Class B	0.93%	1.6%
30079	Shirasu-toge fault zone	10 km	6.5	1,600 years	Class A-B	1.9%	3.1%
30080	Wakatochi-toge fault	14 km	6.7	4,400 years	Class B	0.68%	1.1%
30081	Kuno-gawa fault	15 km	6.8	4,800 years	Class B	0.62%	1.0%
30082	Furukawa fault zone (Toichi-gawa fault)	16 km	6.8	27,000 years	Class C	0.11%	0.19%
30083	Kuchiudo-Yamanokuchi fault	20 km	7.0	33,800 years	Class C	0.089%	0.15%
30084	Byobu-yama fault nanseibu (Byobu-yama fault nanseibu nokori)	16 km	6.8	80,000 years	(Note 5)	0.037%	0.062%
30085	Kasahara fault	16 km	6.8	12,700 years	Class B-C	0.24%	0.39%
30086	Hanadate fault	10 km	6.5	7,900 years	Class [B]	0.38%	0.63%
30087	Fukozu fault zone	11 km	6.6	3,500 years	0.25 mm/y	0%[Note 6)]	0%[Note 6)]
30088	Nagoya-shi-fukin fault	11 km	6.6	8,700 years	0.1 mm/y	0.34%	0.57%
30089	Tenpaku-kako fault	13 km	6.7	150,000 years	(Note 5)	0.020%	0.033%

Table 3.3.3-1 Parameters for modeling active faults other than major active fault zones (part 3)

Code	Modeled fault name (note 1)	Fault length (note 2)	*M*	Recurrence interval	Basis for calculation of recurrence interval (note 3)	Occur. prob. within 30 years	Occur. prob. within 50 years
30090	Bijo-zan fault zone	17 km	6.9	5,400 years	0.25 mm/y	0.55%	0.92%
30091	Tanigumi-Kochibora fault	15 km	6.8	2,000 years	0.6 mm/y	1.5%	2.5%
30092	Ikedayama fault	16 km	6.8	5,100 years	0.25 mm/y	0.59%	0.98%
30093	Tsushima fault zone	31 km	7.3	9,800 years	Class B	0.31%	0.51%
30094	Suzuka-Oki fault	13 km	6.7	4,100 years	Class B	0.73%	1.20%
30095	Yoro-sanchi-seien fault zone	19 km[Note 4)]	7.0	6,000 years	Class B	0.50%	0.83%
30096	Hokyoji fault	17 km	6.9	13,500 years	Class B-C	0.22%	0.37%
30097	Kanakusa-dake fault zone	10 km	6.5	2,600 years	0.3 mm/y	1.1%	1.9%
30098	Okukawanami fault	13 km	6.7	10,300 years	Class B-C	0.29%	0.48%
30099	Sarake fault	12 km	6.6	9,500 years	Class B-C	0.32%	0.52%
30100	Hosenji fault zone	17 km	6.9	13,500 years	Class B-C	0.22%	0.37%
30101	Mihama-wan-Oki fault	21 km	7.0	69,500 years	? (Less than Class C)	0.043%	0.072%
30102	Mimi-kawa fault zone	11 km	6.6	3,500 years	Class B	0.85%	1.4%
30103	Biwako-togan-kotei fault	12 km	6.6	3,800 years	Class B	0.79%	1.3%
30104	Kumagawa fault zone	11 km	6.6	8,700 years	0.1 mm/y	0.34%	0.57%
30105	Biwako-nanbu-kotei fault	14 km	6.7	4,400 years	Class B	0.68%	1.1%
30106	Odorii fault zone	24 km	7.1	40,600 years	Class C	0.074%	0.12%
30107	Suzuka-sakashita fault zone	15 km	6.8	7,900 years	0.15 mm/y	0.38%	0.63%
30108	Kyogamine-minami fault	10 km	6.5	3,200 years	Class B	0.93%	1.6%
30109	Chuo-kozosen Taki	20 km	7.0	33,800 years	Class C	0.089%	0.15%
30110	Ieki fault zone	16 km	6.8	27,000 years	Class C	0.11%	0.19%
30111	Nabari fault zone	29 km[Note 4)]	7.3	49,000 years	Class C	0.061%	0.10%
30112	Shigaraki fault zone	16 km	6.8	5,100 years	0.25 mm/y	0.59%	0.98%
30113	Wazuka-dani fault	14 km	6.7	4,400 years	Class B	0.68%	1.1%
30114	Tahara fault	10 km	6.5	16,900 years	Class C	0.18%	0.30%
30115	Ayame-ike flexure zone	15 km	6.8	4,000 years	0.3 mm/y	0.75%	1.2%
30116	Keihanna-kyuryo flexure zone	24 km	7.1	7,600 years	Class B	0.39%	0.66%
30117	Habikino fault zone	15 km	6.8	4,800 years	Class B	0.62%	1.0%
30118	Izumi-hokuroku fault zone	16 km	6.8	27,000 years	Class C	0.11%	0.19%
30119	Chuo-kozosen Gojo	36 km	7.4	60,800 years	Class [C]	0.049%	0.082%
30120	Habu fault	16 km	6.8	5,100 years	0.25 mm/y	0.59%	0.98%
30121	Nakayama fault zone	11 km	6.6	29,100 years	0.03 mm/y	0.10%	0.17%
30122	Mitakesan fault	10 km	6.5	33,100 years	? (Less than Class C)	0.091%	0.15%
30123	Gosho-dani fault zone	29 km	7.3	9,200 years	Class B	0.33%	0.54%
30124	Takatsuka-yama fault	12 km	6.6	3,800 years	Class B	0.79%	1.3%
30125	Shizuki fault zone	10 km	6.5	7,900 years	Class B-C	0.38%	0.63%
30126	Hansanji fault zone	14 km	6.7	23,700 years	Class C	0.13%	0.21%
30127	Yabu fault zone	21 km[Note 4)]	7.0	6,700 years	Class B	0.45%	0.74%
30128	Akenobe-hoppo fault	12 km	6.6	20,300 years	Class C	0.15%	0.25%
30129	Hikihara fault	10 km	6.5	16,900 years	Class C	0.18%	0.30%
30130	Ametaki-Kamato fault	15 km	6.8	49,600 years	? (Less than Class C)	0.060%	0.10%
30131	Iwatsubo fault zone (Shikano fault)	13 km	6.7	34,400 years	0.03 mm/y	0%[Note 6)]	0%[Note 6)]
30132	Iwatsubo fault zone (Iwatsubo fault)	8 km	6.3	21,200 years	0.03 mm/y	0.14%	0.24%
30133	Kashima fault zone	18 km	6.9	14,300 years	0.1 mm/y	0.21%	0.35%
30134	Yoshii fault	11 km	6.6	1,500 years	0.6 mm/y	2.0%	3.3%
30135	Fukuyama fault zone	11 km	6.6	36,400 years	Less than Class C	0.082%	0.14%
30136	Mitsugi fault	10 km	6.5	33,100 years	? (Less than Class C)	0.091%	0.15%
30137	Shobara fault	10 km	6.5	16,900 years	Class C	0.18%	0.30%
30138	Miyoshi fault zone	11 km	6.6	18,600 years	Class C	0.16%	0.27%

Table 3.3.3-1 Parameters for modeling active faults other than major active fault zones (part 4)

Code	Modeled fault name (note 1)	Fault length (note 2)	*M*	Recurrence interval	Basis for calculation of recurrence interval (note 3)	Occur. prob. within 30 years	Occur. prob. within 50 years
30139	Kamine fault	15 km	6.8	4,800 years	Class B	0.62%	1.0%
30140	Tsutsuga fault zone	16 km	6.8	12,700 years	0.1 mm/y	0.24%	0.39%
30141	Yasaka fault zone	47 km	7.6	124,400 years	0.03 mm/y	0.024%	0.040%
30142	Ohara-ko fault	16 km	6.8	2,500 years	0.5 mm/y	1.2%	2.0%
30143	Shibuki fault	16 km	6.8	53,000 years	? (Less than Class C)	0.057%	0.094%
30144	Tokushima-heiya-nan'en fault zone	13 km	6.7	4,100 years	Class B	0.73%	1.2%
30145	Akui-gawa fault zone	28 km[Note 4)]	7.2	92,700 years	? (Less than Class C)	0.032%	0.054%
30146	Ebata fault zone	22 km	7.1	72,800 years	Less than Class C	0.041%	0.069%
30147	Takanawa-san-kita fault	15 km	6.8	49,600 years	? (Less than Class C)	0.060%	0.10%
30148	Tsunatsukimori fault	11 km	6.6	3,500 years	Class B	0.85%	1.4%
30149	Yasuda fault	23 km	7.1	76,100 years	? (Less than Class C)	0.039%	0.066%
30150	Gyodo-zaki fault	17 km	6.9	5,400 years	Class B	0.55%	0.92%
30151	Kochi-Agawa	22 km	7.1	17,500 years	0.1 mm/y	0.17%	0.29%
30152	Sukumo-Nakamura fault zone	26 km	7.2	86,100 years	? (Less than Class C)	0.035%	0.058%
30153	Tosashimizu-kita fault zone	10 km	6.5	33,100 years	? (Less than Class C)	0.091%	0.15%
30154	Kokura-higashi fault zone	12 km	6.6	31,800 years	0.03 mm/y	0.094%	0.16%
30155	Fukuchiyama fault zone	29 km	7.3	23,000 years	0.1 mm/y	0.13%	0.22%
~~30156~~	~~Kego fault zone~~	~~19 km~~	~~7.0~~	~~15,100 years~~	~~0.1 mm/y~~	~~0.20%~~	~~0.33%~~
30157	Saganoseki fault	12 km	6.6	20,300 years	Class C	0.15%	0.25%
30158	Fukuragi fault	10 km	6.5	33,100 years	? (Less than Class C)	0.091%	0.15%
30159	Taradake-nanseiroku fault zone (Tataradake-nanseiroku fault zone)	15 km	6.8	25,400 years	Class C	0.12%	0.20%
30160	Aso-gairin-nanroku fault group	15 km	6.8	29,800 years	0.04 mm/y	0.10%	0.17%
30161	Midorikawa fault zone	26 km[Note 4)]	7.2	8,300 years	Class B	0.36%	0.60%
30162	Tsurukiba fault zone	11 km	6.6	36,400 years	? (Less than Class C)	0.082%	0.14%
30163	Kunimi-dake fault zone	13 km	6.7	43,000 years	? (Less than Class C)	0.070%	0.12%
30164	Kawaminami-Soyabaru fault	14 km	6.7	4,400 years	Class B	0.68%	1.1%
~~30165~~	~~Hitoyoshi-bonchi fault zone~~	~~22 km~~	~~7.1~~	~~8,700 years~~	~~0.2 mm/y~~	~~0.34%~~	~~0.57%~~
30166	Minamata fault zone	10 km	6.5	16,900 years	Class C	0.18%	0.30%
30167	Nagashima fault group	15 km	6.8	25,400 years	Class C	0.12%	0.20%
30168	Kagoshimawan-toen fault zone	17 km	6.9	5,400 years	Class B	0.55%	0.92%
30169	Kagoshimawan-seien fault zone	15 km	6.8	49,600 years	? (Less than Class C)	0.060%	0.10%
30170	Ichiki fault zone	23 km	7.1	76,100 years	? (Less than Class C)	0.039%	0.066%
30171	Ikedako-nishi fault zone	10 km	6.5	800 years	Class A	3.7%	6.1%
30172	Tanega-shima-hokubu fault	14 km	6.7	5,600 years	0.2 mm/y	0.53%	0.89%
30173	Yaku-shima-nangan fault zone	18 km	6.9	4,800 years	0.3 mm/y	0.62%	1.0%
30174	Kikai-jima fault zone	14 km	6.7	1,100 years	Class A	2.7%	4.4%
30175	Okinoerabu-jima fault zone	13 km	6.7	4,100 years	Class B	0.73%	1.2%
30176	Kinwan-seigan fault zone	11 km	6.6	3,500 years	Class B	0.85%	1.4%
30177	Miyako-jima fault zone	29 km	7.3	9,200 years	Class B	0.33%	0.54%
30178	Yonaguni-jima fault zone	11 km	6.6	3,500 years	Class B	0.85%	1.4%

Table 3.3.3-1 Parameters for modeling active faults other than major active fault zones (part 5)

Code	Modeled fault name (note 1)	Fault length (note 2)	M	Recurrence interval	Basis for calculation of recurrence interval (note 3)	Occur. prob. within 30 years	Occur. prob. within 50 years
30179	Noto-hanto Earthquake fault[Note 7)]	—	6.9	—	—	0%[Note 6)]	0%[Note 6)]
30180	Ube-tobu fault-Shimogo fault	12 km	6.6	39,700 years	? (Less than Class C)	0.076%	0.13%
30181	Ube-nanto-Oki fault zone	16 km	6.8	53,000 years	? (Less than Class C)	0.057%	0.094%
30182	Himeshima-hokuto-Oki fault zone	18 km	6.9	59,600 years	? (Less than Class C)	0.050%	0.084%

Note 1: The modeled fault names are taken from either database if the fault is listed in the database, but if no appropriate name is available, a provisional place name is given. The red characters indicate values changed from those for the period starting 2008, and blue characters indicate names that have been changed from the 2008 version (the names used in the 2008 version are shown in black in parentheses).

Note 2: The fault length shows the value calculated from the coordinates of both edges of the fault.

Note 3: For active faults that indicate "Class XX" in the column for the basis for calculation of the recurrence interval, the recurrence interval is calculated based on the average slip rate obtained from the activity level described in "New Edition: Active Faults of Japan". For active faults that indicate "XX mm/y", the recurrence interval is based on the data of average slip rate described in "Digital Active Fault Map of Japan". See note 5 below for the explanation for "(Note 5)". "? (Less than Class C)" denotes that an activity level of less than Class C is determined due to lack of data.

Note 4: For Noheji fault zone (30014), Toridame fault zone (30022), Tsurukawa fault (30064), Chuo-kozosen-Akaishi-sanchi-seien fault zone (30074), Yoro-sanchi-seien fault zone (30095), Nabari fault zone (30111),Yabu fault zone (30127), Akui-gawa fault zone (30145), and Midorikawa fault zone (30161), fault lines of certainty level III at both edges of the active fault are included in the fault length if they are 5 km or less, but excluded from the fault length if they are more than 5 km.

Note 5: For the Futaba fault nanbu (Haramachi-shi Ohara inan) (30032), since it has been indicated that no displacement has been observed during about 120,000 years in the late Quaternary (Fukushima Prefecture, 1999), the mean recurrence interval used is 120,000 years. For the Kamogawa-teichi fault zone kita fault (30062), since "Digital Active Fault Map of Japan" indicates that "no activity has been observed in the past 10,000 years", the mean recurrence interval used is 10,000 years. For the Byobu-yama fault nanseibu (30084), since it has been indicated that no displacement has been observed since about 80,000 years ago (Gifu Prefecture, 2001), the mean recurrence interval used is 80,000 years. For the Tenpaku-kako fault (30089), for which a survey by Nagoya City has reported that "no activity has been observed in the past 150,000 years" (Nagoya City, 1999), the mean recurrence interval used is 150,000 years.

Note 6: The following active faults are known to have been activated recently, and the possibility of earthquake occurrence in the near future is considered to be low. Therefore, the earthquake occurrence probability is assumed to be 0% for both the period within 30 years and that within 50 years.

Iro-zaki fault (30071): 1974 Izu-hanto-Oki Earthquake
Fukozu fault zone (30087): 1945 Mikawa Earthquake
Iwatsubo fault zone (Shikano fault) (30131): 1943 Tottori Earthquake
Noto-hanto Earthquake fault (30179): 2007 Noto-hanto Earthquake

Note 7: Noto-hanto Earthquake fault is modeled based on a model by the Geospatial Information Authority of Japan, as a reverse fault that is 34.5 km long, 20 km wide, striking 55°, and dipping southeast at a dip angle of 63°.

Note 8: The crossed-out active faults are those that have been removed from this table due to being modeled as major active fault zones.

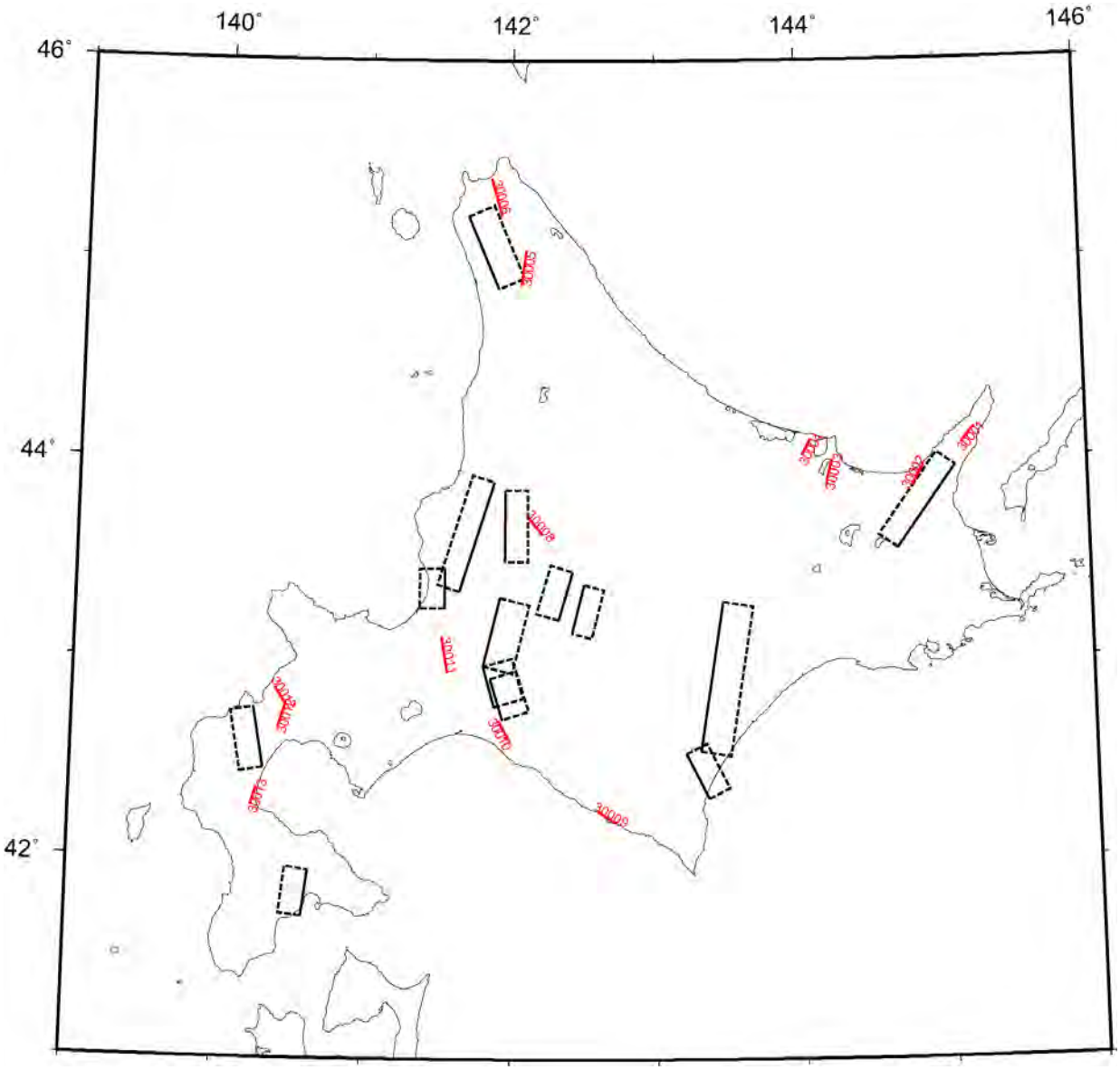

Figure 3.3.3-1 Models of active faults other than major active fault zones (part 1)
Red: Models of active faults other than major active fault zones
Black: Models of major active fault zones

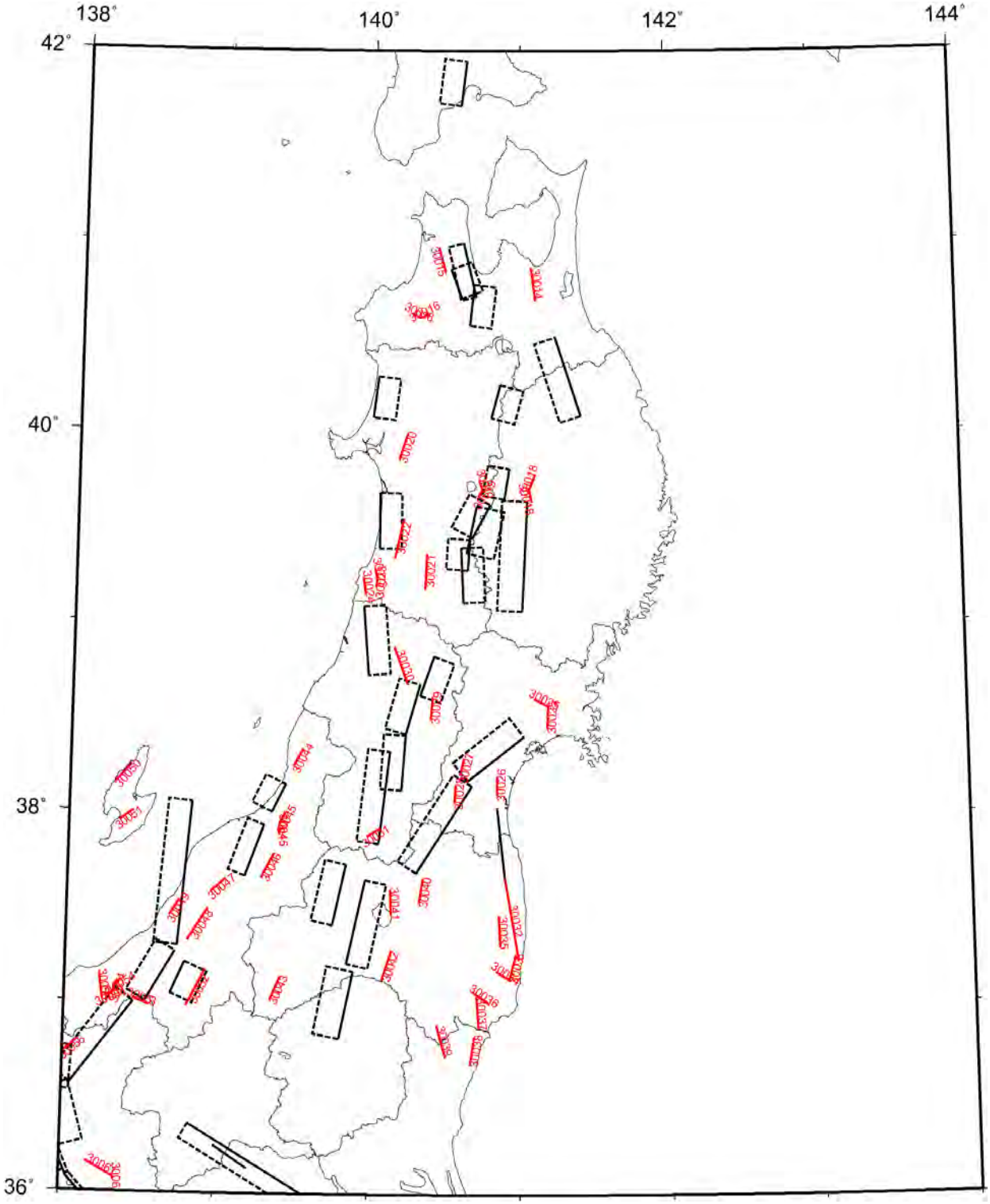

Figure 3.3.3-1 Models of active faults other than major active fault zones (part 2)
Red: Models of active faults other than major active fault zones
Black: Models of major active fault zones

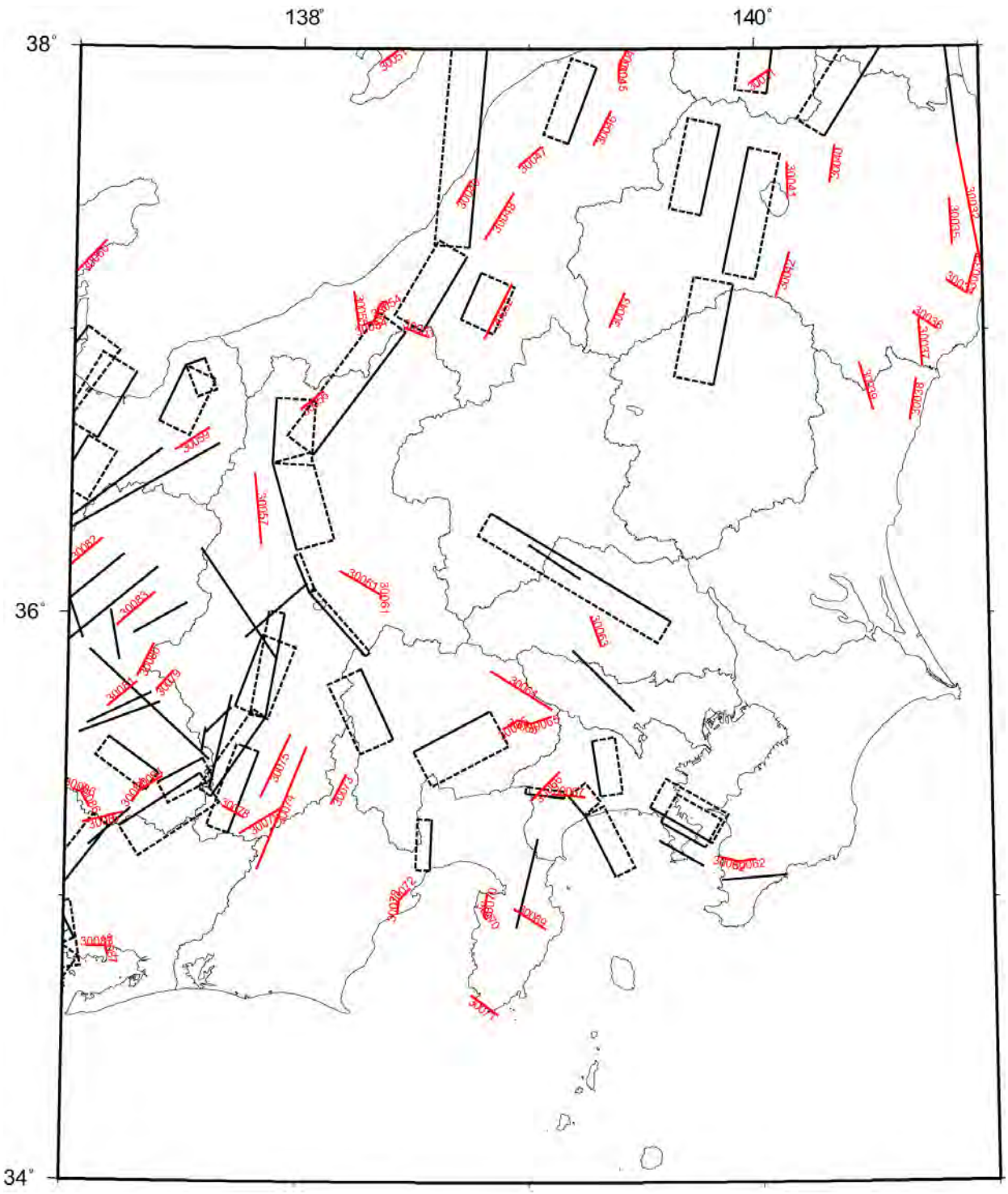

Figure 3.3.3-1 Models of active faults other than major active fault zones (part 3)
Red: Models of active faults other than major active fault zones
Black: Models of major active fault zones

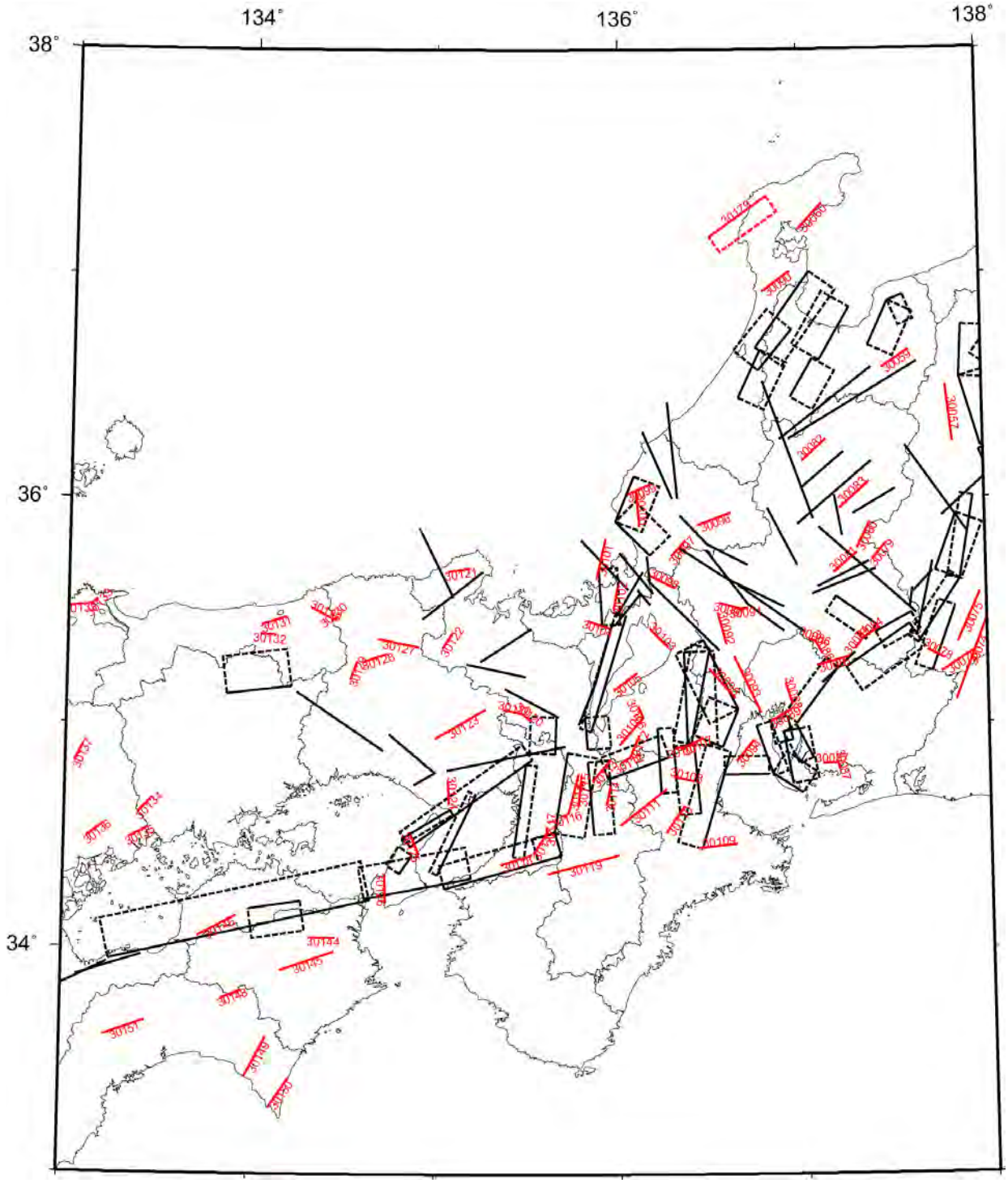

Figure 3.3.3-1 Models of active faults other than major active fault zones (part 4)
Red: Models of active faults other than major active fault zones
Black: Models of major active fault zones

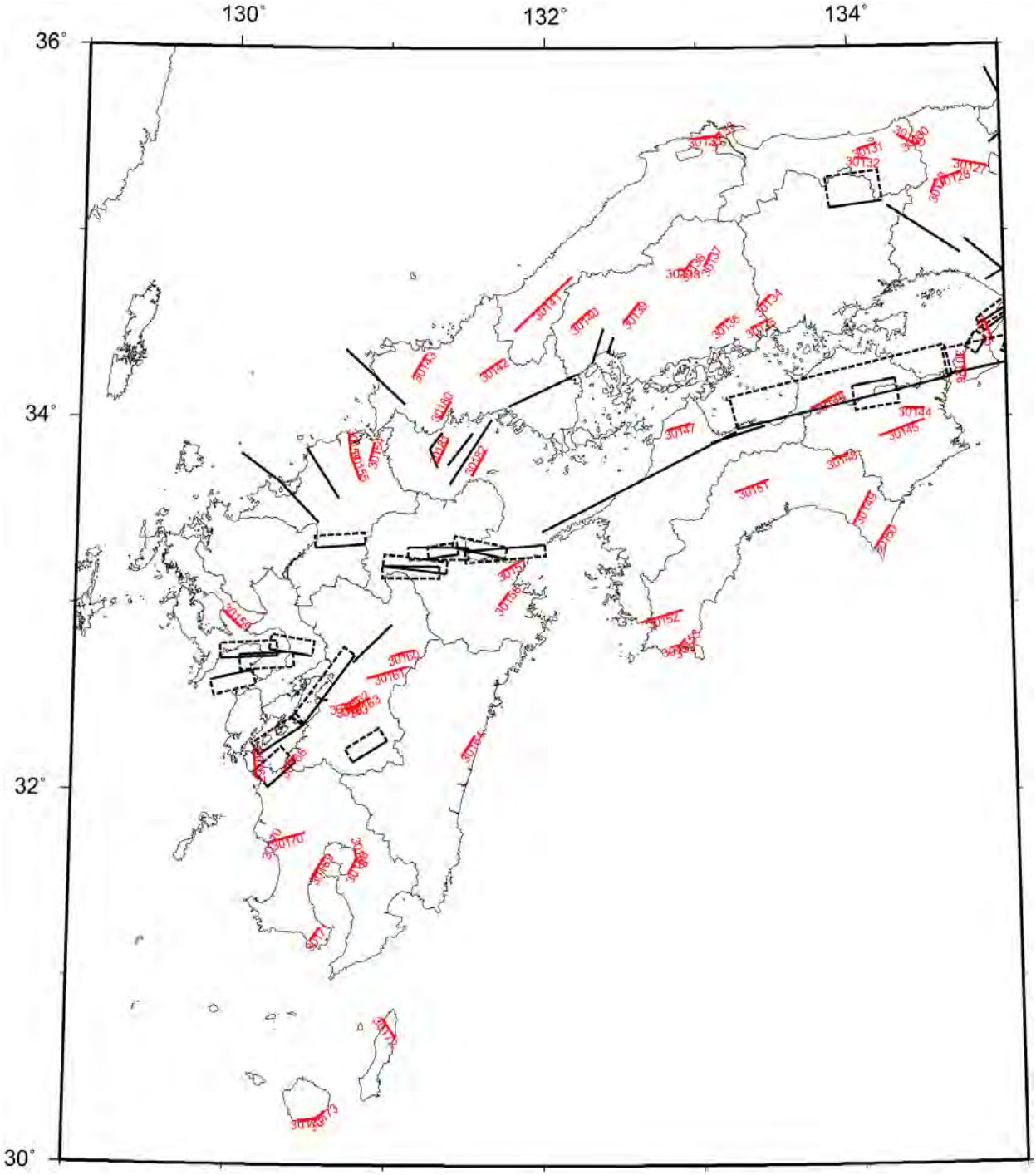

Figure 3.3.3-1 Models of active faults other than major active fault zones (part 5)
Red: Models of active faults other than major active fault zones
Black: Models of major active fault zones

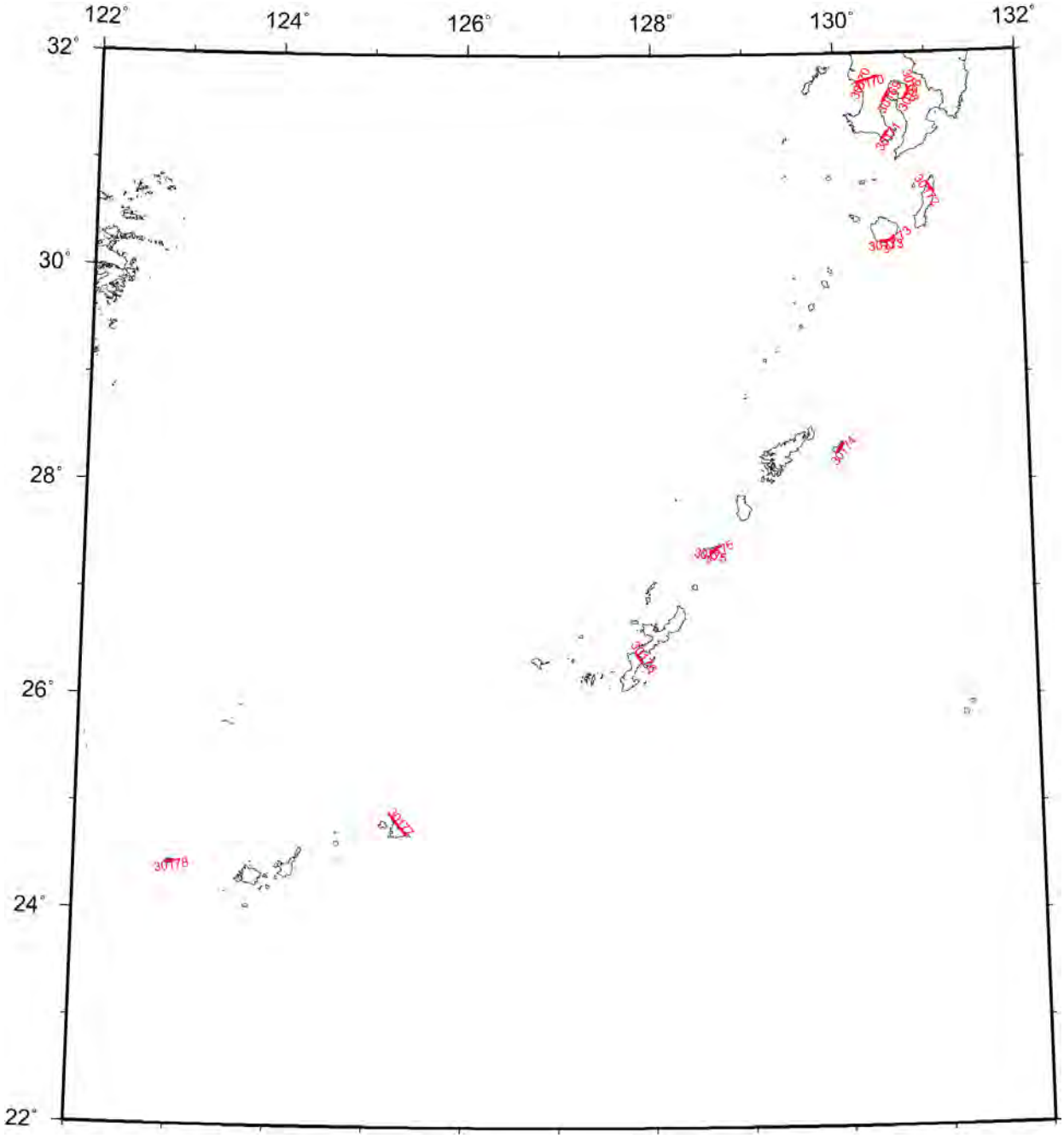

Figure 3.3.3-1 Models of active faults other than major active fault zones (part 6)
Red: Models of active faults other than major active fault zones
Black: Models of major active fault zones

3.3.4 Earthquakes without specified source faults

3.3.4.1 Definition and classification of earthquakes without specified source faults

Apart from the earthquakes which are classified into the groups discussed above, many earthquakes occur in actuality, such as inland shallow earthquakes and small and medium interplate earthquakes that occur at places where no active fault is known to exist. In this report, we call such earthquakes "earthquakes without specified source faults", and consider their influence when creating PSHM. Since it is difficult to specify in advance the place of occurrence, the earthquake magnitude, and the occurrence probability of individual earthquakes without specified source faults, characteristics as earthquake clusters are expressed by probability models. Here, earthquakes without specified source faults are evaluated by classifying them as below according to their place of occurrence.

a) Interplate/intraplate earthquakes without specified source faults for the Pacific plate
   - a-1) Earthquakes on the plate boundaries of the Pacific plate, other than large events
   - a-2) Earthquakes within the subducting Pacific plates, other than large events
b) Interplate/intraplate earthquakes without specified source faults for the Philippine Sea plate
   - b-1) Earthquakes on the plate boundaries of the Philippine Sea plate, other than large events
   - b-2) Earthquakes within the subducting Philippine Sea plate, other than large events
c) Earthquakes occurring at onshore locations where active faults have not been specified
d) Earthquakes without specified source faults in Urakawa-Oki
e) Earthquakes without specified source faults in the eastern margin of the Japan Sea
f) Earthquakes without specified source faults in the southern area of Izu-shoto islands
g) Earthquakes without specified source faults in the vicinity of Nansei-shoto islands

3.3.4.2 Outline of the evaluation method

The evaluation method for earthquakes without specified source faults is the same as that used in the "National Seismic Hazard Maps for Japan" (ERC, 2005b, 2006b, 2007b, 2008b), and basically conforms to the "Preliminary Version of PSHM (Specific Area, Western Japan)" (SLTE/SESGM, ERC, 2004), "Preliminary Version of PSHM (Specific Area, Northern Japan)" (SLTE/SESGM, ERC, 2003), and "Evaluation Method for Earthquakes Without Specified Source Faults, etc. (Interim Report)" (SLTE, ERC, 2002a). While the basic evaluation method is as shown below, different treatment is sometimes applied according to the conditions of the respective earthquakes classified in 3.3.4.1 or the respective regions. Such different treatment is explained in the parts describing individual evaluations.

Major differences from the ERC (2008b) are the following three points:

[1] Whereas the lower limit value of the maximum magnitude was 6.5 uniformly, the following changes are made:
   a) The lower limit value of the maximum magnitude of earthquakes in the sea area without specified source faults that occur at subducting plates is changed from conventional 6.5 to 7.0.
      Basis: According to the long-term evaluation data concerning subduction-zone earthquakes, earthquakes of up to around *M*7.0 have occurred in areas such as Central Sanriku-Oki (Iwate-ken-Oki) where large earthquakes are considered unlikely to occur.
   b) The lower limit value of the maximum magnitude of earthquakes in the sea area without specified source faults that occur in the upper crust of overriding plates and in the southern area of Izu-shoto islands is changed from conventional 6.5 to 7.0.
      Basis: Unlike earthquakes in the land area, active faults have not been identified sufficiently, and have not been modeled as independent seismic source faults.
   c) The lower limit value of the maximum magnitude of earthquakes in the land area without specified source faults from conventional 6.5 to 6.8.
      Basis: Earthquakes of *M*6.8 which do not correspond to the currently modeled active faults have occurred more than a few times.

[2] In the zoning of earthquakes without specified source faults for the Philippine Sea plate, a part of the area from Bungosuido through eastern Kyushu to Nansei-shoto islands where relatively deep earthquakes occur is included in the area of Akinada-Iyonada-Bungosuido.

[3] The period of the JMA earthquake catalog data used is extended by one year to the end of 2007.

With regard to earthquakes without specified source faults, the place of occurrence, magnitude, and frequency of the earthquakes are modeled based on the data of past earthquakes. In doing so, the following two methods are both used: the method of making evaluation for each area divided under the long-term evaluation of subduction-zone earthquakes or each area divided based on seismotectonics, epicenter distribution, etc. (hereinafter referred to as the "zoning method"), and the method of making evaluation for each automatically divided mesh of 0.1 degrees north-south and east-west (hereinafter referred to as the "non-zoning method"). The former method is based on the technique used by the Property and Casualty Insurance Rating Organization (2000), and the latter method is based on the idea of smoothed seismicity by Frankel (1995). The major difference between the two methods is the size

of the area in which the seismic activity level is considered to be uniform. Since an area under the zoning method is generally larger than a 0.1-degree mesh, the variation in the regional distribution of earthquake occurrence frequency (the difference between the maximum and minimum frequencies and the extent of frequency variation based on distance) tends to be stronger under the non-zoning method. At the end, the frequency under the zoning method is converted into frequency for each 0.1-degree mesh, and the mean value between the results under the zoning method and the non-zoning method is used.

While the seismic source data used for calculating the earthquake occurrence frequency is determined by giving consideration to the conditions of each target area, the following data are both used, in principle:

a) Catalog combining data from the Utsu Catalog (Utsu, 1982; Utsu, 1985) for earthquakes of magnitude 6.0 or more that occurred during the period from 1885 to 1925 and data from the JMA's Monthly Report on Earthquakes and Volcanoes in Japan (Catalog), December 2007 issue, published in 2008 (JMA, 2008) for earthquakes of magnitude 5.0 or more that occurred during the period from 1926 to 2007 (hereinafter referred as the "medium earthquake catalog")
b) The JMA earthquake catalog of magnitude 3.0 or more (4.0 or more for earthquakes at the Pacific plate and the Philippine Sea plate) that occurred during the period from 1983 to 2007 (hereinafter referred as the "small earthquake catalog")

The source depth used is 200 km or less. Earthquakes that are separately modeled (earthquakes occurring in major active fault zones, subduction-zone earthquakes, and earthquakes occurring on active faults on land other than major active fault zones) are excluded from these catalogs.

Earthquakes that occur within 90 days from the occurrence of an earthquake of magnitude 6.0 or more, within a circle of Size A (km^2) expressed by the following formula (Public Works Research Institute, Ministry of Construction, 1983) which is centered around the epicenter, are regarded as aftershocks and automatically excluded.

$$\log A = M - 3.2 \qquad (3.3.4.2\text{-}1)$$

Foreshocks and swarm earthquakes are not excluded.

The probability distribution of earthquake magnitude is assumed to follow a Gutenberg-Richter relation with an upper limit, and coefficient b shall be 0.9, which is considered to be a average value for the area surrounding Japan. The minimum magnitude considered in the seismic hazard analysis shall be 5.0,[1] and the maximum magnitude shall be determined for each zoned area, considering the magnitude of past earthquakes and results of related long-term evaluation. The lower limit value of the maximum magnitude is 6.8 for the land area and 7.0 for the sea area.

The time series of occurrence of earthquakes is assumed to follow a stationary Poisson process.

The following section shows the conditions for evaluation and the evaluation results for each category of earthquakes.

3.3.4.3 Interplate/intraplate earthquakes without specified source faults for the Pacific plate

1) Target earthquakes

The earthquakes targeted as interplate/intraplate earthquakes without specified source faults for the Pacific plate are earthquakes associated with the subduction of the Pacific plate, which occur at a site nearer to land from the trench axis, where the depth of the upper surface of the plate is up to around 150 km. Since the following long-term evaluations have been published for subduction-zone earthquakes related to the target areas, these evaluations are taken into account when building the models: "Long-term Evaluation of the Miyagi-ken-Oki Earthquake" (ERC, 2000), "Long-term Evaluation of Seismic Activity from Sanriku-Oki to Boso-Oki" (ERC, 2002b), "Long-term Evaluation of Seismic Activity Along the Sagami Trough" (ERC, 2004c), and "Long-term Evaluation of Seismic Activity Along the Kuril Trench (Second Edition)" (ERC, 2004d). While the specific zoning is indicated in 2), the area targeted here is the area from along the Kuril Trench to the vicinity of Ogasawara-shoto islands.

The relationship with other earthquakes without specified source faults is as follows. First, regarding the land area, earthquakes of which the depth is 25 km or less are separately evaluated as "earthquakes occurring at onshore locations where active faults have not been specified" as discussed later. Therefore, in overlapping areas, earthquakes of which the depth is more than 25 km are evaluated as "interplate/intraplate earthquakes without specified source faults for the Pacific plate". In Urakawa-Oki, earthquakes of which the depth is 25 km to 45 km are separately evaluated as "earthquakes without specified source faults in Urakawa-Oki". Thus, those earthquakes are excluded from evaluation. In southern Kanto, the Pacific plate is subducting under the Philippine Sea plate, and when viewed as a plane, this category not only overlaps with "earthquakes occurring at onshore locations where active faults have not been specified", but also with "interplate/intraplate earthquakes without specified source faults for the Philippine Sea plate". These earthquakes are treated separately as shown in Figure 3.3.4.3-1. Specifically, earthquakes that are deeper than 5 km above the upper surface of the Pacific plate are regarded as Pacific plate earthquakes. Since earthquakes

[1] When using the small earthquake catalog, the occurrence frequency of earthquakes with a minimum magnitude of 5.0 or more used in the analysis is calculated based on the occurrence probability of earthquakes of magnitude 3.0 (or 4.0) or more and a Gutenberg-Richter relation with b=0.9.

in and south of the Boso-Oki region overlap with "earthquakes without specified source faults in the southern area of Izu-shoto islands", those of which the depth is more than 40 km are targeted as earthquakes of the Pacific plate.

2) Zoning

Figure 3.3.4.3-2 shows the zoning of interplate/intraplate earthquakes without specified source faults for the Pacific plate.

The area in and north of the Boso-hanto-Oki region is zoned while taking into account the division of areas and plate depth contours indicated in the long-term evaluations of related subduction-zone earthquakes, as well as Kosuga et al. (1996), the plate depth contours indicated by Katsumata et al. (2002), and Umino et al. (1990). The area is divided into the part shallower and the part deeper than around the 60 km depth contour of the upper surface of the plate. The southern Kanto area is determined to match the area of "*M*7 class earthquakes in Southern Kanto", and the boundary between Area No. 12 and Area No. 13 is the 80 km depth contour of the upper surface of the Philippine Sea plate by Ishida (1992). In the area in and south of the Boso-Oki region, subduction-zone earthquakes have not been evaluated. Thus, the area is divided by the 60 km and 150 km depth contours presumed from the trench axis and the depth contours described in Utsu (2001).

3) Earthquake catalogs

The catalogs of medium earthquakes and small earthquakes (the minimum magnitude of 4.0) are both used, in principle. However, as shown in Figure 3.3.4.3-2, for the area including the Etorofu, Kunashiri, Shikotan and Habomai Islands, the medium earthquake catalog is limited to earthquakes of magnitude 5.0 or more that have occurred since 1960, considering the detection capability of the observation network. For the area around Kanto, earthquakes of magnitude 5.0 or more that have occurred since 1940, when the influence of the 1923 Taisho Kanto Earthquake has diminished, are used as the medium earthquake catalog. For the area in and south of the Boso-Oki region, only earthquakes of magnitude 5.0 or more that have occurred since 1983 are used, and the small and medium earthquake catalogs are not used, considering the detection capability of the observation network.

The source depth covered is up to 200 km, but as mentioned above, data of other earthquakes without specified source faults that overlap, when viewed as a plane, are excluded. In addition, data of earthquakes that are separately evaluated as related subduction-zone earthquakes are excluded from the catalogs.

Figure 3.3.4.3-3 shows the epicenter distribution of earthquakes of magnitude 5.0 or more that have occurred since 1926, and Figure 3.3.4.3-4 shows the epicenter distribution of earthquakes of magnitude 4.0 or more that have occurred since 1983. Figure 3.3.4.3-5 and Figure 3.3.4.3-6 show the cumulative occurrence frequency by earthquake magnitude.

4) Maximum magnitude

The maximum magnitude is determined for each zoned area, while taking into account the magnitude of the largest past earthquake and the long-term evaluations of subduction-zone earthquakes in the related area. However, if the magnitude of the largest past earthquake is less than M_j =7.0, M_j =7.0 is determined as the maximum magnitude for the area. Figure 3.3.4.3-7 and Table 3.3.4.3-1 show the determined maximum magnitudes and the basis for the determination.

5) Occurrence ratio between interplate earthquakes and intraplate earthquakes

In the area north of the Ibaraki-ken-Oki region, the occurrence ratio used in the "Preliminary Version of PSHM (Specific Area, Northern Japan)" (Subcommittee for Long-term Evaluations/Subcommittee for Evaluation of Strong Ground Motion, ERC, 2003) is applied. This ratio has been determined based on the ratio of the number of earthquakes occurring above and those occurring below a boundary that is 20 km deep from the upper surface of the plate, as shown in Figure 3.3.4.3-8 (NIED, 2003). For the area that is deeper than the 60 km depth contour, all earthquakes are regarded as intraplate earthquakes. Meanwhile, with regard to the area in and south of southern Kanto, which was not covered by the "Preliminary Version of PSHM (Specific Area, Northern Japan)", it is not easy to distinguish between the types of earthquakes since the seismic source distribution in the depth direction is complicated due to the presence of the Philippine Sea plate. Thus, the ratio is determined as follows. First, earthquakes in the area deeper than 60 km (80 km for southern Kanto) are all regarded as intraplate earthquakes, and the ratio for the area of southern Kanto of which the depth is 80 km or less is assumed to be 1:1, and the ratios for the remaining two areas are assumed to be the same as the ratio for the north neighboring Ibaraki-Oki region (8:1). The ratios between interplate earthquakes and intraplate earthquakes thus determined are shown in Figure 3.3.4.3-9.

6) Determination of the fault planes

The center of the fault plane for an interplate earthquake is positioned at the depth of the upper surface of the plate, and that for an intraplate earthquake is positioned 30 km deeper than the upper surface of the plate. The shape of the fault plane is circular, and the fault plane for an interplate earthquake is aligned with the upper surface of the plate, while a horizontal fault plane is arranged within the plate for an intraplate earthquake. Size S (km^2) of a circular fault is determined according to the magnitude to satisfy the following formula which has rounded the coefficient of the formula by Utsu and Seki (1955):

$$\log S = M - 4.0 \qquad (3.3.4.3\text{-}1)$$

7) Conversion to moment magnitude M_w

Moment magnitude M_w is assumed to be equal to M_j.

8) Distribution of the earthquake occurrence frequency

Figure 3.3.4.3-10 (a) shows the distribution of occurrence frequency for the total of interplate and intraplate earthquakes (the occurrence frequency of earthquakes of magnitude 5.0 or more within one year in an area of 0.1 degrees × 0.1 degrees). It adopts the mean value of the frequency for the following four cases: 1) the case using the medium earthquake catalog and the zoning method, 2) the case using the medium earthquake catalog and the non-zoning method, 3) the case using the small earthquake catalog and the zoning method, and 4) the case using the small earthquake catalog and the non-zoning method. The results, distinguished between those for interplate earthquakes and those for intraplate earthquakes considering the above-mentioned ratio, are shown in Figure 3.3.4.3-10 (b) and (c).

	(Interplate:Intraplate)
(1) All crustal earthquakes	
(2) All earthquakes occur within the Philippine Sea plate (Maximum *M* of earthquakes without specified source faults is 6.6)	0 : 1
(3) All earthquakes occur on the upper surface or within the Philippine Sea plate (Maximum *M* of earthquakes without specified source faults is 6.6)	1 : 1
(4) Earthquakes occur on the upper surface or within the Pacific plate (Maximum *M* of earthquakes without specified source faults is 6.6 for those on the upper surface, and the largest *M* of past earthquakes for those within the plate)	1 : 1
(5) Earthquakes occur on the upper surface or within the Pacific plate (Maximum *M* of earthquakes without specified source faults is the largest *M* of past earthquakes)	8 : 1
(6) All earthquakes occur within the Pacific plate (Maximum *M* of earthquakes without specified source faults is the largest *M* of past earthquakes)	0 : 1

Bold arrow denotes the area for which earthquakes of around *M*7 are taken into consideration.

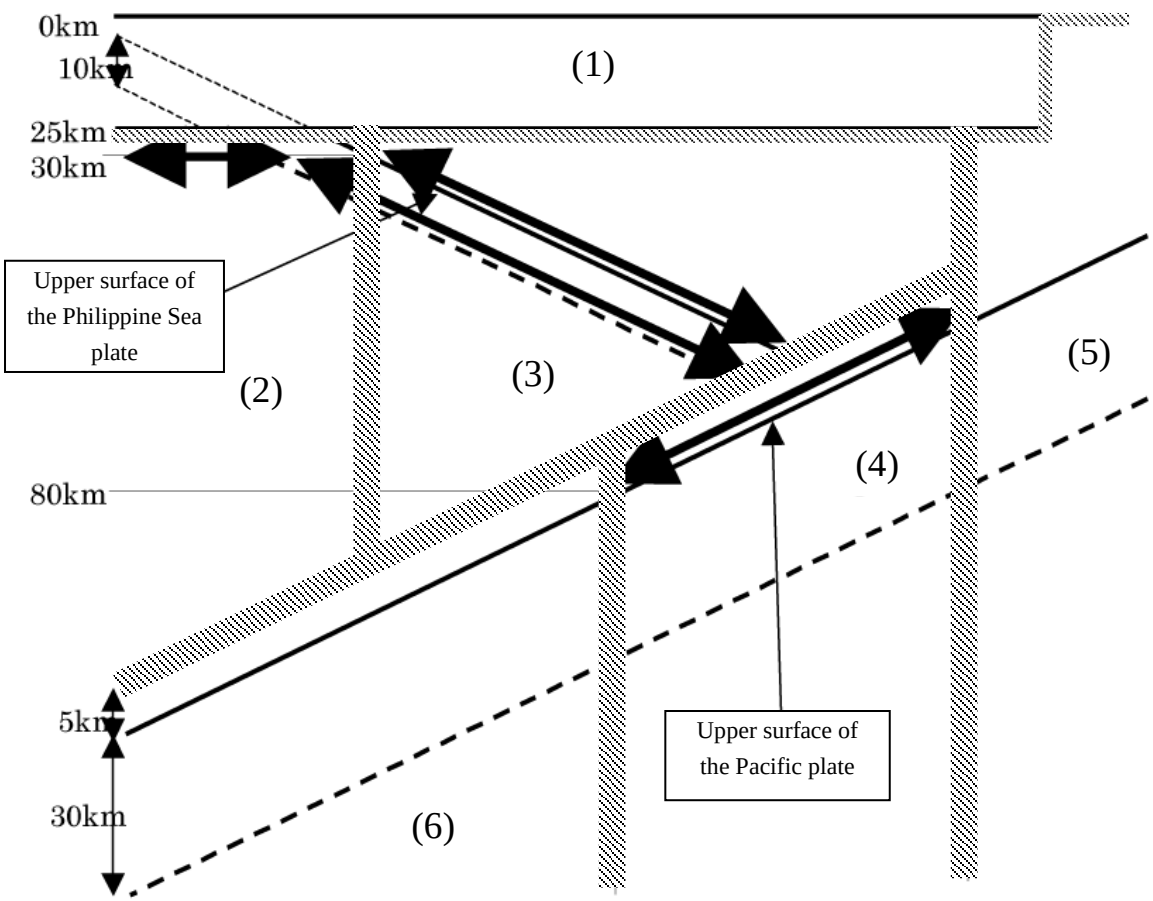

Figure 3.3.4.3-1 Earthquakes treatment schematic for subduction-zone earthquakes of around *M*7 and earthquakes without specified source faults in the vicinity of Kanto plain

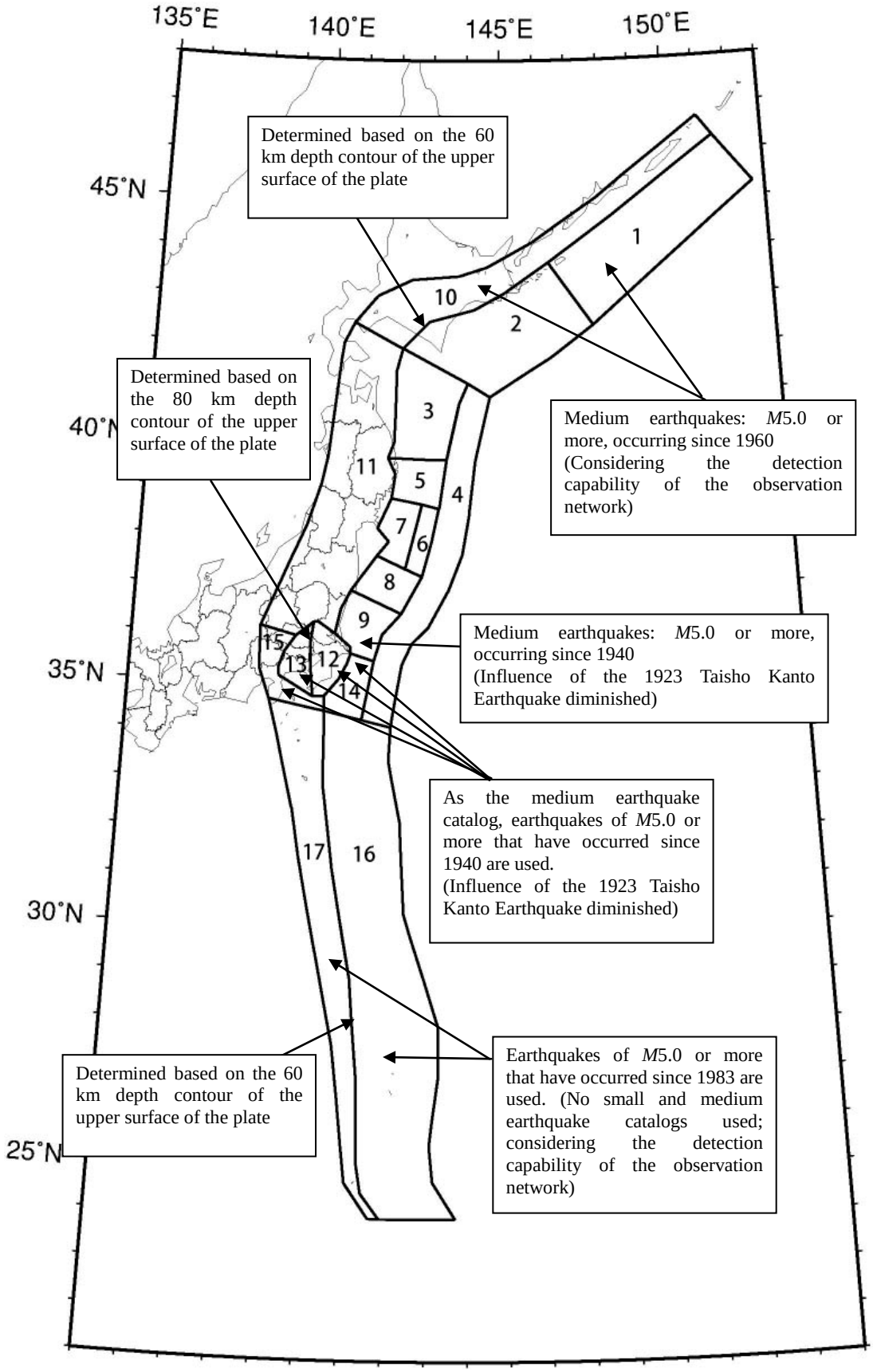

Figure 3.3.4.3-2 Zoning of earthquakes without specified source faults for the Pacific plate. Earthquake catalogs used for calculating the frequency are also shown. A standard catalog is used where no catalog is specified.

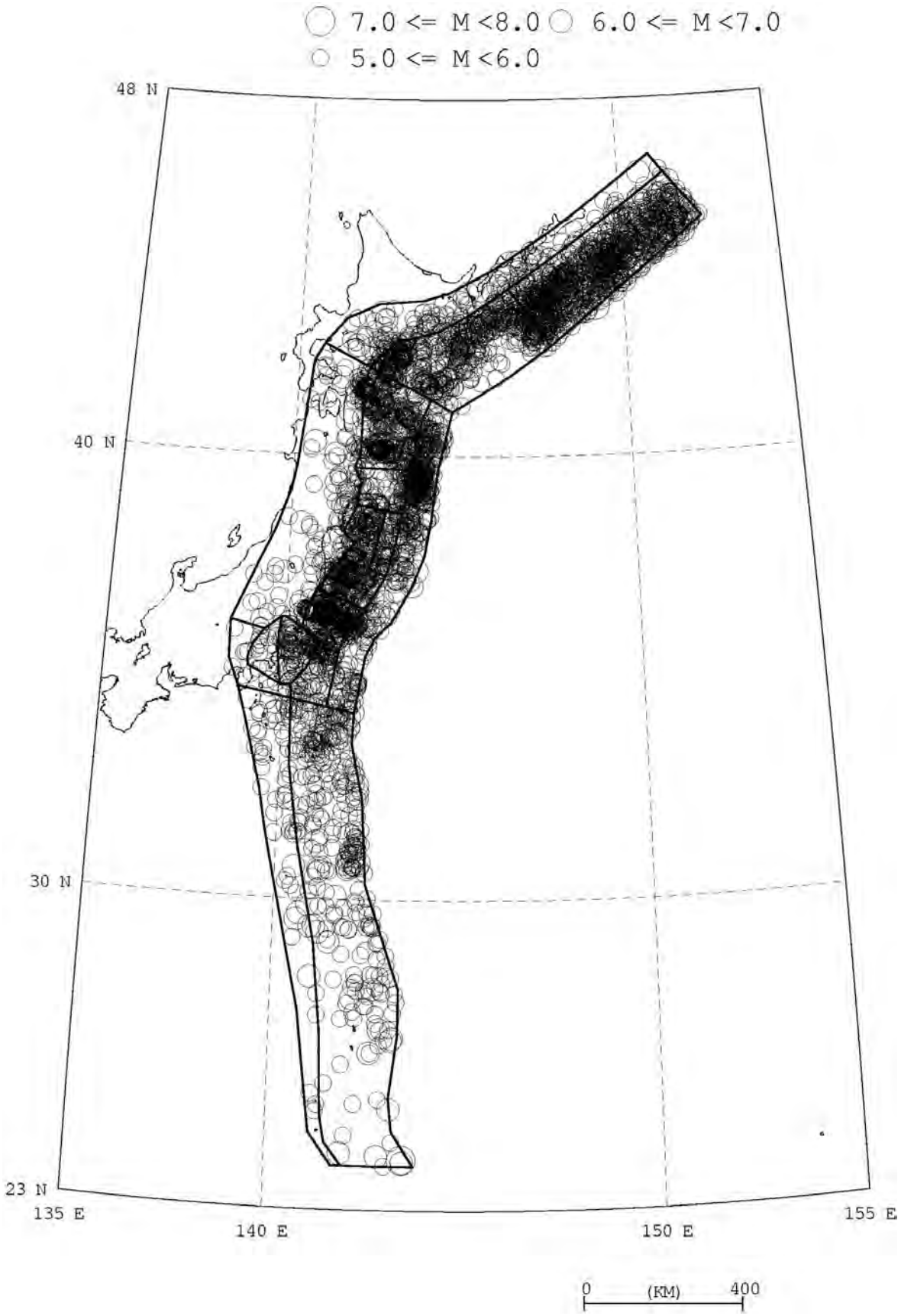

Figure 3.3.4.3-3 Epicenter distribution of earthquakes of *M*≥5.0 since 1926

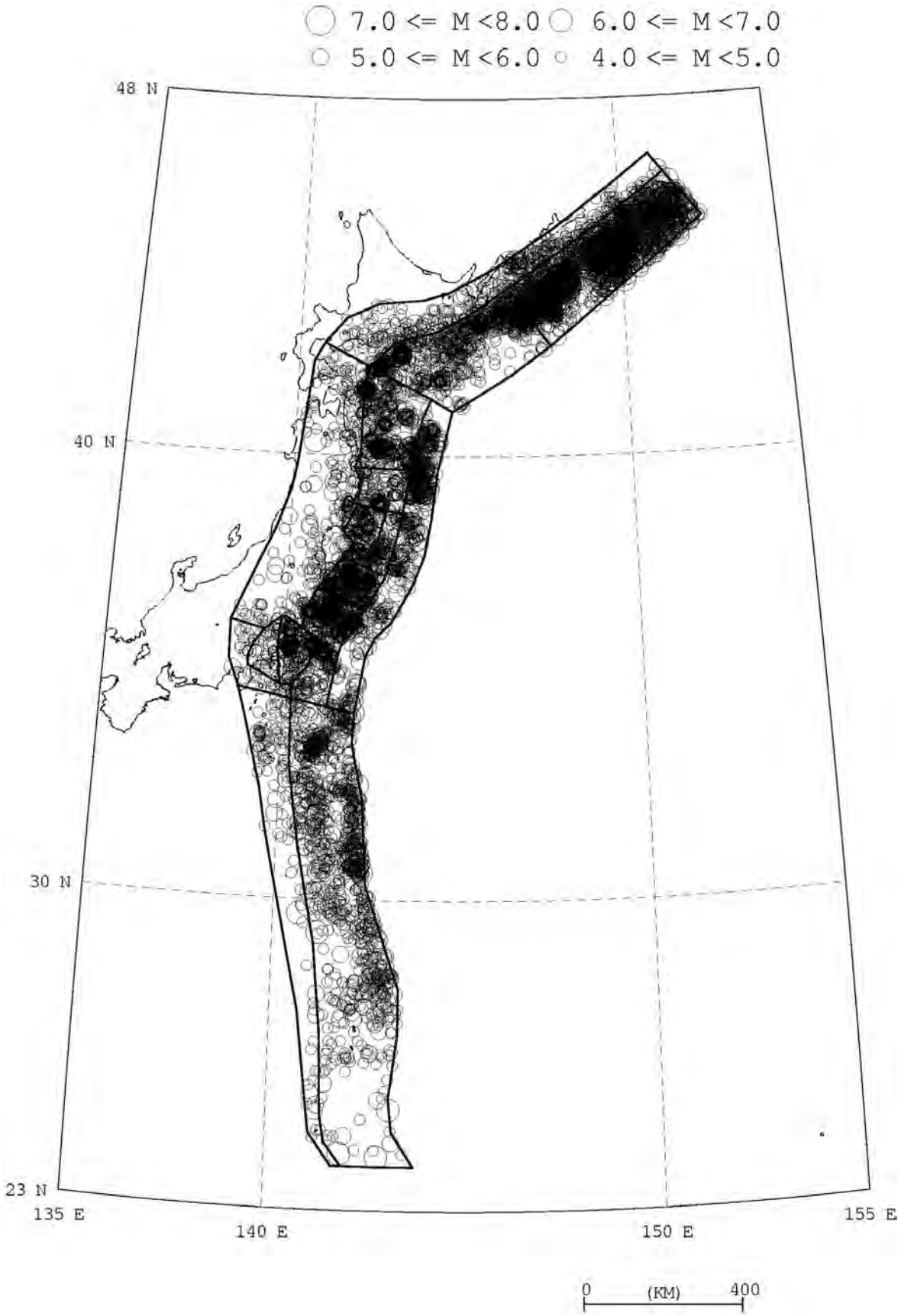

Figure 3.3.4.3-4 Epicenter distribution of earthquakes of *M*≥4.0 since 1983

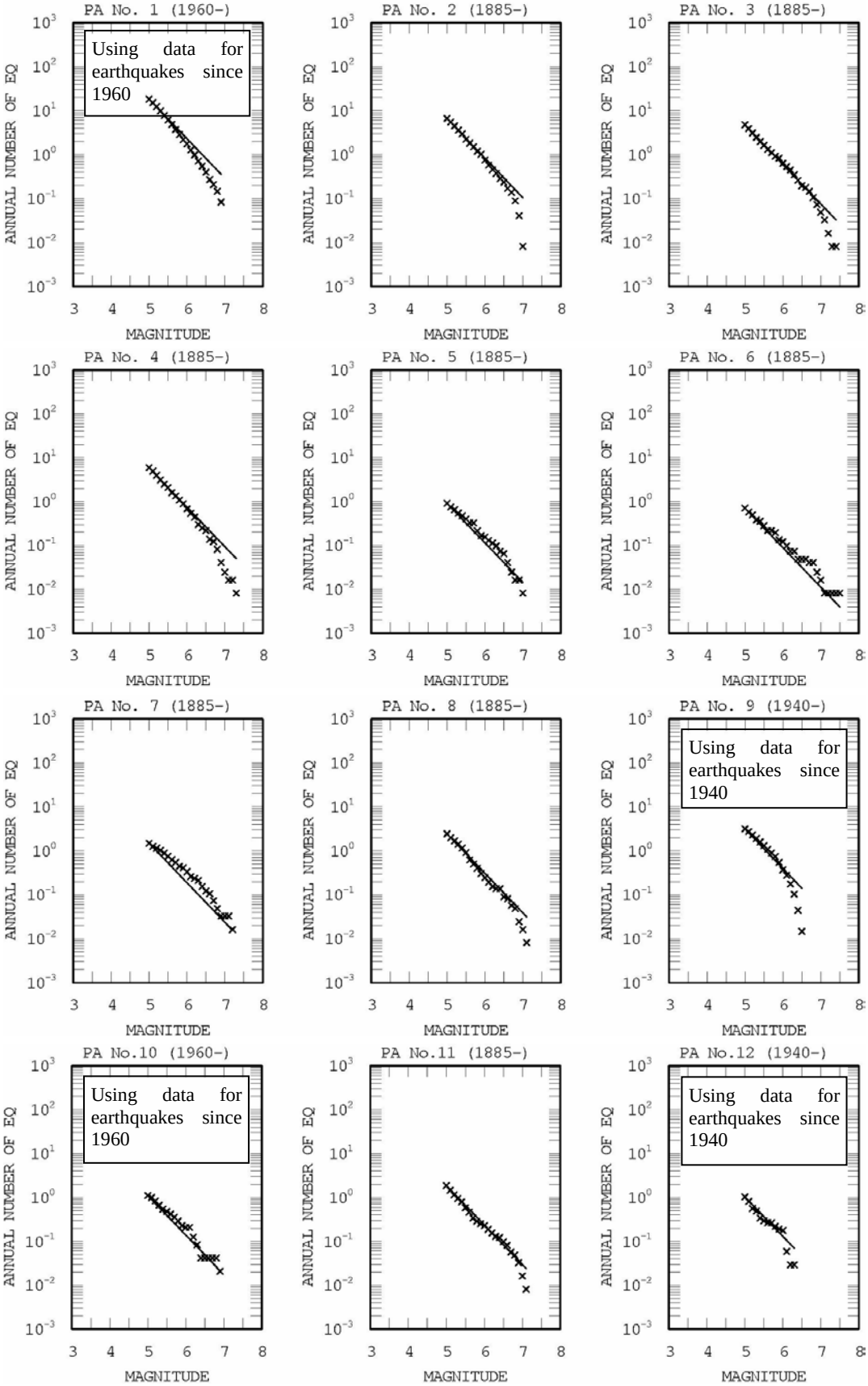

Figure 3.3.4.3-5 Cumulative frequency by earthquake magnitude based on medium earthquake catalog (part 1)

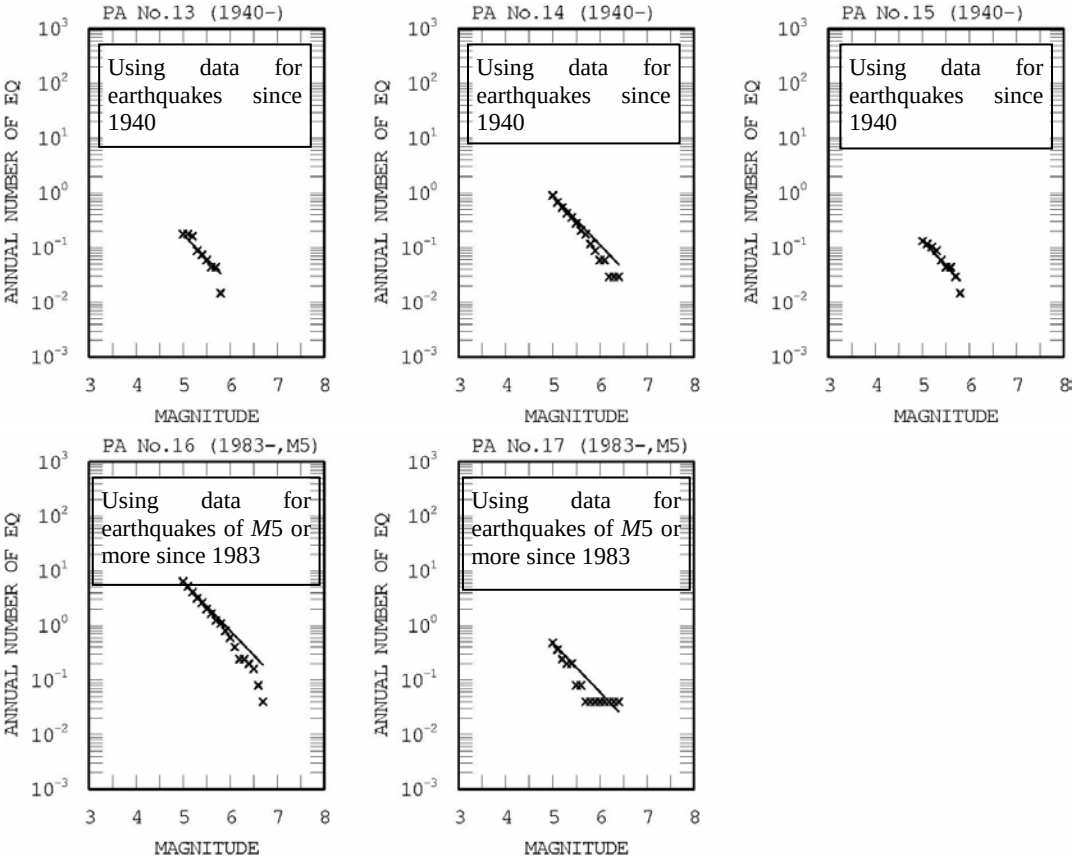

Figure 3.3.4.3-5 Cumulative frequency by earthquake magnitude based on medium earthquake catalog (part 2)

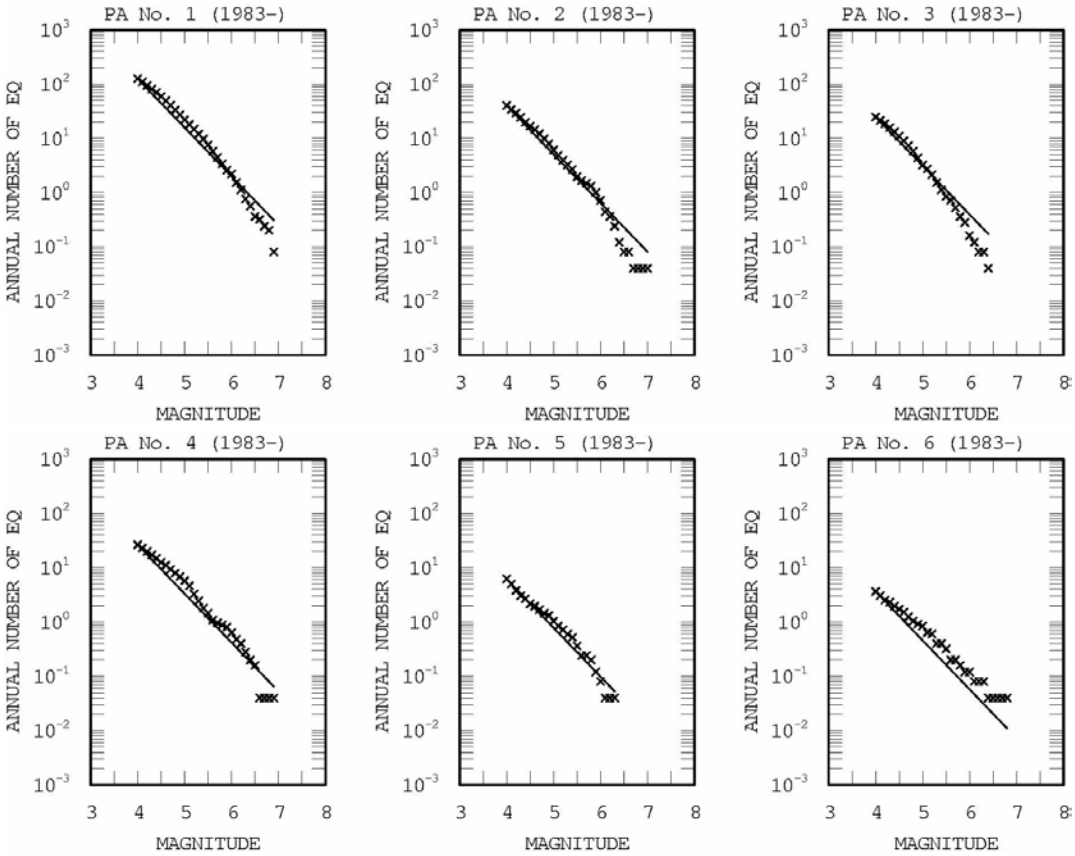

Figure 3.3.4.3-6 Cumulative frequency by earthquake magnitude based on small earthquake catalog (part 1)

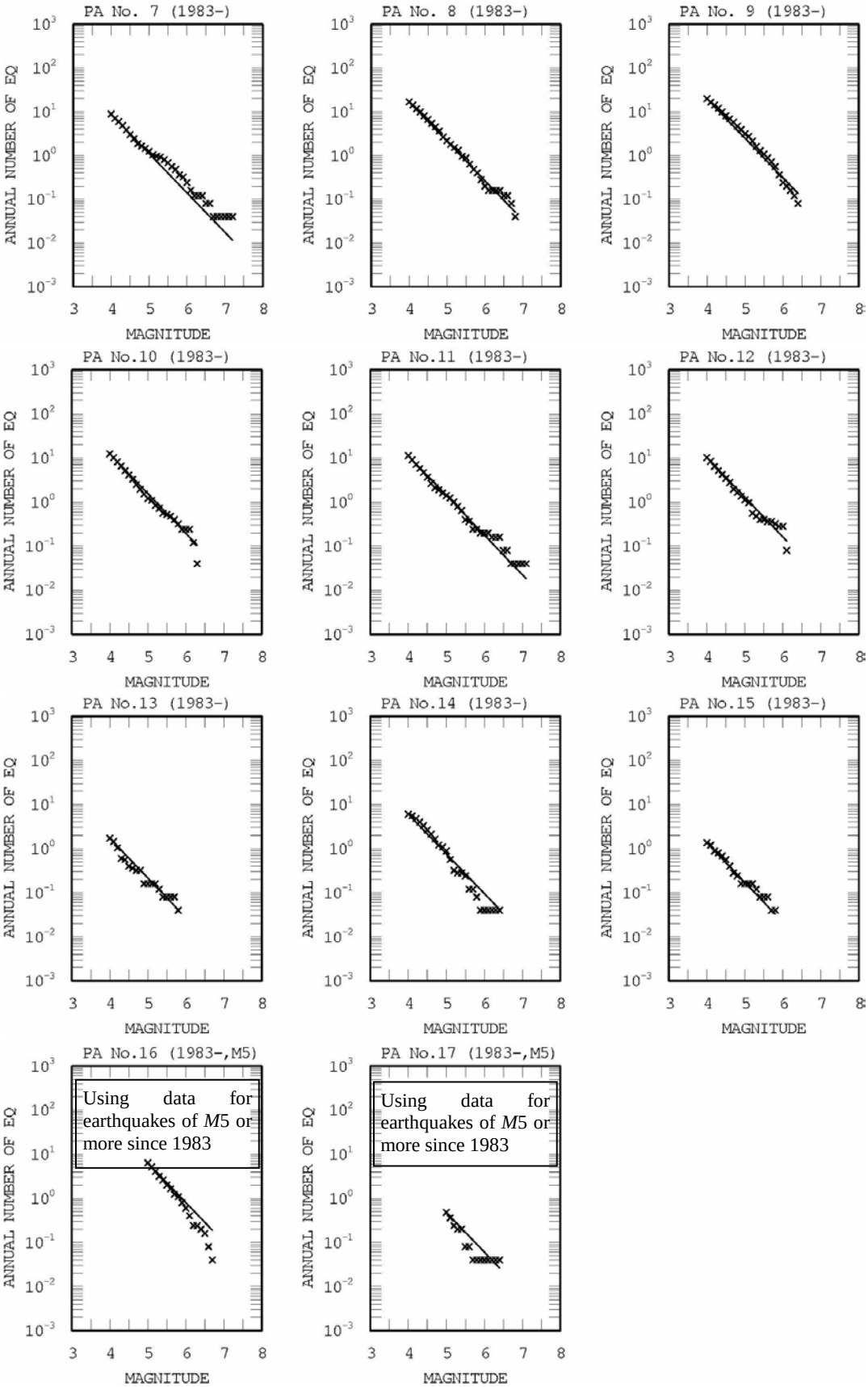

Figure 3.3.4.3-6 Cumulative frequency by earthquake magnitude based on small earthquake catalog (part 2)

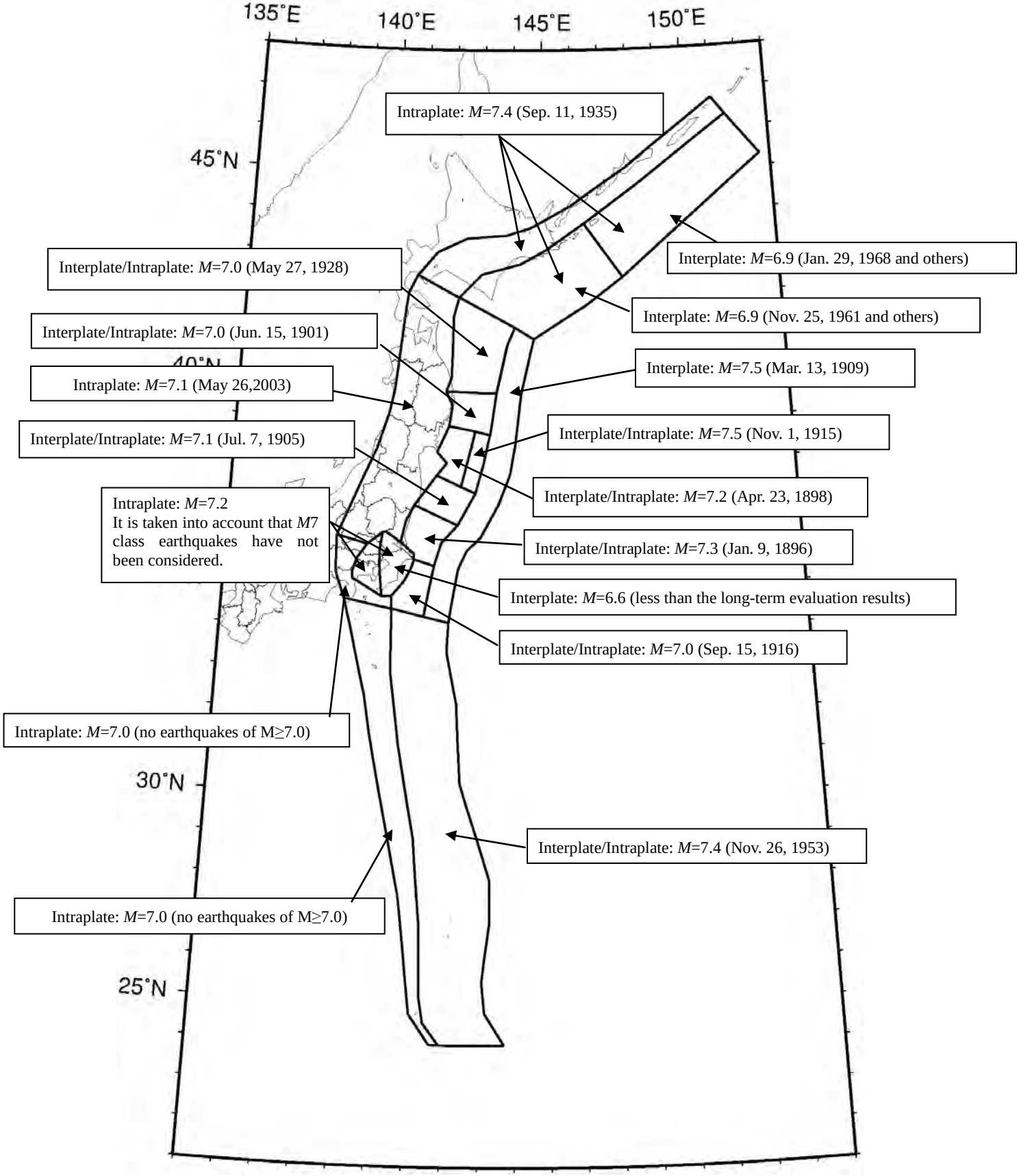

Figure 3.3.4.3-7 Maximum magnitude of earthquakes determined by the zoning area

Table 3.3.4.3-1 Maximum magnitude determined for each area and the basis for the determination (part 1)

Area No.		Maximum *M*	Basis	Remarks
1	Interplate	6.9	Jan. 29, 1968 and others	Earthquakes of around *M*7.1 are separately evaluated as relatively small subduction-zone earthquakes.
	Intraplate	7.4	Sep. 11, 1935 (h=90 km)	Same maximum *M* is determined for intraplate earthquakes in areas No.1, 2, and 10. Earthquake on Feb. 21, 1937 (*M*7.6) is judged to be a shallow earthquake.
2	Interplate	6.9	Nov. 25, 1961 and others	Earthquakes of around *M*7.1 are separately evaluated as relatively small subduction-zone earthquakes.
	Intraplate	7.4	Sep. 11, 1935 (h=90 km)	Same maximum *M* is determined for intraplate earthquakes in areas No.1, 2, and 10.
3	Interplate and intraplate	7.0	May 27, 1928	For interplate earthquakes, earthquakes of *M*7.1-7.6 are evaluated as subduction-zone earthquakes other than characteristic earthquakes. Same maximum *M* is determined for interplate and intraplate earthquakes.
4	Interplate	7.5	Mar. 13, 1909	Earthquakes of approximately *M*8.2 are separately evaluated as subduction-zone earthquakes. Although these earthquakes are mentioned in the long-term evaluation as being Boso-Oki earthquakes, they are evaluated here since they have not been independently modeled.
	Intraplate	—		All earthquakes are assumed to be interplate earthquakes from the viewpoint of ground motion evaluation.
5	Interplate and intraplate	7.0	Jun. 15, 1901	No subduction-zone earthquakes. Same maximum *M* is determined for interplate and intraplate earthquakes.
6	Interplate and intraplate	7.5	Nov. 1, 1915	Earthquakes of approximately *M*7.7 are separately evaluated as subduction-zone earthquakes. Same maximum *M* is determined for interplate and intraplate earthquakes.
7	Interplate and intraplate	7.2	Apr. 23, 1898	Miyagi-ken-Oki earthquakes of around *M*7.3-7.5 are separately evaluated as subduction-zone earthquakes. Same maximum *M* is determined for interplate and intraplate earthquakes.
8	Interplate and intraplate	7.1	Jul. 7, 1905	Earthquakes of approximately *M*7.4 are separately evaluated as subduction-zone earthquakes. Same maximum *M* is determined for interplate and intraplate earthquakes.
9	Interplate	7.3	Jan. 9, 1896	Earthquakes of around *M*6.8 (earthquakes subject to evaluation are those of *M*6.7-7.0) are separately evaluated as subduction-zone earthquakes, but there is a possibility of making re-evaluation by including the earthquake of *M*7.0 that has occurred on May 8, 2008.
	Intraplate	7.3	(Same as above)	Same maximum *M* is determined for interplate and intraplate earthquakes.
10	Interplate	—		(All earthquakes are assumed to be intraplate earthquakes.)
	Intraplate	7.4	Sep. 11, 1935 (h=90 km)	Same maximum *M* is determined for intraplate earthquakes in areas No.1, 2, and 10.
11	Interplate	—		(All earthquakes are assumed to be intraplate earthquakes.)
	Intraplate	7.1	May 26, 2003 Miyagi-ken-Oki	

Table 3.3.4.3-1 Maximum magnitude determined for each area and the basis for the determination (part 2)

Area No.		Maximum *M*	Basis	Remarks
12	Interplate	6.6	Less than the long-term evaluation results	Earthquakes of around *M*6.7-7.2 are separately evaluated as subduction-zone earthquakes.
	Intraplate	7.2		It is taken into account that these earthquakes are not included in the category of "*M*7 class earthquakes" which are subduction-zone earthquakes.
13	Interplate	—		(All earthquakes are assumed to be intraplate earthquakes.)
	Intraplate	7.2		It is taken into account that these earthquakes are not included in the category of "*M*7 class earthquakes" which are subduction-zone earthquakes.
14	Interplate and intraplate	7.0	Sep. 15, 1916	Same maximum *M* is determined for interplate and intraplate earthquakes.
15	Interplate	—		(All earthquakes are assumed to be intraplate earthquakes.)
	Intraplate	7.0	Lowest limit value is applied.	No earthquakes of *M*7.0 or more.
16	Interplate and intraplate	7.4	Nov. 26, 1953	Same maximum *M* is determined for interplate and intraplate earthquakes. Although these earthquakes are mentioned in the long-term evaluation as being Boso-Oki earthquakes, they are evaluated here since they have not been independently modeled.
17	Interplate	—		(All earthquakes are assumed to be intraplate earthquakes.)
	Intraplate	7.0	Lowest limit value is applied.	No earthquakes of *M*7.0 or more.

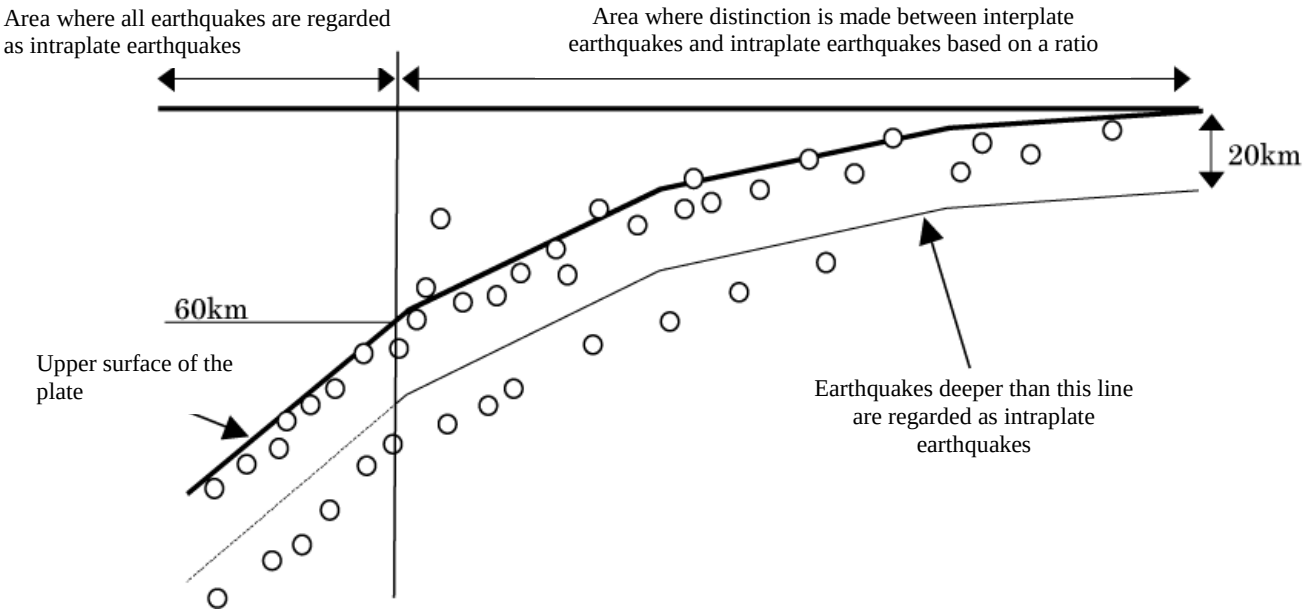

Figure 3.3.4.3-8 Idea of distinguishing between interplate earthquakes and intraplate earthquakes (SLTE/SESGM, ERC, 2003).

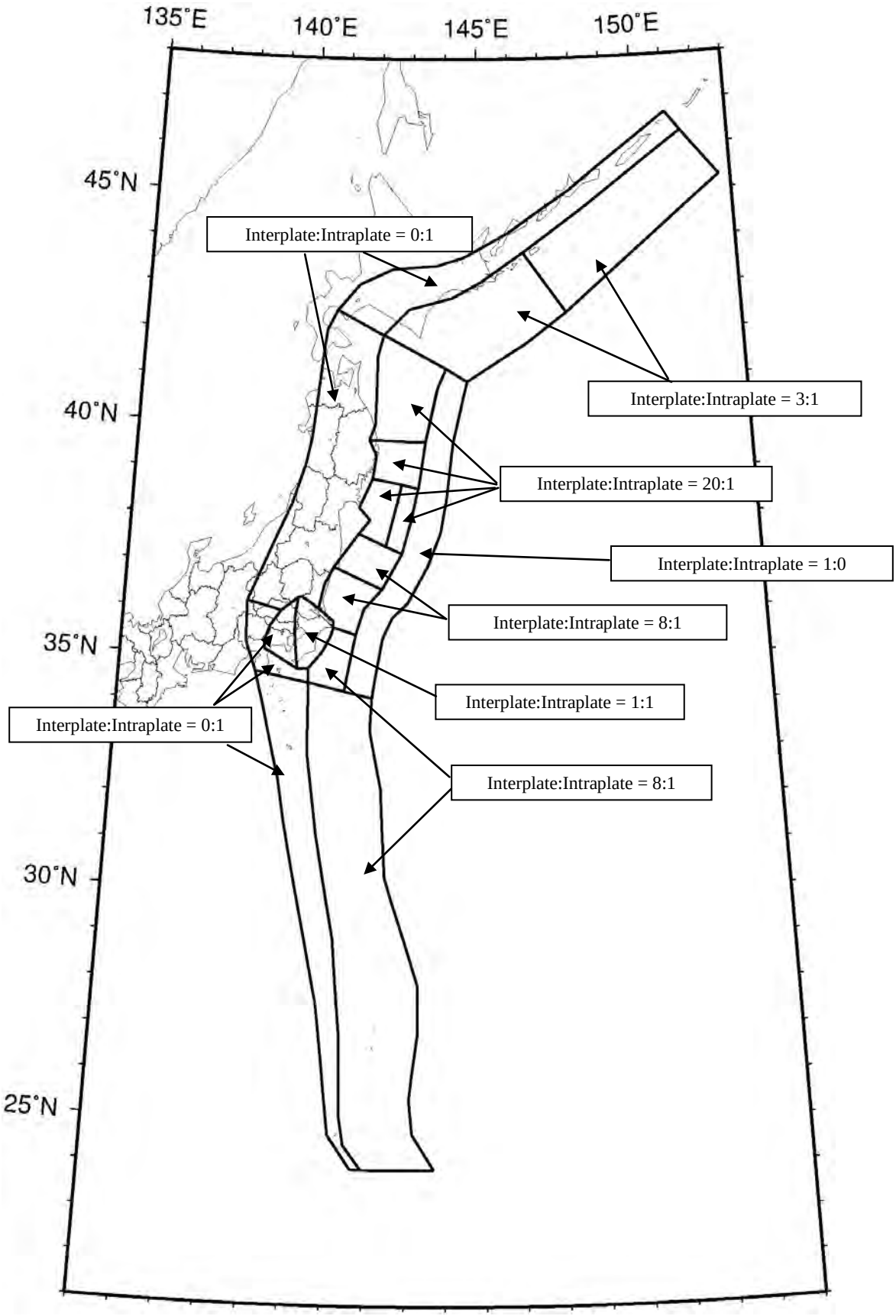

Figure 3.3.4.3-9 Occurrence ratio between interplate earthquakes and intraplate earthquakes by the zoning area

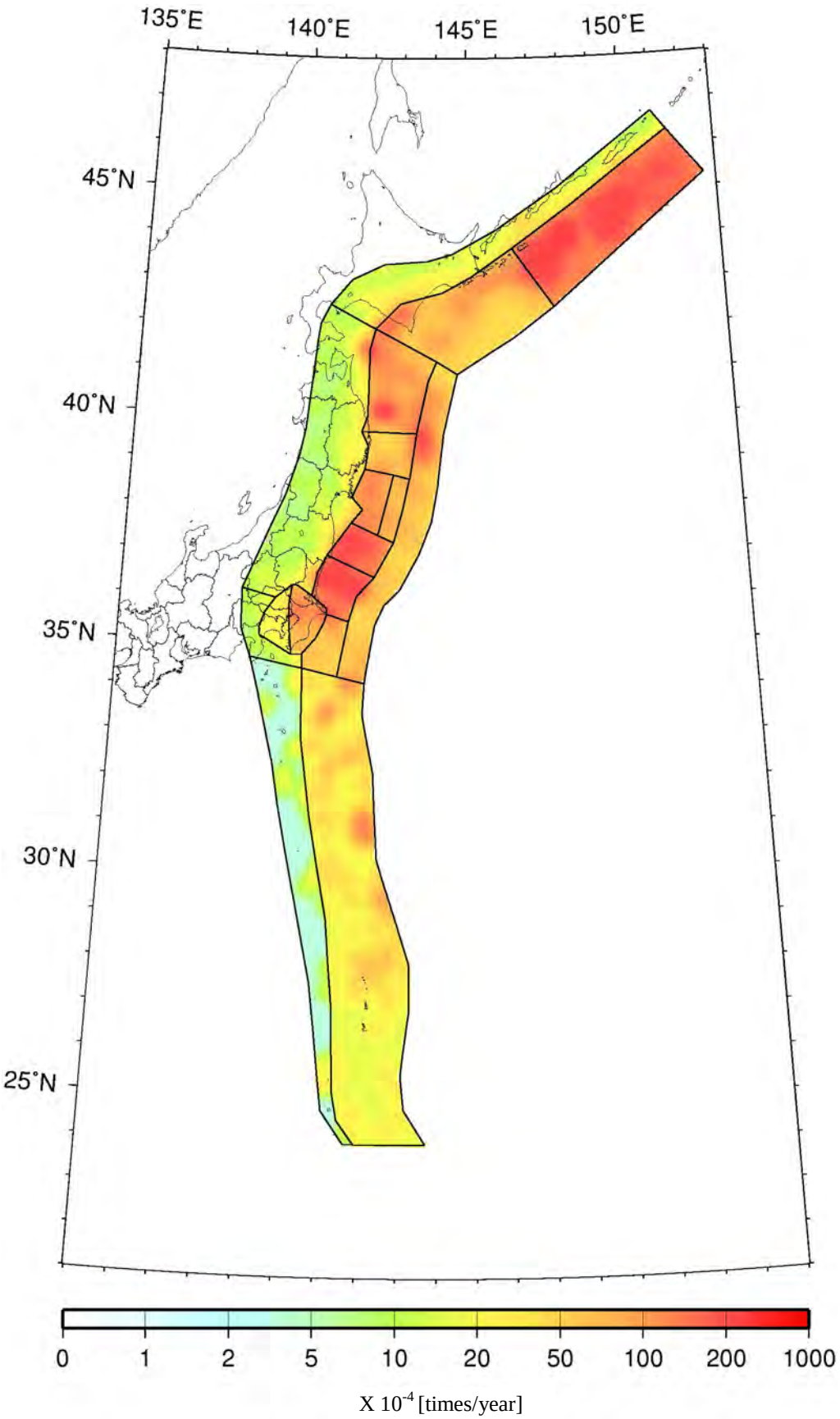

(a) Total for interplate and intraplate earthquakes

Figure 3.3.4.3-10 Occurrence frequency of earthquakes in the Pacific plate (per 0.1-degree square, *M*5.0 or more)

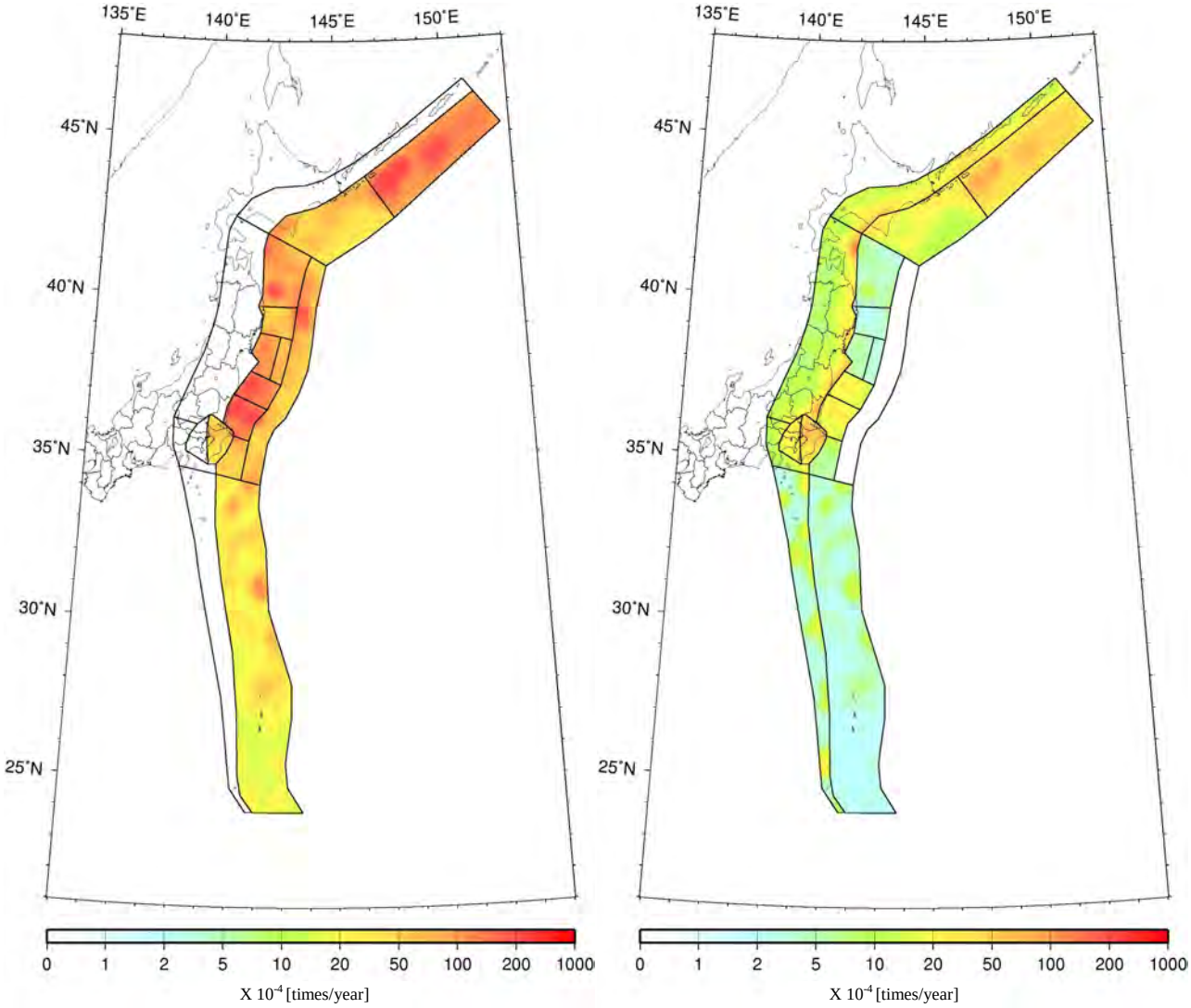

(b) Interplate earthquakes

(c) Intraplate earthquakes

Figure 3.3.4.3-10 Occurrence frequency of earthquakes in the Pacific plate (per 0.1-degree square, *M*5.0 or more)

3.3.4.4 Interplate/intraplate earthquakes without specified source faults for the Philippine Sea plate

1) Target earthquakes

The earthquakes targeted as interplate/intraplate earthquakes without specified source faults for the Philippine Sea plate are earthquakes associated with the subduction of the Pacific plate, which occur at a site nearer to land from the trench axis. Since the following long-term evaluations have been published for subduction-zone earthquakes related to the target areas, these evaluations are taken into account when building the models: "Long-term Evaluation of Nankai Trough Earthquakes" (ERC, 2001b), "Long-term Evaluation of Seismic Activity in Hyuganada and in the Vicinity of Nansei-shoto islands" (ERC, 2004a), and "Long-term Evaluation of Seismic Activity Along the Sagami Trough" (ERC, 2004c). While the specific zoning is indicated in 2), the earthquakes targeted here are roughly divided into those in the following five areas: southern Kanto, along the Nankai Trough, Akinada-Iyonada-Bungosuido, Hyuganada, and a relatively shallow area from Kyushu to Nansei-shoto islands.

The relationship with other earthquakes without specified source faults is as follows. First, regarding the land area, earthquakes of which the depth is 25 km or less are separately evaluated as "earthquakes occurring at onshore locations where active faults have not been specified" as discussed later. Therefore, in overlapping areas, earthquakes of which the depth is more than 25 km are evaluated as "interplate/intraplate earthquakes without specified source faults for the Philippine Sea plate". In southern Kanto, the Pacific plate is subducting under the Philippine Sea plate, and when viewed as a plane, this category overlaps with "interplate/intraplate earthquakes without specified source faults

for the Pacific plate" discussed in 3.3.4.3. Thus, these earthquakes are distinguished from each other based on the depth of the seismic source. The specific distinguishing method is, as explained above in the section about "earthquakes without specified source faults for the Pacific plate", earthquakes that are shallower than 5 km above the upper surface of the Pacific plate are regarded as Philippine Sea plate earthquakes. While the area in the vicinity of Nansei-shoto islands overlaps with that of "earthquakes without specified source faults in the vicinity of Nansei-shoto islands", earthquakes of which the depth is 60 km or more are regarded as earthquakes at the Philippine Sea plate. In the area south from the trench axis, shallow earthquakes have occurred from Izu-shoto islands to Ogasawara-shoto islands. They are inferred to be earthquakes occurring within the Philippine Sea plate, but have been modeled separately as "earthquakes without specified source faults in the southern area of Izu-shoto islands".

2) Zoning

Figure 3.3.4.4-1 shows the zoning of interplate/intraplate earthquakes without specified source faults for the Philippine Sea plate. The areas of Akinada-Iyonada-Bungosuido, Hyuganada, and the area corresponding to relatively deep earthquakes from Kyushu to the vicinity of Nansei-shoto islands are determined by taking into account the areas determined in long-term evaluations. The south-side boundary of the area along the Nankai Tough is determined by taking into account the trench axis, and the north-side boundary is determined by taking into account the northernmost point of the epicenter distribution. The area of southern Kanto is determined to match the area of "*M*7 class earthquakes in Southern Kanto", and the boundary between Area No. 5 and Area No. 6 is the 30 km depth contour of the upper surface of the Philippine Sea plate by Ishida (1992). Since earthquakes in the area including Izu Peninsula are separately modeled as earthquakes without specified source faults in the land area, they are not evaluated as earthquakes at the Philippine Sea plate.

A change from the ERC (2008b) is that a part of the area from Bungosuido through eastern Kyushu to Nansei-shoto islands where relatively deep earthquakes occur is included in the area of Akinada-Iyonada-Bungosuido (see Figure 3.4.4.4-2).

3) Earthquake catalogs

The catalogs of medium earthquakes and small earthquakes (the minimum magnitude of 4.0) are both used, in principle. However, for the area of southern Kanto, earthquakes of magnitude 5.0 or more that have occurred since 1940, when the influence of the 1923 Taisho Kanto Earthquake has diminished, are used as the medium earthquake catalog. For the area from Kyushu to the vicinity of Nansei-shoto islands where relatively deep earthquakes occur, only earthquakes of magnitude 5.0 or more that have occurred since 1983 are used, and the small and medium earthquake catalogs are not used, considering the detection capability of the observation network. With regard to the source depth, earthquakes of which the depth is more than 25 km are used for the area that overlaps with the area of earthquakes without specified source faults in the land area, and earthquakes that correspond to earthquakes without specified source faults for the Pacific plate are excluded for southern Kanto. In addition, earthquakes that are separately evaluated as related subduction-zone earthquakes are excluded from the catalogs.

Figure 3.3.4.4-3 shows the epicenter distribution of earthquakes of magnitude 5.0 or more that have occurred since 1926, and Figure 3.3.4.4-4 shows the epicenter distribution of earthquakes of magnitude 4.0 or more that have occurred since 1983. Figure 3.3.4.4-5 and Figure 3.3.4.4-6 show the cumulative occurrence frequency by earthquake magnitude.

4) Maximum magnitude

The maximum magnitude is determined for each zoned area, while taking into account the magnitude of the largest earthquake that has occurred since 1600 and the long-term evaluations of subduction-zone earthquakes in the related area. Table 3.3.4.4-1 and Table Figure 3.3.4.4-7 show the determined maximum magnitudes and the basis for the determination.

5) Occurrence ratio between interplate earthquakes and intraplate earthquakes

In the area of Hyuganada, the occurrence ratio between interplate earthquakes and intraplate earthquakes is determined as 7:3, referring to Uehira et al. (2001). In the area of southern Kanto, the ratio between interplate earthquakes and intraplate earthquakes is assumed to be 1:1 in the northern area where the upper surface of the plate is deeper than 30 km, and all earthquakes are regarded as intraplate earthquakes in the southern area, taking into account that shallow earthquakes will be evaluated as crustal earthquakes. In other areas, all earthquakes are regarded as intraplate earthquakes. The ratio for each area is shown in Figure 3.3.4.4-8.

6) Determination of the fault planes

After determining the upper surface of the Philippine Sea plate based on the long-term evaluations for the target areas and past research results, the center of the fault plane for an interplate earthquake is positioned at the depth of the upper surface of the plate, and that for an intraplate earthquake is positioned 10 km deeper than the upper surface of the plate. The shape of the fault plane is circular, and the fault plane for an interplate earthquake is aligned with the upper surface of the plate, while a horizontal fault plane is arranged within the plate for an intraplate earthquake. The size of a fault is determined according to the magnitude to satisfy the formula by Utsu and Seki (1955) (Formula 3.3.4.3-1).

7) Conversion to moment magnitude M_w

Moment magnitude M_w is assumed to be equal to M_j.

8) Distribution of the earthquake occurrence frequency

Figure 3.3.4.4-9 (a) shows the distribution of occurrence frequency for the total of interplate and intraplate earthquakes (the occurrence frequency of earthquakes of magnitude 5.0 or more within one year in an area of 0.1 degrees × 0.1 degrees). It adopts the mean value of the frequency for the following four cases: 1) the case using the medium earthquake catalog and the zoning method, 2) the case using the medium earthquake catalog and the non-zoning method, 3) the case using the small earthquake catalog and the zoning method, and 4) the case using the small earthquake catalog and the non-zoning method. The results, distinguished between those for interplate earthquakes and those for intraplate earthquakes considering the above-mentioned ratio, are shown in Figure 3.3.4.4-9 (b) and (c).

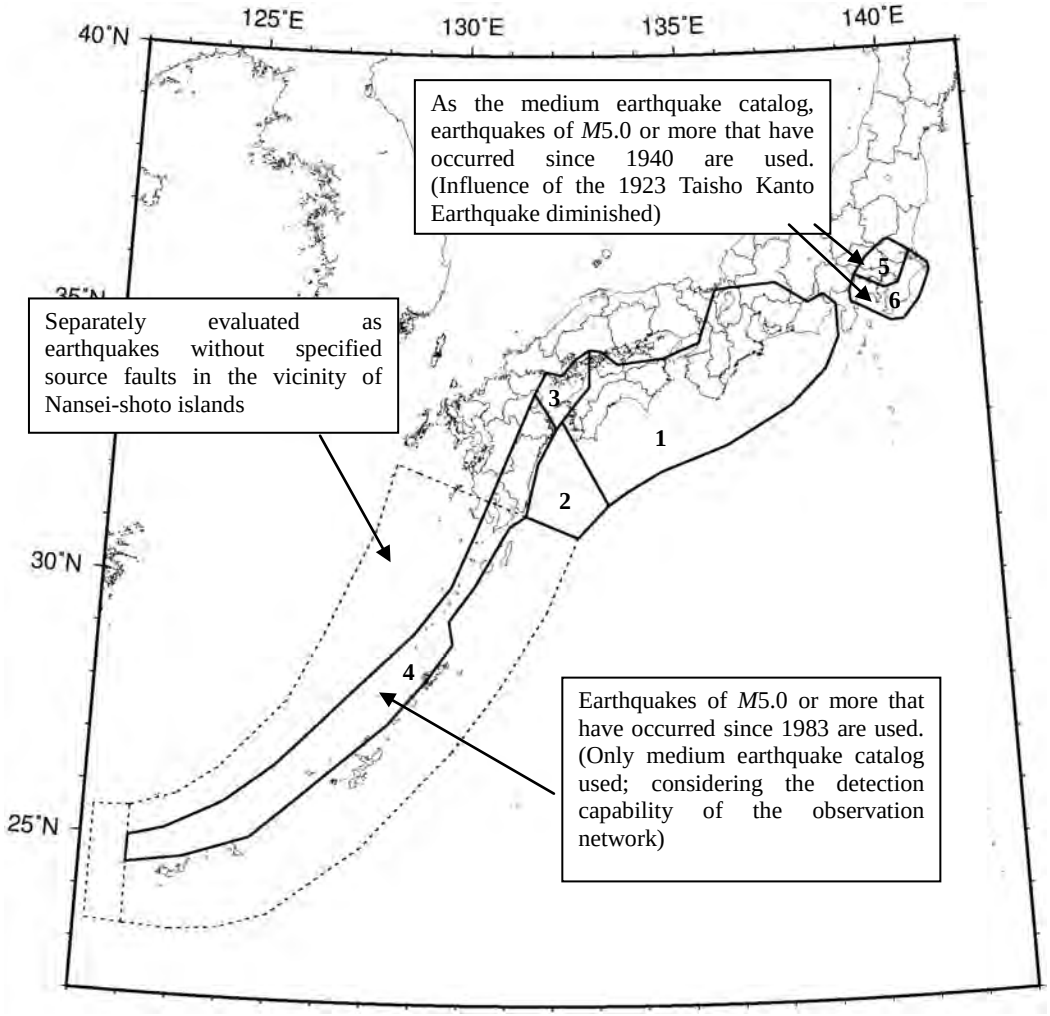

Figure 3.3.4.4-1 Zoning of earthquakes without specified source faults for the Philippine Sea plate. Earthquake catalogs used for calculating the frequency are also shown. A standard catalog is used where no catalog is specified.

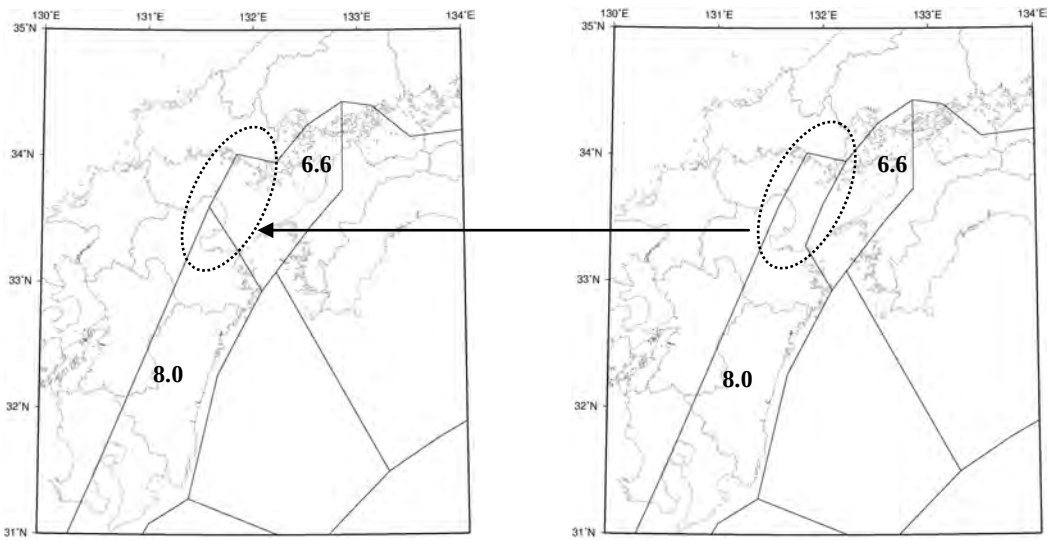

2009 version　　Up to 2008 version

Figure 3.3.4.4-2 Change in the zoning (values shown in the figure denote the maximum magnitudes of earthquakes without specified source faults for the respective areas)

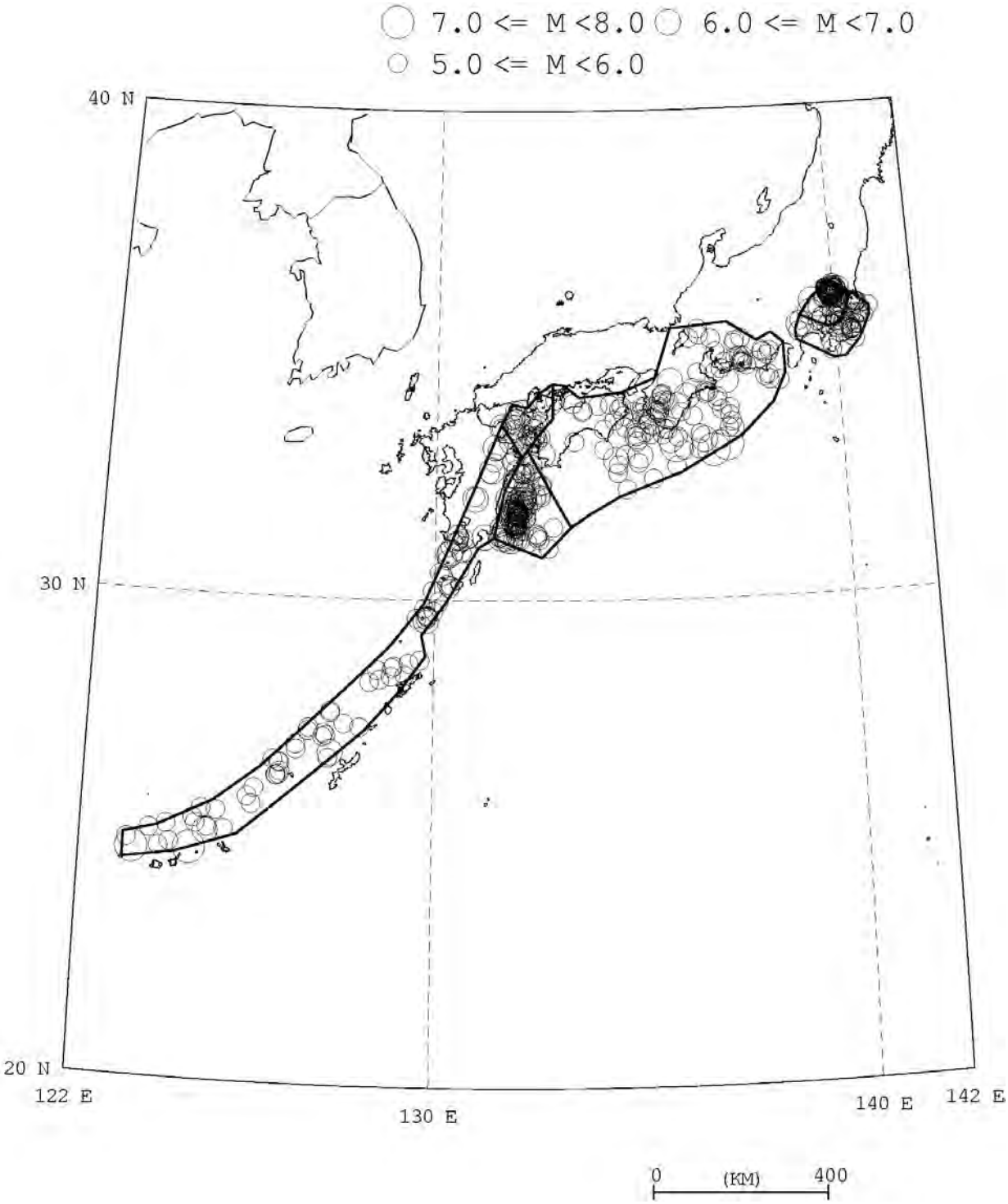

Figure 3.3.4.4-3 Epicenter distribution of earthquakes of M≥5.0 since 1926

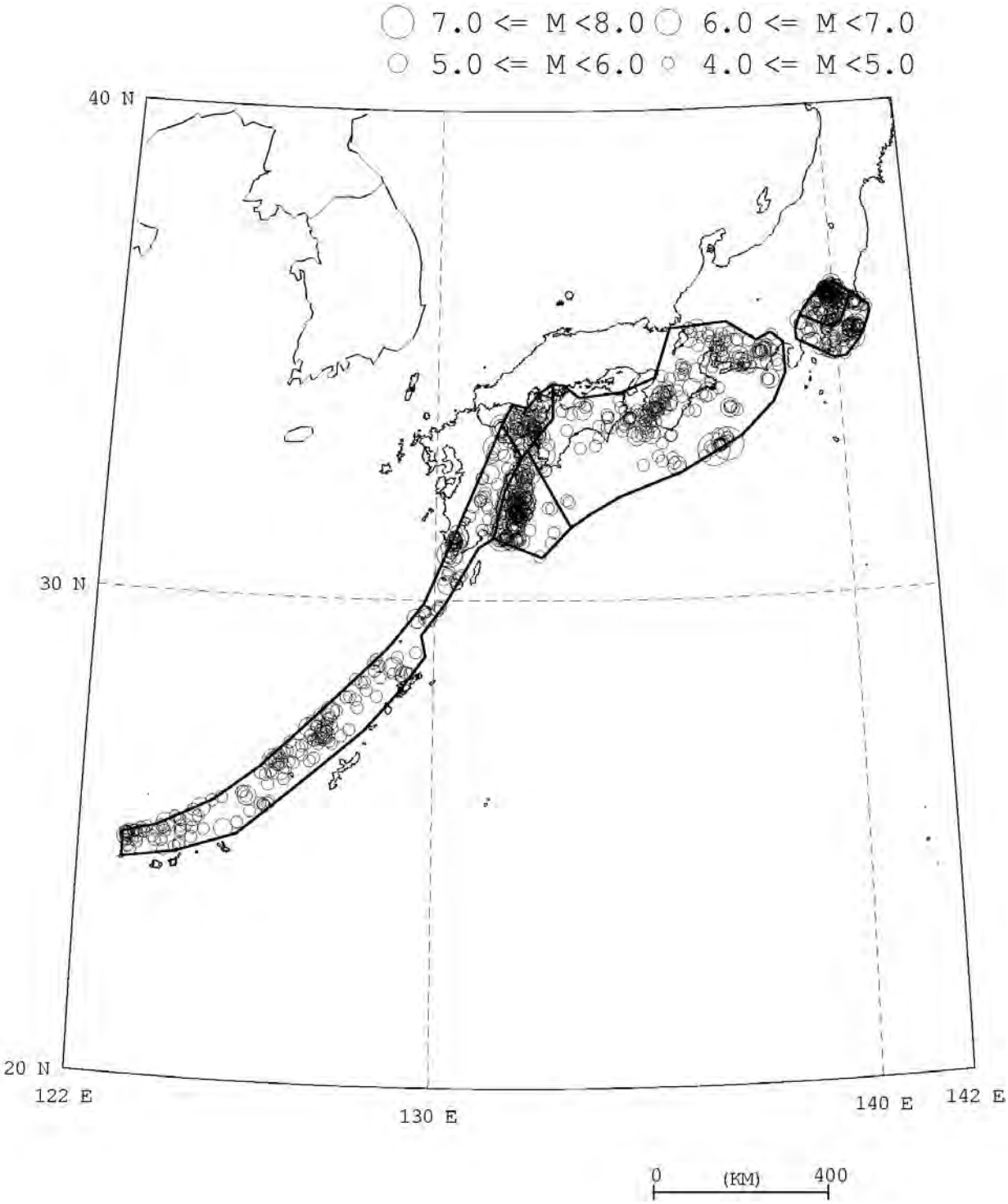

Figure 3.3.4.4-4 Epicenter distribution of earthquakes of M≥4.0 since 1983

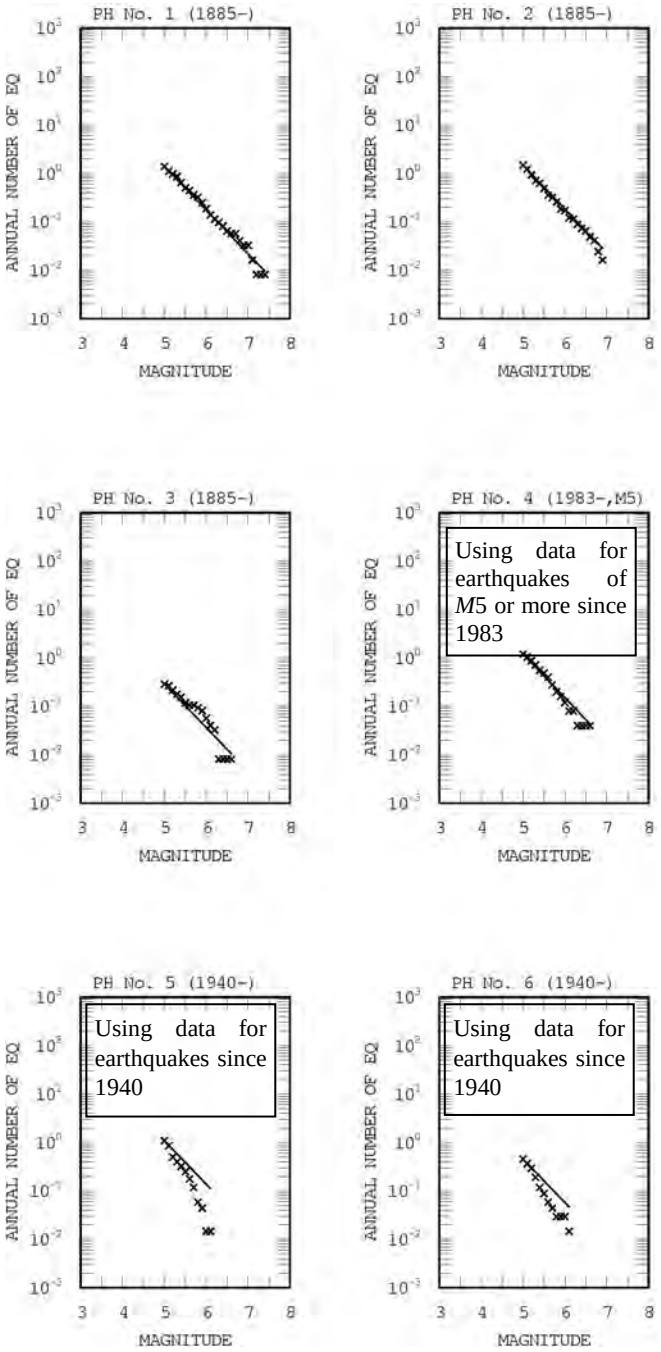

Figure 3.3.4.4-5 Cumulative frequency by earthquake magnitude based on medium earthquake catalog

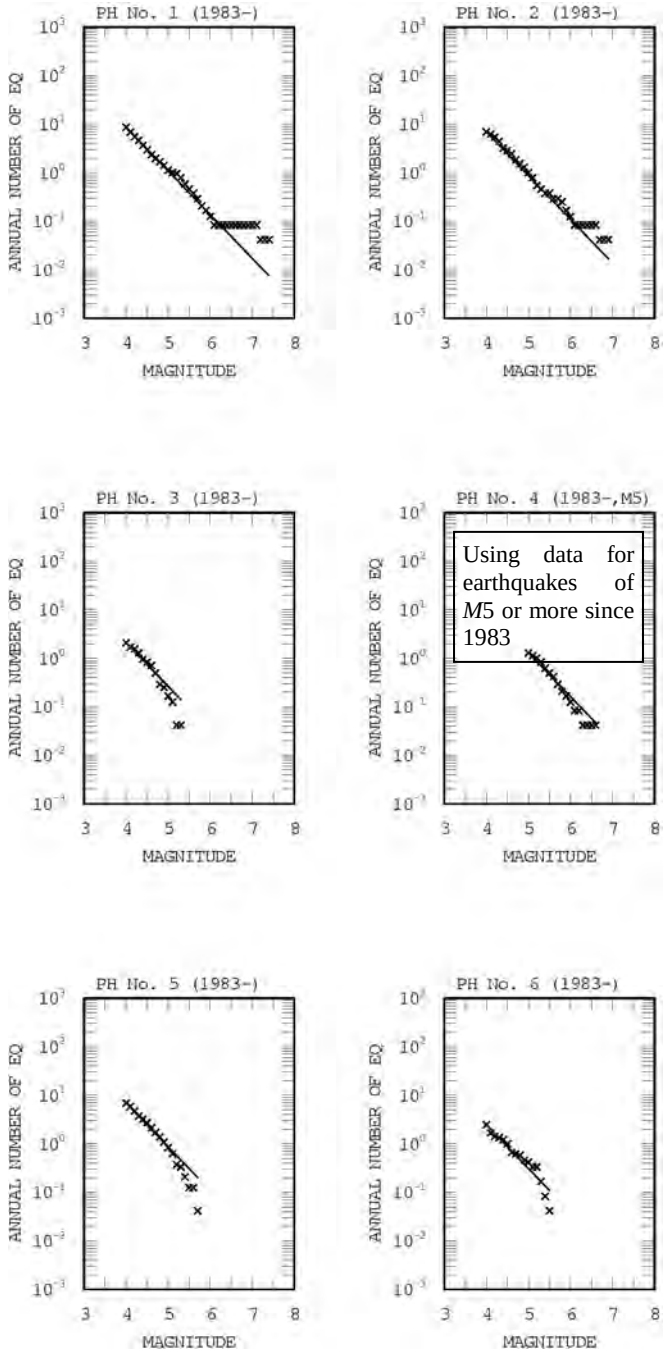

Figure 3.3.4.4-6 Cumulative frequency by earthquake magnitude based on small earthquake catalog

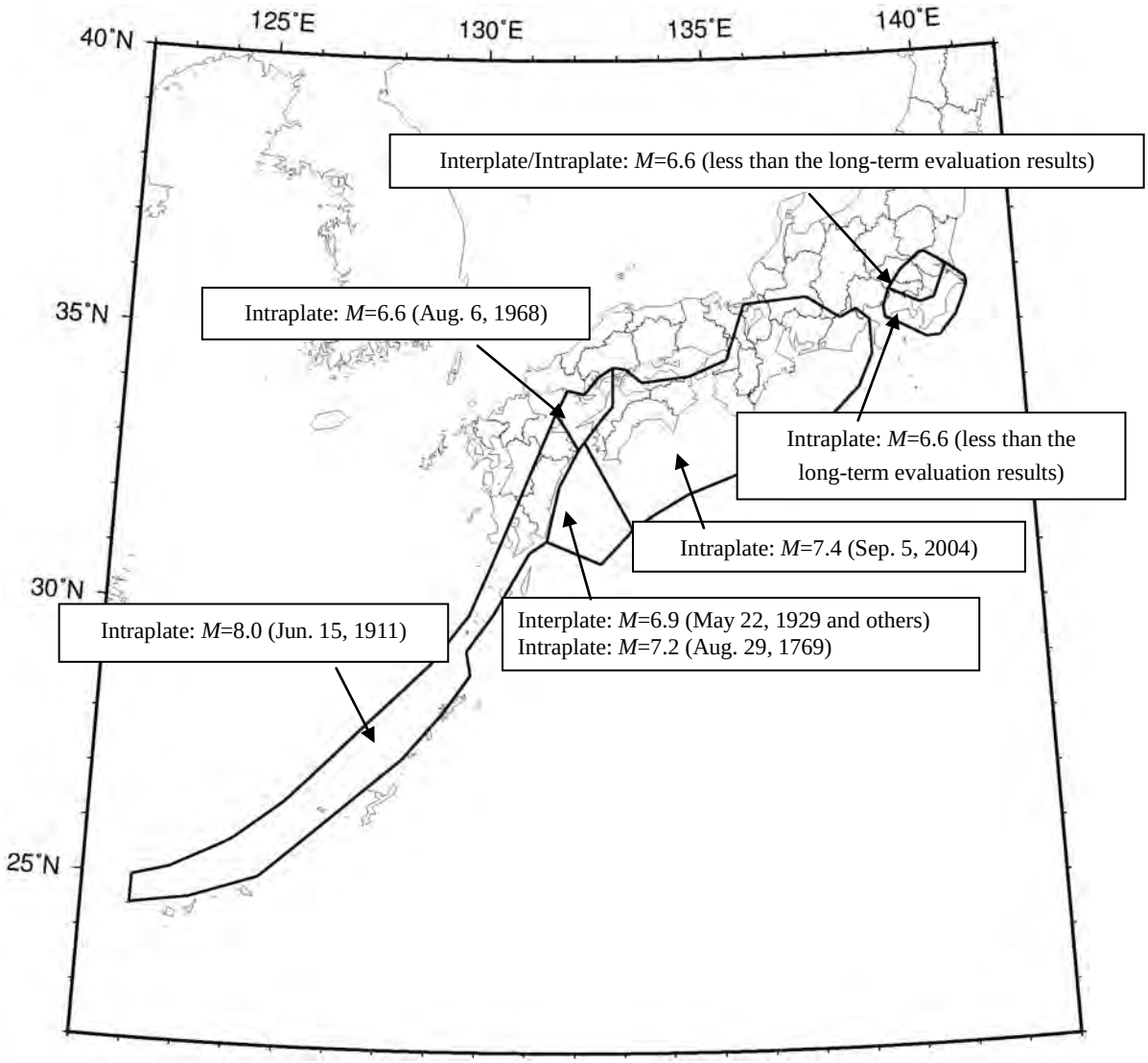

Figure 3.3.4.4-7 Maximum magnitudes of earthquakes without specified source faults for the Philippine Sea plate

Table 3.3.4.4-1 Maximum magnitude determined for each area

Area No.		Maximum *M*	Basis	Remarks
1	Intraplate	7.4	Sep. 5, 2004 Kii-hanto-nansei-Oki	
2	Interplate	6.9	May 22, 1929 Hyuganada Oct. 19, 1996	Earthquakes of *M*7.0 or more are separately evaluated as subduction-zone earthquakes
	Intraplate	7.2	Aug. 29, 1769	Determined based on description in the long-term evaluation.
3	Intraplate	6.6	Aug. 6, 1968 Ehime-ken-seiho-Oki	Earthquakes of *M*6.7 or more are separately evaluated as subduction-zone earthquakes
4	Intraplate	8.0	Jun. 15, 1911 Amami-oshima-kinkai	The location of the epicenter adopts the location in Gutenberg and Richter's catalog, based on the description in the long-term evaluation for the area.
5	Interplate	6.6	(Less than the long-term evaluation results)	Earthquakes of *M*6.7 or more are separately evaluated as subduction-zone earthquakes
	Intraplate	6.6	(Less than the long-term evaluation results)	Earthquakes of *M*6.7 or more are separately evaluated as subduction-zone earthquakes
6	Intraplate	6.6	(Less than the long-term evaluation results)	Earthquakes of *M*6.7 or more are separately evaluated as subduction-zone earthquakes

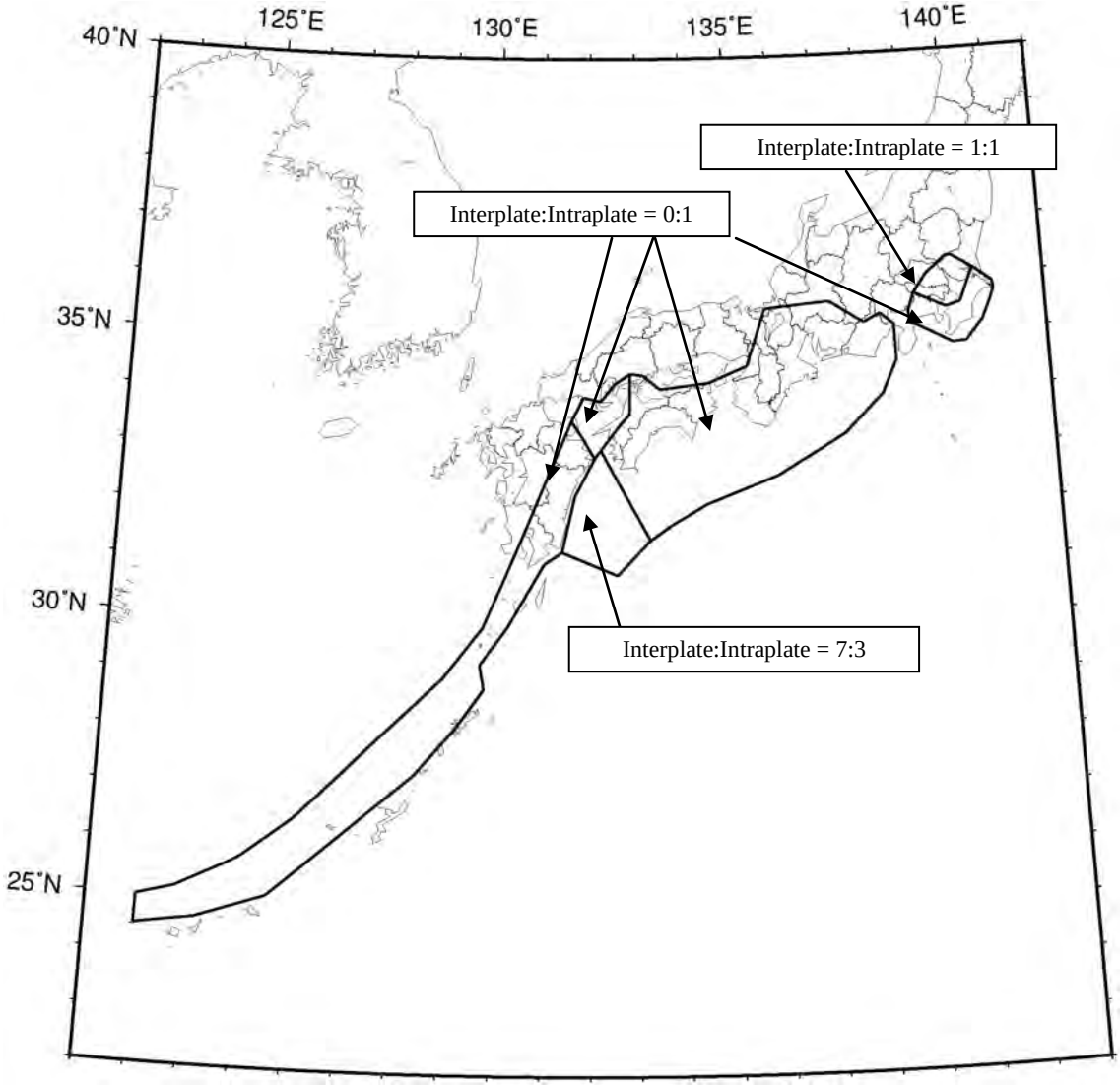

Figure 3.3.4.4-8 Occurrence ratio between interplate earthquakes and intraplate earthquakes

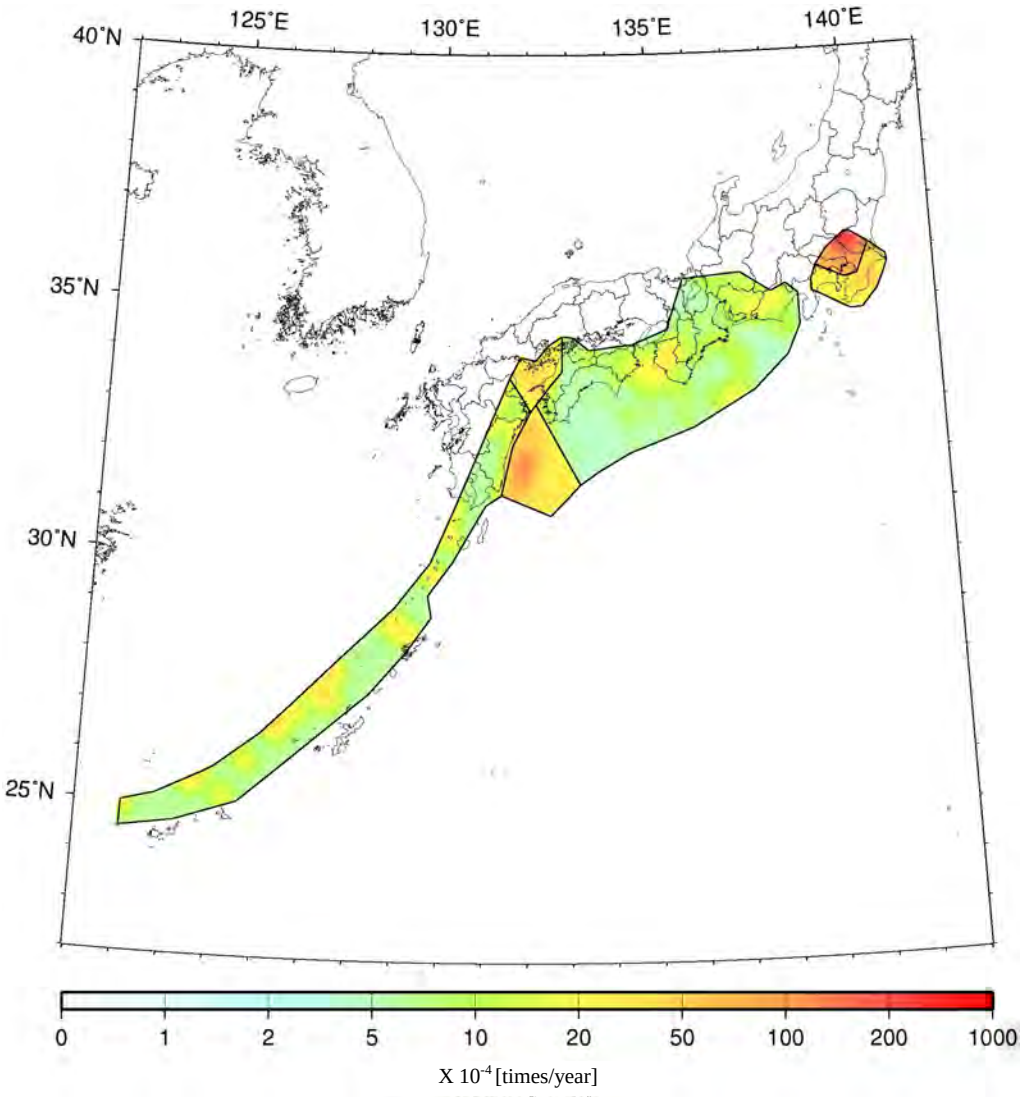

(a) Total for interplate and intraplate earthquakes

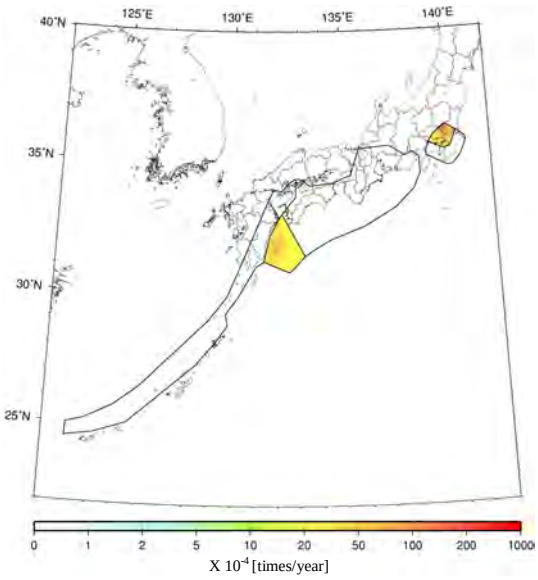

(b) Interplate earthquakes

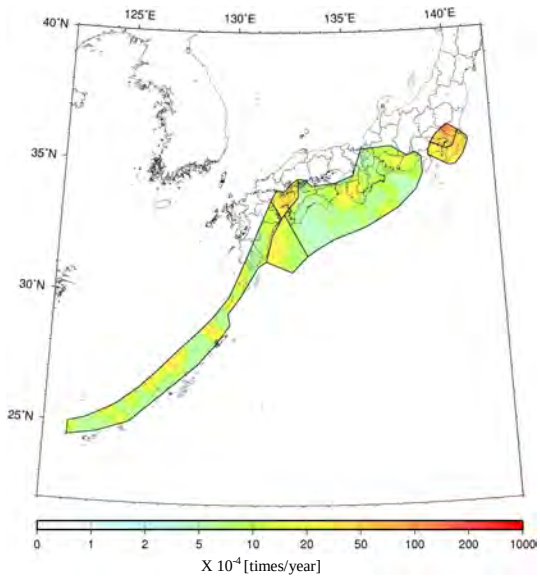

(c) Intraplate earthquakes

Figure 3.3.4.4-9 Occurrence frequency of earthquakes ain the Phillippine Sea plate (per 0.1-degree square, *M*5.0 or more)

3.3.4.5 Earthquakes occurring at onshore locations where active faults have not been specified

1) Target earthquakes

The target earthquakes are those that occur in the seismogenic layer within the upper crust of an overriding plate which are shallow and occur at locations where active faults have not been specified. In land area, characteristic earthquakes that occur in major active fault zones and at other active faults are separately evaluated, and many large earthquakes are considered to be covered by such earthquake categories. However, since earthquakes other than characteristic earthquakes related to active faults have not been modeled, they are evaluated as earthquakes without specified source faults.

Among shallow earthquakes that occur at an overriding plate, those from southern Kyushu to Nansei-shoto islands and those along the eastern margin of the Japan Sea are separately modeled as earthquakes without specified source faults, so they are excluded from this category.

2) Zoning

Areas are zoned based on the seismotectonic province map by Kakimi et al. (2003) (Figure 3.3.4.5-1; hereinafter referred to as the "new Kakimi map"). However, for zones that do not cover the land area, such as those in the Pacific coast from Omaezaki to Shikoku, the boundaries of the zones are corrected to include the land area. Regarding the areas that include the eastern margin of the Japan Sea, boundary lines are added so as to separate the land area near Niigata Prefecture and the eastern margin of the Japan Sea. The determined zones are shown in Figure 3.3.4.5-2. As mentioned in 1) above, the areas along the eastern margin of the Japan Sea and those in and south of southern Kyushu are excluded, since they are separately evaluated.

3) Earthquake catalogs

The catalogs of medium earthquakes and small earthquakes (the minimum magnitude of 3.0) are both used, in principle. However, the period covered by the medium earthquake catalog is partly changed, and for the area including Kanto and the area of Izu Peninsula, earthquakes of magnitude 5.0 or more that have occurred since 1940, when the influence of the 1923 Taisho Kanto Earthquake has diminished, are used as the medium earthquake catalog. For the area from eastern Hokkaido to the Etorofu, Kunashiri, Shikotan and Habomai Islands, earthquakes of magnitude 5.0 or more that have occurred since 1960 are used as the medium earthquake catalog, considering the detection capability of the observation network.

As for the source depth, only earthquakes of which the depth is 25 km or less are used, in principle, but in the sea area of the Japan Sea side of the Japanese archipelago, earthquakes of which the depth is up to 40 km are targeted, considering the accuracy of the source depth. Earthquakes that correspond to characteristic earthquakes occurring in major active fault zones and earthquakes occurring at active faults other than major active fault zones are excluded from earthquake catalogs.

Figure 3.3.4.5-3 shows the epicenter distribution of earthquakes of magnitude 5.0 or more that have occurred since 1926, and Figure 3.3.4.5-4 shows the epicenter distribution of earthquakes of magnitude 3.0 or more that have occurred since 1983. Figure 3.3.4.5-5 and Figure 3.3.4.5-6 show the cumulative occurrence frequency by earthquake magnitude.

4) Maximum magnitude

The maximum magnitude assumed for each zoned area is the maximum magnitude of earthquakes that have occurred since 1600 of which association with major active fault zones and active faults other than major active fault zones is unclear. The lower limit value is M_j =6.8 for the land area and M_j =7.0 for the sea area. The maximum magnitude determined for each area is shown in Figure 3.3.4.5-7 and Table 3.3.4.5-1.

5) Determination of the fault planes

Seismic source faults are assumed to distribute uniformly in the seismogenic layer within the upper crust. The shape of each fault plane shall be a vertical rectangle, and its length is derived from the magnitude by the Matsuda (1975) formula. The width of the fault shall be equal to the length (but not wider than the thickness of the seismogenic layer), and the strike shall be at random. However, when carrying out numerical calculation, the source is assumed to be a point source that is 3 km deep, which gives roughly equivalent results as the study results by NIED (2003).

6) Conversion to moment magnitude M_w

Moment magnitude M_w is converted from M_j using the following formula, based on Takemura (1990):

$$M_w = 0.78\, M_j + 1.08 \qquad (3.3.4.5\text{-}1)$$

7) Distribution of the earthquake occurrence frequency

Figure 3.3.4.5-8 shows the distribution of occurrence frequency for earthquakes occurring at onshore locations where active faults have not been specified (the occurrence frequency of earthquakes of magnitude 5.0 or more within one year in an area of 0.1 degrees × 0.1 degrees). It adopts the mean value of the frequency for the following four cases: 1) the case using the medium earthquake catalog and the zoning method, 2) the case using the medium earthquake catalog and the non-zoning method, 3) the case using the small earthquake catalog and the zoning method, 4) the case using the small earthquake catalog and the non-zoning method.

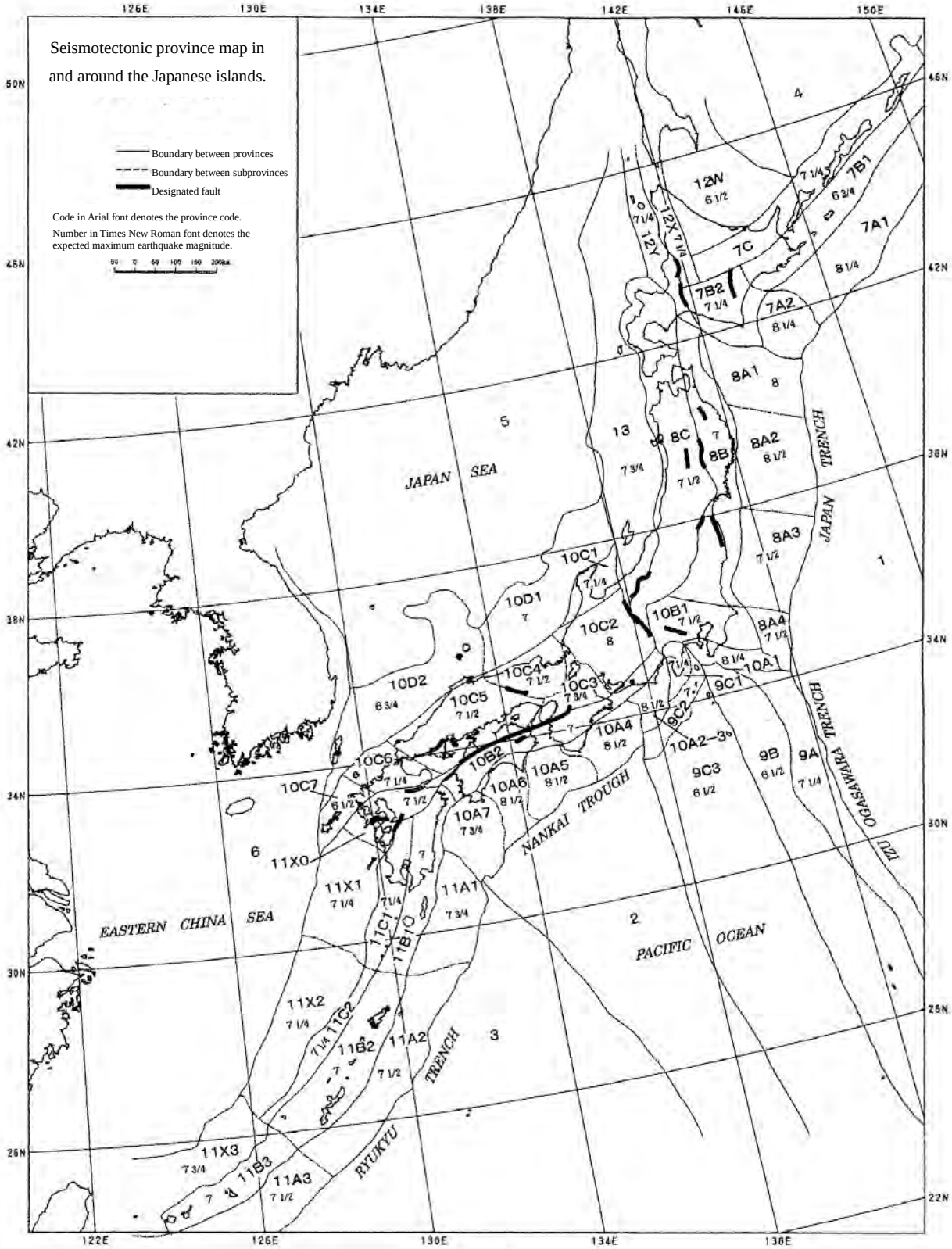

Fig. 1. Seismotectonic province map in and around the Japanese islands. Boldfaced sign is the symbol of province. Roman-type numeral represents the expected maximum earthquake magnitude (M_{max}) assigned to each province. Solid line: boundary between provinces. Broken line: boundary between subprovinces. Bar: the designated fault.

Figure 3.3.4.5-1 Seismotectonic province map by Kakimi et al. (2003) (new Kakimi map)

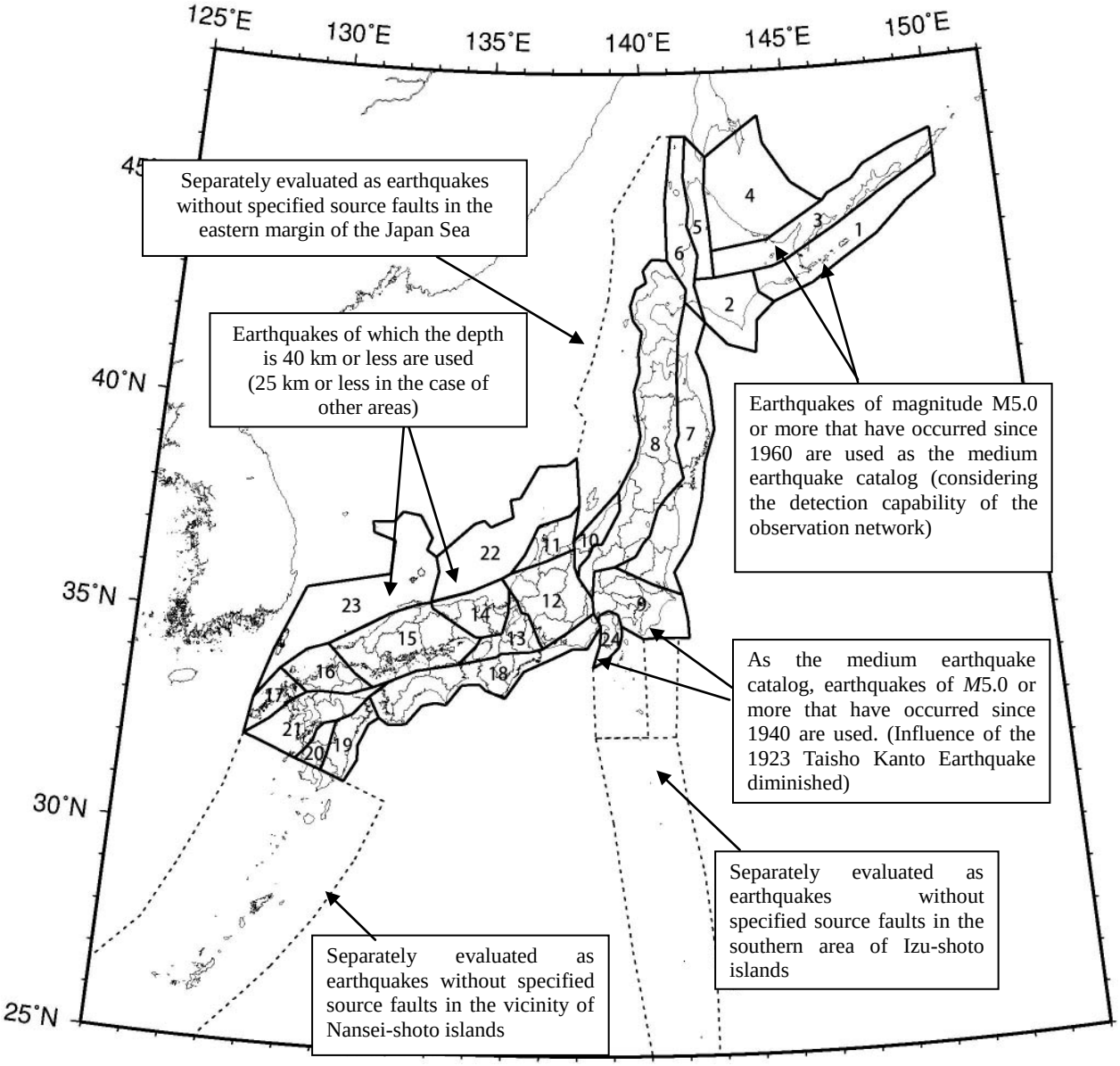

Figure 3.3.4.5-2 Zoning of shallow earthquakes without specified source faults in land area. Earthquake catalogs used for calculating the frequency are also shown. A standard catalog is used where no catalog is specified.

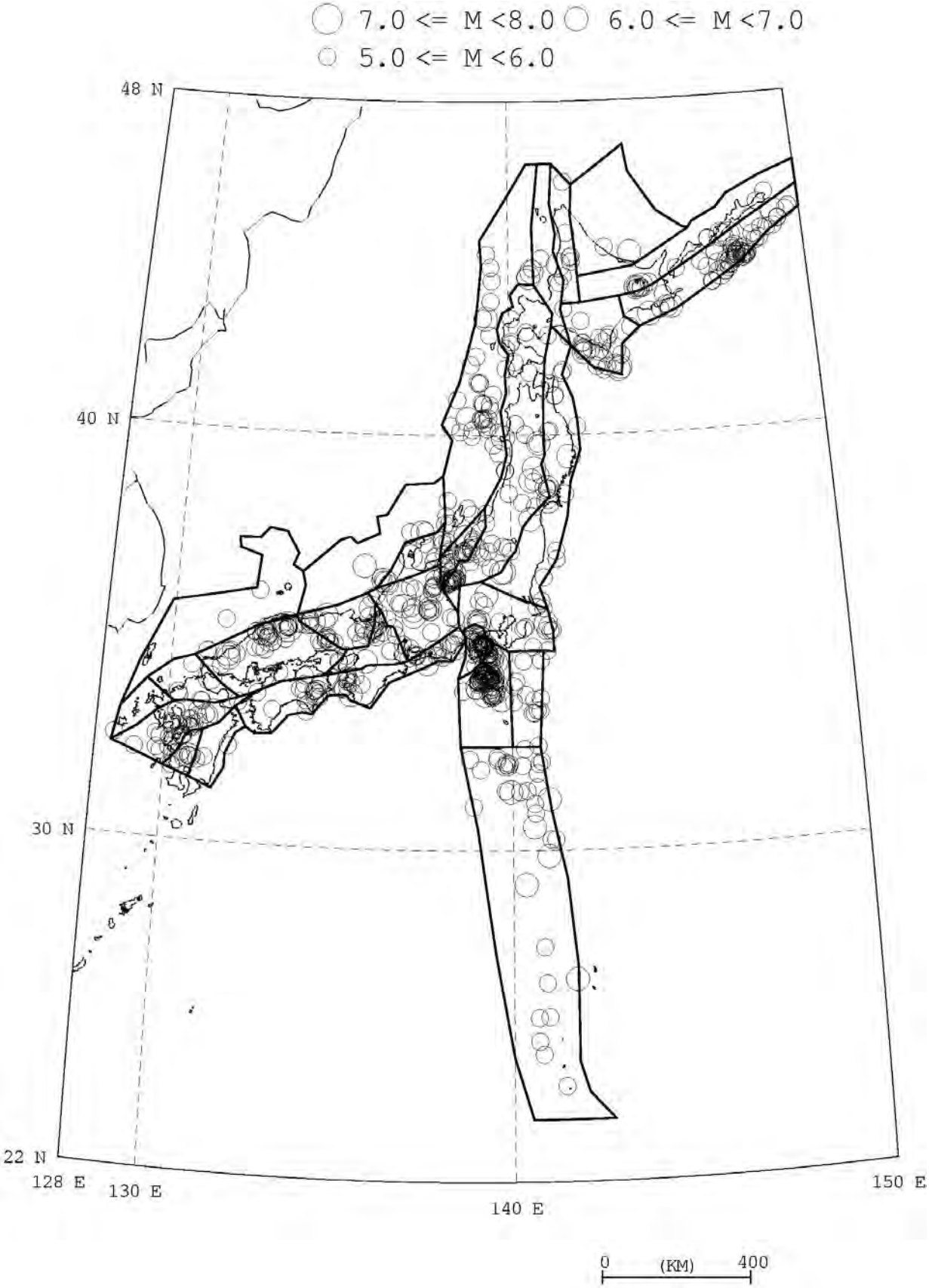

Figure 3.3.4.5-3 Epicenter distribution of earthquakes of *M*≥5.0 since 1926 (Those in the areas of the eastern margin of the Japan Sea and the southern area of Izu-shoto islands are also shown.)

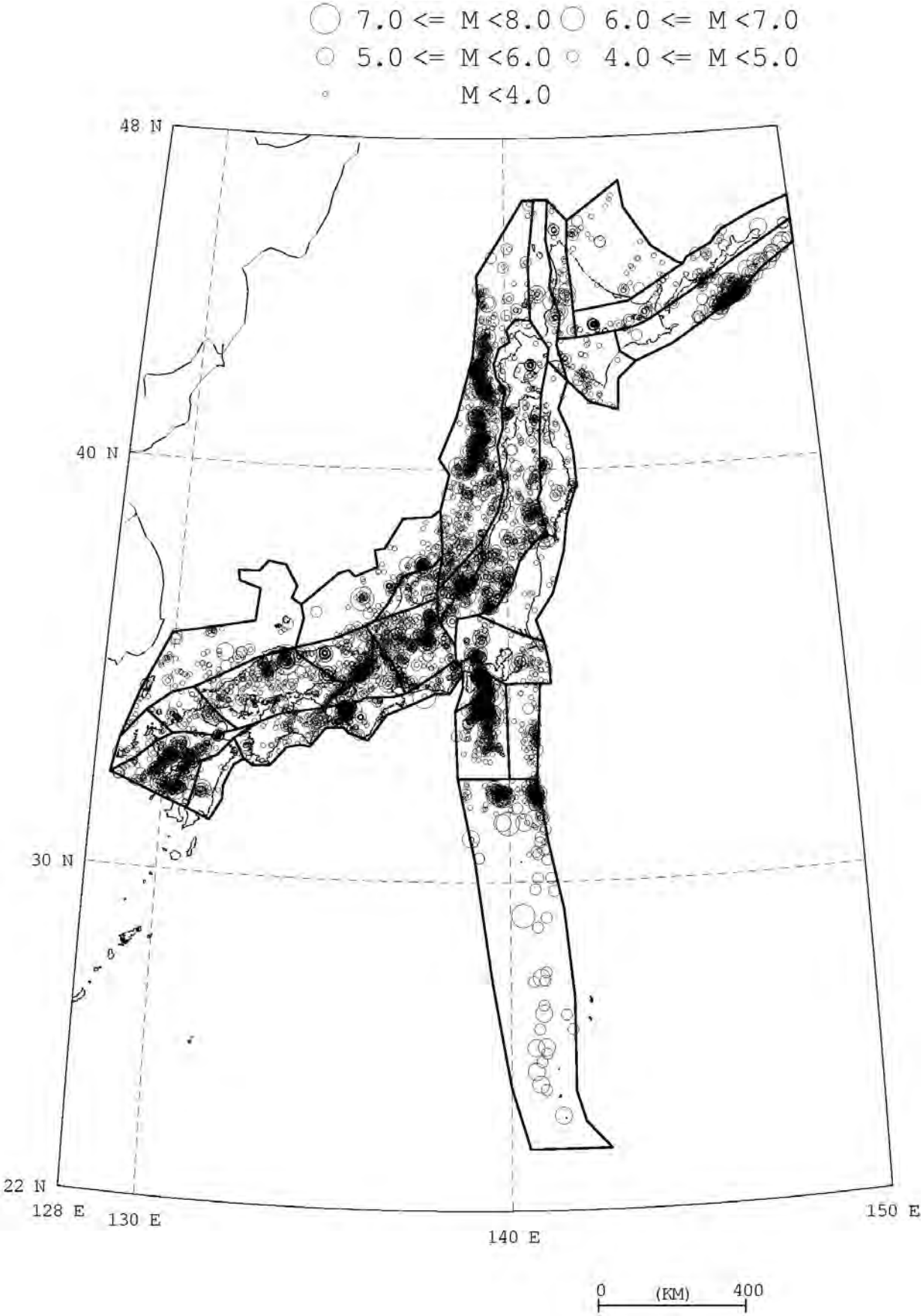

Figure 3.3.4.5-4 Epicenter distribution of earthquakes of *M*≥3.0 since 1983 (Those in the areas of the eastern margin of the Japan Sea and the southern area of Izu-shoto islands are also shown.)

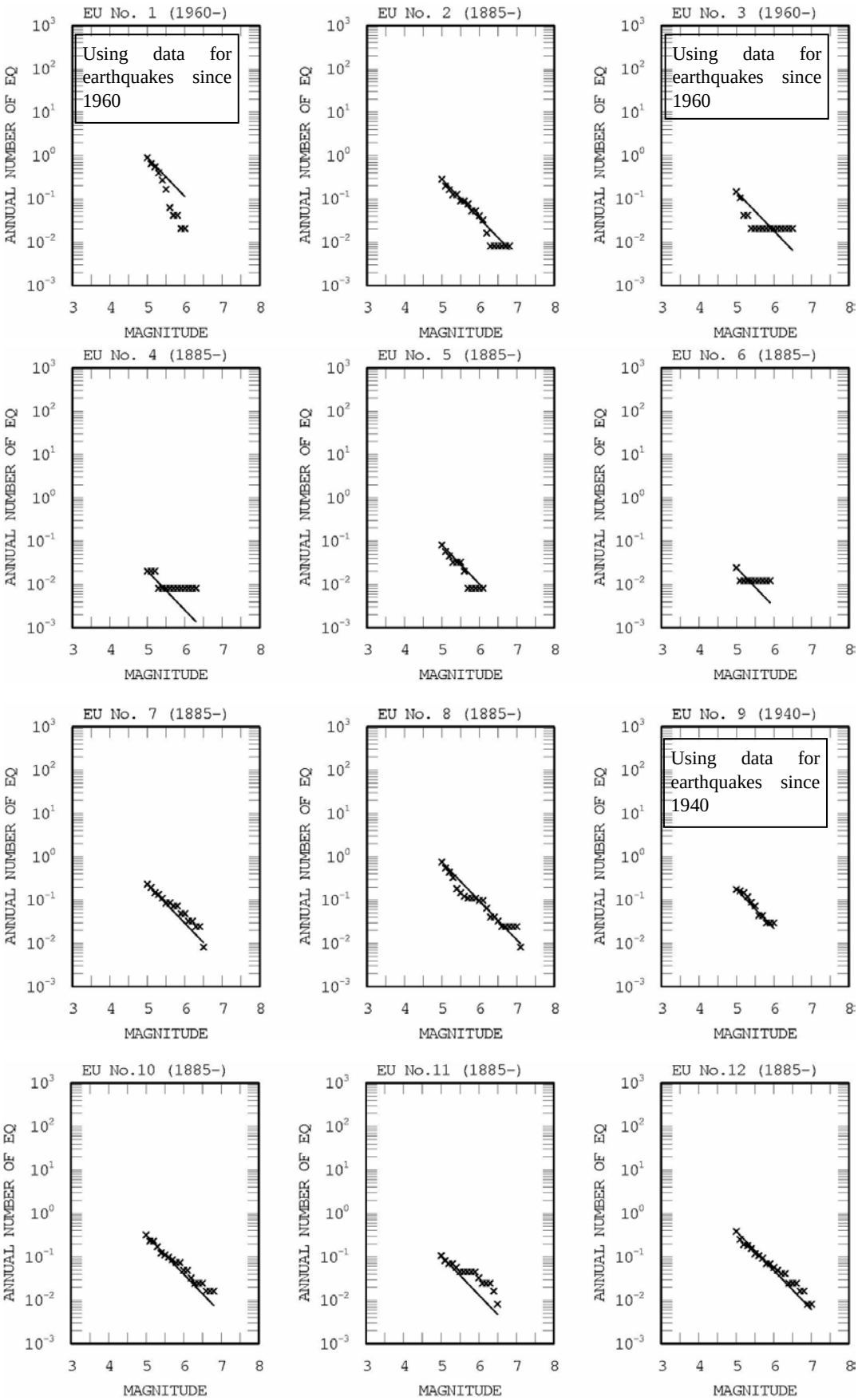

Figure 3.3.4.5-5 Cumulative frequency by earthquake magnitude based on medium earthquake catalog (part 1)

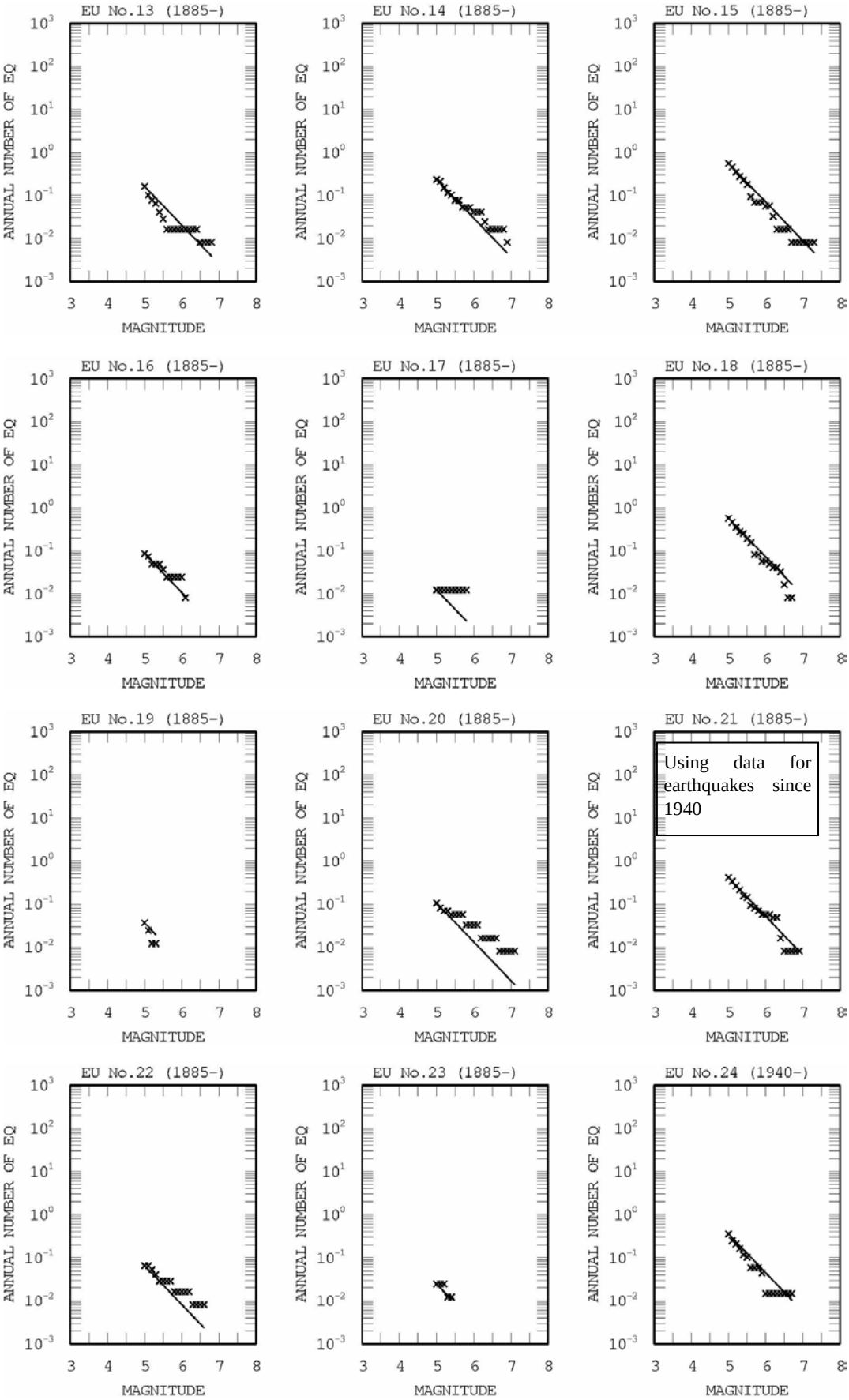

Figure 3.3.4.5-5 Cumulative frequency by earthquake magnitude based on medium earthquake catalog (part 2)

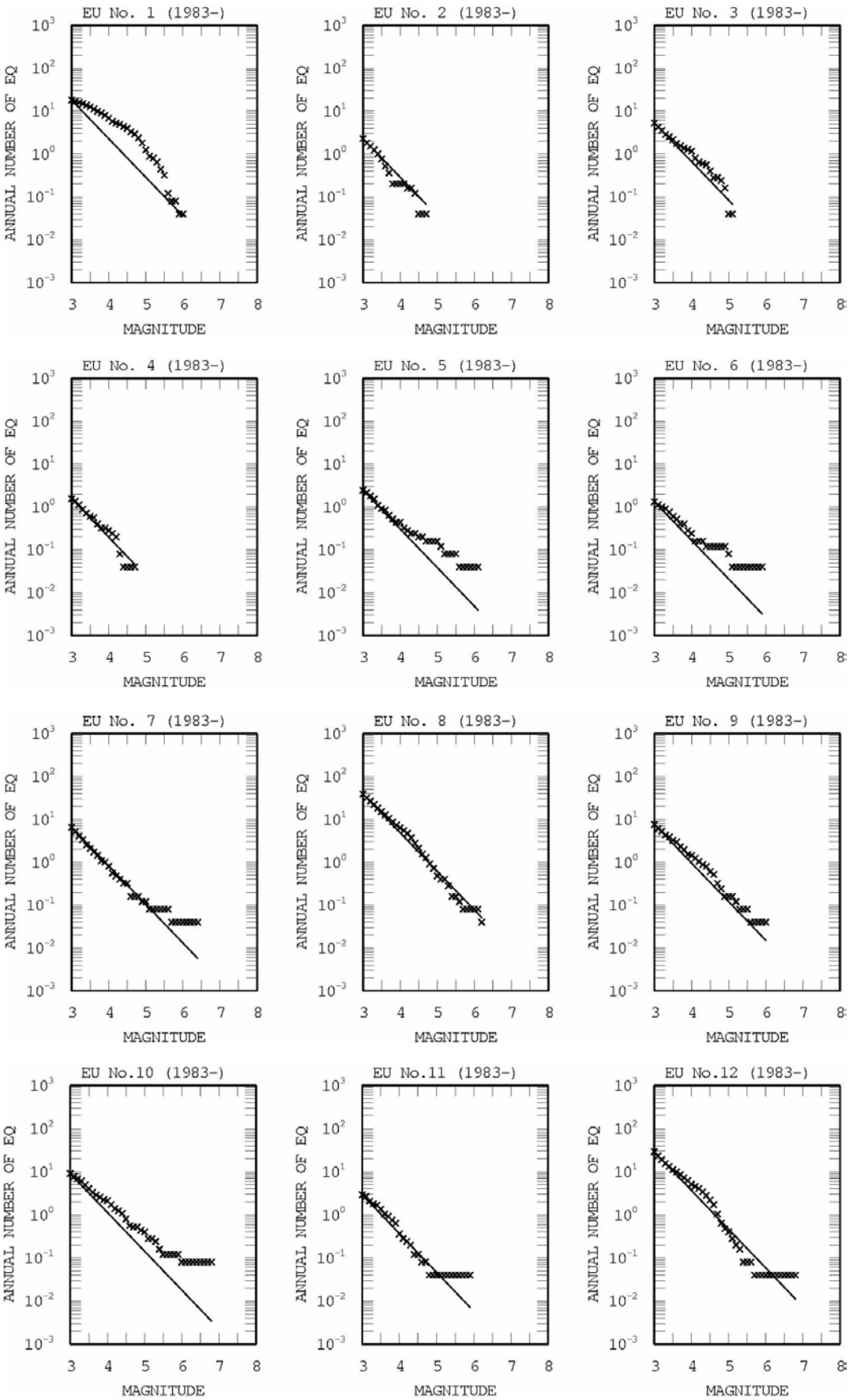

Figure 3.3.4.5-6 Cumulative frequency by earthquake magnitude based on small earthquake catalog (part 1)

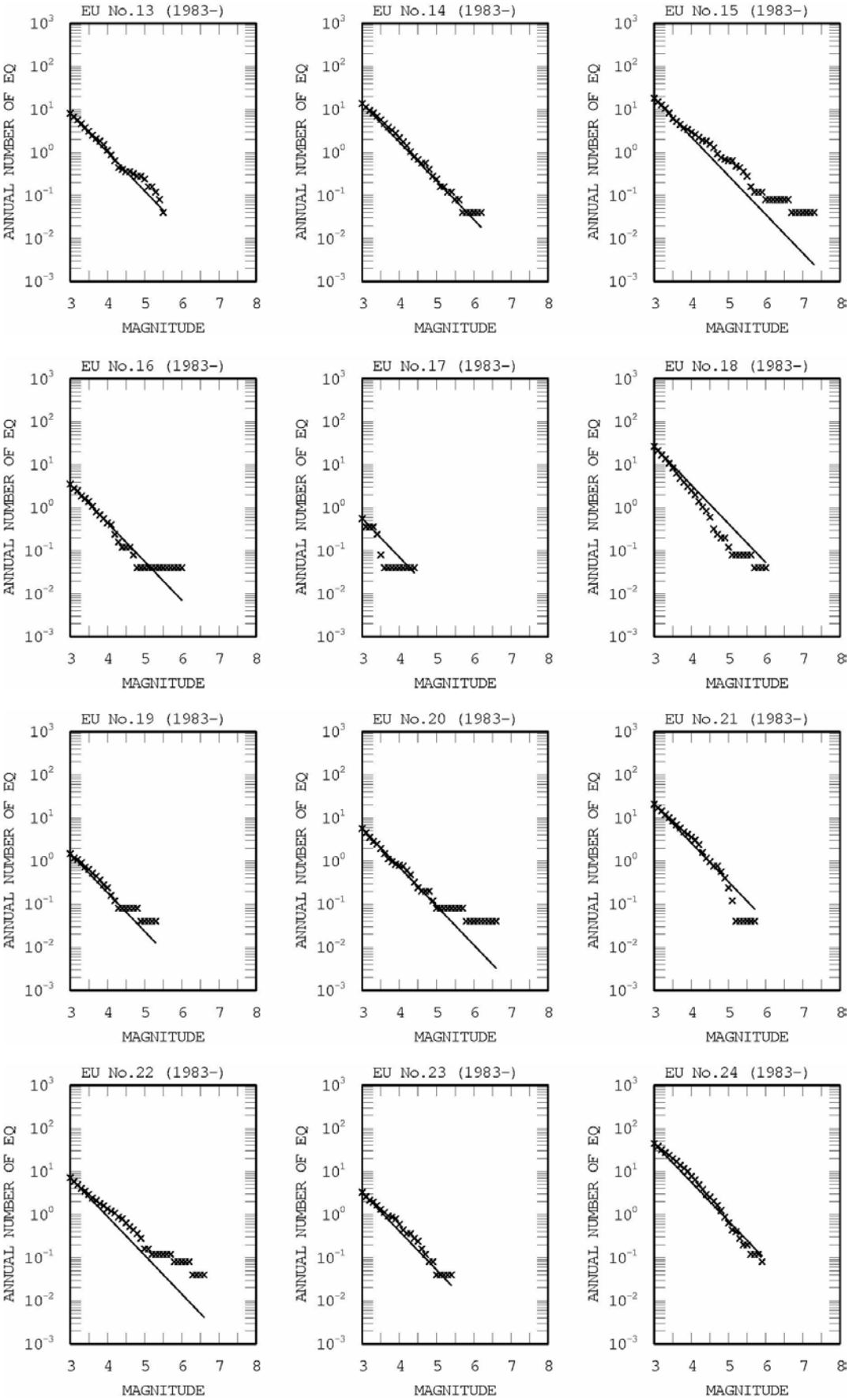

Figure 3.3.4.5-6 Cumulative frequency by earthquake magnitude based on small earthquake catalog (part 2)

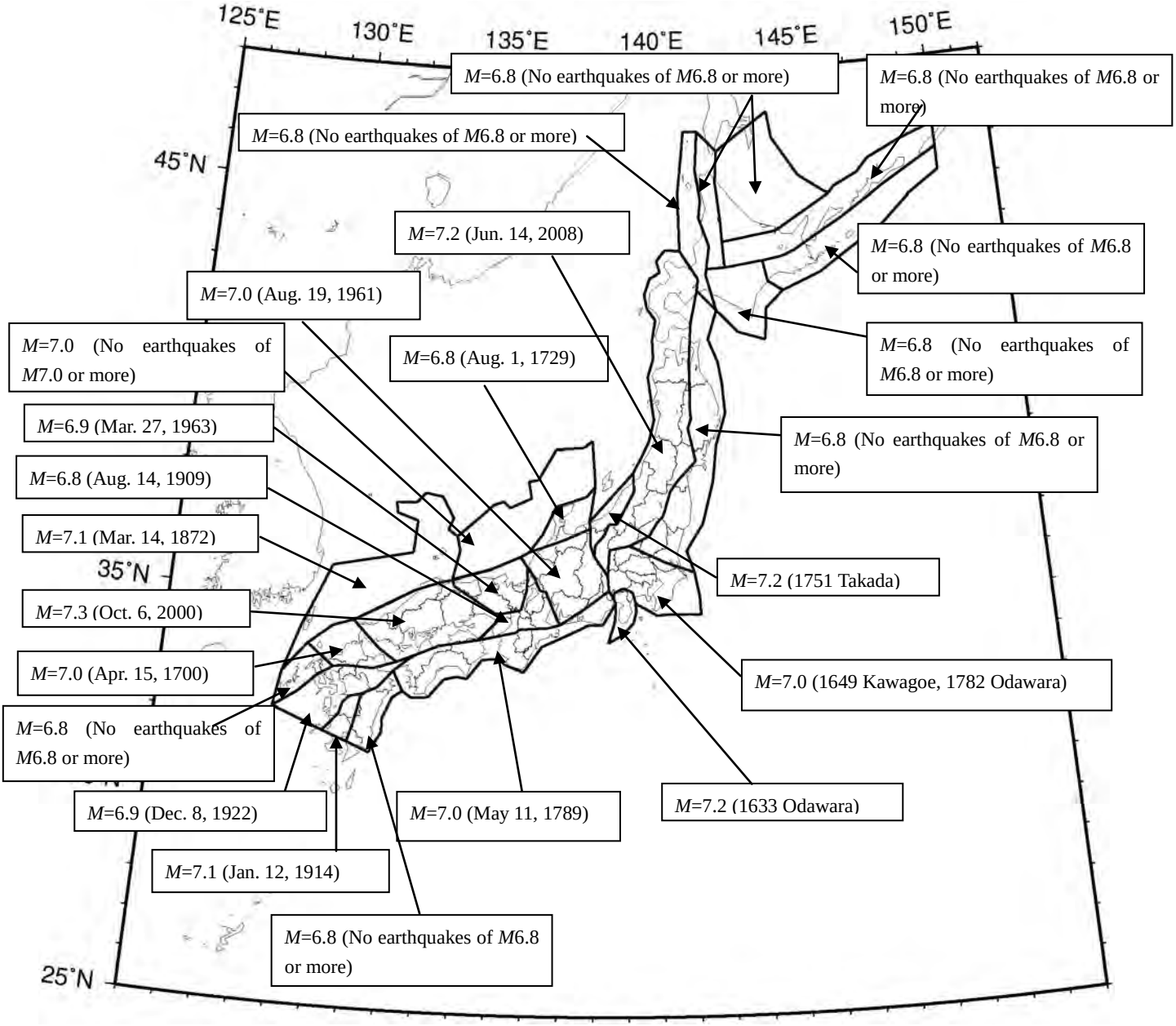

Figure 3.3.4.5-7 Maximum magnitudes of earthquakes without specified source faults in the land area

Table 3.3.4.5-1 Maximum magnitude determined for each area

Area No.	Maximum *M*	Basis	Remarks
1	6.8	(Lower limit value of maximum *M*)	
2	6.8	(Lower limit value of maximum *M*)	
3	6.8	(Lower limit value of maximum *M*)	
4	6.8	(Lower limit value of maximum *M*)	
5	6.8	(Lower limit value of maximum *M*)	
6	6.8	(Lower limit value of maximum *M*)	
7	6.8	(Lower limit value of maximum *M*)	Earthquakes on Jun. 3, 1772 (*M*6.7) and Jul. 8, 1858 (*M*7.3) are judged to be Pacific plate earthquakes.
8	7.2	Jun. 14, 2008 Iwate/Miyagi inland	1766 Tsugaru Earthquake (*M*7.3) and 1896 Rikuu Earthquake (*M*7.2) are associated with active faults.
9	7.0	Jul. 30, 1649 Kawagoe Aug. 23, 1782 Odawara	These earthquakes are taken into consideration, although it is unclear whether they are crustal earthquakes. 1924 Tanzawa Earthquake (*M*7.3) is not evaluated as being an aftershock of the 1923 Taisho Kanto Earthquake.
10	7.2	May 21, 1751 Takada	1847 Zenkoji Earthquake (*M*7.4) is associated with an active fault.
11	6.8	Aug. 1, 1729 Noto/Sado	
12	7.0	Aug. 19, 1961 Kita-Mino Earthquake	1891 Noubi Earthquake (*M*8.0), 1858 Hietsu Earthquake (*M*7.1), and 1948 Fukui Earthquake (M7.1) are all associated with active faults.
13	6.8	Aug. 14, 1909 Anegawa Earthquake	1596 Keicho Earthquake (*M*7.5), 1662 Kanbun Earthquake (*M*7.5), 1854 Iga-ueno Earthquake (*M*7.3), and 1995 Hyogo-ken Nanbu (Kobe) Earthquake (M7.3) are all associated with active faults. Earthquake in the vicinity of Oumi-hachiman in 1819 (*M*7.3) is excluded due to an indication of the possibility that the earthquake was relatively deep.
14	6.9	Mar. 27, 1963 Echize-misaki-Oki	1927 Kita-Tango Earthquake (*M*7.3) and 1943 Tottori Earthquake (*M*7.2) are both associated with active faults.
15	7.3	Oct. 6, 2000 Western Tottori Earthquake	Earthquakes in 1649 (*M*7.0), 1686 (*M*7.2), and 1857 (*M*7.3) are excluded since they are considered to be Philippine Sea plate earthquakes.
16	7.0	Apr. 15, 1700 Iki/Tsushima	2005 West off Fukuoka earthquake (*M*7.0) is associated with the Kego fault zone (northwestern part).
17	6.8	(Lower limit value of maximum *M*)	
18	7.0	May 11, 1789 Awa	1854 Iyo-seibu (*M*7.4) is excluded since it is considered to be a Philippine Sea plate earthquake.
19	6.8	(Lower limit value of maximum *M*)	Earthquake of *M*7.7 in 1769 is judged to be a Philippine Sea plate earthquake, since a tsunami occurred.
20	7.1	Jan. 12, 1914 Sakura-jima	This earthquake is taken into considered when determining the maximum magnitude, despite an indication of the possibility of being a volcanic earthquake.
21	6.9	Dec. 8, 1922 Chijiwa-wan	1596 Keicho-Bungo (*M*7.5) is associated with an active fault.
22	7.0	(Lower limit value of maximum *M* for the sea area)	
23	7.1	Mar. 14, 1872 Hamada Earthquake	
24	7.2	Mar. 1, 1633 Odawara (7±1/4)	1930 Kita-Izu Earthquake (*M*7.3) is associated with an active fault.

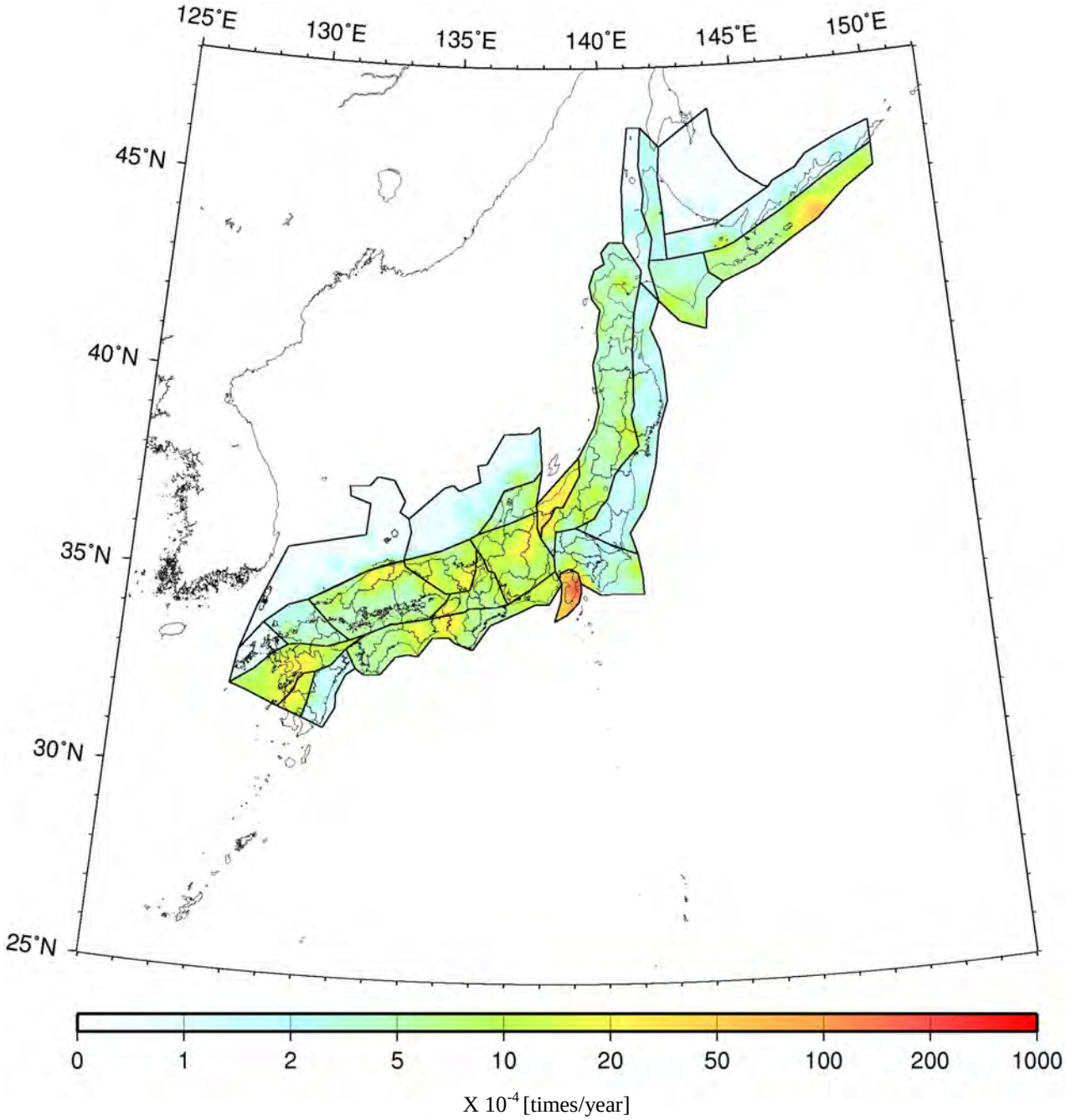

Figure 3.3.4.5-8 Occurrence frequency of shallow earthquakes without specified source faults in the land area (per 0.1-degree square, *M*5.0 or more)

3.3.4.6 Earthquakes without specified source faults in Urakawa-Oki

1) Target earthquakes and zoning

Earthquakes occurring in the vicinity of the source area of the 1982 Urakawa-Oki Earthquake (*M*7.1, h=40 km) are shallower than the upper surface of the Pacific plate, but are deeper than the lower surface of the seismogenic layer of the upper crust in other regions, and their relation with the lower crust of the Kuril arc which is delaminated has been pointed out (Murai et al., 2002). Here, earthquakes occurring in the vicinity of the source area of the 1982 Urakawa-Oki Earthquake are modeled as "earthquakes without specified source faults in Urakawa-Oki" separately from earthquakes without specified source faults at the Pacific plate and in the land area.

Figure 3.3.4.6-1 shows the conceptual drawing of earthquakes without specified source faults in Urakawa-Oki, and Figure 3.3.4.6-2 shows the zoning. The zoning is determined so as to include the 1982 Urakawa-Oki Earthquake and the earthquake of M6.0 in 1927, and the southeastern boundary is determined so that the depth of the upper surface of the plate is about 45 km. Since this zoning overlaps with the zoning for crustal earthquakes without specified source faults in land area, when viewed as a plane, earthquakes of which the source depth is 25 km or more and less than 45 km are used for evaluating the seismic activity level, as shown in Figure 3.3.4.6-1.

2) Earthquake catalogs

While the medium earthquake catalog and the small earthquake catalog are both used, earthquakes cannot be extracted by using the Utsu catalog since the target area is positioned in between the areas for earthquakes within the upper crust and earthquakes at the Pacific plate. Thus, only earthquakes of magnitude 5.0 or more that have occurred since 1926 from the JMA catalog are used as the medium earthquake catalog, and the Utsu catalog is not used in combination. The small earthquake catalog shall be the data for earthquakes of magnitude 3.0 or more that have occurred since 1983 from the JMA catalog. Figure 3.3.4.6-3 shows the epicenter distribution of these earthquakes.

The cumulative occurrence frequency by earthquake magnitude, calculated based on the medium earthquake catalog and the small earthquake catalog, is shown in Figure 3.3.4.6-4.

3) Maximum magnitude

The maximum magnitude shall be *M*7.1 of the 1982 Urakawa-Oki Earthquake.

4) Determination of the fault planes

The *Handbook of Parameters of Seismic Faults in Japan* (written and edited by Sato, 1989) shows four fault models for the 1982 Urakawa-Oki Earthquake. According to the handbook, the strike is within the range of N30W-N60W, and the dip angle is within the range of 30°-60°. Two models are dipping northeast and the other two models are dipping southwest. Using such data as reference, fault planes are assumed to be circular fault planes striking N45W and dipping northeast at a dip angle of 45°, and the depth of the center of the fault is fixed at 35 km, which is about half the depth of the area. The size of the fault is determined according to the magnitude to satisfy the Utsu formula. Planar places of the fault plane are assumed to be distributed uniformly within the zoned area.

5) Conversion to moment magnitude M_w

Moment magnitude *M*w is assumed to be equal to *M*j.

6) Assumed earthquake type

In ground motion evaluation (applying an attenuation relation), formulas for crustal earthquakes are used.

7) Distribution of the earthquake occurrence frequency

Figure 3.3.4.6-5 shows the distribution of occurrence frequency for earthquakes in Urakawa-Oki (the occurrence frequency of earthquakes of magnitude 5.0 or more within one year in an area of 0.1 degrees × 0.1 degrees). It adopts the mean value of the frequency for the following four cases: 1) the case using the medium earthquake catalog and the zoning method, 2) the case using the medium earthquake catalog and the non-zoning method, 3) the case using the small earthquake catalog and the zoning method, 4) the case using the small earthquake catalog and the non-zoning method.

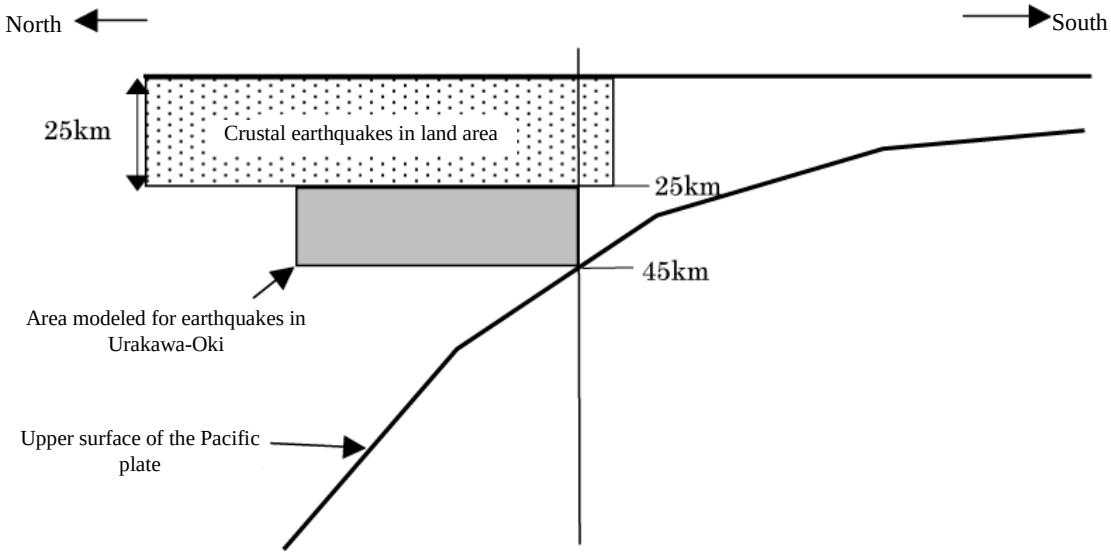

Figure 3.3.4.6-1 Target area of earthquakes without specified source faults in Urakawa-Oki

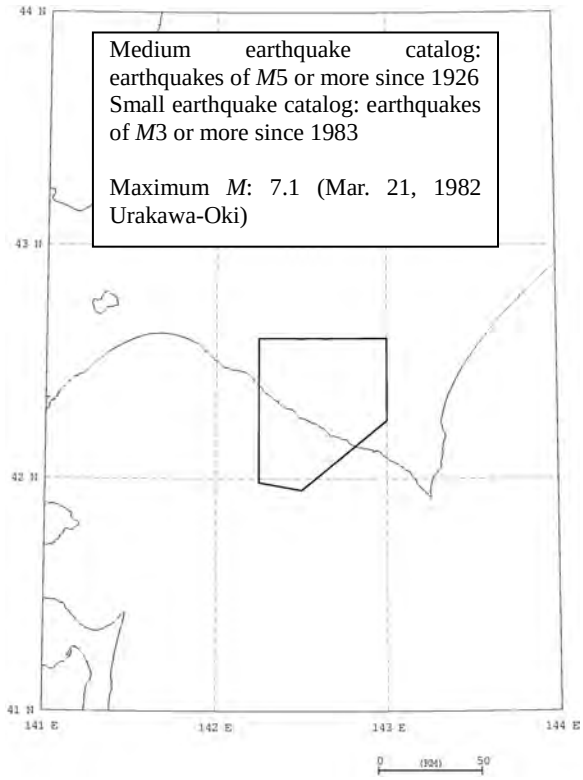

Figure 3.3.4.6-2 Zoning of earthquakes without specified source faults in Urakawa-Oki. Earthquake catalogs used for calculating the frequency, and maximum magnitude are also shown.

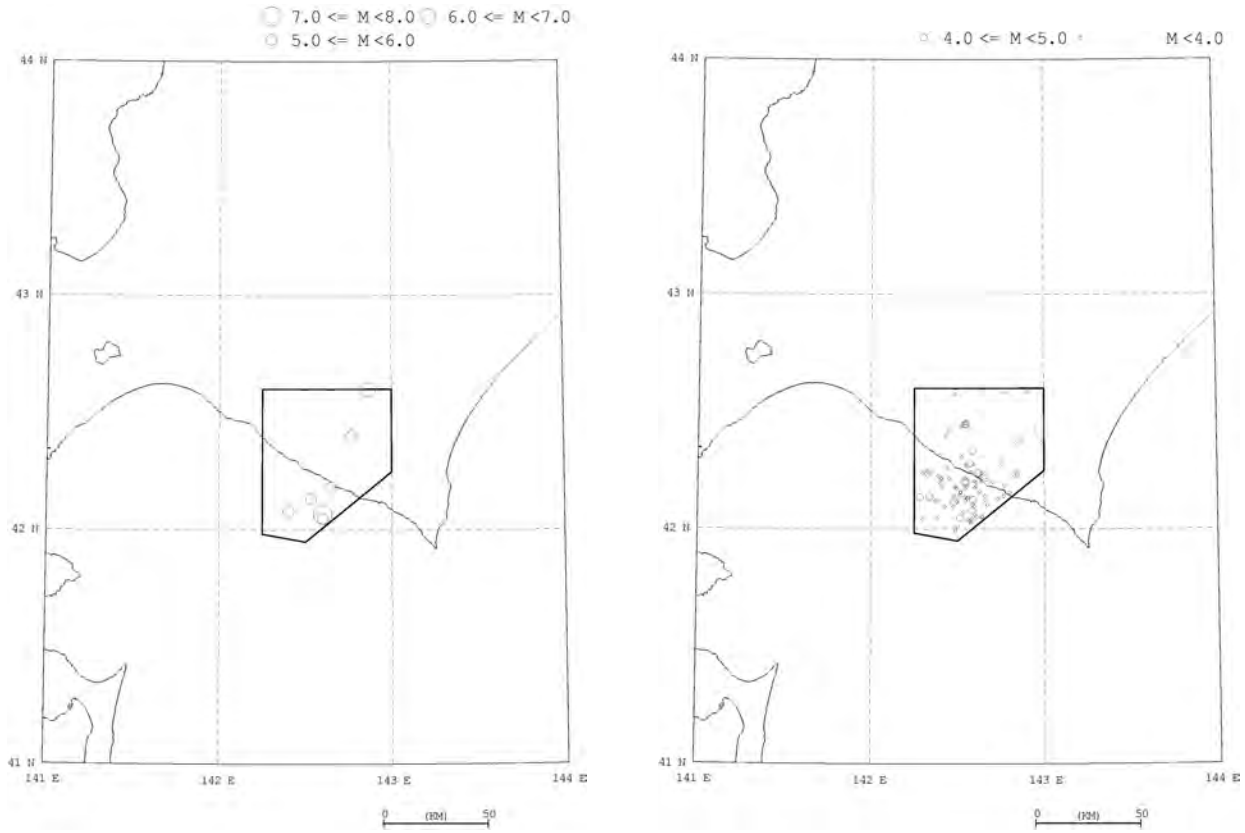

(a) Earthquakes of M≥5.0 since 1926

(b) Earthquakes of M≥3.0 since 1983

Figure 3.3.4.6-3 Epicenter distribution of earthquakes without specified source faults in Urakawa-Oki within the zoned area

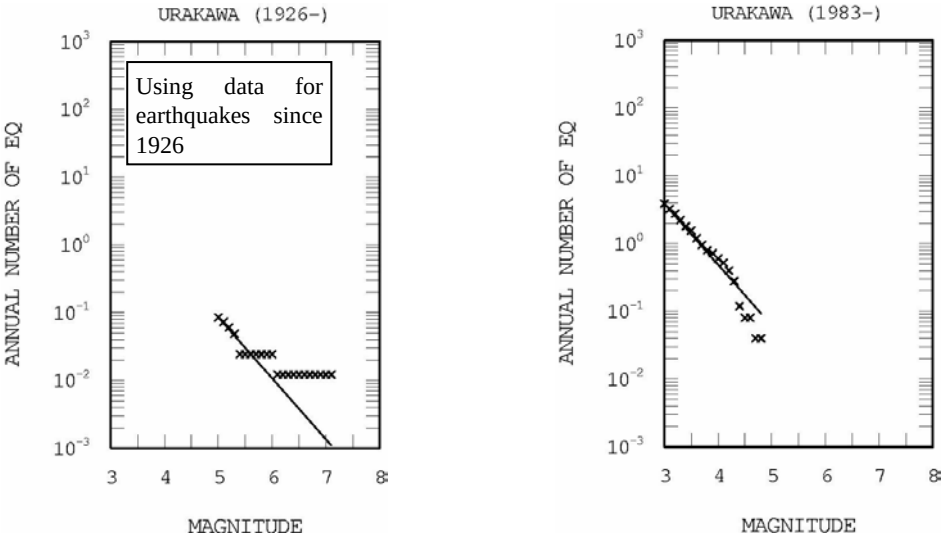

Figure 3.3.4.6-4 Cumulative frequency by earthquake magnitude for earthquakes without specified source faults in Urakawa-Oki (left: medium earthquake catalog, right: small earthquake catalog)

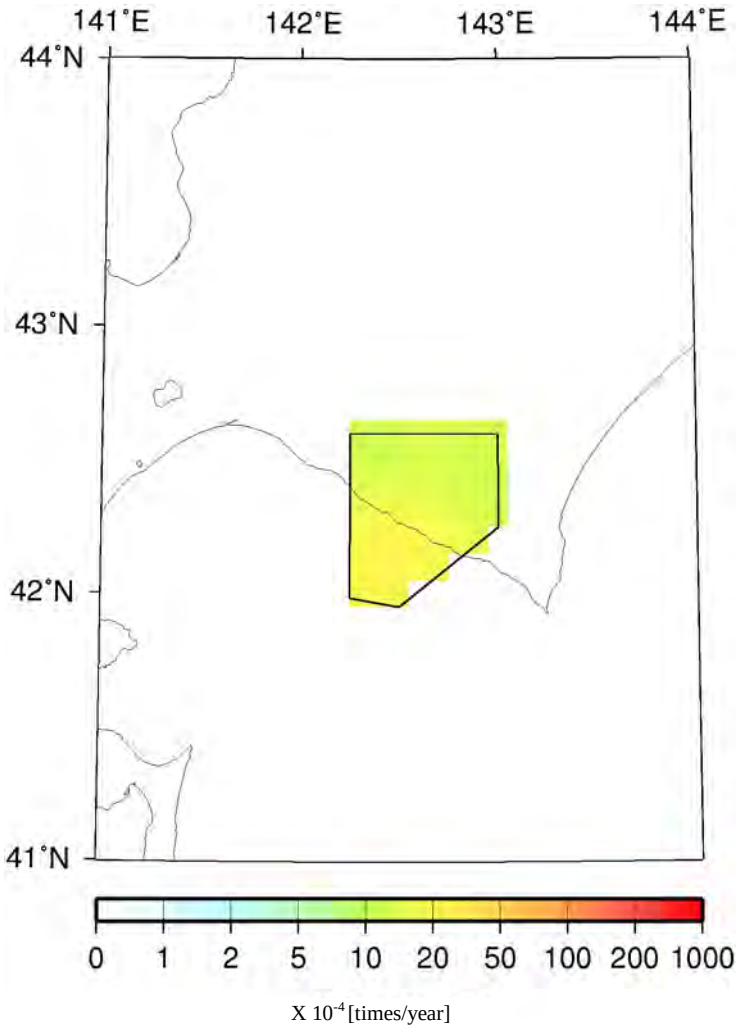

Figure 3.3.4.6-5 Occurrence frequency of earthquakes without specified source faults in Urakawa-Oki (per 0.1-degree square, *M*5.0 or more)

3.3.4.7 Earthquakes without specified source faults in the eastern margin of the Japan Sea

1) Target earthquakes

The earthquakes targeted as earthquakes without specified source faults in the eastern margin of the Japan Sea are those other than subduction-zone earthquakes with a magnitude of around 7.5 or more, which are separately evaluated based on the long-term evaluation of subduction-zone earthquakes in the same area (ERC, 2003c).

2) Zoning

Figure 3.3.4.7-1 shows the zoning of earthquakes without specified source faults in the eastern margin of the Japan Sea. The figure also shows the zoning of shallow earthquakes without specified source faults in land area, for reference. The area is determined while taking into account the area along the eastern margin of the Japan Sea in the seismotectonic province map by Kakimi et al. (2003) (Figure 3.3.4.5-1). However, as the area indicated in the New Kakimi Map extends to the land area of Niigata Prefecture, the area determined here only covers the area in and north of the part around the coastline.

3) Earthquake catalogs

The catalogs of medium earthquakes and small earthquakes (the minimum magnitude of 3.0) are both used, and regarding the source depth, earthquakes shallower than 40 km are extracted. Earthquakes that are separately evaluated as related subduction-zone earthquakes are excluded from the catalogs.

Figure 3.3.4.7-2 shows the epicenter distribution of earthquakes of magnitude 5.0 or more that have occurred since 1926, and Figure 3.3.4.7-3 shows the epicenter distribution of earthquakes of magnitude 3.0 or more that have occurred since 1983. Figure 3.3.4.7-4 shows the cumulative frequency of earthquakes by earthquake magnitude.

4) Maximum magnitude

As indicated in Figure 3.3.4.7-1, the maximum magnitude is assumed to be 7.3. When excluding earthquakes that correspond to separately evaluated subduction-zone earthquakes, the magnitude of the largest earthquake in the past is 7.1, but the maximum magnitude used here is made larger considering that earthquakes evaluated as subduction-zone earthquakes are magnitude 7.5 or more.

5) Determination of the fault planes

The fault planes are treated in the same manner as those of crustal earthquakes without specified source faults in land area. Specifically, vertical faults of which the size changes according to the magnitude are assumed to be distributed in the seismogenic layer within the upper crust. However, when carrying out numerical calculation, the source is assumed to be a point source that is 3 km deep, which gives roughly equivalent results as such fault planes.

6) Conversion to moment magnitude M_w

Moment magnitude Mw is assumed to be equal to Mj. The treatment differs from that for crustal earthquakes without specified source faults in land area, but is determined by taking into account the relationship between M_w and M_j for the Nihonkai-chubu Earthquake and the Hokkaido-nansei-Oki Earthquake.

7) Assumed earthquake type

In ground motion evaluation (applying an attenuation relation), formulas for crustal earthquakes are used.

8) Distribution of the earthquake occurrence frequency

Figure 3.3.4.7-5 shows the distribution of occurrence frequency of earthquakes without specified source faults along the eastern margin of the Japan Sea (the occurrence frequency of earthquakes of magnitude 5.0 or more within one year in an area of 0.1 degrees × 0.1 degrees). It adopts the mean value of the frequency for the following four cases: 1) the case using the medium earthquake catalog and the zoning method, 2) the case using the medium earthquake catalog and the non-zoning method, 3) the case using the small earthquake catalog and the zoning methos, 4) the case using the small earthquake catalog and the non-zoning method.

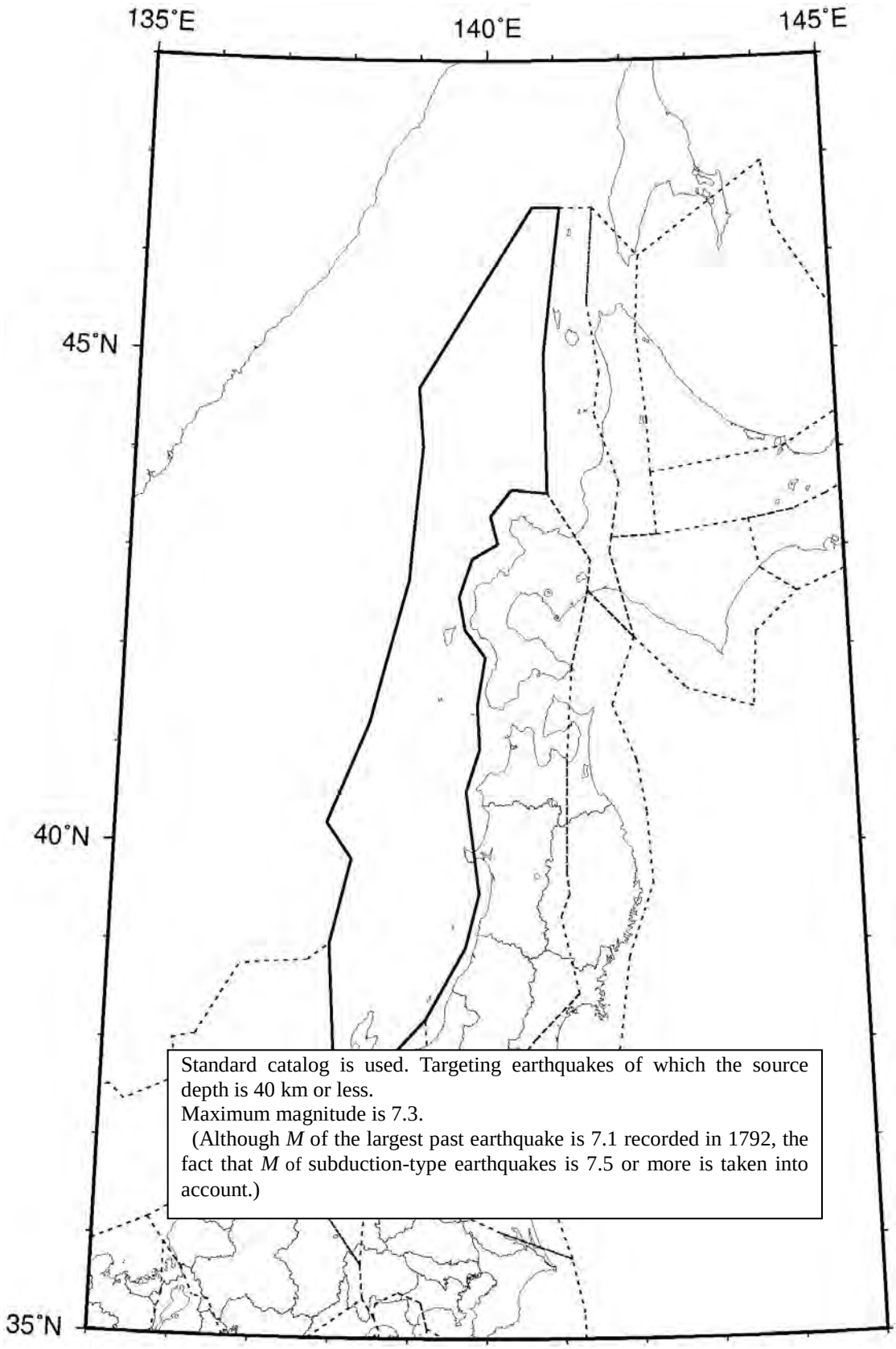

Figure 3.3.4.7-1 Zoning of earthquakes without specified source faults in the eastern margin of the Japan Sea. Earthquake catalogs used, and maximum magnitude are also shown. (Zoning of shallow earthquakes in the land area is also indicated in broken lines.)

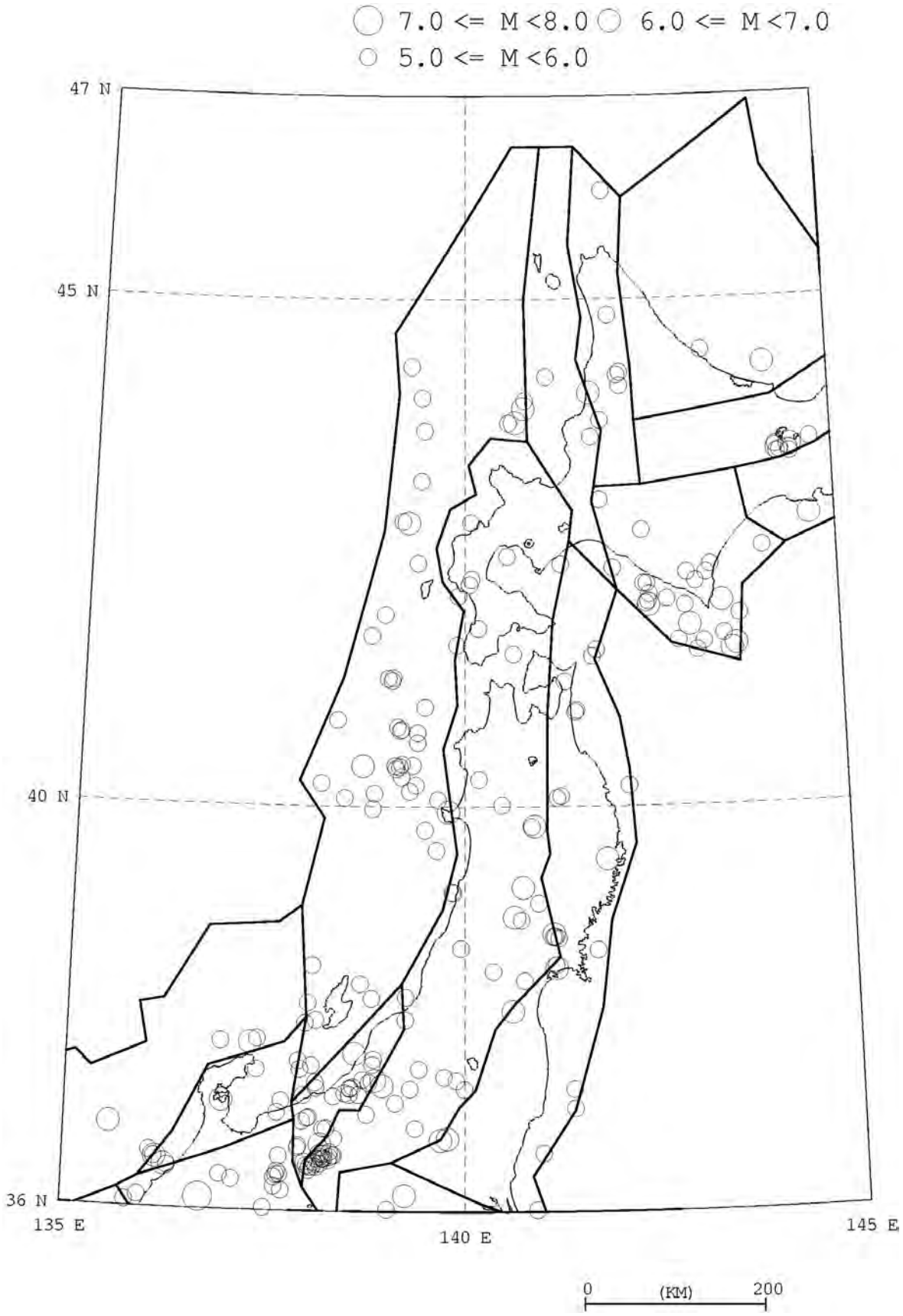

Figure 3.3.4.7-2 Epicenter distribution of earthquakes of M≥5.0 since 1926

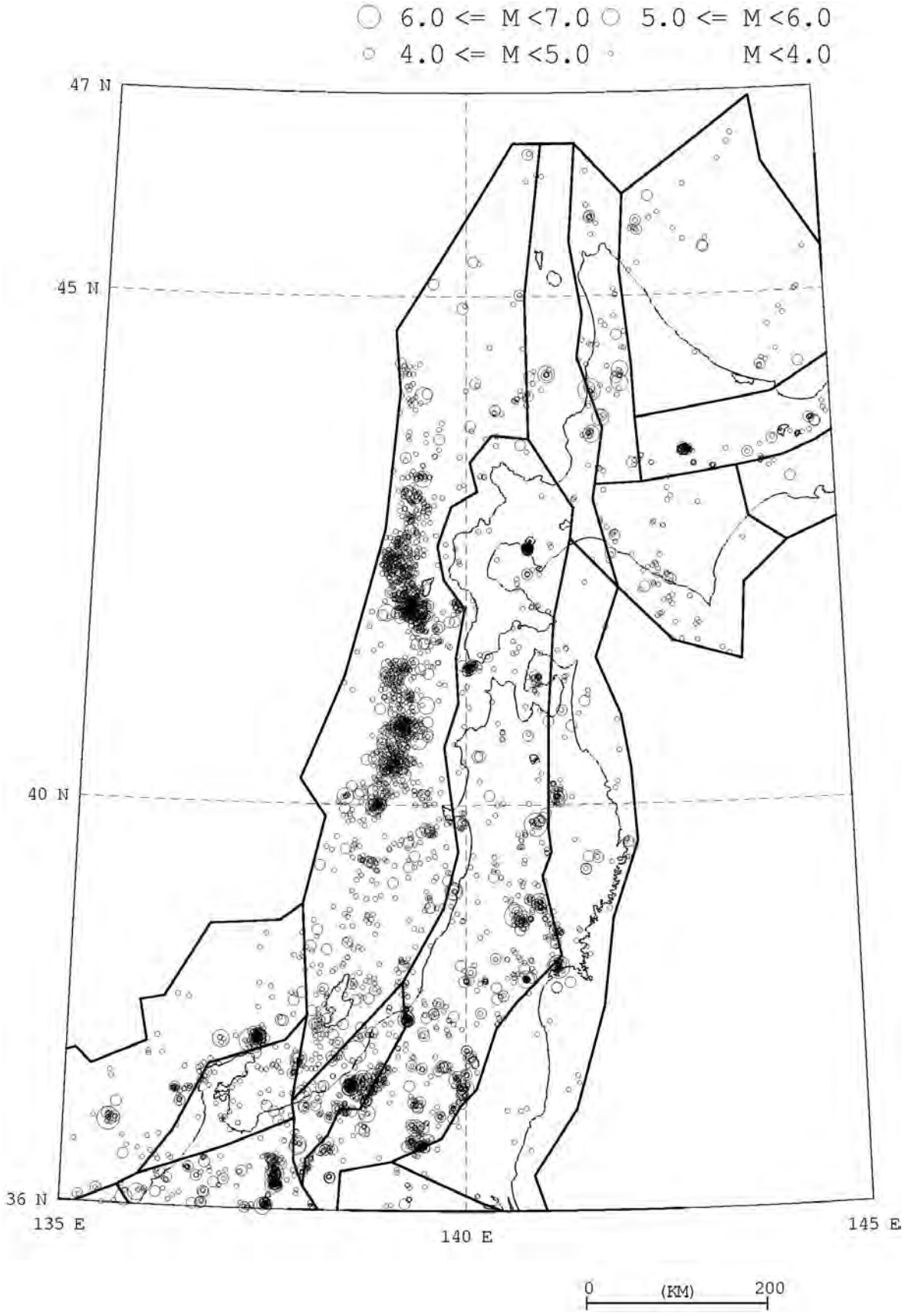

Figure 3.3.4.7-3 Epicenter distribution of earthquakes of *M*≥3.0 since 1983

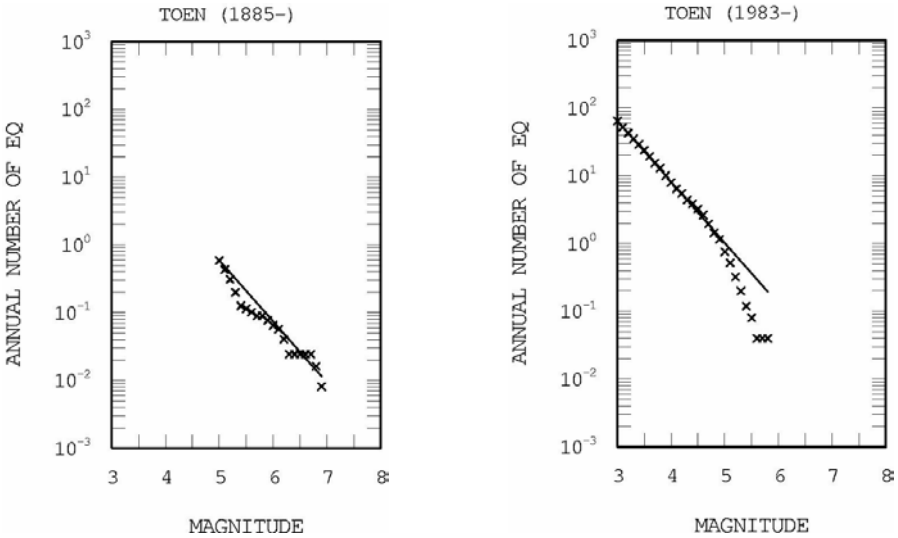

Figure 3.3.4.7-4 Cumulative frequency by earthquake magnitude for earthquakes without specified source faults in the eastern margin of the Japan Sea (left: medium earthquake catalog, right: small earthquake catalog)

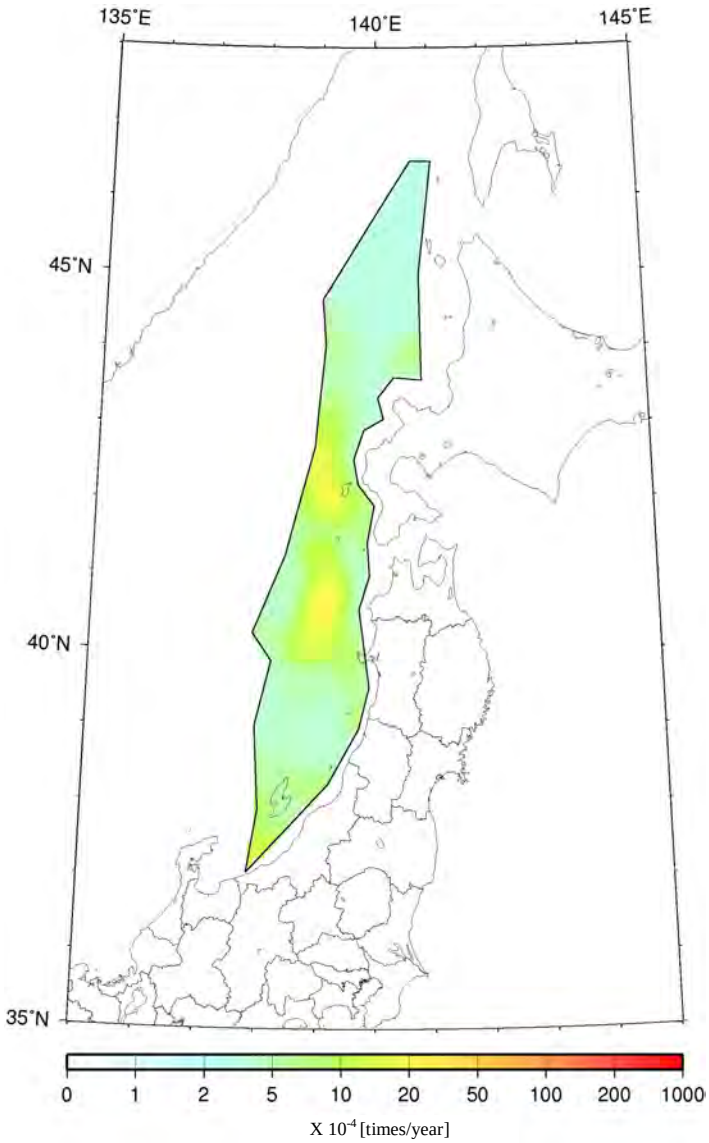

Figure 3.3.4.7-5 Occurrence frequency of earthquakes without specified source faults in the eastern margin of the Japan Sea (per 0.1-degree square, *M*5.0 or more)

3.3.4.8 Earthquakes without specified source faults in the southern area of Izu-shoto islands

1) Target earthquakes

The earthquakes targeted as earthquakes without specified source faults in the southern area of Izu-shoto islands are shallow earthquakes that occur further south from the Izu Peninsula and the Sagami Trough, which are actually assumed to be occurring within the Philippine Sea plate. It includes the area in the vicinity of Izu-shoto islands where seismic activity is active.

Earthquakes without specified source faults for the Pacific plate are related to this category of earthquakes, but they are treated separately as shown in Figure 3.3.4.8-1.

2) Zoning

Figure 3.3.4.8-2 shows the zoning. The north side is joined to the area of shallow earthquakes without specified source faults in land area. The east side of the area is determined so as to be aligned to the 30 km depth contour of the upper surface of the Pacific plate, and the west side boundary is established nearly parallel to the west side. Area No. 1, which is close to the Izu Peninsula, is distinguished from the other areas as an area with an extremely high level of seismic activity.

3) Earthquake catalogs

For the two areas on the north side, the catalogs of medium earthquakes and small earthquakes (the minimum magnitude of 3.0) are both used. However, regarding the target period of the medium earthquake catalog, earthquakes of magnitude 5.0 or more that have occurred since 1940, when the influence of the 1923 Taisho Kanto Earthquake has diminished, are used. For Area No. 3 on the south side, only earthquakes of magnitude 5.0 or more that have occurred since 1983 are used, and the small and medium earthquake catalogs are not used, considering the detection capability of the observation network. As for the source depth, only earthquakes of which the depth is 40 km or less are used, but earthquakes that occur deeper than the upper surface of the Pacific plate are evaluated as earthquakes at the Pacific plate.

Figure 3.3.4.8-3 shows the epicenter distribution of earthquakes of magnitude 5.0 or more that have occurred since 1926, and Figure 3.3.4.8-4 shows the epicenter distribution of earthquakes of magnitude 3.0 or more that have occurred since 1983. Figure 3.3.4.8-5 shows the cumulative frequency of earthquakes by earthquake magnitude.

4) Maximum magnitude

The maximum magnitude uses the largest magnitude of past earthquakes for each zoned area. The lower limit value shall be M_j =7.0. The maximum magnitude determined for each area is shown in Table 3.3.4.8-1. Figure 3.3.4.8-2 above also show the maximum magnitude.

5) Determination of the fault planes

The fault planes are treated in the same manner as those of earthquakes without specified source faults in land area. Specifically, vertical faults are assumed to be positioned at random in the seismogenic layer of which the thickness is between 10-20 km. However, when carrying out numerical calculation, the source is assumed to be a point source that is 3 km deep, which gives roughly equivalent results as such fault planes.

6) Conversion to moment magnitude M_w

Similar to the treatment for earthquakes without specified source faults in land area, moment magnitude M_w is converted from M_j using the following formula, based on Takemura (1990):

$$M_w = 0.78\, M_j + 1.08 \qquad (3.3.4.8\text{-}1)$$

7) Assumed earthquake type

The earthquakes under this category are actually earthquakes within the Philippine Sea plate, but in ground motion evaluation (applying an attenuation relation), they are assumed to have the same characteristics as crustal earthquakes in land area.

8) Distribution of the earthquake occurrence frequency

Figure 3.3.4.8-6 shows the distribution of occurrence frequency of earthquakes without specified source faults in the southern area of Izu-shoto islands (the occurrence frequency of earthquakes of magnitude 5.0 or more within one year in an area of 0.1 degrees × 0.1 degrees). For Area No. 1 and Area No. 2, it adopts the mean value of the frequency for the following four cases: 1) the case using the medium earthquake catalog and the zoning method, 2) the case using the medium earthquake catalog and the non-zoning method, 3) the case using the small earthquake catalog and the zoning method, 4) the case using the small earthquake catalog and the non-zoning method. For Area No. 3, it adopts the mean value of the frequency for 1) the case using the zoning method and 2) the case using the non-zoning method, based on the data of earthquakes of magnitude 5.0 or more that have occurred since 1983.

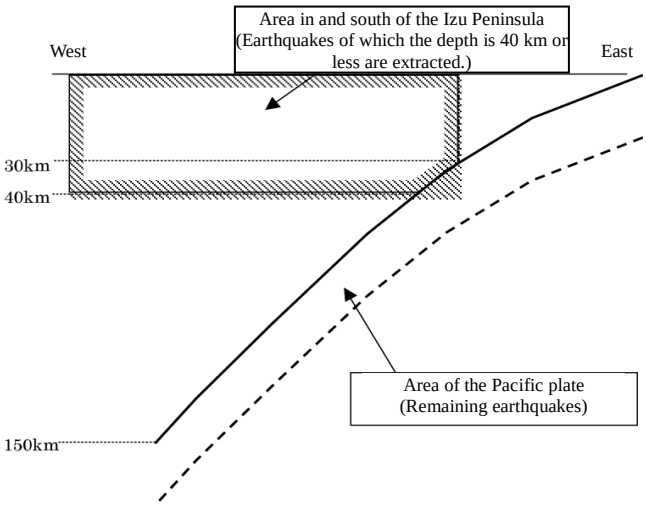

Figure 3.3.4.8-1 Area for extracting shallow earthquakes in and south of the vicinity of Izu-shoto islands

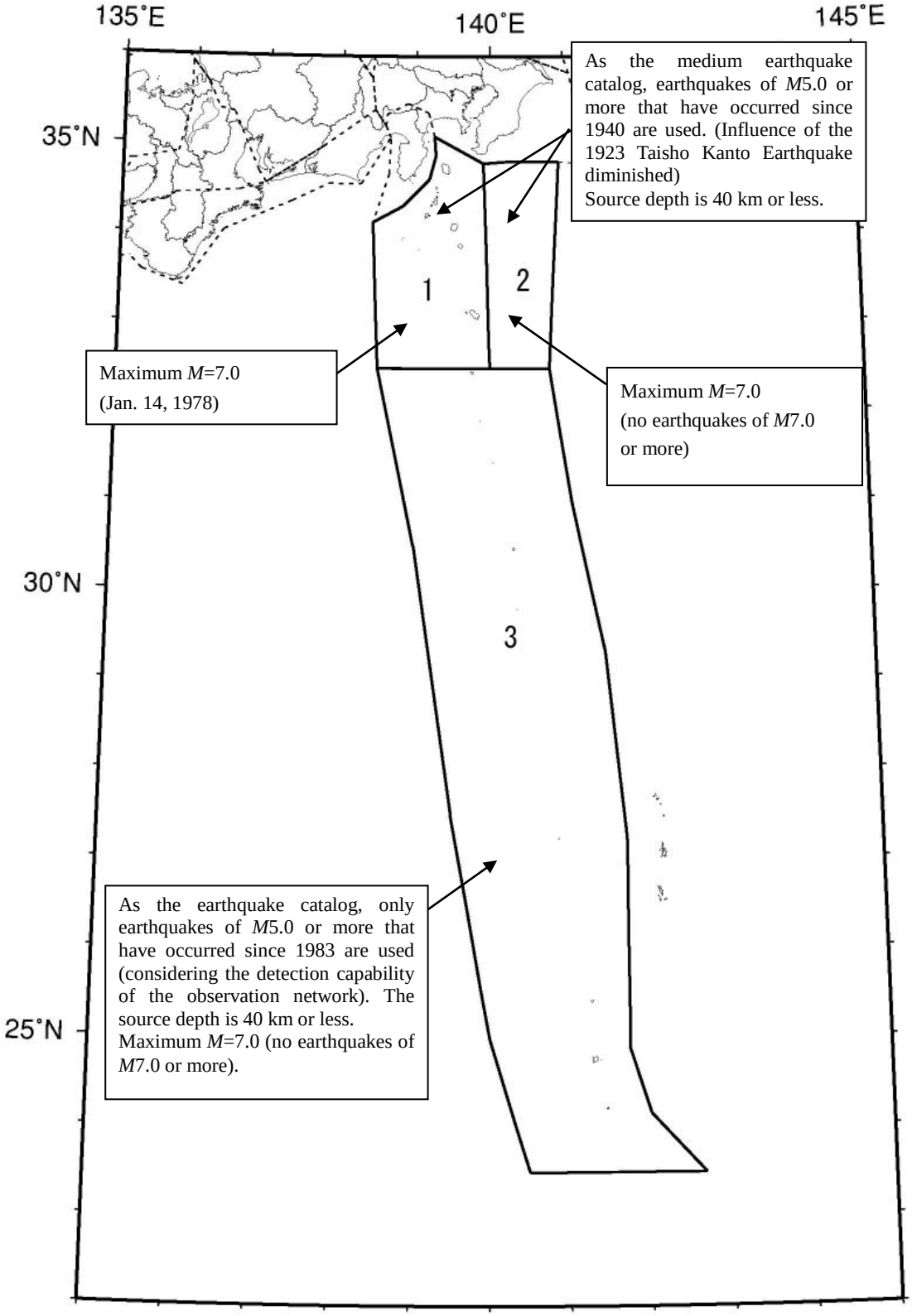

Figure 3.3.4.8-2 Zoning of earthquakes without specified source faults in the southern area of Izu-shoto islands. Earthquake catalogs used, and maximum magnitude are also shown.

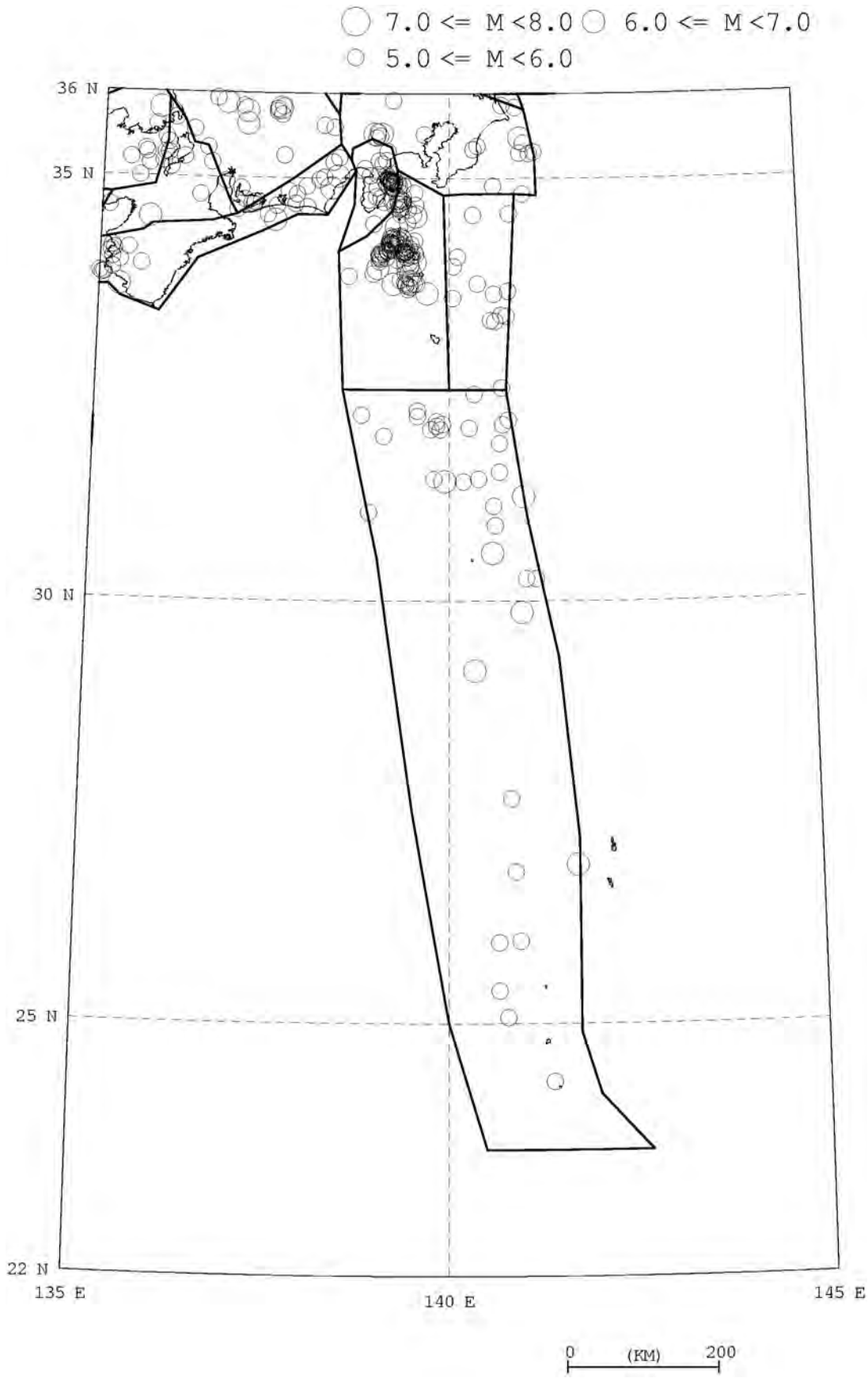

Figure 3.3.4.8-3 Epicenter distribution of earthquakes of M≥5.0 since 1926

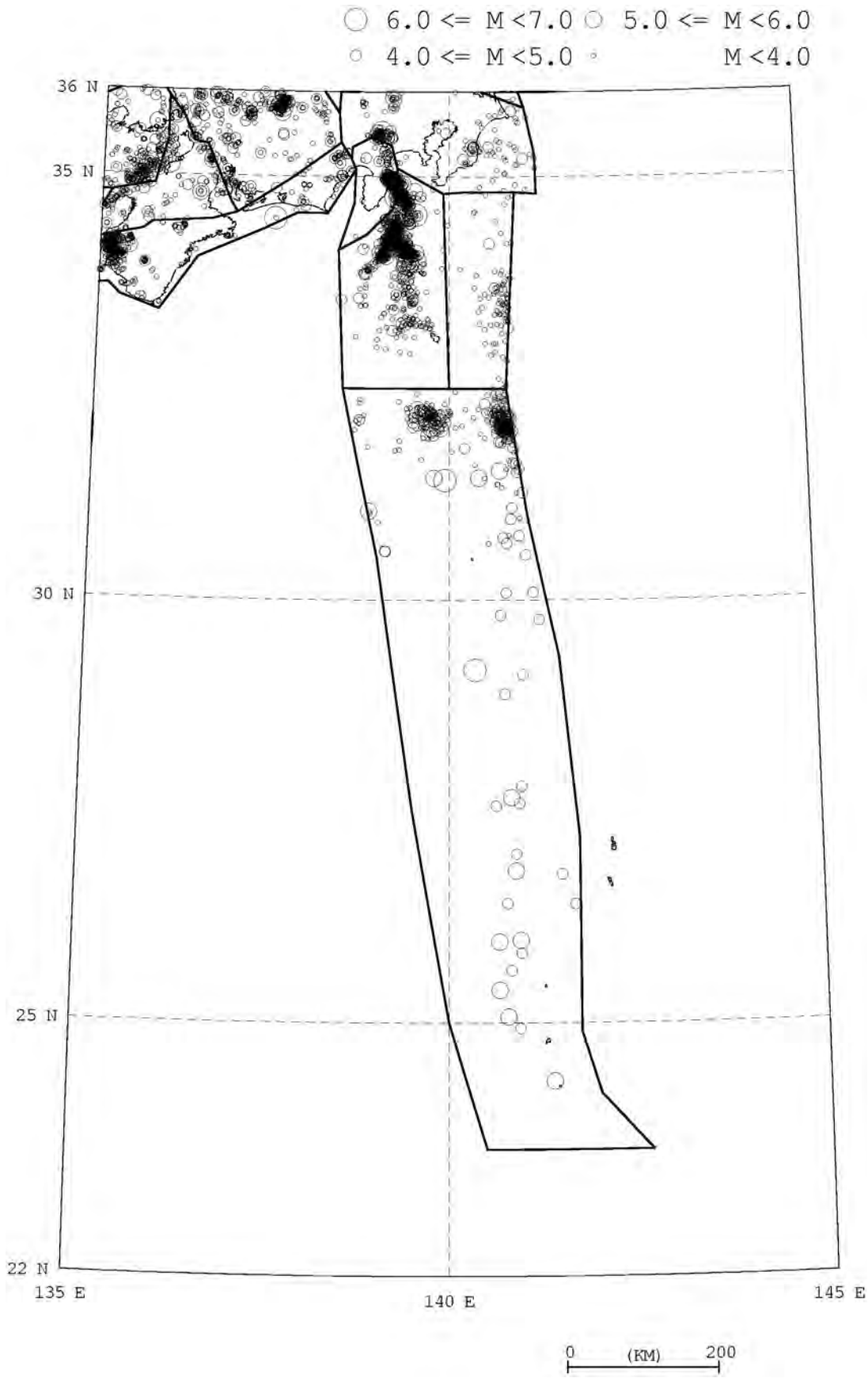

Figure 3.3.4.8-4 Epicenter distribution of earthquakes of *M*≥3.0 since 1983

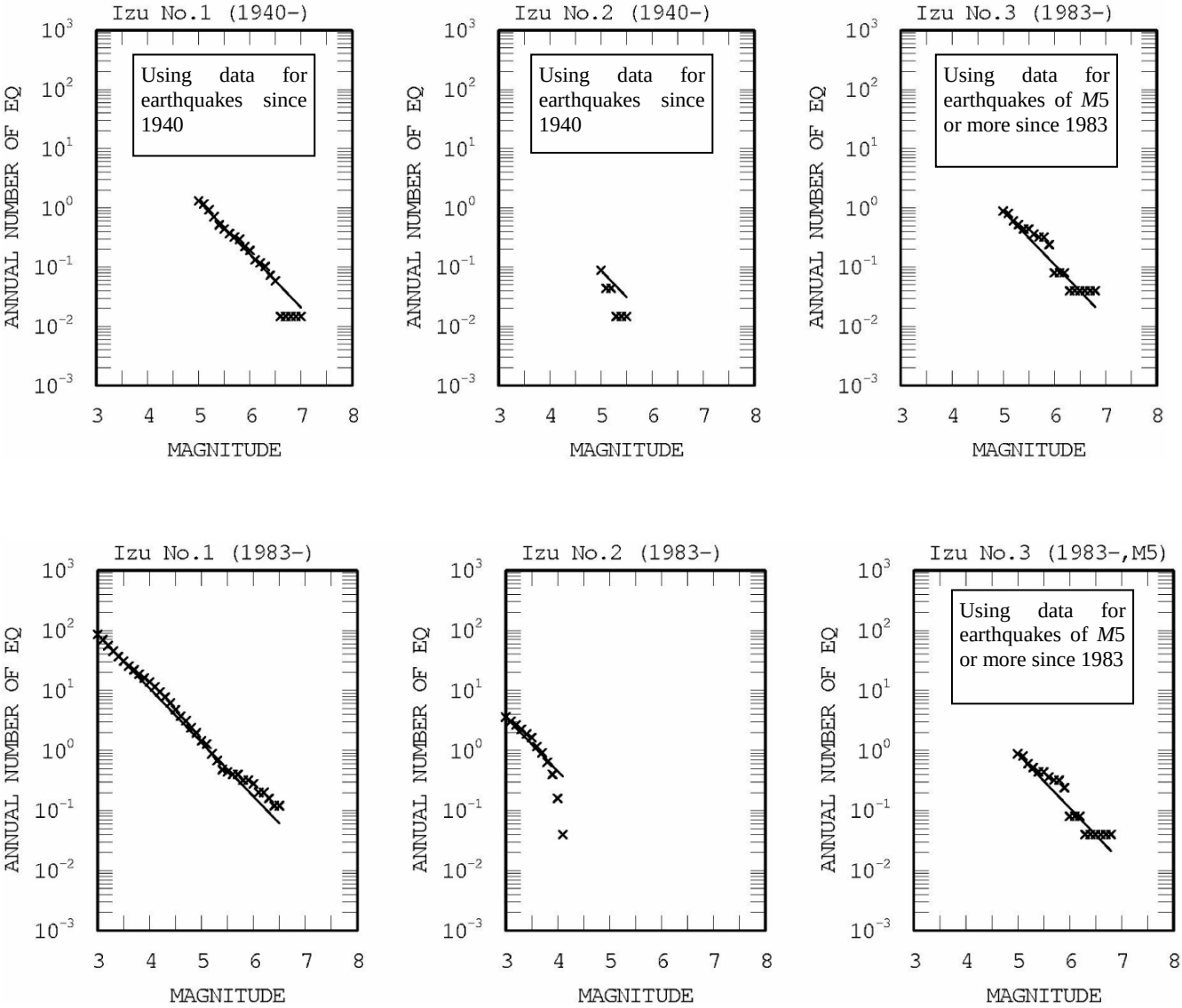

Figure 3.3.4.8-5 Cumulative frequency by earthquake magnitude for earthquakes without specified source faults in the southern area of Izu-shoto islands (upper row: medium earthquake catalog, lower row: small earthquake catalog)

Table 3.3.4.8-1 Maximum magnitude determined for each area

Area No.	Maximum *M*	Basis	Remarks
1	7.0	Jan. 14, 1978 Izu-Oshima-kinkai Earthquake	
2	7.0	(Lower limit value of maximum *M*)	
3	7.0	(Lower limit value of maximum *M*)	

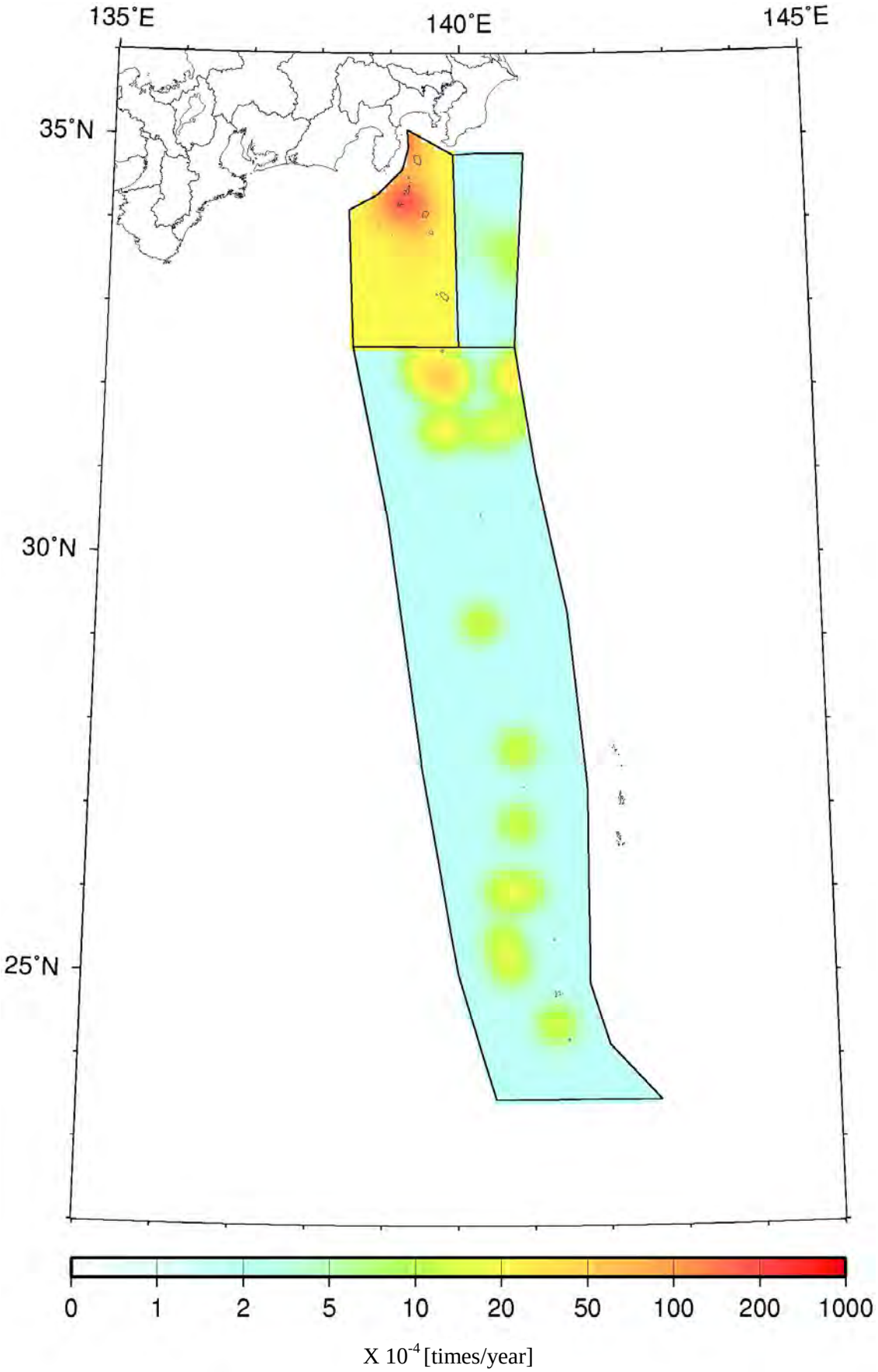

Figure 3.3.4.8-6 Occurrence frequency of earthquakes without specified source faults in the southern area of Izu-shoto islands (per 0.1-degree square, *M*5.0 or more)

3.3.4.9 Earthquakes without specified source faults in the vicinity of Nansei-shoto islands

1) Target earthquakes

With regard to earthquakes in the vicinity of Nansei-shoto islands, the accuracy of the seismic source data is not necessarily sufficient due to limitations in the observation network. Thus, it is difficult to classify past earthquakes into different types. Accordingly, in "Long-term Evaluation of Seismic Activity in Hyuganada and the Vicinity of the Nansei-shoto islands Trench" (ERC, 2004a), earthquakes were evaluated separately between "shallow earthquakes in the vicinity of Nansei-shoto islands (depth: roughly 60 km or less)", ""earthquakes in the vicinity of Yonaguni-jima (depth: roughly 100 km or less)", and "relatively deep earthquakes from Kyushu to the vicinity of Nansei-shoto islands (depth: from roughly around 60 km to around 150 km)". Earthquakes without specified source faults are also modeled to match the above classification. However, since relatively deep earthquakes from Kyushu to the vicinity of Nansei-shoto islands are treated as intraplate earthquakes of the Philippine Sea plate, here, shallow earthquakes in the vicinity of Nansei-shoto islands and earthquakes in the vicinity of Yonaguni-jima which are not large earthquakes are collectively referred to as "earthquakes without specified source faults in the vicinity of Nansei-shoto islands". Figure 3.3.4.9-1 shows the relationship between the target earthquakes and the related earthquakes.

2) Zoning

The area determined in "Long-term Evaluation of Seismic Activity in Hyuganada and the Vicinity of the Nansei-shoto islands Trench" (ERC, 2004a) is zoned as shown in Figure 3.3.4.9-2.

3) Earthquake catalogs

Considering the limitations in the observation network in the target area, only earthquakes of magnitude 5.0 or more that have occurred since 1983 from the JMA catalog are used, and the small and medium earthquake catalogs are not used for this area. The target earthquakes are those of which the source depth is 100 km or less with regard to earthquakes in the vicinity of Yonaguni-jima, and those of which the source depth is 60 km or less with regard to shallow earthquakes in the vicinity of Nansei-shoto islands. While the area of the shallow earthquakes in the vicinity of Nansei-shoto islands and that of relatively deep earthquakes from Kyushu to the vicinity of Nansei-shoto islands overlap when projected on the ground surface, their depth directions and the locational relationship between the two areas are as shown earlier in Figure 3.3.4.9-1. Since the seismic sources tend to be determined to be deep in the east side of the area of relatively deep earthquakes (the right-hand side in Figure 3.3.4.9-1), even earthquakes of which the depth is indicated to be 60 km or more in the earthquake catalog are regarded as earthquakes of which the depth is 60 km or less, prioritizing data on the location of the epicenter. Whereas earthquakes which are separately evaluated as subduction-zone earthquakes are excluded from the earthquake catalog, no such earthquakes are included in earthquakes that have occurred since 1983 which are used for evaluation of the earthquake occurrence frequency. Figure 3.3.4.9-3 shows the epicenter distribution of earthquakes of magnitude 5.0 or more that have occurred since 1983. Figure 3.3.4.9-4 shows the cumulative frequency by earthquake magnitude.

4) Maximum magnitude

For the area of shallow earthquakes in the vicinity of Nansei-shoto islands, there are descriptions concerning past earthquakes in the long-term evaluation concerning the area, but the occurrence probability and other factors have not been evaluated, and earthquakes in the area have not been modeled as subduction-zone earthquakes. Thus, all earthquakes are treated as earthquakes without specified source faults, and the maximum magnitude is assumed to be 7.7.

Earthquakes in the vicinity of Yonaguni-jima with a magnitude of 7.5 or more are separately modeled as subduction-zone earthquake based on long-term evaluation. Therefore, the maximum magnitude of earthquakes without specified source faults is determined to be 7.3, which is the largest magnitude of earthquakes with a magnitude level of 7.4 or less that have occurred in the past. Table 3.3.4.9-1 shows the maximum magnitude by area. Figure 3.3.4.9-2 above also shows the maximum magnitude.

5) Determination of the fault planes

In the long-term evaluation for this area, earthquakes of which the depth is 60 km or less were treated collectively for relatively shallow earthquakes in the vicinity of Nansei-shoto islands, and earthquakes of which the depth is 100 km or less were treated collectively for earthquakes in the vicinity of Yonaguni-jima. In reality, they are likely to be a mix of earthquakes occurring within an overriding plate, earthquakes occurring on the shallow earthquakes of the Philippine Sea plate, and earthquakes occurring within the Philippine Sea plate, but it is difficult to identify the ratio of their occurrence frequency. Thus, the depth of the center of the fault planes is fixed at 30 km for shallow earthquakes in the vicinity of Nansei-shoto islands, and at 40 km for earthquakes in the vicinity of Yonaguni-jima.

The fault planes for shallow earthquakes in the vicinity of Nansei-shoto islands are assumed to be circular fault planes of which the size changes according to the earthquake magnitude, with the center of the fault planes positioned at the depth of 30 km. They are assumed to be striking N45E, taking into account the trench axis in this area, and dipping northwest at a dip angle of 45°. Under these conditions, fault planes do not project above the ground surface even when the maximum magnitude is 7.7.

The fault planes for earthquakes in the vicinity of

Yonaguni-jima are assumed to be circular fault planes of which the size changes according to the earthquake magnitude, with the center of the fault planes positioned at the depth of 40 km. They are assumed to be striking N90E, taking into account the trench axis in this area, and dipping north at a dip angle of 45°.

In both cases above, the size S(km^2) of the circular fault is determined according to the magnitude to satisfy the following formula which has rounded the coefficient of the formula by Utsu and Seki (1955):

$$\log S = M\text{-}4.0 \qquad (3.3.4.9\text{-}1)$$

6) Conversion to moment magnitude M_w

Moment magnitude Mw is assumed to be equal to Mj.

7) Assumed earthquake type

Although different types of earthquakes are considered to be mixed, they are assumed to be interplate earthquakes in ground motion evaluation (applying an attenuation relation).

8) Distribution of the earthquake occurrence frequency

Figure 3.3.4.9-5 shows the distribution of occurrence frequency of earthquakes in the vicinity of Nansei-shoto islands (the occurrence frequency of earthquakes of magnitude 5.0 or more within one year in an area of 0.1 degrees × 0.1 degrees). It adopts the mean value of the frequency for 1) the case using the zoning method and 2) the case using the non-zoning method, based on the data of earthquakes of magnitude 5.0 or more that have occurred since 1983.

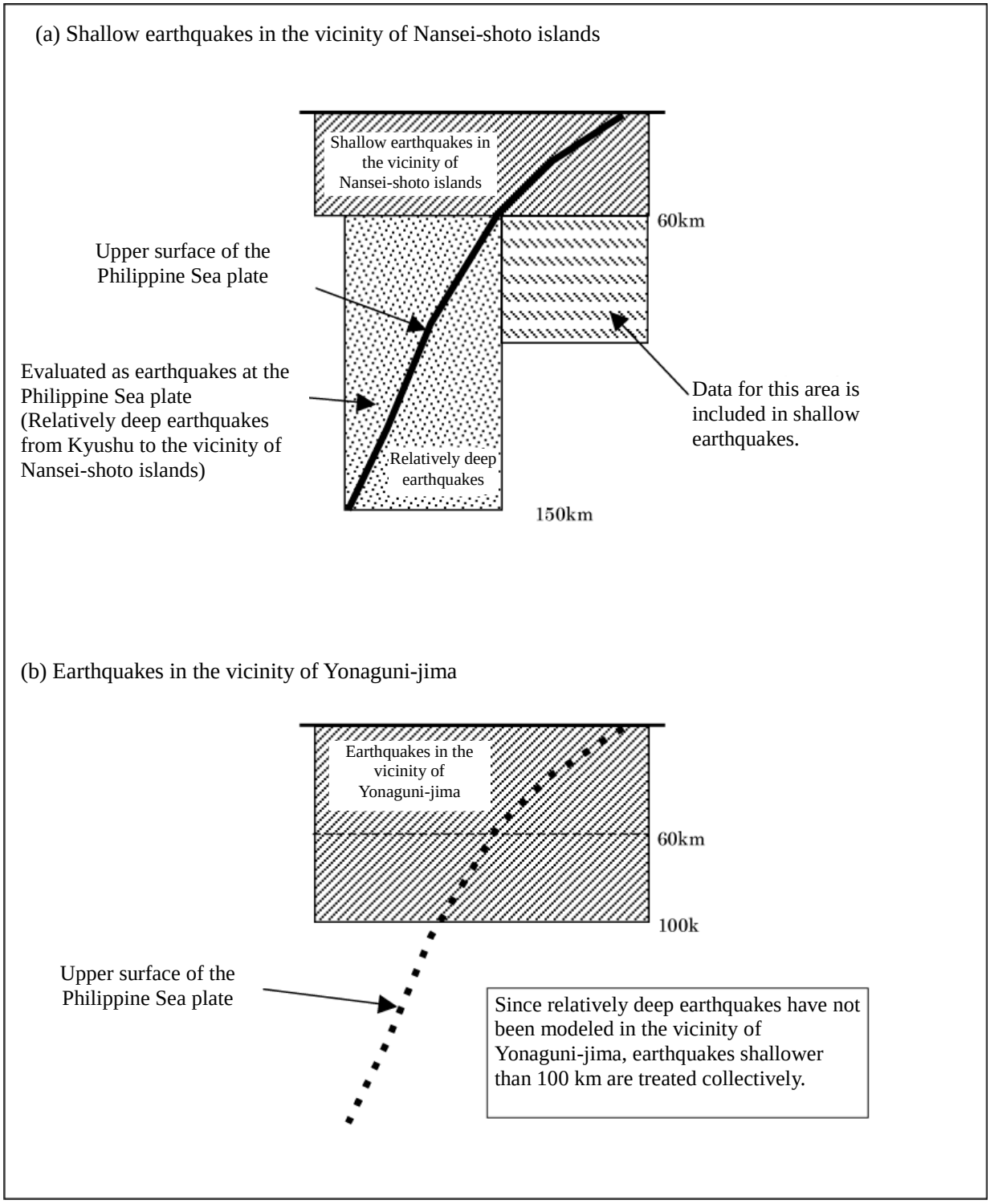

Figure 3.3.4.9-1 Target earthquakes of earthquakes without specified source faults in the vicinity of Nansei-shoto islands

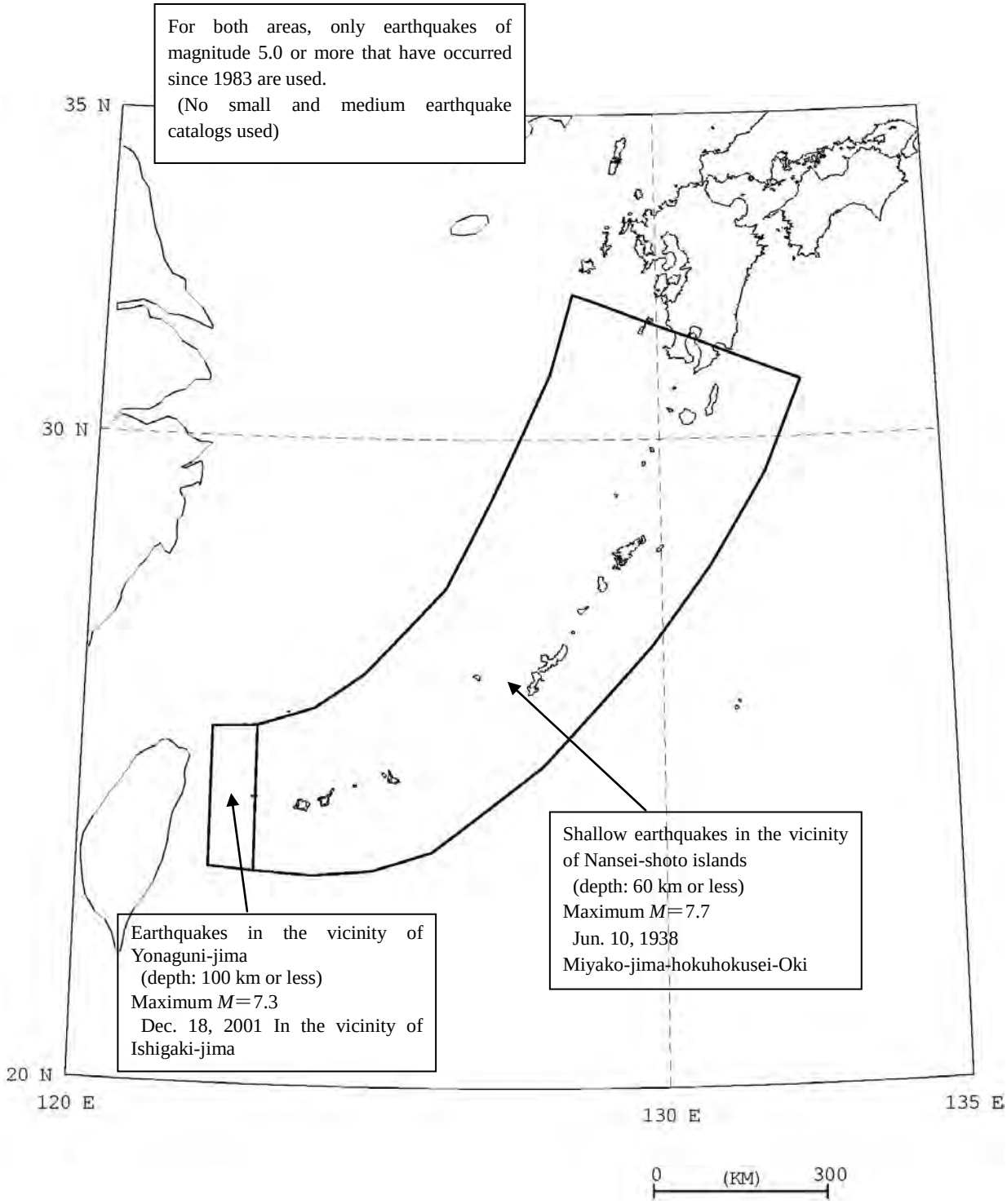

Figure 3.3.4.9-2 Zoning of earthquakes without specified source faults in the vicinity of Nansei-shoto islands. Earthquake catalogs used for calculating the frequency, and maximum magnitude

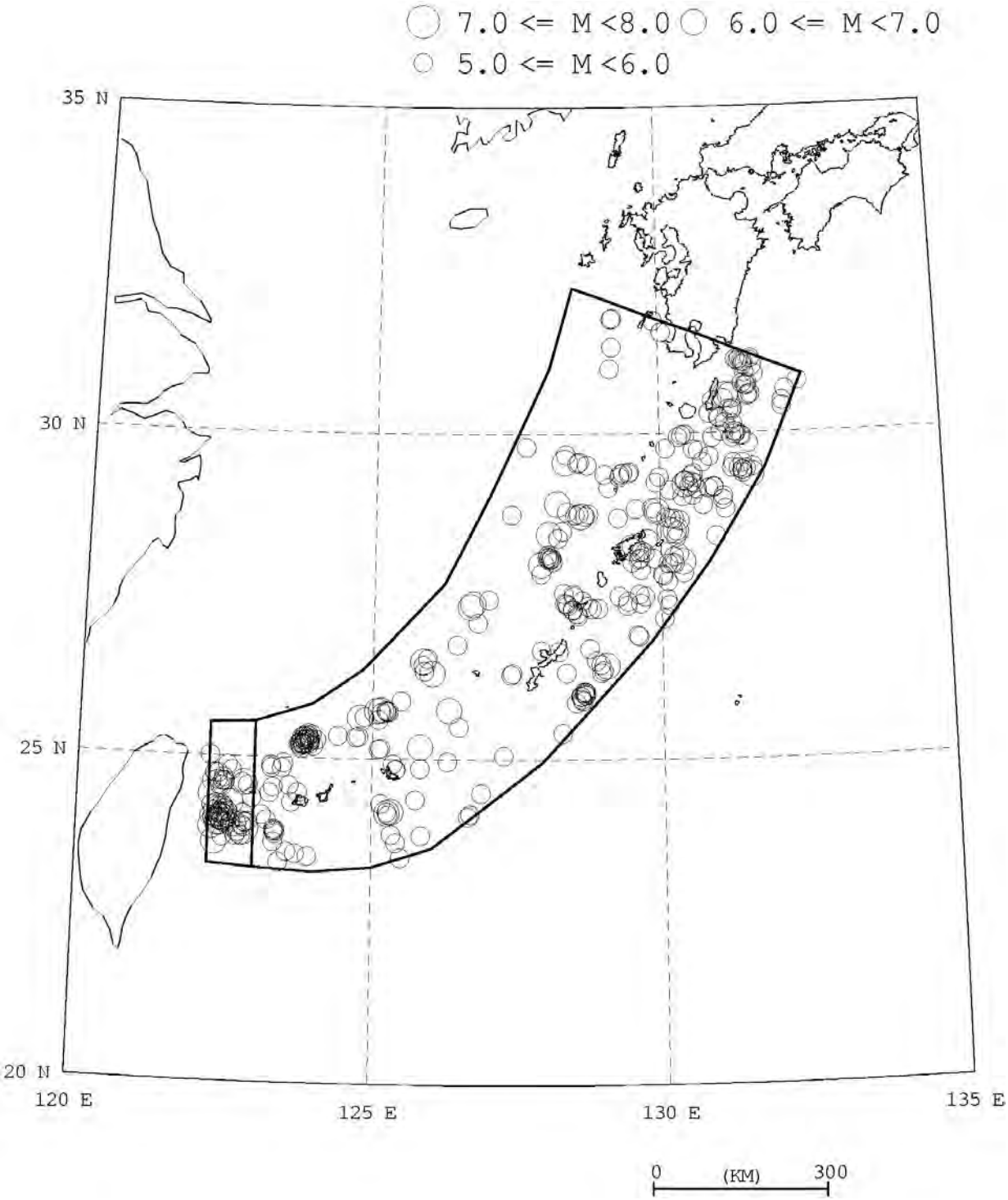

Figure 3.3.4.9-3 Epicenter distribution of earthquakes without specified source faults in the vicinity of Nansei-shoto islands (JMA catalog data for earthquakes since 1983, magnitude 5.0 or more)

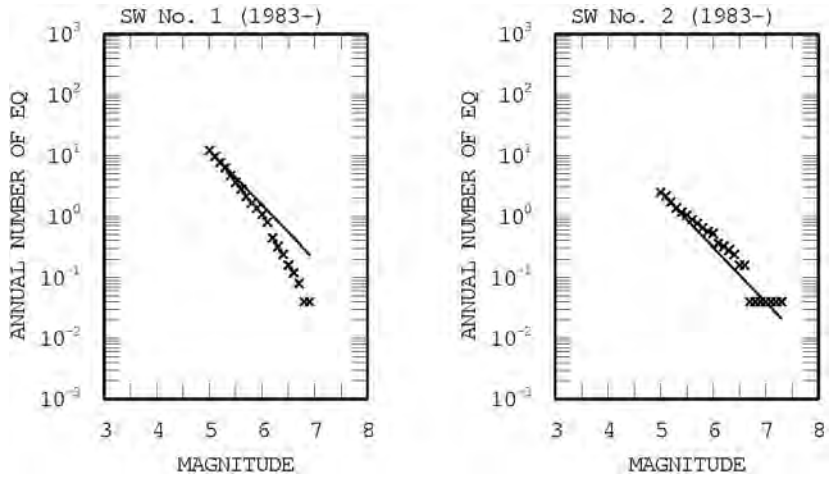

Figure 3.3.4.9-4 Cumulative frequency by earthquake magnitude for each area of earthquakes without specified source faults in the vicinity of Nansei-shoto islands

Table 3.3.4.9-1 Maximum magnitude determined for each area

Area No.	Maximum *M*	Basis	Remarks
1	7.7	Jun. 10, 1938 Miyako-jima-hokuhokusei-Oki	Based on description in the long-term evaluation. *M* is based on Utsu.
2	7.3	Dec. 18, 2001 In the vicinity of Ishigaki-jima	In the long-term evaluation, earthquakes of *M*7.5 or more have been evaluated.

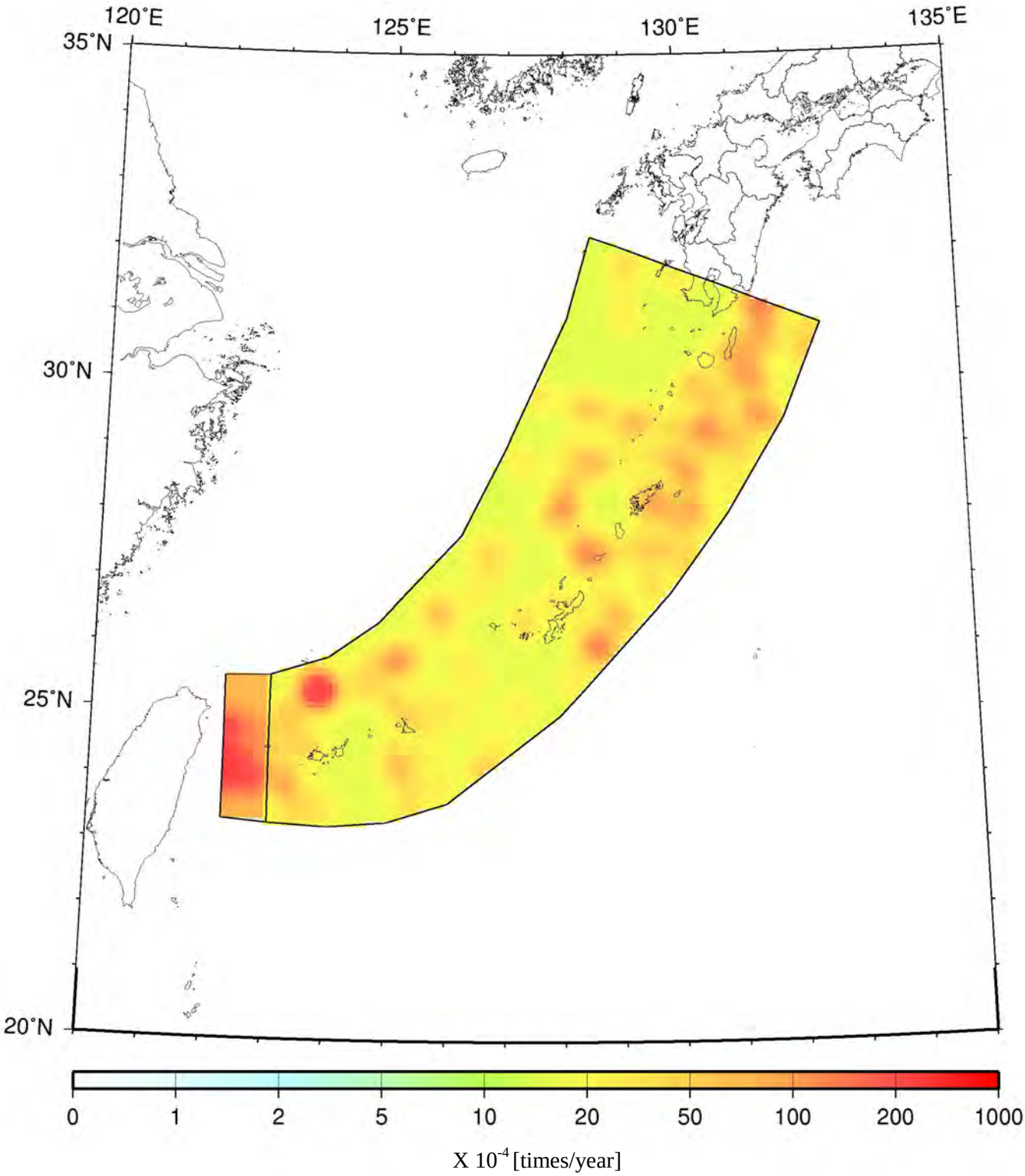

Figure 3.3.4.9-5 Occurrence frequency of earthquakes without specified source faults in the vicinity of Nansei-shoto islands (per 0.1-degree square, *M*5.0 or more)

3.3.4.10 Comparison of the earthquake occurrence frequency between the 2008 version and the 2009 version

Sections 3.3.4.3 through 3.3.4.9 have indicated the details of modeling and the earthquake occurrence frequency for each group of earthquakes. This section compares the earthquake occurrence frequency calculated the 2009 version and the results obtained from the 2008 version. The difference the 2009 version from the 2008 version is the difference in the JMA seismic source data used. The 2008 version uses the data up to the end of 2006, and the 2009 version uses the data up to the end of 2007. Therefore, earthquakes that have occurred during one year from January 2007 to December 2007 are added in the 2009 version, and the periods covered by the catalogs are longer. In addition, if a review of past seismic source data has been reflected in the new seismic source data, that would also affect the results of calculation of the frequency.

The following figures compare the frequency distribution itself as well as the rate of change in the frequency (derived by dividing the increase or decrease from the frequency obtained the 2008 fiscal year by the frequency obtained the 2008 fiscal year: $(\nu_{2009}-\nu_{2008})/\nu_{2008}$). The figures showing the rate of change in the frequency also show the epicenters of earthquakes that occurred during the period from January 2007 to December 2007. In the figures below, the 2008 version denotes the results obtained the 2008 fiscal year and the 2009 version denotes the results obtained the 2009 fiscal year.

The general tendency of changes in the earthquake occurrence frequency is as follows.

- Due to the characteristics of the method for calculation of the occurrence frequency using the zoning method, if earthquakes occur in the target zoned area more frequently in 2007 than the past average frequency, the frequency in the area increases overall.
- Due to the characteristics of the method for calculation of the occurrence frequency using the non-zoning method, the frequency increases in areas around the earthquakes that occurred in 2007.
- When the period covered by the catalog used for calculating the earthquake occurrence frequency is short, the addition of one year of data has a conspicuous influence. For example, in the area in and south of Izushoto and in the vicinity of Nansei-shoto islands where only the data since 1983 are used, the rate of change tends to be emphasized.
- In areas where the occurrence frequency is low, the addition of one year of data has a conspicuous influence.

Figure 3.3.4.10-1 shows comparison of the occurrence frequency of earthquakes without specified source faults for the Pacific plate. The two versions seem hardly different when only comparing the frequency, but the rate of change in the frequency in the middle figure shows the strong influence of individual earthquakes in some locations in and south of the latitude of 34 degrees north. Since this area only uses earthquakes of M5 or more that have occurred since 1983 as the earthquake catalog, the influence of individual earthquakes shows up clearly.

Figure 3.3.4.10-2 shows the comparison results for earthquakes without specified source faults for the Philippine Sea plate. In the area in the vicinity of Kanto, the frequency has risen slightly in the eastern part of the Boso Peninsula, but in the long, narrow area from Kyushu to Nansei-shoto islands, the frequency is low overall. Regarding the area in the vicinity off Bungosuido, the zoning has changed from the 2008 fiscal year's version, so its influence is included in the change in frequency.

Figure 3.3.4.10-3 shows the comparison results for shallow earthquakes in land area, earthquakes along the eastern margin of the Japan Sea, and earthquakes without specified source faults in the southern area of Izu-shoto islands. The frequency has risen slightly in the northeastern part of Hokkaido, the eastern part of the Boso Peninsula, the area off Noto Peninsula, and Ogasawara-shoto islands. These are considered to be the influence of the swarm earthquakes in Kujukuri in August 2007 with regard to the eastern part of the Boso Peninsula, and the aftershocks of the 2007 Noto-hanto Earthquake with regard to the area off Noto Peninsula. It should be noted, however, that in places where the absolute value of the earthquake occurrence frequency is small, such as in the northeastern part of Hokkaido, a minute change could be strongly emphasized.

Figure 3.3.4.10-4 shows the results for earthquakes without specified source faults in Urakawa-Oki. Hardly any change is observed in the frequency.

Figure 3.3.4.10-5 shows the results of earthquakes without specified source faults in the vicinity of Nansei-shoto islands. In this area, the influence of the addition of data is emphasized since the period covered by the catalog used is short at 25 years. The rate of change in the frequency indicates a trend that, in the wide area in the east side, the frequency has risen at places where earthquakes have occurred within the additional one year, and has slightly declined in other places. On the other hand, no large change is observed in the area in the west side.

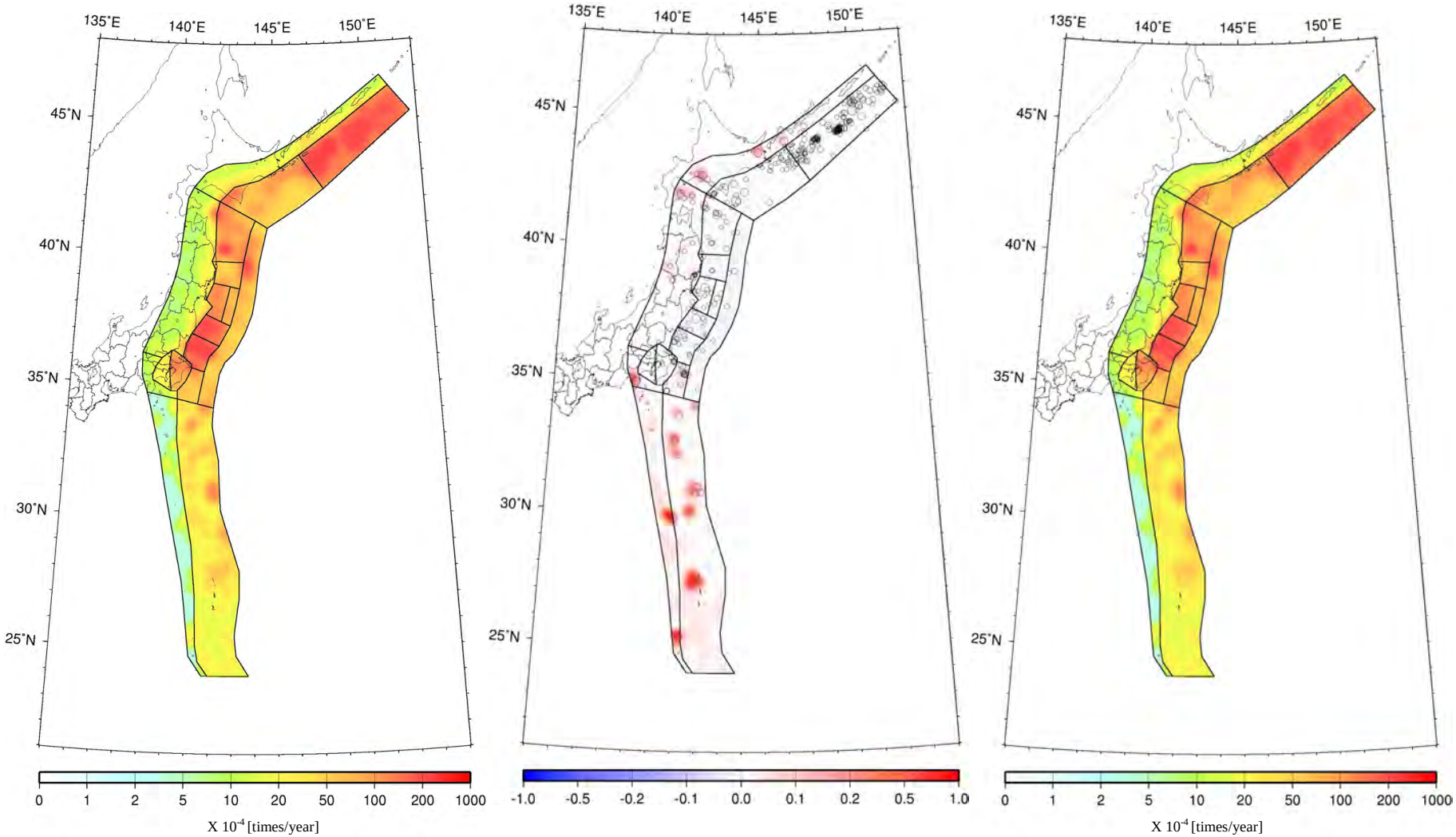

2009 version (data: - Dec. 2007)

Rate of change = (2009-2008)/2008

2008 version (data: - Dec. 2006)

Figure 3.3.4.10-1 Occurrence frequency of earthquakes without specified source faults for the Pacific plate (Total for interplate and intraplate earthquakes)

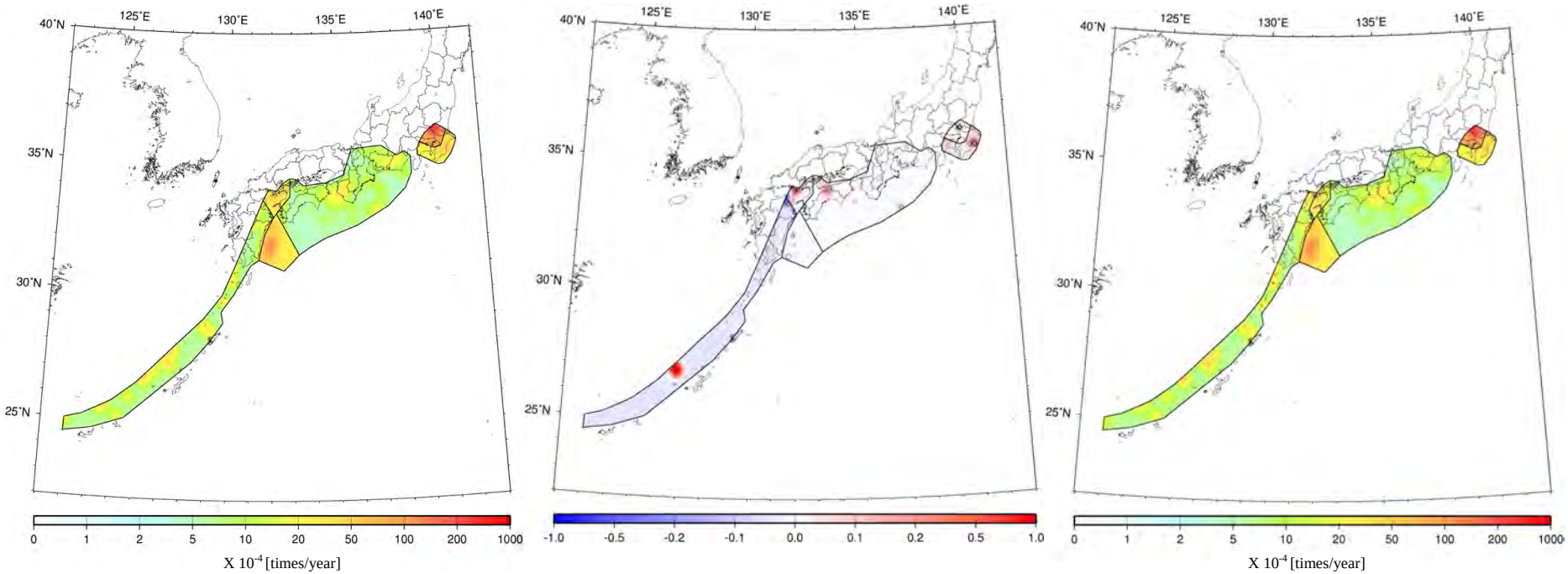

2009 version (data: - Dec. 2007) | Rate of change = (2009-2008)/2008 | 2008 version (data: - Dec. 2006)

Figure 3.3.4.10-2 Occurrence frequency of earthquakes without specified source faults in the Philippine Sea plate (Total for interplate and intraplate earthquakes)

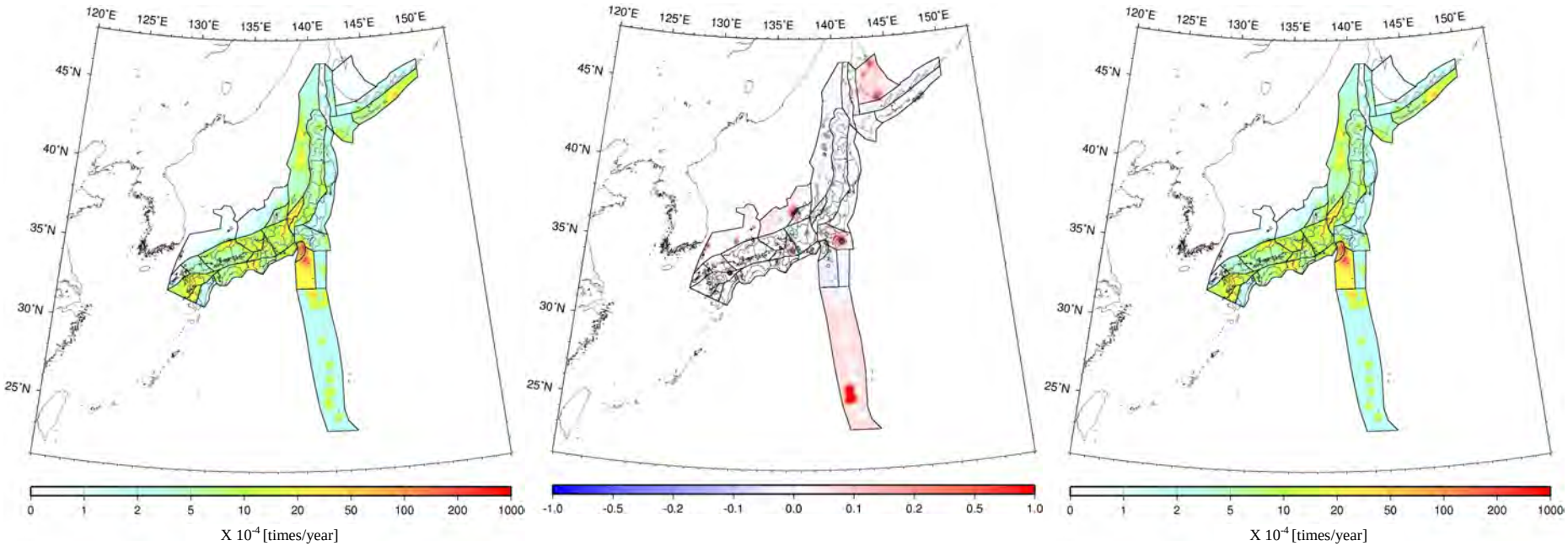

2009 version (data: - Dec. 2007) | Rate of change = (2009-2008)/2008 | 2008 version (data: - Dec. 2006)

Figure 3.3.4.10-3 Occurrence frequency of earthquakes without specified source faults in shallow parts of land area, in the southern area of Izu-shoto islands, and in the eastern margin of the Japan Sea

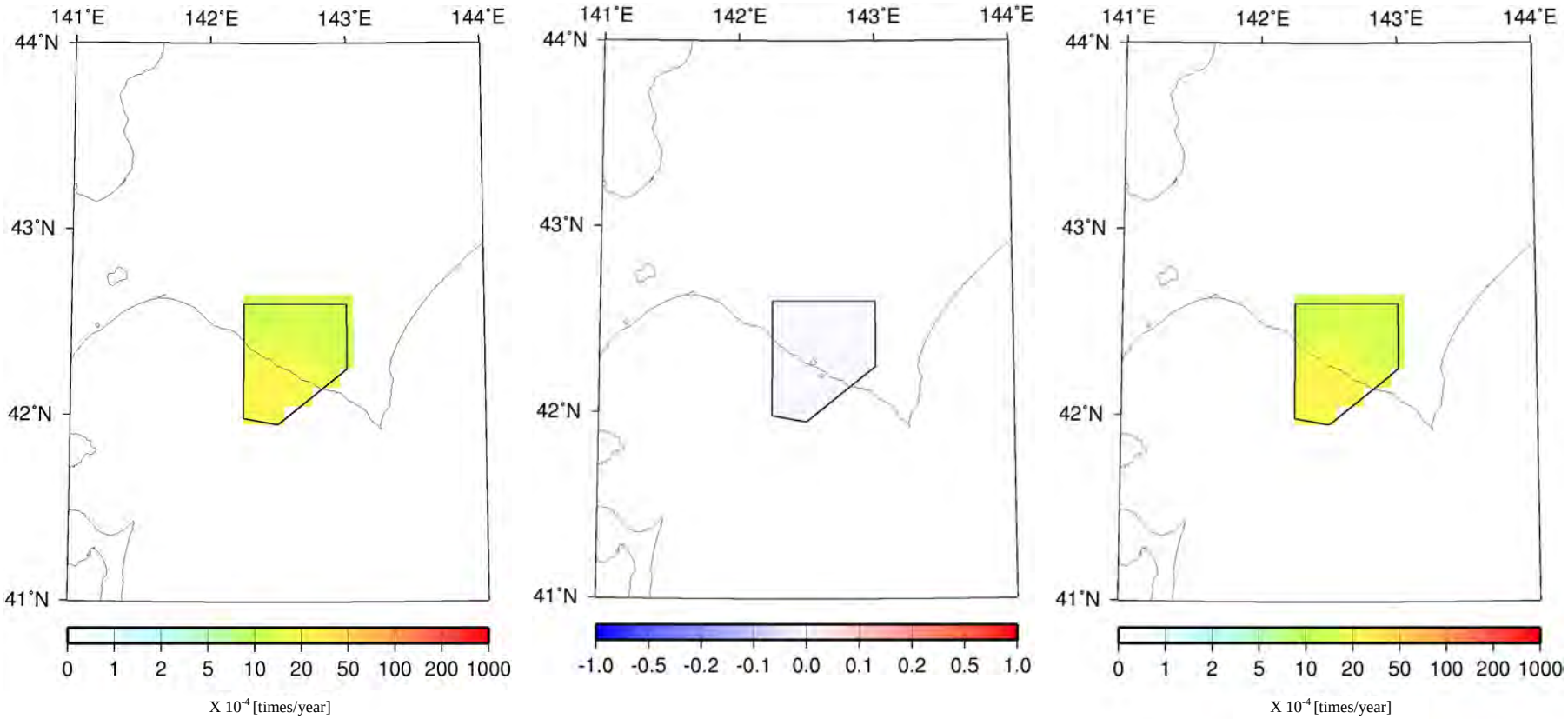

2009 version (data: - Dec. 2007)

Rate of change = (2009-2008)/2008

2008 version (data: - Dec. 2006)

Figure 3.3.4.10-4 Occurrence frequency of earthquakes without specified source faults in Urakawa-Oki

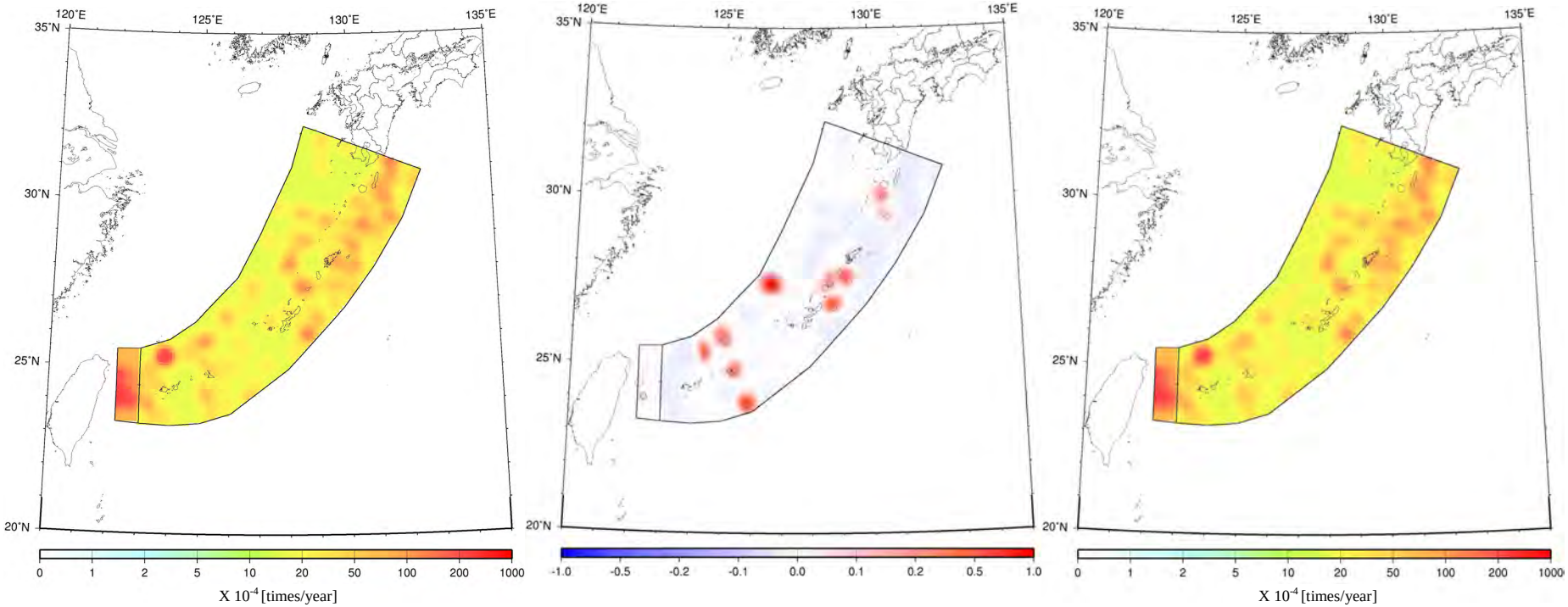

2009 version (data: - Dec. 2007) | Rate of change = (2009-2008)/2008 | 2008 version (data: - Dec. 2006)

Figure 3.3.4.10-5 Occurrence frequency of earthquakes without specified source faults in the vicinity of Nansei-shoto islands

3.4 Earthquake Category

Up to the 2008 version, earthquakes considered for preparing seismic hazard maps had been classified into earthquakes occurring in major active fault zones, subduction-zone earthquakes, and other earthquakes, and had been used for analyzing the characteristics of seismic hazard nationwide in detail. This time, earthquake categories are defined as a new earthquake classification, and maps for individual earthquake categories are also created. Shown below are the three earthquake categories under the new classification system.

Earthquake Category I <Subduction-zone large earthquakes>

(Mega earthquakes in subduction zones with specified source faults with a recurrence interval of several hundred years)

- Nankai Trough earthquakes (Nankai Earthquake/Tonankai Earthquake/Assumed Tokai Earthquake)
- Miyagi-ken-Oki Earthquake/earthquakes close to the offshore trenches in Southern Sanriku-Oki
- Large interplate earthquakes in Northern Sanriku-Oki
- Tokachi-Oki Earthquake/Nemuro-Oki Earthquake
- Shikotanto-Oki Earthquake
- Etorofuto-Oki Earthquake
- Kanto Earthquake of "1923 Taisho" type

Earthquake Category II <Subduction-zone earthquakes without specified source faults>

(Earthquakes without specified source faults that occur in plates at trenches)

- Interplate earthquakes other than characteristic earthquakes in Northern Sanriku-Oki
- Large interplate earthquakes close to the offshore trenches in the Sanriku-Oki to Boso-Oki regions (Tsunami earthquakes)
- Large intraplate earthquakes close to the offshore trenches in the Sanriku-Oki to Boso-Oki regions (normal faults type)
- Interplate earthquakes in Fukushima-ken-Oki
- Interplate earthquakes in Ibaraki-ken-Oki
- Relatively small interplate earthquakes in the Tokachi-Oki and Nemuro-Oki regions
- Relatively small interplate earthquakes in the Shikotanto-Oki and Etorofuto-Oki regions
- Relatively shallow earthquakes within a subducted plate along the Kuril Trench
- Relatively deep earthquakes within a subducted plate along the Kuril Trench
- Intraplate earthquakes in Akinada-Iyonada-Bungosuido
- Interplate earthquakes in Hyuganada
- Relatively small interplate earthquakes in Hyuganada
- Earthquakes in the vicinity of Yonaguni-jima
- Other *M*7 class earthquakes in Southern Kanto
- Interplate/intraplate earthquakes without specified source faults for the Pacific plate
- Interplate/intraplate earthquakes without specified source faults for the Philippine Sea plate
- Earthquakes without specified source faults in Urakawa-Oki

Earthquake Category III <Shallow earthquakes in land area>

(Earthquakes at active fault zones and earthquakes without specified source faults in land area and in the surrounding sea area)

- Characteristic earthquakes occurring in major active fault zones
- Hokkaido-hokusei-Oki Earthquake
- Hokkaido-seiho-Oki Earthquake
- Hokkaido-nansei-Oki Earthquake
- Aomori-ken-seiho-Oki Earthquake
- Akita-ken-Oki Earthquake
- Yamagata-ken-Oki Earthquake
- Niigata-ken-hokubu-Oki Earthquake
- Sadogashima-hoppo-Oki Earthquake
- Earthquakes occurring on active faults other than major active fault zones
- Earthquakes occurring at onshore locations where active faults have not been specified
- Earthquakes without specified source faults in the eastern margin of the Japan Sea
- Earthquakes without specified source faults in the southern area of Izu-shoto islands
- Earthquakes without specified source faults in the vicinity of Nansei-shoto islands

3.5 Ground Motion Evaluation Models

Among the evaluation conditions for creating PSHM for the whole of Japan, this section describes the ground motion evaluation models.

The evaluation of the ground motion intensity is carried out by, while using attenuation relations, considering the mean value of the ground motion intensity evaluated based on the characteristics of the seismic source, such as the magnitude and the distance to the seismic source fault, and the variance included in the evaluation formula. Specifically, after evaluating the peak velocity on the surface of the engineering bedrock, the amplification factor of the shallow subsurface for the peak velocity is multiplied to evaluate the peak ground velocity on the ground surface. The instrumental seismic intensity is evaluated by converting the peak ground velocity on the ground surface by using an empirical relation.

3.5.1 Attenuation relation for the peak velocity on the engineering bedrock

Here, the layer with 400m/s shear wave velocity is assumed to be the engineering bedrock, and the peak velocity on the bedrock is obtained by an attenuation relation by Si and Midorikawa (1999). While Si and Midorikawa (1999) proposes two types of formulas for deriving the distance to the seismic source fault, one for the shortest fault distance and the other for the equivalent hypocentral distance, here, the following formula using the shortest fault distance X (km) is adopted:

$$\begin{aligned}\log PGV &= 0.58M_{\mathrm{w}} + 0.0038H + d - 1.29 \\ &\quad - \log(X + 0.0028\times 10^{0.50M_{\mathrm{w}}}) - 0.002X \\ d &= \begin{cases} 0.0 & \text{crustal earthquake} \\ -0.02 & \text{interplate earthquake} \\ 0.12 & \text{intraplate earthquake} \end{cases}\end{aligned} \tag{3.5.1-1}$$

Here, PV (cm/s) is the peak velocity on a hard layer with 600m/s shear wave velocity, M_{w} is the moment magnitude of the earthquake, and H (km) is the depth of the center of the source fault. The value obtained by first deriving a rate (1.41) from the following amplification factor for the peak velocity based on the average shear wave velocity $AVS30$ (m/s) from the surface layer to the depth of 30 m by Fujimoto and Midorikawa (2006)

$$\log(amp) = 2.367 - 0.852\cdot\log AVS30 \tag{3.5.1-2}$$

and then multiplying the rate by peak velocity PV obtained by Formula (3.5.1-1) is used as peak velocity PV_{b400} on the engineering bedrock with 400m/s shear wave velocity.

The conversion from JMA magnitude M to the moment magnitude is carried out separately for shallow earthquakes in land area and other earthquakes. The relation between seismic moment M_0 and the JMA magnitude

$$\log M_0 = 1.17M + 10.72 \tag{3.5.1-3}$$

by Takemura (1990) and the relation between the seismic moment and the moment magnitude

$$\log M_0 = 1.5M_{\mathrm{w}} + 9.1 \tag{3.5.1-4}$$

(Kanamori, 1977) are used to derive

$$M_w = 0.78M + 1.08 \tag{3.5.1-5}$$

and this formula is used for the conversion for shallow earthquakes in land area. For other earthquakes, the JMA magnitude and the moment magnitude shall be equal, that is, $M = M_{\mathrm{w}}$.

3.5.2 Correction method for regions of anomalous seismic intensity

In deep earthquakes of which the seismic source is on the Japan Sea side of the Japanese archipelago, sometimes larger seismic intensities are observed in the Pacific Ocean side, which is farther from the seismic source than the areas on the Japan Sea side. This is a phenomenon called anomalous seismic intensity distribution. The anomalous seismic intensity distribution is conspicuous in deep earthquakes, but it is also observed for intermediate depth earthquakes of which the seismic source is located directly beneath the Japanese archipelago. Anomalous seismic intensity distribution is not a phenomenon that occurs locally based on differences in the site condition, but is explained by the peculiar seismic wave attenuation (Q value) structure in island arc areas as shown in Figure 3.5.2-1. Since the same ground motion intensity is given to sites with the equal seismic source distance in an attenuation relation, it was difficult to express the anomalous seismic intensity distribution in the past. However, it has become possible to express the phenomenon through recent accumulation of seismic intensity records. The outline of the method is described below.

(1) Correction for northeast Japan

In order to reflect the anomalous seismic intensity distribution that is characteristic in intermediate depth earthquakes that occur in Pacific plate, correction factors V_1 and V_2 of an attenuation relation that follows the method by Morikawa et al. (2003) are introduced. Correction factor V_1 expressed the phenomenon where a larger seismic intensity is observed on the Pacific Ocean side than on the Japan Sea side, and correction factor V_2 expresses the phenomenon where a large seismic intensity is observed even at a far location as a result of the seismic waves passing within a subducting plate (slab) with low attenuation. These factors make it possible to apply the attenuation relation by Si and Midorikawa (1999) to locations that are 300 km or more away from the seismic source, and are expressed by the following formulas respectively:

$$\begin{aligned}\log V_1 &= (-4.021\times 10^{-5}\times X_{\mathrm{tr}} + 9.905\times 10^{-3})\times(H-30) \\ V_2 &= \max\{1.0, (R/300)^{2.064}\times 10^{-0.012}\}\end{aligned} \tag{3.5.2-1}$$

Here, X_{tr} is the distance from the trench axis to the observation point (km; see Figure 3.5.2-1), R is the hypocentral distance (km), and H is the source depth (km). The trench axis for deriving X_{tr} is approximated by a line joining the 11 points indicated in Table 3.5.2-1 by straight lines (Figure 3.5.2-2). Correction factor V_1 is only applied to earthquakes for which source depth H is more than 30 km. The correction is made by multiplying the value of the peak velocity obtained by the attenuation relation (Si and Midorikawa, 1999) by V_1 and V_2. According to Formula (3.5.2-1), the correction factor V_1 becomes 1.0 when the distance from the trench axis to the observation point X_{tr} is about 250 km.

In Morikawa et al. (2003), the correction factors are derived based on a study targeting earthquakes that have occurred in or north of the Ibaraki-ken-Oki region, but here, the same correction is applied to earthquakes that occur at the Pacific plate in or south of the Ibaraki-ken-Oki region. Meanwhile, whereas earthquakes without specified source faults in Urakawa-Oki occur at sites shallower than the upper surface of the Pacific plate, they are made subject to the correction, considering that the depth of the center of the fault is determined to be 35 km in the model and that, in the 1982 Urakawa-Oki Earthquake, the area with JMA seismic intensity 3 reached locations near the prefectural boundary between Miyagi and Iwate Prefectures. As a result, the earthquakes to which such correction is applied are subduction-zone earthquakes at the Pacific plate (including earthquakes of around $M7$ in southern Kanto that occur at the Pacific plate) and earthquakes without specified source faults in Urakawa-Oki.

(2) Correction for southwest Japan

In Philippine Sea plate, where intermediate depth earthquakes with large magnitude occur less frequently than in northeast Japan, correction factors for the attenuation relation had not been derived due in part to the scarceness of strong motion records of such large earthquakes (Morikawa et al., 2003). Under such circumstance, a clear anomalous seismic intensity distribution was observed in the earthquake that occurred in the central part of Oita Prefecture on June 12, 2006 (M=6.2, depth=145 km). Thus, Morikawa et al. (2006) derived a correction factor for the anomalous seismic intensity distribution in southwest Japan to be used in the attenuation relation by Kanno et al. (2006), by also using records of small and medium earthquakes. Using the same data set as Morikawa et al. (2006), the correction factor for the anomalous seismic intensity distribution in southwest Japan to be used in the attenuation relation by Si and Midorikawa (1999) was separately obtained. As a result, the following factor V'_1 has been obtained

$$\log V'_1 = \begin{cases} 4.28\times10^{-5}\times X_{vf}\times(H-30) & (X_{vf}\le 75\text{km}) \\ 3.21\times10^{-3}\times(H-30) & (X_{vf}>75\text{km}) \end{cases} \quad (3.5.2\text{-}2)$$

where X_{vf} is the distance (km) from the volcanic front to the observation point, which takes, as shown in Figure 3.5.2-1, a positive value in the forearc (Pacific Ocean) side of the volcanic front and a negative value in the back arc (Japan Sea, East China Sea) side. Here, the volcanic front is approximated by a line joining the ten points indicated in Table 3.5.2-2 with straight lines (Figure 3.5.2-2). Similar to northeast Japan, the correction is made by multiplying the value of the peak velocity obtained by the attenuation relation (Si and Midorikawa, 1999), by V'_1.

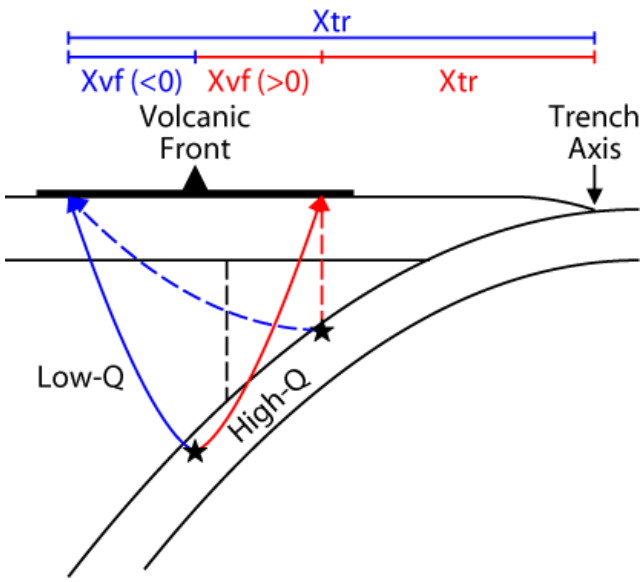

Figure 3.5.2-1 Schematic drawing of the Q value structure in an island arc area and definitions of X_{tr} and X_{vf} (Source: Morikawa et al., 2006)

While this correction factor has been derived targeting earthquakes of which the depth is 30 km, occurring at the Philippine Sea plate at or west of longitude 137 degrees east, earthquakes in southwest Japan for which anomalous seismic intensity distribution occurs conspicuously are limited to earthquakes of which the depth is more than around 80 km occurring in the Kyushu region. Therefore, earthquakes to which this correction applies are only intermediate depth earthquakes from Kyushu to the vicinity of Nansei-shoto (earthquakes occurring in Area No. 4 shown in Figure 3.3.4.4-1) that satisfy such condition.

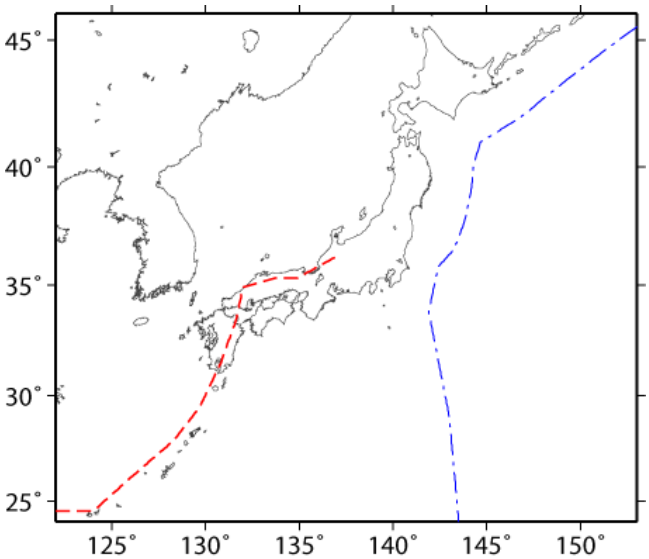

Figure 3.5.2-2 Locations of the trench axis (blue) and the volcanic front (Red) defined for correcting the anomalous seismic intensity distribution

Table 3.5.2-1 Reference points of the trench axis in Northeast Japan

Latitude [°N]	45.50	42.00	41.00	40.10
Longitude [°E]	153.00	146.80	144.65	144.30
Latitude [°N]	39.20	37.70	36.55	35.80
Longitude [°E]	144.20	143.80	143.25	142.40
Latitude [°N]	33.80	29.00	24.00	—
Longitude [°E]	141.90	143.00	143.50	—

Table 3.5.2-2 Reference points of the volcanic front in Southwest Japan

Latitude [°N]	36.20	35.30	35.30	34.90
Longitude [°E]	136.90	134.90	133.70	132.00
Latitude [°N]	33.40	31.50	29.5	27.90
Longitude [°E]	131.60	130.80	129.7	128.30
Latitude [°N]	24.50	24.50	—	—
Longitude [°E]	124.00	122.00	—	—

3.5.3 Evaluation of the peak velocity on ground surface

The peak velocity PGV_s on ground surface is obtained by multiplying the peak velocity PGV_{b400} on the engineering bedrock by the separately calculated amplification factor for the peak velocity from the engineering bedrock to the ground surface (Figure 3.5.3-1). This amplification factor is based on the average shear wave velocity (AVS30; Matsuoka and Wakamatsu, 2008) from the ground surface to the depth of 30m, obtained from the 250m Mesh Engineering Geomorphologic Classification Map created for the whole of Japan by Wakamatsu and Matsuoka (2008). It is obtained by applying the empirical relation (Formula (3.5.1-2)) with AVS30 by Fujimoto and Midorikawa (2006). The amplification factor of the peak velocity is explained in detail in Section 4.4.3.

3.5.4 Evaluation of the JMA instrumental seismic intensity on ground surface

Conventionally, in the "National Seismic Hazard Maps for Japan," the seismic intensity on the ground surface had been evaluated from the peak ground velocity on the ground surface, by using the following empirical relation between the peak ground velocity and the JMA instrumental seismic intensity proposed by Midorikawa et al. (1999)

$$I = 2.68 + 1.72 \cdot \log PGV_S \qquad (3.5.4\text{-}1)$$

where I is the JMA instrumental seismic intensity and PGV_S is the peak ground velocity (cm/s) on the ground surface.

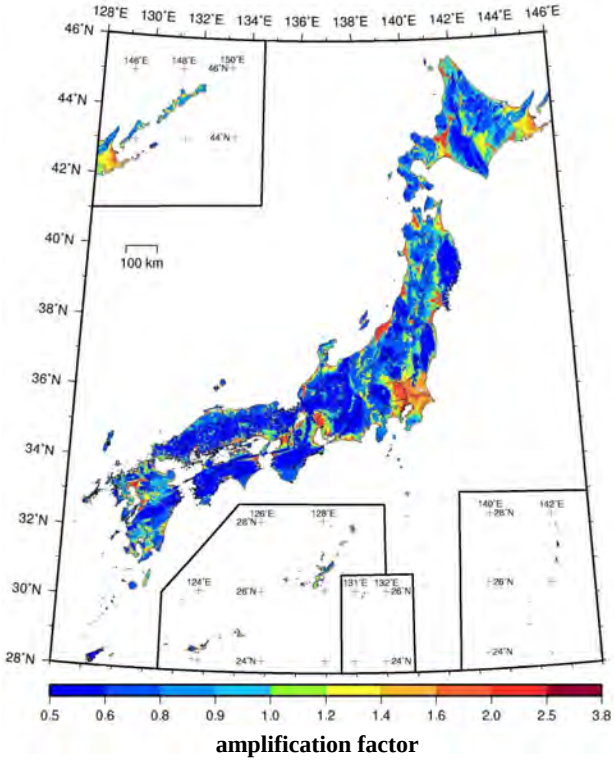

Figure 3.5.3-1 Amplification factor for the peak velocity from the layer equivalent to the engineering bedrock (400m/s shear wave velocity) to ground surface based on the geomorphologic classification

Later, Fujimoto and Midorikawa (2005), considering that strong motion records of recent earthquakes with high seismic intensity have increased due to the development of a high-density strong motion observation network, proposed the

following formula as a new relation between an index of ground motion intensity, such as the peak ground velocity, and the instrumental seismic intensity:

$$I = 2.002 + 2.603 \cdot \log PGV_S - 0.213 \cdot (\log PGV_S)^2 \qquad (3.5.4\text{-}2)$$

However, Fujimoto and Midorikawa (2005) has indicated that in the record for the 2003 Tokachi-Oki Earthquake, which is a subduction-zone earthquake, the peak ground velocity tends to be larger against the instrumental seismic intensity due to the ground motions having a dominant long-period component (mainly two seconds or more). Thus, examination was made on which of the above relations should be used for subduction-zone earthquakes and for inland earthquakes, based on the observation records of recent large earthquakes (Morikawa and Fujiwara, 2009), and the treatment was decided. While the details of the examination are indicated in Appendix 3, it is concluded that Formula (3.5.4-1) is appropriate for subduction-zone earthquakes where large earthquakes of *M*8 class or more occur frequently, and Formula (3.5.4-2) is appropriate for inland earthquakes where most of the earthquakes are *M*7 class. Accordingly, when evaluating the instrumental seismic intensity on the ground surface, Formula (3.5.4-1) is used for evaluating Category I and II earthquakes, which are subduction-zone earthquakes, and Formula (3.5.4-2) is used for Category III earthquakes, which are inland earthquakes.

3.5.5 Variance of the attenuation relation

Conventionally, in the "National Seismic Hazard Maps for Japan," for the purpose of avoid having the ground motion intensity become infinitely large, the distribution of the variance of the peak velocity on the engineering bedrock had been assumed to be a logarithmic normal distribution, and values outside the level three times the logarithmic standard deviation had been cut off at the tail of the distribution. The same treatment is adopted in the creation of the seismic hazard maps this time.

In determining the size of the variance, the types of variance should be divided into those that are to be treated as an essentially random phenomenon (aleatory uncertainty) and those attributable to lack of knowledge or data (epistemic uncertainty), and only those that correspond to aleatory uncertainty need to be considered in hazard curve calculation. As a result of considering such fact, in the "National Seismic Hazard Maps for Japan," the variance (σ) representing the standard deviation of the attenuation relation was determined to be variance dependent on the amplitude of the peak velocity at a stiff site with 600m/s shear wave velocity (PGV_{b600}), as shown below (Figure 3.5.5-1).

$$\sigma = \begin{cases} 0.20 & PGV_{b600} \le 25\text{cm/s} \\ 0.20 - 0.05 \cdot \dfrac{PGV_{b600} - 25}{25} & 25 < PGV_{b600} \le 50\text{cm/s} \\ 0.15 & PGV_{b600} > 50\text{cm/s} \end{cases} \qquad (3.5.5\text{-}1)$$

After that, further research was conducted on the variance to be used for probabilistic seismic hazard evaluation, based on the further accumulated strong motion records and a large amount of ground motion simulations. Accordingly, the variance to be used in the PSHM was examined anew based on the results of such research. While the details are shown in Appendix 3, based on the research result that variance becomes larger near the seismic source, it has been decided that variance (σ_{III}) depending on seismic source distance (*X*) is as follows

$$\text{earthquakes } \sigma_{III} = \begin{cases} 0.23 & X \le 20\text{km} \\ 0.23 - 0.03 \cdot \dfrac{\log(X/20)}{\log(30/20)} & 20 < X \le 30\text{km} \\ 0.20 & X > 30\text{km} \end{cases} \qquad (3.5.5\text{-}2)$$

(the red line in Figure 3.5.5-2). σ_{III} is to be used for Category III earthquakes which are mainly inland, and the conventional variance dependent on amplitude (Formula (3.5.5-1), Figure (3.5.5-1)) is to be used for Category I and II earthquakes which are mainly subduction-zone earthquakes that have no sites near the seismic source and that are substantially influenced by large earthquakes.

In the conventional "National Seismic Hazard Maps for Japan", variance of the peak velocity on the engineering bedrock had been assumed to be a logarithmic normal distribution, and in order to avoid having the ground motion intensity become infinitely large, values outside the level three times the logarithmic standard deviation had been cut off at the tail of the distribution. Since no new findings have been made with regard to this point, the same treatment is adopted for the seismic hazard maps created in this study.

The ground motion evaluation methods, which are used for the respective earthquakes to be evaluated in the PSHM are summarized and shown in Table 3.5.5-1.

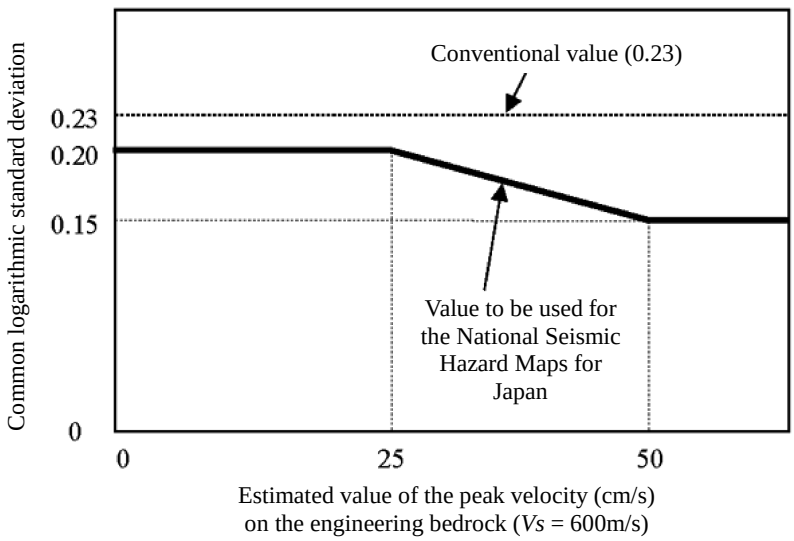

Figure 3.5.5-1 Conventionally used variance dependent on amplitude to be applied to category I and II earthquakes (bold line)

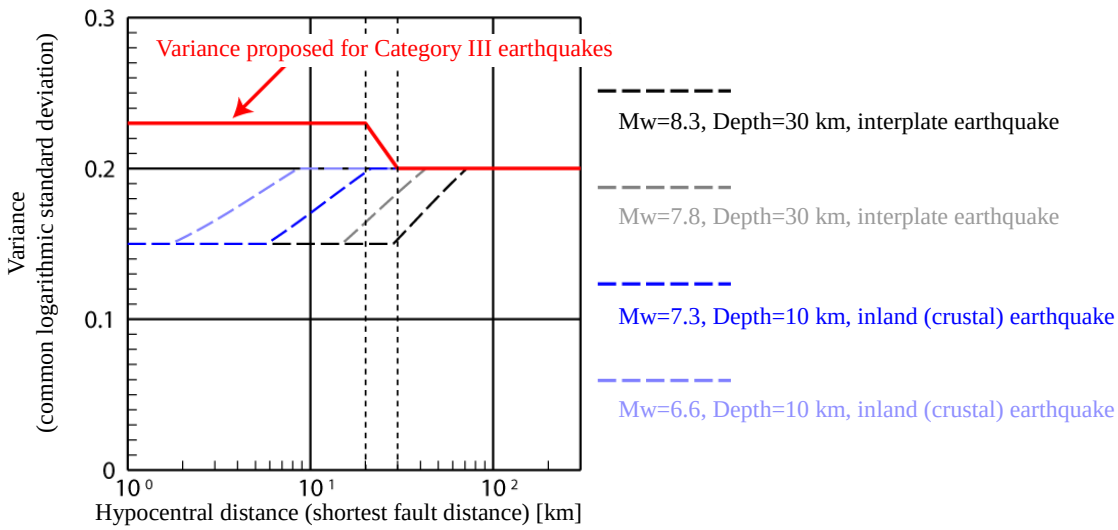

Figure 3.5.5-2 Variance dependent on hypocentral distance to be introduced for category III earthquakes (red line). The broken lines show the conventionally used variance dependent on amplitude, and "depth" represents the depth of the center of the fault plane.

Table 3.5.5-1 List of earthquakes evaluated in the PSHM and the attenuation relations applied (part 1)

Earthquake	Former earthquake classification	Earthquake category	Attenuation relation		
			Factor	Correction	Variance
Characteristic earthquakes occurring in major active fault zones	Major active fault zone	III	Crustal	—	Distance
Nankai Trough earthquakes (Nankai Earthquake + Tonankai Earthquake + Assumed Tokai Earthquake)	Subduction zone	I	Interplate	—	Amplitude
Miyagi-ken-Oki Earthquake and Earthquakes close to the offshore trenches in Southern Sanriku-Oki	Subduction zone	I	Interplate	North Japan	Amplitude
Large interplate earthquakes in Northern Sanriku-Oki	Subduction zone	I	Interplate	North Japan	Amplitude
Large interplate earthquakes close to the offshore trenches in Northern Sanriku-Oki to Boso-Oki regions (Tsunami earthquakes)	Subduction zone	II	Interplate	North Japan	Amplitude
Large intraplate earthquakes close to the offshore trenches in Northern Sanriku-Oki to Boso-Oki regions (normal faults type)	Subduction zone	II	Interplate	North Japan	Amplitude
Interplate earthquakes other than characteristic earthquakes in Northern Sanriku-Oki	Subduction zone	II	Interplate	North Japan	Amplitude
Interplate earthquakes in Fukushima-ken-Oki	Subduction zone	II	Interplate	North Japan	Amplitude
Interplate earthquakes in Ibaraki-ken-Oki	Subduction zone	II	Interplate	North Japan	Amplitude
Tokachi-Oki Earthquake・Nemuro-Oki Earthquake	Subduction zone	I	Interplate	North Japan	Amplitude
Shikotanto-Oki Earthquake	Subduction zone	I	Interplate	North Japan	Amplitude
Etorofuto-Oki Earthquake	Subduction zone	I	Interplate	North Japan	Amplitude
Relatively small interplate earthquakes in the Tokachi-Oki and Nemuro-Oki regions	Subduction zone	II	Interplate	North Japan	Amplitude
Relatively small interplate earthquakes in the Shikotanto-Oki and Etorofuto-Oki regions	Subduction zone	II	Interplate	North Japan	Amplitude
Relatively shallow earthquakes within a subducted plate	Subduction zone	II	Intraplate	North Japan	Amplitude
Relatively deep earthquakes within a subducted plate	Subduction zone	II	Intraplate	North Japan	Amplitude
Hokkaido-hokusei-Oki Earthquake	Subduction zone	III	Interplate	—	Distance
Hokkaido-seiho-Oki Earthquake	Subduction zone	III	Interplate	—	Distance
Hokkaido-nansei-Oki Earthquake	Subduction zone	III	Interplate	—	Distance
Aomori-ken-seiho-Oki Earthquake	Subduction zone	III	Interplate	—	Distance
Akita-ken-Oki Earthquake	Subduction zone	III	Interplate	—	Distance
Yamagata-ken-Oki Earthquake	Subduction zone	III	Interplate	—	Distance

Table 3.5.5-1 List of earthquakes evaluated in the PSHM and the attenuation relations applied (part 2)

Earthquake	Former earthquake classification	Earthquake category	Attenuation relation		
			Factor	Correction	Variance
Niigata-ken-hokubu-Oki Earthquake	Subduction zone	III	Interplate	—	Distance
Sadogashima-hoppo-Oki Earthquake	Subduction zone	III	Interplate	—	Distance
Intraplate earthquakes in Akinada-Iyonada-Bungosuido	Subduction zone	II	Intraplate	—	Amplitude
Interplate earthquakes in Hyuganada	Subduction zone	II	Interplate	—	Amplitude
Relatively small interplate earthquakes in Hyuganada	Subduction zone	II	Interplate	—	Amplitude
Earthquakes in the vicinity of Yonaguni-jima	Subduction zone	II	Interplate	—	Amplitude
Kanto Earthquake of "1923 Taisho" type	Subduction zone	I	Interplate	—	Amplitude
Other *M*7 class earthquakes in Southern Kanto	Subduction zone	II	Interplate /Intraplate	—	Amplitude
Earthquakes occurring on active faults on land other than major active fault zones	Other	III	Crustal	—	Distance
Interplate earthquakes without specified source faults for the Pacific plate	Other	II	Interplate	North Japan	Amplitude
Intraplate earthquakes without specified source faults for the Pacific plate	Other	II	Intraplate	North Japan	Amplitude
Interplate earthquakes without specified source faults for the Philippine Sea plate	Other	II	Interplate	—	Amplitude
Intraplate earthquakes without specified source faults for the Philippine Sea plate	Other	II	Intraplate	West Japan (partial)	Amplitude
Earthquakes occurring at onshore locations where active faults have not been specified	Other	III	Crustal	—	Distance
Earthquakes without specified source faults in Urakawa-Oki	Other	II	Crustal	—	Amplitude
Earthquakes without specified source faults in the eastern margin of the Japan Sea	Other	III	Crustal	—	Distance
Earthquakes without specified source faults in the southern area of Izu-shoto islands	Other	III	Crustal	—	Distance
Earthquakes without specified source faults in the vicinity of Nansei-shoto islands	Other	III	Interplate	—	Distance

Notes: Variance of the attenuation relation: "Distance" denotes that the variance is dependent on the distance, and is large at the source area, and "Amplitude" denotes that the variance is dependent on the amplitude, and is small at the source area.

3.6 Change Logs for the Used Parameters of Creating the PSHM

In March 2005, HERP published the "National Seismic Hazard Maps for Japan" (2005 version). After that, based on updates of various evaluations and chronological changes in the earthquake occurrence probabilities, the PSHM have been updated annually. The 2006 version seismic hazard maps were published in September 2006, the 2007 version in April 2007, and the 2008 version in April 2008.

The following tables summarize the history of change logs in the conditions for creating the maps (Table 3.6-1 to Table 3.6-4). Further, Figure 3.6-1 to Figure 3.6-4 show the distribution of the probability that an earthquake with seismic intensity of 6 Lower or more will occur within 30 years where all earthquakes are considered (average case) in the 2005 version to the 2008 version. The color bar used as the scale for the values of probability differs by version, but here the bar is unified to the most recent one.

Table 3.6-1 Changes in the conditions for creating the PSHM <2006 version>

Earthquake classification	Introduced benchmark and parameters (changed from the 2005 version)
Earthquakes occurring in the 98 major active fault zones	- In the calculation of the earthquake occurrence probability applying a renewal process, the origin of the time axis was changed from "January 1, 2005" to "January 1, 2006." - No change was made to the calculation of the earthquake occurrence probability applying a Poisson process. - The results of partial revision of long-term evaluations that were published by the end of March 2006 were reflected (Furano fault zone (eastern part), Kitayuri fault).
Subduction-zone earthquakes	- In the calculation of the earthquake occurrence probability applying a renewal process or a time-predictable model, the origin of the time axis was changed from "January 1, 2005" to "January 1, 2006." - No change was made to the calculation of the earthquake occurrence probability applying a Poisson process.
Earthquakes with specified source faults (earthquakes occurring on active faults on land other than the 98 major active fault zones)	- No change was made.
Earthquakes without specified source faults	- For JMA catalog used for the distribution of earthquake occurrence frequency, data revisions and updates (data up to the end of 2002→ data up to the end of 2004) were reflected.
Ground motion evaluation	- No change was made.

Table 3.6-2 Changes in the conditions for creating the PSHM <2007 version>

Earthquake classification	Introduced benchmark and parameters (changed from the 2006 version)
Earthquakes occurring in major active fault zones (Name changed)	- In the calculation of the earthquake occurrence probability applying a renewal process, the origin of the time axis was changed from "January 1, 2006" to "January 1, 2007." - No change was made to the calculation of the earthquake occurrence probability applying a Poisson process. - The results of long-term evaluations (including partial revisions) that were published by the end of December 2006 were reflected (Sone-kyuryo fault zone, Hitoyoshi-bonchi-nan'en fault zone, Kushigata-sanmyaku fault zone, Sakaitoge/Kamiya fault zone (main part), Unzen fault group (southeastern part)).
Subduction-zone earthquakes	- In the calculation of the earthquake occurrence probability applying a renewal process or a time-predictable model, the origin of the time axis was changed from "January 1, 2006" to "January 1, 2007." - No change was made to the calculation of the earthquake occurrence probability applying a Poisson process.
Earthquakes with specified source faults (earthquakes occurring on active faults on land other than major active fault zones)	- The results of long-term evaluations that were additionally published by the end of December 2006 were reflected (Kofu-bonchi-nan'en fault zone and Hitoyoshi-bonchi fault zone deleted).
Earthquakes without specified source faults	- For JMA catalog used for the distribution of earthquake occurrence frequency, data revisions and updates (data up to the end of 2004 → data up to the end of 2005) were reflected.
Ground motion evaluation	- In order to deal with the anomalous seismic intensity distribution in southwest Japan, the correction factor of the attenuation relation was introduced.

Table 3.6-3 Changes in the conditions for creating the PSHM <2008 version>

Earthquake classification	Introduced benchmark and parameters (changed from the 2007 version)
Earthquakes occurring in major active fault zones	- In the calculation of the earthquake occurrence probability applying a renewal process, the origin of the time axis was changed from "January 1, 2007" to "January 1, 2008." - No change was made to the calculation of the earthquake occurrence probability applying a Poisson process. - The results of long-term evaluations (including partial revisions) that were published by the end of December 2007 were reflected (Kego fault zone, Uozu fault zone, Yamagata-bonchi fault zone, Inadani fault zone, Sarobetsu fault zone).
Subduction-zone earthquakes	- In the calculation of the earthquake occurrence probability applying a renewal process or a time-predictable model, the origin of the time axis was changed from "January 1, 2007" to "January 1, 2008." - No change was made to the calculation of the earthquake occurrence probability applying a Poisson process.
Earthquakes with specified source faults (earthquakes occurring on active faults on land other than major active fault zones)	- The results of long-term evaluations that were additionally published by the end of December 2007 were reflected (Sarobetsu fault zone, Niino fault, Kurobishiyama fault zone, and Kego fault zone deleted). - The fault model for the 2007 Noto-hanto Earthquake was newly evaluated. However, the earthquake occurrence probability within 30 years and 50 years were both determined to be "Nearly 0%."
Earthquakes without specified source faults	- For JMA catalog used for the distribution of earthquake occurrence frequency, data revisions and updates (data up to the end of 2005 → data up to the end of 2006) were reflected.
Ground motion evaluation	- No change was made.

Table 3.6-4 Changes in the conditions for creating the PSHM <2009 version>

Earthquake classification	Introduced benchmark and parameters (changed from the 2008 version)
Earthquakes occurring in major active fault zones	- In the calculation of the earthquake occurrence probability applying a renewal process, the origin of the time axis was changed from "January 1, 2008" to "January 1, 2009." - No change was made to the calculation of the earthquake occurrence probability applying a Poisson process. - The results of long-term evaluations (including partial revisions) that were published by the end of December 2008 were reflected (Hanawa-higashi fault zone, Tonami-heiya fault zone/Kurehayama fault zone, Aizu-bonchi-seien/-toen fault zone, Ube-oki fault group (Suonada fault group)). - Correction was made to make the fault planes and the magnitude match those in the strong motion evaluation.
Subduction-zone earthquakes	- In the calculation of the earthquake occurrence probability applying a renewal process or a time-predictable model, the origin of the time axis was changed from "January 1, 2008" to "January 1, 2009." - No change was made to the calculation of the earthquake occurrence probability applying a Poisson process. - The model for subduction-zone earthquakes in Ibaraki-ken-Oki was modified.
Earthquakes with specified source faults (earthquakes occurring on active faults on land other than major active fault zones)	- The results of long-term evaluations that were additionally published by the end of December 2008 were reflected (Ube-tobu fault-Shimogo fault, Ube-nanto-Oki fault zone, and Northwestern Hime-shima-Oki fault zone added).
Earthquakes without specified source faults	- For JMA catalog used for the distribution of earthquake occurrence frequency, data revisions and updates (data up to the end of 2006 → data up to the end of 2007) were reflected. - The maximum magnitude was partially modified. - The zoning around Suonada at the Philippine Sea plate was modified.
Ground motion evaluation	- Size of mesh for calculation was modified - The amplification factors were modeified - The variance of attenuation relation and conversion formula peak velocity → seismic intensity which were used for Earthquake Category III were modeified.

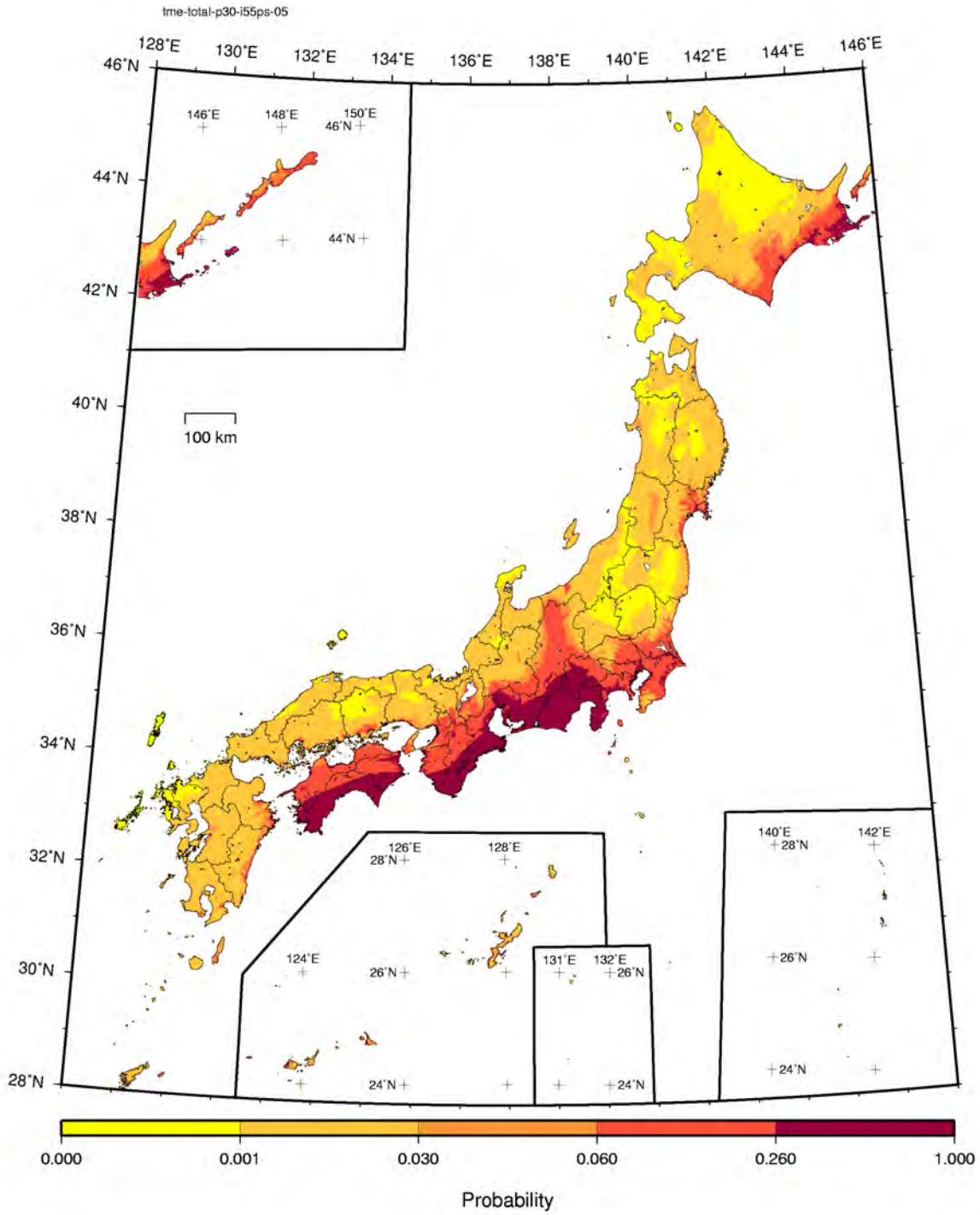

Figure 3.6-1 Total Hazard Considering All Earthquakes (Average Case; 2005 Version)

<Probability for Earthquake of Seismic Intensity 6 Lower or More Within 30 Years>

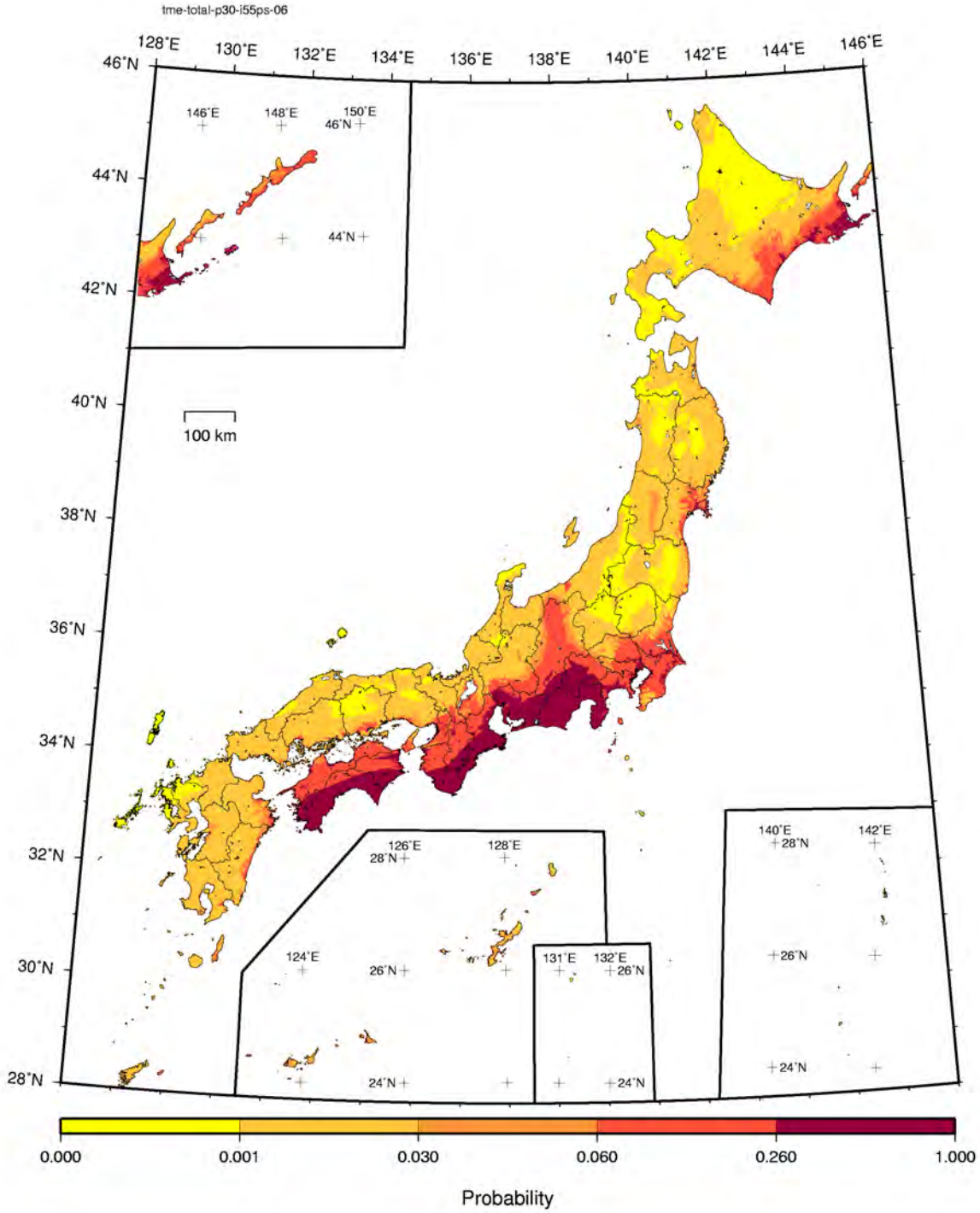

Figure 3.6-2 Total Hazard Considering All Earthquakes (Average Case; 2006 Version)

<Probability for Earthquake of Seismic Intensity 6 Lower or More Within 30 Years>

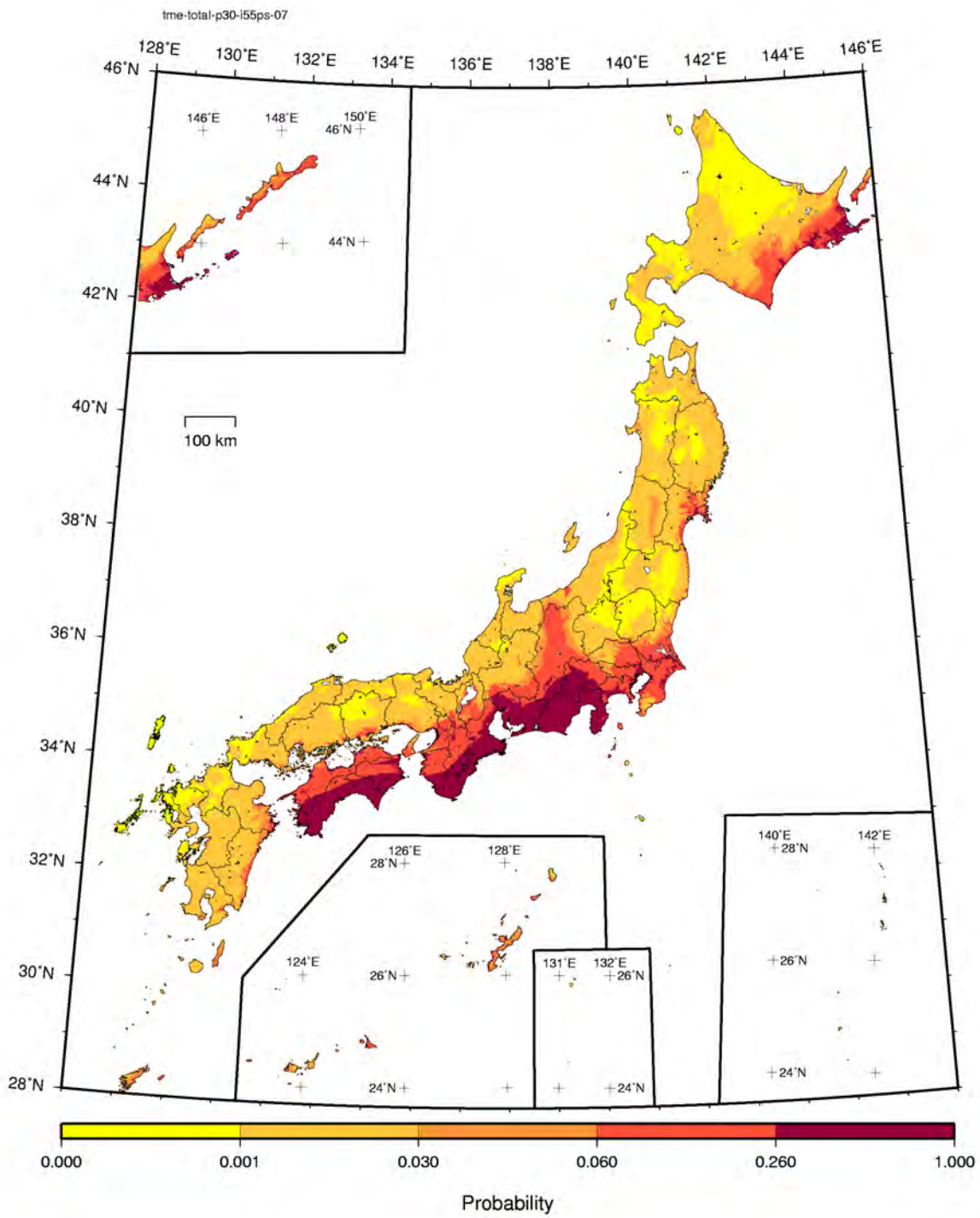

Figure 3.6-3 Total Hazard Considering All Earthquakes (Average Case; 2007 Version)

<Probability for Earthquake of Seismic Intensity 6 Lower or More Within 30 Years>

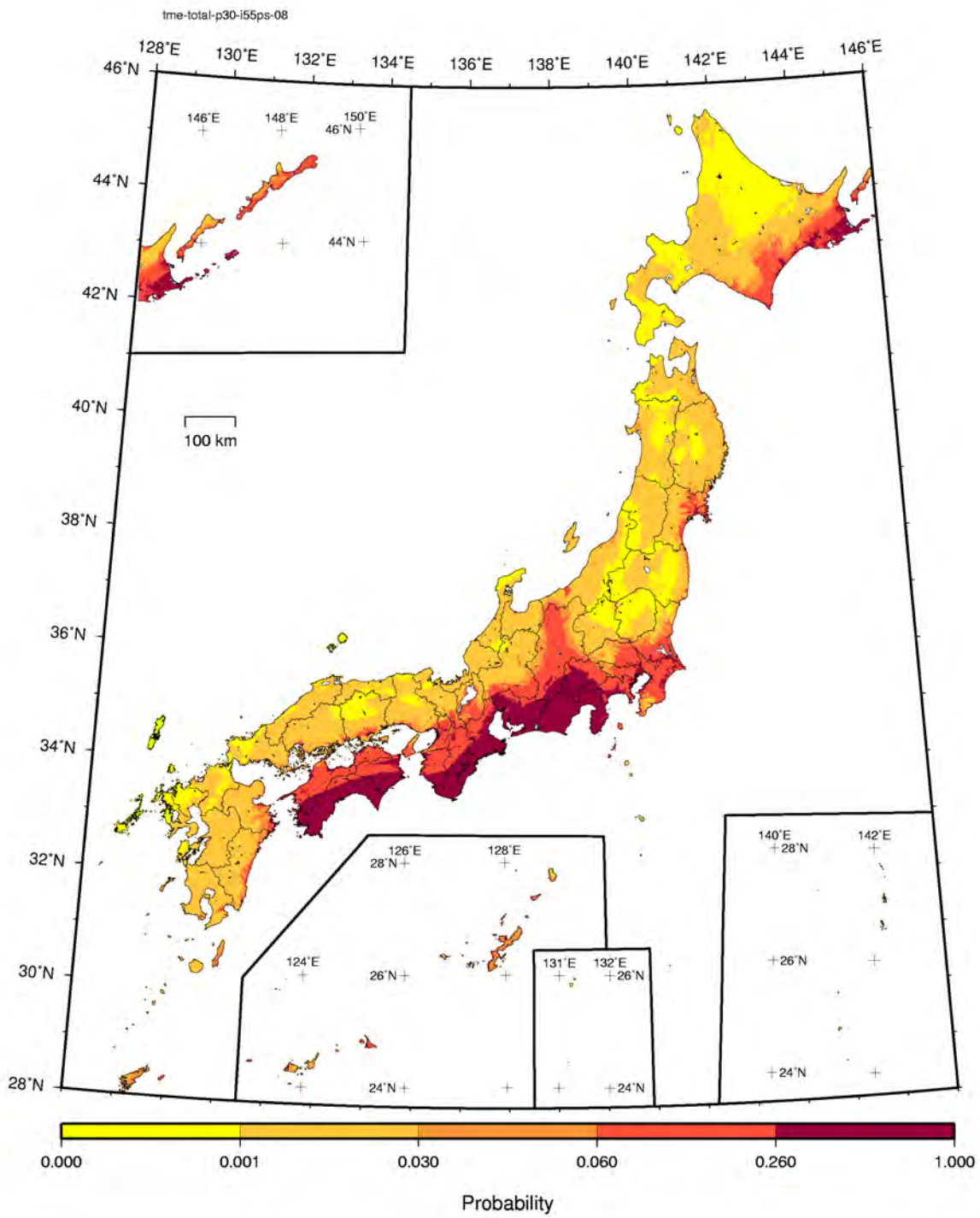

Figure 3.6-4 Total Hazard Considering All Earthquakes (Average Case; 2008 Version)

<Probability for Earthquake of Seismic Intensity 6 Lower or More Within 30 Years>

3.7 Evaluation Results

3.7.1 List of evaluation maps

(0) Site amplification factor

Figure 3.7.2-1: Amplification Factor for Peak Velocity (from engineering bedrock (layer with Vs=400m/s) to ground surface; 2009 version)

Figure 3.7.2-2: Amplification Factor for Peak Velocity (from engineering bedrock (layer with Vs=400m/s) to ground surface; 2008 version)

Figure 3.7.2-3: Ratio of Amplification Factor for Peak Velocity (2009 version/2008 version)

(1) Distribution of ground motion intensity where exceedance probability within 30 years is fixed

a) Total hazard considering all earthquakes (exceedance probability: 6% and 3%)

Figure 3.7.2-4(1): Total Hazard Considering All Earthquakes (Average Case)
<Distribution of Instrumental Seismic Intensity on the Ground Surface (Exceedance Probability: 6%)>

Figure 3.7.2-4(2): Total Hazard Considering All Earthquakes (Average Case)
<Distribution of Instrumental Seismic Intensity on the Ground Surface (Exceedance Probability: 3%)>

Figure 3.7.2-5(1): Total Hazard Considering All Earthquakes (Maximum Case)
<Distribution of Instrumental Seismic Intensity on the Ground Surface (Exceedance Probability: 6%)>

Figure 3.7.2-5(2): Total Hazard Considering All Earthquakes (Maximum Case)
<Distribution of Instrumental Seismic Intensity on the Ground Surface (Exceedance Probability: 3%)>

b) Hazard by earthquake category (exceedance probability: 6% and 3%)

Figure 3.7.2-6(1): Hazard Associated with Subduction-Zone Large Earthquakes
<Distribution of Instrumental Seismic Intensity on the Ground Surface (Exceedance Probability: 6%)>

Figure 3.7.2-6(2): Hazard Associated with Subduction-Zone Large Earthquakes
<Distribution of Instrumental Seismic Intensity on the Ground Surface (Exceedance Probability: 3%)>

Figure 3.7.2-7(1): Hazard Associated with Subduction-Zone Earthquakes without Specified Source Faults
<Distribution of Instrumental Seismic Intensity on the Ground Surface (Exceedance Probability: 6%)>

Figure 3.7.2-7(2): Hazard Associated with Subduction-Zone Earthquakes without Specified Source Faults
<Distribution of Instrumental Seismic Intensity on the Ground Surface (Exceedance Probability: 3%)>

Figure 3.7.2-8(1): Hazard Associated with Inland Shallow Earthquakes (Average Case)
<Distribution of Instrumental Seismic Intensity on the Ground Surface (Exceedance Probability: 6%)>

Figure 3.7.2-8(2): Hazard Associated with Inland Shallow Earthquakes (Average Case)
<Distribution of Instrumental Seismic Intensity on the Ground Surface (Exceedance Probability: 3%)>

Figure 3.7.2-9(1): Hazard Associated with Inland Shallow Earthquakes (Maximum Case)
<Distribution of Instrumental Seismic Intensity on the Ground Surface (Exceedance Probability: 6%)>

Figure 3.7.2-9(2): Hazard Associated with Inland Shallow Earthquakes (Maximum Case)
<Distribution of Instrumental Seismic Intensity on the Ground Surface (Exceedance Probability: 3%)>

(2) Distribution of exceedance probability where ground motion intensity within 30 years is fixed

a) Total hazard considering all earthquakes (seismic intensity: 5 Lower or more, 5 Upper or more, 6 Lower or more, 6 Upper or more)

Figure 3.7.2-10(1): Total Hazard Considering All Earthquakes (Average Case)
<Distribution of Exceedance Probability (Seismic Intensity: 5 Lower or More)>

Figure 3.7.2-10(2): Total Hazard Considering All Earthquakes (Average Case)
<Distribution of Exceedance Probability (Seismic Intensity: 5 Upper or More)>

Figure 3.7.2-10(3): Total Hazard Considering All Earthquakes (Average Case)
<Distribution of Exceedance Probability (Seismic Intensity: 6 Lower or More)>

Figure 3.7.2-10(4): Total Hazard Considering All Earthquakes (Average Case)
<Distribution of Exceedance Probability (Seismic Intensity: 6 Upper or More)>

Figure 3.7.2-11(1): Total Hazard Considering All Earthquakes (Maximum Case)
<Distribution of Exceedance Probability (Seismic Intensity: 5 Lower or More)>

Figure 3.7.2-11(2): Total Hazard Considering All Earthquakes (Maximum Case)
<Distribution of Exceedance Probability (Seismic Intensity: 5 Upper or More)>

Figure 3.7.2-11(3): Total Hazard Considering All Earthquakes (Maximum Case)
<Distribution of Exceedance Probability (Seismic Intensity: 6 Lower or More)>

Figure 3.7.2-11(4): Total Hazard Considering All Earthquakes (Maximum Case)
<Distribution of Exceedance Probability (Seismic Intensity: 6 Upper or More)>

b) Hazard by earthquake category (seismic intensity: 5 Lower or more, 5 Upper or more, 6 Lower or more, 6 Upper or more)

Figure 3.7.2-12(1): Hazard Associated with Subduction-Zone Large Earthquakes
<Distribution of Exceedance Probability (Seismic Intensity: 5 Lower or More)>

Figure 3.7.2-12(2): Hazard Associated with Subduction-Zone Large Earthquakes
<Distribution of Exceedance Probability (Seismic Intensity: 5 Upper or More)>

Figure 3.7.2-12(3): Hazard Associated with Subduction-Zone Large Earthquakes
<Distribution of Exceedance Probability (Seismic Intensity: 6 Lower or More)>

Figure 3.7.2-12(4): Hazard Associated with Subduction-Zone Large Earthquakes
<Distribution of Exceedance Probability (Seismic Intensity: 6 Upper or More)>

Figure 3.7.2-13(1): Hazard Associated with Subduction-Zone Earthquakes without Specified Source Faults
<Distribution of Exceedance Probability (Seismic Intensity: 5 Lower or More)>

Figure 3.7.2-13(2): Hazard Associated with Subduction-Zone Earthquakes without Specified Source Faults
<Distribution of Exceedance Probability (Seismic Intensity: 5 Upper or More)>

Figure 3.7.2-13(3): Hazard Associated with Subduction-Zone Earthquakes without Specified Source Faults
<Distribution of Exceedance Probability (Seismic Intensity: 6 Lower or More)>

Figure 3.7.2-13(4): Hazard Associated with Subduction-Zone Earthquakes without Specified Source Faults
<Distribution of Exceedance Probability (Seismic Intensity: 6 Upper or More)>

Figure 3.7.2-14(1): Hazard Associated with Inland Shallow Earthquakes (Average Case)
<Distribution of Exceedance Probability (Seismic Intensity: 5 Lower or More)>

Figure 3.7.2-14(2): Hazard Associated with Inland Shallow Earthquakes (Average Case)
<Distribution of Exceedance Probability (Seismic Intensity: 5 Upper or More)>

Figure 3.7.2-14(3): Hazard Associated with Inland Shallow Earthquakes (Average Case)
<Distribution of Exceedance Probability (Seismic Intensity: 6 Lower or More)>

Figure 3.7.2-14(4): Hazard Associated with Inland Shallow Earthquakes (Average Case)
<Distribution of Exceedance Probability (Seismic Intensity: 6 Upper or More)>

Figure 3.7.2-15(1): Hazard Associated with Inland Shallow Earthquakes (Maximum Case)
<Distribution of Exceedance Probability (Seismic Intensity: 5 Lower or More)>

Figure 3.7.2-15(2): Hazard Associated with Inland Shallow Earthquakes (Maximum Case)
<Distribution of Exceedance Probability (Seismic Intensity: 5 Upper or More)>

Figure 3.7.2-15(3): Hazard Associated with Inland Shallow Earthquakes (Maximum Case)
<Distribution of Exceedance Probability (Seismic Intensity: 6 Lower or More)>

Figure 3.7.2-15(4): Hazard Associated with Inland Shallow Earthquakes (Maximum Case)
<Distribution of Exceedance Probability (Seismic Intensity: 6 Upper or More)>

c) Hazard by earthquake category in quartiles (seismic intensity: 5 Lower or more, 5 Upper or more, 6 Lower or more, 6 Upper or more)

Figure 3.7.2-16(1): Hazard Associated with Subduction-Zone Large Earthquakes
<Distribution of Exceedance Probability in Quartiles (Seismic Intensity: 5 Lower or More)>

Figure 3.7.2-16(2): Hazard Associated with Subduction-Zone Large Earthquakes
<Distribution of Exceedance Probability in Quartiles (Seismic Intensity: 5 Upper or More)>

Figure 3.7.2-16(3): Hazard Associated with Subduction-Zone Large Earthquakes
<Distribution of Exceedance Probability in Quartiles (Seismic Intensity: 6 Lower or More)>

Figure 3.7.2-16(4): Hazard Associated with Subduction-Zone Large Earthquakes
<Distribution of Exceedance Probability in Quartiles (Seismic Intensity: 6 Upper or More)>

Figure 3.7.2-17(1): Hazard Associated with Subduction-Zone Earthquakes without Specified Source Faults
<Distribution of Exceedance Probability in Quartiles (Seismic Intensity: 5 Lower or More)>

Figure 3.7.2-17(2): Hazard Associated with Subduction-Zone Earthquakes without Specified Source Faults
<Distribution of Exceedance Probability in Quartiles (Seismic Intensity: 5 Upper or More)>

Figure 3.7.2-17(3): Hazard Associated with Subduction-Zone Earthquakes without Specified Source Faults
<Distribution of Exceedance Probability in Quartiles (Seismic Intensity: 6 Lower or More)>

Figure 3.7.2-17(4): Hazard Associated with Subduction-Zone Earthquakes without Specified Source Faults
<Distribution of Exceedance Probability in Quartiles (Seismic Intensity: 6 Upper or More)>
Figure 3.7.2-18(1): Hazard Associated with Inland Shallow Earthquakes (Average Case)
<Distribution of Exceedance Probability in Quartiles (Seismic Intensity: 5 Lower or More)>
Figure 3.7.2-18(2): Hazard Associated with Inland Shallow Earthquakes (Average Case)
<Distribution of Exceedance Probability in Quartiles (Seismic Intensity: 5 Upper or More)>
Figure 3.7.2-18(3): Hazard Associated with Inland Shallow Earthquakes (Average Case)
<Distribution of Exceedance Probability in Quartiles (Seismic Intensity: 6 Lower or More)>
Figure 3.7.2-18(4): Hazard Associated with Inland Shallow Earthquakes (Average Case)
<Distribution of Exceedance Probability in Quartiles (Seismic Intensity: 6 Upper or More)>
Figure 3.7.2-19(1): Hazard Associated with Inland Shallow Earthquakes (Maximum Case)
<Distribution of Exceedance Probability in Quartiles (Seismic Intensity: 5 Lower or More)>
Figure 3.7.2-19(2): Hazard Associated with Inland Shallow Earthquakes (Maximum Case)
<Distribution of Exceedance Probability in Quartiles (Seismic Intensity: 5 Upper or More)>
Figure 3.7.2-19(3): Hazard Associated with Inland Shallow Earthquakes (Maximum Case)
<Distribution of Exceedance Probability in Quartiles (Seismic Intensity: 6 Lower or More)>
Figure 3.7.2-19(4): Hazard Associated with Inland Shallow Earthquakes (Maximum Case)
<Distribution of Exceedance Probability in Quartiles (Seismic Intensity: 6 Upper or More)>

(3) Distribution of ground motion intensity where exceedance probability within 50 years is fixed (exceedance probability: 39%, 10%, 5%, 2%)
Figure 3.7.2-20(1): Total Hazard Considering All Earthquakes (Average Case)
<Distribution of Instrumental Seismic Intensity on the Ground Surface (Exceedance Probability: 39%)>
Figure 3.7.2-20(2): Total Hazard Considering All Earthquakes (Average Case)
<Distribution of Instrumental Seismic Intensity on the Ground Surface (Exceedance Probability: 10%)>
Figure 3.7.2-20(3): Total Hazard Considering All Earthquakes (Average Case)
<Distribution of Instrumental Seismic Intensity on the Ground Surface (Exceedance Probability: 5%)>
Figure 3.7.2-20(4): Total Hazard Considering All Earthquakes (Average Case)
<Distribution of Instrumental Seismic Intensity on the Ground Surface (Exceedance Probability: 2%)>
Figure 3.7.2-21(1): Total Hazard Considering All Earthquakes (Maximum Case)
<Distribution of Instrumental Seismic Intensity on the Ground Surface (Exceedance Probability: 39%)>
Figure 3.7.2-21(2): Total Hazard Considering All Earthquakes (Maximum Case)
<Distribution of Instrumental Seismic Intensity on the Ground Surface (Exceedance Probability: 10%)>
Figure 3.7.2-21(3): Total Hazard Considering All Earthquakes (Maximum Case)
<Distribution of Instrumental Seismic Intensity on the Ground Surface (Exceedance Probability: 5%)>
Figure 3.7.2-21(4): Total Hazard Considering All Earthquakes (Maximum Case)
<Distribution of Instrumental Seismic Intensity on the Ground Surface (Exceedance Probability: 2%)>

(4) Distribution of differences in exceedance probability within 30 years between 2009 version and 2008 version (seismic intensity: 5 Lower or more, 5 Upper or more, 6 Lower or more, 6 Upper or more)
Figure 3.7.2-22(1): Differences in the Total Hazard Taking All Earthquakes into Consideration (Average Case)
<Distribution of Exceedance Probability (Seismic Intensity: 5 Lower or more)>
Figure 3.7.2-22(2): Differences in the Total Hazard Taking All Earthquakes into Consideration (Average Case)
<Distribution of Exceedance Probability (Seismic Intensity: 5 Upper or more)>
Figure 3.7.2-22(3): Differences in the Total Hazard Taking All Earthquakes into Consideration (Average Case)
<Distribution of Exceedance Probability (Seismic Intensity: 6 Lower or more)>

Figure 3.7.2-22(4): Differences in the Total Hazard Taking All Earthquakes into Consideration (Average Case)
<Distribution of Exceedance Probability (Seismic intensity: 6 Upper or more)>
Figure 3.7.2-23(1): Differences in the Total Hazard Taking All Earthquakes into Consideration (Maximum Case)
<Distribution of Exceedance Probability (Seismic intensity: 5 Lower or more)>
Figure 3.7.2-23(2): Differences in the Total Hazard Taking All Earthquakes into Consideration (Maximum Case)
<Distribution of Exceedance Probability (Seismic intensity: 5 Upper or more)>
Figure 3.7.2-23(3): Differences in the Total Hazard Taking All Earthquakes into Consideration (Maximum Case)
<Distribution of Exceedance Probability (Seismic intensity: 6 Lower or more)>
Figure 3.7.2-23(4): Differences in the Total Hazard Taking All Earthquakes into Consideration (Maximum Case)
<Distribution of Exceedance Probability (Seismic intensity: 6 Upper or more)>
Figure 3.7.2-24(1): Differences in the Hazard Associated with Subduction-Zone Large Earthquakes
<Distribution of Exceedance Probability (Seismic intensity: 5 Lower or more)>
Figure 3.7.2-24(2): Differences in the Hazard Associated with Subduction-Zone Large Earthquakes
<Distribution of Exceedance Probability (Seismic intensity: 5 Upper or more)>
Figure 3.7.2-24(3): Differences in the Hazard Associated with Subduction-Zone Large Earthquakes
<Distribution of Exceedance Probability (Seismic intensity: 6 Lower or more)>
Figure 3.7.2-24(4): Differences in the Hazard Associated with Subduction-Zone Large Earthquakes
<Distribution of Exceedance Probability (Seismic intensity: 6 Upper or more)>
Figure 3.7.2-25(1): Differences in the Hazard Associated with Subduction-Zone Earthquakes without Specified Source Faults
<Distribution of Exceedance Probability (Seismic intensity: 5 Lower or more)>
Figure 3.7.2-25(2): Differences in the Hazard Associated with Subduction-Zone Earthquakes without Specified Source Faults
<Distribution of Exceedance Probability (Seismic intensity: 5 Upper or more)>
Figure 3.7.2-25(3): Differences in the Hazard Associated with Subduction-Zone Earthquakes without Specified Source Faults
<Distribution of Exceedance Probability (Seismic intensity: 6 Lower or more)>
Figure 3.7.2-25(4): Differences in the Hazard Associated with Subduction-Zone Earthquakes without Specified Source Faults
<Distribution of Exceedance Probability (Seismic intensity: 6 Upper or more)>
Figure 3.7.2-26(1): Differences in the Hazard Associated with Inland Shallow Earthquakes (Average Case)
<Distribution of Exceedance Probability (Seismic intensity: 5 Lower or more)>
Figure 3.7.2-26(2): Differences in the Hazard Associated with Inland Shallow Earthquakes (Average Case)
<Distribution of Exceedance Probability (Seismic intensity: 5 Upper or more)>
Figure 3.7.2-26(3): Differences in the Hazard Associated with Inland Shallow Earthquakes (Average Case)
<Distribution of Exceedance Probability (Seismic intensity: 6 Lower or more)>
Figure 3.7.2-26(4): Differences in the Hazard Associated with Inland Shallow Earthquakes (Average Case)
<Distribution of Exceedance Probability (Seismic intensity: 6 Upper or more)>
Figure 3.7.2-27(1): Differences in the Hazard Associated with Inland Shallow Earthquakes (Maximum Case)
<Distribution of Exceedance Probability (Seismic intensity: 5 Lower or more)>
Figure 3.7.2-27(2): Differences in the Hazard Associated with Inland Shallow Earthquakes (Maximum Case)
<Distribution of Exceedance Probability (Seismic intensity: 5 Upper or more)>
Figure 3.7.2-27(3): Differences in the Hazard Associated with Inland Shallow Earthquakes (Maximum Case)
<Distribution of Exceedance Probability (Seismic intensity: 6 Lower or more)>
Figure 3.7.2-27(4): Differences in the Hazard Associated with Inland Shallow Earthquakes (Maximum Case)
<Distribution of Exceedance Probability (Seismic intensity: 6 Upper or more)>

(5) Distribution of differences in exceedance probability within 30 years between average case and maximum case (seismic intensity: 5 Lower or more, 5 Upper or more, 6 Lower or more, 6 Upper or more)

Figure 3.7.2-28(1): Differences in the Total Hazard Taking All Earthquakes into Consideration
<Distribution of Exceedance Probability (Seismic Intensity: 5 Lower or more)>

Figure 3.7.2-28(2): Differences in the Total Hazard Taking All Earthquakes into Consideration
<Distribution of Exceedance Probability (Seismic Intensity: 5 Upper or more)>

Figure 3.7.2-28(3): Differences in the Total Hazard Taking All Earthquakes into Consideration
<Distribution of Exceedance Probability (Seismic Intensity: 6 Lower or more)>

Figure 3.7.2-28(4): Differences in the Total Hazard Taking All Earthquakes into Consideration
<Distribution of Exceedance Probability (Seismic Intensity: 6 Upper or more)>

Figure 3.7.2-29(1): Differences in the Hazard Associated with Inland Shallow Earthquakes
<Distribution of Exceedance Probability (Seismic intensity: 5 Lower or more)>

Figure 3.7.2-29(2): Differences in the Hazard Associated with Inland Shallow Earthquakes
<Distribution of Exceedance Probability (Seismic intensity: 5 Upper or more)>

Figure 3.7.2-29(3): Differences in the Hazard Associated with Inland Shallow Earthquakes
<Distribution of Exceedance Probability (Seismic intensity: 6 Lower or more)>

Figure 3.7.2-29(4): Differences in the Hazard Associated with Inland Shallow Earthquakes
<Distribution of Exceedance Probability (Seismic intensity: 6 Upper or more)>

(6) Distribution of differences in peak velocity on bedrock (Vs=600m/s) within 30 years between 2009 version and 2008 version

a) Total hazard considering all earthquakes (exceedance probability within 30 years: 6% and 3%)

Figure 3.7.2-30(1): Total Hazard Considering All Earthquakes (Average Case)
<2009 Version; Peak Velocity on the Bedrock (Vs=600 m/s) (Exceedance Probability: 6%)>

Figure 3.7.2-30(2): Total Hazard Considering All Earthquakes (Average Case)
<2008 Version; Peak Velocity on the Bedrock (Vs=600 m/s) (Exceedance Probability: 6%)>

Figure 3.7.2-30(3): Total Hazard Considering All Earthquakes (Average Case)
<Distribution of Differences in the Peak velocity on the Bedrock (Vs=600 m/s) (Exceedance Probability: 6%)>

Figure 3.7.2-31(1): Total Hazard Considering All Earthquakes (Average Case)
<2009 Version; Peak Velocity on the Bedrock (Vs=600 m/s) (Exceedance Probability: 3%)>

Figure 3.7.2-31(2): Total Hazard Considering All Earthquakes (Average Case)
<2008 Version; Peak Velocity on the Bedrock (Vs=600 m/s) (Exceedance Probability: 3%)>

Figure 3.7.2-31(3): Total Hazard Considering All Earthquakes (Average Case)
<Distribution of Differences in the Peak velocity on the Bedrock (Vs=600 m/s) (Exceedance Probability: 3%)>

Figure 3.7.2-32(1): Total Hazard Considering All Earthquakes (Maximum Case)
<2009 Version; Peak Velocity on the Bedrock (Vs=600 m/s) (Exceedance Probability: 6%)>

Figure 3.7.2-32(2): Total Hazard Considering All Earthquakes (Maximum Case)
<2008 Version; Peak Velocity on the Bedrock (Vs=600 m/s) (Exceedance Probability: 6%)>

Figure 3.7.2-32(3): Total Hazard Considering All Earthquakes (Maximum Case)
<Distribution of Differences in the Peak velocity on the Bedrock (Vs=600 m/s) (Exceedance Probability: 6%)>

Figure 3.7.2-33(1): Total Hazard Considering All Earthquakes (Maximum Case)
<2009 Version; Peak Velocity on the Bedrock (Vs=600 m/s) (Exceedance Probability: 3%)>

Figure 3.7.2-33(2): Total Hazard Considering All Earthquakes (Maximum Case)
<2008 Version; Peak Velocity on the Bedrock (Vs=600 m/s) (Exceedance Probability: 3%)>

Figure 3.7.2-33(3): Total Hazard Considering All Earthquakes (Maximum Case)
<Distribution of Differences in the Peak velocity on the Bedrock (Vs=600 m/s) (Exceedance Probability: 3%)>

b) Hazard by earthquake category (exceedance probability within 30 years: 6% and 3%)

Figure 3.7.2-34(1): Hazard Associated with Subduction-Zone Large Earthquakes
<2009 Version; Peak Velocity on the Bedrock (Vs=600 m/s) (Exceedance Probability: 6%)>

Figure 3.7.2-34(2): Hazard Associated with Subduction-Zone Large Earthquakes
<2008 Version; Peak Velocity on the Bedrock (Vs=600 m/s) (Exceedance Probability: 6%)>

Figure 3.7.2-34(3): Hazard Associated with Subduction-Zone Large Earthquakes
<Distribution of Differences in the Peak velocity on the Bedrock (Vs=600 m/s) (Exceedance Probability: 6%)>

Figure 3.7.2-35(1): Hazard Associated with Subduction-Zone Large Earthquakes
<2009 Version; Peak Velocity on the Bedrock (Vs=600 m/s) (Exceedance Probability: 3%)>

Figure 3.7.2-35(2): Hazard Associated with Subduction-Zone Large Earthquakes
<2008 Version; Peak Velocity on the Bedrock (Vs=600 m/s) (Exceedance Probability: 3%)>

Figure 3.7.2-35(3): Hazard Associated with Subduction-Zone Large Earthquakes
<Distribution of Differences in the Peak velocity on the Bedrock (Vs=600 m/s) (Exceedance Probability: 3%)>

Figure 3.7.2-36(1): Hazard Associated with Subduction-Zone Earthquakes without Specified Source Faults
<2009 Version; Peak Velocity on the Bedrock (Vs=600 m/s) (Exceedance Probability: 6%)>

Figure 3.7.2-36(2): Hazard Associated with Subduction-Zone Earthquakes without Specified Source Faults
<2008 Version; Peak Velocity on the Bedrock (Vs=600 m/s) (Exceedance Probability: 6%)>

Figure 3.7.2-36(3): Hazard Associated with Subduction-Zone Earthquakes without Specified Source Faults
<Distribution of Differences in the Peak velocity on the Bedrock (Vs=600 m/s) (Exceedance Probability: 6%)>

Figure 3.7.2-37(1): Hazard Associated with Subduction-Zone Earthquakes without Specified Source Faults
<2009 Version; Peak Velocity on the Bedrock (Vs=600 m/s) (Exceedance Probability: 3%)>

Figure 3.7.2-37(2): Hazard Associated with Subduction-Zone Earthquakes without Specified Source Faults
<2008 Version; Peak Velocity on the Bedrock (Vs=600 m/s) (Exceedance Probability: 3%)>

Figure 3.7.2-37(3): Hazard Associated with Subduction-Zone Earthquakes without Specified Source Faults
<Distribution of Differences in the Peak velocity on the Bedrock (Vs=600 m/s) (Exceedance Probability: 3%)>

Figure 3.7.2-38(1): Hazard Associated with Inland Shallow Earthquakes (Average Case)
<2009 Version; Peak Velocity on the Bedrock (Vs=600 m/s) (Exceedance Probability: 6%)>

Figure 3.7.2-38(2): Hazard Associated with Inland Shallow Earthquakes (Average Case)
<2008 Version; Peak Velocity on the Bedrock (Vs=600 m/s) (Exceedance Probability: 6%)>

Figure 3.7.2-38(3): Hazard Associated with Inland Shallow Earthquakes (Average Case)
<Distribution of Differences in the Peak velocity on the Bedrock (Vs=600 m/s) (Exceedance Probability: 6%)>

Figure 3.7.2-39(1): Hazard Associated with Inland Shallow Earthquakes (Average Case)
<2009 Version; Peak Velocity on the Bedrock (Vs=600 m/s) (Exceedance Probability: 3%)>

Figure 3.7.2-39(2): Hazard Associated with Inland Shallow Earthquakes (Average Case)
<2008 Version; Peak Velocity on the Bedrock (Vs=600 m/s) (Exceedance Probability: 3%)>

Figure 3.7.2-39(3): Hazard Associated with Inland Shallow Earthquakes (Average Case)
<Distribution of Differences in the Peak velocity on the Bedrock (Vs=600 m/s) (Exceedance Probability: 3%)>

Figure 3.7.2-40(1): Hazard Associated with Inland Shallow Earthquakes (Maximum Case)
<2009 Version; Peak Velocity on the Bedrock (Vs=600 m/s) (Exceedance Probability: 6%)>

Figure 3.7.2-40(2): Hazard Associated with Inland Shallow Earthquakes (Maximum Case)
<2008 Version; Peak Velocity on the Bedrock (Vs=600 m/s) (Exceedance Probability: 6%)>

Figure 3.7.2-40(3): Hazard Associated with Inland Shallow Earthquakes (Maximum Case)
<Distribution of Differences in the Peak velocity on the Bedrock (Vs=600 m/s) (Exceedance Probability: 6%)>
Figure 3.7.2-41(1): Hazard Associated with Inland Shallow Earthquakes (Maximum Case)
<2009 Version; Peak Velocity on the Bedrock (Vs=600 m/s) (Exceedance Probability: 3%)>
Figure 3.7.2-41(2): Hazard Associated with Inland Shallow Earthquakes (Maximum Case)
<2008 Version; Peak Velocity on the Bedrock (Vs=600 m/s) (Exceedance Probability: 3%)>
Figure 3.7.2-41(3): Hazard Associated with Inland Shallow Earthquakes (Maximum Case)
<Distribution of Differences in the Peak velocity on the Bedrock (Vs=600 m/s) (Exceedance Probability: 3%)>

(7) Distribution of maximum contribution factor on exceedance probability within 30 years considering all earthquakes (seismic intensity: 5 Lower or more, 5 Upper or more, 6 Lower or more, 6 Upper or more)
Figure 3.7.2-42(1): Maximum Contribution factor by Earthquake Category
(Seismic Intensity: 5 Lower or More; Average Case)
Figure 3.7.2-42(2): Maximum Contribution factor by Earthquake Category
(Seismic Intensity: 5 Upper or More; Average Case)
Figure 3.7.2-42(3): Maximum Contribution factor by Earthquake Category
(Seismic Intensity: 6 Lower or More; Average Case)
Figure 3.7.2-42(4): Maximum Contribution factor by Earthquake Category
(Seismic Intensity: 6 Upper or More; Average Case)
Figure 3.7.2-43(1): Maximum Contribution factor by Earthquake Category
(Seismic Intensity: 5 Lower or More; Maximum Case)
Figure 3.7.2-43(2): Maximum Contribution factor by Earthquake Category
(Seismic Intensity: 5 Upper or More; Maximum Case)
Figure 3.7.2-43(3): Maximum Contribution factor by Earthquake Category
(Seismic Intensity: 6 Lower or More; Maximum Case)
Figure 3.7.2-43(4): Maximum Contribution factor by Earthquake Category
(Seismic Intensity: 6 Upper or More; Maximum Case)

(8) Evaluation results by prefecture/region
Figure 3.7.2-44:Seismic Hazard Maps by Region (Hokkaido)
Figure 3.7.2-45: Seismic Hazard Maps by Region (Four Northern Islands).
Figure 3.7.2-46: Seismic Hazard Maps by Region (Ishikari Subprefecture, Hokkaido)
Figure 3.7.2-47: Seismic Hazard Maps by Region (Oshima Subprefecture, Hokkaido)
Figure 3.7.2-48: Seismic Hazard Maps by Region (Hiyama Subprefecture, Hokkaido)
Figure 3.7.2-49: Seismic Hazard Maps by Region (Shiribeshi Subprefecture, Hokkaido)
Figure 3.7.2-50: Seismic Hazard Maps by Region (Sorachi Subprefecture, Hokkaido)
Figure 3.7.2-51: Seismic Hazard Maps by Region (Kamikawa Subprefecture, Hokkaido)
Figure 3.7.2-52: Seismic Hazard Maps by Region (Rumoi Subprefecture, Hokkaido)
Figure 3.7.2-53: Seismic Hazard Maps by Region (Souya Subprefecture, Hokkaido)
Figure 3.7.2-54: Seismic Hazard Maps by Region (Abashiri Subprefecture, Hokkaido)
Figure 3.7.2-55: Seismic Hazard Maps by Region (Iburi Subprefecture, Hokkaido)
Figure 3.7.2-56: Seismic Hazard Maps by Region (Hidaka Subprefecture, Hokkaido)
Figure 3.7.2-57: Seismic Hazard Maps by Region (Tokachi Subprefecture, Hokkaido)
Figure 3.7.2-58: Seismic Hazard Maps by Region (Kushiro Subprefecture, Hokkaido)
Figure 3.7.2-59: Seismic Hazard Maps by Region (Nemuro Subprefecture, Hokkaido)
Figure 3.7.2-60: Seismic Hazard Maps by Region (Aomori Prefecture)
Figure 3.7.2-61: Seismic Hazard Maps by Region (Iwate Prefecture)
Figure 3.7.2-62: Seismic Hazard Maps by Region (Miyagi Prefecture)
Figure 3.7.2-63: Seismic Hazard Maps by Region (Akita Prefecture)
Figure 3.7.2-64: Seismic Hazard Maps by Region (Yamagata Prefecture)

Figure 3.7.2-65: Seismic Hazard Maps by Region (Fukushima Prefecture)
Figure 3.7.2-66: Seismic Hazard Maps by Region (Ibaraki Prefecture)
Figure 3.7.2-67: Seismic Hazard Maps by Region (Tochigi Prefecture)
Figure 3.7.2-68: Seismic Hazard Maps by Region (Gunma Prefecture)
Figure 3.7.2-69: Seismic Hazard Maps by Region (Saitama Prefecture)
Figure 3.7.2-70: Seismic Hazard Maps by Region (Chiba Prefecture)
Figure 3.7.2-71: Seismic Hazard Maps by Region (Metropolitan Tokyo)
Figure 3.7.2-72: Seismic Hazard Maps by Region (Izu-shoto)
Figure 3.7.2-73: Seismic Hazard Maps by Region (Ogasawara-shoto)
Figure 3.7.2-74: Seismic Hazard Maps by Region (Kanagawa Prefecture)
Figure 3.7.2-75: Seismic Hazard Maps by Region (Niigata Prefecture)
Figure 3.7.2-76: Seismic Hazard Maps by Region (Toyama Prefecture)
Figure 3.7.2-77: Seismic Hazard Maps by Region (Ishikawa Prefecture)
Figure 3.7.2-78: Seismic Hazard Maps by Region (Fukui Prefecture)
Figure 3.7.2-79: Seismic Hazard Maps by Region (Yamanashi Prefecture)
Figure 3.7.2-80: Seismic Hazard Maps by Region (Nagano Prefecture)
Figure 3.7.2-81: Seismic Hazard Maps by Region (Gifu Prefecture)
Figure 3.7.2-82: Seismic Hazard Maps by Region (Shizuoka Prefecture)
Figure 3.7.2-83: Seismic Hazard Maps by Region (Aichi Prefecture)
Figure 3.7.2-84: Seismic Hazard Maps by Region (Mie Prefecture)
Figure 3.7.2-85: Seismic Hazard Maps by Region (Shiga Prefecture)
Figure 3.7.2-86: Seismic Hazard Maps by Region (Kyoto Prefecture)
Figure 3.7.2-87: Seismic Hazard Maps by Region (Osaka Prefecture)
Figure 3.7.2-88: Seismic Hazard Maps by Region (Hyogo Prefecture)
Figure 3.7.2-89: Seismic Hazard Maps by Region (Nara Prefecture)
Figure 3.7.2-90: Seismic Hazard Maps by Region (Wakayama Prefecture)
Figure 3.7.2-91: Seismic Hazard Maps by Region (Tottori Prefecture)
Figure 3.7.2-92: Seismic Hazard Maps by Region (Shimane Prefecture)
Figure 3.7.2-93: Seismic Hazard Maps by Region (Okayama Prefecture)
Figure 3.7.2-94: Seismic Hazard Maps by Region (Hiroshima Prefecture)
Figure 3.7.2-95: Seismic Hazard Maps by Region (Yamaguchi Prefecture)
Figure 3.7.2-96: Seismic Hazard Maps by Region (Tokushima Prefecture)
Figure 3.7.2-97: Seismic Hazard Maps by Region (Kagawa Prefecture)
Figure 3.7.2-98: Seismic Hazard Maps by Region (Ehime Prefecture)
Figure 3.7.2-99: Seismic Hazard Maps by Region (Kochi Prefecture)
Figure 3.7.2-100: Seismic Hazard Maps by Region (Fukuoka Prefecture)
Figure 3.7.2-101: Seismic Hazard Maps by Region (Saga Prefecture)
Figure 3.7.2-102: Seismic Hazard Maps by Region (Nagasaki Prefecture)
Figure 3.7.2-103: Seismic Hazard Maps by Region (Kumamoto Prefecture)
Figure 3.7.2-104: Seismic Hazard Maps by Region (Oita Prefecture)
Figure 3.7.2-105: Seismic Hazard Maps by Region (Miyazaki Prefecture)
Figure 3.7.2-106: Seismic Hazard Maps by Region (Kagoshima Prefecture)
Figure 3.7.2-107: Seismic Hazard Maps by Region (Amami region)
Figure 3.7.2-108: Seismic Hazard Maps by Region (Okinawa Prefecture)
Figure 3.7.2-109: Seismic Hazard Maps by Region (Miyako-jima/Yaeyama region)
Figure 3.7.2-110: Seismic Hazard Maps by Region (Daito-jima region)

Uncolored locations in the distribution maps of the exceedance probability indicate that the probability at those locations is zero. The boundaries of administrative districts shown in the maps are those as of January 1, 2009.

3.7.2 Evaluation results

This section indicates the evaluation results of the PSHM for the period starting January 2009 and overviews the characteristics of the results as well as analyzes the differences from the evaluation results for the 2008 year.

The differences in the conditions for creating the PSHM this time and for creating the PSHM 2008 year for the period starting January 2008 are summarized in Section 3.6. The changes are extremely extensive, including changes in the earthquake occurrence probability due to the origin of the time axis being shifted by one year, reflecting of the results of long-term evaluations published by December 2008, modification in the model for the Ibaraki-ken-Oki Earthquake, modification in fault planes of major active fault zones, partial changes in the values of maximum magnitude and zoning of earthquakes without specified source faults, a change in the amplification factor, as well as a change in the grid resolution, and changes in the ground motion evaluation method (variance of the attenuation relation, and the formula for converting the peak ground velocity to the instrumental seismic intensity) to be applied to earthquakes in land area and coastal area. Among these, the change that has a particularly large influence is the change in the ground motion evaluation method.

(1) Site amplification factor

Figure 3.7.2-1 shows the amplification factor for the peak velocity from the engineering bedrock (*Vs*=400m/s) to the ground surface used this time, and Figure 3.7.2-2 shows the amplification factor used in the 2008 version created last fiscal year. Figure 3.7.2-3 shows the ratio between the two (2009 version/2008 version). These figures indicate that the amplification factor in the 2009 version is wider in range than that used in the 2008 version, and that it tends to be smaller in mountainous areas, and larger in plains and basins. In other words, the contrast of the amplification factors is larger than in the 2008 version.

(2) Distribution of instrumental seismic intensity on ground surface where exceedance probability is fixed

Figure 3.7.2-4 and Figure 3.7.2-5 show distribution of the instrumental seismic intensity on the ground surface that considers all earthquakes, where the exceedance probability within 30 years starting January 2009 is 6% and 3%. Figure 3.7.2-4 shows the distribution where the earthquake occurrence probability for major active fault zones is based on the average case, and Figure 3.7.2-5 shows the distribution where the earthquake occurrence probability for major active fault zones is based on the maximum case.

According to Figure 3.7.2-4 showing the values for the average case, when the exceedance probability is 6%, areas of seismic intensity 6 Lower or more (orange - red) are found in the east coast of Hokkaido, areas around Sendai, Pacific coasts from southern Kanto to Shikoku, areas around Nagano Prefecture, and some other plains, and when the exceedance probability is 3%, the areas of seismic intensity 6 Lower or more expand.

When comparing the average case and the maximum case where the exceedance probability is 6%, the results for the maximum case are larger in the following areas: Ishikari Lowlands (Tobetsu fault: occurrence probability within 30 years 0.082%→2.5%, Ishikari-teichi-toen fault zone (main part): 1.7% → 5.8%); Yamagata Prefecture (Yamagata-bonchi fault zone (northern part): 2.2%→7.6%, Shonai-heiya-toen fault zone: 0.020%→6.5%), areas around the Niigata Plain (Kushigata-sanmyaku fault zone: 1.9%→4.9%, Nagaoka-heiya-seien fault zone: nearly 0%→2.2%), Toyama Prefecture – Ishikawa Prefecture (Tonami-heiya fault zone (western part): 0.017%→2.3%, Tonami-heiya fault zone (eastern part): 1.1%→5.9%, Kurehayama fault zone: 0.29%→4.8%, Morimoto/Togashi fault zone: 0.31%→5.5%, etc.), and the Kinki and Chubu regions (Biwako-seigan fault zone: 1.9%→9.4%, Chuo-kozosen fault zone (Kongo-sanchi-toen-Izumi-sanmyaku-nan'en): nearly 0%→5.5%).

Figure 3.7.2-6 to Figure 3.7.2-9 show the hazard by earthquake category. These figures indicate that subduction-zone large earthquakes (Category I) have a large influence on the eastern part of Hokkaido, areas around the Sendai Plain, and areas from southern Kanto to Shikoku, that subduction-zone earthquakes without specified source faults (Category II) have a large influence on the Pacific coast of Hokkaido, southern Kanto, and areas from the western part of Shikoku to the eastern part of Kyushu, and that shallow earthquakes in land area (Category III) have a large influence on areas around Niigata Prefecture – Nagano Prefecture – Izu Peninsula and the Kinki region.

Figure 3.7.2-20 to Figure 3.7.2-21 shows the distribution of the instrumental seismic intensity on the ground surface considering all earthquakes where the exceedance probability within 50 years is 39%, 10%, 5%, and 2%. The 10% exceedance probability within 50 years corresponds to the 6% exceedance probability within 30 years, and the 5% exceedance probability within 50 years corresponds to the 3% exceedance probability within 30 years, producing the same results if the earthquake occurrence is at random on the time axis. However, when the results for such exceeding probability within 50 years are compared with the results for the corresponding exceedance probability within 30 years (Figure 3.7.2-4, etc.), the results, though generally similar, differ in some areas such as regions influenced by Nankai Trough earthquakes and regions from Tohoku to Hokkaido. The reason for such difference is that, when the period is changed from 30 years to 50 years, the degree of change in the earthquake occurrence probability becomes larger or smaller than 50/30 times for some earthquakes. For example, in the case of large interplate earthquakes in Northern Sanriku-Oki, the earthquake occurrence probability within 30 years is 4.5%, while the earthquake occurrence probability within 50 years is 39%, which is more than eight times the probability within 30 years. Therefore, the map for the period of 50 years shows strong

ground motions in wider areas in the region from Tohoku to Hokkaido compared to the map for the period of 30 years.

(3) Distribution of exceedance probability where instrumental seismic intensity on ground surface is fixed

Figure 3.7.2-10 and Figure 3.7.2-11 show the results of distribution of the probability that an earthquake with seismic intensity 5 Lower, seismic intensity 5 Upper, seismic intensity 6 Lower, and seismic intensity 6 Upper or more will occur within 30 years starting January 2009, considering all earthquakes. Figure 3.7.2-10 shows the distribution where the earthquake occurrence probability for major active fault zones is based on the average case, and Figure 3.7.2-11 shows the distribution where the earthquake occurrence probability for major active fault zones is based on the maximum case.

The probability of an earthquake with seismic intensity 5 Lower or more is shown in dark colors of 3% or more in most of the regions nationwide. In contrast, the regions with a high probability of an earthquake with seismic intensity 6 Lower or more are limited to the eastern part of Hokkaido, areas around the Sendai Plain, areas in the Pacific Ocean side from southern Kantoto Shikoku, Nagano Prefecture, and some plains.

Figure 3.7.2-12 to Figure 3.7.2-15 show these results by earthquake category. For Category I (subduction-zone large earthquakes), the hazard level is high in the eastern part of Hokkaido, the Sanriku coast including Miyagi Prefecture, and the Pacific coast from southern Kanto to Shikoku. The results clearly show the extent of spread of the influence of the historically repeating subduction-zone large earthquakes (large earthquakes from the Kuril Trench to the Japan Trench and along the Nankai Trough). The results for Category II (subduction-zone earthquakes without specified source faults) show that these earthquakes have an influence on wide areas on the Pacific coast nationwide. The hazard level is particularly high in the eastern part of Hokkaido and southern Kanto, indicating that close attention needs to be paid not only to subduction-zone large earthquakes, but also to subduction-zone earthquakes without specified source faults in these regions. The results for Category III (shallow earthquakes in land area) show that these earthquakes have an influence on wide areas nationwide. The hazard level is particularly high around major active fault zones where the occurrence probability is high. In maps for total hazard considering all earthquakes, Category III earthquakes tend to be disregarded behind the more noticeable influence of Category I (subduction-zone large earthquakes). However, the results for Category III alone reveal that this category of earthquakes is important particularly in areas other than the Pacific Ocean side of the Japanese archipelago.

Figure 3.7.2-16 to Figure 3.7.2-19 show the distribution of exceedance probability by earthquake category, not based on the absolute values of the probability, but based on quartiles* of the values of the probability in color scale. Here, meshes for which the probability is zero are excluded. The results for the probability of an earthquake with seismic intensity 6 Lower or more in quartiles show that the deep-colored areas indicating a high hazard level are found mainly in areas influenced by Nankai Trough earthquakes in the case of Category I, mainly in the Pacific Ocean side from Hokkaido to Kyushu in the case of Category II, and mainly in the Chubu region but also spread nationwide in the case of Category III.

(4) Distribution of differences in exceedance probability between 2009 version and 2008 version

Figure 3.7.2-22 to Figure 3.7.2-27 show the distribution of differences in the exceedance probability within 30 years between the 2009 version and the 2008 version. The figures show not only the results of total hazard considering all earthquakes, but also results by earthquake category. The difference in the probability is the value obtained by subtracting the exceedance probability for the period starting January 2008 from the exceedance probability for the period starting January 2009. The areas where the probability has risen for the period starting January 2009 are shown in red, and areas where the probability has declined are shown in blue. The values are the real numbers, and not percentages.

The results reveal that, in the data for total hazard considering all earthquakes based on the average case, the differences in the probability for an earthquake with a seismic intensity exceeding 5 Lower are strongly attributable to the difference in the amplification factor between the 2009 version and the 2008 version (see Figure 3.7.2-3). When the target seismic intensity becomes larger, the regions showing large differences become limited. In the case of the probability for an earthquake with seismic intensity 6 Lower or more, plains are shown in red (the probability is larger in the 2009 version), and mountainous areas from the Chubu region to Kii Peninsula and to Shikoku are shown in blue (the probability is smaller in the 2009 version).

A characteristic point in the results by earthquake category is the fact that, for shallow earthquakes in land area (Category III) with a large seismic intensity, the results in the 2009 version are larger than those in the 2008 version in almost all areas. This is considered to be attributable to the difference in the ground motion evaluation method (the difference in the treatment of variance and in the formula for converting the peak ground velocity into the instrumental seismic intensity).

(5) Distribution of differences in exceedance probability between maximum case and average case

Figure 3.7.2-28 shows the distribution of differences in the exceedance probability within 30 years where the earthquake occurrence probability for major active fault zones is based on the

* Different color is allocated to each of the four equal parts of the data set where the data is sorted from small to large.

maximum case and where it is based on the average case. In addition to the results for total hazard considering all earthquakes, the results for shallow earthquakes in land area (Category III) alone are also shown in Figure 3.7.2-29. The areas where the differences in the probability are large are located around fault zones where the differences in earthquake occurrence probability are large between the maximum case and the average case. Main such areas include the following (main related fault zones are shown in parentheses): northern part of Hokkaido (Sarobetsu fault zone); Ishikari Lowlands in Hokkaido (Ishikari-teichi-toen fault zone (main part), etc.); Yamagata Prefecture (Yamagata-bonchi fault zone (northern part), Shonai-heiya-toen fault zone); areas around the Niigata Plain (Kushigata-sanmyaku fault zone, Nagaoka-heiya-seien fault zone); Kanagawa Prefecture (Kannawa/Kozu-Matsuda fault zone, etc.); Toyama Prefecture to Ishikawa Prefecture (Tonami-heiya fault zone, Morimoto/Togashi fault zone, etc.); Nagano Prefecture to Gifu Prefecture (Sakaitoge/Kamiya fault zone (main part), Kokufu fault zone, Atera fault zone (northern segment of the main part), etc.); the Kinki and Chubu regions (Biwako-seigan fault zone, Chuo-kozosen fault zone (Kongo-sanchi-toen-Izumi-sanmyaku-nan'en), etc.); Fukuoka Prefecture (Kego fault zone (southeastern part)); Oita Prefecture (Oita-heiya-Yufuin fault zone); and Kumamoto Prefecture to Nagasaki Prefecture (Futagawa/Hinagu fault zone, Unzen fault group).

(6) Distribution of differences in peak velocity on bedrock (*Vs*=600m/s) between 2009 version and 2008version

Figure 3.7.2-30 and Figure 3.7.2-31 show the values of the peak velocity on the bedrock for which the exceedance probability within 30 years is 6％ and 3％. The figures show the results for the 2009 version, the results for the 2008 version, and the difference between the two (the value obtained by subtracting the peak velocity in the 2008 version from the peak velocity in the 2009 version) for the average case. Figure 3.7.2-32 and Figure 3.7.2-33 show the results for the maximum case. Figure 3.7.2-34 to Figure 3.7.2-41 show the results by earthquake category. Since the comparison is made by the values on the bedrock, the influence of the difference in the amplification factor between the 2008 version and the 2009 version is excluded. In other words, it is possible to see the influence of the differences in seismic activity or the ground motion evaluation models, out of the various differences between the 2009 version and the 2008 version.

Looking at the results by earthquake category where the exceedance probability within 30 years is 3%, for Category I (subduction-zone large earthquakes), the results in the 2009 version are larger than those in the 2008 version in areas from the southern part of Hokkaido to the vicinity of Aomori Prefecture, which is attributable to an increase in the occurrence probability for large interplate earthquakes in Northern Sanriku-Oki from 3.8% to 4.5% as a result of shifting the origin of the time axis by one year. Meanwhile, the reason that the results in the 2009 version are slightly larger in wide areas centering on Kii Peninsula to Shikoku is that the occurrence probability for Nankai Trough earthquakes has increased.

In the case of Category II (subduction-zone earthquakes without specified source faults), the results in the 2009 version are large around Ibaraki Prefecture, and small around Akinada. The former is attributable to the fact that, from among the earthquakes without specified source faults at the Pacific plate, the maximum magnitude for the area of earthquakes in Ibaraki-ken-Oki has been changed from 6.6 to 7.3. The latter is attributable to the fact that, from among the earthquakes without specified source faults at the Philippine Sea plate, the zoning of the areas from Bungosuido to the vicinity of Akinada has been changed, and the maximum magnitude has also been changed accordingly.

In the case of Category III (shallow earthquakes in land area), the influence of the following factors is observed: publication and revision of long-term evaluations of major active fault zones; changes in the fault parameters of major active fault zones (changes in the depth of the upper edge of the fault in particular); updating of the frequency and changes in the maximum magnitude of earthquakes without specified source faults; and changes in the variance of the attenuation relation. Overall, the hazard level tends to be higher in the 2009 version since the variance of the attenuation relation for earthquakes that occur at a short distance has become larger. However, since the extent of influence of other factors differs by location, there are also regions where the hazard level has barely changed (shown in white) and regions where the hazard level has declined (shown in blue). In most of the regions in red, the rise in the hazard level is attributable to the increase in the variance of the attenuation relation, but in areas around Suonada, the rise is attributable to the fact that long-term evaluation of the Ube-oki fault group (Suonada fault group) has been newly published. In the blue regions from Ishikawa Prefecture to the western part of Toyama Prefecture, the decline in the hazard level is considered to be attributable to the revision of the long-term evaluation of the Tonami-heiya fault zone/Kurehayama fault zone and an increase in the depth of the upper edge of the fault.

The results for total hazard mostly reflect the differences by category discussed above.

(7) Distribution of earthquake categories having maximum contribution factor

Figure 3.7.2-42 and Figure 3.7.2-43 show the earthquake categories having the largest contribution factor on the probability of occurrence of an earthquake with specific seismic intensity within 30 years, in color scale for the whole of Japan, for the average case and the maximum case.

The contribution factor on the probability of an earthquake with seismic intensity 5 Lower or more for the average case is largest

for subduction-zone large earthquakes (Category I) from the southern part of Iwate Prefecture to the whole area of Miyagi Prefecture, and from the western part of Kanto to the regions of Chubu-Kinki-Chugoku/Shikoku-the northwestern part of Kyushu. The degree is largest for subduction-zone earthquakes without specified source faults (Category II) in the Pacific coasts from the central part/southeastern part of Hokkaido to Kanto excluding the area around Miyagi Prefecture, and the southeastern part of Kyushu. Further, the degree is largest for shallow earthquakes in land area (Category III) in most of the areas on the Japan Sea side, and the whole area of Nansei-shoto. When the target seismic intensity becomes larger, the regions where shallow earthquakes in land area (Category III) have the largest contribution factor expand. In the case of a seismic intensity of 6 Upper or more, Category III earthquakes are the most influential in wide areas, excluding the Pacific coasts from the Etorofu Island to Hokkaido (Category II), the Pacific coasts in Aomori Prefecture to the eastern part of Miyagi Prefecture (Category I), southern Kanto (Category II), the Tokai region-southern part of the Kinki region-the whole area of Shikoku (Category I), and Miyagi Prefecture (Category II). These results show that, in many regions in Japan, ground motions of seismic intensity 6 Upper or more are likely to be caused by shallow earthquakes in land area (including earthquakes that occur at active faults).

(8) Seismic hazard maps by region

Figure 3.7.2-44 to Figure 3.7.2-110 show, as the results by region, the distribution of the probability of occurrence of an earthquake with seismic intensity 6 Lower or more within 30 years starting January 2009 for the average case, the distribution of the instrumental seismic intensity where the exceedance probability within 30 years is 3%, and the amplification factor for the peak velocity from the engineering bedrock to the ground surface. In addition to maps by prefecture, maps by subprefecture are created for Hokkaido, and individual maps are created for some islands.

(Figures are shown in the following pages.)

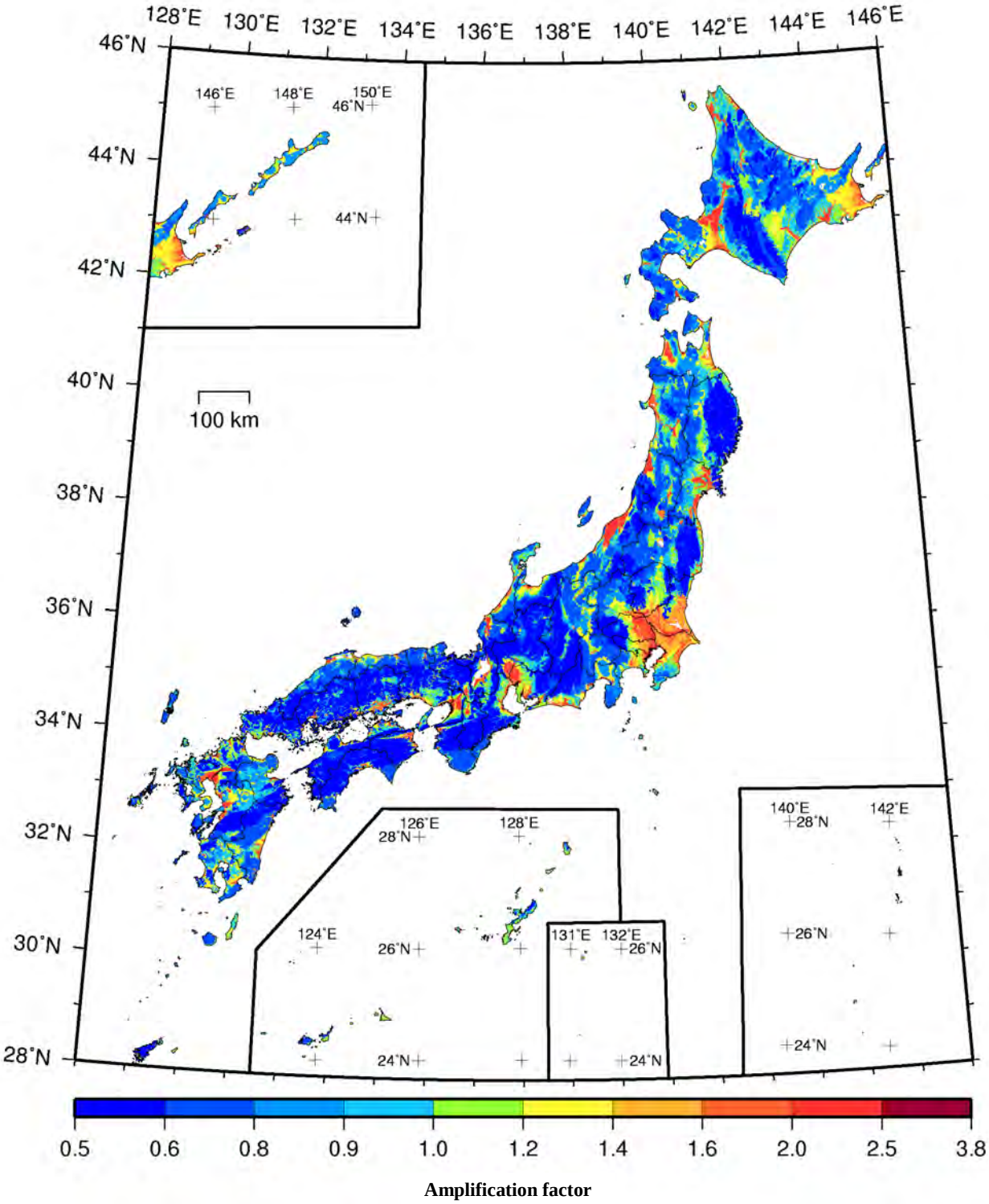

Figure 3.7.2-1 Amplification factor for peak velocity (from engineering bedrock (layer with Vs=400m/s) to ground surface; 2009 version)

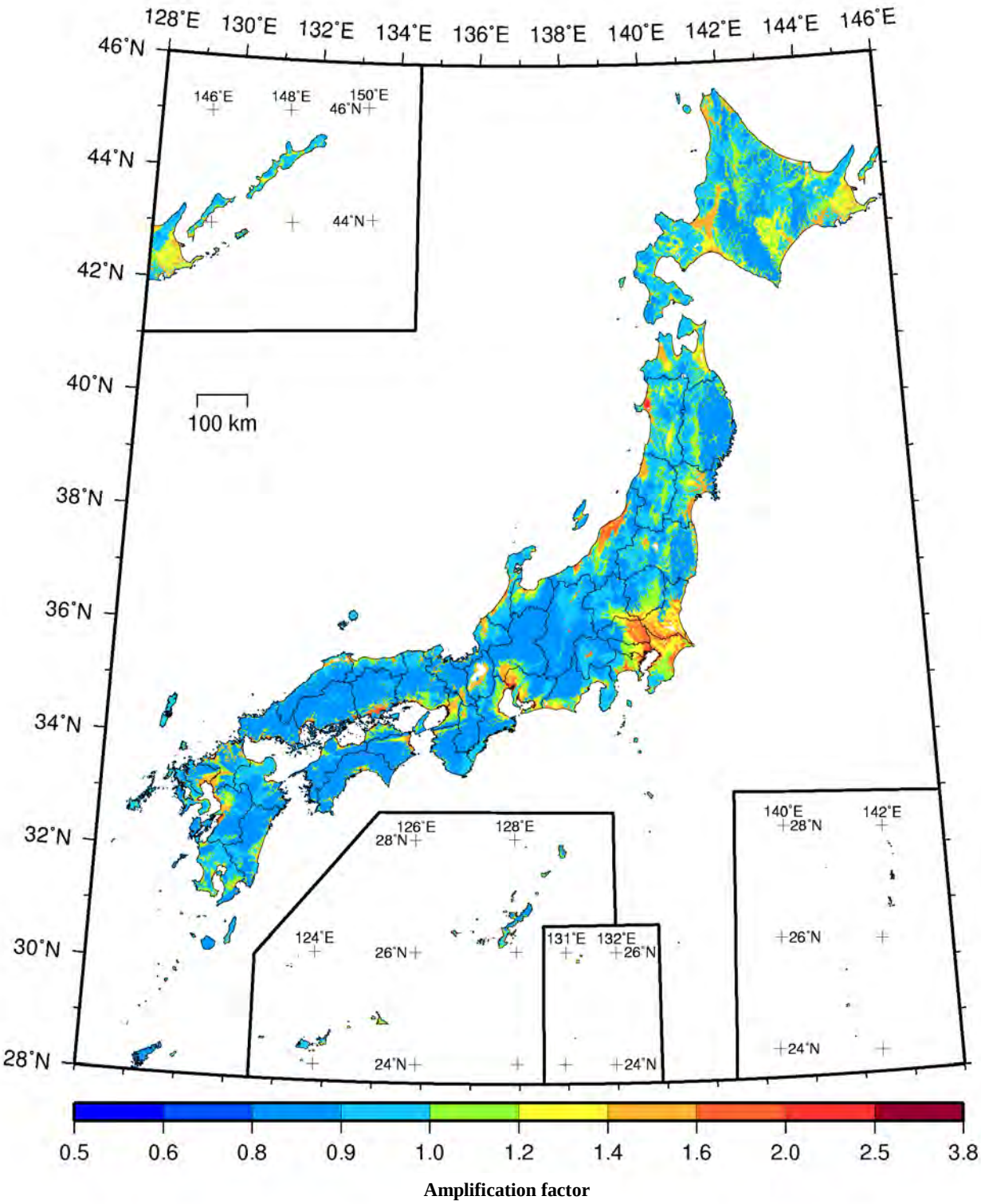

Figure 3.7.2-2 Amplification factor for peak velocity (from engineering bedrock (layer with Vs=400m/s) to ground surface; 2008 version)

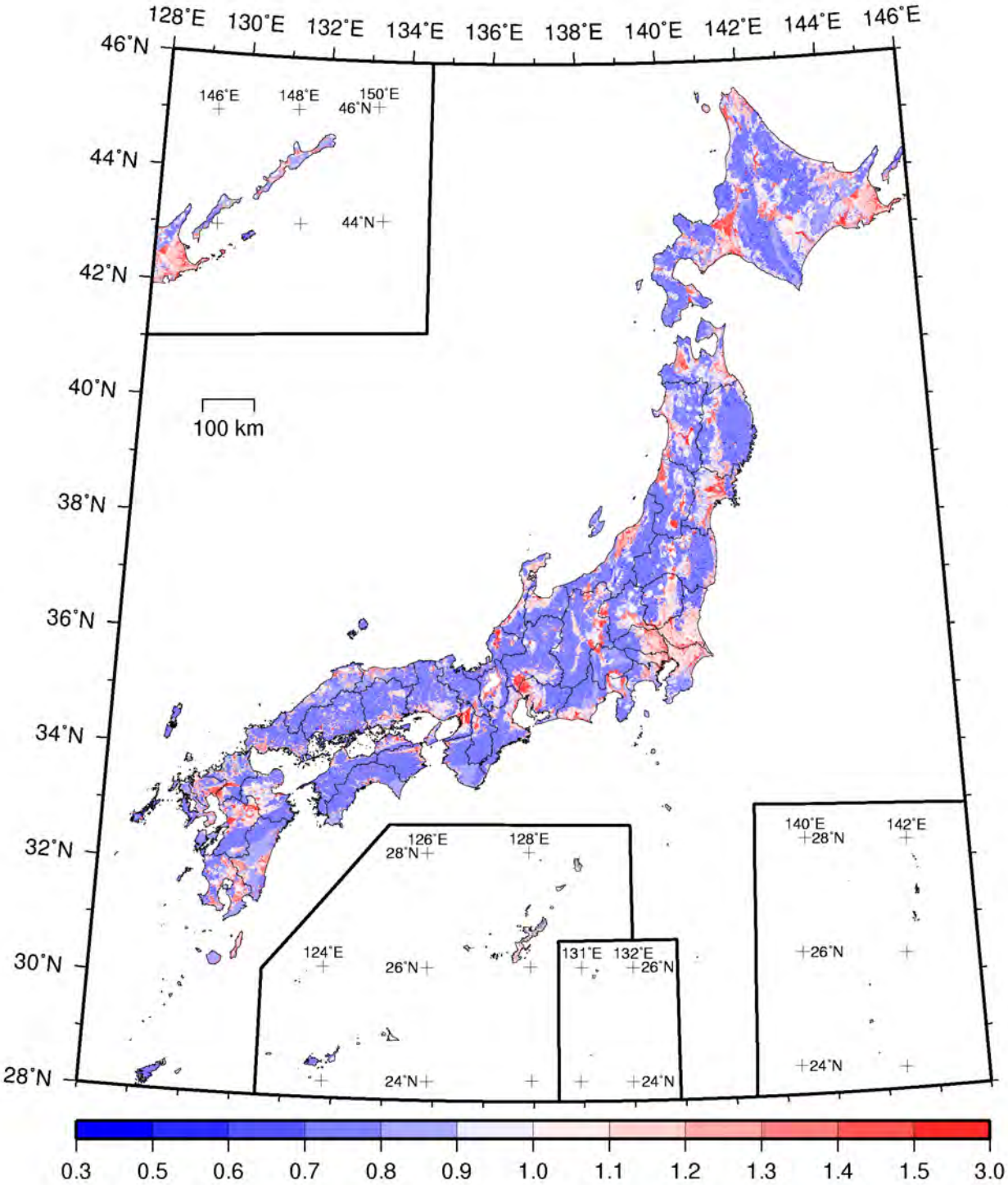

Ratio of amplification factor (2009 version/2008 version)

Figure 3.7.2-3 Ratio of amplification factor for peak velocity (2009 version/2008 version)

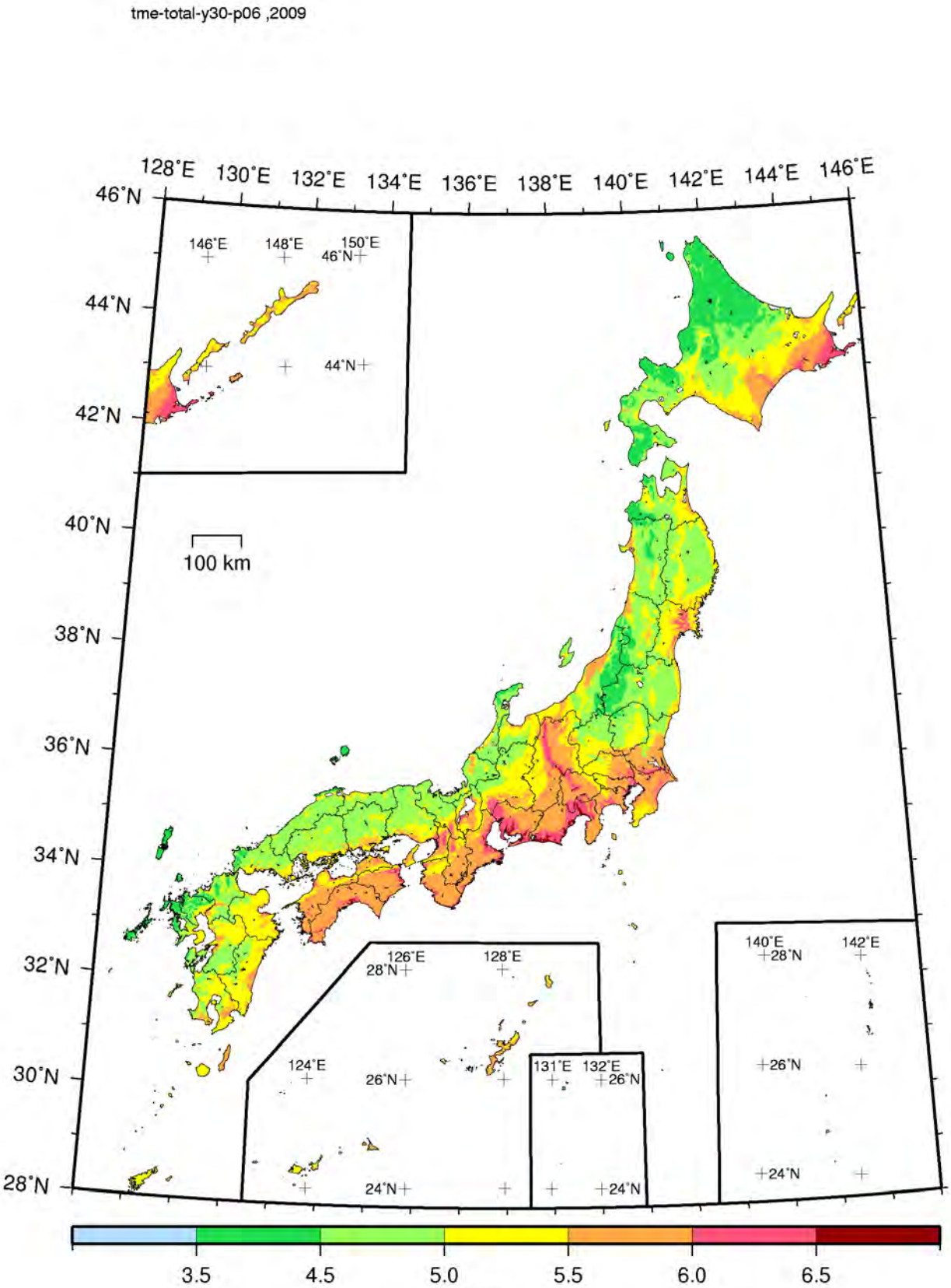

JMA seismic intensity
(Exceedance probability within 30 years: 6%)

Figure 3.7.2-4 (1) JMA seismic intensity on the ground surface considering all earthquakes (Exceedance probability within 30 years: 6%; average case)

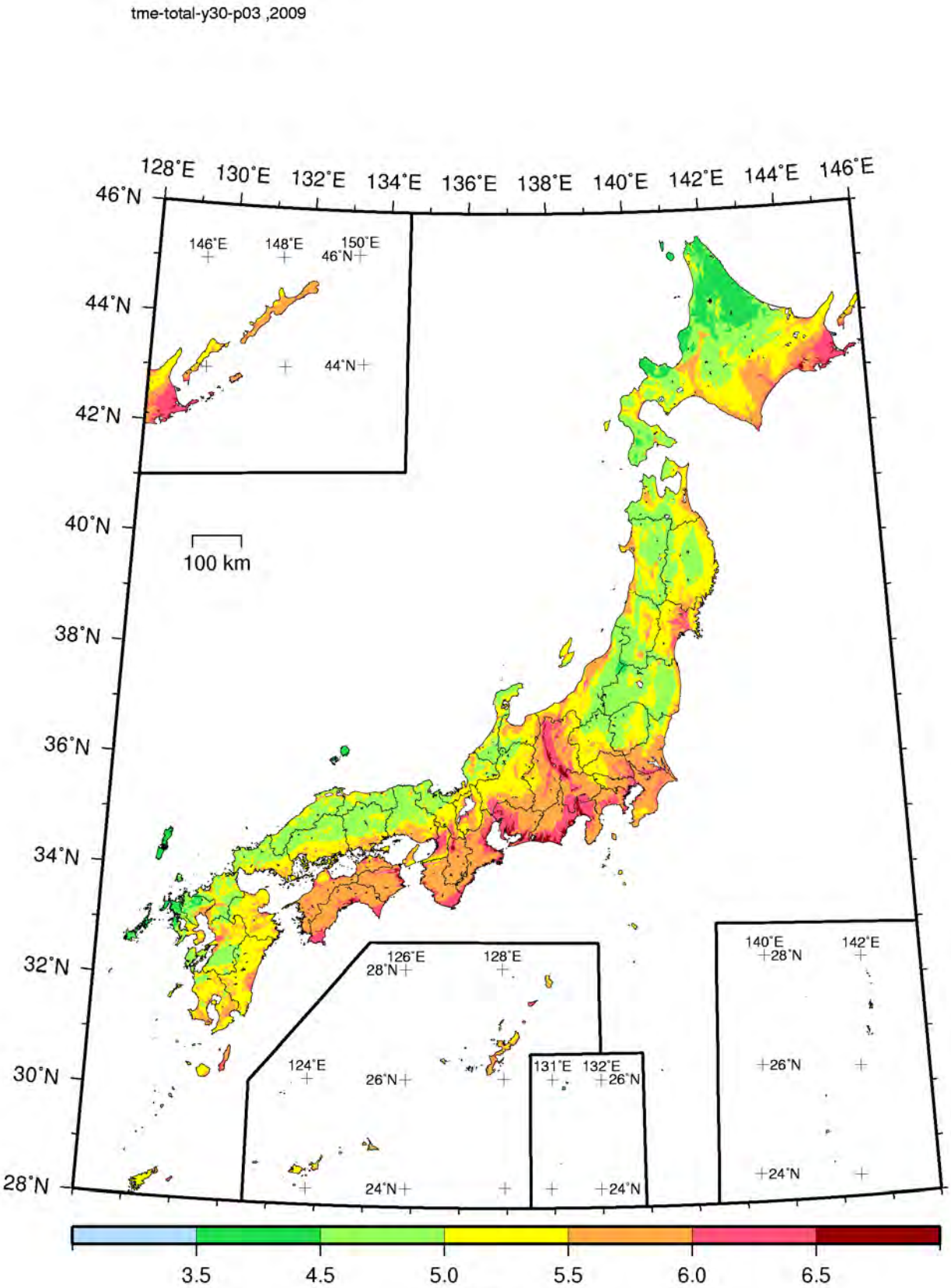

JMA seismic intensity
(Exceedance probability within 30 years: 3%)

Figure 3.7.2-4 (2) JMA seismic intensity on the ground surface considering all earthquakes (Exceedance probability within 30 years: 3%; average case)

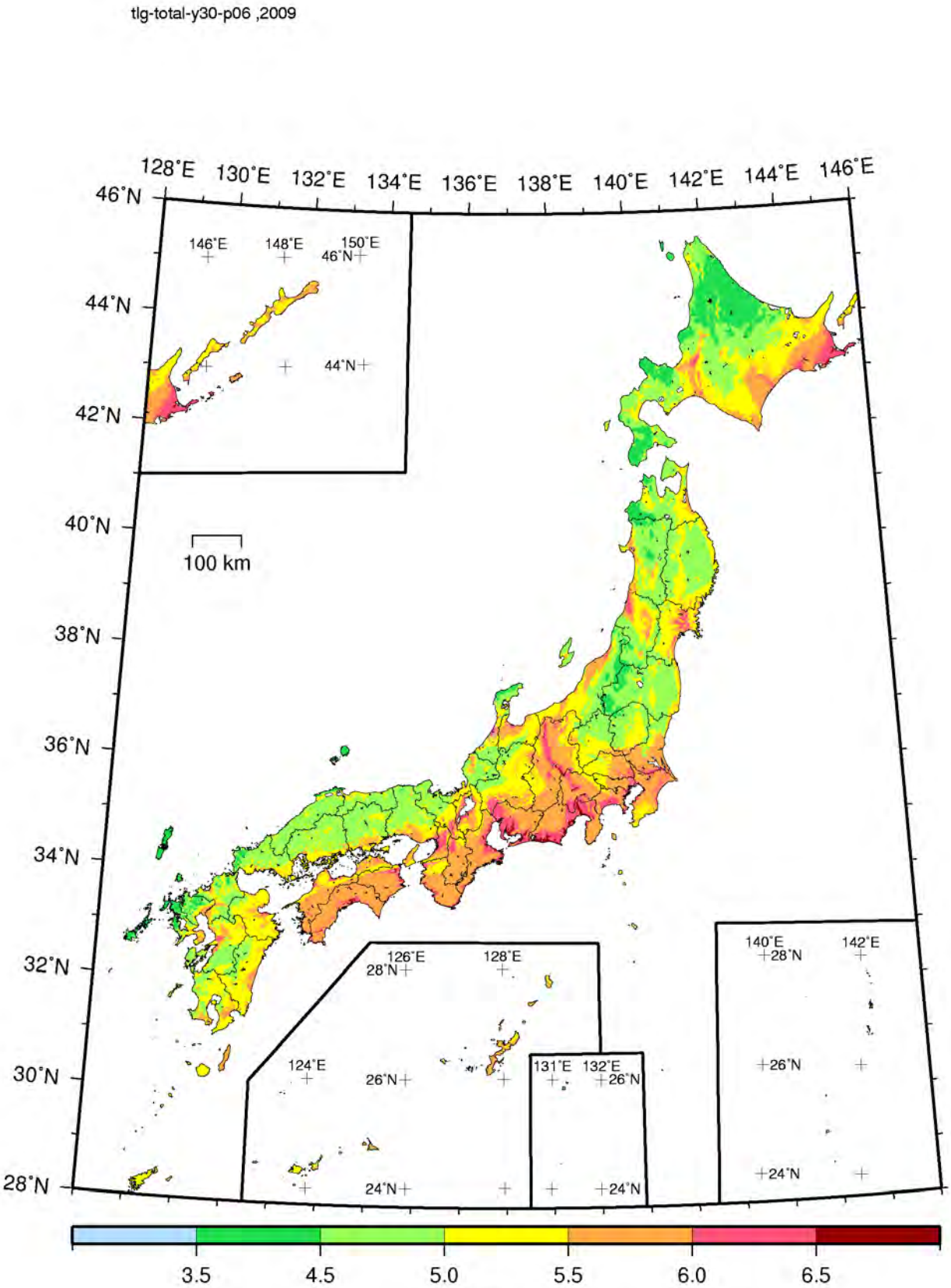

JMA seismic intensity
(Exceedance probability within 30 years: 6%)

Figure 3.7.2-5 (1) JMA seismic intensity on the ground surface considering all earthquakes (Exceedance probability within 30 years: 6%; maximum case)

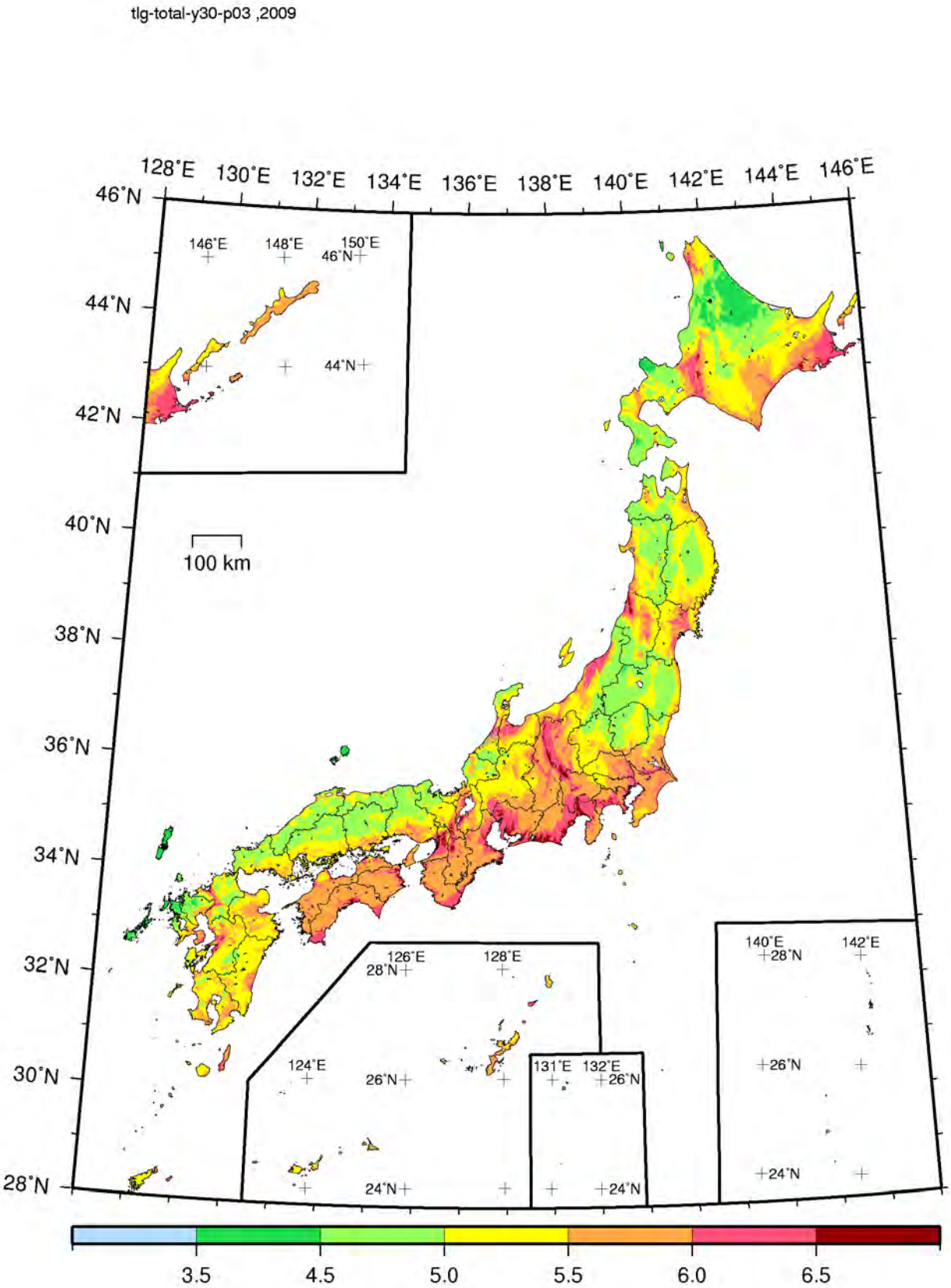

JMA seismic intensity
(Exceedance probability within 30 years: 3%)

Figure 3.7.2-5 (2) JMA seismic intensity on the ground surface considering all earthquakes (Exceedance probability within 30 years: 3%; maximum case)

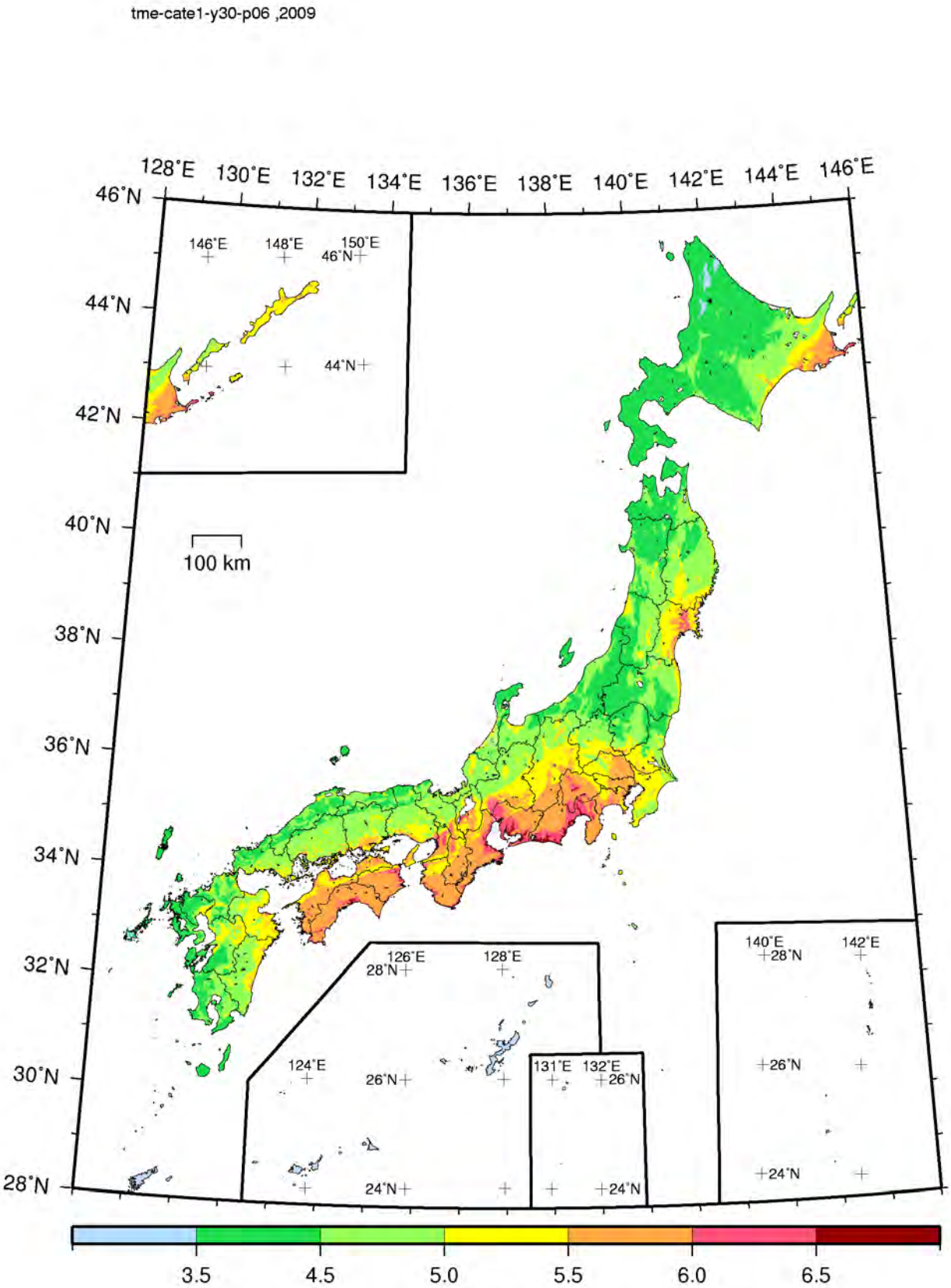

JMA seismic intensity
(Exceedance probability within 30 years: 6%)

Figure 3.7.2-6 (1) JMA seismic intensity on the ground surface associated with earthquake category I (Exceedance probability within 30 years: 6%)

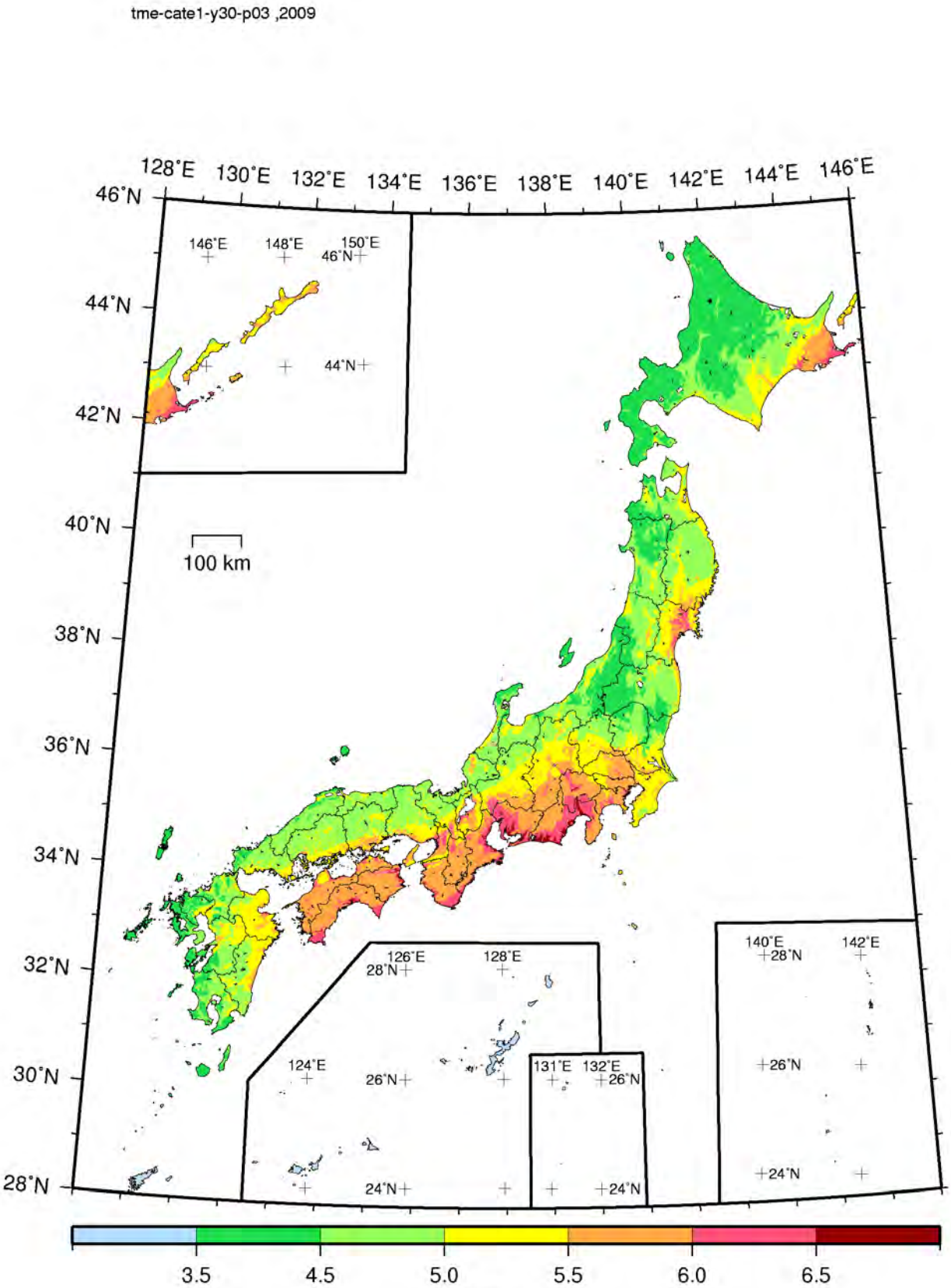

JMA seismic intensity
(Exceedance probability within 30 years: 3%)

Figure 3.7.2-6 (2) JMA seismic intensity on the ground surface associated with earthquake category I (Exceedance probability within 30 years: 3%)

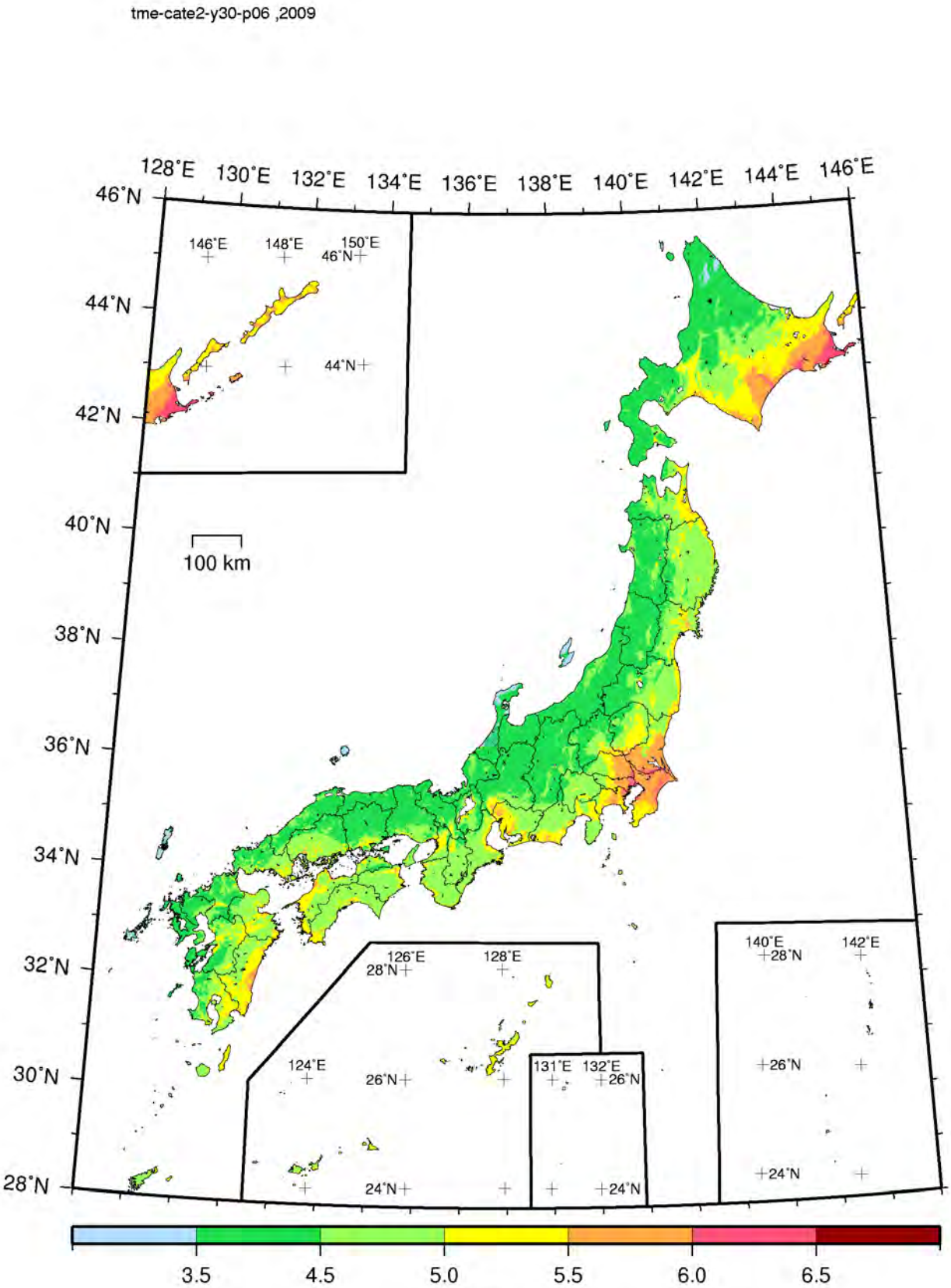

JMA seismic intensity
(Exceedance probability within 30 years: 6%)

Figure 3.7.2-7 (1) JMA seismic intensity on the ground surface associated with earthquake category II (Exceedance probability within 30 years: 6%)

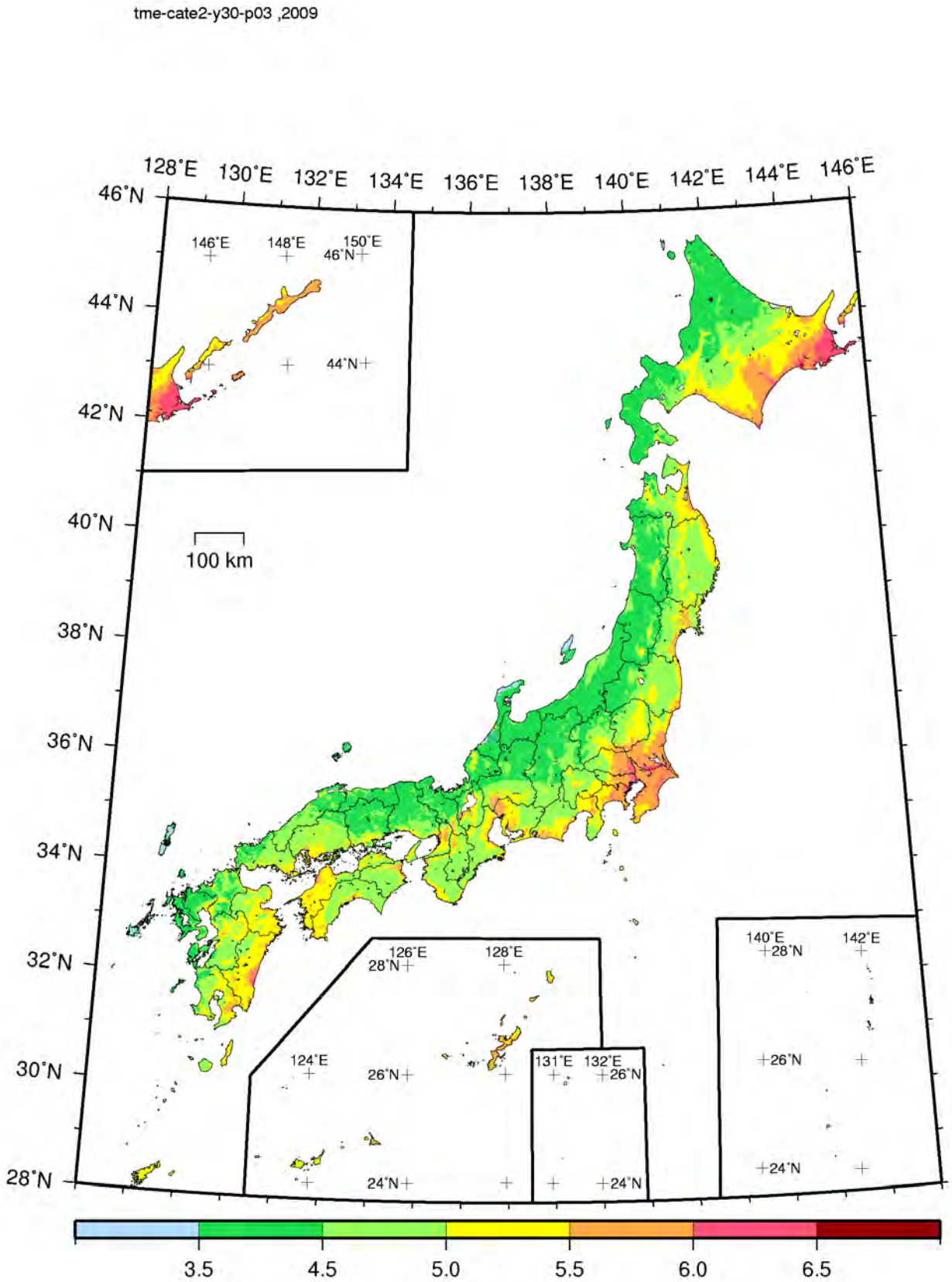

JMA seismic intensity
(Exceedance probability within 30 years: 3%)

Figure 3.7.2-7 (2) JMA seismic intensity on the ground surface associated with earthquake category II (Exceedance probability within 30 years: 3%)

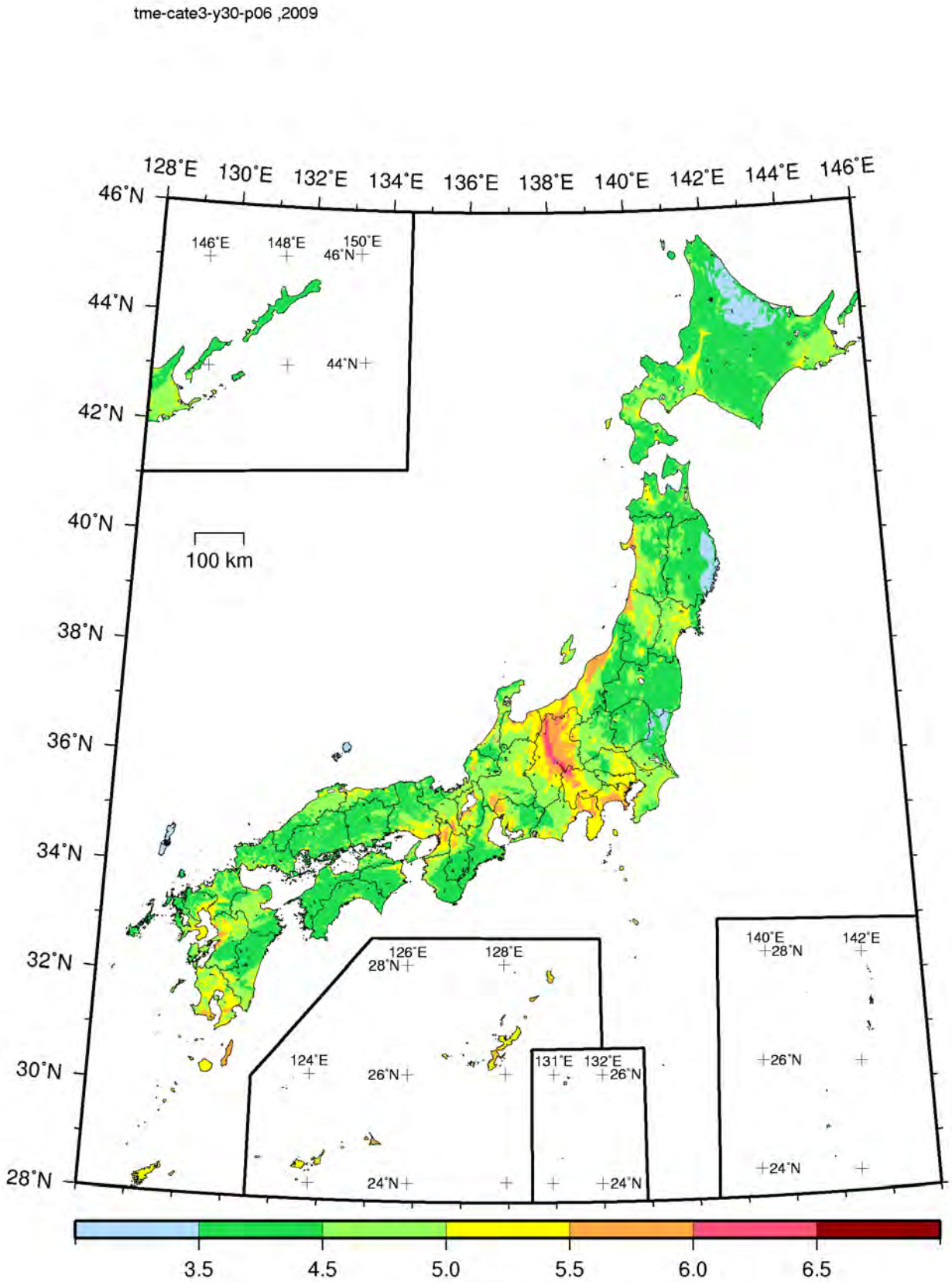

JMA seismic intensity
(Exceedance probability within 30 years: 6%)

Figure 3.7.2-8 (1) JMA seismic intensity on the ground surface associated with earthquake category III (Exeedance probability within 30 years: 6%; average case)

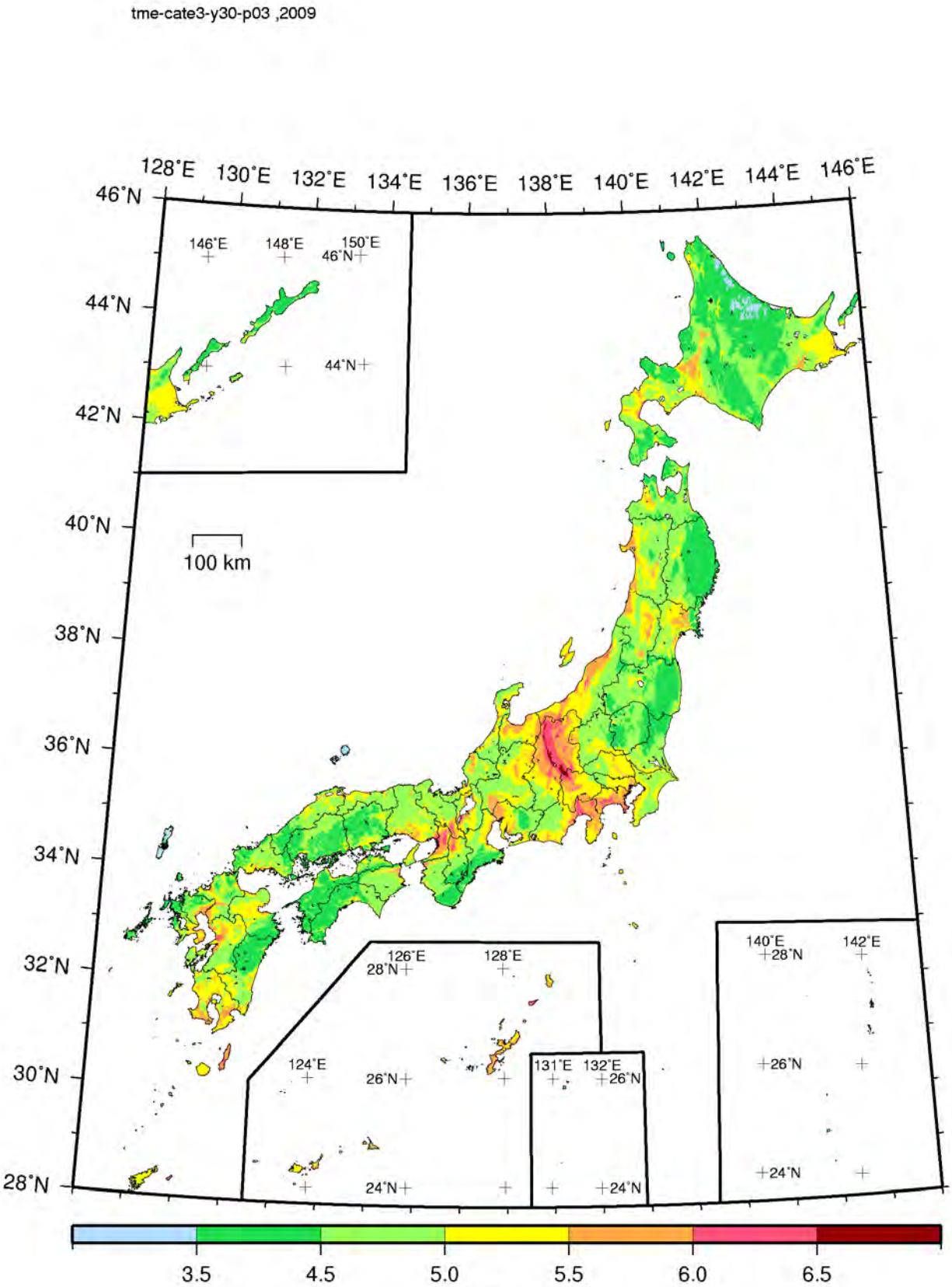

JMA seismic intensity
(Exceedance probability within 30 years: 3%)

Figure 3.7.2-8 (2) JMA seismic intensity on the ground surface associated with earthquake category III (Exeedance probability within 30 years: 3%; average case**)**

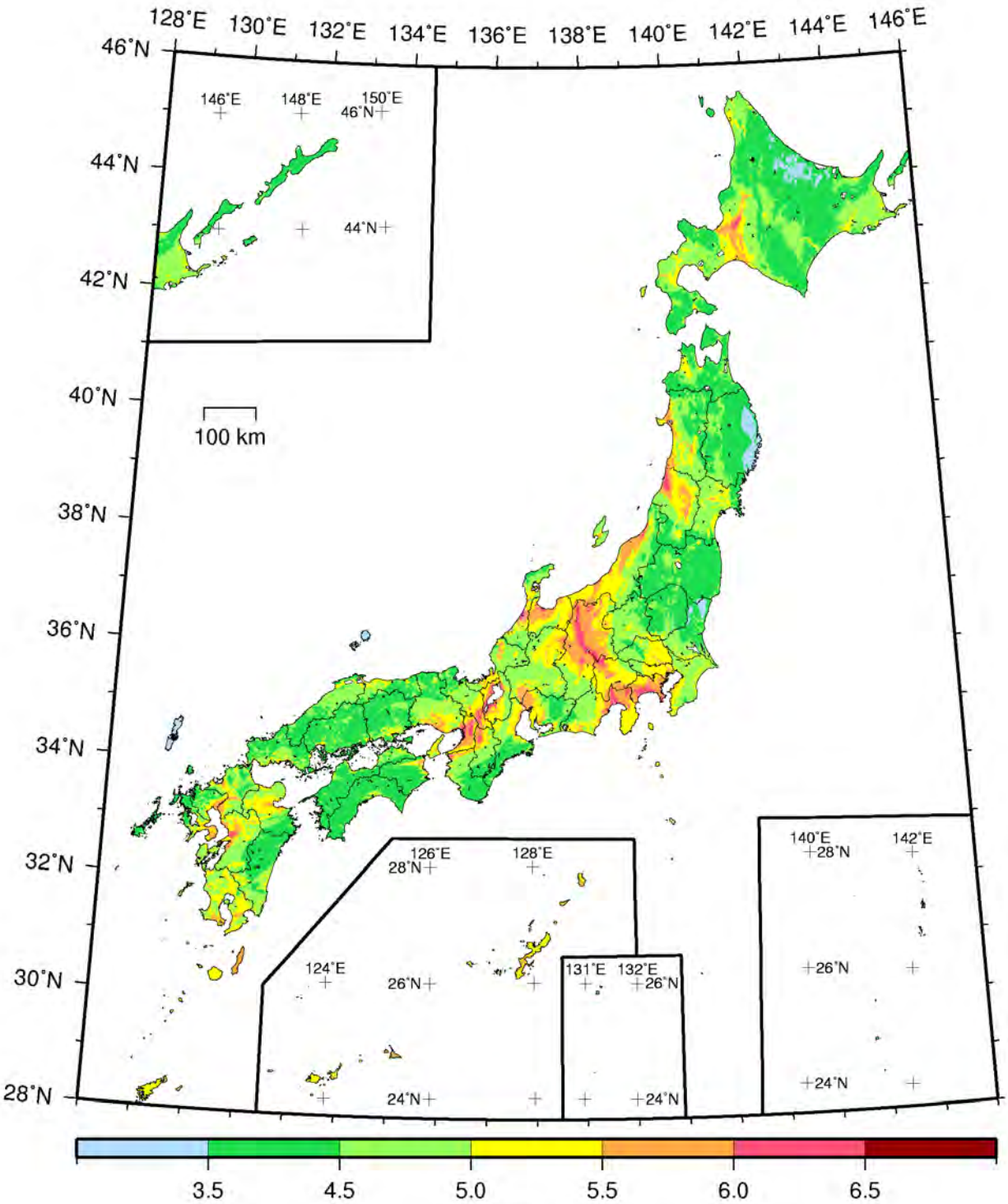

JMA seismic intensity
(Exceedance probability within 30 years: 6%)

Figure 3.7.2-9 (1) JMA seismic intensity on the ground surface associated with earthquake category III (Exeedance probability within 30 years: 6%; maximum case)

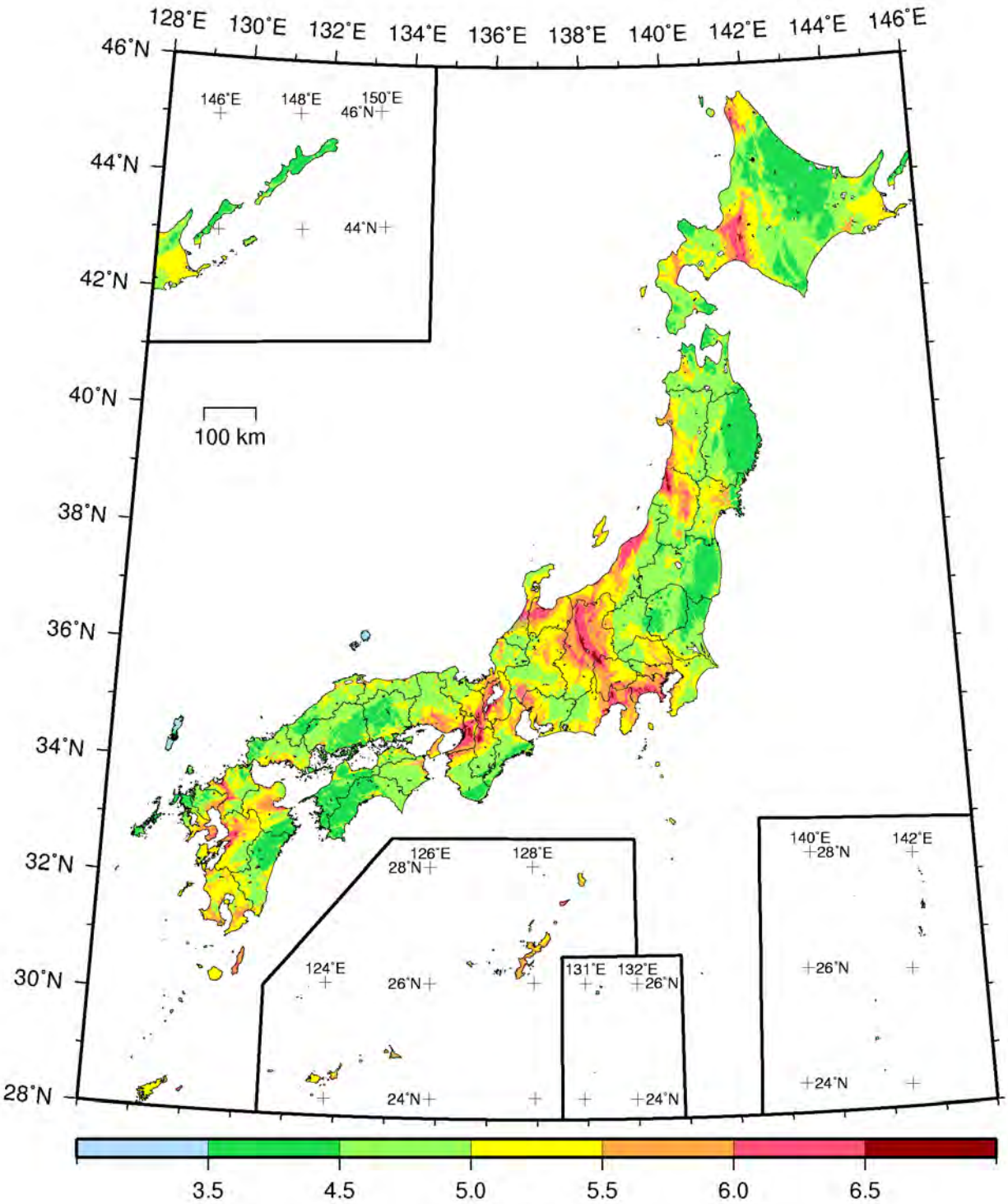

JMA seismic intensity
(Exceedance probability within 30 years: 3%)

Figure 3.7.2-9 (2) JMA seismic intensity on the ground surface associated with earthquake category III (Exeedance probability within 30 years: 3%; maximum case)

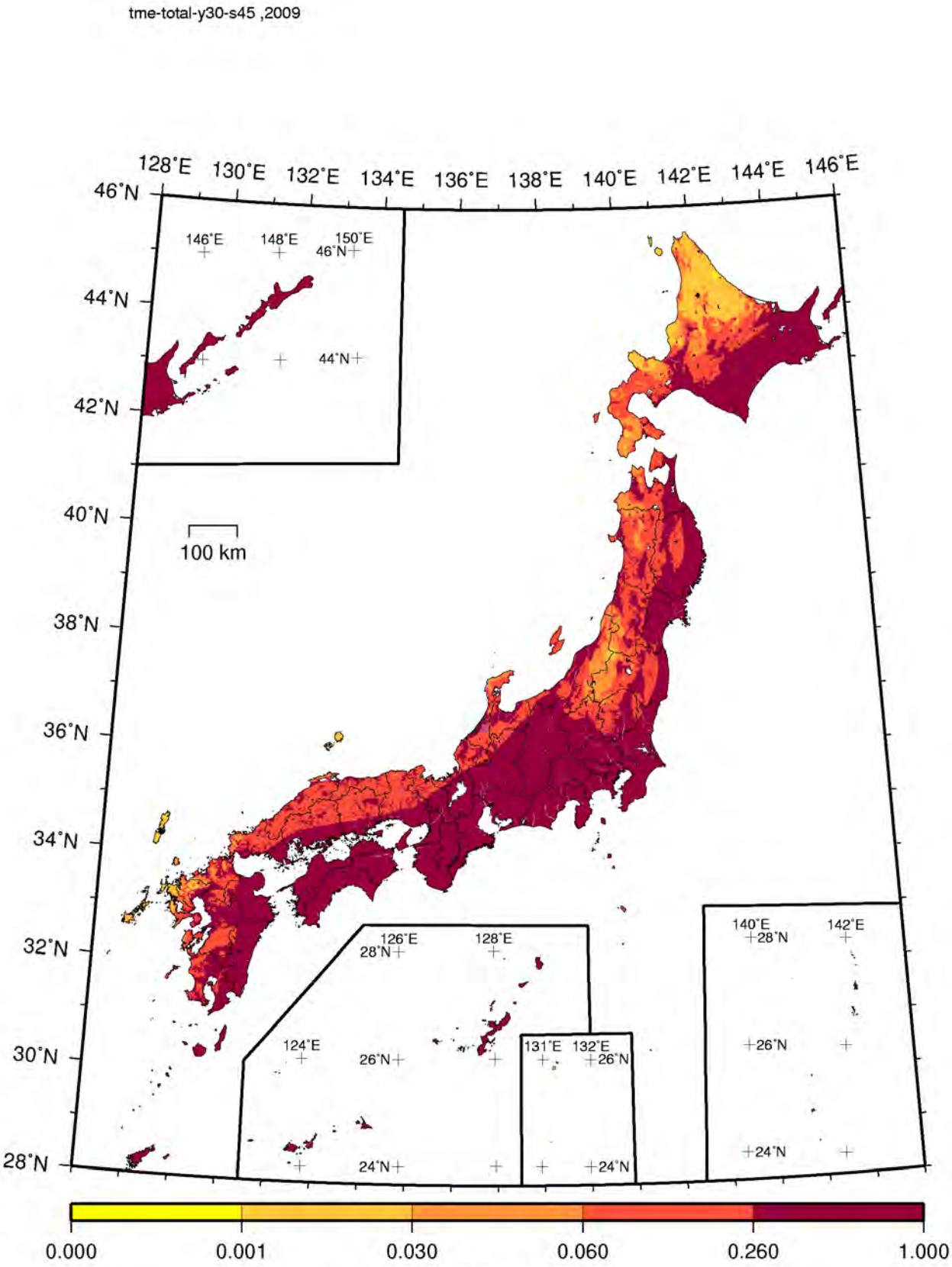

Exceedance probability within 30 years
(JMA seismic intensity: 5 Lower or more)

Figure 3.7.2-10 (1) Exceedance probability within 30 years considering all earthquakes (JMA seismic intensity: 5 Lower or more; average case)

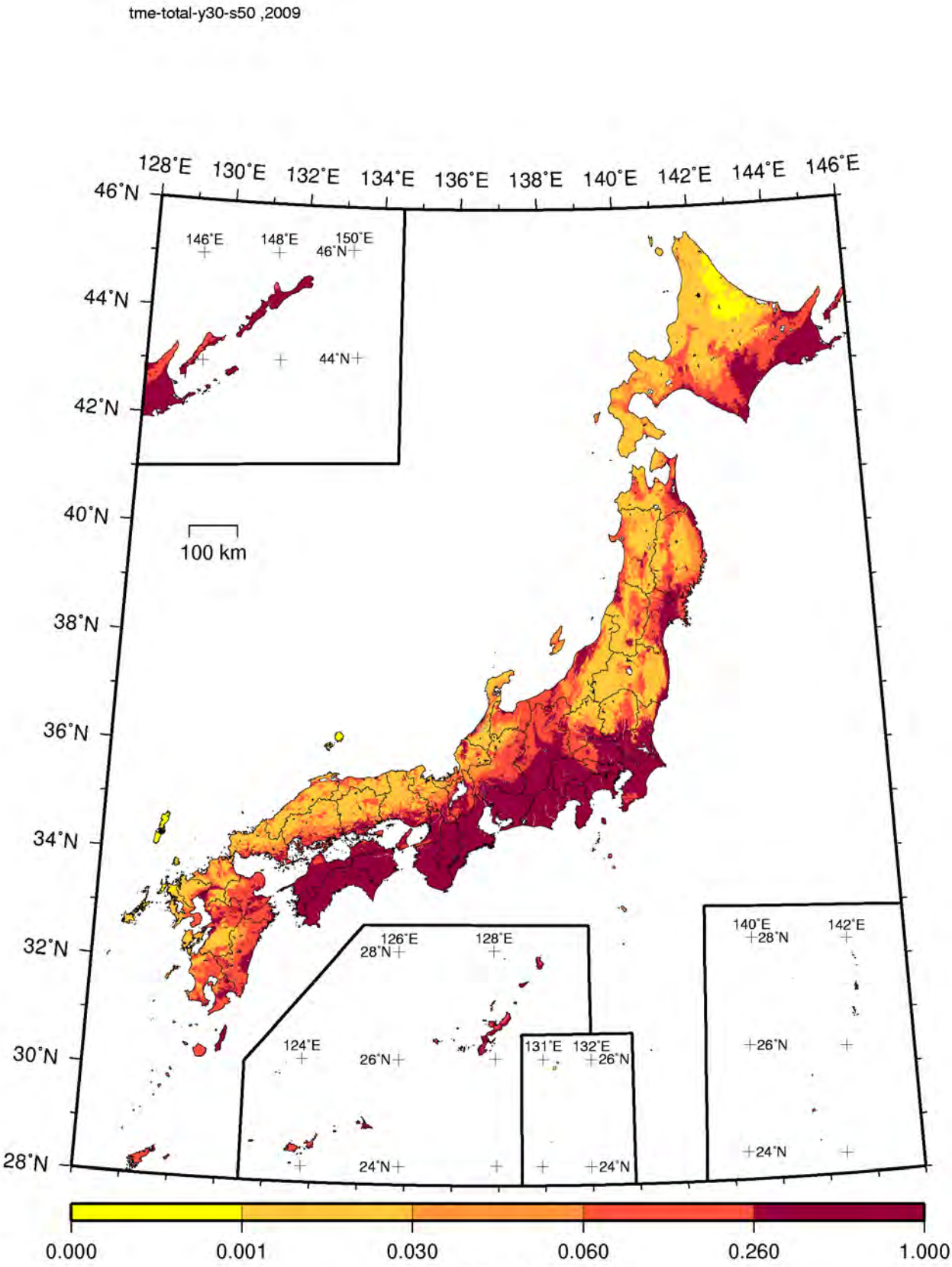

Exceedance probability within 30 years
(JMA seismic intensity: 5 Upper or more)

Figure 3.7.2-10 (2) Exceedance probability within 30 years considering all earthquakes (JMA seismic intensity: 5 Upper or more; average case)

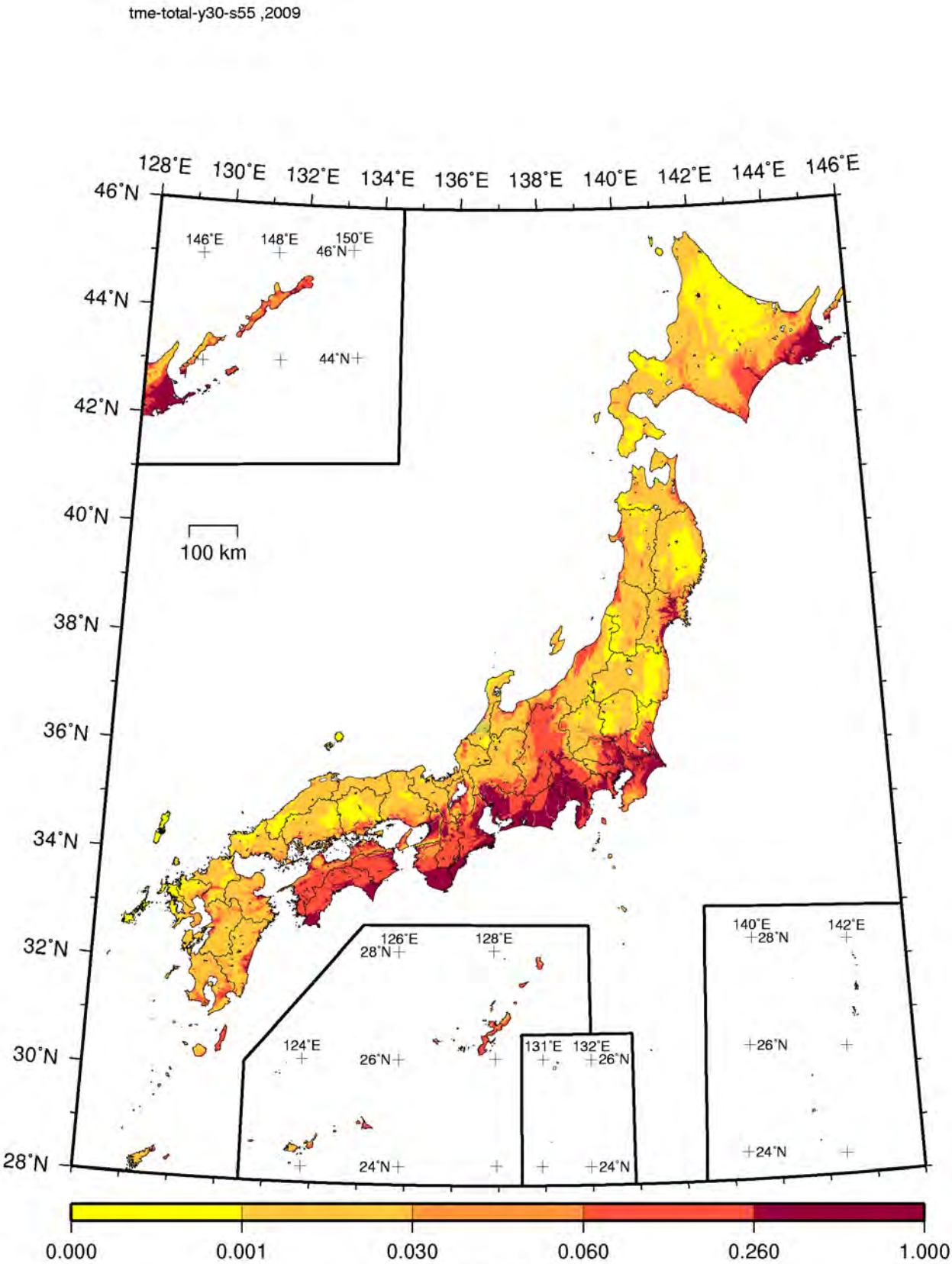

Exceedance probability within 30 years
(JMA seismic intensity: 6 Lower or more)

Figure 3.7.2-10 (3) Exceedance probability within 30 years considering all earthquakes (JMA seismic intensity: 6 Lower or more; average case)

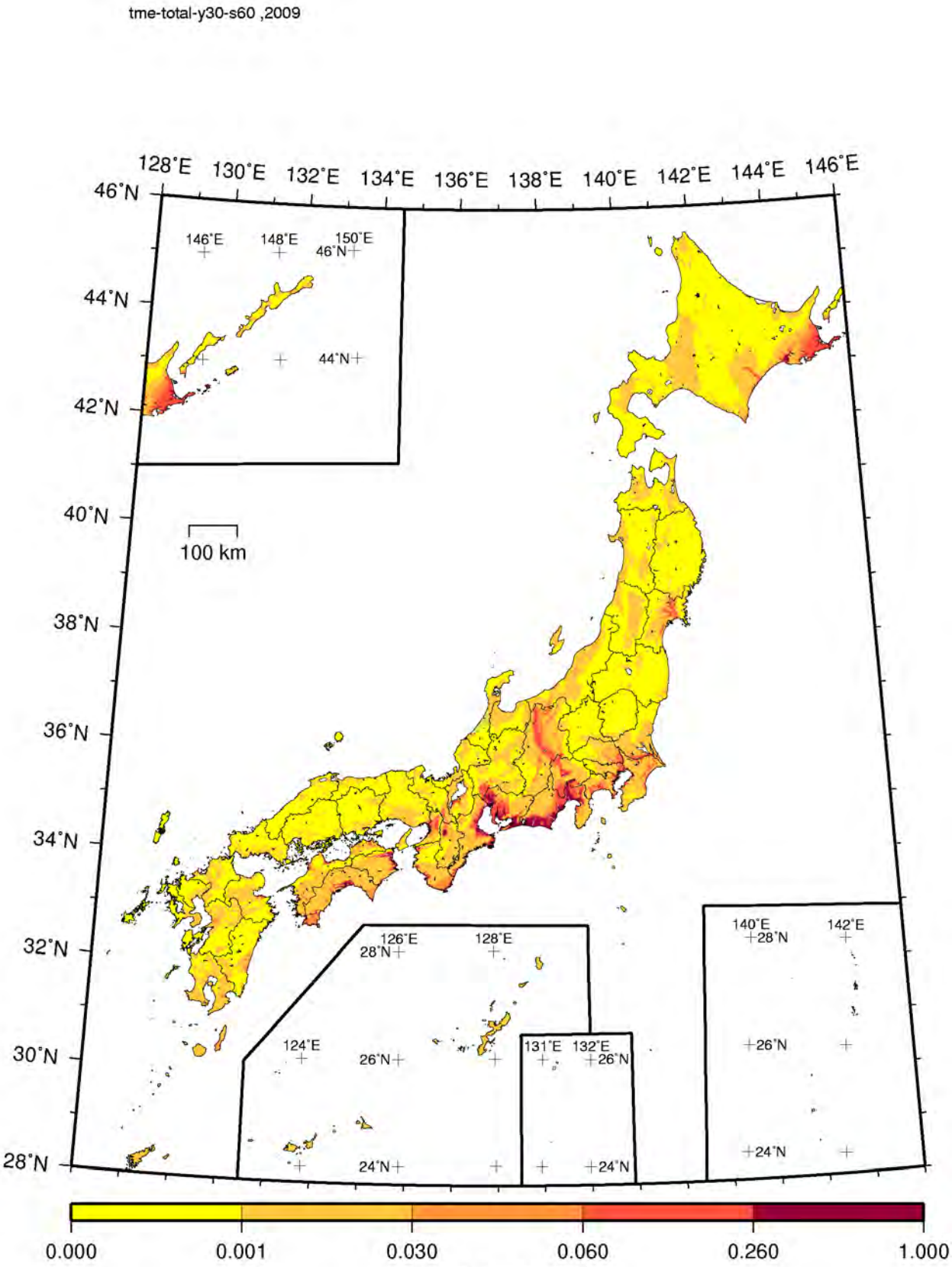

Exceedance probability within 30 years
(JMA seismic intensity: 6 Upper or more)

Figure 3.7.2-10 (4) Exceedance probability within 30 years considering all earthquakes (JMA seismic intensity: 6 Upper or more; average case)

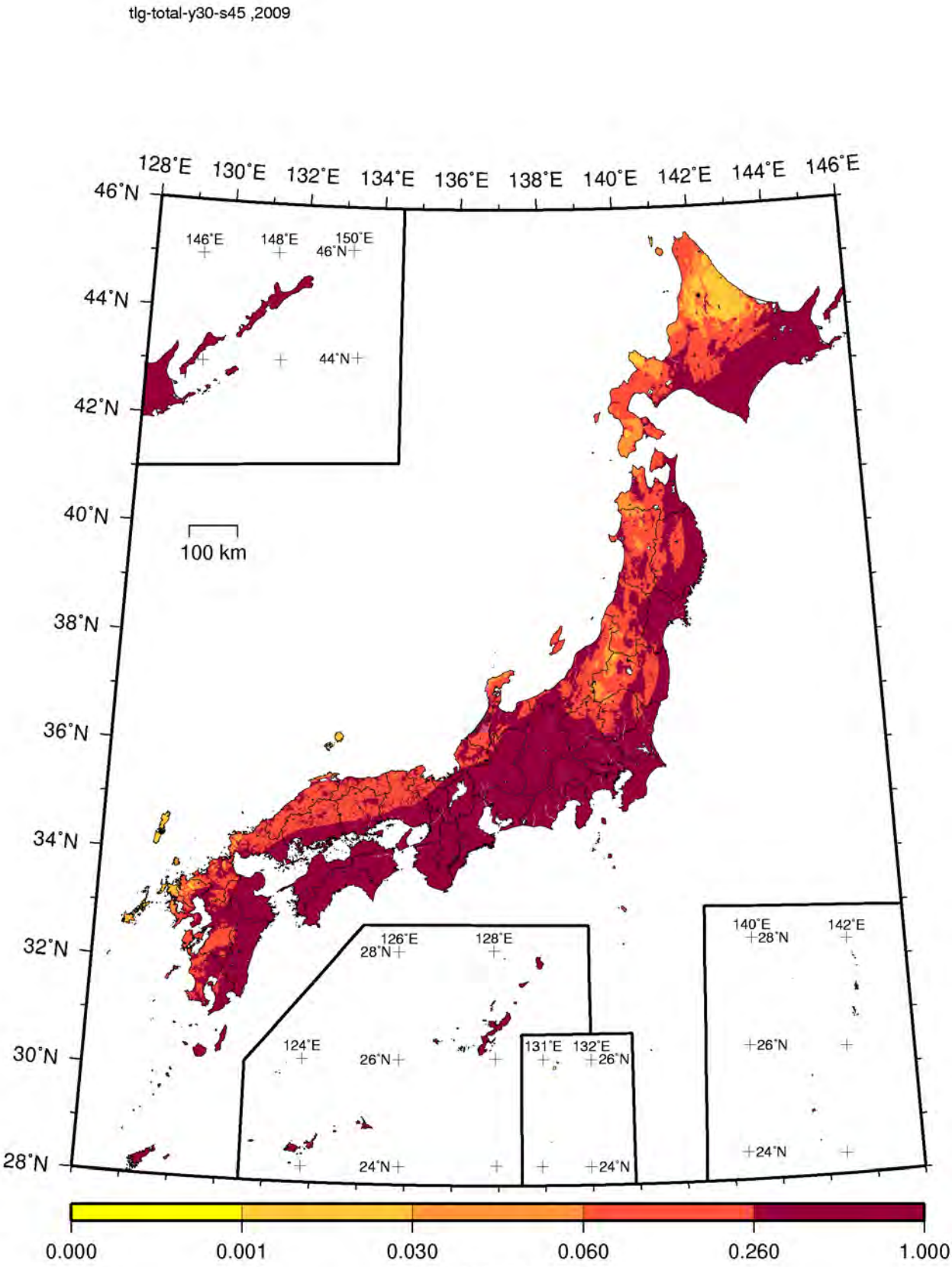

Exceedance probability within 30 years
(JMA seismic intensity: 5 Lower or more)

Figure 3.7.2-11 (1) Exceedance probability within 30 years considering all earthquakes (JMA seismic intensity: 5 Lower or more; maximum case)

tlg-total-y30-s50 ,2009

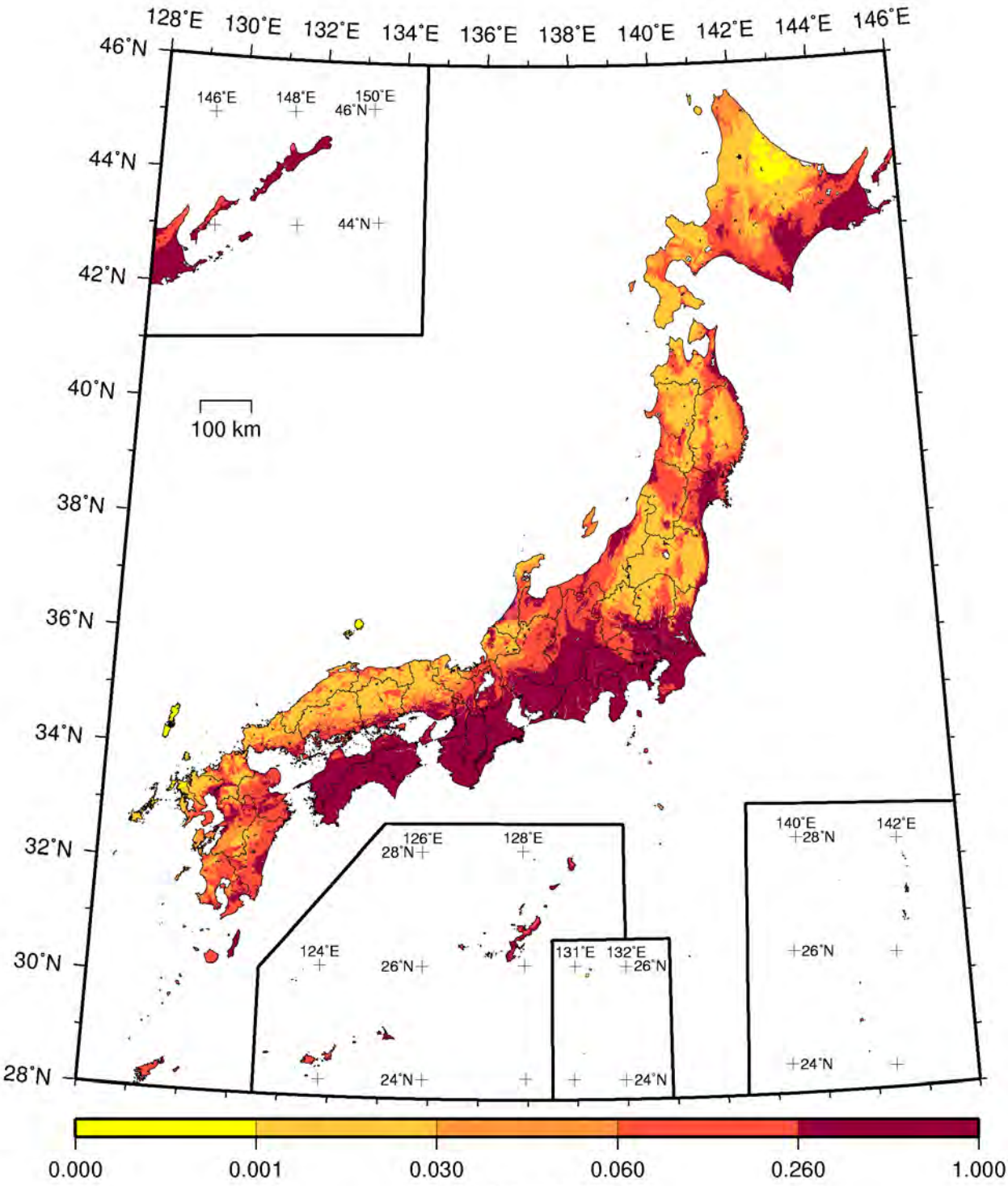

Exceedance probability within 30 years
(JMA seismic intensity: 5 Upper or more)

Figure 3.7.2-11 (2) Exceedance probability within 30 years considering all earthquakes (JMA seismic intensity: 5 Upper or more; maximum case)

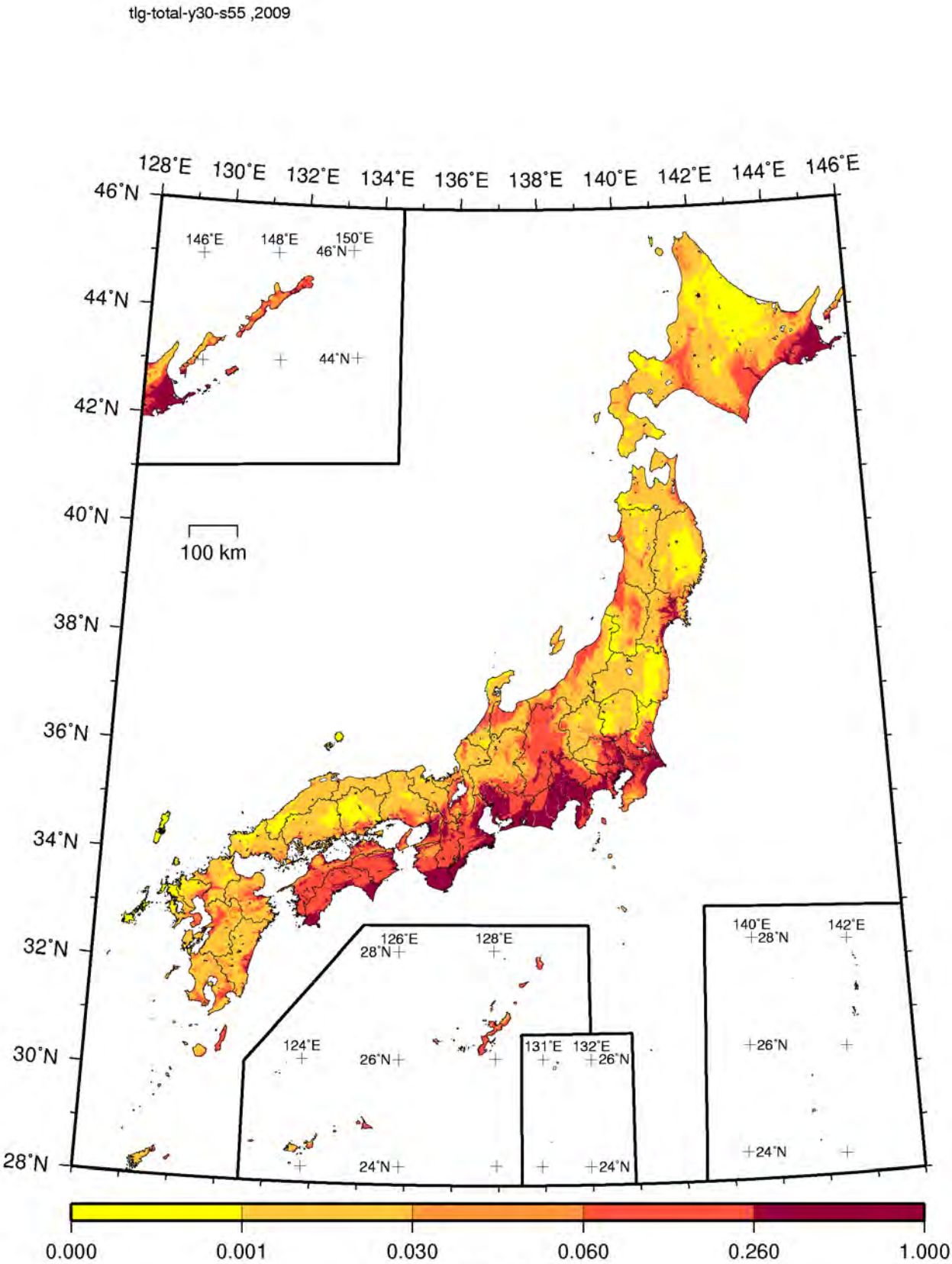

Exceedance probability within 30 years
(JMA seismic intensity: 6 Lower or more)

Figure 3.7.2-11 (3) Exceedance probability within 30 years considering all earthquakes (JMA seismic intensity: 6 Lower or more; maximum case)

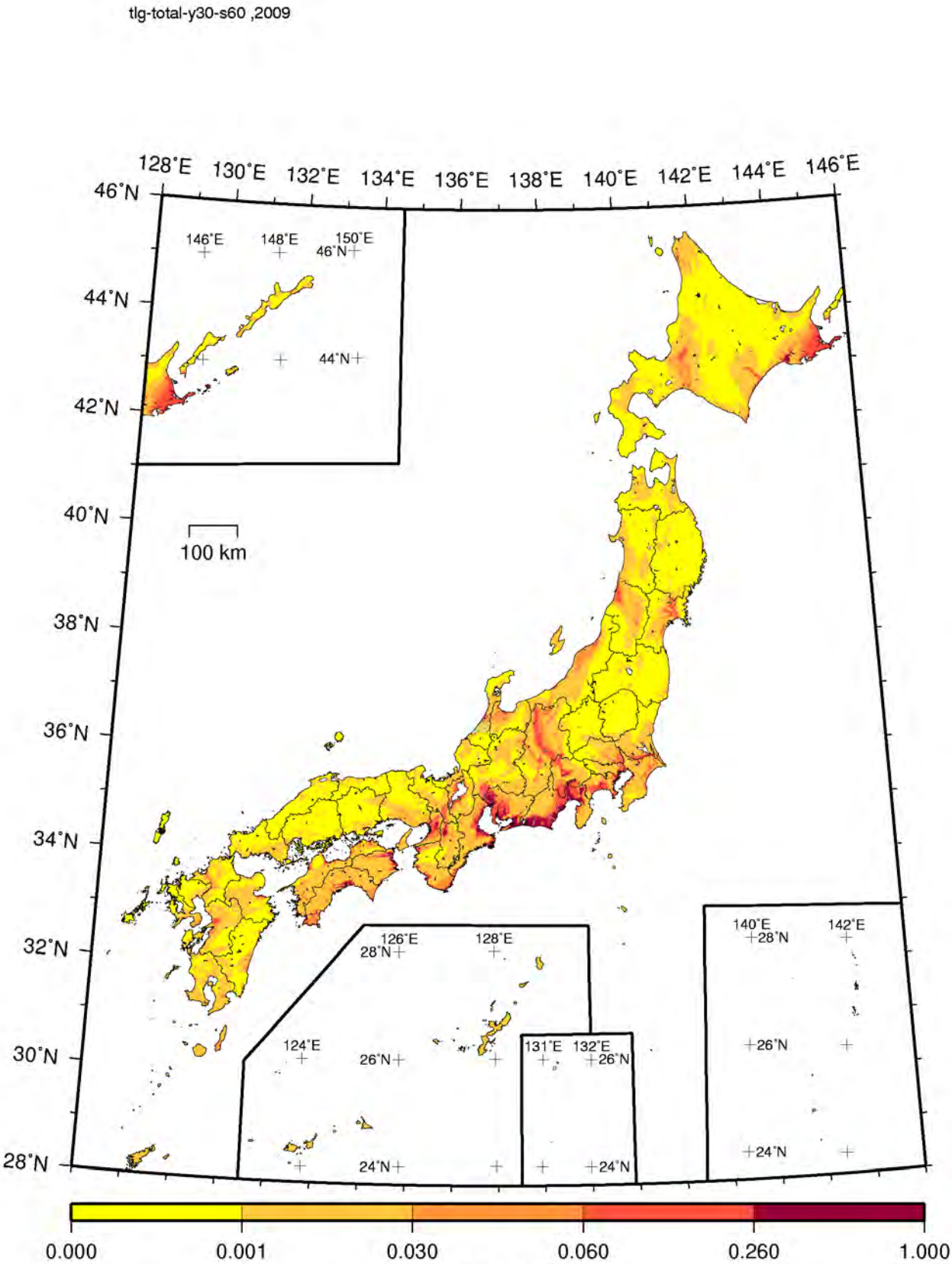

Exceedance probability within 30 years
(JMA seismic intensity: 6 Upper or more)

Figure 3.7.2-11 (4) Exceedance probability within 30 years considering all earthquakes (JMA seismic intensity: 6 Upper or more; maximum case)

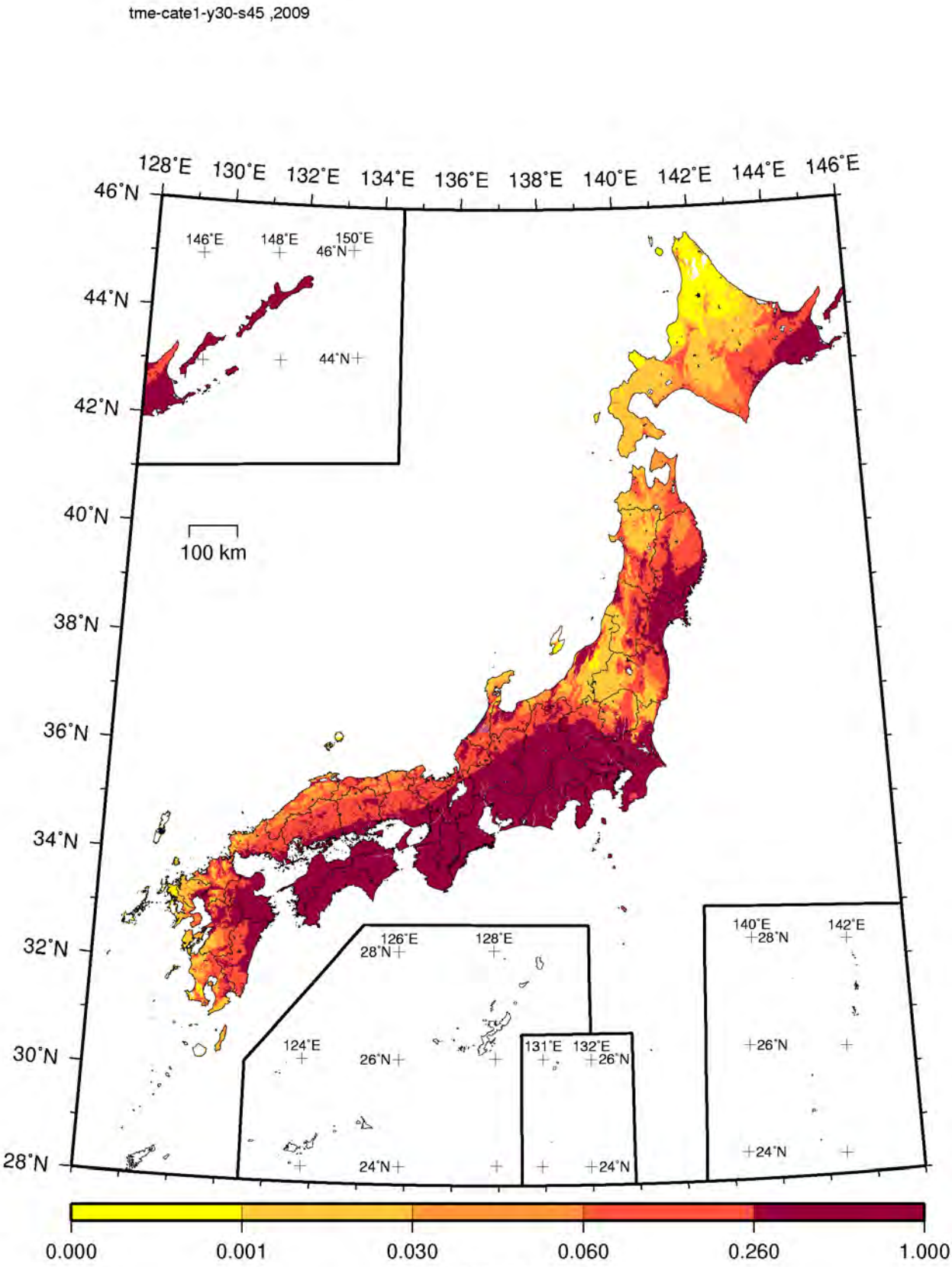

Exceedance probability within 30 years
(JMA seismic intensity: 5 Lower or more)

Figure 3.7.2-12 (1) Exceedance probability within 30 years associated with earthquake category I (JMA seismic intensity: 5 Lower or more)

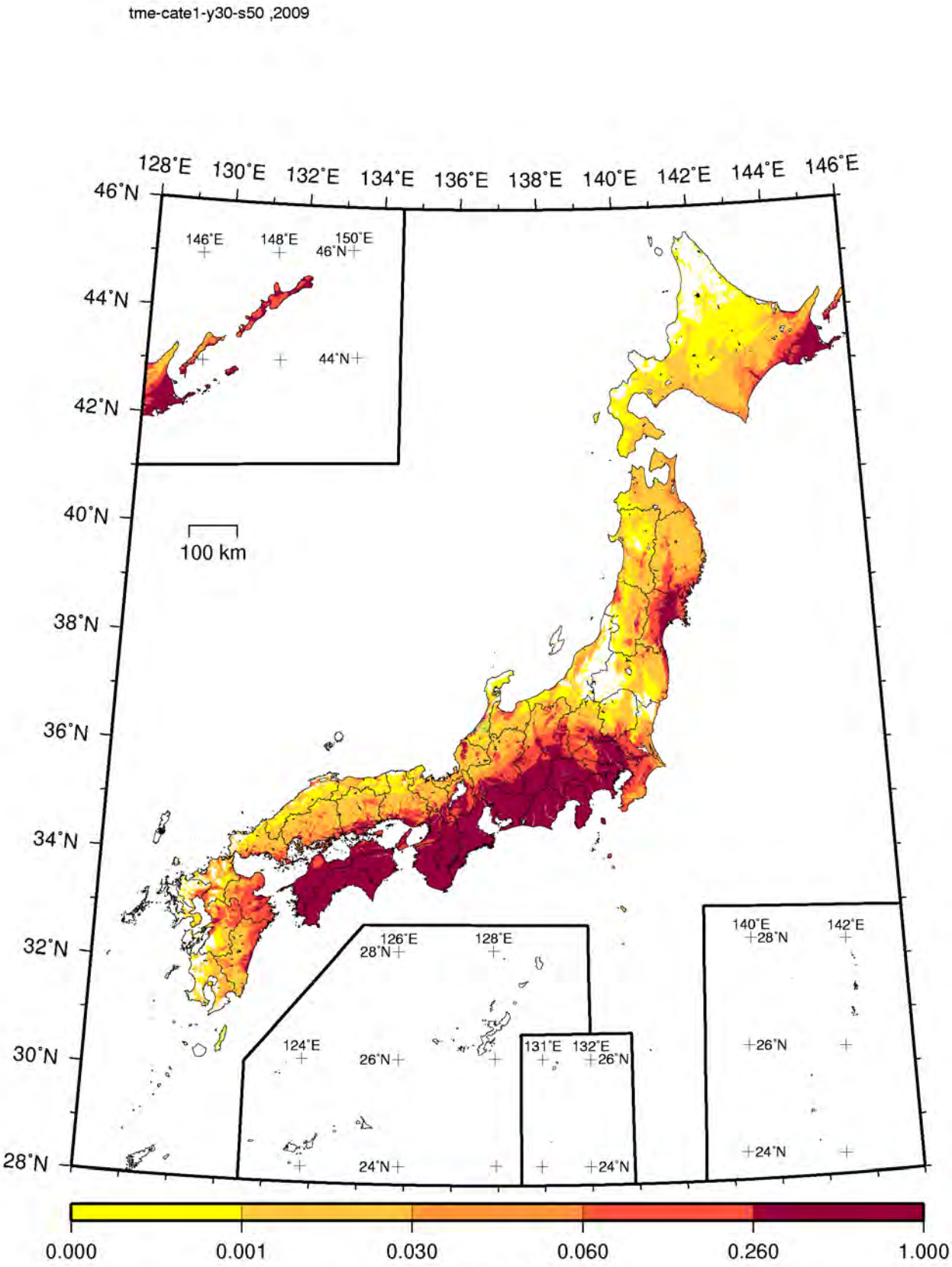

Exceedance probability within 30 years
(JMA seismic intensity: 5 Upper or more)

Figure 3.7.2-12 (2) Exceedance probability within 30 years associated with earthquake category I (JMA seismic intensity: 5 Upper or more)

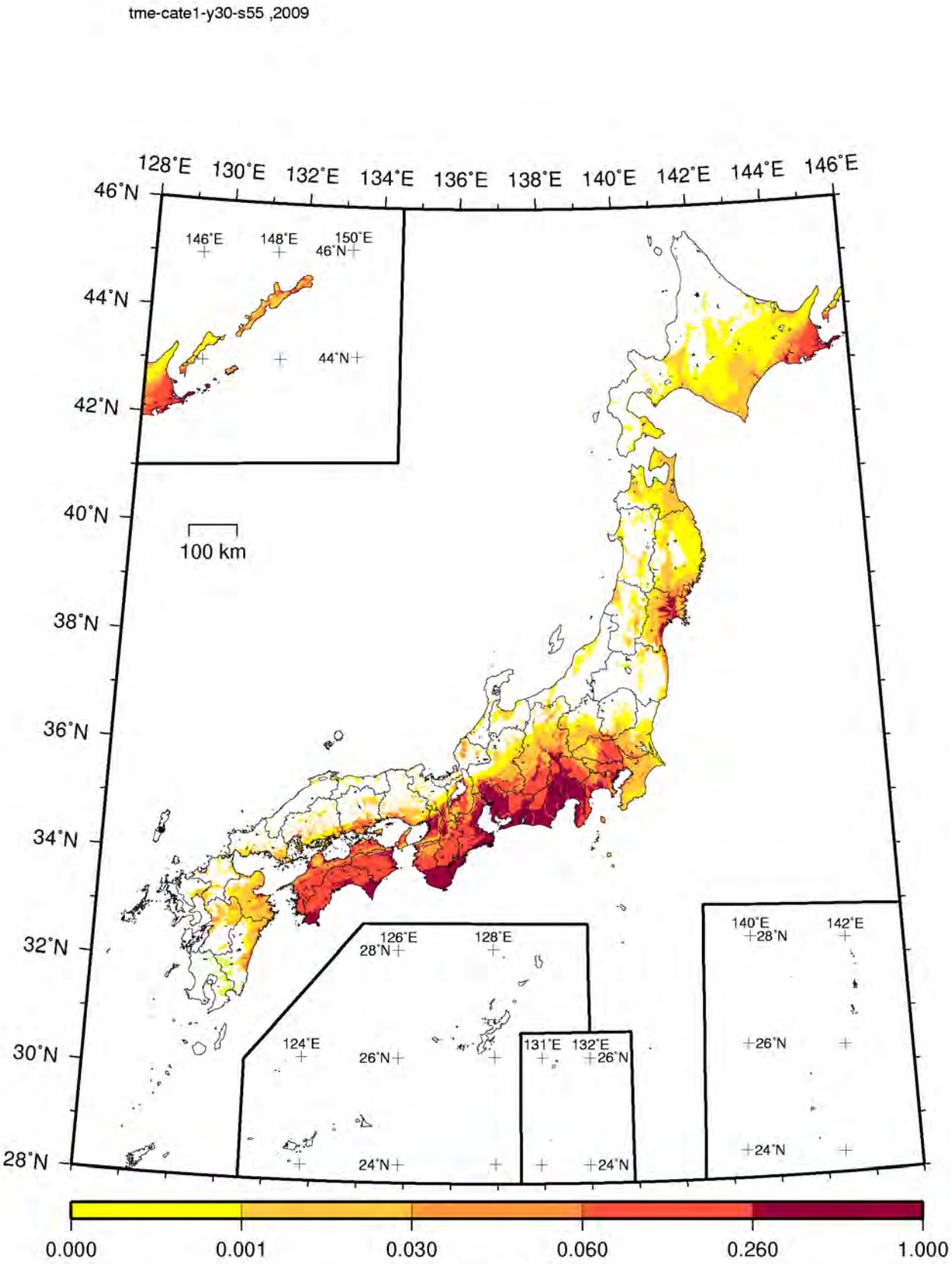

Exceedance probability within 30 years
(JMA seismic intensity: 6 Lower or more)

Figure 3.7.2-12 (3) Exceedance probability within 30 years associated with earthquake category I (JMA seismic intensity: 6 Lower or more)

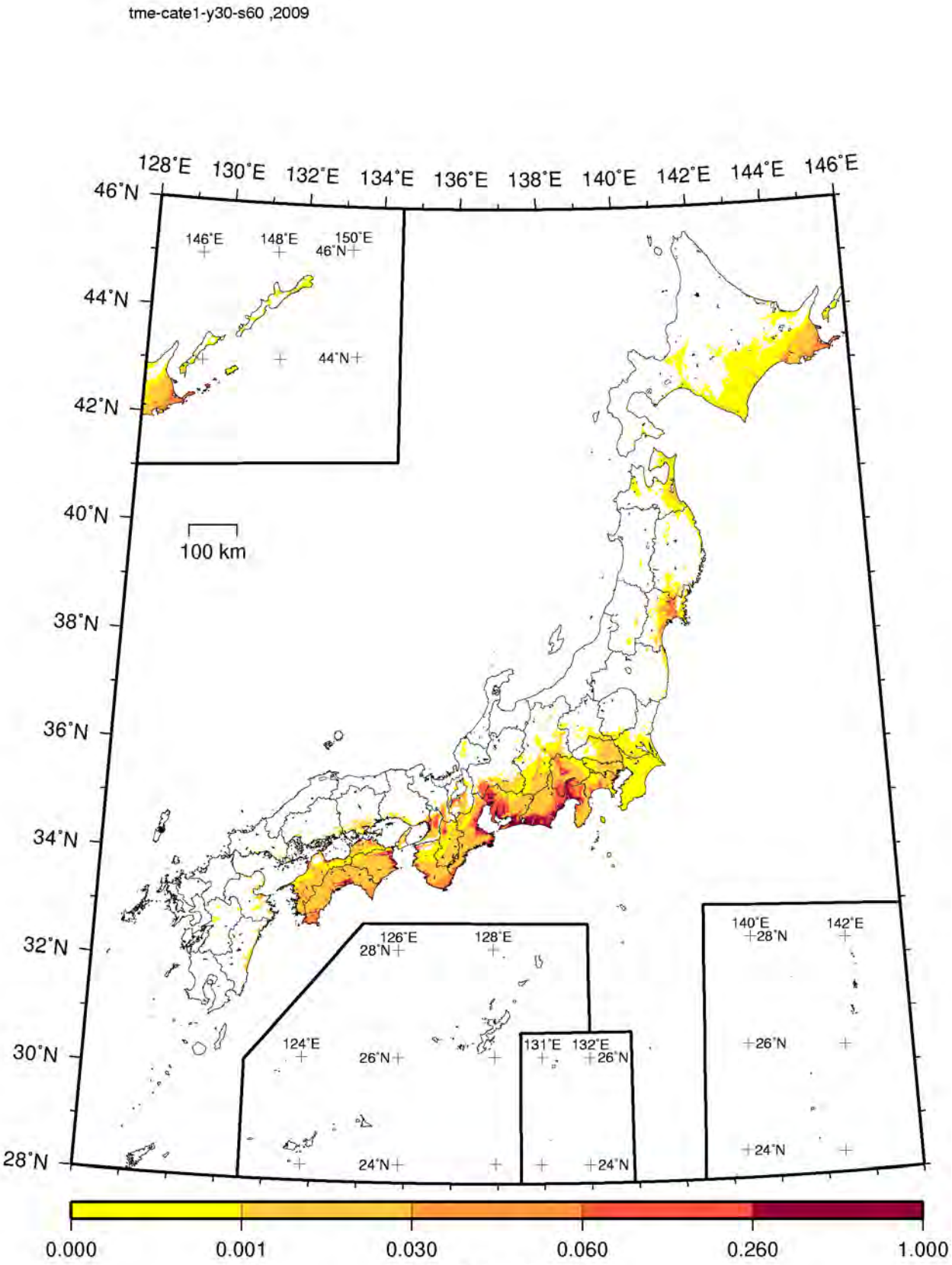

Exceedance probability within 30 years
(JMA seismic intensity: 6 Upper or more)

Figure 3.7.2-12 (4) Exceedance probability within 30 years associated with earthquake category I
(JMA seismic intensity: 6 Upper or more)

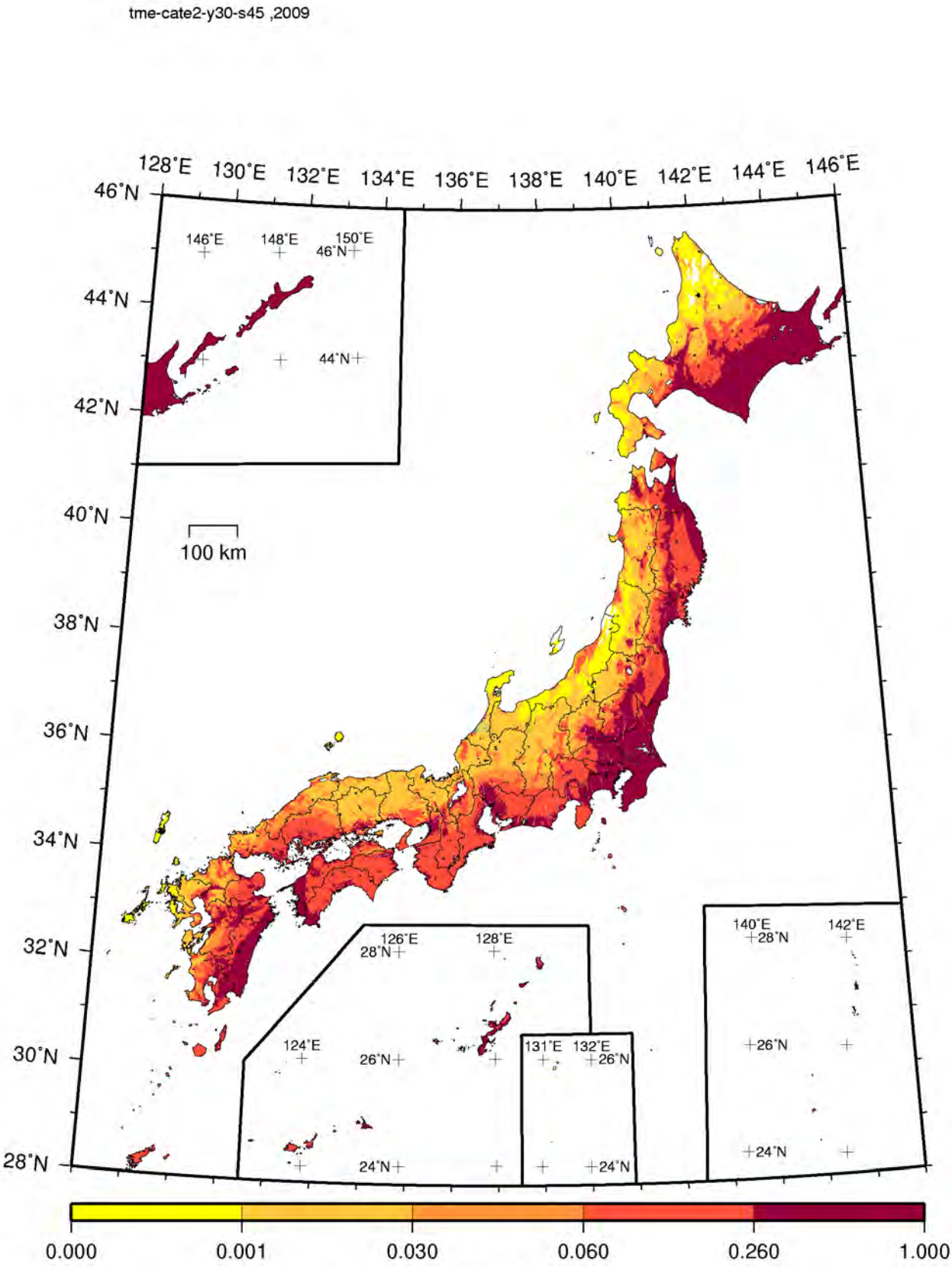

Exceedance probability within 30 years
(JMA seismic intensity: 5 Lower or more)

Figure 3.7.2-13 (1) Exceedance probability within 30 years associated with earthquake category II (JMA seismic intensity: 5 Lower or more)

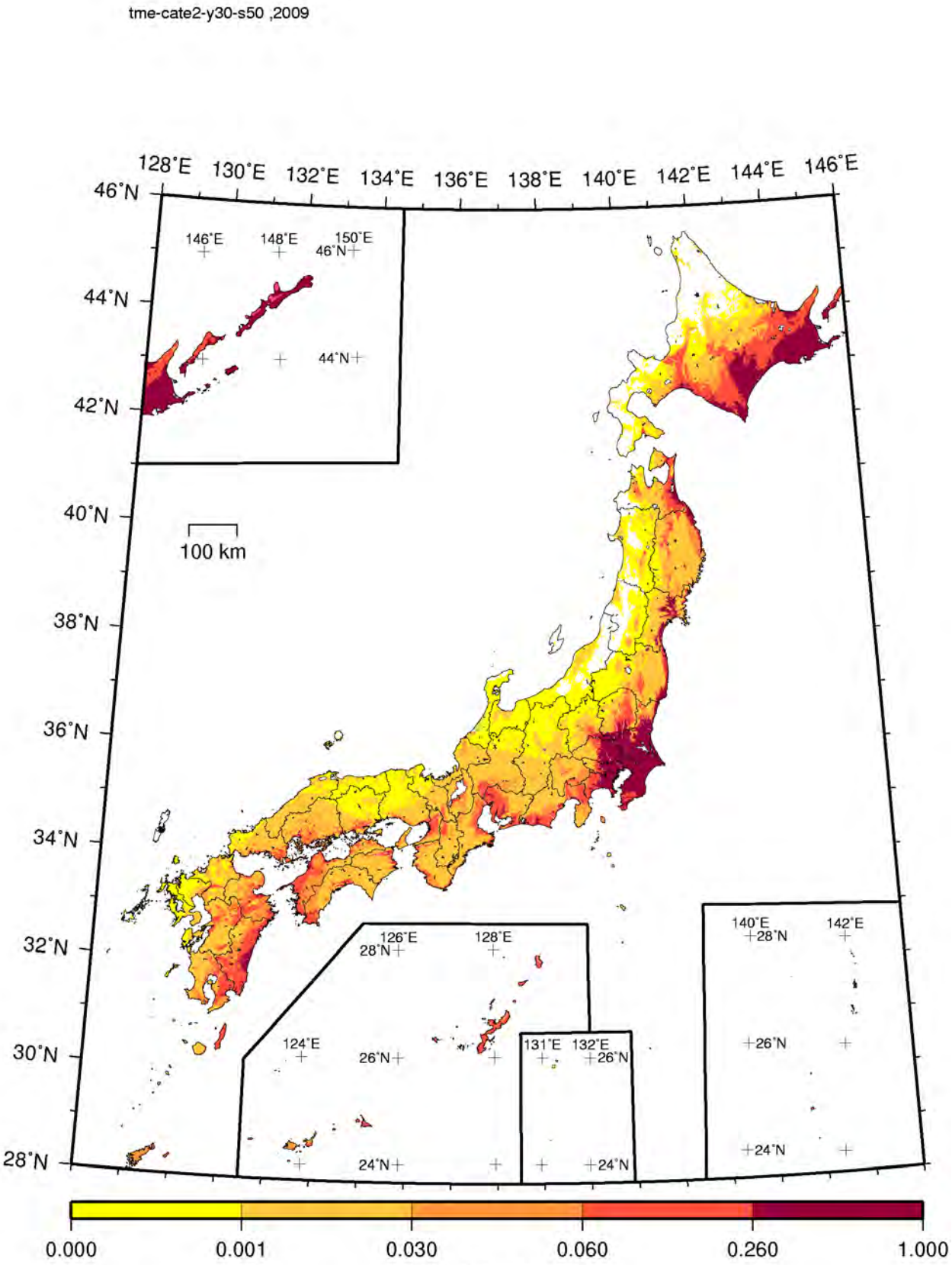

Exceedance probability within 30 years
(JMA seismic intensity: 5 Upper or more)

Figure 3.7.2-13 (2) Exceedance probability within 30 years associated with earthquake category II
(JMA seismic intensity: 5 Upper or more)

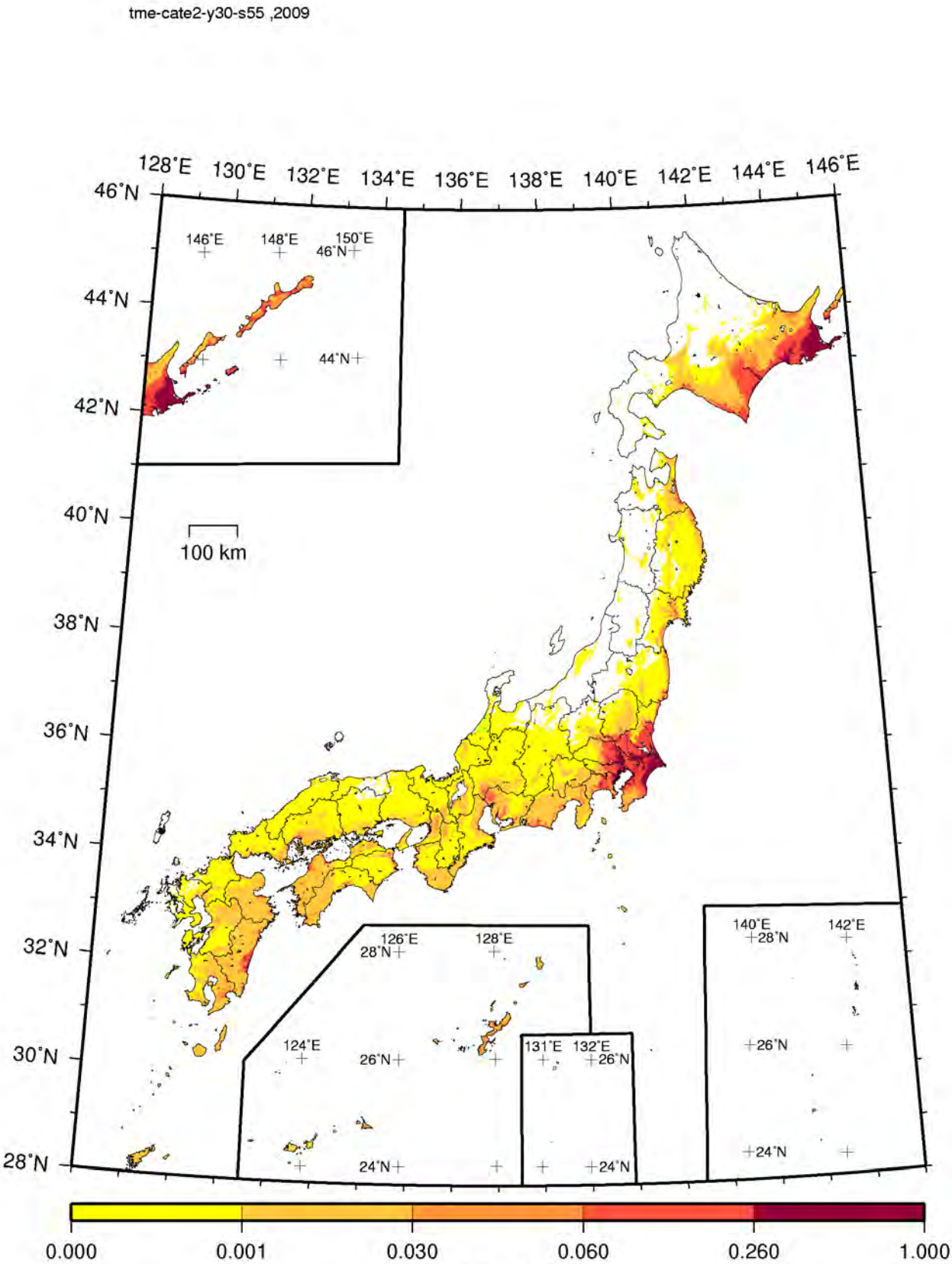

Exceedance probability within 30 years
(JMA seismic intensity: 6 Lower or more)

Figure 3.7.2-13 (3) Exceedance probability within 30 years associated with earthquake category II (JMA seismic intensity: 6 Lower or more)

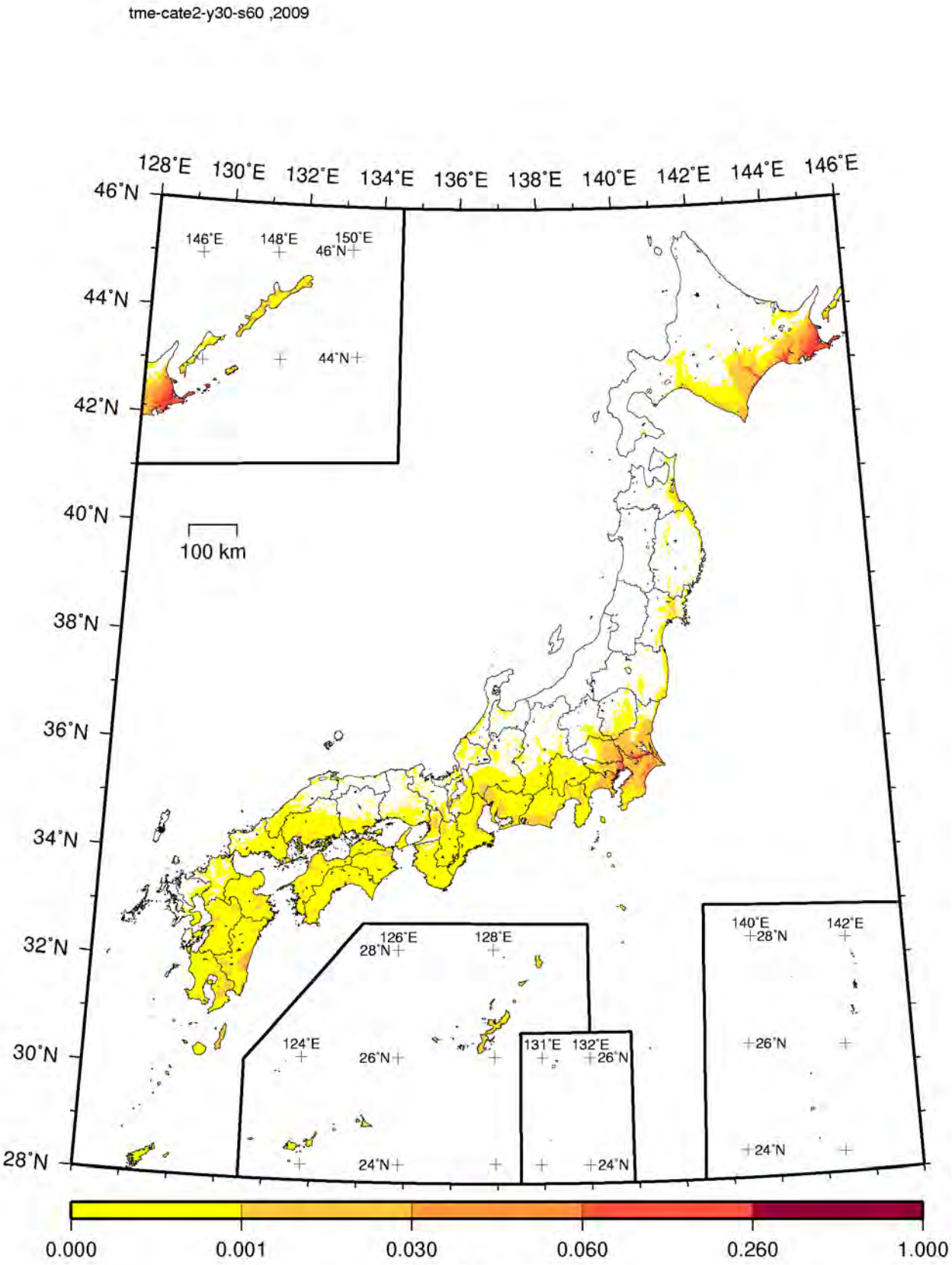

Exceedance probability within 30 years
(JMA seismic intensity: 6 Upper or more)

Figure 3.7.2-13 (4) Exceedance probability within 30 years associated with earthquake category II (JMA seismic intensity: 6 Upper or more)

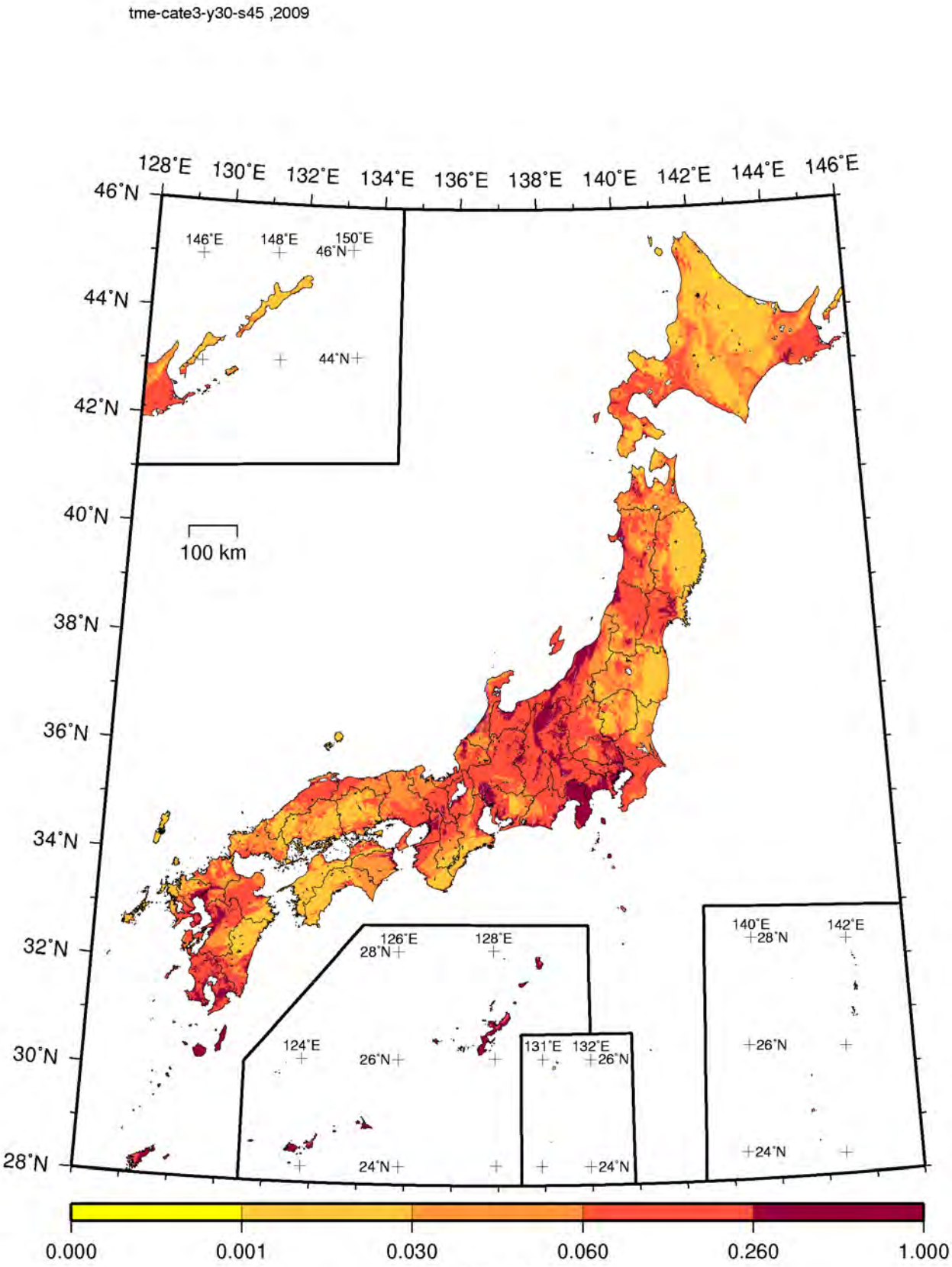

Exceedance probability within 30 years
(JMA seismic intensity: 5 Lower or more)

Figure 3.7.2-14 (1) Exceedance probability within 30 years associated with earthquake category III (JMA seismic intensity: 5 Lower or more; average case)

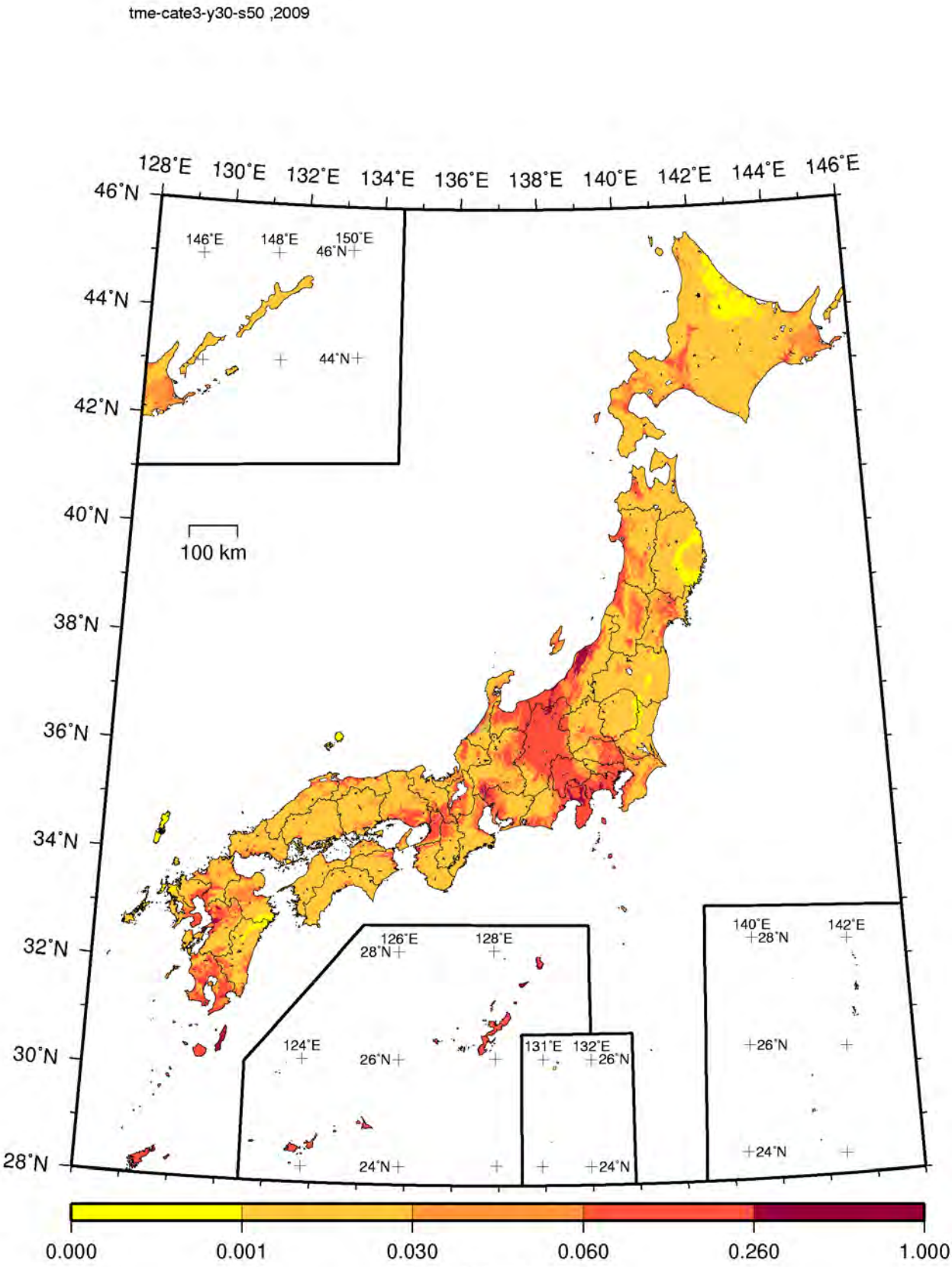

Exceedance probability within 30 years
(JMA seismic intensity: 5 Upper or more)

Figure 3.7.2-14 (2) Exceedance probability within 30 years associated with earthquake category III (JMA seismic intensity: 5 Upper or more; average case)

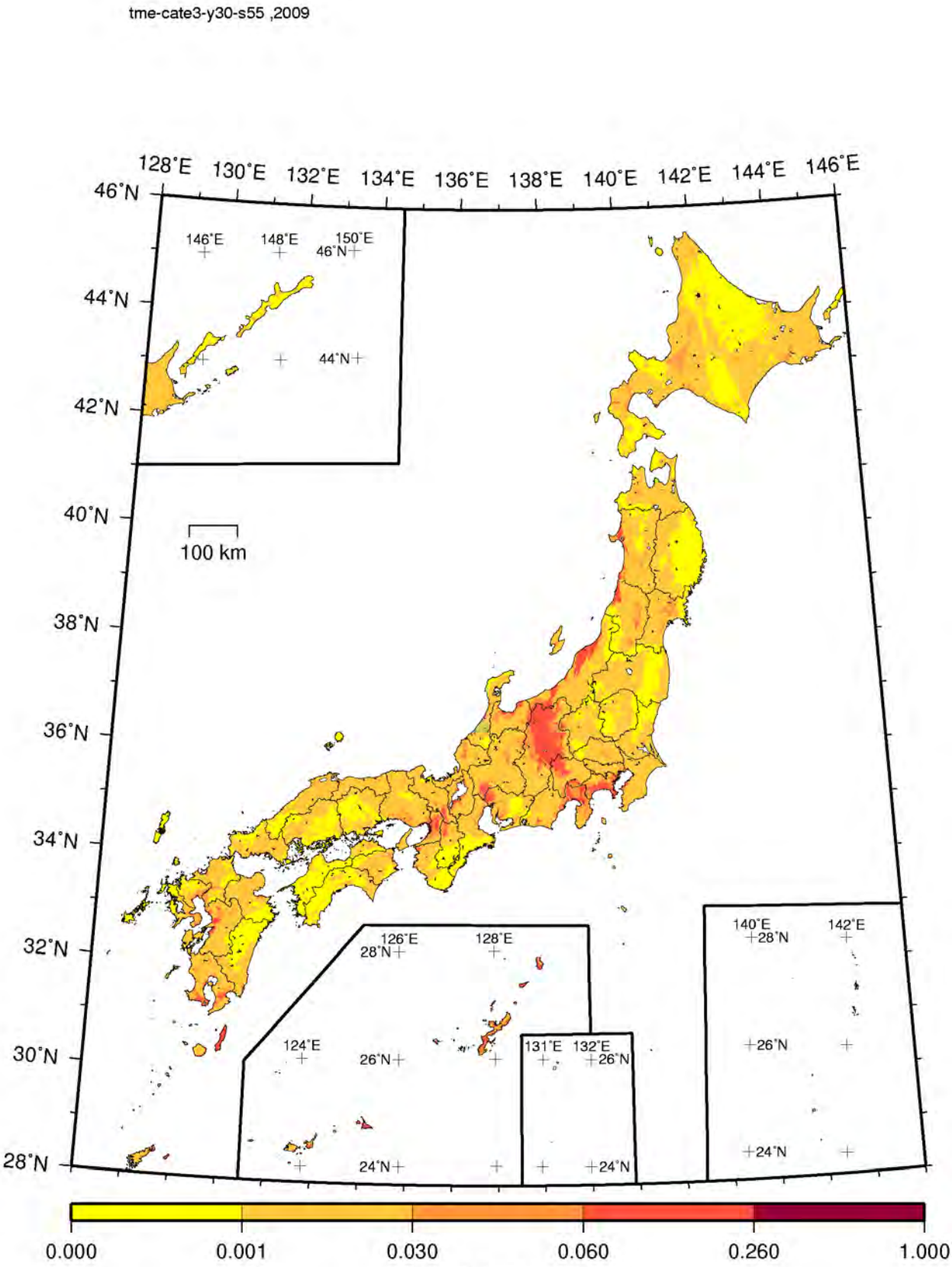

Exceedance probability within 30 years
(JMA seismic intensity: 6 Lower or more)

Figure 3.7.2-14 (3) Exceedance probability within 30 years associated with earthquake category III (JMA seismic intensity: 6 Lower or more; average case)

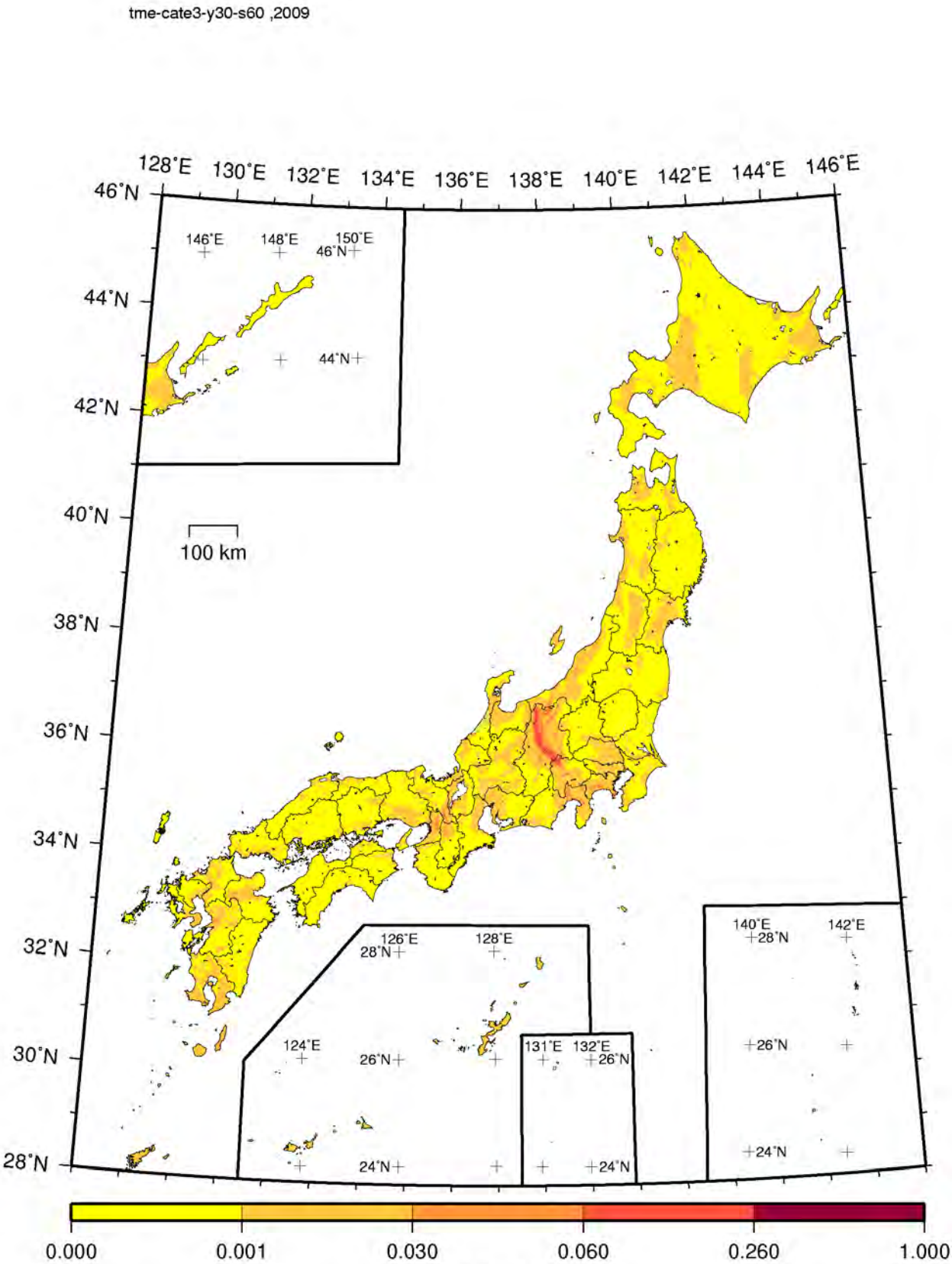

Exceedance probability within 30 years
(JMA seismic intensity: 6 Upper or more)

Figure 3.7.2-14 (4) Exceedance probability within 30 years associated with earthquake category III (JMA seismic intensity: 6 Upper or more; average case)

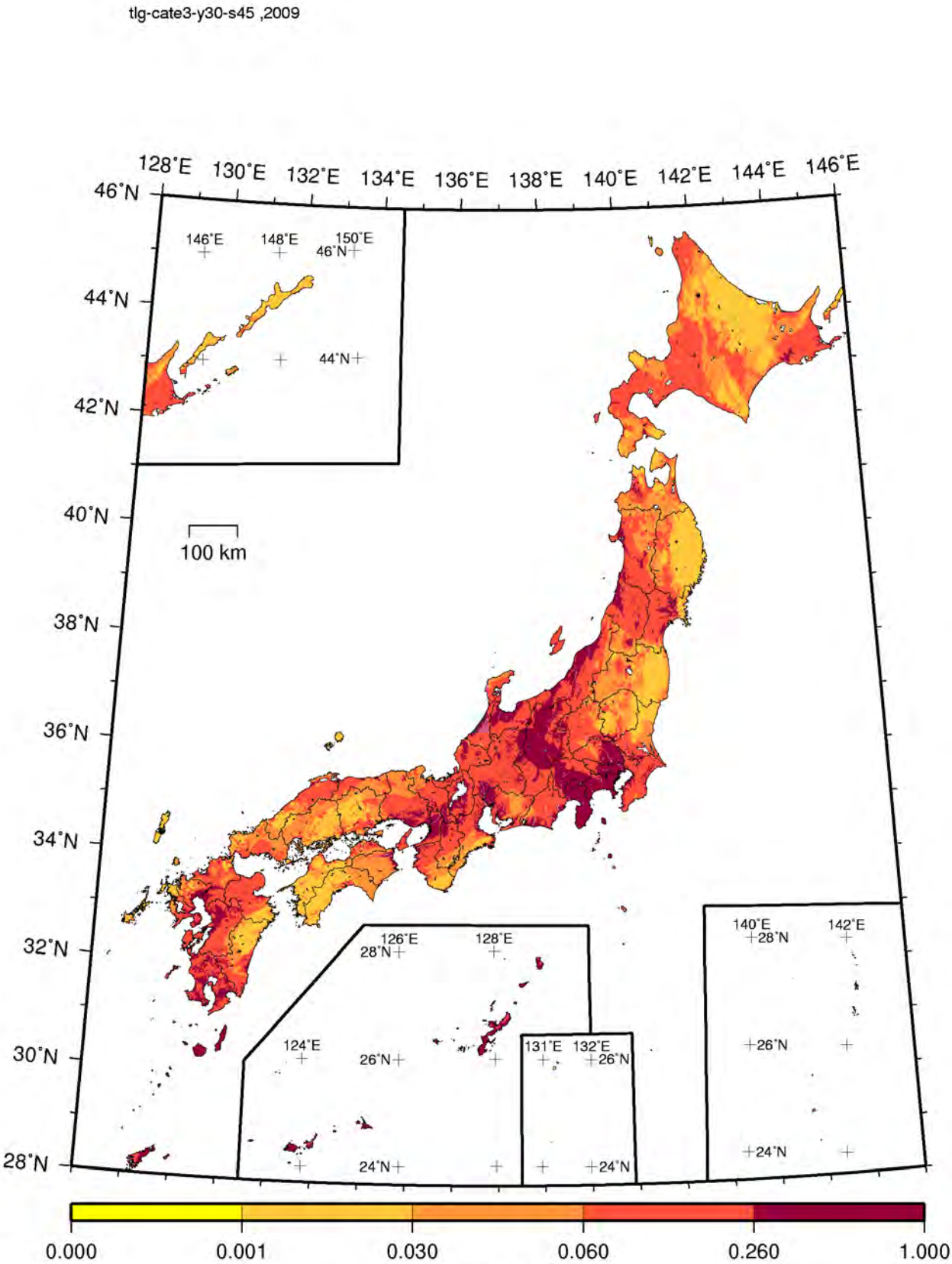

Exceedance probability within 30 years
(JMA seismic intensity: 5 Lower or more)

Figure 3.7.2-15 (1) Exceedance probability within 30 years associated with earthquake category III (JMA seismic intensity: 5 Lower or more; maximum case)

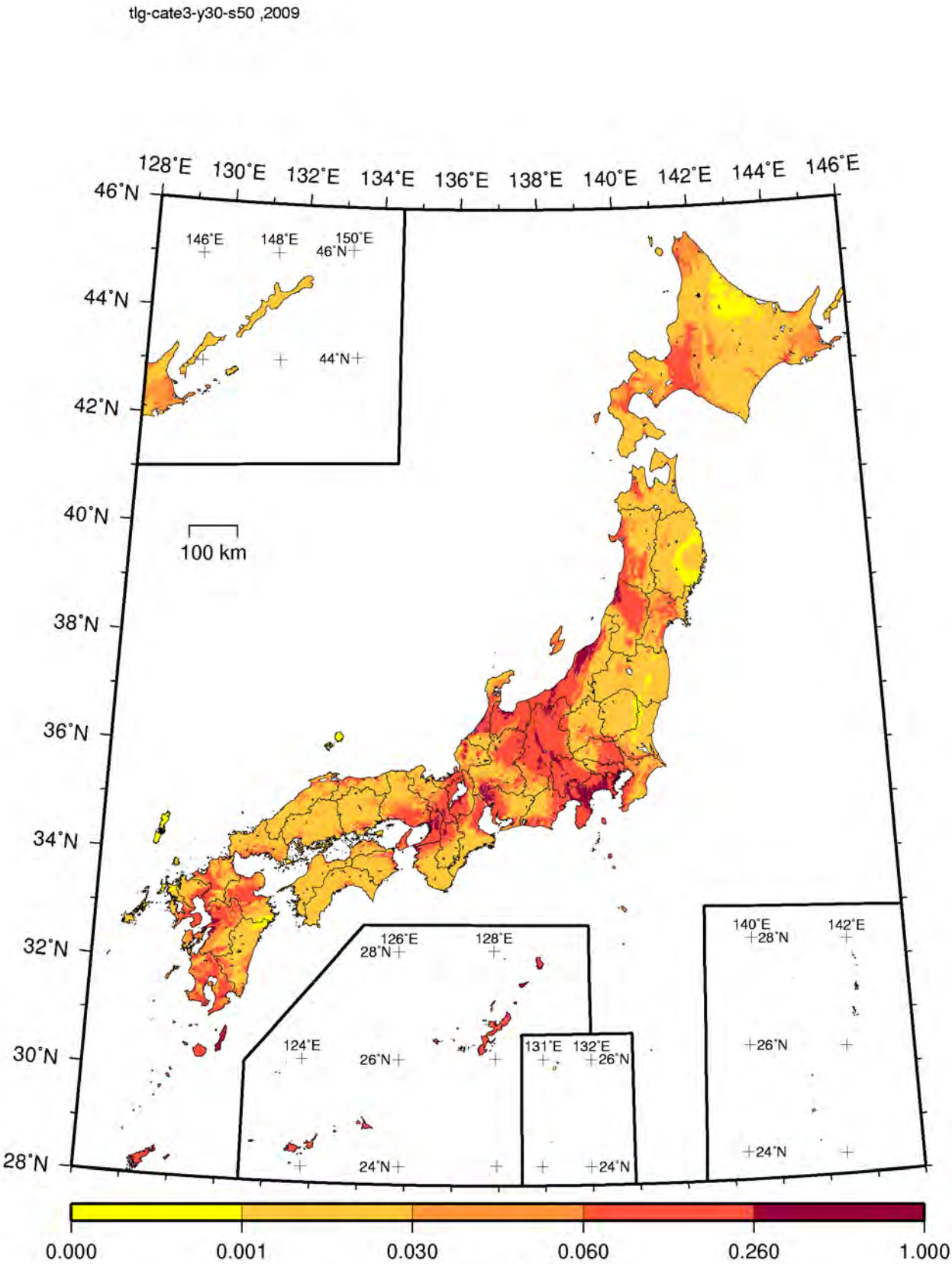

Exceedance probability within 30 years
(JMA seismic intensity: 5 Upper or more)

Figure 3.7.2-15 (2) Exceedance probability within 30 years associated with earthquake category III (JMA seismic intensity: 5 Upper or more; maximum case)

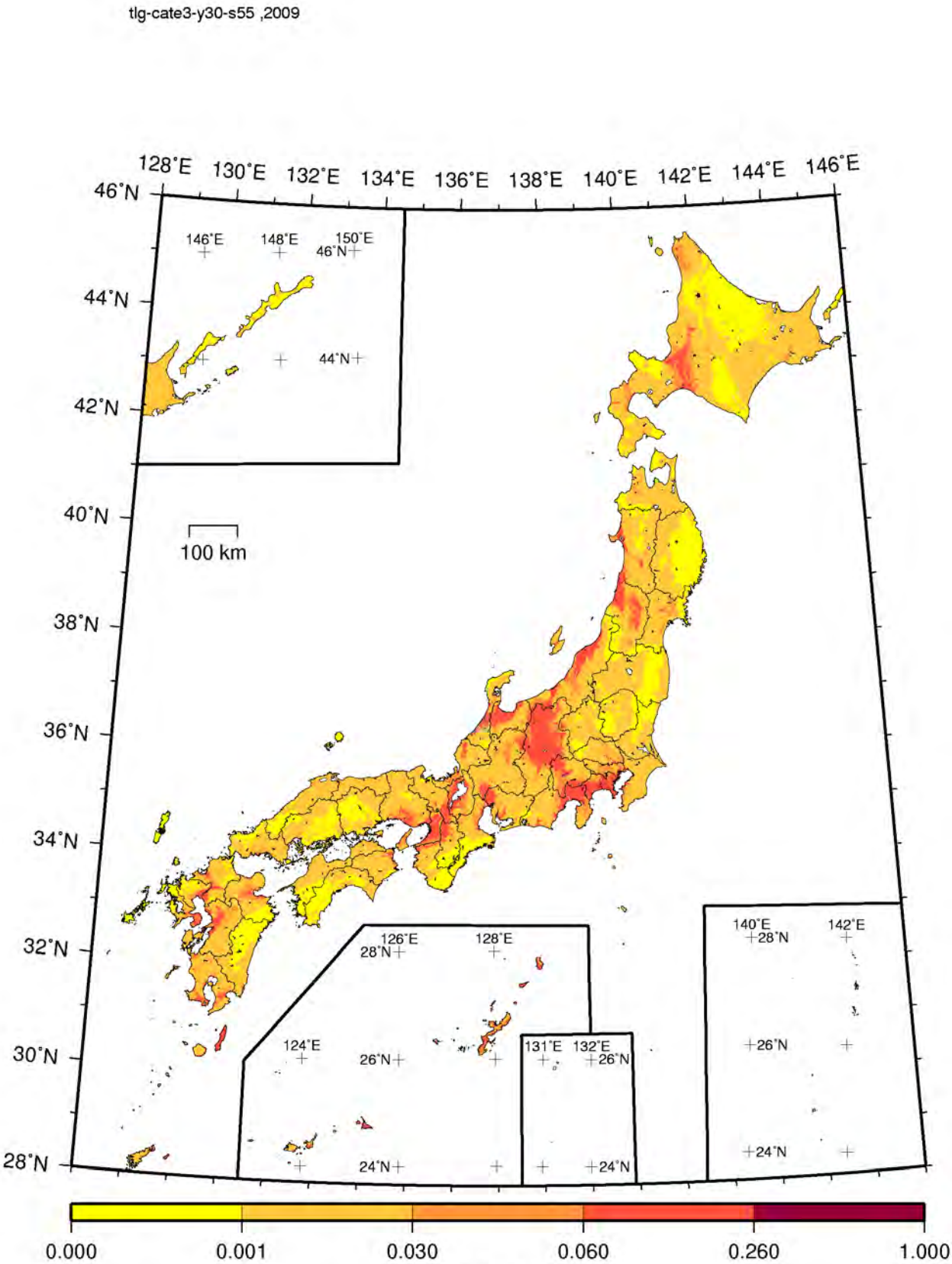

Exceedance probability within 30 years
(JMA seismic intensity: 6 Lower or more)

Figure 3.7.2-15 (3) Exceedance probability within 30 years associated with earthquake category III (JMA seismic intensity: 6 Lower or more; maximum case)

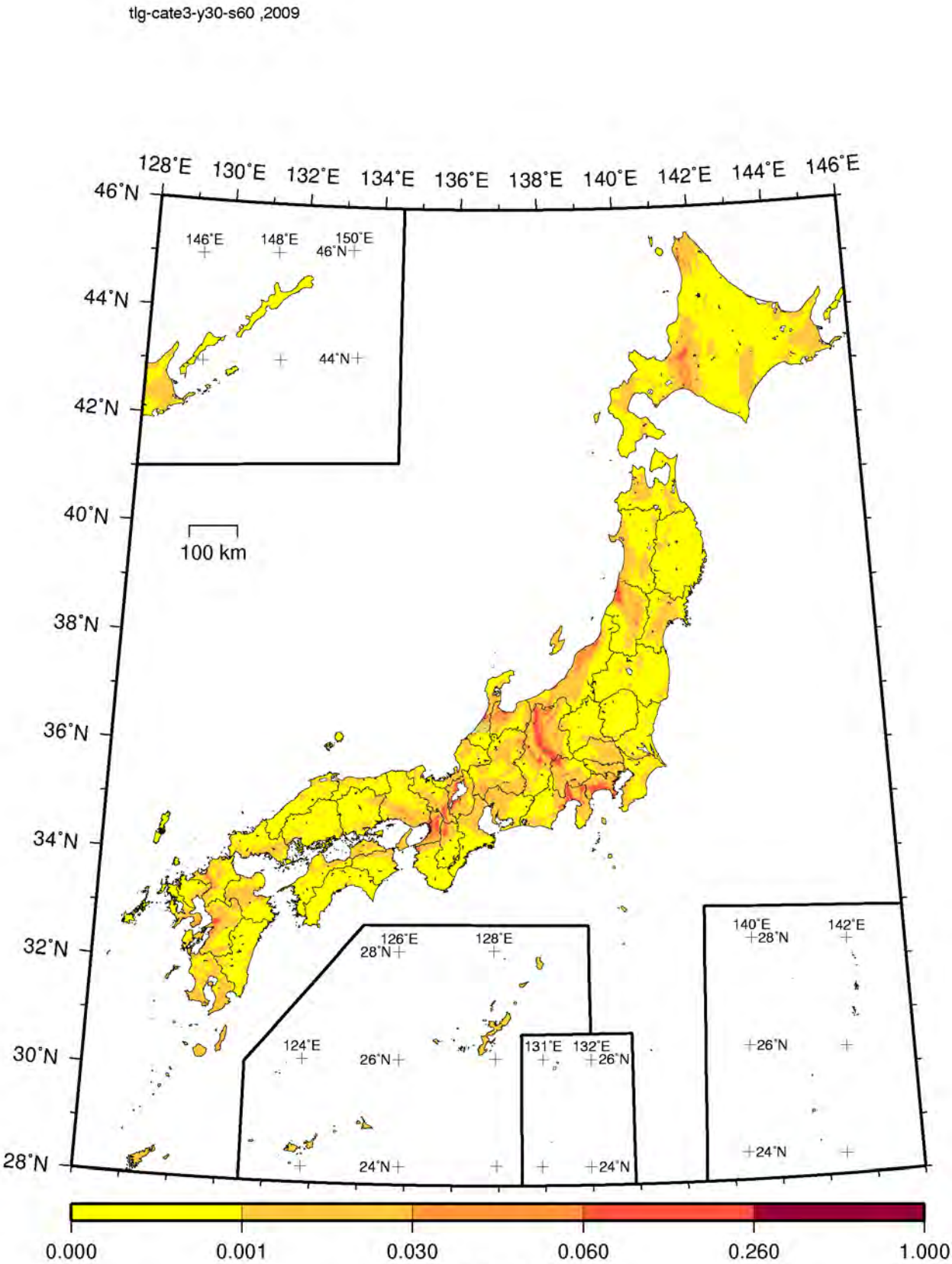

Exceedance probability within 30 years
(JMA seismic intensity: 6 Upper or more)

Figure 3.7.2-15 (4) Exceedance probability within 30 years associated with earthquake category III (JMA seismic intensity: 6 Upper or more; maximum case)

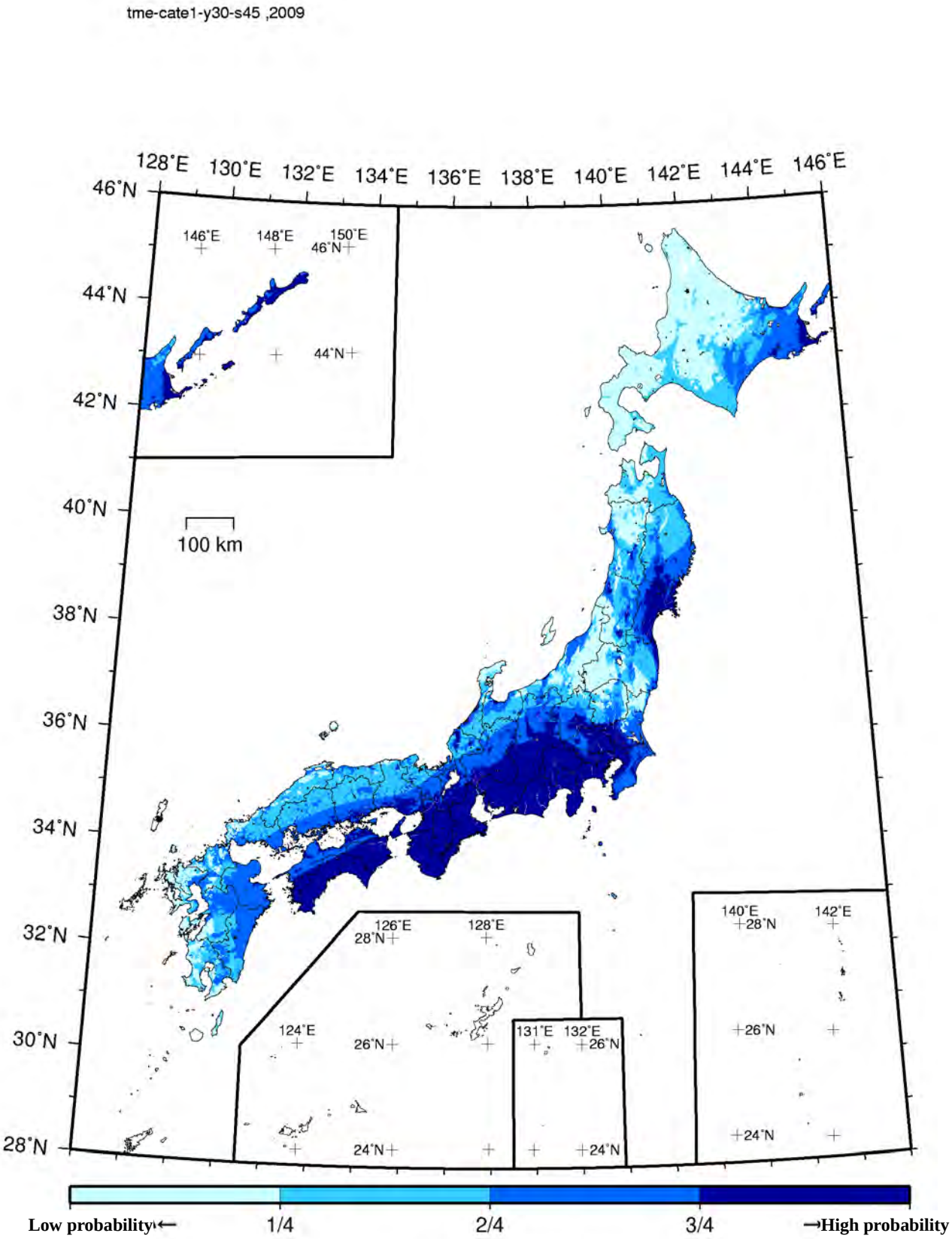

Exceedance probability within 30 years (in quartiles)
(JMA seismic intensity: 5 Lower or more)

Figure 3.7.2-16 (1) Exceedance probability within 30 years in quartiles associated with earthquake category I (JMA seismic intensity: 5 Lower or more)

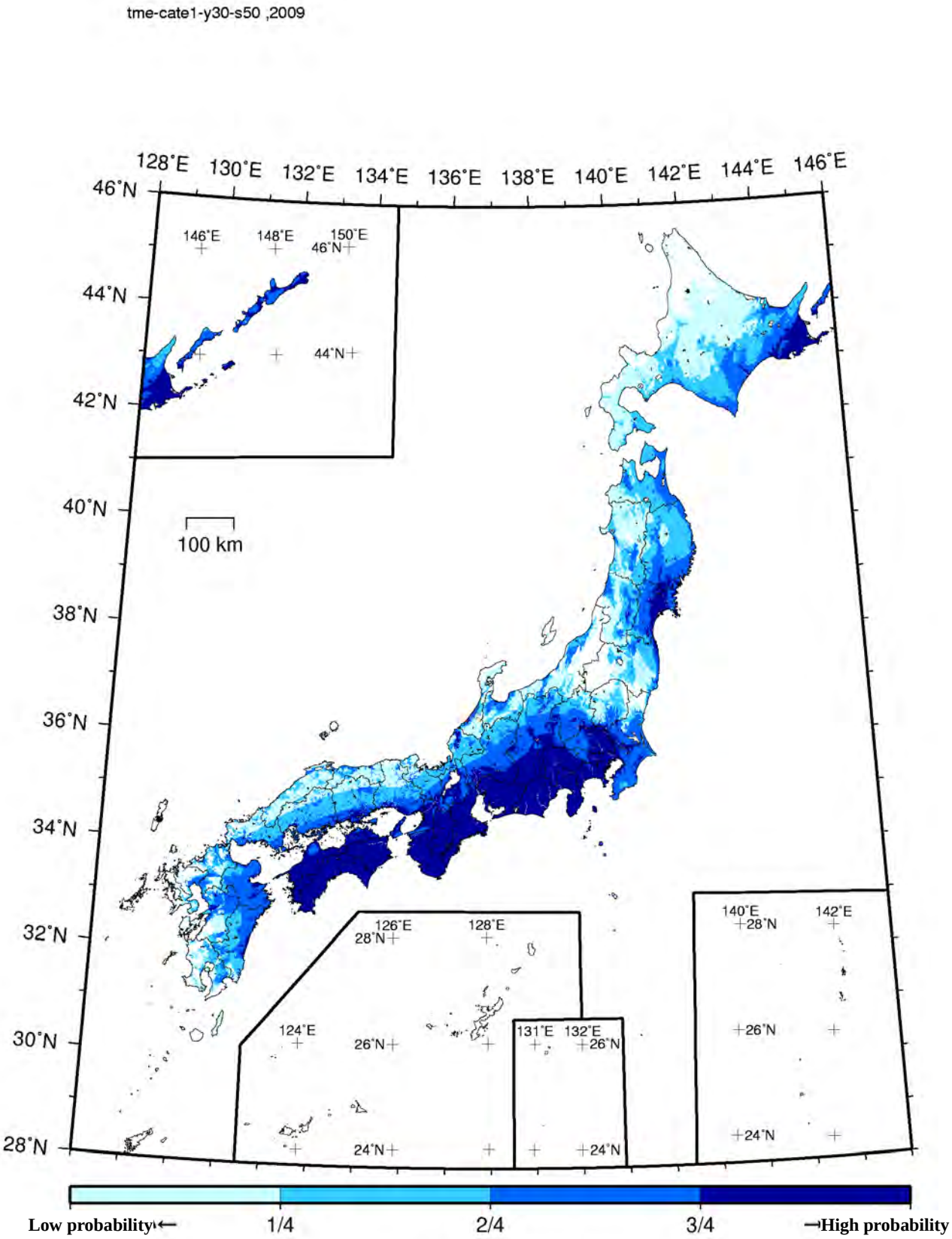

Exceedance probability within 30 years (in quartiles)
(JMA seismic intensity: 5 Upper or more)

Figure 3.7.2-16 (2) Exceedance probability within 30 years in quartiles associated with earthquake category I (JMA seismic intensity: 5 Upper or more)

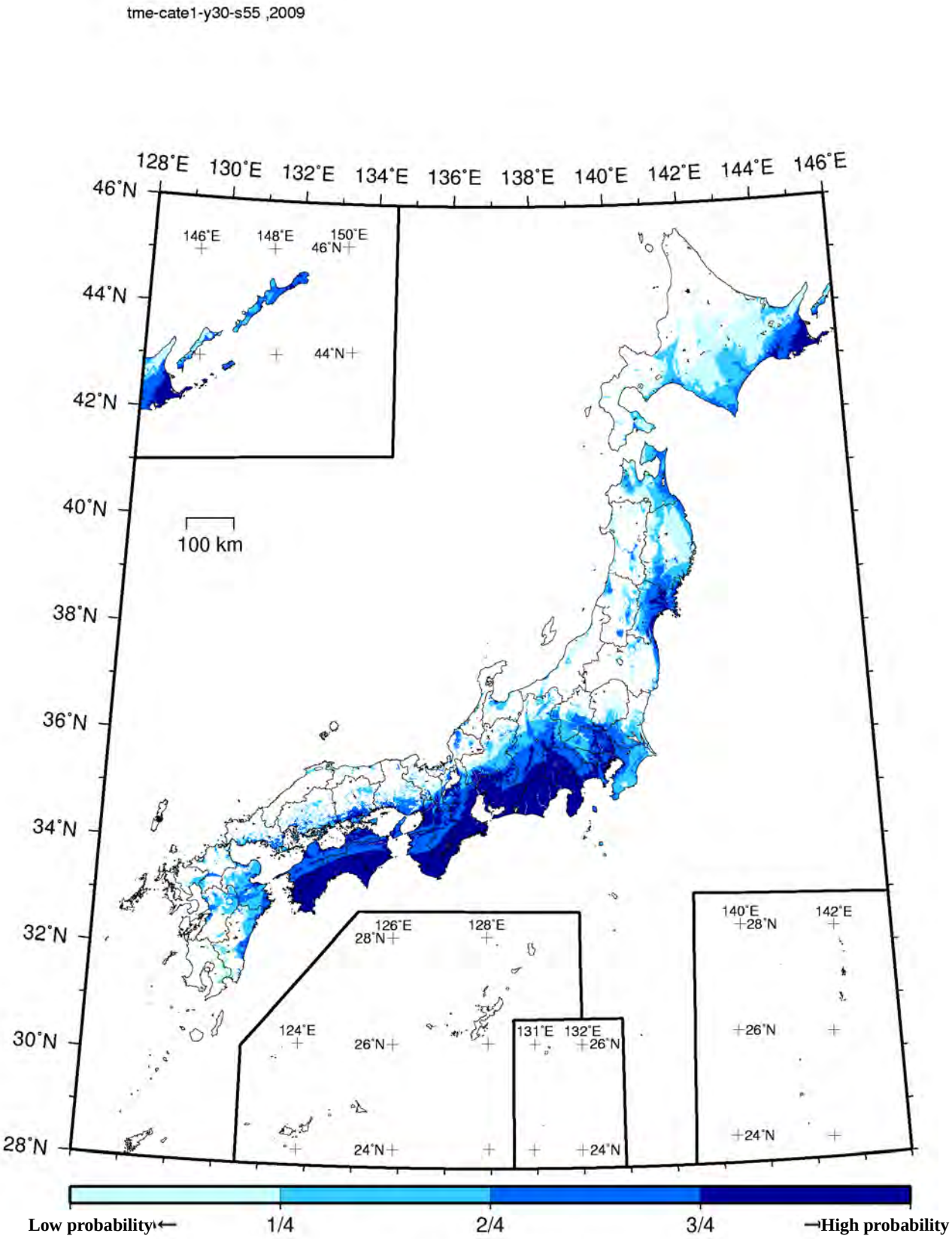

Exceedance probability within 30 years (in quartiles)
(JMA seismic intensity: 6 Lower or more)

Figure 3.7.2-16 (3) Exceedance probability within 30 years in quartiles associated with earthquake category I (JMA seismic intensity: 6 Lower or more)

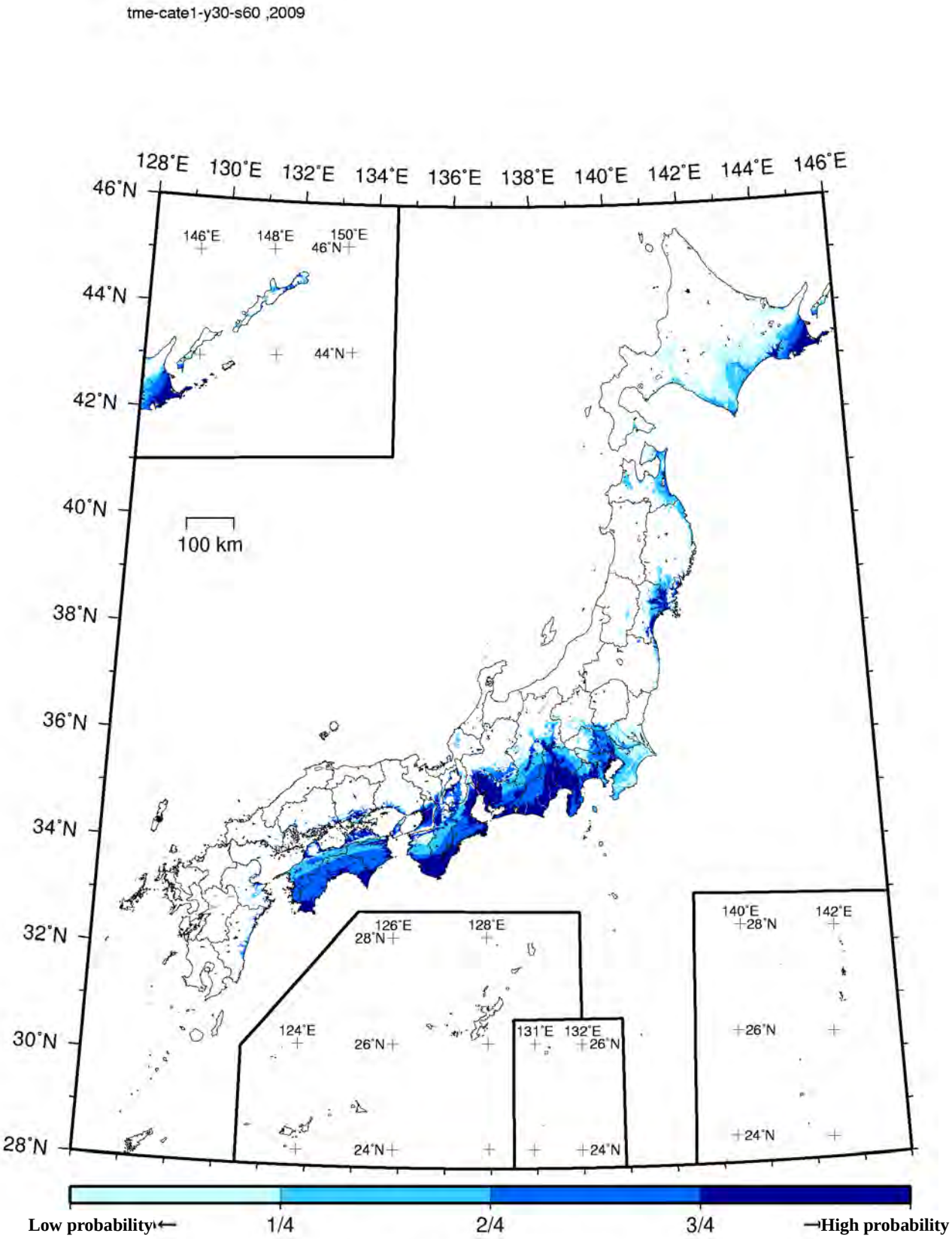

Exceedance probability within 30 years (in quartiles)
(JMA seismic intensity: 6 Upper or more)

Figure 3.7.2-16 (4) Exceedance probability within 30 years in quartiles associated with earthquake category I (JMA seismic intensity: 6 Upper or more)

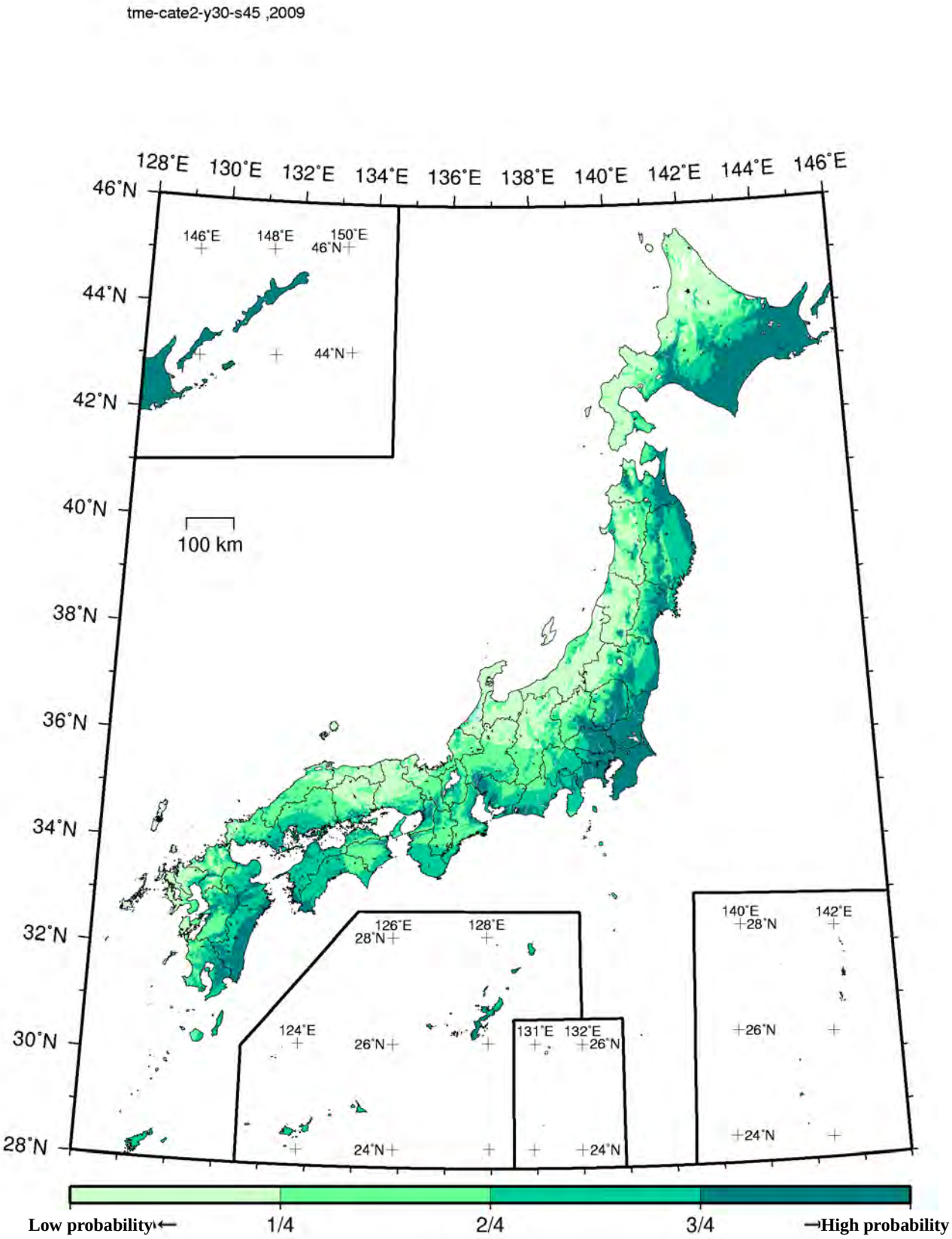

Exceedance probability within 30 years (in quartiles)
(JMA seismic intensity: 5 Lower or more)

Figure 3.7.2-17 (1) Exceedance probability within 30 years in quartiles associated with earthquake category II (JMA seismic intensity: 5 Lower or more)

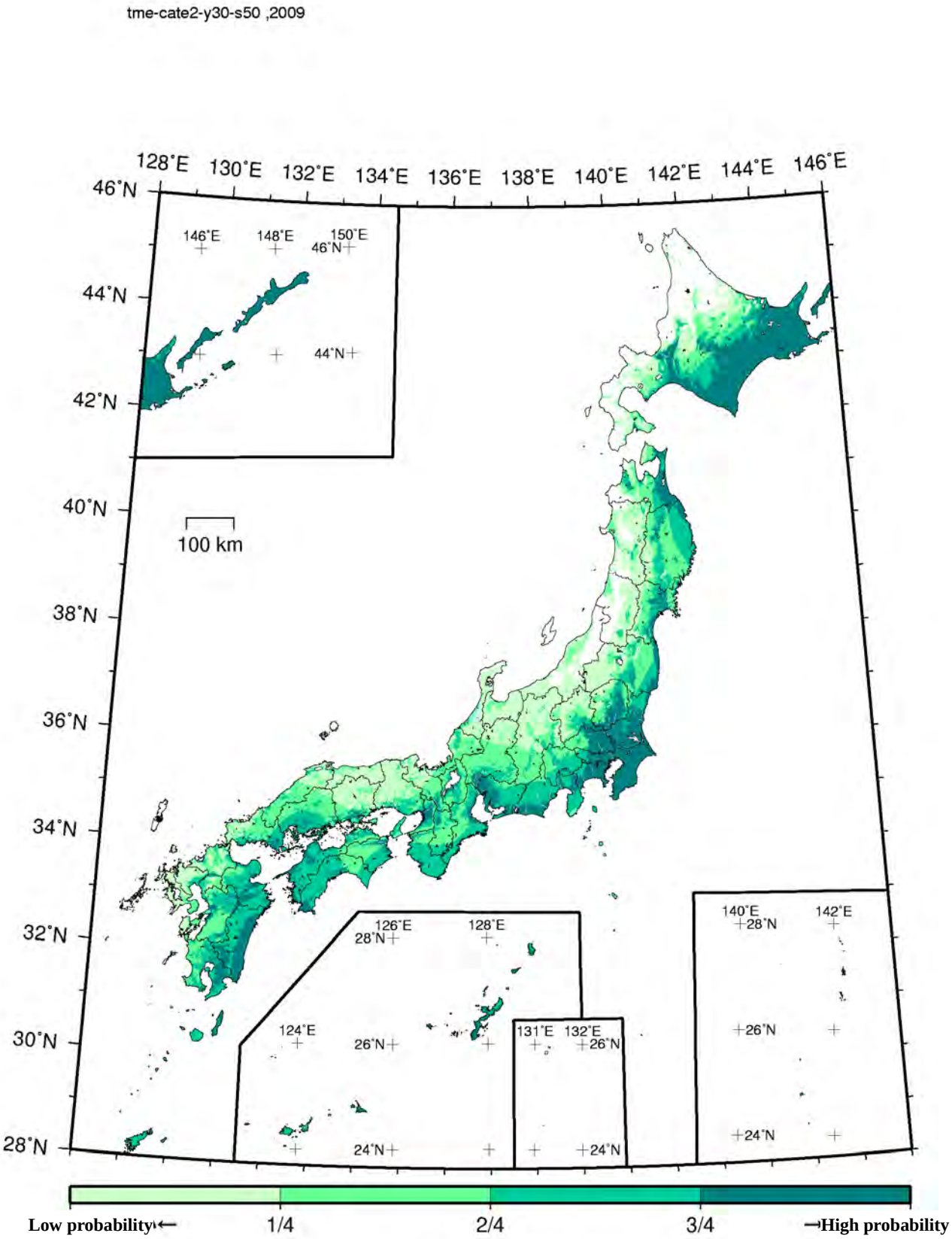

Exceedance probability within 30 years (in quartiles)
(JMA seismic intensity: 5 Upper or more)

Figure 3.7.2-17 (2) Exceedance probability within 30 years in quartiles associated with earthquake category II (JMA seismic intensity: 5 Upper or more)

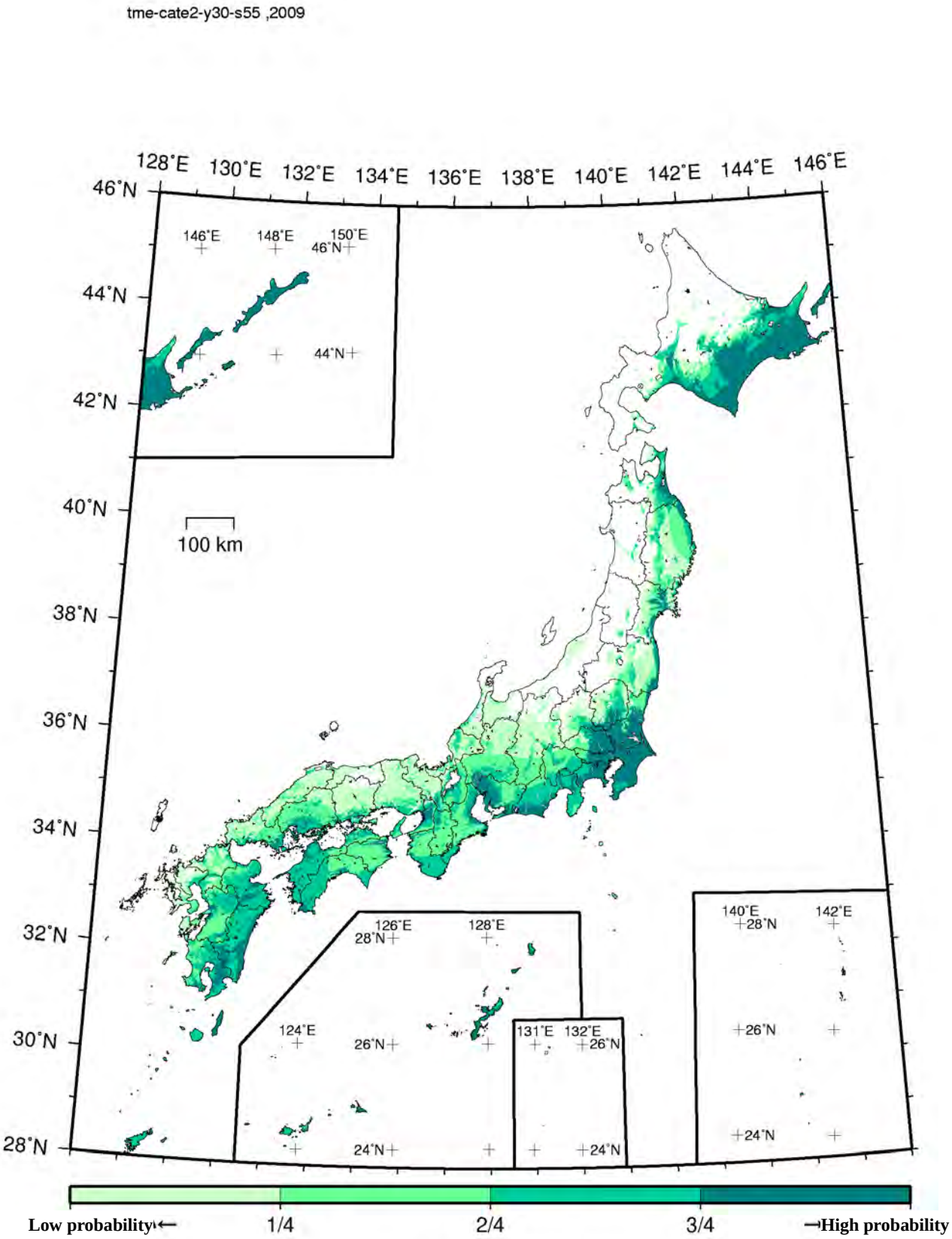

Exceedance probability within 30 years (in quartiles)
(JMA seismic intensity: 6 Lower or more)

Figure 3.7.2-17 (3) Exceedance probability within 30 years in quartiles associated with earthquake category II (JMA seismic intensity: 6 Lower or more)

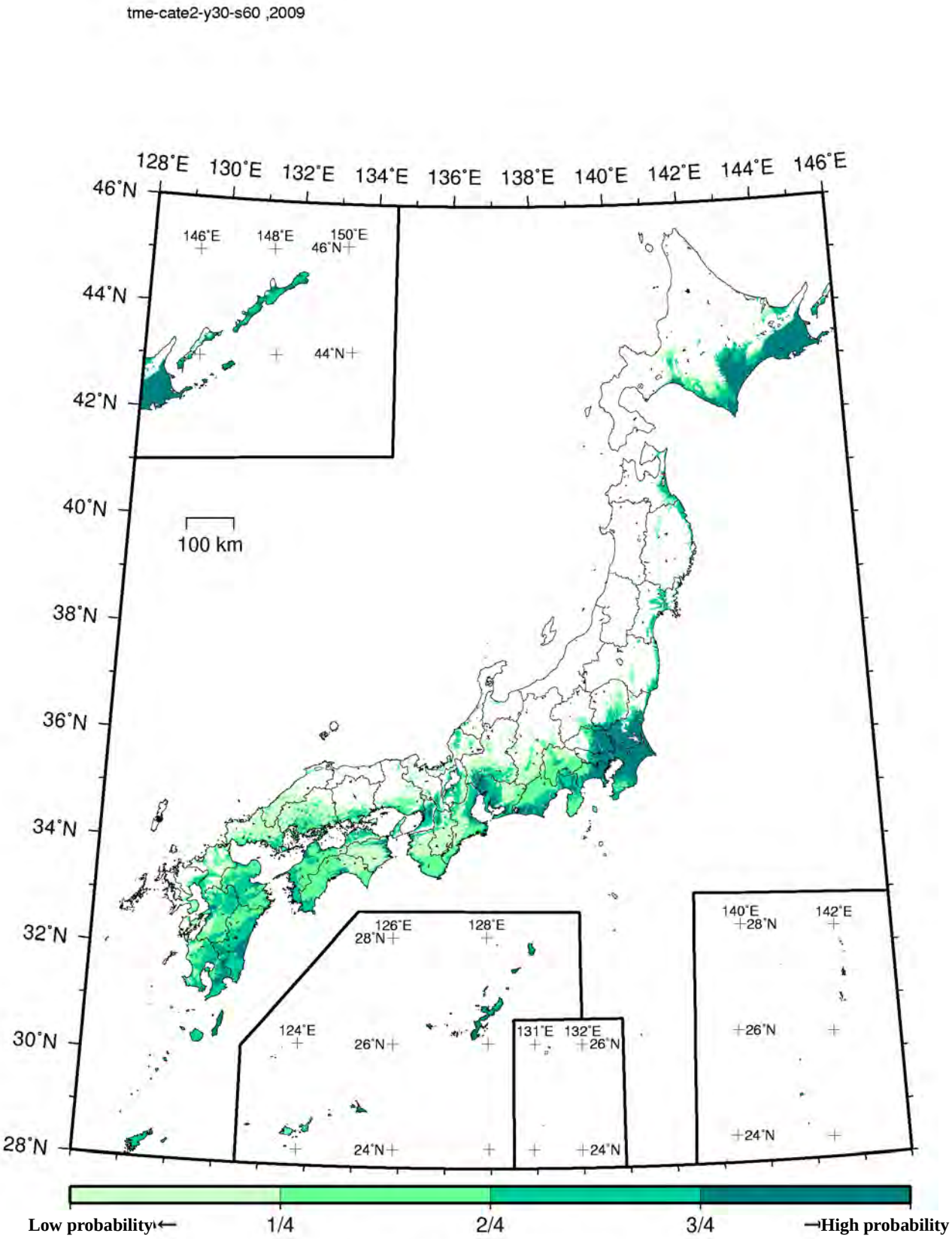

Exceedance probability within 30 years (in quartiles)
(JMA seismic intensity: 6 Upper or more)

Figure 3.7.2-17 (4) Exceedance probability within 30 years in quartiles associated with earthquake category II (JMA seismic intensity: 6 Upper or more)

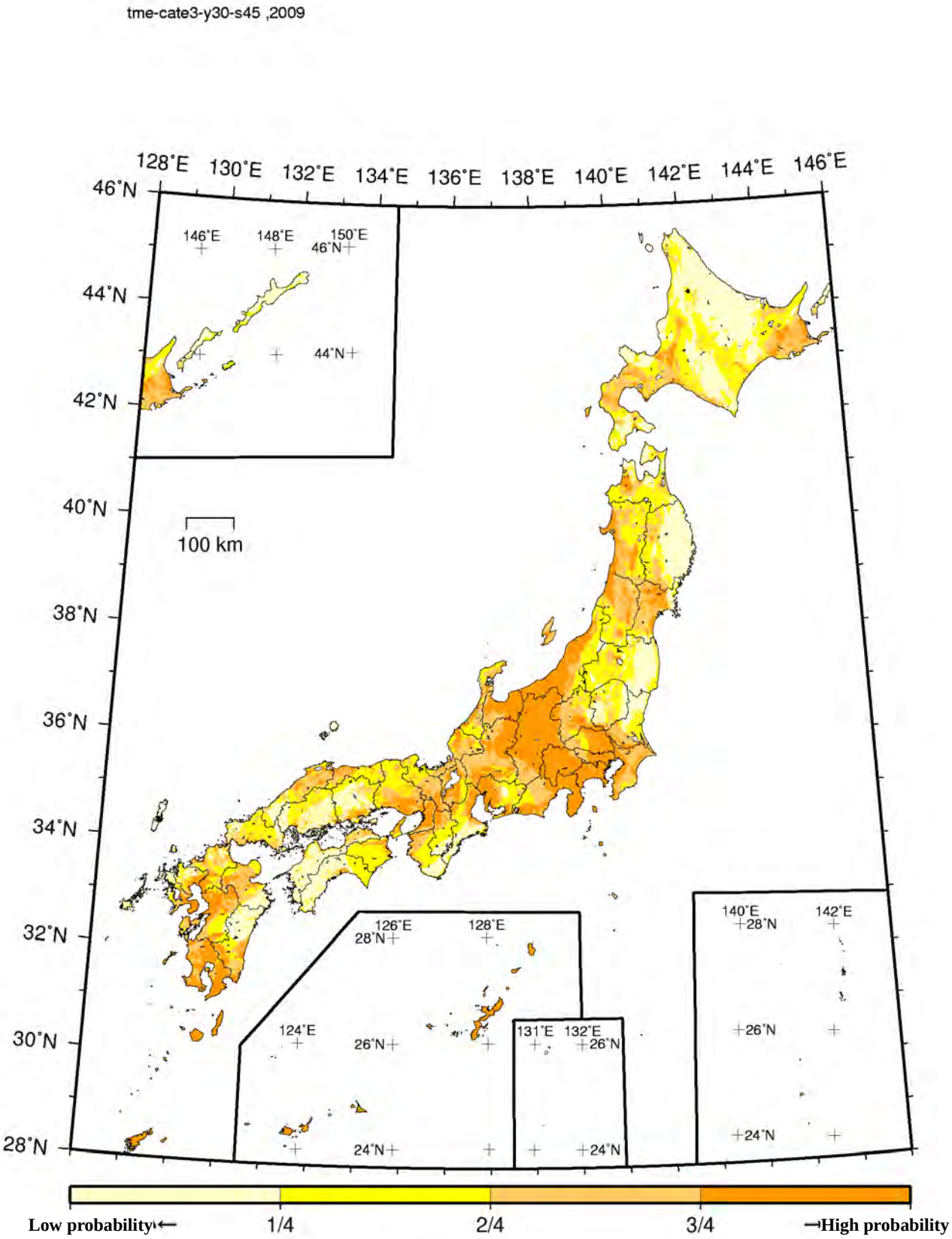

Exceedance probability within 30 years (in quartiles)
(JMA seismic intensity: 5 Lower or more)

Figure 3.7.2-18 (1) Exceedance probability within 30 years in quartiles associated with earthquake category III (JMA seismic intensity: 5 Lower or more; average case)

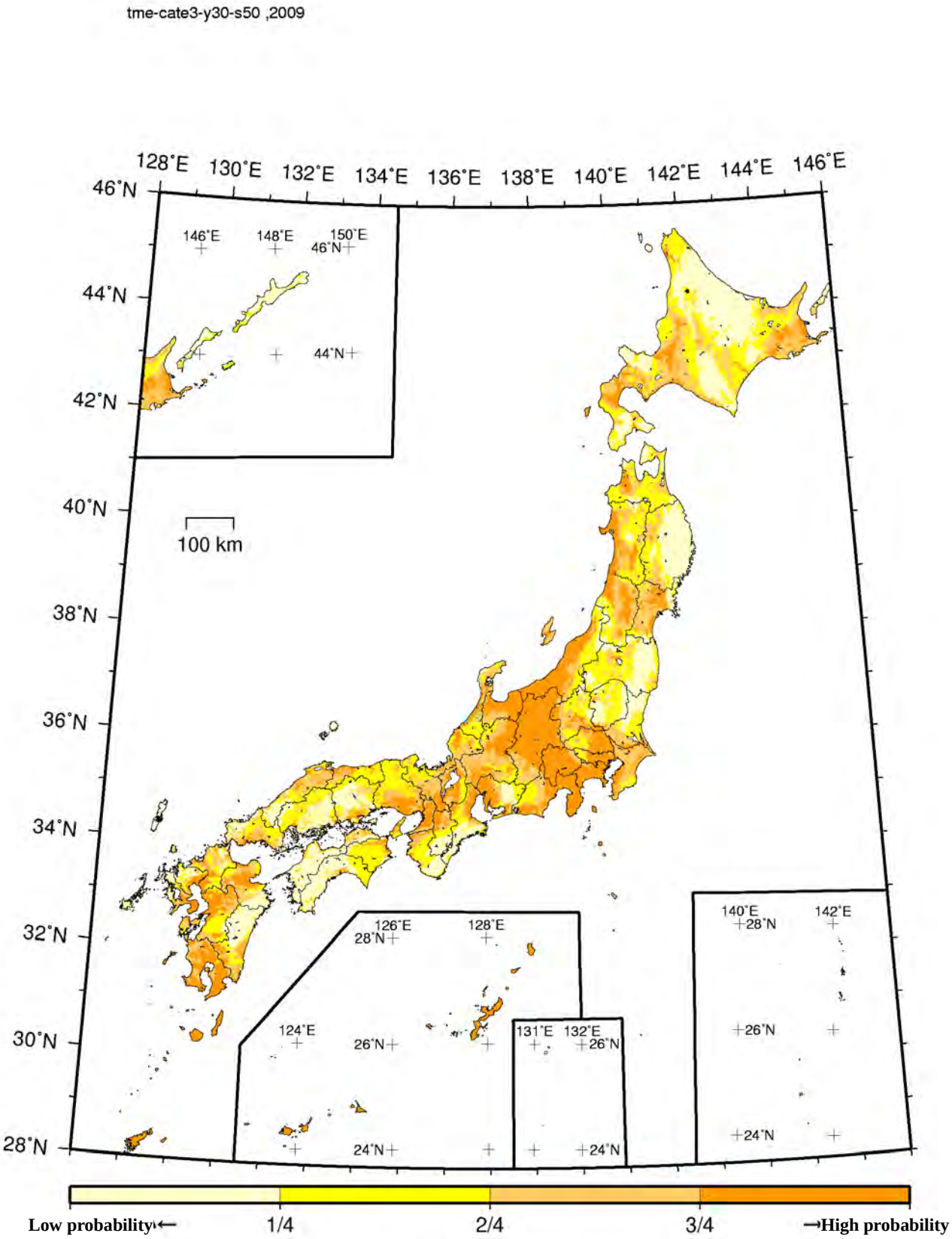

Exceedance probability within 30 years (in quartiles)
(JMA seismic intensity: 5 Upper or more)

Figure 3.7.2-18 (2) Exceedance probability within 30 years in quartiles associated with earthquake category III (JMA seismic intensity: 5 Upper or more; average case)

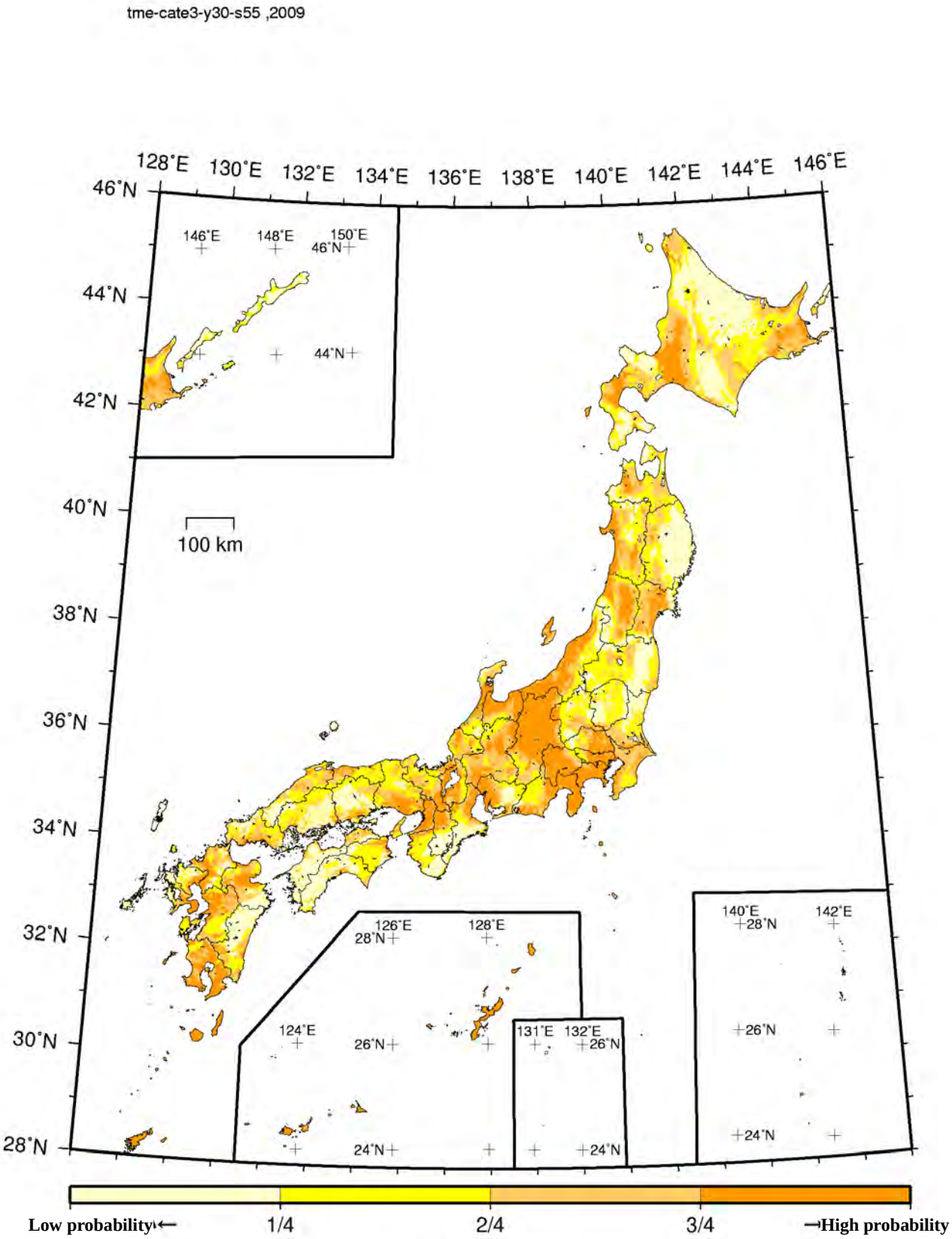

Exceedance probability within 30 years (in quartiles)
(JMA seismic intensity: 6 Lower or more)

Figure 3.7.2-18 (3) Exceedance probability within 30 years in quartiles associated with earthquake category III (JMA seismic intensity: 6 Lower or more; average case)

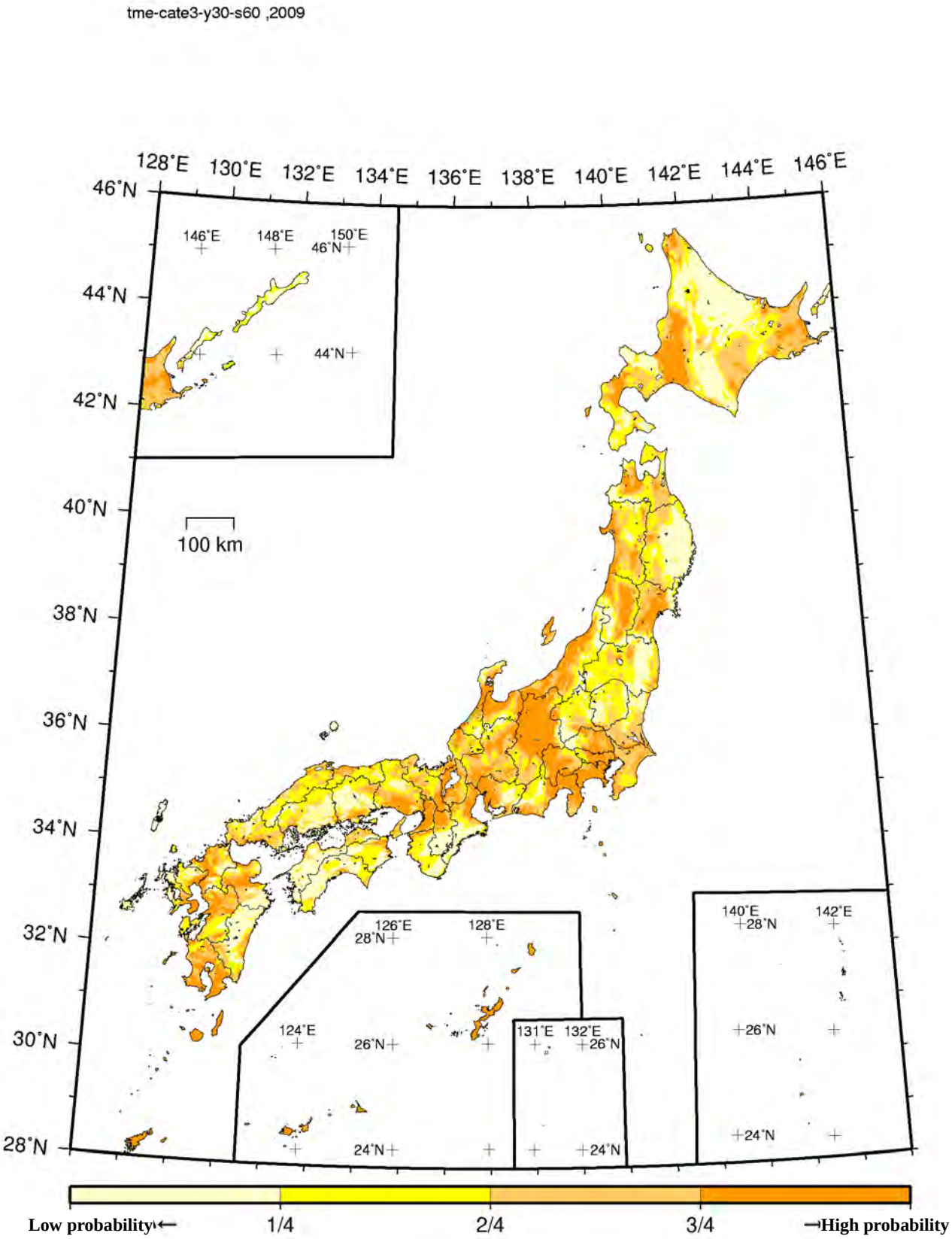

Exceedance probability within 30 years (in quartiles)
(JMA seismic intensity: 6 Upper or more)

Figure 3.7.2-18 (4) Exceedance probability within 30 years in quartiles associated with earthquake category III (JMA seismic intensity: 6 Upper or more; average case)

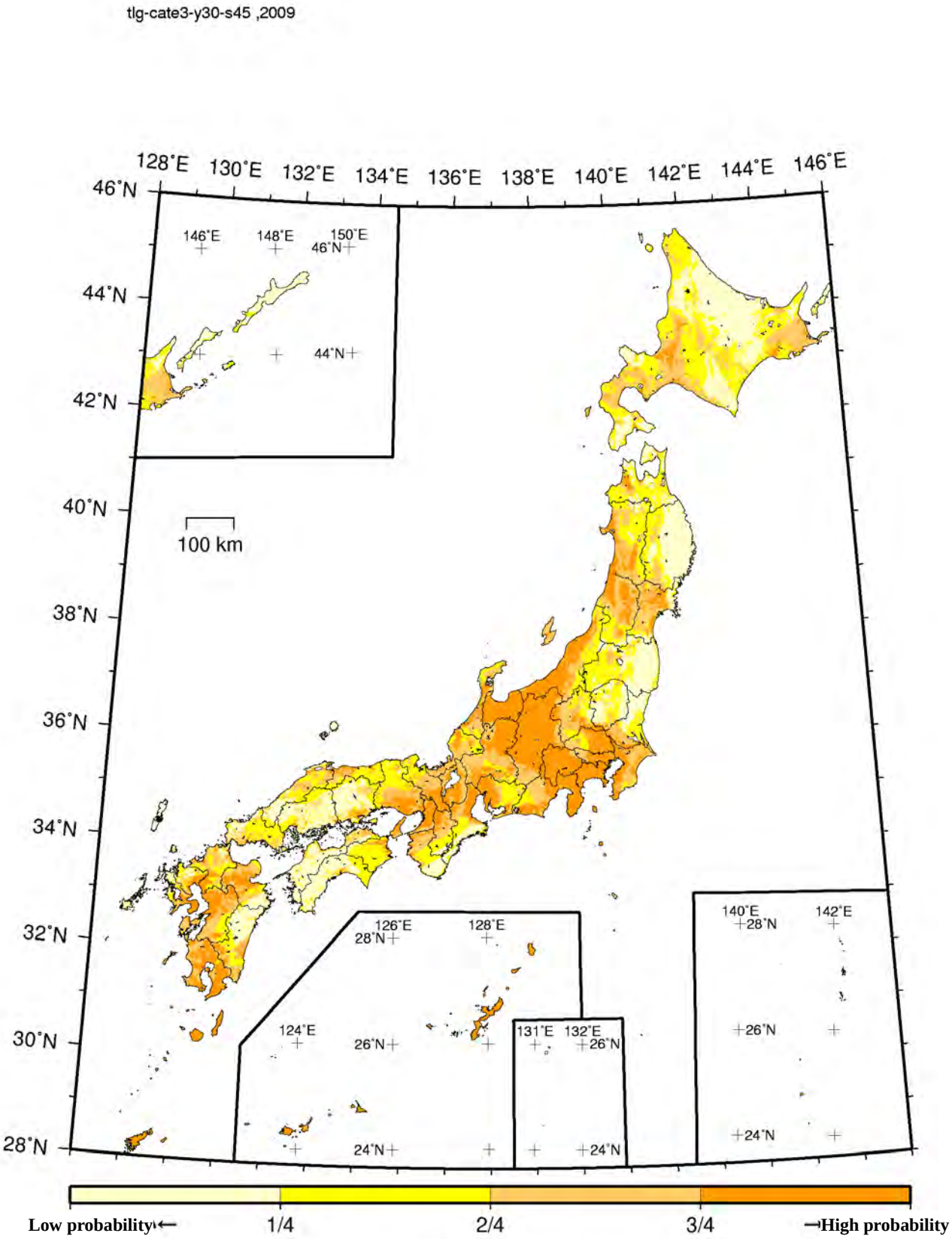

Exceedance probability within 30 years (in quartiles)
(JMA seismic intensity: 5 Lower or more)

Figure 3.7.2-19 (1) Exceedance probability within 30 years in quartiles associated with earthquake category III (JMA seismic intensity: 5 Lower or more; maximum case)

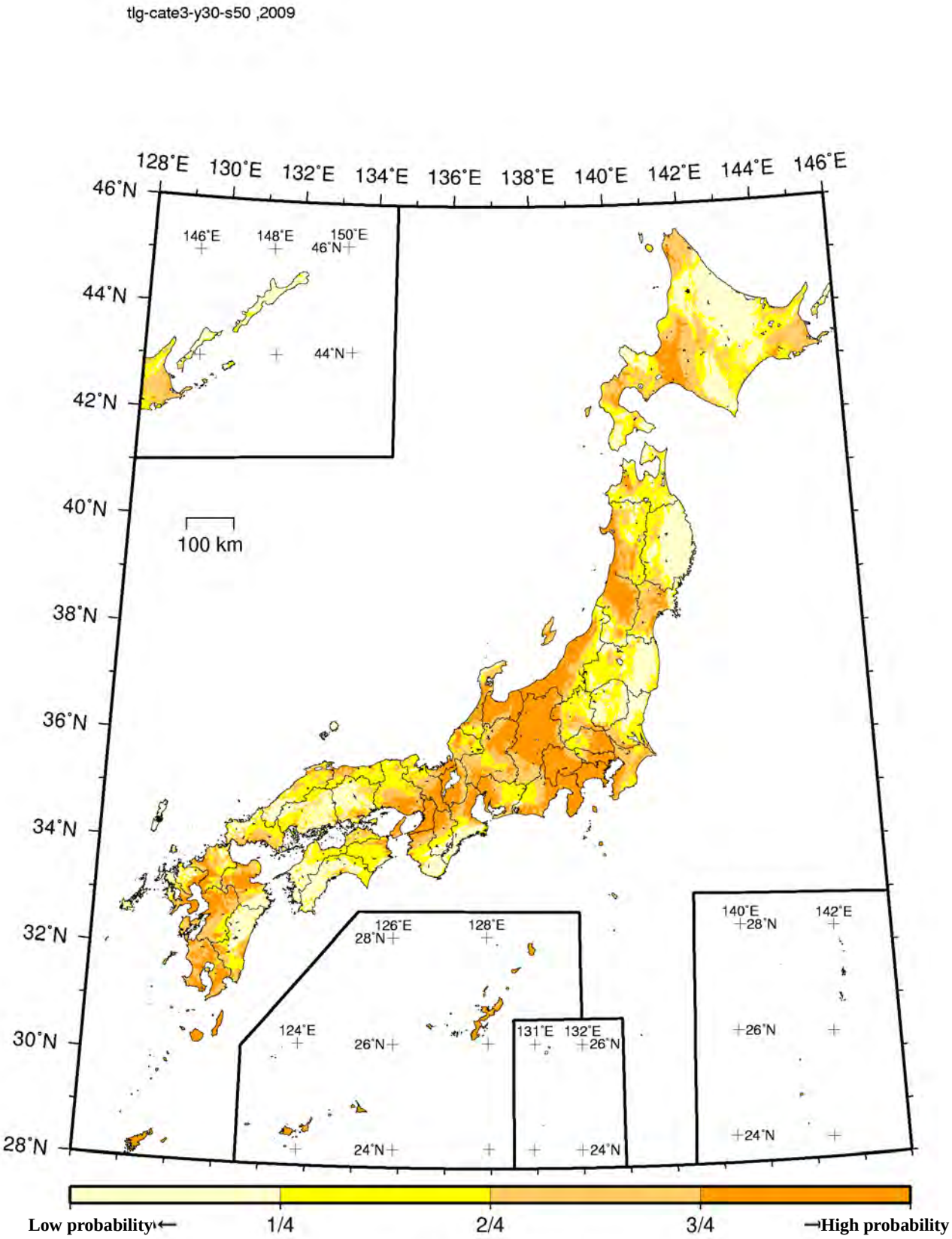

Exceedance probability within 30 years (in quartiles)
(JMA seismic intensity: 5 Upper or more)

Figure 3.7.2-19 (2) Exceedance probability within 30 years in quartiles associated with earthquake category III (JMA seismic intensity: 5 Upper or more; maximum case)

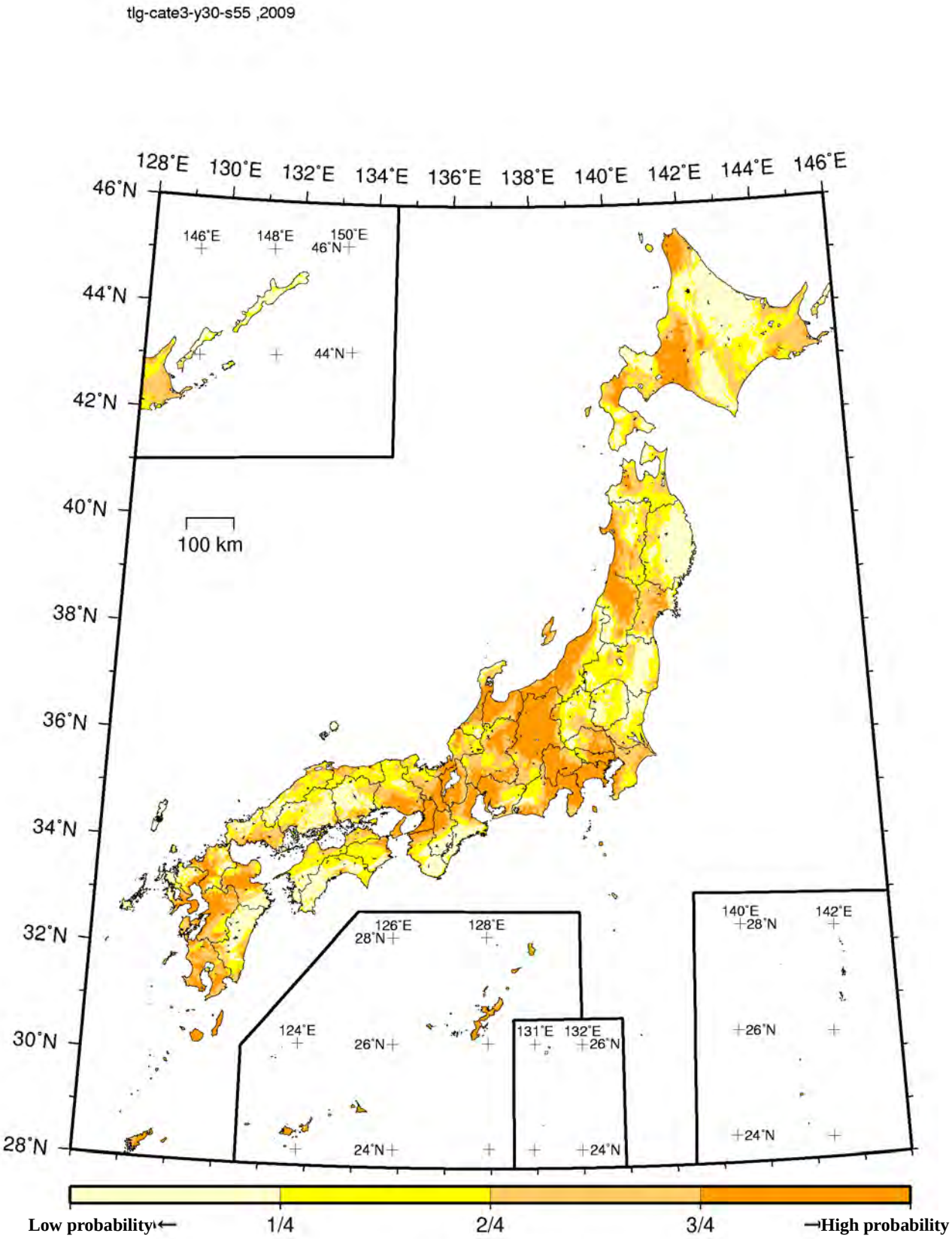

Exceedance probability within 30 years (in quartiles)
(JMA seismic intensity: 6 Lower or more)

Figure 3.7.2-19 (3) Exceedance probability within 30 years in quartiles associated with earthquake category III (JMA seismic intensity: 6 Lower or more; maximum case)

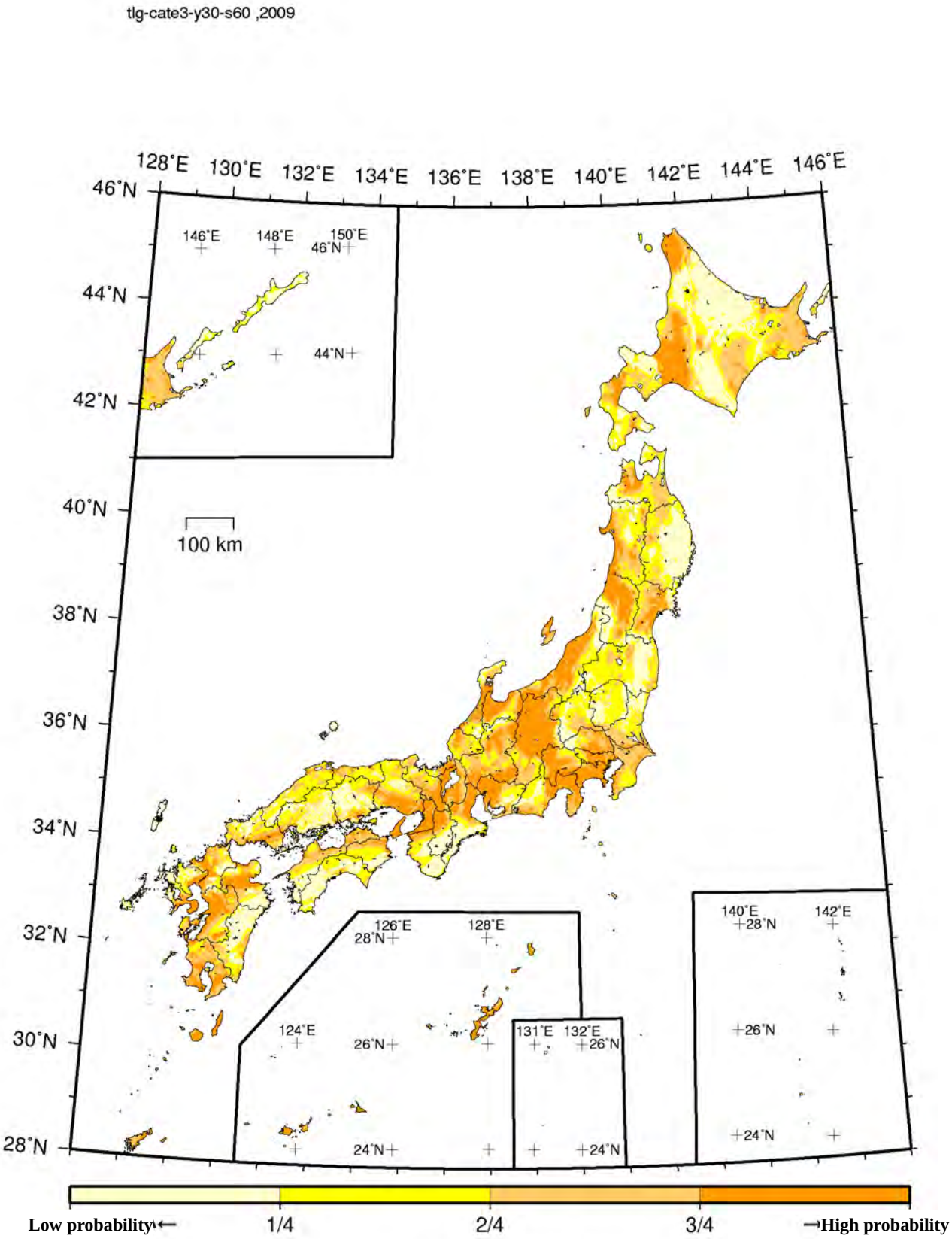

Exceedance probability within 30 years (in quartiles)
(JMA seismic intensity: 6 Upper or more)

Figure 3.7.2-19 (4) Exceedance probability within 30 years in quartiles associated with earthquake category III (JMA seismic intensity: 6 Upper or more; maximum case)

tme-total-y50-p39 ,2009

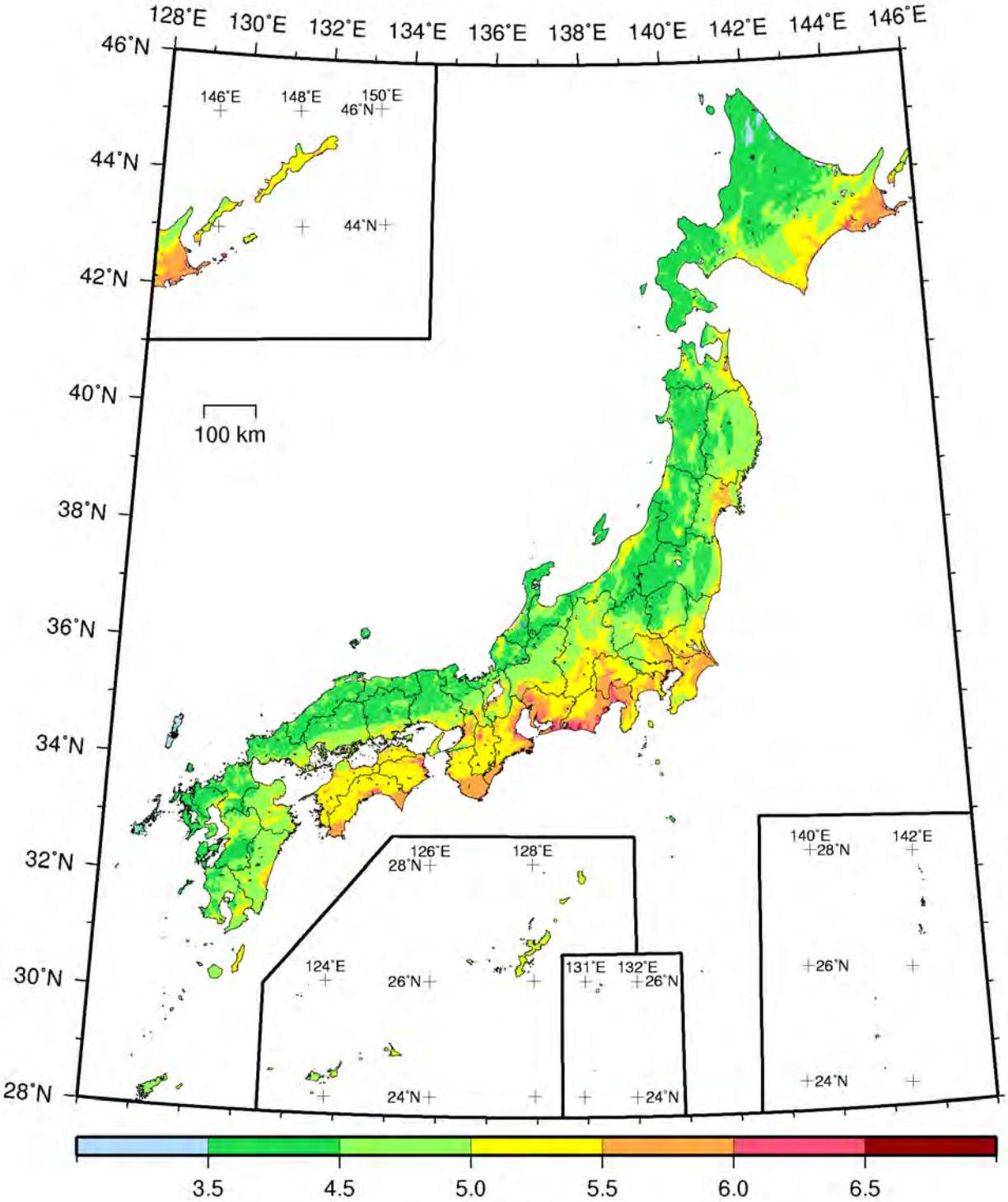

JMA seismic intensity
(Exceedance probability within 50 years: 39%)

Figure 3.7.2-20 (1) JMA seismic intensity on the ground surface considering all earthquakes (Exceedance probability within 50 years: 39%; average case)

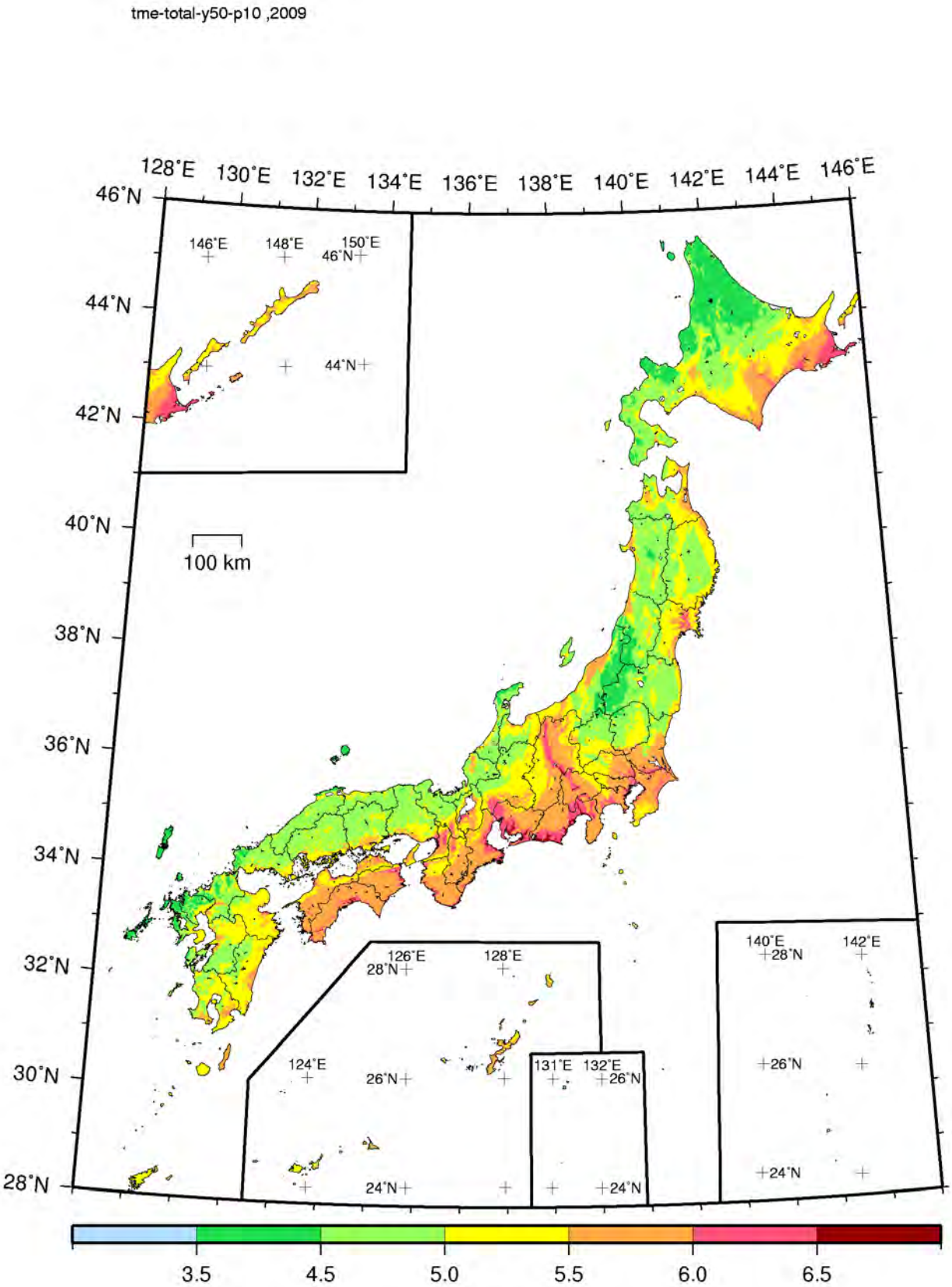

JMA seismic intensity
(Exceedance probability within 50 years: 10%)

Figure 3.7.2-20 (2) JMA seismic intensity on the ground surface considering all earthquakes (Exceedance probability within 50 years: 10%; average case)

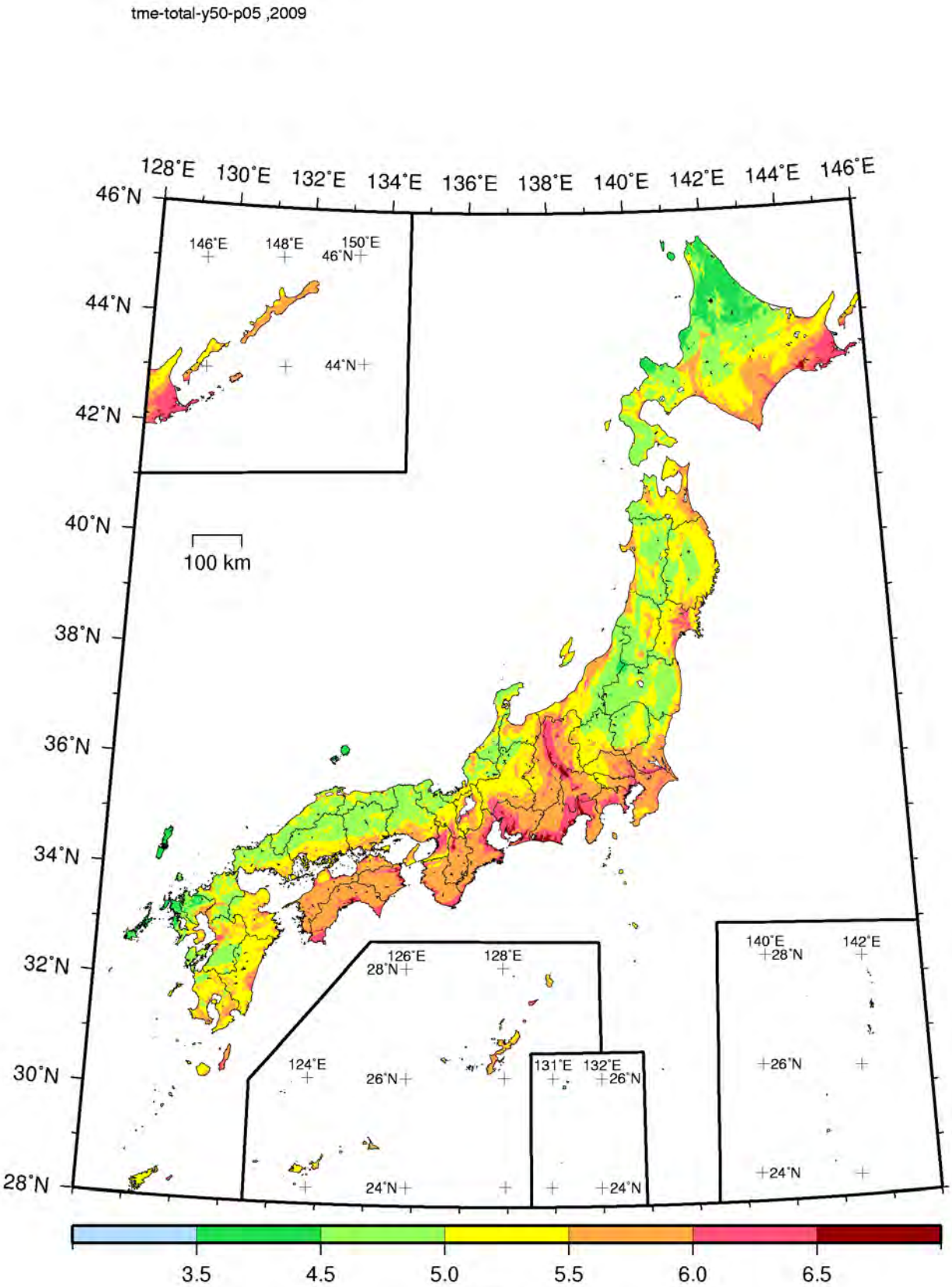

JMA seismic intensity
(Exceedance probability within 50 years: 5%)

Figure 3.7.2-20 (3) JMA seismic intensity on the ground surface considering all earthquakes (Exceedance probability within 50 years: 5%; average case)

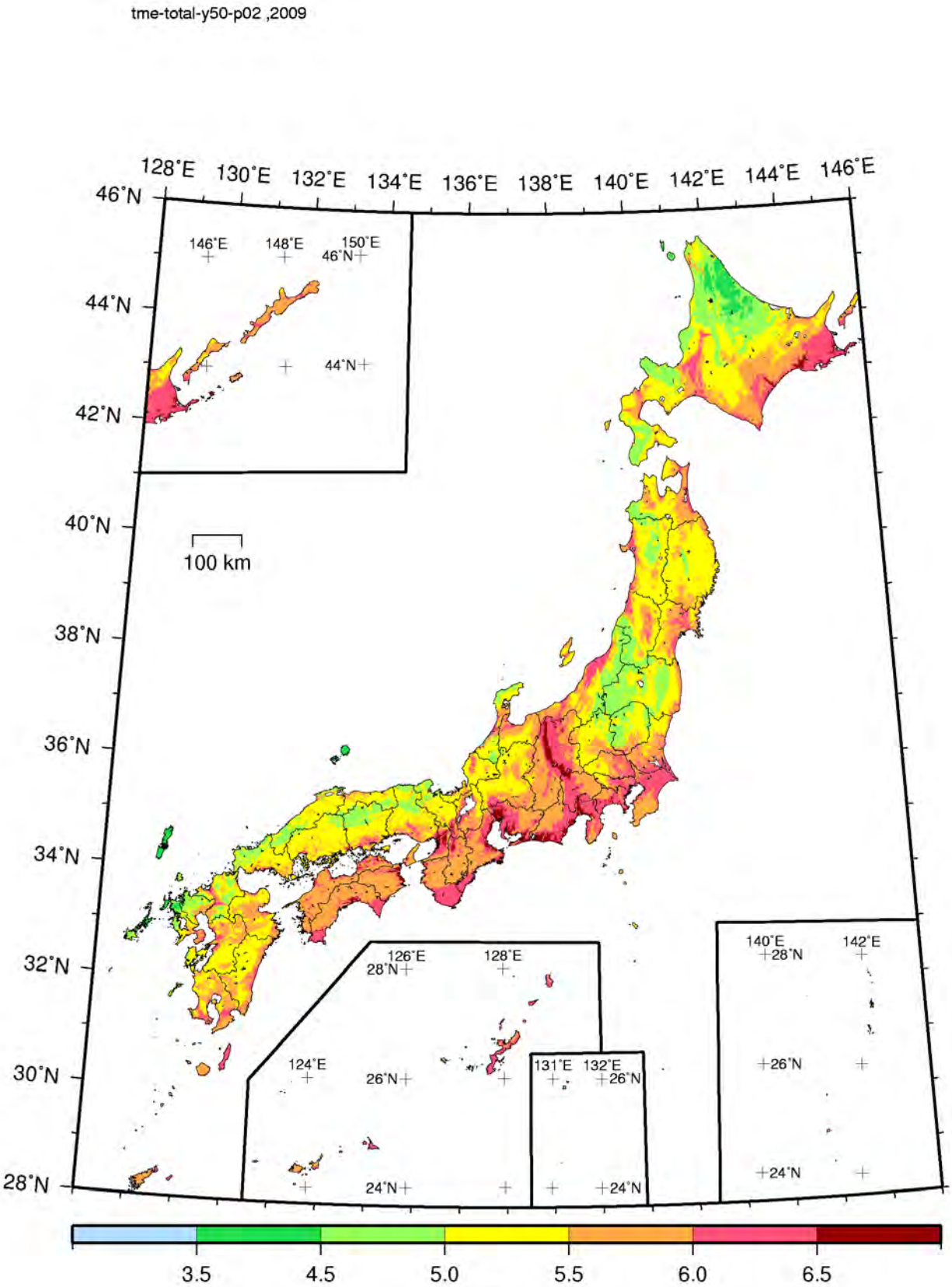

JMA seismic intensity
(Exceedance probability within 50 years: 2%)

Figure 3.7.2-20 (4) JMA seismic intensity on the ground surface considering all earthquakes (Exceedance probability within 50 years: 2%; average case)

tlg-total-y50-p39 ,2009

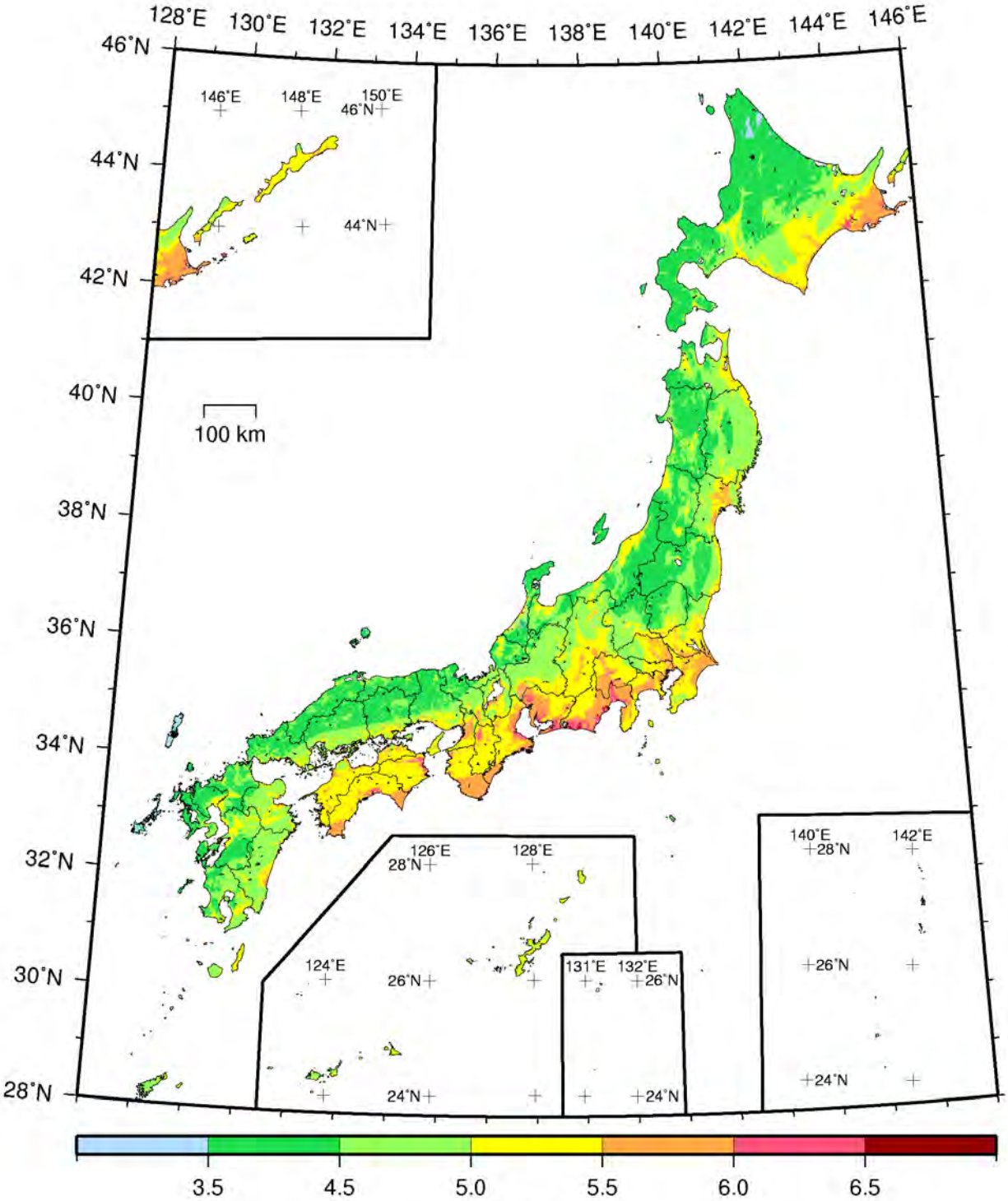

JMA seismic intensity
(Exceedance probability within 50 years: 39%)

Figure 3.7.2-21 (1) JMA seismic intensity on the ground surface considering all earthquakes (Exceedance probability within 50 years: 39%; maximum case)

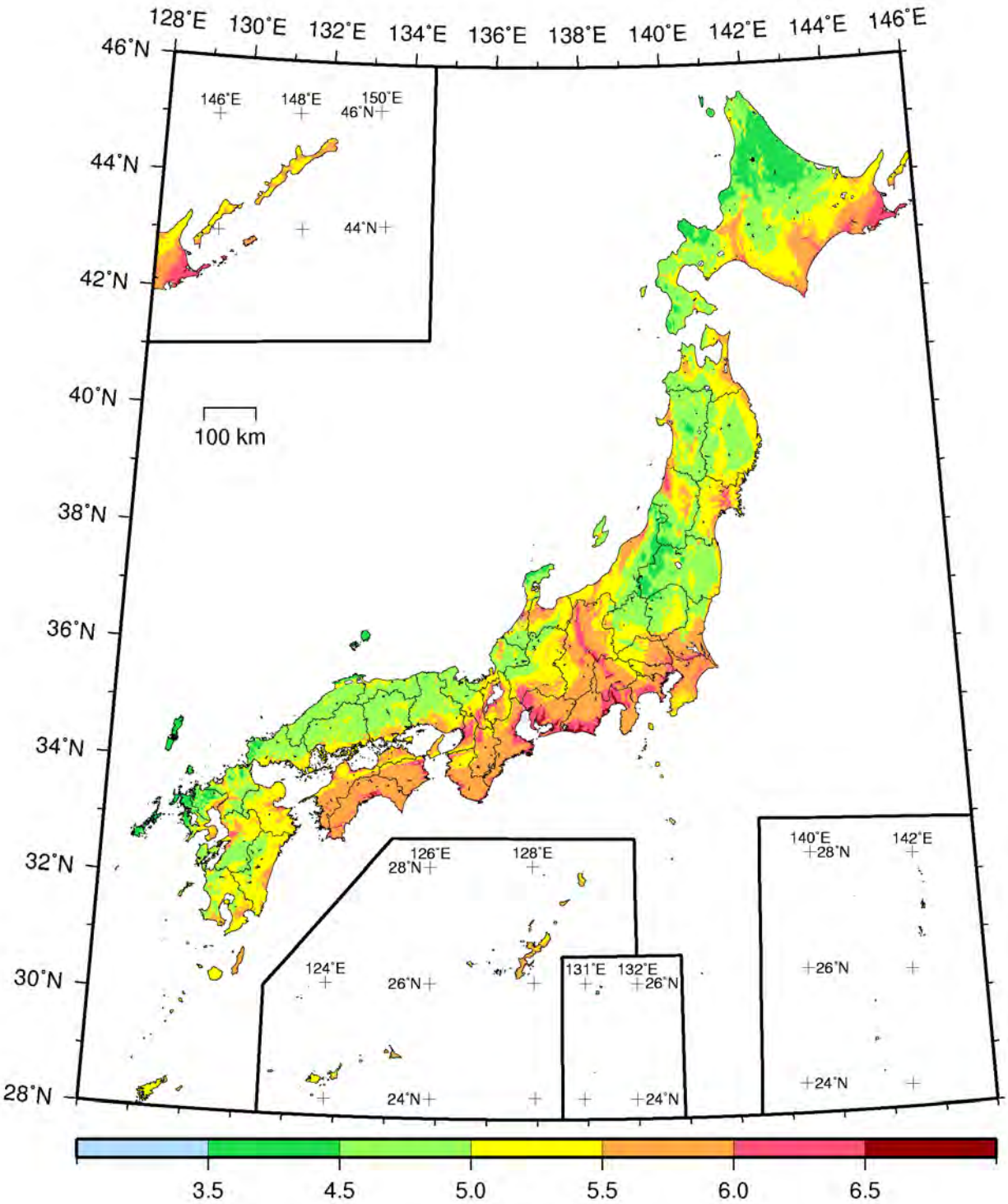

JMA seismic intensity
(Exceedance probability within 50 years: 10%)

Figure 3.7.2-21 (2) JMA seismic intensity on the ground surface considering all earthquakes (Exceedance probability within 50 years: 10%; maximum case)

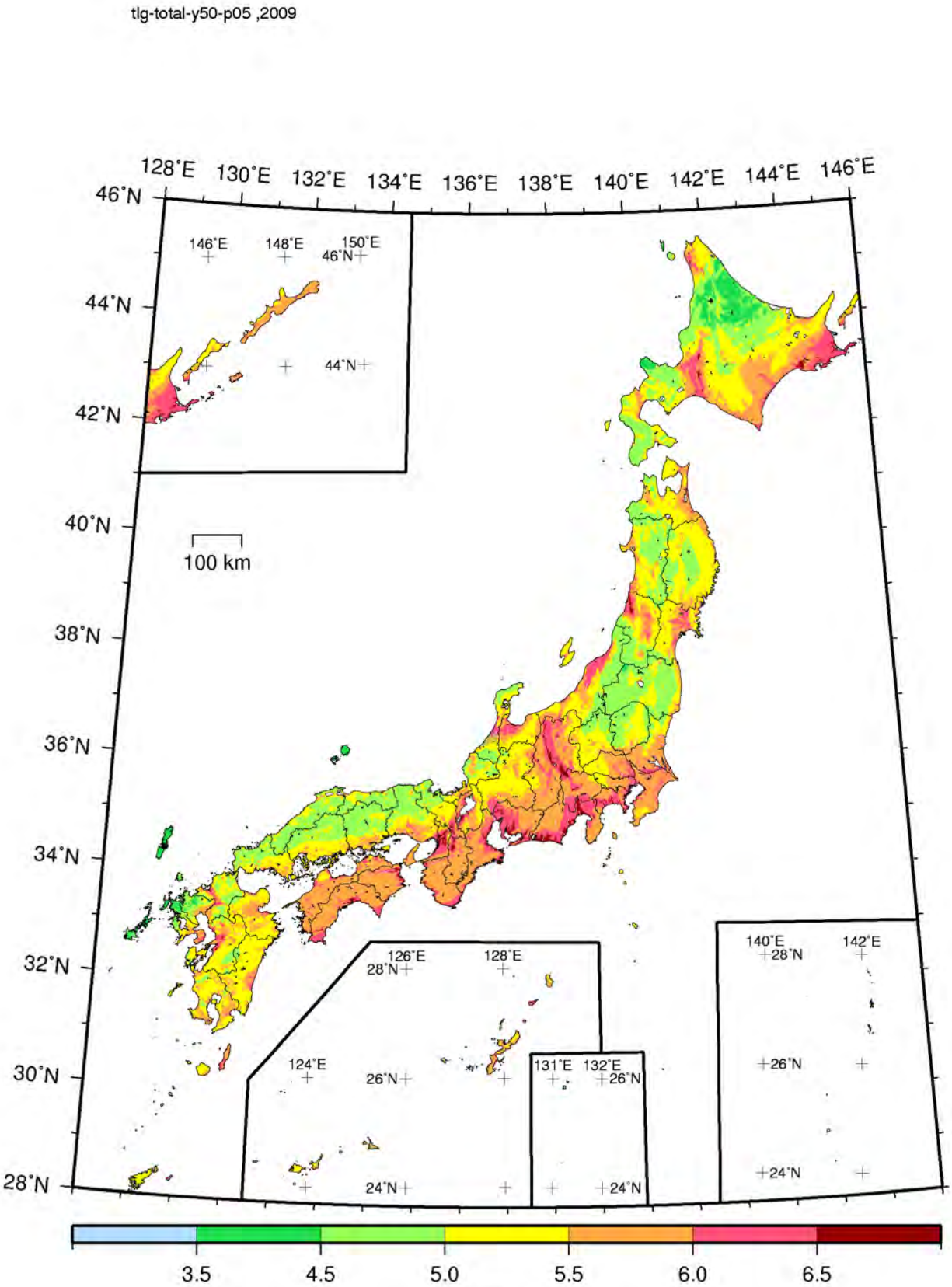

JMA seismic intensity
(Exceedance probability within 50 years: 5%)

Figure 3.7.2-21 (3) JMA seismic intensity on the ground surface considering all earthquakes (Exceedance probability within 50 years: 5%; maximum case)

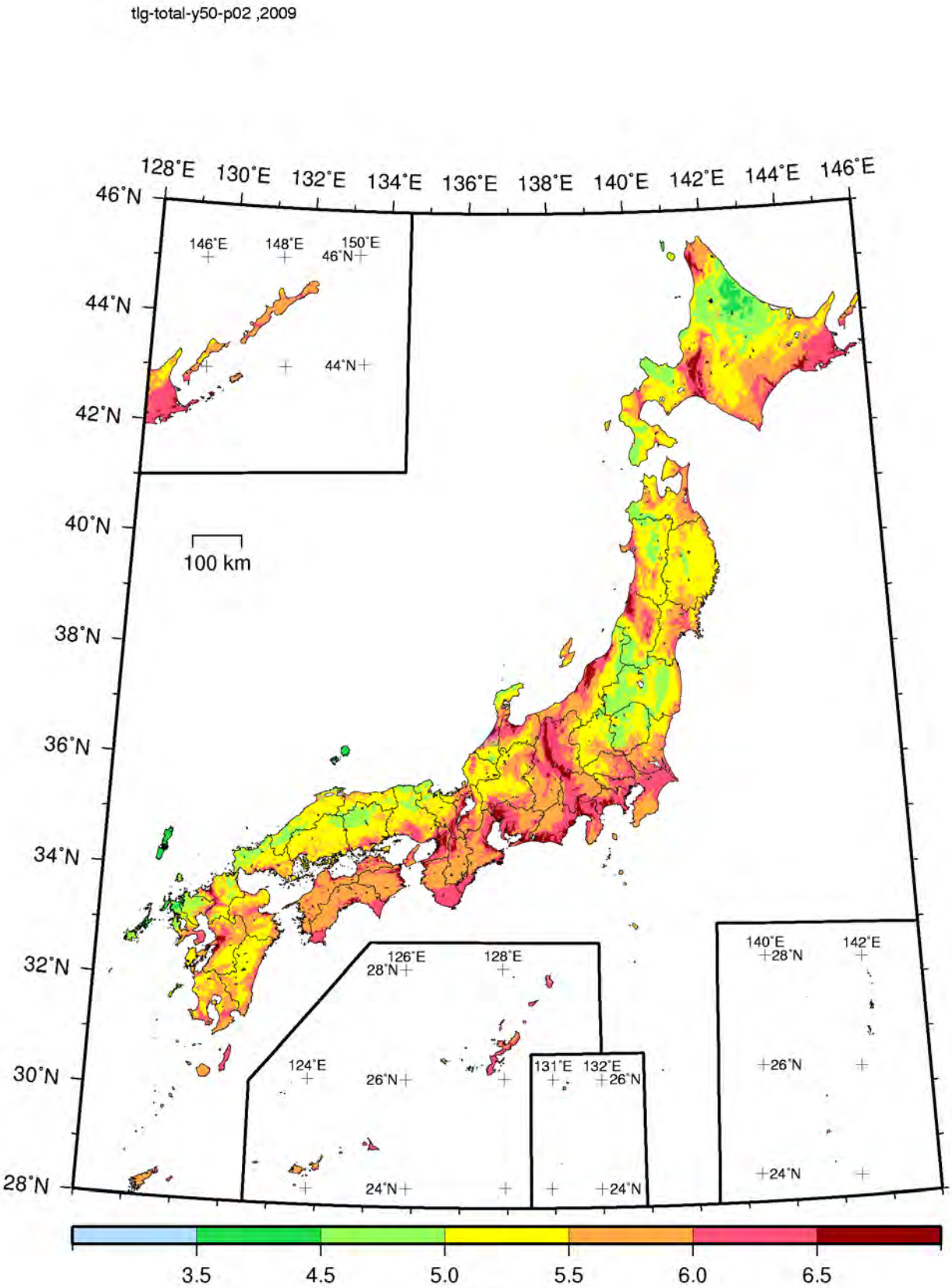

JMA seismic intensity
(Exceedance probability within 50 years: 2%)

Figure 3.7.2-21 (4) JMA seismic intensity on the ground surface considering all earthquakes (Exceedance probability within 50 years: 2%; maximum case)

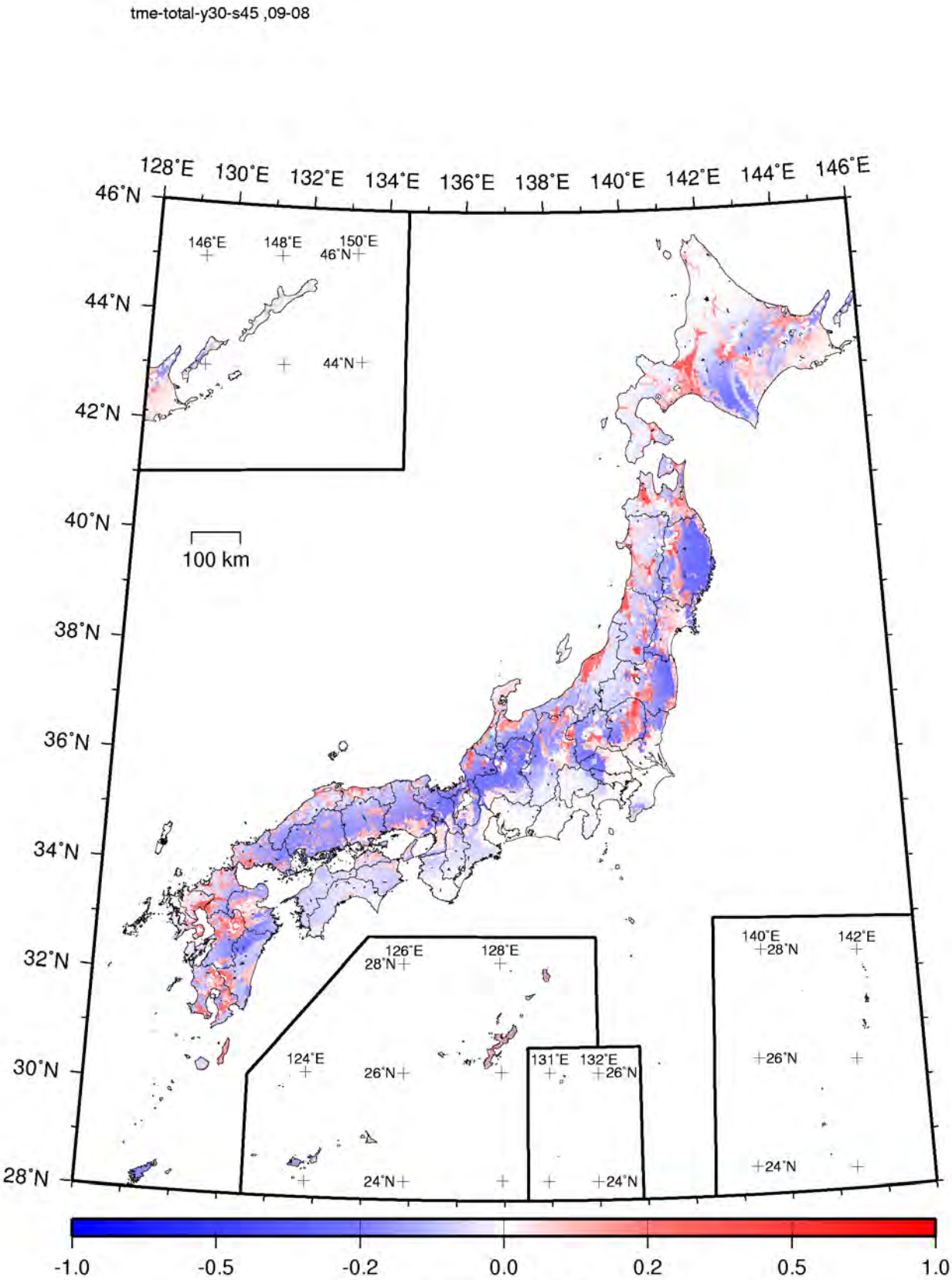

Difference in the exceedance probability within 30 years
(JMA seismic intensity: 5 Lower or more)

Figure 3.7.2-22 (1) Differences in the exceedance probability within 30 years taking all earthquakes into consideration (JMA seismic intensity: 5 Lower or more; average case)

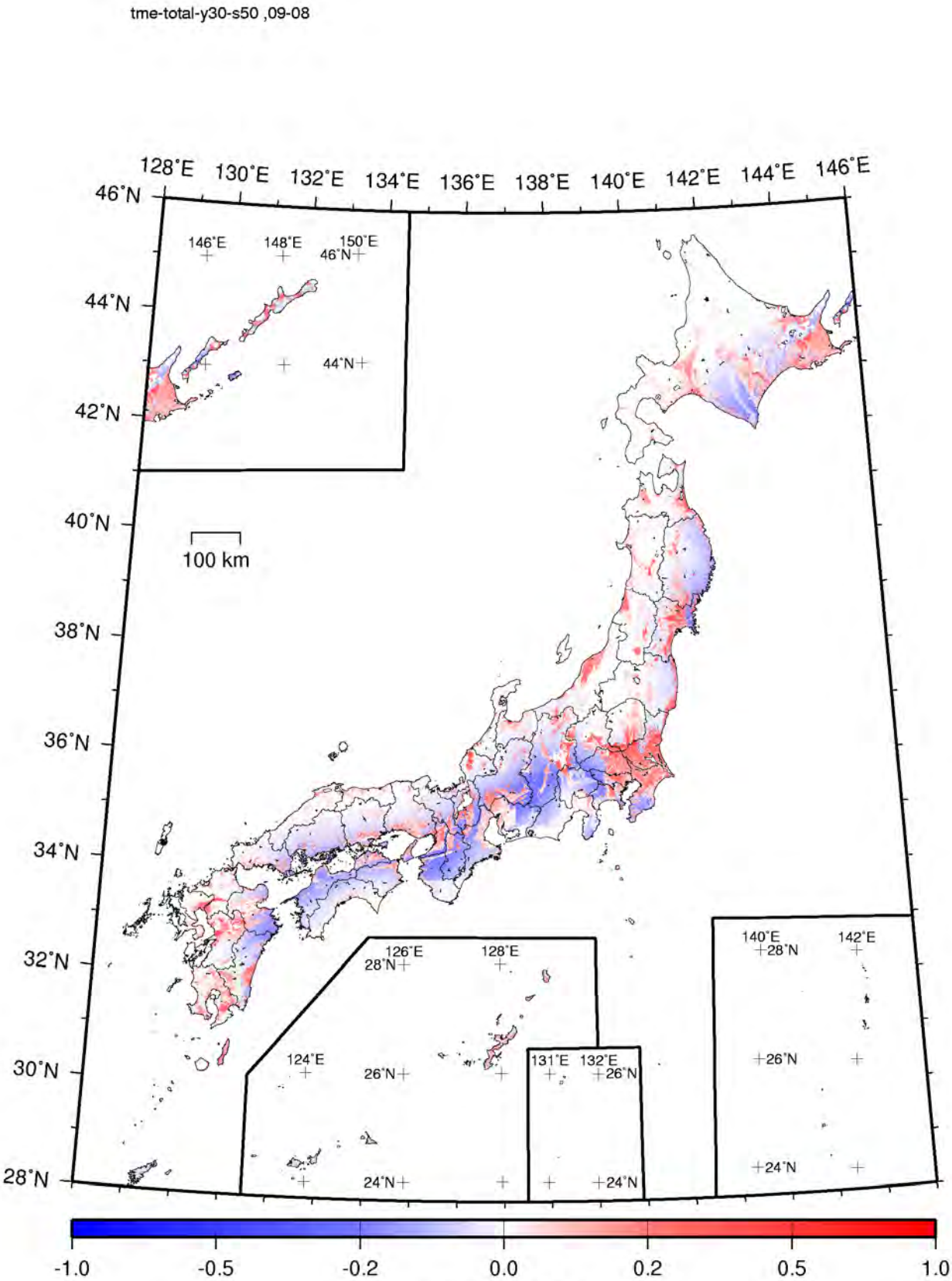

Difference in the exceedance probability within 30 years
(JMA seismic intensity: 5 Upper or more)

Figure 3.7.2-22 (2) Differences in the exceedance probability within 30 years taking all earthquakes into consideration (JMA seismic intensity: 5 Upper or more; average case)

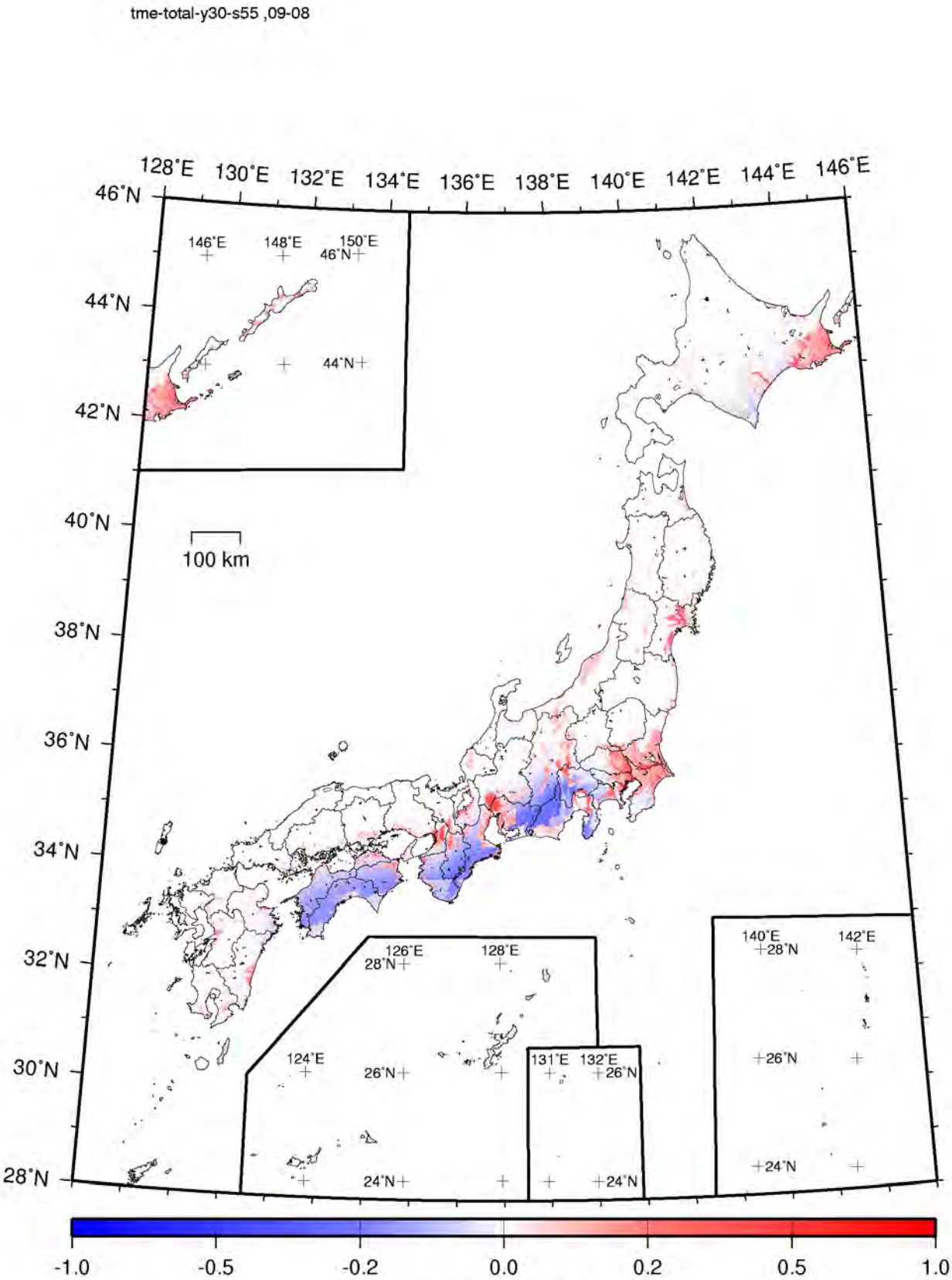

Difference in the exceedance probability within 30 years
(JMA seismic intensity: 6 Lower or more)

Figure 3.7.2-22 (3) Differences in the exceedance probability within 30 years taking all earthquakes into consideration (JMA seismic intensity: 6 Lower or more; average case)

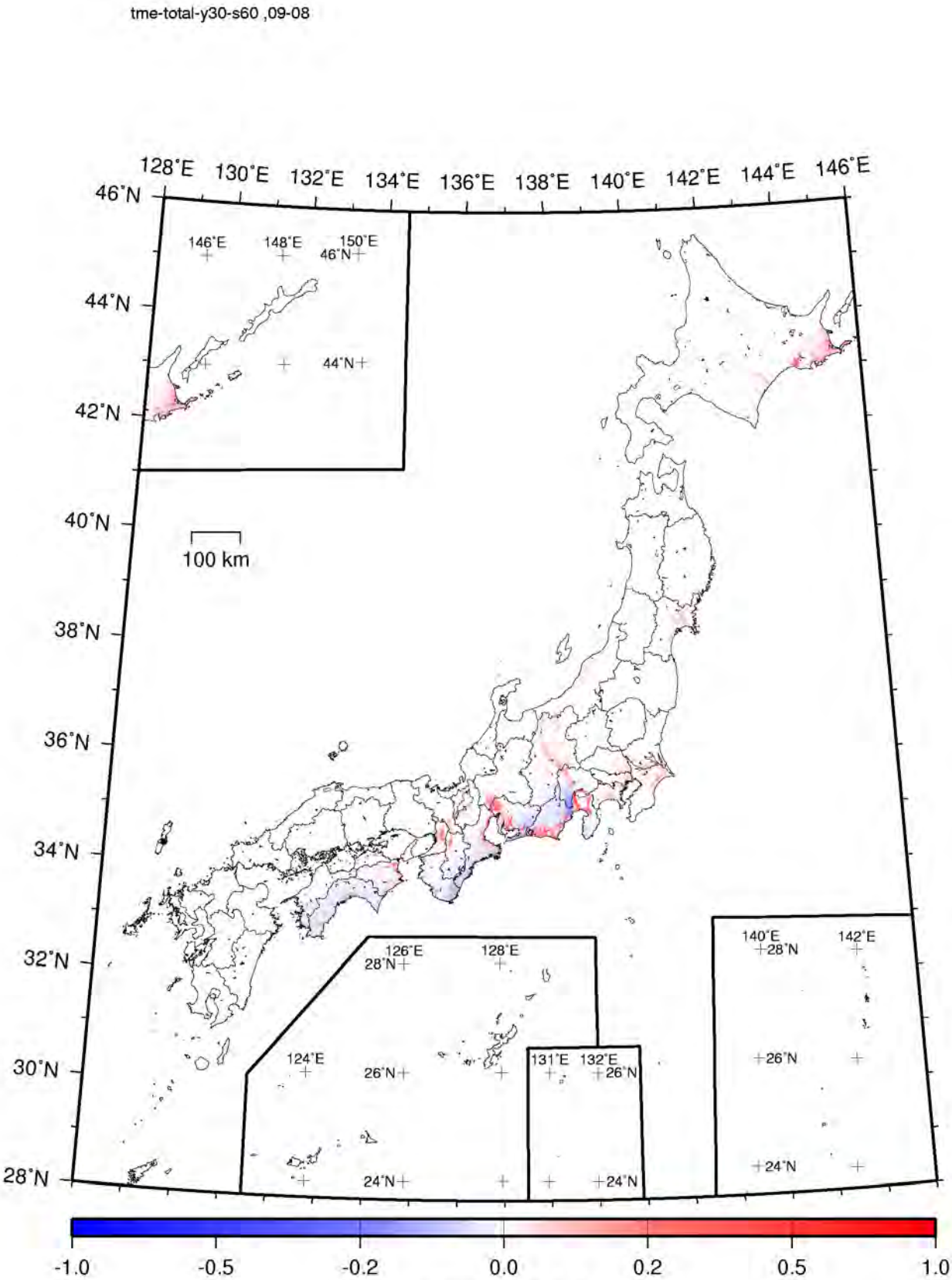

Difference in the exceedance probability within 30 years
(JMA seismic intensity: 6 Upper or more)

Figure 3.7.2-22 (4) Differences in the exceedance probability within 30 years taking all earthquakes into consideration (JMA seismic intensity: 6 Upper or more; average case)

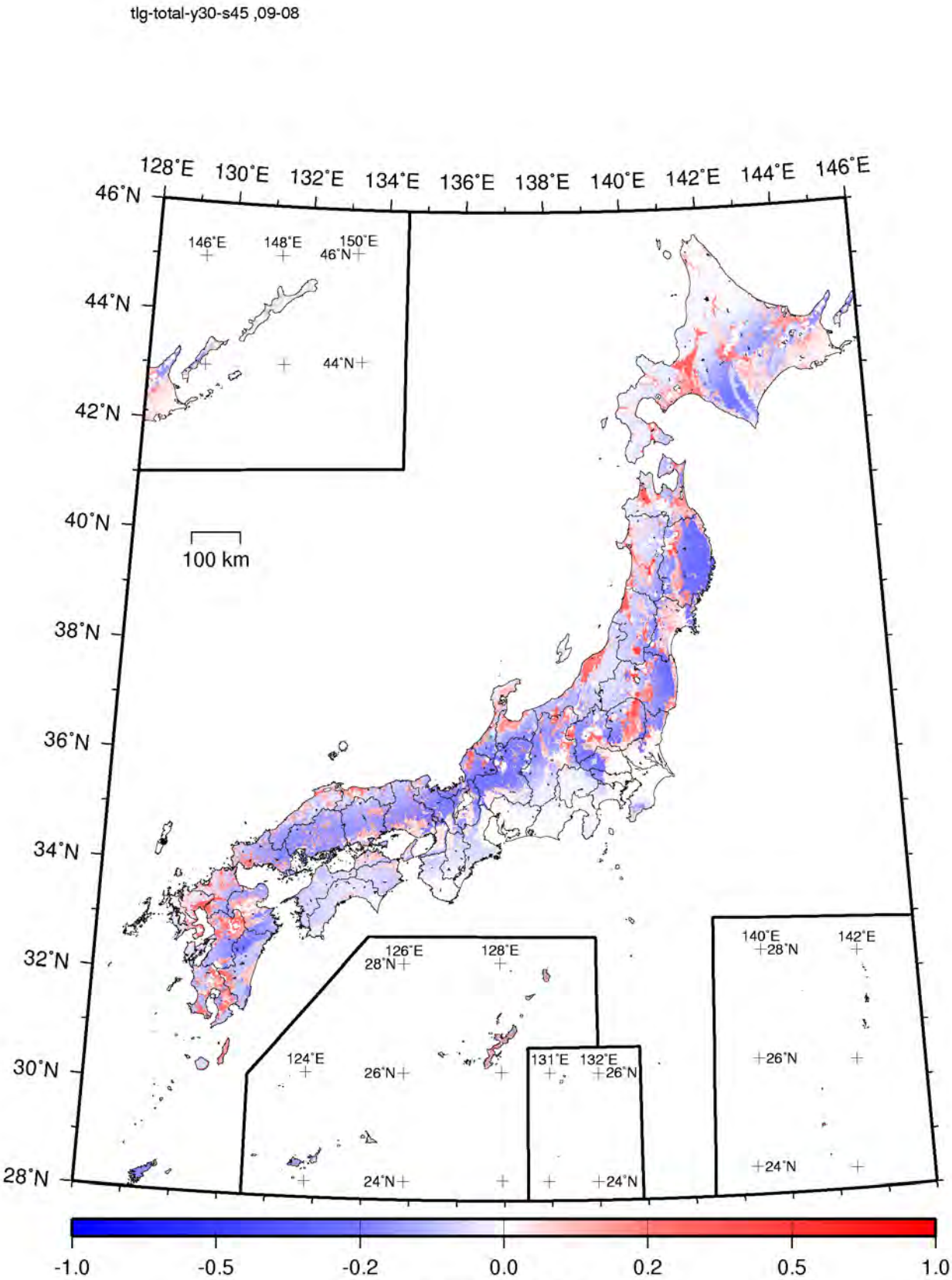

Difference in the exceedance probability within 30 years
(JMA seismic intensity: 5 Lower or more)

Figure 3.7.2-23 (1) Differences in the exceedance probability within 30 years taking all earthquakes into consideration (JMA seismic intensity: 5 Lower or more; maximum case)

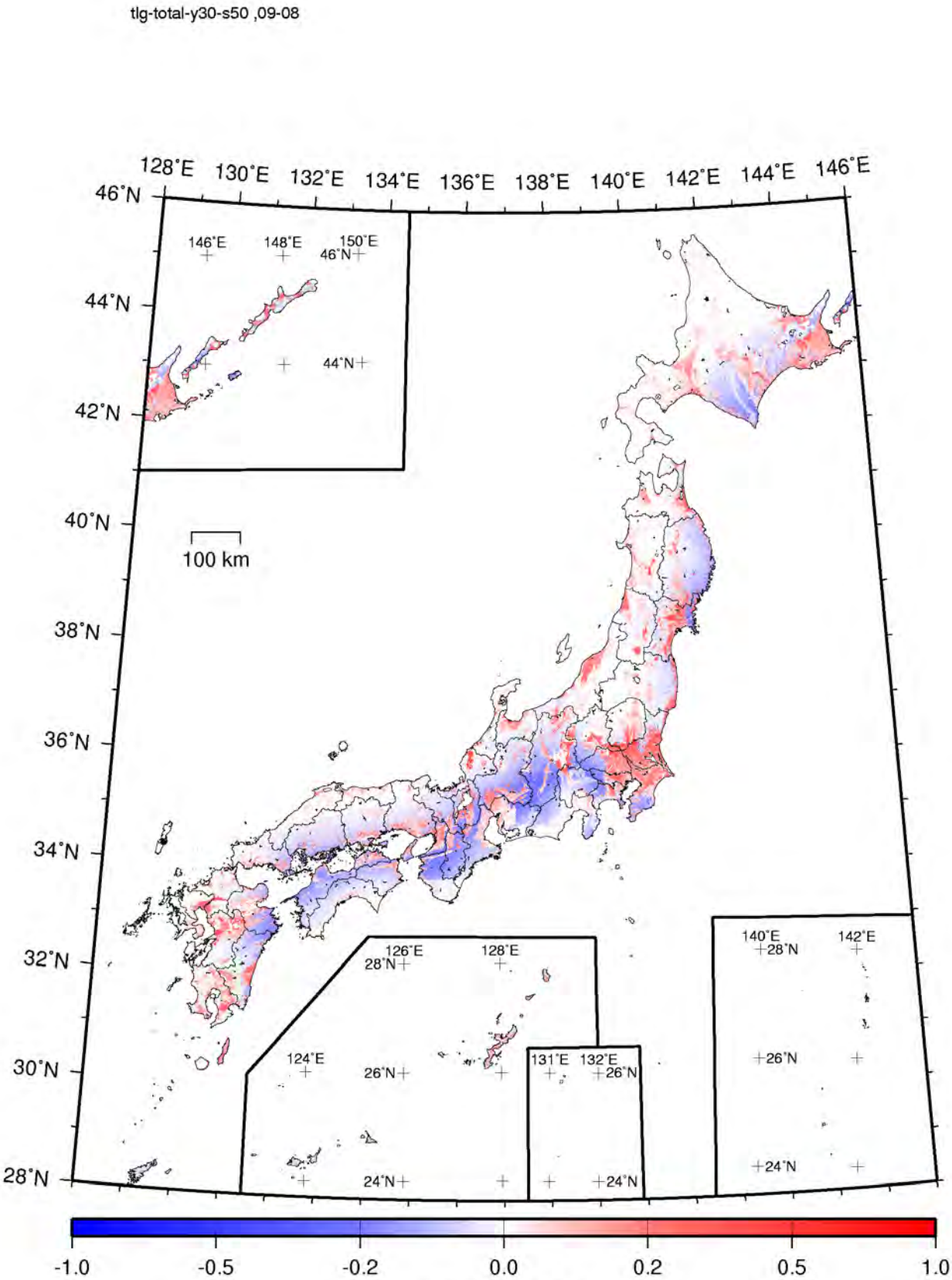

Difference in the exceedance probability within 30 years
(JMA seismic intensity: 5 Upper or more)

Figure 3.7.2-23 (2) Differences in the exceedance probability within 30 years taking all earthquakes into consideration (JMA seismic intensity: 5 Upper or more; maximum case)

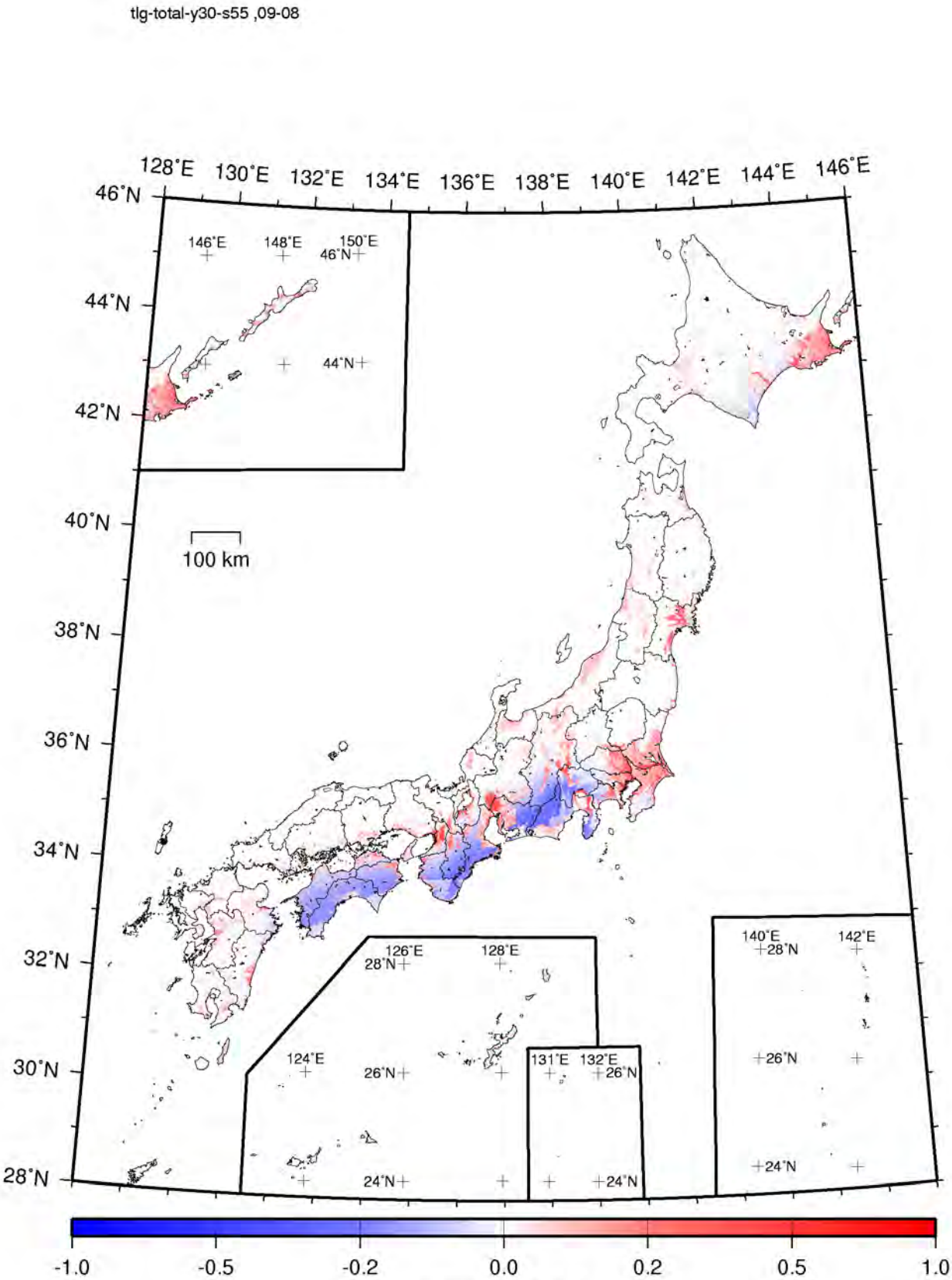

Difference in the exceedance probability within 30 years
(JMA seismic intensity: 6 Lower or more)

Figure 3.7.2-23 (3) Differences in the exceedance probability within 30 years taking all earthquakes into consideration (JMA seismic intensity: 6 Lower or more; maximum case)

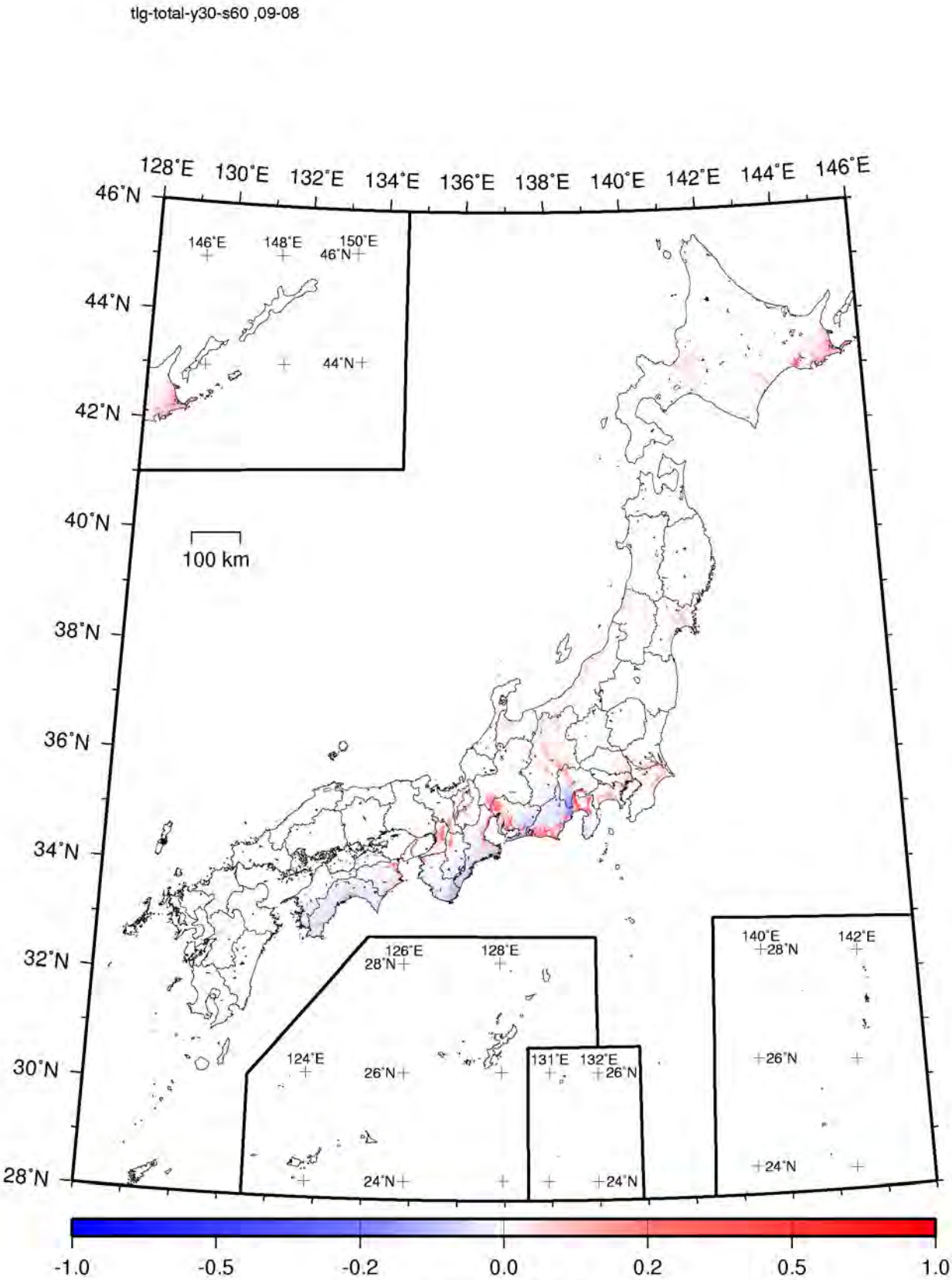

Difference in the exceedance probability within 30 years
(JMA seismic intensity: 6 Upper or more)

Figure 3.7.2-23 (4) Differences in the exceedance probability within 30 years taking all earthquakes into consideration (JMA seismic intensity: 6 Upper or more; maximum case)

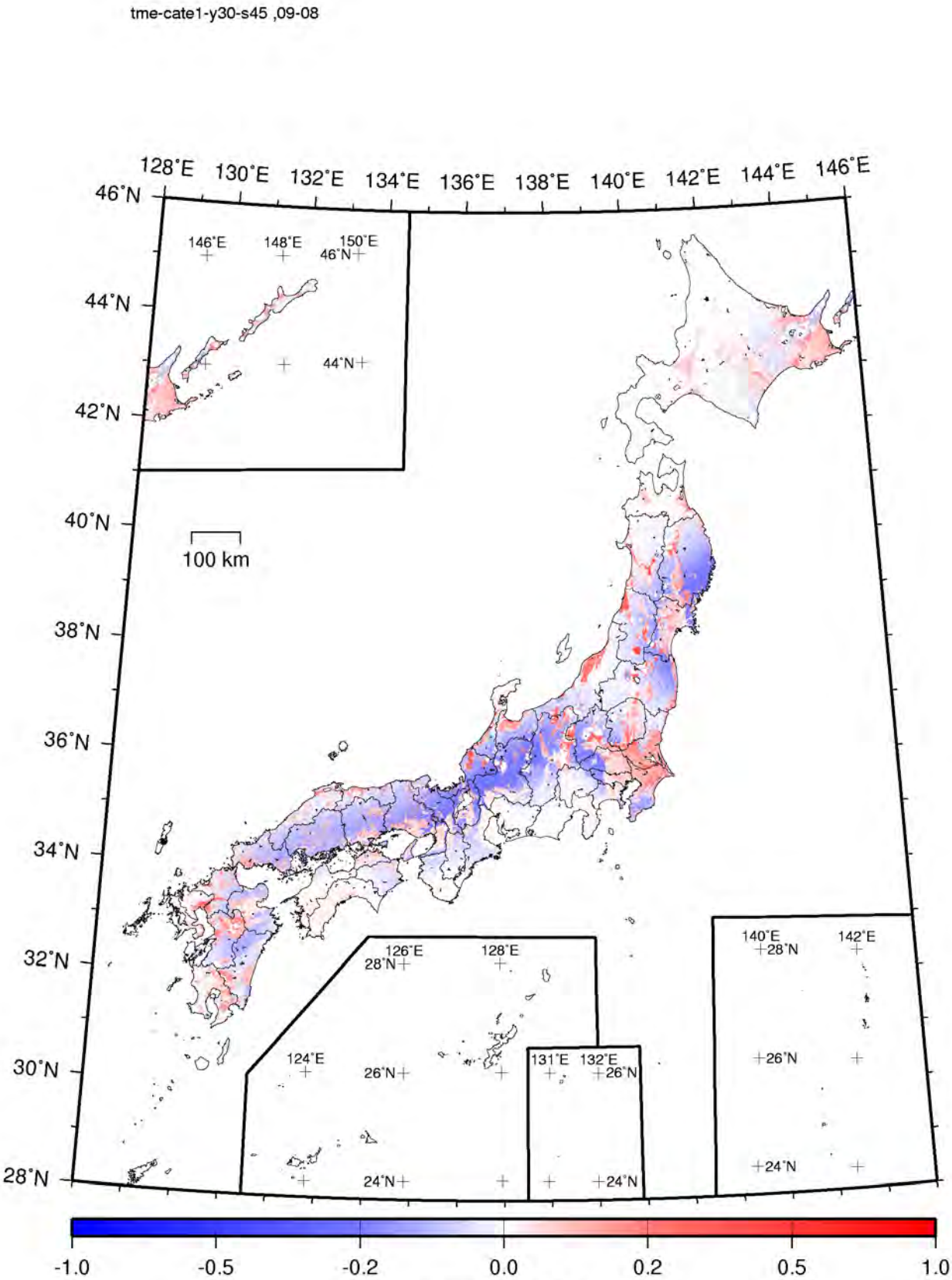

Difference in the exceedance probability within 30 years
(JMA seismic intensity: 5 Lower or more)

Figure 3.7.2-24 (1) Differences in the exceedance probability within 30 years associated with earthquake category I (JMA Seismic intensity: 5 Lower or more)

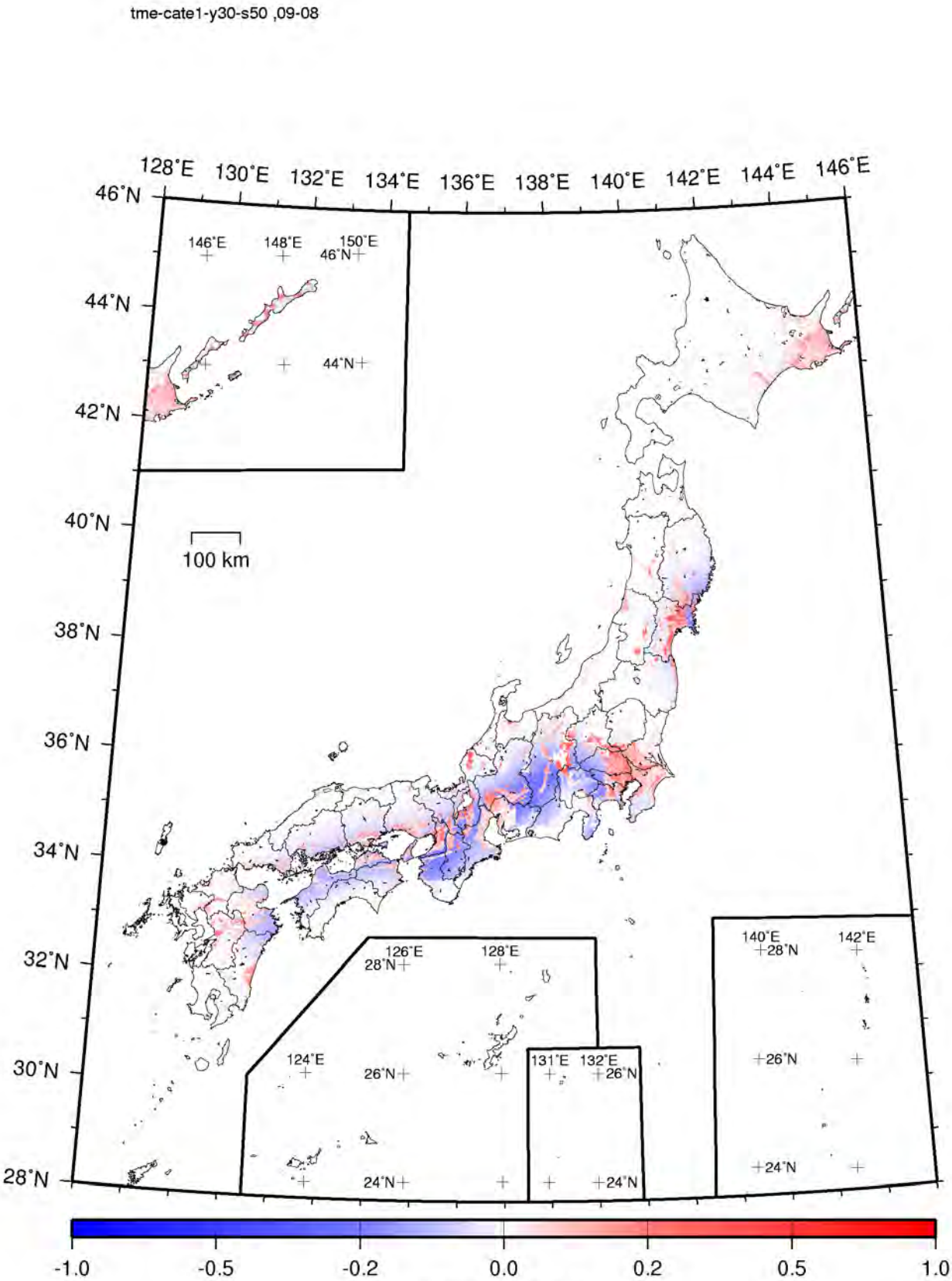

Difference in the exceedance probability within 30 years
(JMA seismic intensity: 5 Upper or more)

Figure 3.7.2-24 (2) Differences in the exceedance probability within 30 years associated with earthquake category I (JMA Seismic intensity: 5 Upper or more)

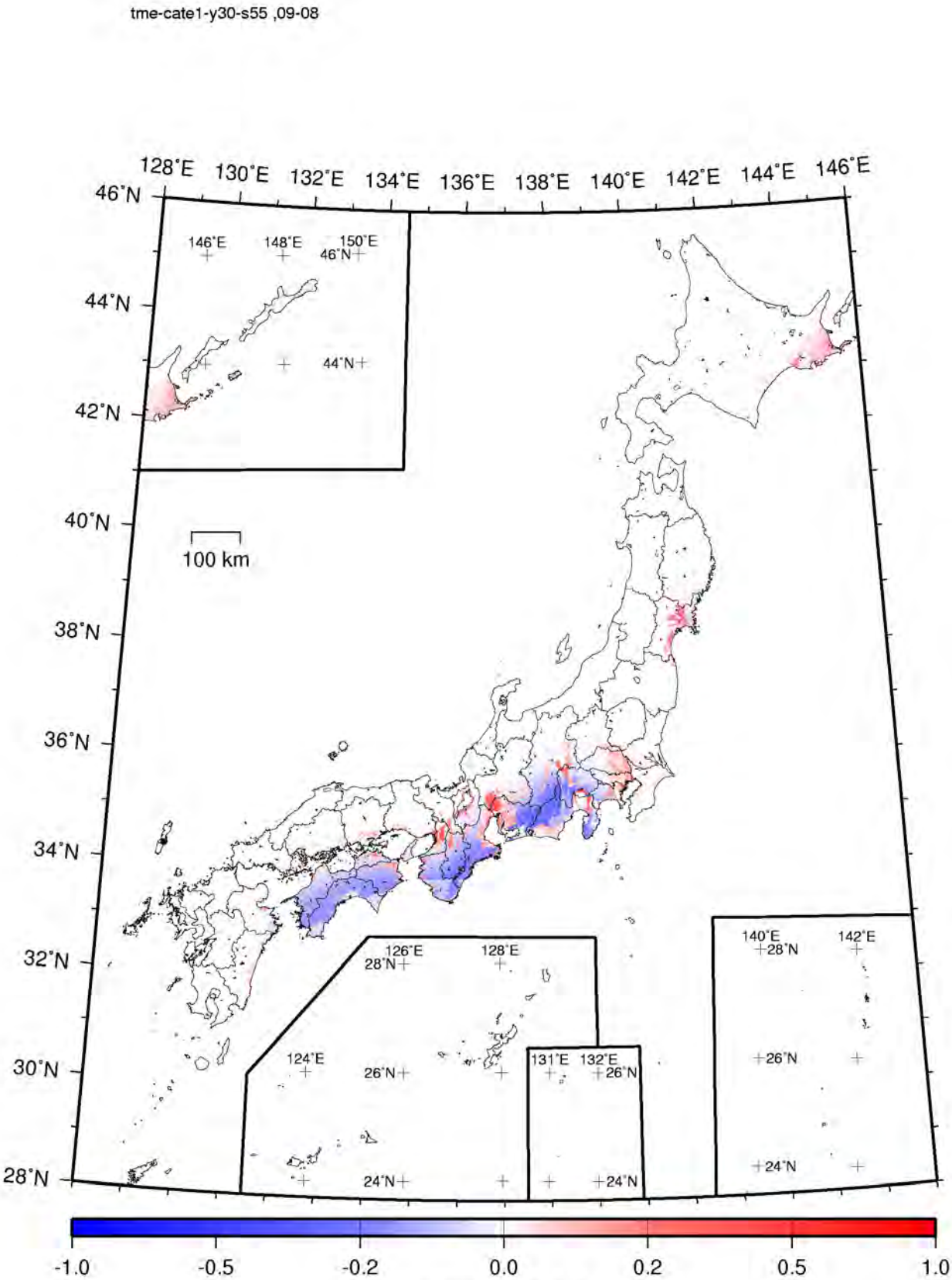

Difference in the exceedance probability within 30 years
(JMA seismic intensity: 6 Lower or more)

Figure 3.7.2-24 (3) Differences in the exceedance probability within 30 years associated with earthquake category I (JMA Seismic intensity: 6 Lower or more)

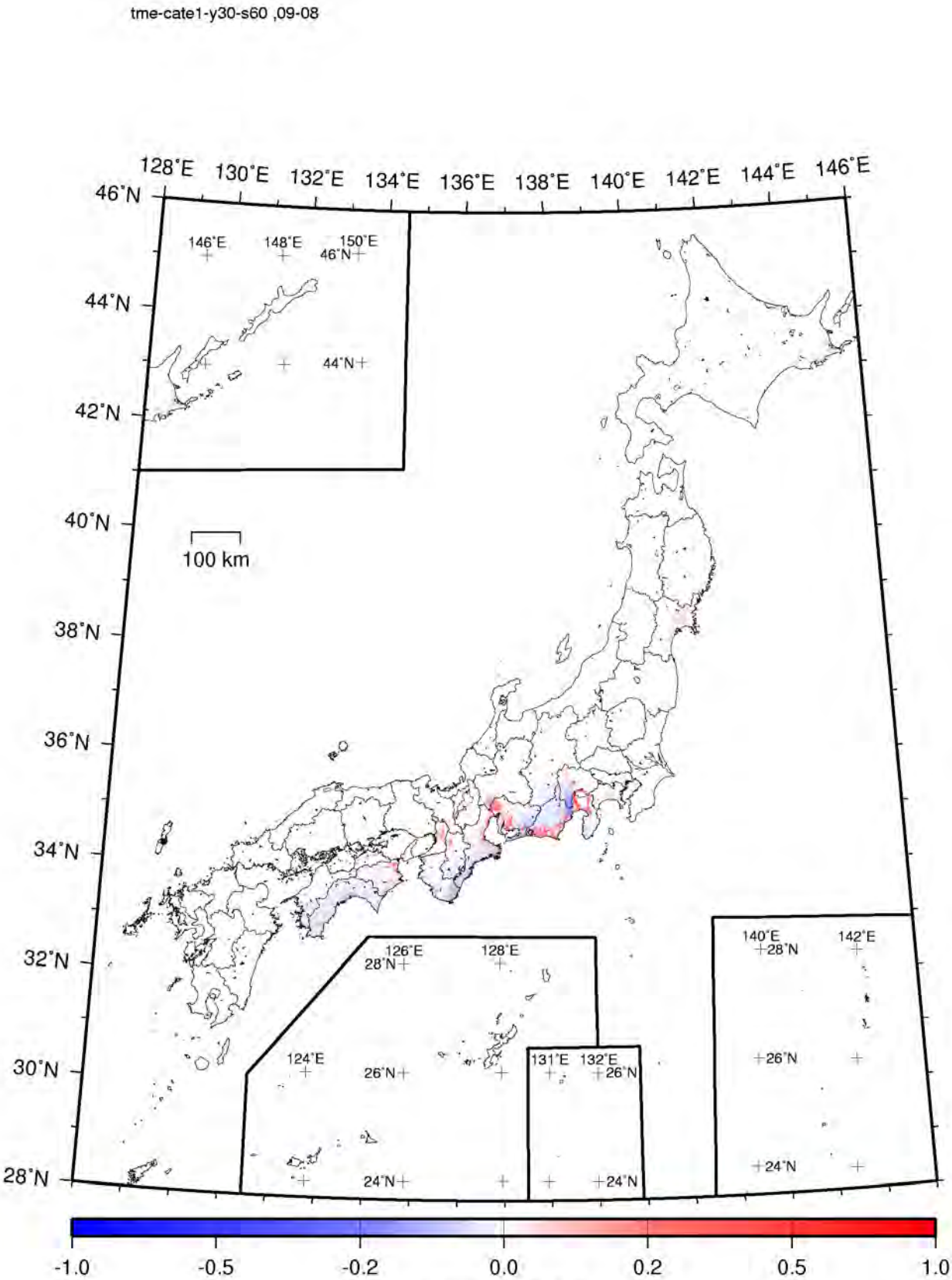

Difference in the exceedance probability within 30 years
(JMA seismic intensity: 6 Upper or more)

Figure 3.7.2-24 (4) Differences in the exceedance probability within 30 years associated with earthquake category I (JMA Seismic intensity: 6 Upper or more)

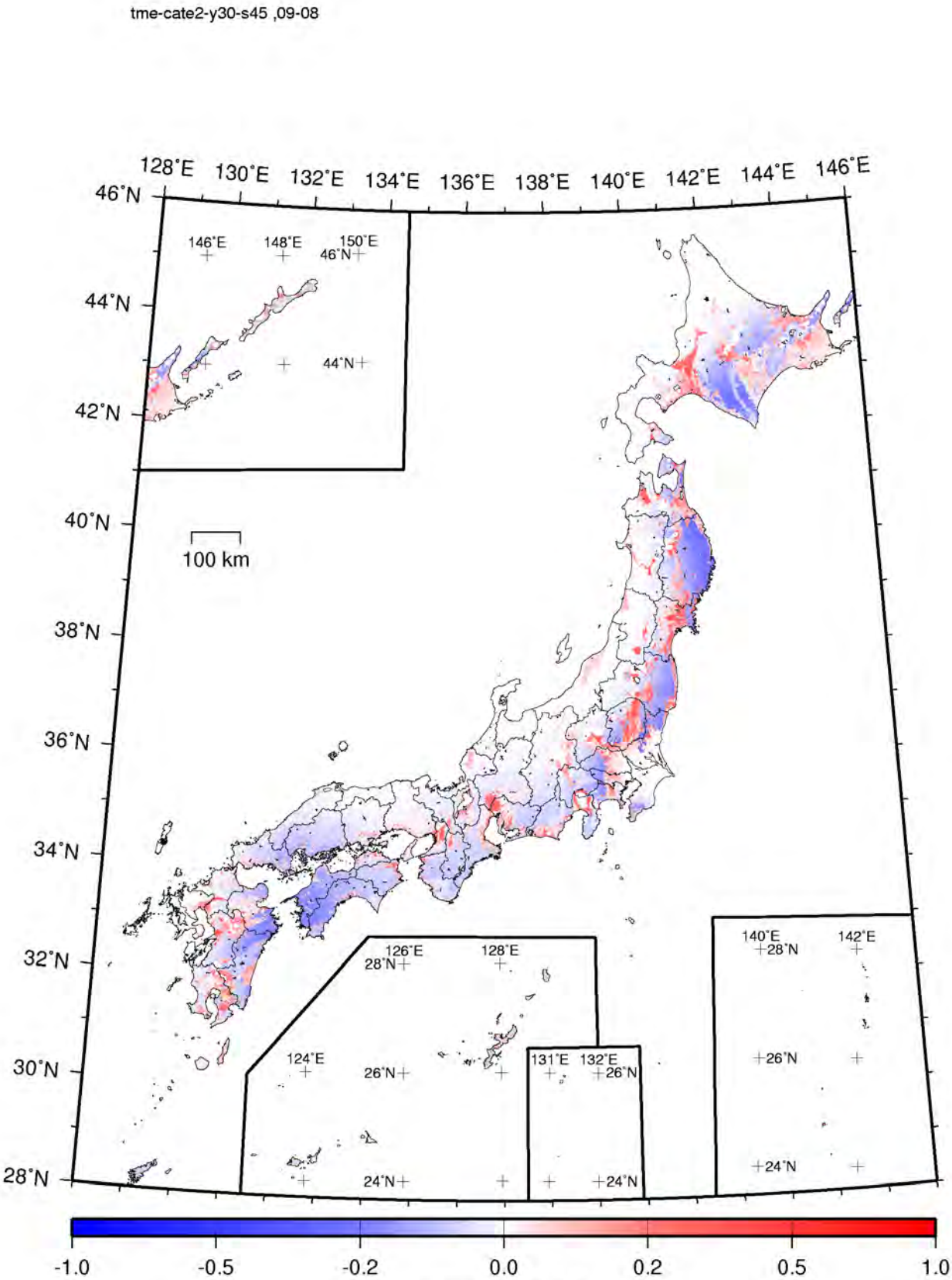

Difference in the exceedance probability within 30 years
(JMA seismic intensity: 5 Lower or more)

Figure 3.7.2-25 (1) Differences in the exceedance probability within 30 years associated with earthquake category II (JMA Seismic intensity: 5 Lower or more)

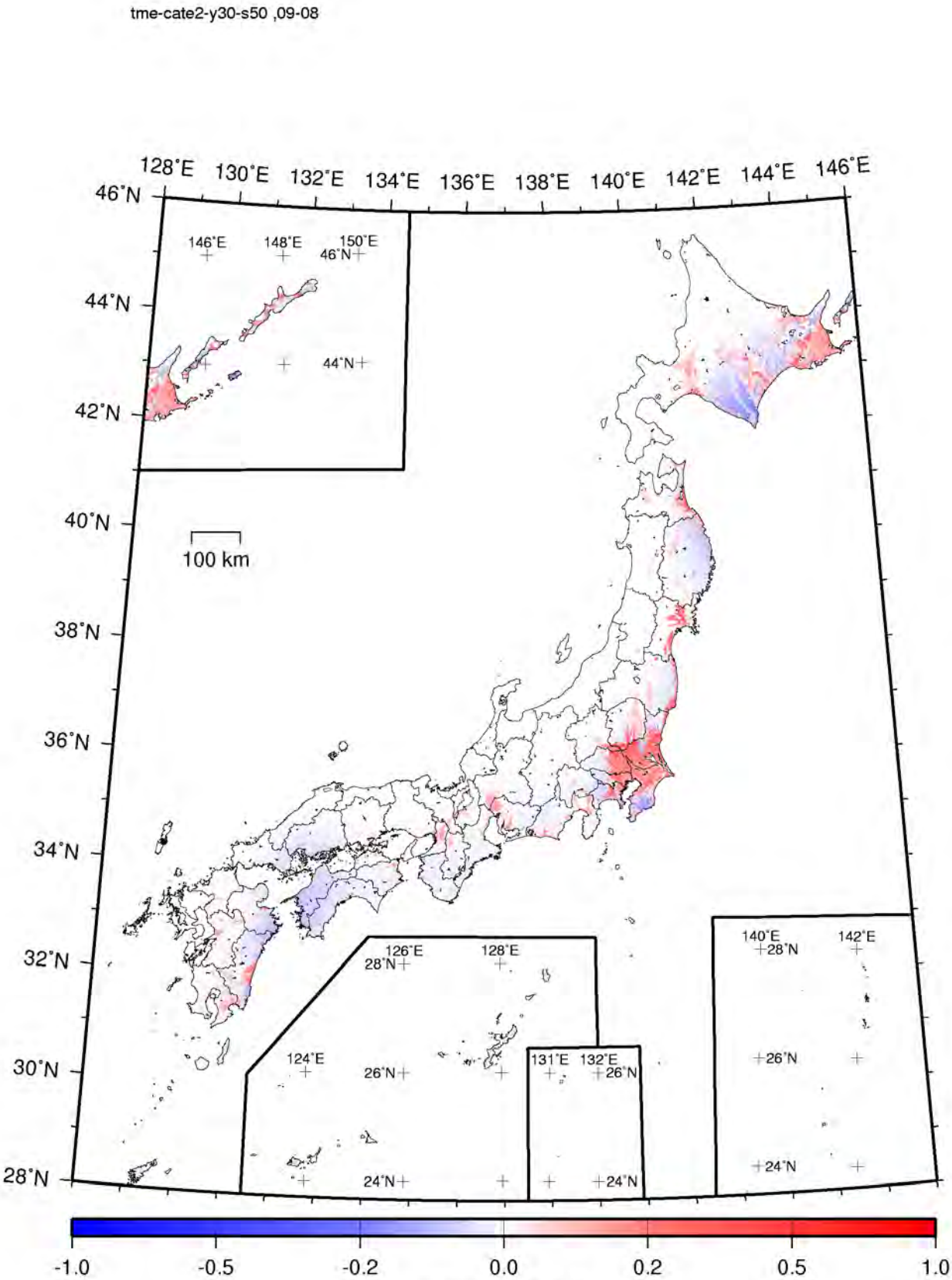

Difference in the exceedance probability within 30 years
(JMA seismic intensity: 5 Upper or more)

Figure 3.7.2-25 (2) Differences in the exceedance probability within 30 years associated with earthquake category II (JMA Seismic intensity: 5 Upper or more)

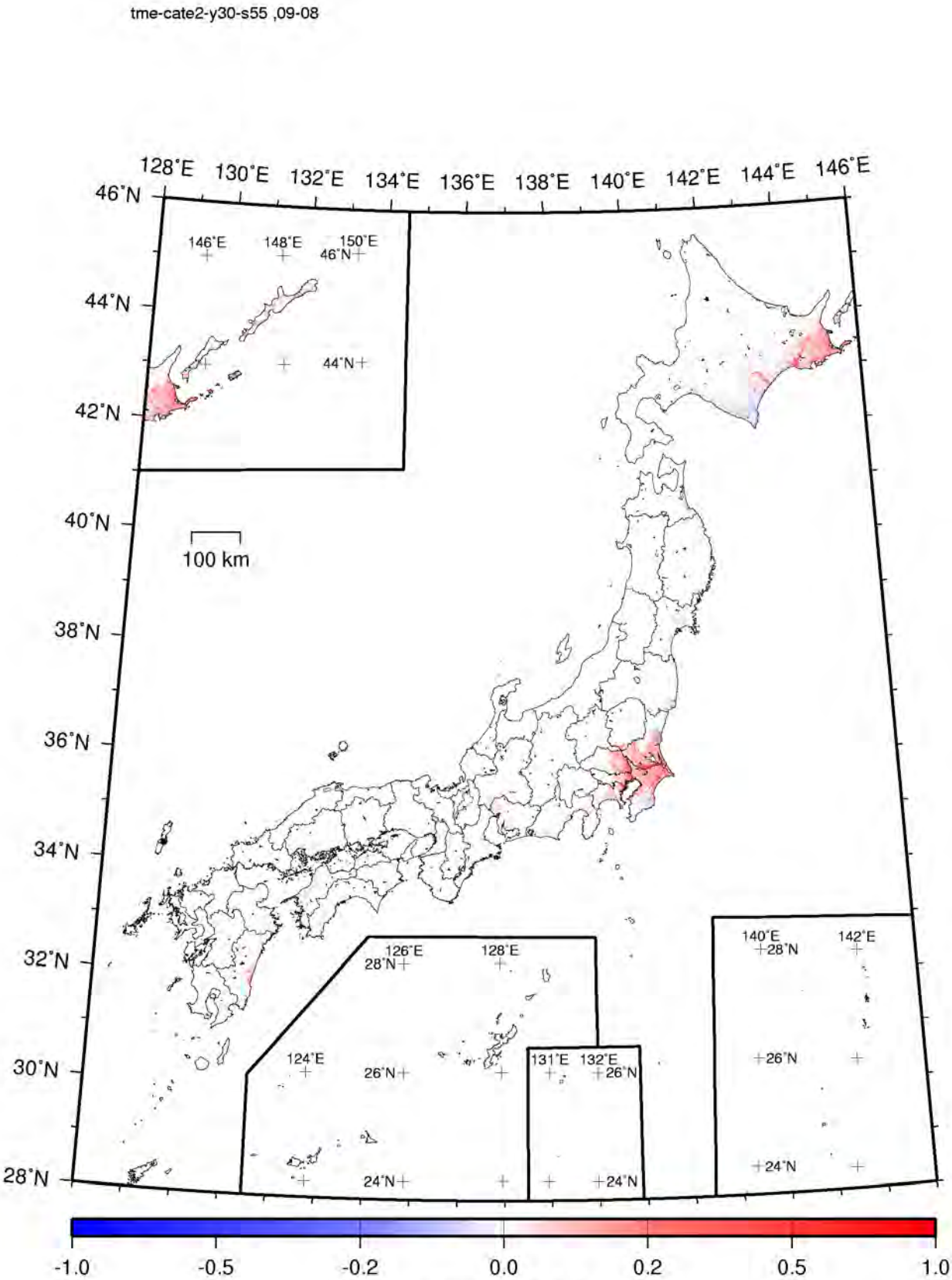

Difference in the exceedance probability within 30 years
(JMA seismic intensity: 6 Lower or more)

Figure 3.7.2-25 (3) Differences in the exceedance probability within 30 years associated with earthquake category II (JMA Seismic intensity: 6 Lower or more)

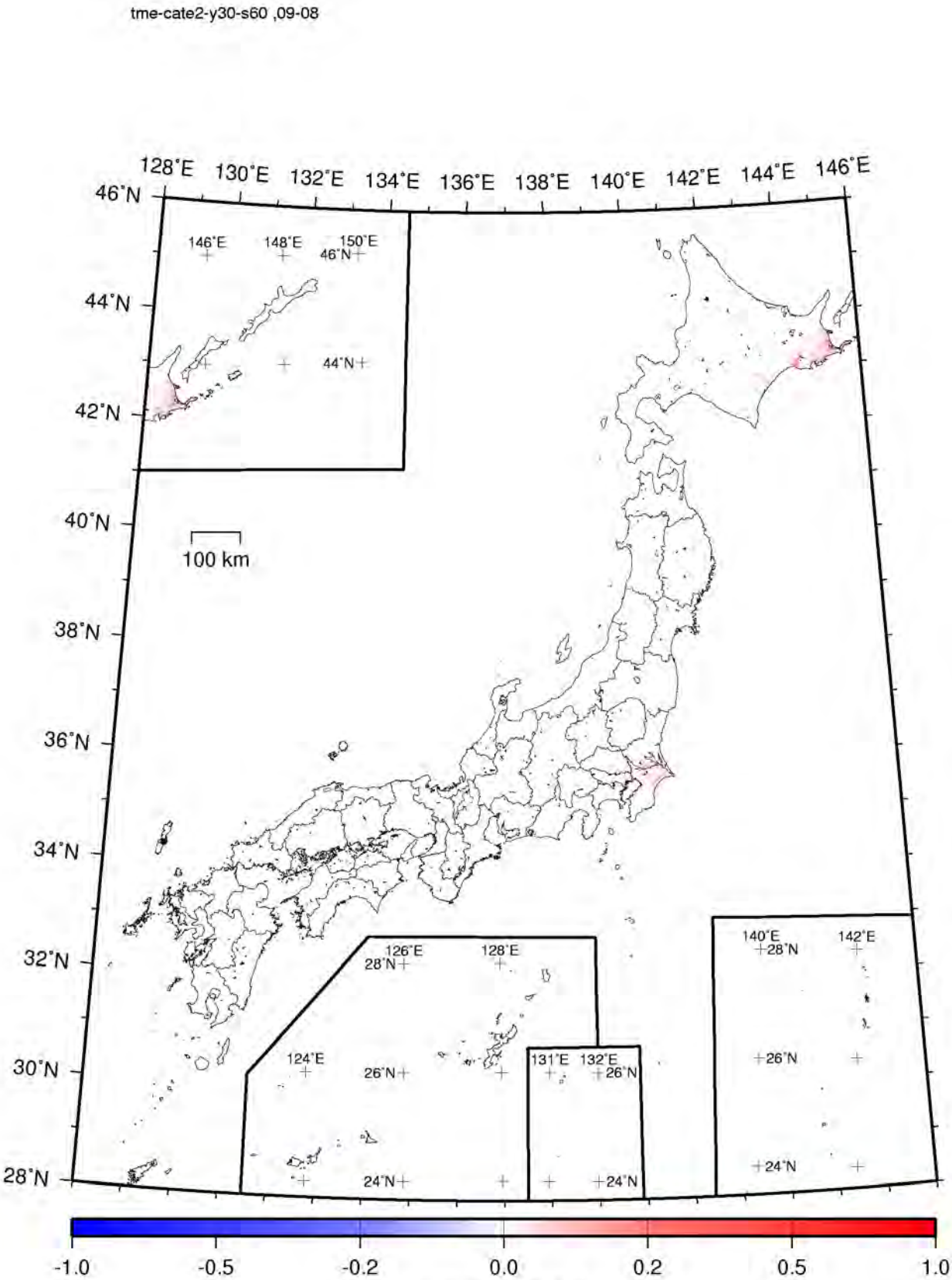

Difference in the exceedance probability within 30 years
(JMA seismic intensity: 6 Upper or more)

Figure 3.7.2-25 (4) Differences in the exceedance probability within 30 years associated with earthquake category II (JMA Seismic intensity: 6 Upper or more)

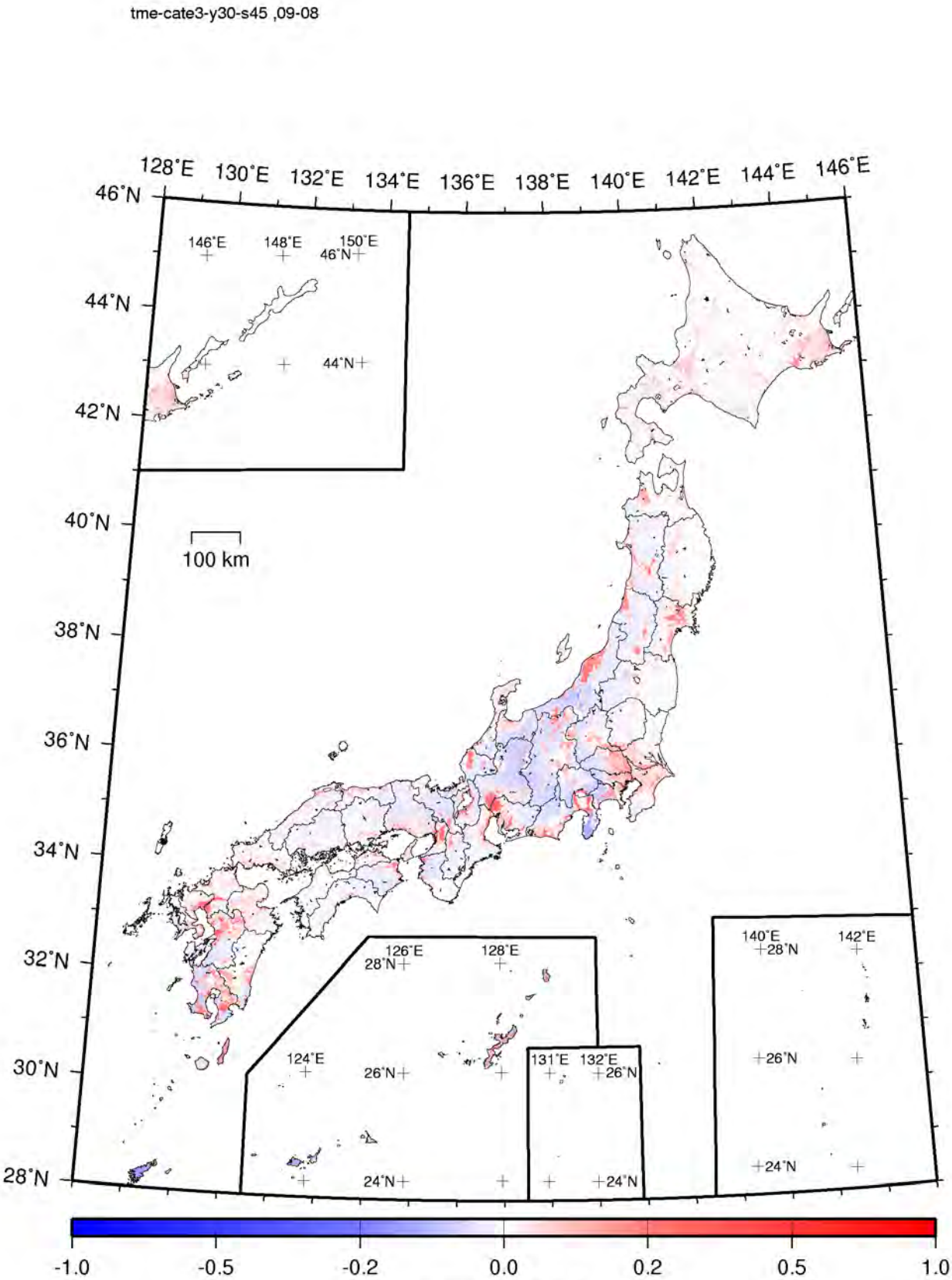

Difference in the exceedance probability within 30 years
(JMA seismic intensity: 5 Lower or more)

Figure 3.7.2-26 (1) Differences in the exceedance probability within 30 years associated with earthquake category III (JMA Seismic intensity: 5 Lower or more; average case)

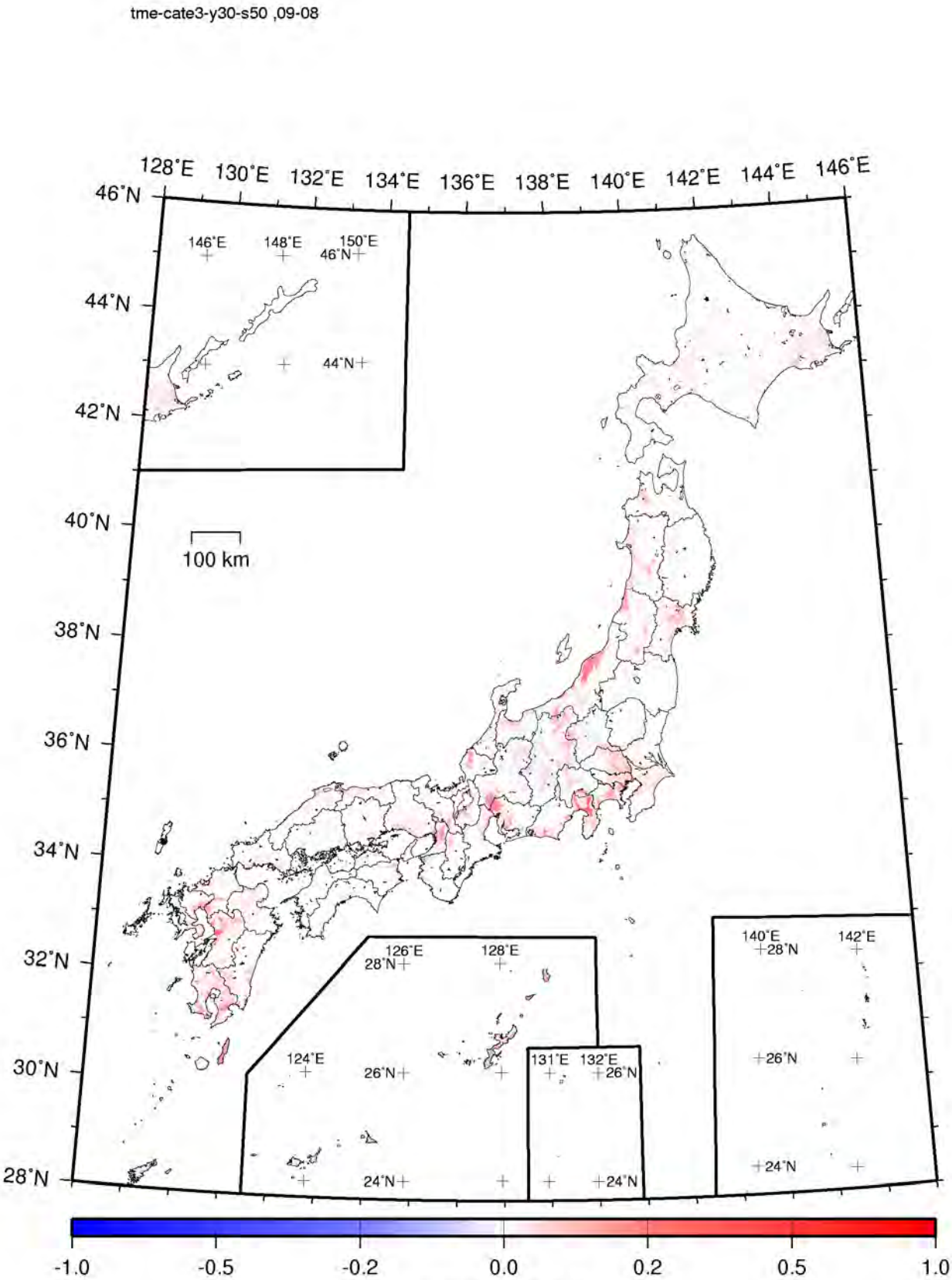

Difference in the exceedance probability within 30 years
(JMA seismic intensity: 5 Upper or more)

Figure 3.7.2-26 (2) Differences in the exceedance probability within 30 years associated with earthquake category III (JMA Seismic intensity: 5 Upper or more; average case)

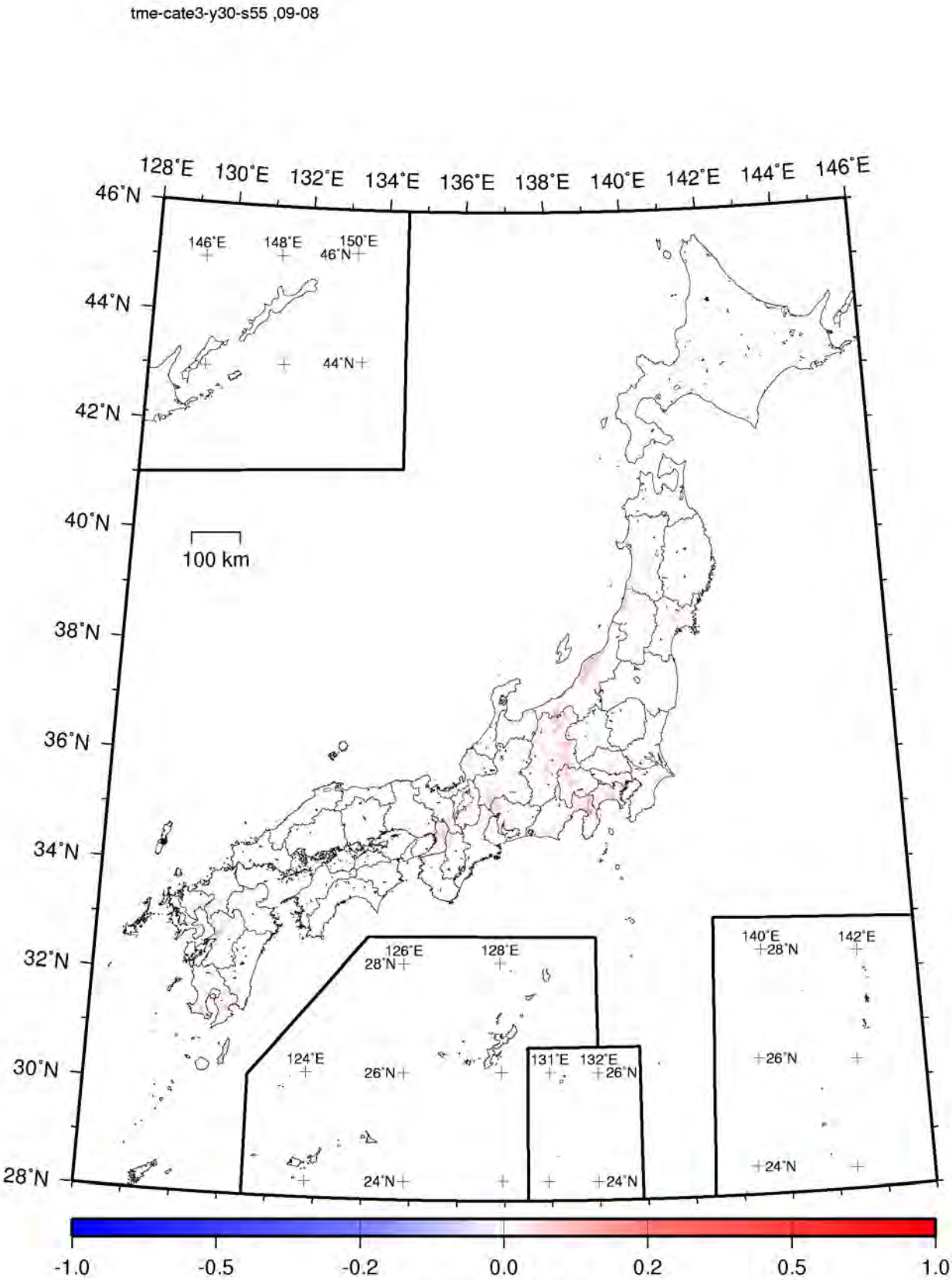

Difference in the exceedance probability within 30 years
(JMA seismic intensity: 6 Lower or more)

Figure 3.7.2-26 (3) Differences in the exceedance probability within 30 years associated with earthquake category III (JMA Seismic intensity: 6 Lower or more; average case)

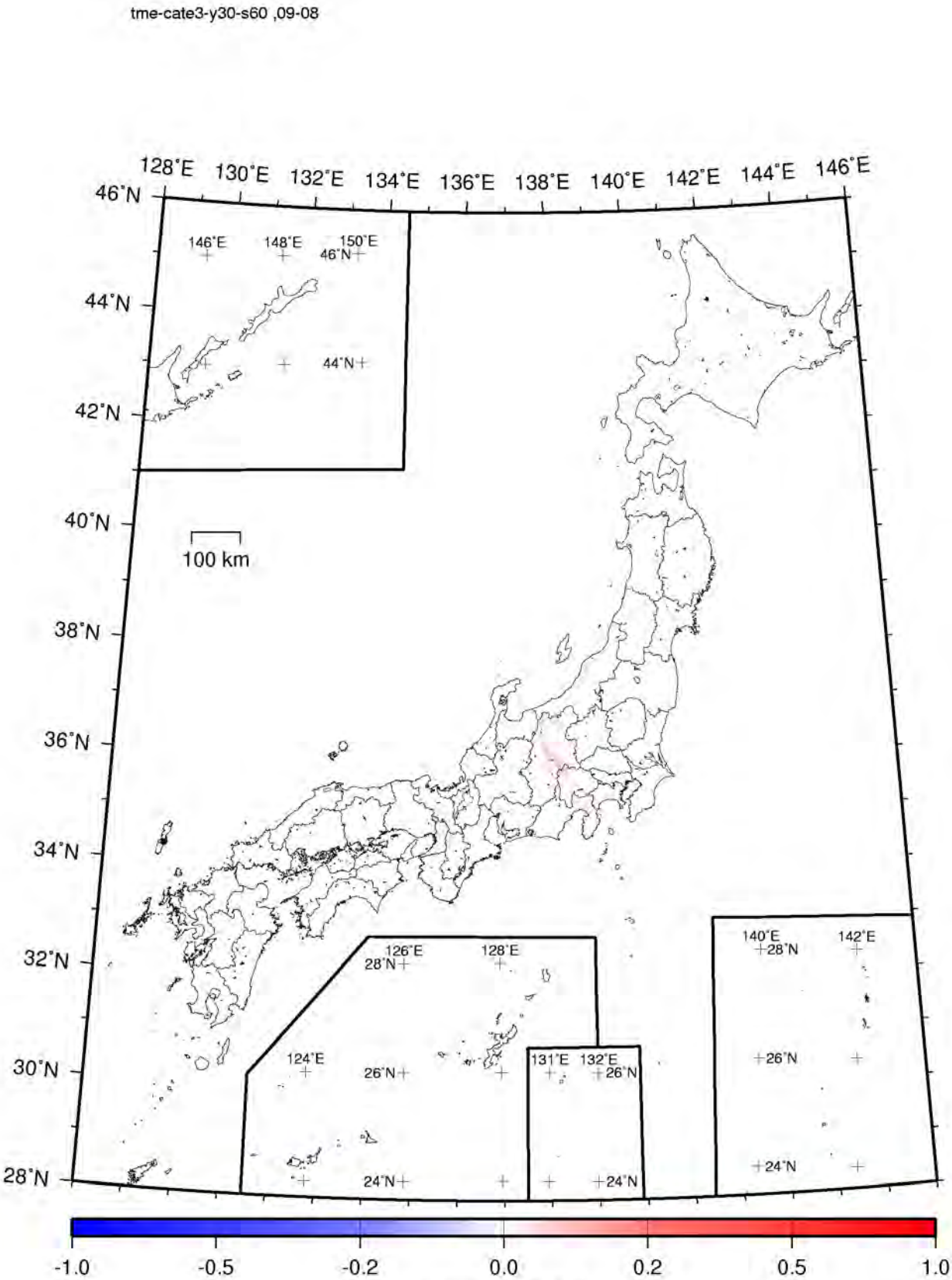

Difference in the exceedance probability within 30 years
(JMA seismic intensity: 6 Upper or more)

Figure 3.7.2-26 (4) Differences in the exceedance probability within 30 years associated with earthquake category III (JMA Seismic intensity: 6 Upper or more; average case)

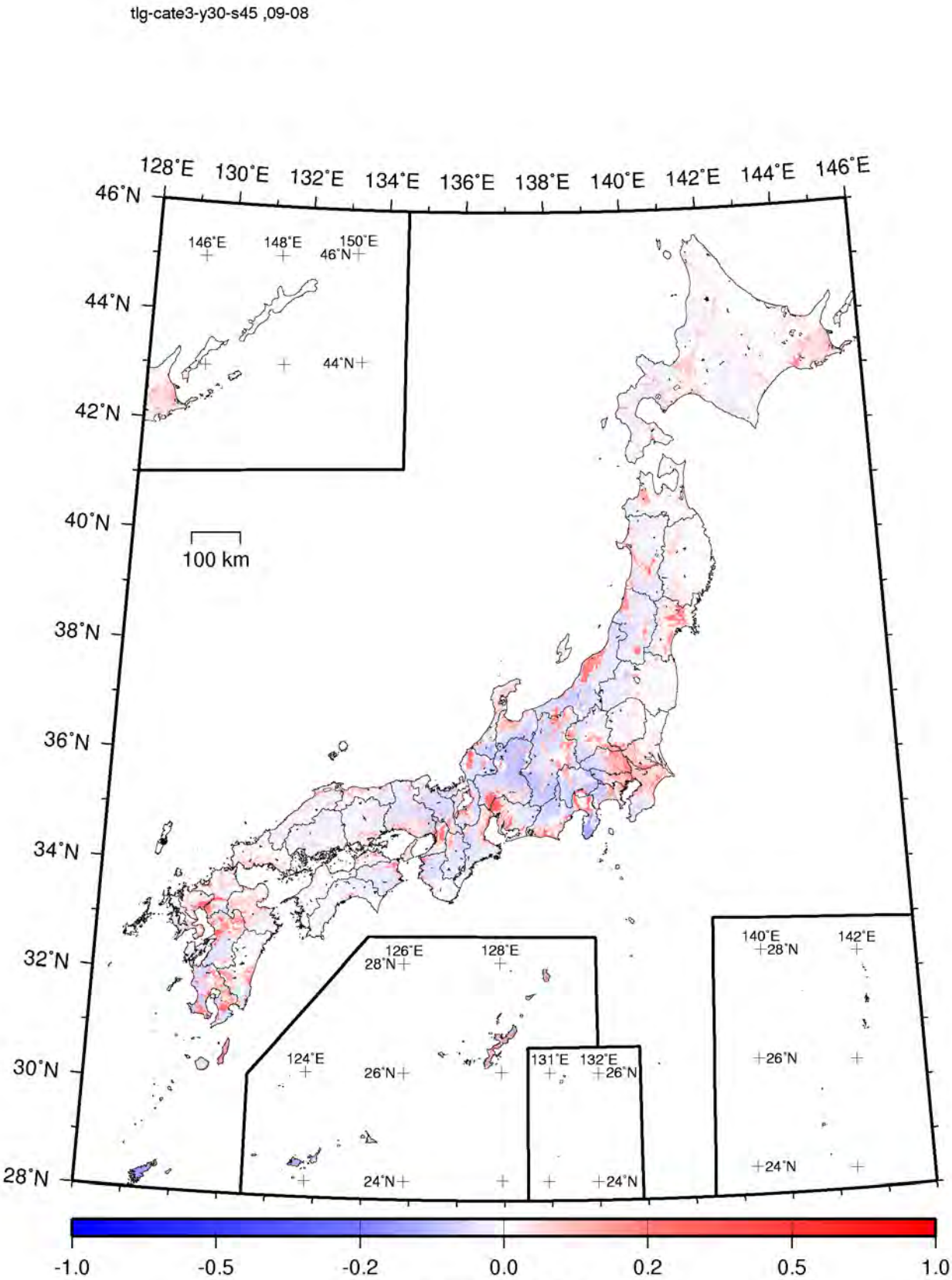

Difference in the exceedance probability within 30 years
(JMA seismic intensity: 5 Lower or more)

Figure 3.7.2-27 (1) Differences in the exceedance probability within 30 years associated with earthquake category III (JMA Seismic intensity: 5 Lower or more; maximum case)

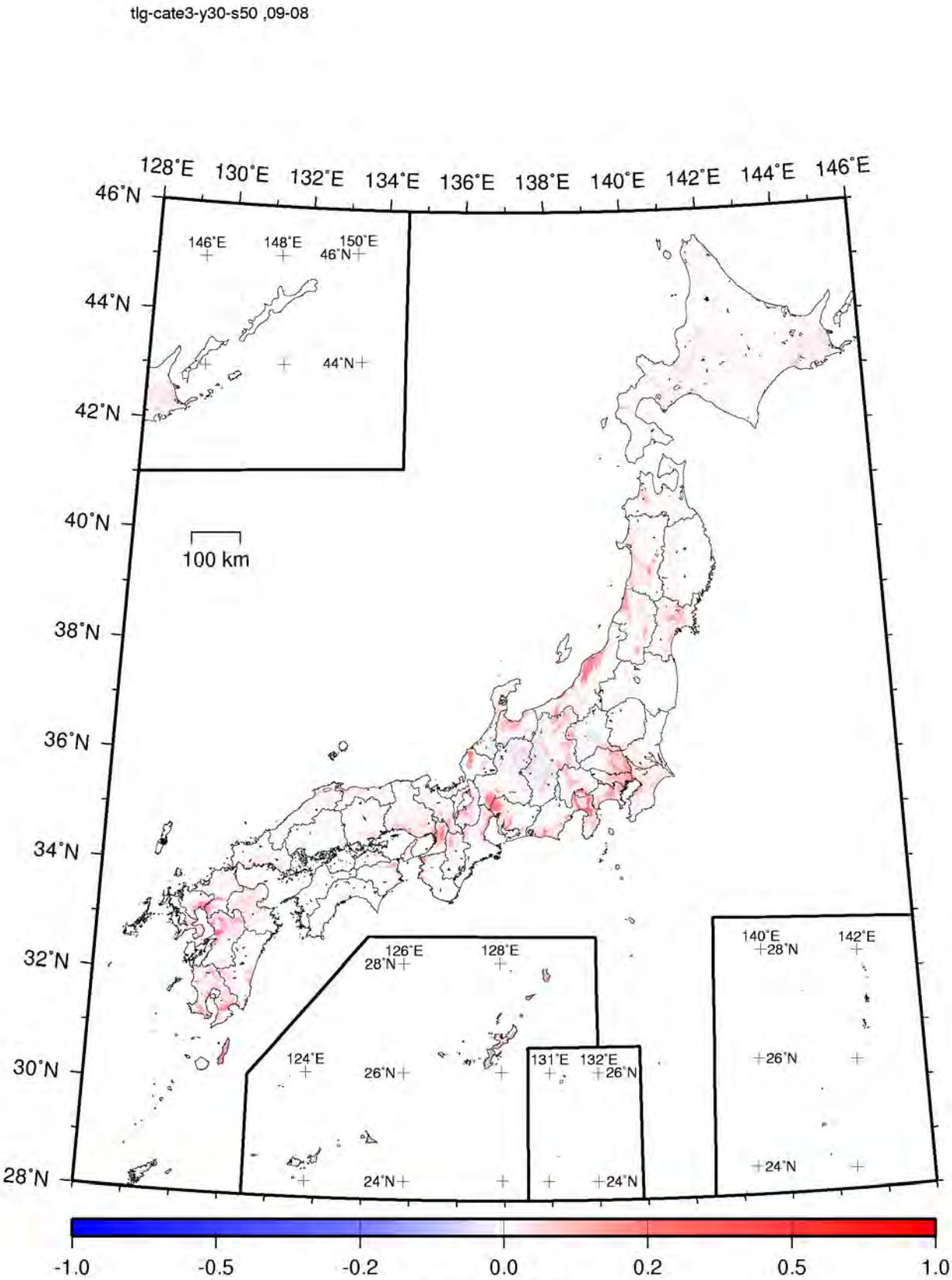

Difference in the exceedance probability within 30 years
(JMA seismic intensity: 5 Upper or more)

Figure 3.7.2-27 (2) Differences in the exceedance probability within 30 years associated with earthquake category III (JMA Seismic intensity: 5 Upper or more; maximum case)

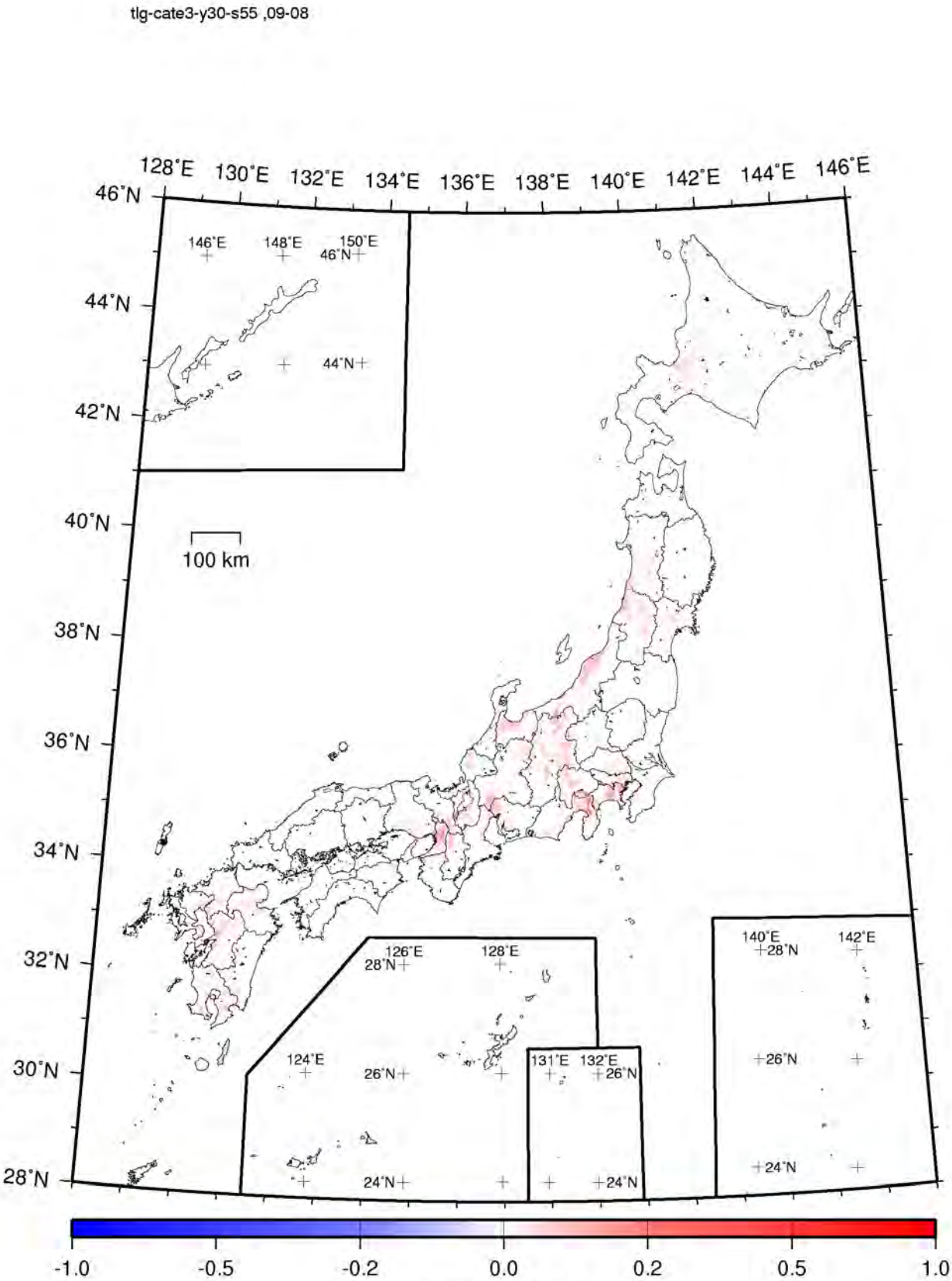

Difference in the exceedance probability within 30 years
(JMA seismic intensity: 6 Lower or more)

Figure 3.7.2-27 (3) Differences in the exceedance probability within 30 years associated with earthquake category III (JMA Seismic intensity: 6 Lower or more; maximum case)

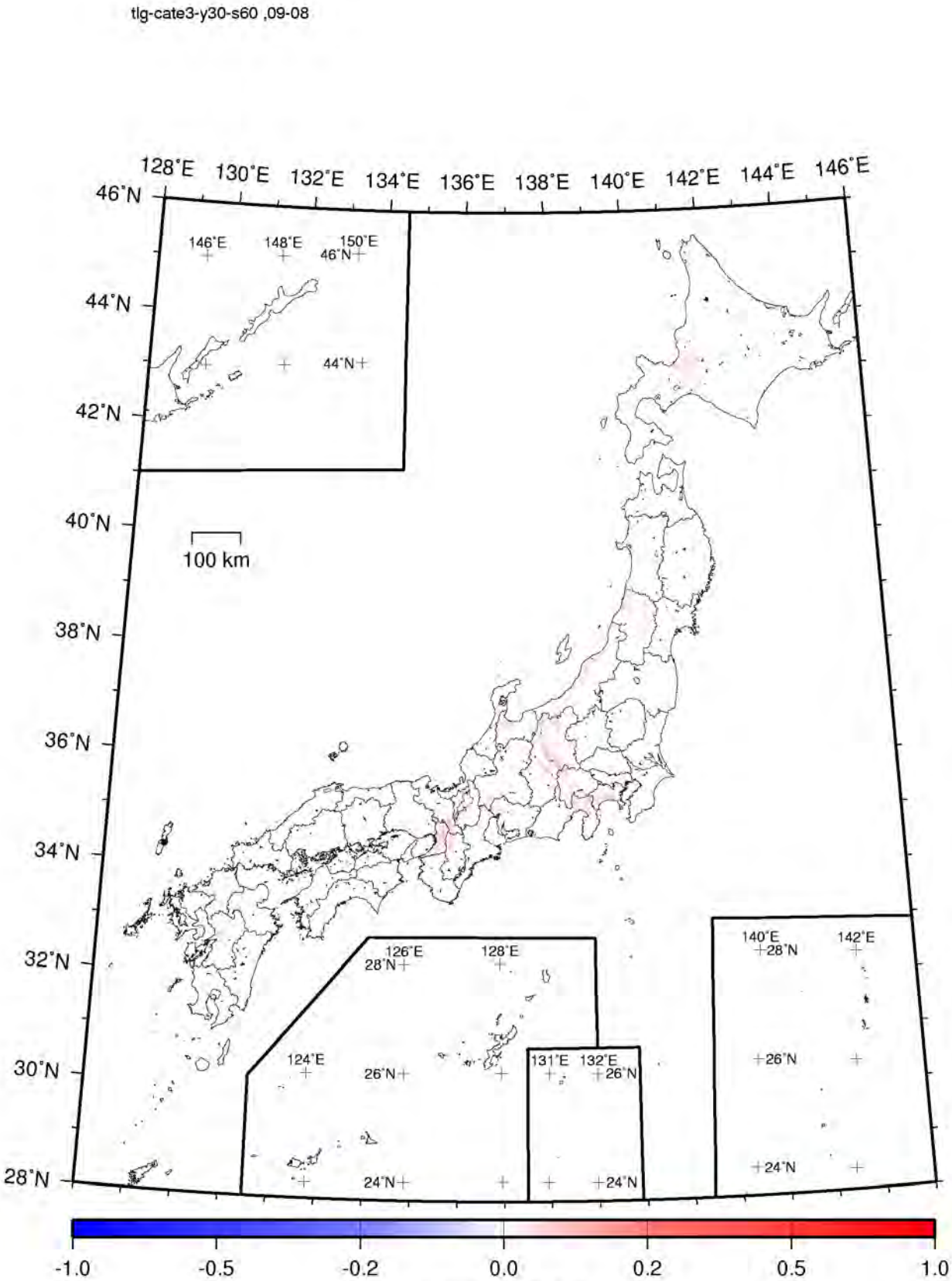

Difference in the exceedance probability within 30 years
(JMA seismic intensity: 6 Upper or more)

Figure 3.7.2-27 (4) Differences in the exceedance probability within 30 years associated with earthquake category III (JMA Seismic intensity: 6 Upper or more; maximum case)

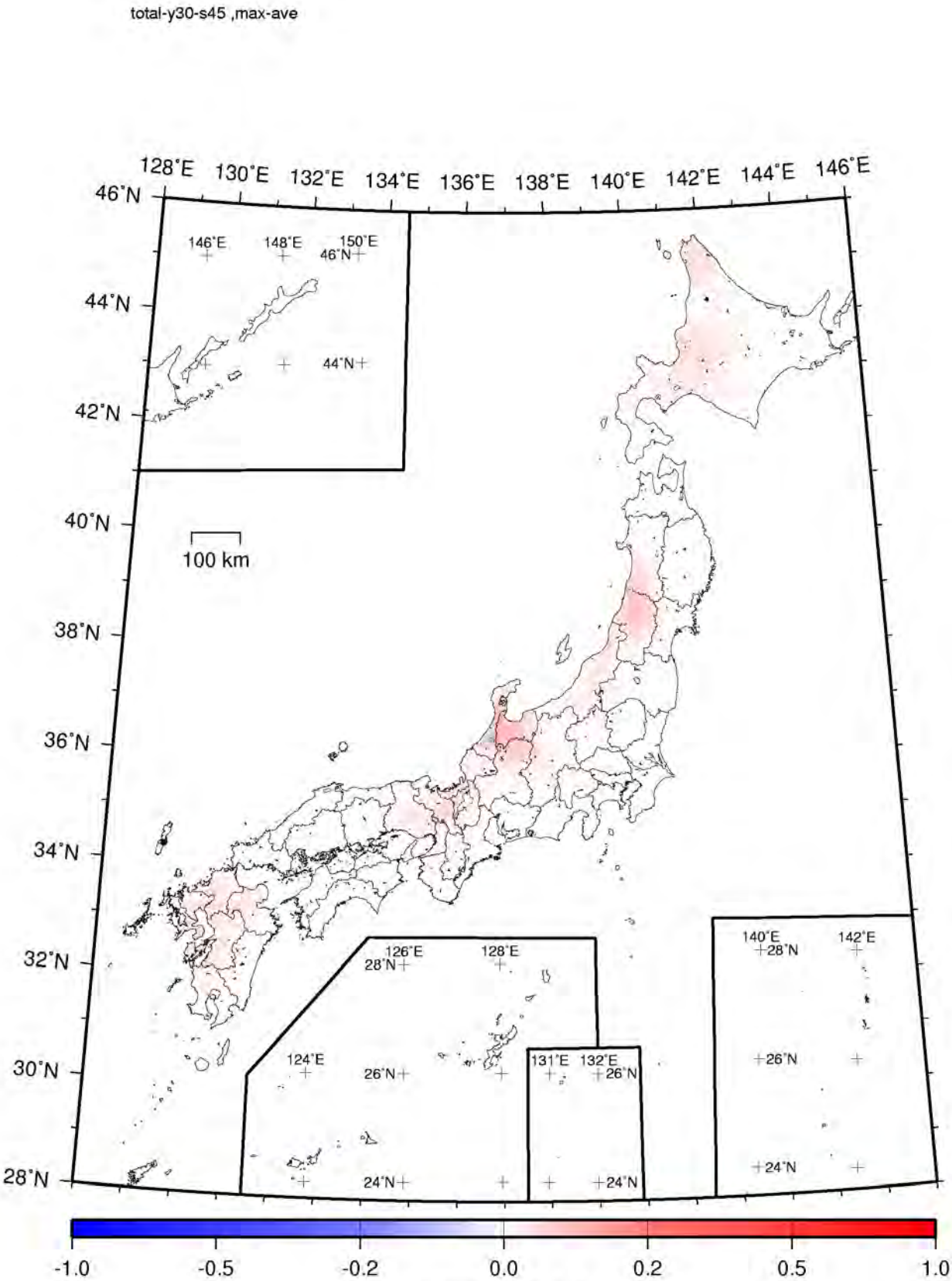

Difference in the exceedance probability within 30 years
(JMA seismic intensity: 5 Lower or more)

Figure 3.7.2-28 (1) Differences in the exceedance probability within 30 years taking all earthquakes into consideration (JMA seismic intensity: 5 Lower or more; "maximum case" - "average case")

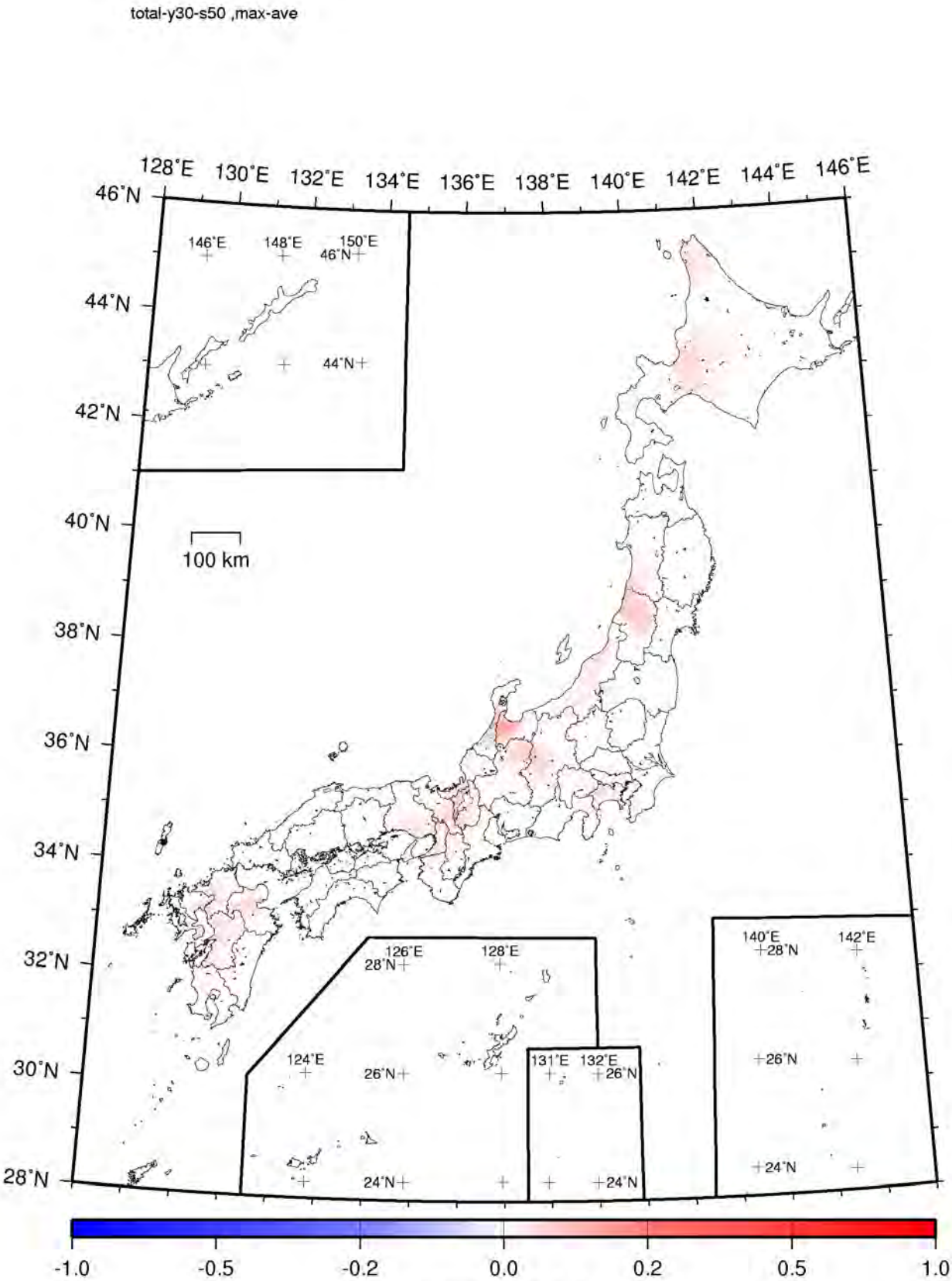

Difference in the exceedance probability within 30 years
(JMA seismic intensity: 5 Upper or more)

Figure 3.7.2-28 (2) Differences in the exceedance probability within 30 years taking all earthquakes into consideration (JMA seismic intensity: 5 Upper or more; "maximum case" - "average case")

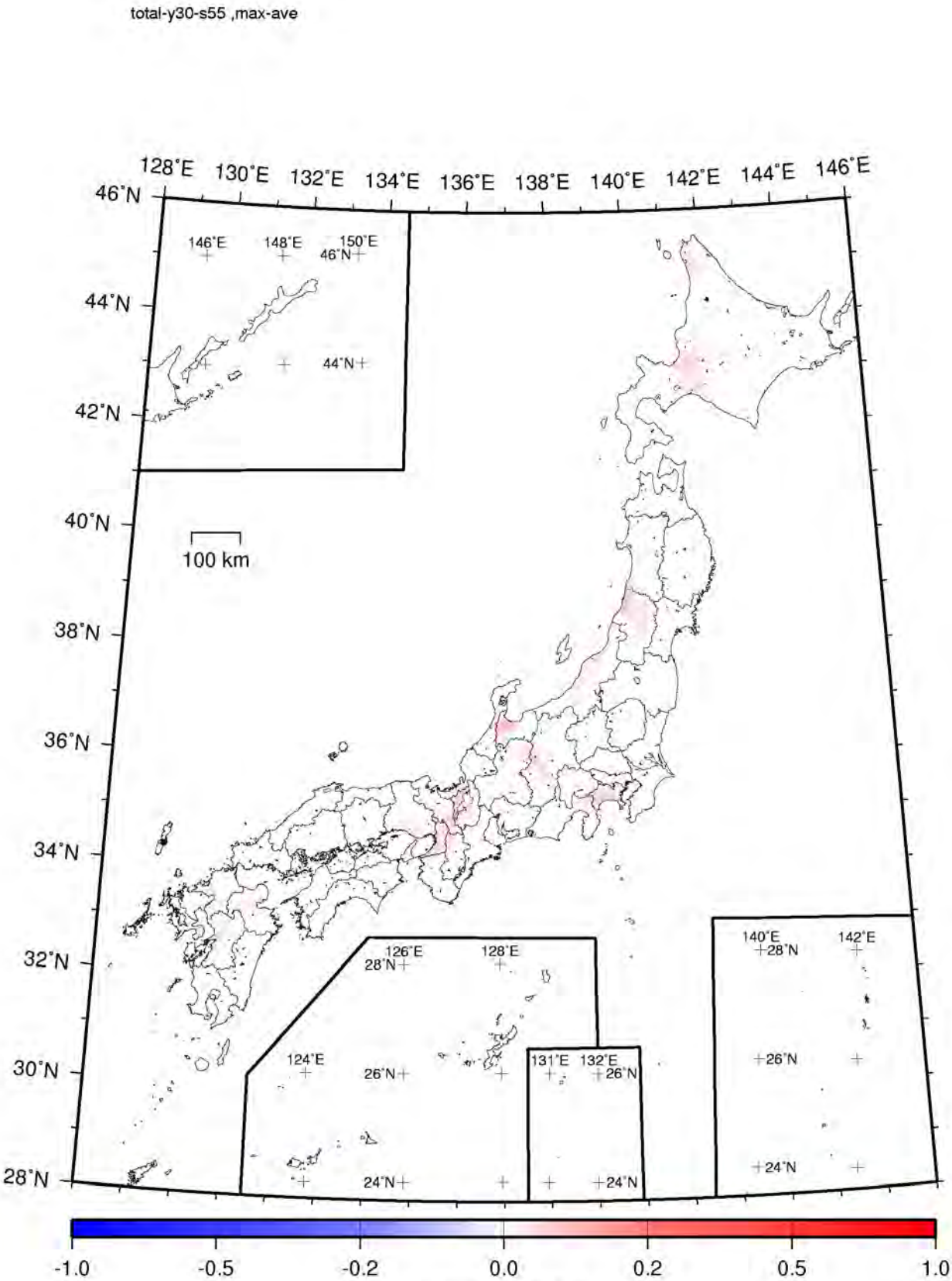

Difference in the exceedance probability within 30 years
(JMA seismic intensity: 6 Lower or more)

Figure 3.7.2-28 (3) Differences in the exceedance probability within 30 years taking all earthquakes into consideration (JMA seismic intensity: 6 Lower or more; "maximum case" - "average case")

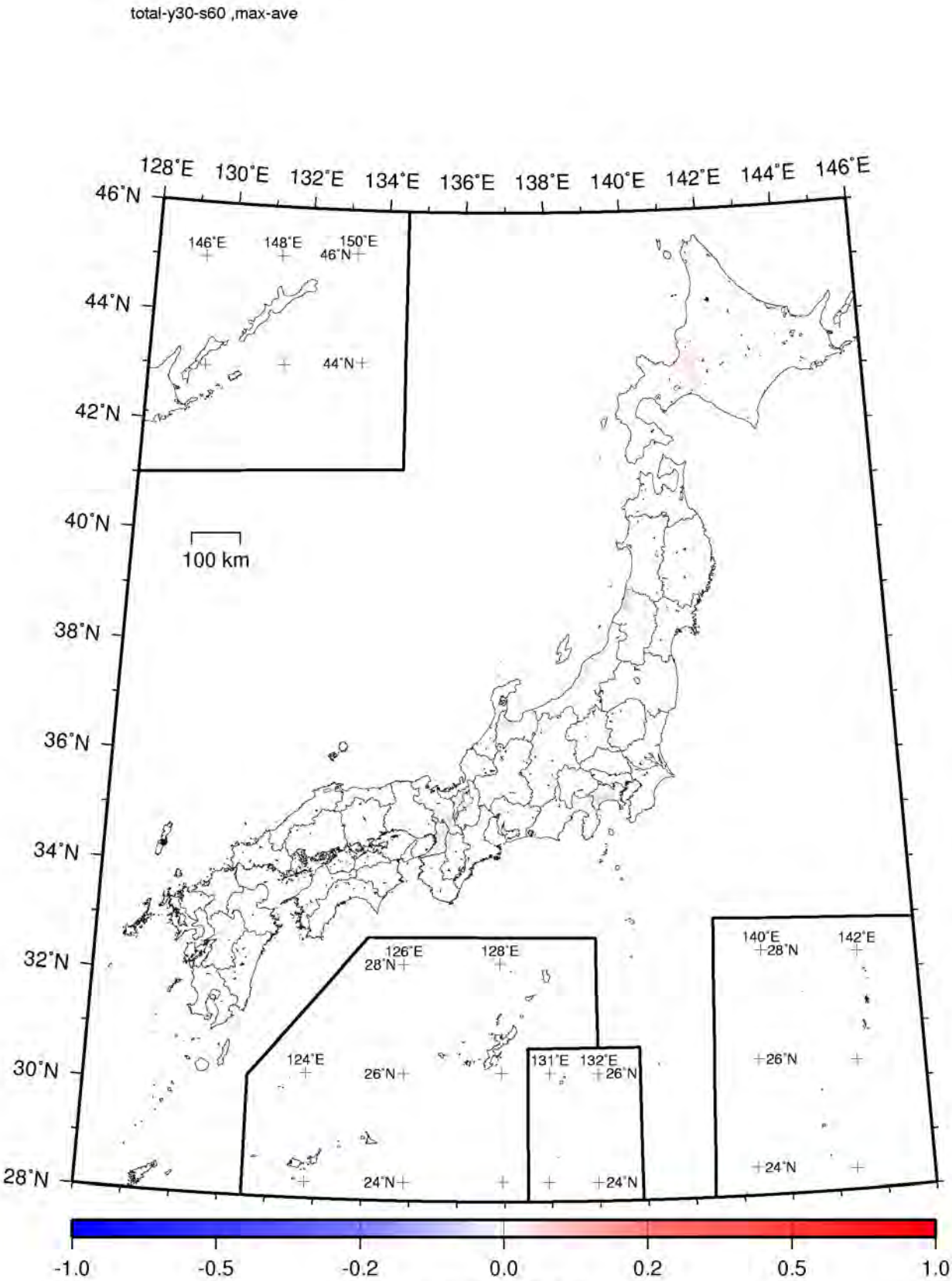

Difference in the exceedance probability within 30 years
(JMA seismic intensity: 6 Upper or more)

Figure 3.7.2-28 (4) Differences in the exceedance probability within 30 years taking all earthquakes into consideration (JMA seismic intensity: 6 Upper or more; "maximum case" - "average case")

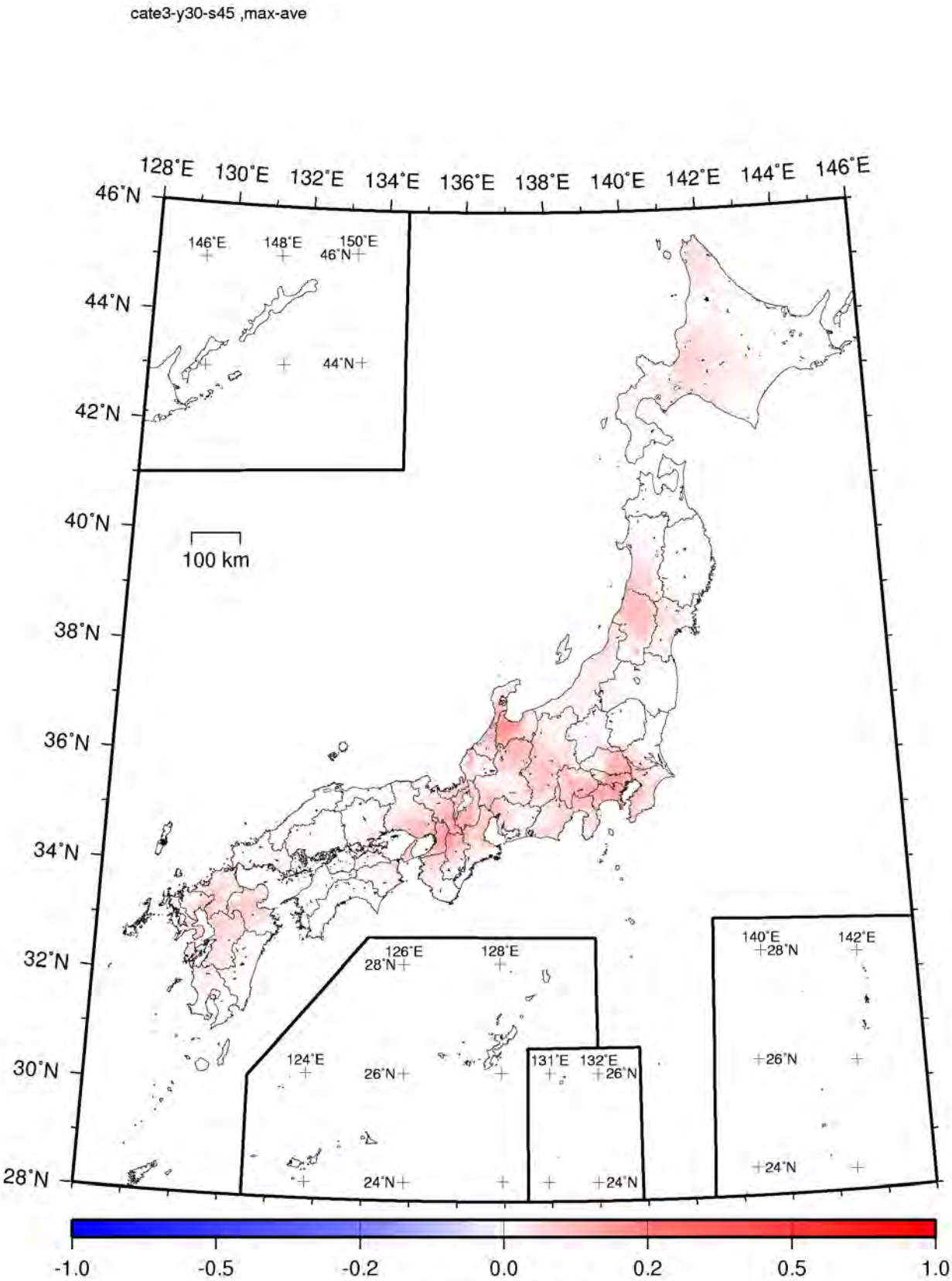

Difference in the exceedance probability within 30 years
(JMA seismic intensity: 5 Lower or more)

Figure 3.7.2-29 (1) Differences in the exceedance probability within 30 years associated with earthquake category III (JMA Seismic intensity: 5 Lower or more; "maximum case" - "average case")

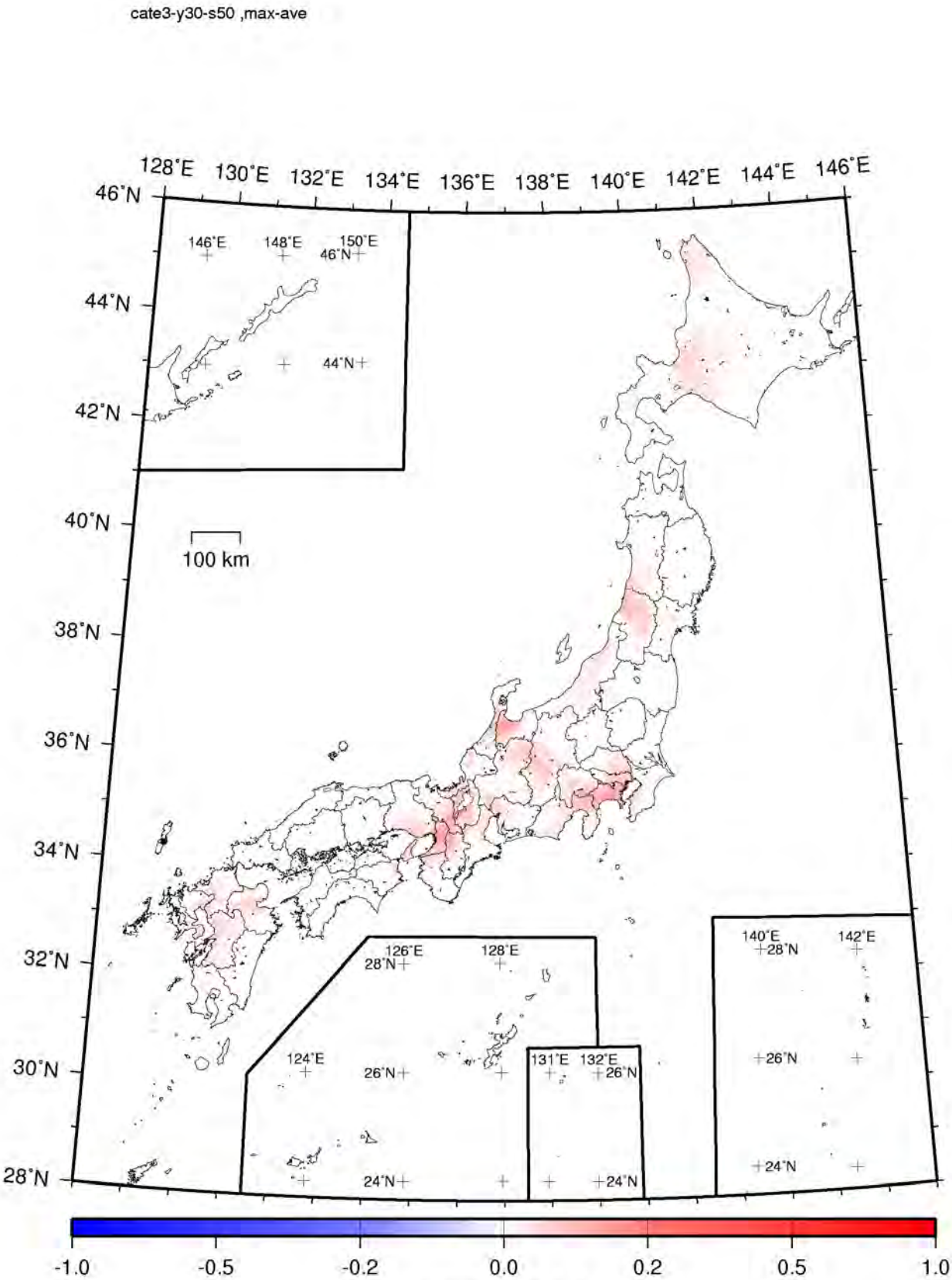

Difference in the exceedance probability within 30 years
(JMA seismic intensity: 5 Upper or more)

Figure 3.7.2-29 (2) Differences in the exceedance probability within 30 years associated with earthquake category III (JMA Seismic intensity: 5 Upper or more; "maximum case" - "average case")

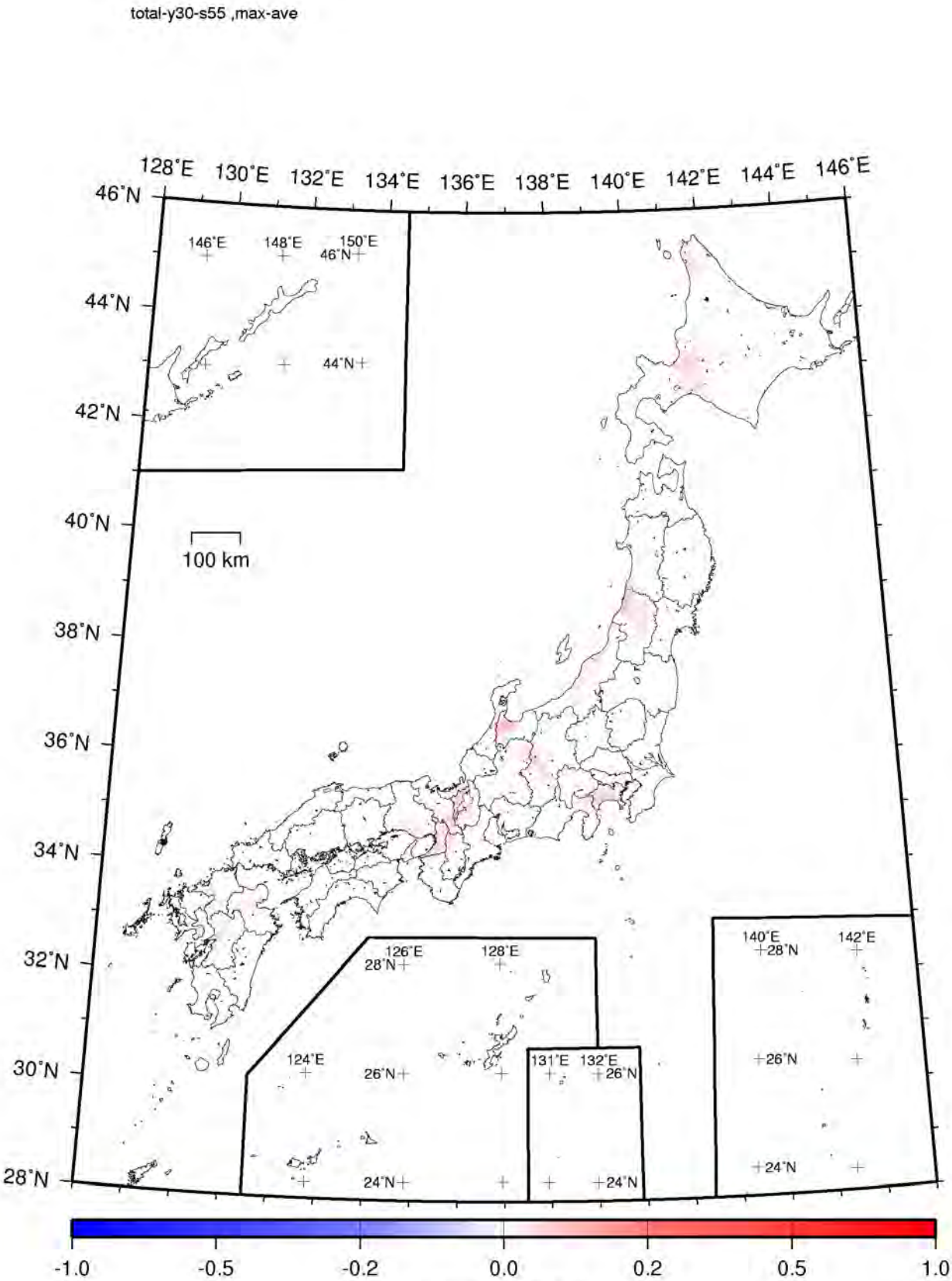

Difference in the exceedance probability within 30 years
(JMA seismic intensity: 6 Lower or more)

Figure 3.7.2-29 (3) Differences in the exceedance probability within 30 years associated with earthquake category III (JMA Seismic intensity: 6 Lower or more; "maximum case" - "average case")

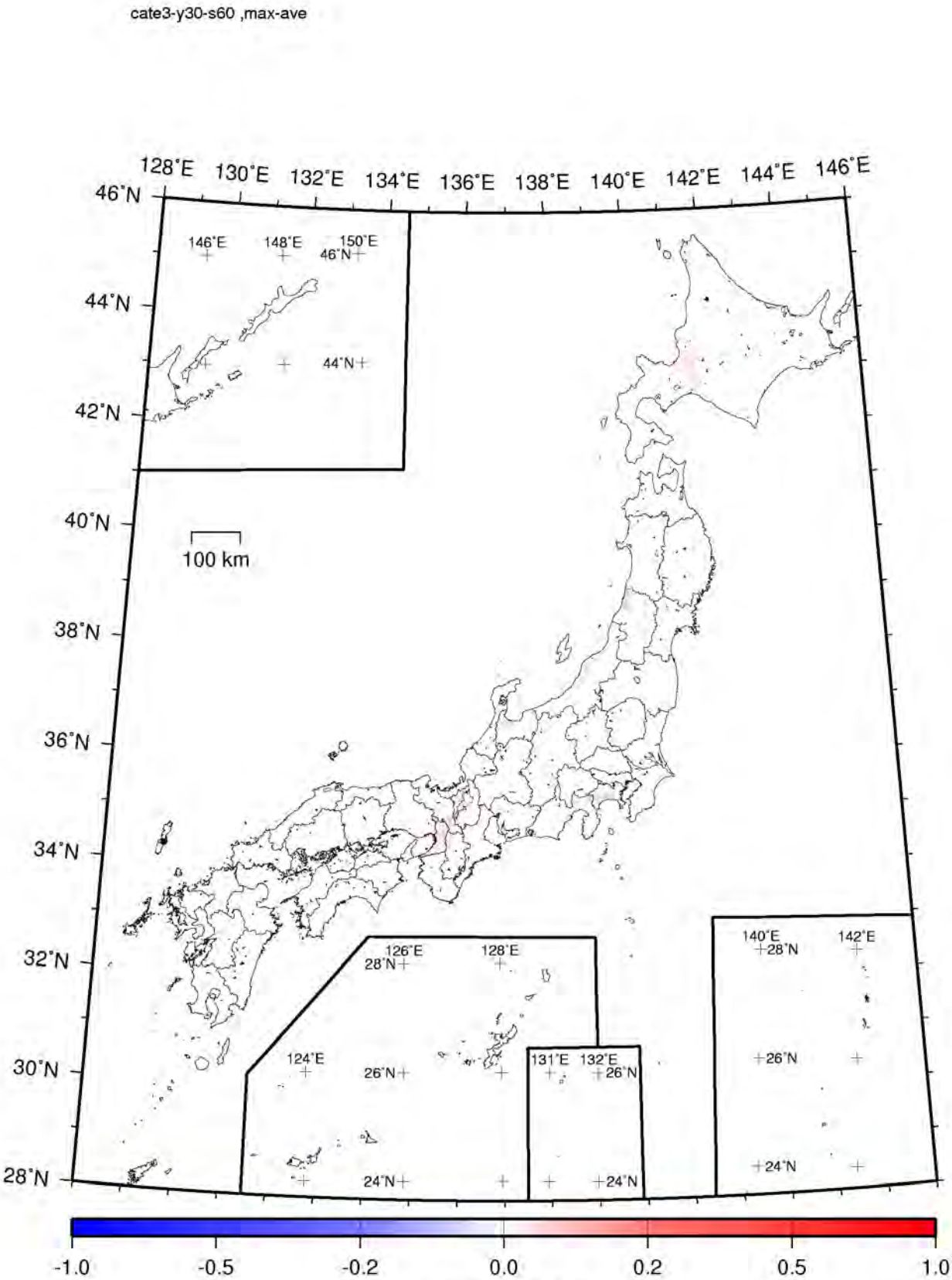

Difference in the exceedance probability within 30 years
(JMA seismic intensity: 6 Upper or more)

Figure 3.7.2-29 (4) Differences in the exceedance probability within 30 years associated with earthquake category III (JMA Seismic intensity: 6 Upper or more; "maximum case" - "average case")

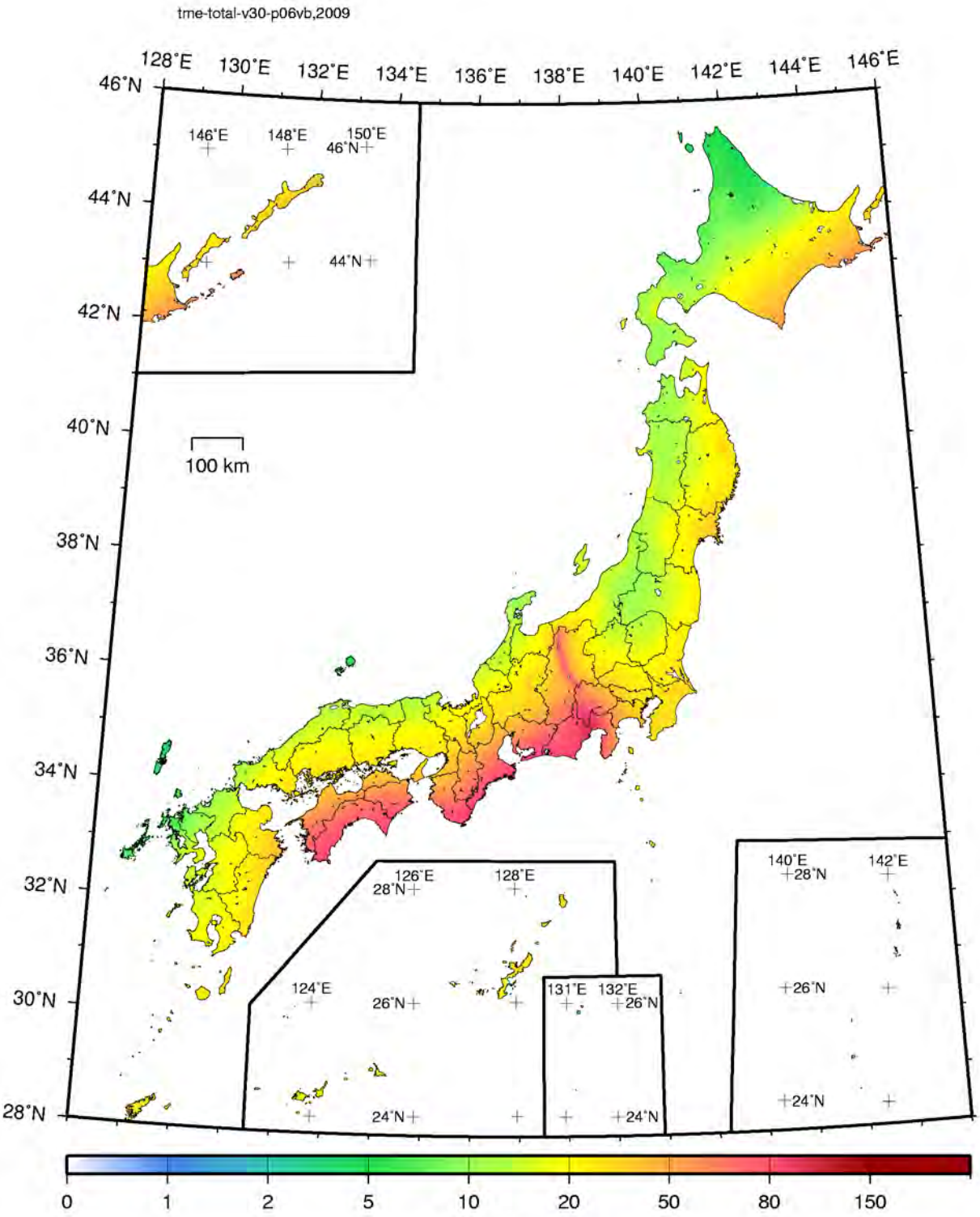

Peak ground velocity (cm/s)
(Exceedance probability within 30 years: 6%)

Figure 3.7.2-30 (1) Peak ground velocity on the bedrock (Vs=600 m/s) considering all earthquakes (2009 version; exceedance probability within 30 years: 6%; average case)

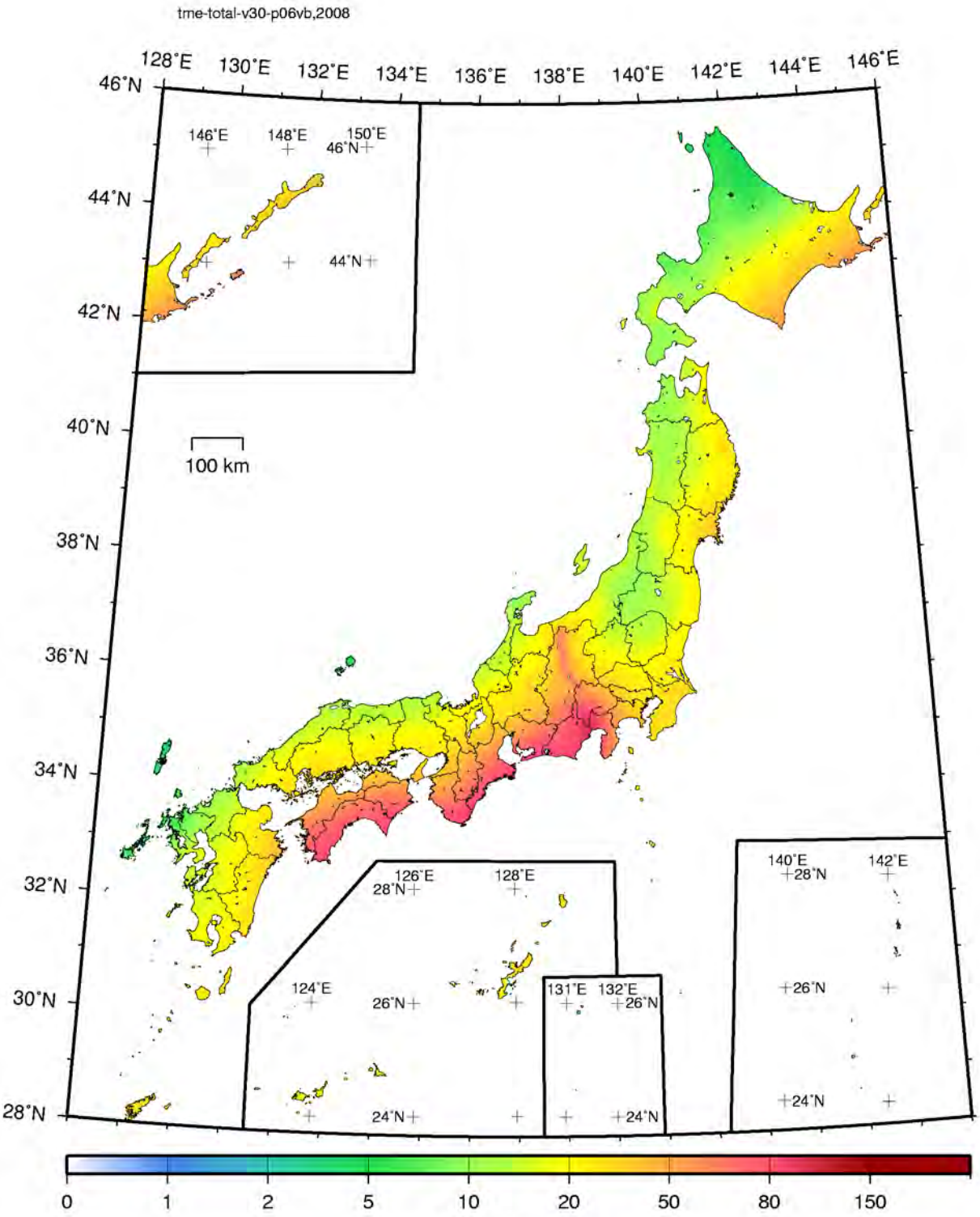

Peak ground velocity (cm/s)
(Exceedance probability within 30 years: 6%)

Figure 3.7.2-30 (2) Peak ground velocity on the bedrock (Vs=600 m/s) considering all earthquakes (2008 version; exceedance probability within 30 years: 6%; average case)

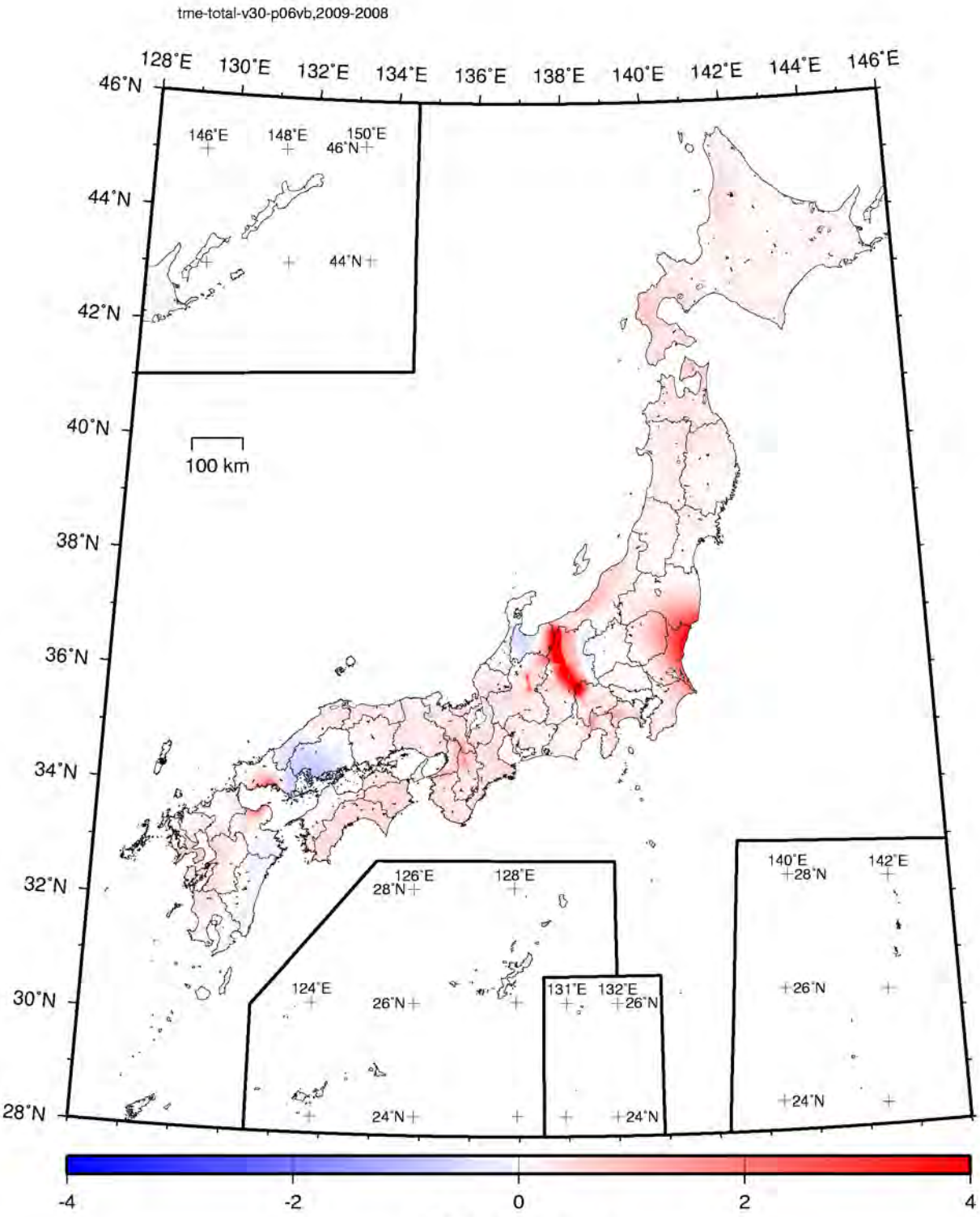

Difference in the peak ground velocity (cm/s)
(Exceedance probability within 30 years: 6%)

Figure 3.7.2-30 (3) Differences in the peak ground velocity on the bedrock (Vs=600 m/s) considering all earthquakes (Exceedance probability within 30 years: 6%; average case)

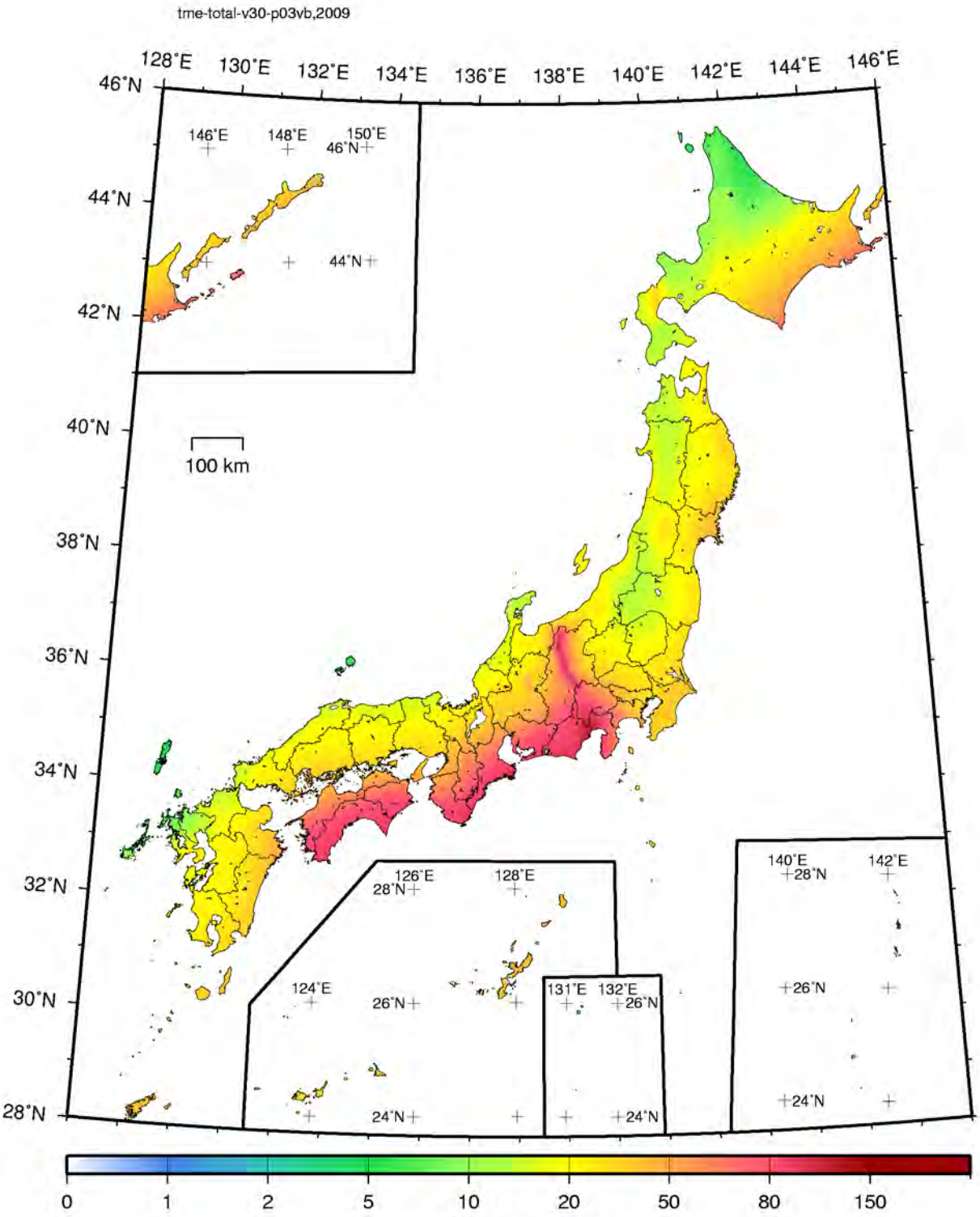

Peak ground velocity (cm/s)
(Exceedance probability within 30 years: 3%)

Figure 3.7.2-31 (1) Peak ground velocity on the bedrock (Vs=600 m/s) considering all earthquakes (2009 version; exceedance probability within 30 years: 3%; average case)

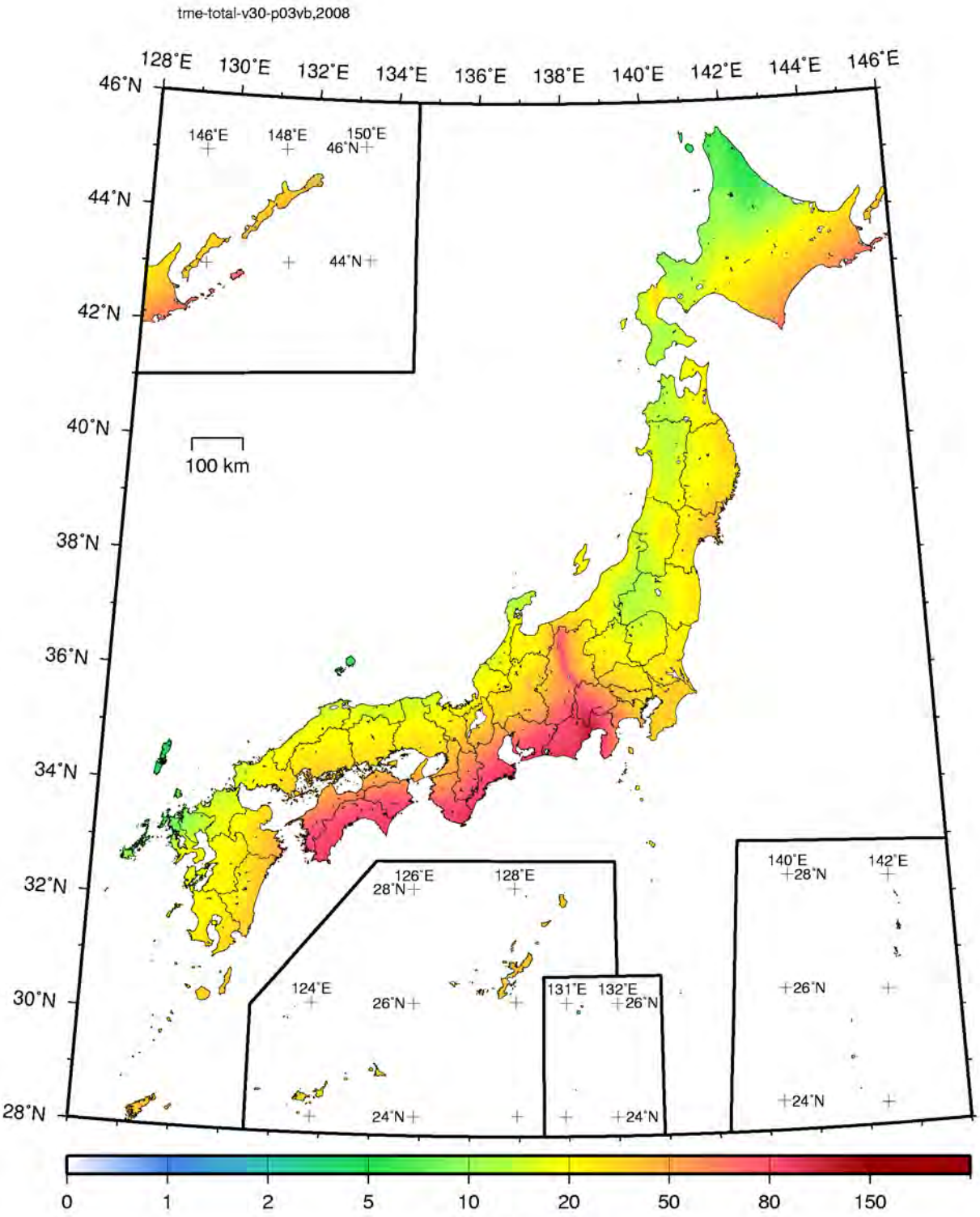

Peak ground velocity (cm/s)
(Exceedance probability within 30 years: 3%)

Figure 3.7.2-31 (2) Peak ground velocity on the bedrock (Vs=600 m/s) considering all earthquakes (2008 version; exceedance probability within 30 years: 3%; average case)

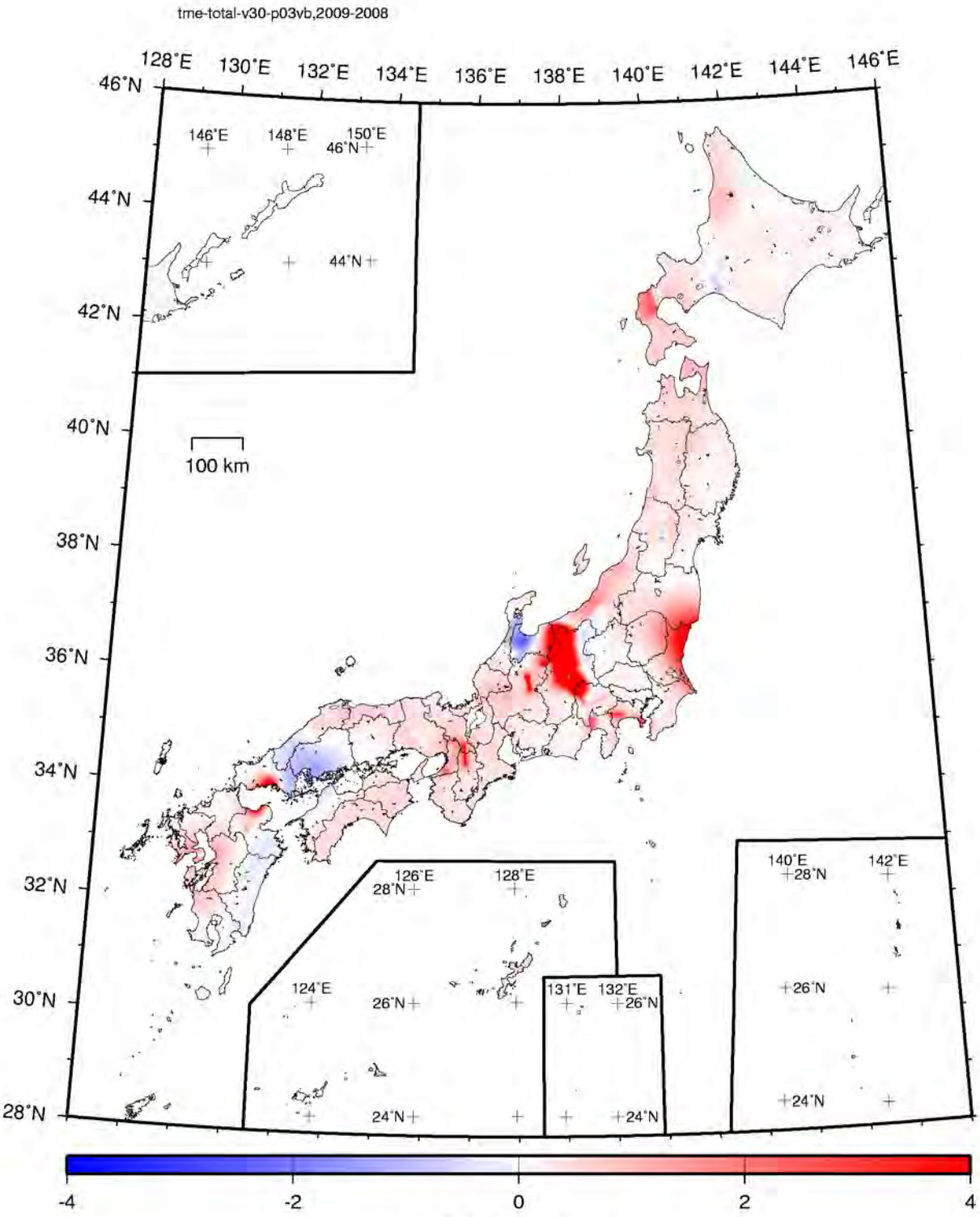

Difference in the peak ground velocity (cm/s)
(Exceedance probability within 30 years: 3%)

Figure 3.7.2-31 (3) Differences in the peak ground velocity on the bedrock (Vs=600 m/s) considering all earthquakes (Exceedance probability within 30 years: 3%; average case)

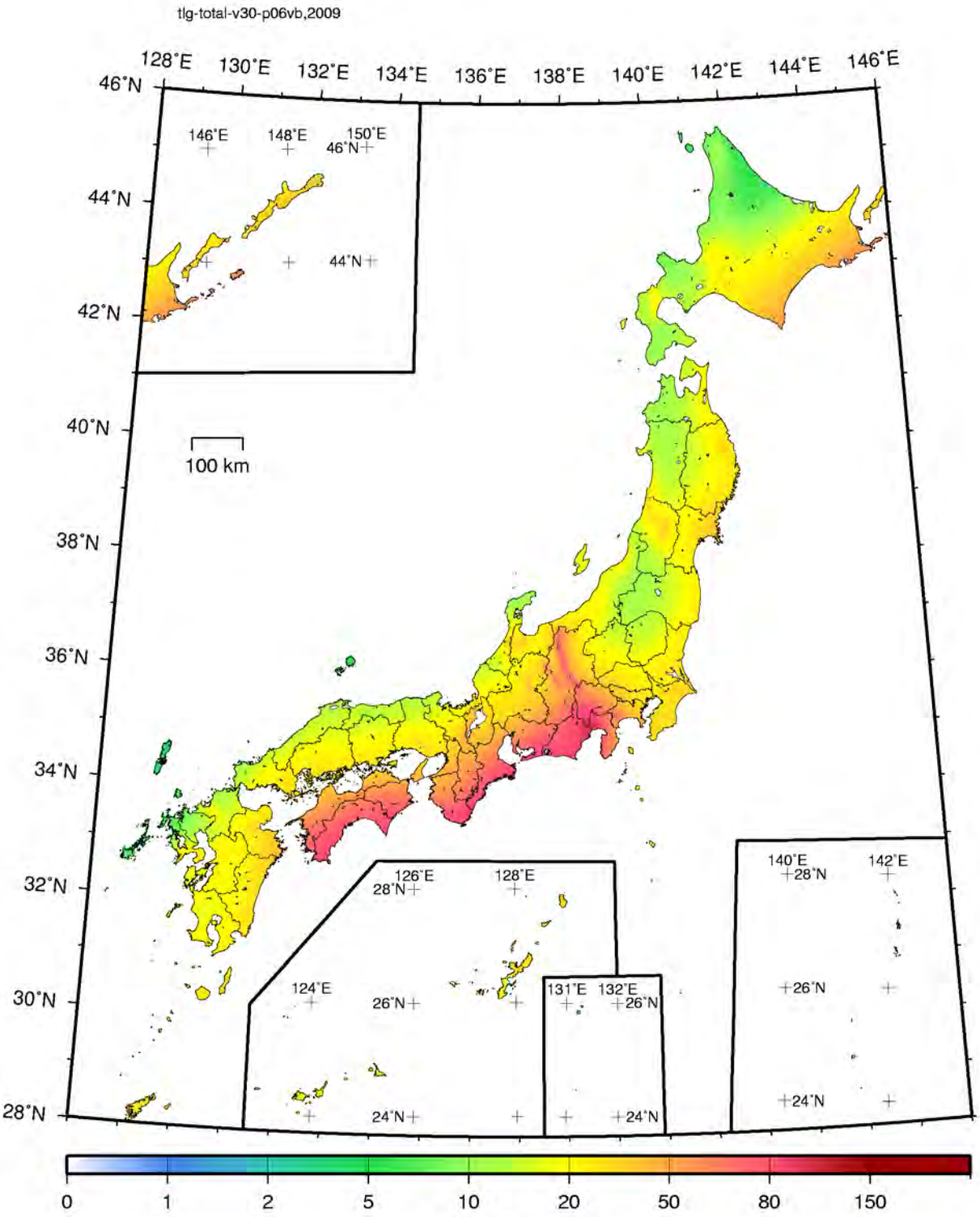

Peak ground velocity (cm/s)
(Exceedance probability within 30 years: 6%)

Figure 3.7.2-32 (1) Peak ground velocity on the bedrock (Vs=600 m/s) considering all earthquakes (2009 version; exceedance probability within 30 years: 6%; maximum case)

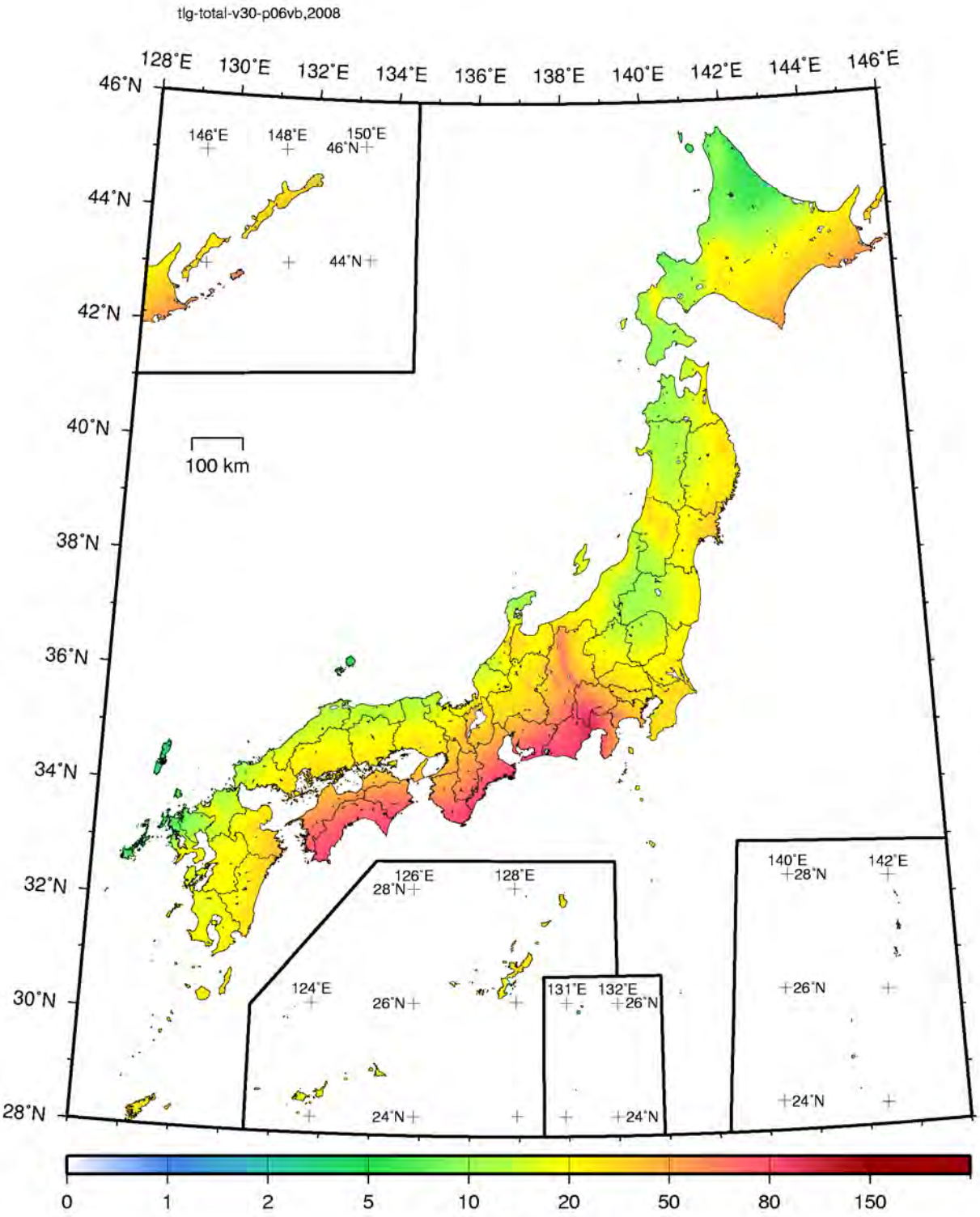

Peak ground velocity (cm/s)
(Exceedance probability within 30 years: 6%)

Figure 3.7.2-32 (2) Peak ground velocity on the bedrock (Vs=600 m/s) considering all earthquakes (2008 version; exceedance probability within 30 years: 6%; maximum case)

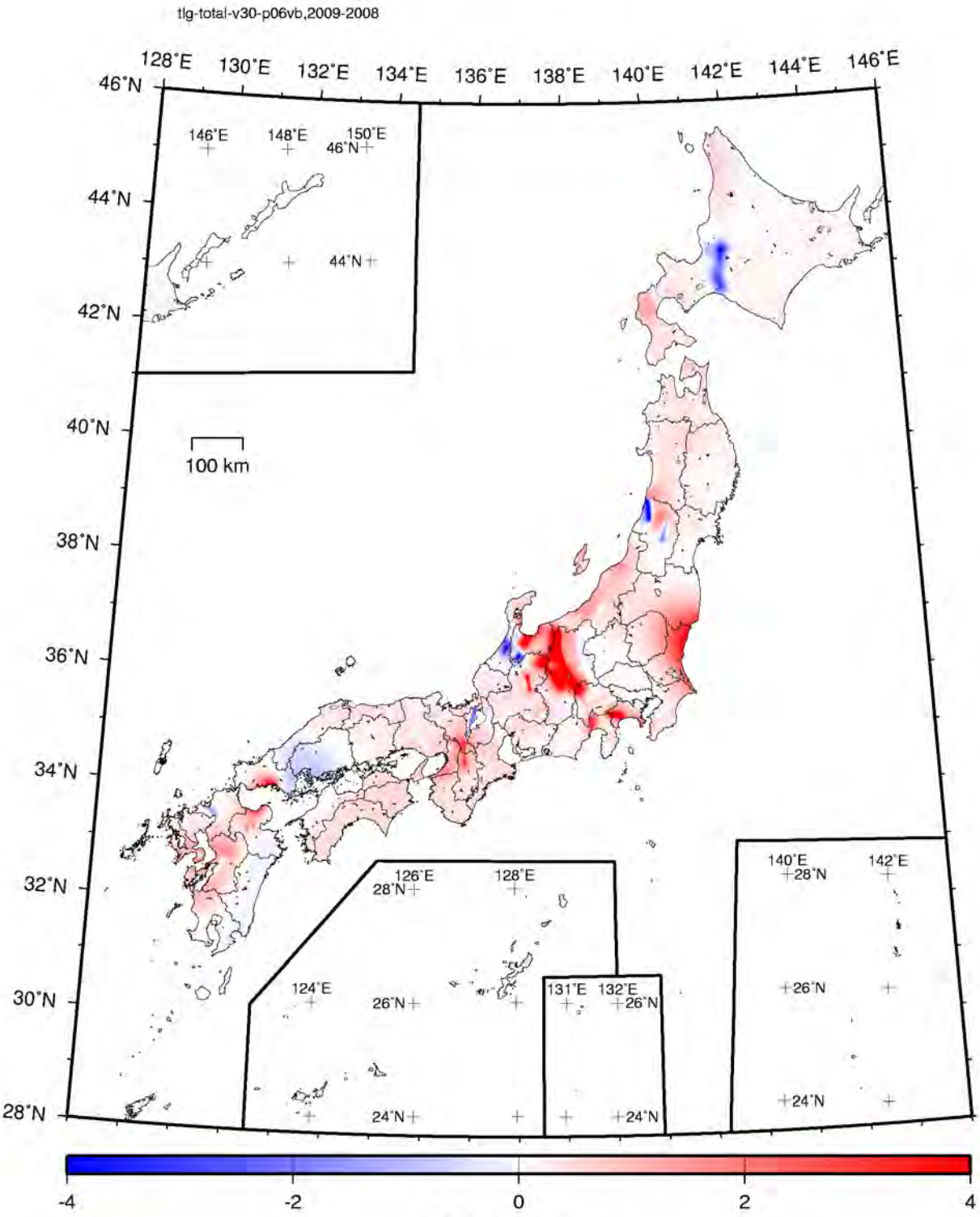

Difference in the peak ground velocity (cm/s)
(Exceedance probability within 30 years: 6%)

Figure 3.7.2-32 (3) Differences in the peak ground velocity on the bedrock (Vs=600 m/s) considering all earthquakes (Exceedance probability within 30 years: 6%; maximum case)

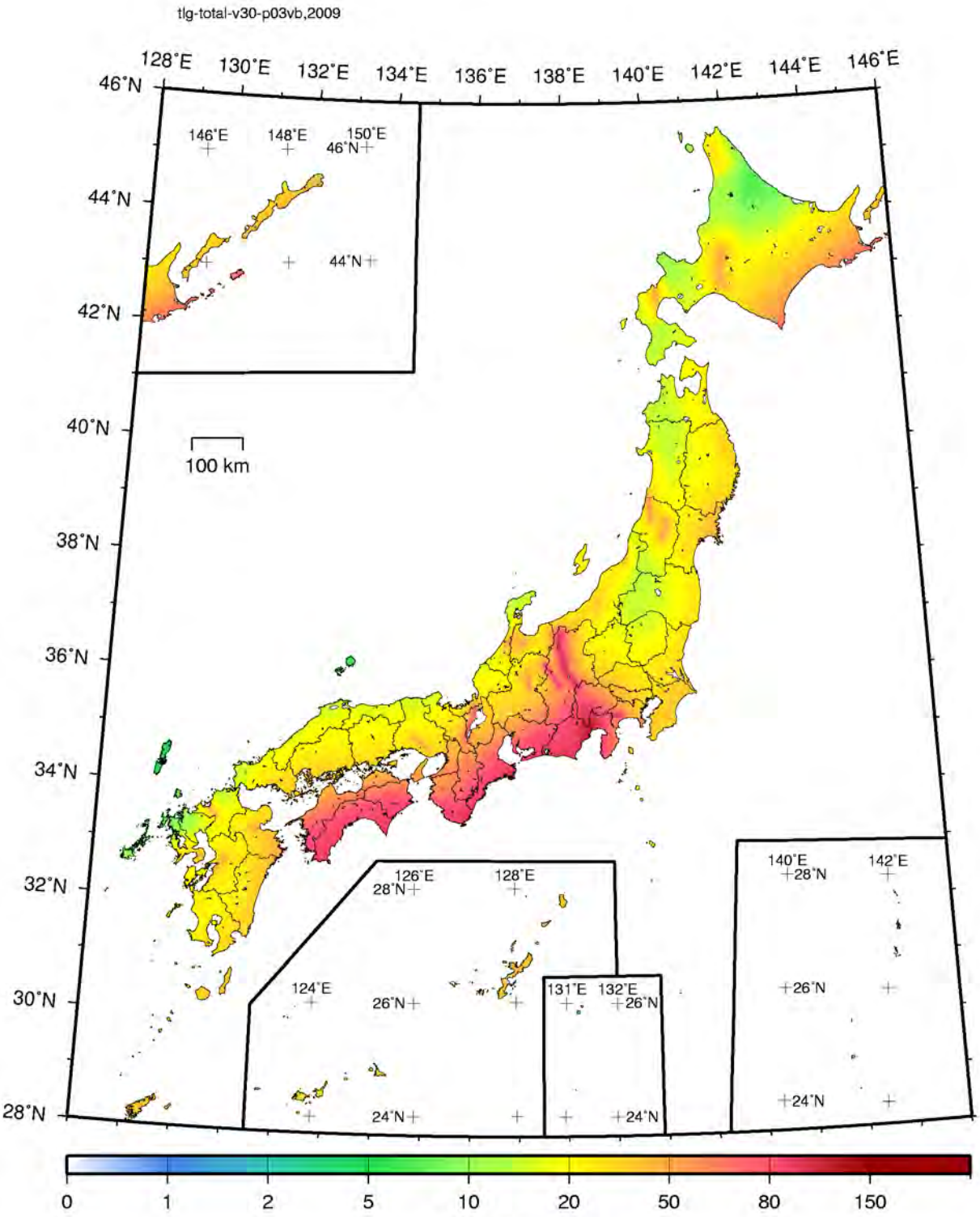

Peak ground velocity (cm/s)
(Exceedance probability within 30 years: 3%)

Figure 3.7.2-33 (1) Peak ground velocity on the bedrock (Vs=600 m/s) considering all earthquakes (2009 version; exceedance probability within 30 years: 3%; maximum case)

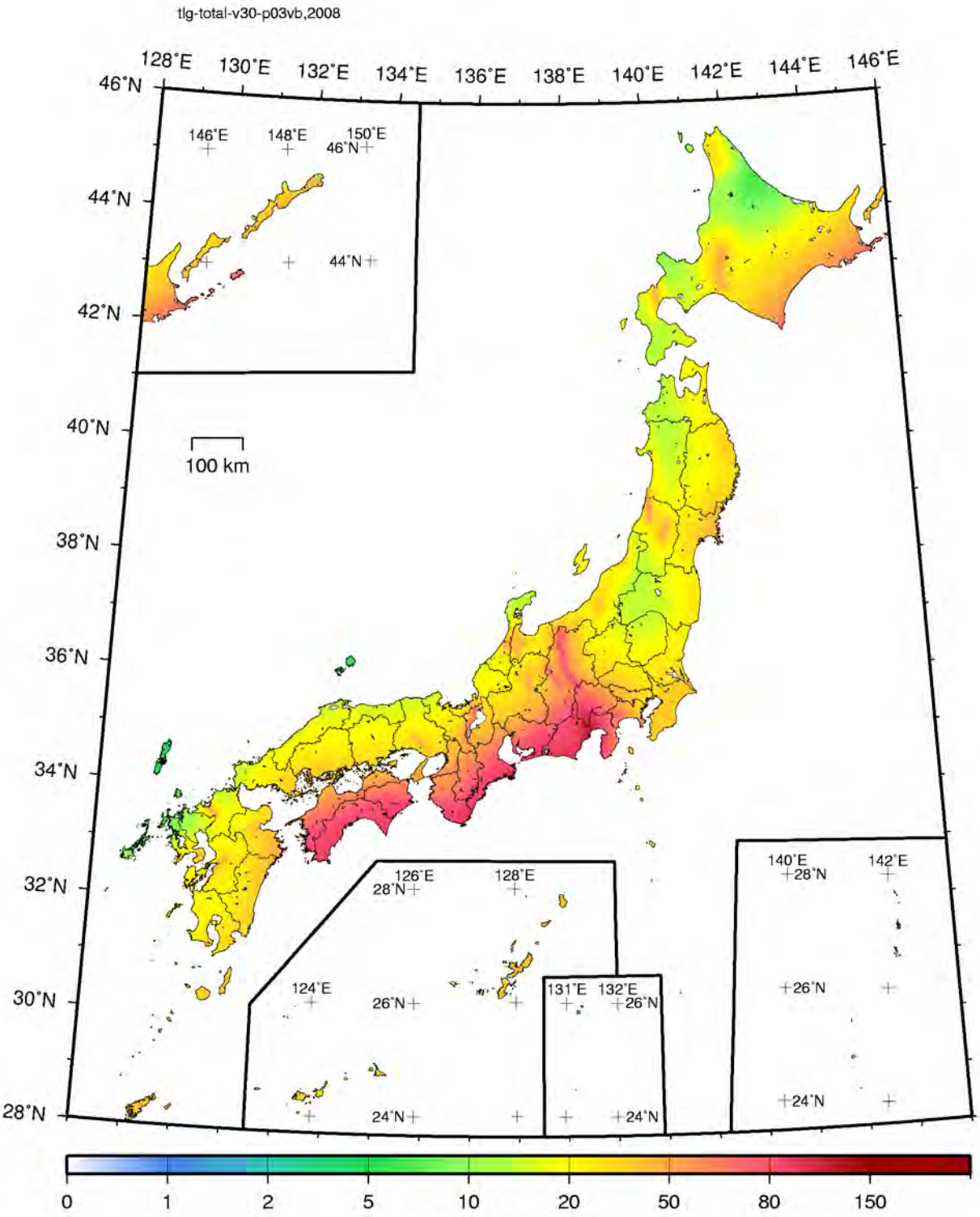

Peak ground velocity (cm/s)
(Exceedance probability within 30 years: 3%)

Figure 3.7.2-33 (2) Peak ground velocity on the bedrock (Vs=600 m/s) considering all earthquakes (2008 version; exceedance probability within 30 years: 3%; maximum case)

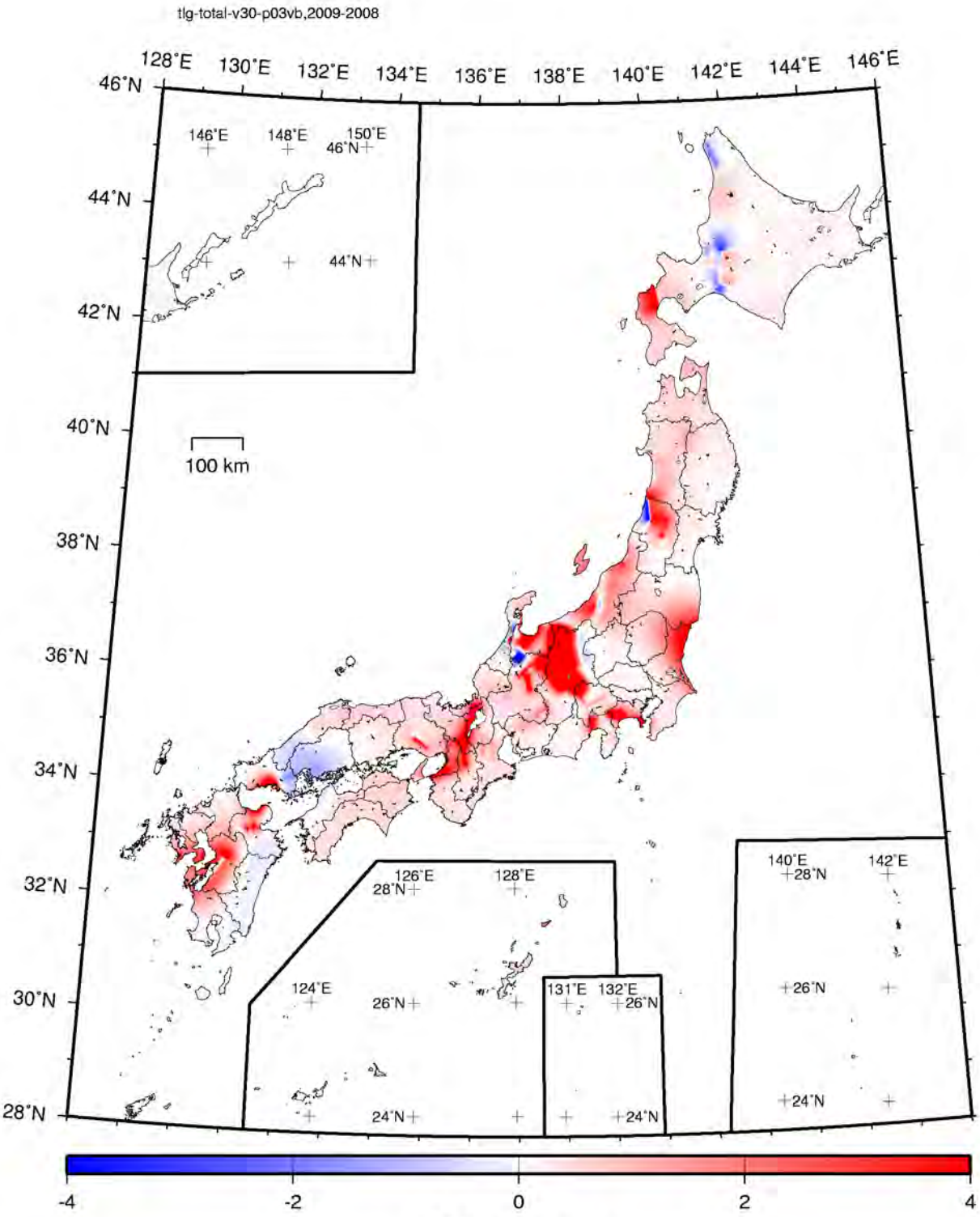

Difference in the peak ground velocity (cm/s)
(Exceedance probability within 30 years: 3%)

Figure 3.7.2-33 (3) Differences in the peak ground velocity on the bedrock (Vs=600 m/s) considering all earthquakes (Exceedance probability within 30 years: 3%; maximum case)

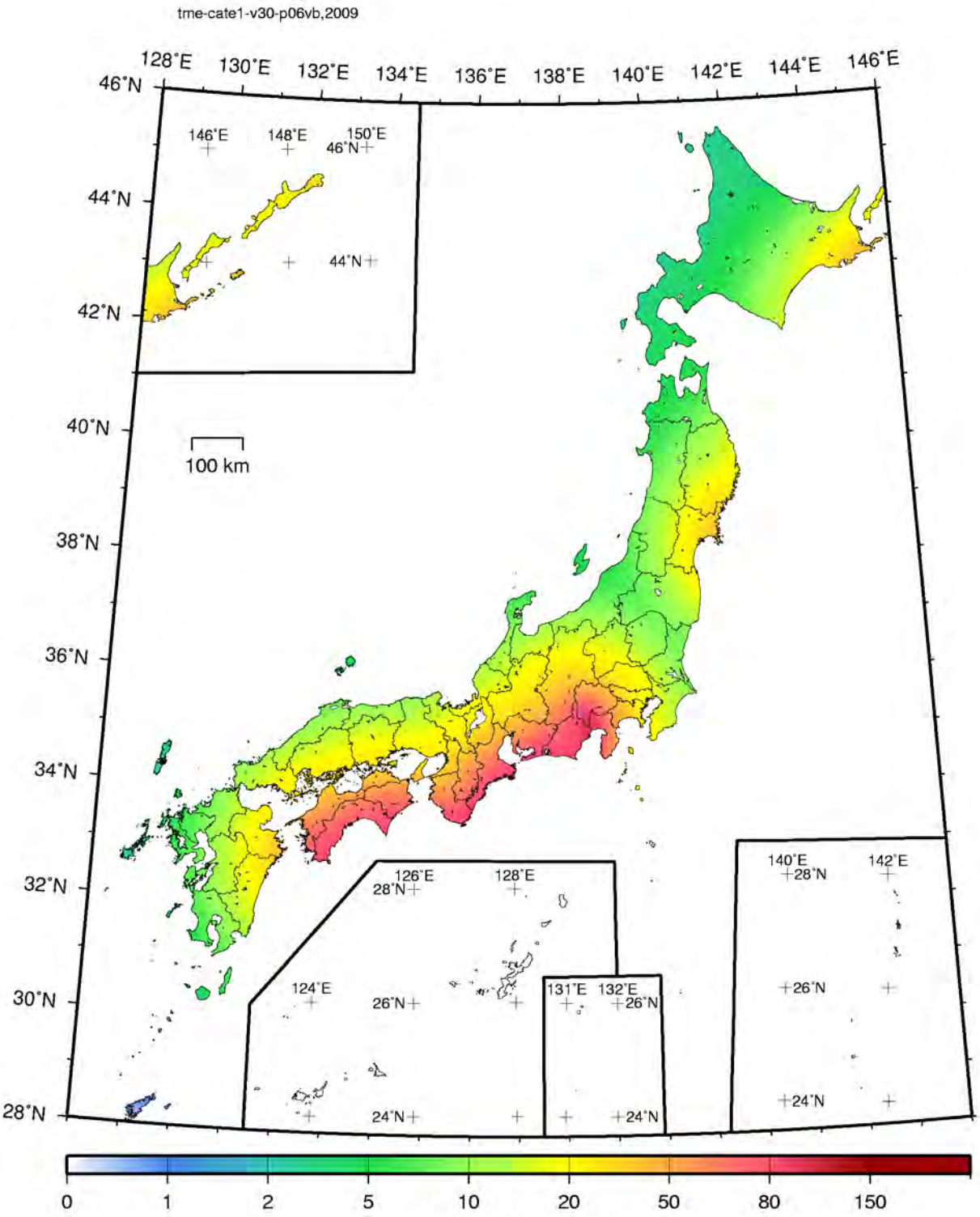

Peak ground velocity (cm/s)
(Exceedance probability within 30 years: 6%)

Figure 3.7.2-34 (1) Peak ground velocity on the bedrock (Vs=600 m/s) associated with earthquake category I (2009 version; exceedance probability within 30 years: 6%)

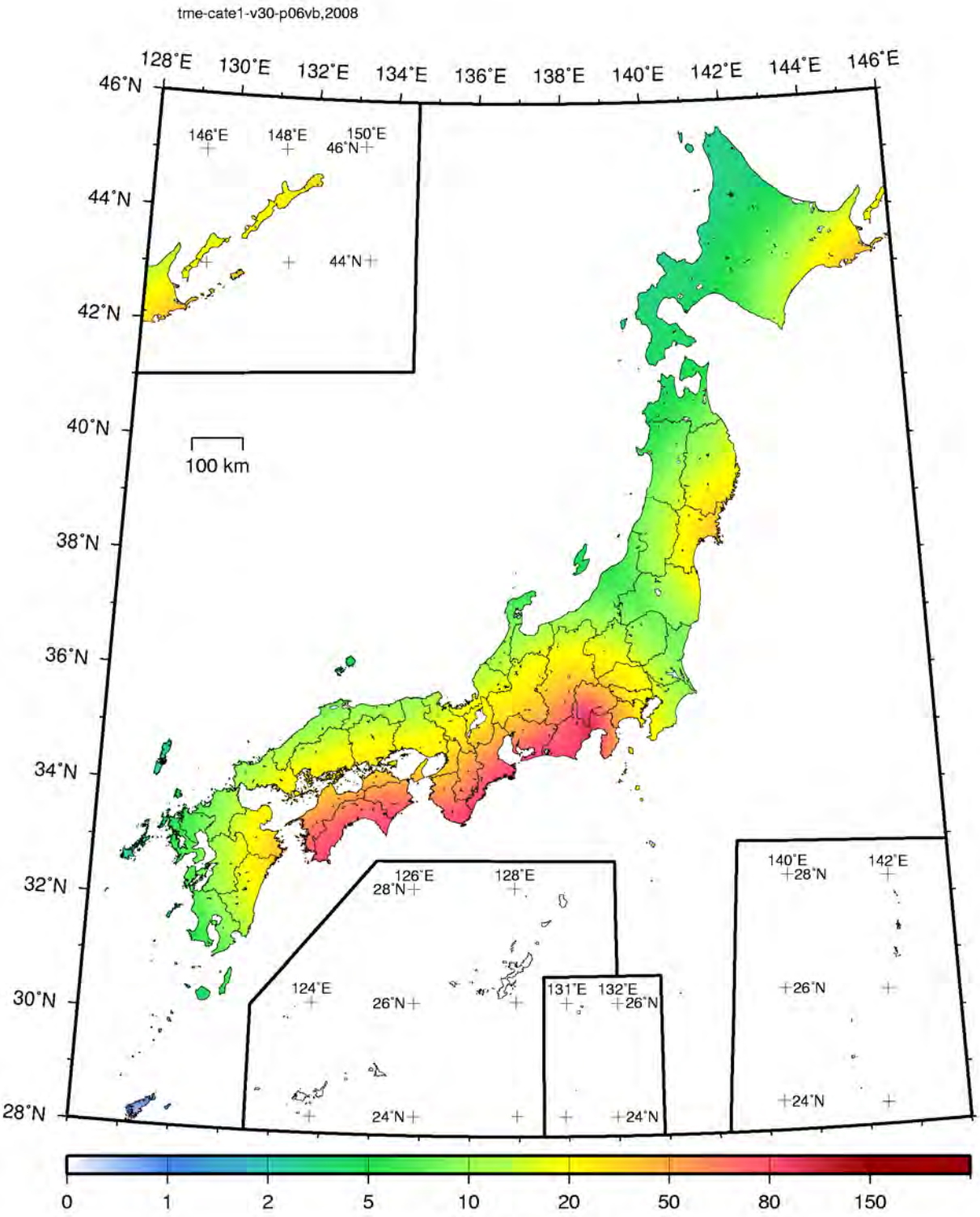

Peak ground velocity (cm/s)
(Exceedance probability within 30 years: 6%)

Figure 3.7.2-34 (2) Peak ground velocity on the bedrock (Vs=600 m/s) associated with earthquake category I (2008 version; exceedance probability within 30 years: 6%)

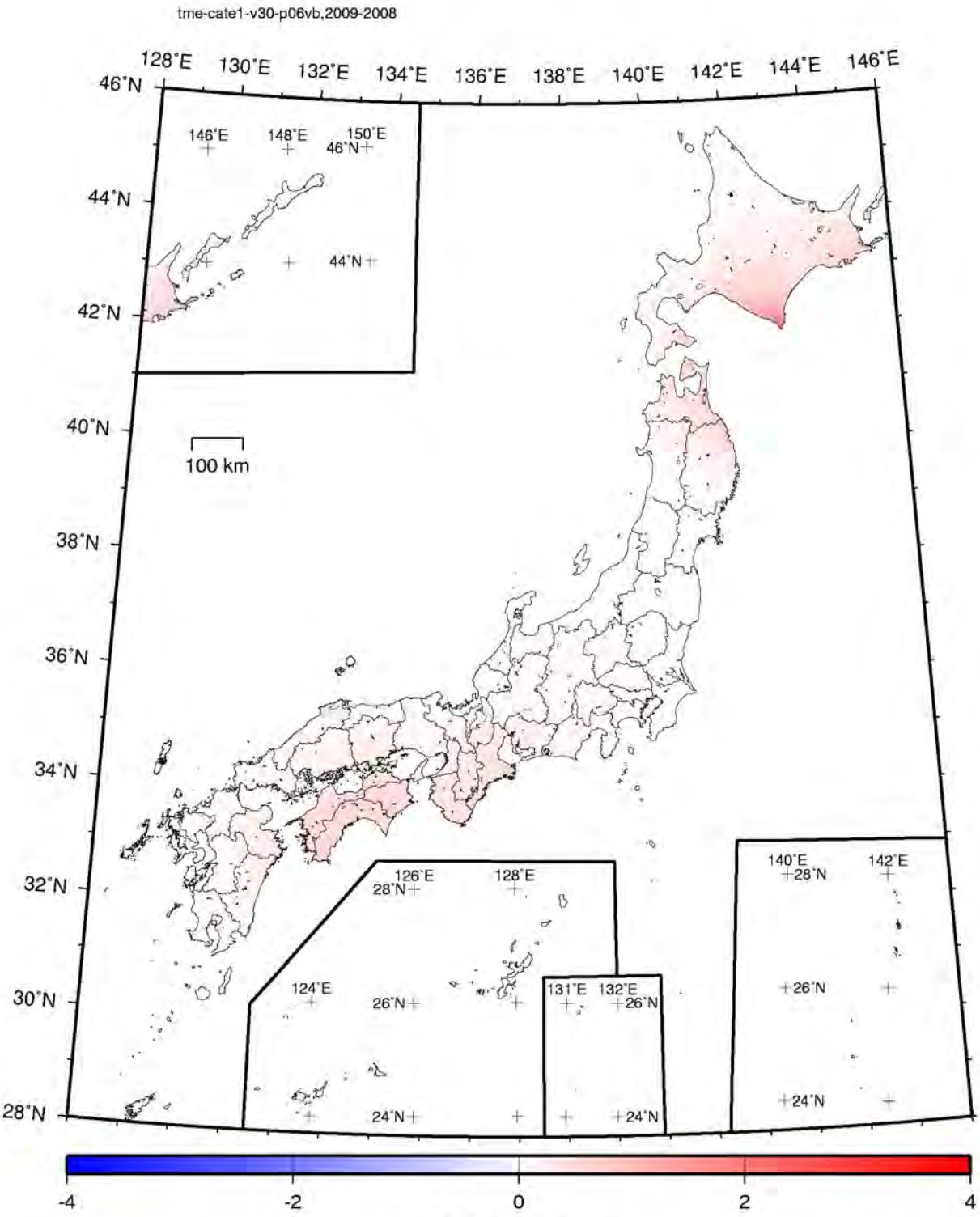

Difference in the peak ground velocity (cm/s)
(Exceedance probability within 30 years: 6%)

Figure 3.7.2-34 (3) Differences in the peak ground velocity on the bedrock (Vs=600 m/s) associated with earthquake category I (Exceedance probability within 30 years: 6%)

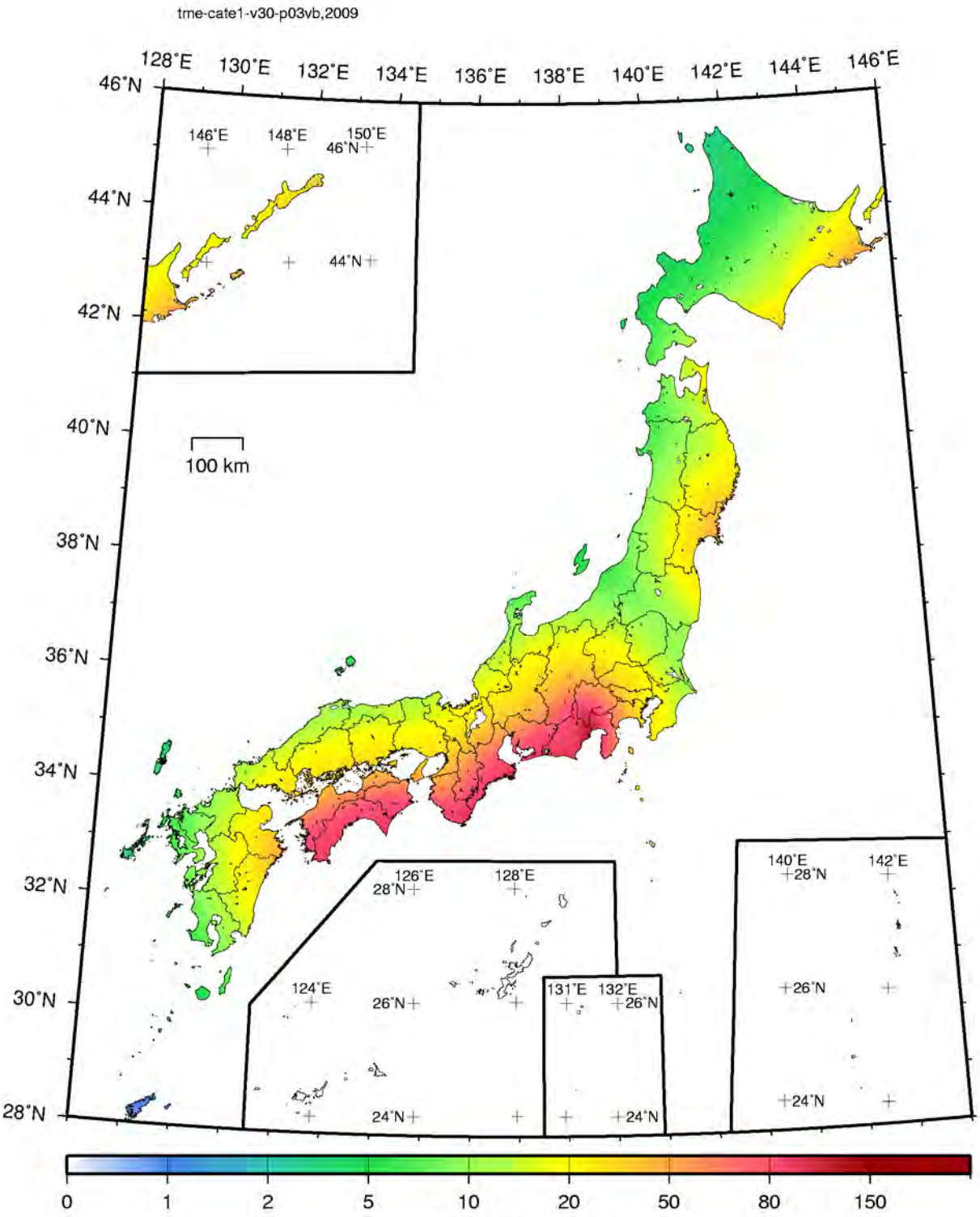

Peak ground velocity (cm/s)
(Exceedance probability within 30 years: 3%)

Figure 3.7.2-35 (1) Peak ground velocity on the bedrock (Vs=600 m/s) associated with earthquake category I (2009 version; exceedance probability within 30 years: 3%)

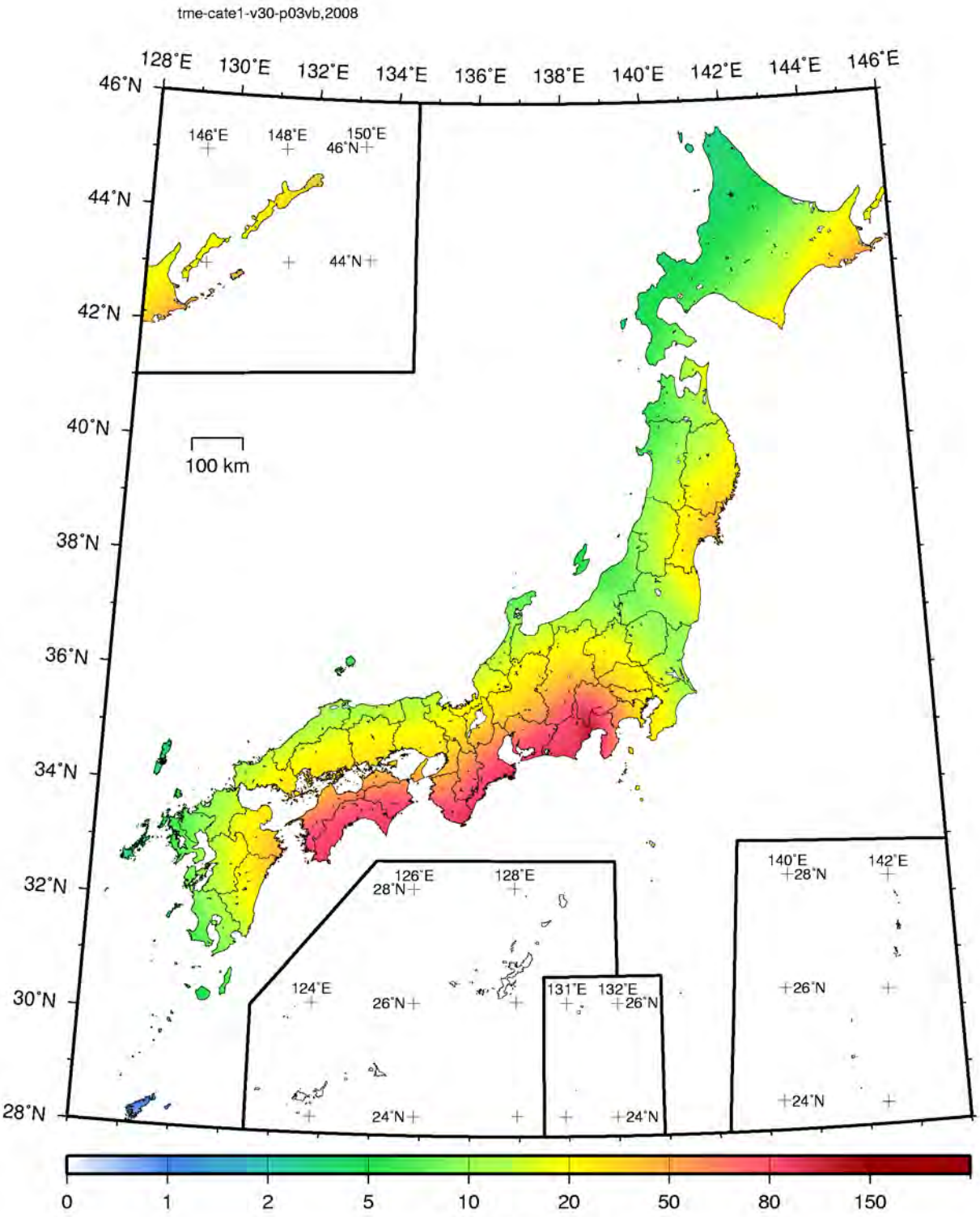

Peak ground velocity (cm/s)
(Exceedance probability within 30 years: 3%)

Figure 3.7.2-35 (2) Peak ground velocity on the bedrock (Vs=600 m/s) associated with earthquake category I (2008 version; exceedance probability within 30 years: 3%)

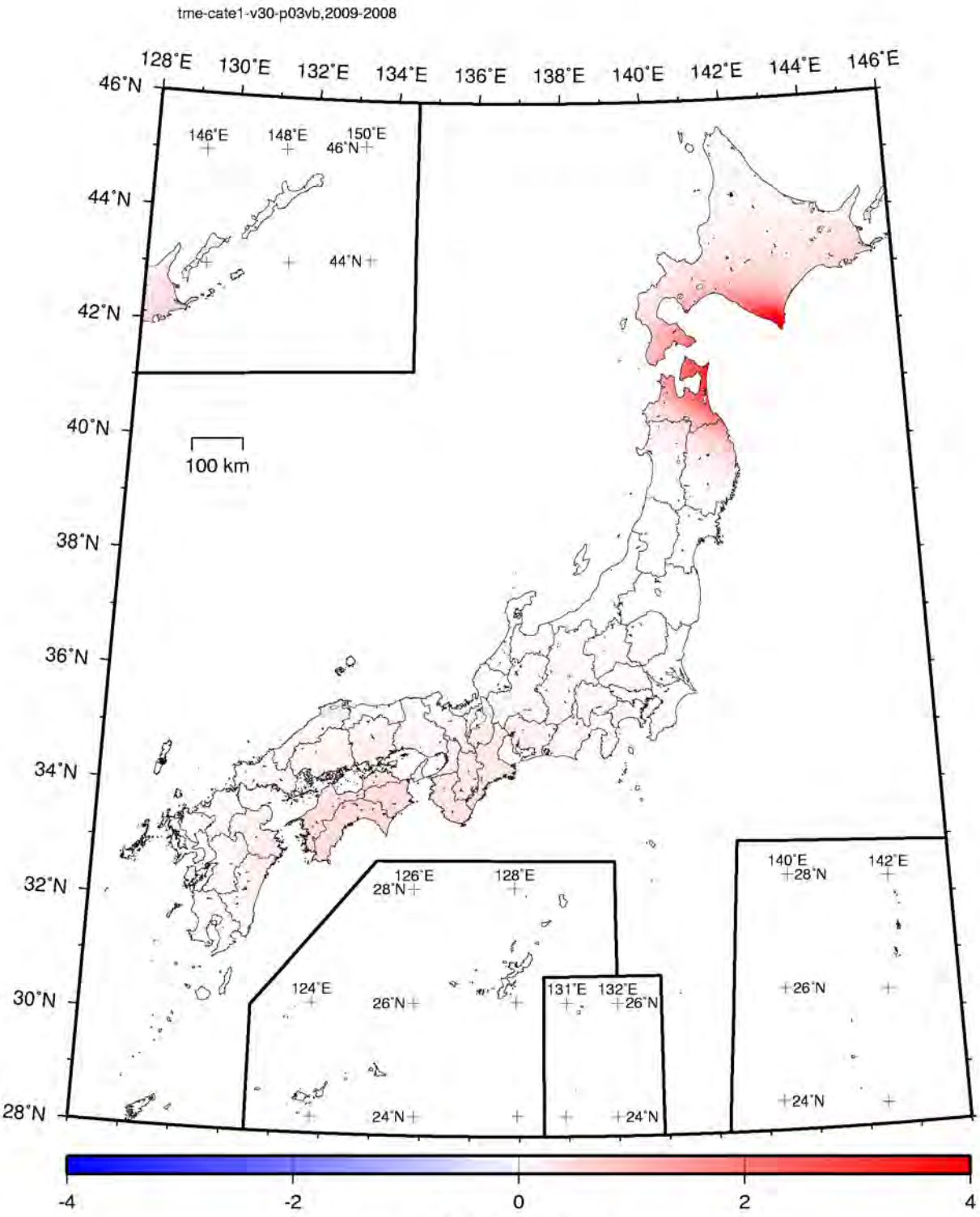

Difference in the peak ground velocity (cm/s)
(Exceedance probability within 30 years: 3%)

Figure 3.7.2-35 (3) Differences in the peak ground velocity on the bedrock (Vs=600 m/s) associated with earthquake category I (Exceedance probability within 30 years: 3%)

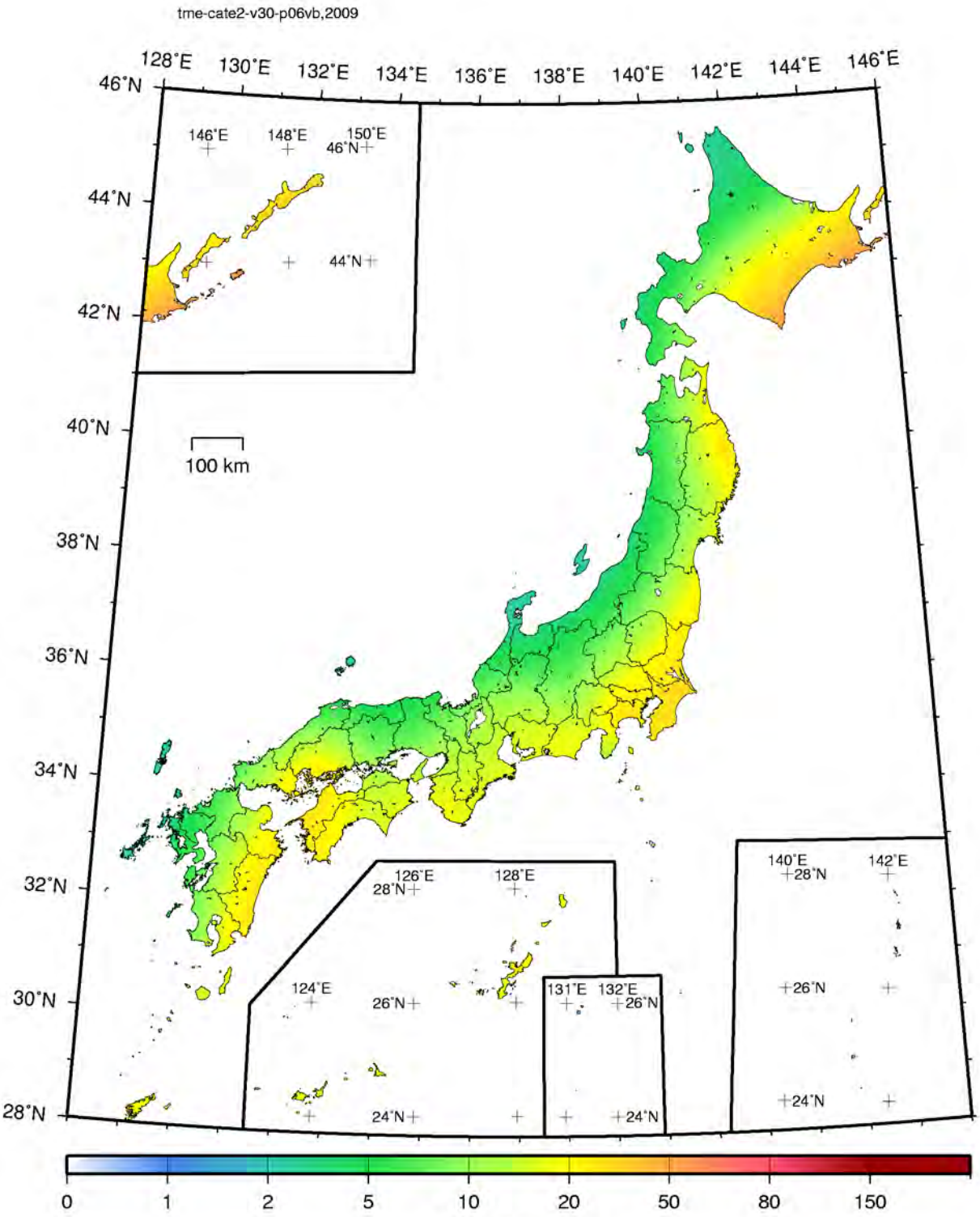

Peak ground velocity (cm/s)
(Exceedance probability within 30 years: 6%)

Figure 3.7.2-36 (1) Peak ground velocity on the bedrock (Vs=600 m/s) associated with earthquake category II (2009 version; exceedance probability within 30 years: 6%)

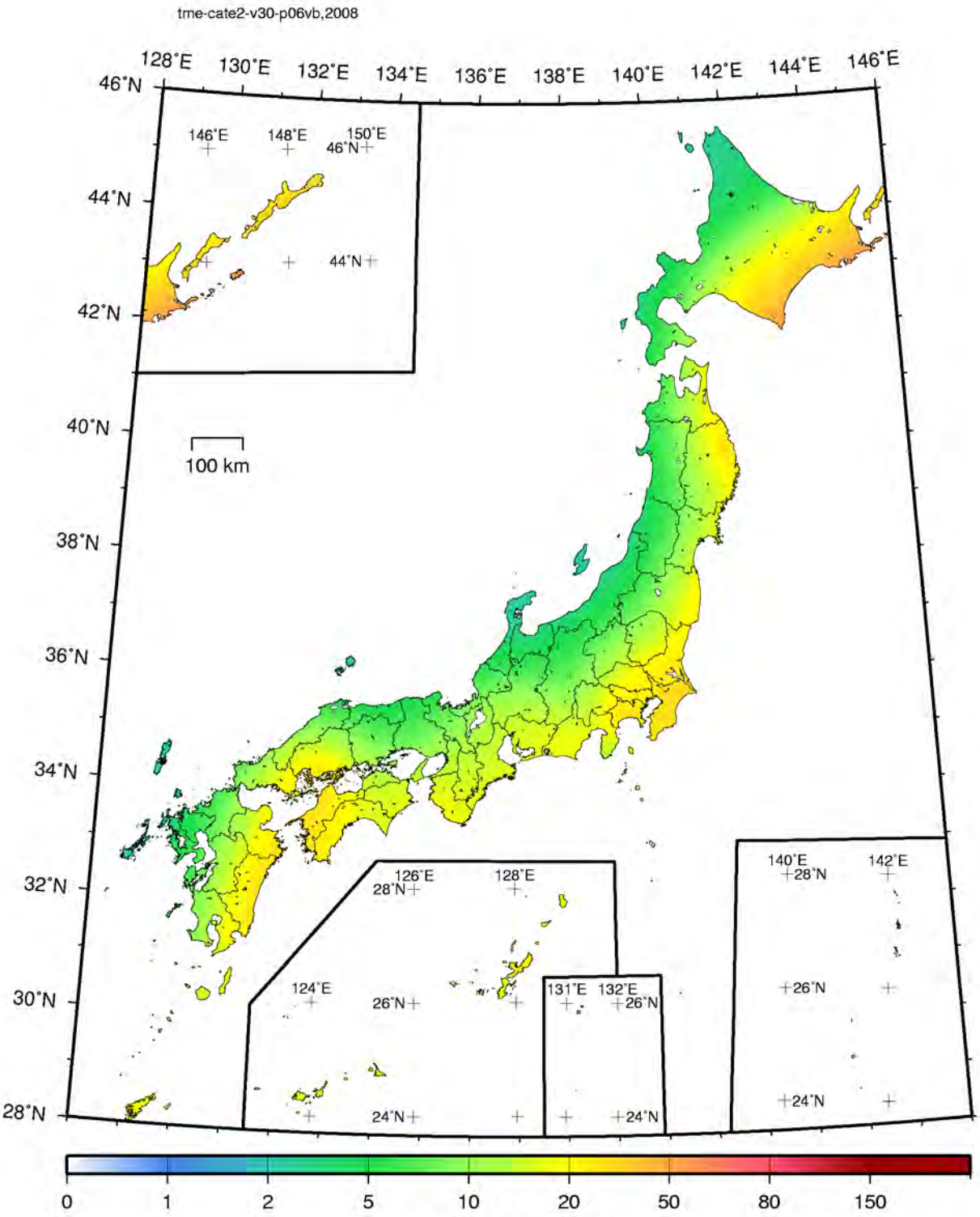

Peak ground velocity (cm/s)
(Exceedance probability within 30 years: 6%)

Figure 3.7.2-36 (2) Peak ground velocity on the bedrock (Vs=600 m/s) associated with earthquake category II (2008 version; exceedance probability within 30 years: 6%)

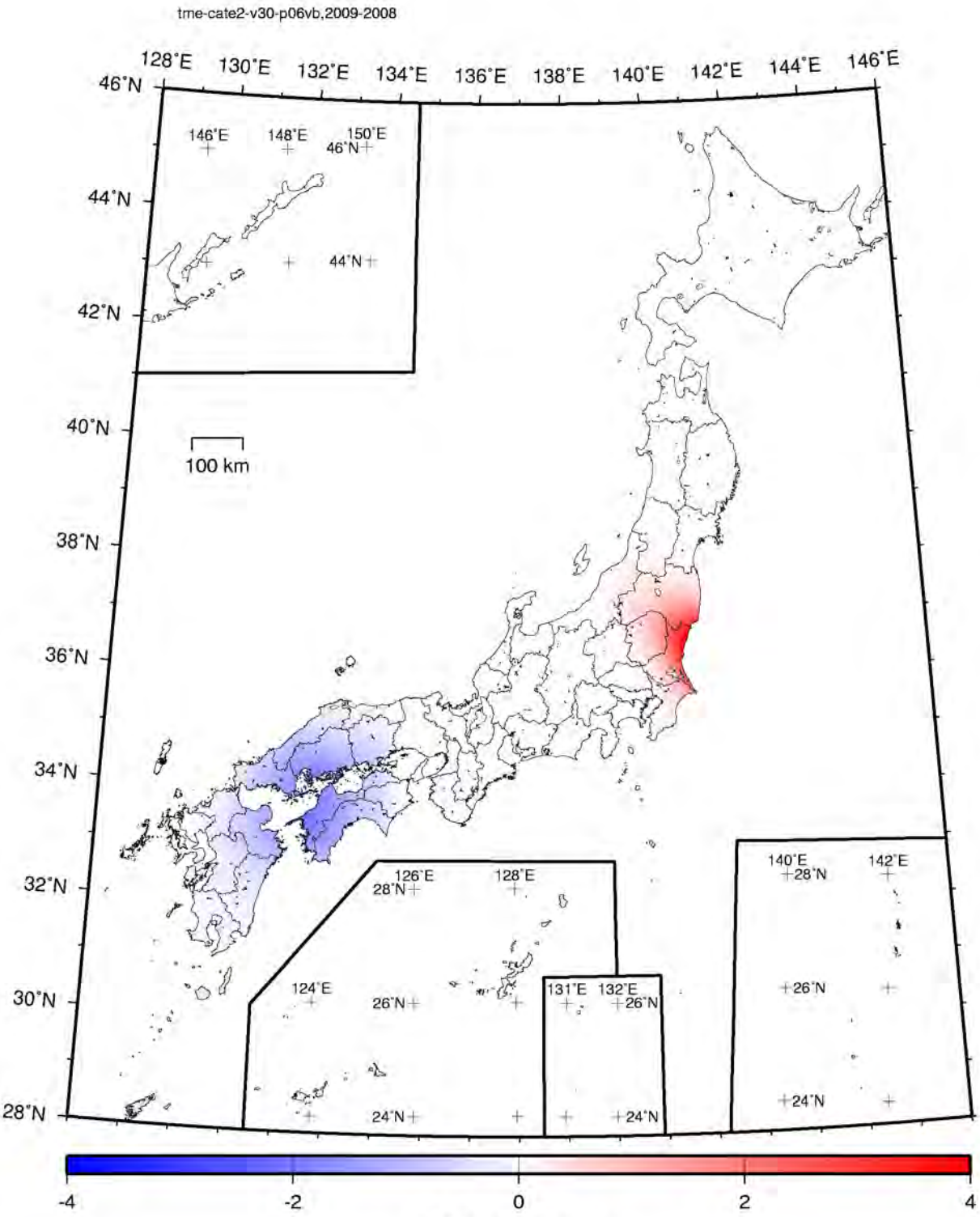

Difference in the peak ground velocity (cm/s))
(Exceedance probability within 30 years: 6%)

Figure 3.7.2-36 (3) Differences in the peak ground velocity on the bedrock (Vs=600 m/s) associated with earthquake category II (Exceedance probability within 30 years: 6%)

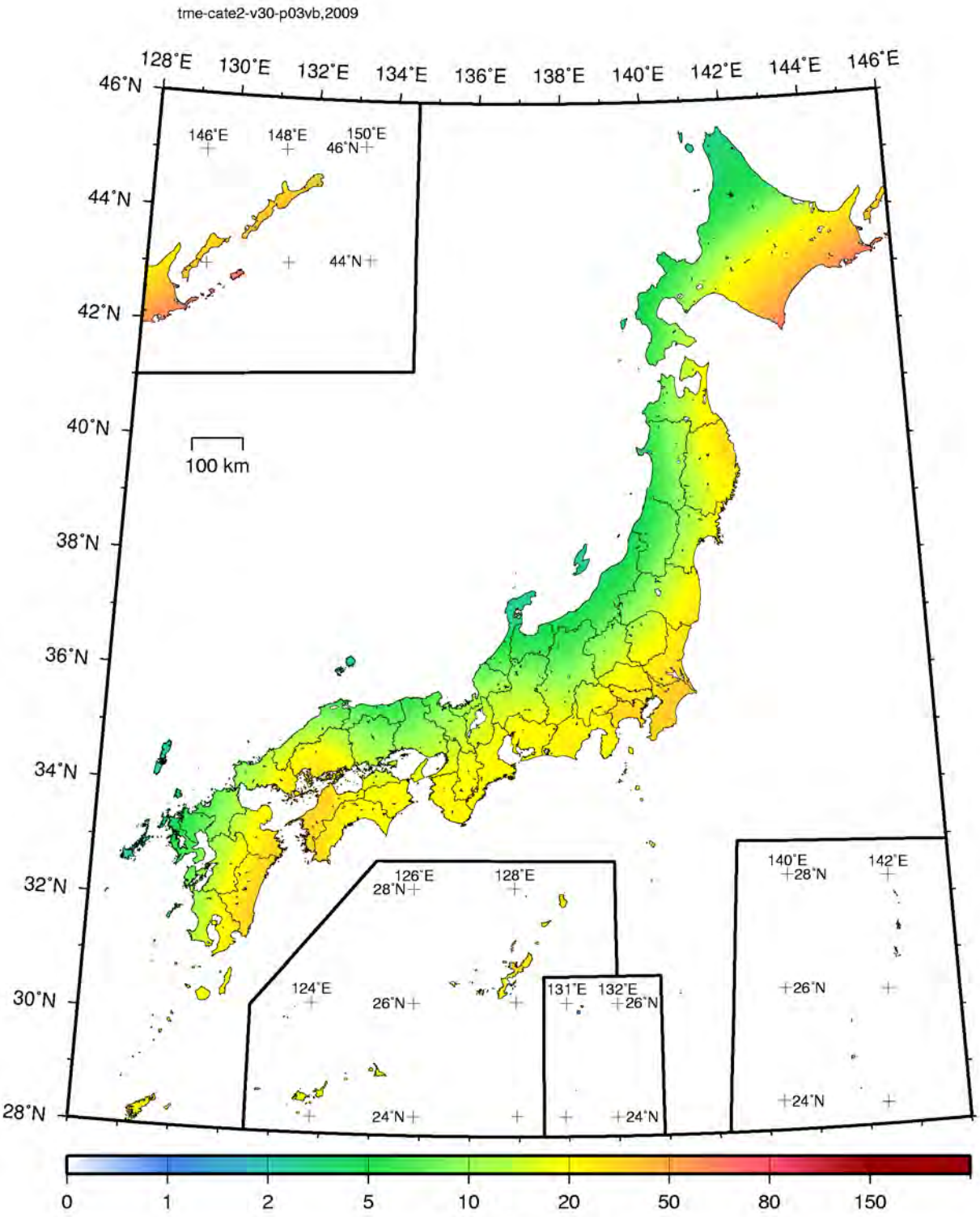

Peak ground velocity (cm/s)
(Exceedance probability within 30 years: 3%)

Figure 3.7.2-37 (1) Peak ground velocity on the bedrock (Vs=600 m/s) associated with earthquake category II (2009 version; exceedance probability within 30 years: 3%)

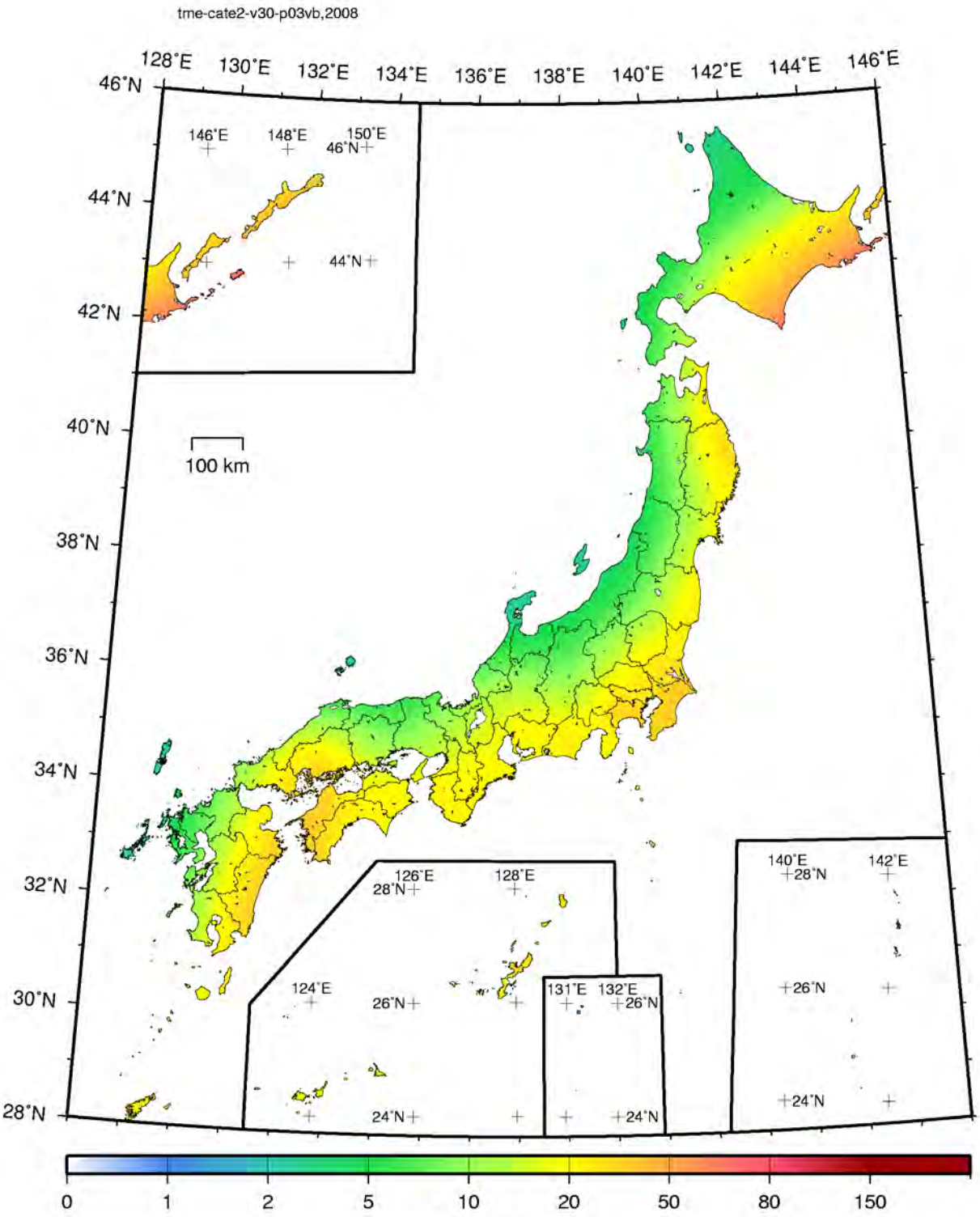

Peak ground velocity (cm/s)
(Exceedance probability within 30 years: 3%)

Figure 3.7.2-37 (2) Peak ground velocity on the bedrock (Vs=600 m/s) associated with earthquake category II (2008 version; exceedance probability within 30 years: 3%)

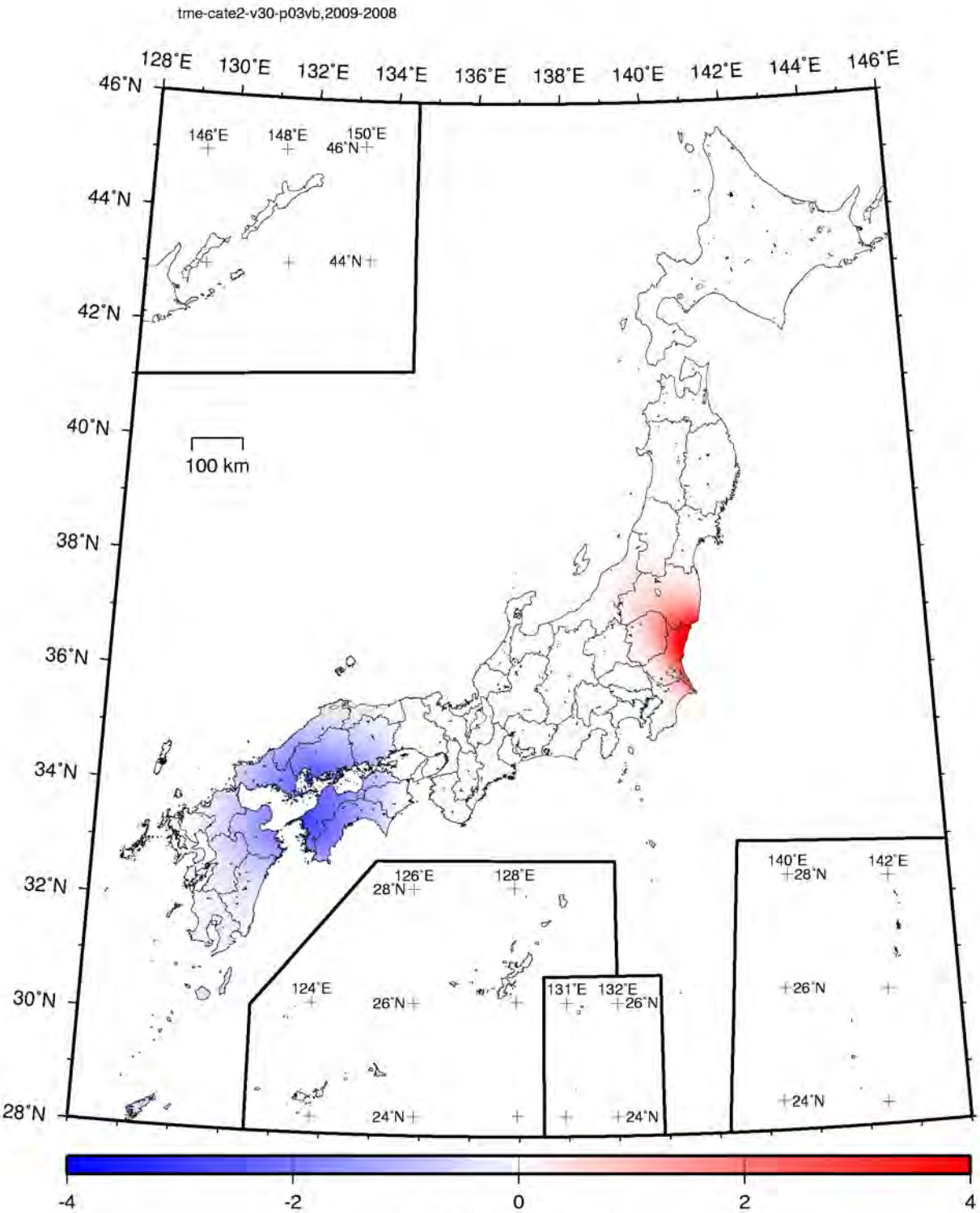

Difference in the peak ground velocity (cm/s)
(Exceedance probability within 30 years: 3%)

Figure 3.7.2-37 (3) Differences in the peak ground velocity on the bedrock (Vs=600 m/s) associated with earthquake category II (Exceedance probability within 30 years: 3%)

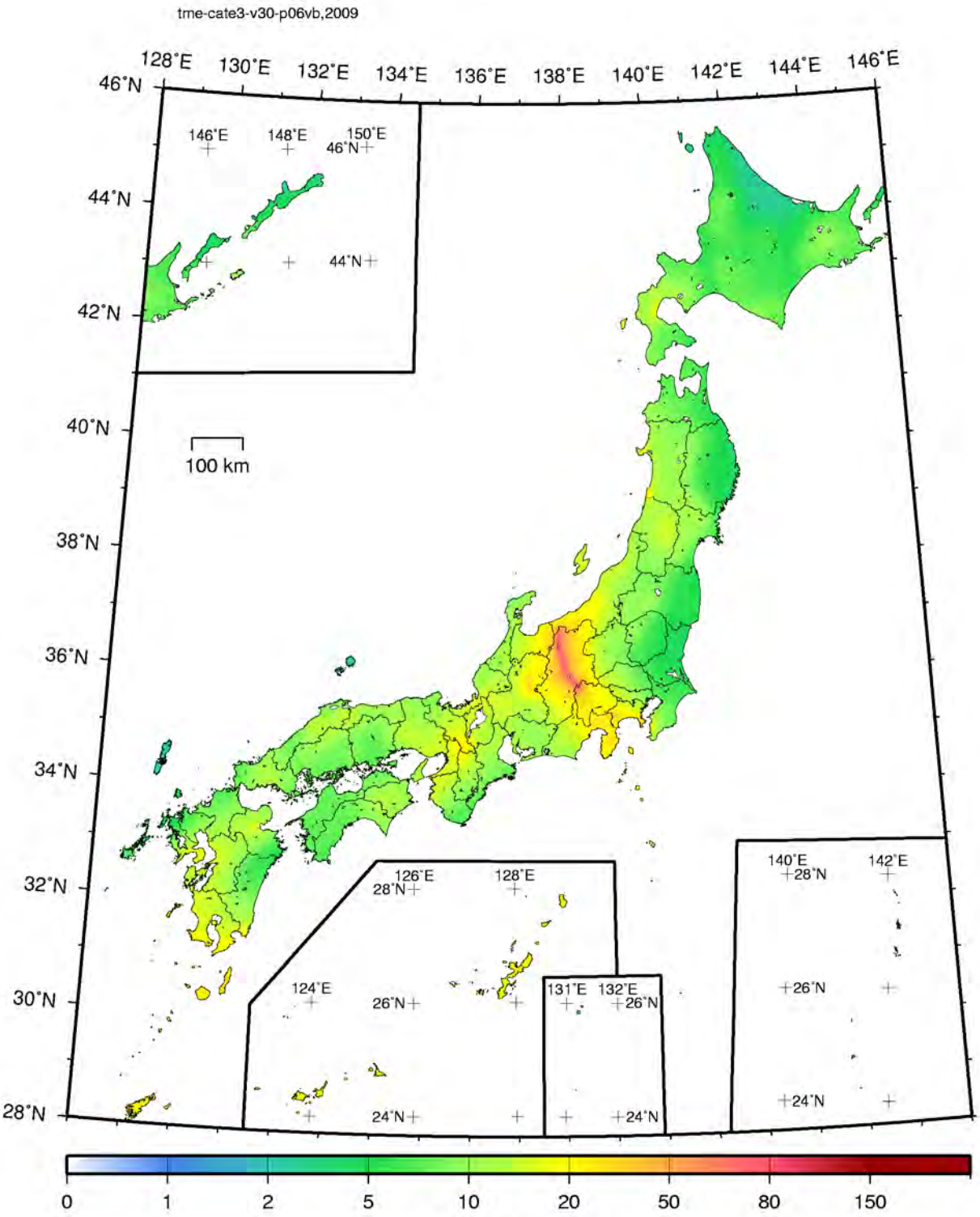

Peak ground velocity (cm/s)
(Exceedance probability within 30 years: 6%)

Figure 3.7.2-38 (1) Peak ground velocity on the bedrock (Vs=600 m/s) associated with earthquake category III (2009 version; exceedance probability within 30 years: 6%; average case)

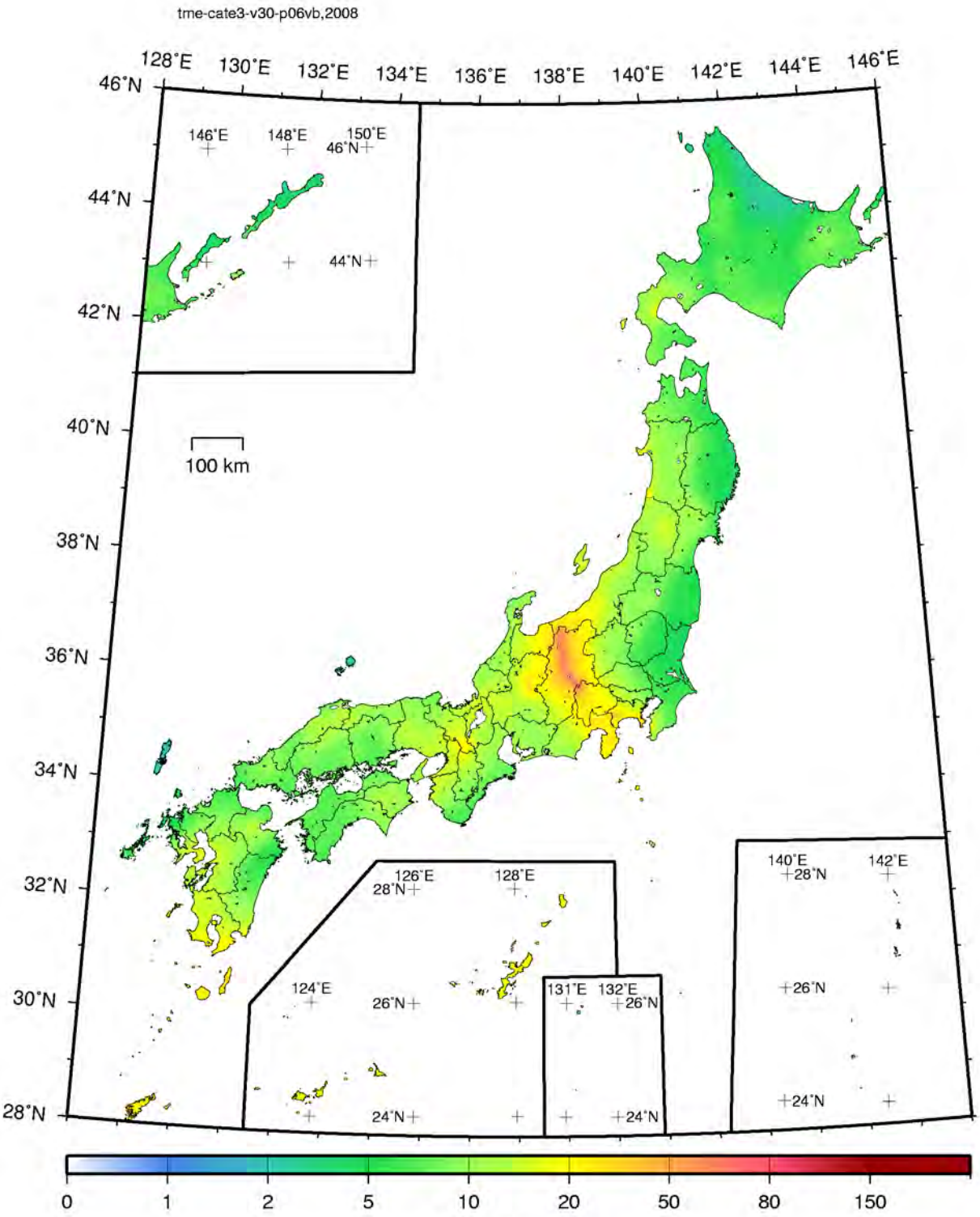

Peak ground velocity (cm/s)
(Exceedance probability within 30 years: 6%)

Figure 3.7.2-38 (2) Peak ground velocity on the bedrock (Vs=600 m/s) associated with earthquake category III (2008 version; exceedance probability within 30 years: 6%; average case)

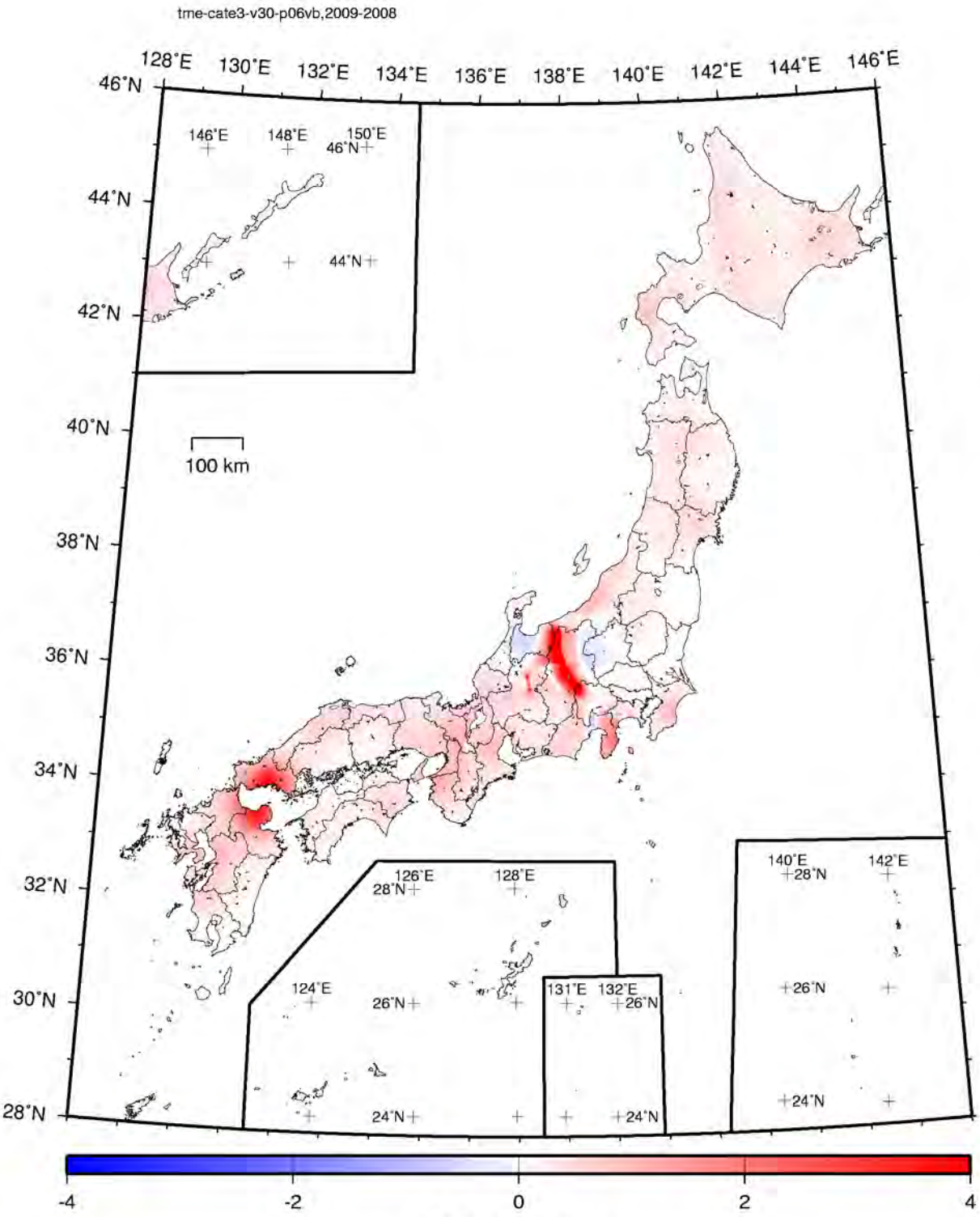

Difference in the peak ground velocity (cm/s)
(Exceedance probability within 30 years: 6%)

Figure 3.7.2-38 (3) Differences in the peak ground velocity on the bedrock (Vs=600 m/s) associated with earthquake category III (Exceedance probability within 30 years: 6%; average case)

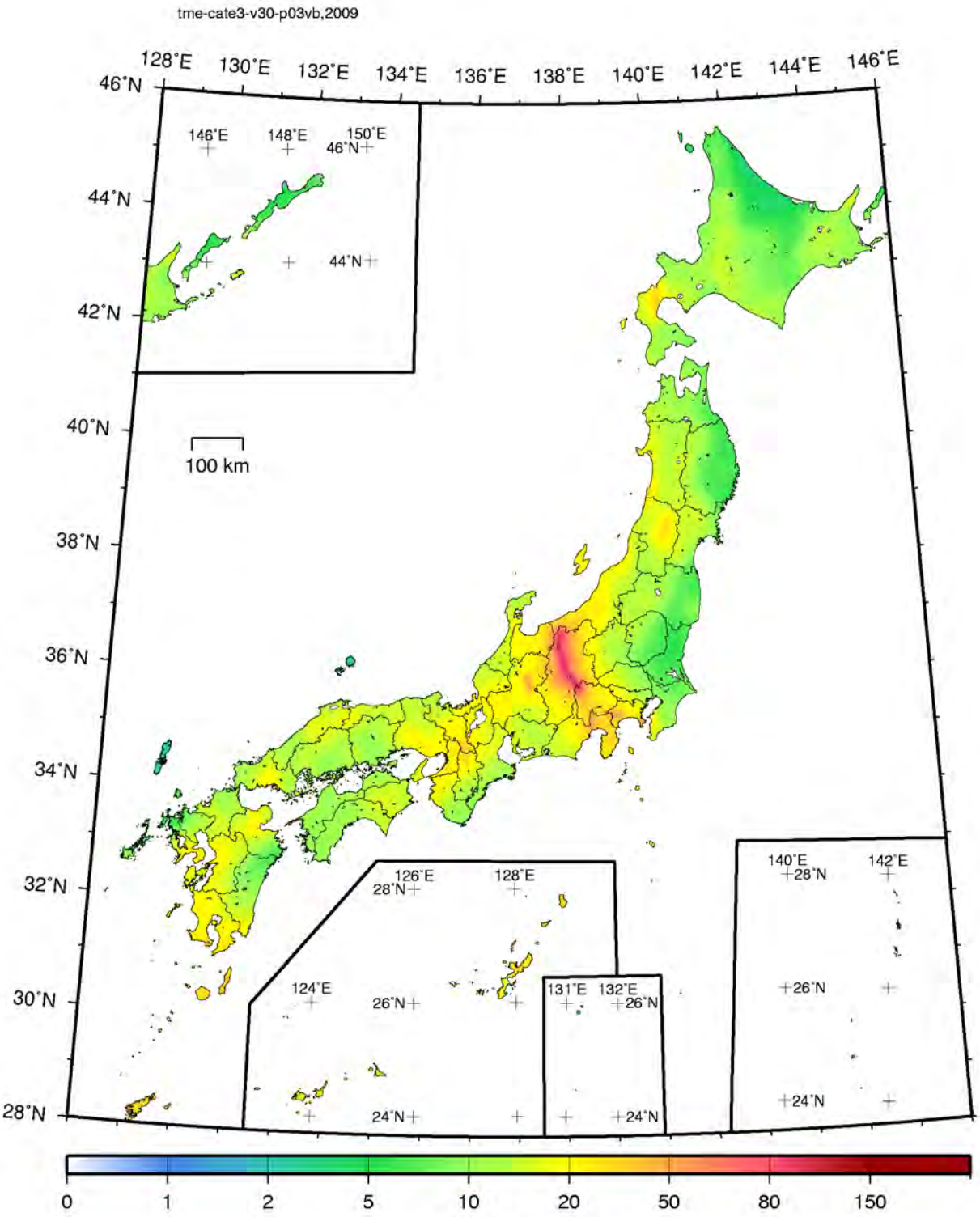

Peak ground velocity (cm/s)
(Exceedance probability within 30 years: 3%)

Figure 3.7.2-39 (1) Peak ground velocity on the bedrock (Vs=600 m/s) associated with earthquake category III (2009 version; exceedance probability within 30 years: 3%; average case)

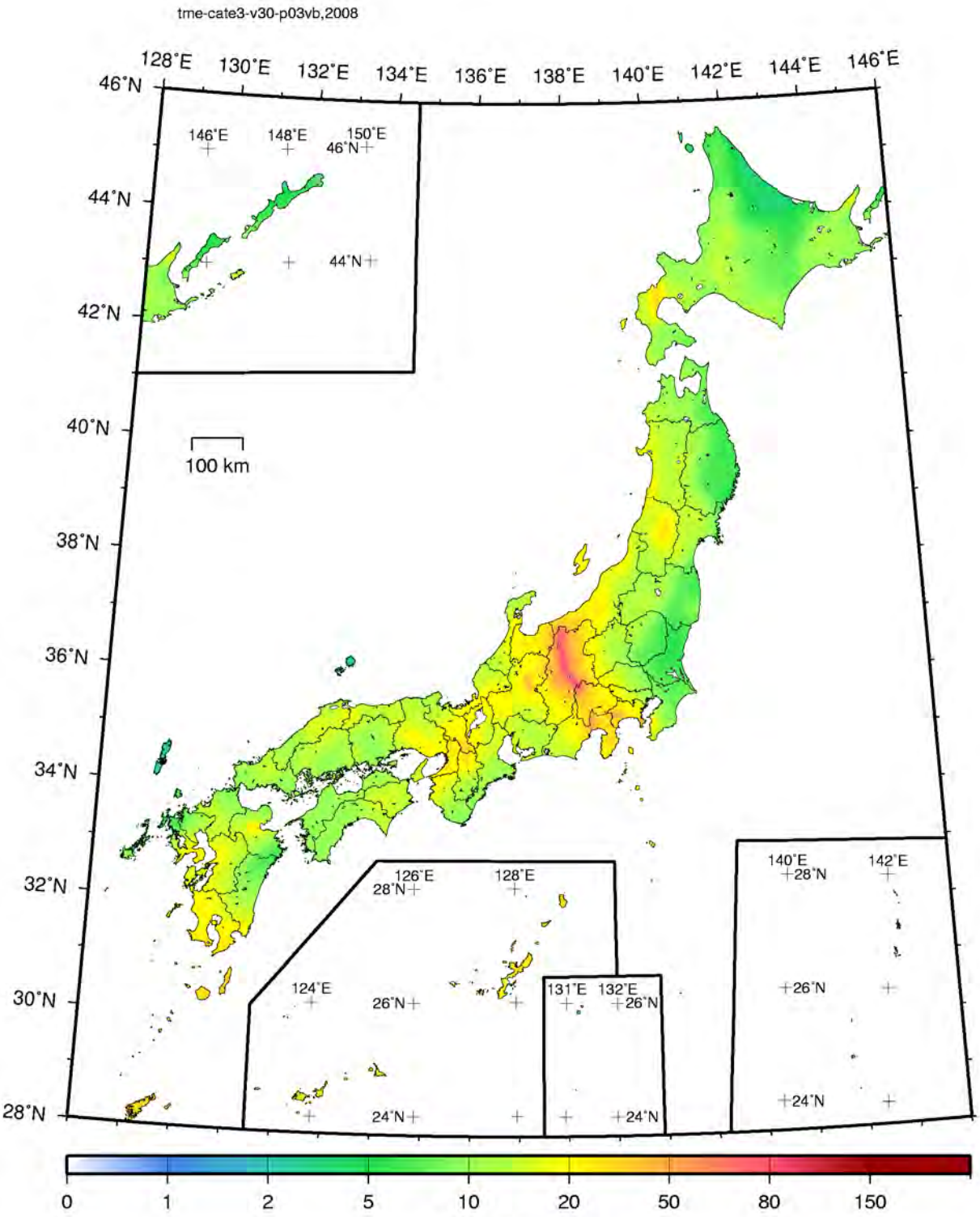

Peak ground velocity (cm/s)
(Exceedance probability within 30 years: 3%)

Figure 3.7.2-39 (2) Peak ground velocity on the bedrock (Vs=600 m/s) associated with earthquake category III (2008 version; exceedance probability within 30 years: 3%; average case)

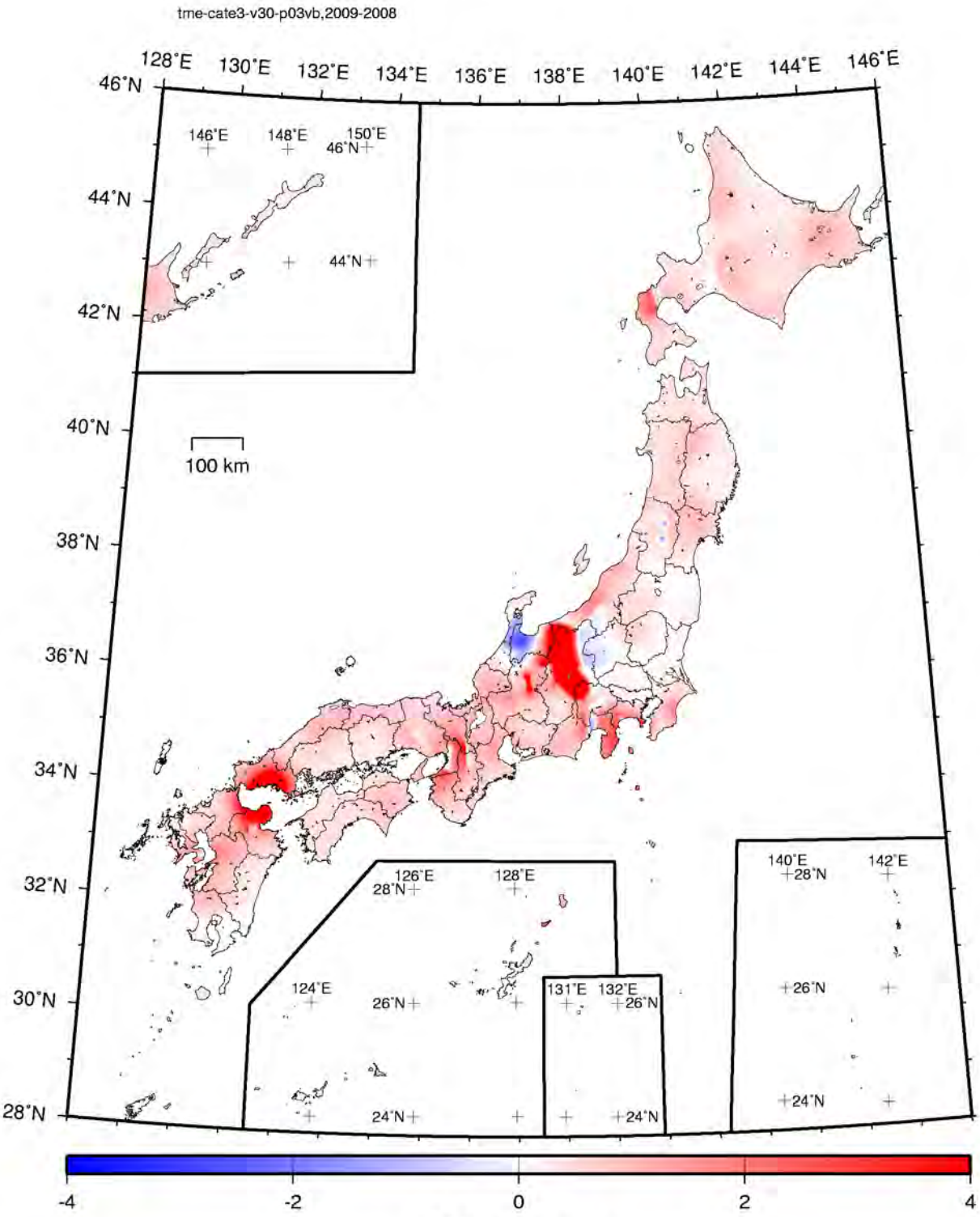

Difference in the peak ground velocity (cm/s)
(Exceedance probability within 30 years: 3%)

Figure 3.7.2-39 (3) Differences in the peak ground velocity on the bedrock (Vs=600 m/s) associated with earthquake category III (Exceedance probability within 30 years: 3%; average case)

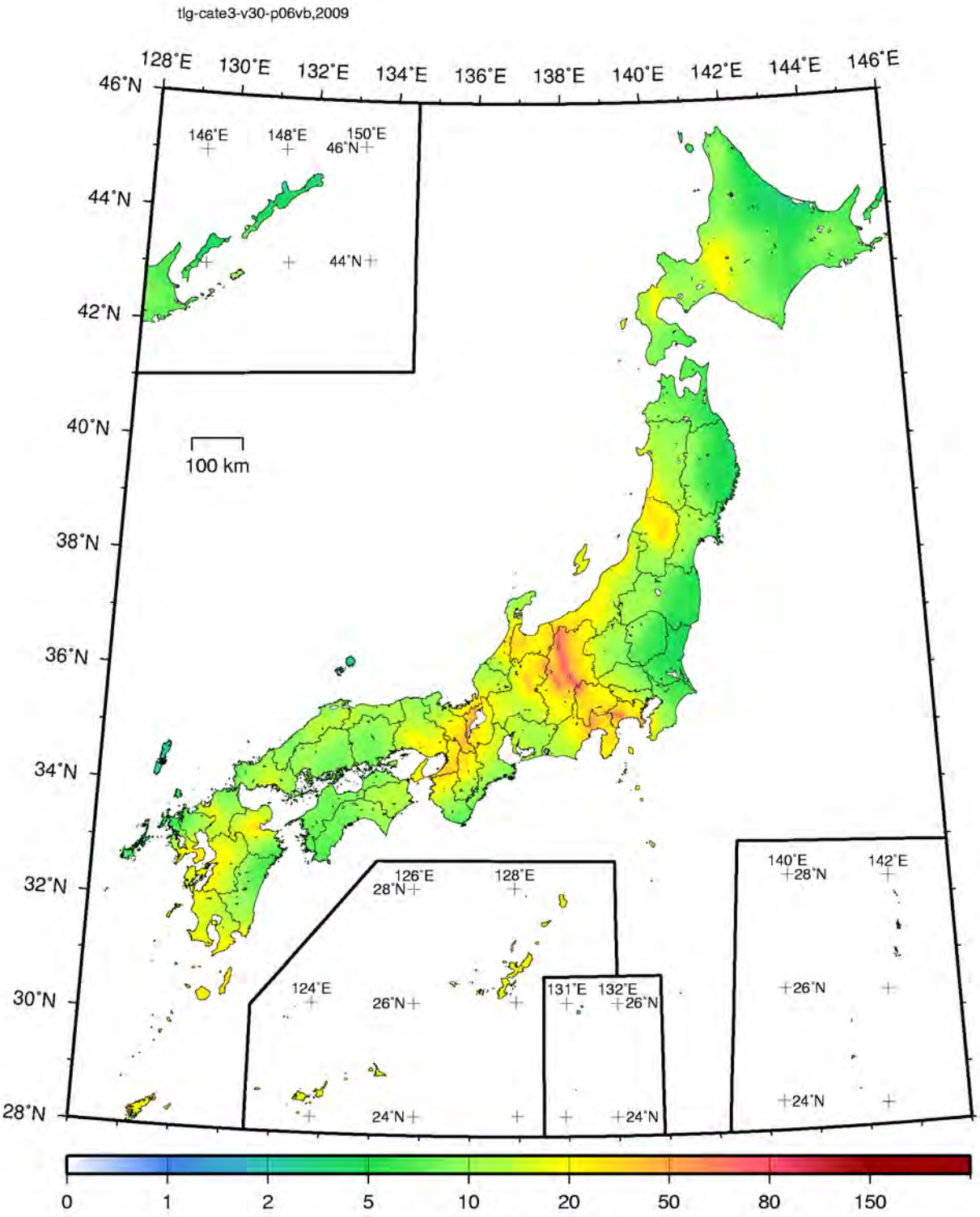

Peak ground velocity (cm/s)
(Exceedance probability within 30 years: 6%)

Figure 3.7.2-40 (1) Peak ground velocity on the bedrock (Vs=600 m/s) associated with earthquake category III (2009 version; exceedance probability within 30 years: 6%; maximum case)

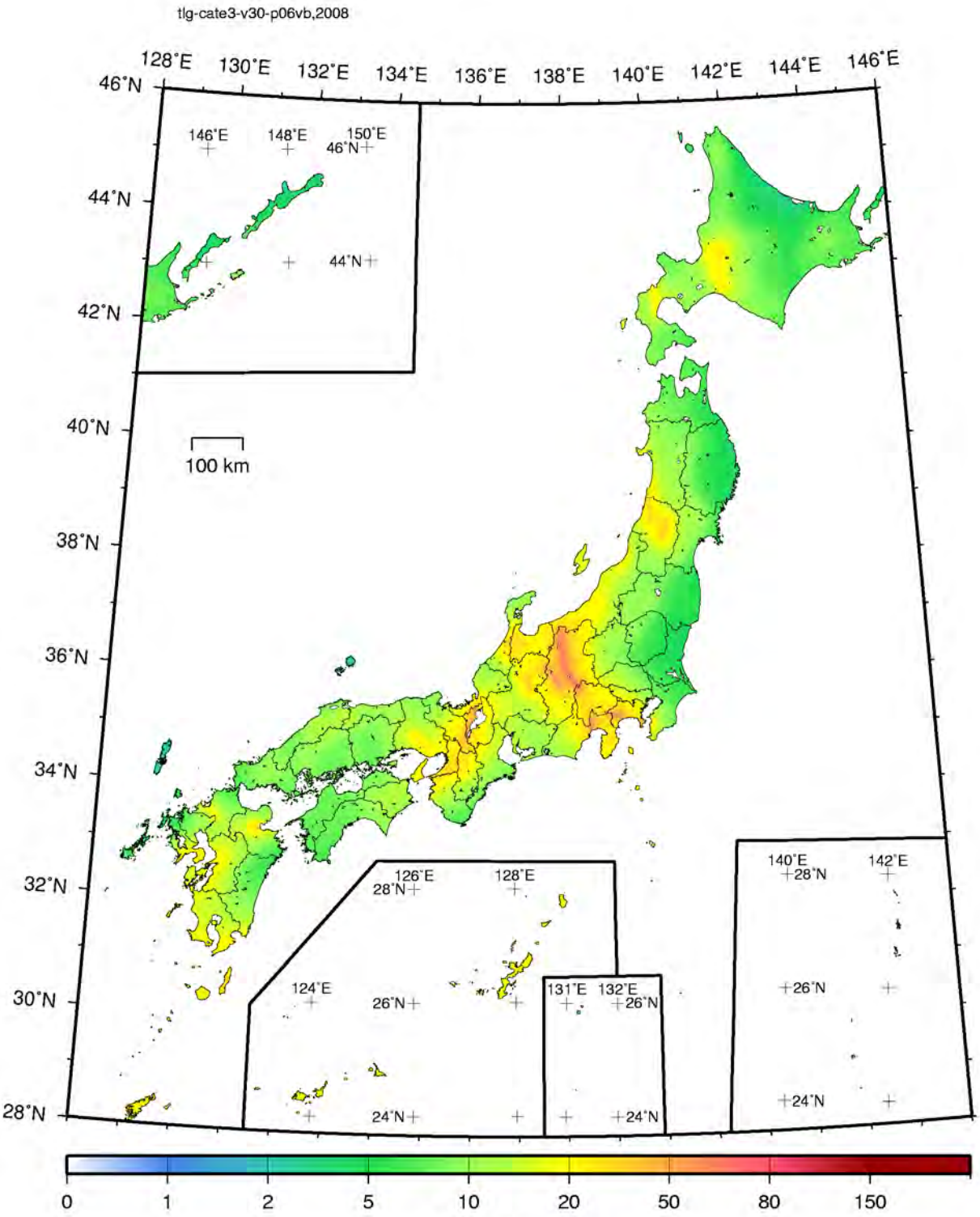

Peak ground velocity (cm/s)
(Exceedance probability within 30 years: 6%)

Figure 3.7.2-40 (2) Peak ground velocity on the bedrock (Vs=600 m/s) associated with earthquake category III (2008 version; exceedance probability within 30 years: 6%; maximum case)

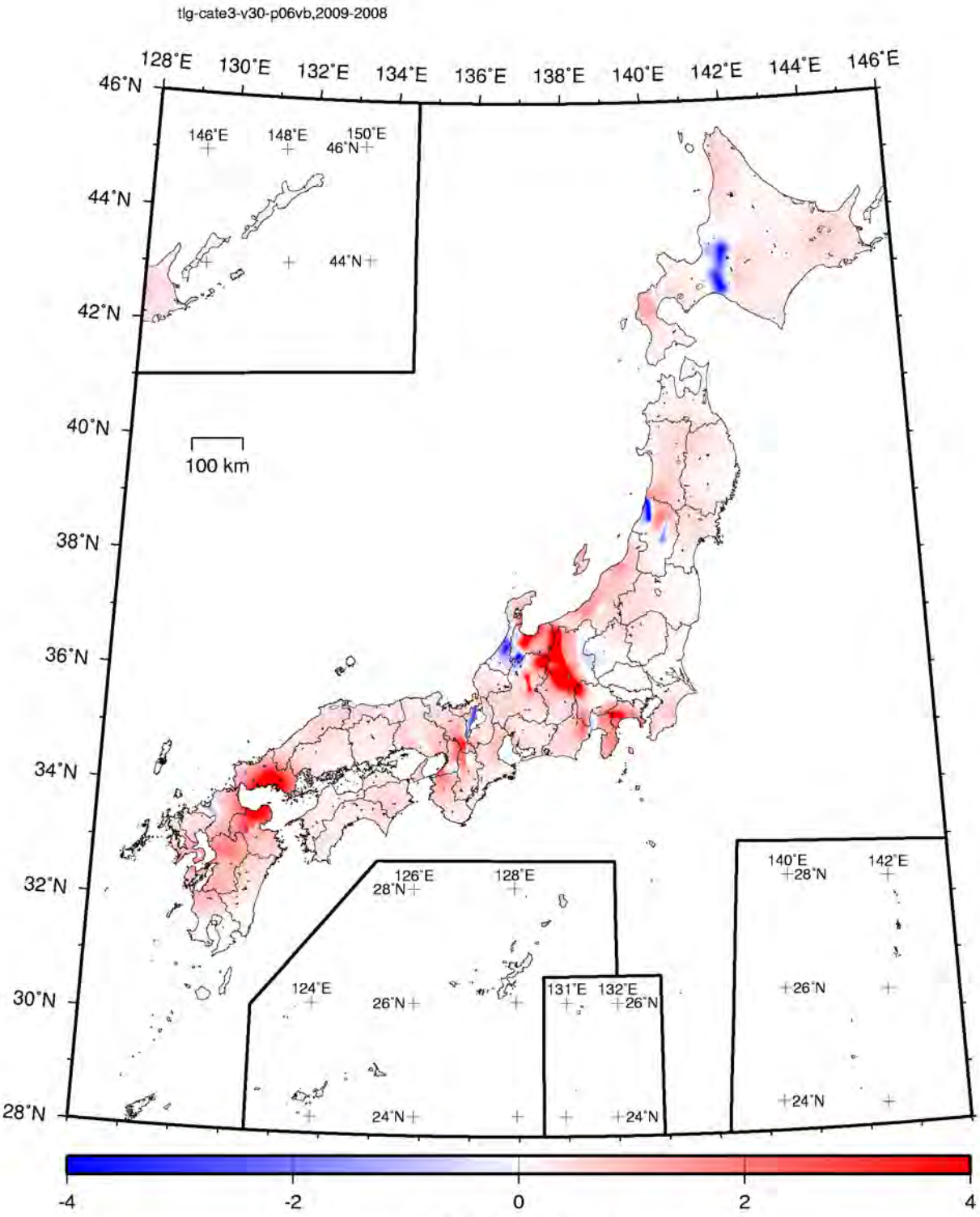

Difference in the peak ground velocity (cm/s)
(Exceedance probability within 30 years: 6%)

Figure 3.7.2-40 (3) Differences in the peak ground velocity on the bedrock (Vs=600 m/s) associated with earthquake category III (Exceedance probability within 30 years: 6%; maximum case)

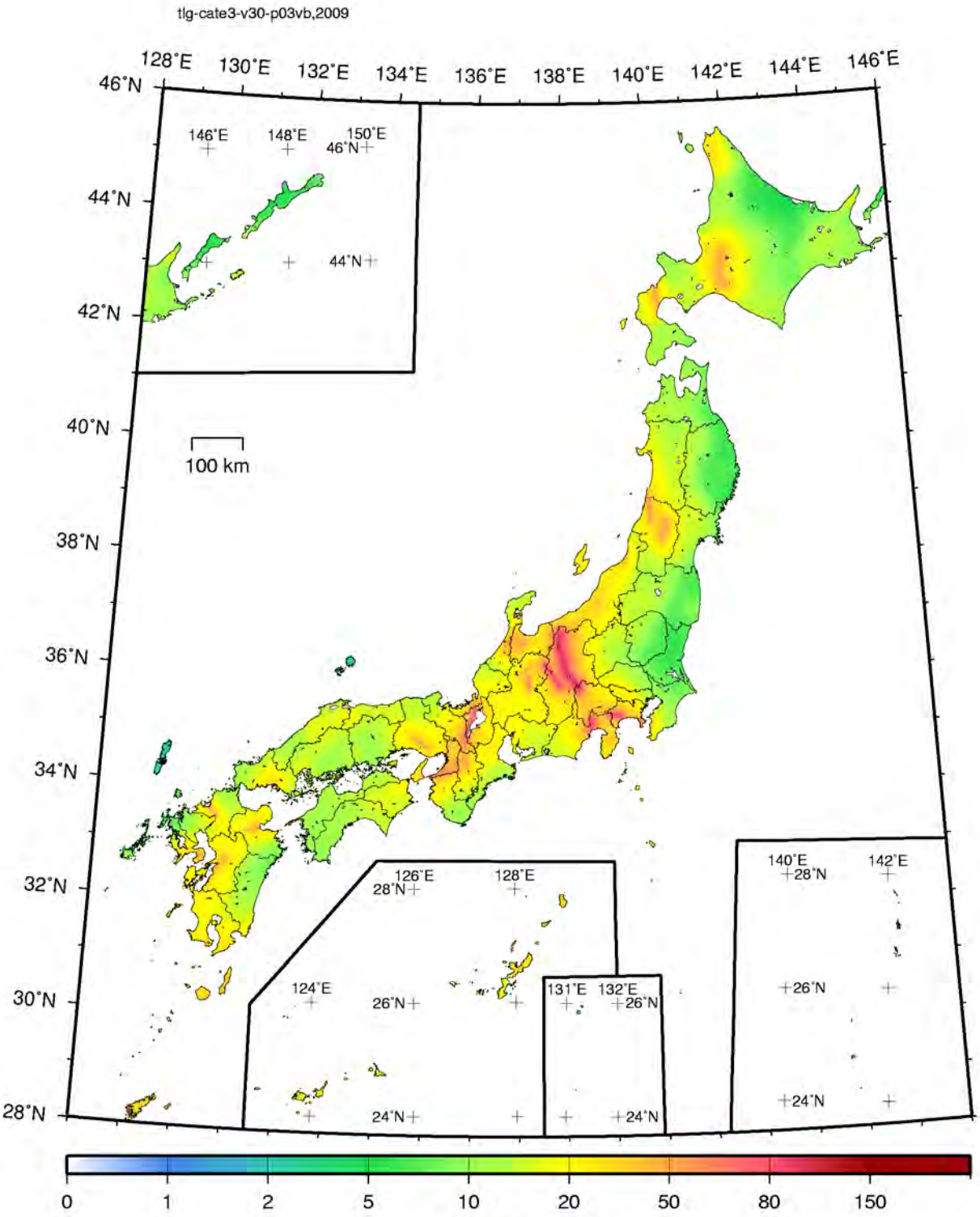

Peak ground velocity (cm/s)
(Exceedance probability within 30 years: 3%)

Figure 3.7.2-41 (1) Peak ground velocity on the bedrock (Vs=600 m/s) associated with earthquake category III (2009 version; exceedance probability within 30 years: 3%; maximum case)

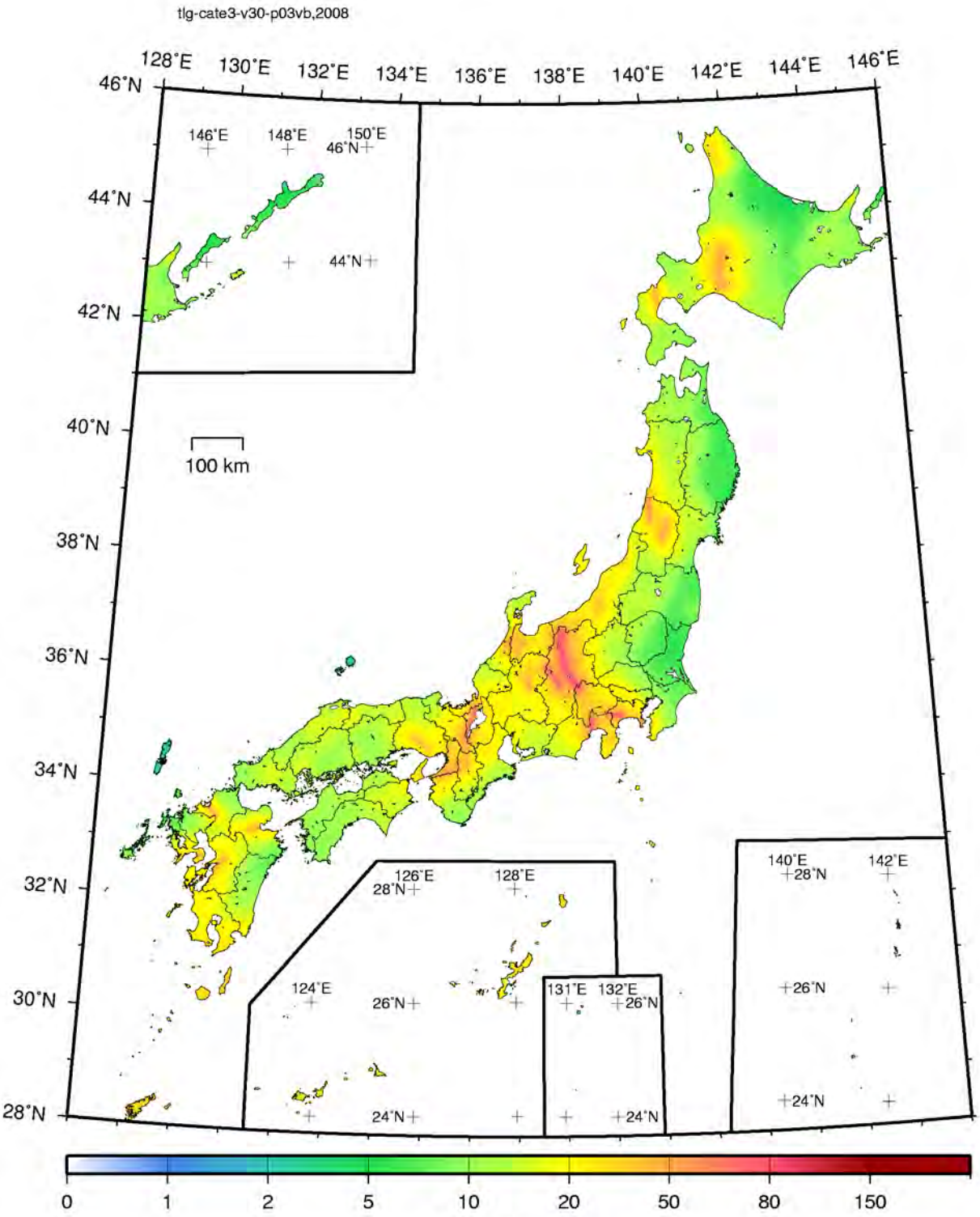

Peak ground velocity (cm/s)
(Exceedance probability within 30 years: 3%)

Figure 3.7.2-41 (2) Peak ground velocity on the bedrock (Vs=600 m/s) associated with earthquake category III (2008 version; exceedance probability within 30 years: 3%; maximum case)

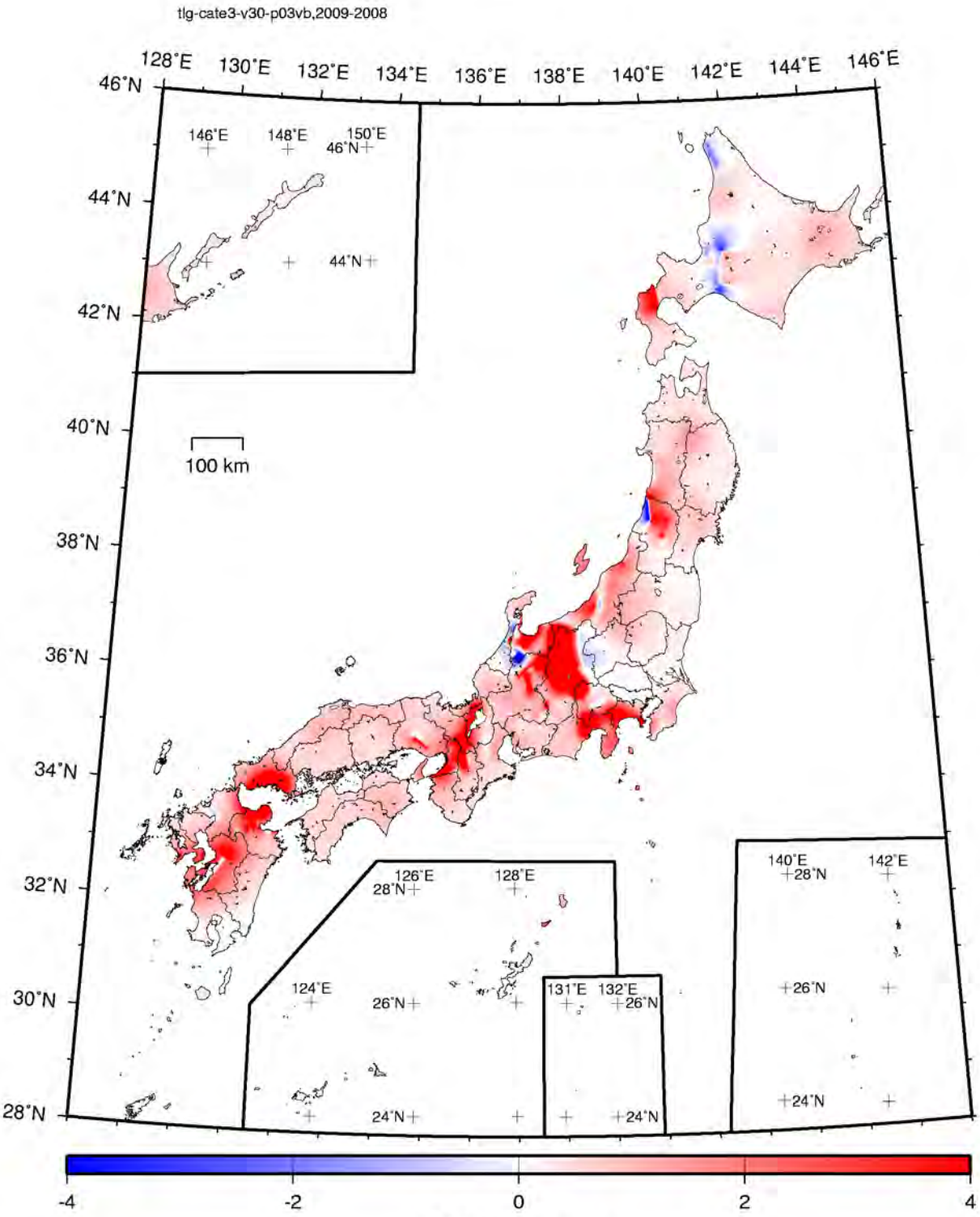

Difference in the peak ground velocity (cm/s)
(Exceedance probability within 30 years: 3%)

Figure 3.7.2-41 (3) Differences in the peak ground velocity on the bedrock (Vs=600 m/s) associated with earthquake category III (Exceedance probability within 30 years: 3%; maximum case)

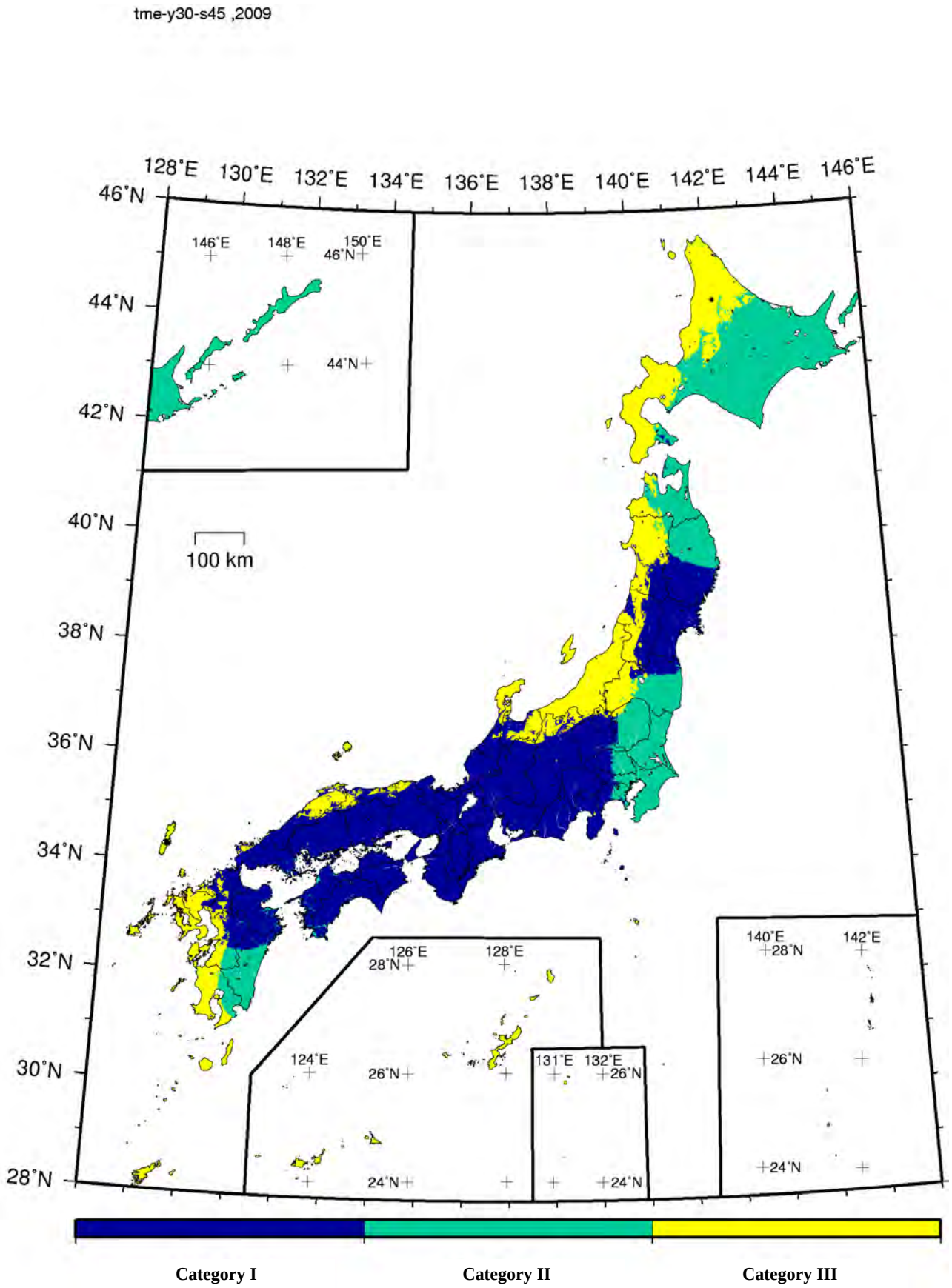

Figure 3.7.2-42 (1) earthquake category of maximum contribution
(JMA seismic intensity: 5 Lower or more; average case)

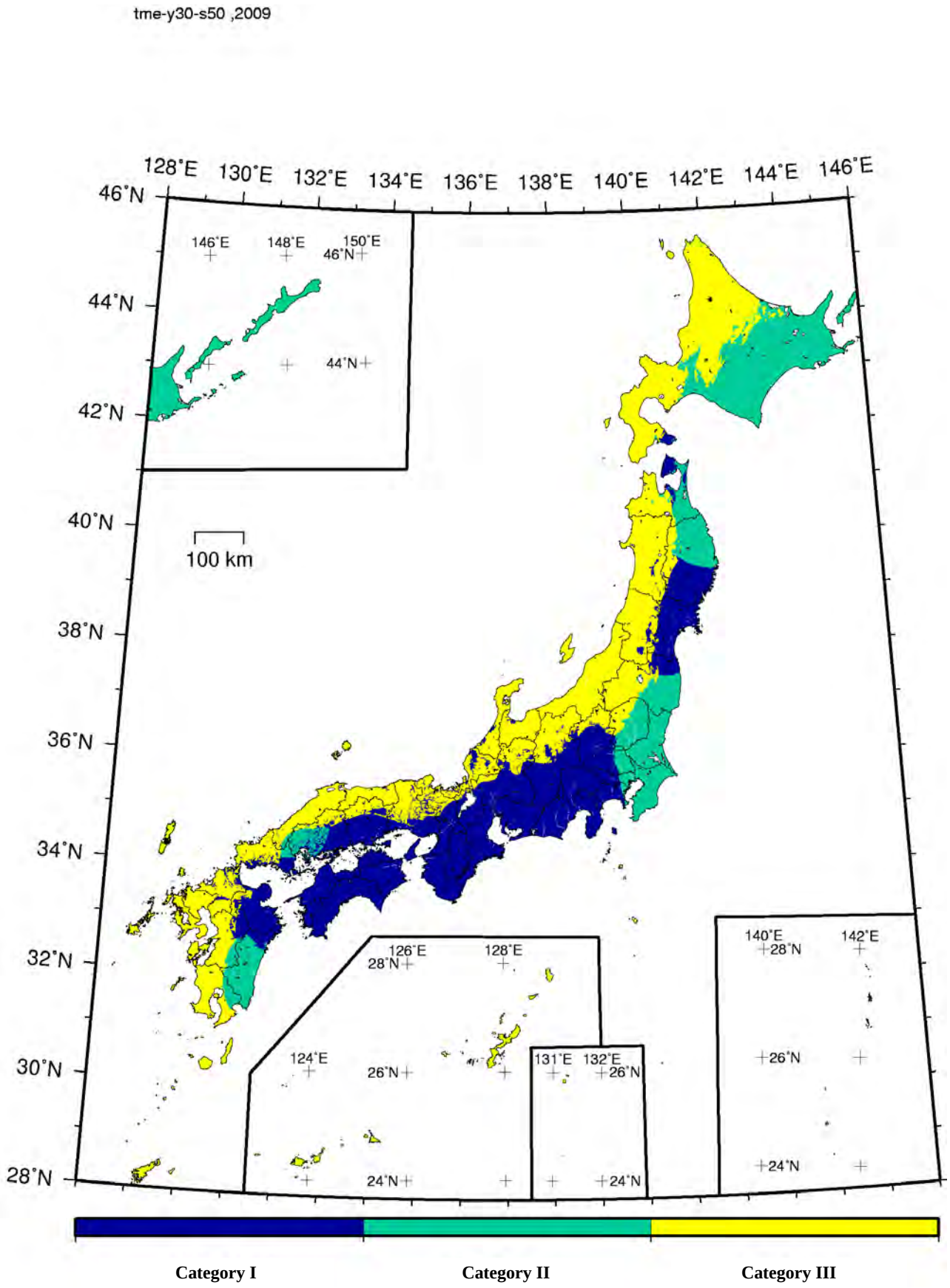

Figure 3.7.2-42 (2) earthquake category of maximum contribution
(JMA seismic intensity: 5 Upper or more; average case)

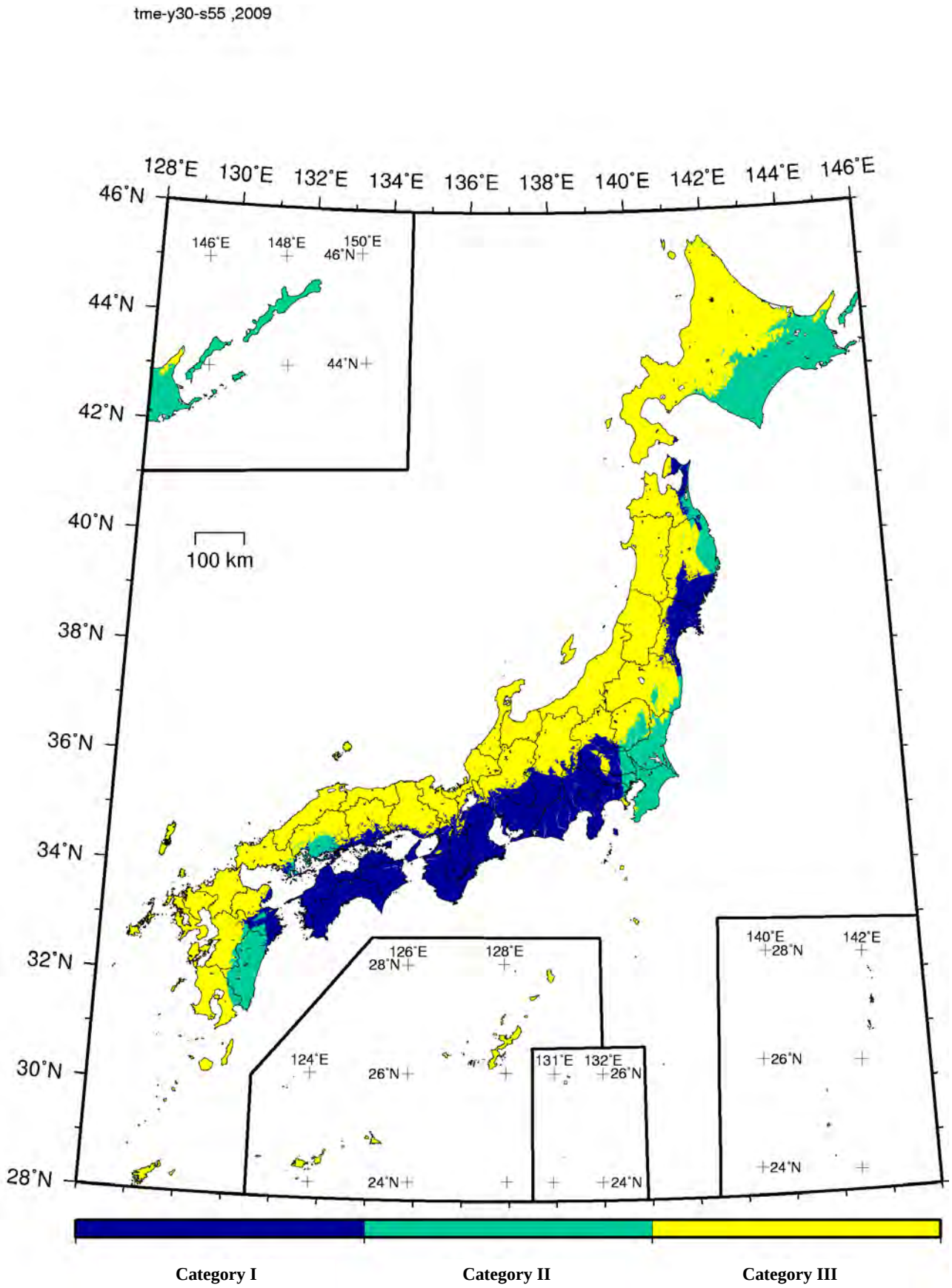

Figure 3.7.2-42 (3) earthquake category of maximum contribution
(JMA seismic intensity: 6 Lower or more; average case)

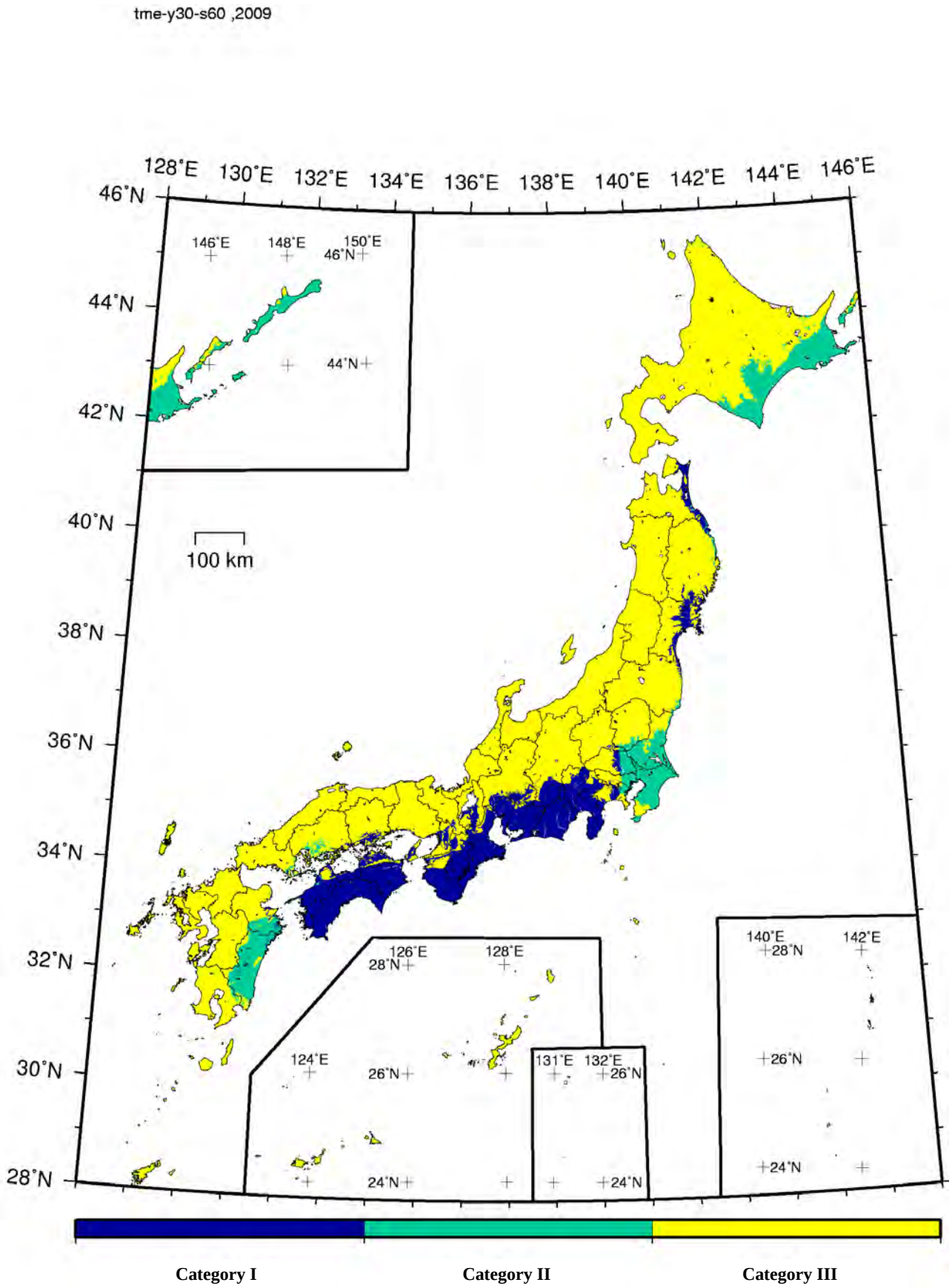

Figure 3.7.2-42 (4) earthquake category of maximum contribution
(JMA seismic intensity: 6 Upper or more; average case)

tlg-y30-s45 ,2009

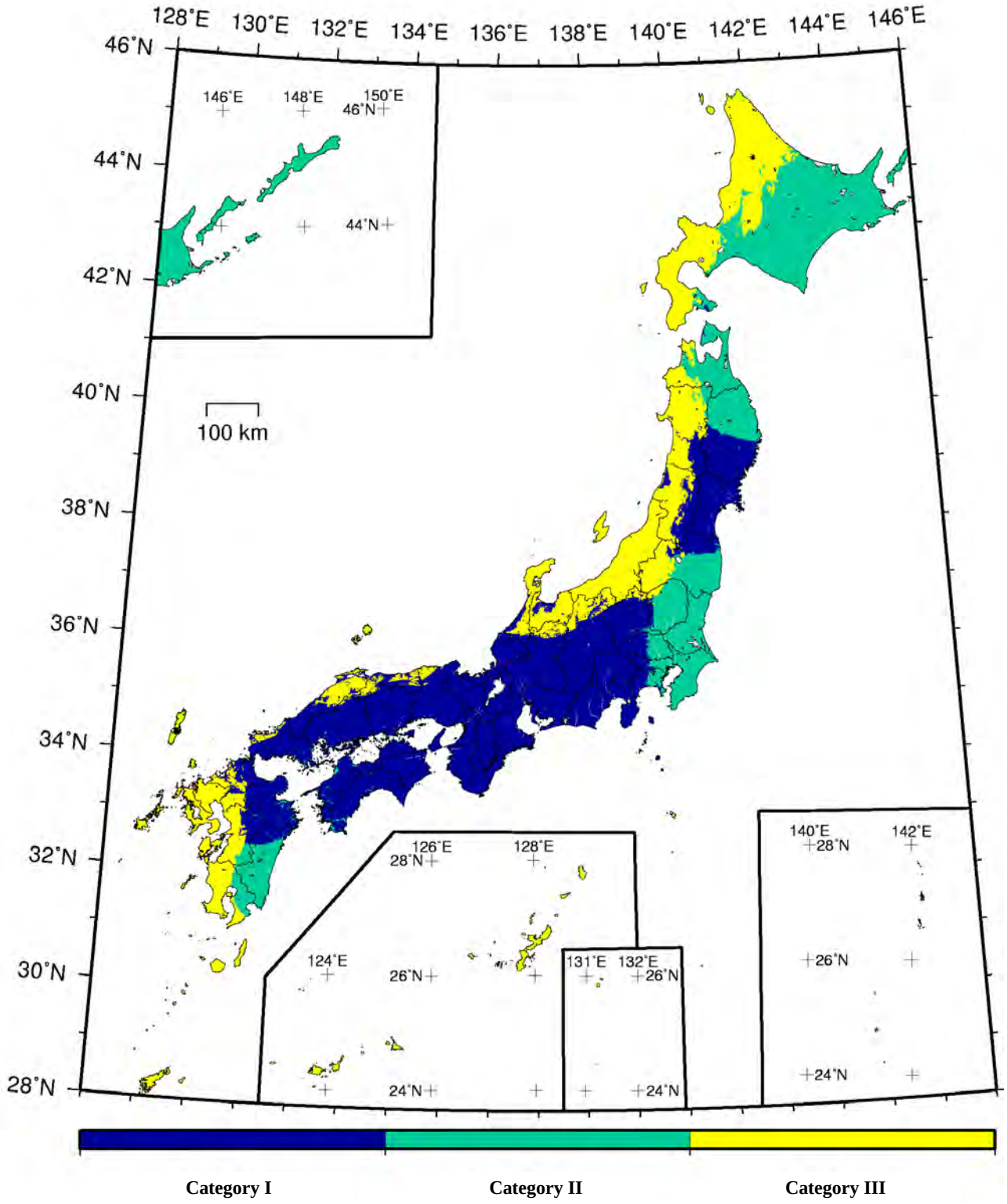

Figure 3.7.2-43 (1) earthquake category of maximum contribution
(JMA seismic intensity: 5 Lower or more; maximum case)

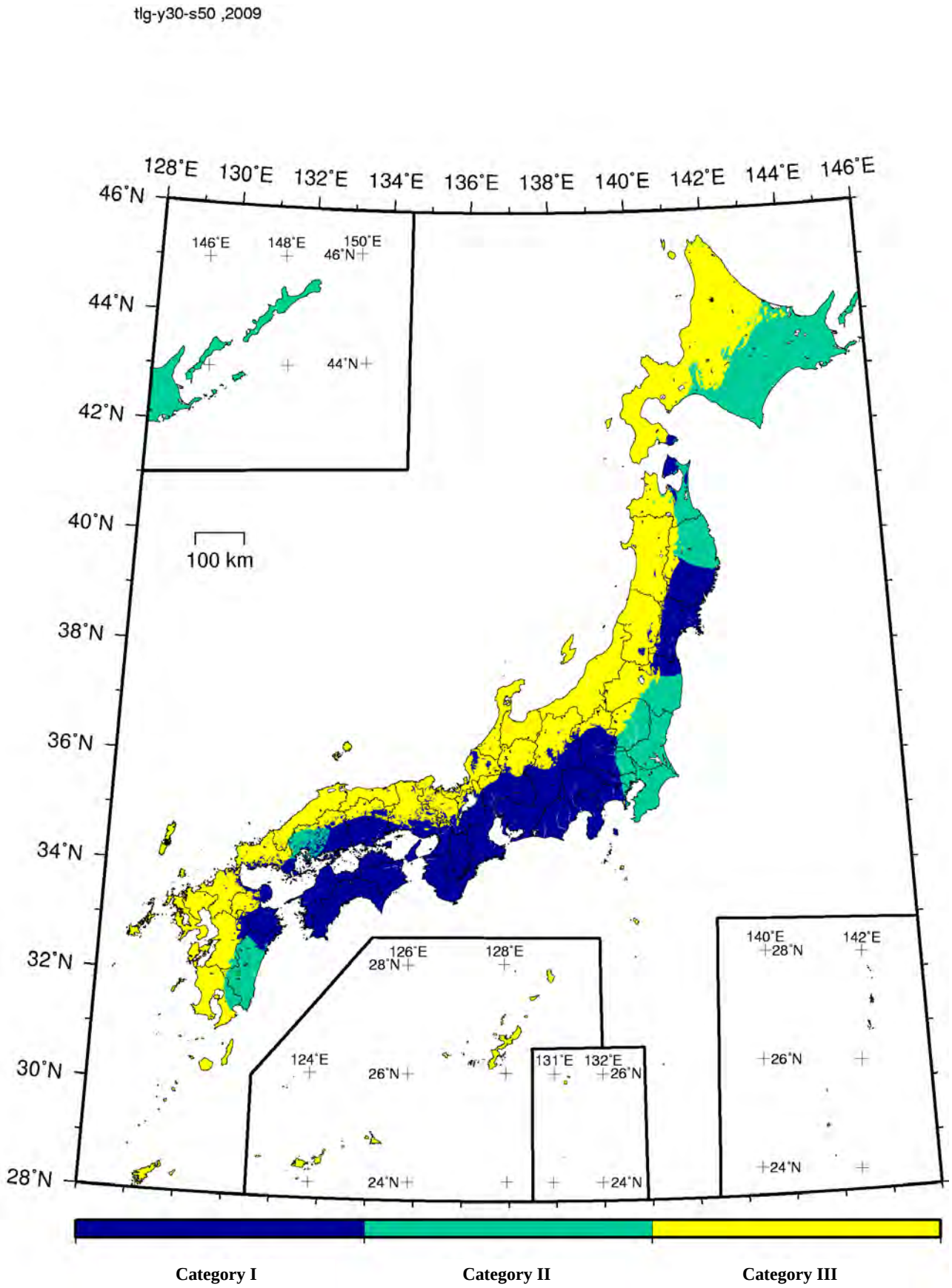

Figure 3.7.2-43 (2) earthquake category of maximum contribution
(JMA seismic intensity: 5 Upper or more; maximum case)

tlg-y30-s55 ,2009

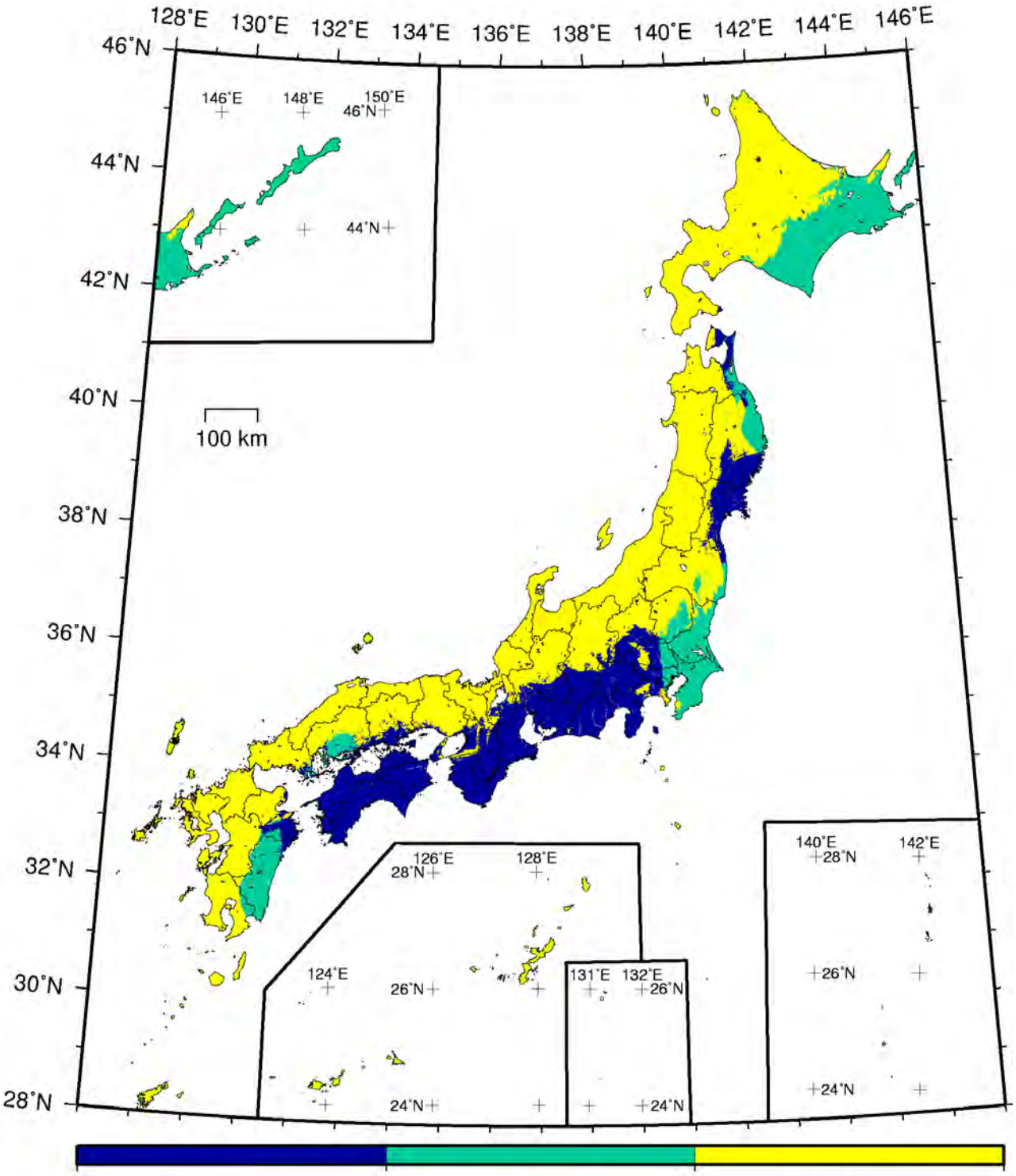

Category I **Category II** **Category III**

Figure 3.7.2-43 (3) earthquake category of maximum contribution
(JMA seismic intensity: 6 Lower or more; maximum case)

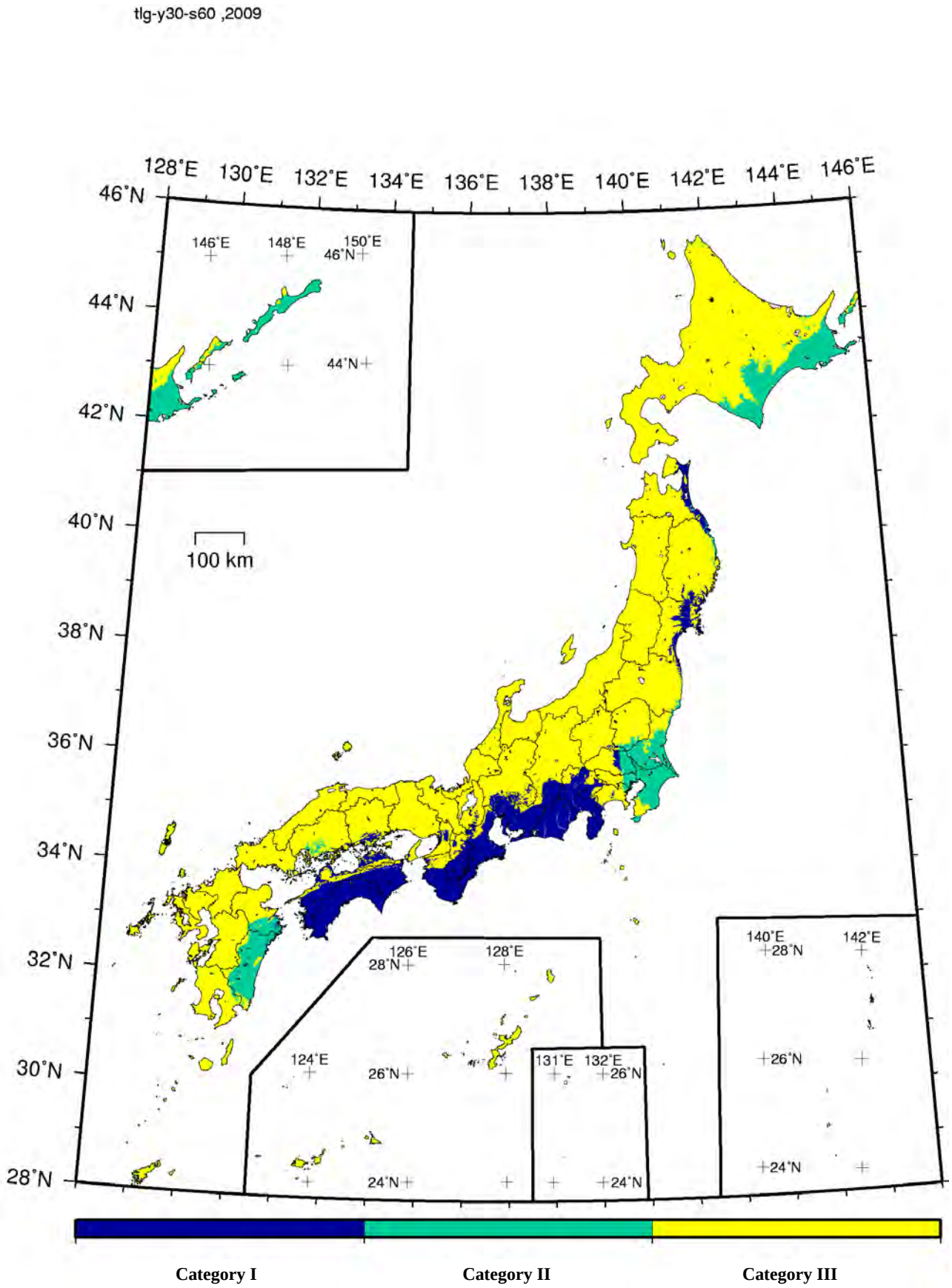

Figure 3.7.2-43 (4) earthquake category of maximum contribution
(JMA seismic intensity: 6 Upper or more; maximum case)

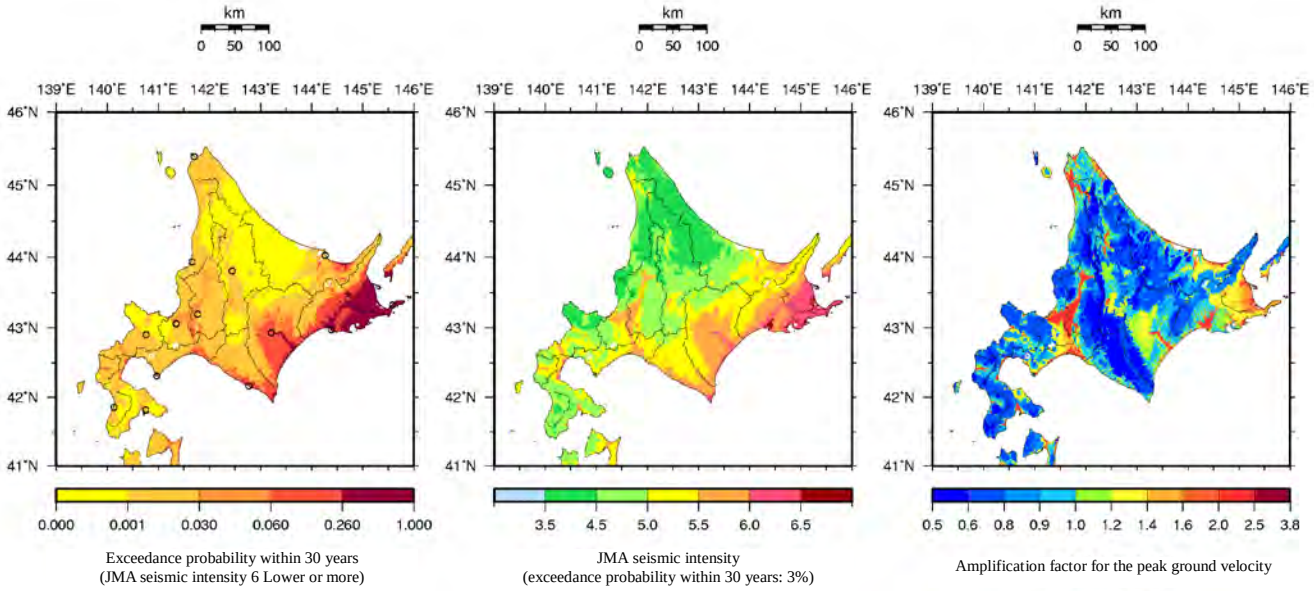

Figure 3.7.2-44 Seismic hazard maps for Hokkaido

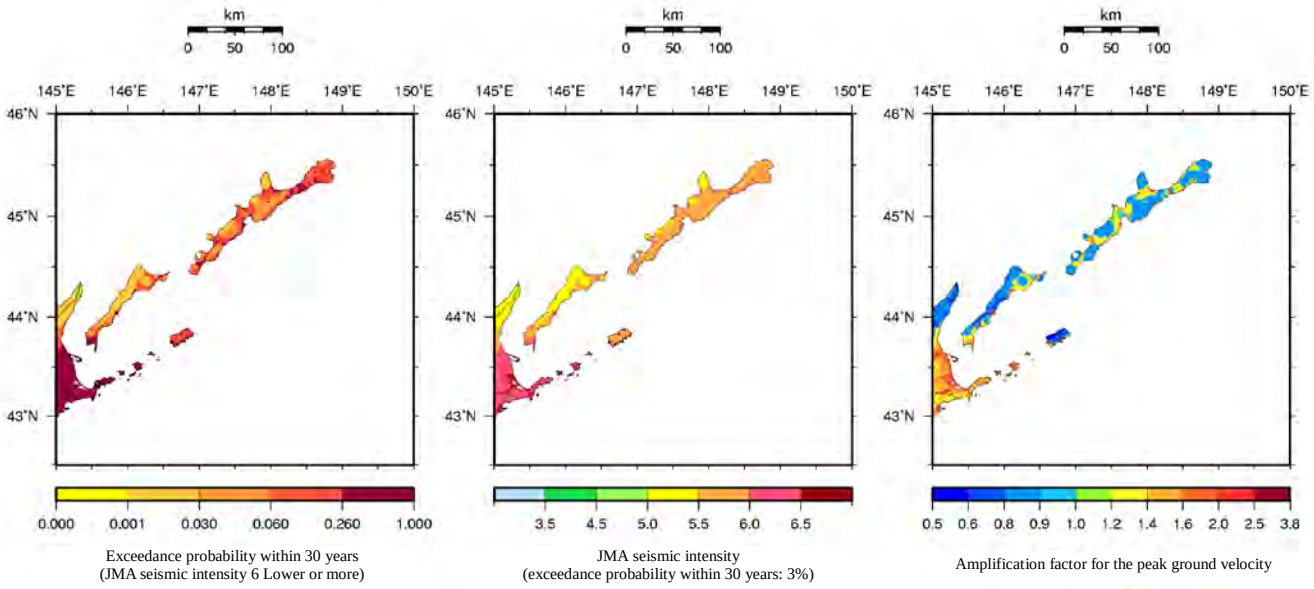

Figure 3.7.2-45 Seismic hazard maps for Etrorofu, Kunashiri, Shikotan and Habomai islands

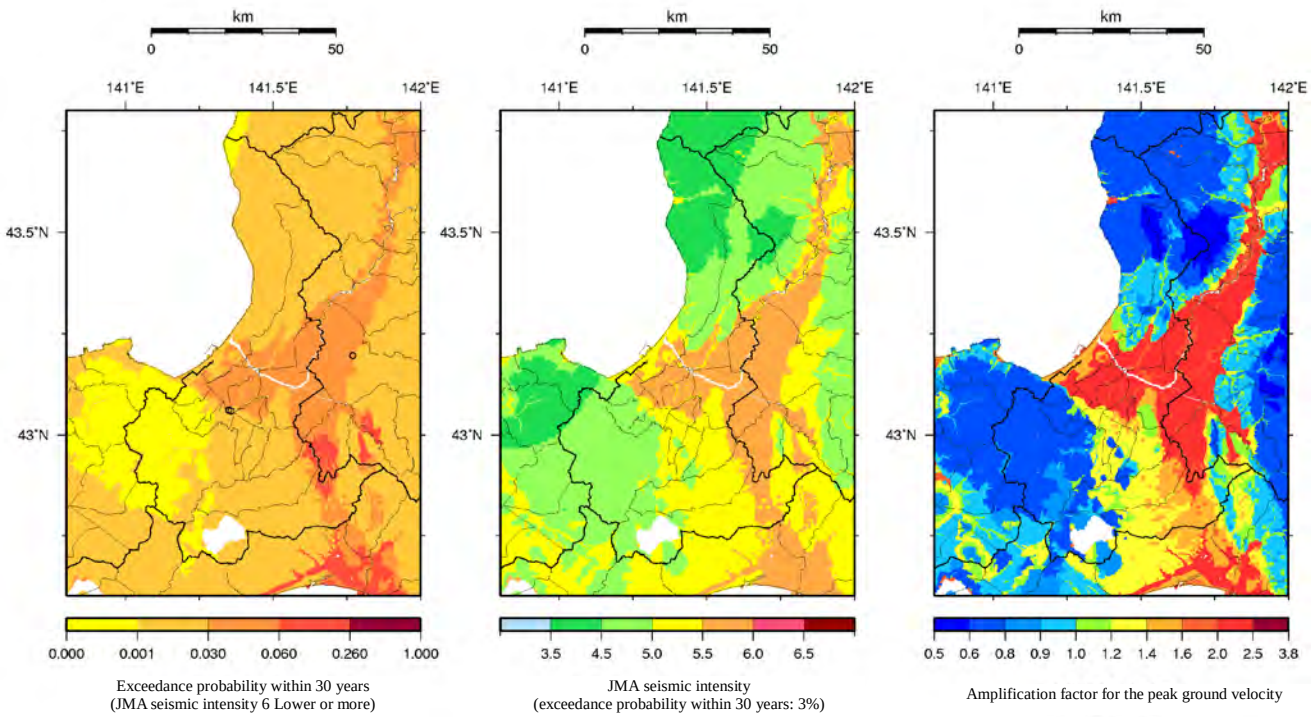

Figure 3.7.2-46 Seismic hazard maps for Ishikari subprefecture, Hokkaido

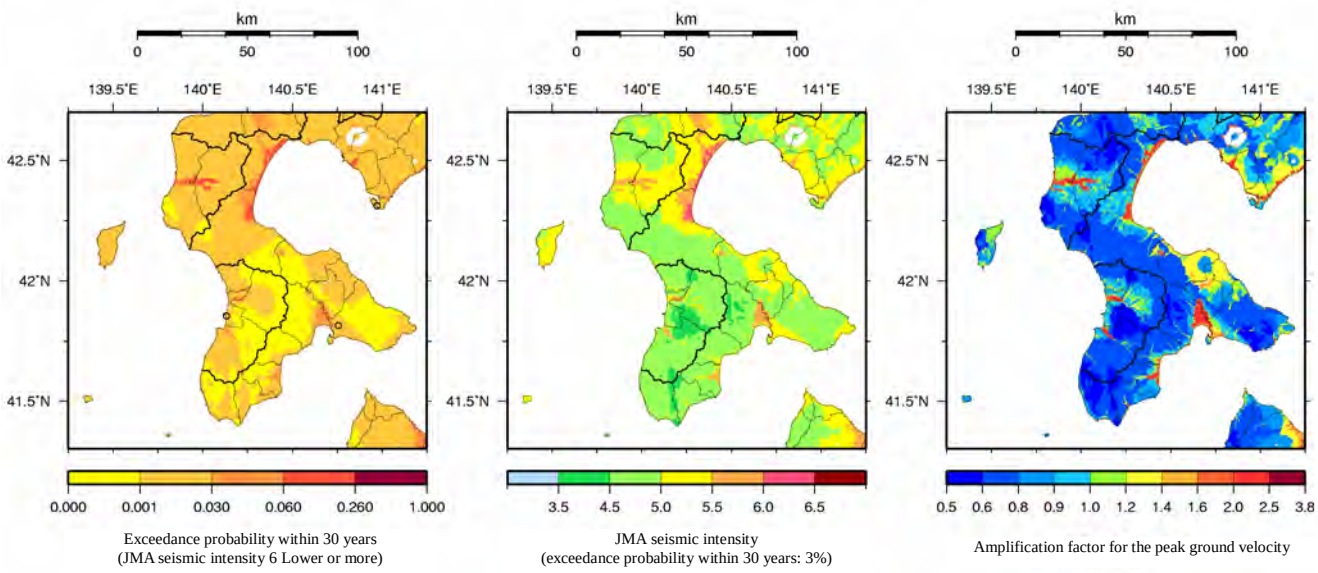

Figure 3.7.2-47 Seismic hazard maps for Oshima subprefecture, Hokkaido

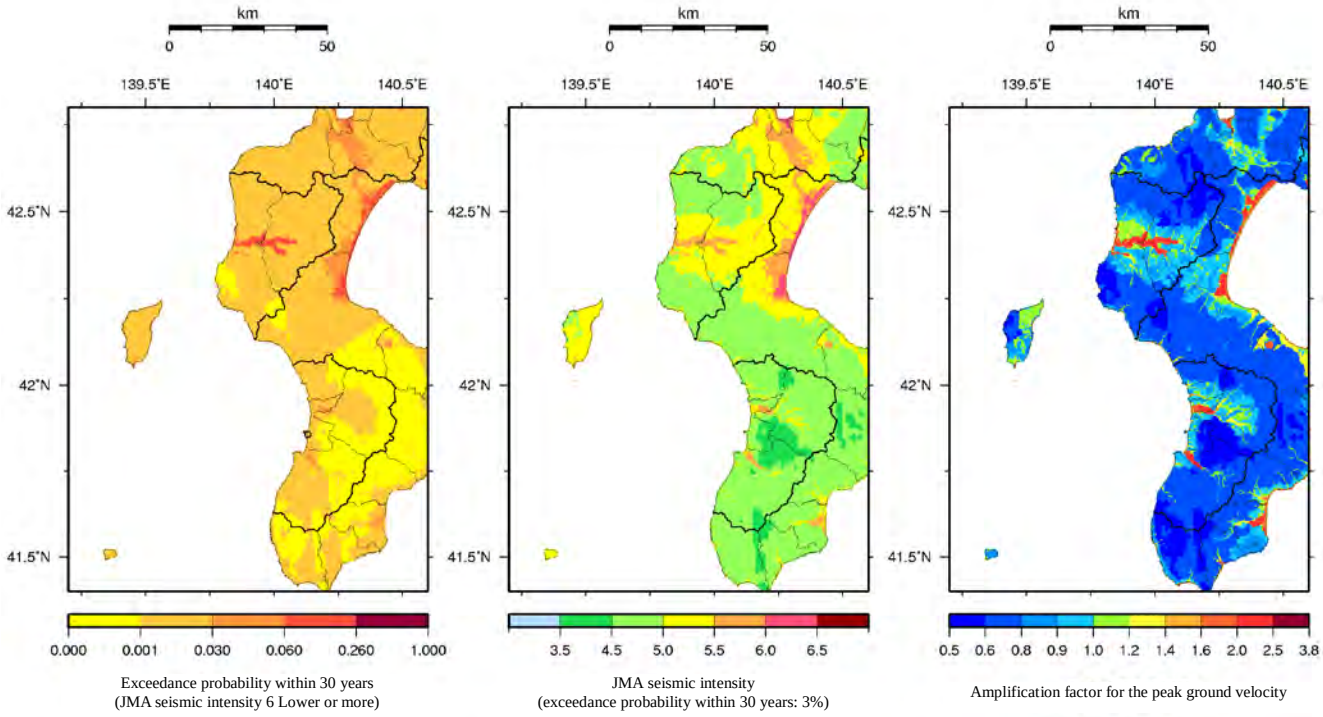

Figure 3.7.2-48 Seismic hazard maps for Hiyama subprefecture, Hokkaido

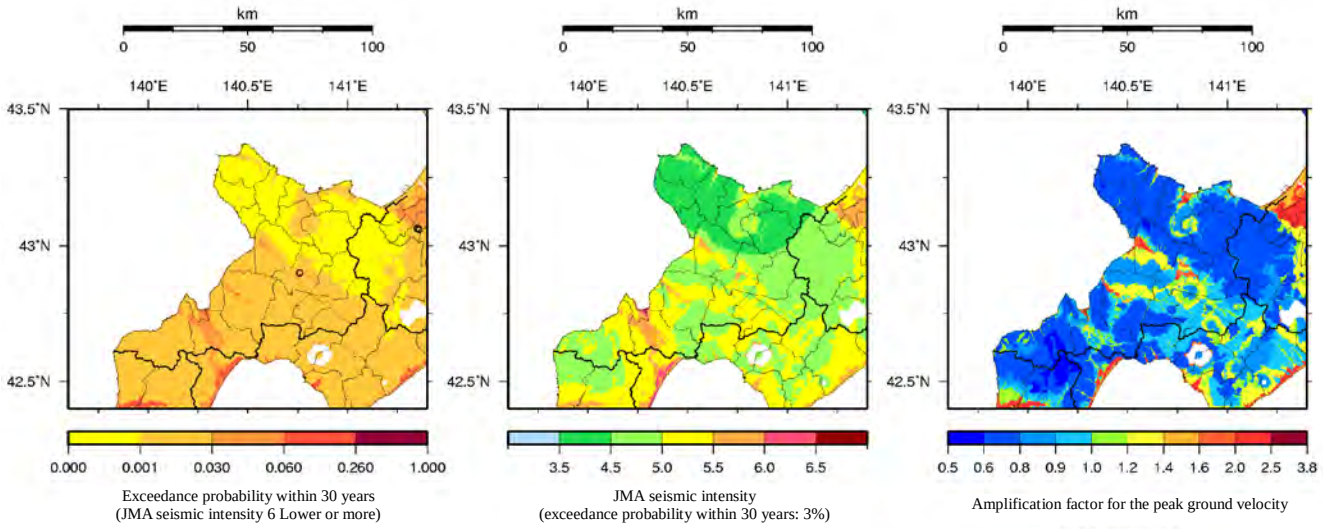

Figure 3.7.2-49 Seismic hazard maps for Shiribeshi subprefecture, Hokkaido

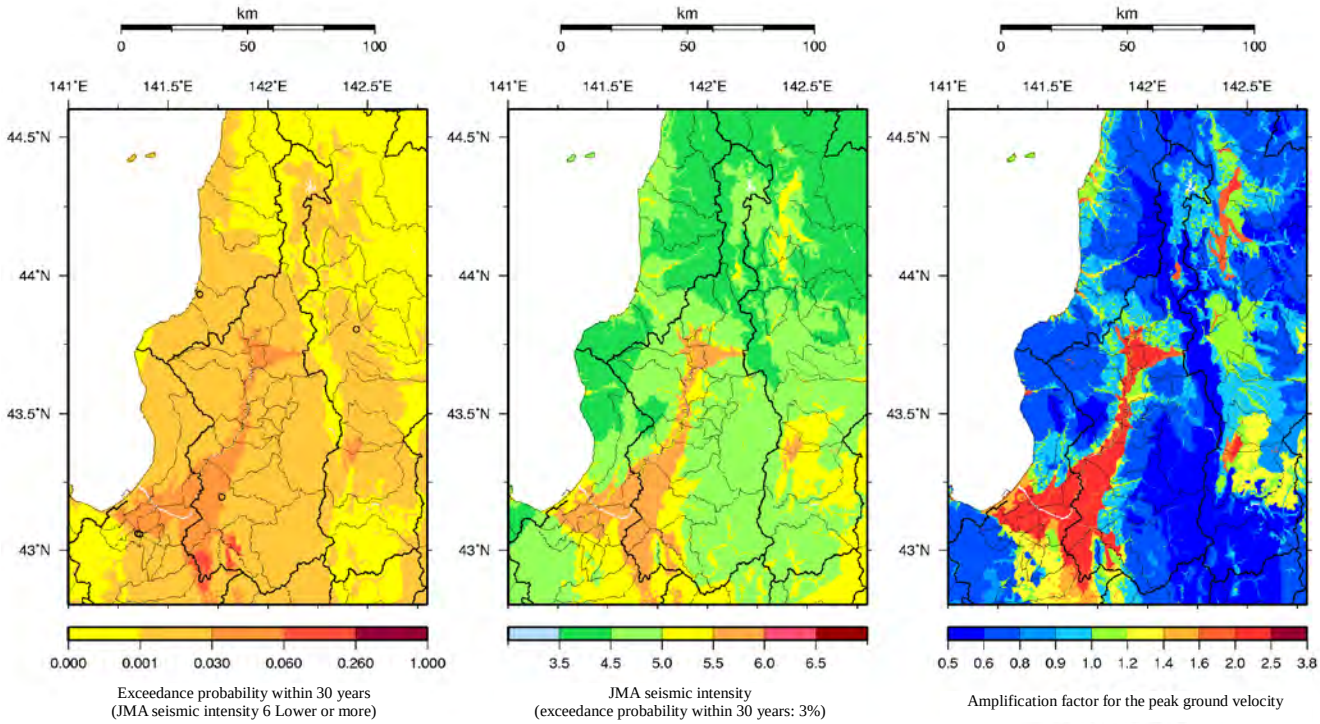

Figure 3.7.2-50 Seismic hazard maps for Sorachi subprefecture, Hokkaido

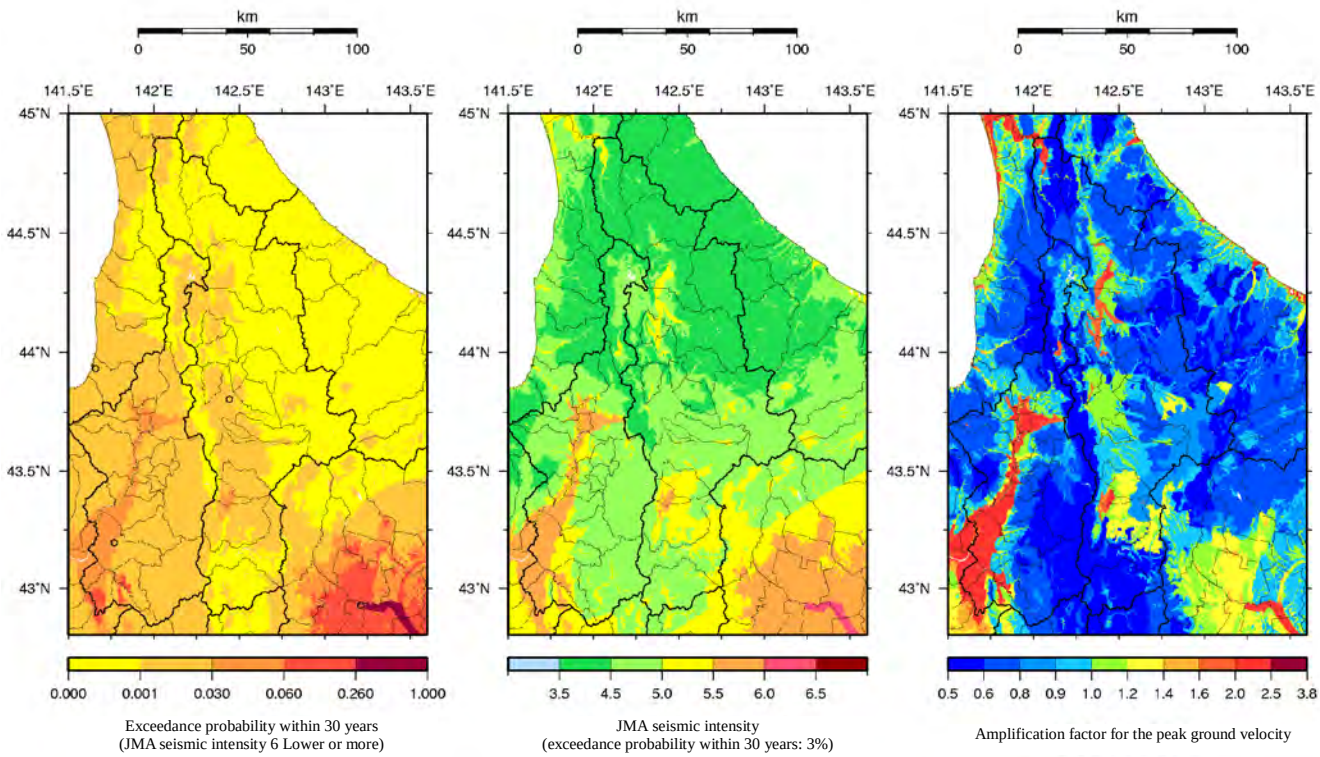

Figure 3.7.2-51 Seismic hazard maps for Kamikawa subprefecture, Hokkaido

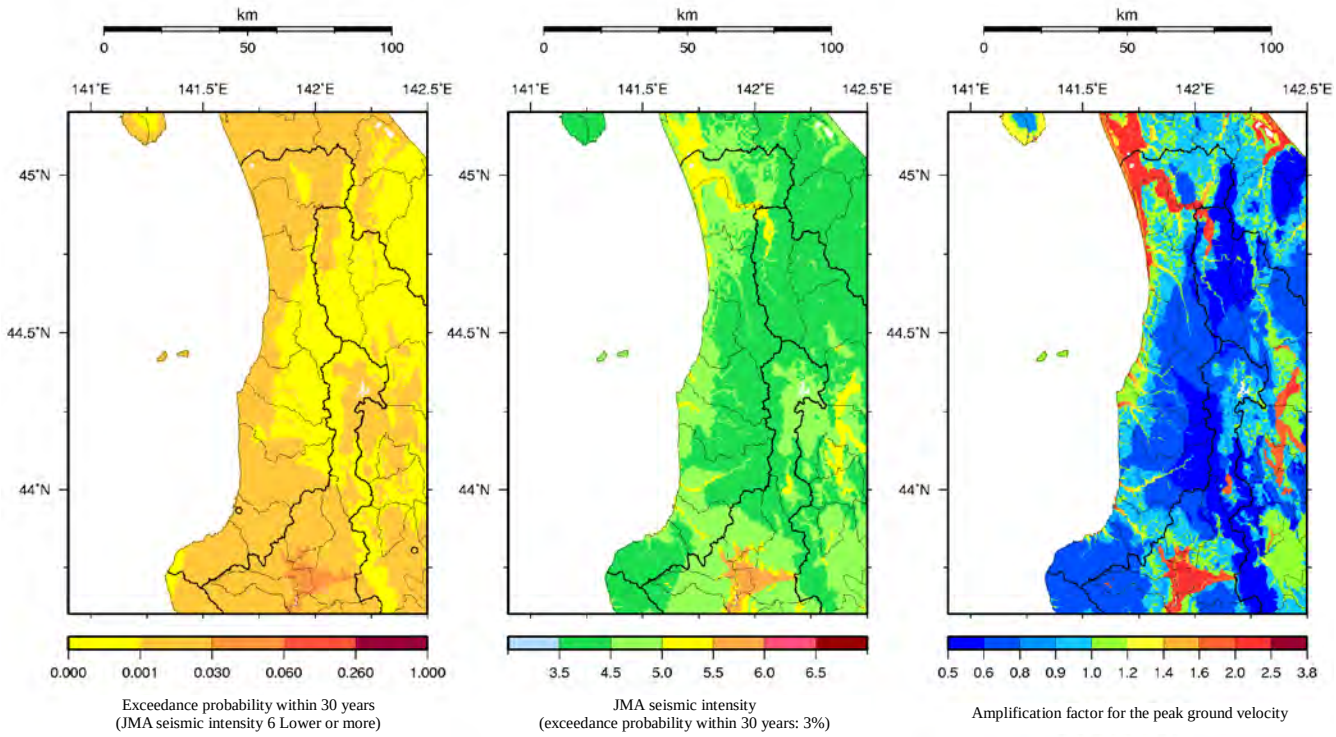

Figure 3.7.2-52 Seismic hazard maps for Rumoi subprefecture, Hokkaido

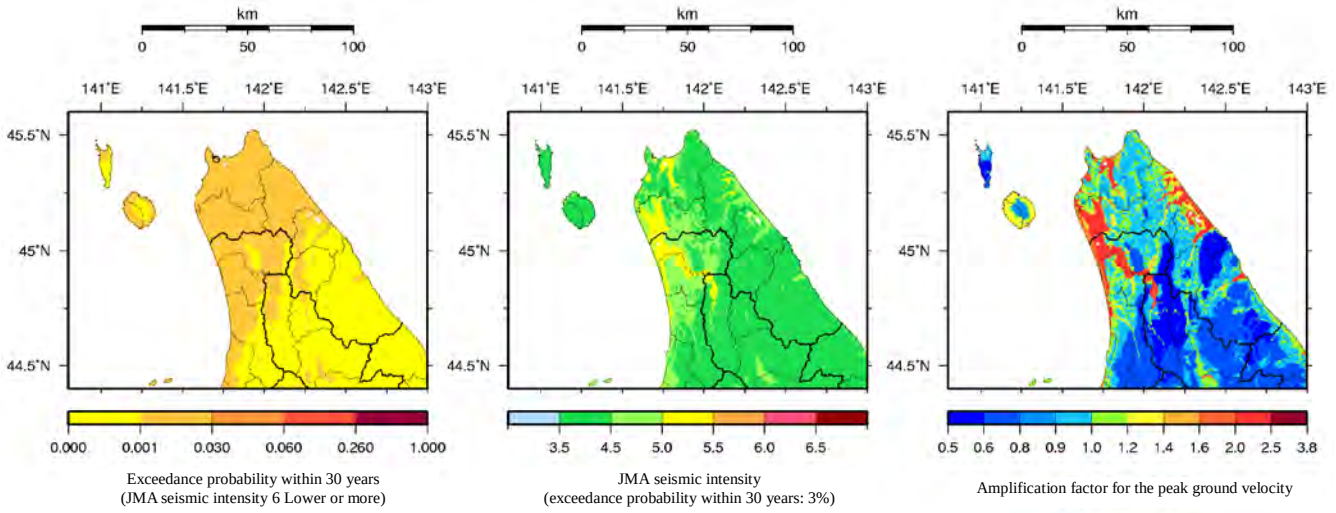

Figure 3.7.2-53 Seismic hazard maps for Souya subprefecture, Hokkaido

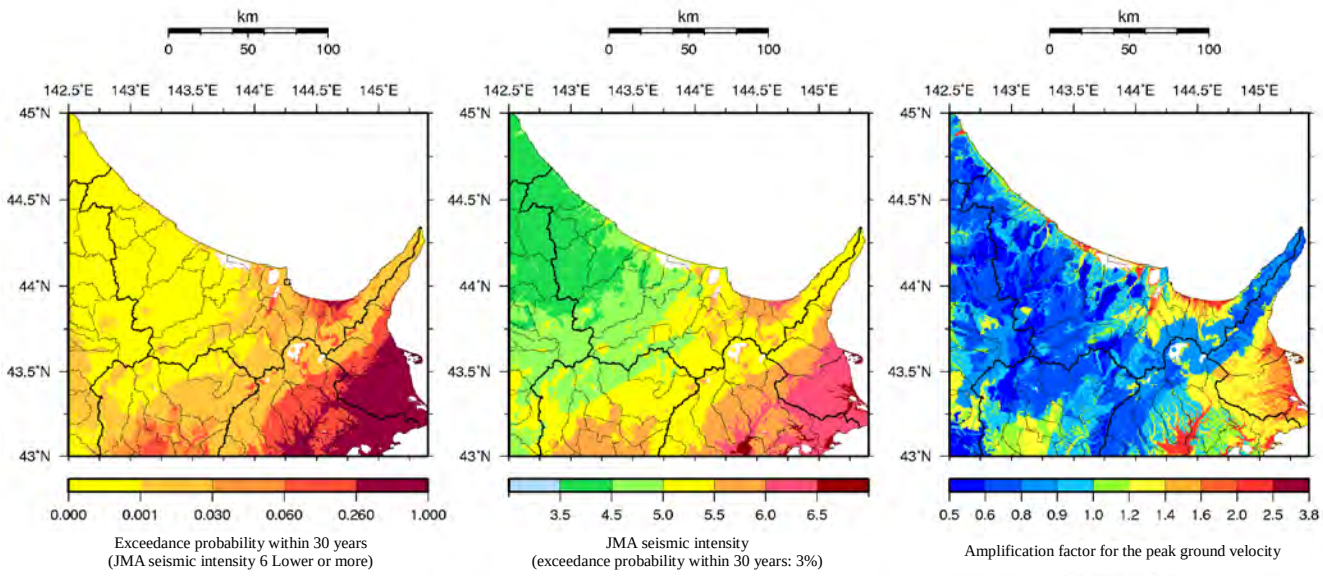

Figure 3.7.2-54 Seismic hazard maps for Abashiri subprefecture, Hokkaido

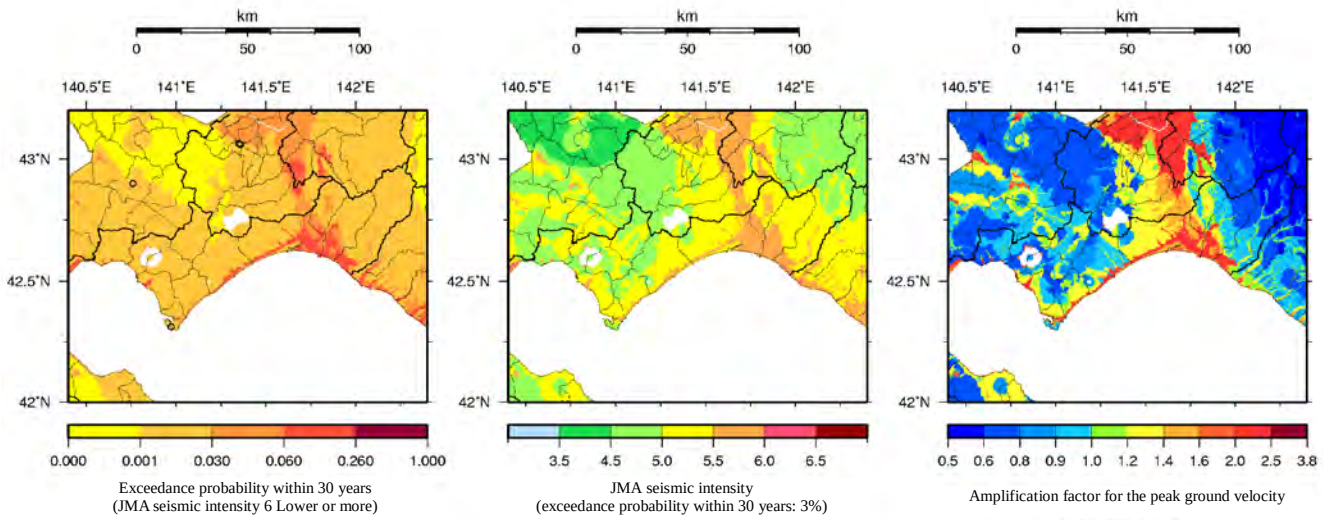

Figure 3.7.2-55 Seismic hazard maps for Iburi subprefecture, Hokkaido)

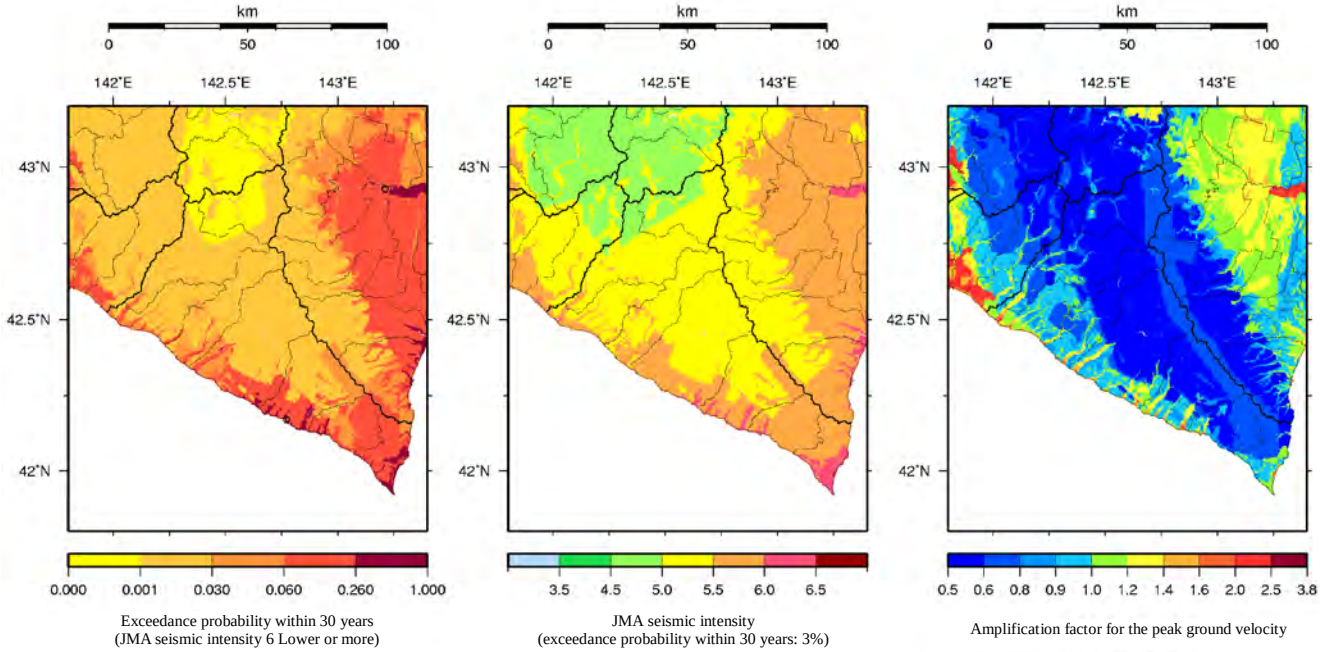

Figure 3.7.2-56 Seismic hazard maps for Hidaka subprefecture, Hokkaido

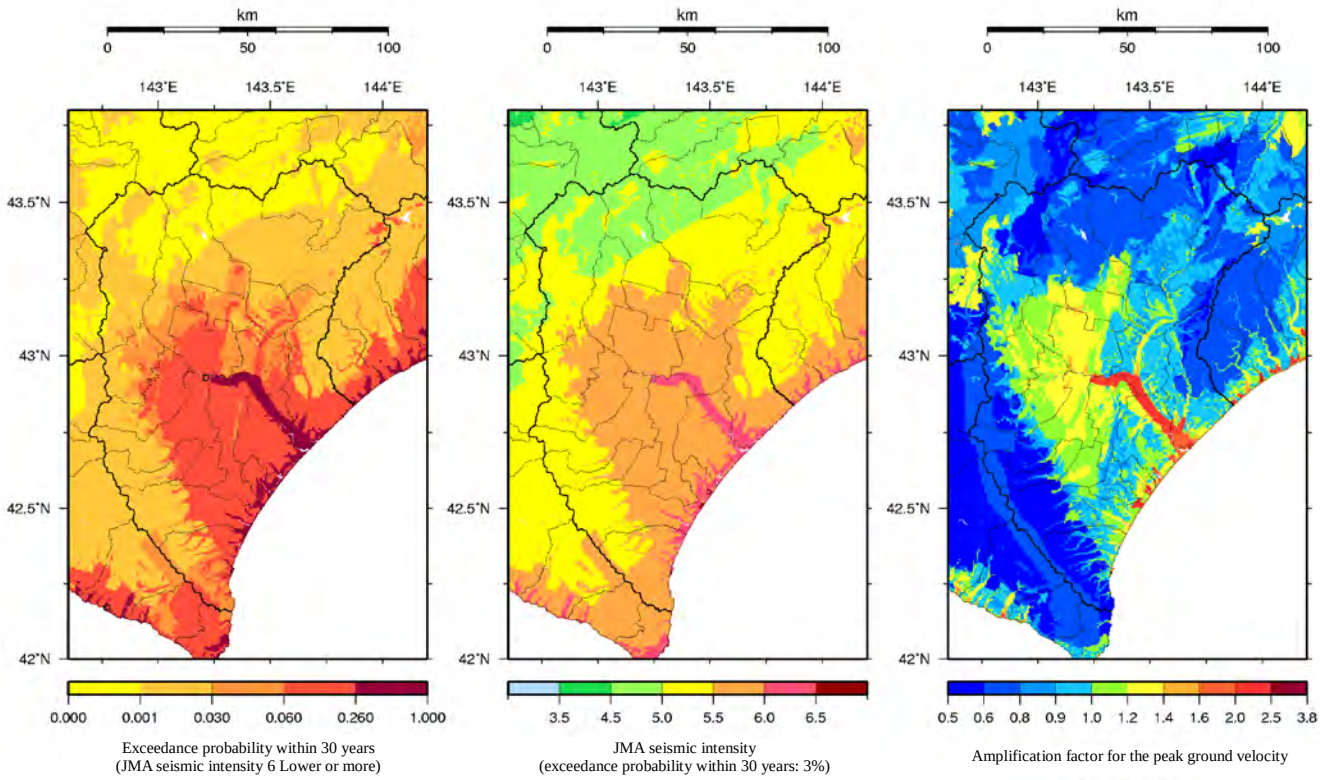

Figure 3.7.2-57 Seismic hazard maps for Tokachi subprefecture, Hokkaido

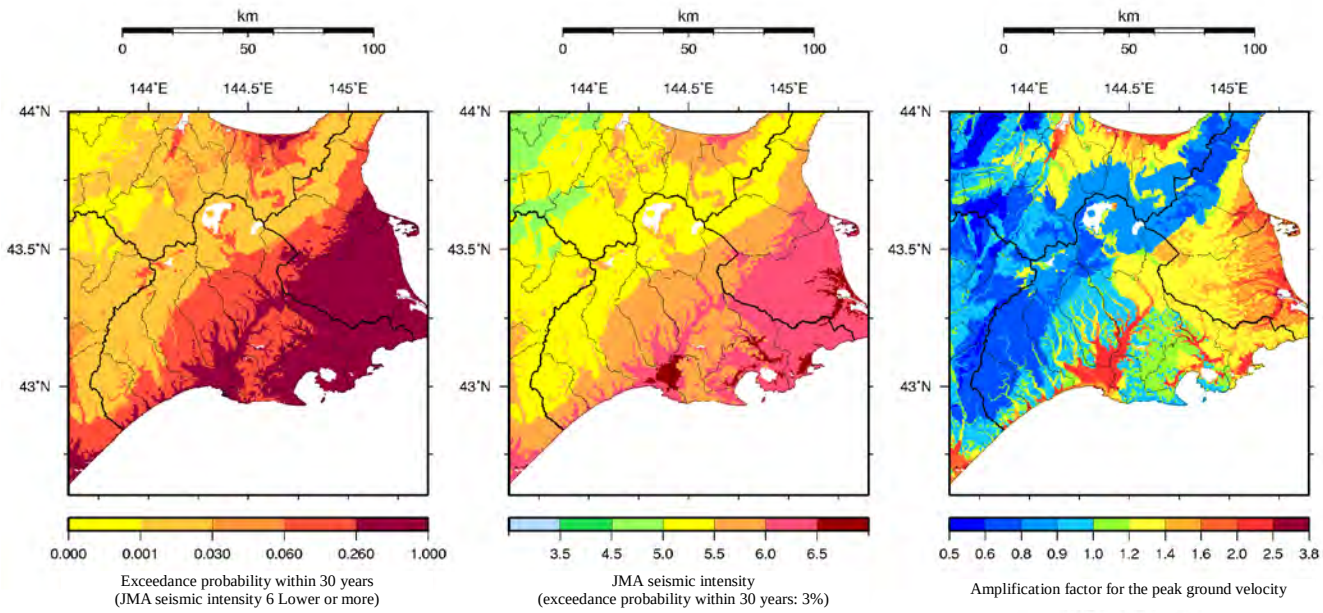

Figure 3.7.2-58 Seismic hazard maps for Kushiro subprefecture, Hokkaido

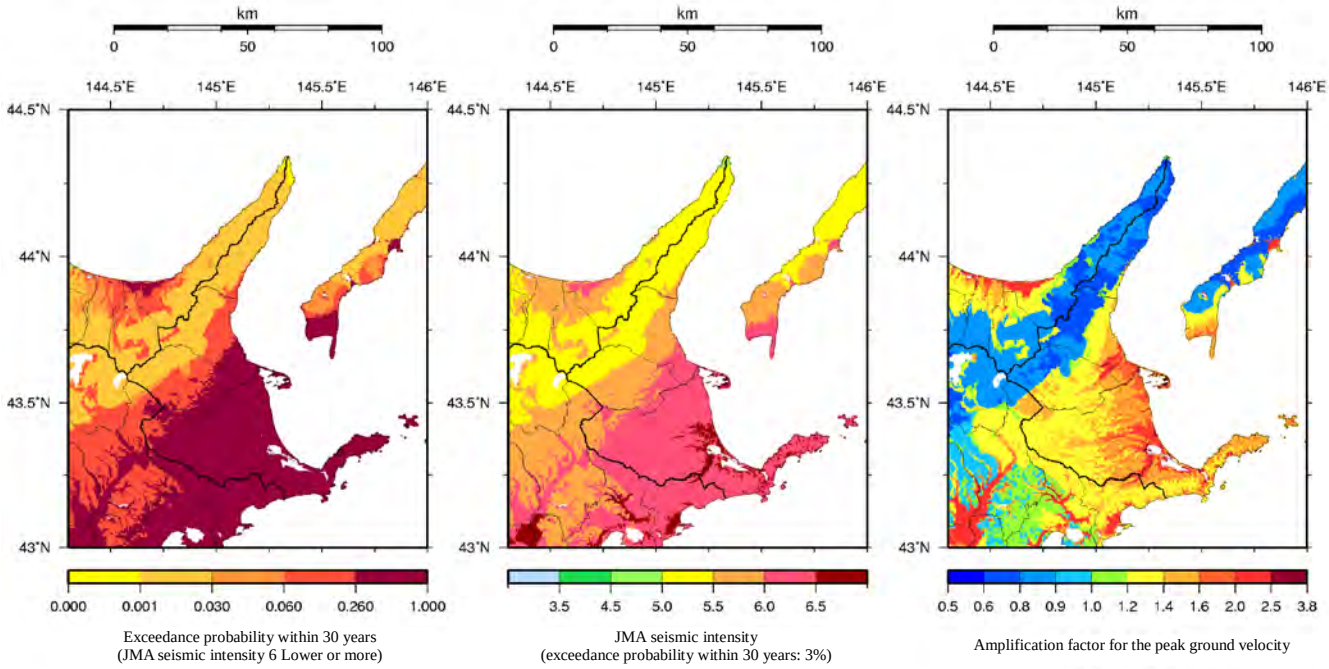

Figure 3.7.2-59 Seismic hazard maps for Nemuro subprefecture, Hokkaido

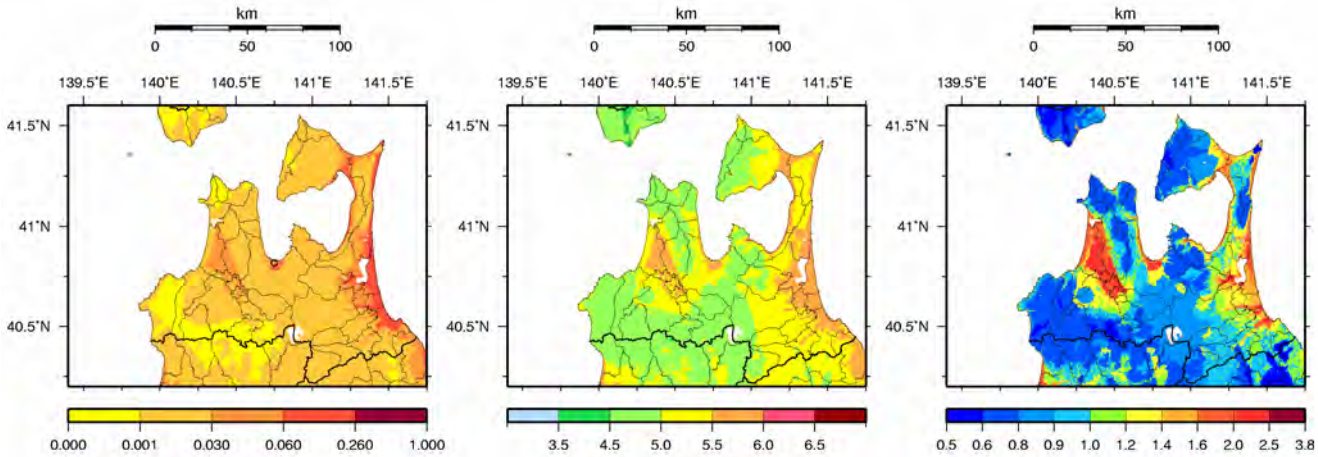

Exceedance probability within 30 years
(JMA seismic intensity 6 Lower or more)

JMA seismic intensity
(exceedance probability within 30 years: 3%)

Amplification factor for the peak ground velocity

Figure 3.7.2-60 Seismic hazard maps for Aomori prefecture

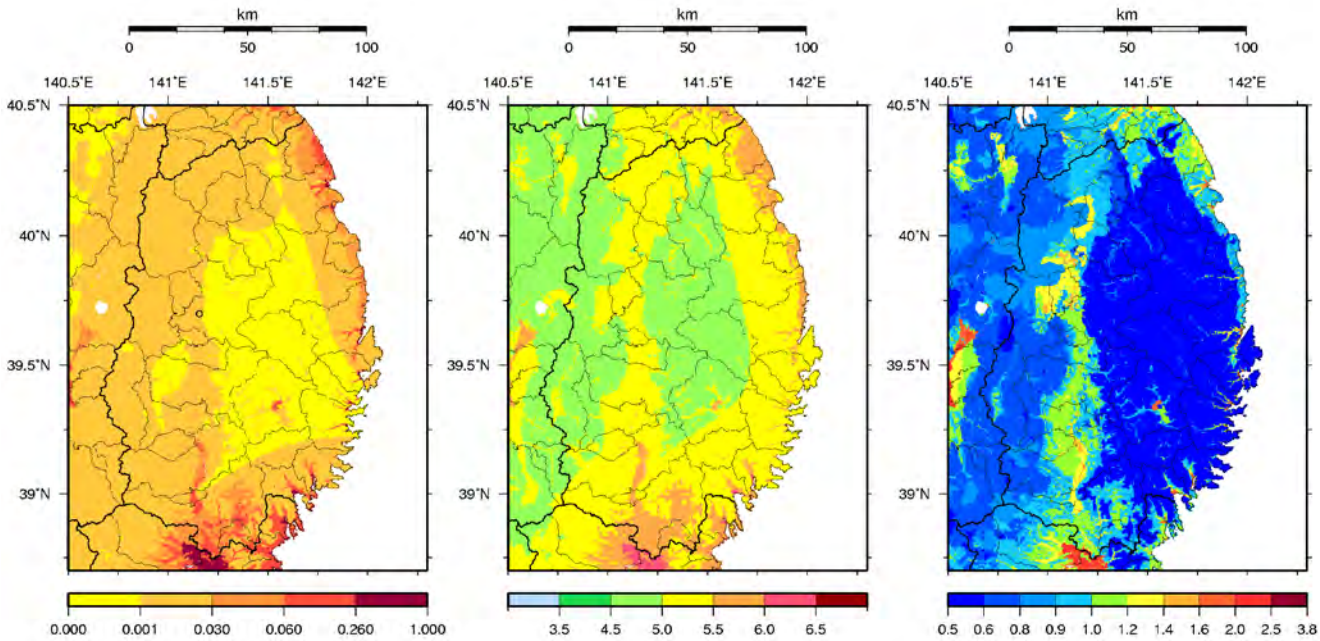

Exceedance probability within 30 years
(JMA seismic intensity 6 Lower or more)

JMA seismic intensity
(exceedance probability within 30 years: 3%)

Amplification factor for the peak ground velocity

Figure 3.7.2-61 Seismic hazard maps for Iwate prefecture

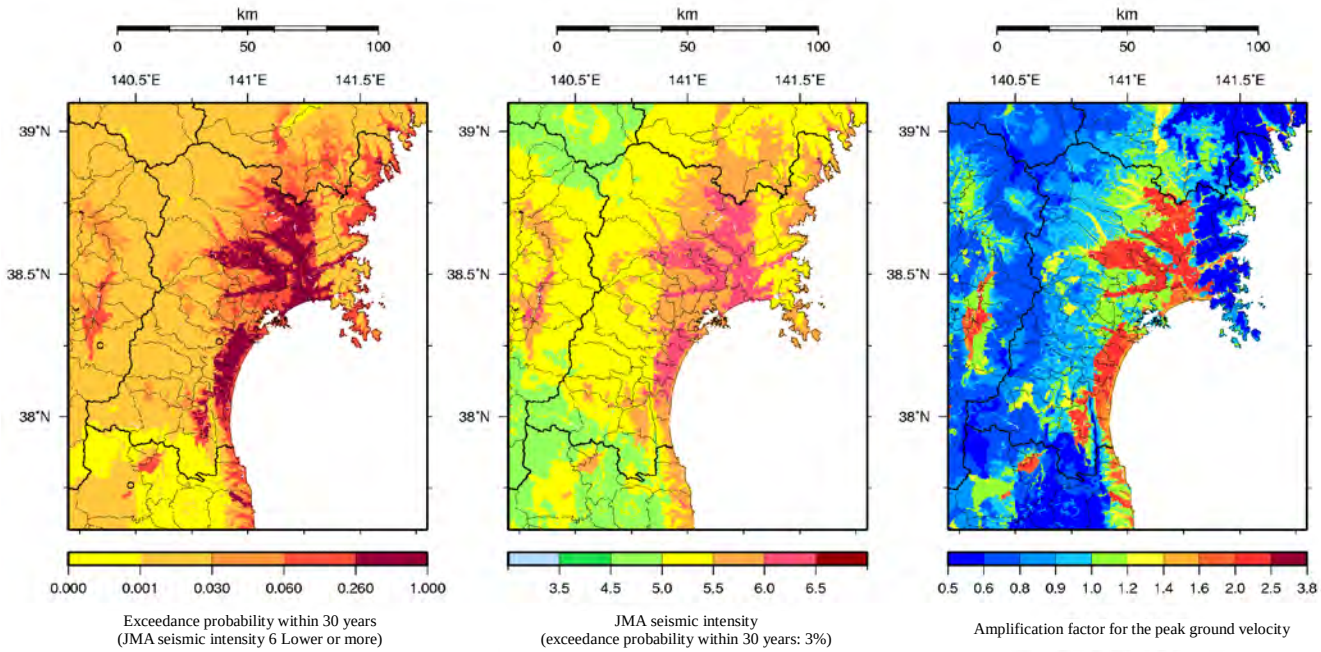

Figure 3.7.2-62 Seismic hazard maps for Miyagi prefecture

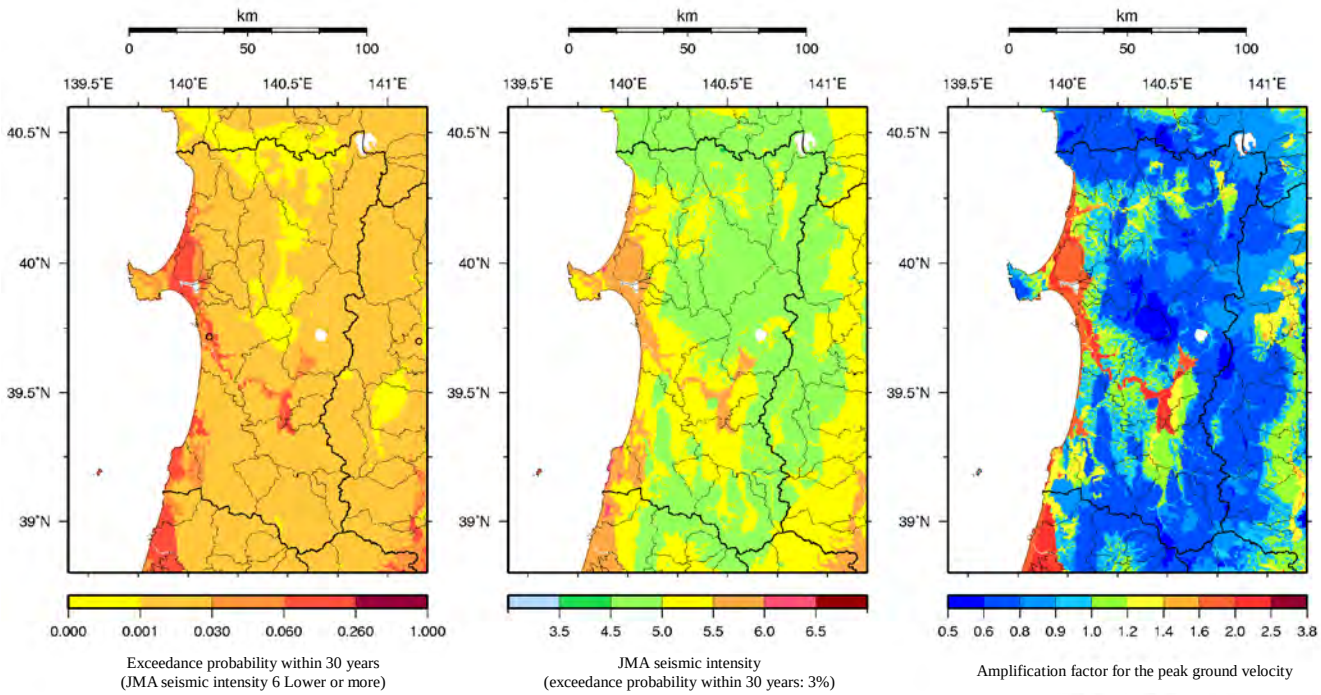

Figure 3.7.2-63 Seismic hazard maps for Akita prefecture

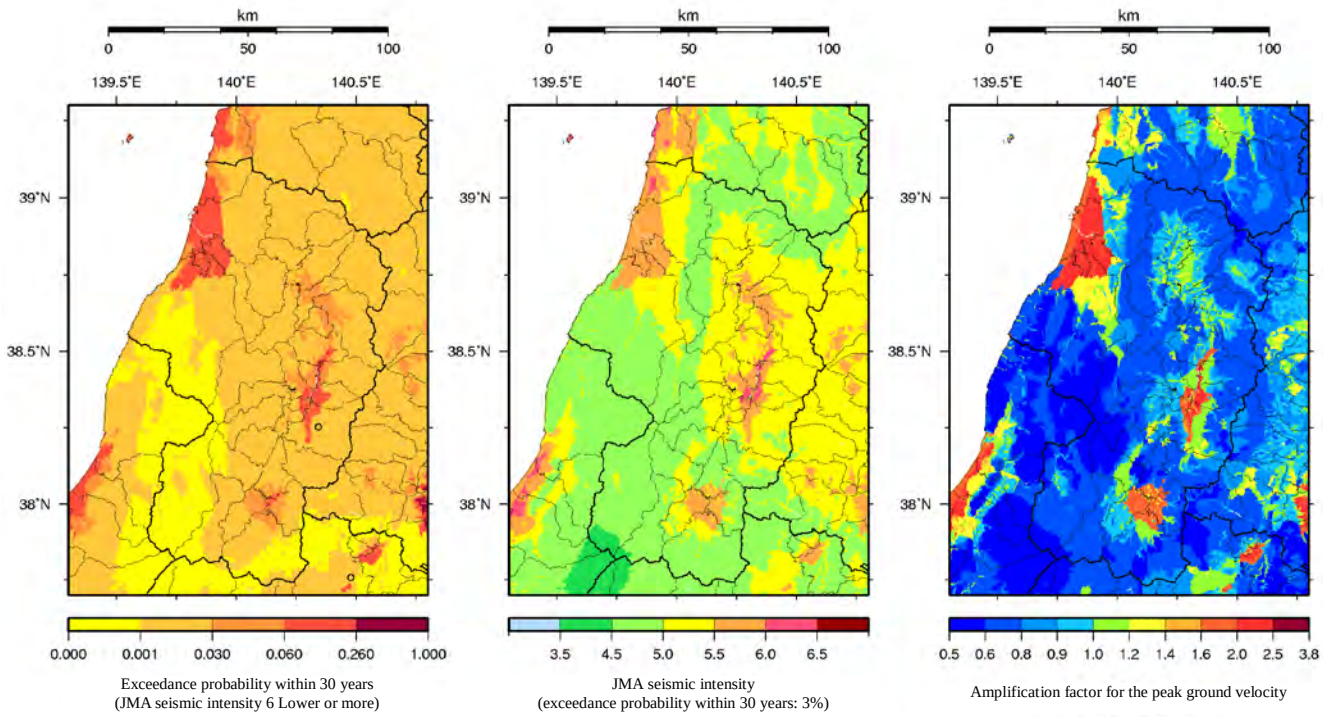

Figure 3.7.2-64 Seismic hazard maps for Yamagata prefecture

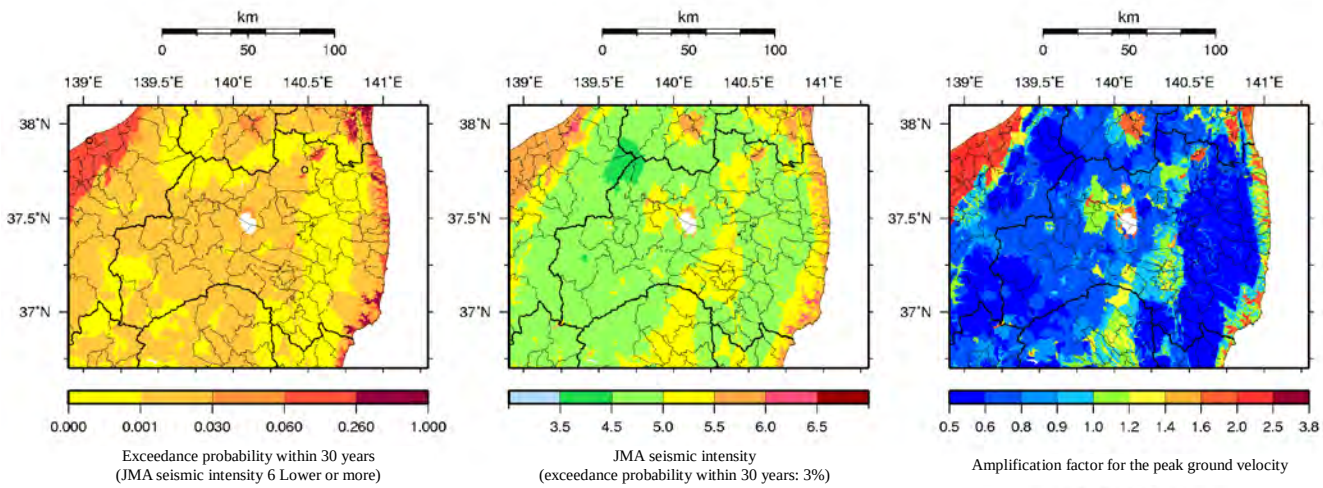

Figure 3.7.2-65 Seismic hazard maps for Fukushima prefecture

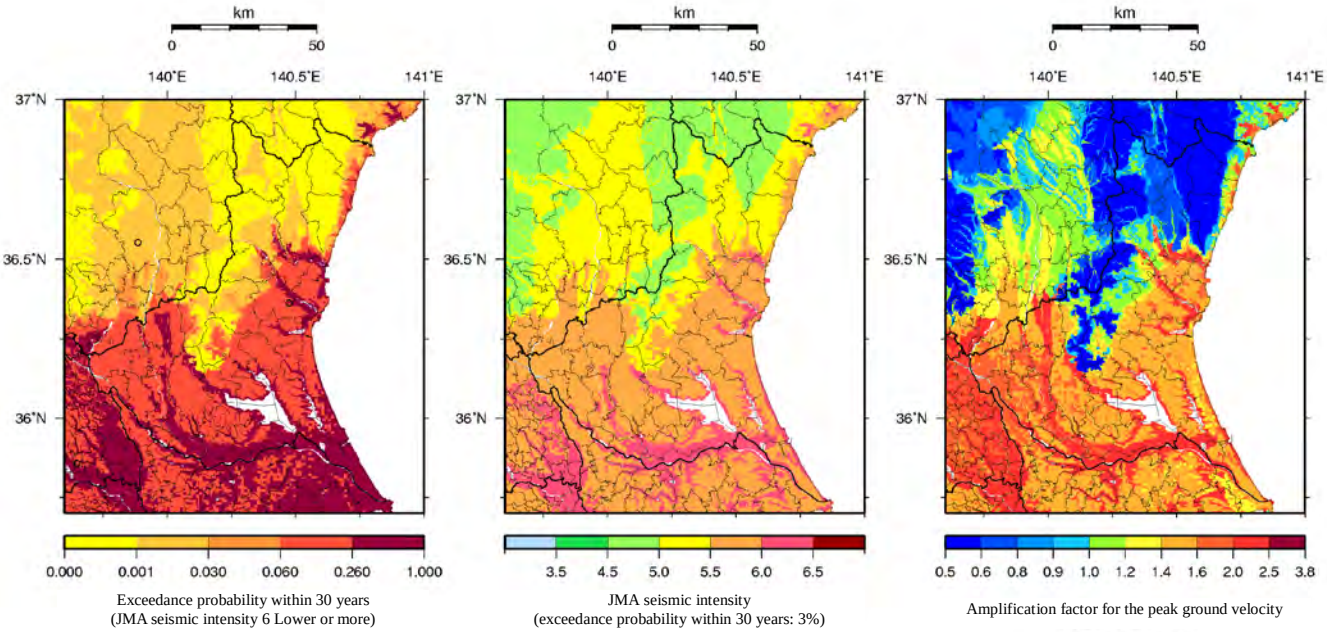

Figure 3.7.2-66 Seismic hazard maps for Ibaraki prefecture

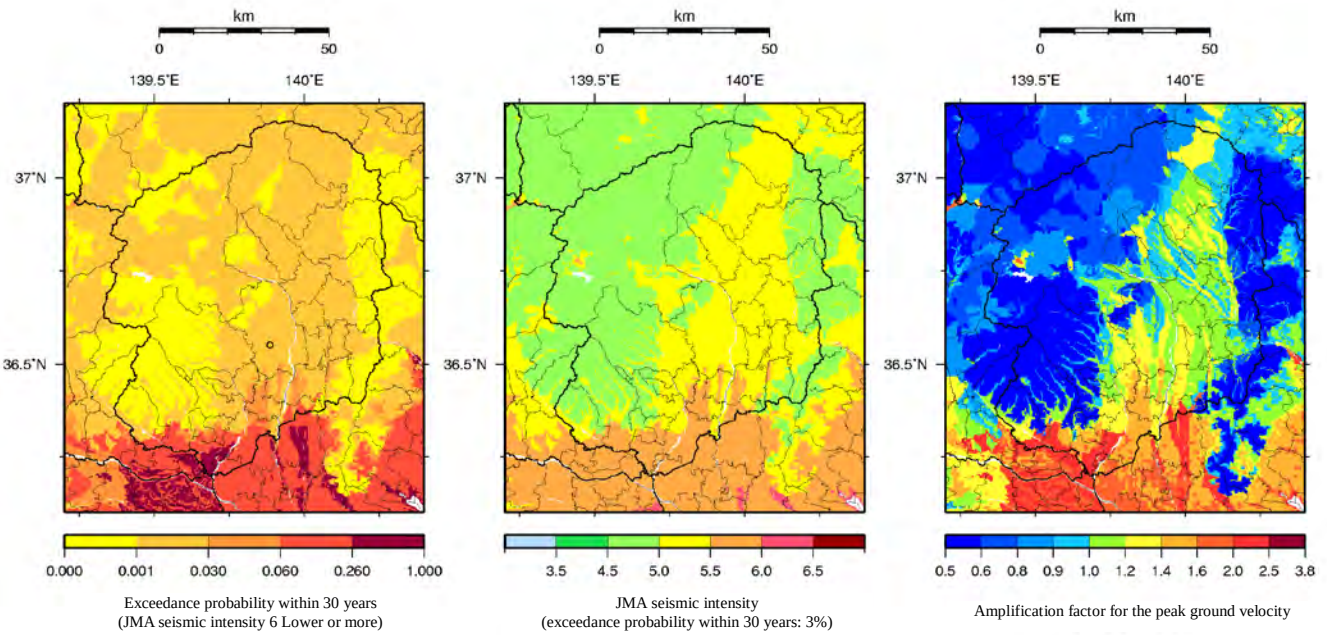

Figure 3.7.2-67 Seismic hazard maps for Tochigi prefecture

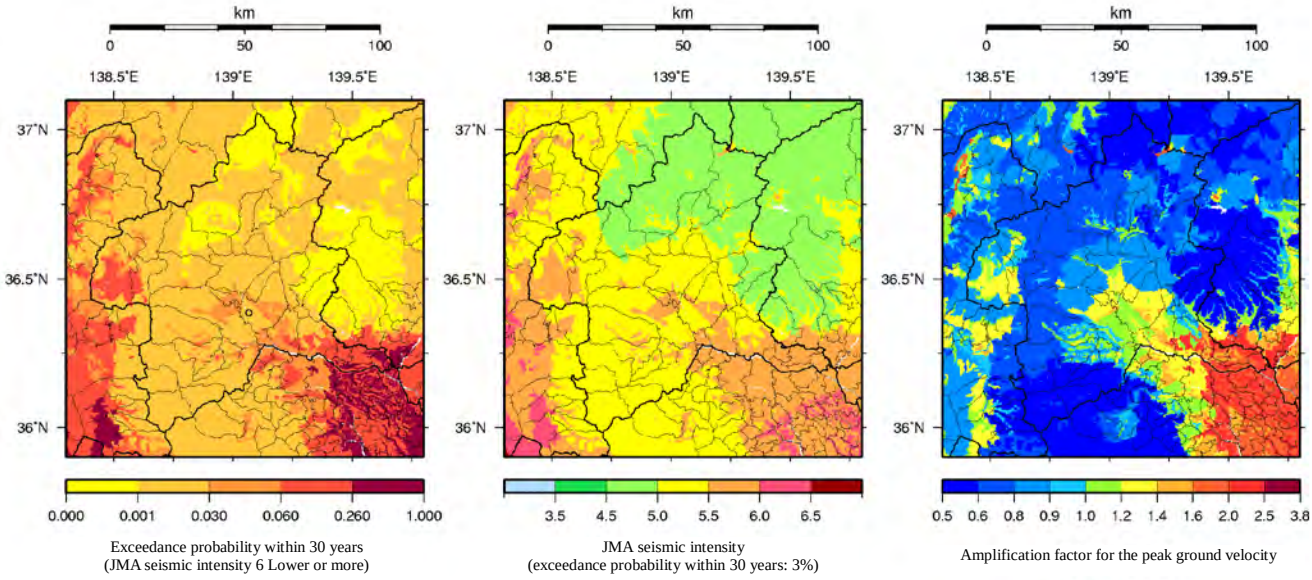

Figure 3.7.2-68 Seismic hazard maps for Gunma prefecture

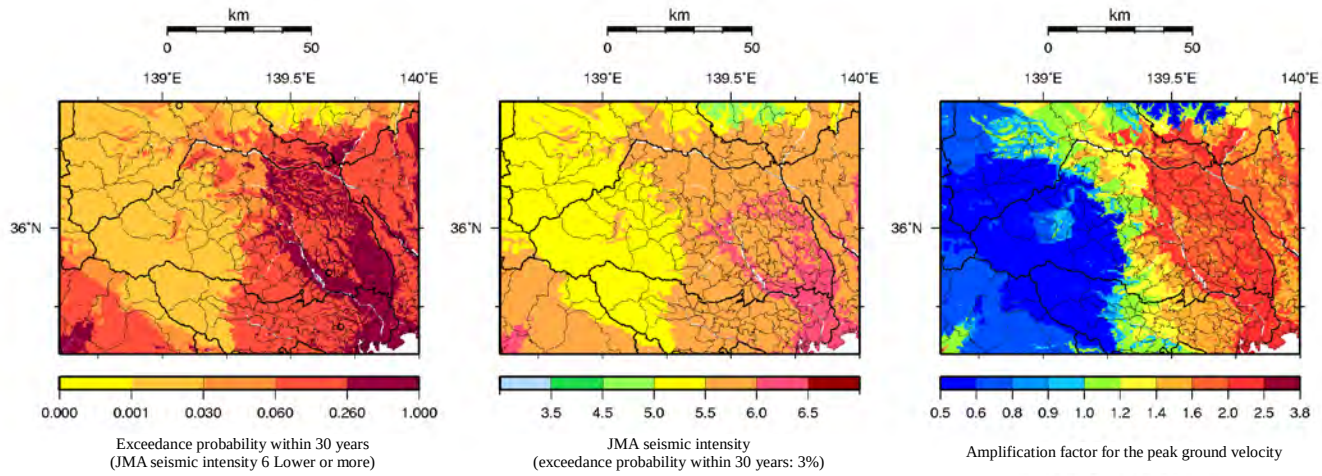

Figure 3.7.2-69 Seismic hazard maps for Saitama prefecture

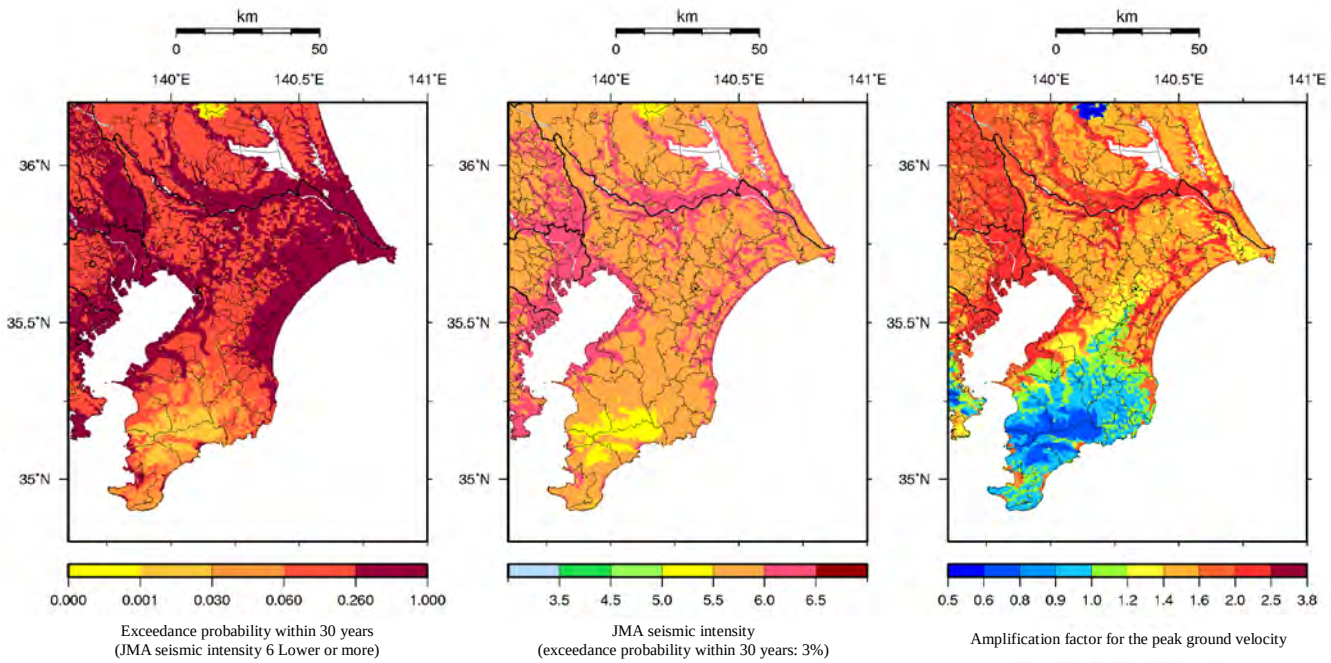

Figure 3.7.2-70 Seismic hazard maps for Chiba prefecture

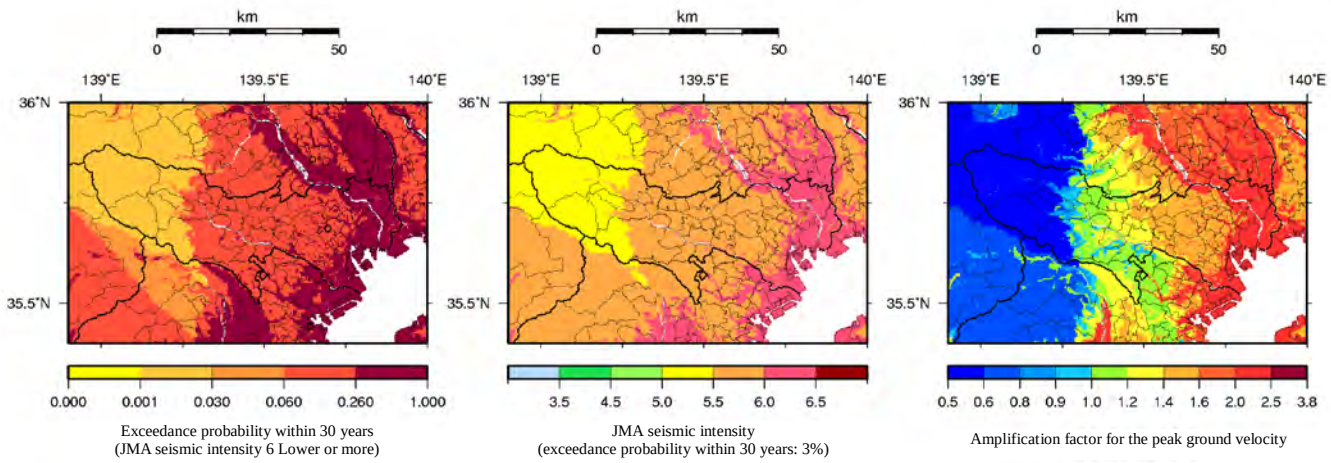

Figure 3.7.2-71 Seismic hazard maps for metropolitan Tokyo

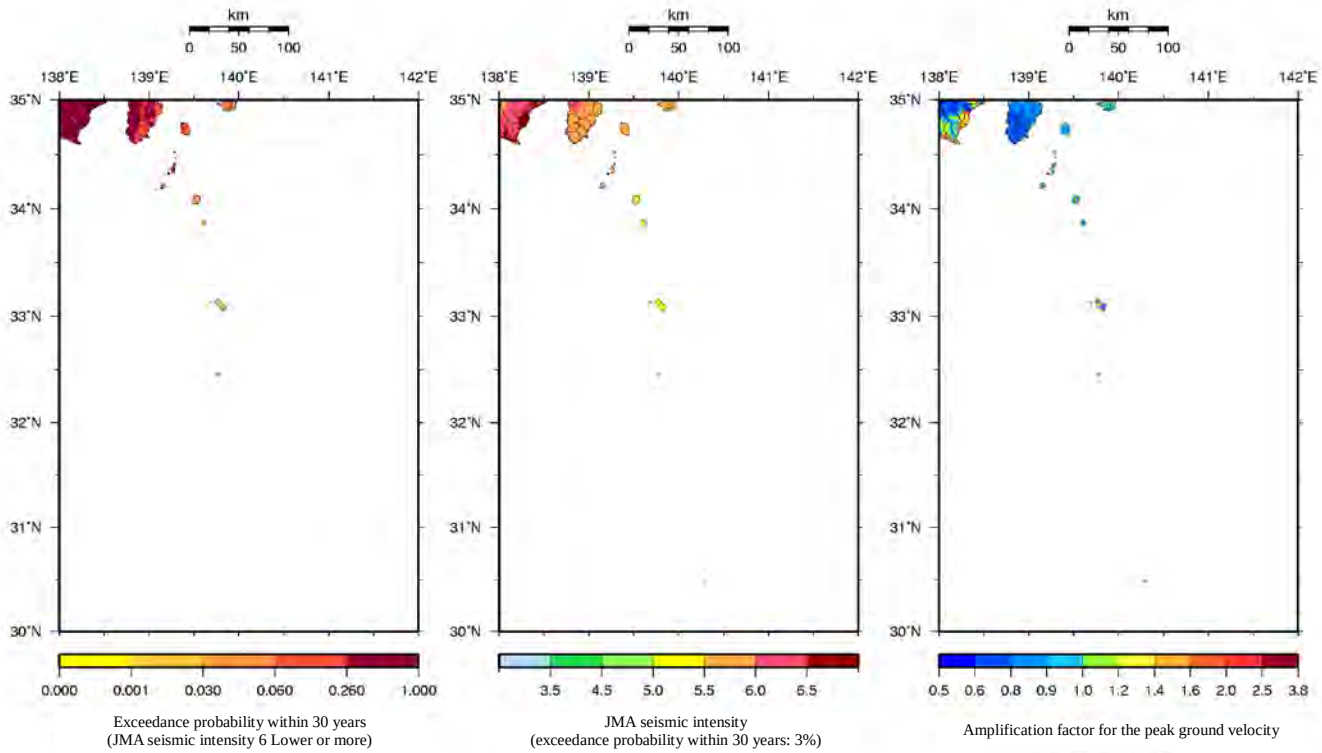

Figure 3.7.2-72 Seismic hazard maps for the Izu-shoto islands

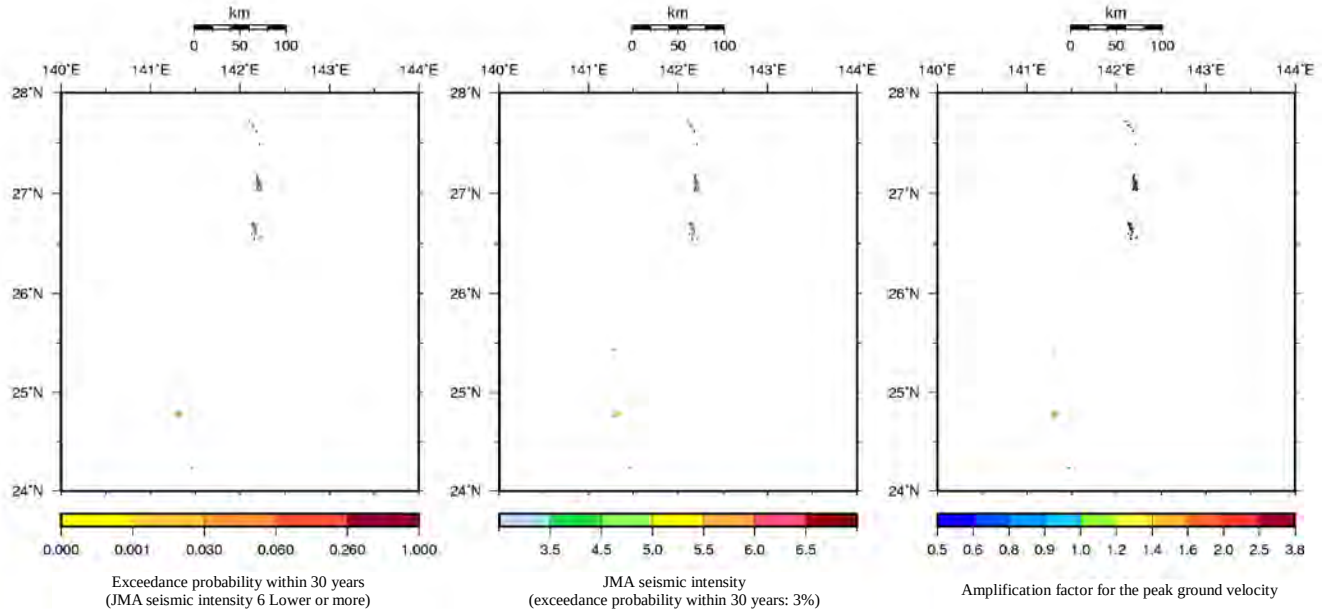

Figure 3.7.2-73 Seismic hazard maps for the Ogasawara-shoto (Bonin) islands

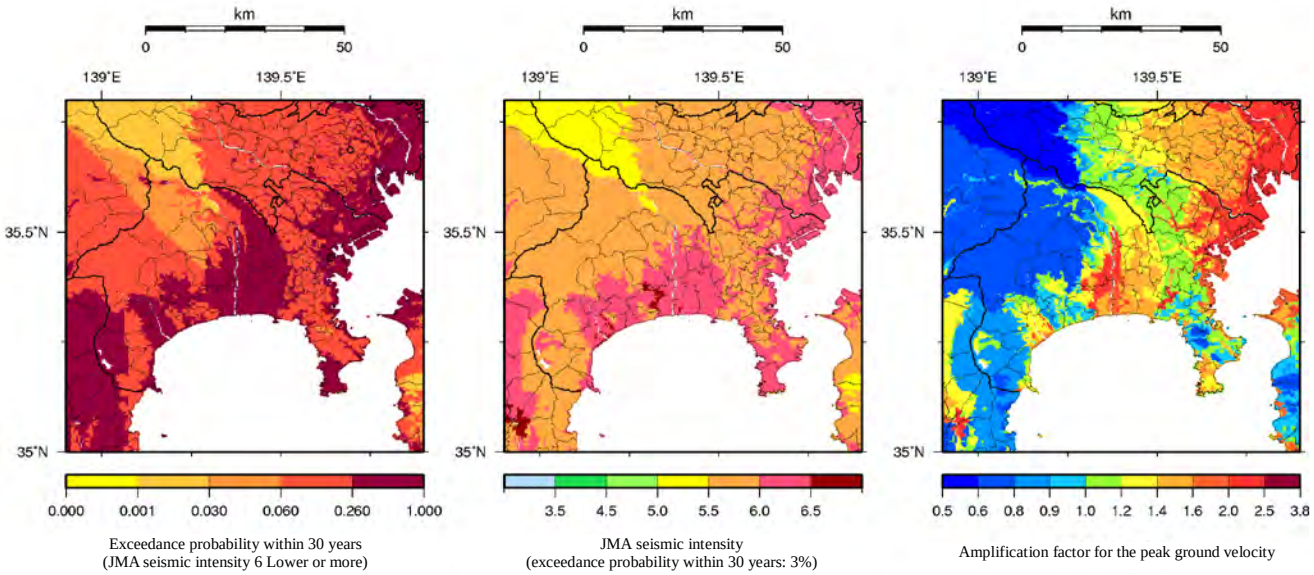

Figure 3.7.2-74 Seismic hazard maps for Kanagawa prefecture

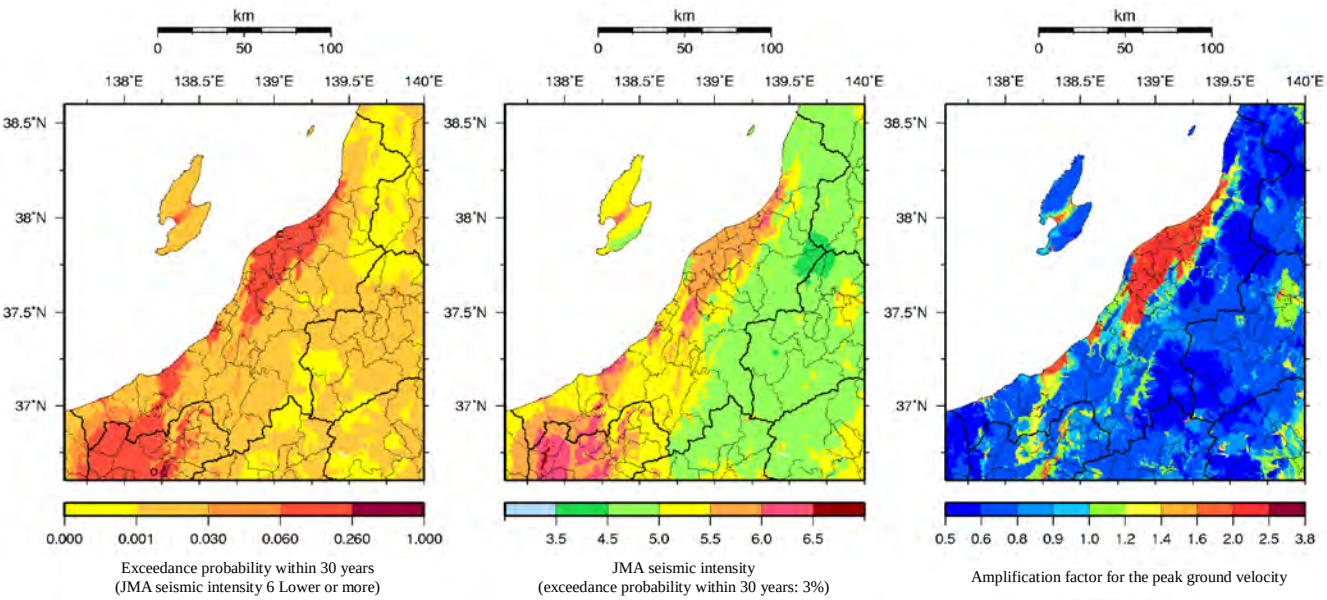

Figure 3.7.2-75 Seismic hazard maps for Niigata prefecture

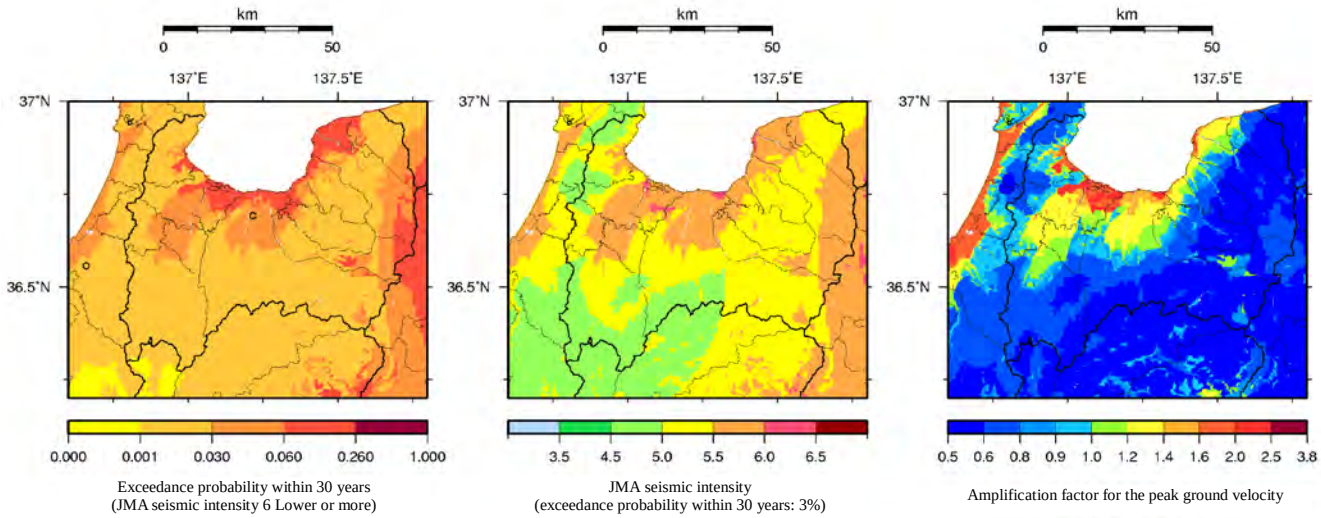

Figure 3.7.2-76 Seismic hazard maps for Toyama prefecture

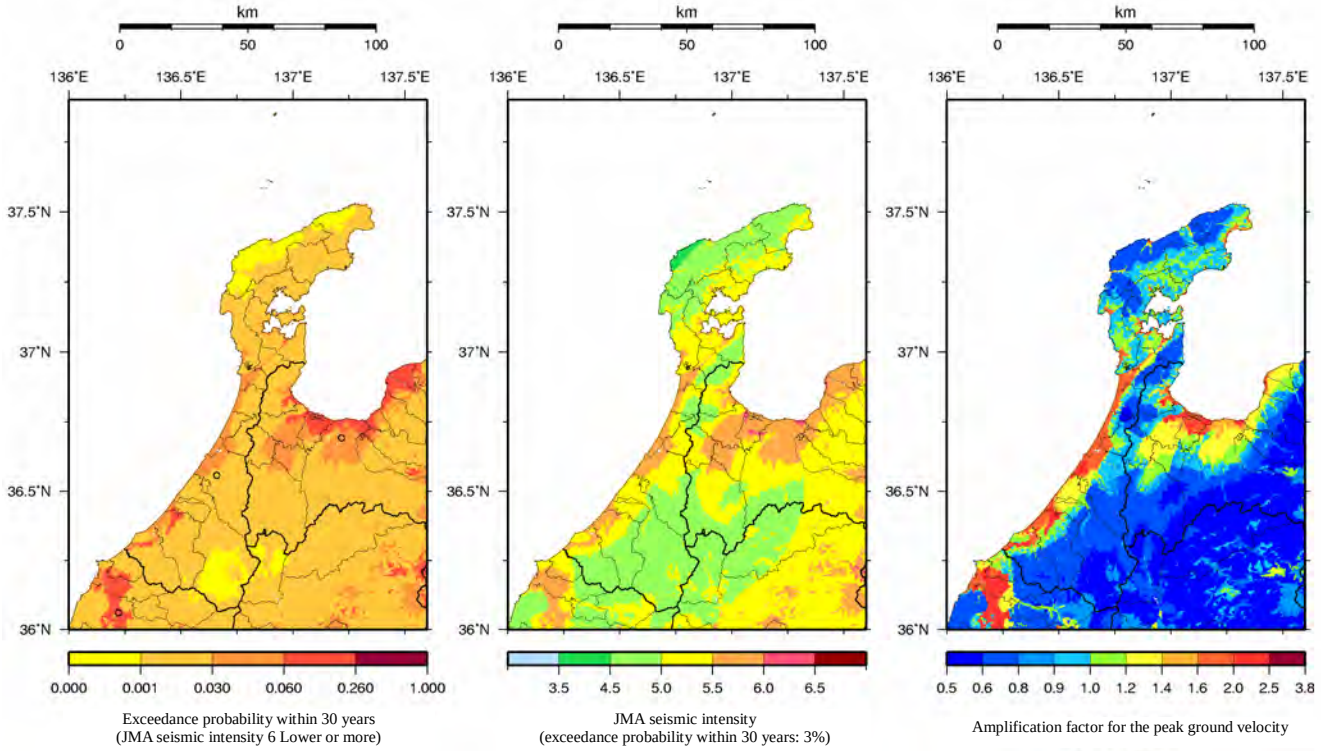

Figure 3.7.2-77 Seismic hazard maps for Ishikawa prefecture

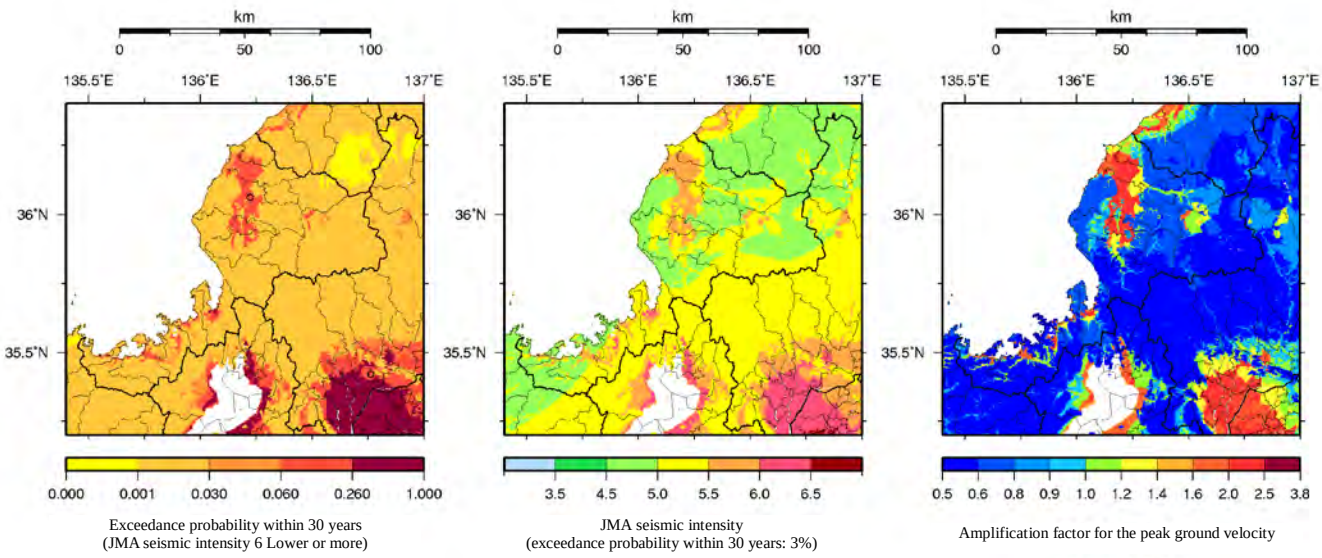

Figure 3.7.2-78 Seismic hazard maps for Fukui prefecture

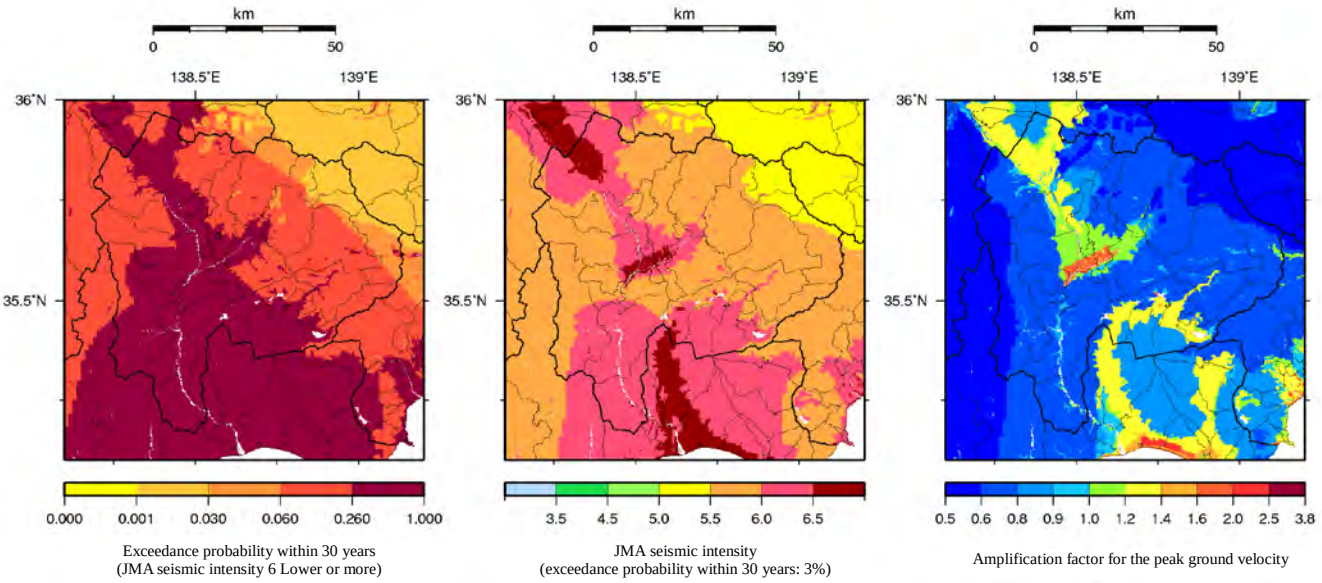

Figure 3.7.2-79 Seismic hazard maps for Yamanashi prefecture

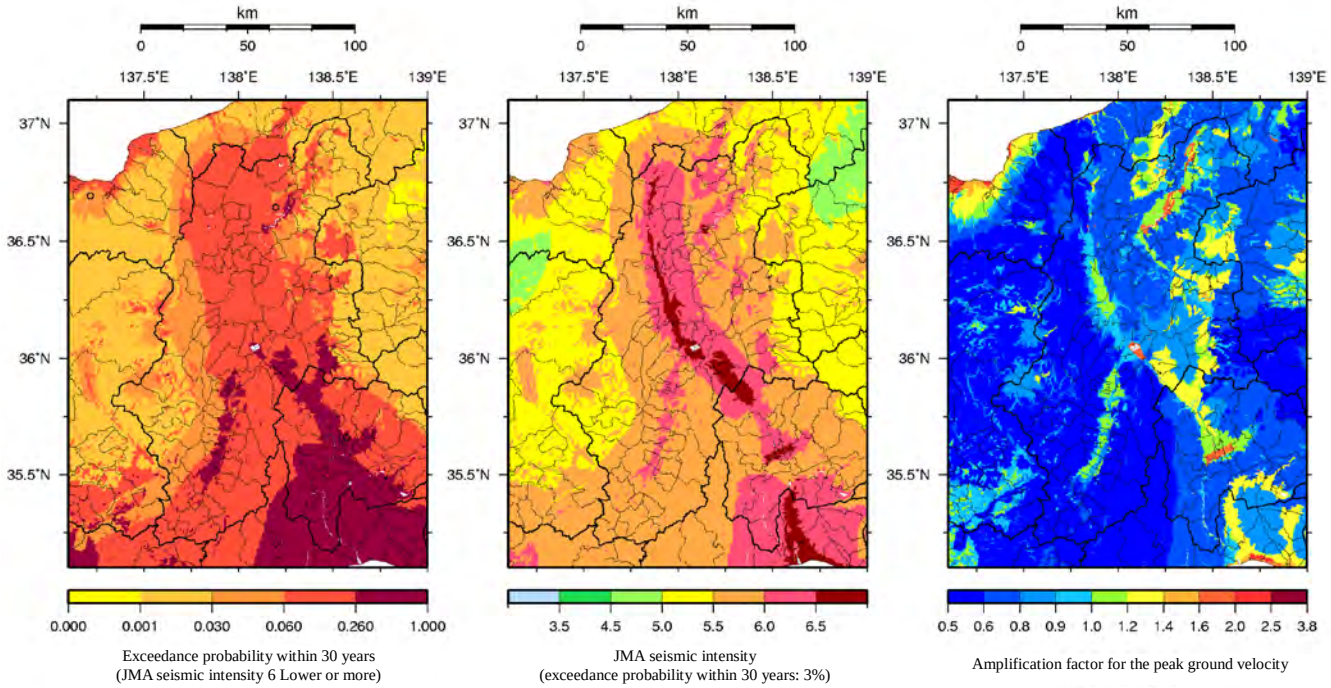

Figure 3.7.2-80 Seismic hazard maps for Nagano prefecture

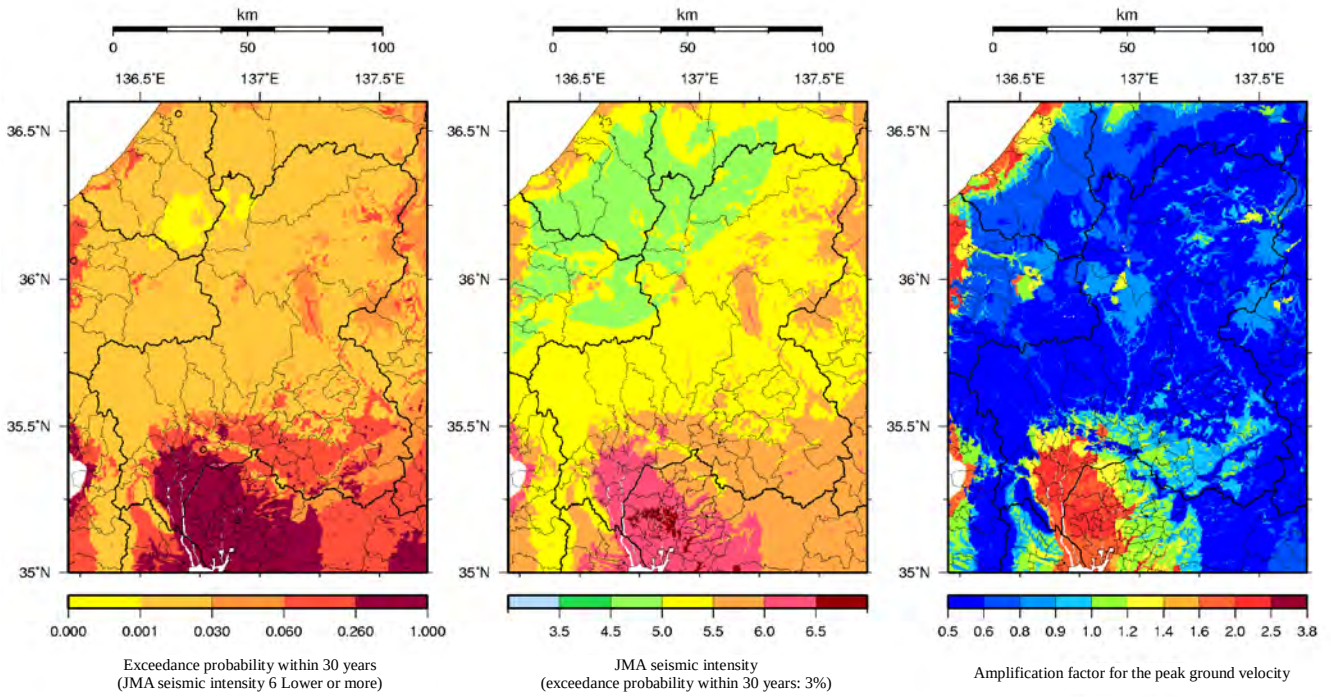

Figure 3.7.2-81 Seismic hazard maps for Gifu prefecture

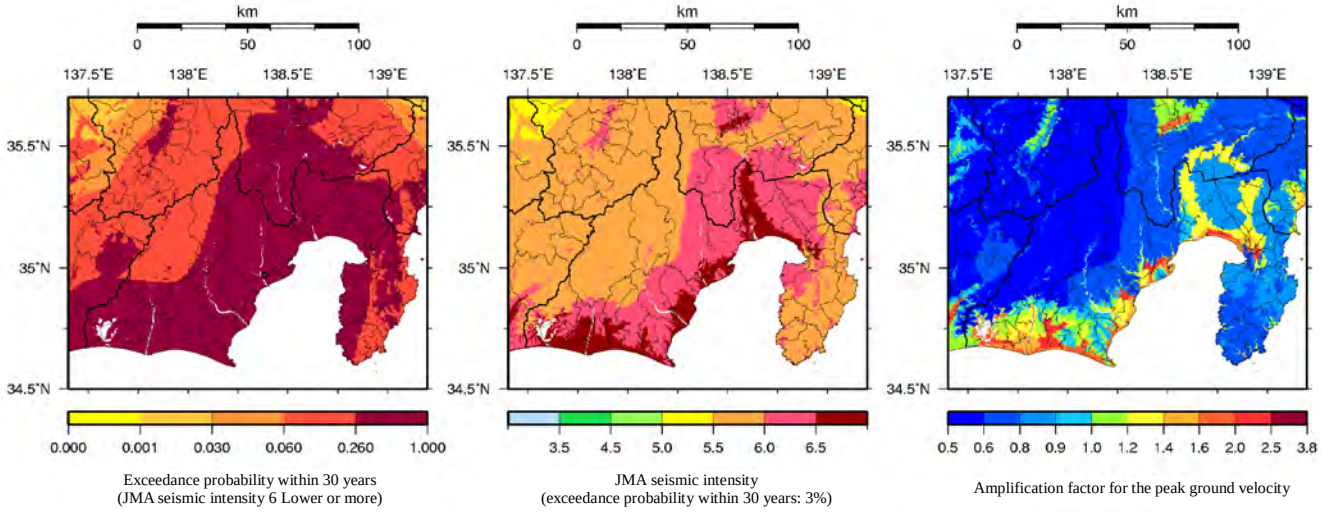

Figure 3.7.2-82 Seismic hazard maps for Shizuoka prefecture

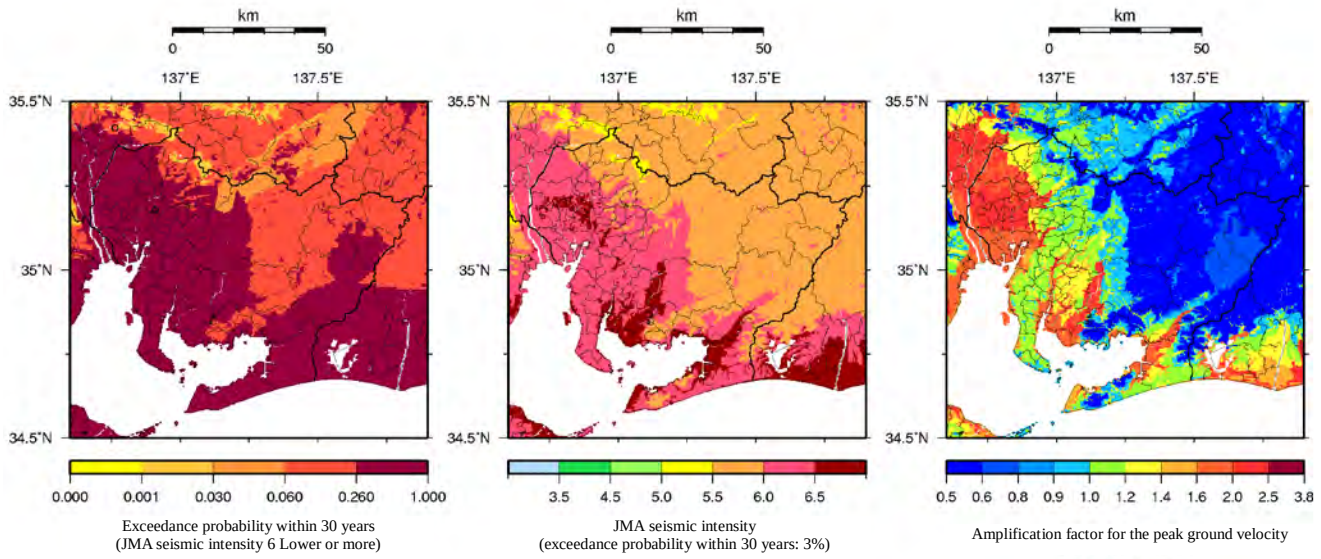

Figure 3.7.2-83 Seismic hazard maps for Aichi prefecture

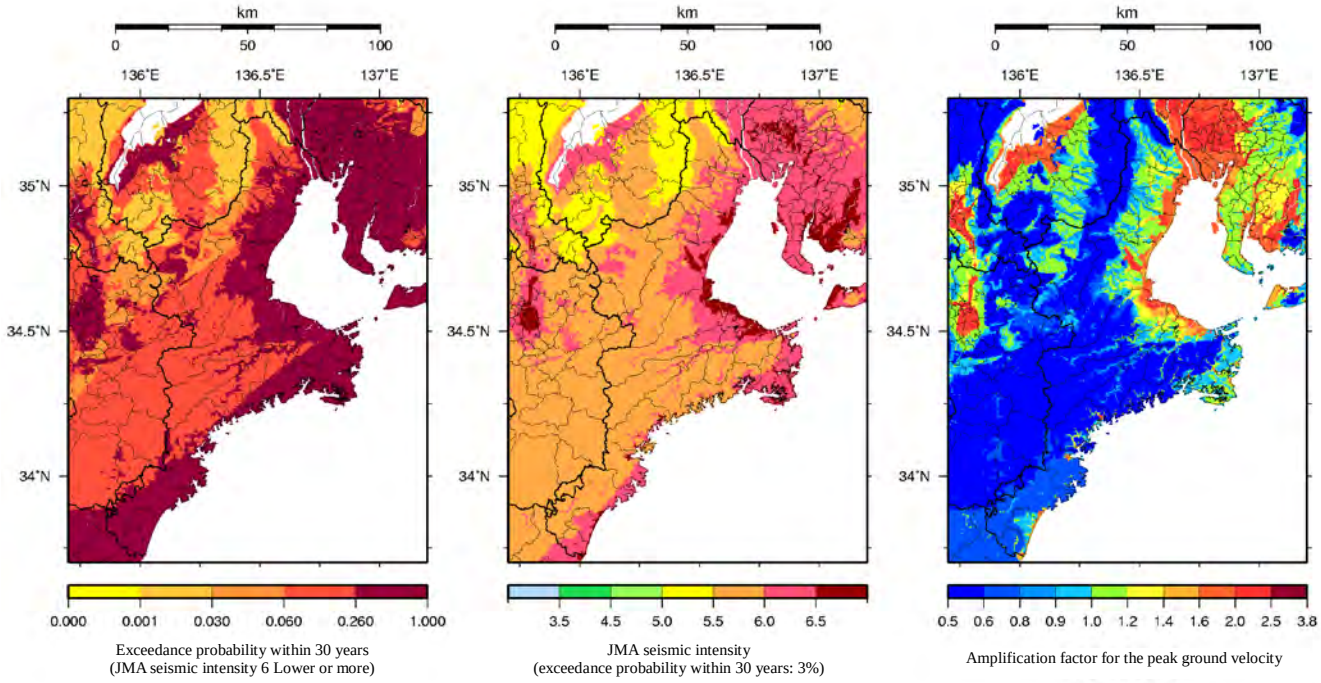

Figure 3.7.2-84 Seismic hazard maps for Mie prefecture

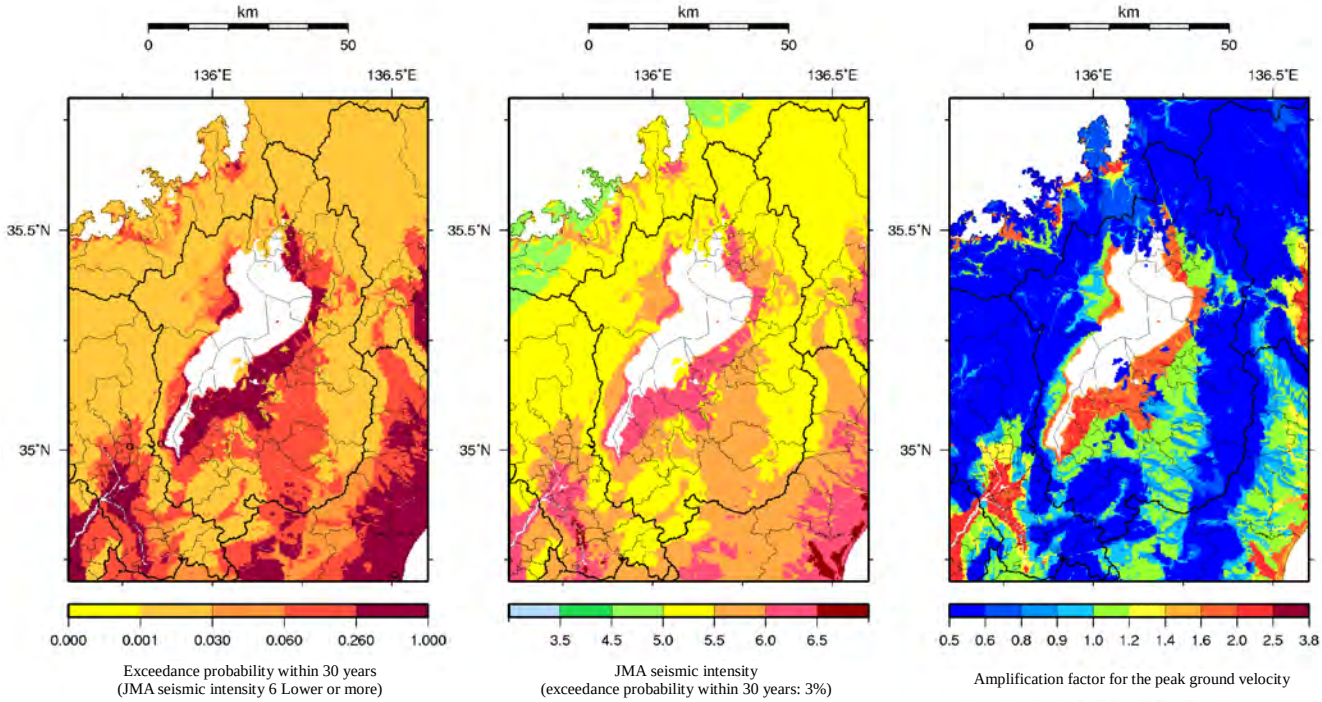

Figure 3.7.2-85 Seismic hazard maps for Shiga prefecture

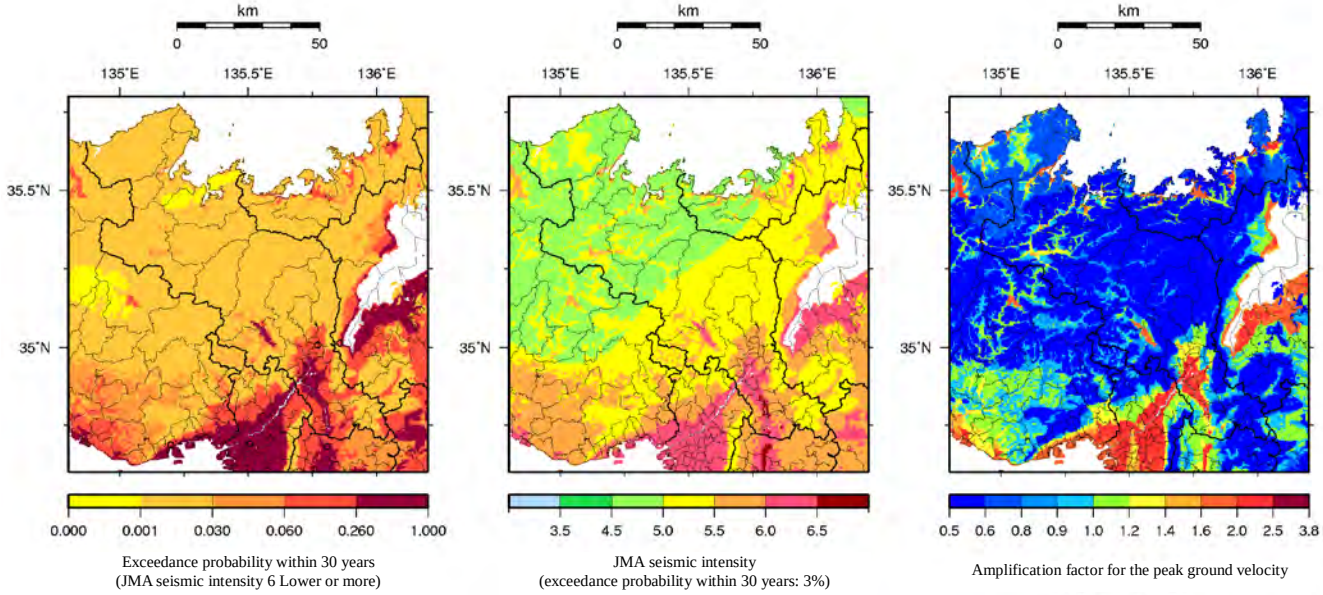

Figure 3.7.2-86 Seismic hazard maps for Kyoto prefecture

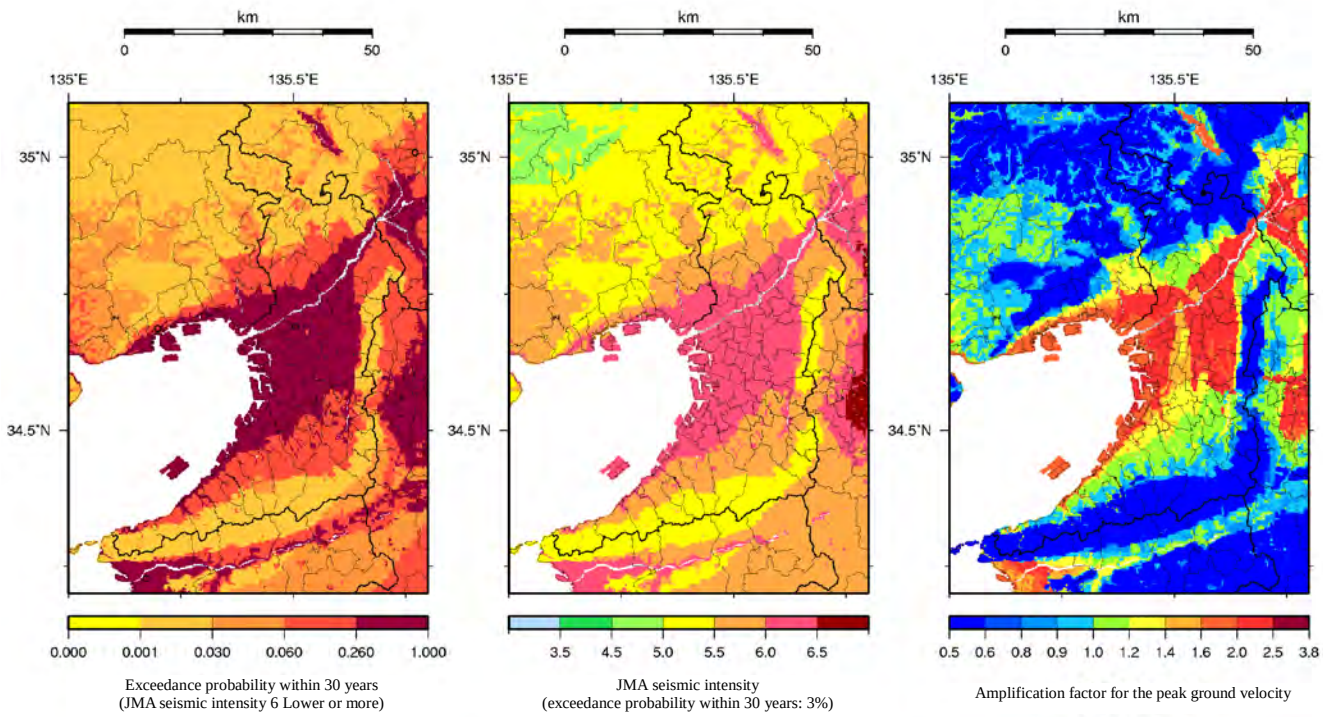

Figure 3.7.2-87 Seismic hazard maps for Osaka prefecture

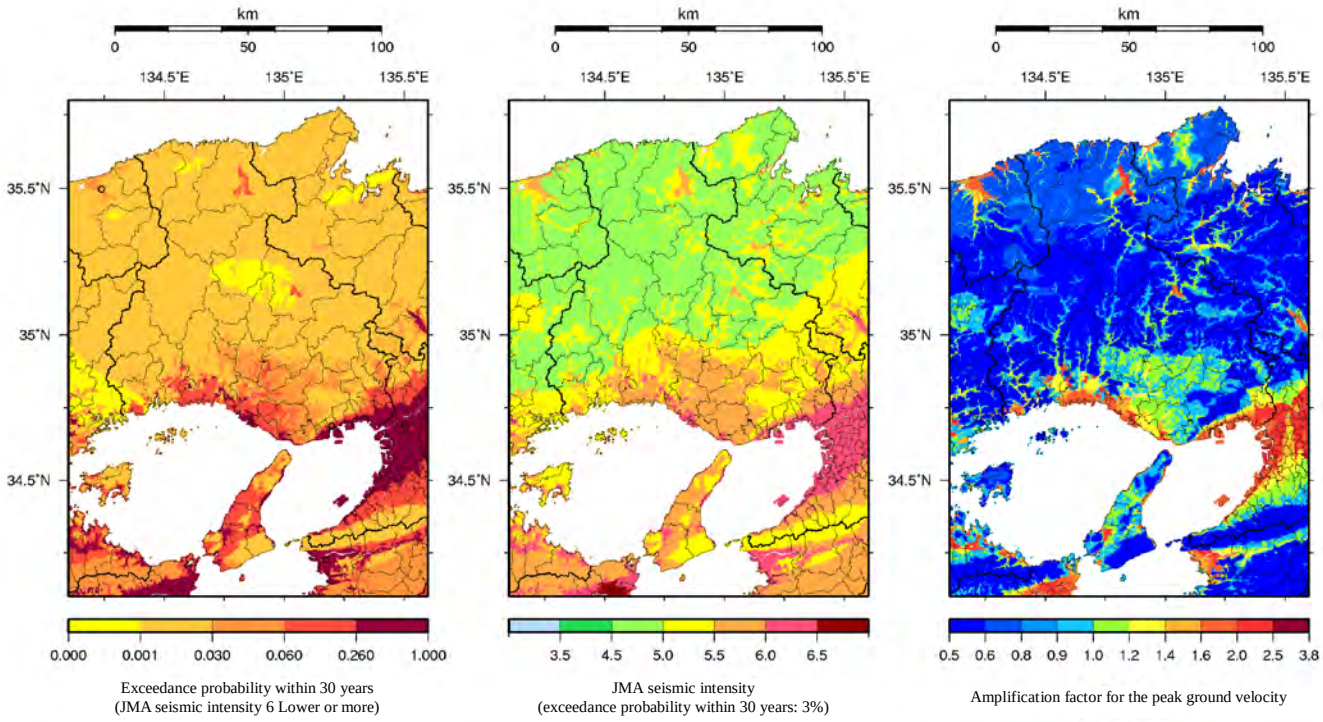

Figure 3.7.2-88 Seismic hazard maps for Hyogo prefecture

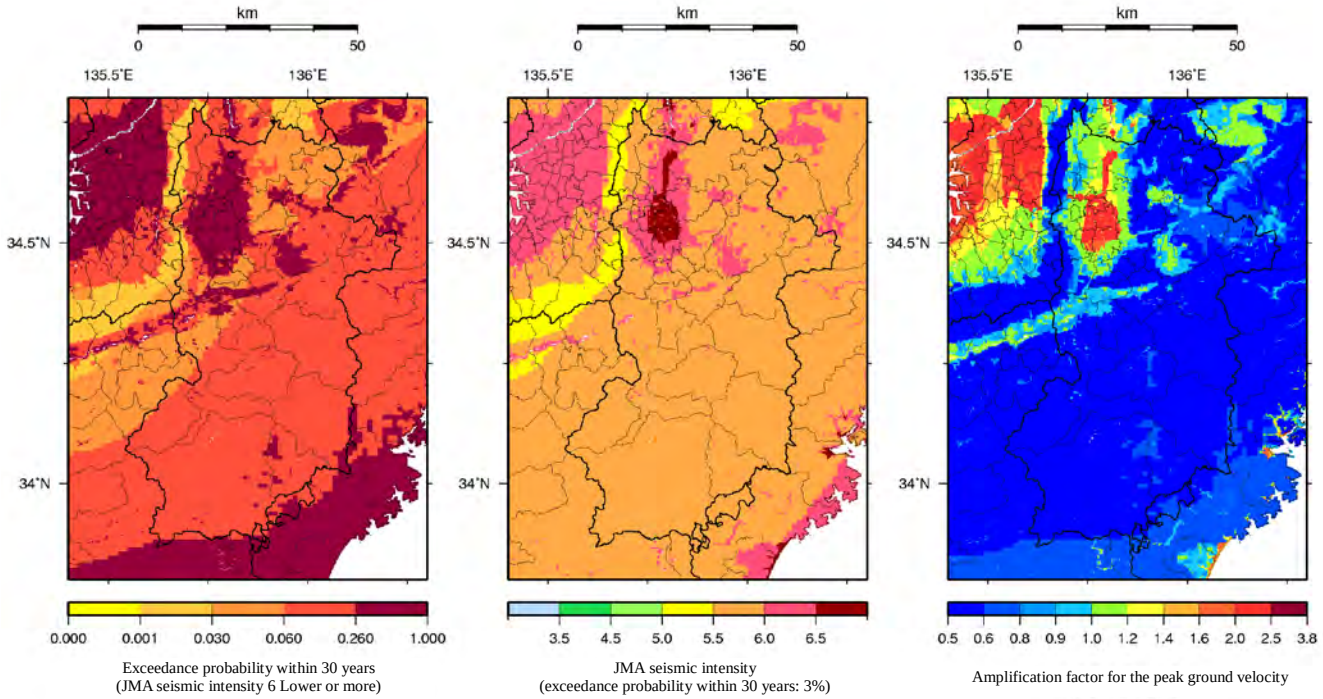

Figure 3.7.2-89 Seismic hazard maps for Nara prefecture

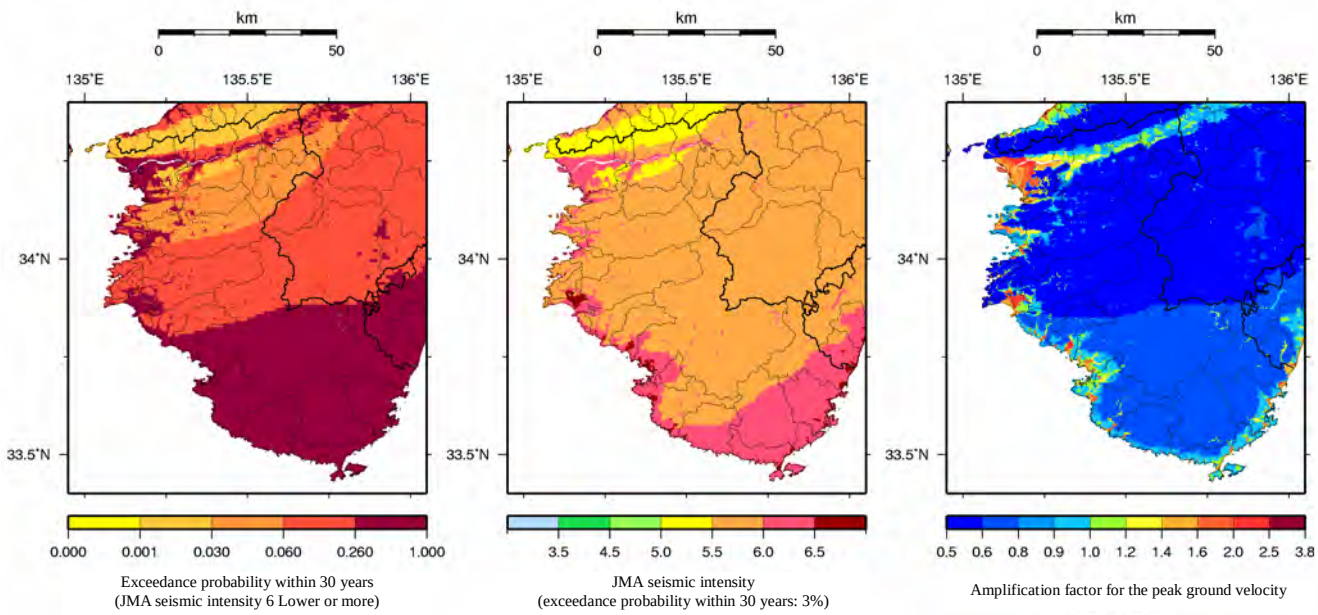

Figure 3.7.2-90 Seismic hazard maps for Wakayama prefecture

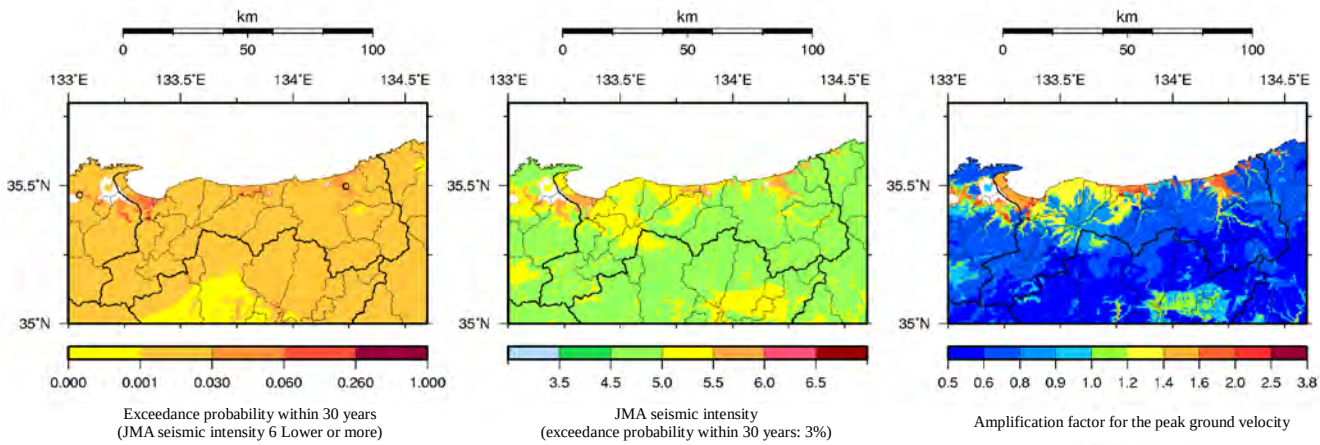

Figure 3.7.2-91 Seismic hazard maps for Tottori prefecture

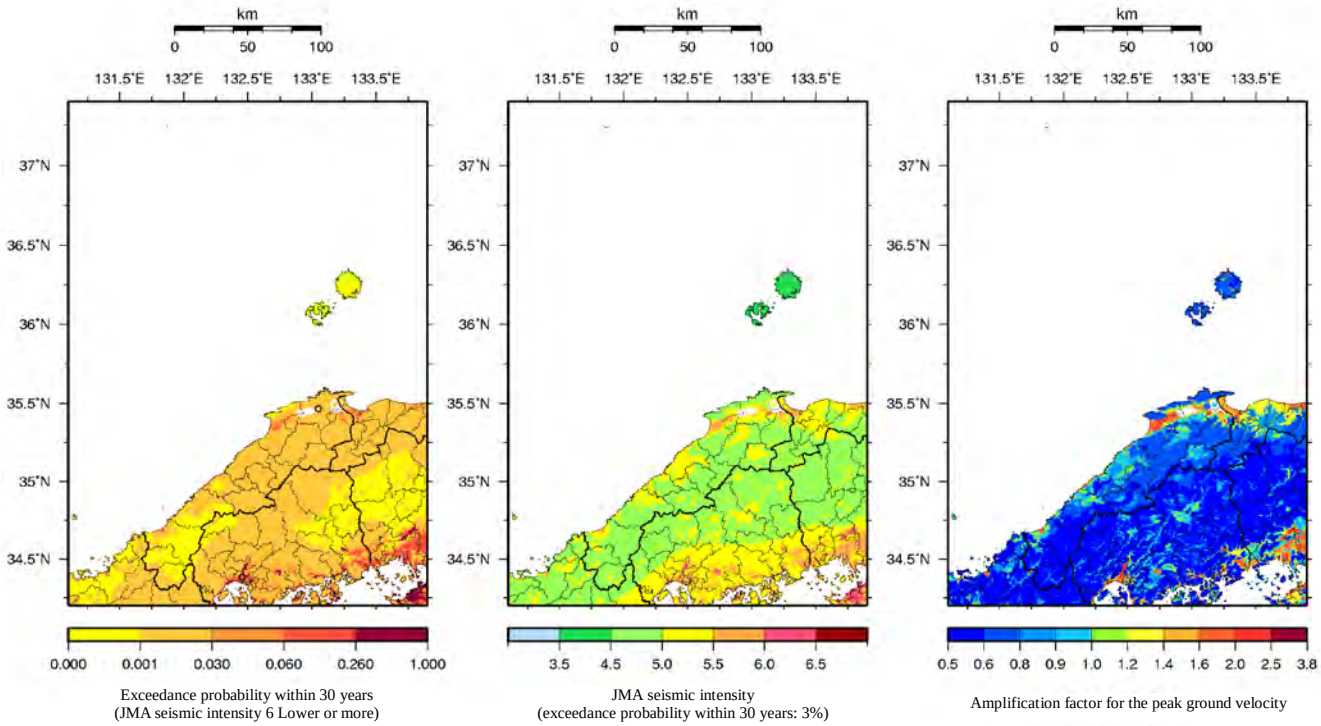

Figure 3.7.2-92 Seismic hazard maps for Shimane prefecture

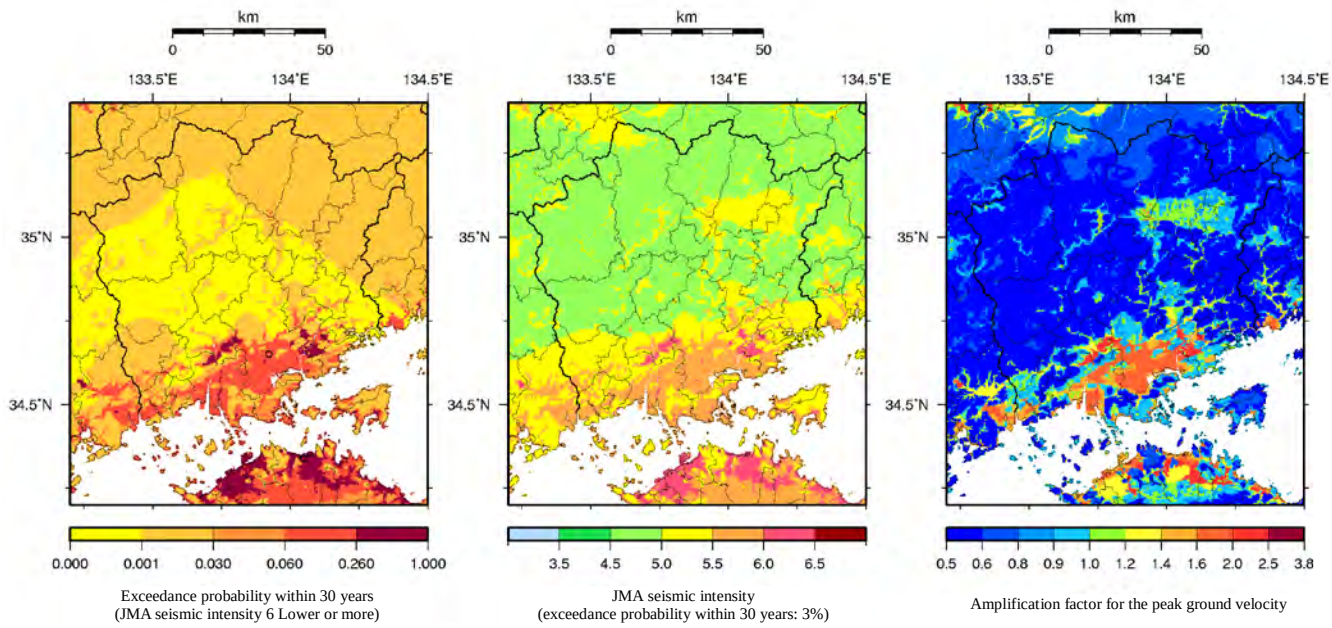

Figure 3.7.2-93 Seismic hazard maps for Okayama prefecture

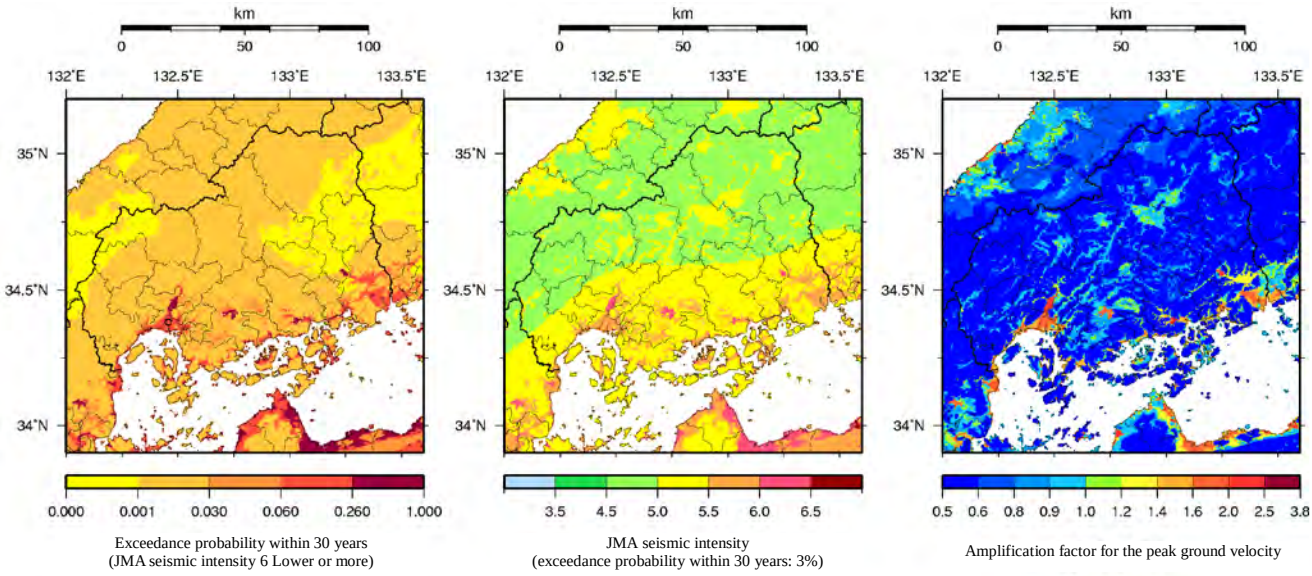

Figure 3.7.2-94 Seismic hazard maps for Hiroshima prefecture

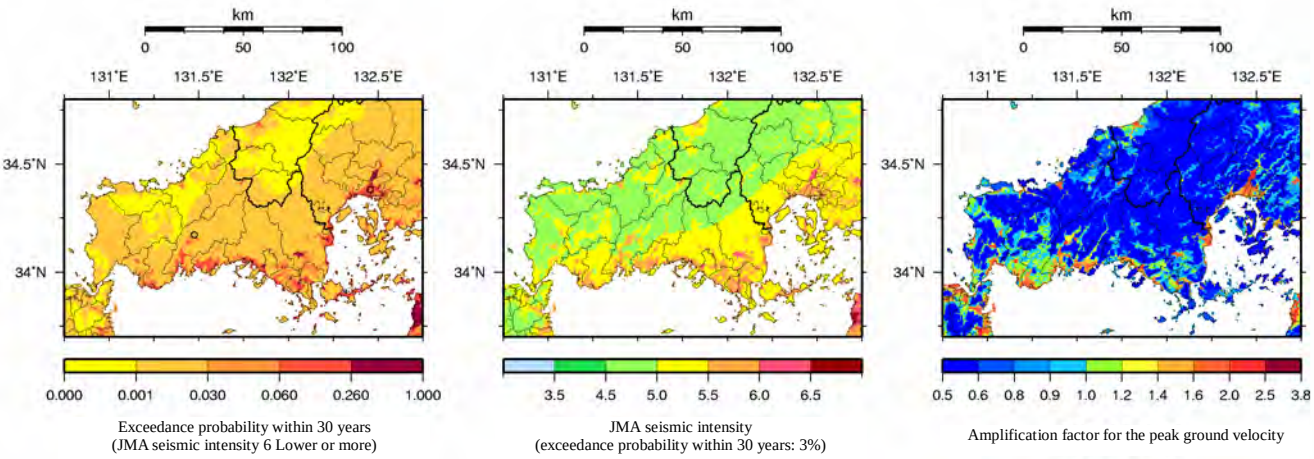

Figure 3.7.2-95 Seismic hazard maps for Yamaguchi prefecture

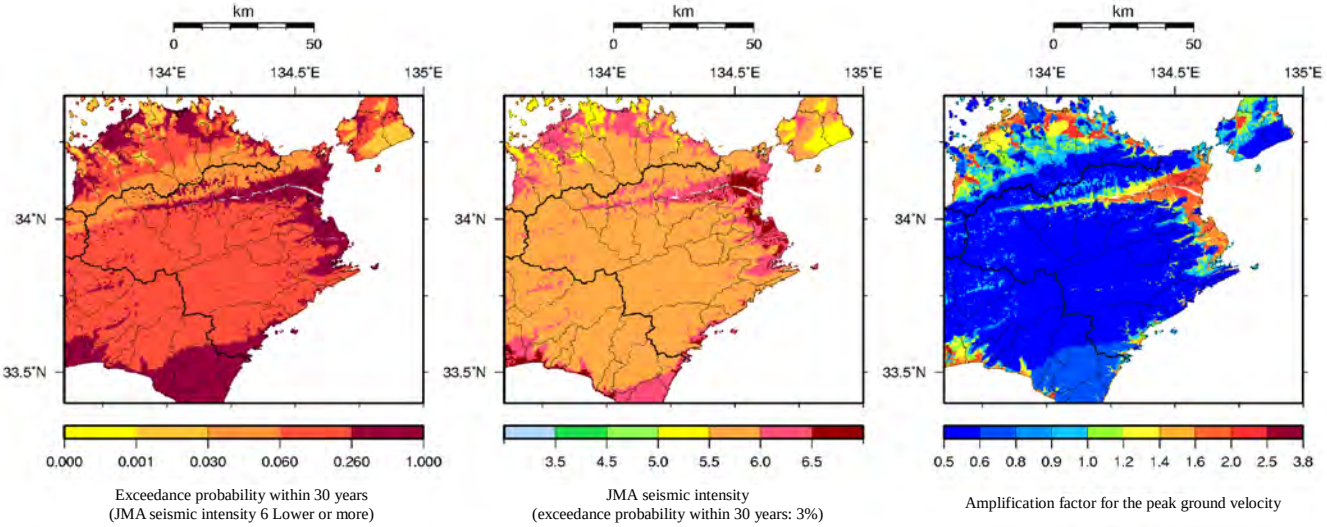

Figure 3.7.2-96 Seismic hazard maps for Tokushima prefecture

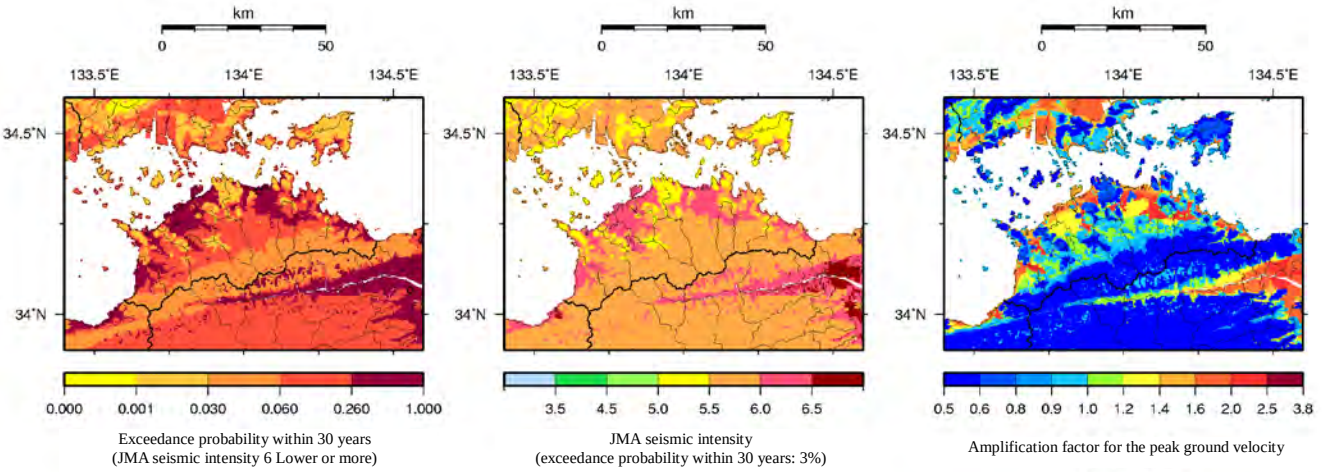

Figure 3.7.2-97 Seismic hazard maps for Kagawa prefecture

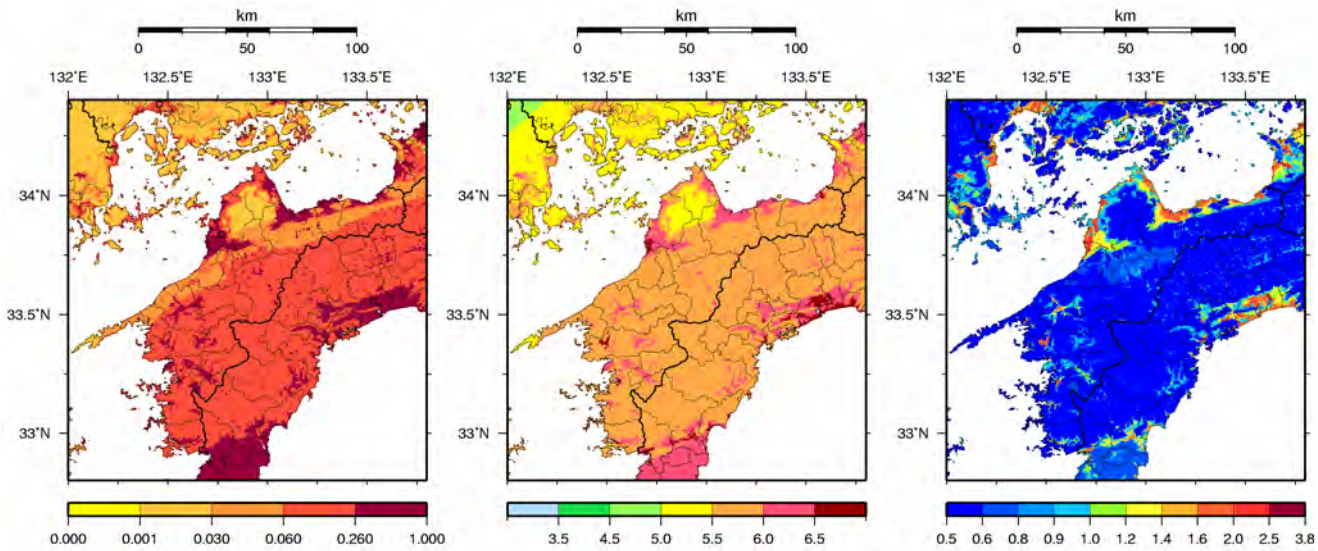

Figure 3.7.2-98 Seismic hazard maps for Ehime prefecture

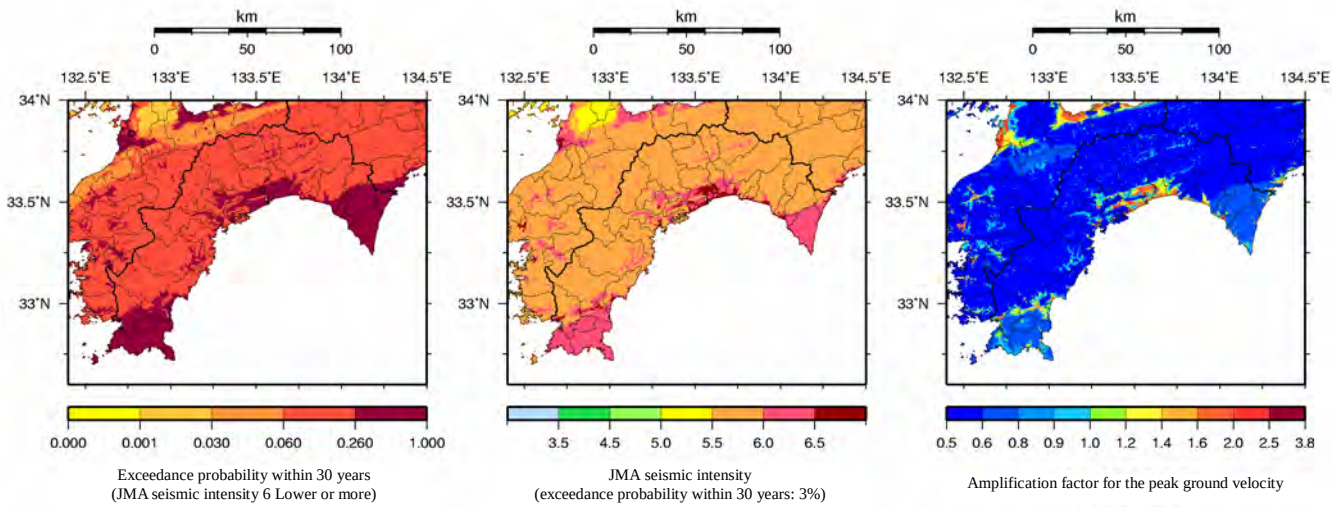

Figure 3.7.2-99 Seismic hazard maps for Kochi prefecture

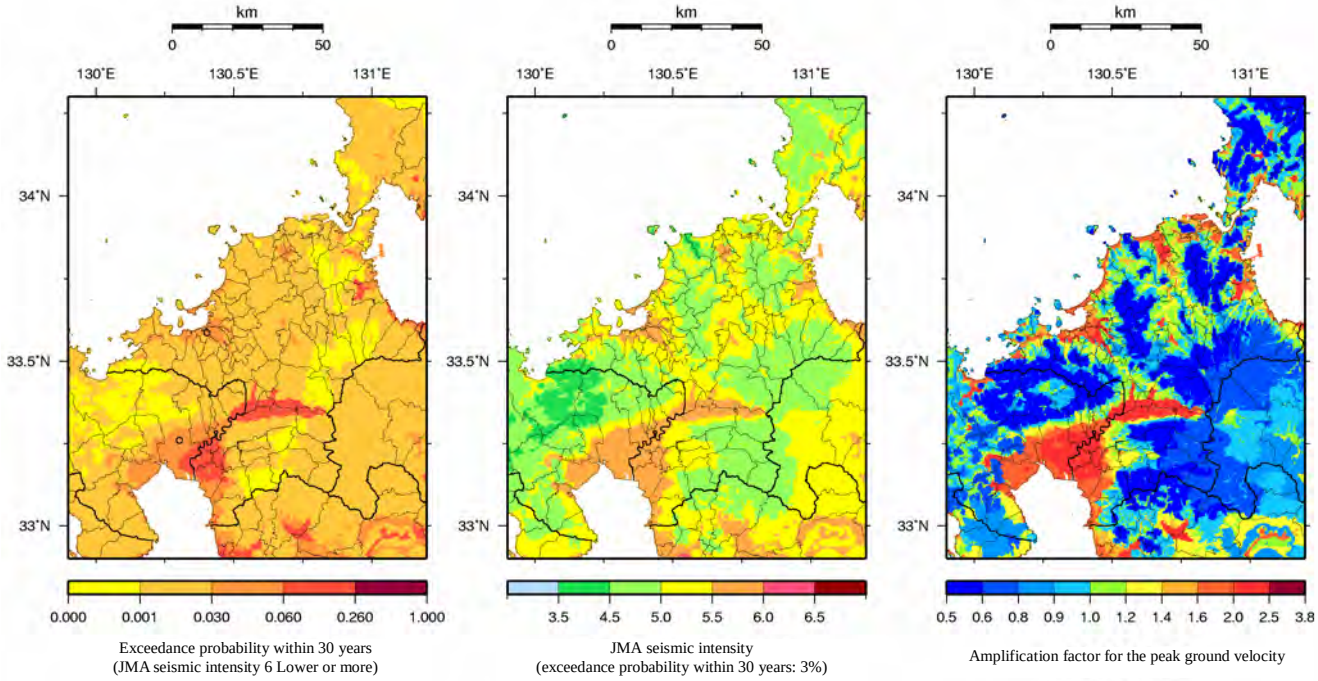

Figure 3.7.2-100 Seismic hazard maps for Fukuoka prefecture

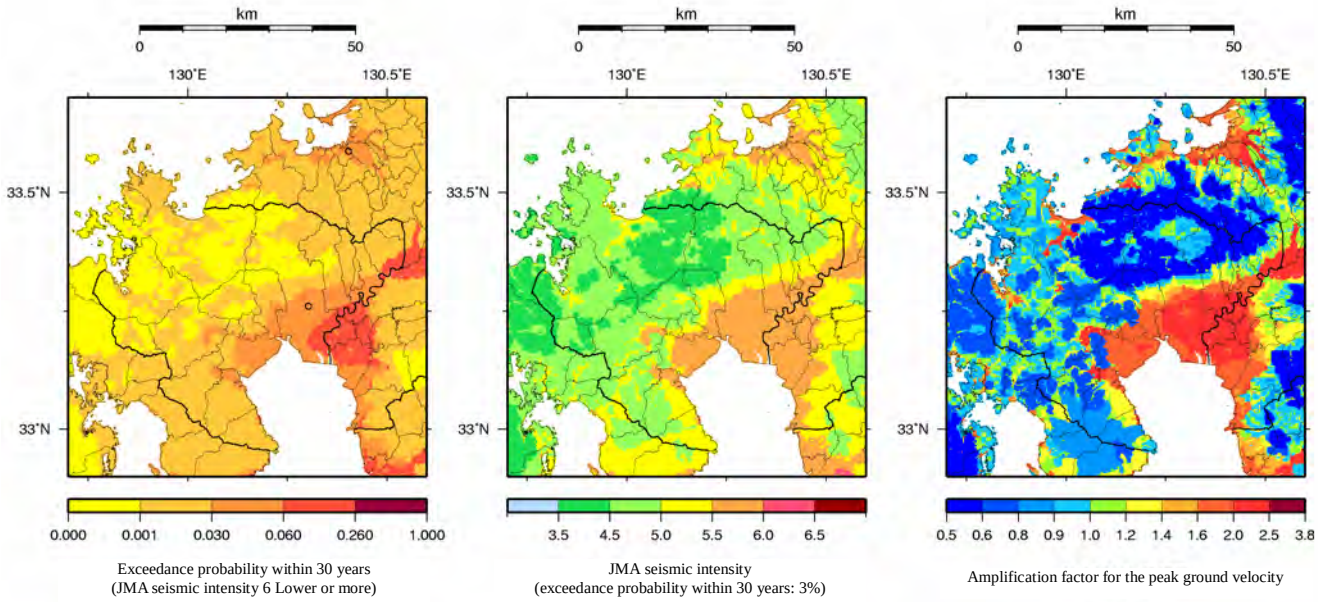

Figure 3.7.2-101 Seismic hazard maps for Saga prefecture

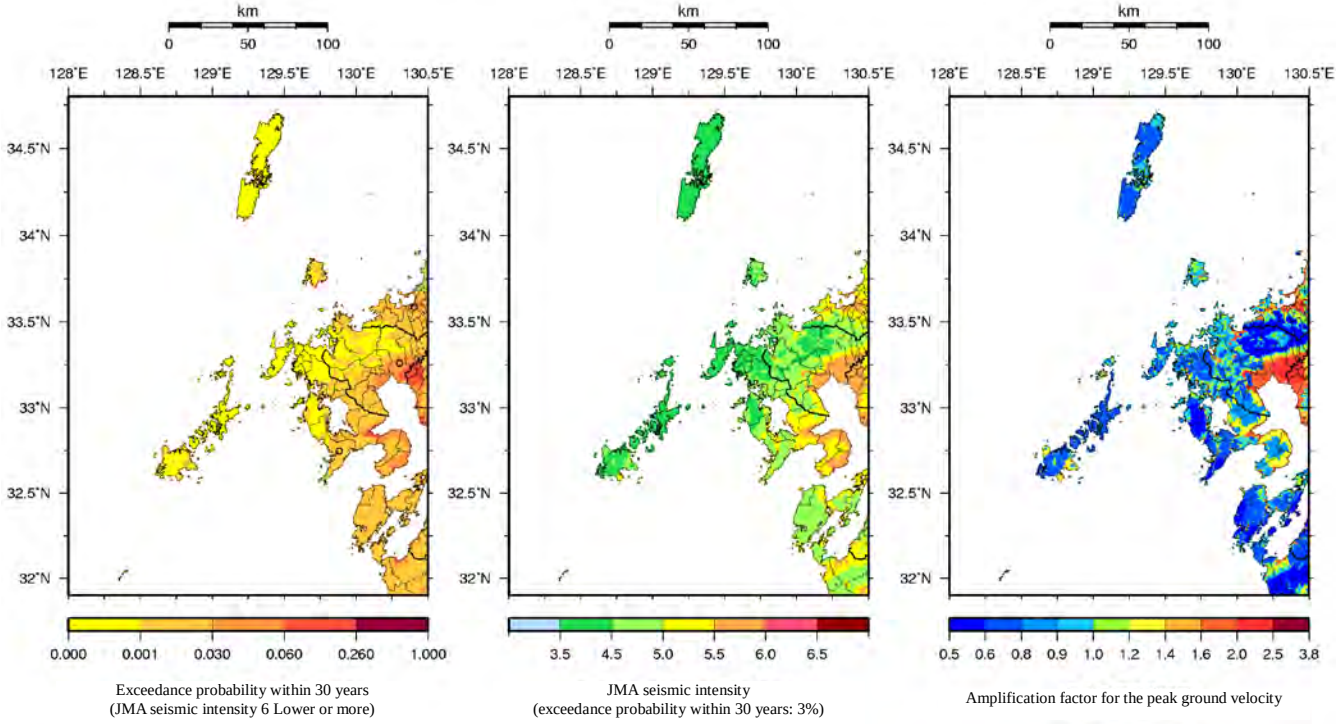

Figure 3.7.2-102 Seismic hazard maps for Nagasaki prefecture

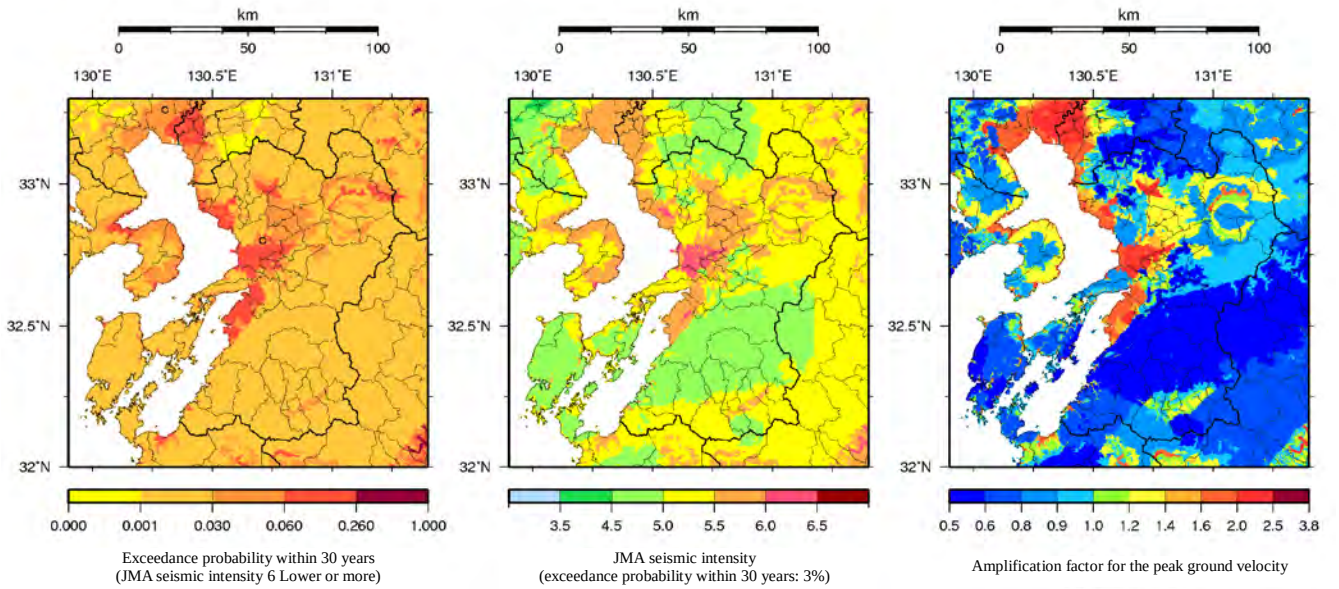

Figure 3.7.2-103 Seismic hazard maps for Kumamoto prefecture

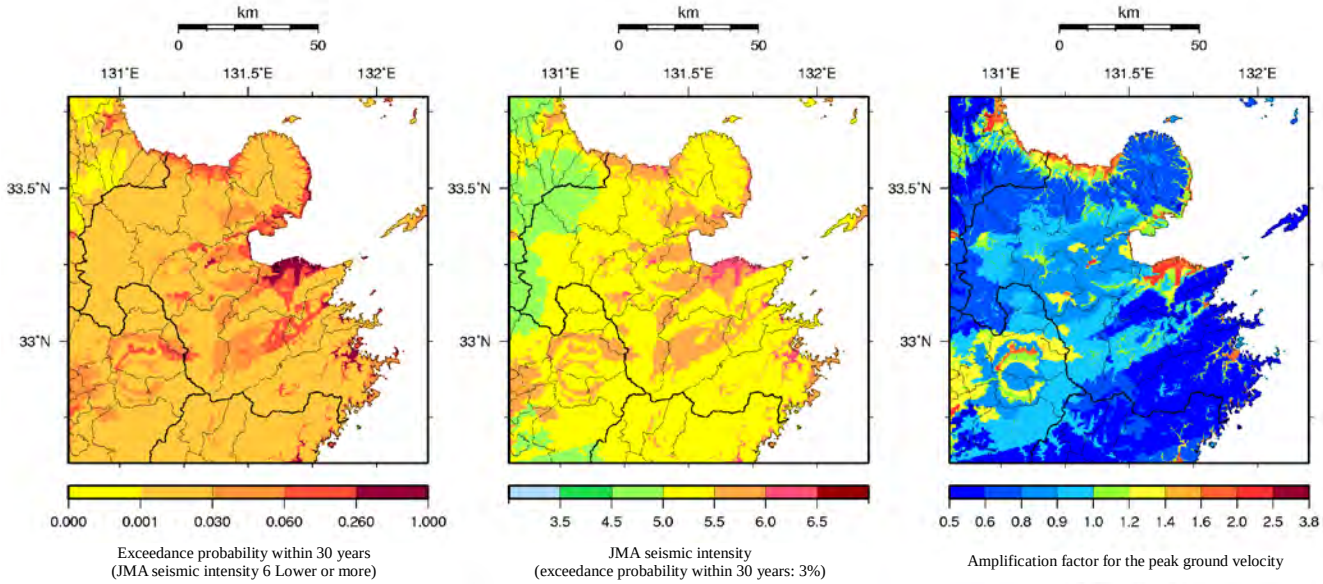

Figure 3.7.2-104 Seismic hazard maps for Oita prefecture

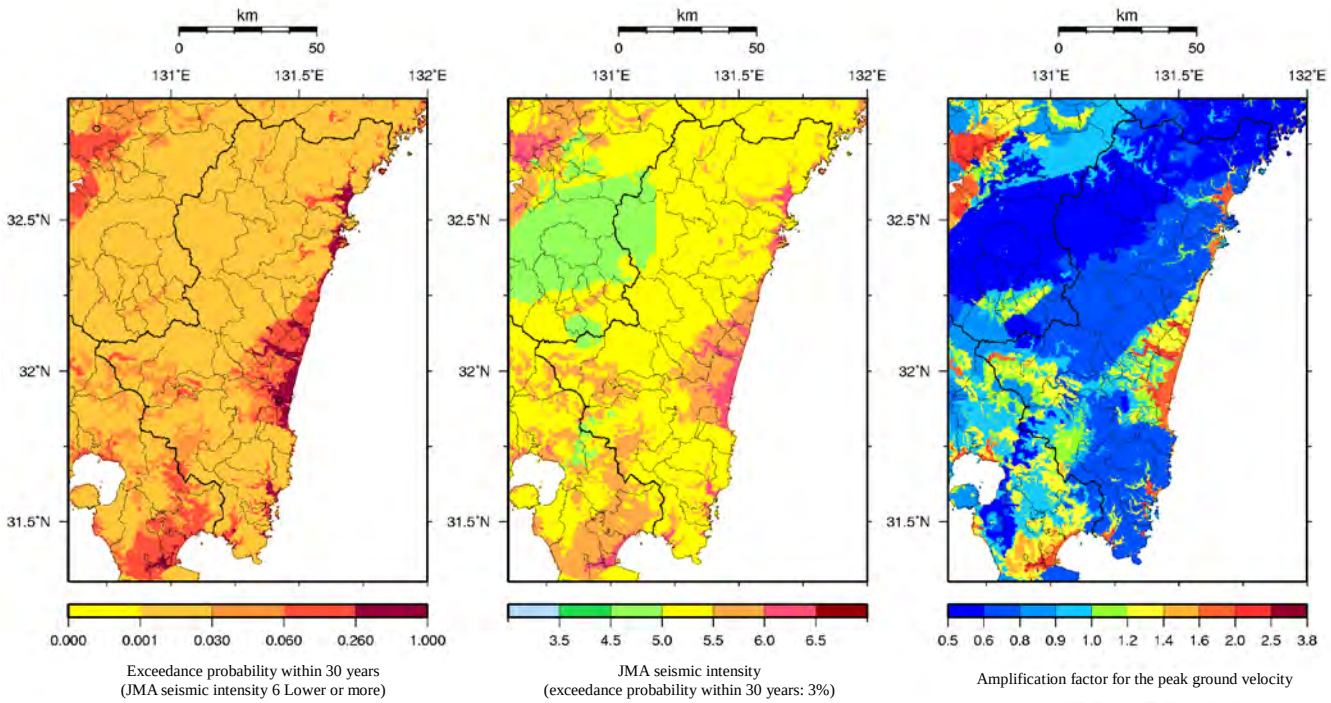

Figure 3.7.2-105 Seismic hazard maps for Miyazaki prefecture

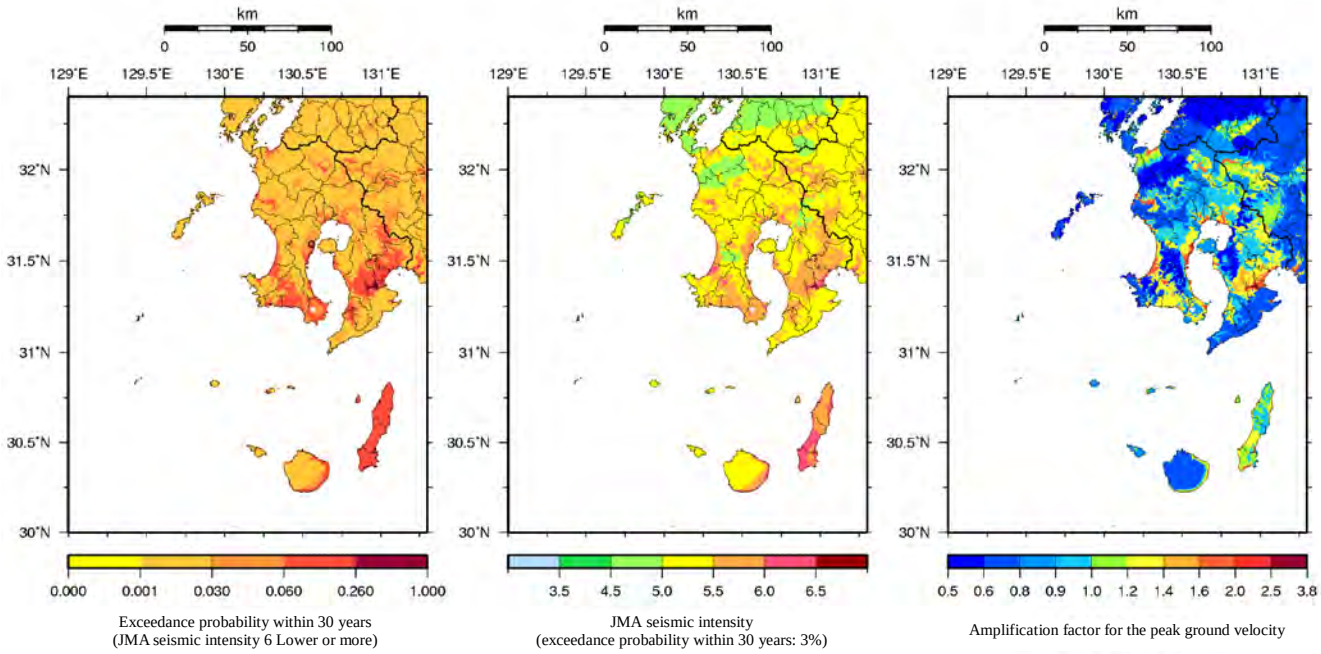

Figure 3.7.2-106 Seismic hazard maps for Kagoshima prefecture

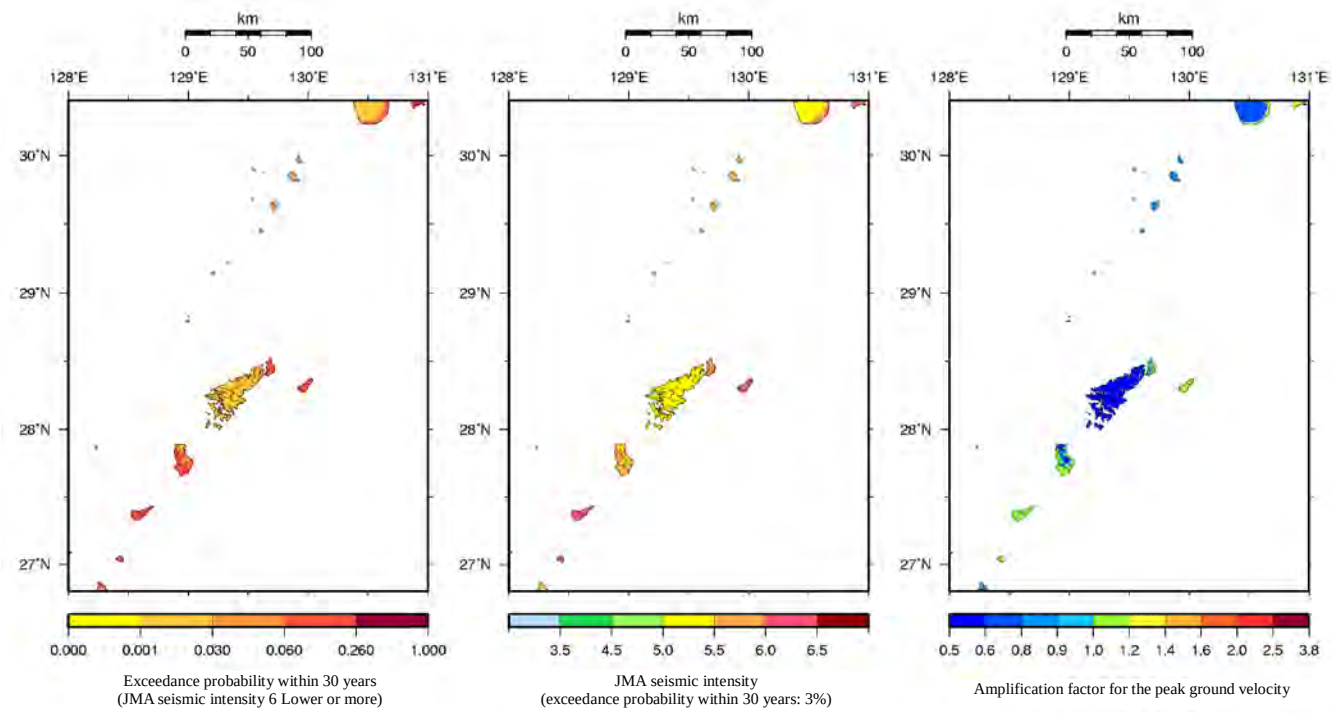

Figure 3.7.2-107 Seismic hazard maps for Amami region

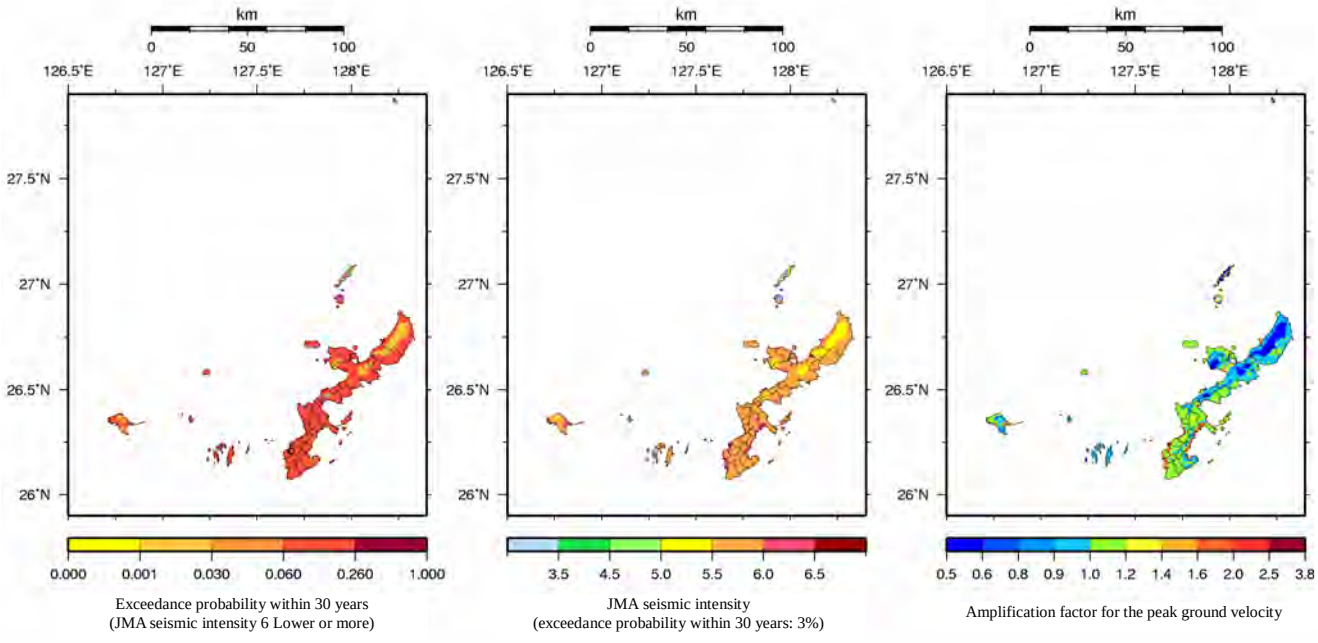

Figure 3.7.2-108 Seismic hazard maps for Okinawa prefecture

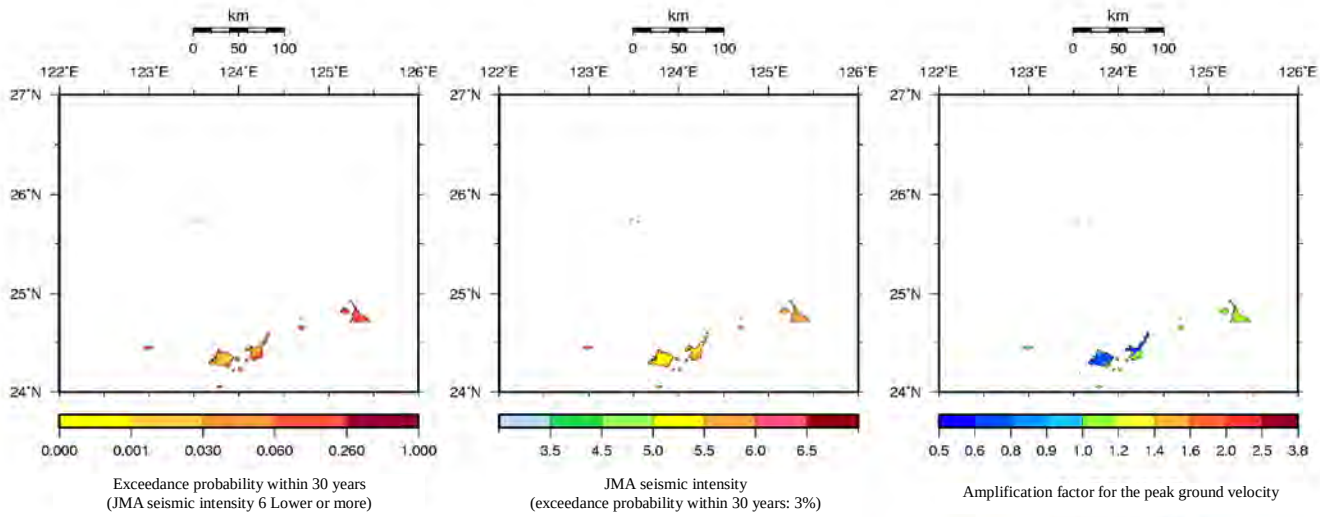

Figure 3.7.2-109 Seismic hazard maps for the Miyako and Yaeyama islands

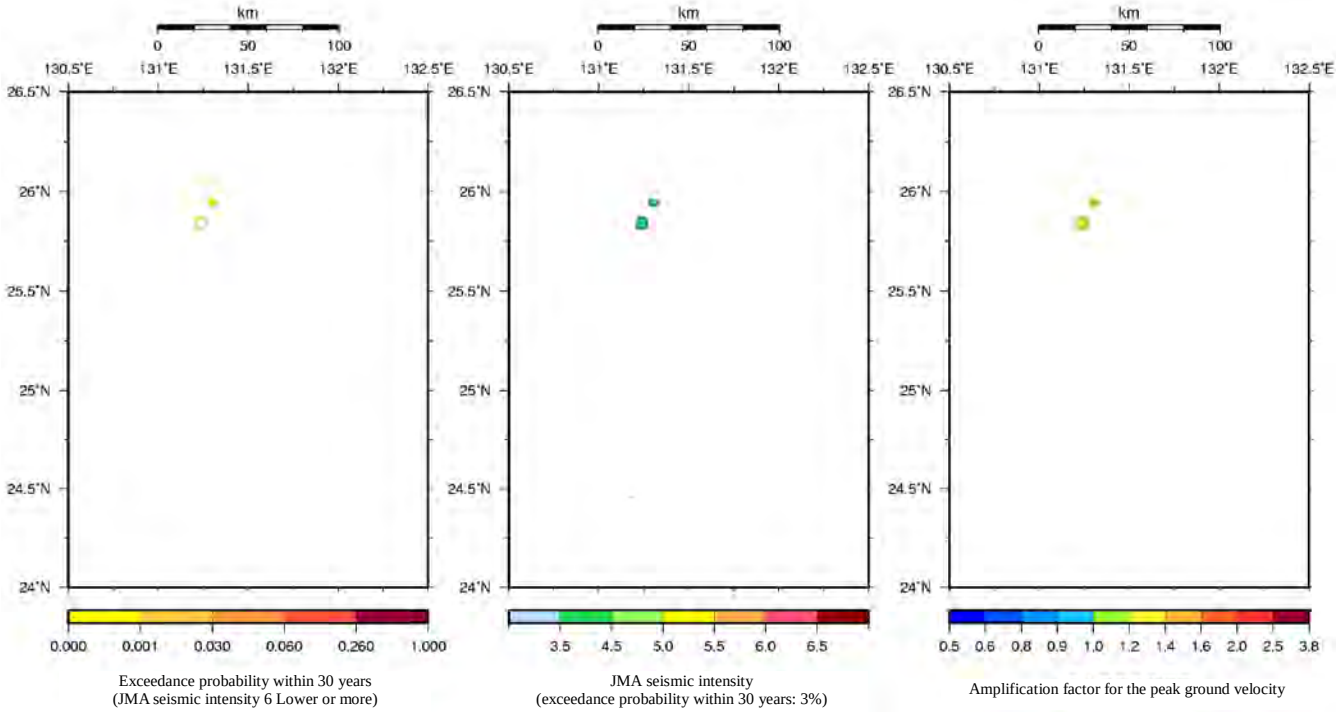

Figure 3.7.2-110 Seismic hazard maps for the Daito-shoto islands

3.7.3 Exceedance probability of JMA seismic intensity 6 Lower within 30 years at representative sites

This section compares the results in the 2008 version and the results in the 2009 version with regard to the exceedance probability of JMA seismic intensity 6 Lower within 30 years at representative sites in Japan. The target sites are the location of the municipal office in the capital city of each prefecture and the location of each subprefecture in Hokkaido, totaling 61 sites.

Table 3.7.3-1 shows the site amplification factor and the exceedance probability of JMA seismic intensity 6 Lower within 30 years for the 61 sites. The table also indicates the results in the 2008 version, and the differences in the exceedance probability. Figure 3.7.3-1 shows the graphs of the exceedance probability of JMA seismic intensity 6 Lower within 30 years and the site amplification factor. In that figure, (a) and (b) are the same graphs but only the scaling of the vertical axis differs. Figure 3.7.3-2 shows the contribution factor by earthquake category at each site.

Out of the 61 sites, the exceedance probability of JMA seismic intensity 6 Lower within 30 years declined from the results in the 2008 version in only three sites: Kofu, Abashiri, and Hidaka. The probability has risen for the remaining 58 sites. For many of these sites, the site amplification factor has become larger than in the 2008 version, and its influence has been directly reflected in the results. For some sites, the exceedance probability has risen despite that the site amplification factor has become smaller. The main reason for this is the renewal of the ground motion evaluation method (variance of the attenuation relation, and the formula for the conversion between velocity and JMA instrumental seismic intensity).The renewal of the ground motion evaluation method has pushed up the exceedance probability of JMA seismic intensity 6 Lower within 30 years, particularly notably at sites where the influence of inland earthquakes is dominant (sites where the yellow indication is dominant in Figure 3.7.3-2).

Figure 3.7.3-3 analyzes the causes for the differences between the 2008 version and the 2009 version. Case 1 denotes the results in the 2008 version. Case 2 denotes the results based on Case 1 where only the site amplification factor and the ground motion evaluation method have been renewed (variance of the attenuation relation and the formula for the conversion between velocity and JMA instrumental seismic intensity). Case 3 denotes the results based on Case 2 where earthquakes without specified source faults have been renewed. Case 4 denotes the results based on Case 3 where subduction-zone earthquakes have been renewed. Case 5 denotes the results based on Case 4 where earthquakes at major active fault zones and other active faults have been renewed. Case 5 is equivalent to the results in the 2009 version. For most sites, the differences between Case 1 and Case 2 are substantial, indicating that the renewal of the site amplification factor and the ground motion evaluation method has had the strongest influence among the changes made to the conditions when creating the 2009 version. The influence of the renewal of earthquakes without specified source faults was not so large, but difference is found in the results for Mito where the maximum magnitude was changed in the surrounding area. The one-year shift of the origin of the time axis of the occurrence probability for subduction-zone earthquakes has shown some influence, but not so large. In Mito, the probability has declined slightly due to the renewal of subduction-zone earthquakes, but this is attributable to the modification of the model for subduction-zone earthquakes in Ibaraki-ken-Oki. The only influence of the renewal of earthquakes at major active fault zones and other active faults was the slight influence of the long-term evaluation of the Suonada fault group observed in Yamaguchi.

Figure 3.7.3-4 shows the hazard curves for the above-mentioned characteristic sites. In that figure, the purple line denotes the results in the 2008 version (Case 1), and the red line denotes the results in the 2009 version (Case 5). The blue dotted line denotes the results in the 2008 version where only the site amplification factor and the ground motion evaluation method have been renewed (Case 2). Figure (a) shows the results for Osaka. It indicates that the hazard level is high across the curve in the 2009 version. Since the results for Case 2 and Case 5 are almost overlapping, it is found that the cause for the difference is the renewal of the site amplification factor and the ground motion evaluation method. Figure (b) shows the results for Nagasaki. For Nagasaki as well, the results for case 2 and case 5 are almost overlapping, but the curve for the 2008 version and that for the 2009 version cross each other. Since the site amplification factor is small in Nagasaki, the cause that the hazard level in the 2009 version becomes high in areas where the JMA instrumental seismic intensity is high is considered to be the renewal of the ground motion evaluation method. Figure (c) shows the results for Mito and Figure (d) shows the results for Yamaguchi. Differences are found between the results for case 2 and case 5 in both of these figures. While the renewal of the maximum magnitude of earthquakes without specified source faults has influenced the results in Mito, and the renewal of earthquakes at major active fault zones and other active faults has influenced the results in Yamaguchi, such influences are observed across the hazard curves.

Table 3.7.3-1 Comparison of site amplification factor and exceedance probability of JMA seismic intensity 6 Lower within 30 years at each site (part 1)

Site name	Site amplification factor		Exceedance probability of JMA seismic intensity 6 Lower within 30 years		Difference in exceedance probability
	2008 version	2009 version	2008 version	2009 version	(2009-2008)
Sapporo	1.36	1.31	5.4E-03	1.2E-02	6.7E-03
Aomori	1.54	1.44	1.4E-02	2.0E-02	6.5E-03
Morioka	1.04	1.13	1.5E-03	6.8E-03	5.2E-03
Sendai	1.04	1.03	2.8E-02	4.1E-02	1.2E-02
Akita	1.54	2.21	1.5E-02	7.7E-02	6.1E-02
Yamagata	1.04	1.10	7.8E-03	2.3E-02	1.5E-02
Fukushima	1.04	1.19	1.2E-03	8.9E-03	7.7E-03
Mito	1.52	1.86	8.3E-02	3.2E-01	2.3E-01
Utsunomiya	1.09	1.30	2.8E-03	1.6E-02	1.3E-02
Maebashi	1.11	1.19	9.1E-03	2.5E-02	1.6E-02
Saitama	1.49	1.63	1.2E-01	2.3E-01	1.1E-01
Chiba	1.67	2.23	2.7E-01	6.4E-01	3.7E-01
Tokyo	1.35	1.44	1.1E-01	2.0E-01	8.3E-02
Yokohama	1.67	2.19	3.3E-01	6.7E-01	3.4E-01
Niigata	1.88	1.85	3.4E-02	7.6E-02	4.3E-02
Toyama	1.29	1.40	2.5E-02	5.7E-02	3.2E-02
Kanazawa	1.15	1.12	1.0E-02	1.8E-02	8.1E-03
Fukui	1.45	2.19	1.4E-02	1.2E-01	1.0E-01
Kofu	1.85	1.06	8.2E-01	5.5E-01	-2.7E-01
Nagano	0.95	1.04	5.7E-02	1.2E-01	6.5E-02
Gifu	1.08	1.20	8.1E-02	1.7E-01	8.9E-02
Shizuoka	1.16	1.29	8.7E-01	9.0E-01	2.8E-02
Nagoya	1.28	1.28	3.8E-01	4.4E-01	6.7E-02
Tsu	1.48	2.21	6.3E-01	8.5E-01	2.3E-01
Otsu	1.05	1.10	7.2E-02	1.2E-01	4.9E-02
Kyoto	1.08	1.22	6.5E-02	1.5E-01	8.0E-02
Osaka	1.45	2.15	2.3E-01	6.0E-01	3.6E-01
Kobe	1.27	1.40	8.2E-02	1.8E-01	9.6E-02
Nara	1.03	2.05	1.6E-01	6.7E-01	5.1E-01
Wakayama	1.36	1.44	3.5E-01	4.8E-01	1.2E-01
Tottori	1.45	1.75	7.5E-03	4.1E-02	3.4E-02
Matsue	1.45	1.44	7.7E-03	2.1E-02	1.3E-02
Okayama	1.45	1.81	9.1E-02	2.2E-01	1.3E-01
Hiroshima	1.45	1.71	1.0E-01	1.9E-01	9.2E-02
Yamaguchi	1.12	1.21	6.9E-03	3.0E-02	2.3E-02
Tokushima	1.44	1.75	4.6E-01	6.0E-01	1.3E-01
Takamatsu	1.33	1.75	2.1E-01	4.1E-01	1.9E-01
Matsuyama	1.11	1.24	2.3E-01	3.3E-01	1.1E-01
Kochi	1.39	2.18	5.4E-01	6.2E-01	8.0E-02

Table 3.7.3-1 Comparison of site amplification factor and exceedance probability of JMA seismic intensity 6 Lower within 30 years at each site (part 2)

Site name	Site amplification factor		Exceedance probability of JMA seismic intensity 6 Lower within 30 years		Difference in exceedance probability
	2008 version	2009 version	2008 version	2009 version	(2009-2008)
Fukuoka	1.45	1.81	2.3E-02	3.8E-02	1.6E-02
Saga	1.45	2.05	5.6E-03	5.0E-02	4.4E-02
Nagasaki	1.20	0.98	7.1E-03	1.3E-02	6.4E-03
Kumamoto	1.36	1.53	2.0E-02	7.1E-02	5.1E-02
Oita	1.45	2.25	1.6E-01	4.8E-01	3.3E-01
Miyazaki	1.40	2.13	1.3E-01	4.6E-01	3.2E-01
Kagoshima	1.45	2.05	3.7E-02	1.6E-01	1.2E-01
Naha	1.69	1.78	1.5E-01	2.5E-01	9.6E-02
Sapporo City	1.39	1.32	5.5E-03	1.2E-02	6.6E-03
Hakodate City	1.04	1.07	1.5E-03	5.0E-03	3.5E-03
Esashi Town	1.04	0.90	1.3E-03	3.4E-03	2.1E-03
Kutchan Town	1.05	1.97	9.8E-04	3.1E-02	3.0E-02
Iwamizawa City	1.36	2.07	2.0E-02	4.6E-02	2.7E-02
Asahikawa City	1.08	1.14	3.3E-04	2.3E-03	2.0E-03
Rumoi City	1.16	1.25	3.3E-03	9.8E-03	6.5E-03
Wakkanai City	1.54	1.52	5.2E-03	9.3E-03	4.1E-03
Abashiri City	1.54	1.11	1.7E-02	7.9E-03	-9.3E-03
Muroran City	0.91	1.75	6.4E-04	2.8E-02	2.7E-02
Urakawa Town	1.54	0.99	3.3E-01	1.4E-01	-1.8E-01
Obihiro City	1.25	1.25	8.4E-02	1.1E-01	2.4E-02
Kushiro City	0.99	1.45	1.8E-01	4.6E-01	2.8E-01
Nemuro City	1.21	1.43	4.6E-01	6.3E-01	1.7E-01

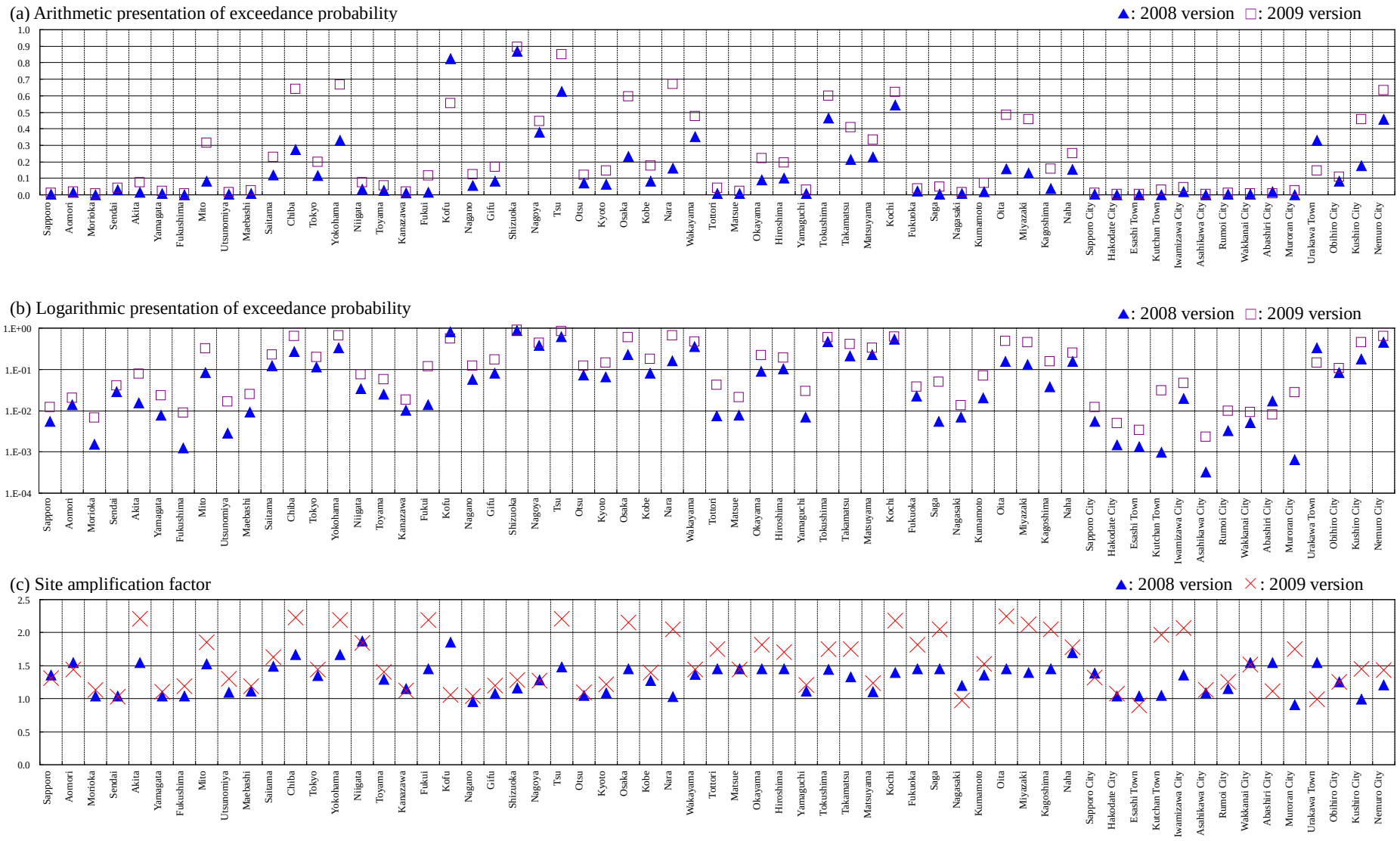

Figure 3.7.3-1 Comparison of exceedance probability of JMA seismic intensity 6 Lower within 30 years between 2008 version and 2009 version

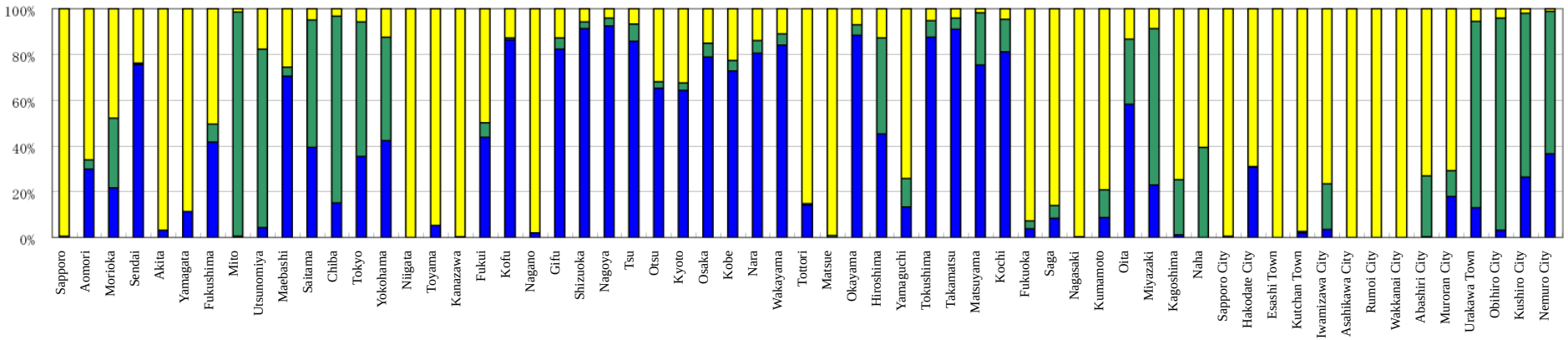

- **Earthquake Category I <Mega earthquakes in subduction zones with specified source faults with a recurrence interval of several hundred years>**

  Nankai Trough earthquakes (Nankai Earthquake/Tonankai Earthquake/Assumed Tokai Earthquake), Miyagi-ken-Oki Earthquake/earthquakes close to the offshore trenches in Southern Sanriku-Oki, large interplate earthquakes in Northern Sanriku-Oki, Tokachi-Oki Earthquake/Nemuro-Oki Earthquake, Shikotanto-Oki Earthquake, Etorofuto-Oki Earthquake, Kanto Earthquake of "1923 Taisho" type

  Note: Subduction-zone earthquakes in Ibaraki-ken-Oki are included in Category II.

- **Earthquake Category II <Earthquakes without specified source faults that occur at plates at trenches>**

  Interplate earthquakes other than characteristic earthquakes in Northern Sanriku-Oki, large interplate earthquakes close to the offshore trenches in the Sanriku-Oki to Boso-Oki regions (Tsunami earthquakes), large intraplate earthquakes close to the offshore trenches in the Sanriku-Oki to Boso-Oki regions (normal faults type), interplate earthquakes in Fukushima-ken-Oki, interplate earthquakes in Ibaraki-ken-Oki, relatively small interplate earthquakes in the Tokachi-Oki and Nemuro-Oki regions, relatively small interplate earthquakes in the Shikotanto-Oki and Etorofuto-Oki regions, relatively shallow earthquakes within a subducted plate along the Kuril Trench, relatively deep earthquakes within a subducted plate along the Kuril Trench, intraplate earthquakes in Akinada-Iyonada-Bungosuido, interplate earthquakes in Hyuganada, relatively small interplate earthquakes in Hyuganada, earthquakes in the vicinity of Yonaguni-jima, other *M*7 class earthquakes in Southern Kanto, interplate/intraplate earthquakes without specified source faults for the Pacific plate, interplate/intraplate earthquakes without specified source faults for the Philippine Sea plate, earthquakes without specified source faults in Urakawa-Oki

- **Earthquake Category III <Earthquakes at active fault zones and earthquakes without specified source faults in land area and in the surrounding sea area>**

  Characteristic earthquakes occurring in major active fault zones, Hokkaido-hokusei-Oki Earthquake, Hokkaido-seiho-Oki Earthquake, Hokkaido-nansei-Oki Earthquake, Aomori-ken-seiho-Oki Earthquake, Akita-ken-Oki Earthquake, Yamagata-ken-Oki Earthquake, Niigata-ken-hokubu-Oki Earthquake, Sadogashima-hoppo-Oki Earthquake, earthquakes occurring on active faults other than major active fault zones, earthquakes occurring at onshore locations where active faults have not been specified, earthquakes without specified source faults in the eastern margin of the Japan Sea, earthquakes without specified source faults in the southern area of Izu-shoto islands, earthquakes without specified source faults in the vicinity of Nansei-shoto islands

Figure 3.7.3-2 Contribution factor by earthquake category

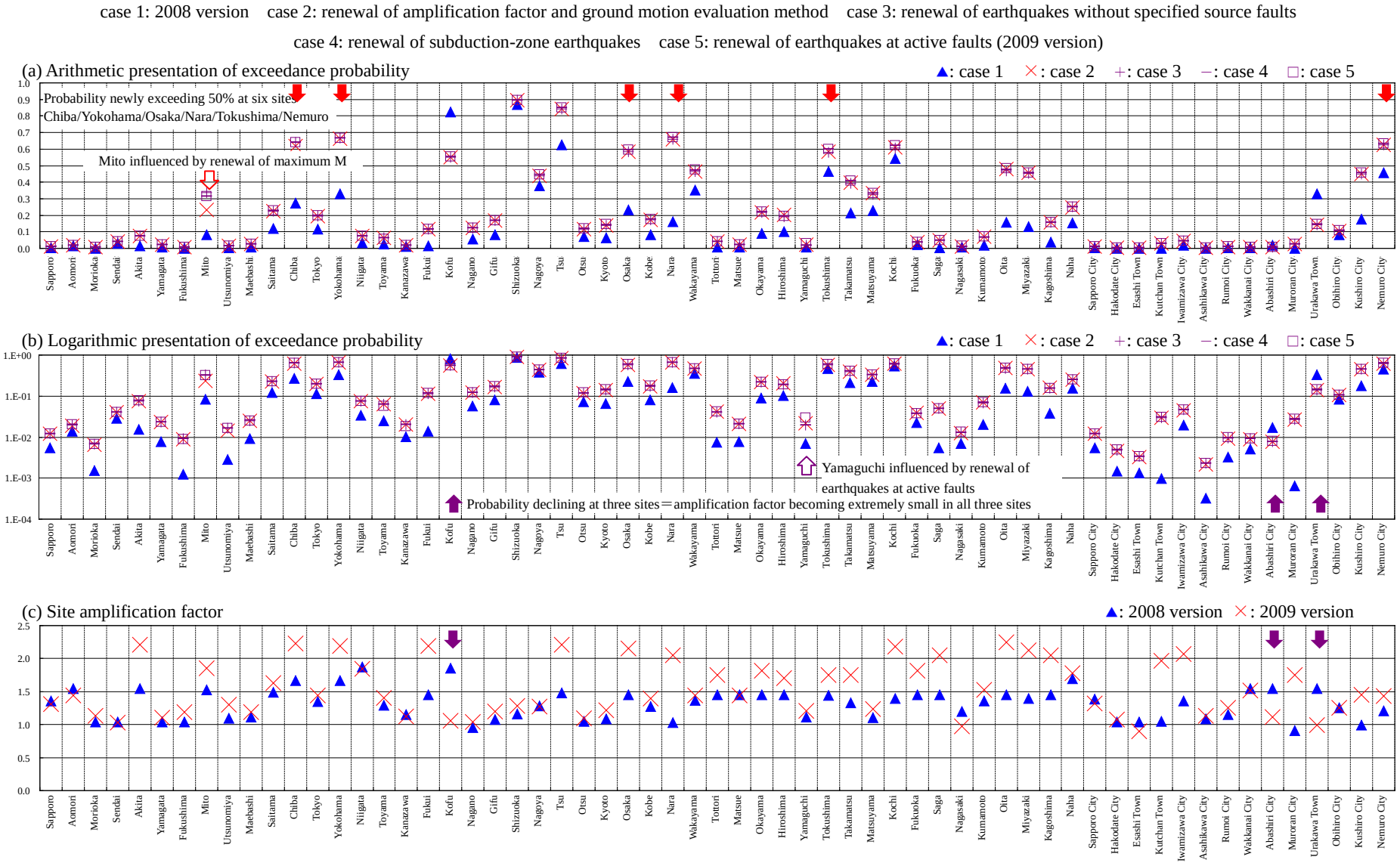

Figure 3.7.3-3 Analysis of causes for differences in exceedance probability of JMA seismic intensity 6 Lower within 30 years between 2008 version and 2009 version

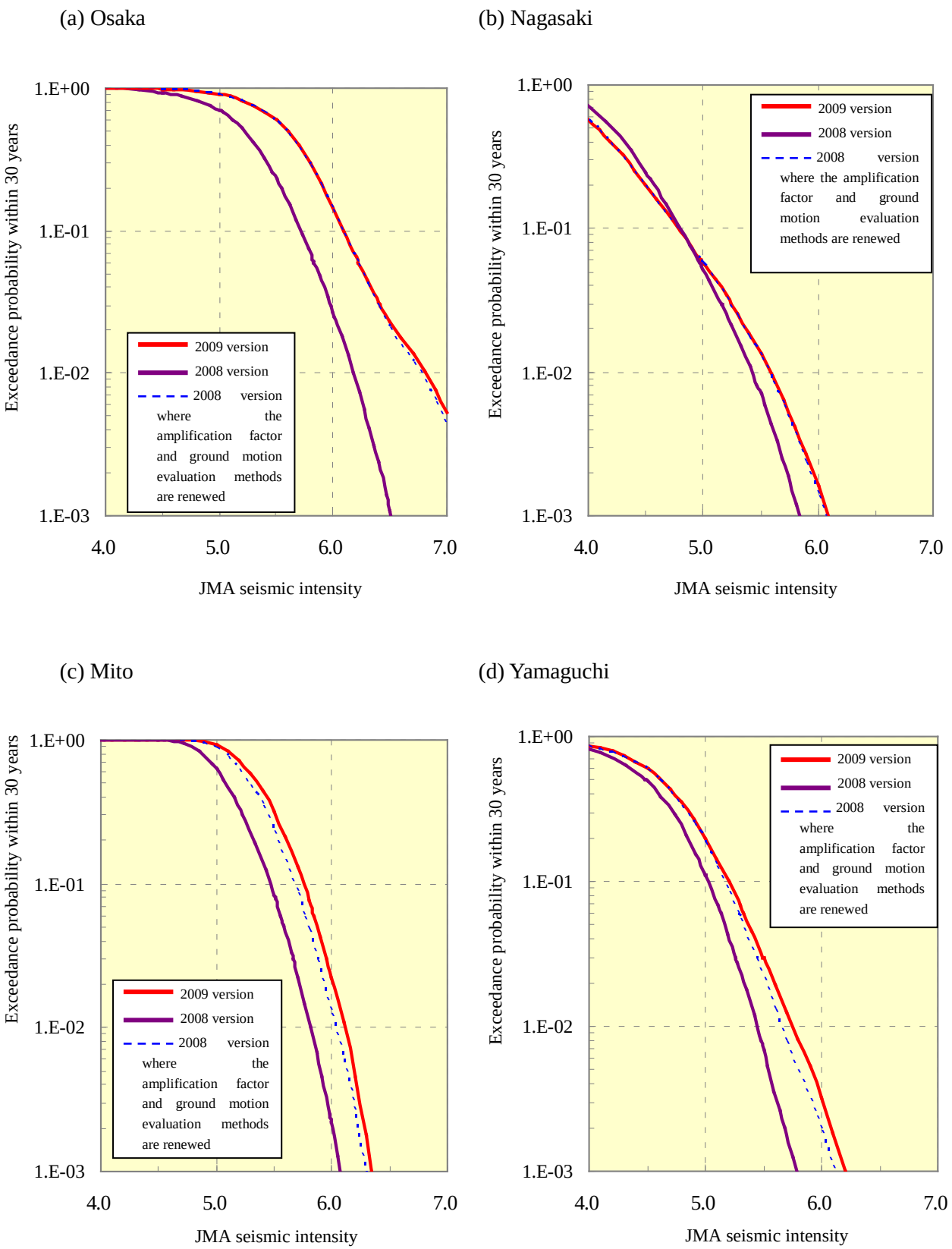

Figure 3.7.3-4 Comparison of characteristic hazard curves

References for Chapter 3

1) Abe, K. (1975): “Re-examination of the Fault Model for the Niigata Earthquake of 1964", *J. Phys. Earth*, **23**, 349-366.

2) Abe, K. (1987): “Source Model and Characteristics of a Small Tsunami On the Tsunami Accompanying the Largest Aftershock (June 21, 1983) of Japan Sea", *Journal of the Seismological Society of Japan* (Second Series), **40**, 349-363 (in Japanese with English abstract).

3) Aida, I. (1989): “Tenpo Yonen no Shonai-oki jishin ni yoru tsunami ni kansuru jissuu jikken” (Numerical experiment on the tsunami generated by the Shonai-Oki Earthquake in 1833), *Zoku kojisin: jitsuzo to kyozo* (Paleoseismicity [Part 2]: Real and virtual image) (written and edited by Hagiwara, T.), 204-213.

4) NIED (2003): “A Study on Preliminary Versions of Probabilistic Seismic Hazard Map in Northern Part of Japan", *Technical Note of the National Research Institute for Earth Science and Disaster Prevention*, **246**, 259pp. (in Japanese).

5) Central Disaster Prevention Council “Special investigation council concerning the Tokai Earthquake” (2001): *Chuo Bosai Kaigi Tokai jishin ni kansuru senmon chosakai hokoku* (Report of the Special Survey Committee for the Tokai Earthquake), December 11, 2001 (in Japanese).

6) Frankel, A. (1995): “Mapping Seismic Hazard in the Central and Eastern United States", *Seism. Res. Lett.*, **66**-4, 8-21.

7) Fujimoto, K and Midorikawa, S. (2005): “Empirical Method for Estimating J.M.A. Instrumental Seismic Intensity from Ground Motion Parameters Using Strong Motion Records during Recent Major Earthquakes", *Journal of social safety science*, **7**, 1-6 (in Japanese with English abstract).

8) Fujimoto, K and Midorikawa, S. (2006): “Relationship between Average Shear-Wave Velocity and Site Amplification Inferred from Strong Motion Records at Nearby Station Pairs", *Journal of Japan Association for Earthquake Engineering*, **6**-1, 11-22 (in Japanese with English abstract).

9) Fukushima Prefecture (1999): *Heisei 10 nendo jishin kankei kiso chosa kofukin: Futaba danso ni kansuru chosa seika hokokusho* (FY1998 Subsidy for basic survey related to earthquakes: Report on the research results concerning the Futaba fault), 109pp. (in Japanese).

10) Gifu Prefecture (2001): *Heisei 12 nendo jishin kankei kiso chosa kofukin: Byobuyama/Enasan dansotai ni kansuru chosa seika hokokusho* (FY2000 Subsidy for basic survey related to earthquakes: Report on the research results concerning the Byobuyama/Enasan fault zone), 164pp. (in Japanese).

11) Ide, S. and Takeo, M. (1996): “The Dynamic Rupture Process of the 1993 Kushiro-oki Earthquake", *J. Geophys. Res.*, **101**-B3, 5661-5675.

12) Irikura, K. and Miyake, H. (2001): “Prediction of Strong Ground Motions for Scenario Earthquakes", *Journal of Geography*, **110**, 849-875.

13) Ishida, M. (1992): “Geometry and Relative Motion of the Philippine Sea Plate and Pacific Plate Beneath the Kanto-Tokai District, Japan", *J. Geophys. Res.*, **97**-B1, 489-513.

14) Ishikawa, Y. and Okumura, T. (2001): "Risk-based Determination of Scenario Earthquakes for Regional Disaster Mitigation", *Journal of social safety science*, **3**, 199-206 (in Japanese with English abstract).

15) Ishikawa, Y., Okumura, T., and Saito, T. (2002): “Probabilistic Seismic Hazard Analysis Considering the Plural Earthquake Occurrence", *The 57th Annual Conference of the Japan Society of Civil Engineers*, I-737, 1473-1474 (in Japanese).

16) Ishikawa, Y., Fujiwara, H., Nojima, N., Okumura, T., and Miyakoshi, J. (2008): “Jishin kategori betsu no kakuritsu-ron-teki jishindo yosoku chizu” (Probabilistic seismic hazard maps by earthquake category), *Proceedings of the 6th annual meeting of Japan Association for Earthquake Engineering*, 220-221 (in Japanese).

17) Ito, K. (1997): “Upper Cutoff Depth of Seismicity in the Crust", *Programme and abstracts Seismological Society of Japan 1997, Fall Meeting*, 69 (in Japanese).

18) Earthquake Research Committee (2000): “Miyagi-ken-oki jishin no choki hyoka” (Long-term evaluation of the Miyagi-ken-Oki Earthquake), published on November 27, 2000 (in Japanese).

19) Earthquake Research Committee (2001a): “Choki-teki najishin hassei kakuritsu no kyoka shuho ni tsuite” (Regarding Methods for Evaluating Long-term Probability of Earthquake Occurrence), published on June 8, 2001.

20) Earthquake Research Committee (2001b): “Nankai torafu no jishin no choki hyoka nit suite” (Long-term evaluation of Nankai Trough earthquakes), published on September 27, 2001 (in Japanese).

21) Earthquake Research Committee (2002a): “Futagawa/Hinagu dansotai no hyoka” (Evaluation of the Futagawa/Hinagu fault zone), published on May 8, 2002 (in Japanese).

22) Earthquake Research Committee (2002b): “Sanriku-oki kara Boso-oki ni kakete no jishin katsudo no choki hyoka ni tsuite” (Long-term evaluation of seismic activity from Sanriku-Oki to Boso-Oki), published on July 31, 2002 (in Japanese).

23) Earthquake Research Committee (2003a): “Chishima kaiko zoi no jishin katsudo no choki hyoka nit suite” (Long-term evaluation of seismic activity along the Kuril Trench), published on March 24, 2003 (in Japanese).

24) Earthquake Research Committee (2003b): “Miyagi-ken-oki jishin wo sotei shita kyosindo hyoka nit suite” (Strong motion evaluation assuming a Miyagi-ken-Oki Earthquake), published on June 18, 2003 (in Japanese).

25) Earthquake Research Committee (2003c): “Nihonkai toen-bu no jishin katsudo no choki hyoka nit suite” (Long-term evaluation of seismic activity in the eastern margin of the Japan Sea), published on June 20, 2003 (in Japanese).

26) Earthquake Research Committee (2004a): “Hyuganada oyobi Nansei-shoto kaiko shuhen no jishin katsudo no choki hyoka nit suite” (Long-term evaluation of seismic activity in Hyuganada and the vicinity of the Nansei-shoto Trench), published on February 27, 2004 (in Japanese).
27) Earthquake Research Committee (2004b): “Sanriku-oki hokubu no jishin wo sotei shita kyoshindo hyoka ni tsuite” (Strong motion evaluation assuming earthquakes in northern Sanriku-Oki), published on May 21, 2004 (in Japanese).
28) Earthquake Research Committee (2004c): “Sagami torafu zoi no jishin katsudo no choki hyoka nit suite” (Long-term evaluation of seismic activity along the Sagami Trough), published on August 23, 2004 (in Japanese).
29) Earthquake Research Committee (2004d): “Chishima kaiko zoi no jishin katsudo no choki hyoka (dai ni han) nit suite” (Long-term evaluation of seismic activity along the Kuril Trench [second edition]), published on December 20, 2004.
30) Earthquake Research Committee (2005a): “Choki hyokani okeru kakuritsuchi no koshin to katsudanso no jishin kibo no hyoki nit suite” (Renewal of the probability values and indication of earthquake magnitude for active faults in the long-term evaluation), published on January 12, 2005 (in Japanese).
31) Earthquake Research Committee (2005b): “‘Zenkoku wo gaikan shita jishindo yosoku chizu’ hokokusho” (Report: “National Seismic Hazard Maps for Japan”), published on March 23, 2005 (in Japanese).
32) Earthquake Research Committee (2006a): “Choki hyoka ni yoru jishin hassei kakuritsuchi no koshin nit suite” (Renewal of earthquake occurrence probability values in long-term evaluation), published on January 11, 2006 (in Japanese).
33) Earthquake Research Committee (2006b): “‘Zenkoku wo gaikan shita jishindo yosoku chizu’ hokokusho” (Report: “National Seismic Hazard Maps for Japan”), revised on September 25, 2006 (in Japanese).
34) Earthquake Research Committee (2007a): “Choki hyoka ni yoru jishin hassei kakuritsuchi no koshin nit suite” (Renewal of earthquake occurrence probability values in long-term evaluation), published on January 10, 2007 (in Japanese).
35) Earthquake Research Committee (2007b): “‘Zenkoku wo gaikan shita jishindo yosoku chizu’ 2007 nen ban” (“National Seismic Hazard Maps for Japan” 2007 version), published on April 18, 2007 (in Japanese).
36) Earthquake Research Committee (2008a): “Choki hyoka ni yoru jishin hassei kakuritsuchi no koshin nit suite” (Renewal of earthquake occurrence probability values in long-term evaluation), published on January 11, 2008 (in Japanese).
37) Earthquake Research Committee (2008b): “‘Zenkoku wo gaikan shita jishindo yosoku chizu’ 2008 nen ban” (“National Seismic Hazard Maps for Japan” 2008 version), published on April 24, 2008 (in Japanese).
38) Earthquake Research Committee (2009a): “Choki hyoka ni yoru jishin hassei kakuritsuchi no koshin nit suite” (Renewal of earthquake occurrence probability values in long-term evaluation), published on January 9, 2009 (in Japanese).
39) Earthquake Research Committee (2009b): “Sanriku-oki kara Boso-oki ni kakete no jishin katsudo no choki hyoka no ichibu kaitei ni tsuite” (Partial revision of long-term evaluation of seismic activity from Sanriku-Oki to Boso-Oki), published on March 9, 2009 (in Japanese).
40) Subcommittee for Long-term Evaluations, Earthquake Research Committee (2002a): “Shingen wo arakajime tokutei shinikui jishiin to no hyoka shuho nit suite (Chukan hokoku)” (Evaluation methods for earthquakes without specified source faults, etc. [Interim report]), published on May 29, 2002 (in Japanese).
41) Subcommittee for Long-term Evaluations, Earthquake Research Committee (2002b): “Tsugi no Miyagi-ken-oki jishin no shingen danso no keijo hyoka ni tsuite” (Evaluation of the seismic source fault shape of the next Miyagi-ken-Oki Earthquake), published on October 15, 2002 (in Japanese).
42) Subcommittee for Long-term Evaluations/Subcommittee for Evaluation of Strong Ground Motion, Earthquake Research Committee (2003): “Kakuritsu-ron-teki jishindo yosoku chizu no shisakuban (Chiiki gentei: Kita Nihon)” (Preliminary Version of Probabilistic Seismic Hazard Maps [Specific Area, Northern Japan]), published on March 25, 2003 (in Japanese).
43) Subcommittee for Long-term Evaluations/Subcommittee for Evaluation of Strong Ground Motion, Earthquake Research Committee (2004): “Kakuritsu-ron-teki jishindo yosoku chizu no shisakuban (Chiiki gentei: Nishi Nihon)” (Preliminary Version of Probabilistic Seismic Hazard Maps [Specific Area, Western Japan]), published on March 25, 2004 (in Japanese).
44) Working Group for Advancement of Seismic Hazard Maps, Subcommittee for Long-term Evaluations/Subcommittee for Evaluation of Strong Ground Motion, Earthquake Research Committee (2008): “Zenkoku jishindo yosoku chizu ni okeru Ibaraki-ken-oki no jishin no atsukai nit suite” (Treatment of the Ibaraki-ken-Oki Earthquake in the National Seismic Hazard Maps for Japan) (conference material, Map 25 (7)), December 17, 2008 (in Japanese).
45) Kameda, H., Ishikawa, Y., Okumura, T, and Nakajima, M. (1997): “Probabilistic Scenario Earthquakes-Definition and Engineering Applications", *Journal of geological engineering*, **577**/I-41, 75-87.
46) The Research Group for Active Faults of Japan ed. (1991): *Active Faults in Japan (revised edition)*, University of Tokyo Press, 437pp. (in Japanese).
47) Kakimi, T., Matsuda, T., Aida, I., and Kinugasa, Y. (2003): “A Seismotectonic Province Map in and around the Japanese Islands", *Journal of the Seismological Society of Japan* (Second Series), **55**, 389-406 (in Japanese with English abstract).
48) Kanno, T., Narita, A., Morikawa, N., Fujiwara, H. and

Fukushima, Y. (2006): “A new attenuation relation for strong ground motion in Japan based on recorded data", *Bull. Seism. Soc. Am.*, **96**, 879-897.

49) Katsumata, K., Kasahara, M., and Wada, N. (2002): “Chumitsu jishin kansoku-mo ni yotte mietekita Taiheiyo pureto-nai Tokachi-Oki danretsu-tai” (Tokachi-Oki fracture zone within the Pacific plate revealed by a dense seismic network), *Chikyu Monthly*, **24-**7, 499-503 (in Japanese).

50) Ground Vibration Division, Department of Earthquake Disaster Prevention, Public Works Research Institute, Ministry of Construction (1983): “Zen/yoshin no hindo oyobi kibo ni kansuru chosa” (Research on the frequency and magnitude of foreshocks and aftershocks), *Technical Note of the Public Works Research Institute* No.1995 (in Japanese).

51) Kikuchi, M. and Kanamori, H. (1995): “Kotaiiki jishin kiroku ni yoru 1994 nen Hokkaido toho-oki jishin no singen mekanizumu” (Source mechanism of the 1994 Eastern Hokkaido-Oki Earthquake revealed by broadband seismic records), *Chikyu Monthly*, **17** (5), 322-328 (in Japanese).

52) JMA (2008): *Monthly Report on Earthquakes and Volcanoes in Japan [Catalog]*, December 2007 issue.

53) Kosuga, M., T. Sato, A. Hasegawa, T. Matsuzawa, S. Suzuki, and Y. Motoya (1996): “Spatial Distribution of Intermediate-depth Earthquakes with Horizontal or Vertical Nodal Planes beneath Northeastern Japan", *Phys. Earth Planet. Inter.*, **93**, 63-89.

54) Matsuda, T. (1975): "Magnitude and Recurrence Interval of Earthquakes from a Fault", *Journal of the Seismological Society of Japan* (Second Series), **28**, 269-283 (in Japanese with English abstract).

55) Matsuda, T., Tsukazaki, T., and Haginoya, M. (2000): “Distribution of Active Faults and Historical Shallow Earthquakes of Japanese Islands, with a Catalog of On-land Seismogenic Faults and Earthquakes", *Active Fault Research*, **19**, 33-54 (in Japanese).

56) Matsuoka, M. and Wakamatsu, K. (2008): “Site Amplification Capability Map based on 7.5-arc-second Japan Engineering Geomorphologic Classification Map”, National Instituter of Advanced Industrial Science and Technology, Intellectual property management no. H20PRO-936.

57) Midorikawa, S., Fujimoto, K., and Muramatsu, I. (1999): "Correlation of New J.M.A. Instrumental Seismic Intensity with Former J.M.A. Seismic Intensity and Ground Motion Parameters", *Journal of social safety science*, **1**, 51-56 (in Japanese with English abstract).

58) Mochizuki, K., Yamada, T., Shinohara, M., Yamanaka, Y. and Kanazawa, T. (2008): “Weak interplate coupling by seamounts and repeating M~7 earthquakes", *Science*, **321**, 1194-1197.

59) Morikawa, N., Kanno, T., Narita, A., Fujiwara, H., and Fukushima, Y. (2003): “Additional Correction Terms for Attenuation Relations Corresponding to the Anomalous Seismic Intensity in Northeast Japan", *Journal of Japan Association for Earthquake Engineering*, **3-**4, 14-26 (in Japanese with English abstract).

60) Morikawa, N., Kanno, T., Narita, A., Fujiwara, H., and Fukushima, Y. (2006): “New Additional Correction Terms for Attenuation Relations of Peak Amplitudes and Response Spectra Corresponding to the Anomalous Seismic Intensity in Northeastern Japan", *Journal of Japan Association for Earthquake Engineering*, **6-**1, 23-41 (in Japanese with English abstract).

61) Morikawa, N. and Fujiwara, H. (2009): “On the relationship between peak ground velocity and seismic intensity", *Abstract Submissions for Japan Geoscience Union Meeting 2009*, S152-P024.

62) Murai, Y., Akiyama, S., Katsumata, K., Takanami, T., Yamashina, T., Watanabe, T., Cho, I., Tanaka, M., Kuwano, A., Wada, N., Shimamura, H., Furuya, I., Zhao, D., and Sanda, R. (2002): “Collision structure beneath the Hidaka Mountains deduced from observations with ocean bottom seismometers and land stations", *Chikyu Monthly*, **24-**7, 495-498 (in Japanese).

63) Murotani, T., Kikuchi, M., and Yamanaka, Y. (2003): “Source process of the 1982 Ibaraki ken oki earthquake inferred from JMA strong motion records", *Seismological Society of Japan 2003 Fall Meeting*, P029 (in Japanese).

64) Murotani, S., Miyake, H. and Koketsu, K. (2008): “Scaling of characterized slip models for plate-boudary earthquakes", *Earth Planets Space*, **60**, 987-991.

65) Nagoya University (2008): “Source process of Off-Ibaraki earthquake on May 8, 2008 (Mj6,4, 7.0)", *Report of the Coordinating Committee for Earthquake Prediction, Japan*, **80**, 101-110 (in Japanese).

66) Nagoya City (1999): *Heisei 10 nendo jishin kankei kiso chosa kofukin: Tenpaku-kako danso ni kansuru chosa seika hokokusho* (FY1998 Subsidy for basic survey related to earthquakes: Report on the research results concerning the Tenpaku-kako fault), 119pp. (in Japanese).

67) Nakata, T. and Imaizumi, T. ed. (2002): *Digital Active Fault Map of Japan*, University of Tokyo Press (in Japanese).

68) Okumura, T. and Ishikawa, Y. (1998): “Katsudanso no katsudo-do kara suitei sareru heikin hen’i sokudo ni kansuru kento” (Study on the average displacement velocity inferred from the activity level of an active fault), *The 53rd Annual Conference of the Japan Society of Civil Engineers*, Part I (B), 554-555 (in Japanese).

69) Satake, K. (1986): “Re-examination of the 1940 Shakotan-oki Earthquake and the Fault Parameters of the Earthquakes along the Eastern Margin of the Japan Sea", *Phys. Earth Planet. Inter.*, **43**, 137-147.

70) Written and edited by Sato, R. (1989): *Handbook of Parameters of Seismic Faults in Japan*, Kajimia Institute Publishing, 390pp. (in Japanese).

71) Sato, T. (1985): “Rupture Characteristics of the 1983

Nihonkai-chubu (Japan Sea) Earthquake as Inferred from Strong Motion Accelerograms", *J. Phys. Earth*, **33**, 525-557.

72) Subcommittee for Survey and Observation Plans, Policy Committee (2003): “Plan for Strengthening Survey and Observation of the Tonankai/Nankai Earthquakes [First Report]", June 26, 2003.

73) Si, H. and Midorikawa, S.(1999): “New Attenuation Relationships for Peak Ground Acceleration and Velocity Considering Effects of Fault Type and Site Condition", *Journal of structural and construction engineering (Transactions of AIJ)*, **523**, 63-70 (in Japanese with English abstract).

74) Property and Casualty Insurance Rating Organization (2000): “Katsudanso to rekishi jishin towo koryo shita jishin kikendo hyoka no kenkyu: Jishin hazado mappu no teian” (Research on seismic hazard evaluation taking into consideration active faults and historical earthquakes: Proposal for seismic hazard maps), *Research report for earthquake insurance*, 47 (in Japanese).

75) Takemura, M. (1990): “Magnitude-seismic moment relations for the shallow earthquakes in and around Japan", *Journal of the Seismological Society of Japan* (Second Series), **43**, 257-265 (in Japanese with English abstract).

76) Tanioka, Y., Satake, K. and Ruff, L.(1995): “Total Analysis of the 1993 Hokkaido Nansei-oki Earthquake Using Seismic Wave, Tsunami, and Geodetic Data", *Geophys. Res. Lett.*, **22-**1, 9-12.

77) Uehira, K., Shimizu, H., Matsuo, N., and Goto, K. (2001): “The Detailed Structure of the Deep Seismic Zone and Focal Mechanism Solutions from the Western End of Chugoku Shikoku District to the Kyushu District)", *Chikyu Monthly*, **23**-10, 669-673 (in Japanese).

78) Umino, N., Hasegawa, A. and Takagi, A. (1990): “The Relationship between Seismicity Patterns and Fracture Zones beneath Northeastern Japan", *Tohoku Geophys. Jour.*, **33-**2, 149-162.

79) Usami, T. (1996): *Materials for Comprehensive List of Destructive Earthquakes in Japan, 416-1995: Revised and Enlarged Edition*, University of Tokyo Press, 493pp. (in Japanese).

80) Utsu, T. and Seki, A. (1955): “A Relation Between the Area of After-shock Region and the Energy of Main-shock", *Journal of the Seismological Society of Japan* (Second Series), **7,** 233-240 (in Japanese with English abstract).

81) Utsu, T. (1982): “Catalog of Large Earthquakes in the Region of Japan from 1885 through 1980", *Bulletin of the Earthquake Research Institute, University of Tokyo*, **57,** 401-463 (in Japanese with English abstract).

82) Utsu, T. (1985): “Catalog of Large Earthquakes in the Region of Japan from 1885 through 1980 [Revision and addition]", *Bulletin of the Earthquake Research Institute, University of Tokyo*, **60,** 639-642 (in Japanese with English abstract).

83) Utsu, T. (2001): *Jishingaku (Dai 3 pan)* (Seismology [Third edition]), Kyoritsu Shuppan, 392pp. (in Japanese).

84) Wakamatsu, K. and Matsuoka, M. (2008): “Development of nationwide GIS-based 7.5-arc-second Japan Engineering Geomorphologic Classification Map”, *Proceedings of the 6th annual meeting of Japan Association for Earthquake Engineering*, 222-223 (in Japanese).

4. Seismic Hazard Maps (SHM) for Specified Seismic Source Faults

4.1 Procedure and Results of Evaluation and Presentation Method

4.1.1 Target earthquakes

The Seismic Hazard Maps (SHM) for Specified Seismic Source Faults target characteristic earthquakes that have undergone long-term evaluation as indicated in Chapter 2. For target earthquakes that occur in major active fault zones, inner source parameters are determined, and strong motion waveform simulation is carried out using the detailed method. In addition, calculation using the conventional method (the method using an attenuation relation) is also carried out. Fault zones of which the length in the long-term evaluation is less than 20 km, which are excluded from application of the Recipe, are excluded from target earthquakes here since the method for determining the outer/inner source parameters has not been established. However, if the occurrence probability in the long-term evaluation is high, the calculation is made for such earthquakes by exceptionally applying the current Recipe. For subduction-zone earthquakes, not a waveform simulation using the detailed method, but only a strong motion simulation using the conventional method is carried out, since the method for determining the inner source parameters is still in the process of improvement, and subsurface structure models such as the deep subsurface structure are insufficient both qualitatively and quantitatively in the sea area.

4.1.2 Outline of the evaluation method

Strong motion simulation using the detailed method targeting major active fault zones is carried out following the procedures indicated in the Recipe. The brief outline is as shown below.

1) Outer/inner source parameters and subsurface structure models (crustal structure model for the seismic bedrock and deeper, deep subsurface structure model) are determined.
2) The strong motion waveforms on the "engineering bedrock in the detailed method" are simulated.
3) Ground motions on the ground surface are evaluated based on the shallow subsurface structure model.

Meanwhile, the brief outline of the strong motion simulation using the conventional method is as shown below.

i) Outer source parameters are determined.
ii) Ground motions on the "engineering bedrock in the detailed method" are calculated based on an attenuation relation.
iii) Ground motions on ground surface are evaluated based on the shallow subsurface structure model.

Here, ground with a shear wave velocity of 600m/s is defined as the "engineering bedrock in the detailed method", and is distinguished from the engineering bedrock (ground with a shear wave velocity of 400m/s) used for PSHM that was discussed in the previous chapter.

4.1.3 Method for presenting the results

As the results of simulation using the detailed method, the distribution of the peak ground velocity on the "engineering bedrock in the detailed method" and the distribution of the seismic intensity on the ground surface are shown on maps. In addition, major sites are selected from within the area covered by the map, and the velocity waveforms on the "engineering bedrock in the detailed method" as well as the pseudo velocity response spectrum (attenuation: 5%) in the mesh containing the municipal office of that site are indicated.

As the results of simulation using the conventional method, the distribution of the seismic intensity on the ground surface and the distribution of the probabilities that the target earthquake would generate ground motions with seismic intensity 5 Lower or more, seismic intensity 5 Upper or more, seismic intensity 6 Lower or more, and seismic intensity 6 Upper or more are shown on maps.

4.2 Areas Covered by the SHM and Its Specifications

4.2.1 Areas covered by the SHM

The areas covered by the SHM for Specified Seismic Source Faults are determined separately for each target fault zone. A map created by using the detailed method covers a rectangular area including locations within a horizontal distance of about 50 km from the edges of the fault. The target area generally encompasses an area where an earthquake of around *M*7 occurring in a major active fault zone is assumed to generate ground motions of intensity 5 Upper according to the prediction results using an attenuation relation. While taking into consideration the locational relationships with the seismic source fault and the population, ten cities are selected from within the area covered by the map as major sites, and the waveforms on the engineering bedrock as well as the pseudo velocity response spectrum (attenuation: 5%) in the meshs containing the municipal offices of those cities are indicated.

The area covered by maps using the conventional method is a rectangular area, slightly wider than in the map using the detailed method, which generally encompasses an area where the seismic intensity will be 5 Lower. The area for an earthquake in a major active fault zone and that for a subduction-zone earthquake is a rectangular area including locations within a horizontal distance of 80 km and 300 km, respectively, from the edges of the fault.

4.2.2 Map specifications

For the SHM using the detailed method, the following maps are created as a set for each target fault zone:

- Topographic map and map of the fault plane locations
- Comparison with the attenuation relation by Si and Midorikawa (1999) for the peak velocity on the "engineering bedrock in the detailed method"

- Distribution of the peak velocity on the "engineering bedrock in the detailed method"
- Distribution of the seismic intensity on the "engineering bedrock in the detailed method"
- Distribution of the site amplification factor for JMA seismic intensity from the "engineering bedrock in the detailed method" to the ground surface
- Distribution of the seismic intensity on ground surface

For the SHM using the conventional method, the following maps are created as a set:

- Topographic map and map of the fault plane locations
- Geomorphologic classification map
- Distribution of the peak velocity on the "engineering bedrock in the detailed method"
- Distribution of the amplification factor for the peak ground velocity from the "engineering bedrock in the detailed method" to the ground surface
- Distribution of the peak ground velocity on ground surface
- Distribution of the seismic intensity the ground surface
- Distribution of probability that the target earthquake would generate ground motions of a specific seismic intensity or more (conditional exceedance probability, four types: JMA seismic intensity 5 Lower or more, JMA seismic intensity 5 Upper or more, JMA seismic intensity 6 Lower or more, and JMA seismic intensity 6 Upper or more)

In all of the maps above, the site for evaluating the ground motions on the ground surface is the center of each quarter mesh (about 250 m × 250 m), which is one-sixteenth of the Third mesh (about 1 km × 1 km), within the target area. However, the site for evaluating the ground motions on the "engineering bedrock in the detailed method" is the center of each 1 km mesh. The latitudes and longitudes of the maps are based on the Tokyo Datum before the revision of the Survey Act.

4.3 Determination of the Inner Source parameters and Others of Characteristic Earthquakes Occurring in Major Active Fault Zones

In order to carry out a strong motion simulation using the detailed method, inner source parameters and others are determined for major active fault zones of which the length in the long-term evaluation is 20 km or more, according to the standardized method described in the Recipe (note: the version updated on April 11, 2008), based on the outer source parameters determined in Chapter 2. The determined parameters are summarized in Table 4.3-1. The details are described below.

4.3.1 Determination of inner source parameters

Figure 4.3.1-1 shows the overall flow of the determination process. The method for determining individual parameters is as follows.

a) Locations and number of asperities

The following principles were formulated for determining the locations of asperities by the standardized modeling method applicable nationwide.

○ Regarding the depth (fault width) direction:

- The asperity is positioned in the middle.
- The asperity is not positioned in the shallowest or deepest fault model mesh.
- Where the mesh in the background area is odd-numbered, the asperity is moved toward the shallower direction from the middle.

○ Regarding the length (strike) direction:

- Where the distribution of displacement has been indicated in the long-term evaluation, the asperity is positioned so that a place with a large displacement comes to be middle.
- Where such information does not exist, the asperity is positioned in the central part of the fault plane.
- The asperity is not positioned in the meshs at both ends of the fault model.

The number of asperities is determined based on the fault segments. If the active segment has been divided in the long-term evaluation, such divided parts are replaced as segments. If the fault model length is 60 km or more, the model is divided into two segments, referring to the descriptions in the long-term evaluation. If a fault model cannot be divided based on the long-term evaluation, the length of the fault model is roughly halved as segments for strong motion simulation. If the fault has an bending point, the fault is divided into segments at the inflexion point. In any other cases, a single fault zone shall be a single segment. If the segment length is less than 25 km, one asperity is allocated. If the length is 30 km or more, two asperities are allocated, and if the length is 25km to 30km, either one or two asperities are allocated. If a fault zone consists of a single segment and the segment length is 25km to 30km, two models are built: one with one asperity, and the other with two asperities.

b) Total size of the asperities S_a [km^2]

The total size of the asperities is obtained from the short-period level A (N・m/s^2) of the acceleration source spectrum, in principle. The short-period level is calculated by using the empirical relation with seismic moment M_0 (N・m) by Dan et al. (2001) (Formula (11) of the Recipe)

$$A = 2.46 \times 10^{10} \times (M_0 \times 10^7)^{1/3} \tag{4.3-1}$$

(Irikura et al., 2002). Where the asperity is assumed to be circular, its equivalent radius r (km) is obtained by

$$r = \frac{7\pi}{4} \cdot \frac{M_0}{A \cdot R} \cdot \beta^2 \tag{4.3-2}$$

(Formula (12) of the Recipe) where R (km) is the radius supposing that the whole fault model has been replaced with a circle of an equivalent size, and β (km/s) is the shear wave velocity within the seismogenic layer. As a result, the total size of the asperities can be obtained by

$$S_a = \pi r^2 \tag{4.3-3}$$

In the case of a fault zone (such as the Uozu fault zone) where bending two fault planes are joined underground, the simulation is made by determining the inner source parameters for both the original size and the smaller size that excludes the overlapping part.

Where the fault model length is extremely larger than the fault model width, such as in the case of a super-long fault, if the total size of the asperities is obtained through the procedure above, its percentage to the size of the whole fault plane may differ substantially from the value indicated by an empirical relation, the 22% indicated by Somerville et al. (1999), the 15-37% indicated by Miyakoshi et al. (2001), or the 37% indicated by Ishii et al. (2000). This means that it is not appropriate to assume the whole fault plane to be circular in shape (Earthquake Research Committee, 2005). Therefore, in such case, the total size of the asperities is assumed to be 22% of the size of the whole seismic source fault model S_{model}, based on Somerville et al. (1999).

If one segment has two asperities, the ratio of their size shall be 2:1 based on the research results of Ishii and Sato (2000). When presenting individual asperities in the fault model meshs, the asperities are determined to be in a shape close to a square of which the size is insofar as possible no smaller than the size obtained above. The length/width of the asperity shall be roughly around 1.0 to 1.5.

c) Average slip of the asperities/background area D_a, D_b [m]

The average slip of all asperities D_a is obtained by using the following formula (Formula (15) of the Recipe) where D_a is ξ times the average slip of the whole seismic source fault model D_{model} (m)

$$D_a = \xi \cdot D_{model} \tag{4.3-4}$$

while applying ξ=2 based on Somerville et al. (1999) and Ishii et al. (2000). The slip of the background area D_b is calculated by the following formulas (Formulas (16) to (18) of the Recipe) after deriving the seismic moment of the background area M_{0b} (N・m) which excludes seismic moment of the asperity M_{0a} (N・m) from seismic moment of the whole fault M_0 (N・m):

$$M_{0a} = \mu \cdot D_a \cdot S_a \tag{4.3-5}$$

$$M_{0b} = M_0 - M_{0a} \tag{4.3-6}$$

$$D_b = \frac{M_{0b}}{\mu \cdot S_b} = \frac{M_{0b}}{\mu \cdot (S_{model} - S_a)} \tag{4.3-7}$$

Here, μ is the rigidity of the seismogenic layer (see Formula (2.1.2-10), and Formula (10) of the Recipe). If there are multiple asperities, the slip of each asperity D_{ai} is calculated by the following formula (Formula (19) of the Recipe)

$$D_{ai} = \frac{\gamma_i}{\sum \gamma_i^3} \cdot D_a \tag{4.3-8}$$

$$\gamma_i = \frac{r_i}{r} \tag{4.3-9}$$

d) Static stress drop and effective stress of the whole seismic source fault and asperity, and the effective stress of the background area $\Delta\sigma$, $\Delta\sigma_a$, σ_a, σ_b [MPa]

In the case of a fault for which a circular fracture plane can be assumed, the static stress drop of the whole seismic source fault and the asperity ($\Delta\sigma$ and $\Delta\sigma_a$) are obtained by the following formulas based on Eshelby (1957) (Formulas (21-2) and (20-2) of the Recipe)

$$\Delta\sigma = \frac{7}{16} \cdot \frac{M_0}{R^3} \tag{4.3-10}$$

$$\Delta\sigma_a = \frac{7}{16} \cdot \frac{M_0}{r^2 \cdot R} \tag{4.3-11}$$

However, for fault zones such as a super-long fault for which the total size of the asperities is assumed to be 22% of the total size of the whole fault plane and for which a circular fracture plane cannot be assumed, the static stress drop of the asperity is determined by the following formula by Madariaga (1979) (Formula (20-1) of the Recipe):

$$\Delta\sigma_a = \frac{S_{model}}{S_a} \cdot \Delta\sigma \quad (\fallingdotseq 14.1 \text{ MPa}) \tag{4.3-12}$$

assuming $\Delta\sigma$=3.1 MPa by applying the research results of Fujii and Matsu'ura (2000).

If there are multiple asperities, unless detailed information on the source area is available, the stress drop of each asperity is deemed to coincide with the stress drop of overall asperities, and the effective stress of the asperities (σ_a) is deemed to be equal to the static stress drop.

The effective stress of the background area (σ_b) is, based on Dan et al. (2002), expressed as

$$\sigma_b = \frac{D_b}{W_b} \cdot \frac{W_a}{D_a} \cdot \sigma_a \tag{4.3-13}$$

(Formula (22) of the Recipe) when the segment has one asperity, and expressed as

$$\sigma_b = \frac{D_b}{W_b} \cdot \frac{\sqrt{\pi}}{D_a} \cdot r \cdot \left(\sum \gamma_i^3\right) \cdot \sigma_a \qquad (4.3\text{-}14)$$

(Formula (23) of the Recipe) when the segment has multiple asperities. Here, γ_i is given by Formula (4.3-9), W_a (km) is the asperity width, and W_b (km) is the width in the case of assuming the background area to be rectangular.

e) f_{max} [Hz]

f_{max} is, as defined by Hanks (1982), the frequency at which an acceleration spectrum begins to fall off at high frequencies. The value that has been used in the strong motion simulation targeting active faults, which is f_{max}=6Hz proposed by Tsurugi et al. (1997), is also used here for all fault zones subject to simulation.

f) Average rupture velocity V_r [km/s]

Average rupture velocity V_r is, unless detailed information on the target area is available, determined by the following empirical relation with the shear wave velocity of the seismogenic layer β (km/s) proposed by Geller (1976) (Formula (24) of the Recipe):

$$V_r = 0.72 \cdot \beta \qquad (4.3\text{-}15)$$

4.3.2 Determination of other source parameters

A) Rupture starting point

Though it is desirable to model the rupture starting point based on the branching of active faults proposed by Nakata et al. (1998), the branching is unclear for many fault zones at present. Here, the rupture starting point is determined based on the basic case in the Recipe (Figure 4.3.2-1). Specifically, if the strike-slip component is dominant, the starting points are assumed to be at the corners of the lower edge of the asperity. If there is only one asperity, the starting points are at both corners of the lower edge, and if there are multiple asperities, two cases are assumed where the starting point is at the outside corner of the lower edge of either of the asperities at far ends. If the dip-slip component is dominant (normal fault, reverse fault), the starting points are assumed to be in the middle of the lower edge of the asperity. If there are multiple asperities, the same number of cases as the number of asperities are assumed where the rupture starting point is in the middle of the lower edge of any one of the asperities.

B) Rupture pattern

The rupture is assumed to propagate radially from the rupture starting point at a specific rupture velocity V_r. Between different segments, the rupture is assumed to propagate radially from the spot where the rupture reaches first. However, if the dip angle differs between segments, the rupture is assumed to propagate from the spot at the same depth as the rupture starting point and where the rupture reaches first.

A total of 490 cases have been modeled for 167 fault zones. Fault zones that are treated as exceptions to the standardized method (e.g., the stress drop for the whole seismic source fault is obtained by Formula (4.3-12)) are those indicated with colored background in Table 4.3-1. With regard to the Kannawa/Kozu-Matsuda fault and the Fujikawa-kako fault zone, no inner source parameters are determined, and no simulation using the detailed method is carried out, since the earthquake magnitude is too large against the fault length indicated in the long-term evaluation. The long-term evaulations for these fault zones mention that the relationship between the fault zones and subduction-zone earthquakes is a matter that requires further study.

For details of each fault model, see the list of parameters and the schematic drawings compiled at the end of this study report. Since each model is expressed in 2 km square meshs, note that the finally determined seismic moment may differ slightly from the value initially obtained.

Table 4.3-1 Parameters used in strong motion simulation using the detailed method for major active fault zones (part 1)

		Whole fault															All asperities				Background are	
		L	M	M_0	M_w	S	W	D_{us}	D_{ls}	d	L_{model}	W_{model}	S_{model}	D_{model}	Ds	A	S_a	D_a	Ds_a	S_a/S	S_b	D_b
		km		N·m		km^2	km	km	km	deg.	km	km	km^2	m	MPa	N·m/s^2	km^2	m	MPa		km^2	m
0101	Shibetsu fault zone	52	7.7	5.26E+19	7.1	972.2	18.7	3	15	45	56	18	1008	1.7	4.0	1.99E+19	277.6	3.4	14.5	0.28	730.4	1.0
0201	Tokachi-heiya fault zone (main part)	84	-	2.26E+20	7.5	2016.0	24.0	4	19	45	84	24	2016	3.6	3.1	-	443.5	—	14.1	0.22	1572.5	—
0202	Kochien fault	26	7.2	1.36E+19	6.7	495.1	19.0	3	20	45	28	18	504	0.9	2.9	1.27E+19	91.6	1.8	16.1	0.18	412.4	0.7
9901	Sarobetsu fault zone	44	7.6	3.80E+19	7.0	826.0	18.8	7	25	30	44	18	792	1.5	4.1	1.78E+19	227.0	3.0	14.5	0.29	565.0	0.9
0301	Furano fault zone (western part)	27	7.2	1.47E+19	6.7	513.4	19.0	2	15	45	28	18	504	0.9	3.1	1.30E+19	102.1	1.8	15.5	0.20	401.9	0.7
0302	Furano fault zone (eastern part)	25	7.2	1.26E+19	6.7	476.1	19.0	2	15	45	28	18	504	0.8	2.7	1.23E+19	81.7	1.6	16.7	0.16	422.3	0.6
0401	Mashike-sanchi-toen fault zone	60	7.8	6.96E+19	7.2	1118.4	18.6	3	20	45	64	18	1152	1.9	4.4	2.18E+19	353.0	—	14.2	0.31	799.0	—
0402	Numata-Sunagawa area fault zone	38	7.5	2.85E+19	6.9	716.1	18.8	3	20	45	40	18	720	1.3	3.6	1.62E+19	172.0	2.6	15.1	0.24	548.0	0.9
0501	Tobetsu fault	20	7.0	8.17E+18	6.5	383.3	19.2	3	20	40	22	18	396	0.7	2.5	1.07E+19	58.1	1.4	17.3	0.15	337.9	0.5
0601	Ishikari-teichi-toen fault zone (main part)	66	—	1.23E+20	7.3	1487.0	—	7	30	45	68	24	1487	2.7	5.2	2.64E+19	581.1	5.4	13.3	0.39	905.9	0.9
0602	Ishikari-teichi-toen fault zone (southern part)	23	7.1	1.07E+19	6.6	439.2	19.1	7	30	30	24	18	432	0.8	2.9	1.17E+19	78.5	1.6	16.0	0.18	353.5	0.6
0701	Kuromatsunai-teichi fault zone	32	7.3	2.04E+19	6.8	605.9	18.9	2	15	45	34	18	612	1.1	3.3	1.45E+19	128.7	2.2	15.6	0.21	483.3	0.8
0801	Hakodate-heiya-seien fault zone	24	7.1	1.17E+19	6.6	457.9	19.1	2	15	45	26	18	468	0.8	2.8	1.20E+19	81.7	1.6	16.1	0.17	386.3	0.6
0901	Aomori-wan-seigan fault zone	31	7.3	1.92E+19	6.8	587.5	19.0	3	18	60	32	18	576	1.1	3.4	1.42E+19	128.7	2.2	15.2	0.22	447.3	0.7
1001	Tsugaru-sanchi-seien fault zone (northern part)	16	6.8	5.28E+18	6.4	313.9	19.6	3	18	45	18	18	324	—	—	—	—	—	—	—	—	—
1002	Tsugaru-sanchi-seien fault zone (southern part)	23	7.1	1.07E+19	6.6	439.2	19.1	3	18	45	24	18	432	0.8	2.9	1.17E+19	78.5	1.6	16.0	0.18	353.5	0.6
1101	Oritsume fault	47	7.6	4.32E+19	7.0	881.2	18.7	2	15	45	48	18	864	1.6	4.1	1.86E+19	248.8	3.2	14.4	0.29	615.2	1.0
10101	Hanawa-higashi fault zone	19	7.0	7.40E+18	6.5	393.0	20.7	3	15	45	20	20	400	—	—	—	—	—	—	—	—	—
1201	Noshiro fault zone	22	7.1	9.84E+18	6.6	420.6	19.1	3	18	45	24	18	432	0.7	2.7	1.14E+19	69.4	1.4	16.7	0.16	362.6	0.6
1301	Kitakami-teichi-seien fault zone	62	7.8	7.42E+19	7.2	1155.2	18.6	3	14	35	64	18	1152	2.1	4.7	2.23E+19	387.1	—	13.8	0.34	764.9	—
1401	Shizukuishi-bonchi-seien fault zone	17	6.9	5.95E+18	6.4	339.7	20.0	2	14	45	18	18	324	—	—	—	—	—	—	—	—	—
1402	Mahiru-sanchi-toen fault zone (northern part)	21	7.0	8.98E+18	6.6	401.8	19.1	3	17	40	22	18	396	0.7	2.8	1.10E+19	66.5	1.4	16.6	0.17	329.5	0.6
1403	Mahiru-sanchi-toen fault zone (southern part)	17	6.9	5.95E+18	6.4	339.7	20.0	3	19	45	18	18	324	—	—	—	—	—	—	—	—	—
1501	Yokote-bonchi-toen fault zone (northern part)	26	7.2	1.36E+19	6.7	495.1	19.0	3	17	25	28	18	504	0.9	2.9	1.27E+19	91.6	1.8	16.1	0.18	412.4	0.7
1502	Yokote-bonchi-toen fault zone (southern part)	30	7.3	1.80E+19	6.8	568.8	19.0	3	15	45	32	18	576	1.0	3.2	1.39E+19	116.9	2.0	15.7	0.20	459.1	0.7
1601	Kitayuri fault	30	7.3	1.80E+19	6.8	568.8	19.0	3	24	45	32	18	576	1.0	3.2	1.39E+19	116.9	2.0	15.7	0.20	459.1	0.7
1701	Shinjo-bonchi fault zone	23	7.1	1.07E+19	6.6	439.2	19.1	3	20	45	24	18	432	0.8	2.9	1.17E+19	78.5	1.6	16.0	0.18	353.5	0.6
1801	Yamagata-bonchi fault zone (northern part)	29	7.3	1.69E+19	6.8	550.7	19.0	4	16	45	30	18	540	1.0	3.3	1.36E+19	113.1	2.0	15.6	0.21	426.9	0.7
1802	Yamagata-bonchi fault zone (southern part)	31	7.3	1.92E+19	6.8	587.5	19.0	4	16	45	32	18	576	1.1	3.4	1.42E+19	128.7	2.2	15.2	0.22	447.3	0.7
1901	Shonai-heiya-toen fault zone	38	7.5	2.85E+19	6.9	716.1	18.8	3	20	45	40	18	720	1.3	3.6	1.62E+19	172.0	2.6	15.1	0.24	548.0	0.9
2001	Nagamachi-Rifu-sen fault zone	40	7.5	3.15E+19	6.9	752.7	18.8	3	16	40	42	18	756	1.3	3.7	1.67E+19	186.3	2.6	15.0	0.25	569.7	0.9
2101	Fukushima-bonchi-seien fault zone	57	7.8	6.30E+19	7.1	1064.1	18.7	2	15	45	60	18	1080	1.9	4.4	2.11E+19	333.3	—	14.0	0.31	746.7	—
2201	Nagai-bonchi-seien fault zone	51	7.7	5.06E+19	7.1	954.1	18.7	2	15	45	54	18	972	1.7	4.1	1.96E+19	271.7	3.4	14.6	0.28	700.3	1.0
2301	Futaba fault	40	7.5	3.15E+19	6.9	752.7	18.8	2	19	90	42	18	756	1.3	3.7	1.67E+19	186.3	2.6	15.0	0.25	569.7	0.9
2401	Aizu-bonchi-seien fault zone	34	7.4	2.30E+19	6.8	642.9	18.9	2	20	45	36	18	648	1.1	3.4	1.51E+19	141.0	2.2	15.6	0.22	507.0	0.8
2402	Aizu-bonchi-toen fault zone	49	7.7	4.68E+19	7.0	917.5	18.7	2	18	45	50	18	900	1.7	4.2	1.91E+19	265.9	3.4	14.3	0.30	634.1	0.9
2501	Kushigata-sanmyaku fault zone	16	6.8	5.28E+18	6.4	313.9	19.6	3	23	45	18	18	324	0.5	2.2	9.23E+18	40.7	1.0	17.5	0.13	283.3	0.5
2601	Tsukioka fault zone	30	7.3	1.80E+19	6.8	568.8	19.0	3	24	55	32	18	576	1.0	3.2	1.39E+19	116.9	2.0	15.7	0.20	459.1	0.7
2701	Nagaoka-heiya-seien fault zone	83	-	2.06E+20	7.5	1925.6	23.2	6	23	55	84	24	2016	3.3	3.1	-	443.5	—	14.1	0.22	1572.5	—
2901	Kamogawa-teichi fault zone	25	7.2	1.26E+19	6.7	476.1	19.0	2	18	90	26	18	468	0.9	3.0	1.23E+19	88.2	1.8	16.1	0.19	379.8	0.6

Table 4.3-1 Parameters used in strong motion simulation using the detailed method for major active fault zones (part 2)

		Whole fault															All asperities				Background are	
		L	M	M_0	M_w	S	W	D_{us}	D_{ls}	d	L_{model}	W_{model}	S_{model}	D_{model}	Ds	A	S_a	D_a	Ds_a	S_a/S	S_b	D_b
		km		N·m		km^2	km	km	km	deg.	km	km	km^2	m	MPa	N·m/s^2	km^2	m	MPa		km^2	m
3001	Sekiya fault	38	7.5	2.85E+19	6.9	716.1	18.8	2	13	30	40	18	720	1.3	3.6	1.62E+19	172.0	2.6	15.1	0.24	548.0	0.9
3101	Kanto-heiya-hokuseien fault zone (main part)	82	-	1.44E+20	7.4	1607.2	19.6	5	20	60	82	20	1640	2.8	3.1	-	360.8	—	14.1	0.22	1279.2	—
3102	Hirai-Kushibiki fault zone	23	7.1	1.07E+19	6.6	439.2	19.1	2	20	90	24	18	432	0.8	2.9	1.17E+19	78.5	1.6	16.0	0.18	353.5	0.6
3401	Tachikawa fault zone	33	7.4	2.17E+19	6.8	624.2	18.9	2	18	90	34	18	612	1.1	3.5	1.48E+19	141.0	2.2	15.1	0.23	471.0	0.8
3501	Isehara fault	21	7.0	8.98E+18	6.6	401.8	19.1	1	15	60	22	18	396	0.7	2.8	1.10E+19	66.5	1.4	16.6	0.17	329.5	0.6
3601	Kannawa/Kozu-Matsuda fault zone	—	7.5	—	—	—	—	3	10	—	—	—	631	—	—	—	—	—	—	—	—	—
3701	Miura-hanto fault group (Kinugasa/Kitatake fault zone of the main part)	14	—	1.41E+19	6.7	—	—	3	15	45	28	18	504	0.9	3.0	1.28E+19	95.0	1.8	16.1	0.19	409.0	0.7
3702	Miura-hanto fault group (Takeyama fault zone of the main part)	11	—	7.21E+18	6.5	—	—	3	15	45	20	18	360	0.6	2.6	1.02E+19	55.4	1.2	16.7	0.15	304.6	0.5
3703	Miura-hanto fault group (southern part)	20	7.0	—	—	—	—	3	15	90	20	12	240	—	—	—	—	—	—	—	—	—
3801	Kitaizu fault zone	32	7.3	2.04E+19	6.8	605.9	18.9	3	11	90	36	10	360	1.8	3.1	-	79.2	3.6	14.1	0.22	280.8	1.3
3901	Tokamachi fault zone (western part)	33	7.4	2.17E+19	6.8	624.2	18.9	5	25	45	34	18	612	1.1	3.5	1.48E+19	141.0	2.2	15.1	0.23	471.0	0.8
3902	Tokamachi fault zone (eastern part)	19	7.0	7.40E+18	6.5	393.0	20.7	5	20	45	20	20	400	—	—	—	—	—	—	—	—	—
10401	Sone-kyuryo fault zone	32	7.3	2.04E+19	6.8	605.9	18.9	2	16	30	34	18	612	1.1	3.3	1.45E+19	128.7	2.2	15.6	0.21	483.3	0.8
4001	Nagano-bonchi-seien fault zone	58	7.8	6.50E+19	7.1	1081.4	18.6	4	18	45	60	18	1080	1.9	4.5	2.13E+19	346.4	3.8	14.0	0.32	733.6	1.0
4101	Itoigawa-Shizuoka-kozosen fault zone (central part/northern part)	112	—	1.50E+20	7.4	—	—	2	15	40 80	62 50	20 14	1240 700	2.5	4.4	2.82E+19	589.6	—	14.1	0.30	1350.4	—
4202	Itoigawa-Shizuoka-kozosen fault zone (southern part)	30	7.3	—	—	—	—	2	15	45	30	20	600	—	—	—	—	—	—	—	—	—
4301	Fujikawa-kako fault zone	20	8.0	—	—	—	—	3	10	45	20	8	160	—	—	—	—	—	—	—	—	—
4501	Kiso-sanmyaku-seien fault zone (northern segment of the main part)	40	7.5	3.15E+19	6.9	752.7	18.8	2	16	40 90	30 14	18 16	540 224	1.3	3.6	1.67E+19	186.3	—	14.9	0.24	577.7	—
4502	Kiso-sanmyaku-seien fault zone (southern segment of the main part)	8	6.3	—	—	—	—	3	20	90	9.4	9	84.6	—	—	—	—	—	—	—	—	—
4503	Seinaiji-toge fault zone	34	7.4	2.30E+19	6.8	642.9	18.9	2	16	90	38	16	608	1.2	3.7	1.51E+19	153.9	2.4	14.8	0.25	454.1	0.8
4601	Sakaitoge/Kamiya fault zone (main part)	47	7.6	4.32E+19	7.0	881.2	18.7	2	16	90	52	16	832	1.7	4.4	1.86E+19	260.2	3.4	14.0	0.31	571.8	0.9
4602	Kiritoyama-Narai fault zone	28	7.2	1.57E+19	6.7	531.7	19.0	2	16	90	32	16	512	1.0	3.3	1.33E+19	109.4	2.0	15.4	0.21	402.6	0.7
4701	Atotsugawa fault zone	69	7.9	9.13E+19	7.2	1281.4	18.6	2	16	90	74	16	1184	2.5	5.5	2.39E+19	490.9	—	13.2	0.41	693.1	—
4801	Kokufu fault zone	27	—	8.55E+18	6.6	—	—	2	17	90	28	14	392	0.7	2.7	1.08E+19	63.6	1.4	16.5	0.16	328.4	0.6
4802	Takayama fault zone	48	—	2.51E+19	6.9	—	—	2	17	90	48	14	672	1.2	3.5	1.55E+19	153.9	2.4	15.3	0.23	518.1	0.8
4803	Inohana fault zone	24	—	6.28E+18	6.5	—	—	2	17	90	24	14	336	0.6	2.5	9.78E+18	50.3	1.2	16.7	0.15	285.7	0.5
4901	Ushikubi fault zone	54	7.7	5.67E+19	7.1	1009.6	18.7	2	16	90	58	16	928	2.0	4.9	2.04E+19	333.3	4.0	13.6	0.36	594.7	0.8
5001	Shokawa fault zone	67	7.9	8.63E+19	7.2	1245.7	18.6	2	15	90	72	14	1008	2.7	3.1	-	221.8	—	14.1	0.22	786.2	—
5101	Inadani fault zone (main part)	79	8.0	1.19E+20	7.3	1462.3	18.5	2	20	70	80	18	1440	2.6	5.3	2.61E+19	581.1	—	13.1	0.40	858.9	—
5102	Inadani fault zone (southeastern part)	32	7.3	2.04E+19	6.8	605.9	18.9	2	20	60	34	18	612	1.1	3.3	1.45E+19	128.7	2.2	15.6	0.21	483.3	0.8
5201	Atera fault zone (northern segment of the main part)	17	6.9	5.95E+18	6.5	339.7	20.0	2	17	90	20	16	320	0.6	2.5	9.60E+18	47.8	1.2	16.9	0.15	272.2	0.5
5202	Atera fault zone (southern segment of the main part)	60	7.8	6.96E+19	7.2	1118.4	18.6	2	17	90	64	16	1024	2.2	5.1	2.18E+19	394.1	—	13.4	0.38	629.9	—
5203	Sami fault zone	25	7.2	1.26E+19	6.7	476.1	19.0	2	17	90	28	16	448	0.9	3.3	1.23E+19	95.0	1.8	15.3	0.21	353.0	0.7
5204	Shirakawa fault zone	31	7.3	1.92E+19	6.8	587.5	19.0	2	17	90	34	16	544	1.1	3.7	1.42E+19	132.7	2.2	15.1	0.24	411.3	0.8
5301	Byobuyama fault zone	15	6.8	4.65E+18	6.4	288.5	19.2	2	22	60	20	18	360	—	—	—	—	—	—	—	—	—
5302	Akako fault zone	23	7.1	1.07E+19	6.6	439.2	19.1	2	20	60	24	18	432	0.8	2.9	1.17E+19	78.5	1.6	16.0	0.18	353.5	0.6
5303	Enasan-Sanageyama-kita fault zone	60	7.8	6.96E+19	7.2	1118.4	18.6	2	20	40 90	38 22	18 18	684 396	2.1	4.8	2.18E+19	380.1	—	13.7	0.35	699.9	—

Table 4.3-1 Parameters used in strong motion simulation using the detailed method for major active fault zones (part 3)

		Whole fault															All asperities				Background are	
		L	M	M_0	M_w	S	W	D_{us}	D_{ls}	d	L_{model}	W_{model}	S_{model}	D_{model}	Ds	A	S_a	D_a	Ds_a	S_a/S	S_b	D_b
		km		N·m		km^2	km	km	km	deg.	km	km	km^2	m	MPa	N·m/s^2	km^2	m	MPa		km^2	m
5304	Sanage-Takahama fault zone	51	7.7	5.06E+19	7.1	954.1	18.7	2	22	65	52	18	936	1.7	4.3	1.96E+19	153.9	—	31.4	0.16	782.1	—
5305	Kagiya fault zone	35	7.4	2.43E+19	6.9	661.4	18.9	2	16	60	38	18	684	1.1	3.3	1.54E+19	145.3	—	15.6	0.21	538.7	—
10501	Uozu fault zone	32	7.3	2.04E+19	6.8	605.9	18.9	3	18	43	34	18	612	1.1	3.3	1.45E+19	128.7	—	15.6	0.21	483.3	—
5501	Ochigata fault zone	44	7.6	3.80E+19	7.0	826.0	18.8	2	18	30	46	18	828	1.5	3.9	1.78E+19	221.7	3.0	14.5	0.27	606.3	0.9
5601	Tonami-heiya fault zone(western part)	26	—	1.82E+19	6.8	572.0	—	4	20	45	26	22	572	1.0	3.2	1.39E+19	116.9	2.0	15.9	0.20	455.1	0.8
5602	Tonami-heiya fault zone (eastern part)	21	7.0	8.98E+18	6.6	401.8	19.1	4	20	45	22	18	396	0.7	2.8	1.10E+19	66.5	1.4	16.6	0.17	329.5	0.6
5603	Kurehayama fault zone	22	—	2.42E+19	6.9	659.6	—	4	20	45	30	22	660	1.2	3.5	1.53E+19	149.6	2.4	15.4	0.23	510.4	0.8
5701	Morimoto/Togashi fault zone	26	—	1.13E+19	6.6	450.7	—	4	18	45	26	20	520	0.7	2.3	1.19E+19	69.4	1.4	17.3	0.13	450.6	0.6
5801	Fukui-heiya-toen fault zone (main part)	45	7.6	3.97E+19	7.0	845.1	18.8	2	17	90	48	16	768	1.7	4.6	1.81E+19	254.5	3.4	13.8	0.33	513.5	0.8
5802	Fukui-heiya-toen fault zone (western part)	33	7.4	2.17E+19	6.8	624.2	18.9	2	17	90	36	16	576	1.2	3.9	1.48E+19	149.6	2.4	14.8	0.26	426.4	0.8
5901	Nagaragawa-joryu fault zone	29	7.3	1.69E+19	6.8	550.7	19.0	2	17	90	32	16	512	1.1	3.5	1.36E+19	120.8	2.2	15.0	0.24	391.2	0.7
6001	Nukumi fault zone (northwestern part)	16	6.8	5.28E+18	6.4	313.9	19.6	2	13	90	20	12	240	—	—	—	—	—	—	—	—	—
6002	Nukumi fault zone (southeastern part)	21	7.0	8.98E+18	6.6	401.8	19.1	2	18	90	22	18	396	0.7	2.8	1.10E+19	66.5	1.4	16.6	0.17	329.5	0.6
6003	Nobi fault zone (Neodani fault zone of the main part)	30	7.3	1.80E+19	6.8	568.8	19.0	2	15	90	34	14	476	1.2	4.2	1.39E+19	141.0	2.4	14.3	0.30	335.0	0.7
6004	Nobi fault zone (Umehara fault zone of the main part)	36	7.4	2.57E+19	6.9	679.5	18.9	2	19	90	40	18	720	1.1	3.3	1.56E+19	149.6	2.2	15.6	0.21	570.4	0.9
6005	Nobi fault zone (Mitabora fault zone of the main part)	19	7.0	7.40E+18	6.5	393.0	20.7	2	19	90	22	18	396	—	—	—	—	—	—	—	—	—
6006	Ibigawa fault zone	24	7.1	1.17E+19	6.6	457.9	19.1	2	15	90	28	14	392	1.0	3.6	1.20E+19	95.0	2.0	15.1	0.24	297.0	0.6
6007	Mugigawa fault zone	29	7.3	1.69E+19	6.8	550.7	19.0	2	19	90	32	18	576	0.9	3.0	1.36E+19	105.7	1.8	16.3	0.18	470.3	0.7
—	1891 Nobi Earthquake	76	8.0	1.10E+20	7.3	1408.1	18.5	2	22	65	80	14	1120	3.2	3.1	2.54E+19	246.4	—	14.1	0.22	873.6	—
6101	Yanagase/Sekigahara fault zone (northern segment of the main part)	48	7.6	4.50E+19	7.0	899.2	18.7	2	15	40	52	18	936	1.5	3.8	1.88E+19	243.3	3.0	14.7	0.26	692.7	1.0
6102	Yanagase/Sekigahara fault zone (central segment of the main part)	12	6.6	—	—	—	—	2	17	90	13	12	156	—	—	—	—	—	—	—	—	—
6103	Yanagase/Sekigahara fault zone (southern segment of the main part)	45	7.6	3.97E+19	7.0	845.1	18.8	2	17	90	48	16	768	1.7	4.6	1.81E+19	254.5	3.4	13.8	0.33	513.5	0.8
6104	Urazoko-Yanagaseyama fault zone	25	7.2	1.26E+19	6.7	476.1	19.0	2	22	90	26	18	468	0.9	3.0	1.23E+19	88.2	1.8	16.1	0.19	379.8	0.6
6301	Nosaka fault zone	31	7.3	1.92E+19	6.8	587.5	19.0	2	17	90	34	16	544	1.1	3.7	1.42E+19	132.7	2.2	15.1	0.24	411.3	0.8
6302	Shufukuji fault	10	6.5	—	—	—	—	2	17	90	9.6	10	96	—	—	—	—	—	—	—	—	—
6401	Kohoku-sanchi fault zone (northwestern part)	25	7.2	1.26E+19	6.7	476.1	19.0	2	22	90	26	18	468	0.9	3.0	1.23E+19	88.2	1.8	16.1	0.19	379.8	0.6
6402	Kohoku-sanchi fault zone (southeastern part)	16	6.8	5.28E+18	6.4	313.9	19.6	2	16	90	20	16	320	—	—	—	—	—	—	—	—	—
6501	Biwako-seigan fault zone	59	—	5.13E+19	7.1	960.3	—	3	18	70	60	16	960	1.7	4.2	1.97E+19	283.5	3.4	14.2	0.30	676.5	1.0
6701	Yoro-Kuwana-Yokkaichi fault zone	60	7.8	6.96E+19	7.2	1118.4	18.6	2	17	30	62	18	1116	2.0	4.6	2.18E+19	366.4	—	13.9	0.33	749.6	—
6801	Suzuka-toen fault zone	47	7.6	4.32E+19	7.0	881.2	18.7	2	17	60	48	18	864	1.6	4.1	1.86E+19	248.8	3.2	14.4	0.29	615.2	1.0
6901	Suzuka-seien fault zone	44	7.6	3.80E+19	7.0	826.0	18.8	1	20	35	46	18	828	1.5	3.9	1.78E+19	221.7	3.0	14.5	0.27	606.3	0.9
7001	Tongu fault	31	7.3	1.92E+19	6.8	587.5	19.0	1	17	65	32	18	576	1.1	3.4	1.42E+19	128.7	2.2	15.2	0.22	447.3	0.7
7101	Nunobiki-sanchi-toen fault zone (western part)	33	7.4	2.17E+19	6.8	624.2	18.9	2	17	55	34	18	612	1.1	3.5	1.48E+19	141.0	2.2	15.1	0.23	471.0	0.8
7102	Nunobiki-sanchi-toen fault zone (eastern part)	48	7.6	4.50E+19	7.0	899.2	18.7	2	20	45	50	18	900	1.6	4.1	1.88E+19	254.5	3.2	14.4	0.28	645.5	1.0
7201	Kizugawa fault zone	31	7.3	1.92E+19	6.8	587.5	19.0	1	14	50	32	18	576	1.1	3.4	1.42E+19	128.7	2.2	15.2	0.22	447.3	0.7
7301	Mikata fault zone	26	7.2	1.36E+19	6.7	495.1	19.0	1	16	60	28	18	504	0.9	2.9	1.27E+19	91.6	1.8	16.1	0.18	412.4	0.7
7302	Hanaore fault zone (northern part)	26	7.2	1.36E+19	6.7	495.1	19.0	1	20	90	30	18	540	0.8	2.7	1.27E+19	84.9	1.6	16.8	0.16	455.1	0.7
7303	Hanaore fault zone (central-southern part)	35	7.4	2.43E+19	6.9	661.4	18.9	1	20	90	38	18	684	1.1	3.3	1.54E+19	145.3	—	15.6	0.21	538.7	—
7401	Yamada fault zone (main part)	33	7.4	2.17E+19	6.8	624.2	18.9	1	15	90	38	16	608	1.1	3.5	1.48E+19	141.0	2.2	15.2	0.23	467.0	0.8
7402	Gomura fault zone	34	7.4	2.30E+19	6.8	642.9	18.9	1	16	90	38	16	608	1.2	3.7	1.51E+19	153.9	2.4	14.8	0.25	454.1	0.8

Table 4.3-1 Parameters used in strong motion simulation using the detailed method for major active fault zones (part 4)

		Whole fault															All asperities				Bacground area	
		L	M	M_0	M_w	S	W	D_{us}	D_{ls}	d	L_{model}	W_{model}	S_{model}	D_{model}	Ds	A	S_a	D_a	Ds_a	S_a/S	S_b	D_b
		km		N・m		km^2	km	km	km	deg.	km	km	km^2	m	MPa	N・m/s^2	km^2	m	MPa		km^2	m
7501	Nara-bonchi-toen fault zone	35	7.4	2.43E+19	6.9	661.4	18.9	1	15	55	36	18	648	1.2	3.6	1.54E+19	153.9	2.4	15.1	0.24	494.1	0.8
7601	Arima-Takatsuki fault zone	55	7.7	5.87E+19	7.1	1027.4	18.7	1	16	90	60	16	960	2.0	4.8	2.06E+19	339.8	—	13.6	0.35	620.2	—
7701	Ikoma fault zone	38	7.5	2.85E+19	6.9	716.1	18.8	2	15	35	40	18	720	1.3	3.6	1.62E+19	172.0	2.6	15.1	0.24	548.0	0.9
7801	Kanbayashigawa fault	26	7.2	1.36E+19	6.7	495.1	19.0	1	15	90	30	16	480	0.9	3.1	1.27E+19	95.0	1.8	15.9	0.20	385.0	0.7
7802	Mitoke fault	26	7.2	1.36E+19	6.7	495.1	19.0	1	15	90	30	16	480	0.9	3.1	1.27E+19	95.0	1.8	15.9	0.20	385.0	0.7
7803	Kyoto-Nishiyama fault zone	48	7.6	4.50E+19	7.0	899.2	18.7	1	19	90 45	30 18	18 18	540 324	1.7	4.3	1.88E+19	260.2	—	14.3	0.30	603.8	—
7901	Rokko/Awajishima fault zone (Rokko-sanchi-nan'en-Awajishima-togan segment of the main part)	71	7.9	9.67E+19	7.3	1318.2	18.6	1	16	60	74	18	1332	2.3	4.8	2.43E+19	475.3	4.6	13.6	0.36	856.7	1.1
7902	Rokko/Awajishima fault zone (Awajishima-seigan segment of the main part)	23	7.1	1.07E+19	6.6	439.2	19.1	1	16	80	28	16	448	0.8	2.8	1.17E+19	75.4	1.6	16.4	0.17	372.6	0.6
7903	Senzan fault zone	12	6.6	—	—	—	—	1	16	45	11	11	121	—	—	—	—	—	—	—	—	—
8001	Uemachi fault zone	42	7.5	3.47E+19	7.0	790.1	18.8	2	15	70	46	16	736	1.5	4.2	1.73E+19	216.4	3.0	14.4	0.29	519.6	0.9
9701	Ise-wan fault zone (northern segment of the main part)	25	7.2	1.26E+19	6.7	476.1	19.0	3	23	65	26	18	468	0.9	3.0	1.23E+19	88.2	1.8	16.1	0.19	379.8	0.6
9702	Ise-wan fault zone (southern segment of the main part)	17	6.9	5.95E+18	6.4	339.7	20.0	2	19	45	18	18	324	—	—	—	—	—	—	—	—	—
9703	Shiroko-Noma fault	21	7.0	8.98E+18	6.6	401.8	19.1	2	21	60	22	18	396	0.7	2.8	1.10E+19	66.5	1.4	16.6	0.17	329.5	0.6
9801	Osaka-wan fault zone	39	7.5	3.00E+19	6.9	734.7	18.8	4	15	70	44	12	528	1.8	6.0	1.65E+19	248.8	3.6	12.8	0.47	279.2	0.2
8101	Kongo-sanchi-toen-Izumi-sanmyaku-nan'en	72	—	5.19E+19	7.1	966.0	—	4	15	43	72	16	966	1.7	4.2	1.98E+19	283.5	3.4	14.4	0.29	682.5	1.0
8102	Kitan-kaikyo-Naruto-kaikyo	51	7.7	5.06E+19	7.1	954.1	18.7	4	15	30	54	18	972	1.7	4.1	1.96E+19	271.7	3.4	14.6	0.28	700.3	1.0
8103	Sanuki-sanmyaku-nan'en-Ishizuchi-sanmyaku-hokuen-tobu	131	—	3.41E+20	7.6	3196.4	24.4	4	16	35	132	24	3168	3.4	3.1	—	697.0	—	14.1	0.22	2471.0	—
8103	Sanuki-sanmyaku-nan'en-Ishizuchi-sanmyaku-hokuen-tobu*	131	—	5.06E+19	7.4	—	—	4	16	35	136	18	2448	—	3.1	—	538.6	—	14.1	0.22	1909.4	—
8104	Ishizuchi-sanmyaku-hokuen	30	7.3	1.80E+19	6.8	568.8	19.0	4	17	90	34	14	476	1.2	4.2	1.39E+19	141.0	2.4	14.3	0.30	335.0	0.7
8105	Ishizuchi-sanmyaku-hokuen-seibu-Iyonada	129	—	1.81E+20	7.4	1806.0	14.0	4	16	90	130	14	1820	3.2	3.1	—	400.4	—	14.1	0.22	1419.6	—
8105	Ishizuchi-sanmyaku-hokuen-seibu-Iyonada*	129	—	1.66E+20	7.4	—	—	4	16	90	138	14	1932	—	3.1	—	425.0	—	14.1	0.22	1507.0	—
8201	Nagisen fault zone	32	—	3.85E+19	7.0	831.9	—	2	21	45	32	26	832	1.5	3.9	1.79E+19	221.7	3.0	14.6	0.27	610.3	0.9
8202	Yamasaki fault zone (northwestern segment of the main part)	52	—	4.87E+19	7.1	935.7	—	2	21	90	52	18	936	1.7	4.1	1.94E+19	265.9	3.4	14.6	0.28	670.1	1.0
8203	Yamasaki fault zone (southeastern segment of the main part)	30	—	1.62E+19	6.7	539.7	—	2	21	90	30	18	540	1.0	3.2	1.34E+19	109.4	2.0	15.6	0.20	430.6	0.7
-	Yamasaki fault zone (southeastern segment of the main part)/Kusatani fault	44	—	3.49E+19	7.0	792.1	—	2	21	90	44	18	792	1.4	3.8	1.73E+19	206.1	2.8	14.6	0.26	585.9	0.9
-	(Ohara/Hijima/Yasutomi/southeastern segm	80	—	1.15E+20	7.3	1437.9	—	2	21	90	80	18	1440	2.6	3.1	—	316.8	5.2	14.4	0.22	1123.2	1.8
8204	Kusatani fault	13	6.7	—	—	—	—	2	21	90	12	12	144	—	—	—	—	—	—	—	—	—
8401	Nagao fault zone	24	7.1	1.17E+19	6.6	457.9	19.1	3	12	35	26	18	468	0.8	2.8	1.20E+19	81.7	1.6	16.1	0.17	386.3	0.6
8701	Itsukaichi fault	20	7.0	8.17E+18	6.5	383.3	19.2	2	23	90	22	18	396	0.7	2.5	1.07E+19	58.1	1.4	17.3	0.15	337.9	0.5
8702	Koi-Hiroshima-seien fault zone	10	6.5	—	—	—	—	2	25	90	9.7	10	97	—	—	—	—	—	—	—	—	—
8801	Iwakuni fault zone	44	7.6	3.80E+19	7.0	826.0	18.8	2	18	90	46	18	828	1.5	3.9	1.78E+19	221.7	3.0	14.5	0.27	606.3	0.9
9001	Kikukawa fault zone	44	7.6	3.80E+19	7.0	826.0	18.8	2	16	90	48	16	768	1.6	4.4	1.78E+19	237.8	3.2	14.1	0.31	530.2	0.9
10601	Suonada fault zone (main part)	44	7.6	3.80E+19	7.0	826.0	18.8	2	18	90	46	18	828	1.5	3.9	1.78E+19	221.7	3.0	14.5	0.27	606.3	0.9
10602	Akiho-oki fault zone	23	7.1	1.07E+19	6.6	439.2	19.1	2	18	90	24	18	432	0.8	2.9	1.17E+19	78.5	1.6	16.0	0.18	353.5	0.6
10603	Southern Ube-Oki fault zone	22	7.1	9.84E+18	6.6	420.6	19.1	2	18	90	24	18	432	0.7	2.7	1.14E+19	69.4	—	16.7	0.16	362.6	—
9101	Nishiyama fault zone	31	7.3	1.92E+19	6.8	587.5	19.0	2	16	90	36	16	576	1.1	3.4	1.42E+19	128.7	2.2	15.2	0.22	447.3	0.7
9201	Beppu-wan-Hijiu fault zone (eastern part)	43	7.6	3.64E+19	7.0	808.4	18.8	3	14	60	48	14	672	1.7	5.1	1.76E+19	254.5	3.4	13.4	0.38	417.5	0.7
9202	Beppu-wan-Hijiu fault zone (western part)	32	7.3	2.04E+19	6.8	605.9	18.9	3	14	60	36	14	504	1.3	4.4	1.45E+19	158.4	2.6	14.0	0.31	345.6	0.7

Table 4.3-1 Parameters used in strong motion simulation using the detailed method for major active fault zones (part 5)

		Whole fault															All asperities				Background are	
		L	M	M_0	M_w	S	W	D_{us}	D_{ls}	d	L_{model}	W_{model}	S_{model}	D_{model}	Ds	A	S_a	D_a	Ds_a	S_a/S	S_b	D_b
		km		N・m		km^2	km	km	km	deg.	km	km	km^2	m	MPa	N・m/s^2	km^2	m	MPa		km^2	m
9203	Oita-heiya-Yufuin fault zone (eastern part)	27	7.2	1.47E+19	6.7	513.4	19.0	3	14	60	32	14	448	1.0	3.8	1.30E+19	113.1	2.0	15.0	0.25	334.9	0.7
9204	Oita-heiya-Yufuin fault zone (western part)	14	6.7	4.08E+18	6.3	264.2	18.9	3	14	60	18	14	252	0.5	2.4	8.47E+18	36.3	1.0	17.1	0.14	215.7	0.4
9205	Noinedake-Haneyama fault zone	30	7.3	1.80E+19	6.8	568.8	19.0	3	14	60	34	14	476	1.2	4.2	1.39E+19	141.0	2.4	14.3	0.30	335.0	0.7
9206	Kuenohirayama-Kameishiyama fault zone	34	7.4	2.30E+19	6.8	642.9	18.9	3	14	60	38	14	532	1.4	4.6	1.51E+19	176.7	2.8	13.8	0.33	355.3	0.7
9301	Futagawa/Hinagu fault zone (northeastern part)	27	7.2	1.47E+19	6.7	513.4	19.0	3	16	90	32	14	448	1.0	3.8	1.30E+19	113.1	2.0	15.0	0.25	334.9	0.7
9302	Futagawa/Hinagu fault zone (central part)	47	7.6	4.32E+19	7.0	881.2	18.7	3	16	60	52	16	832	1.7	4.4	1.86E+19	260.2	3.4	14.0	0.31	571.8	0.9
9302	Futagawa/Hinagu fault zone (southwestern part)	27	7.2	1.47E+19	6.7	513.4	19.0	3	16	60	32	16	512	0.9	3.1	1.30E+19	98.5	1.8	16.0	0.19	413.5	0.7
9302	a/Hinagu fault zone (central part + southwest	74	7.9	1.05E+20	7.3	1372.6	18.5	3	16	60	84	16	1344	2.5	5.2	2.50E+19	522.8	—	13.3	0.39	821.2	—
10801	Kego fault zone (northwestern part)	25	—	1.12E+19	6.6	—	—	3	19	87	28	16	448	0.8	2.9	1.19E+19	80.0	1.6	16.1	0.18	368.0	0.6
10802	Kego fault zone (southeastern part)	27	7.2	1.47E+19	6.7	513.4	19.0	2	17	90	32	16	512	0.9	3.1	1.30E+19	112.6	1.8	14.1	0.22	399.4	0.7
9401	Minou fault zone	26	7.2	1.36E+19	6.7	495.1	19.0	3	14	60	30	14	420	1.0	3.8	1.27E+19	109.4	2.0	14.8	0.26	310.6	0.7
9501	Unzen fault group (northern part)	30	7.3	1.80E+19	6.8	568.8	19.0	3	18	60	32	18	576	1.0	3.2	1.39E+19	116.9	2.0	15.7	0.20	459.1	0.7
9502	Unzen fault group (southeastern part)	23	7.1	1.07E+19	6.6	439.2	19.1	3	18	60	26	18	468	0.7	2.6	1.17E+19	72.4	1.4	16.7	0.15	395.6	0.6
9503	Unzen fault group (northern segment of the southwestern part)	31	7.3	1.92E+19	6.8	587.5	19.0	3	18	60	34	18	612	1.0	3.1	1.42E+19	116.9	2.0	16.1	0.19	495.1	0.8
9504	Unzen fault group (southern segment of the southwestern part)	23	7.1	1.07E+19	6.6	439.2	19.1	3	18	60	26	18	468	0.7	2.6	1.17E+19	72.4	1.4	16.7	0.15	395.6	0.6
9601	Izumi fault zone	20	7.0	8.17E+18	6.5	383.3	19.2	3	15	45	22	18	396	0.7	2.5	1.07E+19	58.1	1.4	17.3	0.15	337.9	0.5
10901	Hitoyoshi-bonchi-nan'en fault zone	22	7.1	9.84E+18	6.6	420.6	19.1	2	17	60	24	18	432	0.7	2.7	1.14E+19	69.4	1.4	16.7	0.16	362.6	0.6

Notes: For fault zones marked with an asterisk (*), the parameters have been determined by the segmenting and aggregating method (adjustment method II).

Parameters (see also the main text)

L: Fault length　M: Magnitude　M_0: Seismic moment,　M_w: Moment magnitude

S: Fault size　W: Fault plane width　D_{us}: Depth of the upper edge of the fault plane　D_{ls}: Depth of the lower edge of the seismogenic layer

δ: Dip angle of the fault plane　L_{model}: Fault model length　W_{model}: Fault model width　S_{model}: Fault model size

D_{model}: Average slip of the fault model　Δσ: Static stress drop　A: Short-period level of the acceleration source spectrum

S_a: Total asperity size　D_a: Average slip of the asperities　$\Delta\sigma_a$: Static stress drop of the asperity

S_a/S: Rate of asperity size/fault size　S_b: Background area size　D_b: Average slip of the background area

Background color

Purple: Fault treated as a super-long fault.

Light blue: Fault modeled based on the model used in the strong motion evaluation (verification of the strong motion prediction method).

Orange: Fault with multiple segments (the average slip of all asperities and of the background area are not shown since they differ by segment).

Light purple: Fault modeled so that bent fault planes are joined underground (two sets of inner parameters are determined).

Pink: Fault for which Fujii and Matsu'ura (2000) is applied to the static stress drop of the whole fault plane (other than a super-long fault and a model used in the strong motion evaluation).

Green: Fault for which a simulation using the detailed method is carried out (inner parameters are determined by exceptionally extrapolating the Recipe).

Gray: Short fault for which a simulation using the detailed method is not carried out.

Yellow: Fault which uses the model that has been used in the 2005 - 2008 versions of PSHM (a simulation using the detailed method is not carried out).

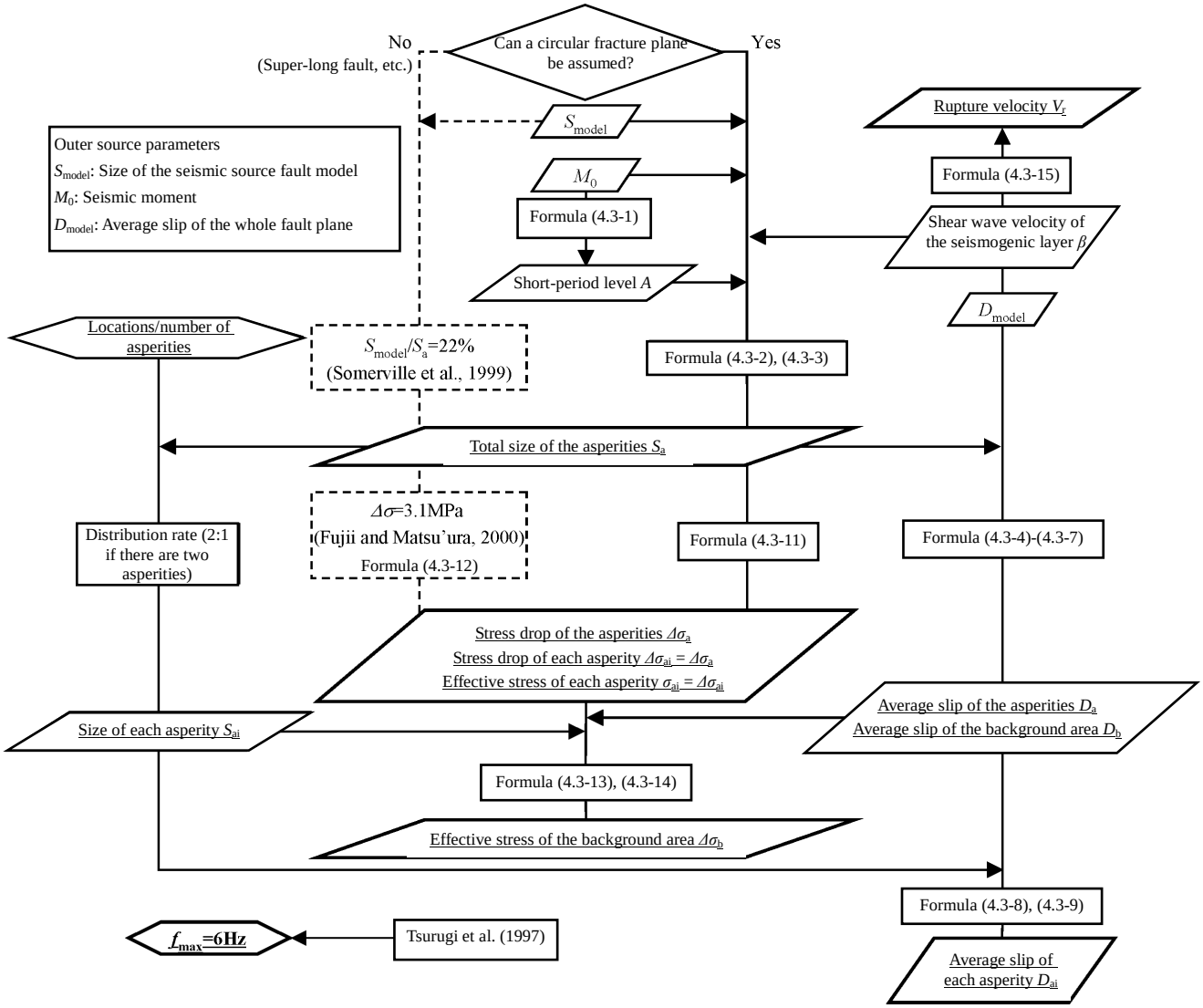

Figure 4.3.1-1 Flow chart of determination of inner source parameters (created based on appended Figure 2 of the Recipe)

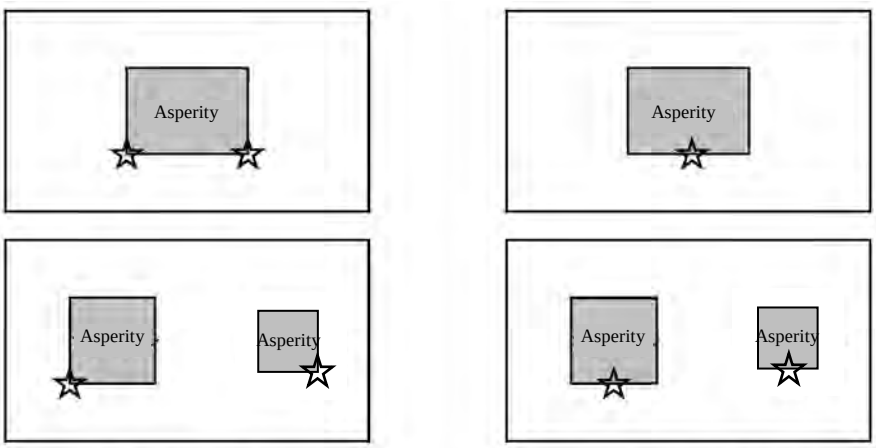

Strike-slip component is dominant. Dip-slip component is dominant.

Example of the positions of the rupture starting points (star) and asperities

Figure 4.3.2-1 Method for determining the rupture starting points (source: Recipe)

4.4 Modeling of Subsurface Structures

As subsurface structure models to be used in the strong motion simulation, the following three types of models are built and applied according to HERP's Recipe: "crustal structure model for the seismic bedrock and deeper", "deep subsurface structure models", and "shallow subsurface structure model" (Figure 4.4-1). The following sections outline each type of models.

4.4.1 Crustal structure of the seismic bedrock and deeper

In conventional SHM, the crustal structure of the seismic bedrock and deeper had been determined by referring to the Conrad discontinuity (boundary between the upper crust and the lower crust) and Moho discontinuity (boundary between the crust and the mantle) by Zhao et al. (1994). Recently, Matsubara et al. (2008) has obtained the detailed 3D velocity structure for the crust and mantle beneath the Japanese archipelago, using the records of NIED's High Sensitivity Seismograph Network Japan (Hi-net). In this study, the three-layer structure shown in Figure 4.4.1-1 and Table 4.4.1-1 is determined as the crustal structure model for the seismic bedrock and deeper, based on the results of Matsubara et al. (2008).

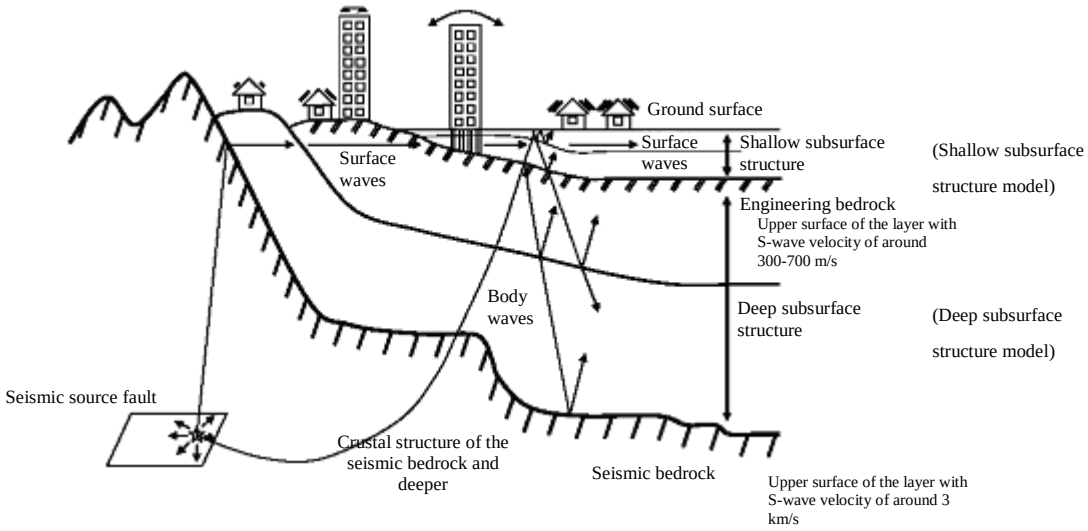

Figure 4.4-1 Schematic drawing of the subsurface structure models (source: Recipe)

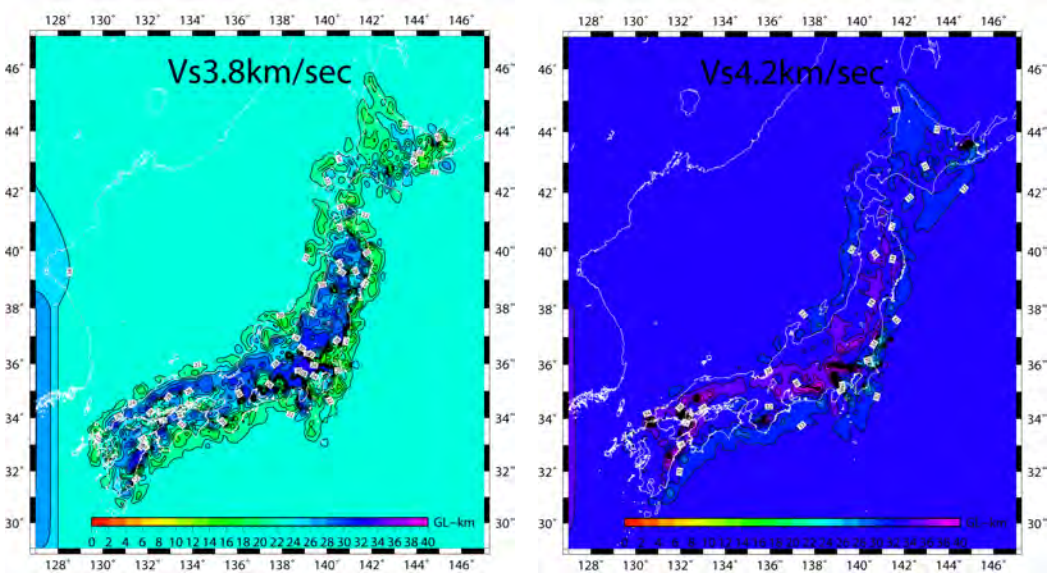

Figure 4.4.1-1 Crustal structure models for the seismic bedrock and deeper based on Matsubara et al. (2008) (distribution of the upper surface depth of each layer)

Table 4.4.1-1 Phydical properties of crustal structure models for the seismic bedrock and deeper. Q values are those at the frequency of 1 Hz used in finite-difference method (see Section 4.5.2)

Classification	Primary wave velocity [km/s]	Shear wave velocity [km/s]	Density [g/cm^3]	Qp, Qs
1	5.8	3.4	2.70	300
2	6.5	3.8	2.80	300
3	7.2	4.2	2.90	300

4.4.2 Deep subsurface structure models

The deep subsurface structure model refers to the ground between the engineering bedrock to the seismic bedrock shown in Figure 4.4-1. When creating the "National Seismic Hazard Maps for Japan", deep subsurface structure models were built for the whole of Japan in order to carry out the strong motion simulation of major active fault zones. These models, which have basically been created by following the procedure in the Recipe and have incorporated models created by past research, etc., are expressed as a 3D structure consisting of 33 layers as shown in Table 4.4.2-1. However, in the strong motion simulation in this study, the "engineering bedrock in the detailed method" is determined to be a layer with shear wave velocity 600m/s. Thus, layers with lower velocity (layer no. 1 to layer no. 5) are not used in the simulation.

Figure 4.4.2-1 shows the distribution of the upper surface depth of each layer. Here, the seismic bedrock is layer no. 29 or a deeper layer. For details about the creation of the deep subsurface structure models, see Fujiwara et al. (2009).

Table 4.4.2-1 Physical properties of deep subsurface structure models. Q values are those at the frequency of 1 Hz used in finite-difference method (see Section 4.5.2) and those used in stochastic Green's function method (constant values)

Layer classification	Primary wave velocity [km/s]	Shear wave velocity [km/s]	Density [g/cm^3]	Qp, Qs	Former layer classification*
1	1.6	0.35	1.85	60	-
2	1.7	0.40	1.85	60	-
3	1.8	0.45	1.9	60	-
4	1.8	0.50	1.9	60	-
5	1.8	0.55	1.9	60	-
6	2.0	0.60	1.9	100	Layer no. 1
7	2.0	0.65	1.95	100	-
8	2.1	0.70	2.0	100	-
9	2.1	0.75	2.0	100	-
10	2.2	0.80	2.0	100	-
11	2.3	0.85	2.05	100	-
12	2.4	0.90	2.05	100	-
13	2.4	0.95	2.1	150	-
14	2.5	1.00	2.1	150	-
15	2.5	1.1	2.15	150	Layer no. 2
16	2.6	1.2	2.15	150	-
17	2.7	1.3	2.2	150	-
18	3.0	1.4	2.25	150	Layer no. 3
19	3.2	1.5	2.25	150	-
20	3.4	1.6	2.3	150	-
21	3.5	1.7	2.3	150	Layer no. 4
22	3.6	1.8	2.35	150	-
23	3.7	1.9	2.35	150	-
24	3.8	2.0	2.4	200	-
25	4.0	2.1	2.4	200	Layer no. 5
26	4.0	2.1	2.4	200	Layer no. 6
27	5.0	2.7	2.5	300	Layer no. 7
28	4.6	2.9	2.55	300	-
29	5.0	2.7	2.5	300	-
30	5.5	3.1	2.6	300	Layer no. 8
31	5.5	3.2	2.65	300	-
32	5.7	3.3	2.7	300	-
33	6.0	3.4	2.75	300	-

*Classification used in the initial models (Fujiwara et al., 2006).

Layer no. 6 (Vs 0.60 km/s) upper surface

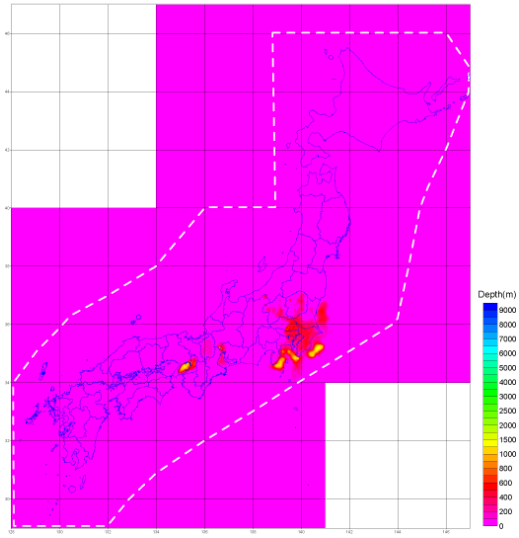

Layer no. 7 (Vs 0.65 km/s) upper surface

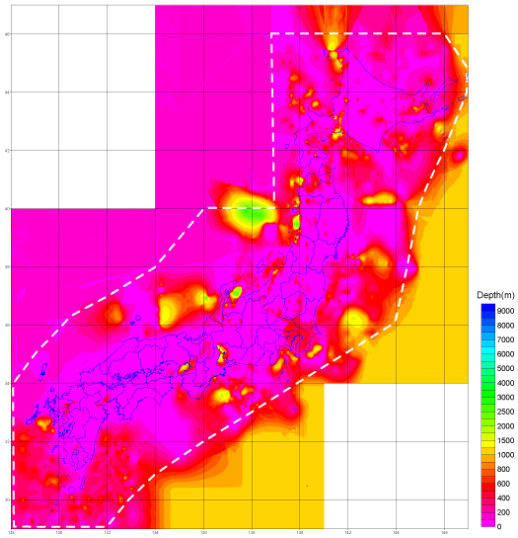

Layer no. 8 (Vs 0.70 km/s) upper surface

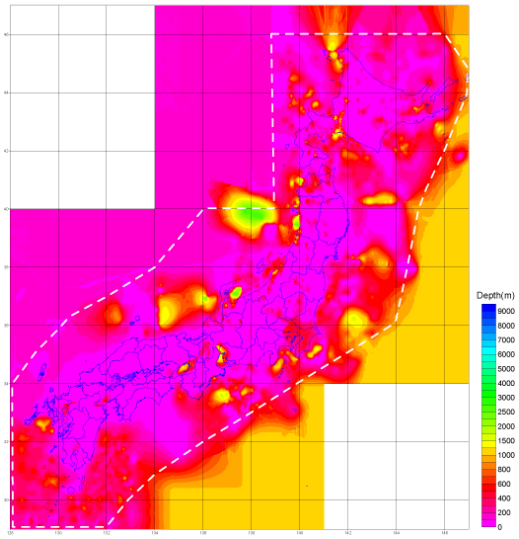

Layer no. 9 (Vs 0.75 km/s) upper surface

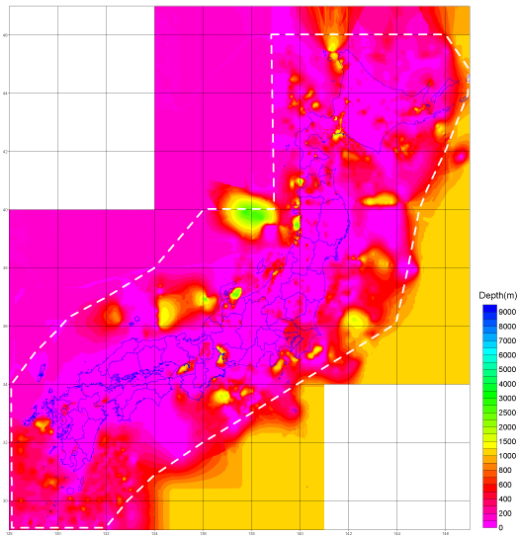

Layer no. 10 (Vs 0.80 km/s) upper surface

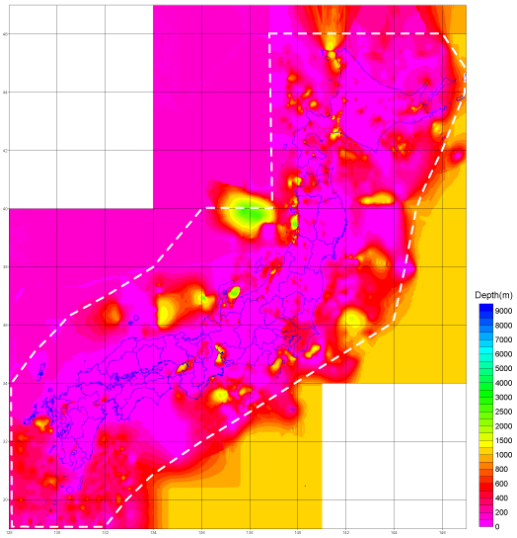

Layer no. 11 (Vs 0.85 km/s) upper surface

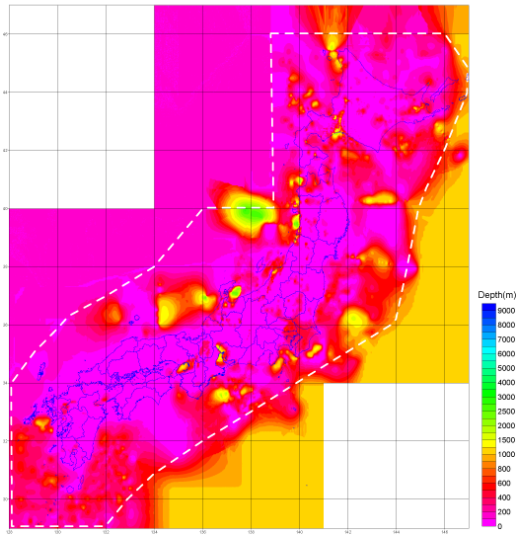

Figure 4.4.2-1 Depth distribution of the upper surface of each layer of the deep subsurface structure models (part 1)

Layer no. 12 (Vs 0.90 km/s) upper surface

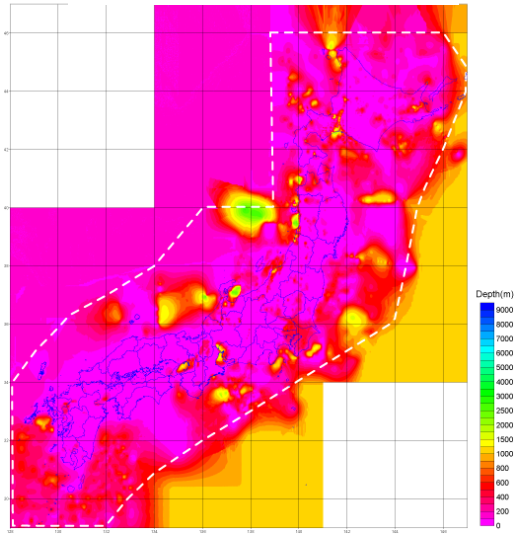

Layer no. 13 (Vs 0.95 km/s) upper surface

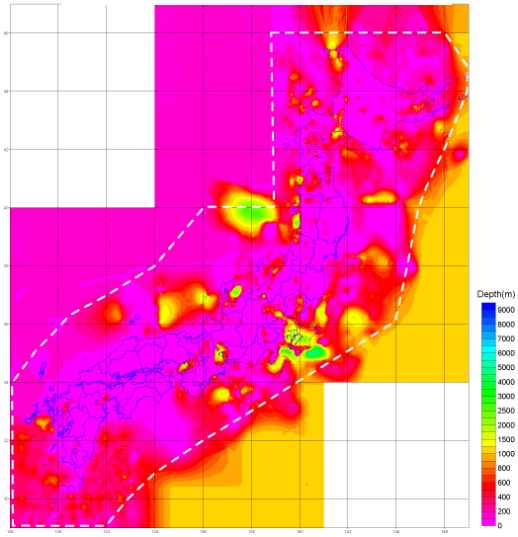

Layer no. 14 (Vs 1.00 km/s) upper surface

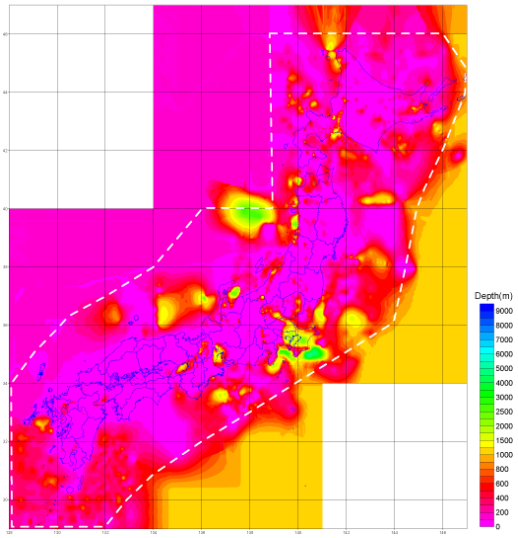

Layer no. 15 (Vs 1.1 km/s) upper surface

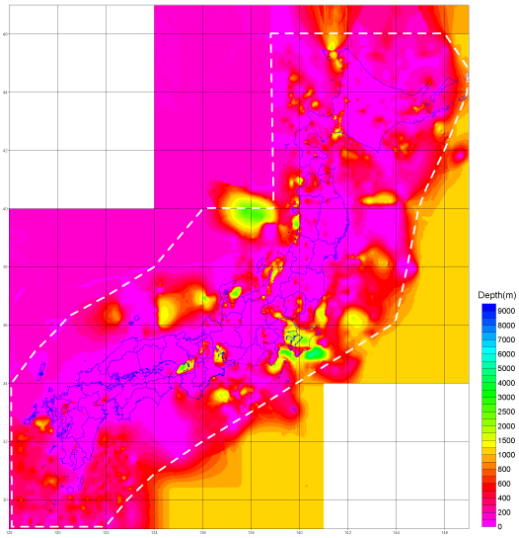

Layer no. 16 (Vs 1.2 km/s) upper surface

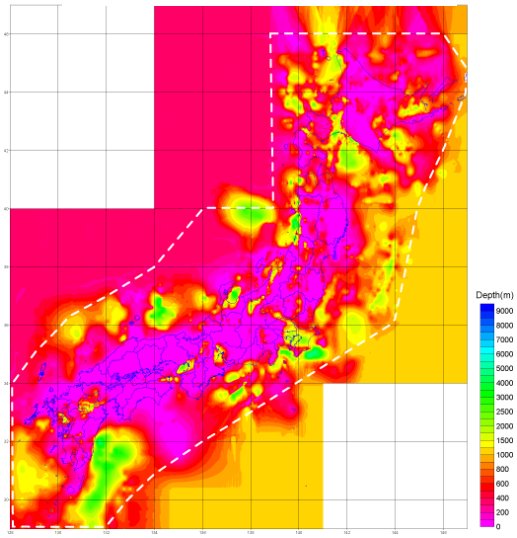

Layer no. 17 (Vs 1.3 km/s) upper surface

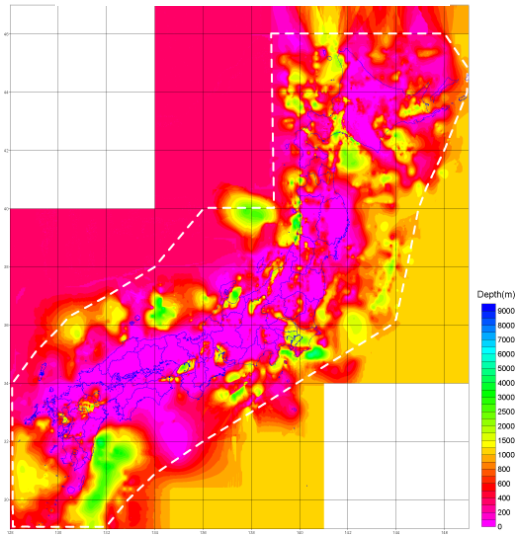

Figure 4.4.2-1 Depth distribution of the upper surface of each layer of the deep subsurface structure models (part 2)

Layer no. 18 (Vs 1.4 km/s) upper surface

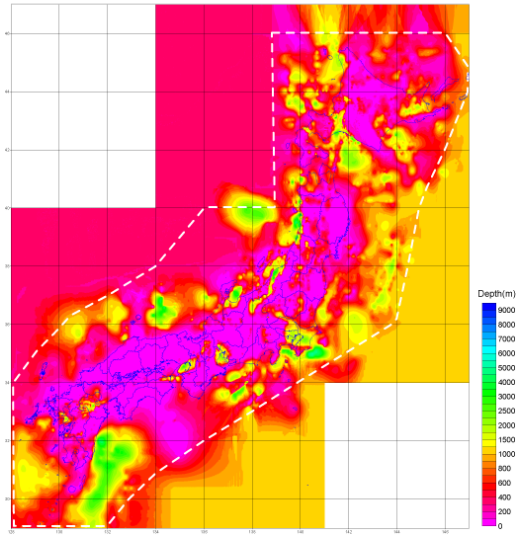

Layer no. 19 (Vs 1.5 km/s) upper surface

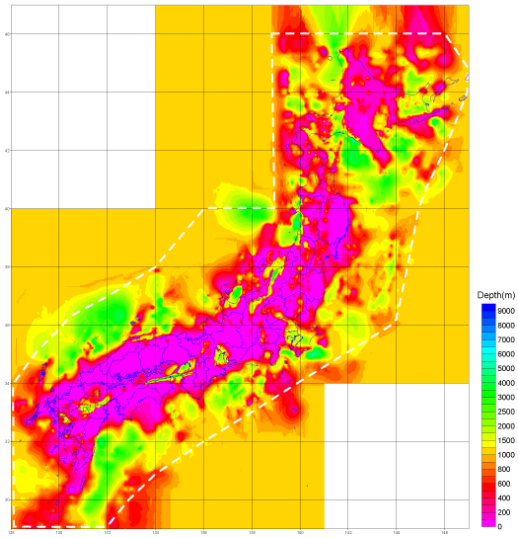

Layer no. 20 (Vs 1.6 km/s) upper surface

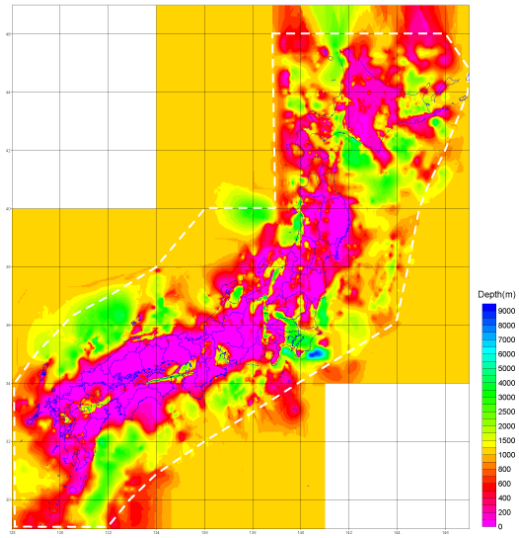

Layer no. 21 (Vs 1.7 km/s) upper surface

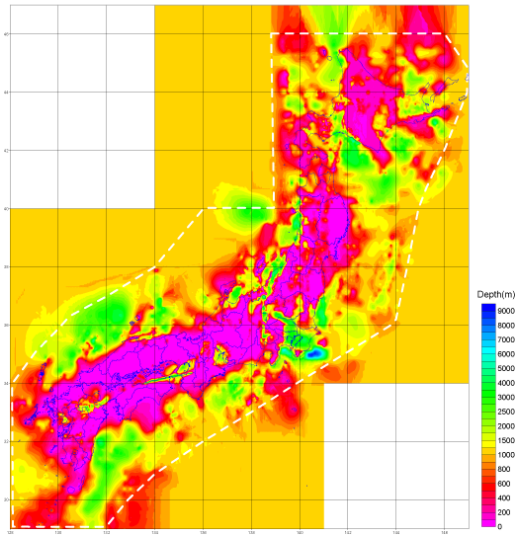

Layer no. 22 (Vs 1.8 km/s) upper surface

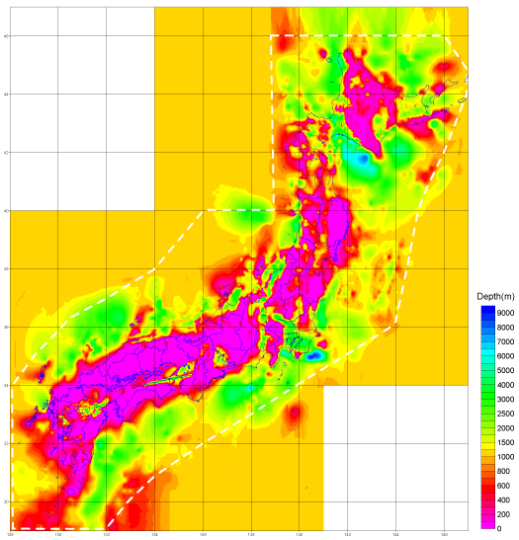

Layer no. 23 (Vs 1.9 km/s) upper surface

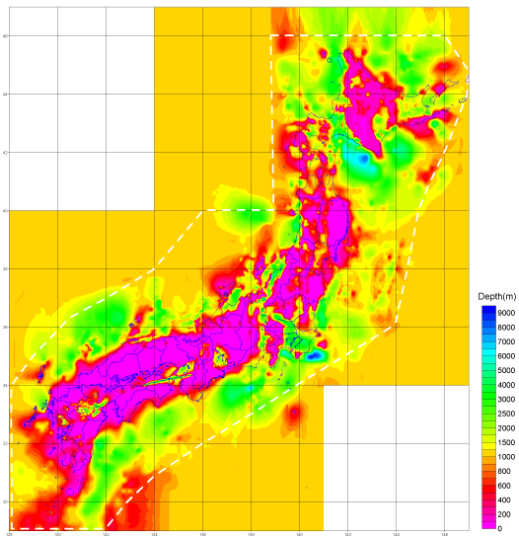

Figure 4.4.2-1 Depth distribution of the upper surface of each layer of the deep subsurface structure models (part 3)

Layer no. 24 (Vs 2.0 km/s) upper surface

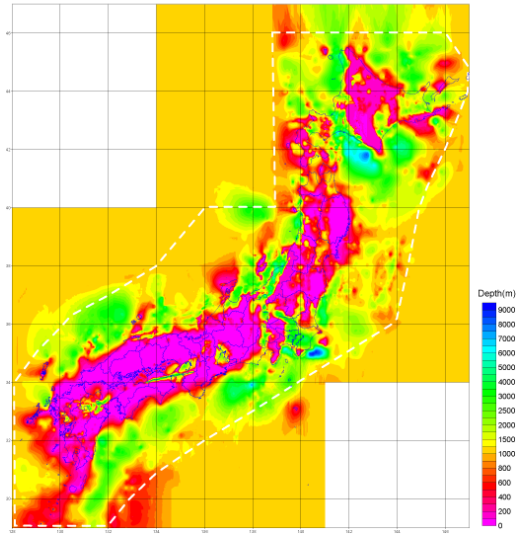

Layer no. 25 (Vs 2.1 km/s) upper surface

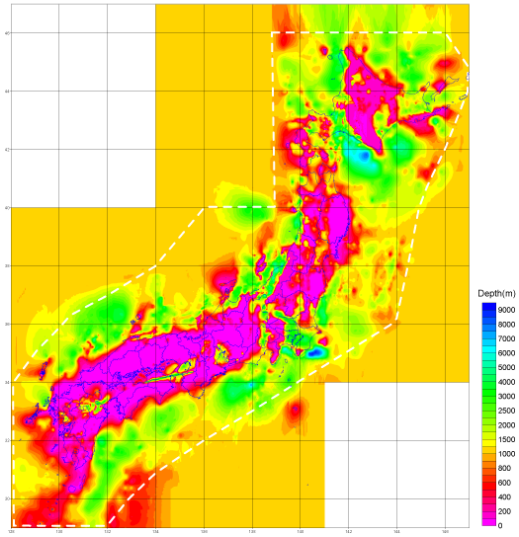

Layer no. 26 (Vs 2.1 km/s) upper surface

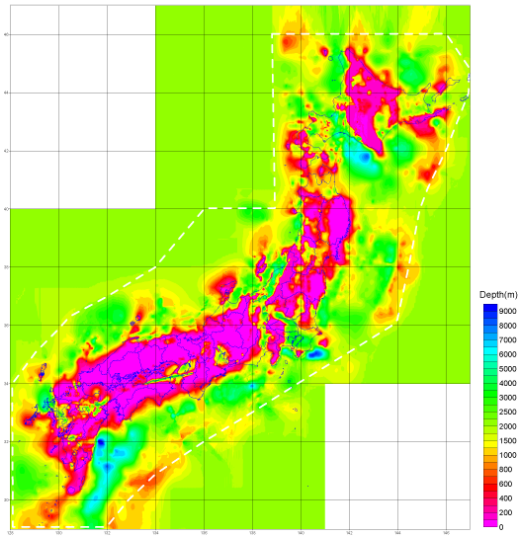

Layer no. 27 (Vs 2.7 km/s) upper surface

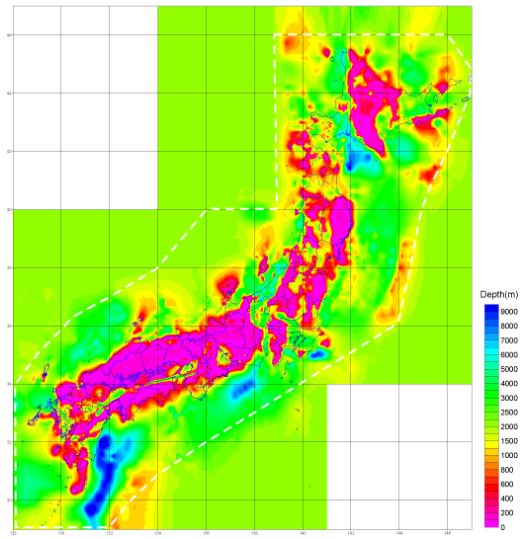

Layer no. 28 (Vs 2.9 km/s) upper surface

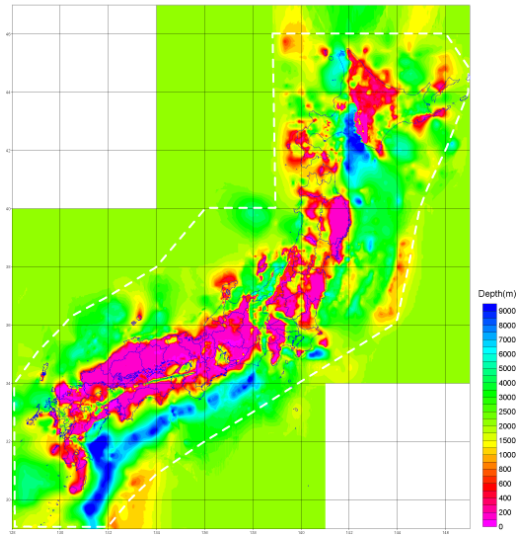

Figure 4.4.2-1 Depth distribution of the upper surface of each layer of the deep subsurface structure models (part 4)

Upper surface of the seismic bedrock

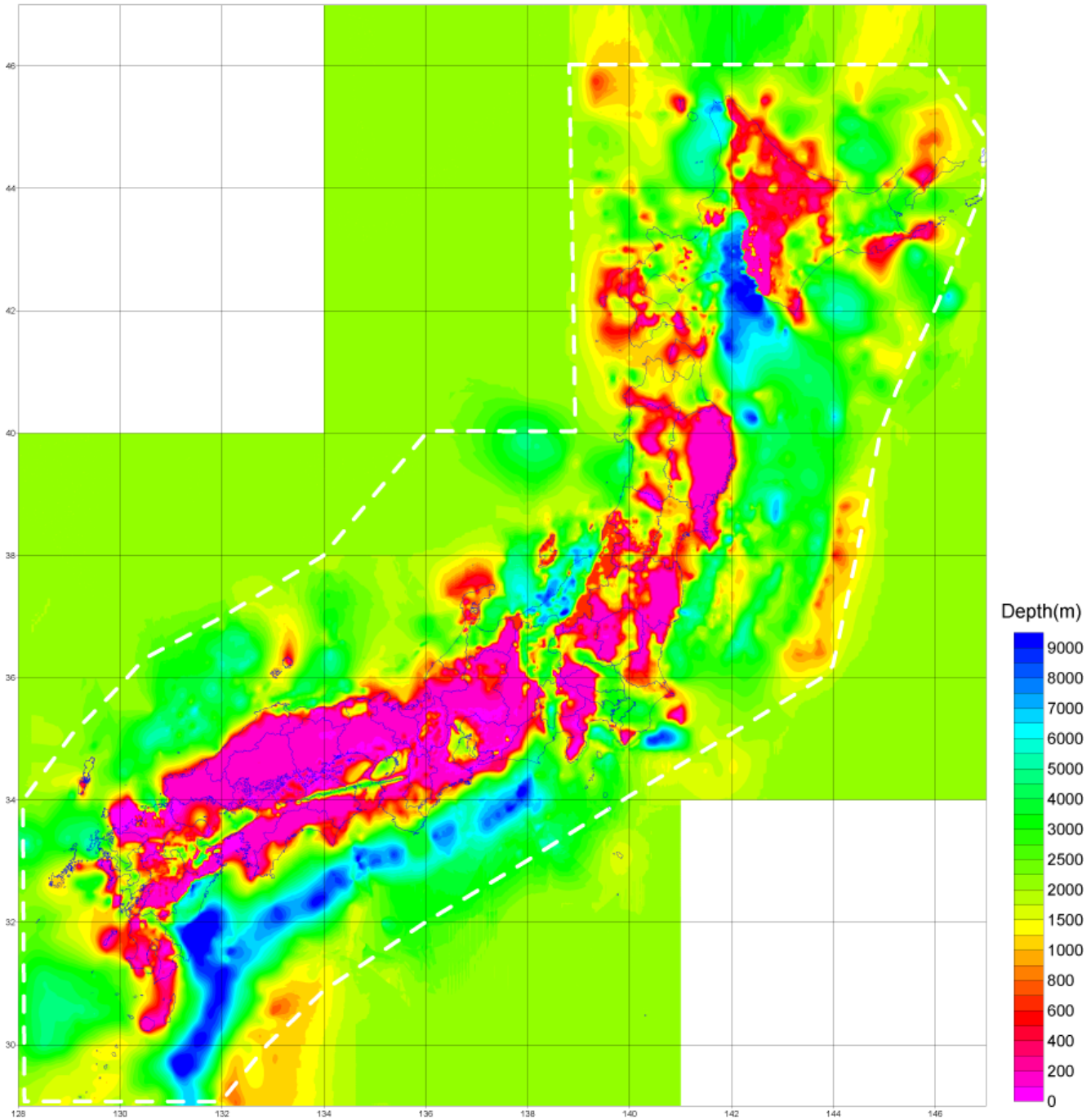

Figure 4.4.2-1 Depth distribution of the upper surface of each layer of the deep subsurface structure models (part 5)

4.4.3 Shallow subsurface structure models

(1) Basic approach

While there are various methods for creating shallow subsurface structure models, ranging from the conventional method to the detailed method, here, the amplification factor of the ground is conentionally obtained by the method for the whole of Japan in a simple manner.

The shallow subsurface structure is evaluated by the following method. First, using the geomorphologic classifications, etc. based on a 250m grid engineering geomorphologic classification map, which is a database expressing the characteristics of shallow subsurface structures of the whole of Japan, distribution of the shear wave velocity (AVS30) from the ground surface to the depth of 30m is inferred. Then, the amplification degree of the ground is obtained from the derived velocity, and finally the ground motion intensity on the ground surface is obtained by multiplying the ground motion intensity (peak ground velocity) on the engineering bedrock by the amplification degree.

(2) The 250 m-grid engineering geomorphologic classification map used for evaluating the amplification factor

Wakamatsu et al. (2004, 2005) proposed engineering geomorphologic classification criteria for classifying the ground conditions of the whole of Japan in a unified manner, by overcoming the problems in the existing geotechnical information databases and, based on those criteria, constructed a GIS database for wide-area hazard evaluation - a 1 km-grid engineering geomorphologic classification map, or, the 30-arc-second Japan Engineering Geomorphologic Classification Map (JEGM). Furthermore, Wakamatsu and Matsuoka (2008) interpreted and stored data on the geomorphologic classification for each 250 m mesh, based on the 30-arc-second JEGM, and constructed a 250 m-grid engineering geomorphologic classification map, or, the 7.5-arc-second JEGM with improved spatial resolution. The 7.5-arc-second JEGM covers areas from Etorofu Island in the north to Okinotori Island in Tokyo Prefecture in the south, and from Yonaguni in the west to Minami-tori Island in the east (20.41875 - 45.5541667 degrees north latitude, 122.934375 - 153.9875 degrees east longitude).

The grid system complies with the quarter grid square under the "Standard Grid Square and Grid Square Code Used for the Statistics" (Announcement No. 143 by the Administrative Management Agency on July, 12, 1973), which is a square grid of 7.5 arc-seconds latitude×11.25 arc-seconds longitude (about 250 m × 250 m). The latitudes and longitudes are in decimal degrees to an accuracy of six decimal places (up to +/- 30 cm). This geographical coordinate system adopts the standard grid square (grid square code N) based on the Tokyo Datum, with different grid square boundary locations from the standard grid square (grid square code) based on the Japanese Geodetic Datum 2000 (JGD2000) which entered into force on April 1, 2002. The reason for the use of the Tokyo Datum was that, because the construction of grid square data was launched in 2002, the JGD2000 version of the required topographic maps on scales of 1:50,000 and 1:25,000 held by the Geospatial Information Authority of Japan were still unavailable at the time.

Each 250 m mesh carries the attributes of the geomorphologic classification indicated in Table 4.4.3-1. This classification complies with the classification criteria proposed by Wakamatsu et al. (2005), which follows purely geomorphologic classification criteria as well as considers an engineering application to evaluating the characteristics of shallow subsurface structures. Since the grid resolution is fine with meshs of about 250 m square, geomorphologic classifications for small areas−"lowland between coastal dunes and/or bars", "rock shore, rock reef", "dry riverbed", and "river bed"−which do not appear on 1 km meshs have been added. When multiple geomorphologic classifications apply to a single mesh, the category that accounts for the largest area within the mesh is determined as the attribute of that mesh, in principle. Only in the case of a valley bottom lowland between mountains or hills, the mesh attribute is determined to be a "valley bottom lowland" as long as the valley bottom lowland accounts for one-third or more of the total area of the mesh, considering that human activity is more active in the valley bottom lowland than in mountains or hills. Even if most of a mesh is a water area, as long as some land exists, however small, the geomorphologic classification for that land area is applied.

In this manner, the geomorphologic classification codes from no. 1 to no. 24 shown in Table 4.4.3-1 have been given to meshs totaling 5,955,179. Figure 4.4.3-1 shows a sample image.

(3) Inference of the average shear wave velocity from the ground surface to the depth of 30 m

In order to infer the average shear wave velocity (AVS30) in the upper 30 m at a given site in any part of Japan, Matsuoka et al. (2005) studied the relation between AVS30 and the geomorphologic classifications by Wakamatsu et al. (2004, 2005) for about 2,000 sites nationwide for which survey data on the shear wave velocity are available. As a result, AVS30 for each geomorphologic classification showed differences that are considered to be attributable to the ground formation process and the sedimentary environment. The study indicated that AVS30 can be inferred with a relatively high accuracy by applying a regression formula which uses the geomorphologic classifications as the basic variable, and elevation, slope gradient, and distance from the mountain or hill of pre-Tertiary period or Tertiary as additional explanatory variables. Further, the study showed that the distribution of AVS30 nationwide can be obtained by using the 30-arc-second JEGM. The regression formula is shown below, and Table 4.4.3-2 shows the regression coefficients and the standard deviation.

$$\log \mathrm{AVS30} = a + b \log E\mathrm{v} + c \log S\mathrm{p} + d \log D\mathrm{m} \pm \sigma \qquad (4.4.3\text{-}1)$$

Here, *a*, *b*, *c*, and *d* are regression coefficients, σ is the standard deviation, *E*v is the elevation (meters), *S*p is the slope gradient (1000 times the tangent), and *D*m is the distance from the mountain or hill of pre-Tertiary period or Tertiary (kilometers).

The regression coefficients in Table 4.4.3-2 generally suggest that the higher the elevation, the steeper the slope gradient, and the shorter the distance from the mountain or hill, AVS30 values become larger. In the upstream region of a river (an area at a high altitude with steep slope gradient), the AVS30 becomes larger as the grain size of deposits is larger, and the closer to the mountain or hill, the shallower the depth to a bedrock. The trend of the obtained regression coefficients is considered to be consistent with the sedimentary environment of the geomorphologic classification.

Formula (4.4.3-1) was originally proposed to infer AVS30 by using the 30-arc-second JEGM. Due to the release of the 7.5-arc-second JEGM which has a finer 250 m resolution, "lowland between coastal dunes and/or bars", "rock shore, rock reef", "dry riverbed", and "river bed", which had not been included in the 1 km grid data, were added as mentioned above (Table 4.4.3-1). Here, "lowland between coastal dunes and/or bars" is treated as "sand dune", and "rock shore, rock reef", "dry riverbed", and "river bed" are excluded from the simulation. Among the geographic indices necessary for AVS30 estimation, elevation (*E*v) and slope gradient (*S*p) use the values from the 30-arc-second JEGM (Wakamatsu et al., 2005). The geochronological information necessary for calculating the distance from the mountain or hill of pre-Tertiary or Tertiary is also extracted from the 30-arc-second JEGM, and where the value of an explanatory variable is 1 or less, the value is fixed at 1. Figure 4.4.3-2 shows the results of the inferred AVS30 distribution.

Table 4.4.3-1 Geomorphologic classification codes and classification criteria (part 1; Wakamatsu and Matsuoka, 2008).

No.	Geomorphologic map unit	Definition and general characteristics	Subsurface soil condition
1	Mountain	Steeply to very steeply sloping topography with highest elevation and relative relief within a mesh of approximately more than 200 m. Moderately to severely dissected.	Pre-Quaternary hard to soft rock.
2	Mountain footslope	Gently sloping topography adjoining mountains and comprised of material sourced from the mountains such as colluvium, talus, landslide, and debris flow deposits.	Loose debris and soils consisting of colluvium, talus, landslide, and debris flow deposits.
3	Hill	Steeply to moderately sloping topography with higher elevation and relative relief within a mesh of approximately 200 m or less. Moderately dissected.	Pre- Quaternary and Quaternary hard to soft rock.
4	Volcano	Steeply to moderately sloping topography with higher elevation and larger relative relief, comprised of Quaternary volcanic rocks and deposits.	Quaternary hard to soft volcanic rock and/or deposits.
5	Volcanic footslope	Gently sloping topography located around skirt of volcano including pyroclastic-, mud- and lava-flow fields, and volcanic fan produced by dissection of volcanic body. Slightly dissected.	Quaternary loose to dense volcanic deposits consisting of ash, scoria, pumice, pyroclastic flow, lava, debris avalanche, etc.
6	Volcanic hill	Moderately sloping topography comprised of pyroclastic flow deposits. Moderately to severely dissected.	Loose to moderately loose pyroclastic flow deposits such as ash, scoria and pumice.
7	Rocky strath terrace	Fluvial or marine terrace with flat surface and step-like form, including limestone terrace of emerged coral reef. Thickness of subsurface soil deposits is less than 5 m.	Hard to soft rock.
8	Gravelly terrace	Fluvial or marine terrace with flat surface and step-like form. Covered with subsurface deposits (gravel or sandy soils) more than 5 m thick.	Dense gravelly soil.
9	Terrace covered with volcanic ash soil	Fluvial or marine terrace with flat surface and step-like form. Covered with cohesive volcanic ash soil of more than 5 m in thickness.	Stiff volcanic ash (cohesive soil).
10	Valley bottom lowland	Long and narrow lowland formed by river or stream between steep to extremely steep slopes of mountain, hill, volcano and terrace.	Moderately dense to dense gravel or boulder in mountain, but loose sandy soil to very soft cohesive soil in plain.

Table 4.4.3-1 Geomorphologic classification codes and classification criteria (part 2; Wakamatsu and Matsuoka, 2008)

No.	Geomorphologic map unit	Definition and general characteristics	Subsurface soil condition
11	Alluvial fan	Semi-cone-like form composed of coarse materials, which is formed at the boundary between mountains and lowland. Slope gradient is more than 1/1000.	Dense gravel with boulders to moderately dense sandy gravel.
12	Natural levee	Slightly elevated area formed along the riverbank by fluvial deposition during floods.	Loose sandy soil.
13	Back marsh	Swampy lowland formed behind natural levees and lowlands surrounded by mountains, hills and terraces.	Very soft cohesive soil containing peat or humus.
14	Abandoned river channels	Swampy shallow depression along former river course with elongate shape.	Very loose sandy soil occasionally covered with soft cohesive soil.
15	Delta and coastal lowland	Delta: flat lowland formed at the river mouth by fluvial accumulation. Coastal lowland: flat lowland formed along shoreline by emergence of shallow submarine deposits, including discontinuous lowlands along sea- or lake- shore.	Loose fluvial sandy soil over-lying very soft cohesive soil.
16	Marine sand and gravel bars	Slightly elevated topography formed along shoreline, composed of sand and gravel, which was washed ashore by ocean wave and/or current action.	Moderately dense to dense marine sand or gravel occasionally with boulder.
17	Sand dune	Wavy topography usually formed along shoreline or river, comprised of fine to moderately aeolian sand, generally overlies sandy lowland.	Very loose to loose fine to medium sand.
18	Lowland between coastal dunes and/or bars	Swampy lowland formed behind dunes or bars	Very soft cohesive soil containing peat or humus.
19	Reclaimed land	Former bottom flat of sea, lake, lagoon, and river that has been reclaimed as land by drainage.	Loose sand overlying very soft cohesive soil, sometimes covered with loose sandy fill.
20	Filled land	Former water body such as sea, lake, lagoon, or river that has been reclaimed as land by drainage.	Very loose to loose sandy fill, overlying very soft cohesive soil or loose sandy soils.
21	Rock shore, Rock reef	Irregular topography of rock or coral around beach zone	Pre- Quaternary and Quaternary hard to soft rock.
22	Dry riverbed	Nearly flat, irregular topography without water in normal time	Moderately dense gravel or very loose sandy soil.
23	River bed	Nearly flat, irregular topography with varying water cover and having erosion and accumulation parts	Water zone.
24	Lake	Inland water body	Water zone.

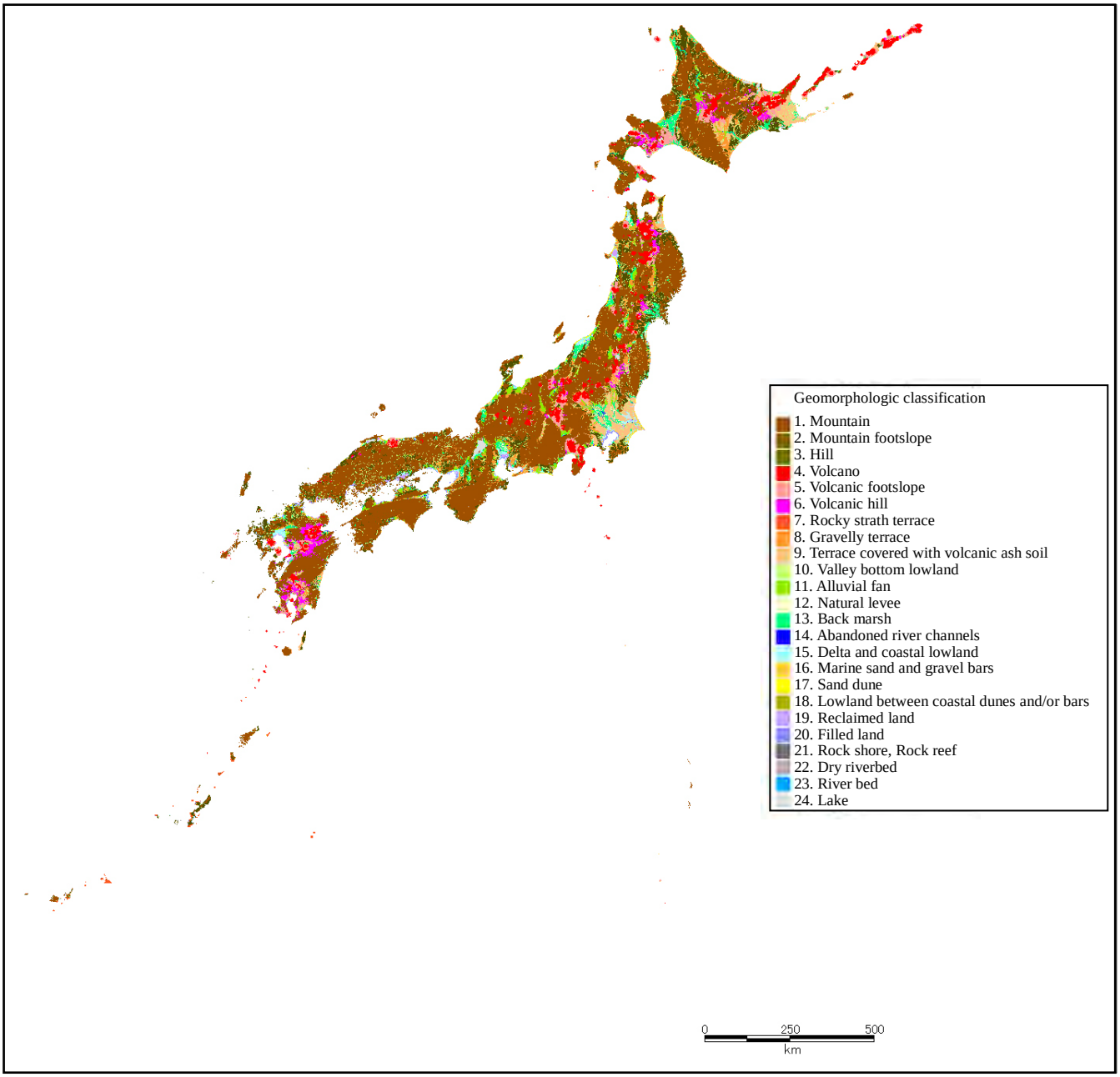

Figure 4.4.3-1 Sample image of the 7.5-arc-second JEGM (Wakamatsu and Matsuoka, 2008).

Table 4.4.3-2 Regression coefficient obtained by multiple linear regression analysis (values in parentheses are standard regression coefficients) (Matsuoka et al., 2005 partially modified)

ID	Geomorphologic classification	Regression coefficient (Standard regression coefficient)				Standard deviation
		a	*b*	*c*	*d*	σ
1p	Mountain (pre-Tertiary)	2.900	0	0	0	0.139
1t	Mountain (Tertiary)	2.807	0	0	0	0.117
2	Mountain footslope	2.602	0	0	0	0.092
3	Hill	2.349	0	0.152 (0.219)	0	0.175
4	Volcano	2.708	0	0	0	0.162
5	Volcanic footslope	2.315	0	0.094 (0.382)	0	0.100
6	Volcanic hill	2.608	0	0	0	0.059
7	Rocky strath terrace	2.546	0	0	0	0.094
8	Gravelly terrace	2.493	0.072 (0.270)	0.027 (0.101)	-0.164 (-0.336)	0.122
9	Terrace covered with volcanic ash soil	2.206	0.093 (0.269)	0.065 (0.223)	0	0.115
10	Valley bottom lowland	2.266	0.144 (0.447)	0.016 (0.040)	-0.113 (-0.265)	0.158
11	Alluvial fan	2.350	0.085 (0.419)	0.015 '0.059)	0	0.116
12	Natural levee	2.204	0.100 (0.368)	0	0	0.124
13	Back marsh	2.190	0.038 (0.178)	0	-0.041 (-0.152)	0.116
14	Abandoned river channels	2.264	0	0	0	0.091
15	Delta and coastal lowland	2.317	0	0	-0.103 (-0.403)	0.107
16	Marine sand and gravel bars	2.415	0	0	0	0.114
17	Sand dune	2.289	0	0	0	0.123
18	Reclaimed land	2.373	0	0	-0.124 (-0.468)	0.123
19	Filled land	2.404	0	0	-0.139 (-0.418)	0.120

$\log AVS30 = a + b\log Ev + c\log Sp + d\log Dm \pm \sigma$

AVS30: Average shear wave velocity (m/s), *Ev*: elevation (m), *Sp*: (tangent of slope) *1000, *Dm*: distance (km) from mountain or hill of pre-Tertiary or Tertiary

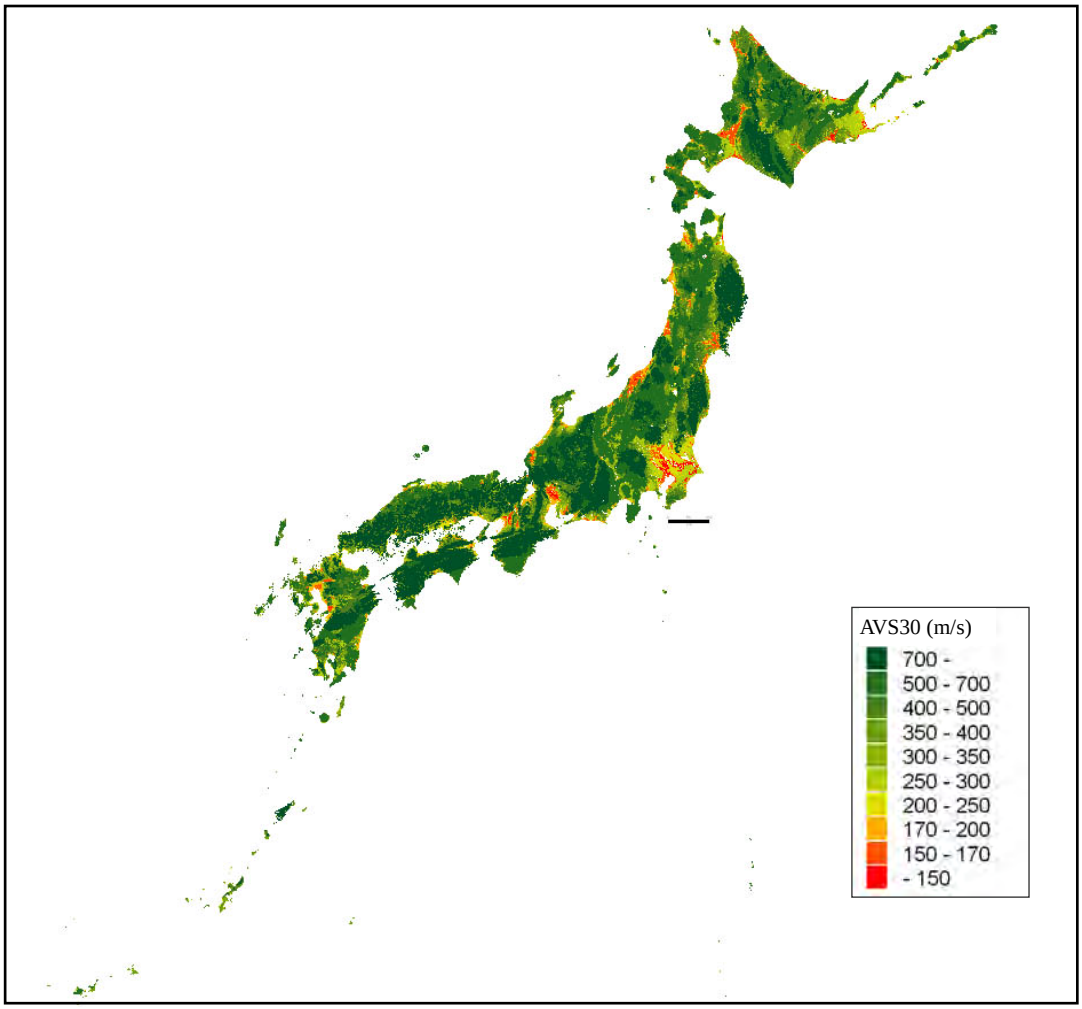

Figure 4.4.3-2 Average shear wave velocity distribution inferred from the 7.5-arc-second JEGM (Matsuoka and Wakamatsu, 2008 partially modified)

4.5 Method of Strong Motion Simulation

To simulate strong motions, first the ground motions on the "engineering bedrock in the detailed method" are obtained, after which the ground motions on the ground surface are calculated based on the former. This rough procedure of the SHM is basically the same between the detailed method and the method using an attenuation relation. Figure 4.5-1 shows the flow of simulation in both methods.

4.5.1 Simulation of waveforms on the "engineering bedrock in the detailed method"

Strong motions on the "engineering bedrock in the detailed method" are simulated using the hybrid method, which is a proven method that has been used in many broad frequency band waveform simulations. Using the three-dimensional finite difference method for the low-frequency (long-periodic) component to which the deterministic approach is applied, and using the stochastic Green's function method for the high-frequency (short periodic) component to which the semiempirical method is applied, the two components are synthesized in time domain.

As discussed in Section 4.2.2, waveforms on the "engineering bedrock in the detailed method" are simulated for the center of the 1 km mesh. This is a measure to reduce the amount of calculation, considering that the accuracy of the "deep subsurface structure" is not necessarily secured for 250 m meshs.

4.5.1.1 Three-dimensional finite difference method

The finite difference method, along with the finite element method, is a typical method for solving a problem by discretizing the whole analytical domain (a domain method). The recent improvement in computer performance has made it possible to simulate large-scale three-dimensional wave fields. However, when treating a low-velocity layer near the ground surface, the domain needs to be divided into fine meshs, and use of a grid with homogenous spacing generates an enormous load on the computer. In order to reduce the load on the computer, computation methods using a heterogeneous grid have been developed (e.g., Aoi and Fujiwara, 1999, and Pitarka, 1999). This study carries out the simulating by the fourth-order spatial finite difference method (Levander, 1988) using the discontinuous grid proposed by Aoi and Fujiwara (1999).

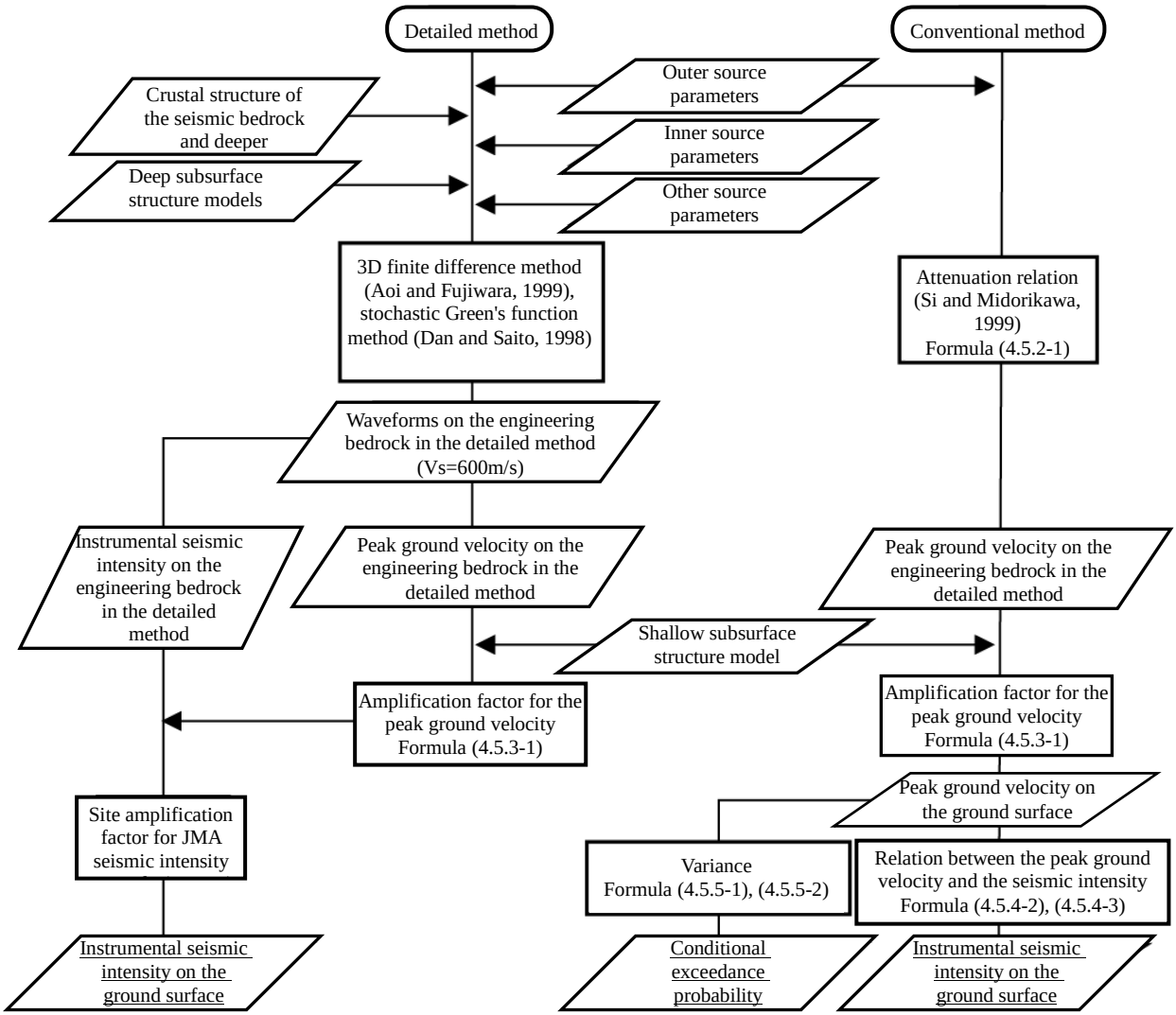

Figure 4.5-1 Flowchart of strong motion simulation for SHM for Specified Seismic Source Faults

In the finite difference method by Aoi and Fujiwara (1999), the grid spacing at the deep part comprising a high-velocity layer (Domain II) is three times the spacing at the shallow part comprising a low-velocity layer (Domain I). Also, the method uses a staggered grid (e.g., Virieux and Madariaga, 1982), where the grid points for evaluating displacement (or velocity) are staggered by half the grid spacing from the grid points for evaluating stress. In order to achieve stability of the numerical simulation, since a grid with equal spacing is used within each domain, the time step Δt (s) used for the simulation needs to satisfy

$$\Delta t < \frac{0.495h}{v_{\max}} \qquad (4.5.1.1\text{-}1)$$

(Graves, 1996), and the maximum frequency f_{upper} (Hz) to be simulated needs to satisfy

$$f_{upper} < \frac{v_{\min}}{5h} \qquad (4.5.1.1\text{-}2)$$

where $v_{\max}$ (m/s) and $v_{\min}$ (m/s) are respectively the maximum and minimum velocities within each domain, and h (m) is the grid spacing. In this study, Δt is 0.0083333 seconds and the grid spacing for Domain I is 100m. Since $v_{\min}$ in Formula (4.5.1.1-2) is the shear wave velocity (600m/s) on the "engineering bedrock in the detailed method" (see Section 4.4.2), the simulation can be made for the frequency band of up to 1.14Hz (wave period: about 0.88 seconds or more).

As a measure to minimize the artificial reflected waves from the boundaries of the simulated domain, an absorbing boundary condition by Cerjan et al. (1985)

$$Atn = \exp\{-\alpha(J_0 - j)^2\}, \text{ (j=1,2,}\cdots\text{,}J_0\text{)} \quad (4.5.1.1\text{-}3)$$

is applied. This is a method to gradually attenuate the wave amplitude at each time step while using the J_0 number of grid points from the boundary as a strip of absorbing boundary. Parameters α and J_0 are determined to be 0.005 and 60, respectively, for Domain I (shallow part), and 0.015 and 20, respectively, for Domain II (deep part), in compliance with Aoi and Fujiwara (1999)

As for the inelastic attenuation of the medium (Q-value), this study uses the method of introducing the spatially varying effect of Q-values into the finite difference method through approximate treatment (Graves, 1996). In this method, Q-values are assumed to be proportional to the frequency, and to be the same between primary waves and shear waves (see Table 4.4.1-1 and Table 4.4.2-1).

The seismic source is modeled by the method of adding moment to the stress term (e.g., Coutant et al., 1995; Pitarka, 1999). As the source time function, the approximation formula of the slip velocity function by Nakamura and Miyatake (2000) (Formula (25) of the Recipe)

$$\frac{dD(t)}{dt} = \begin{cases} \frac{2V_m}{t_d} \cdot t \cdot (1 - \frac{t}{2t_d}) & 0 \le t < t_b \\ \frac{b}{\sqrt{t - \varepsilon}} & t_b \le t < t_r \\ c - a_r(t - t_r) & t_r \le t < t_s \\ 0 & t < 0, t \ge t_s \end{cases} \quad (4.5.1.1\text{-}4)$$

is used, following the Recipe. The parameters necessary for calculating this approximation formula are given by

$$\varepsilon = \frac{5t_b - 6t_d}{4(1 - t_d / t_b)} \quad (4.5.1.1\text{-}5)$$

$$b = 2V_m \cdot \frac{t_b}{t_d} \cdot \sqrt{t_b - \varepsilon} \cdot (1 - \frac{t_b}{2t_d}) \quad (4.5.1.1\text{-}6)$$

$$t_d \cong \frac{1}{\pi \cdot f_{\max}} \quad (4.5.1.1\text{-}7)$$

$$t_r \cong \alpha \frac{W'}{V_r}, \quad \alpha = 0.5 \quad (4.5.1.1\text{-}8)$$

$$V_m = \Delta\sigma \cdot \frac{\sqrt{2 f_c \cdot W' \cdot V_r}}{\mu}, \quad f_c = f_{\max} \quad (4.5.1.1\text{-}9)$$

(Nakamura and Miyatake, 2000, 2001). Here, W'(km) is the asperity width (W_a) in the case of the asperity area, and the width of the whole fault (W_{model}) in the case of the background area. The time t_b(s) in which the slip velocity shifts to the Kostrov-type function is obtained by using the bisection method based on the final slip (Nakamura and Miyatake, 2001).

The actual simulation in this study uses the GMS (Aoi et al., 2004).

4.5.1.2 Stochastic Green's function method

The empirical Green's function method is a simulation method for reproducing strong motion waveforms generated by a large earthquake, whereby the observation record of a small earthquake that has occurred in the vicinity of the source area of the target large earthquake is superpositioned as a Green's function. This is based on the idea that the path effects and the site effects are included in the record of a small earthquake that occurs in the same region as the target large earthquake. After being proposed by Hartzell (1978), the method has been applied to actual earthquakes by Irikura (1983) and others, and the validity of the method has been indicated. The advantage of this method is that it can express the fracture process at the seismic source of a large earthquake to a certain extent, and that even the short periodic component which is difficult to simulate deterministically can be simulated despite having no or insufficient information on the subsurface structure.

Meanwhile, Boore (1983) extended the method by Hanks and McGuire (1981) that had been used for predicting maximum values such as the maximum acceleration, and proposed a method to generate a time domain waveform by adding the envelop curve of the waveform, which has been stochastically obtained from observation records, to the ω^{-2} source spectrum by Brune (1970, 1971) (Aki, 1967). The stochastic Green's function method simulates the ground motion waveform by regarding the waveform generated by the method by Boore (1983) to be a record of a small earthquake, and superpositioning it in the same manner as in the empirical Green's function method. This method is advantageous in that it enables waveform simulation even for a site where no observation record is available. In particular, it has been used for strong motion predictions that take into consideration the short periodic component, which is difficult to simulate by a deterministic approach (e.g., Kamae et al., 1991; Dan et al., 2000).

This study applies the stochastic Green's function method by Dan and Sato (1998) and Dan et al. (2000) to carry out strong motion waveform simulation of the short periodic component. The outline is shown below.

(1) Generation of a stochastic Green's function on the seismic bedrock

A stochastic Green's function on the seismic bedrock is generated by using a similar method as Boore (1983) based on the spectrum model and envelope model using the parameters by Sato et al. (1994a, 1994b), inferred from records of subduction-zone earthquakes observed mainly in the Sendai region.

The shear wave spectrum ($A_s(f)$) of a small earthquake on the seismic bedrock is expressed by the model of Fourier

acceleration spectra of ground motions as shown in the following formula.

$$A_s(f) = \frac{F}{4\pi\rho_s\beta_s^3} \cdot \frac{M_{0s} \cdot (2\pi f)^2}{1+(f/f_{cs})^2} \cdot \frac{1}{\sqrt{1+(f/f_{\max})^m}} \times \frac{1}{r_s}\exp\left(-\frac{\pi f r_s}{Q(f)\cdot\beta_s}\right) \times 2\sqrt{\frac{\rho_s\beta_s}{\rho_{sb}\beta_{sb}}} \quad (4.5.1.2\text{-}1)$$

Here, s is an index concerning the fault of a small earthquake, F is the radiation pattern of the seismic wave, ρ_s (kg/m^3) and β_s (m/s) are the medium density and the shear wave velocity in the fault of the small earthquake, M_{0s} (N・m) is the seismic moment, f_{cs} (Hz) is the critical frequency, r_s (m) is the distance from the seismic source to the target site, $Q(f)$ is the average Q-value for the whole propagation path, and ρ_{sb} (kg/m^3) and β_{sb} (m/s) are the density and shear wave velocity of the seismic bedrock. The last term takes into consideration the influence of the free surface, and the impedance contrast between the medium and the seismic bedrock of the element fault (Sato, 1978) (Dan et al., 2000).

With regard to $Q(f)$, due to the recent accumulation of strong motion records, regional Q-values have been introduced in some recent studies (e.g., Kawase and Matsuo, 2004), but this study adopts

$$Q(f) = \begin{cases} 110 f^{0.69} & f \geq 1Hz \\ 110 & f < 1Hz \end{cases} \quad (4.5.1.2\text{-}2)$$

by Sato (1994b), which has been used in the past SHM, for all fault zones.

For F in Formula (4.5.1.2-1), considering that the radiation pattern is unclear in the high frequency component of ground motions, the mean value of shear waves on the entire source sphere indicated by Boore and Boatwright (1984), which is 0.63, is regarded as the root mean square of the two horizontal components, and the value obtained by dividing such value by $2^{1/2}$, which is 0.445, is adopted. As for m, which is a constant expressing the degree of attenuation of the seismic spectrum in the high frequency domain, 4.2 by Sato et al. (1994b) is used. The values concerning the size of the seismic source, M_{0s} and f_{cs}, are obtained by the following relations:

$$M_{0s} = \mu_s L_s W_s D_s \quad (4.5.1.2\text{-}3)$$

$$f_{cs} = \frac{(7/16)^{1/6}}{\sqrt{\pi}} \cdot \beta_s \cdot \left(\frac{\sigma_s}{M_{0s}}\right)^{1/3} \quad (4.5.1.2\text{-}4)$$

$$\mu_s = \rho_s \beta_s^2 \quad (4.5.1.2\text{-}5)$$

$$\sigma_s = \frac{7\pi}{16} \cdot \frac{\mu_s D_s}{\sqrt{L_s W_s / \pi}} \quad (4.5.1.2\text{-}6)$$

Here, L_s and W_s are the length and width of the fault of a small earthquake, both of which correspond to the fault model grid size (2km; see Section 2.1.2) in this study, while μ_s (N・m/s^2) and σ_s (Pa) are the modulus of rigidity of the medium and the effective stress in the fault of a small earthquake.

Generation of a time history waveform requires aging characteristics, or phase characteristics of the spectrum. These should be determined based on study results that consider regional characteristics, but sufficient research results have not been attained at present. Thus, this study applies the following empirical envelope model ($E(t)$) that has been obtained from seismic records for the engineering bedrock in the Sendai region by Sato et al. (1994a):

$$E(t) = \begin{cases} \left(\dfrac{t-t_a}{t_b-t_a}\right)^2 & (t_a \leq t < t_b) \\ 1 & (t_b \leq t < t_c) \\ \exp\left\{-\dfrac{(\ln 10)\cdot(t-t_c)}{t_d-t_c}\right\} & (t_c \leq t < t_d) \end{cases} \quad (4.5.1.2\text{-}7)$$

where

$$\begin{aligned} \log(t_b - t_a) &= 0.229M - 1.112 \\ \log(t_c - t_b) &= 0.433M - 1.936 \\ \log(t_d - t_c) &= 0.778\log r_s - 0.34 \end{aligned} \quad (4.5.1.2\text{-}8)$$

The stochastic Green's function is generated by the following procedure (Senna et al., 2004):

[1] The time history waveform is generated by performing an inverse Fourier transform after uniformly giving the phase between -π and π to the Fourier amplitude in Formula (4.5.1.2-1) by using a random number.

[2] The phase information is obtained by performing a Fourier transform after multiplying the time history waveform by the aging characteristics in Formula (4.5.1.2-7).

[3] An inverse Fourier transform is performed once again after giving the Fourier amplitude in Formula (4.5.1.2-1) to the phase in [2], to derive the time history waveform.

[4] Envelope processing is carried out so as not to change the phase information in [3].

As a result of separate consideration, the one and only random number that corresponds to average amplitude of the simulated waveform is selected and applied in this study.

(2) Stochastic Green's function on the "engineering bedrock in the detailed method"

A one-dimensional (horizontally layered) ground model directly under each simulated site is built based on the three-dimensional deep subsurface structure model built in Section 4.4.2. By assuming the stochastic Green's function on the seismic bedrock to be waves vertically incident on this structure, the stochastic Green's function on the "engineering bedrock in the detailed method" is simulated by using the one-dimensional multiple reflection theory for SH waves.

(3) Waveform synthesis by the stochastic Green's function method on the "engineering bedrock in the detailed method"

Waveform synthesis is carried out by regarding the stochastic Green's function generated in (2) to be the record of a small earthquake, and following the semi-empirical waveform synthesis method by Dan and Sato (1998) which considers the variable slip of the fault.

If

$$\frac{L_l}{L_s} = a\ ,\ \ \frac{W_l}{W_s} = b \qquad (4.5.1.2\text{-}9)$$

then the waveform of a large earthquake $u_l(t)$ is expressed as

$$u_l(t) = \sum_{p=1}^{a}\sum_{q=1}^{b} u_{pq}(t)\ ,\ \ u_{pq}(f) = F_{pq}(f)\cdot u_s(f) \qquad (4.5.1.2\text{-}10)$$

where l is an index concerning the large earthquake, L and W are the length and width of the fault, respectively, $u_{pq}(f)$ is a Fourier transform of $u_{pq}(t)$, and $u_s(f)$ is the stochastic Green's function regarded as the record of the small earthquake. The method by Dan and Sato (1998) considers the final slip (D_{pq}) and maximum slip velocity (V_{pq}) of the element fault (index pq), and $F_{pq}(f)$ which corrects the difference in seismic spectrum between the small earthquake and the large earthquake in each element fault is expressed as

$$F_{pq}(f) = \frac{D_{pq}}{D_s}\cdot\frac{(1+j\cdot f/f_{cs})^2}{(1+j\cdot f/f_{Dpq})(1+j\cdot f/f_{Spq})} \times\frac{r_s}{r_{pq}}\cdot\exp\{\frac{2\pi f}{2Q(f)\beta}(r_s - r_{pq})\} \qquad (4.5.1.2\text{-}11)$$

$$f_{Dpq} = \frac{1}{2\pi}\frac{V_{pq}}{D_{pq}} = \frac{2\beta\sigma_{pq}}{2\pi\mu D_{pq}} \qquad (4.5.1.2\text{-}12)$$

$$f_{Spq} = \frac{1}{2\pi}\frac{\beta}{\lambda_{pq}} \qquad (4.5.1.2\text{-}13)$$

Here, j is the imaginary unit, r (m) is the distance from the seismic source, and λ (m) is the radius in the case of deeming the fault to be a circular fault of the same size.

In this study, the waveform simulation only targets SH waves. Therefore, vertical seismic motions are not simulated.

4.5.1.3 Hybrid method

The hybrid method is a method of evaluating broadband strong motionss by synthesizing the two results that have been calculated for the high-frequency (short periodic) component and for the low-frequency (long periodic) component (e.g., Kawase and Matsushima, 1998; Sato et al., 1998; Irikura and Kamae, 1999). The waveforms on the "engineering bedrock in the detailed method" that have been simulated by the two methods discussed in Section 4.5.1.1 and Section 4.5.1.2 are synthesized. After applying a matching filter combining two types of filters with a specific filter frequency to the respective time history waveforms, the two are superpositioned in the time domain. This study uses the filter frequency of one second, and adopts a matching filter of the combination shown Figure 4.5.1.3-1. Since a waveform simulation using the stochastic Green's function method is not carried out for vertical component, the waveforms simulated by the hybrid method are also limited to the two horizontal components. In the waveforms simulated by the stochastic Green's function method, the same waveforms are used for both horizontal components in this study.

Under this method, the peak velocity on the "engineering bedrock in the detailed method" adopts a value obtained by conducting vector synthesis of the two horizontal components of the waveforms simulated by the procedure above.

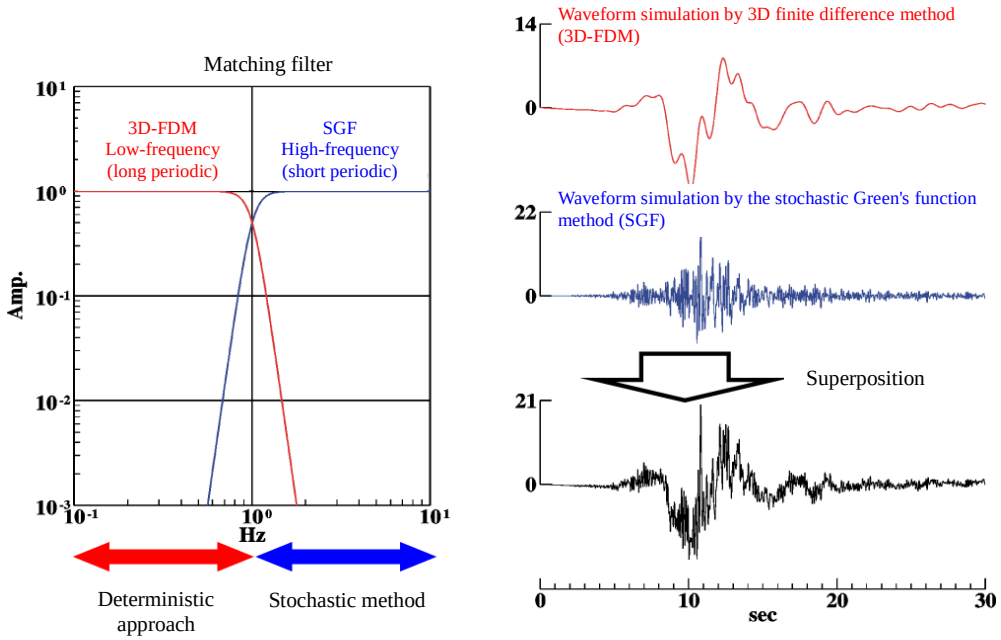

Figure 4.5.1.3-1 Concepts of the hybrid method (right) and the matching filter used in this study (left)

4.5.2 Simulation of the peak velocity on the engineering bedrock using an attenuation relation

The conventional method is basically the same as the ground motion simulation for the PSHM. However, here, the peak ground velocity on the "engineering bedrock in the detailed method" (Vs=600m/s) *PGV* (cm/s) is obtained. In other words, this method directly uses the value computed by the attenuation relation by Si and Midorikawa (1999)

$$\log PGV = 0.58M_w + 0.0038H + d - 1.29 - \log(X + 0.0028 \times 10^{0.50M_w}) - 0.002X \quad (4.5.2\text{-}1)$$

where H (km) is the central depth of the seismic source fault models, and X (km) is the shortest distance to the fault. Factor d by fault type used for earthquakes in major active fault zones is 0.0, which is the value for inland crustal earthquakes, and that used for subduction-zone earthquakes is -0.02 which is the value for interplate earthquakes. If correction concerning regions of anomalous seismic intensity is necessary for subduction-zone earthquakes, the correction is made in the same manner as for the PSHM. Specifically, such correction is made for the Etorofuto-Oki Earthquake, Shikotanto-Oki Earthquake, Nemuro-Oki Earthquake, Tokachi-Oki Earthquake, Miyagi-ken-Oki Earthquake, and Ibaraki-ken-Oki Earthquake. Since these are all earthquakes occurring at the Pacific plate, the correction factors

$$\log V_1 = (-4.021 \times 10^{-5} \times X_{tr} + 9.905 \times 10^{-3}) \times (H - 30)$$
$$V_2 = \max\{1.0, (R/300)^{2.064} \times 10^{-0.012}\} \quad (4.5.2\text{-}2)$$

(the same as Formula (3.5.2-1)) are applied by multiplying them by the peak ground velocity obtained by Formula (4.5.2-1). For details, see Section 3.5.2 or Appendix 3.

4.5.3 Evaluation of the peak ground velocity on ground surface

Based on the average shear wave velocity in the upper 30 m, *AVS*30 (m/s), obtained for the "shallow subsurface structure" (see Section 4.4.3) (Figure 4.4.3-2), the amplification factor (*amp*) for the peak ground velocity from the "engineering bedrock in the detailed method" to the ground surface can be obtained by using the empirical relation proposed by Fujimoto and Midorikawa (2006) (Formula (32) of the Recipe)

$$\log(amp) = 2.367 - 0.852 \cdot \log AVS30 \quad (4.5.3\text{-}1)$$

The peak ground velocity on the ground surface is evaluated by multiplying this value by the peak ground velocity on the "engineering bedrock in the detailed method". This is a common method for both the detailed method and the method using an attenuation relation. In the detailed method, the peak ground velocity on the engineering bedrock is obtained for the center of the 1 km mesh. However, the peak ground velocity on the ground surface is calculated for 250 m meshs. Therefore, in all of the 16 meshs of 250 m contained in a single 1 km mesh, which is a waveform simulation site, the peak ground velocity on the ground surface is evaluated using the same value (waveform).

4.5.4 Evaluation of the JMA instrumental seismic intensity on the ground surface

A different approach is used between the detailed method and the method using an attenuation relation, for calculating the JMA instrumental seismic intensity on the ground surface.

In the detailed method, the instrumental seismic intensity on the "engineering bedrock in the detailed method" is calculated first according to the definition by JMA (1996) from the waveform simulated above, in order to utilize the frequency characteristics of the simulated waveform. Since no simulation is made for vertical seismic motions in this process, the amplitude is assumed to be zero in the simulation. As characteristics of amplitude by the "shallow subsurface structure", the average shear wave velocity in the upper 30 m (*AVS*30, m/s) calculated based on the engineering geomorphologic classification is used. Specifically, the instrumental seismic intensity on the ground surface is obtained by adding to the instrumental seismic intensity on the "engineering bedrock in the detailed method" the following site amplification factor for JMA seismic intensity (ΔI)

$$\begin{aligned}\Delta I &= 2.603\cdot\log(amp) - 0.213\cdot\{\log(amp)\}^2 \\ &\quad - 0.426\cdot\log(PGV_{\mathrm{b}})\cdot\log(amp)\end{aligned} \qquad (4.5.4\text{-}1)$$

(ERC, 2008a; Formula (35) of the Recipe) derived by combining the relation between *AVS*30 and the amplification factor for the peak ground velocity (Formula (4.5.3-1)) and the relation between the peak ground velocity and the instrumental seismic intensity (Formula (3.5.4-2)). Here, PGV_{b} (cm/s) is the peak ground velocity on the engineering bedrock with shear wave velocity 600m/s. Since simulations using the detailed method only target earthquakes in major active fault zones which are Category III earthquakes, this study adopts

$$I = 2.002 + 2.603\cdot\log PGV_S - 0.213\cdot(\log PGV_S)^2 \qquad (4.5.4\text{-}2)$$

(Fujimoto and Midorikawa, 2005; the same as Formula (33) of the Recipe and Formula (3.5.4-2)) as the relation between the peak ground velocity and the instrumental seismic intensity.

On the other hand, in the conventional method, the instrumental seismic intensity on the ground surface is calculated from the peak ground velocity on the ground surface (PGV_{s}) obtained in the previous section, by using an empirical relation between the peak ground velocity and the instrumental seismic intensity. In the same manner as for the PSHM, the relation used is

$$I = 2.68 + 1.72\cdot\log PGV_S \qquad (4.5.4\text{-}3)$$

(Midorikawa et al. (1999); the same as Formula (3.5.4-1)) for Category I and Category II earthquakes, and Formula (4.5.4-2) above is used for Category III earthquakes. While both formulas target ground motions of seismic intensity 4 or more, even where the seismic intensity will be less than 4, this study obtains the seismic intensity by directly applying both formulas as they are, in the same manner as for the PSHM.

4.5.5 Evaluation of the conditional exceedance probability

In the conventional method, by considering variance, the probability that the occurrence of the target earthquake would generate ground motion intensity at certain level or greater can be obtained as in Formula (3.1.2-4). Here, the probabilities that the occurrence of the target earthquake would generate shaking of four levels from seismic intensity 5 Lower or more to seismic intensity 6 Upper or more are calculated and presented on maps.

The method for calculating the seismic intensity on the ground surface is the same as in the ground motion evaluation method for the PSHM. Specifically, the distribution shape of variance of the peak ground velocity on the engineering bedrock is assumed to be logarithmic normal distribution, and values outside the level three times the logarithmic standard deviation are cut off. Variance of the attenuation relation (logarithmic standard deviation) is variance dependent on the peak ground velocity on the engineering bedrock PGV_{b} (cm/s)

$$\sigma_{\mathrm{I,II}} = \begin{cases} 0.20 & PGV_{\mathrm{b}} \le 25\text{cm/s} \\ 0.20 - 0.05\cdot\dfrac{PGV_{\mathrm{b}} - 25}{25} & 25 < PGV_{\mathrm{b}} \le 50\text{cm/s} \\ 0.15 & PGV_{\mathrm{b}} > 50\text{cm/s} \end{cases}$$

(4.5.5-1)

(the same as Formula (3.5.5-1); see Figure 3.5.5-1) for Category I and Category II earthquakes, and variance dependent on the shortest distance to the fault X (km)

$$\sigma_{\mathrm{III}} = \begin{cases} 0.23 & X \le 20\text{km} \\ 0.23 - 0.03\cdot\dfrac{\log(X/20)}{\log(30/20)} & 20 < X \le 30\text{km} \\ 0.20 & X > 30\text{km} \end{cases} \qquad (4.5.5\text{-}2)$$

(the same as Formula (3.5.5-2); see the red line in Figure 3.5.5-2) for Category III earthquakes.

Table 4.5.2-1 shows the earthquake types, correction for regions of anomalous seismic intensity, variance, and the formula for conversion between the peak ground velocity and the instrumental seismic intensity applied when simulating the ground motion distribution and the conditional exceedance probability distribution using the conventional method.

4.6 Evaluation Results

The figures showing the evaluation results are compiled in a separate volume.

4.6.1 Characteristic earthquakes occurring in major active fault zones

The results of evaluation using the detailed method are shown in Figure 4.6.1-1 to Figure 4.6.1-490. Each figure consists of the following data: a ground motion distribution map (Part 1); velocity waveforms at a major sites (Part 2); and pseudo velocity response spectra (attenuation: 5%) at a major sites (Part 3). However, the figure for the Kego fault zone only shows the ground motion distribution map based on "Verification of the Strong Motion Evaluation Method Based on the Observation Records of the 2005 West Off Fukuoka Earthquake" (ERC, 2008a; see also Appendix 4) and "Strong Motion Evaluation Assuming Earthquakes in the Kego Fault Zone (Southeastern Part)" (ERC, 2008b).

The results of evaluation using the conventional method are shown in Figure 4.6.1-491 to Figure 4.6.1-661. Each figure consists of the following data: a ground motion distribution map (Part 1) and a conditional exceedance probability distribution map (Part 2).

4.6.2 Subduction-zone earthquakes and earthquakes in the eastern margin of the Japan Sea

The results of evaluation using the conventional method are shown in Figure 4.6.2-1 to Figure 4.6.2-25. Each figure consists of the following data: a ground motion distribution map (Part 1), and a conditional exceedance probability distribution map (Part 2).

As for the PSHM, the boundaries of administrative districts shown in the figures are those as of January 1, 2009.

Table 4.5.5-1 List of computational schemes applied in the conventional method

Earthquake	Earthquake category	Attenuation relation			Peak ground velocity ↔ instrumental seismic intensity
		Factor	Correction	Variance	
Characteristic earthquakes occurring in major active fault zones	III	Crustal	—	Distance	Fujimoto
Etorofuto-Oki Earthquake	I	Interplate	Northern Japan	Amplitude	Midorikawa
Shikotanto-Oki Earthquake	I	Interplate	Northern Japan	Amplitude	Midorikawa
Nemuro-Oki Earthquake	I	Interplate	Northern Japan	Amplitude	Midorikawa
Tokachi-Oki Earthquake	I	Interplate	Northern Japan	Amplitude	Midorikawa
Tokachi-Oki Earthquake + Nemuro-Oki Earthquake	I	Interplate	Northern Japan	Amplitude	Midorikawa
Miyagi-ken-Oki Earthquake (A1, A2)	I	Interplate	Northern Japan	Amplitude	Midorikawa
Earthquakes close to the offshore trenches in Southern Sanriku-Oki (B)	I	Interplate	Northern Japan	Amplitude	Midorikawa
Miyagi-ken-Oki Earthquake	I	Interplate	Northern Japan	Amplitude	Midorikawa
Large interplate earthquakes in Northern Sanriku-Oki	I	Interplate	Northern Japan	Amplitude	Midorikawa
Interplate characteristic earthquakes in Ibaraki-ken-Oki	II	Interplate	Northern Japan	Amplitude	Midorikawa
Western Hokkaido-Oki Earthquake	III	Interplate	—	Distance	Fujimoto
Southwestern Hokkaido-Oki Earthquake	III	Interplate	—	Distance	Fujimoto
Western Aomori-ken-Oki Earthquake	III	Interplate	—	Distance	Fujimoto
Yamagata-ken-Oki Earthquake	III	Interplate	—	Distance	Fujimoto
Northern Niigata-ken-Oki Earthquake	III	Interplate	—	Distance	Fujimoto
Kanto Earthquake of "1923 Taisho" type	I	Interplate	—	Amplitude	Midorikawa
Assumed Tokai Earthquake	I	Interplate	—	Amplitude	Midorikawa
Tonankai Earthquake	I	Interplate	—	Amplitude	Midorikawa
Nankai Earthquake	I	Interplate	—	Amplitude	Midorikawa
Tonankai Earthquake + Assumed Tokai Earthquake	I	Interplate	—	Amplitude	Midorikawa
Nankai Earthquake + Tonankai Earthquake	I	Interplate	—	Amplitude	Midorikawa
Nankai Earthquake + Tonankai Earthquake + Assumed Tokai Earthquake	I	Interplate	—	Amplitude	Midorikawa

Notes: Factor: "Crustal" - Crustal earthquakes, "Interplate" - Interplate earthquakes (type for factor *d* in Formula (4.5.2-1)).

Correction: Correction for regions of anomalous seismic intensity, "Northern Japan" - Formula (4.5.2-1) and Formula (4.5.2-2) by Morikawa et al. (2003).

Variance: "Distance" - Distance-dependent Formula (4.5.5-2), "Amplitude" - Amplitude-dependent Formula (4.5.5-1).

Peak ground velocity ↔ instrumental seismic intensity: "Fujimoto" - Formula (4.5.4-2) by Fujimoto and Midorikawa (2005), "Midorikawa" - Formula (4.5.4-3) by Midorikawa et al. (1999).

References for Chapter 4

1) Aki, K. (1967): "Scaling law of seismic spectrum", *J. Geophys. Res.*, **72**, 1217-1231.

2) Aoi, S. and Fujiwara, H. (1999): "3D finite-difference method using discontinuous grids", *Bull. Seism. Soc. Am.*, **89**, 918-930.

3) Aoi, S., Hayakawa, T., and Fujiwara, H. (2004): "Ground Motion Simulator: GMS", *Butsuri-Tansa (Geophysical Exploration)*, **57**, 651-666.

4) Boore, D. M. (1983): "Stochastic simulation of high-frequency ground motions based on seismological models of the radiated spectra", *Bull. Seism. Soc. Am.*, **73**, 1865-1894.

5) Boore, D. M. and Boatwright, J. (1984): "Average body-wave radiation coefficients", *Bull. Seism. Soc. Am.*, **74**, 1615-1621.

6) Brune, J. N. (1970): "Tectonic stress and the spectra of seismic share waves from earthquakes", *J. Geophys. Res.*, **75**, 4997-5009.

7) Brune, J. N. (1971): "Correction", *J. Geophys. Res.*, **76**, 5002.

8) Cerjan, C., Kosloff, D., Kosloff, R. and Reshef, M. (1985): "A nonreflecting boundary condition for discrete acoustic and elastic wave equations", *Geophysics*, **50**, 705-708.

9) Coutant, O., Virieux, J. and Zollo, A. (1995): "Numerical source implementation in a 2D finite difference scheme for wave propagation", *Bull. Seism. Soc. Am.*, **85**, 1507-1512.

10) Dan, K. and Sato, T. (1998): "Strong-Motion Prediction by Semi-empirical Method Based on Variable-slip Rupture Model of Earthquake Fault", *Journal of structural and construction engineering (Transactions of AIJ)*, **509**, 49-60 (in Japanese with English abstract).

11) Dan, K., Watanabe, M., and Sato, T., Miyakoshi, J., Sato, T. (2000): "Isoseismal Map of Strong Motions for the 1923 Kanto Earthquake (M_{JMA} 7.9) by Stochastic Green's Function Method", *Journal of structural and construction engineering (Transactions of AIJ)*, **530**, 53-62 (in Japanese with English abstract).

12) Dan, K., Watanabe, M., Sato, T., and Ishii, T. (2001): "Short-period Source Spectra Inrefrred from Variable-slip Rupture Models and Modeling of Eearthquake Faults for Strong Motion Prediction by Semi-empirical Method", *Journal of structural and construction engineering (Transactions of AIJ)*, **545**, 51-62 (in Japanese with English abstract).

13) Dan, K., Sato, T., and Irikura, K. (2002): "Characterizing Source Model for Strong Motion Prediction Based on Asperity Model", *Proceedings of the 11th Japan Earthquake Engineering Symposium*, 555-560 (in Japanese with English abstract).

14) Eshelby, J. D. (1957): "The determination of the elastic field of an ellipsoidal inclusion, and related problems", *Proceedings of the Royal Society*, A241, 376-396.

15) Fujii, Y. and Matsu'ura, M. (2000): "Regional difference in scaling laws for large earthquakes and its tectonic implication", *Pure Appl. Geophys.*, **157**, 2283-2302.

16) Fujimoto, K. and Midorikawa, S. (2005): "Empirical Method for Estimating J.M.A. Instrumental Seismic Intensity from Ground Motion Parameters Using Strong Motion Records during Recent Major Earthquakes", *Journal of social safety science*, **7**, 1-6 (in Japanese with English abstract).

17) Fujimoto, K. and Midorikawa, S. (2006): "Relationship between Average Shear-Wave Velocity and Site Amplification Inferred from Strong Motion Records at Nearby Station Pairs", *Journal of Japan Association for Earthquake Engineering*, **6**-1, 11-22 (in Japanese with English abstract).

18) Fujiwara, H., Kawai, S., Aoi, S., Senna, S., Ooi, M., Matsuyama, H., Iwamoto, K., Suzuki, H., and Hayakawa, Y. (2006): "A Subsurface Structure Modeling of Whole of Japan for Strong Motion Evaluation", *Proceedings of the 12th Japan earthquake engineering symposium*, 0340, 1466-1469 (in Japanese with English abstract).

19) Fujiwara, H. et al. (2009), A Study on subsurface structure model for deep sedimentary layers of Japan for strong-motion evaluation, *Technical Note of the National Research Institute for Earth Science and Disaster Prevention*, **337** (in Japanese).

20) Geller, R. J. (1976): "Scaling relations for earthquake source parameters and magnitudes", *Bull. Seism. Soc. Am.*, **66**, 1501-1523.

21) Graves, R. W. (1996): "Simulating seismic wave propagation in 3D elastic media using staggered-grid finite differences", *Bull. Seism. Soc. Am.*, **86**, 1091-1106.

22) Hanks, T. C. (1982): "fmax", *Bull. Seism. Soc. Am.*, **72**, 1867-1879.

23) Hanks, T. C. and McGuire, R. K. (1981): "The character of high-frequency strong ground motion", *Bull. Seism. Soc. Am.*, **71**, 2071-2095.

24) Hartzell, S. H. (1978): "Earthquake aftershocks as Green's functions", *Geophys. Res. Lett.*, **5**, 1-4.

25) Irikura, K. (1983): "Semi-empirical estimation of strong ground motions during large earthquakes", *Bull. Disas. Prev. Inst., Kyoto Univ.*, **33**, 63-104.

26) Irikura, K. and Kamae, K. (1999): "Strong Ground Motions during the 1948 Fukui Earthquake Estimation of Broad band Ground Motion Using a Hybrid Simulation Technique", *Journal of the Seismological Society of Japan* (Second Series), **52**, 129-150 (in Japanese with English abstract).

27) Irikura, K., Miyake, H., Iwata, T., Kamae, K., and Kawabe, H. (2002): "Revised Recipe for Predicting Strong Ground Motion and. Its Validation", *Proceedings of the 11th Japan Earthquake Engineering Symposium*, 567-572 (in Japanese with English abstract).

28) Ishii, T., Sato, T., and Somerville, P. G. (2000): "Identification of Main Rupture Areas of Heterogeneous Fault Models for Strong-motion Estimation", *Journal of structural and construction engineering (Transactions of AIJ)*, **527**, 61-70 (in Japanese with English abstract).

29) Ishii, T. and Sato, T. (2000): "Relations between the Main

Rupture Areas and their Moments of Heterogeneous Fault Models for Strong motion Estimation", *Programme and abstracts Seismological Society of Japan 2000, Fall Meeting*, B09 (in Japanese).

30) Earthquake Research Committee (2005): "Yamasaki dansotai no jishin wo sotei shita kyoshindo hyoka ni tsuite" (Strong motion evaluation assuming the Yamasaki fault zone), published on January 31, 2005 (in Japanese).

31) Earthquake Research Committee (2008a): "2005 nen Fukuoka-ken seiho-oki no jishin no kansoku kiroku ni motozuku kyoshindo hyoka shuho no kensho ni tsuite" (Verification of the strong motion evaluation method based on the observation records of the 2005 Fukuoka-ken Seiho Oki Earthquake), published on April 11, 2008 (in Japanese).

32) Earthquake Research Committee (2008b): "Kego dansotai (nanto-bu) no jishin wo sotei shita kyoshindo hyoka ni tsuite" (Strong motion evaluation assuming earthquakes in the Kego fault zone (southeastern part)), published on April 11, 2008 (in Japanese).

33) Earthquake Research Committee (2008c): "Shingen danso wo tokutei shita jishin no kyoshindo yosoku shuho (Reshipi)" (Strong ground motion prediction method (Recipe) for earthquakes with specified source faults) (updated on April 11, 2008), published on April 11, 2008 (in Japanese).

34) Kamae, K., Irikura, K., and Fukuchi, Y. (1991): "Prediction of Strong Ground Motion Based on Scaling Law of Earthquake: By stochastic synthesis method", *Journal of structural and construction engineering (Transactions of AIJ)*, **430**, 1-9.

35) Kawase, H. and Matsuo, H. (2004): "Separation of Source, Path, and Site Effects based on the Observed Data by K-NET, KiK-net, and JMA Strong Motion Network", *Journal of Japan Association for Earthquake Engineering*, **4**-1, 33-52 (in Japanese with English abstract).

36) Kawase, H. and Matsushima, S. (1998): "Strong motion simulation by a semi-empirical method, a theoretical method, and a hybrid method of the two: A case study on the 1995 Hyogo-ken Nambu earthquake", *Summaries of Technical Papers of Annual Meeting Architectural Institute of Japan*, B-II, 171-172 (in Japanese).

37) JMA (1996): Public Notice No. 4 of the Japan Metrological Agency.

38) Levander, A. R. (1988): "Fourth-order finite-difference P-SV seismograms", *Geophysics*, **53**, 1425-1436.

39) Madariaga, R. (1979): "On the relation between seismic moment and stress drop in presence of stress and strength heterogeneity", *J. Geophys. Res.*, **84**, 2243-2250.

40) Matsubara, M., Obara, K. and Kasahara, K. (2008): "Three-dimensional P- and S-wave velocity structures beneath the Japan islands obtained by high-density seismic stations by seismic tomography", *Tectonophysics*, **454**, 86-103.

41) Matsuoka, M. and Wakamatsu, K. (2008): “Site Amplification Capabiliti Map based on the 7.5-arc-second Japan Engineering Geomorpholigic Classification Map”, National Institute of Advanced Industrial Science and Technology, Intellectual property management no. H20PRO-936.

42) Matsuoka, M., Wakamatsu, K., Fujimoto, K., and Midorikawa, S. (2005): "Average Shear-wave Velocity Mapping Using Japan Engineering Geomorphologic Classification Map", Journal of geological engineering, No.794/I-72, 239-251 (in Japanese with English abstract).

43) Midorikawa, S., Fujimoto, K., and Muramatsu, I. (1999): "Correlation of New J.M.A. Instrumental Seismic Intensity with Former J.M.A. Seismic Intensity and Ground Motion Parameters", *Journal of social safety science*, **1**, 51-56 (in Japanese with English abstract).

44) Miyakoshi, K., Sekiguchi, H., Iwata, T. (2001): "Suberi no kukan-teki fukinshitsusei no chushutsu" (Extraction of the spatial heterogeneity of slip), FY2000 Special Coordination Fund for Science and Technology "Master Model of Strong Motion Prediction for Mitigating Earthquake Disasters" Research Report, 99-109 (in Japanese).

45) Morikawa, N., Kanno, T., Narita, A., Fujiwara, H., and Fukushima, Y. (2003): "Additional Correction Terms for Attenuation Relations Corresponding to the Anomalous Seismic Intensity in Northeast Japan", *Journal of Japan Association for Earthquake Engineering*, **3**-4, 14-26 (in Japanese with English abstract).

46) Nakamura, H. and Miyatake, T. (2000): "An Approximate Expression of Slip Velocity Time Function for Simulation of Near-field Strong Ground Motion", *Journal of the Seismological Society of Japan* (Second Series), **53**, 1-9 (in Japanese with English abstract).

47) Nakamura, H. and Miyatake, T. (2001): "An Approximate Expression of Slip Velocity Time Function for Simulation of Near field Strong Ground Motion (2) Fortran Program", http://www.eri-u-tokyo.ac.jp/miyatake/SlipFunc-Prog.html, January 2001 (in Japanese).

48) Nakata, T., Shimazaki, K., Suzuki, Y., and Tsukuda, E. (1998): "Fault Branching and Directivity of Rupture Propagation", *Journal of Geography*, **107**, 512-528 (in Japanese with English abstract).

49) Pitarka, A. (1999): "3D elastic finite-difference modeling of seismic motion using staggered grids with nonuniform spacing", *Bull. Seism. Soc. Am.*, **89**, 54-68.

50) Sato, T., Dan, K., Graves, R. W. and Somerville, P. G. (1998): "Broadband Strong-Motion Simulation in Tokyo during the Great 1923 Kanto Earthquake (Ms 8.2)by Hybrid Technique of 3-D Finite-Difference Method and Semi-Empirical Method Based on Variable-Slip Rupture Model", *Proceedings of the 10th Japan earthquake engineering symposium*, Vol.1, 679-684 (in Japanese with English abstract).

51) Sato, T. and Kawase, H. and Sato, T. (1994a): "Engineerring Bedrock Waves Obtained through the Identification Analysis Based on Borehole Records and Their Statistical Envelope

Characteristics", *Journal of structural and construction engineering (Transactions of AIJ)*, **461**, 19-28 (in Japanese with English abstract).

52) Sato, T., Kawase, H. and Sato, T. (1994b): "Statistical Spectral Characteristics for Engineering Bedrock Waves in Which Local Site Effects of Surface Geology are Removed. Based on the ground motion records of small and medium earthquakes observed in the boreholes in Sendai", *Journal of structural and construction engineering (Transactions of AIJ)*, **462**, 79-89 (in Japanese with English abstract).

53) Sato, Y. (1978): *Dansei hado-ron* (Elastic wave propagation), Iwanami Shoten (in Japanese).

54) Senna, S., Fujiwara, H., Kawai, S., Aoi, S., Kunugi, T., Ishii, T., Hayakawa, Y., Morikawa, N., Honda, R., Kobayashi, K., Oi, M., Yasoshima, Y., Kanno, T., Okumura, N. (2004): "A Study on Strong-Motion Maps for Scenario Earthquakes in Morimoto-Togashi Fault Zone", *Technical Note of the National Research Institute for Earth Science and Disaster Prevention*, **255** (in Japanese).

55) Si, H. and Midorikawa, S. (1999): “New Attenuation Relationships for Peak Ground Acceleration and Velocity Considering Effects of Fault Type and Site Condition", *Journal of structural and construction engineering (Transactions of AIJ)*, **523**, 63-70 (in Japanese with English abstract).

56) Somerville, P. G., Irikura, K., Graves, R., Sawada, S., Wald, D., Abrahamson, N., Iwasaki, Y., Kagawa, T., Smith, N. and Kowada, A. (1999): Characterizing crustal earthquake slip models for prediction of strong ground motion, Seismol. Res. Lett., 70, 59-80.

57) Tsurugi, M., Kagawa, T., Irikura, K., and Kowada, A. (1997): "Cutoff frequency fmax of earthquakes occurring in Kinki district", *Abstracts 1997: Japan Earth and Planetary Science joint meeting*, 103.

58) Virieux, J. and Madariaga, R. (1982): "Dynamic faulting studied by a finite difference method", *Bull. Seism. Soc. Am.*, 72, 345-369.

59) Wakamatsu, K. and Matsuoka, M. (2008): “Development of nationwide GIS-based 7.5-arc second Japan Engineering Geomorphologic Classification Map”, *Proceedings of the 6th annual meeting of Japan Association for Earthquake Engineering*, 222-223 (in Japanese).

60) Wakamatsu, K., Matsuoka, M., Kubo, S., Hasegawa, K., and Sugiura, M. (2004): "Development of GIS-based Japan Engineering Geomorphologic Classification Map", Journal of geological engineering, No.759/I-67 (in Japanese with English abstract).

61) Wakamatsu, K., Kubo, S., Matsuoka, M., Hasegawa, K., and Sugiura, M. (2005): *Japan Engineering Geomorphologic Classification Map*, University of Tokyo Press (in Japanese).

62) Zhao, D., Hasegawa, A. and Kanamori, H. (1994): "Deep structure of Japan subduction zone as derived from local, regional, and teleseismic events", *J. Geophys. Res.*, **122**, 313-327.

5. Japan Seismic Hazard Information Station (J-SHIS)

5.1 Outline

The National Seismic Hazard Maps for Japan consist of two types of maps different in nature: the PSHM that combine long-term probabilistic evaluations of earthquake occurrence and strong motion evaluations, and the Seismic Hazard Maps for Specified Seismic Source Faults which are based on detailed strong motion evaluation for scenarios assumed for specific earthquakes. Whereas HERP was established based on the lessons learned from the 1995 Hyogo-ken Nanbu (Kobe) Earthquake, the National Seismic Hazard Maps for Japan can be regarded as a comprehensive compilation of HERP's past ten years of achievements in seismic hazard evaluation based on its survey and research activities. Therefore, including the data required for mapping such as seismic activity models, seismic source fault models, subsurface structure models, etc., they contain an enormous amount of information.

As a part of its studies on utilization of seismic hazard maps, NIED has set up the Study Committee for Engineering Applications of the National Seismic Hazard Maps to explore the issue. The Committee's report recommends that the seismic hazard maps should be considered as seismic hazard information sharing bases by regarding the maps as a group of information incorporating the underlying data used in the evaluation process, such as the seismic activity models, seismic source models, and subsurface structure models, rather than mere maps as final products. In order to put this recommendation into practice, NIED started the operation of the "Japan Seismic Hazard Information Station (J-SHIS)," on May 9, 2005 (http://www.j-shis.bosai.go.jp).

Four years have passed since the launch of operation of the J-SHIS. During that time, remarkable progress has been made in the technology to distribute map data via the Internet. By incorporating such latest technology, NIED developed a new J-SHIS system that is capable of providing the following data in a user-friendly manner by overlaying the data on background maps: the new National Seismic Hazard Maps for Japan which consist of the PSHM for the whole of Japan with a 250 m mesh resolution; the Seismic Hazard Maps for Specified Seismic Source Faults based on detailed strong motion prediction of earthquakes that occur at major active fault zones; and the deep subsurface structure models for the whole of Japan and 250 m mesh geomorphological land classification models used for the required calculations.

5.2 Objectives

In publishing seismic hazard maps, the publication system should not only contain the results (maps and data) of probabilistic seismic hazard evaluations and scenario-type ground motion evaluations for major assumed earthquakes, but should offer some scheme for complementing the disadvantages of the two types of evaluations, and for helping users understand their respective characteristics, and procedures for objectively determining and explaining future ground motions based on them. In addition, the system should provide links to various databases, such as long-term evaluation results for each earthquake, information on past earthquakes, geomorphologic information on active faults, etc., information on shallow/deep subsurface structures, earthquake observation records, and records of seismic damage, so as to allow users to easily understand the seismic environment around the target site (region). The J-SHIS is a system aimed at achieving these objectives.

Further, the Study Committee for Engineering Applications of the National Seismic Hazard Maps presented the following recommendations to makers of seismic hazard maps:

- Significance as seismic hazard information sharing bases—Making earthquake and bedrock motion databases of the highest scientific standard
- Diversity of displayed items—Providing interfaces that allow diverse technical activities on the engineering side (allowing a high degree of freedom in activities)
- Disclosure of not only the results, but also the process−Making the process of uncertainty evaluation open
- Creation of the publication system—Developing effective user interfaces/Allowing users to scrutinize the conditions to be determined
- Importance of appropriate updating—Reflecting scholarly and technical progress on the system
- Fostering the viewpoint of low frequency-high impact disasters and correct awareness of disaster tendencies that change according to the earthquake characteristics, in the understanding of seismic hazard maps

In response to these recommendations, the J-SHIS has been constructed as a system with the following objectives:

➢ Database forming seismic hazard information sharing bases

The system shall be a database serving as seismic hazard information sharing bases, which does not only display maps generated from the seismic hazard map creating process, but also accumulates all parameters and simulation results for creating seismic hazard maps, and offers seismic hazard information as geospatial information.

➢ Interfaces that realize diverse expressions of seismic hazard maps

Since users of seismic hazard maps are wide-ranging, the system should provide interfaces that offer access to diverse expressions, such as detailed information on a site and qualitative probability ranking information, in addition to the PSHM and the Seismic Hazard Maps for Specified Seismic Source Faults.

➢ Visualization and provision of parameters for creating seismic hazard maps

The system should provide interface for visualizing the parameters

used for seismic activity evaluation models, the shapes of seismic source faults, shallow subsurface structures, deep subsurface structures, etc., and allowing access to such data.

- Visualization of influences of high-frequency subduction-type earthquakes that influence wide areas and low-frequency inland (active fault) earthquakes that influence limited areas

With regard to PSHM, maps should be created and presented by earthquake category so as utilize their advantage of accumulating the effects of diverse seismic sources of different types, complement their disadvantage of concealing the influences of individual earthquakes, and ensure that the evaluation results would be used without any misunderstanding. Contribution factor maps should be created and presented in order to identify earthquake category that have the largest influence to a certain site.

5.3 Technical Background

The J-SHIS provides PSHM, Seismic Hazard Maps for Specified Seismic Source Faults, and geospatial information on shallow subsurface structure, etc. via the Internet. Geospatial information, defined in Article 2, paragraph (1) of the Basic Act on the Advancement of Utilizing Geospatial Information (Act No. 63 of 2007) that entered into force in 2007, is either of the following:

[1] Information that represents the position of a specific point or extent in geospace

[2] Information consisting of a combination of the information above and any information associated thereto

At present, it has become possible to use numerical map data (raster data, vector data) on computers or mutually use such data on networks due to enhancement of the Internet environment, improvement of computer performance, and an increase in publicly disclosed geospatial information. Because of this, it has become easier to overlay multiple maps on a computer, and such data have come to be used more frequently together with geospatial information managed by organizations. Examples of application of geospatial information include Google Maps, car navigation system maps, numerical maps 25000/2500 issued by the Geospatial Information Authority of Japan, digital maps created by local public entities, and geographical statistical information maps being developed by research institutes. The usage is wide-ranging from city planning, and business strategy, to personal information transmission, and users and usage are diversifying. Under the trend of the e-Japan Strategy promoted by the national government, geospatial information held by local public entities has gradually been developed in the form of integrated geographical information systems (GIS), and there are growing cases where such information is also made accessible by general users.

At the same time, development of standards for mutual use of numerical map data via networks is also under way. Open Geospatial Consortium, Inc. (OGC), which is an industrial consortium promoting standardization of GIS-related technology, is developing standards for spatial data models and their representation schemes, as well as the method of combining GIS-supporting software as OpenGIS®. In particular, there have been a growing number of commercial and non-commercial applications and libraries supporting service standards such as WMS (Web Mapping Service), WFS (Web Feature Service), and WCS (Web Coverage Service). From the OpenGIS® standards, a factor that is playing a significant role in promoting the mutual use of geospatial information via networks is an increase of open-source software for GIS and Web mapping. Open-source software is software of which the distribution terms comply with mainly the following criteria (Open Source Initiative, "The Open Source Definition," http://www.opensource.org/docs/osd).

(1) Free redistribution
(2) Source code
(3) Derived works
(4) Integrity of the author's source code
(5) No discrimination against persons or groups
(6) No discrimination against fields of endeavor
(7) Distribution of license
(8) License must not be specific to a product
(9) License must not restrict other software
(10) License must be technology-neutral

One of the greatest merits of using open-source software is reduction of the introduction cost. The introduction cost can be reduced by selecting open-source software that has functions equivalent to commercial software. In addition, since no license cost is required, it is also possible to reduce the financial burden to be borne in later years. Open-source software has been actively used by research institutions, etc., because due to the open source code their system configuration can be easily examined in detail and they can be easily customized for realizing functions. In recent years, leading IT companies have widely come to make technological investments in open source development or release their products as open source. Also, there have been increasing cases where general companies build their enterprise system with open-source software. However, as software maintenance and customer support are not available, they need to be applied after estimating the future cost for investigations and implementation required for realizing functions.

Conventional Web mapping systems, both commercial software and open-source software, usually had the GIS engine or the mapping server (ESRI ArcGIS, MapServer, etc.) on the server side, and after dynamically creating images on the server in response to user requests, returned the images to the clients. However, the disclosure of the Google Maps API (http://code.google.com/intl/ja/apis/maps/) brought about a

substantial change in the approach of Web mapping systems. While the approach of having the GIS engine on the server side and providing services can respond to users' various GIS processing requests, the response speed is generally slow, and the server load is high. Therefore, in order to respond to many users, high-performance hardware would be required. In contrast, the method provided by the Google Maps API transfers the map information around the desired display area from the server to the client in the form of small tile images, and the client side combines the tile images and reconstructs the image on the Web browser. The transmission of the multiple tiles is conducted asynchronously. By preparing the tile images in advance, the server load has been reduced and the response speed to user requests has increased by this method. Also, as a result of providing the process for controlling the user interface for map display as API, users can construct original interfaces. However, the clients' processing load increases, since the map image for the display area is reconstructed from tile images and the map interface control is processed on the Web browser side.

The types of maps currently provided by Google are limited to street maps, satellite maps (air photos), terrain maps, and hybrid maps. Similar services include Yahoo! Maps, etc.

As a system that provides original map information in the form of tile images similar to Google Maps, ka-Map (http://ka-map.maptools.org/) has been published as open source. ka-Map smoothly moves or zooms the map layer information defined by the MapServer (http://mapserver.org/) as maps similar to Google Maps. By using ka-Map's functions, users can use original maps as tile images.

The progress in Web interface-related technology is also remarkable. Such progress can be seen, in part, in the increase in Web pages using AJAX (Asynchronous Javascript + XML). In order to acquire system-specific information for a site designated on a map via the Web, a server request is made, and a process is executed to return information to the client and display it.

Generally, the execution results of server requests were returned in the form of HTML elements, and the HTML was rendered. Therefore, users could not conduct any other processing until the execution results were returned. However, with the use of AJAX, which enables asynchronous requests, users can continue processing that is unrelated to the request. Further, many rich client libraries that combine dynamic HTML, which can change page content without server access, and provide an interface similar to desktop applications have been released as open source (e.g., Ext, RICO, MochiKit, Dojo, script.aculo.us, and Yahoo! User Interface Library).

In particular, OpenLayers (http://openlayers.org/) is an open-source library that is capable of displaying various types of maps and GIS information on the Web by overlaying such data in layers. It is published as a library that can show maps in various different styles, while providing interfaces with the following: OpenGIS®-specified schemes for using numerical maps on networks, such as WMS and WFS; GIS files such as GML (Geography Markup Language); applications such as ka-Map, MapServer, and MapGuide; and services such as Google Maps, Yahoo! Maps, and VirtualEarth.

The J-SHIS needs to stably provide the annually updated seismic hazard maps irrespective of external factor risk including a rise in updating, licensing, and maintenance fees. Also, it needs to be capable of flexibly adapting to hardware enhancement or improvement of system scalability associated with an increase in the amount of information published in line with enhancement of information provision related to earthquake risk. Because of this, use of open-source software was investigated, and the software configuration was decided. The J-SHIS represents one of various presentation methods of seismic hazard maps, and it is a system that helps users navigate to original information held by the seismic hazard maps. Thus, in order to smoothly display all of the maps contained in the J-SHIS, a selection was made for such open-source software related to Web interface, GIS, and Web mapping that are necessary for displaying seismic hazard maps by using tile images, as in the case of Google Map, and for smoothly moving to or zooming the area around the target site as well as switching between maps or displaying site information with a user-friendly interface.

5.4 J-SHIS System

The J-SHIS system is a data management/Web mapping system. This system manages PSHM, Seismic Hazard Maps for Specified Seismic Source Faults, and information on shallow/deep subsurface structures in a centralized manner, and is based on open-source software which allows general users to easily view such information on their Web browsers. The characteristics of the J-SHIS as a Web mapping system are shown below.

- Seismic hazard map viewing function supporting 250 m mesh
- Smooth map scroll function (moving, zooming in/out)
- Image overlay function (layer transparency function) between seismic hazard maps and the Google Map service
- Function for polygonal representation of seismic source fault on the browser
- Interface for displaying conditional probability of exceedance maps and scenario earthquake maps by using seismic source fault polygons
- Function to present/download hazard curves for all Third-mesh
- Map distribution function using WMS (trial operation)
- Geospatial information distribution function using WFS (trial operation)

Figure 5.4-1 shows the outline of the J-SHIS system. The numerical data of seismic hazard maps and information on shallow/deep subsurface structures are accumulated in the data

acquisition tier of the J-SHIS, and stored in the seismic hazard map numerical database in the data accumulation tier according to the rules defined in the system. Public data files (CSV format) and GIS data files (ESRI Shapefile, GeoTiff) are created from the information stored in the database. Also, in order to reduce the access load to seismic hazard maps by Web interface, the tile images (cache images) are generated in advance.

General users can use the J-SHIS by accessing the Web contents (J-SHIS Web system) published in the application tier and the service tier by using a Web browser. In addition, by using a download interface, users are able to download the numerical data of seismic hazard maps that are allocated in the application tier of the J-SHIS as batch data for the whole of Japan and in the scale of the First-mesh. The format of the public files is CSV. While provision of the files as general-purpose GIS contents is under consideration, it is currently difficult to provide data via the Internet since the data size of information on 250 m mesh seismic hazard maps is enormous. Studies will be made in the future on development of GIS data and advancement of the data provision interface from the viewpoint of users, such as providing GIS contents in units of administrative districts.

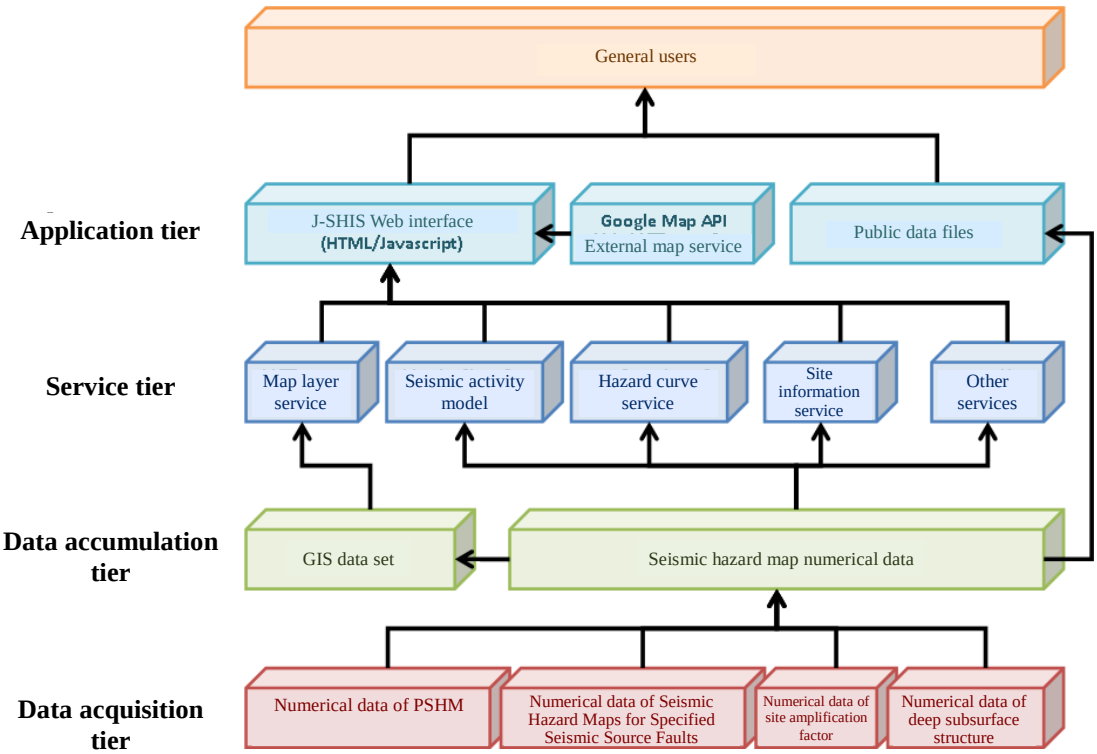

Figure 5.4-1 Outline of the J-SHIS system

5.4.1 Functions

The J-SHIS has a Web mapping function for viewing and downloading information on seismic hazard maps. Table 5.4.1-1 shows the map information concerning seismic hazard maps that can be viewed by using the J-SHIS.

PSHM can present the following maps in a mesh of about 250 m nationwide: maps of probability of ground motions of JMA seismic intensity 5 Lower, 5 Upper, 6 Lower, or 6 Upper or more within 30 years for "all earthquakes," "earthquake category I," "earthquake category II," and "earthquake category III"; maps of ground motions at a certain intensity for a 3% or 6% probability of exceedance (or JMA instrumental seismic intensity, peak ground velocity, and peak velocity on the engineering bedrock); maps of ground motions for a 2%, 5%, 10%, or 39% probability of exceedance within 50 years (JMA instrumental seismic intensity, peak ground velocity, and peak velocity on the engineering bedrock). In addition, maps for the "average case" and the "maximum case" can be presented for "all earthquakes" and "earthquake category III." However, there are no maps of probability of ground motions of JMA seismic intensity 5 Upper and 6 Upper or more within 30 years in the 2008 version (starting date: January 1, 2008). It should be noted that the 2008 version, which has been developed based on the Third-mesh nationwide, greatly differs from the 2009 version.

The PSHM by earthquake category are maps that show the probability of exceedance of a specific JMA seismic intensity within 30 years in quartiles, using a color scale of four levels. They present the probability of ground motions of JMA seismic intensity 5 Lower, 5 Upper, 6 Lower, or 6 Upper or more for earthquake categories I, II, and III in four colors according to the

level of probability. The 2008 version does not provide maps by earthquake category.

Contribution factor of PSHM indicate the earthquake category that has the largest influence on each site in different colors. They show the earthquake category which accounts for the highest probability of ground motions of JMA seismic intensity 5 Lower, 5 Upper, 6 Lower, or 6 Upper or more within 30 years for the average case and for the maximum case. The 2008 version does not provide maps that show the degree of influence of the probability of ground motions of JMA seismic intensity 5 Upper or 6 Upper or more within 30 years.

Maps of conditional probability of exceedance consist of maps of the probability of ground motions of JMA seismic intensity 5 Lower, 5 Upper, 6 Lower, or 6 Upper or more where the designated earthquake occurs, and maps of expected values of JMA instrumental seismic intensity. The earthquakes for which maps of conditional probability of exceedance are available are earthquakes occurring in major active fault zones, earthquakes occurring at other active faults, and subduction-type earthquakes without specified source faults.

Maps of scenario earthquakes are shortened terms for Seismic Hazard Maps for Specified Seismic Source Faults. They present the simulation results of strong motion prediction under the hybrid method for major active fault zones. In the simulation, the JMA instrumental seismic intensity on the engineering bedrock for the Third-mesh is simulated, and then the distribution of the JMA instrumental seismic intensity on the ground surface for the 250 m mesh is obtained based on the site amplification factor for JMA seismic intensity evaluated for the 250 m mesh. The maps available are those of the peak velocity on the engineering bedrock and those of the JMA instrumental seismic intensity on the ground surface.

Maps of the site amplification factor show the geomorphologic classification, the 30 m average shear wave velocity, and the shallow subsurface amplification factor (amplification factor for peak velocity from the engineering bedrock with shear wave velocity 400m/s to the ground surface) in a mesh of about 250 m (quarter mesh) nationwide.

Maps of the deep subsurface structure present the geological boundaries in a 1 km mesh nationwide based on the depth and elevation. Maps of scenario earthquake are calculated based on the deep subsurface structure models.

Table 5.4.1-1 Map information in the J-SHIS

Map information	Explanation
PSHM	Nationwide PSHM in 250 m mesh (Figure 5.4.1-1)
PSHM by earthquake category	Map of ranking of exceedance probability in quartiles (Figure 5.4.1-2)
Contribution factor of PSHM	Area map of the largest degree of influence (Figure 5.4.1-3)
Conditional probability of exceedance	Map of exceedance probability and map of expected values of the JMA instrumental seismic intensity where a designated earthquake occurs (Figure 5.4.1-4)
Maps of scenario earthquakes	Seismic Hazard Map for Specified Seismic Source Faults (Figure 5.4.1-5)
Site amplification factor	Area map of the geomorphological classification, the 30 m average shear wave velocity, and the amplification factor of the shallow subsurface layers in the 250 m mesh (Figure 5.4.1-6)
Deep subsurface structure	Area map of the deep subsurface used in the simulation for Seismic Hazard Maps for Specified Seismic Source Faults (Figure 5.4.1-7)

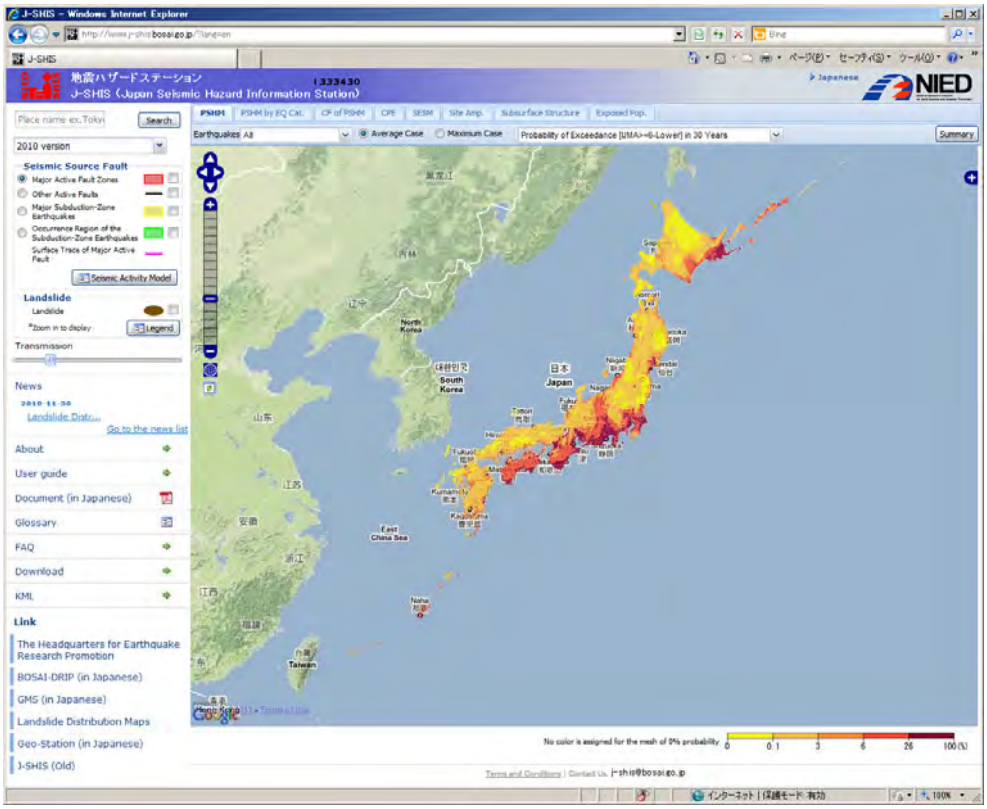

Figure 5.4.1-1 PSHM.

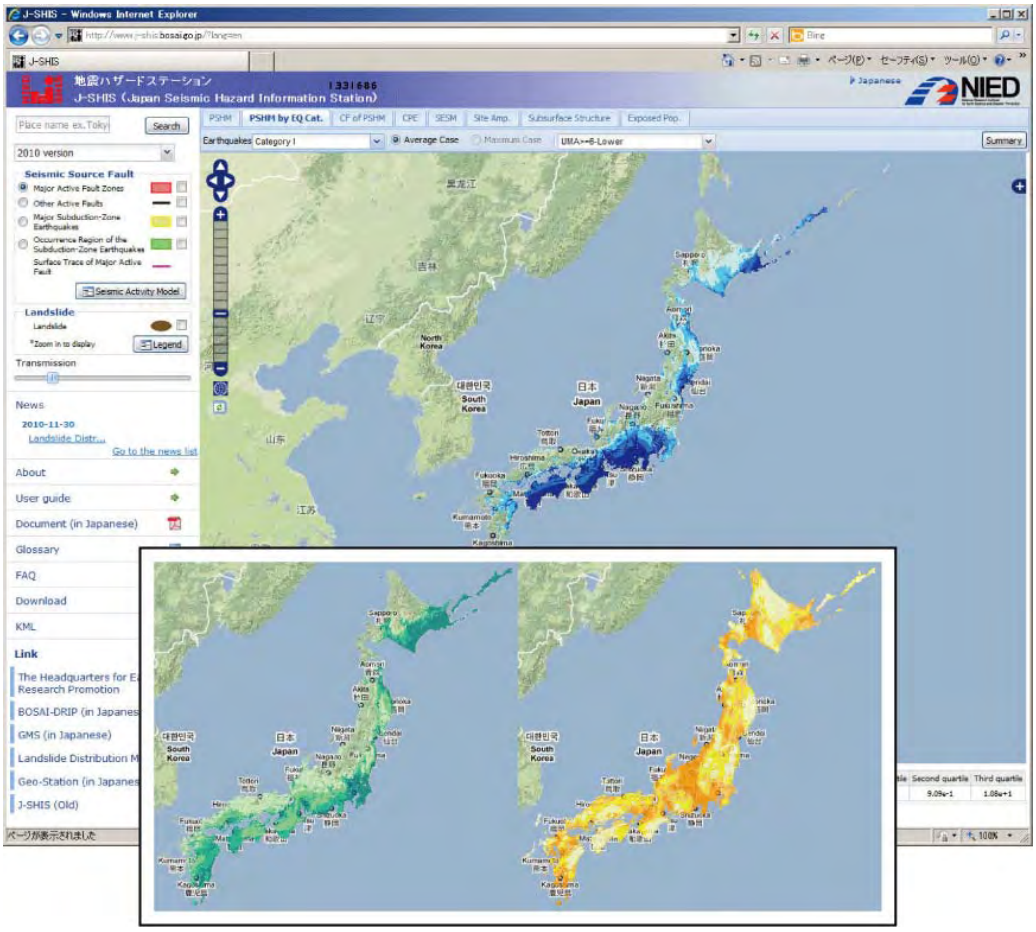

Figure 5.4.1-2 PSHM by earthquake category.

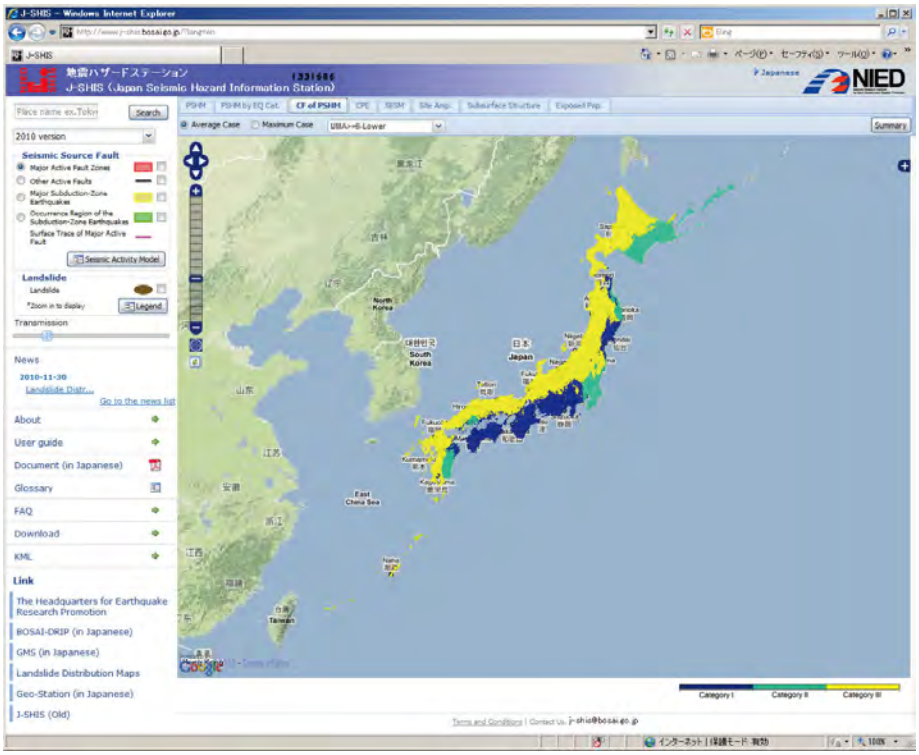

Figure 5.4.1-3 Contribution factor of PSHM

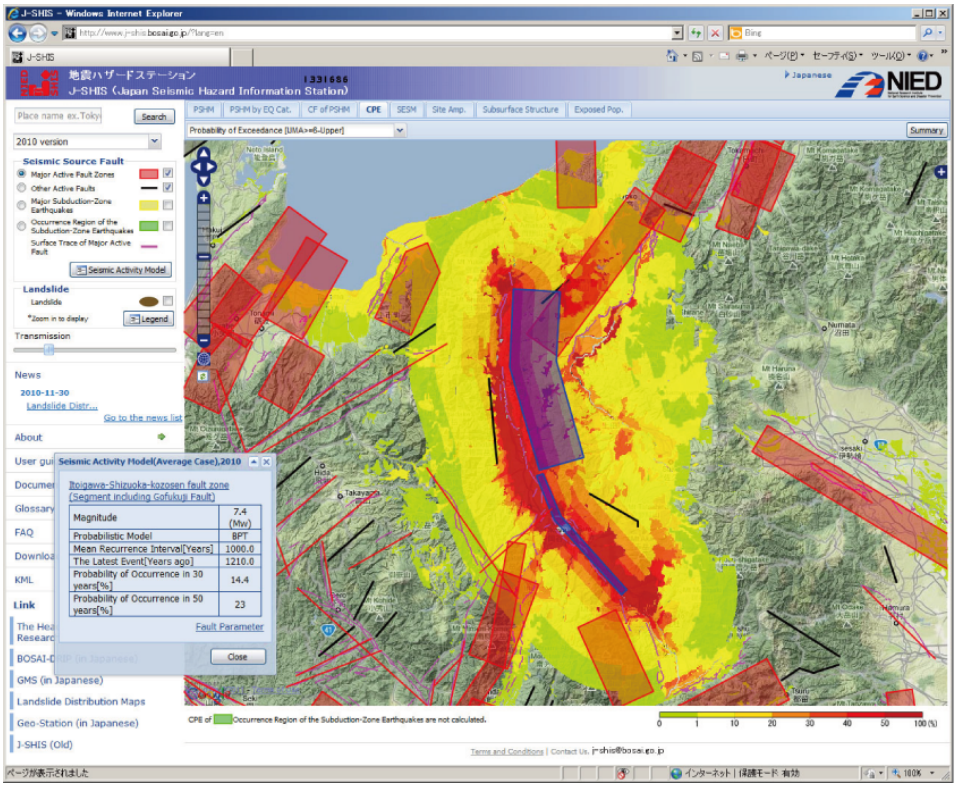

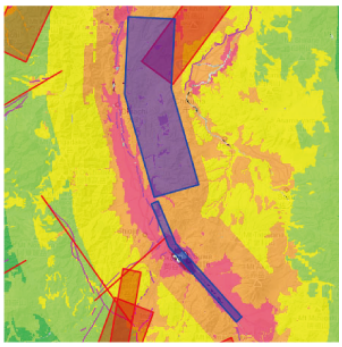

Figure 5.4.1-4 Conditional probability of exceedance.

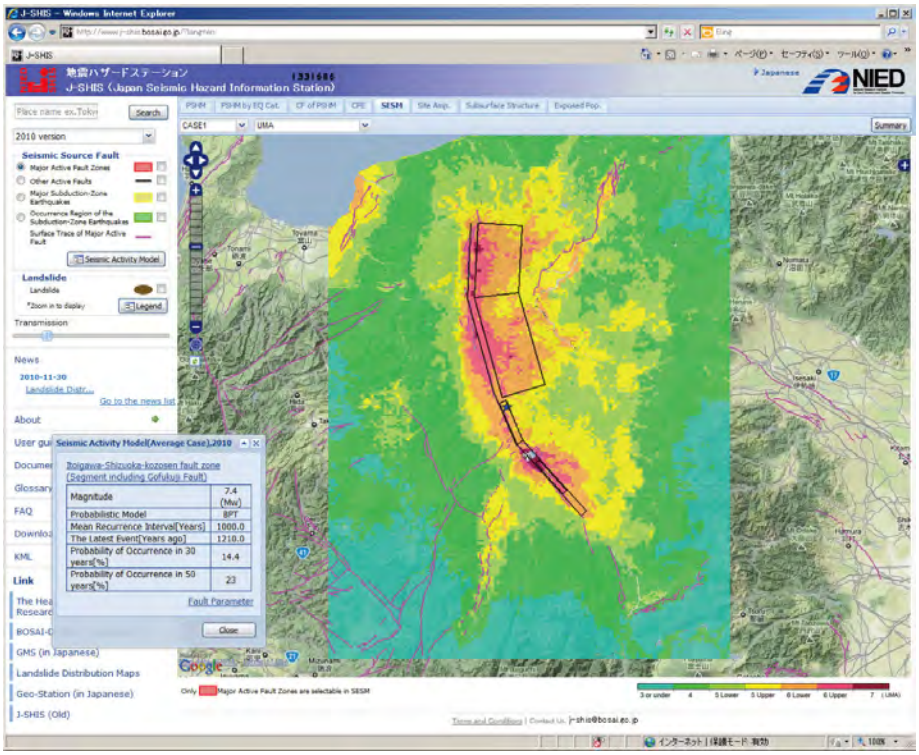

Figure 5.4.1-5 Scenario earthquakes

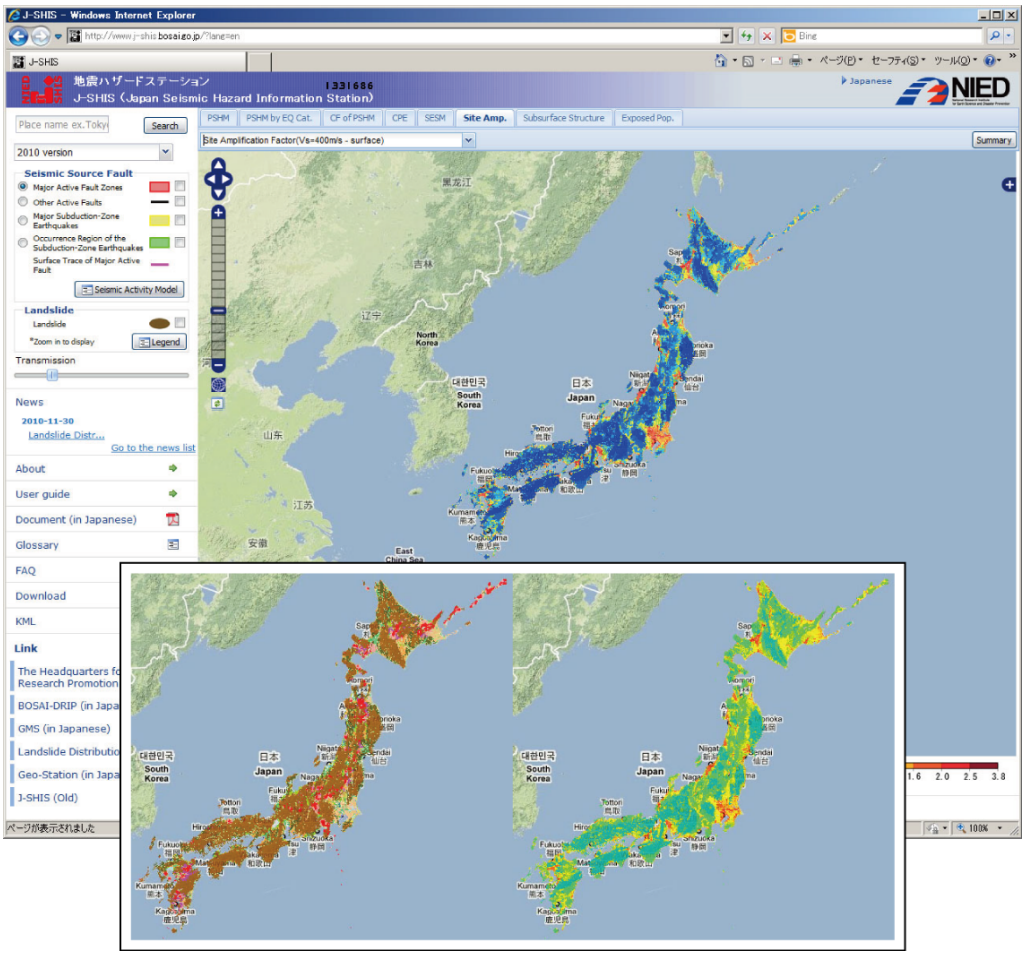

Figure 5.4.1-6 Site amplification factor

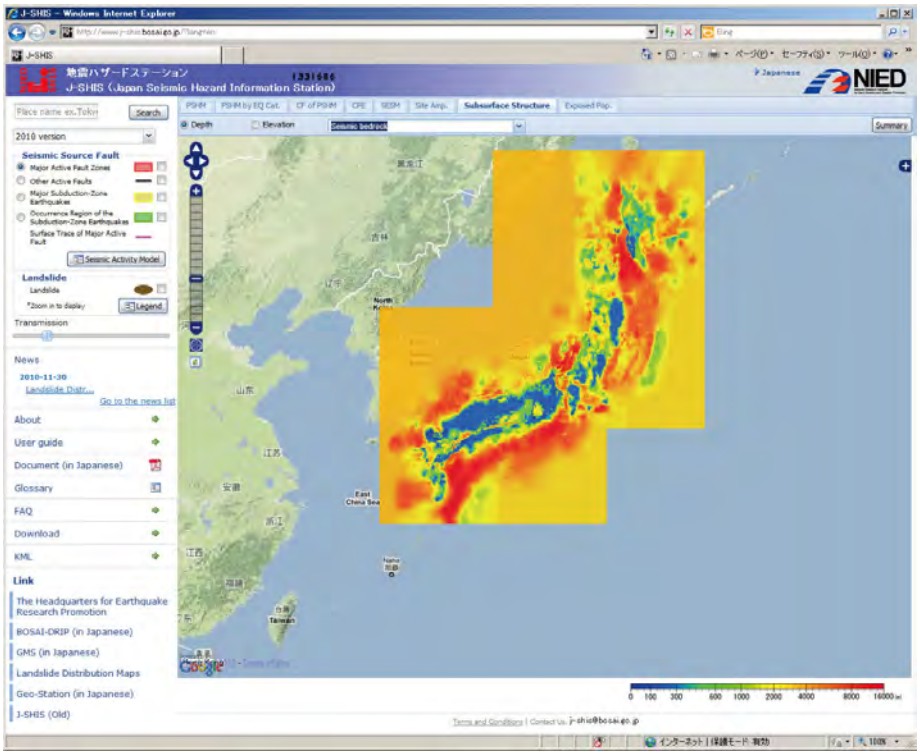

Figure 5.4.1-7 Deep subsurface.

The functions of the J-SHIS for general users are provided in the form of Web contents through the services of the J-SHIS Web system shown in Table 5.4.1-2. The respective Web contents are linked together through user interfaces.

Table 5.4.1-2 Service outline

Service	Explanation
Map layer service	Service of overlaying the map images tiled on the Web interface on top of Google Maps by designating the layer code defined in the J-SHIS (Figure 5.4.1-8)
Seismic activity model service	Service of searching the seismic activity models associated with a selected fault shape from the database, and presenting them in the Web interface (Figure 5.4.1-9)
Site information service	Service of searching the site information (exceedance probability, site amplification factor, etc.) within the mesh corresponding to a designated 250 m mesh code from the database, and presenting them in the Web interface (Figure 5.4.1-10)
Hazard curve service	Service of searching the hazard curve for the Third-mesh corresponding to a designated 250 m mesh code from the database, and presenting the hazard curve graph and the graph of the degree of influence in the Web interface. It is also a service for creating and downloading numerical data of hazard curves. (Figure 5.4.1-11)
Data download service	Service for downloading numerical information and data rules associated with the seismic hazard maps (Figure 5.4.1-12)
Other services	WMS and WFS services are provided within NIED on a trial basis. The server load and other aspects are investigated. The system configuration and software configuration are studied, and as well, the possibility for providing these services to general users is considered. (Figure 5.4.1-13)

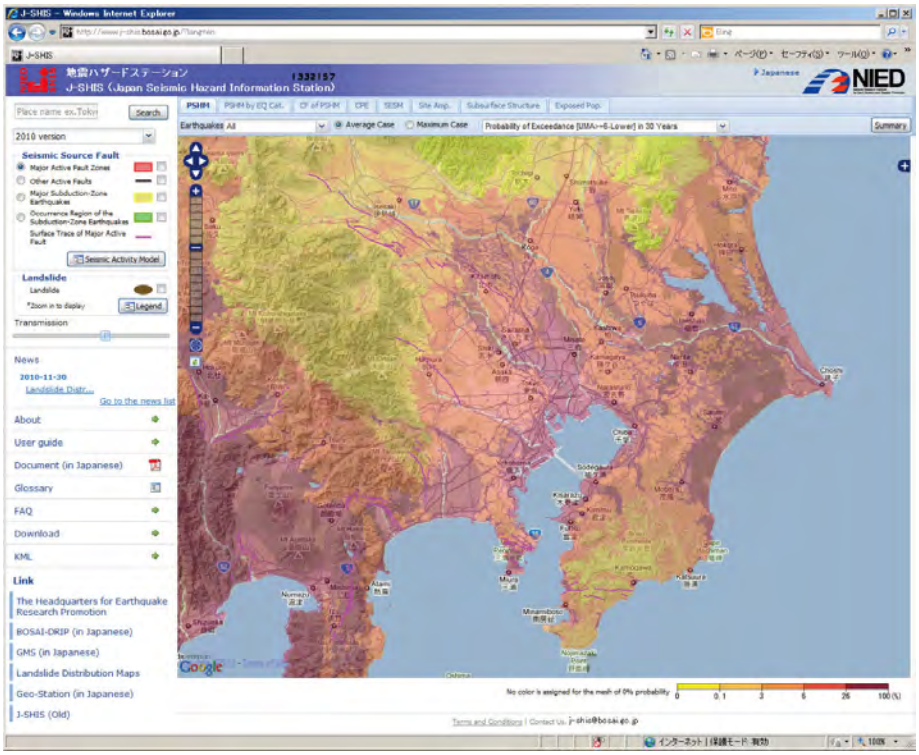

Figure 5.4.1-8 Map layer service

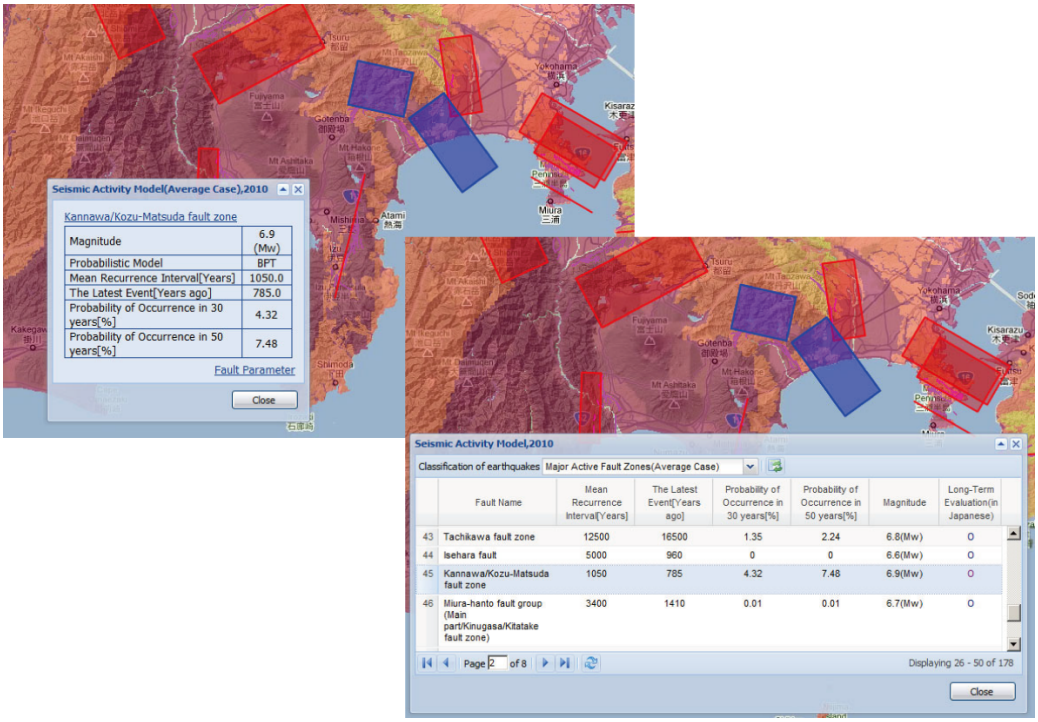

Figure 5.4.1-9 Seismic activity model service

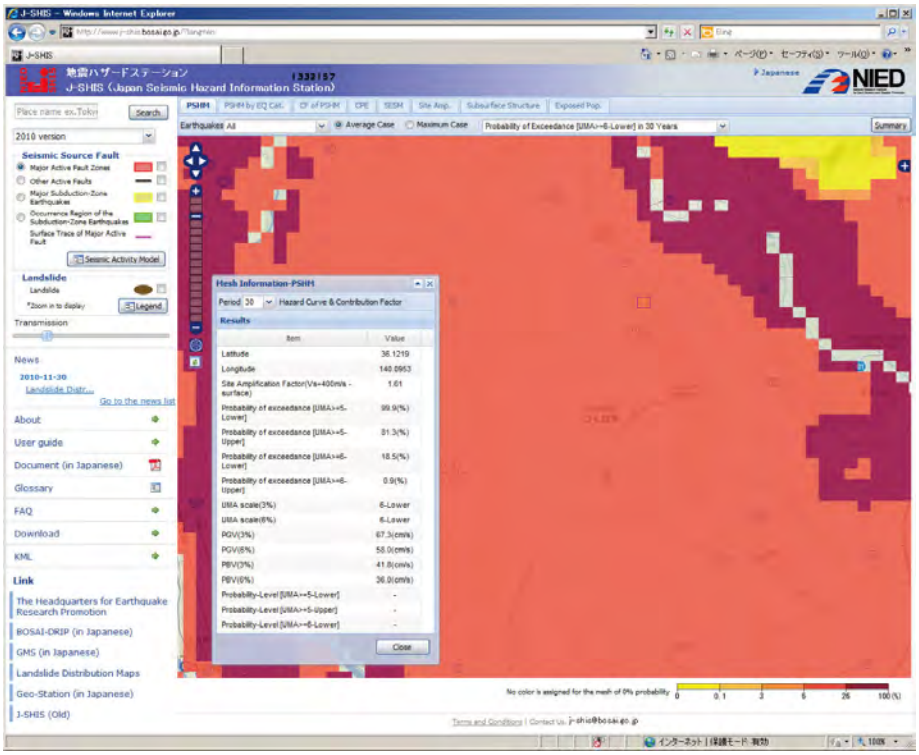

Figure 5.4.1-10 Site information service

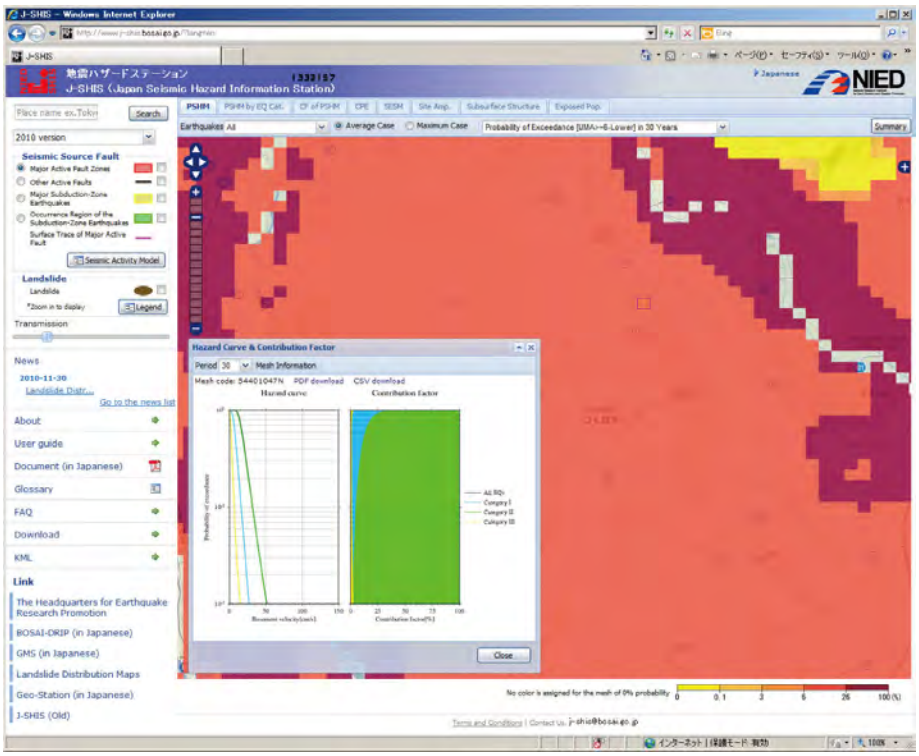

Figure 5.4.1-11 Hazard curve service

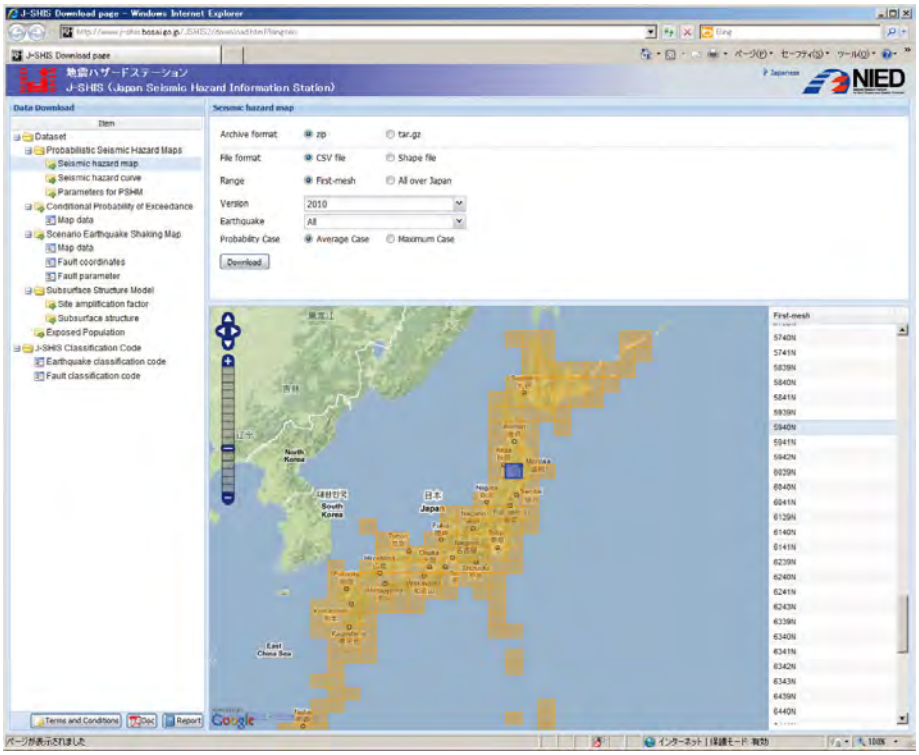

Figure 5.4.1-12 Data download service

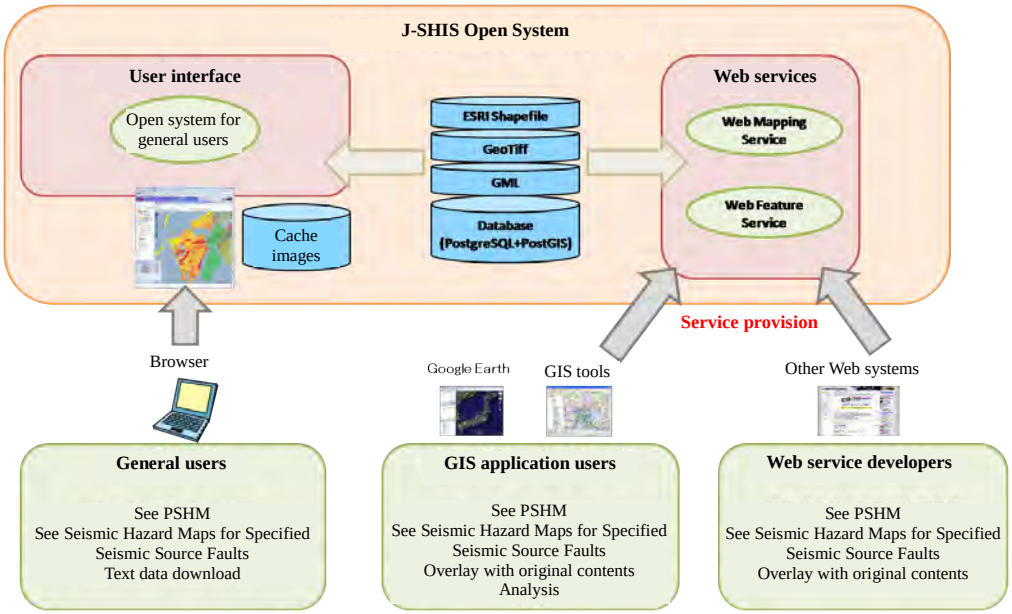

Figure 5.4.1-13 WMS service

[Map layer - seismic activity model service linkage interface]

The map layer - seismic activity model service linkage interface offers the function to link together the maps related to PSHM (PSHM, maps by earthquake category, maps of the degree of influence) and maps related to Seismic Hazard Maps for Specified Seismic Source Faults (maps of scenario earthquakes, maps of conditional probability of exceedance) based on the shape of the evaluated seismic source fault. For contents using the map layer service, the interface presents the map images related to the seismic hazard maps and the fault shapes on top of each other. Since the seismic activity model service is associated with the fault shapes, if the user selects a fault shape, the seismic activity model of the selected fault shape is presented. Also, the user can shift to the map of conditional probability of exceedance and the

map of scenario earthquake that are associated with the selected fault, without changing the displayed area (Figure 5.4.1-14).

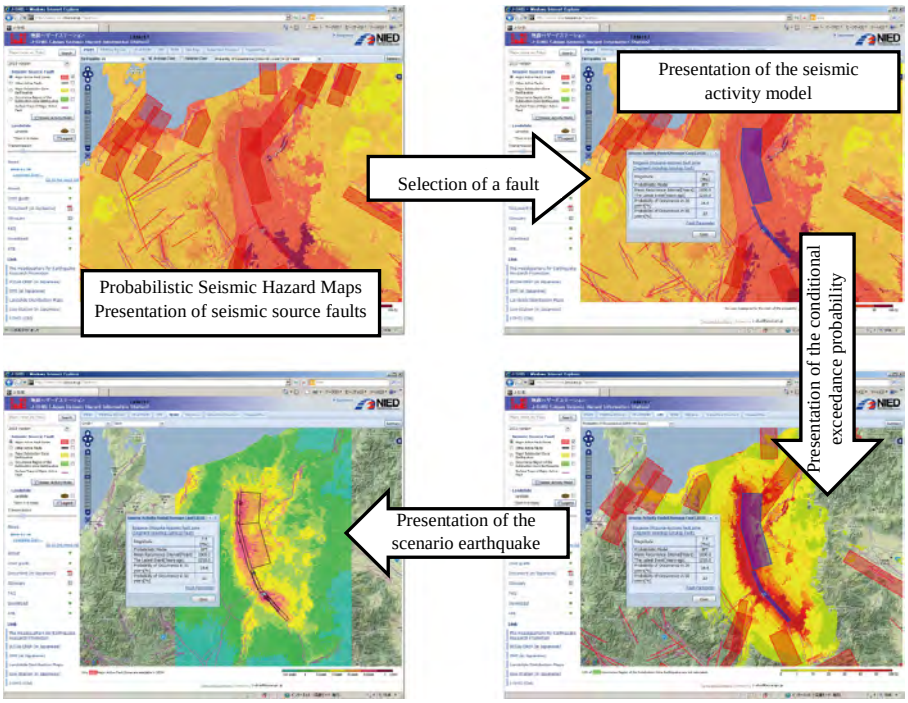

Figure 5.4.1-14 Linkage of maps based on seismic activity model

[Map layer - site information service linkage interface]

The map layer - site information service linkage interface offers the function to present the site information related to the target site on the presented map layer. Since the map layer is made transparent and is presented over Google Maps, it is easy to identify the location. The transparency rate can be changed dynamically. Different site information is shown depending on the presented map layer (Figure 5.4.1-15).

[Site information - hazard curve service linkage interface]

The site information - hazard curve service linkage interface offers the function to show the hazard curves and the graph of the degree of influence when site information is presented while the Probabilistic Seismic Hazard Map layer is displayed. This interface can be used to download numerical information and image information of the hazard curves for a selected site (Figure 5.4.1-16).

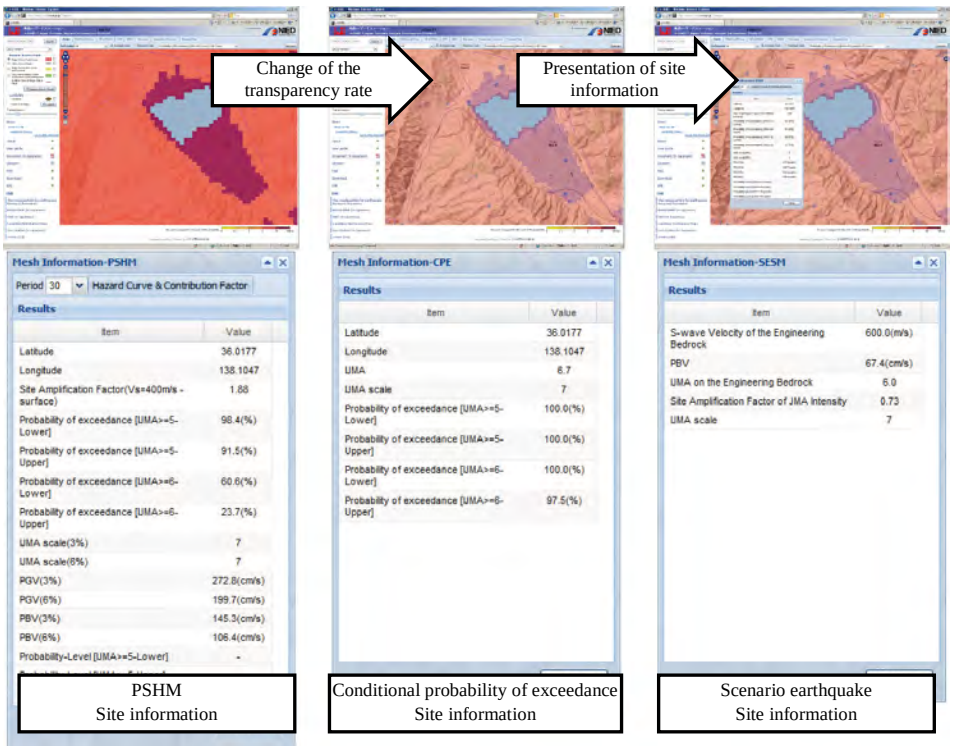

Figure 5.4.1-15 Presentation of Site Information

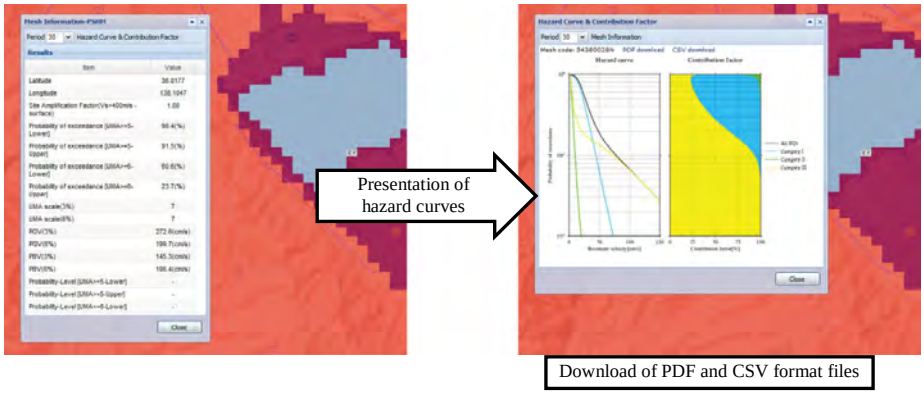

Figure 5.4.1-16 Download of hazard curves

5.4.2 Public data

In order to respond to the recommendation by the Study Committee for Engineering Applications of the National Seismic Hazard Maps, which is "Disclosure of not only the results, but also the process—Making the process of uncertainty evaluation open," the J-SHIS publishes information used in the process of making the PSHM and the Seismic Hazard Maps for Specified Seismic Source Faults. The published information is shown in Table 5.4.2-1.

Table 5.4.2-1 Public data (part 1)

Public data	Explanation
[PSHM] Map data files	Files are provided for the respective earthquake types of "all earthquakes," "earthquake category I," "earthquake category II," and "earthquake category III," and the respective probability cases of "average case" and "maximum case." They are CSV files containing the following values, corresponding to 250 m mesh codes: the probability of ground motions of JMA seismic intensity 5 Lower, 5 Upper, 6 Lower, or 6 Upper or more within 30 years; the JMA instrumental seismic intensity for a 3% or 6% probability of exceedance; the peak ground velocity; the peak velocity on the engineering bedrock; the JMA instrumental seismic intensity for a 2%, 5%, 10%, or 39% probability of exceedance within 50 years; the peak ground velocity; and the peak velocity on the engineering bedrock. Selection can be made between batch download files for the whole of Japan and download files for each First-mesh.
[PSHM] Hazard curve data files	Files are provided for the respective target Third-mesh codes, the respective probability cases of "average case" and "maximum case," and the respective evaluation periods of "30 years" and "50 years." They are CSV files containing the exceedance probability relating to each earthquake for the simulated peak velocity on the engineering bedrock. The files can be downloaded with respect to all Third-meshs for which hazard curves have been simulated.
[PSHM] Other data files	The following parameters used for simulating PSHM can be downloaded in a batch: ・ Fault shape data ・ Seismic activity evaluation parameters ・ Occurrence frequency data ・ Zone shape data ・ Interplate/intraplate earthquake ratio data ・ Parameters for the attenuation relation ・ Plate shape data
[Conditional probability of exceedance] Map data files	Files are provided for the respective target earthquakes (earthquakes in major active fault zones, earthquakes at other active faults, subduction-type earthquake). They are CSV files containing the values of the probability of ground motions of JMA seismic intensity 5 Lower, 5 Upper, 6 Lower, or 6 Upper or more, and the expected values of the JMA instrumental seismic intensity on the ground surface, corresponding to the 250 m mesh. * Subduction-type earthquakes only include those with specified source faults.
[Conditional probability of exceedance] Fault parameter files	Files are provided for the respective target earthquakes (earthquakes in major active fault zones, earthquakes at other active faults, subduction-type earthquake). They are CSV files containing the fault parameters (reference position, fault length, fault width, strike angle, dip angle, magnitude) of the target earthquake.

Table 5.4.2-1 Public data (part 2)

Public data	Explanation
[Seismic Hazard Maps for Specified Seismic Source Faults] Map data files	Files are provided for the respective target earthquakes (earthquakes in major active fault zones). They are CSV files containing the following values, corresponding to the 250 m mesh: the peak velocity on the engineering bedrock; the JMA instrumental seismic intensity on the engineering bedrock; the site amplification factor for JMA seismic intensity; and the JMA instrumental seismic intensity on the ground surface.
[Seismic Hazard Maps for Specified Seismic Source Faults] Fault coordinate data files	Files are provided for the respective target earthquakes (earthquakes in major active fault zones). They are CSV files containing the position of the surface trace of the fault, fault vertex coordinates, asperity vertex coordinates, and element source position.
[Seismic Hazard Maps for Specified Seismic Source Faults] Fault parameter files	Files are provided for the respective target earthquakes (earthquakes in major active fault zones) in PDF format.
[Site information] Shallow subsurface data files	Shallow subsurface data files are CSV files containing geomorphologic classification codes corresponding to the 250 m mesh, the 30 m average shear wave velocity values, and amplification factor values (amplification factor for the peak velocity from Vs=400m/s to the ground surface). Selection can be made between batch download files for the whole of Japan and download files for each First-mesh.
[Site information] Deep subsurface data files	Deep subsurface data files are divided into those containing elevation values and those containing depth values. Each file contains the elevation values or depth values of the upper surface of layers 1 to 33 for the Third-mesh. Selection can be made between batch download files for the whole of Japan and download files for each First-mesh.
[Site information] Deep subsurface media data files	Deep subsurface media data files are CSV files containing the primary wave velocity values, shear wave velocity values, density, Qp values, and Qs values for the respective layers of deep subsurface data.

5.4.3 Seismic hazard map numerical database

The J-SHIS system is a system which manages PSHM, Seismic Hazard Maps for Specified Seismic Source Faults, and information on shallow/deep subsurface structures in a centralized manner, and allows creation of contents for general users. At present, the total database size including the tables for management purposes and indices for increasing the database search speed is about 260 gigabytes. The outline of data managed by the seismic hazard map numerical database and the estimated data size are described below.

As basic data of PSHM, seismic activity evaluation models, seismic source fault models, and the numerical data of hazard curves simulated based on the Third-mesh nationwide are accumulated and managed by using a relational database system.

The hazard curves for all meshs are stored in the database as numerical data of exceedance probability corresponding to the Third-mesh codes, the earthquake codes that uniquely identify the earthquake to be considered, the evaluation period, and the peak velocity on the engineering bedrock]. Thus, the J-SHIS system can create an area map of strong motion indices corresponding to a designated exceedance probability or an exceedance probability map corresponding to designated strong motion indices, while considering a given number of earthquakes. In the same way, the J-SHIS system is able to create a map of the contribution factor of PSHM which shows the distribution of earthquakes that have the largest degree of influence in the respective 250 m meshs, and maps by earthquake category which present the exceedance probability in the form of a quartile ranking. Among the map data above, those concerning "earthquake category I," "earthquake category II", and "earthquake category III" are stored in the database and are utilized as basic information on earthquake disaster risk.

Also, as simulation-related information, parameters used for evaluating seismic activity are managed using the database. The fault shape data are classified into those of rectangular faults, non-rectangular faults, and discretized rectangular source faults, and the numerical data and GIS data are stored in the database.

Table 5.4.3-1 and Table 5.4.3-2 show the number of hazard

curve records and the number of map data records of Probabilistic Seismic Hazard Maps for which the starting date is January 1, 2009.

As basic data of conditional probability of exceedance maps, output results, namely, the probability of ground motions of JMA seismic intensity 5 Lower, 5 Upper, 6 Lower, or 6 Upper or more in a 250 m mesh and expected values of the JMA instrumental seismic intensity on the ground surface are accumulated and managed by using the database. Conditional probability of exceedance maps are managed based on the fault code that uniquely identifies an earthquake and the version number, considering the case where parameters used in the simulation are changed. The number of data records is shown in Table 5.4.3-3.

As basic data of scenario earthquake maps, the fault coordinate data that have been input, and output results which are strong motion indices in a 250 m mesh (values of the peak velocity on the engineering bedrock, values of the velocity on the engineering bedrock, values of the JMA instrumental seismic intensity on the ground surface, values of the JMA instrumental seismic intensity on the engineering bedrock, and values of site amplification factor for JMA seismic intensity) are accumulated and managed by using a relational database. Scenario earthquake maps are managed based on the fault code that uniquely identifies an earthquake and the version number, considering the case where parameters used in the simulation are changed. The number of data records is shown in Table 5.4.3-4.

As basic data of maps of the shallow subsurface structure, the shallow subsurface information based on the Third-mesh, which was used from the 2005 version to the 2008 version and the shallow subsurface information based on the 250 m mesh that was used in the 2009 version are accumulated and managed as indices corresponding to 250 m mesh codes (geomorphologic classification, 30 m average shear wave velocity, and amplification factor) by using a relational database. The shallow subsurface information based on the Third-mesh can be treated equivalently as the shallow subsurface information based on the 250 m mesh by dividing the information into information based on the 250 m mesh and registering it in the database. The number of data records is shown in Table 5.4.3-5.

As basic data of maps of the deep subsurface structure, the deep subsurface information developed based on the Third-mesh covering the whole of Japan is accumulated and managed as indices corresponding to Third-mesh codes (elevations and depths of layers 1 to 33) by using a relational database. The number of data records is shown in Table 5.4.3-6.

Table 5.4.3-1 Number of hazard curve records for the 2009 version

Item	Number of data	Remarks
Third-mesh codes	384,948	Number of Third-mesh codes for the land area of the whole of Japan
Earthquake types	40	Maximum case: 3
Evaluation period types	2	30 years, 50 years
Samples of the peak velocity on the engineering bedrock	46	0 m/s - 300 m/s
Total	1,416,608,640	Among these, 406,834,996 records for which the exceedance probability is not zero are registered in the database. Database size: 26 GB Index size: 34 GB Total size: 60 GB

Table 5.4.3-2 Number of map data records for the 2009 version

Item	Number of data	Remarks
250 m mesh codes	5,955,180	Number of 250 m mesh codes for the land area of the whole of Japan
Earthquake types	4	Average case: "earthquake categories I, II, and III" Maximum case: "earthquake category III"
Map types	22	Exceedance probability within 30 years (4)
Total	524,055,840	Among these, 82,215,956 records for which the exceedance probability is not zero are registered in the database. Database size: 5 GB Index size: 6 GB Total size: 11 GB

Table 5.4.3-3 Number of map data records for the conditional probability of exceedance maps

Item	Number of data	Remarks
250 m mesh codes	—	Differs for each scenario earthquake
Number of simulated earthquakes	369	Earthquakes occurring in major active fault zones, earthquakes occurring at other active faults, and subduction-zone earthquakes
Total	308,121,829	Database size: 28 GB Index size: 15 GB Total size: 43 GB

Table 5.4.3-4 Number of map data records for the scenario earthquake maps

Item	Number of data	Remarks
250 m mesh codes	—	Differs for each scenario earthquake
Number of scenario earthquakes	149	Earthquakes occurring in major active fault zones (484 cases in total)
Total		Database size: 15 GB Index size: 7 GB Total size: 22 GB

Table 5.4.3-5 Number of map data records for the maps of the shallow subsurface structure

Item	Number of data	Remarks
250 m mesh codes	6,168,976 (2008 version) 6,208,787 (2009 version)	Including meshs for which the geomorphologic classification is 0 (30 m average shear wave velocity: 0)
Total	6,168,976 (2008 version) 6,208,787 (2009 version)	Database size: 1 GB Index size: 1 GB Total size: 2 GB

Table 5.4.3-6 Number of map data records for the maps of the deep subsurface structure

Item	Number of data	Remarks
Third-mesh codes	2,701,360	Including the sea area
Total	2,701,360	Database size: 850 MB Index size: 150 MB Total size: 1 GB

5.4.4 Hardware configuration

As indicated in Section 5.4.3, the J-SHIS is a seismic hazard information web system with a large database, and every year, data related to the PSHM with the data size shown in Table 5.4.3-1 and Table 5.4.3-2 are added to the database. In addition, the system creates cache map images of about 1 terabyte in

advance so as to enable smooth viewing of the various maps through Web interfaces. However, it is not the type of system where the database is updated frequently. Therefore, the system area is configured with highly reliable disks (SAS), and disk arrays are configured by using low-cost, large-capacity disks (SATA) with RAID 6 and hot swap in order to increase hardware fault tolerance. Since it is difficult to back up the large database with a general-purpose backup medium, a redundant system using two units is adopted. By configuring two exactly identical systems below the load balancer, the system achieves the backup function and the load distribution as Web server.

Table 5.4.4-1 shows the hardware configuration of the J-SHIS.

5.4.5 Software configuration

The J-SHIS system is configured as a system that operates on Redhat Linux ES5. Since all applications are not dependent on Redhat Linux, they can also be operated on other Linux systems (Fedora, CentOS, etc.). Table 5.4.5-1 shows the software configuration of the data acquisition tier, the service tier, and the application tier of the J-SHIS system (see Figure 5.4-1).

5.5 Toward Sending Information on Earthquake Risk

The J-SHIS system has been built as a platform for providing information pertaining to seismic hazard maps in an easy-to-understand manner, based on the recommendations by the Study Committee for Engineering Applications of the National Seismic Hazard Maps. Under such circumstances, the long-term strategy guidelines "Innovation 25" was adopted by the Cabinet on June 1, 2007. "Innovation 25" covers the years up to 2025, discusses how to create the future of Japan with prosperity and hopes, and sets out the policies to be addressed on a short- and long-term basis, including research and development, social reform and human resources development. One of the specific measures of the roadmap for the technology innovation strategy is "Projects for Accelerating the Transfer to Society." As one such project, "Construction of the information and communication system which gives detailed disaster information to each resident, and helps disaster countermeasures" was mentioned in "Innovation 25." In response to this, NIED launched research and development of a "disaster risk information platform" with the aim of creating a society where any person could learn about the "risk" of natural disasters they may incur and plan/implement "disaster prevention measures" suitable for that person, and in order to provide "materials (disaster risk information)" and "tools/means (platform)" to that end.

For the purpose of "construction of disaster risk information platforms," activities are being planned where the research target is stretched from the conventional seismic hazard to also cover earthquake risk evaluation. It is expected that these efforts will contribute to "strengthening bridge functions to promote engineering and sociological research for disaster prevention and mitigation" which is one of the basic goals set out in HERP's "New Policy for Earthquake Research: The second basic comprehensive policy for the promotion of earthquake observation, measurement, surveys and research."

Table 5.4.4-1 Hardware configuration

Item	Component	Quantity
Server A	ProLiant DL380 G5	1
	(1) Quad Core Intel® X-X5460 3.16 GHz 2x6MB L2	2
	(2) 2GB PC2-5300 FB-DIMM DDR2-667	4
	(3) 146GB hot-plug 10krpm 2.5” SAS hard disk drive	3
Storage A	StorageWorks MSA60	2
	(1) Smart Array P800/512 BBWC controller	2
	(2) Modular Smart Array60	2
	(3) 1TB hard disk drive (SATA)	24
Server B	ProLiant DL380 G5	1
	(1) Quad Core Intel® X-X5460 3.16 GHz 2x6MB L2	2
	(2) 2GB PC2-5300 FB-DIMM DDR2-667	4
	(3) 146 GB hot-plug 10 krpm 2.5” SAS hard disk drive	3
Storage B	StorageWorks MSA60	2
	(1) Smart Array P800/512 BBWC controller	2
	(2) Modular Smart Array60	2
	(3) 1TB hard disk drive (SATA)	24

Table 5.4.5-1 Software configuration

Software	Name	Remarks
OS	Redhat Linux ES5	Operating system
Web server	Apache-2.2.9	[Service tier]
Script language	PHP-5.2.6	[Data acquisition tier] [Data accumulation tier] [Service tier] Script languages for CGI/operational application development
	Perl-5.8.8	
Map server WMS server WFS server	Mapserver-5.2.1	[Service tier] Map service server
Tile server	Ka-Map-1.0	[Service tier] Tile image creation/access program
GIS	GRASS-6.3.0	[Data accumulation tier] Open-source GIS system. The J-SHIS system uses it for converting vector data into raster data.
Database	PostgreSQL-8.3.3	[Data accumulation tier] Open-source relational database management system
GIS add-on	PostGIS-1.3.3	[Data accumulation tier] Add-on for handling GIS information in the PostgreSQL database
Library	proj-4.6.1	[Data accumulation tier] Geodetic system conversion library
	shapelib-1.2.10	[Data accumulation tier] ESRI Shapefile library
	gdal-1.6.0	[Data accumulation tier] GIS data conversion library
	geos-3.0.0	[Data accumulation tier] Computational geometry library
	libgeotiff-1.2.5	[Data accumulation tier] Library for GeoTiff
Javascript library	OpenLayers-2.7	[application tier] Map service overlay library
	Ext-2.2	[application tier] Rich client library
External map access API	Google Map API	[application tier] Javascript API for accessing Google Maps

6. Toward the Future

The accomplishments to date and future challenges concerning seismic hazard maps are summarized in Table 6-1. In the future, it is essential to not only solve problems related to creation of seismic hazard maps, but to also promote efforts for putting the maps to effective use and for bridging to earthquake disaster prevention.

References for Chapter 6

1) Fujimoto, K. and Midorikawa, S. (2005): " Empirical Method for Estimating J.M.A. Instrumental Seismic Intensity from Ground Motion Parameters Using Strong Motion Records during Recent Major Earthquakes," *Journal of social safety science*, **7**, 1-6 (in Japanese with English abstract).
2) Fujimoto, K. and Midorikawa, S. (2006): "Relationship between Average Shear-Wave Velocity and Site Amplification Inferred from Strong Motion Records at Nearby Station Pairs," *Journal of Japan Association for Earthquake Engineering*, **6**-1, 11-22 (in Japanese with English abstract).
3) Koketsu, K. and Miyake, H. (2007): "Proposal for a standard procedure of modeling 3-D velocity structures in Japan," *Proceedings of the 2nd International Workshop on Long-Period Ground Motion Simulation and Velocity Structures*, 41-44.
4) Matsubara, M., Obara, K. and Kasahara, K. (2008): "Three-dimensional P- and S-wave velocity structures beneath the Japan islands obtained by high-density seismic stations by seismic tomography," *Tectonophysics*, **454**, 86-103.
5) Matsuoka, M., Wakamatsu, K., Fujimoto, K., and Midorikawa, S. (2005): "Average Shear-wave Velocity Mapping Using Japan Engineering Geomorphologic Classification Map," Journal of geological engineering, No.794/I-72, 239-251.
6) Wakamatsu, K. and Matsuoka, M. (2008): “Development of nationwide GIS-based 7.5-arc-second Japan Engineering Geomorphologic Classification Map”, *Proceedings of the 6th annual meeting of Japan Association for Earthquake Engineering*, 222-223 (in Japanese).

Table 6-1 Products and remaining challenges concerning seismic hazard maps (part 1)

		Accomplishments	Remaining challenges
Modeling of seismic activity	Application of long-term evaluations	・Modeling of characteristic earthquakes occurring in major active fault zones and subduction zones	・Incorporation of new long-term evaluation results ・Systematization of models with an eye on their effective use
	Modeling of earthquakes without specified source faults	・Use of both the zoning method and the non-zoning method ・Automatic removal of aftershocks from earthquake catalogs	・Improvement of models in respect to zoning, maximum magnitude, etc. ・Study on the method of treating foreshocks and aftershocks
	Interaction between earthquakes	・Treated as an independent event	・Modeling of correlated earthquakes ・Interaction between large subduction-zone earthquakes and inland earthquakes
Modeling of seismic sources for strong motion prediction	Advancement of the Recipe	・Establishment of "standardized modeling method applicable nationwide" for seismic source fault models ・Establishment of the procedure for determining parameters for obtaining average prediction results	・Establishment of methods for modeling super-long faults and short faults ・Evaluation of parameter uncertainty and its influence on variance in the prediction results ・Introduction of rupture velocity heterogeneity ・Study on the method for determining the stress drop
Modeling of subsurface structures	Crustal structure of the seismic bedrock and deeper	・Use of nationwide models based on Hi-net data (Matsubara et al., 2008)	・Building of models including island areas such as Nansei-shoto islands and Ogasawara-shoto islands
	Deep subsurface structure models	・Creation of a Recipe of modeling and modification methods (Koketsu and Miyake, 2007) and application of the Recipe ・Creation and improvement of deep subsurface structure models nationwide	・Improvement of models by incorporating new seismic data, etc. (including expansion of island areas) ・Modeling of velocity inversion layers
	Shallow subsurface structure models	・Construction of 250 m mesh Japan Engineering Geomorphologic Classification Map (JEGM) (Wakamatsu and Matsuoka, 2008)	・Shift to the new datum (JGD2000)
	Integrated models		・Integration of shallow/deep subsurface structure models

Table 6-1 Products and remaining challenges concerning seismic hazard maps (part 2)

		Accomplishments	Remaining challenges
Strong motion simulation methods	Conventional method (attenuation relation for ground motion)	・Simulation of distribution of the seismic intensity on the ground surface based on an attenuation relation and geomorphologic classification ・<u>Introduction of a new variance model based on observation records</u>	・Introduction of hanging-wall effects and rupture directivity ・Further study on variance including distribution shape and cut-off ・Introduction of the seismic bedrock depth
	Detailed method	・Waveform simulation using the hybrid method ・<u>Calculation of the seismic intensity on the ground surface from the seismic intensity increment</u>	・Simulation of vertical motions using the stochastic Green's function method ・Study on the simulation method for areas in close vicinity of the seismic source
	Method for calculating ground motions on the ground surface	・<u>Application of various empirical formulas (Fujimoto and Midorikawa, 2005, 2006; Matsuoka et al., 2005) that have been improved based on observation records</u> ・Evaluation of nonlinear site response through application of the equivalent linear method	・Further improvement of various empirical formulas ・Study on the applicability of nonlinear site response to the conventional method ・Prediction of ground liquefaction
	Verification of the simulation methods	・Verification based on strong motion records of actual earthquakes (such as the 2003 Tokachi-Oki Earthquake and the 2005 west off Fukuoka Earthquake) and reflection of the results on the Recipe	・Further verification based on strong motion records of recent large earthquakes ・Comparison with the seismic intensity distribution of historical earthquakes
Publication of data and their effective use	Data publication	・Yearly renewal of the Probabilistic Seismic Hazard Maps ・Publication of maps and data by the J-SHIS ・<u>Introduction of earthquake categories</u>	・Further advancement of the J-SHIS ・Study on more easy-to-understand publication methods
	Bridging to disaster prevention/ mitigation measures	・Use and reference of J-SHIS for earthquake insurance ・Use and reference of data by local public entities and companies	・Establishment of a method for determining scenario earthquakes based on probabilistic seismic hazard ・Implementation of earthquake risk evaluation based on seismic hazard maps ・Development of basic data such as buildings and population, and construction of an updating system

* Underlined accomplishments are new products introduced in the National Seismic Hazard Maps for Japan (2009).

7. Closing Remarks

The National Seismic Hazard Maps for Japan have been prepared based on "The Promotion of Earthquake Research: Basic comprehensive policy for the promotion of earthquake observation, measurement, surveys and research" compiled by HERP in April 1999. The maps are considered to have mostly achieved the original goal of summing up seismic hazard evaluation covering the whole of Japan. However, in order to mitigate earthquake disasters, the National Seismic Hazard Maps for Japan must not only be regarded as mere seismic hazard evaluation, but be effectively used in actual disaster mitigation activities.

In June 2007, long-term strategic guidelines "Innovation 25" was approved by the Cabinet. "Innovation 25" indicates the policies to be implemented in the short term and in the medium-to-long term in areas including promotion of R&D and reform of social systems, for the time period up to 2025. The guidelines set out that six projects entitled "Projects for Accelerating the Transfer to Society" be launched in April 2008 for showing outcomes of technologies by verification with a bird's eye view of the entire process, from basic research to the transfer of science and technology to society. One of such projects was "Construction of an information and communications system which provides each citizen with detailed disaster information and which is useful for disaster response." This project is to be carried out in a coordinated manner by relevant ministries, under the leadership of the Council for Science and Technology Policy. MEXT's share of role in this project was to implement "development of a disaster risk information platform of NIED (BOSAI-DRIP)," and it was decided that NIED is to undertake the development of such platform.

The "BOSAI-DRIP" aims to develop a system which can give information on major disaster risks, such as earthquake disasters, volcanic disasters, wind and flood disasters, landslide disasters, and snow and ice disasters, to each citizen, and which can actually be used for disaster response, while achieving compatibility with other disaster information systems. Specific objectives are to consolidate information on natural disasters held by relevant ministries, local public entities, research institutions, etc. in coordination with these organizations, to develop risk evaluation methods and methods for utilizing disaster risk information, and to create and distribute hazard risk maps covering the whole of Japan. There is also a plan to create and distribute detailed regional hazard risk maps in cooperation with specific regions, and to carry out empirical research for contributing to improving regional disaster prevention abilities.

In April 2009, HERP compiled "New Policy for Earthquake Research: The second basic comprehensive policy for the promotion of earthquake observation, measurement, surveys and research." (hereinafter referred to as the "New Basic Comprehensive Policy") The new policy sets out, as its basic objectives, to promote various research for further advancing seismic hazard maps as well as "strengthening bridge functions to promote engineering and sociological research for disaster prevention and mitigation."

In order to mitigate earthquake damage, it is essential to raise each individual's awareness of earthquakes and to encourage them to be prepared for future earthquakes. The first necessary step to this end is to prepare highly realistic, detailed hazard maps and risk information covering earthquakes that occur in all parts of Japan, based on which each individual can consider earthquake risk as his/her own personal issue. There are calls for consolidating such information and constructing a seismic hazard/risk information station which can provide easy-to-understand, reliable information to each citizen by applying the latest technology, thereby widely publishing and disseminating such information and using such information for disaster prevention and mitigation measures. Therefore, the research for the "BOSAI-DRIP" is planned to expand its target from conventional seismic hazard to also cover seismic risk evaluation. Such research is expected to contribute to "strengthening bridge functions to promote engineering and sociological research for disaster prevention and mitigation," which is one of the basic objectives of the New Basic Comprehensive Policy.

Acknowledgments

This study has been carried out under the guidance of HERP's ERC and relevant subcommittees and section meetings. The data of the average shear wave velocity to the depth of 30 m (AVS30) based on geomorphological land classification has been kindly provided by Mr. Masashi Matsuoka from the National Institute of Advanced Industrial Science and Technology (AIST). In addition, the following persons generously cooperated in the consideration process: Mr. Masajiro Imoto, Ms. Naoko Okumura, and Mr. Yutaka Yasoshima, as well as Mr. Toshiaki Sato, Mr. Jun'ichi Miyakoshi, Mr. Satoshi Fujikawa, Mr. Motofumi Watanabe, Mr. Yoshimitsu Fukushima, and Mr. Masafumi Mori (currently at Nagoya University) from Shimizu Corporation, Mr. Tatsuo Kanno from Hiroshima University, Mr. Hisanori Matsuyama, Mr. Hideaki Shinohara, Mr. Yoshiaki Inagaki, Mr. Haruhiko Suzuki, Mr. Michio Morino, Mr. Koji Iwamoto, and Mr. Ying Liu from Oyo Corporation, Mr. Toshihiko Hayakawa, Mr. Takashi Chiba, Ms. Mari Takahashi Mr. Yuta Asaka, and Mr. Kenji Sugimoto from Mitsubishi Space Software Co., Ltd., and Mr. Nobuoto Nojima from Gifu University.

(Accepted October 2, 2009)

Appendix[1]

Strong Ground Motion Prediction Method ("Recipe") for Earthquakes with Specified Source Faults

Revised on December 21, 2009

The "Strong Ground Motion Prediction Method ("Recipe") for Earthquakes with Specified Source Faults" (hereinafter referred to as the "Recipe") puts together the currently used methods for modeling source parameters, modeling the subsurface structure, simulating strong ground motions, and verifying the prediction results, all of which constitute the strong ground motion prediction method, as well as the approach for determining the source parameters, based on the results of the Earthquake Research Committee's study on strong ground motion evaluation to date. Up until now, the Earthquake Research Committee (ERC) has conducted strong ground motion evaluations for a total of 15 earthquakes (11 earthquakes occurring on active faults, and four subduction-zone earthquakes occurring on plate boundaries), and has published the results.[2] The Committee has also conducted verification of the strong ground motion prediction method using the observation records of the 2000 Western Tottori Earthquake, the 2003 Tokachi-Oki Earthquake, and the 2005 West off Fukuoka Earthquake obtained from the K-NET and KiK-net observation networks and observation networks of the seismic intensity meters of the Japan Meteorological Agency (JMA) and municipalities (Subcommittee for Evaluation of Strong Ground Motion of the ERC, 2002; 2004; 2008).

The Recipe aims to establish a "standardized methodology whereby anybody can obtain the same results" for predicting, with high accuracy, the strong ground motions that occur in the case of earthquakes with specified source faults. The Recipe is to be reviewed and revised in the future through further studies on strong ground motion evaluations.

Appended Figure 1 shows the flow of strong ground motion prediction under the Recipe. The Recipe consists of the following four processes: (1) set up the parameters for characterized source model;[3] (2) modeling the subsurface structure; (3) conducting strong ground motion simulation; and (4) verifying the prediction results. Each of these processes is explained below in the order the processes are carried out.

The abovementioned Recipe is designed as a recipe that serves as a reference in conducting detailed strong ground motion evaluation for each individual fault. However, when collectively simulating the strong ground motions assumed for earthquakes that occur in the over-100 major active fault zones, it is considered more effective and efficient to use a method that determines some fault parameters in a slightly simplified manner, while basically following the Recipe. Thus, such simplified method is also explained below.

---

[1] The original is in http://www.jishin.go.jp/main/chousa/09_yosokuchizu/g_furoku3.pdf written in Japanese which is published on the website of the Headquarters for Earthquake Research Promotion.

[2] The results of the strong ground motion evaluations are published on the website of the Headquarters for Earthquake Research Promotion (http://www.jishin.go.jp/main/index.html).

[3] The "characterized source model" refers to a source model that expresses the source parameters necessary for reproducing the strong ground motions, by using major parameters. The characterized source model is, in the case of an active fault, a source fault model that takes into consideration the outer source characteristics indicating the shape and area of the source fault, the inner source parameters indicating the heterogeneity of the fault, and other source parameters indicating the rupture process. The term "characterized" originates from the term "characterization" used in Somerville *et al*. (1999).

1. Characterized source model

In the characterized source model, the source parameters are determined while giving consideration to the following three source characteristics: outer source parameters indicating the shape and area of the whole fault; inner source parameters indicating mainly the heterogeneity of the source fault; and other source paramters indicating the rupture process.

The method for determining the source parameters explained below represents the basic policy for building a characterized source model for earthquakes that occur on an assumed source fault, and aims to achieve reproducibility in the determination of standard values of source fault parameters for strong ground motion predictions.

The following sections describe the method for determining the source parameters for the characterized source model for the respective types of earthquakes (earthquakes occurring on active faults and subduction-zone interplate earthquakes).

1.1 Characterized source model for earthquakes occurring on active faults

Strong motion observation records of the latest event are rarely available for earthquakes occurring on active faults, which have longer recurrence intervals than subduction-zone interplate earthquakes. Accordingly, when assuming an earthquake occurring on an active fault, a characterized source model must be merely based on the traces of past seismic activity revealed through tectonic geomorphological surveys and trenching surveys. Thus, the uncertainty of the model tends to be larger than that for subduction-zone interplate earthquakes. Considering such uncertainty, it is desirable to assume multiple characterized source models for earthquakes occurring on active faults.

Here, different methods of determining outer source parameters are described for the following cases: the case of using a source fault based on past earthquake records or assuming a source fault based on detailed survey results (see 1.1.1 (A)); and the case of assuming a source fault from ground surface information about the active fault by using a simplified method (see 1.1.1 (B)). Appended Figure 2 shows the flow chart of determination of source parameters for earthquakes occurring on active faults.

1.1.1 Outer source parameters

The following are determined as outer source parameters for source fault models of earthquakes occurring on active faults:

- Location and structure of the source fault model (location, strike, segments[4])
- Area (length/width), depth, and dip angle of the source fault model
- Earthquake magnitude
- Average slip of the source fault model

[4] Within an active fault which is a unit that generates earthquakes of a maximum magnitude, a segment represents a unit that generates slightly smaller earthquakes as segmented-release-type earthquakes. Segments are classified into earthquake segments, geometric segments, and behavioral segments, depending on the data used as the basis. In strong motion evaluation, the expression "segment" is used without defining the term in detail.

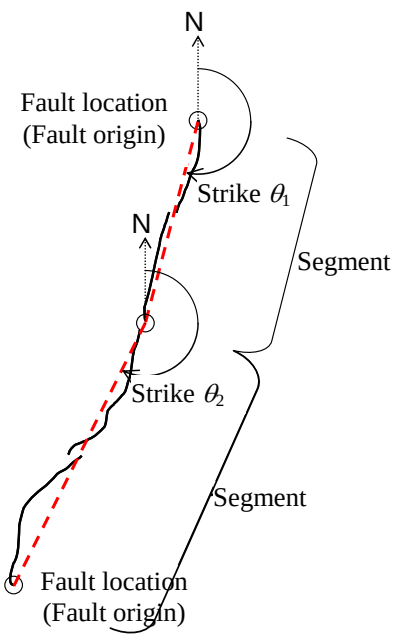

Location, strike, segments

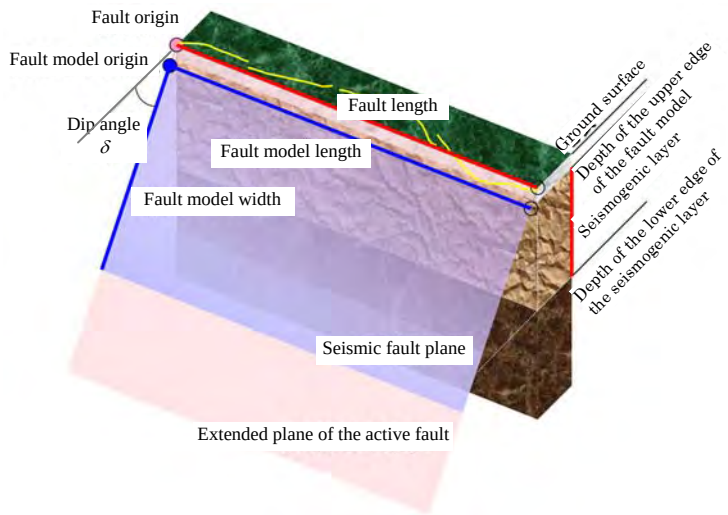

Length, width, depth, and dip angle of the fault model

(a) Location and structure of the source fault model

When determining the location of a source fault model, the active fault map indicated in the long-term evaluation results by the ERC (hereinafter referred to as the "long-term evaluation") is used, in principle. However, both ends of a fault indicated in the long-term evaluation merely show both ends of the location where distribution of an active fault (zone) has been confirmed. Therefore, when determining the location and strike of the source fault model, the model does not necessarily have to be aligned with the strike of the straight line joining such both ends of the active fault (zone). Sometimes, consideration is made on extending the source fault model beyond both ends of the active fault (zone) (ERC, 2003d; 2004a) or shifting the source fault model parallel to the straight line joining both ends of the active fault (zone) (ERC, 2004d) by referring to the descriptions in the long-term evaluation. Where an active fault (zone) is bent and a part of the active fault (zone) is positioned 5 km or more away from the abovementioned line joining both ends of the active fault (zone), the source fault may be modeled by using multiple straight lines along the active fault (zone) (ERC, 2003e; 2004e).

When determining the segments, if an active fault (zone) is divided into active segments in the long-term evaluation, those active segments are basically used as the segments in the strong ground motion evaluation, but the later-mentioned number and locations of asperities[5] are also taken into consideration.

If no long-term evaluation results are available for an active fault (zone), the segments are determined based on the results of tectonic geomorphological surveys or materials compiling existing data, such as "Active Faults in Japan, New Edition" (The Research Group for Active Faults of Japan ed., 1991), "Active Fault Map in Urban Area" (Geospatial Information Authority of Japan (GSI)), and "Digital Active Fault Map of Japan" (Nakata and Imaizumi ed., 2002). In

[5] An asperity is a region of a source fault that generates particularly strong seismic waves (a region where the slip or the stress drop is large).

that process, if multiple faults exist in the vicinity, the seismogenic fault is determined according to the criteria by Matsuda (1990).

(A) The case of using a source fault based on past earthquake records or assuming a source fault based on detailed survey results

In the case of using a source fault based on past earthquake records or assuming a source fault based on detailed survey results, the fault model is determined in such a manner to make use of such findings.

(b) Area (length *L*/width *W*), depth, and dip angle (*δ*) of the source fault model

The modeled source fault length L (km) is determined based on the shape of the modeled source fault assumed in **(a)**. For determining the width W (km), the following empirical relations between W and L by Irikura and Miyake (2001) are used:

$$W = L \qquad (L < W_{\max}) \quad \text{(1-a)}$$

$$W = W_{\max} \qquad (L \geq W_{\max}) \quad \text{(1-b)}$$

where

$$W_{\max} = T_s / \sin\delta$$

$$T_s = H_d - H_s$$

T_s: thickness of the seismogenic layer (km) ($T_s \leqq 20$km)

δ: dip angle of the fault

H_d, H_s: respectively, the lower edge of the seismogenic layer and the upper edge of the fault model (km) (which can be determined from distribution of microearthquakes (Ito, 1999))

Formula (1) indicates that the modeled source fault width W for an earthquake occurring on an active fault saturates to give a constant value according to the thickness of the seismogenic layer T_s.

Relationship between the thickness of the seismogenic layer T_s and the fault model width W

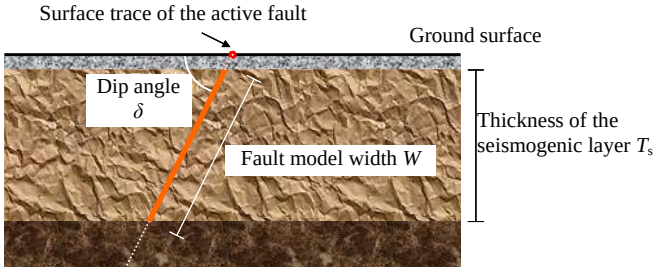

The dip angle of the source fault model must be determined carefully, because although the shape of the entire active fault from the ground surface to the bottom of the seismogenic layer has rarely been ascertained in reality, it substantially influences the next process, which is

assumption of the earthquake magnitude. If any data is available for estimating the dip angle of the fault, such as the results of a seismic reflection survey of the target fault, such information is used (e.g., ERC, 2004a). If the dip angle can be estimated from the same type of fault in the vicinity, the data on such fault is used. If none of these data are available, one of the following dip angles is used, in principle, according to the slip type (slip direction):

Reverse fault: 45°
Normal fault: 45°
Strike-slip fault: 90°

As a point to note, consideration should be given to the surrounding geological structure, particularly the distribution of active faults, and the relationship between the target fault and the surrounding geological structure should be made clear. Where the long-term evaluation indicates either "low angle" or "high angle", the dip angle is determined within the scope of 0°-30° or 60°-90°, respectively, while noting the point above.

The depth of the upper edge of the source fault model is to be the same as the depth of the upper surface of the seismogenic layer of microearthquakes (the shallow limit of microearthquakes). This is because recent studies on dynamic models of seismic sources have revealed that, even when hardly any stress drop occurs in the sedimentary rock layer lying in the upper several kilometers of the subsurface structure, a rupture emitting seismic energy in the bedrock part beneath that layer is transmitted to the sedimentary rock layer and reaches the ground surface in the form of a fault displacement (e.g., Dalguer *et al*., 2001).

(c) Earthquake magnitude (seismic moment M_0)

The earthquake magnitude is calculated by an empirical relation between the seismic moment M_0 (Nm) and the source fault area S (km^2). According to Somerville *et al.* (1999), the relation between the seismic moment and the source fault area can be expressed by the following formula:[6]

$$M_0 = \left(S / 2.23\times10^{15}\right)^{3/2} \times 10^{-7} \quad \text{.....} \quad (2)$$

However, the formula above is based on the results of source inversion using strong motion records of past large earthquakes, which do not include data for M8-class mega-earthquakes. On the other hand, Wells and Coppersmith (1994) includes data of M8-class mega-earthquakes that have been analyzed based on data of aftershocks and crustal movements. In Wells and Coppersmith (1994), the source fault area corresponding to a given seismic moment becomes systematically smaller than that derived by the formula above, as the earthquake magnitude becomes larger. Accordingly, the magnitude of an earthquake with a large source fault area is calculated by using the following formula, which is based on data from studies including Wells and Coppersmith (1994) and proposed by Irikura and Miyake (2001):

$$M_0 = \left(S / 4.24\times10^{11}\right)^{2} \times 10^{-7} \qquad (3)$$

Formula (3) should be applied to earthquakes of M_0=7.5×10^{18} (Nm) (equivalent to moment magnitude M_w6.5) or more, but only up to M_0=1.0×10^{21} (Nm), considering the distribution of the

[6] Whereas Somerville *et al.* (1999) and Irikura and Miyake (2001) use the CGS system of units, this Recipe uses the MKS system of units.

data underlying Formula (3).

*** For convenience, the threshold value is given above for determining which of the two formulae should be used, so that the earthquake magnitude can be obtained in an automatic manner. However, since the scaling law varies depending on whether or not the fault width is saturated in principle, it is more reasonable to use Formula (2) when the fault width is unsaturated (Formula (1-a)) and to use Formula (3) when the fault width is saturated (Formula (1-b)). When calculating the source fault aera, the formula to be used may be selected by also taking this point into consideration.**

(B) The case of assuming a source fault from ground surface information about the active fault by using a simplified method

The modeled fault area is assumed by an empirical relation to match the earthquake magnitude inferred from the active fault length L (km) on the ground surface indicated in the long-term evaluation. The flow chart of the process of assuming the modeled fault area is shown in Appended Figure 3. This flow chart is to be applied to earthquakes of M7 or more. For earthquakes of a smaller magnitude, an appropriate method is to be selected case by case. It is also desirable to model the fault by an appropriate method selected case by case when the active fault length exceeds roughly 80 km.

(d) Earthquake magnitude (seismic moment M_0)

The seismic moment M_0 (Nm) is calculated by using the following empirical relation between the earthquake magnitude (magnitude M) indicated in the long-term evaluation and the seismic moment M_0 (Takemura, 1990):

$$\log M_0 = 1.17 \cdot M + 10.72 \quad \text{.....} \quad (4)$$

Here, M is obtained by M = (log$L$+2.9)/0.6 (Matsuda, 1975). Hereinafter, the earthquake magnitude M indicated in the long-term evaluation is deemed to be equivalent to the Japan Meteorological Agency (JMA) magnitude M_{JMA}.

(e) Source fault area S

The source fault area is calculated by an empirical relation between the source fault area S (km^2) and the seismic moment M_0 (Nm). The following formula, which is based on data from studies including Wells and Coppersmith (1994) and proposed by Irikura and Miyake (2001), is used:

$$S = 4.24 \cdot 10^{-11} \cdot \left(M_0 \times 10^7\right)^{1/2} \quad \text{.....} \quad (3)'$$

Formula (3)' should be applied to earthquakes of M_0=7.5×10^{18} (Nm) (equivalent to M_w6.5) or more, but only up to M_0=1.0×10^{21} (Nm), considering the distribution of the data underlying Formula (3)'. For earthquakes smaller than M_0=7.5×10^{18} (Nm), the source fault area is calculated by the following relation between the seismic moment and the source fault area derived by Somerville *et al.* (1999) based on the results of source inversion using strong motion records of past large earthquakes:

$$S = 2.23 \cdot 10^{-15} \cdot \left(M_0 \times 10^7\right)^{2/3} \quad \text{(2)'}$$

However, as described in (1.1.1 (c)), a special consideration is required when the earthquake is M7 (about M_w6.5) or less.

(f) Modeled source fault width W_{model} and modeled source fault length L_{model}

The source fault width W (km) is obtained by the following formula, which divides the source fault area S (km^2) derived by Formula (3)' or Formula (2)' by the active fault length L (km):

$$W = S / L \quad (5)$$

Here, different methods are used for calculating the modeled source fault width depending on whether or not the lower edge of the fault model extends below the seismogenic layer when considering the obtained source fault width W (km) and the dip angle δ (º). The depth of the lower edge of the seismogenic layer is determined based on the distribution of the depths of microearthquakes (Ito, 1999). The depth of the upper edge of the seismogenic layer is to be approximately between the deep subsurface structure and the layer with V_s=3.0km/s.

i) The case where the lower edge of the source fault model does not extend below the seismogenic layer
Modeled source fault width (km) W_{model} = a multiple of the fault model mesh size[7] that is smaller than W
Modeled source fault length (km)

$$L_{model} = S / W_{model} \quad (6)$$

where L_{model} is a multiple of the fault model mesh size that is larger than L.

ii) The case where the lower edge of the source fault model extends below the seismogenic layer
Modeled source fault width (km) W_{model} = a multiple of the fault model mesh size where the depth of the lower edge of the fault model would be shallower than the seismogenic layer + 2 km
Modeled fault length is obtained by Formula (6) where L_{model} (km) is a multiple of the fault model mesh size that is larger than L (km) but no more than L+5km.

The dip angle is to be based on the long-term evaluation, but if the long-term evaluation results are not available, the flow chart shown in Appended Figure 4 is to be followed.

[7] Assuming use in the hybrid method, the source fault model is calculated by deeming the mesh size to be used in the stochastic Green's function method as the smallest unit. Since the currently adopted mesh size is 2 km square, the length and width of the source fault model are treated here as multiples of 2. This value needs to be reviewed in the future in line with the progress of the calculation method for the stochastic Green's function method.

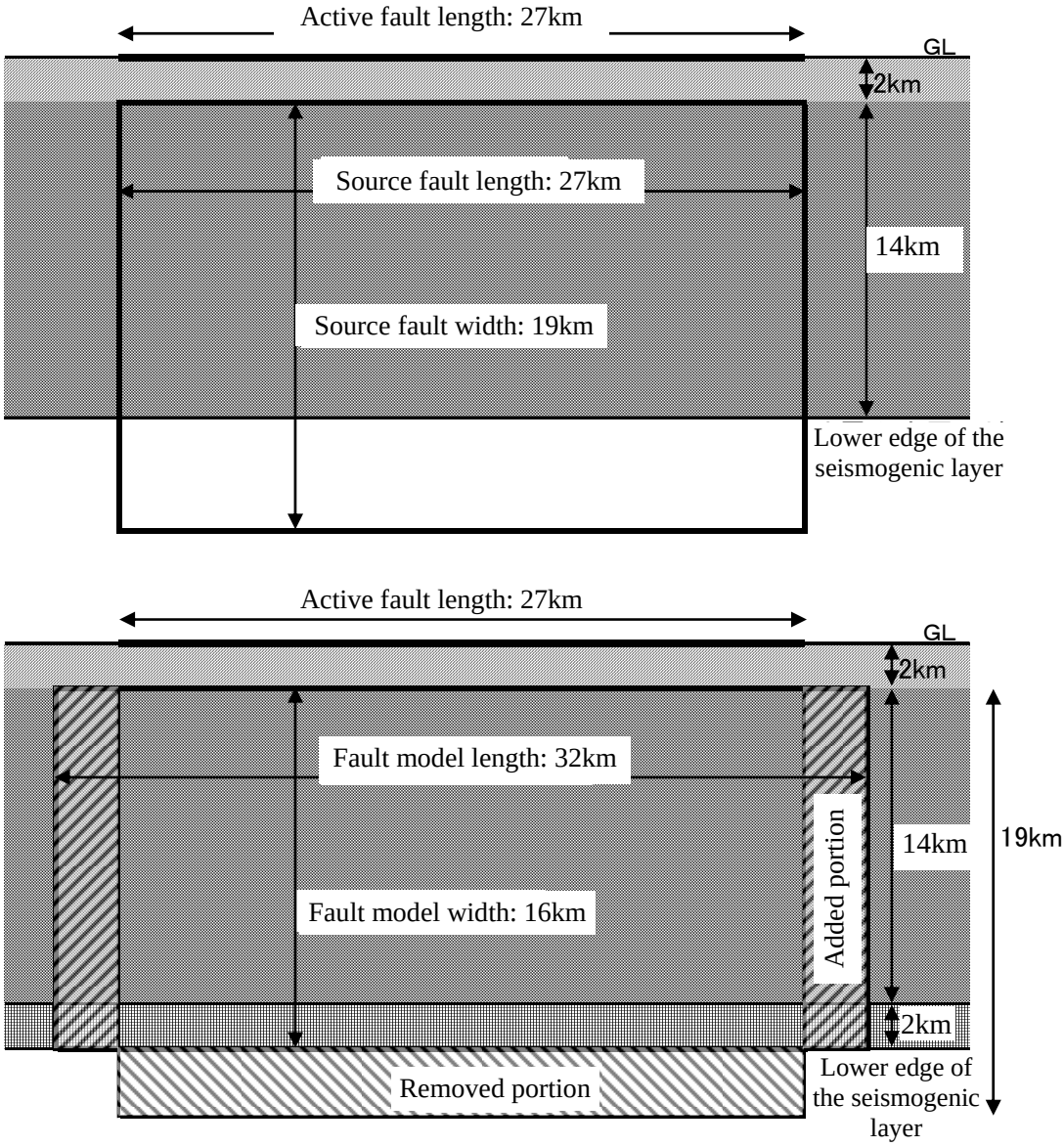

Conceptual diagram of the fault model length and width
(Above) initial model, (below) corrected model

(g) Modeled source fault area $S_{\mathbf{model}}$

The modeled source fault area S_{model} (km^2) is obtained by the following formula from the modeled source faultlength L_{model} (km) and the modeled source fault width W_{model} (km):

$$S_{\text{model}} = L_{\text{model}} \cdot W_{\text{model}} \quad \text{.....} \quad (7)$$

The parameters for **1.1.2** are determined by deeming the modeled source fault area S_{model} (km^2) to be equivalent to the source fault area.

(C) Common to (A) and (B)

(h) Seismic moment M_0 for each segment

When multiple segments move simultaneously, the total area of the segments is to be the

source fault area, and the overall seismic moment M_0 (Nm) is calculated by using Formula (2) or (3). The seismic moment is distributed among the individual segments weighted by the segment area to the power of 1.5 as shown in the following formula so that the average stress drop will be the same for each segment:

$$M_{0i} = M_0 \cdot S_i^{3/2} \Big/ \sum S_i^{3/2} \quad \text{.....} \quad (8)$$

M_{0i}: seismic moment of the i-th segment
S_i : area of the i-th segment

*** Some studies that have analyzed data of recent large earthquakes with rupture of multiple segments have reported that the cascade model is suitable since it assumes the same amount of displacement for each segment even where multiple segments cause an earthquake in a correlated manner (e.g., Awata, 2004; Toda, 2004). Such approach is sometimes used along with the long-term evaluation particularly in the case of evaluating a super-long active fault zone. However, methods for determining the scaling law or the characterized source model in the case where the segments are evaluated individually are still under study.**

(i) Average slip *D*

The relation between the average slip D (m) and the seismic moment M_0 (Nm) of the whole source fault is expressed by the following formula, using the source fault area S (km^2) (or the modeled source fault area S_{model} (km^2)) and the rigidity μ (N-m^2):

$$D = M_0 / (\mu \cdot S) \quad \text{.....} \quad (9)$$

The modulus of rigidity is calculated from the density of the seismogenic layer ρ (kg/m^3) and the shear-wave velocity β (km/s).

$$\mu = \rho \cdot \beta^2 \quad \text{.....} \quad (10)$$

1.1.2 Inner source parameters

The following are determined as inner source parameters of a source fault model for an earthquake occurring on an active fault:

- Asperity locations and the number of asperities
- Asperity area
- Average slip of the asperities and the background region
- Effective stress of the asperities and the background region
- $f_{\max}$[8]
- Average rupture velocity
- Slip velocity time function
- Slip angle

(a) Asperity locations and the number of asperities

[8] $f_{\max}$ is, one of the source spectral characteristics, the frequency at which an acceleration spectrum begins to fall off at high frequencies.

With regard to the asperity locations, a recent study surveying the distribution of displacement of the seismogenic fault in detail has revealed that distribution of displacement of the shallow part of the source fault corresponds closely with the distribution of displacement of the seismogenic fault (Sugiyama *et al.*, 2002). Accordingly, the asperity locations of a source fault model are determined based on the distribution of displacement associated with a single seismic event that has been obtained from an active fault survey or based on the distribution of the average slip rate.

Specifically, the asperity locations are determined by methods including the following:

- When the long-term evaluation provides a description on the distribution of displacement or a description that indirectly indicates regional differences in displacement, such information is to be used (e.g., ERC, 2002; 2004a).
- The value of (or a value equivalent to) the average slip rate is calculated from data indicating the distribution of displacement or historical activities of the fault (e.g., ERC, 2003a; 2004c).

The assuming method above involves a high level of uncertainty, such as the inability to assume asperity locations in the deep part of the source fault. However, strong ground motion evaluation results have revealed that differences in the asperity locations substantially influence the results of strong ground motion prediction (e.g., ERC, 2002; 2003a). Therefore, it is desirable, also from the disaster prevention viewpoint, to determine multiple cases in order to identify the extent of differences in the strong ground motion prediction results depending on the asperity locations.

The number of asperities is 2.6 per earthquake on average, according to Somerville *et al.* (1999) that has organized the results of source inversion of past inland earthquakes. In addition, more segments tend to move simultaneously and the number of asperities increases as the assumed earthquake magnitude becomes larger. For example, research results show that, while the number of asperities is two for the 2000 Western Tottori Earthquake (M_w=6.8) and three for the 1995 Hyogoken Nanbu Earthquake (M_w=6.9), the number is five for the 1999 Kocaeli Earthquake in Turkey (M_w=7.4) and six for the 1999 Chi-Chi Earthquake in Taiwan (M_w=7.6) (Iwata *et al.*, 2001; Miyakoshi *et al.*, 2001). By referring to these research results, the number of asperities is to be determined as one or two per segment, according to the situation.

*** When no information on the asperity locations, the asperity is to be positioned near the center of the fault if there is only one asperity, and the asperities are to be arranged in a balanced manner if there are multiple asperities. In this case as well, it is desirable to determine multiple cases as needed.**

(b) Short-period level *A* and the total area of the asperities S_a

The total area of the asperities S_a (km^2) is closely related to the acceleration source spectrum level in the short-period range (hereinafter referred to as the "short-period level") which directly affects the strong ground motion prediction. Therefore, the total area of the asperities S_a (km^2) is obtained after determining the short-period level for the source fault model. The short-period level can be inferred based on the seismic waveform at observation points on firm ground that is hardly affected by the shallow subsurface structure or at observation points where the effects of the shallow subsurface structure have been ascertained quantitatively. However, since earthquakes occurring on active faults have extremely long recurrence intervals,

it is currently impossible to assume the short-period level from the latest event. In the meantime, if the area is not restricted to the source area of the assumed earthquake, an empirical relation between the short-period level and the seismic moment is available from analyses of recent earthquakes. Thus, when calculating the short-period level, the following empirical relation between the seismic moment M_0 (Nm) and the short-period level A (Nm/s^2) by Dan *et al.* (2001) is used (Irikura *et al.*, 2002):

$$A = 2.46 \times 10^{10} \times \left(M_0 \times 10^7\right)^{1/3} \quad \text{(11)}$$

The total area of the asperities S_a (km^2) can be obtained by $S_a = \pi r^2$. For convenience, the shapes of the source fault and the asperities are assumed to be circles of an equivalent area. The equivalent radius r (km) where the total area of the asperities is deemed to be circular is obtained by Formula (12), using the short-period level A (Nm/s^2) inferred by Formula (11):

$$r = (7\pi/4) \cdot \{M_0/(A \cdot R)\} \cdot \beta^2 \quad \text{(12)}$$

The formula above is derived from the following Formula (13) (Boatwright, 1988) and Formula (14) (Dan *et al.*, 2001) based on the theoretical relation between M_0 and A in a single-asperity model (a model having only one asperity):

$$M_0 = (16/7) \cdot r^2 \cdot R \cdot \Delta\sigma_a \quad \text{(13)}$$

$$A = 4\pi \cdot r \cdot \Delta\sigma_a \cdot \beta^2 \quad \text{(14)}$$

where R (km) is the equivalent radius corresponding to the fault area S (km^2), $\Delta\sigma_a$ (MPa) is the stress drop of the asperities, and β (km/s) is the shear-wave velocity in the source area. Formula (13) and Formula (14) can be extensively applied to a multiple-asperity model (a model having multiple asperities). Irikura *et al.* (2002) has indicated that the values of both formulae are not dependent on the number of asperities. Where there are multiple asperities, the equivalent radius r (km) is given by $\sqrt{\sum_{i=1}^{N} r_i^2}$ (assuming N number of asperities with a radius of $r_1, r_2, \ldots, r_N$).

Meanwhile, recent research results show that the percentage of the total area of the asperities for an inland earthquake to the total fault area is 22% on average (Somerville *et al.*, 1999) or 15%-27% (Miyakoshi et al., 2001). Although these values are not restraint conditions, they need to be taken into account. It should be noted that there is also a view stating that, when a single segment has two asperities, the area would be distributed between those asperities at the ratio of 16:6 (Irikura and Miyake, 2001) or 2:1 (Ishii and Sato, 2000) based on recent researches .

Studies have indicated that it is not necessarily appropriate to assume a circular crack for a super-long fault for which the source fault length is sufficiently long in comparison to the source fault width. The Recipe infers the seismic moment M_0 (Nm), which is an outer source parameter, by Formula (3)', which does not assume a circular fault plane. However, it infers the total area of the asperities, which is an inner source parameters, by Formulae (11) to (14) derived from a scaling law assuming a circular crack. With such a method, the total area of the asperities tends to be overestimated in comparison to existing survey/research results, as the area of the whole source fault becomes larger. Therefore, a scaling law that does not assume a circular fault plane needs to be applied also for inner source paraemeters. However, scaling laws concerning

asperities of mega faults have been have been an unsolved research topic due in part to the scarceness of the data available. Accordingly, in such a case, there is a method of not using Formulae (11) to (14), but instead inferring the total area of the asperities from the percentage of the total area of the asperities to the area of the whole source fault proposed by Somerville *et al.* (1999), which is about 22%. In this case, special attention must be paid to the method for calculating the stress drop of the asperities. This method will be explained in **(d)**.

(c) Average slip of the asperities/background region D_a ,D_b

The average slip of all asperities D_a (m) is to be ξ times the average slip of the whole source fault D (m), and ξ=2 is used based on the results of summing up analyses of recent inland earthquakes (Somerville *et al.*, 1999; Ishii et al., 2000).

$$D_a = \xi \cdot D \quad \text{.....} \quad (15)$$

Based on this, the average slip of the background region D_b (m) can be calculated by the following formulae using the seismic moment of the background region M_{0b} (Nm), obtained by excluding the seismic moment of the asperities M_{0a} (Nm) from the seismic moment of the whole fault M_0 (Nm), and using the area of the background region S_b (km^2):

$$M_{0a} = \mu \cdot D_a \cdot S_a \quad \text{.....} \quad (16)$$

$$M_{0b} = M_0 - M_{0a} \quad \text{.....} \quad (17)$$

$$D_b = M_{0b} / (\mu \cdot S_b) \quad \text{.....} \quad (18)$$

Here, μ in Formula (10) is the modulus of rigidity (Nm^2).

The average slip of each asperity D_{ai} (m) is obtained by the following formula, empirically assuming that, where each asperity is assumed to be a circular crack for convenience, the percentage to the radius r_i (km) (the radius of the i-th asperity) calculated from the area of each asperity S_{ai} (km^2) (the area of the i-th asperity) is the same for all asperities (D_{ai}/r_i = constant):

$$D_{ai} = \left(\gamma_i / \sum \gamma_i^3\right) \cdot D_a \quad \text{.....} \quad (19)$$

where γ_i is r_i / r, D_{ai} (m) is the average slip of the i-th asperity, and the equivalent radius r (km) of all asperities can be obtained by Formula (12).

*** However, where the average slip of the largest asperity obtained above and the slip inferred in a trench survey differ considerably, value ξ in Formula (15) will be adjusted as required.**

(d) Static stress drop and the effective stress of the whole source fault and asperities, and the effective stress of the background region $\Delta\sigma$, $\Delta\sigma_a$, σ_a, σ_b

For the static stress drop of the asperity $\Delta\sigma_a$ (MPa), Madariaga (1979) has proposed the following formula:

$$\Delta\sigma_a = (S/S_a) \cdot \Delta\sigma \quad \text{.....} \quad (20\text{-}1)$$

$\Delta\sigma$: static stress drop (MPa) of the whole source fault
S: area of the whole source fault (km^2)

S_a: total area of the asperities (km^2)

Using Formula (20-1), the static stress drop of the asperities $\Delta\sigma_a$ (MPa) can be obtained by giving the percentage of the total area of the asperities S_a (km^2) to the area of the whole source fault S (km^2), and the static stress drop of the whole source fault $\Delta\sigma$ (MPa).

For a source fault of which the area is appropriate for assuming a circular crack, the seismic moment M_0 (Nm) of the whole source fault is proportional to the area of the whole source fault S (=πR^2) (km^2) to the power of 1.5 (Eshelby, 1957). Therefore, $\Delta\sigma_a$ can be calculated by the following formula obtained by modifying Formula (13) as a formula equivalent to Formula (20-1):

$$\Delta\sigma_a = (7/16)\cdot M_0 / (r^2 \cdot R) \quad \text{.....(20-2)}$$

Here, the equivalent radius r (km) of all asperities can be obtained by Formula (12).

Meanwhile, as mentioned in **(b)**, there is a problem in using, for a mega fault, the method of calculating the equivalent radius r (km) using Formula (12) that has been derived by assuming a circular crack. Thus, Formula (20-2) cannot be used. In such a case, the static stress drop of the asperities $\Delta\sigma_a$ (MPa) is obtained by Formula (20-1). The percentage of the total area of the asperities S_a (km^2) to the area of the whole source fault S (km^2) is to be about 22% based on Somerville *et al.* (1999). As for the static stress drop of the whole source fault $\Delta\sigma$ (MPa), research results by Fujii and Matsu'ura (2000) propose the following formula as a relation between the seismic moment M_0 (Nm) and the fault shape (the fault width W (km) and the fault length L (km)) for a mega fault:

$$M_0 = \{WL^2/(aL+b)\}\cdot \Delta\sigma \quad \text{.....(21-1)}$$

W: fault width (km)
L: fault length (km)
a, b: structure-dependent parameters (given by numerical simulation)

As a relation for a super-long inland strike-slip fault, $\Delta\sigma$=3.1 (MPa) has been derived by regression calculation based on collected observation data, while assuming W=15km, a=1.4×10^{-2}, and b=1.0. For example, if this 3.1MPa is used as the static stress drop of the whole source fault $\Delta\sigma$ (MPa), $\Delta\sigma_a$ will be about 14.4MPa by Formula (20-1), which roughly corresponds to the existing survey/research results (ERC, 2005). Since the value 3.1MPa proposed by Fujii and Matsu'ura (2000) targets a strike-slip fault, and has been derived under a number of conditions as described above, the scope of its application needs to be sufficiently considered in the future (Irikura, 2004), but until a new finding is obtained about the static stress drop $\Delta\sigma$ (MPa) of a super-longt fault, $\Delta\sigma$ = 3.1 (MPa) is to be given as a provisional value.

As for a source fault of which the area is appropriate for assuming a circular crack, the static stress drop of the whole source fault $\Delta\sigma$ (MPa) can be calculated by the following formula, derived in the same manner as Formula (20-2) based on Eshelby (1957):

$$\Delta\sigma = (7/16)\cdot M_0 / R^3 \quad \text{.....(21-2)}$$

When there are multiple asperities, unless detailed information on the source area is available, the stress drop of each asperity is deemed to be equal to all others and to coincide with the stress drop of overall asperities. In addition, the effective stress of the asperities σ_a (MPa) is

empirically deemed to be almost equal to the static stress drop of the asperities $\Delta\sigma_a$ (MPa). The effective stress of the background region σ_b (MPa) is, based on Dan *et al.* (2002) and according to the proportional relation/approximation relation

Effective stress ∝ slip velocity ∝ (slip/rise time)

Rise time = width of the source fault (when deemed to be rectangular)/(rupture velocity × 2)

calculated by the following formula using the width of the asperity area W_a (km) if a segment has only one asperity:

$$\sigma_b = (D_b/W_b)/(D_a/W_a)\cdot\sigma_a \quad \text{..... (22)}$$

and calculated by the following formula if a segment has multiple asperities:

$$\sigma_b = (D_b/W_b)\cdot(\sqrt{\pi}/D_a)\cdot r\cdot\sum\gamma_i^3\cdot\sigma_a \quad \text{..... (23)}$$

Here, W_b (km) is the width where the background region is deemed to be rectangular. If the source fault has an irregular shape, the fault width is obtained from source fault area S (km^2), giving consideration to the appropriate aspect ratio (L/W) of the fault, for convenience (e.g., if the aspect ratio is 2, $W_b = \sqrt{S/2}$).

*** In some cases, the seismic waveform or the seismic intensity distribution simulated by using the source parameters determined as above may not coincide with the past earthquake data used for verification. In such a case, the parameters are to be determined again by prioritizing the uniquely inferred earthquake magnitude or short-period level. If past seismic waveform data is available, it may be possible to assume individual asperity areas from the pulse width of the waveform.**

(e) f_{max}

The Subcommittee for Evaluation of Strong Ground Motion of the ERC (2001) has assumed and compared the following two cases: f_{max} = 6Hz (Tsurugi *et al.*, 1997) and f_{max} = 13.5Hz (Sato *et al.*, 1994). Since the study has found that the case of f_{max} = 6Hz corresponded more closely to the existing attenuation relation, f_{max} = 6Hz is to be used.

(f) Average rupture velocity V_r

The average rupture velocity V_r (km/s) is, unless detailed information on the source area is available, inferred by the following empirical relation with the S-wave velocity of the seismogenic layer β (km/s) proposed by Geller (1976):

$$V_r = 0.72\cdot\beta \quad \text{..... (24)}$$

*** Recent studies have obtained values slightly larger than the coefficient 0.72 proposed by Geller (1976). For instance, Somerville *et al.* (1999) has obtained a rupture velocity of 2.4km/s - 3.0km/s from the collected 15 inland earthquake source models, and its mean value is 2.7km/s. This value would be about 0.8 times the S-wave velocity of the seismogenic layer β, if β is assumed to be 3.4km/s, (Kataoka *et al.*, 2003). It has also been confirmed that, in a simulation following the**

Recipe, the simulation results of particularly the long-period component vary substantially if the rupture velocity is changed (Subcommittee for Evaluation of Strong Ground Motion of the ERC, 2008).

(g) Slip velocity time function *dD*(*t*)/*dt*

The approximation formula by Nakamura and Miyatake (2000) is used for the slip velocity time function. The approximation formula by Nakamura and Miyatake (2000) is expressed as

$$dD(t)/dt = \begin{cases} (2V_m/t_d)\cdot t\cdot\{1-(t/2t_d)\} & 0<t<t_b \\ b/\sqrt{t-\varepsilon} & t_b<t<t_r \\ c-a_r(t-t_r) & t_r<t<t_s \\ 0 & t<0 \text{ or } t>t_s \end{cases} \quad \text{..... (25)}$$

$$\varepsilon = (5t_b - 6t_d)/\{4(1-t_d/t_b)\}$$

$$b = 2V_m\cdot(t_b/t_d)\cdot\sqrt{t_b-\varepsilon}\cdot(1-t_b/2t_d)$$

c, a_r: coefficients
t_r:(t_s-t_r)=2:1
V_r: rupture velocity (km/s)

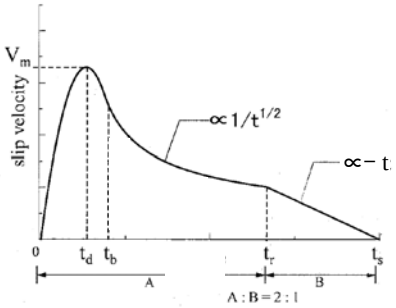

Conceptual diagram of the slip velocity time function

The following four parameters are given to calculate this approximation formula:

- Time of reaching the peak slip velocity t_d (s)
- Time of shifting to the Kostrov-type function where the amplitude of the slip velocity is proportional to $1/\sqrt{t}$ t_b (s)
- Rise time t_r (s)
- Maximum amplitude of the slip velocity V_m (m/s)

Each parameter is determined as below.

- Time of reaching the peak slip velocity t_d (s)

$$t_d \cong 1/(\pi\cdot f_{max}) \text{ ..... (26)}$$

- Time of shifting to the Kostrov-type function where the amplitude of the slip velocity is proportional to $1/\sqrt{t}$ t_b (s)

This can be given automatically by giving the final slip in Formula (25).

- Rise time t_r (s)

$$t_r \cong \alpha\cdot W/V_r \text{ ..... (27)}$$

α=0.5

- Maximum amplitude of the slip velocity V_m (m/s)

$$V_m = \Delta\sigma\cdot\sqrt{2f_c\cdot W\cdot V_r}/\mu \text{ ..... (28)}$$

The parameters used here are as follows:

f_c: corner frequency of the low-pass filter (equivalent to f_{max}) (Hz)

$W = W_a$ (the asperity width in the case of an asperity area) (km)
$= W_b$ (the width of the whole fault in the case of the background region) (km)

*** The ERC has used the superpositioning proposed by Dan and Sato (1998) in its strong ground motion evaluation. According to Kataoka *et al.* (2003), when using the superpositioning proposed by Kamae *et al.* (1991), α with which the seismic waveform obtained by simulation analysis can best reproduce the observation records is about 0.2-0.4 for inland earthquakes (four earthquakes) and about 0.25-0.6 for subduction-zone earthquakes (two earthquakes). "Verification of the Strong Ground Motion Evaluation Method Using the Observation Records of the 2000 Western Tottori Earthquake" (Subcommittee for Evaluation of Strong Ground Motion of the ERC, 2002), which used the superpositioning proposed by Kamae et al. (1991), indicated that the observation records are reproduced well when α is 0.42-0.49. The value of α may be determined by taking these values into account, while also looking at which superpositioning method is used. It should be noted that ground motions simulated by using a function of $1/\sqrt{t}$ as the slip velocity time function tends to be predicted to have smaller amplitude in the short-period range.**

(h) Slip angle λ

As for the slip angle λ (°), if the angle is provided in the long-term evaluation, such angle is used. If no data is available, the following slip angle is to be basically used according to the fault slip type (slip direction):

reverse fault: 90°
normal fault: -90°
left-lateral strike-slip fault: 0°
right-lateral strike-slip fault: 180°

*** In an actual earthquake, the slip angle λ (°) of the source fault varies by location. If the same slip angle λ (°) is assumed for the whole fault in a source fault model, the directivity effect tends to show overly strongly in the strong ground motion prediction results.**

1.1.3 Other source parameters

The following are determined as the other source parameters:

- Rupture starting point
- Rupture pattern

(a) Rupture starting point

The location of the rupture starting point is assumed based on the modeling of the relationship between the branching pattern of the active fault and the rupture starting point and rupture directivity proposed by Nakata et al. (1998). Since the location of the rupture starting point substantially influences the results of the strong ground motion prediction results, if the distribution pattern is unclear, it is desirable to build multiple cases as needed (e.g., ERC, 2003c;

2004c). With regard to the relationship between the location of the rupture starting point and asperity locations, according to Somerville *et al.* (1999) and Kikuchi and Yamanaka (2001), the rupture starting point should not be positioned within an asperity, because it tends to exist outside asperities. Also, according to Kikuchi and Yamanaka (2001), the depth of the rupture starting point should be positioned in the lower part of the source fault, since the rupture tends to propagate from deep to shallow in the case of inland strike-slip faults.

*** When assuming average ground motions and where the rupture starting point cannot be determined based on such information as the shape of the active fault, basically, the rupture starting point is to be positioned at the corners of the lower edge of the asperity if the strike-slip component is dominant, and positioned in the middle of the lower edge of the asperity if the dip-slip component is dominant, as a rather simplified parameter determination method. In this case as well, it is desirable to determine multiple cases as needed.**

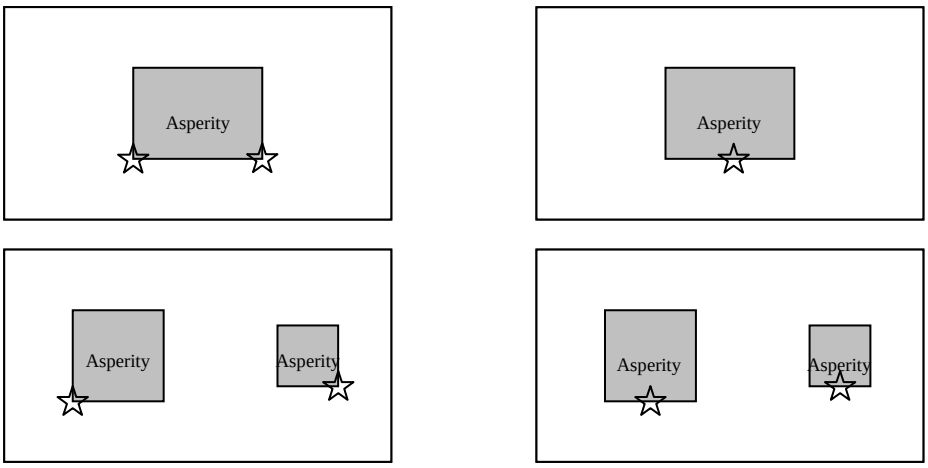

Strike-slip component is dominant Dip-slip component is dominant

Example of the positions of the rupture starting points (star) and asperities

(b) Rupture pattern

The rupture is assumed to propagate radially from the rupture starting point. Between different segments, the rupture is assumed to propagate radially from the site where the rupture reaches first. The time differences in rupture propagation between segments are obtained as follows:

- If the segments are continuous, continuous rupture propagation is assumed.
- If the segments are not continuous, but are separated from each other, the rupture propagation is obtained by assuming the propagation of S-waves between the segments.

1.2 Characterized source model for subduction-zone interplate earthquakes

Subduction-zone interplate earthquakes have shorter recurrence intervals than earthquakes occurring on active faults. Therefore, information showing the conditions of past earthquakes remains available for some regions, and such information can be used when building a characterized source model. Meanwhile, as explained again in **4.**, a characterized source model

is verified in each phase, using past earthquake-related data, and the source parameters are reviewed as needed. In such process of reviewing a characterized source model, there may be a case of stretching the interpretation of the Recipe below as a result of ascertaining source parameters that can explain the observed waveforms, etc. In such case, past earthquake-related data (earthquake magnitude, source area, seismic waveform records, seismic intensity, seismic damage, etc.) may not all be consistent, so the data to be used needs to be prioritized according to the purpose of analysis. Appended Figure 5 shows the flow chart of determination of source parameters for subduction-zone interplate earthquakes.

1.2.1 Outer source parameters

The following are determined as outer source parameters for source fault models of subduction-zone interplate earthquakes:

- Location and structure of the source fault model (location, strike, depth)
- Area of the source fault model/earthquake magnitude
- Average slip of the source fault model

(a) Location and structure of the source fault model (location, strike θ, depth)

As for the location of a source fault, if the source area of a past earthquake has been inferred, a source fault is determined based on the source area. With regard to the depth, the depth from the upper edge to the lower edge of the seismogenic area is determined based on the depth distribution of the upper surface of the oceanic plate in the assumed source area inferred from an elastic wave exploration, microearthquake distribution, etc.

If the long-term evaluation provides an source area, it is desirable to use such estimated shape, while taking into account the grounds for the estimation.

(b) Area of the source fault model/earthquake magnitude (fault area S, seismic moment M_0)

The source fault area and the earthquake magnitude are determined by either of the following methods:

- The method of clearly determining the source area according to **(a)**, then calculating the fault area from the extent of the source area, and inferring the earthquake magnitude by the empirical relation between the earthquake magnitude and the fault area.
- The method of determining the earthquake magnitude based on the value assumed from past earthquakes, and determining the source fault area by the empirical relation between the earthquake magnitude and the fault area.

For the above-mentioned empirical relation of the earthquake magnitude (between the seismic moment M_0 (Nm) and the fault area S (km^2)), if some data of past earthquakes are available, a formula that considers regional characteristics is used. For example, a regional empirical relation between the seismic moment M_0 (Nm) and the fault area S (km^2) is determined by inferring the average stress drop $\Delta\sigma$ (MPa) of the source area based on the following relation that assumes a circular crack, in the same manner as in Kanamori and Anderson (1975):

$$M_0 = 16/\left(7 \cdot \pi^{3/2}\right) \cdot \Delta\sigma \cdot S^{3/2} \quad \text{.....} \quad (29)$$

On the other hand, if data of past earthquakes are scarce, the empirical relation to be used is that between the earthquake magnitude and the fault area (e.g., Utsu, 2001; Ishii and Sato, 2000) or between the seismic moment M_0 (Nm) and the fault area S (km^2) (e.g., Sato, 1989; Yamanaka and Shimazaki, 1990) that show average characteristics. When using these formulae, it is necessary to take note of how the source fault area, which constitutes part of the data set for the empirical formulae, has been assumed.

If the long-term evaluation provides an estimated shape of the source area, it is desirable to use such estimated shape, while taking into account the grounds for the estimation.

(c) Average slip *D*

See 1.1.1(i).

1.2.2 Inner source parameters

The following are determined as inner source parameters of a source fault of a subduction-zone earthquake:

- Asperity locations and the number of asperities
- Asperity area
- Average slip of the asperities and the background region
- Effective stress of the asperities and the background region
- f_{max}
- Average rupture velocity
- Slip velocity time function
- Slip angle

(a) Asperity locations and the number of asperities

Recent research (Kikuchi and Yamanaka, 2001) and a series of studies on the 2003 Tokachi-Oki Earthquake (e.g., Yamanaka and Kikuchi, 2003; Koketsu *et al.*, 2004; and Yagi, 2004) have found that the locations of the asperities of earthquakes that repeatedly occur at the same source area are very likely to coincide. Therefore, if an earthquake has occurred recently in an assumed source area, the asperity locations can be presumed by analyzing the observation records of that earthquake. Even in the absence of recent observation records, if the distribution of back slips (slip deficits) can be inferred from crustal movement data, the locations with large back slips can be assumed to be the asperity locations, since the interplate coupling is considered to be stronger at asperities than in the surrounding area. Alternatively, since Wells *et al.* (2003) and Sugiyama (2004) point out the existence of a correlation between areas of negative gravity anomaly and asperity locations in the source area of interplate earthquakes, data on gravity anomaly can be used for reference.

If asperity locations have been inferred, the number of asperities corresponds to the number of asperities included in the assumed source area. Generally, the number of asperities increases as the assumed source area/earthquake magnitude becomes larger.

(b) Short-period level *A* and total area of the asperities S_a

The total area of the asperities S_a (km^2) is closely related to the acceleration source

spectrum level in the short-period range (hereinafter referred to as the "short-period level") which directly affects the strong ground motion prediction. Therefore, the total area of the asperities S_a (km^2) is obtained after determining the short-period level A (Nm/s^2) for the source fault model. The short-period level A (Nm/s^2) has been inferred for some earthquakes, based on the seismic waveform at observation points on firm ground that is hardly affected by the shallow subsurface structure or at observation points where the effects of the shallow subsurface structure have been ascertained quantitatively. In the meantime, if the area is not restricted to the source area of the assumed earthquake, the empirical relation between the short-period level A (Nm/s^2) and the seismic moment M_0 (Nm) is available from analysis results of recent earthquakes. Thus, the value of the short-period level is to be obtained by either of the following methods according to circumstances (Irikura et al., 2002):

- If the short-period level A (Nm/s^2) of the latest event in the assumed source area has not been inferred, the short-period level is determined by the empirical relation between the seismic moment M_0 (Nm) and the short-period level A (Nm/s^2) proposed by Dan et al. (2001) (Formula (11)).
- If the short-period level A (Nm/s^2) of the latest event in the assumed source area has been inferred, the short-period level is determined according to the seismic moment of the assumed earthquake by considering the tendency of the empirical relation between the inferred value and the seismic moment M_0 (Nm) (ERC, 2003b; 2004b).

The total area of the asperities S_a (km^2) is calculated by using the short-period level A (Nm/s^2) inferred above and earlier-mentioned Formula (12). If there is only one asperity, the total area of the asperities S_a ($=\pi\times r^2$) (km^2) is obtained by deeming the source fault shape to be a circular crack with a radius R (km) and the asperity to be a single circular crack with an equivalent radius r (km), for convenience.

Meanwhile, recent researches have revealed that the proportion of the total area of the asperities caused by seven subduction-zone interplate earthquakes to the total area of the faults is about 35% ± 11% (Ishii et al., 2000). Although these values are not restraint conditions, they need to be taken into account.

When a single segment has two asperities, it is desirable to distribute the area between those asperities according to how large the asperities were or the back slips were in the latest event. If no such resolution is available, the ratio in which the area should be distributed is determined by considering a view suggesting that, according to recent researches , the ratio would be 2:1 if there are two asperities and 2:1:0.5 if there are three asperities (Ishii and Sato, 2000).

(c) Average slip of the asperities and the background region D_a, D_b

See 1.1.2(c).

*** It is desirable to confirm that the average slip of the largest asperity obtained here complies with the upper limit of co-seismic slip for an earthquake inferred from the relative slip rate between the plates in the source area of the subduction-zone interplate earthquakes and the recurrence interval of the earthquake, and with the maximum slip inferred for past earthquakes.**

(d) Static stress drop of the whole source fault, average static stress drop and average

effective stress of the asperities, and effective stress of the background region $\Delta\sigma$, $\Delta\sigma_a$, σ_a, σ_b

See 1.1.2(d).

*** When the earthquake magnitude, the fault area, and the short-period level are given, the total area of the asperities and the effective stress are uniquely determined from the relations above. If the seismic waveform or the seismic intensity distribution simulated by using those parameters does not coincide with the past earthquake data used for verification, the parameters are to be determined again by prioritizing the uniquely inferred earthquake magnitude or short-period level. If past seismic waveform data is available, it may be possible to assume individual asperity areas from the pulse width of the waveform.**

(e) f_{max}

Since it is difficult to determine f_{max} by considering regional characteristics due to lack of data, etc., f_{max} = 13.5Hz inferred by Sato *et al.* (1994) from the observation records of small and medium earthquakes in the Sendai region is used at present (ERC, 2003b; 2004b).

(f) Average rupture velocity V_r

See 1.1.2(f).

(g) Slip velocity time function $dD(t)/dt$

See 1.1.2(g).

(h) Slip angle λ

See 1.1.2(h).

*** In an actual earthquake, the slip angle of the source fault varies by location. If the same slip angle is assumed for the whole fault in a source fault model, the directivity effect tends to show overly strongly in the strong ground motion prediction results.**

1.2.3 Other source parameters

The following are determined as the outer source parameters:

- Rupture starting point
- Rupture pattern

(a) Rupture starting point

It is appropriate to make the location of the rupture starting point the same as that in past earthquakes if it is known. According to Kikuchi and Yamanaka (2001), the rupture directivity has regional characteristics, and the rupture tends to propagate from shallow to deep in the Sanriku-Oki region, and from deep to shallow in the Nankai trough. If such tendency becomes clear for various sea areas in the future, the location of the rupture starting point can be determined with consideration to the regional characteristics, even for a source area for which the conditions of past earthquakes are unclear.

(b) Rupture pattern

See 1.1.3(b).

2. Subsurface structure models

Major parameters of the subsurface structure model used in a detailed strong ground motion evaluation include the density, the P-wave/S-wave velocity, the Q-value, and the interface shape of each layer, when assuming a stratified structure. The subsurface structure model is built separately for the following three structures:

- The crustal structure of the seismic bedrock[9] and deeper, including the upper mantle, which serves as the propagation path of seismic waves (hereinafter referred to as the "crustal structure of the seismic bedrock and deeper")
- The subsurface structure from the seismic bedrock to the engineering bedrock,[10] which mainly affects the amplification of the long-period component of seismic waves (hereinafter referred to as the "deep subsurface structure").
- The subsurface structure from the engineering bedrock to the ground surface, which mainly affects the amplification of the short-period component of seismic waves (hereinafter referred to as the "shallow subsurface structure")

The concept of the modeling method for each of these structures is explained below. Meanwhile, the later-mentioned hybrid method requires a three-dimensional subsurface structure model that combines the "crustal structure of the seismic bedrock and deeper" and the "deep subsurface structure".

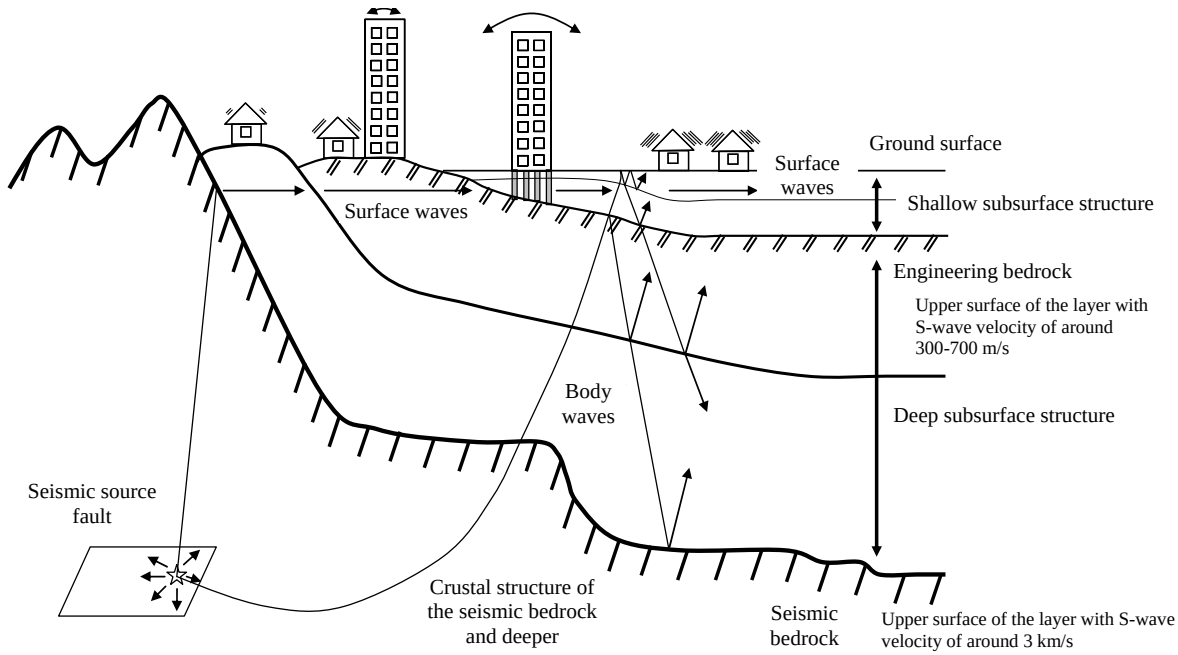

Schematic drawing of the subsurface structure models

[9] The seismic bedrock is the hard bedrock with a S-wave velocity of around 3km/s in the uppermost part of the crust.

[10] The engineering bedrock is the hard soils that serves as the basis for determining ground motions when designing structures in the engineering field, such as architecture and civil engineering. Its S-wave velocity is usually around 300m/s-700m/s although it varies by structure type and ground conditions.

2.1 "Crustal structure of the seismic bedrock and deeper"

The "crustal structure of the seismic bedrock and deeper" from the upper mantle to the seismic bedrock is modeled by taking into consideration such information as the model used in a source inversion analysis, the results of large-scale elastic wave exploration and deep borehole drilling such as MITI well drilling, or three-dimensional seismic wave velocity structure using seismic observation data (e.g., Zhao *et al*., 1994; Matsubara *et al*., 2005). Also, when a model in the sea area is needed for subduction-zone earthquakes, etc., the model is obtained by the same method (e.g., Tanaka *et al.*, 2006).

2.2 "Deep subsurface structure"

2.2.1 Ordinary case

When modeling the "deep subsurface structure", first a 0th-order model[11] is obtained by procedure (1) - (2) of the standard modeling method shown below (Koketsu, 2006; Koketsu *et al*., 2009), using geological information and various structural exploration data. Next, a 0.5th-order model with a more accurate layer interface shape is obtained by procedure (3) - (5), using existed exploration data. However, if no exploration data is available, the 0.5th-order model is obtained by conducting procedure (6) in advance, using the spectrum ratio, etc. of the seismic observation records. Lastly, the final model is obtained by procedure (6) - (7), using the waveforms and spectrum ratio, etc. of the seismic observation records. In the modeling process, it is possible to go back to the lower-order modeling depending on circumstances. Such flow of modeling the "deep subsurface structure" is shown in Appended Figure 6.

Procedure (1)

The velocity structure and the geological structure are compared by comprehensively determining from geological information such as the subsurface geological data and boring logs, as well as various structural exploration results (for the process of "comprehensive determination", see Suzuki, 1996; Fujiwara *et al*. 2006).

[11] As a result of the strong motion evaluations conducted to date and the efforts of the National Research Institute for Earth Science and Disaster Prevention, a nationwide 0th-order model (Fujiwara *et al.*, 2006) of the "deep subsurface structure" is near completion, and can be used. A nationwide first-order model is also being built with completion targeted by the end of FY2009 (Koketsu *et al.*, 2008).

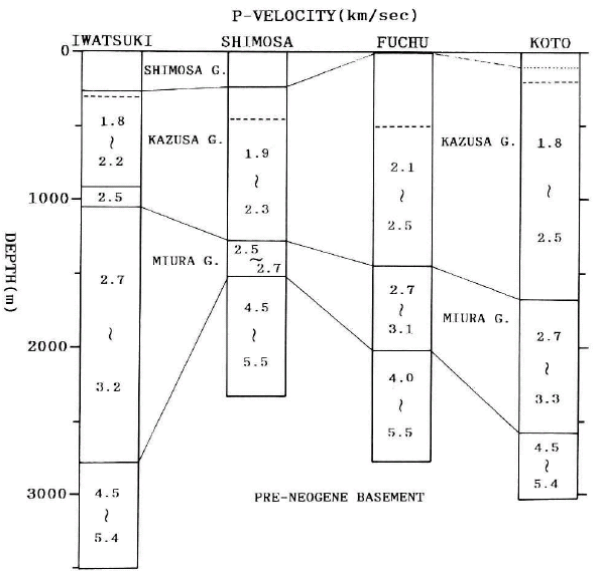

Comparison between the primary-wave velocity distribution at a deep borehole observatory and geological layers; Suzuki (1996)

	Hyuganada (HERP)	Northern Kyushu (HERP)	Miyagi-ken	Sanriku-Oki (HERP)
Lay1(0.35)				
Lay2(0.5)				①0.5
Lay3(0.6)	②0.6	①0.6		
Lay4(0.7)			①0.7	
Lay5(0.8)				
Lay6(0.9)				②0.8
Lay7(1.0)		②1.1		
Lay8(1.3)		③1.4	②1.3	
Lay9(1.5)	③1.5			
Lay10(1.7)		④1.7		
Lay11(2.0)	④2.1	⑤2.1	③2.0	③1.9
Lay12(2.4)				④2.3
Lay13(2.9)	⑤2.7	⑥2.7		
Lay14(3.2)	⑥3.1	⑦3.1	④3.0	⑤3.4

Correspondence of the layer classification in the existing model
Fujiwara, *et al.* (2006)

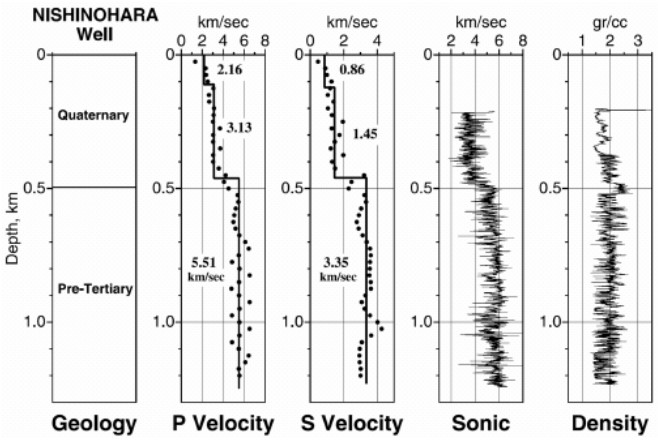

Well logging results using mesopelagic crustal activity observatory; Yamamizu (2004)

Procedure (2)

Based on the comparison results in procedure (1), the P-wave and S-wave velocity and density are given for each layer, taking into consideration the results of seismic refraction surveys, seismic reflection surveys, borehole logging, microtremor explorations, and spectrum ratio analysis of seismograms.

Procedure (3)

The shape of the upper plane of the engineering bedrock is obtained by interpolating micromotion exploration results, boring information, etc. Also, if necessary, a weathered layer is assumed also for areas with a very shallow bedrock.

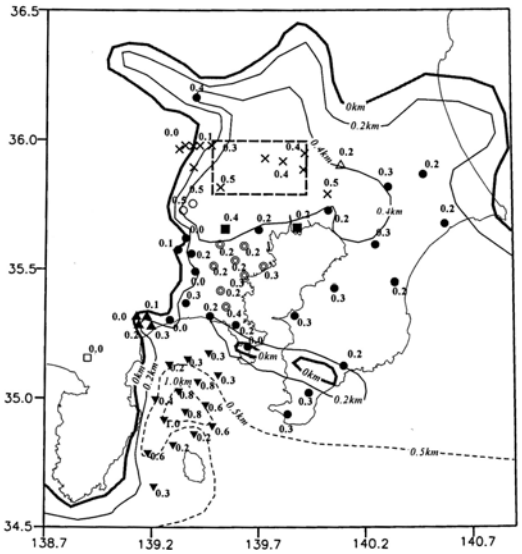

Depth distribution of the upper surface of the engineering bedrock
Yamanaka and Yamada (2002)

Procedure (4)

Information on discontinuity such as the shape of the fault or a fold is collected. The data of the reflection method and the boring well logging are converted into depth while paying attention to the fact that the velocity structure complies with the velocity in procedure (2).

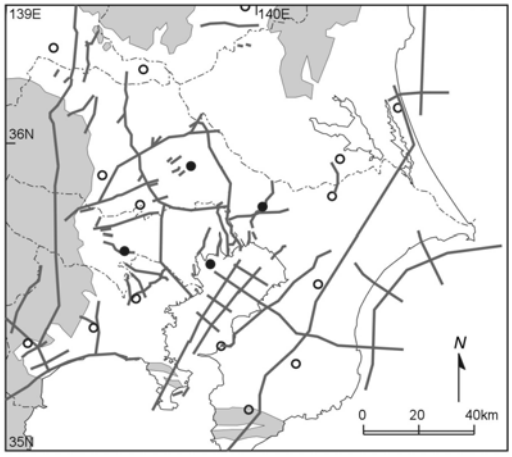

Deep boreholes (dots; black dots denote boreholes reaching the bedrock) and seismic reflection survey lines (gray solid lines) in the Kanto region. The bedrock almost crops out in the gray areas.
Koketsu (2006)

Procedure (5)

The interface shape of each velocity layer is determined by using existed exploration data (seismic refraction survey, gravity survey, etc.) and geological contour maps. The determination is made by inversion, but if sufficient data is not available, a forward solver such as interpolation is used. The information and data in procedure (4) are treated as restraint conditions for inversion or as additional data for interpolation.

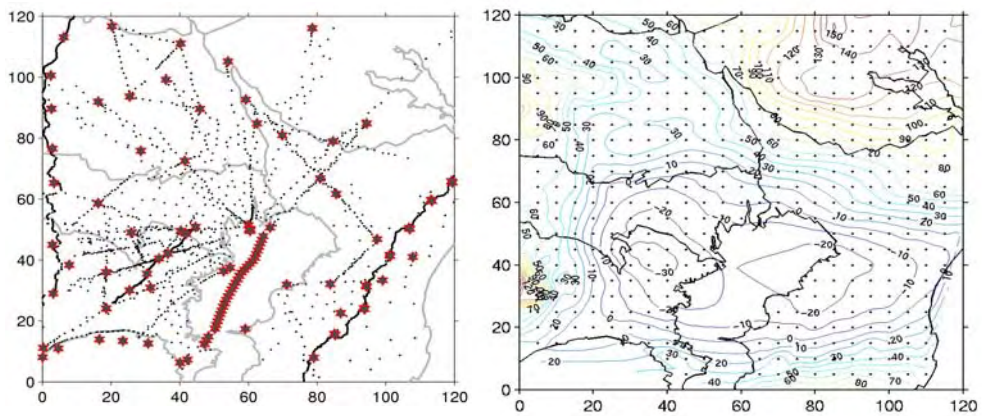

Left-hand chart: Structural exploration lines in the Metropolitan area Afnimar *et al.* (2002)

Right-hand chart: Free-air anomaly map Afnimar *et al.* (2003)

Procedure (6)

The subsurface structure model is adjusted/corrected by using the velocity structures at multiple observation points obtained by applying spectrum ratio analysis (again, by inversion if possible) to natural earthquake records such as those of the K-NET or the KiK-net.

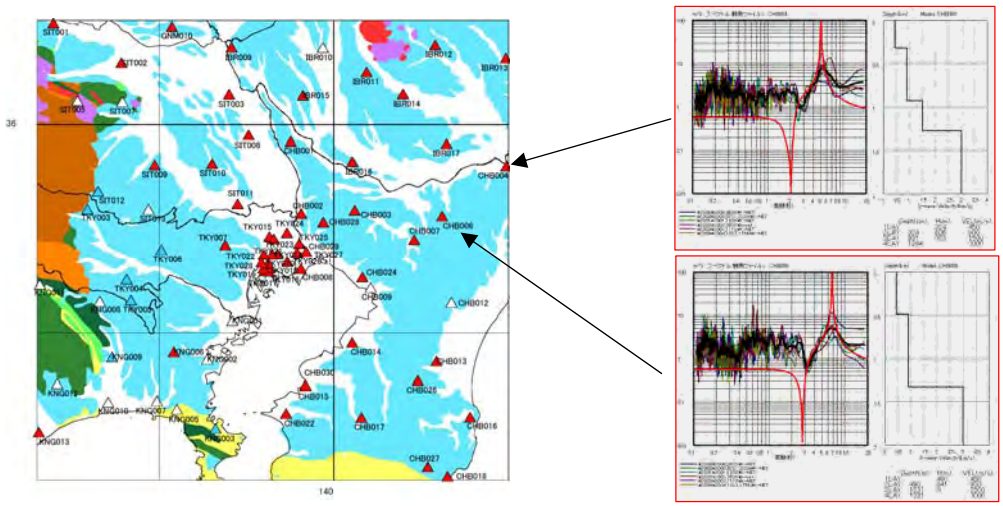

H/V spectrum ratio of seismic observation records and simulated waveforms Tanaka *et al.* (2005)

Procedure (7)

Some moderate size earthquakes (about M5) for which observation records are available are selected, and ground motions at each observation point are simulated by using the subsurface structure model adjusted in procedure (6). The model is further adjusted so that the obtained results coincide with the observation records (again, by inversion if possible).

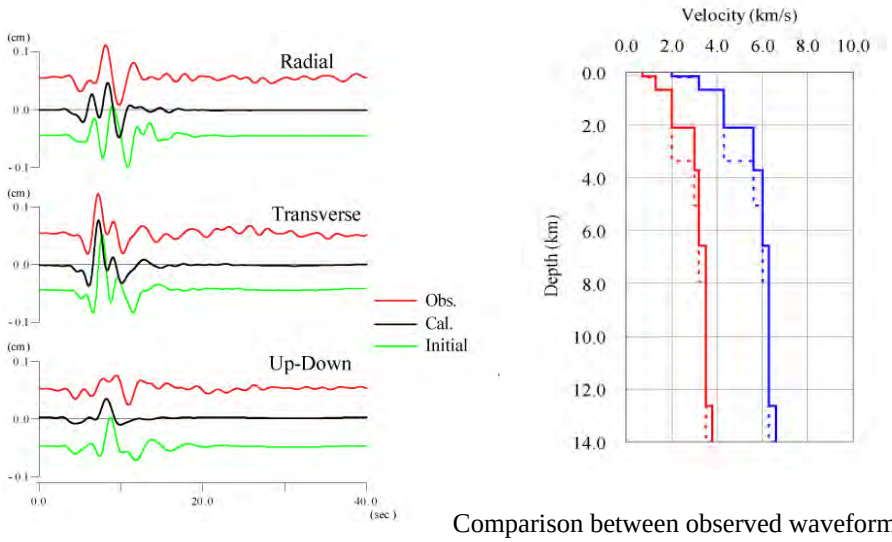

Comparison between observed waveforms and waveforms obtained by ground motion simulation, and the correction result of the velocity model
Hikima and Koketsu (2004)

An appropriate value needs to be determined for the Q-value so as to be able to explain the seismic observation records. For reference, the values used in the strong ground motion evaluations conducted by the ERC to date are shown in the figure below, in comparison to existing research.

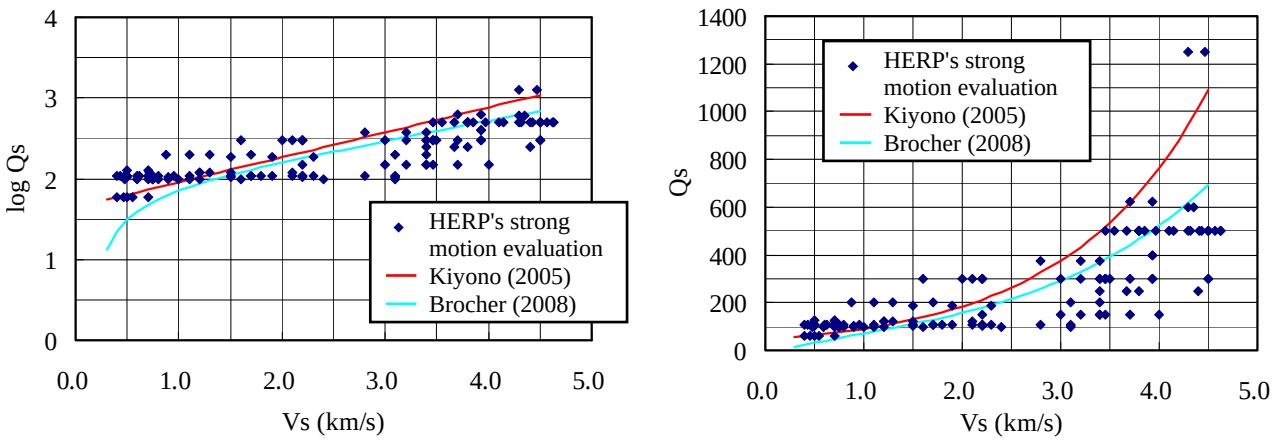

Relation between shear-wave velocity (V_S) and Q-value (Q_S)

2.2.2 Case where the horizontally layered structure can be assumed

When it is known in advance that the horizontally layered structure can be assumed, it is not appropriate to create a three-dimesional heterogeneous model, since it is far easier to theoretically simulate strong ground motions for the horizontally layered structure. The horizontally layered structure is modeled with the same method as that used for the "crustal structure of the seismic bedrock and deeper", by taking into consideration the model used in seismic source inversion analysis, the model used for determining the seismic source, and results

of large-scale elastic wave exploration and deep borehole drilling such as MITI well drilling.

2.3 "Shallow subsurface structure"

With regard to the subsurface structure model for the "shallow subsurface structure", a one-dimensional velocity structure is modeled, in principle, by collecting subsurface geological data and boring data used in ground surveys. Such modeling is necessary also for evaluating, with high accuracy, the nonlinear phenomena which may occur in the shallow subsurface structure at the time of strong ground motions. However, since the "shallow subsurface structure" often substantially changes locally in a horizontal direction, an enormous amount of data and efforts are needed for building an accurate, detailed, area-based model. There are also many areas that have hardly any boring information available.[12] Thus, in order to make an area-based evaluation of the "shallow subsurface structure", modeling methods that simulate the amplification factor empirically based on geomorphologic classification such as digital national land information have been developed. As methodologies that can be used, a method of modeling the "shallow subsurface structure" by using boring data and a method of modeling the structure by area-based evaluation are explained below.

2.3.1 Method of modeling by using boring data

In the method of modeling based on boring data, the density of the one-dimensional layer structure, the P-/S-wave velocity, the layer thickness, and attenuation characteristics of the boring site are determined (e.g., Takahashi and Fukuwa, 2006). Moreover, since the "shallow subsurface structure" shows nonlinear movements when it receives a large strain from a large earthquake, parameters representing nonlinear characteristics need to be determined. It is desirable to determine such parameters by conducting soil tests, but if no soil test results are obtained for the ground in question, existing soil test results are used for determining the parameters.

Under this method, evaluation is generally possible only at sites for which boring data exist. However, when conducting area-based evaluation, it is possible to collect a large amount of boring data and geomorphologic data, extract the typical boring log for each area zoned based on geomorphologic characteristics, and apply such log to each segmented area. In this case, the area of the segmented area is often about 500 m or 250 m square (East-West/South-North).

2.3.2 Method of modeling by area-based evaluation

The typical method of modeling by area-based evaluation is the method of using digital national land information as proposed by Matsuoka and Midorikawa (1994) and Fujimoto and

[12] Even if boring data actually exist, the data are often merely scattered in reality due to the insufficiency of systems for effectively using such data. For regional disaster prevention measures as well, there is a need for developing a system to systematically and continuously integrate data and develop a subsurface structure database through government-industry-academia collaborations in the future. Studies such as the project of "Development of an Integrated Geophysical and Geological Information Database" (Fujiwara, 2007) expected to make achievements in this area.

Midorikawa (2003). This method simulates the amplification factor of the peak velocity by the "shallow subsurface structure" based on the geomorphologic classification data newly prepared by using data including the topography data and elevation data from the digital national land information for each of the mesh areas of about 1 km covering the whole of Japan.

Recently, a Japan Engineering Geomorphologic Classification Map (JEGM) has been developed by reevaluating the geomorphologic characteristics of the whole of Japan by a unified classification standard (Wakamatsu et al., 2004; see 3.2.1). By using such method, the "shallow subsurface structure" can be modeled relatively easily for each of the 1 km or 250 m meshes covering the whole of Japan.

3. Strong ground motion simulation

With regard to strong ground motion simulation, the simulation method for layers up to the upper surface of the engineering bedrock and that for the upper surface of the engineering bedrock to the ground surface differ from each other due to differences in the ground modeling and parameter determinations. Therefore, each of these methods is explained below. The results of a strong ground motion simulation include waveform, peak acceleration, peak velocity, and response spectrum.

3.1 Simulation method for layers up to the upper surface of the engineering bedrock

The strong ground motion simulation methods for layers up to the upper surface of the engineering bedrock can roughly be divided into the empirical method, semi-empirical method, theoretical method, and hybrid method, and the method is selected according to the data size and purpose (e.g., Kagawa *et al.*, 1998). The characteristics of each method are outlined below.

Empirical method

This is the simple method whereby values such as the peak acceleration, peak velocity, and acceleration response spectrum are calculated by a relation between the magnitude and the distance, based on past data. Since the evaluation is made with average values, the influences of the rupture process and the influences of the asperities are not considered individually. As the attenuation relation for obtaining peak velocity on the upper surface of the engineering bedrock, the following empirical formula proposed by Si and Midorikawa (1999) is frequently used.

$$\log PV_b = 0.58M_{\mathrm{w}} + 0.0038D - 1.29 - \log\left(X + 0.0028 \cdot 10^{0.50M_{\mathrm{w}}}\right) - 0.002X \quad \cdots\cdots\cdots\cdots\cdots\cdots (30)$$

PV_{b}: peak velocity(cm/s) on the upper surface of the engineering bedrock
M_w: moment magnitude M_{w}=(logM_0-9.1)/1.5 (Kanamori, 1977)
D: focal depth (km)
X: shortest distance to fault (km)

Semi-empirical method

This is a method of synthesizing the waveform of a large earthquake from the waveform of an existing small earthquake. There are the empirical Green's function method and the

stochastic Green's function method. The empirical Green's function method is a method to deem the observed waveform of a small or moderate size earthquake that has occurred at the source region of the assumed fault as the elementary wave (Green's function), and to sum up the elementary wave according to the rupture process on the assumed fault. The time history waveform can be predicted, and the influences of the rupture process and the influences of the asperities can be considered. However, an appropriate, observed waveform needs to be available in advance for the evaluation site. The stochastic Green's function method deems a waveform that has the average characteristics of a large amount of observation records to be the elementary wave. There is no need to obtain an appropriate, observed waveform for the evaluation site. However, shaking characteristics specific to the evaluation site are difficult to be reflected. The time history waveform is simulated by the same method as that in the empirical Green's function method.

Theoretical method

This is a method to simulate the propagation characteristics of the seismic wave and the amplification characteristics of the shallow subsurface structure by the theory of elastic wave propagation. The time history waveform can be predicted, and the influences of the rupture process and the influences of the asperities can be considered. This method can be used to make evaluation for the long-period domain which is hardly affected by the heterogeneity of the source fault, but due to the difficulty of inferring the rupture process and the subsurface structure related to generation of short-period ground motions, it would be difficult to evaluate the short-period domain.

Hybrid method

This is a method where the long-period domain is simulated by the theoretical method, and the short-period domain where the random phenomenon is dominant by semi-empirical method, and the two are synthesized. The time history waveform can be calculated, and the influences of the rupture process and the influences of the asperities can be considered. The method can be used for broadband evaluation.

In an area where a characterized source model and a detailed subsurface structure model can be used, a hybrid method (e.g., Irikura and Kamae, 1999) that combines the stochastic Green's function method, which is a semi-empirical method, (e.g., Kamae *et al.*, 1991; Dan and Sato, 1998) and the three-dimensional finite difference method (e.g., Aoi and Fujiwara, 1999; Graves, 1996; Pitarka, 1999), which is a theoretical method, is frequently used for conducting area-based strong ground motion simulation. This is because of the following advantages of this hybrid method:

- The influences of the characterized source model and the three-dimensional subsurface structure model can be directly incorporated.
- An area-based prediction is possible.
- The method can be applied to the periodic band (0.1 sec. - 10 sec.) subject to strong ground motion evaluation.

The reason that the stochastic Green's function method is used as the semi-empirical method is that area-based prediction is easy (whereas the empirical Green's function method can only be applied at sites where waveform has been observed, in principle). Also, the reason for using the three-dimensional finite difference method as the theoretical method is that, compared to other

simulation methods for irregular subsurface structure (e.g., finite element method, boundary element method), large-scale numerical operations can be easily conducted and the computation is quick when treating a large-scale subsurface structure. However, if a horizontal, multilayered structure can be assumed for an area, a method using wavenumber integration, which can only be applied to a horizontally layered structure, can be used as the theoretical method (e.g., Kohketsu, 1985; Hisada, 1995). This method is the most frequently used method for the Green's function simulation of a horizontally layered structure; the modeling and simulation are relatively easy, and it has been confirmed from many case examples that, if the source fault model and the horizontally layered structure model are appropriate, the body wave and the surface wave can be reproduced well. For details on the hybrid method, etc., see for example "A Study on Strong Motion Maps for Scenario Earthquakes in Morimoto Togashi Fault Zone" (Senna *et al.*, 2004).

***When using the hybrid method, it is desirable to determine the cross frequency of a matching filter by taking into account the limits of accuracy of the theoretical method and the effectiveness of the semi-empirical method.**

3.2 Simulation method for layers up to the ground surface

Since the simulation method for layers up to the ground surface differs by whether the subsurface structure model for the "shallow subsurface structure" has been built by using boring data or by area-based evaluation, each of these cases is explained below.

3.2.1 Case of a "shallow subsurface structure" modeled by using boring data

Based on a detailed model built by using boring data, the time history waveform on the ground surface is simulated by carrying out one-dimensional seismic response simulation, using the time history waveform on the engineering bedrock as an input. The main methods of one-dimensional seismic response simulation are the linear analysis method (e.g., Haskell, 1960), the equivalent linear analysis method (e.g., Schnabel *et al.*, 1972), and the sequential nonlinear analysis method (e.g., Yoshida and Tohata, 1991). Each method is characterized as follows.

linear analysis method

The simulation is carried out by using the multiple reflection theory. Since nonlinear characteristics of soil are not taken into consideration, if nonlinear characteristics occur as a result of a large earthquake, correct results cannot be obtained.

Equivalent linear analysis method

Based on the multiple reflection theory, the nonlinear characteristics of soil are replaced with an equivalent linear relationship, and certain soil characteristics are used during analysis. When the strain level rises, the accuracy lowers. The extent of the permissible strain level is generally 0.1-1%, although it depends on the required accuracy and the conditions of the ground. If liquefaction, etc. occurs by strong shaking, correct results cannot be obtained.

Sequential nonlinear analysis method

This is a method which attempts to obtain the behavior while expressing the nonlinear characteristics of soil by a mathematical model or a dynamic model, and sequentially simulating the changes in the soil characteristics. Therefore, it is applicable even at a large strain level exceeding 1%. On the other hand, as a large number of parameters need to be determined, it is important that a person having expert knowledge engages in the analysis.

The equivalent linear analysis method has been frequently used for simulation of a wide-area ground motion distribution to date. The reason is that the equivalent linear analysis method is easy to used with only few parameters, and that the obtained ground motion distribution (seismic intensity, acceleration) could comprehensively explain the ground motion distribution of past damaging earthquakes. Meanwhile, the sequential nonlinear analysis method has often been used for each target site in order to verify observed waveforms and to confirm a rise in the excess pore water pressure or an increase in strain of liquefied ground, and has rarely been used for wide-area ground motion evaluation. Wide-area ground motion simulation by the sequential nonlinear analysis method still faces many challenges, such as the need to carry out individual analyses based on expert judgments, such as the determination of the stress-strain relation to be adopted and the parameters to be used. Accordingly, application of the sequential nonlinear analysis method to wide-area ground motion evaluation has only started, and requires further studies.

3.2.2 Case of a "shallow subsurface structure" modeled by area-based evaluation

The peak velocity on the ground surface is calculated by multiplying the value of the peak velocity on the engineering bedrock by the amplification factor *amp* obtained from the geomorphologic unit.

The amplification factor *amp* obtained from the geomorphologic unit is evaluated by following the procedure below.

(1) The geomorphologic classification data for each of the 1 km meshes (e.g., Wakamatsu et al., 2005) or 250 m meshes (e.g., Wakamatsu and Matsuoka, 2007) covering the whole of Japan is used.

(2) The following empirical relation between the elevation and the average S-wave velocity in the upper 30 m *AVS30* (e.g., Matsuoka et al., 2005) is applied to that geomorphologic classification:

$$\log AVS30 = a + b \cdot \log E_{\mathrm{v}} + c \cdot \log S_{\mathrm{p}} + d \cdot \log D_{\mathrm{m}} \pm \sigma \quad \text{.....} (31)$$

*AVS*30: average S-wave velocity in the upper 30 m(m/s)
E_{V}: elevation (m)
S_{p}: slope gradient * 1000 (slope gradient: tangent)
D_{m}: the distance from the mountain or hill of pre-Tertiary period or Tertiary (km)
σ: standard deviation
a, b, c, d: regression coefficients given for each geomorphologic classification

(3) The amplification factor *amp* for the peak velocity from the engineering bedrock to the ground surface is found to correlate with the average S-wave velocity in the upper 30 m *AVS*30. Thus, the amplification factor *amp* for the peak velocity is simulated from *AVS*30 by using the following formula (e.g., Fujimoto and Midorikawa, 2006):

$$\log(amp) = 2.367 - 0.852 \cdot \log AVS30 \pm 0.166 \quad (100 < AVS30 < 1500) \quad \text{..... (32)}$$

amp: amplification factor for the peak velocity on the engineering bedrock with average S-wave velocity 600m/s

Next, the seismic intensity *I* on the ground surface is obtained. The method differs between the case where the maximum value of ground motions on the engineering bedrock has been obtained by an empirical relation such as an attenuation relation for ground motion, and the case where the waveforms on the engineering bedrock has been obtained by the hybrid method, etc. For each case, the seismic intensity *I* on the ground surface is obtained by the following procedures.

i) Case where the peak velocity on the engineering bedrock has been obtained by an empirical relation such as an attenuation relation

The peak ground velocity PGV (cm/s) is simulated by multiplying the peak velocity on the engineering bedrock PV_b (cm/s) by the abovementioned amplification factor for the peak velocity *amp*.

$$PGV = amp \cdot PV_b \quad \text{..... (33)}$$

The seismic intensity *I* on the ground surface is obtained by substituting the peak ground velocity *PGV* into the "relation between the peak velocity and the Japan Meteorological Agency (JMA) instrumental seismic intensity" (e.g., Fujimoto and Midorikawa, 2005).

$$\begin{aligned} I &= 2.002 + 2.603 \cdot \log(PGV) - 0.213 \cdot \{\log(PGV)\}^2 \quad (4 \le I) \\ I &= 2.165 + 2.262 \cdot \log(PGV) \quad (I < 4) \end{aligned} \quad \text{..... (34)}$$

ii) Case where the waveform on the engineering bedrock has been obtained by the hybrid method, etc

First, the site amplification factor for JMA seismic intensity ΔI from the engineering bedrock to the ground surface is evaluated. Where the ground surface seismic intensity is *I*, the peak ground velocity is *PGV* (cm/s), the peak velocity on the engineering bedrock is PV_b (cm/s), and the amplification factor for the peak velocity is *amp*, Formula (35), which applies the relation between the peak velocity and the JMA instrumental seismic intensity (Fujimoto and Midorikawa, 2005) to the JMA seismic intensity I_b on the engineering bedrock, is expressed as:

$$I_{\mathrm{b}} = 2.002 + 2.603 \cdot \log(PV_{\mathrm{b}}) - 0.213 \cdot \{\log(PV_{\mathrm{b}})\}^2 \qquad (4 \le I) \quad \text{..... (35)}$$

From the relationship between Formula (35) and the abovementioned PGV = amp・PV_{b}, the site amplification factor for JMA seismic intensity ΔI is expressed as:

$$\Delta I = I - I_{\mathrm{b}} = 2.603 \cdot \log(amp) - 0.213 \cdot \{\log(amp)\}^2 - 0.426 \cdot \log(PV_{\mathrm{b}}) \cdot \log(amp)$$

$$\text{..... (36)}$$

Therefore, when the "JMA instrumental seismic intensity I_{b} on the engineering bedrock" is calculated from the waveform on the engineering bedrock, according to the method by the JMA (1996), the seismic intensity on the ground surface is obtained as:

$$I = I_{\mathrm{b}} + \Delta I \quad \text{..... (37)}$$

***The amplification factor *amp* for the peak velocity from the upper surface of the engineering bedrock to the ground surface is calculated based on the relation of the average S-wave velocity in the upper 30 m *AVS*30. However, in mountains and hills, the engineering bedrock often appears at a depth much shallower than 30 m. It has been pointed out that the amplification factor *amp* obtained would be underestimated and cannot explain well the influences of the weak layers shallower than the engineering bedrock. Thus, proposals have been made on an amplification factor using average S-wave velocity at a depth other than the upper 30 m (e.g., Kawase and Matsuo, 2004; Hamada *et al.*, 2007). Accordingly, if the engineering bedrock of a mountain or a hill appears at a depth shallower than 30 m, a separate consideration would be required.**

*** If boring data can be collected, results with more regional characteristics can be expected by independently evaluating *AVS*30 for each geomorphologic unit or the relation between *AVS*30 and the amplification factor (e.g., Central Disaster Prevention Council, 2001; 2003).**

*** Formula (35) for obtaining the "seismic intensity on the engineering bedrock" is applicable to seismic intensity 4 or more. However, the "Seismic Hazard Maps for Specified Seismic Source Faults" by the Headquarters for Earthquake Research Promotion (HERP) use Formula (35) also in cases where the seismic intensity is 3 or less for convenience, due in part to the focus of the maps on sites where the seismic intensity is 5-Lower or more (e.g., ERC, 2008).**

*** Since Formula (34) has been inferred mainly from inland earthquakes that have occurred in recent years, when it is used for large subduction-zone earthquakes with a dominant long-period component, the peak velocity tends to be slightly overestimated. In such a case, a separate consideration would be required, such as using the formula proposed by Midorikawa *et al.* (1999) (Morikawa and Fujiwara, 2009).**

4. Verification of the prediction results

This section about verification of the prediction results explains the methods for confirming whether or not the strong ground motion prediction results are appropriate. Verification of the prediction results is conducted by comparing the prediction results and the facts observed in the past. However, since there is a difference in the earthquake recurrence intervals as well as the amount of available data between earthquakes occurring on active faults and subduction-zone interplate earthquakes, the verification method for each type of earthquake is shown below.

4.1 Verification of strong ground motion prediction results for earthquakes occurring on active faults

Since earthquakes occurring on active faults have long recurrence intervals, seismic intensity information and observation information at the time of the latest event are not available in most cases. Therefore, basically, verification of the strong motion prediction results for earthquakes occurring on active faults is conducted through comparison with values inferred by using an attenuation relation for ground motion.

4.1.1 Comparison with values inferred by using an attenuation relation

The results of simulation by the semi-empirical method or the theoretical method are compared with values inferred by using an attenuation relation, and confirmation is made that the simulation results fall within the variance of values estimated by using an attenuation relation (hereinafter referred to as the "variance of attenuation relation").

When comparing values inferred by using an attenuation relation and strong ground motion prediction results, it is desirable to use an attenuation relation that considers the regional characteristics. If an attenuation relation that considers the regional characteristics has not been prepared, a comparison is made with an existing attenuation relation. In this case, if the determined source parameters or subsurface structure model characteristics differ from average characteristics, the tendency of variance in prediction results would also differ. Accordingly, it is important to conduct comparison or verification while sufficiently paying attention to such point.

*** If, as a result of verification, the strong ground motion prediction results considerably differ from the attenuation relation, and there is a problem in the appropriateness of the prediction results, the determined characterized source model or subsurface structure model should be modified.**

4.1.2 Comparison with the seismic intensity distribution

The seismic intensity distribution is the most frequently used index for making area-based verification of strong ground motion prediction results at present. Seismic intensity distribution since the end of the 19th century (the middle of the Meiji Era) can be directly used

in the comparison. For earthquakes that have occurred since the early 17th century (the Edo Era), information on earthquake damage is fairly available. Therefore, the seismic intensity distribution has been inferred based on such information. Verification based on the seismic intensity distribution is conducted by using an empirical method or a semi-empirical method at a relatively early phase in determining the source parameters.

*** If the seismic intensity distribution and the simulation results do not match each other, the source parameters or the subsurface structure model should be reviewed.**

4.1.3 Comparison with observed waveform records

Due to the development of the K-NET and KiK-net observation networks since 1997, it has become possible to verify strong ground motion prediction results by comparing the waveform of the prediction results and observation records. The extent to which the simulated waveform can be made to match the observation records in the comparison with observation records depends case by case on the quality of the observed waveform and how much information on the seismic source and the ground conditions at the observation point are available. At present, as long as the conditions are right, it is possible to make the simulated waveform match even with the phase characteristics of the observation records with high accuracy. However, given that it is an area-based prediction, the verification is deemed to be successful if the maximum value of the time history waveform, duration, predominant period, and spectral characteristics can be explained to a certain extent.

*** In order to make the simulation results match the observed waveform, the inner source parameters and the subsurface structure model would need to be reviewed. Since the inner source parameters can only be ascertained with strong-motion records near the seismic source, and strong-motion records are essential for verification of the subsurface structure model, further expansion and development of the K-NET and KiK-net observation networks and observation networks of seismic intensity meters installed by the JMA and local public entities are desired.**

4.2 Verification of strong ground motion prediction results for subduction-zone interplate earthquakes

Since subduction-zone interplate earthquakes have shorter recurrence intervals than earthquakes occurring on active faults, information on earthquake damage and observation information at the time of the latest event are available in many cases. Therefore, strong motion prediction results can be verified and source parameters can be reviewed by comparing such information and the strong ground motion prediction results that assume past earthquakes. Verification methods include comparison with the seismic intensity distribution, observed waveform records, and values inferred by using an attenuation relation for ground motion.

4.2.1 Comparison with the seismic intensity distribution

See 4.1.2.

4.2.2 Comparison with observed waveform records

As digital strong-motion records have been obtained since the 1960s, when assuming the 1968 Tokachi-Oki Earthquake or any subsequent subduction-zone earthquake, the strong ground motion prediction results can be verified by comparing the time history waveform of the prediction results and observation records. Also, more observation records have become accessible since 1997 due to the development of the K-NET and KiK-net observation networks. The extent to which the simulated waveform can be made to match the observation records in the comparison with observation records depends case by case on the quality of the observed waveform and how much information on the seismic source and the ground conditions are available. At present, as long as the conditions are right, it is possible to make the simulated waveform match even with the phase characteristics of the observation records with high accuracy. However, given that it is an area-based prediction, the verification is deemed to be successful if the maximum value of the time history waveform, duration, predominant period, and spectral characteristics can be explained to a certain extent.

*** In order to make the simulation results match the observed waveform, the inner source parameters and the subsurface structure model would need to be reviewed. Since the inner source parameters can only be ascertained with strong-motion records near the seismic source, and strong-motion records are essential for verification of the subsurface structure model, further expansion and development of the K-NET and KiK-net observation networks and observation networks of seismic intensity meters installed by the JMA and local public entities are desired.**

*** Since the purpose of a strong ground motion evaluation is not in making the simulated waveform match the observed waveform, attention should be paid so as not to overly focus on this comparison process.**

4.2.3 Comparison with values inferred by using an attenuation relation

See 4.1.1.

Past research results have confirmed that observation records of large earthquakes can be reproduced with a relatively high accuracy by the empirical Green's function method using observation records of small and moderate size earthquakes (e.g., Kamae and Irikura, 1998; Ikeda et al., 2002). Therefore, as a method of verifying the strong motion prediction results by the hybrid method, it is also possible to compare the results obtained by the empirical Green's function method and those obtained by the hybrid method for a site for which observation records of a small or medium earthquake that has occurred in the vicinity of the target source fault are available in advance.

References

Afnimar, Koketsu, K. and Komazawa, M. (2003): "3-D structure of the Kanto basin, Japan from joint inversion of refraction and gravity data", *Proceedings of the 2003 IUGG Meeting*, Abstract SS04/07A/A03-002.

Afnimar, Koketsu, K. and Nakagawa, K. (2002): "Joint inversion of refraction and gravity data for the three-dimensional topography of a sediment-basement interface", *Geophys. J. Int.*, **151**, 243-254.

Aoi, S. and Fujiwara, H. (1999): "3D Finite-Difference Method using discontinuous grids", *Bull. Seism. Soc. of Am.*, **89**, 918-930.

Awata, Y. (2004): "Katsudanso kara hassei suru jishin kibo no yosoku shuho ni kansuru shomondai" (Problems on prediction method of earthquake magnitude occurring on active faults), *Chikyu Monthly*, **46** special issue, 163-167 (in Japanese).

Boatwright, J. (1988): "The seismic radiation from composite models of faulting", *Bull. Seism. Soc. Am.*, **78**, 489-508.

Brocher, T. M. (2008): "Key elements of regional seismic velocity models for ground motion simulations", *Journal of Seismology*, **12**, doi:10.1007/s10950-007-9061-3.

Central Disaster Prevention Council (2001): 11th Special investigation council concerning the Tokai Earthquake, shiryo3-1, December 11, 2001 (in Japanese).

Central Disaster Prevention Council (2003): 16th Special investigation council concerning the Tonankai-Nankai Earthquakes and others, sankoushiryo2, December 16, 2003 (in Japanese).

Dalguer, L. A., Irikura, K., Riera, J. and Chiu, H. C. (2001): "Fault Dynamic Rupture Simulation of the Hypocenter area of the Thrust Fault of the 1999 Chi-Chi (Taiwan) Earthquake, *Geophys. Res. Lett.*, **28**-7, 1327-1330.

Dan., K. and Sato, T. (1998): "Strong-Motion Prediction by Semi-empirical Method Based on Variable-slip Rupture Model of Earthquake Fault", *J. Struct. Constr. Eng., AIJ*, **509**, 49-60 (in Japanese with English abstract).

Dan, K., Watanabe, M., Sato, T. and Ishii, T. (2001): "Short-period Source Spectra Inferred from Variable-slip Rupture Models and Modeling of Earthquake Faults for Strong Motion Prediction by Semi-empirical Method", *J. Struct. Constr. Eng., AIJ*, **545**, 51-62 (in Japanese with English abstract).

Dan, K., Sato, T. and Irikura, K. (2002): "Characterizing Source Model for Strong Motion Prediction Based on Asperity Model", *Proceedings of the 11th Japan Earthquake Engineering Symposium*, 555-560 (in Japanese with English abstract).

Earthquake Research Committee (2002): "Strong motion evaluation assuming earthquakes at the Itoigawa-Shizuoka-kozosen fault zone (northern part, central part)", published on October 31, 2002 (in Japanese).

Earthquake Research Committee (2003a): "Strong motion evaluation assuming earthquakes at the Morimoto/Togashi fault zone", published on March 12, 2003 (in Japanese).

Earthquake Research Committee (2003b): "Strong motion evaluation assuming earthquakes at the Miyagi-oki", published on June 18, 2003 (in Japanese).

Earthquake Research Committee (2003c): "Strong motion evaluation assuming earthquakes at the Futagawa/Hinagu fault zone", published on July 31, 2003 (in Japanese).

Earthquake Research Committee (2003d): "Strong motion evaluation assuming earthquake at the Miura-hanto fault group", published on October 28, 2003 (in Japanese).

Earthquake Research Committee (2003e): "Strong motion evaluation assuming earthquakes at the Yamagata-bonchi fault zone", published on November 25, 2003 (in Japanese).

Earthquake Research Committee (2004a): "Strong motion evaluation assuming earthquakes at the Tonami-heiya fault zone", published on March 22, 2004 (in Japanese).

Earthquake Research Committee (2004b): "Strong motion evaluation assuming earthquakes at

the northern Sanriku-oki", published on May 21, 2004 (in Japanese).
Earthquake Research Committee (2004c): "Strong motion evaluation assuming earthquakes at the Biwako-seigan fault zone", published on June 21, 2004 (in Japanese).
Earthquake Research Committee (2004d): "Strong motion evaluation assuming earthquakes at the Takayama-Oppara fault zone", published on September 27, 2004 (in Japanese).
Earthquake Research Committee (2004e): "Strong motion evaluation assuming earthquakes at the Ishikari-teichi-toen fault zone", published on November 29, 2004 (in Japanese).
Earthquake Research Committee (2005): "Strong motion evaluation assuming earthquakes at the Yamazaki fault zone", published on January 31, 2005 (in Japanese).
Earthquake Research Committee (2008): "Strong motion evaluation assuming earthquakes at the Kego fault zone (southeastern part)", publishd on April 11, 2008 (in Japanese).
Eshelby, J. D. (1957): "The determination of the elastic field of an ellipsoidal inclusion, and related problems", *Proceedings of the Royal Society*, A241, 376-396.
Fujii, Y. and Matsu'ura, M. (2000): "Regional difference in scaling laws for large earthquakes and its tectonic implication", *Pure Appl. Geophys.*, **157**, 2283-2302.
Fujimoto, K. and Midorikawa, S. (2003): "Average Shear-Wave Velocity Mapping throughout Japan Using the Digital National Land Information", *Journal of Japan Association for Earthquake Engineering*, **3**-3, 13-27 (in Japanese with English abstract).
Fujimoto, K. and Midorikawa, S. (2005): "Empirical Method for Estimating J.M.A. Instrumental Seismic Intensity from Ground Motion Parameters Using Strong Motion Records during Recent Major Earthquakes", *Journal of Social Safety Science*, **7**, 1-6 (in Japanese with English abstract).
Fujimoto, K. and Midorikawa, S. (2006): "Relationship between Average Shear-Wave Velocity and Site Amplification Inferred from Strong Motion Records at Nearby Station Pairs", *Journal of Japan Association for Earthquake Engineering*, **6**-1, 11-22 (in Japanese with English abstract).
Fujiwara, H. (2007): "Development of an Integrated Geophysical and Geological Information Database", *Proceedings of first symposium on the Development of an Integrated Geophysical and Geological Information Database*, 9-22 (in Japanese).
Fujiwara, H., Kawai, S., Aoi, S., Senna, S., Ooi, M., Matusyama, H., Iwamoto, K., Suzuki, H. and Hayakawa, Y. (2006): "A Subsurface Structure Modeling of Whole of Japan for Strong Motion Evaluation", *Proceedings of the 12th Japan Earthquake Engineering Symposium*, 0340, 1466-1469 (in Japanese with English abstract).
Geller, R. J. (1976): "Scaling relations for earthquake source parameters and magnitudes", *Bull. Seism. Soc. Am.*, **66**, 1501-1523.
Graves, R. W. (1996): "Simulating seismic wave propagation in 3D elastic media using staggered-grid finite differences, *Bull. Seism. Soc. Am.*, **86**, 1091-1106.
Hamada, S., Miyata, Y., Takahashi, H., Kaneko, F, Kato, T., Morita, Y. and Fukuwa, N. (2007): "For Accuracy Improvement of Seismic Hazard Maps in Semi-Mountainous Area", *Journal of Social Safety Science*, **9**, 131-136 (in Japanese with English abstract).
Haskell, N. A. (1960): "Crustal reflection of plane SH waves", J. Geophys. Res., 65, 4147-4150.
Hikima, K. and Koketsu, K. (2004): "3-D Velocity Structure Modeling and Source Processes Inversion: The 2003 Miyagi-ken Hokubu, Japan Earthquake Sequence", *EOS Trans. AGU*, **85**(47), Fall Meet. Suppl., Abstract S54A-06.
Hisada, Y. (1995): "An efficient method for computing Green's functions for a layered half-space with sources and receivers at close depth (part2)", *Bull. Seism. Soc. Am.*, **85**,

1080-1093.
Ikeda, T., Kamae, K., Miwa, S. and Irikura, K. (2002): "Source Characterization and Strong Ground Motion Simulation of the 2000 Tottori-ken Seibu Earthquake Using the Empirical Green's Function Method", *J. Struct. Constr. Eng., AIJ*, **561**, 37-45 (in Japanese with English abstract).
Irikura, K. and Kamae, K. (1999): "Strong Ground Motions during the 1948 Fukui Earthquake Estimation of Broad band Ground Motion Using a Hybrid Simulation Technique", *J. Seism. Soc. Japan (Second Series)*, **52**, 129-150 (in Japanese with English abstract).
Irikura, K. and Miyake, H. (2001): "Prediction of Strong Ground Motions for Scenario Earthquakes", *Journal of Geography*, **110**, 849-875 (in Japanese with English abstract).
Irikura, K., Miyake, H., Iwata, T., Kamae, K. and Kawabe, H. (2002): "Revised Recipe for Predicting Strong Ground Motion and Its Validation", *Proceedings of the 11th Japan Earthquake Engineering Symposium*, 567-572 (in Japanese with English abstract).
Irikura, K. (2004): "Recipe for Predicting Strong Ground Motion from Future Large Earthquake", *Annual of Disas. Prev. Inst., Kyoto Univ.*, No.47A, 317-322 (in Japanese).
Ishii, T., Sato, T. and Somerville, P. G. (2000): "Identification of Main Rupture Areas of Heterogeneous Fault Models for Strong-Motion Estimation", *J. Struct. Constr. Eng., AIJ*, **527**, 61-70 (in Japanese with English abstract).
Ishii, T. and Sato, T. (2000): "Relation between the Main Rupture Areas and their Moments of Heterogeneous Fault Models for Strong Motion Estimation", *Programme and Abstracts Seism. Soc. Japan 2000, Fall Meeting*, B09 (in Japanese).
Ito, K. (1999): "Seismogenic layer, reflective lower crust, surface heat flow and large inland-earthquakes", *Tectonophysics*, **306**, 423-433.
Iwata, T., Sekiguchi, H. and Miyakoshi, K. (2001): "Characterization of source process of recent destructive earthquake inverted from strong motion records in the dense network", *Proceedings of US-Japan Joing Workshop and third grantees meeting for US-Japan Cooperative Research on Urban Earthquake Disaster Mitigation*, 53-59.
Japan Meteorological Agency (1996): Public Notice No. 4 of the Japan Meteorological Agency.
Kagawa, T., Irikura, K. and Takemura, M. (1998): "Estimation of Strong Ground Motion -Present Status and Future-", *J. Seism. Soc. Japan (Second Series)*, **51**, 339-354 (in Japanese with English abstract).
Kamae, K., Irikura, K. and Fukuchi, Y. (1991): "Prediction of Strong Ground Motion Based on Scaling Law of Earthquake", *J. Struct. Constr. Eng., AIJ*, **430**, 1-9.
Kamae, K. and Irikura, K. (1998): "Source model of the 1995 Hyogo-ken Nanbu earthquake and simulation of near-source ground motion", *Bull. Seism. Soc. Am.*, **88**, 400-412.
Kanamori, H. (1977): "The energy release in great earthquakes", *J. Geophys. Res.*, **82**, 2981-2987.
Kanamori, H. and Anderson, D. L. (1975): "Theoretical basis of some empirical relations in seismology", *Bull. Seism. Soc. Am.*, **65**, 1073-1095.
Kataoka, S., Kusakabe, T., Murakoshi, J. and Tamura, K. (2003): "Study on a Procedure for Formulating Level 2 Earthquake Motion Based on Scenario Earthquakes", *Research Report of National Institute for Land and Infrastructure Management*, **15**, 32pp. (in Japanese)
Kawase, H. and Matuo H. (2004): "Separation of Source, Path, and Site Effects based on the Observed Data by K-NET, KiK-net, and JMA Strong Motion Network", *Journal of Japan Association for Earthquake Engineering*, **4**-4, 126-145 (in Japanese with English abstract).

Kikuchi, M. and Yamanaka, Y. (2001): "Kiou oojishin no hakai katei = asuperitii no doutei" (Rupture processes of past large earthquakes = identification of asperities), *Saisumo*, **5**-7, 6-7 (in Japanese).

Kiyono, J. (2005): "Fuseikei jiban no simyureishon kaiseki" (Simulation analysis of irregular ground), Earthquake Ground Motions -phenomenon and theory-, 252-267 (in Japanese).

Kohketsu, K. (1985): "The extended reflectivity method for synthetic near-field seismograms", *J. Phys. Earth*, **33**, 121-131.

Koketsu, K. (2006): "Chika kouzou to choushuki jisindo" (Subsurface structure and long-period ground motion), *Bulletin of Japan Association for Earthquake Engineering*, **4**, 12-15 (in Japanese).

Koketsu, K., Hikima, K., Miyazaki, S. and Ide, S (2004): "Joint inversion of strong motion and geodetic data for the source process of the 2003 Tokachi-oki, Hokkaido, earthquake", *Earth, Planets and Space*, **56**-3, 329-334.

Koketsu, K., Miyake, H., Afnimar and Tanaka, Y. (2009): "A proposal for a standard procedure of modeling 3-D velocity structures and its application to the Tokyo metropolitan area, Japan", *Tectonophysics*, **472**, 290-300.

Koketsu, K., Miyake, H. and Hikima, K. (2008): "Current Status of the Japan Integrated Velocity Structure Model", *Proceedings of second symposium on the Development of an Integrated Geophysical and Geological Information Database*, 63-64 (in Japanese).

Geospatial Information Authority of Japan: *Active Fault Map in Urban Area (1:25,000).*

Matsubara, M., Hayashi, H., Obara, K. and Kasahara, K. (2005): "Low-velocity oceanic crust at the top of the Philippine Sea and Pacific plates beneath Kanto region , central Japan, imaged by seismic tomography", *J. Geophys. Res.*, **110**, B12304, dio:10.1029/2005JB003673.

Madariaga, R. (1979): On the relation between seismic moment and stress drop in the presence of stress and strength heterogeneity", *J. Geophys. Res.*, **84**, 2243-2250.

Matsuda, T. (1975): "Magnitude and Recurrence Interval of Earthquakes from a Fault", *J. Seism. Soc. Japan (Second Series)*, **28**, 269-283 (in Japanese with English abstract).

Matsuda, T. (1990): "Seismic Zoning Map of Japanese Islands, with Maximum Magnitudes Derived from Active Fault Data", *Bull. Earthq. Res. Inst., Univ. Tokyo*, 65, 289-319 (in Japanese with English abstract).

Matsuoka, M. and Midorikawa, S. (1994): "Digital national land information and seismic microzoning", *Proceedings of the 22nd Symposium of Earthquake Ground Motion, AIJ*, 23-34 (in Japanese with English abstract).

Matsuoka, M., Wakamatsu, K., Fujimoto, K. and Midorikawa, S. (2005): "Average Shear-wave Velocity Mapping Using Japan Engineering Geomorphologic Classification Map", *Journal of Geological Engineering*, No.794/I-72, 239-251 (in Japanese with English abstract).

Midorikawa, S., Fujimoto, K. and Muramatsu, I. (1999): "Correction of New J.M.A. Instrumental Seismic Intensity with Former J.M.A. Seismic Intensity and Ground Motion Parameters", *Journal of Social Safety Science*, **1**, 51-56 (in Japanese with English abstract).

Miyakoshi, K., Sekiguchi, H. and Iwata, T. (2001): "Extraction of the spatial heterogeneity of slip", FY2000 Special Coordination Fund for Science and Technology "Master Model of Strong Motion Prediction for Mitigating Earthquake Disasters" Research Report, 99-109 (in Japanese).

Morikawa, N. and Fujiwara, H. (2009): "On the relationship between peak ground velocity and seismic intensity", *Abstract Submissions for Japan Geoscience Union Meeting 2009*,

S152-P024.
Nakata, T., Shimazaki, K., Suzuki, Y. and Tsukuda, E. (1998): "Fault Branching and Directivity of Rupture Propagation", *Journal of Geography*, **107**, 512-528 (in Japanese with English abstract).
Nakata, T. and Imaizumi, T. ed. (2002): *Digital Active Fault Map of Japan*, University of Tokyo Press (in Japanese).
Nakamura, H. and Miyatake, T. (2000): "An Approximate Expression of Slip Velocity Time Function for Simulation of Near Field Strong Ground Motion", *J. Seism. Soc. Japan (Second Series)*, **53**, 1-9 (in Japanese with English abstract).
Pitarka, A. (1999): "3D Elastic Finite-Difference Modeling of Seismic Motion Using Staggered Grids with Nonuniform Spacing", *Bull. Seism. Soc. Am.*, **89**, 54-68.
Sato, R. ed. (1989): *Fault Parameter Handbook in Japan*, Kajima Institute Publishing Co., Ltd, 390pp. (in Japanese).
Sato, T., Kawase, H. and Sato. T. (1994): "Statistical Spectral Characteristics for Engineering Bedrock Waves in Which Local Site Effects of Surface Geology are Removed. Based on the ground motion records of small and medium earthquakes observed in the boreholes in Sendai", *J. Struct. Constr. Eng., AIJ*, **462**, 79-89 (in Japanese with English abstract).
Schnabel, P. B., Lysmer, J. and Seed, H. B. (1972): "SHAKE, a Computer Program for Earthquake Response Analysis of Hirozontally Layered Sites", Report No. EERC 72-12, University of California, Berkeley.
Senna, S., Fujiwara, H., Kawai, S., Aoi, S., Kunugi, T., Ishii, T., Hayakawa, Y., Morikawa, N., Honda, R., Kobayashi, K., Ooi, M., Yasoshima, Y., Kanno, T. and Okumuar, N. (2004): "A Study on Strong-Motion Maps for Scenario Earthquakes in Morimoto-Togashi Fault Zone", *Technical Note of the National Research Institute for Earth Science and Disaster Prevention*, **255** (in Japanese).
Si, H. and Midorikawa, S. (1999): "New Attenuation Relationships for Peak Ground Acceleration and Velocity Considering Effects of Fault Type and Site Condition", *J. Struct. Constr. Eng., AIJ*, **523**, 63-70 (in Japanese with English abstract).
Somerville, P. G., Irikrua, K., Graves, R., Sawada, S., Wald, D., Abrahamson, N., Iwasaki, Y., Kagawa, T., Smith, N. and Kowada, A. (1999): "Characterizing crustal earthquake slip models for the prediction of strong ground motion", *Seism. Res. Lett.*, **70**, 59-80.
Subcommittee for Evaluation of Strong Ground Motion, Earthquake Research Committee (2001): "Strong motion evaluation method assuming earthquakes at the Itoigawa-Shizuoka kozosen fault zone (north part, central part) (interim report)", published on May 25, 2001 (in Japanese).
Subcommittee for Evaluation of Strong Ground Motion, Earthquake Research Committee (2002): "Verification of strong ground motion evaluation method using the observation record of the 2000 Western Tottori Earthquake", published on October 31, 2002 (in Japanese).
Subcommittee for Evaluation of Strong Ground Motion, Earthquake Research Committee (2004): "Verification of strong ground motion evaluation method using the observation record of the 2003 Tokachi-oki Earthquake", published on December 20, 2004 (in Japanese).
Subcommittee for Evaluation of Strong Ground Motion, Earthquake Research Committee (2008): "Verification of strong ground motion evaluation method using the observation record of the 2005 West off Fukuoka Earthquake", published on April 11, 2008 (in

Japanese).
Sugiyama, Y., Sekiguchi, H., Awata, Y., Fusejima, Y. and Shimokawa, K. (2002): "Relationship between active fault information and heterogeneous source characteristics", FY2001 Special Coordination Fund for Science and Technology "Master Model of Strong Motion Prediction for Mitigating Earthquake Disasters" Research Report, 119-129 (in Japanese).
Sugiyama, Y. (2004): "Asperities and Multi-Segment Ruptures in Subduction Zones and Inland Active Fault Systems", *Proceedings of International Conference in Commemoration of 5th Anniversary of the 1999 Chi-Chi Earthquake*, Taiwan, 1-9.
Suzuki, H. (1996): "Geology of the Koto Deep Borehole Observatory and Geological Structure beneath the Metropolitan Area, Japan", *Report of the National Research Institute for Earth Science and Disaster Prevention*, **56**, 77-123 (in Japanese with English abstract).
Takemura, M. (1990): "Magnitude-seismic moment relations for the shallow earthquakes in and around Japan", J. *Seism. Soc. Japan (Second Series)*, **43**, 257-265 (in Japanese with English abstract).
Takahashi, H. and Fukuwa, N. (2006): "Proposal and Verification of Modeling of the Surface Layers for Strong Motion Prediction", *J. Struct. Constr. Eng., AIJ*, **599**, 51-59 (in Japanese with English abstract).
Tanaka, Y., Koketsu, K., Miyake, H., Furumura, T., Sato, H., Hirata, N., Suzuki, H. and Masuda, T. (2005): "The Daidaitoku community model of the velocity structure beneath the Tokyo metropolitan area (1)", Abstracts 2005: *Japan Earth and Planetary Science Joint Meeting*, S079-P010.
Tanaka, Y., Miyake, H., Koketsu, K., Furumura, T., Hayakawa, T., Baba, T., Suzuki, H. and Masuda, T. (2006): "The DaiDaiToku Integrated Model of the Velocity Structure beneath the Tokyo Metropolitan Area (2)", *Abstracts: Japan Geoscience Union Meeting 2006*, S116-P014.
The Research Group for Active Faults of Japan ed. (1991): Active Faults in Japan (revised edition), University of Tokyo Press, 448pp. (in Japanese).
Toda, S. (2004): "Research issues in predicting inland earthquakes", *Chikyu Monthly*, **46** special issue, 108-111 (in Japanese).
Tsurugi, M., Kagawa, T., Irikura, K. and Kowada, A. (1997): "Cutoff frequency fmax of earthquakes occurring in Kinki district", *Abstracts 1997: Japan Earth and Planetary Science Joint Meeting*, 103.
Utsu, T. (2001): *Seismology* [Third edition], Kyoritsu shuppan, 392pp. (in Japanese).
Wakamatsu, K., Matsuoka, M., Kubo, J., Hasegawa, K. and Sugiura, M. (2004): "Development of GIS-based Japan Engineering Geomorphologic Classification Map", *Journal of Geological Engineering*, No.759/I-67 (in Japanese with English abstract).
Wakamatsu, K., Matsuoka, M., Sugiura, M., Kubo, J. and Hasegawa, K. (2005): *Japan Engineering Geomorphologic Classification Map*, University of Tokyo Press (in Japanese).
Wakamatsu, K. and Matsuoka, M. (2007): "Development of GIS-based 7.5-arc-second geomorphologic land classification map for Kyushu region", *Proceedings of the 5th Annual Meeting of Japan Association for Earthquake Engineering*, 102-103 (in Japanese).
Wells, D. L. and Coppersmith, K. J. (1994): "New empirical relationships among magnitude, rupture length, rupture width, rupture area, and surface displacement", *Bull. Seism. Soc. Am.*, **84**, 974-1002.
Wells, R. E., Blakely, R. J., Sugiyama, Y., Scholl, D. W. and Dinterman, P. A. (2003):

"Basin-Centered Asperities in Great Subduction Zone Earthquake: A Link between Slip, Subsidence, and Subduction Erosion", *J. Geophys. Res.*, **108**, B10, 2507, dio:10.1029/2002JB002072.

Yagi, Y. (2004): "Source rupture process of the 2003 Tokachi-oki earthquake determined by joint inversion of teleseismic body wave and strong ground motion data", *Earth, Planets and Space*, **56**-3, 311-316.

Yamamizu, F. (2004): "Seismic Wave Velocity Structures in Kanto Area as Revealed by the Crustral Activity Observation Well VSP" *Technical Note of the National Research Institute for Earth Science and Disaster Prevention*, **251** (in Japanese).

Yamanaka, Y. and Shimazaki, K. (1990): "Scaling relationship between the number of aftershocks and the size of the main shock", *J. Phys. Earth*, **38**, 305-324.

Yamanaka, Y. and Kikuchi, M. (2003): "Source process of the recurrent Tokachi-oki earthquake on September 26, 2003, inferred from teleseismic body waves", *Earth, Planets and Space*, **55**-12, e21-e24.

Yamanaka, H. and Yamada, N. (2002): "Estimation of 3D S-wave velocity model of deep sedimentary layers in Kanto plain, Japan, using microtremor array measurements", Butsuri Tansa, 55, 53-65 (in Japanese with English abstrat).

Yoshida, N. and Tohata, I. (1991): *YUSAYUSA-2 theory and usage* (in Japanese).

Zhao, D., Hasegawa, A. and Kanamori, H. (1994): "Deep structure of Japan subduction zone as derived from local, regional, and teleseismic events", *J. Geophys. Res.*, **122**, 313-327.

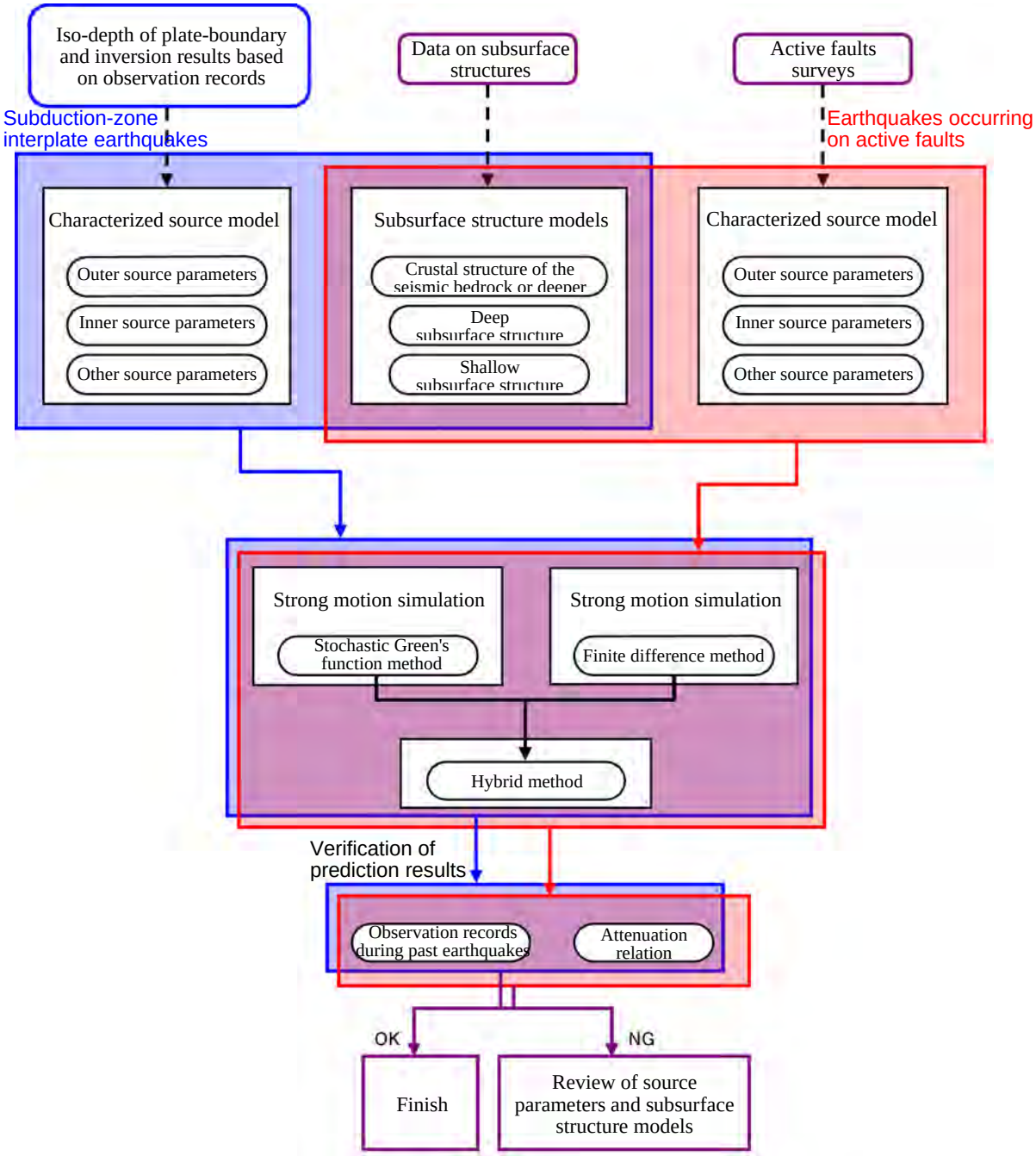

Appended Figure 1 Flow chart of strong motion prediction method (hybrid method) for earthquakes with specified source fault.

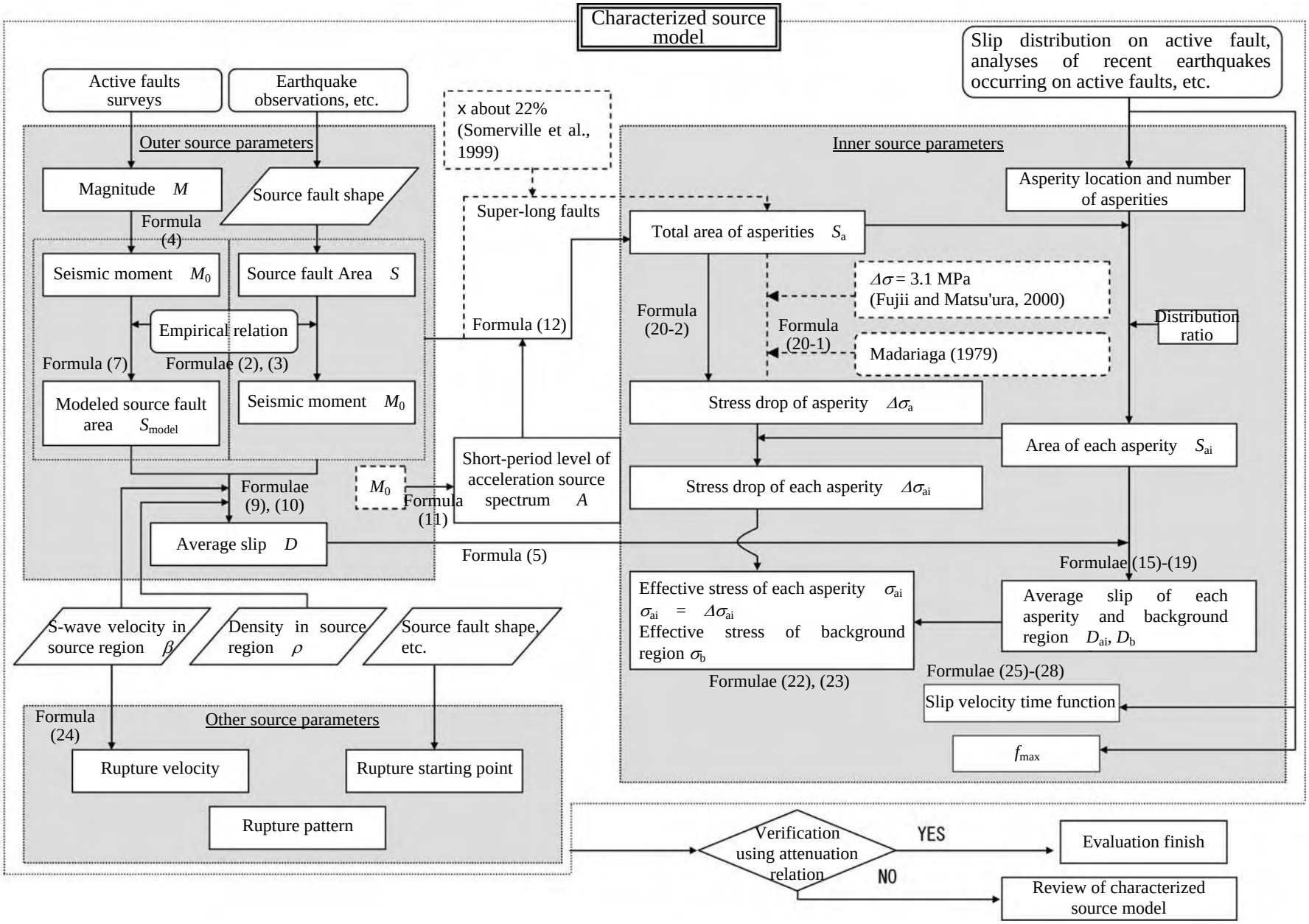

Appended Figure 2 Flow chart of determination of source parameters for earthquakes occurring on active faults. (The case of using a source fault based on past earthquake records or assuming a source fault based on detailed survey results.)

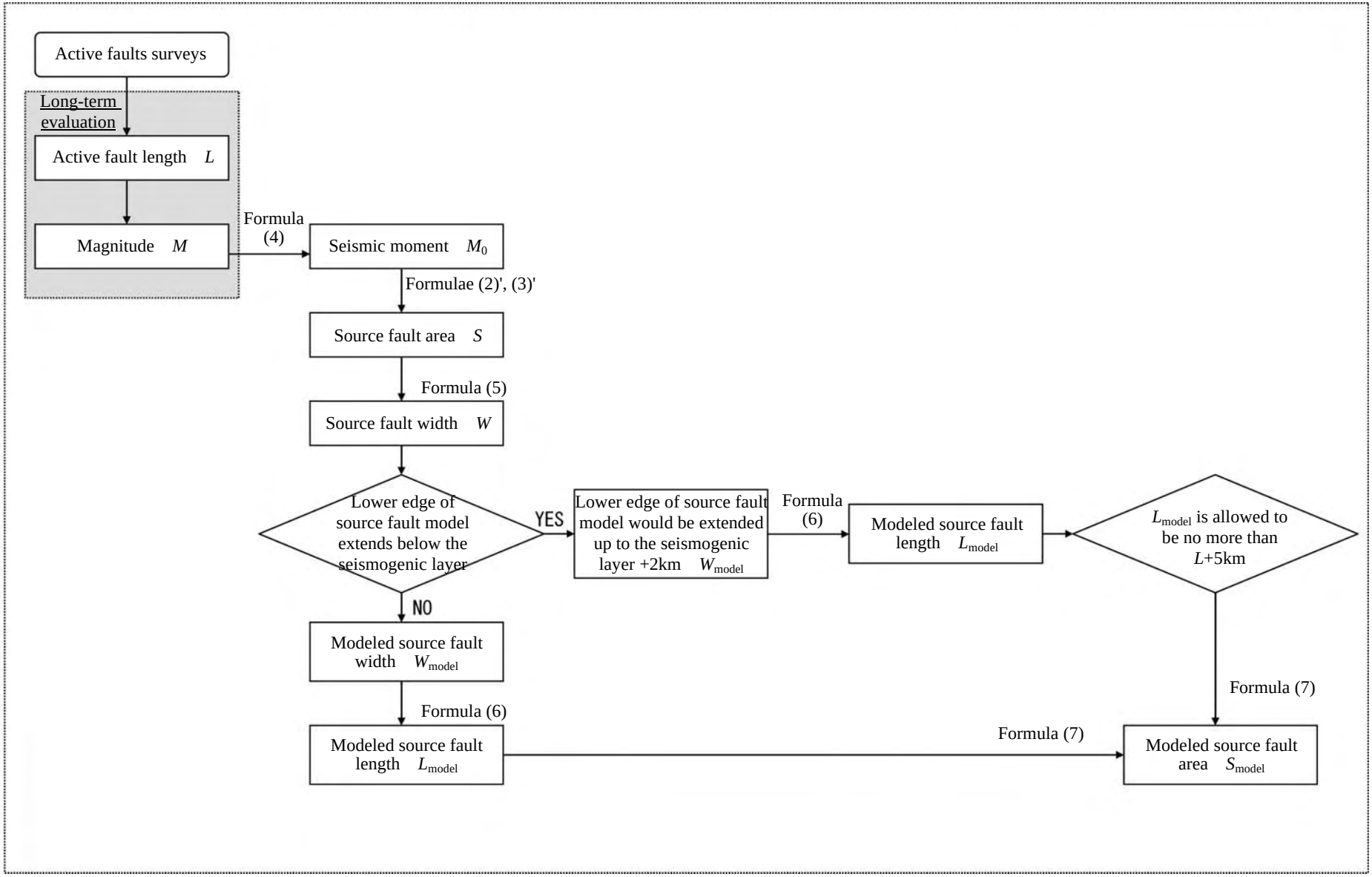

Appended Figure 3 Flow chart of determination of source parameters for earthquakes occurring on active faults. (The case of assuming a source fault from ground surface information about the active fault by using a simplified method.)

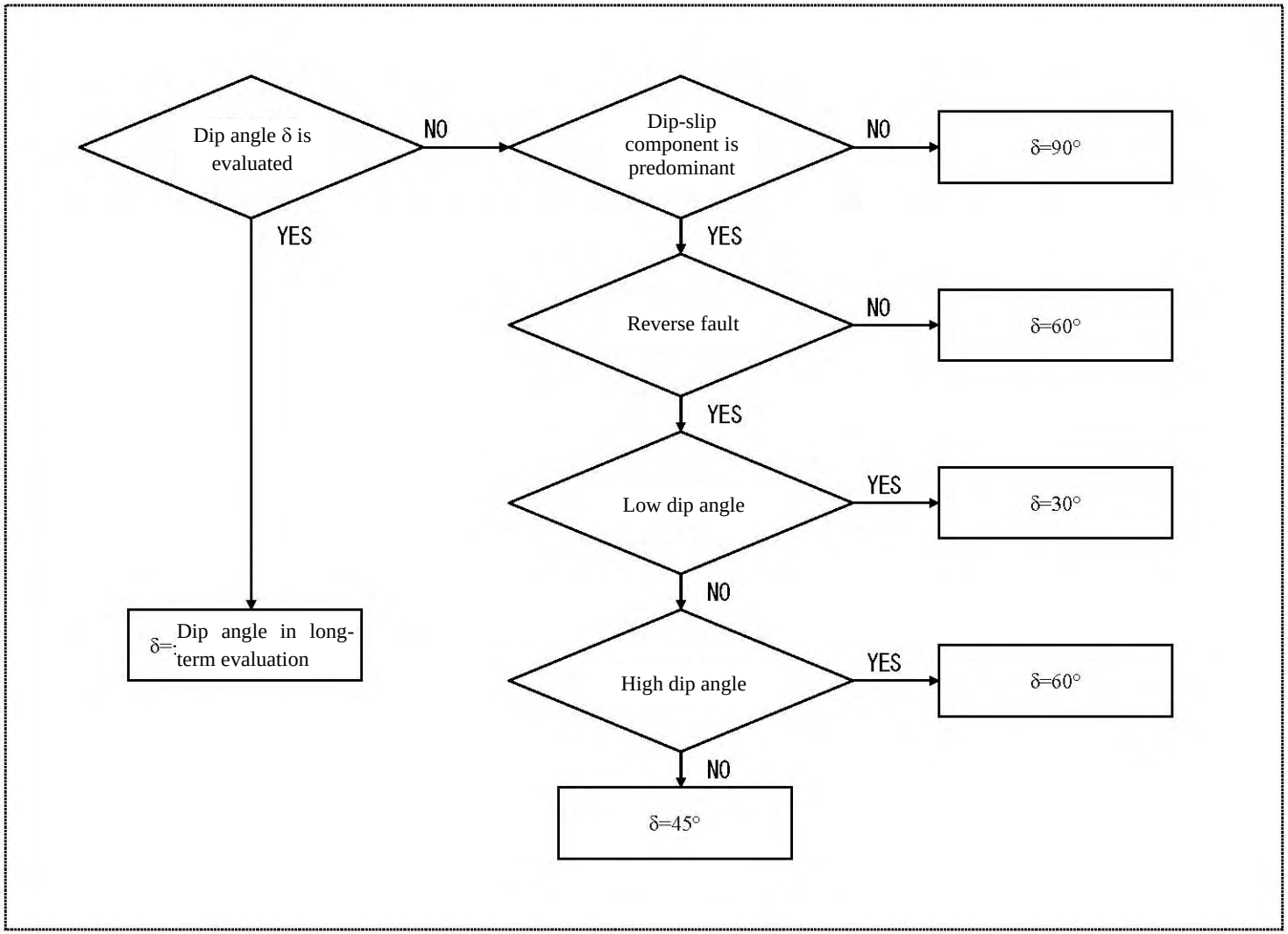

Appended Figure 4 Flow chart of determination of dip angle of source fault for earthquakes occurring on active faults.

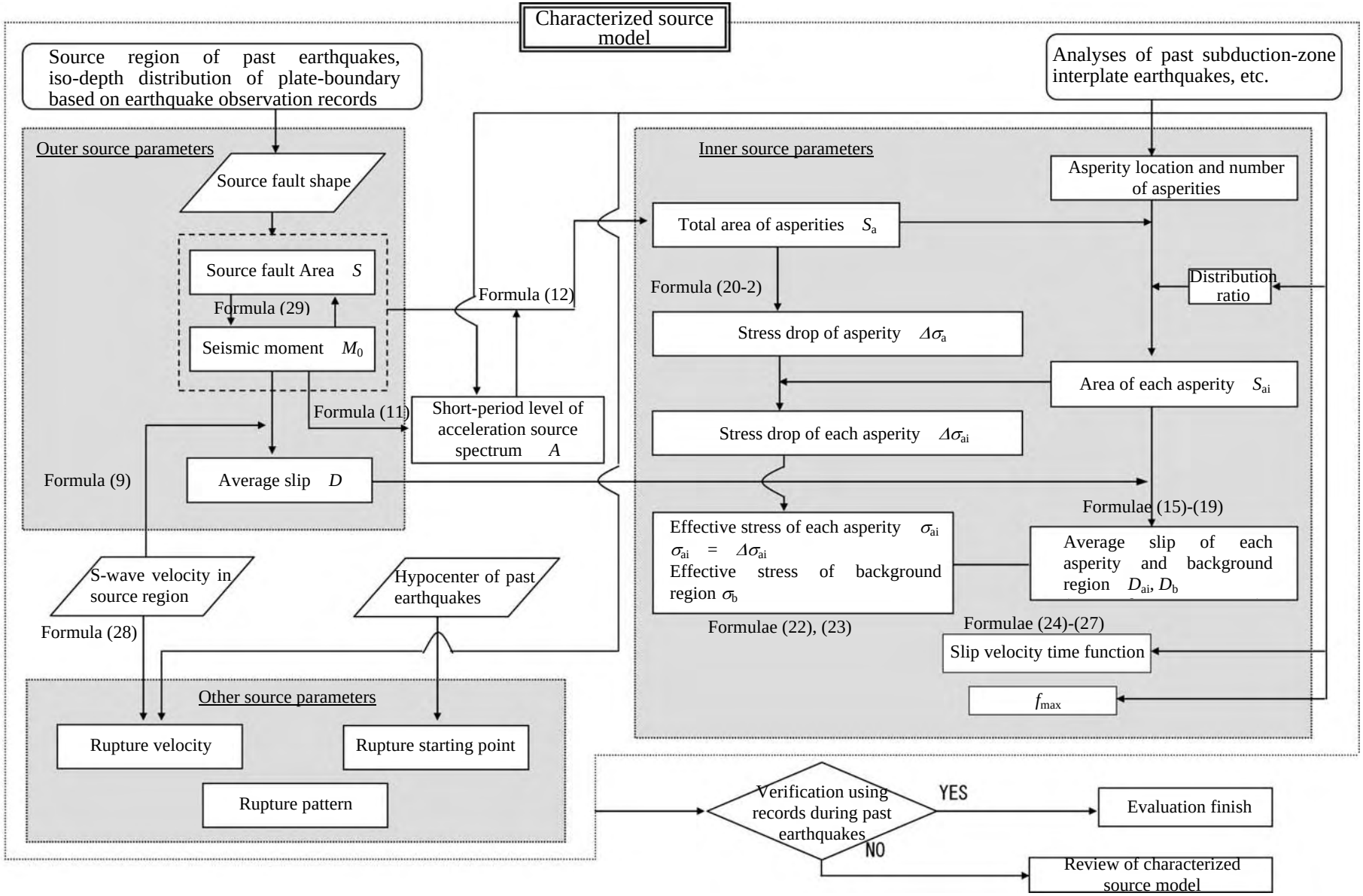

Appended Figure 5 Flow chart of determination of source parameters for subduction-zone interplate earthquakes.

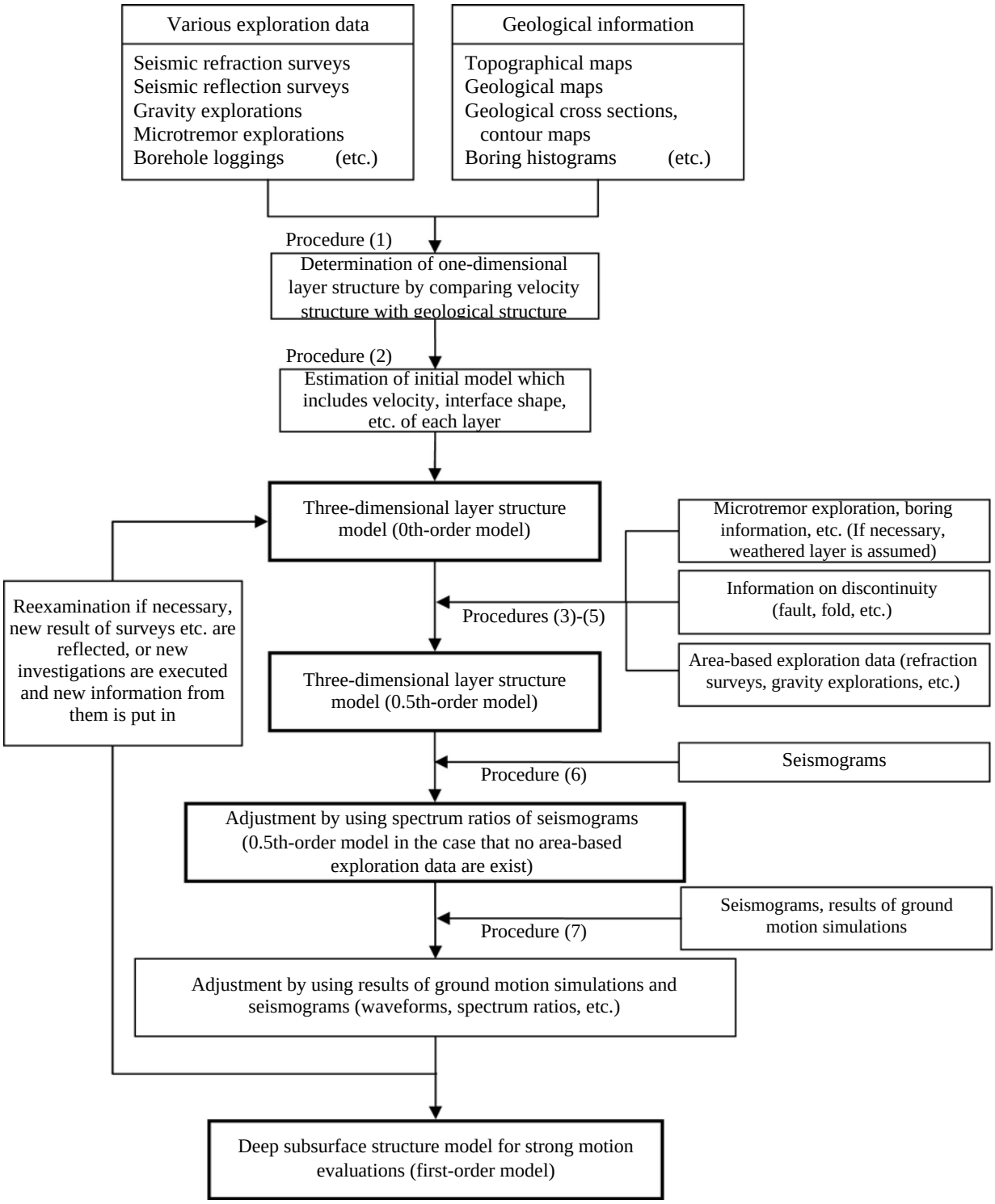

Appended Figure 6 Flow chart of modeling deep subsurface structure for strong motion evaluations.

National Research Institute for Earth Science and Disaster Prevention
Tennodai 3-1, Tsukuba, Ibaraki, 305-0006 Japan